

CRC Series in  
CONTEMPORARY FOOD SCIENCE

# Food Emulsions

Principles, Practices, and Techniques

**Second Edition**

David Julian McClements



CRC PRESS

# **Food Emulsions**

Principles, Practices, and Techniques

**Second Edition**

# CRC Series in CONTEMPORARY FOOD SCIENCE

Fergus M. Clydesdale, Series Editor  
University of Massachusetts, Amherst

## Published Titles:

*New Food Product Development: From Concept to Marketplace*  
Gordon W. Fuller

*Food Properties Handbook*  
Shafiur Rahman

*Aseptic Processing and Packaging of Foods: Food Industry Perspectives*  
Jarius David, V. R. Carlson, and Ralph Graves

*Handbook of Food Spoilage Yeasts*  
Tibor Deak and Larry R. Beauchat

*Getting the Most Out of Your Consultant: A Guide to Selection  
Through Implementation*  
Gordon W. Fuller

*Food Emulsions: Principles, Practice, and Techniques*  
David Julian McClements

*Antioxidant Status, Diet, Nutrition, and Health*  
Andreas M. Papas

*Food Shelf Life Stability*  
N.A. Michael Eskin and David S. Robinson

*Bread Staling*  
Pavinee Chinachoti and Yael Vodovotz

*Food Consumers and the Food Industry*  
Gordon W. Fuller

*Interdisciplinary Food Safety Research*  
Neal M. Hooker and Elsa A. Murano

*Automation for Food Engineering: Food Quality Quantization and Process Control*  
Yanbo Huang, A. Dale Whittaker, and Ronald E. Lacey

*Introduction to Food Biotechnology*  
Perry Johnson-Green

*The Food Chemistry Laboratory: A Manual for Experimental Foods, Dietetics,  
and Food Scientists, Second Edition*  
Connie M. Weaver and James R. Daniel

*Modeling Microbial Responses in Food*  
Robin C. McKellar and Xuewen Lu

*Food Emulsions: Principles, Practice, and Techniques, Second Edition*  
David Julian McClements

# Food Emulsions

Principles, Practices, and Techniques

Second Edition

David Julian McClements



**CRC PRESS**

---

Boca Raton London New York Washington, D.C.



### Library of Congress Cataloging-in-Publication Data

---

McClements, D. J.

Food emulsions : principles, practice, and techniques / David Julian

McClements.— 2nd ed.

p. cm.

Includes bibliographical references and index.

ISBN 0-8493-2023-2 (alk. paper)

1. Emulsions. 2. Food. I. Title.

TP156.E6M35 2004

664—dc22

2004054209

This book contains information obtained from authentic and highly regarded sources. Reprinted material is quoted with permission, and sources are indicated. A wide variety of references are listed. Reasonable efforts have been made to publish reliable data and information, but the author and the publisher cannot assume responsibility for the validity of all materials or for the consequences of their use.

Neither this book nor any part may be reproduced or transmitted in any form or by any means, electronic or mechanical, including photocopying, microfilming, and recording, or by any information storage or retrieval system, without prior permission in writing from the publisher.

The consent of CRC Press does not extend to copying for general distribution, for promotion, for creating new works, or for resale. Specific permission must be obtained in writing from CRC Press for such copying.

Direct all inquiries to CRC Press, 2000 N.W. Corporate Blvd., Boca Raton, Florida 33431.

**Trademark Notice:** Product or corporate names may be trademarks or registered trademarks, and are used only for identification and explanation, without intent to infringe.

**Visit the CRC Press Web site at [www.crcpress.com](http://www.crcpress.com)**

---

© 2005 by CRC Press

No claim to original U.S. Government works

International Standard Book Number 0-8493-2023-2

Library of Congress Card Number 2004054209

Printed in the United States of America 1 2 3 4 5 6 7 8 9 0

Printed on acid-free paper

# *Dedication*

---

*This book is dedicated to my wife Jayne and daughter Isobelle.*



---

# Preface

A wide variety of food products, both natural and manufactured, exist either partly or wholly as emulsions, or have been in an emulsified form sometime during their production. Common examples of these *food emulsions* include milk, flavored milks, creams, whipped cream, butter, yogurt, cheese, salad dressings, mayonnaise, dips, coffee whitener, ice cream, desserts, soups, sauces, margarine, infant formula, and fruit beverages. Even though these products differ widely in their appearances, textures, tastes, and shelf lives they all consist (or once consisted) of small droplets of one liquid dispersed in another liquid. Consequently, many of their physicochemical and sensory properties can be understood by applying the fundamental principles, concepts, and techniques of a discipline known as *emulsion science*. Knowledge of this discipline is also essential for the rational development of ingredients capable of encapsulating, protecting, and delivering functional food components, such as flavors, antioxidants, vitamins, antimicrobials, and bioactive lipids. It is for these reasons that anybody working in the food industry with these types of products should have at least an elementary understanding of emulsion science.

The primary objective of this book is to present the basic principles, concepts, and techniques of emulsion science and show how they can be used to better understand, predict, and control the properties of a wide variety of food products and functional ingredients. Rather than describing the specific methods and problems associated with the creation of each particular type of emulsion-based food product, I have concentrated on an explanation of the basic concepts of emulsion science, as these are applicable to all types of food emulsions. In particular, this book focuses on developing a fundamental understanding of the major factors that determine the stability, texture, appearance, and flavor of food emulsions. Having said this, the second edition of this book does contain a final chapter that demonstrates the practical use of emulsion science by using it to understand the formulation, formation, and physicochemical properties of some real food emulsions (beverages, dairy emulsions, and dressings).

The second edition of the book has been revised and expanded considerably to reflect recent developments in the field of food emulsions and to provide a more accurate, comprehensive, and up-to-date discussion of the most important topics relevant to the field. In particular, the chapter on emulsion ingredients has been revised extensively to provide a detailed discussion of the origin, properties, and characteristics of the different kinds of functional ingredients (emulsifiers, surfactants, lipids, texture modifiers, and so on) that can be used to produce food emulsions. The second edition also contains two additional chapters. The *Appearance and Flavor* chapter in the first edition has been divided into two separate chapters in the second edition to reflect the considerable advances that have been made in these two important areas. In addition, a chapter on practical applications of emulsion science in the food industry has been included in the second edition, which highlights the importance of emulsion science for understanding, controlling, and improving the quality of dairy products, beverage emulsions, and dressings.

It is a great pleasure to acknowledge the contributions of all those who helped bring this book to fruition. I could never have completed this book without the love, support, and understanding of my wife Jayne, my daughter Isobelle, and my family. I must also thank all of my students, Post-Docs, and coworkers who have been a continual source of stimulating ideas and constructive criticism, and my teachers for providing me with the academic foundations on which I have attempted to build. I also thank all of the scientists who have helped me put together this new edition of the book by providing useful comments on the text or by providing figures that demonstrate useful and important concepts, including Dr. Marc Anton, Prof. John Coupland, Dr. Julia DesRocher, Prof. Eric Dickinson, Mr Robert Engel, Prof. Douglas Goff, Prof. Yoshinori Mine, Dr. Luis Pagnaloni, Prof. Helmar Schubert, Prof. Pieter Walstra, and Dr. Peter Wilde. Finally, I thank all those at CRC Press for their help in the preparation of this book.

---

## About the Author

Dr. David Julian McClements has been an Assistant or Associate Professor at the Department of Food Science at the University of Massachusetts since 1994. He received a *B.Sc. (Hons)* in *Food Science* (1985) and a *Ph.D.* in *Ultrasonic Characterization of Fats and Emulsions* (1989) at the University of Leeds (United Kingdom). He then did Post Doctoral Research at the University of Leeds, University of California (Davis), and the University College Cork (Ireland), before starting at the University of Massachusetts.

Dr. McClements has coauthored a book entitled *Advances in Food Colloids* with Prof. Eric Dickinson, coedited a book entitled *Developments in Acoustics and Ultrasonics* with Dr. Malcolm Povey, and is the sole author of the first edition of *Food Emulsions: Principles, Practice and Techniques*. In addition, he has published over 220 scientific articles as journal manuscripts, book chapters, encyclopedia entries, and conference proceedings. Dr. McClements has received awards from the American Chemical Society and Institute of Food Technologists in recognition of his scientific achievements.



---

# Contents

<b>Chapter 1</b>	<b>Context and background .....</b>	<b>1</b>
1.1	Emulsion science in the food industry.....	1
1.1.1	Development of a more rigorous scientific approach to understanding food emulsion properties .....	2
1.1.2	Development of new analytical techniques to characterize food properties.....	2
1.2	General characteristics of food emulsions .....	3
1.2.1	Definitions .....	3
1.2.2	Mechanisms of emulsion instability .....	5
1.2.3	Ingredient partitioning in emulsions .....	6
1.2.4	Dynamic nature of emulsions .....	7
1.2.5	Complexity of food emulsions .....	7
1.3	Emulsion properties .....	8
1.3.1	Disperse phase volume fraction.....	8
1.3.2	Particle size distribution.....	9
1.3.3	Interfacial properties .....	17
1.3.4	Droplet charge.....	17
1.3.5	Droplet crystallinity.....	18
1.3.6	Droplet interactions.....	19
1.4	Hierarchy of emulsion properties .....	20
1.5	Understanding food emulsion properties .....	21
1.5.1	Factors influencing topics and directions of research .....	21
1.5.2	General approaches used to study food emulsions.....	23
1.6	Overview and philosophy.....	26
<b>Chapter 2</b>	<b>Molecular characteristics .....</b>	<b>27</b>
2.1	Introduction .....	27
2.2	Forces of nature .....	28
2.3	Origin and nature of molecular interactions.....	28
2.3.1	Covalent interactions.....	28
2.3.2	Electrostatic interactions .....	29
2.3.3	van der Waals interactions.....	33
2.3.4	Steric overlap interactions.....	35
2.4	Overall intermolecular pair potential.....	35
2.5	Molecular structure and organization is determined by a balance of interaction energies and entropy effects .....	38
2.6	Thermodynamics of mixing .....	41
2.6.1	Potential energy change on mixing.....	42
2.6.2	Entropy change on mixing.....	43



2.6.3	Overall free energy change on mixing.....	43
2.6.4	Complications.....	44
2.7	Molecular conformation.....	45
2.8	Compound interactions .....	47
2.8.1	Hydrogen bonds .....	47
2.8.2	Hydrophobic interactions.....	48
2.9	Computer modeling of liquid properties .....	48
2.9.1	Monte Carlo techniques.....	49
2.9.2	Molecular dynamics techniques.....	50
2.10	Measurement of molecular characteristics .....	50
<b>Chapter 3</b>	<b>Colloidal interactions .....</b>	<b>53</b>
3.1	Introduction .....	53
3.2	Colloidal interactions and droplet aggregation.....	53
3.3	van der Waals interactions .....	56
3.3.1	Origin of van der Waals interactions .....	56
3.3.2	Modeling van der Waals interactions .....	56
3.3.3	General features of van der Waals interactions.....	62
3.4	Electrostatic interactions .....	63
3.4.1	Origins of electrostatic interactions.....	63
3.4.2	Modeling electrostatic interactions .....	63
3.4.3	General characteristics of electrostatic interactions .....	68
3.5	Steric interactions.....	69
3.5.1	Origin of steric interactions .....	69
3.5.2	Modeling steric interactions.....	69
3.5.3	General characteristics of steric interactions.....	73
3.6	Depletion interactions .....	74
3.6.1	Origin of depletion interactions .....	74
3.6.2	Modeling of depletion interactions .....	75
3.6.3	General characteristics of depletion interactions .....	77
3.7	Hydrophobic interactions.....	78
3.7.1	Origin of hydrophobic interactions.....	78
3.7.2	Modeling hydrophobic interactions .....	79
3.7.3	General characteristics of hydrophobic interactions .....	81
3.8	Hydration interactions .....	81
3.8.1	Origin of hydration interactions .....	81
3.8.2	Modeling hydration interactions.....	81
3.8.3	General characteristics of hydration interactions.....	82
3.9	Thermal fluctuation interactions .....	83
3.9.1	Origin of thermal fluctuation interactions.....	83
3.9.2	Modeling thermal fluctuation interactions.....	84
3.9.3	General characteristics of fluctuation interactions.....	84
3.10	Nonequilibrium effects .....	85
3.10.1	Molecular rearrangements at the interface.....	85
3.10.2	Hydrodynamic flow of continuous phase.....	85
3.10.3	Gibbs–Marangoni effect.....	86
3.11	Total interaction potential.....	86
3.11.1	van der Waals and steric .....	87
3.11.2	van der Waals, steric, and electrostatic .....	88
3.11.3	van der Waals, steric, electrostatic, and hydrophobic.....	91
3.11.4	van der Waals, steric, electrostatic, and depletion.....	91

3.12	Measurement of colloidal interactions .....	92
3.13	Prediction of colloidal interactions in food emulsions.....	93
<b>Chapter 4</b>	<b>Emulsion ingredients .....</b>	<b>95</b>
4.1	Introduction .....	95
4.2	Fats and oils.....	96
4.2.1	Molecular structure and organization .....	98
4.2.2	Bulk physicochemical properties .....	98
4.2.3	Fat crystallization .....	100
4.2.4	Chemical changes .....	109
4.2.5	Selection of an appropriate lipid .....	110
4.3	Water.....	112
4.3.1	Molecular structure and organization .....	112
4.3.2	Bulk physicochemical properties .....	113
4.3.3	Influence of solutes on the organization of water molecules .....	114
4.3.4	Influence of solutes on the physicochemical properties of solutions .....	121
4.3.5	Selection of an appropriate aqueous phase .....	121
4.4	Emulsifiers.....	122
4.4.1	Surfactants .....	122
4.4.2	Amphiphilic biopolymers .....	137
4.4.3	Selection of an appropriate emulsifier .....	146
4.5	Texture modifiers .....	148
4.5.1	Thickening agents .....	148
4.5.2	Gelling agents.....	153
4.5.3	Commonly used texture modifiers .....	158
4.5.4	Selection of an appropriate texture modifier .....	167
4.6	Other food additives .....	168
4.6.1	pH control .....	168
4.6.2	Minerals .....	168
4.6.3	Sequestrants (chelating agents) .....	169
4.6.4	Antioxidants .....	169
4.6.5	Antimicrobial agents .....	171
4.6.6	Flavors .....	171
4.6.7	Colorants .....	172
4.6.8	Weighting agents .....	172
4.6.9	Fat replacers .....	173
4.7	Factors influencing ingredient selection .....	173
<b>Chapter 5</b>	<b>Interfacial properties and their characterization.....</b>	<b>175</b>
5.1	Introduction .....	175
5.2	General characteristics of interfaces .....	176
5.2.1	Interfaces separating two pure liquids .....	176
5.2.2	Interfaces in the presence of solutes .....	179
5.3	Adsorption of solutes to interfaces.....	182
5.3.1	Definition of surface excess concentration .....	182
5.3.2	Relationship between adsorbed and bulk solute concentrations .....	184
5.3.3	Stipulating interfacial properties of surface-active solutes .....	187
5.3.4	Adsorption kinetics .....	187

5.4	Electrical characteristics of interfaces .....	191
5.4.1	Origin of interfacial charge .....	191
5.4.2	Ion distribution near a charged interface .....	193
5.4.3	Factors influencing interfacial electrical properties of emulsions .....	198
5.4.4	Characterization of interfacial electrical properties .....	199
5.5	Interfacial composition and its characterization.....	199
5.5.1	Factors influencing interfacial composition .....	199
5.5.2	Characterization of interfacial composition in emulsions .....	202
5.6	Interfacial structure.....	204
5.6.1	Factors influencing interfacial structure .....	204
5.6.2	Characterization of interfacial structure in emulsions .....	208
5.7	Interfacial tension and its measurement.....	214
5.7.1	Factors influencing interfacial tension .....	214
5.7.2	Characterization of interfacial tension .....	214
5.8	Interfacial rheology.....	221
5.8.1	Factors influencing interfacial rheology .....	221
5.8.2	Characterization of interfacial rheology .....	222
5.9	Practical implications of interfacial phenomena .....	225
5.9.1	Properties of curved interfaces .....	225
5.9.2	Contact angles and wetting .....	226
5.9.3	Capillary rise and meniscus formation .....	229
5.9.4	Interfacial phenomenon in food emulsions .....	230

<b>Chapter 6</b>	<b>Emulsion formation.....</b>	<b>233</b>
6.1	Introduction .....	233
6.2	Overview of homogenization .....	233
6.3	Flow profiles in homogenizers .....	236
6.4	Physical principles of emulsion formation.....	237
6.4.1	Droplet disruption .....	237
6.4.2	Droplet coalescence .....	246
6.4.3	The role of the emulsifier .....	248
6.5	Homogenization devices .....	249
6.5.1	High-speed mixers .....	249
6.5.2	Colloid mills .....	250
6.5.3	High-pressure valve homogenizers .....	251
6.5.4	Ultrasonic homogenizers .....	253
6.5.5	Microfluidization .....	255
6.5.6	Membrane and microchannel homogenizers .....	256
6.5.7	Homogenization efficiency .....	257
6.5.8	Comparison of homogenizers .....	259
6.6	Factors that influence droplet size.....	261
6.6.1	Emulsifier type and concentration .....	261
6.6.2	Energy input .....	263
6.6.3	Properties of component phases .....	263
6.6.4	Temperature .....	264
6.7	Demulsification.....	265
6.7.1	Nonionic surfactants .....	265
6.7.2	Ionic surfactants .....	266
6.7.3	Biopolymer emulsifiers .....	266

6.7.4	General methods of demulsification .....	267
6.7.5	Selection of most appropriate demulsification technique .....	267
6.8	Future developments.....	267
<b>Chapter 7</b>	<b>Emulsion stability .....</b>	<b>269</b>
7.1	Introduction .....	269
7.2	Thermodynamic and kinetic stability of emulsions.....	270
7.2.1	Thermodynamic stability .....	270
7.2.2	Kinetic stability .....	272
7.3	Gravitational separation .....	273
7.3.1	Physical basis of gravitational separation .....	274
7.3.2	Methods of controlling gravitational separation .....	284
7.3.3	Experimental characterization of gravitational separation .....	286
7.4	General features of droplet aggregation .....	289
7.4.1	Droplet–droplet encounters .....	290
7.4.2	Film thinning .....	290
7.4.3	Thin film formation .....	291
7.4.4	Film rupture .....	291
7.5	Flocculation .....	292
7.5.1	Physical basis of flocculation.....	292
7.5.2	Methods of controlling flocculation .....	298
7.5.3	Structure and properties of flocculated emulsions .....	305
7.5.4	Experimental measurement of flocculation .....	309
7.6	Coalescence .....	310
7.6.1	Physical basis of coalescence .....	311
7.6.2	Methods of controlling coalescence .....	319
7.6.3	Factors affecting coalescence .....	320
7.6.4	Measurement of droplet coalescence .....	322
7.7	Partial coalescence .....	324
7.7.1	Physical basis of partial coalescence .....	325
7.7.2	Methods of controlling partial coalescence .....	327
7.7.3	Experimental characterization of partial coalescence .....	329
7.8	Ostwald ripening .....	330
7.8.1	Physical basis of Ostwald ripening .....	331
7.8.2	Methods of controlling Ostwald ripening .....	333
7.8.3	Experimental characterization of Ostwald ripening .....	335
7.9	Phase inversion .....	335
7.9.1	Physical basis of phase inversion .....	336
7.9.2	Methods of controlling phase inversion .....	337
7.9.3	Characterization of phase inversion .....	338
7.10	Chemical and biochemical stability .....	339
<b>Chapter 8</b>	<b>Emulsion rheology .....</b>	<b>341</b>
8.1	Introduction .....	341
8.2	Rheological properties of materials .....	342
8.2.1	Solids .....	342
8.2.2	Liquids .....	345
8.2.3	Plastics .....	351
8.2.4	Viscoelastic materials .....	353

8.3	Measurement of rheologic properties.....	356
8.3.1	Simple compression and elongation .....	357
8.3.2	Shear measurements .....	360
8.3.3	Empirical techniques .....	364
8.4	Rheologic properties of emulsions.....	365
8.4.1	Dilute suspensions of rigid spherical particles .....	366
8.4.2	Dilute suspensions of fluid spherical particles .....	367
8.4.3	Dilute suspensions of rigid nonspherical particles .....	368
8.4.4	Dilute suspensions of flocculated particles .....	370
8.4.5	Concentrated suspensions of nonflocculated particles in the absence of long-range colloidal interactions .....	372
8.4.6	Suspensions of nonflocculated particles with repulsive interactions .....	374
8.4.7	Concentrated suspensions with attractive interactions: flocculated systems .....	376
8.4.8	Emulsions with semisolid continuous phases .....	380
8.5	Computer simulation of emulsion rheology .....	381
8.6	Major factors influencing emulsion rheology .....	382
8.6.1	Disperse phase volume fraction .....	382
8.6.2	Rheology of component phases .....	383
8.6.3	Droplet size .....	384
8.6.4	Colloidal interactions .....	384
8.6.5	Droplet charge .....	385
8.7	Future Trends.....	386

## **Chapter 9 Emulsion flavor .....389**

9.1	Introduction .....	389
9.1.1	Physicochemical processes .....	389
9.1.2	Physiologic processes .....	390
9.1.3	Psychologic processes .....	390
9.1.4	General aspects.....	390
9.2	Flavor partitioning.....	391
9.2.1	Partitioning between a homogenous liquid and a vapor .....	391
9.2.2	Influence of flavor ionization .....	394
9.2.3	Influence of flavor binding on partitioning .....	395
9.2.4	Influence of surfactant micelles on partitioning .....	397
9.2.5	Partitioning in emulsions in the absence of an interfacial membrane.....	397
9.2.6	Partitioning in emulsions in the presence of an interfacial membrane.....	399
9.3	Flavor release.....	401
9.3.1	Overview of physicochemical process of flavor release .....	401
9.3.2	Release of nonvolatile compounds (taste) .....	402
9.3.3	Release of volatile compounds (aroma) .....	407
9.4	Emulsion mouthfeel .....	415
9.5	Measurement of emulsion flavor .....	417
9.5.1	Analysis of volatile flavor compounds .....	417
9.5.2	Analysis of nonvolatile flavor compounds .....	419
9.5.3	Sensory analysis .....	421
9.6	Overview of factors influencing emulsion flavor.....	422
9.6.1	Disperse phase volume fraction .....	422

9.6.2	Droplet size .....	424
9.6.3	Interfacial characteristics .....	426
9.6.4	Oil phase characteristics .....	427
9.6.5	Aqueous phase characteristics .....	428
9.7	Concluding remarks and future directions .....	429
<b>Chapter 10</b>	<b>Appearance .....</b>	<b>431</b>
10.1	Introduction .....	431
10.2	General aspects of optical properties of materials.....	432
10.2.1	Interaction of light with matter .....	432
10.2.2	Human vision .....	438
10.2.3	Quantitative description of appearance .....	438
10.3	Mathematical modeling of emulsion color.....	439
10.3.1	Calculation of scattering characteristics of emulsion droplets .....	440
10.3.2	Calculation of spectral transmittance or reflectance of emulsions .....	442
10.3.3	Relationship of tristimulus coordinates to spectral reflectance and transmittance .....	445
10.3.4	Influence of polydispersity .....	446
10.3.5	Numerical calculations of emulsion color .....	446
10.3.6	Influence of measurement cell .....	449
10.4	Measurement of emulsion color.....	450
10.4.1	Spectrophotometric colorimeters .....	451
10.4.2	Trichromatic colorimeters .....	453
10.4.3	Light scattering .....	454
10.4.4	Sensory analysis .....	454
10.5	Major factors influencing emulsion color.....	454
10.5.1	Droplet concentration and size .....	455
10.5.2	Relative refractive index of droplets .....	456
10.5.3	Colorant type and concentration .....	456
10.5.4	Factors affecting color of real food emulsions .....	458
10.6	Concluding remarks and future directions .....	458
<b>Chapter 11</b>	<b>Characterization of emulsion properties.....</b>	<b>461</b>
11.1	Introduction .....	461
11.2	Testing emulsifier effectiveness .....	461
11.2.1	Emulsifying capacity .....	462
11.2.2	Emulsion stability index .....	463
11.3	Microstructure and droplet size distribution .....	465
11.3.1	Microscopy .....	465
11.3.2	Static light scattering .....	475
11.3.3	Dynamic light scattering and diffusing wave spectroscopy .....	481
11.3.4	Electrical pulse counting .....	485
11.3.5	Sedimentation techniques .....	487
11.3.6	Ultrasonic spectrometry .....	488
11.3.7	Nuclear magnetic resonance .....	492
11.3.8	Neutron scattering .....	493
11.3.9	Dielectric spectroscopy .....	495
11.3.10	Electroacoustics .....	495
11.4	Disperse phase volume fraction.....	495
11.4.1	Proximate analysis .....	495

11.4.2	Density measurements .....	496
11.4.3	Electrical conductivity .....	498
11.4.4	Alternative techniques .....	499
11.5	Droplet crystallinity .....	499
11.5.1	Dilatometry .....	499
11.5.2	Nuclear magnetic resonance .....	501
11.5.3	Thermal analysis .....	504
11.5.4	Ultrasonics .....	506
11.6	Droplet charge .....	508
11.6.1	Particle electrophoresis .....	508
11.6.2	Electroacoustics .....	510
11.7	Droplet interactions .....	512
<b>Chapter 12</b>	<b>Food emulsions in practice .....</b>	<b>515</b>
12.1	Introduction .....	515
12.2	Milk and cream .....	515
12.2.1	Composition .....	515
12.2.2	Microstructure .....	518
12.2.3	Production .....	519
12.2.4	Physicochemical properties .....	520
12.2.5	Dairy products .....	522
12.3	Beverage emulsions .....	526
12.3.1	Composition .....	526
12.3.2	Microstructure .....	529
12.3.3	Production .....	530
12.3.4	Physicochemical properties .....	530
12.4	Dressings .....	533
12.4.1	Composition .....	534
12.4.2	Microstructure .....	537
12.4.3	Production .....	539
12.4.4	Physicochemical properties .....	539
<b>References</b>	<b>.....</b>	<b>545</b>
<b>Index</b>	<b>.....</b>	<b>597</b>

## chapter one

---

# Context and background

### 1.1 Emulsion science in the food industry

A considerable number of natural and processed foods consist either partly or wholly as emulsions, or have been in an emulsified state sometime during their production, including milk, cream, fruit beverages, infant formula, soups, cake batters, salad dressings, mayonnaise, cream-liqueurs, sauces, deserts, salad cream, ice cream, coffee whitener, spreads, butter, and margarine (Krog et al., 1983; Jaynes, 1983; Dickinson and Stainsby, 1982; Dickinson, 1992; Swaisgood, 1996; Friberg and Larsson, 1997; Goff, 1997a–c; Stauffer, 1999; Friberg et al., 2004). The wide diversity of physicochemical and sensory characteristics exhibited by emulsion-based food products is the result of the different kinds of ingredients and processing conditions used to create them. Despite this diversity, there are a number of underlying features that are common to this group of products that makes them amenable to study by a scientific discipline known as *emulsion science*. Emulsion science combines aspects of physics, chemistry, biology, and engineering. Traditionally, the fundamental principles of emulsion science were largely derived from the disciplines of polymer science, colloid science, interfacial chemistry, and fluid mechanics (Hunter, 1986, 1989, 1993; Evans and Wennerstrom, 1994; Hiemenz and Rajagopalan, 1997). Nevertheless, as emulsion science has evolved within the food industry it has incorporated a variety of other disciplines, such as sensory science and physiology, as researchers attempt to correlate organoleptic qualities of food emulsions (such as taste, odor, mouthfeel, and appearance) to their composition and physicochemical properties. In addition, there is a strong tendency within current research on food emulsions toward the integration of knowledge from traditionally separate fields of study, for example, establishing the interrelationships among perceived mouthfeel (sensory science and physiology), emulsion rheology (fluid mechanics), droplet characteristics (colloidal science), and interfacial properties (interfacial chemistry).

The manufacture of an emulsion-based food product with specific quality attributes depends on the selection of the most suitable types and concentrations of raw materials (e.g., water, oil, emulsifiers, thickening agents, minerals, acids, bases, vitamins, flavors, colorants, preservatives) and the most appropriate processing, storage, transport, and usage conditions (e.g., mixing, homogenization, pasteurization, sterilization, chilling, freezing, cooking). Traditionally, the food industry largely relied on craft and tradition for the formulation of food products and the establishment of processing conditions. This approach is unsuitable for the modern food industry, which must rapidly respond to changes in consumer preferences for a greater variety of cheaper, higher quality, healthier, more exotic, and more convenient foods (Sloan, 2003; Mermelstein, 2002).



In addition, the modern food industry relies increasingly on large-scale production operations to produce vast quantities of foods at relatively low cost. The development of new foods, the improvement of existing foods, and the efficient operation of food processing operations require a more systematic and rigorous approach than was used previously (Hollingsworth, 1995; Walstra, 2003). Two major recent trends within food science that have been of particular importance in establishing the more rational development of emulsion-based food products are highlighted below.

### *1.1.1 Development of a more rigorous scientific approach to understanding food emulsion properties*

There has been an increasing tendency within the food industry toward relating the bulk physicochemical and organoleptic properties of food emulsions to the type, concentration, structure, and interactions of their constituent components. Research in this area is carried out at many different structural levels, ranging from the study of the structure and interactions of molecules and colloidal particles, to the study of the rheology, stability, and optical properties of emulsions, to the study of the taste, smell, mouthfeel, and appearance of final products. In particular, there is a growing emphasis on integrating information determined at different structural levels, so as to obtain a more holistic understanding of the properties of the whole system. The improved understanding of the physicochemical basis of food emulsion properties that has resulted from this approach has enabled manufacturers to create low-cost high-quality food products in a more systematic and reliable fashion.

### *1.1.2 Development of new analytical techniques to characterize food properties*

The boundaries of our understanding of the physicochemical basis of food emulsion properties are often determined by the availability of analytical techniques that are capable of investigating the appropriate characteristics of the system. As analytical instrumentation progresses we are able to study things that were not possible earlier, which often results in a deeper and broader understanding of the subject. In recent years, many new and improved analytical techniques for probing the molecular, interfacial, colloidal, and bulk physicochemical properties of emulsions have become available. The application of these techniques has led to considerable advances in basic research, product development, and quality control within the food industry. These analytical techniques are used in research laboratories to enhance the fundamental understanding of the physicochemical basis of emulsion properties. They are also used in factories to monitor the properties of foods during processing so as to ensure that they meet the required quality specifications and to provide information that can be used to optimize the processing conditions required to produce consistently high quality products. As new analytical instrumentation continues to become available there will certainly be further developments in the abilities of food scientists to understand, predict, and control the properties of emulsion-based food products. In addition, the study of food emulsions can provide an excellent paradigm for the study of more structurally complex food materials, since many of the concepts, theories, and techniques developed to model or probe emulsion properties can be applied (with some modification) to understanding these systems.

Ultimately, the aim of the emulsion scientist working in the food industry is to use the basic principles and techniques of emulsion science to enhance the quality of the food

supply and the efficiency of food production. This book presents the conceptual and theoretical framework required by food scientists to understand and control the properties of emulsion-based food products.

## 1.2 General characteristics of food emulsions

### 1.2.1 Definitions

An emulsion consists of two immiscible liquids (usually oil and water), with one of the liquids dispersed as small spherical droplets in the other (Figure 1.1). In most foods, the diameters of the droplets usually lie somewhere between 0.1 and 100  $\mu\text{m}$  (Dickinson and Stainsby, 1982; Dickinson, 1992; Friberg and Larrson, 1997). Emulsions can be conveniently classified according to the relative spatial distribution of the oil and aqueous phases. A system that consists of oil droplets dispersed in an aqueous phase is called an *oil-in-water* or O/W emulsion, for example, milk, cream, dressings, mayonnaise, beverages, soups, and sauces. A system that consists of water droplets dispersed in an oil phase is called a *water-in-oil* or W/O emulsion, for example, margarine and butter. The substance that makes up the droplets in an emulsion is referred to as the *dispersed*, *discontinuous*, or *internal phase*, whereas the substance that makes up the surrounding liquid is called the *continuous* or *external phase*. To be consistent, we will refer to the droplets as the dispersed phase and the surrounding liquid as the continuous phase throughout this book. The concentration of droplets in an emulsion is usually described in terms of the *disperse phase volume fraction*,  $\phi$  (Section 1.3.1).

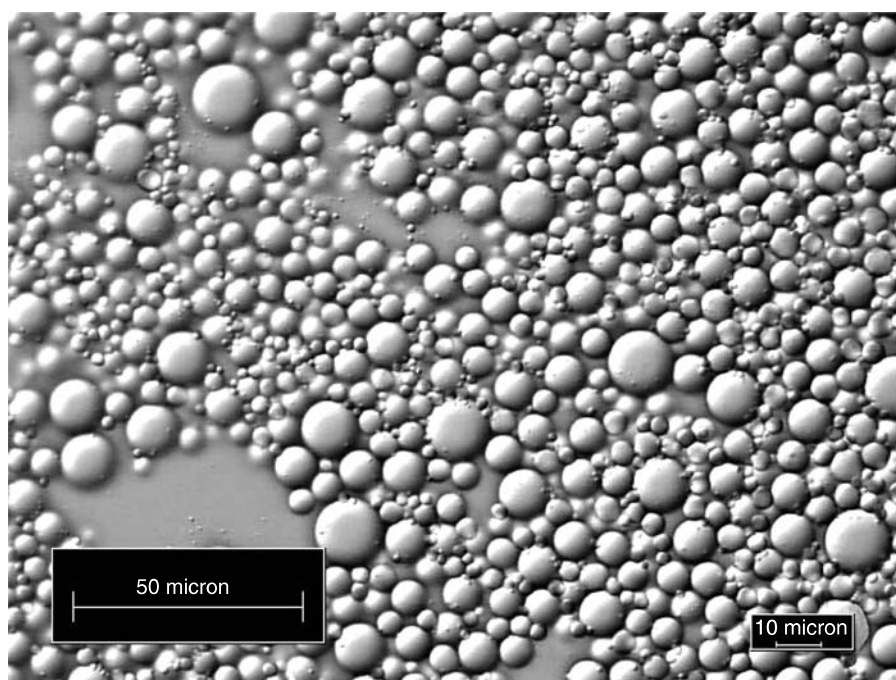


**Figure 1.1** An example of a food oil-in-water emulsion (salad dressing) consisting of oil droplets dispersed in an aqueous medium. Evaluated using differential interference contrast (DIC), a general contrast enhancement optical method that highlights differences in refractive indices in heterogeneous samples (courtesy of Kraft Foods).

In addition to the conventional O/W or W/O emulsions described above, it is also possible to prepare various types of *multiple emulsions*, for example, oil-in-water-in-oil (O/W/O) or water-in-oil-in-water (W/O/W) emulsions (Garti, 1997; Garti and Bisperink, 1998; Garti and Benichou, 2004). For example, a W/O/W emulsion consists of water droplets dispersed within larger oil droplets, which are themselves dispersed in an aqueous continuous phase (Evison et al., 1995; Benichou et al., 2002a). Recently, research has been carried out to create stable multiple emulsions that can be used to control the release of certain ingredients, reduce the total fat content of emulsion-based food products, or to isolate one ingredient from another ingredient that it might normally interact with (Dickinson and McClements, 1995; Garti and Bisperink, 1998; Garti and Benichou, 2001; 2004). Multiple emulsions are likely to find increasing usage within the food industry because of their potential advantages over conventional emulsions. Nevertheless, researchers are still trying to develop multiple emulsions that can be economically produced using food-grade ingredients and that have desirable quality attributes and sufficiently long shelf lives (Garti and Benichou, 2004).

The process of converting two separate immiscible liquids into an emulsion, or of reducing the size of the droplets in a preexisting emulsion, is known as *homogenization*. In the food industry, this process is usually carried out using mechanical devices known as *homogenizers*, which usually subject the liquids to intense mechanical agitation, for example, high speed blenders, high-pressure valve homogenizers, and colloid mills (Chapter 6).

It is possible to form an emulsion by homogenizing pure oil and pure water together, but the two phases usually rapidly separate into a system that consists of a layer of oil (lower density) on top of a layer of water (higher density). This is because droplets tend to merge with their neighbors when they collide with them, which eventually leads to complete phase separation. The driving force for this process is the fact that the contact between oil and water molecules is thermodynamically unfavorable (Israelachvili, 1992), so that emulsions are *thermodynamically unstable* systems (Chapter 7). It is possible to form emulsions that are *kinetically stable* (metastable) for a reasonable period of time (a few days, weeks, months, or years), by including substances known as *stabilizers* (Chapter 4). A stabilizer is any ingredient that can be used to enhance the stability of an emulsion and may be classified as either an *emulsifier* or a *texture modifier* depending on its mode of action. Emulsifiers are *surface-active* molecules that absorb to the surface of freshly formed droplets during homogenization, forming a protective membrane that prevents the droplets from coming close enough together to aggregate (Chapters 6 and 7). Most emulsifiers are *amphiphilic* molecules, that is, they have polar and nonpolar regions on the same molecule. The most common emulsifiers used in the food industry are small-molecule surfactants, phospholipids, proteins, and polysaccharides (Section 4.4). Texture modifiers can be divided into two categories depending on their mode of operation and the rheological characteristics of their solutions: *thickening agents* and *gelling agents* (Section 4.5). Thickening agents are ingredients that are used to increase the viscosity of the continuous phase of emulsions, whereas gelling agents are ingredients that are used to form a gel in the continuous phase of emulsions. Texture modifiers therefore enhance emulsion stability by retarding the movement of the droplets. In the food industry, the most commonly used thickening and gelling agents are usually polysaccharides or proteins in O/W emulsions and fat crystals in W/O emulsions (Section 4.5).

An appreciation of the difference between the thermodynamic stability of a system and its kinetic stability is crucial for an understanding of the properties of food emulsions (Dickinson, 1992). Consider a system that consists of a large number of molecules that can occupy two different free energy states:  $G_{\text{low}}$  and  $G_{\text{high}}$  (Figure 1.2.). The state with the lowest free energy is the one that is thermodynamically favorable, and therefore the one

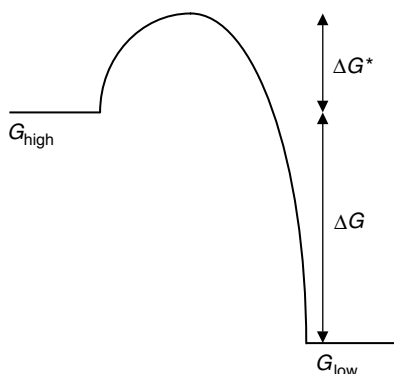


**Figure 1.2** Schematic demonstration of the difference between thermodynamic and kinetic stability. A system will remain in a thermodynamically unstable or metastable state for some time if there is a sufficiently large free energy barrier preventing it from reaching the state with the lowest free energy.

that the molecules are most likely to occupy. At thermodynamic equilibrium, the two states are populated according to the Boltzmann distribution (Atkins, 1994):

$$\frac{n_{\text{high}}}{n_{\text{low}}} = \exp\left(-\frac{(G_{\text{high}} - G_{\text{low}})}{kT}\right) \quad (1.1)$$

where  $n_{\text{low}}$  and  $n_{\text{high}}$  are the number of molecules that occupy the energy levels  $G_{\text{low}}$  and  $G_{\text{high}}$ ,  $k$  is Boltzmann's constant ( $k = 1.38 \times 10^{-23} \text{ J K}^{-1}$ ), and  $T$  is the absolute temperature. The larger the difference between the two free energy levels compared to the thermal energy of the system ( $kT$ ), the greater the fraction of molecules in the lower free energy state. In practice, a system may not be able to reach equilibrium during the timescale of an observation because of the presence of a free energy barrier,  $\Delta G^*$ , between the two states (Figure 1.2). A system in the high free energy state must acquire a free energy greater than  $\Delta G^*$  before it can move into the low energy state. The rate at which a transformation from a high to a low free energy state occurs therefore decreases as the height of the free energy barrier increases. When the free energy barrier is sufficiently large, the system may remain in a thermodynamically unstable state for a considerable length of time, in which case it is said to be *kinetically stable* or *metastable* (Atkins, 1994). In food emulsions, there are actually a large number of intermediate metastable states between the initial emulsion and the completely separated phases, and there are free energy barriers associated with transitions between each of these states. Nevertheless, it is often possible to identify a single free energy barrier, which is associated with a particular physicochemical process that is the most important factor determining the overall kinetic stability of an emulsion (Chapter 7).

### 1.2.2 Mechanisms of emulsion instability

The term “emulsion stability” is broadly used to describe the ability of an emulsion to resist changes in its properties with time (Chapter 7). Nevertheless, there are a variety of physicochemical mechanisms that may be responsible for alterations in emulsion properties, and it is usually necessary to establish which of these mechanisms are important in the particular system under consideration before effective strategies can be developed to improve the stability. A number of the most common physical mechanisms that are

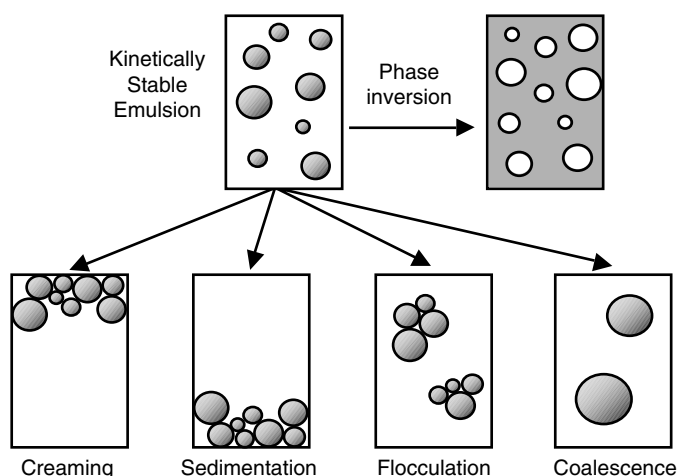


**Figure 1.3** Food emulsions may become unstable through a variety of physical mechanisms, including creaming, sedimentation, flocculation, coalescence, and phase inversion.

responsible for the instability of food emulsions are shown schematically in Figure 1.3. *Creaming* and *sedimentation* are both forms of *gravitational separation*. Creaming describes the upward movement of droplets due to the fact that they have a lower density than the surrounding liquid, whereas sedimentation describes the downward movement of droplets due to the fact that they have a higher density than the surrounding liquid. *Flocculation* and *coalescence* are both types of droplet aggregation. Flocculation occurs when two or more droplets come together to form an aggregate in which the droplets retain their individual integrity, whereas coalescence is the process whereby two or more droplets merge together to form a single larger droplet. Extensive droplet coalescence can eventually lead to the formation of a separate layer of oil on top of a sample, which is known as “oiling-off.” *Phase inversion* is the process whereby an O/W emulsion is converted into a W/O emulsion or vice versa. The physicochemical origin of these and the other major forms of emulsion instability are discussed in Chapter 7, along with factors that influence them, strategies for controlling them, and analytical techniques for monitoring them. In addition to the physical processes mentioned above, it should be noted that there are also various chemical, biochemical, and microbiological processes that occur in food emulsions that can also adversely affect their shelf life and quality, for example, lipid oxidation, enzyme hydrolysis, and bacterial growth.

### 1.2.3 Ingredient partitioning in emulsions

Emulsions are microheterogeneous materials whose composition and properties vary from region to region when examined at length scales of the order of nanometers or micrometers. To a first approximation, most food emulsions can be conveniently considered to consist of three distinct regions that have different physicochemical properties: the interior of the droplets, the continuous phase, and the interface (Figure 1.4). The molecules in an emulsion distribute themselves among these three regions according to their concentration and polarity (Chapter 9). Nonpolar molecules tend to be located primarily in the oil phase, polar molecules in the aqueous phase, and amphiphilic molecules at the interface. It should be noted that even at equilibrium, there is a continuous exchange of molecules between the different regions, which occurs at a rate that depends on the mass transport of the molecules through the different regions in the system. Molecules may also move from one

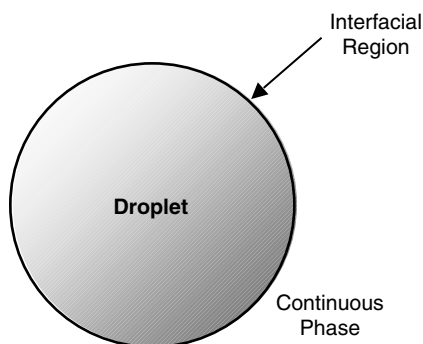


**Figure 1.4** The ingredients in an emulsion partition themselves among the oil, water, and interfacial regions according to their concentration and interactions with the local environment.

region to another when there is some alteration in the environmental conditions of an emulsion, for example, a change in temperature or dilution within the mouth. The location and mass transport of the molecules within an emulsion has a significant influence on the flavor and physicochemical stability of food products (Chapters 7 and 9).

#### 1.2.4 *Dynamic nature of emulsions*

Many of the properties of emulsions can only be understood with reference to their dynamic nature. The formation of emulsions by homogenization is usually a highly dynamic process that involves the violent disruption of droplets and the rapid movement of surface-active molecules from the bulk liquids to the interfacial region (Chapter 6). Even after their formation, the droplets in an emulsion are in continual motion and frequently collide with one another because of their Brownian motion, gravity, or applied mechanical forces (Chapter 7). The continual movement and interactions of droplets causes the properties of emulsions to evolve over time due to the various destabilization mechanisms mentioned earlier (Section 1.2.2). Biopolymers adsorbed to the surface of emulsion droplets may undergo relatively slow conformational changes over time, which result in alterations in the stability and physicochemical properties of the overall system. Surface-active molecules in the continuous phase may exchange with those adsorbed to the droplet surfaces, thus changing the composition and properties of the droplet interfaces. The properties of the system may also change over time due to chemical reactions that occur in the droplet interior, interfacial region, or continuous phase, for example, oxidation of lipids or proteins, or hydrolysis of proteins or polysaccharides. An appreciation of the dynamic processes that occur in food emulsions is therefore extremely important for a thorough understanding of their bulk physicochemical and organoleptic properties.

#### 1.2.5 *Complexity of food emulsions*

Most food emulsions are much more complex than the simple three-component (oil, water, and emulsifier) systems described earlier (Section 1.2.1). The aqueous phase may contain a variety of water-soluble ingredients, including sugars, salts, acids, bases, alcohols, surfactants, proteins, and polysaccharides. The oil phase usually contains a complex mixture of lipid-soluble components, such as triacylglycerols, diacylglycerols, monoacylglycerols, free fatty acids, sterols, and vitamins. The interfacial region may contain a mixture of various surface-active components, including proteins, polysaccharides, phospholipids, surfactants, alcohols, and molecular complexes. In addition, these components may form

various types of structural entities in the oil, water, or interfacial regions (such as fat crystals, ice crystals, biopolymer aggregates, air bubbles, liquid crystals, and surfactant micelles), which in turn may associate to form larger structures (such as biopolymer or particulate networks). A further complicating factor is that foods are subjected to variations in their temperature, pressure, and mechanical agitation during their production, storage, and handling, which can cause significant alterations in their overall properties.

It is clear from the above discussion that food emulsions are compositionally, structurally, and dynamically complex materials, and that many factors contribute to their overall properties. One of the major objectives of this book is to present the conceptual framework needed by food scientists to understand these complex systems in a more systematic and rigorous fashion. Much of our knowledge about these complex systems has come from studies of simple model systems (Section 1.5). Nevertheless, there is an increasing awareness of the need to elucidate the factors that determine the properties of actual emulsion-based food products. For this reason, many researchers are now systematically focusing on understanding at a fundamental level the factors that determine the properties of real food emulsions, such as ingredient interactions (e.g., biopolymer–biopolymer, biopolymer–surfactant, biopolymer–water) and processing conditions (e.g., homogenization, freezing, chilling, cooking, sterilization, pasteurization, mechanical agitation, pressurization, drying).

## 1.3 Emulsion properties

### 1.3.1 Disperse phase volume fraction

The concentration of droplets in an emulsion plays an important role in determining its cost, appearance, texture, flavor, and stability (Chapters 7–10). It is therefore important to be able to clearly, specify, and reliably report the droplet concentration of emulsions. The droplet concentration is usually described in terms of the *disperse phase volume fraction* ( $\phi$ ), which is equal to the volume of emulsion droplets ( $V_D$ ) divided by the total volume of the emulsion ( $V_E$ ):  $\phi = V_D/V_E$ . In some situations, it is more convenient to express the droplet concentration in terms of the disperse phase mass fraction ( $\phi_m$ ), which is equal to the mass of emulsion droplets ( $m_D$ ) divided by the total mass of the emulsion ( $m_E$ ):  $\phi_m = m_D/m_E$ . Frequently, the droplet concentration is expressed as a volume or mass percentage, rather than as a volume or mass fraction. The mass fraction and volume fraction are related to each other through the following equations:

$$\phi_m = \frac{\phi \rho_2}{\rho_2 \phi + (1 - \phi) \rho_1} \quad (1.2a)$$

$$\phi = \frac{\phi_m \rho_1}{\rho_1 \phi_m + (1 - \phi_m) \rho_2} \quad (1.2b)$$

where  $\rho_1$  and  $\rho_2$  are the densities of the continuous and dispersed phases, respectively. When the densities of the two phases are equal, the mass fraction is equivalent to the volume fraction. It should be noted that if the thickness of the interfacial membrane ( $\delta$ ) surrounding the droplets is significant compared to the droplet radius ( $r$ ), then the effective volume fraction of the droplets will be larger than their actual volume fraction:  $\phi_{\text{eff}} = \phi(1 + \delta/r)^3$ . This increase could have important consequences for the stability and rheology of some emulsions (Chapters 7 and 8).

The disperse phase volume fraction of an emulsion is often known because the concentration of the ingredients used to prepare it is carefully controlled. Nevertheless, local variations in disperse phase volume fraction occur within emulsions when the droplets accumulate at either the top or bottom of an emulsion due to creaming or sedimentation. In addition, the disperse phase volume fraction of an emulsion may vary during a food processing operation, for example, if a mixer or valve is not operating efficiently. Consequently, it is often important to have analytical techniques to measure disperse phase volume fraction (Chapter 11).

### 1.3.2 Particle size distribution

Many of the most important properties of emulsion-based food products are determined by the size of the droplets that they contain, for example, shelf life, appearance, texture, and flavor (Chapters 7–10). Consequently, it is important for food scientists to be able to reliably control, predict, measure, and report the size of the droplets in emulsions. In this section, the most important methods of reporting droplet sizes are discussed. Methods of controlling, predicting, and measuring droplet size are covered in later chapters (Chapters 6, 7, and 11).

If all the droplets in an emulsion are of the same size it is referred to as a *monodisperse* emulsion, but if there is a range of droplet sizes present it is referred to as a *polydisperse* emulsion (Figure 1.5). The droplet size ( $x$ ) of a monodisperse emulsion can be completely characterized by a single number, such as the droplet diameter ( $d$ ) or radius ( $r$ ). Monodisperse emulsions are sometimes prepared and used for fundamental studies because the interpretation of experimental measurements is much simpler than for polydisperse emulsions. Nevertheless, real food emulsions always contain a distribution of droplet sizes, and so the specification of their droplet size is more complicated than for monodisperse systems. In some situations, it is important to have information about the full *particle size distribution* of an emulsion (i.e., the fraction of droplets in different specified size ranges), whereas in other situations knowledge of the average droplet size and the width of the distribution is often sufficient. It should be noted that a common error that occurs when particle size data are presented is that the investigator neglects to say whether the size is reported as a radius or a diameter. Obviously, this practice should be avoided because it can cause considerable confusion and lead to misleading interpretations of reported data.

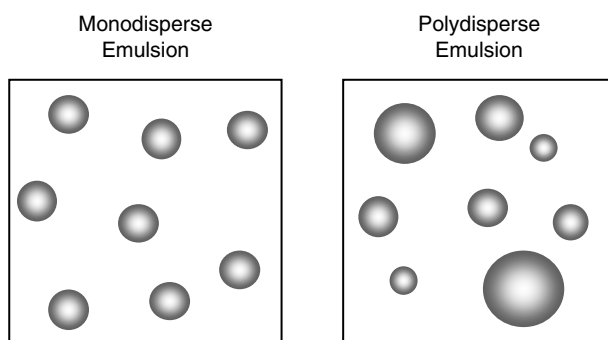


**Figure 1.5** Schematic representation of monodisperse and polydisperse emulsions. In a monodisperse emulsion all the droplets have the same size, but in a polydisperse emulsion they have a range of different sizes.



**Table 1.1** Effect of Particle Size on the Physical Characteristics of 1 g of Oil Dispersed in Water in the Form of Spherical Droplets. Values were Calculated Assuming the Oil had a Density of 920 kg m<sup>-3</sup> and the End-to-End Length of an Individual Oil Molecule was 6 nm.

Droplet Radius (μm)	Number of Droplets per Gram Oil (g <sup>-1</sup> )	Droplet Surface Area per Gram Oil (m <sup>2</sup> g <sup>-1</sup> )	Percentage of Oil Molecules at Droplet Surface (vol%)
100	2.6 × 10 <sup>5</sup>	0.03	0.02
10	2.6 × 10 <sup>8</sup>	0.3	0.2
1	2.6 × 10 <sup>11</sup>	3	1.8
0.1	2.6 × 10 <sup>14</sup>	30	18

1.3.2.1 Presenting particle size data

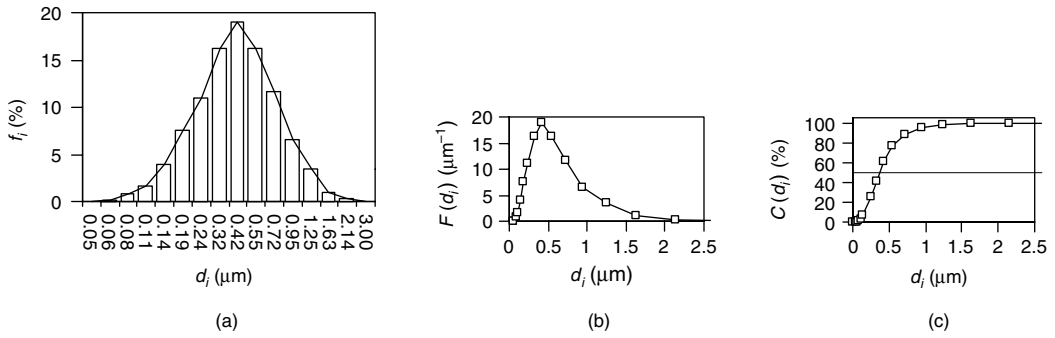
The number of droplets in most emulsions is extremely large (Table 1.1), and so their size can be considered to vary continuously from some minimum value to some maximum value (Walstra, 2003a). When presenting particle size data it is usually convenient to divide the full size range into a number of discrete size-classes and stipulate the amount of droplets that fall into each class (Hunter, 1986). The resulting data can then be presented in tabular form (Table 1.2) or as a histogram (Figure 1.6a). Histograms are usually plotted so that the height of each bar represents the amount of particles in the stipulated size-class, and the central position ( $x_i$ ) of each bar on the  $x$ -axis represents the average size of the particles within the size-class, for example,  $x_i = (x_{\text{low}} + x_{\text{high}})/2$ , where  $x_{\text{low}}$  and  $x_{\text{high}}$  are

**Table 1.2** The Particle Size Distribution of an Emulsion can be Conveniently Represented in Tabular Form. Note that the Volume Frequency is Much More Sensitive to Larger Droplets than the Number Frequency.

$d_{\text{min}}$ (μm)	$d_{\text{max}}$ (μm)	$d_i$ (μm)	$n_i$	$f_i$ (%)	$\phi_i$ (%)	$F(d_i)$ (μm <sup>-1</sup> )	$C(d_i)$ (%)
0.041	0.054	0.048	0	0.0	0.0	0.0	0.0
0.054	0.071	0.063	2	0.1	0.0	117.6	0.1
0.071	0.094	0.082	20	0.9	0.0	888.9	1.0
0.094	0.123	0.108	38	1.7	0.0	1333.3	2.7
0.123	0.161	0.142	89	4.0	0.0	2342.1	6.7
0.161	0.211	0.186	166	7.5	0.2	3320.0	14.3
0.211	0.277	0.244	243	11.0	0.5	3681.8	25.3
0.277	0.364	0.320	360	16.3	1.8	4161.8	41.6
0.364	0.477	0.421	420	19.0	4.7	3716.8	60.6
0.477	0.626	0.551	361	16.3	9.1	2431.0	76.9
0.626	0.821	0.724	256	11.6	14.5	1312.8	88.5
0.821	1.077	0.949	145	6.6	18.6	566.4	95.1
1.077	1.414	1.245	78	3.5	22.6	231.8	98.6
1.414	1.855	1.634	23	1.0	15.1	52.2	99.7
1.855	2.433	2.144	6	0.3	8.9	10.4	100.0
2.8125	3.192	3.002	1	0.0	4.1	2.6	100.0
3.191	3.620	3.406	0	0.0	0.0	0.0	100.0
3.620	4.107	3.864	0	0.0	0.0	0.0	100.0

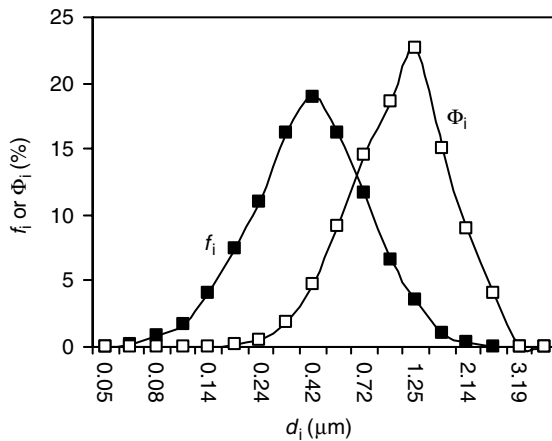
  

Selected mean particle diameters and relative standard deviations			
$d_{10}$	0.49 (μm)	$c_0$	0.63
$d_{20}$	0.57 (μm)	$c_1$	0.59
$d_{30}$	0.67 (μm)	$c_2$	0.55
$d_{32}$	0.92 (μm)		
$d_{43}$	1.20 (μm)		



**Figure 1.6** The particle size distribution of an emulsion can be represented in a number of different ways, for example, a histogram, a frequency distribution  $F(d)$ , or a cumulative distribution  $C(d)$ . These different ways of representing the particle size distribution are described in the text.

the lower and upper boundaries of the size-class. Ideally, the width of the bars on the histogram should be proportional to the width of the size-classes (which may be the same or different for each size-class). In practice, this is often not done because the graphic programs used to plot data are not sufficiently flexible. It is usually more convenient to represent the amount of particles in each size-class as a fraction rather than as an absolute value because it is then possible to directly compare particle size distributions of emulsions containing different total amounts of droplets. The fraction of particles in a size-class can be defined in a number of different ways, e.g., the number ratio,  $f_i = n_i/N$ , where  $n_i$  is the number of droplets in the  $i$ th size class and  $N$  is the total number of droplets, or the volume ratio,  $\Phi_i = v_i/V_N$ , where  $v_i$  is the volume of the droplets in the  $i$ th size class and  $V_N$  is the total volume of all the droplets. The actual volume fraction of droplets in each size-class can be calculated from the volume ratio and the disperse phase volume fraction:  $\phi_i = \phi\Phi_i$ . It should be noted that the shape of a particle size distribution changes appreciably depending on whether it is presented as a number or volume ratio (Table 1.2, Figure 1.7). The volume of a droplet is proportional to  $x^3$ , and so a volume distribution is skewed more toward the larger droplets, whereas a number distribution is skewed more toward the smaller droplets.



**Figure 1.7** Comparison of the particle size distribution of an emulsion plotted as either number or volume ratio vs. diameter (see Table 1.2). The data are plotted as curves, rather than as a histogram, to facilitate comparison.

A particle size distribution can also be represented as a smooth curve, such as the frequency distribution  $F(x_i)$  or the cumulative distribution  $C(x_i)$  (Figure 1.6b and c). For a continuous particle size distribution, the number of particles in a given size-class can be calculated from the frequency distribution by the following equation (Walstra, 2003a):

$$n_i = \int_{x_i - \frac{1}{2}\Delta x_i}^{x_i + \frac{1}{2}\Delta x_i} F(x) d(x) \quad (1.3)$$

where  $\Delta x_i$  is the width of the size-class and  $x_i$  is the value of the particle size at the mid-point of the size-class. For a discrete particle size distribution, the number of particles in a size-class is given by  $n_i \approx F_i \Delta x_i$ , where  $F_i$  and  $\Delta x_i$  are the number frequency distribution and width of the  $i$ th size-class. The number frequency distribution is therefore constructed so that the area under the curve between two droplet sizes is approximately equal to the number of droplets  $n_i$  in that size range (Hunter, 1986). This relationship can be used to convert a histogram to a frequency distribution curve or vice versa. The number ratio in a particular size-class can be related to the number frequency distribution by the equation:  $f_i = F_i \Delta x_i / N$ .

The cumulative distribution represents the percentage of droplets that are smaller than  $x_i$  (Figure 1.6c). The resulting curve usually has an S-shape that varies from 0 to 100% as the particle size increases from the smallest value. The particle size at which half the droplets are smaller and the other half are larger is known as the median particle size,  $x_m$ . The size-class that contains the largest amount of particles is called the mode or modal particle size ( $x_{\text{modal}}$ ). The numerical values of the median and the modal droplet sizes depend on the way that the amount of droplets in each size-class is expressed, for example, number or volume. Hence, there are number and volume median sizes, and number and volume modal sizes of a distribution.

### 1.3.2.2 Mean and standard deviation

It is often convenient to represent the size of the droplets in a polydisperse emulsion by one or two numbers, rather than stipulating the full particle size distribution (Hunter, 1986; Rawle, 2004). The most useful numbers are the mean particle size,  $\bar{x}$ , which is a measure of the central tendency of the distribution, and the standard deviation,  $\sigma$ , which is a measure of the width of the distribution. The mean and standard deviation of a particle size distribution can be calculated using the following equations:

$$\bar{x} = \frac{\sum_{i=1} n_i x_i}{N} \quad (1.4a)$$

$$\sigma = \sqrt{\frac{\sum_{i=1} n_i (x_i - \bar{x})^2}{N}} \quad (1.4b)$$

where the summations are carried out over the total number of size-classes used to represent the distribution. Nevertheless, this is only one way of expressing the mean and standard deviation, and there are a number of other ways that emphasize different physical characteristics of the particle size distribution that are usually more appropriate (Hunter, 1986; Walstra, 2003a). To understand these different ways of representing the mean and

standard deviation of particle size distributions it has proved useful to define the concept of the “moment of a distribution” (Walstra, 2003a):

$$S_n = \int_0^{\infty} x^n F(x) dx \approx \sum_{i=1} n_i x_i^n \quad (1.5)$$

where  $S_n$  is the  $n$ th moment of the distribution.\* The mean particle size and relative standard deviation can then be defined as

$$x_{ab} = \left( \frac{S_a}{S_b} \right)^{1/(a-b)} \quad (1.6)$$

$$c_n = \left( \frac{S_n S_{n+2}}{S_{n+1}^2} - 1 \right)^{1/2} \quad (1.7)$$

where  $a$  and  $b$  are integers (usually between 0 and 6) and  $c_n$  is the (dimensionless) relative standard deviation weighted with the  $n$ th power of  $x$  (Walstra, 2003a). The moment of the distribution has no physical meaning itself, but it can often be simply related to important physical characteristics of the distribution. For example, if the particle size is expressed as the diameter ( $d_i$ ) of the particles in each size-class and  $n_i$  is expressed as the number of particles in each size-class per unit volume of emulsion:

$$S_0 \approx \sum_{i=1} n_i \approx N \quad (1.8a)$$

$$S_1 \approx \sum_{i=1} n_i d_i = L_N \quad (1.8b)$$

$$S_2 \approx \sum_{i=1} n_i d_i^2 = \frac{A_N}{\pi} \quad (1.8c)$$

$$S_3 \approx \sum_{i=1} n_i d_i^3 = \frac{6V_N}{\pi} = \frac{6\phi}{\pi} \quad (1.8d)$$

where  $L_N$ ,  $A_N$ , and  $V_N$  are the total length, surface area, and volume of the droplets per unit emulsion volume, and  $\phi$  is the disperse phase volume fraction. Some of the most important ways of expressing the mean droplet size of particle size distributions are highlighted in Table 1.3. Each of these mean sizes has dimensions of length (meters), but stresses a different physical aspect of the distribution. For example,  $d_{10}$ ,  $d_{20}$ , and  $d_{30}$  are the diameters of individual spheres that have the same average length, surface area, and volume per droplet as the whole distribution. In other words, if there were  $N$  equal-sized droplets of diameter  $d_{10}$  (or  $d_{20}$  or  $d_{30}$ ), then they would have the same total length (or surface area or volume) as the sum of all the droplets in the system. A widely used method of expressing the mean particle size is the area-volume mean diameter ( $d_{32}$ ), which is

\* Note: One must be careful here to distinguish between the “ $n$ ” that represents the number of droplets in a size-class ( $n_i$ ) from the “ $n$ ” that represents the  $n$ th moment of the distribution.

**Table 1.3** Different ways of expressing the mean particle diameter of polydisperse emulsions. Here  $N$ ,  $L$ ,  $A$ ,  $V$  and  $\phi$  represent number, length, surface area, volume and volume fraction, respectively.

Name of Mean	Symbol	Definition	Definition
Number-length mean diameter	$d_{NL}$ or $d_{10}$	$d_{10} = S_1/S_0$	$d_{10} = \frac{\sum_{i=1} n_i d_i}{\sum_{i=1} n_i}$
Number-area mean diameter	$d_{NA}$ or $d_{20}$	$d_{20} = (S_2/S_0)^{1/2}$	$d_{20} = \sqrt{\frac{\sum_{i=1} n_i d_i^2}{\sum_{i=1} n_i}}$
Number-volume mean diameter	$d_{NV}$ or $d_{30}$	$d_{30} = (S_3/S_0)^{1/3}$	$d_{30} = \sqrt[3]{\frac{\sum_{i=1} n_i d_i^3}{\sum_{i=1} n_i}}$
Area-volume mean diameter	$d_{AV}$ or $d_{32}$	$d_{32} = S_3/S_2$	$d_{32} = \frac{\sum_{i=1} n_i d_i^3}{\sum_{i=1} n_i d_i^2}$
Volume fraction-length mean diameter	$d_{\phi L}$ or $d_{43}$	$d_{43} = S_4/S_3$	$d_{43} = \frac{\sum_{i=1} n_i d_i^4}{\sum_{i=1} n_i d_i^3} = \sum_{i=1} \phi_i d_i$

Source: Adapted from Hunter (1986) and Walstra (2003a).

related to the average surface area of droplets exposed to the continuous phase per unit volume of emulsion,  $A_N$ :

$$A_N = \frac{6\phi}{d_{32}} \quad (1.9)$$

This relationship is particularly useful for calculating the total surface area of droplets in an emulsion from knowledge of the mean diameter of the droplets and the disperse phase volume fraction. Another commonly used method of expressing the mean particle size of a polydisperse emulsion is the volume-length diameter ( $d_{43}$ ), which is the sum of the volume ratio of droplets in each size-class multiplied by the mid-point diameter of the size-class. It should be noted that  $d_{43}$  is more sensitive to the presence of large particles in an emulsion than  $d_{32}$ , hence it is often more sensitive to phenomenon such as flocculation.

In general, the higher the order of the mean ( $a + b$ , Equation 1.6) used to describe the particle size distribution, the higher its numerical value. For narrow particle size distributions the different mean values are fairly similar, but for wide particle size distributions they may differ appreciably (Table 1.2). For narrow particle size distributions it is often sufficient to report only the mean particle size, but for wide particle size distributions it is often important to provide some measure of the width of the distribution also. The width of a particle size distribution can be conveniently represented by the *relative* standard deviation with  $n = 2$ , that is,  $c_2$  (Equation 1.7). This is the standard deviation of the size distribution weighted with the particle surface area divided by  $d_{32}$  (Walstra, 2003a). In general,  $c_2$  ranges from around 0.1 for a very narrow distribution to 1.3 for a very wide distribution, but in most food emulsions it usually ranges from around 0.5 to 1. It should be noted that the *absolute* standard deviation (Equation 1.4b) is not a good representation of the width of a distribution, since it is highly sensitive to the mean particle size. For example, consider two particle size distributions with an absolute standard deviation of 0.1  $\mu\text{m}$ , but with mean particle diameters of 0.2 and 20  $\mu\text{m}$ . The droplets in the emulsion with the smallest mean diameter span a relatively wide range compared to the mean ( $\sim 0.1\text{--}0.3 \mu\text{m}$ ,  $c_2 = 0.5$ ), whereas those in the emulsion with the largest mean diameter span a fairly narrow range ( $\sim 19.9\text{--}20.1 \mu\text{m}$ ,  $c_2 = 0.05$ ).

Another important reason for being aware of the various ways of calculating and reporting the mean particle size is that different particle characterization techniques determine different mean values (Hunter, 1986; Orr, 1988; Heimenz and Rajagopalan, 1997; Rawle, 2004). For example, analysis of polydisperse emulsions using microscopy measurements of droplet length gives  $d_{10}$ , imaging processing of droplet area gives  $d_{20}$ , electrical pulse counting gives  $d_{30}$ , and low angle laser light scattering gives  $d_{43}$  (Rawle, 2004). Consequently, it is always important to be clear about which mean size has been determined in an experiment when using or quoting particle size data. In addition, one must be particularly careful in using data determined by one type of particle sizing technique to calculate a mean particle size that is different from the one that the technique is most sensitive to (Rawle, 2004). For example, low angle laser light scattering is much more sensitive to the volume of particles in each size-class than to the number of particles. Hence, there could be a large number of small particles (but with a small total volume) that would not be accurately detected by light scattering, so that a calculation of  $d_{10}$  from the data would not be particularly accurate.

Finally, it should be stressed that one must also be careful when choosing either a mode, median, or mean diameter to represent a full particle size distribution in a polydisperse emulsion (Rawle, 2004). For a normal or Gaussian distribution the mode, median, and mean have similar values, but for a nonsymmetrical or multimodal distribution they have very different values. One must therefore select one or more of these parameters to represent the full particle size distribution based on the physical property that is most pertinent to the person who is going to use the information.

### 1.3.2.3 Mathematical models

The particle size distribution of an emulsion can often be modeled using a mathematical theory, which is convenient because it means that the full data set can be described by a small number of parameters (Hunter, 1986). In addition, many analytical instruments designed to measure particle size distributions assume that the distribution has a certain mathematical form so as to facilitate the conversion of the measured physical parameters (e.g., light intensity vs. scattering angle) into a particle size distribution (Hunter, 1986). If a plot of frequency distribution versus droplet size is symmetrical about the mean droplet size the curve can often be described by a *normal* frequency distribution function (Figure 1.8a):

$$F(x) = \frac{1}{\sigma\sqrt{2\pi}} \exp\left[-\frac{(x - \bar{x})^2}{2\sigma^2}\right] \quad (1.10)$$

This function has a maximum value when  $x = \bar{x}$ . Most (~68%) of the droplets fall within one standard deviation of the mean ( $\bar{x} \pm \sigma$ ), while the vast majority (~99.7%) fall within three standard deviations ( $\bar{x} \pm 3\sigma$ ). Only two parameters are needed to describe the full particle size distribution of an emulsion that can be approximated by a normal distribution: the mean and the standard deviation. The number ratio of droplets within a particular size range ( $x_{\text{low}}$  to  $x_{\text{high}}$ ) can be calculated from Equation 1.10:  $f_i = \int_{x_{\text{low}}}^{x_{\text{high}}} F(x) dx / N$ .

The particle size distribution of most food emulsions is not symmetrical about the mean, but tends to extend much further at the high droplet size end than at the low droplet size end (Figure 1.8b). This type of distribution can often be described by a *log-normal* frequency distribution function (Heimenz and Rajagopalan, 1997):

$$F(\ln x) = \frac{1}{\ln \sigma_g \sqrt{2\pi}} \exp\left[-\frac{(\ln x - \ln \bar{x}_g)^2}{2 \ln^2 \sigma_g}\right] \quad (1.11)$$

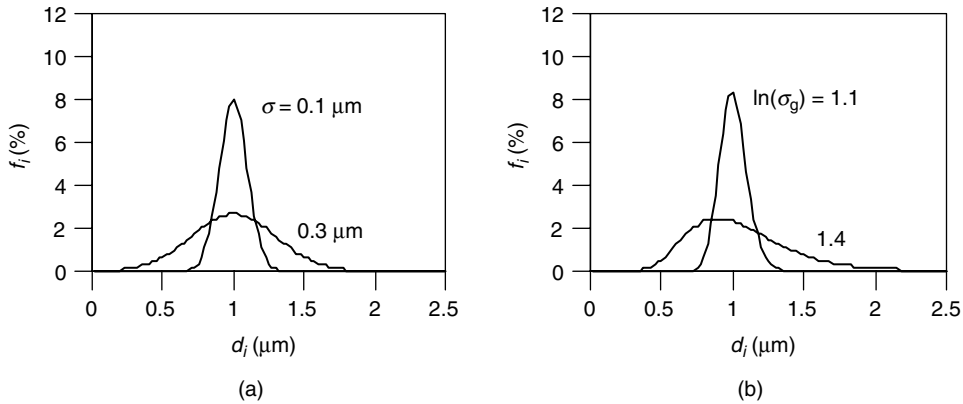


**Figure 1.8** Particle size distributions, represented as droplet number percentage ( $f_i$ ) vs. droplet diameter ( $d_i$ ) calculated assuming different standard deviations for normal and log-normal distributions. For both emulsions, the mean droplet diameter was assumed to be  $1 \mu\text{m}$ . (a) Normal distribution:  $f_i = F(d_i)d(d_i)/N$ ; (b) log-normal distribution:  $f_i = F(\ln d_i)d(\ln d_i)/N$ .

where  $\bar{x}_g$  and  $\sigma_g$  are the geometric mean and the standard deviation of the geometric mean, which are given by the following expressions:

$$\ln \bar{x}_g = \frac{\sum_{i=1} n_i \ln x_i}{N} \quad (1.12a)$$

$$\ln \sigma_g = \sqrt{\frac{\sum_{i=1} n_i (\ln x_i - \ln \bar{x}_g)^2}{N}} \quad (1.12b)$$

If the log-normal curve shown in Figure 1.8 was plotted as  $f_i$  versus  $\ln d_i$  rather than as  $f_i$  versus  $d_i$ , it would be symmetrical about  $\ln \bar{x}_g$ .

It should be stressed that the particle size distribution of many food emulsions cannot be adequately described by the simple mathematical models given above. Bimodal distributions that are characterized by two peaks (Figure 1.9), are often encountered in food

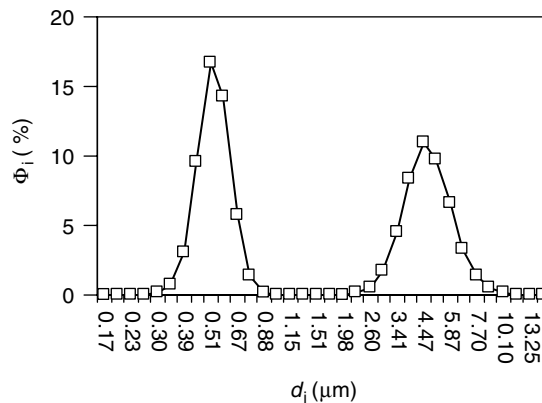


**Figure 1.9** Example of a bimodal distribution resulting from the heat-induced flocculation of droplets in a hexadecane oil-in-water emulsions stabilized by  $\beta$ -lactoglobulin (Kim et al., 2002b).

emulsions, for example, when extensive droplet flocculation occurs or when there is insufficient emulsifier present in an emulsion to stabilize all of the droplets formed during homogenization (Chapters 6 and 7). For these systems, it is often better to present the data as the full particle size distribution, otherwise considerable errors may occur if an inappropriate mathematical model is used. This kind of problem can occur when one is using an analytical instrument that assumes a particular mathematical model when calculating the particle size distribution, for example, a light scattering or ultrasonic spectrometry instrument. If the mathematical model is inappropriate, then the instrument may still report a particle size distribution, but this distribution will be incorrect. The user of the instrument should therefore be aware of this potential problem, and if necessary ensure that the mathematical model is correct by using some independent technique to verify the particle size distribution (e.g., microscopy).

### 1.3.3 *Interfacial properties*

The droplet interface consists of a narrow region (usually a few nanometers thick) that surrounds each emulsion droplet, and contains a mixture of oil, water, and surface-active molecules (Hunter, 1986, 1989). The interfacial region only makes up a significant fraction of the total volume of an emulsion when the droplet radius is less than about 1  $\mu\text{m}$  (Table 1.1). Even so, it plays a major role in determining many of the most important bulk physicochemical and organoleptic properties of food emulsions. For this reason, food scientists are particularly interested in elucidating the factors that determine the composition, structure, thickness, rheology, and charge of the interfacial region, and in elucidating how these interfacial characteristics are related to the bulk physicochemical and sensory properties of emulsions. The composition and structure of the interfacial region are determined by the type and concentration of surface-active species present in the system prior to emulsion formation, as well as by the events that occur during and after emulsion formation, for example, competitive adsorption and displacement (Chapters 5 and 6). The thickness and rheology of the interfacial region may influence the stability of emulsions to gravitational separation, coalescence, and flocculation (Chapters 3 and 7), the rheology of emulsions (Chapter 8), and the mass transport rate of molecules in or out of droplets, for example, Ostwald ripening, compositional ripening, and flavor release (Chapters 7 and 9). The interface acts as a region where surface-active components accumulate, which may lead to acceleration of certain types of chemical reactions (e.g., oxidation), either by increasing the local concentration of molecules or by bringing together different reactive species (McClements and Decker, 2000). The major factors that determine the characteristics of the interfacial region are discussed in Chapter 5, along with experimental techniques to characterize its properties. The electrical characteristics of the interface are discussed in the following section.

### 1.3.4 *Droplet charge*

The bulk physicochemical and organoleptic properties of many food emulsions are governed by the magnitude and sign of the electrical charge on the droplets (Chapters 7–10). The origin of this charge is normally the adsorption of emulsifier molecules that are ionized or ionizable\* (Section 4.4). Surfactants have hydrophilic head groups that may be neutral, positively charged, or negatively charged. Proteins may also be neutral, positively charged, or negatively charged depending on the pH of the solution compared to their isoelectric

\* There is experimental evidence that even oil droplets stabilized by nonionic surfactants have an electrical charge because the oil preferentially adsorbs either  $\text{OH}^-$  or  $\text{H}_3\text{O}^+$  ions from water or contains ionic impurities (Pashely, 2003).



point. Surface-active polysaccharides may also have an electrical charge depending on the type of functional groups along their backbone. Consequently, emulsion droplets may have an electrical charge that depend on the types of surface-active molecules present and the pH of the aqueous phase. The electrical charge on a droplet can be characterized in a number of different ways (Hunter, 1986), that is, the surface charge density ( $\sigma$ ); the electrical surface potential ( $\psi_0$ ), and the zeta-potential ( $\zeta$ ). The surface charge density is the amount of electrical charge per unit surface area, whereas the surface potential is the free energy required to increase the surface charge density from 0 to  $\sigma$ . The  $\zeta$ -potential is the effective surface potential of a droplet suspended in a medium, which takes into account that charged species in the surrounding medium may adsorb to the surface of the droplet and alter its net charge. The  $\zeta$ -potential can be conveniently measured in the laboratory using commercially available analytical instrumentation (Chapter 11).

The charge on a droplet is important because it determines the nature of its interactions with other charged species (Chapters 2–4) or its behavior in the presence of an electrical field (Chapter 11). Two species that have charges of opposite sign are attracted toward each other, whereas two species that have charges of similar sign are repelled (Chapters 2 and 3). All of the droplets in an emulsion are usually coated with the same type of emulsifier and so they have the same electrical charge (if the emulsifier is ionized). When this charge is sufficiently large, the droplets are prevented from aggregating because of the electrostatic repulsion between them (Chapter 3). The properties of emulsions stabilized by ionized emulsifiers are particularly sensitive to the pH and ionic strength of the aqueous phase. If the pH of the aqueous phase is adjusted so that the emulsifier loses its charge, or if salt is added to “screen” the electrostatic interactions between the droplets, the repulsive forces may no longer be strong enough to prevent the droplets from aggregating (Chapters 3 and 7). Droplet aggregation often leads to a large increase in emulsion viscosity (Chapter 8), and may cause the droplets to cream more rapidly (Chapter 7).

Electrostatic interactions also influence the interactions between emulsion droplets and other charged species, such as biopolymers, surfactants, vitamins, antioxidants, flavors, and minerals (Chapters 3, 4, 7, and 9). These interactions often have significant implications for the overall quality of an emulsion product. For example, the volatility of a flavor is reduced when it is electrostatically attracted to the surface of an emulsion droplet, which alters the flavor profile of a food (Landy et al., 1996), or the susceptibility of oil droplets to lipid oxidation depends on whether the catalyst is electrostatically attracted to the droplet surface (Mei et al., 1998a,b). The accumulation of charged species at a droplet surface and the rate at which this accumulation takes place depends on the sign of their charge relative to that of the surface, the strength of the electrostatic interaction, their concentration, and the presence of any other charged species that might compete for the surface.

The above discussion has highlighted the importance of droplet charge in determining both the physical and chemical properties of food emulsions. It is therefore important for food scientists to be able to predict, control, and measure droplet charge. For most food emulsions, it is difficult to accurately predict droplet charge because of the complexity of their composition and the lack of suitable theories. Nevertheless, there is a fairly good understanding of the major factors that influence droplet charge (Chapters 3–5) and of the effect of droplet charge on the stability and rheology of emulsions (Chapters 7 and 8). In addition, a variety of experimental techniques have been developed to measure the magnitude and sign of the charge on emulsion droplets (Chapter 11).

### 1.3.5 Droplet crystallinity

The physical state of the droplets in an emulsion can influence a number of its most important bulk physicochemical and organoleptic properties, including appearance,

rheology, flavor, and stability (Chapters 7–10). The production of margarine, butter, whipped cream, and ice cream depends on a controlled destabilization of an O/W emulsion containing partly crystalline droplets (Chapter 12). The stability of cream to shear and temperature-cycling depends on the crystallization of the milk fat droplets. The rate that milk fat droplets cream depends on their density, which is determined by the fraction of each droplet that is solidified. The cooling sensation that occurs when fat crystals melt in the mouth contributes to the characteristic mouthfeel of many food products (Walstra, 1987, 2003a). Knowledge of the factors that determine the crystallization and melting of emulsified substances, and of the effect that droplet phase transitions have on the properties of emulsions, is therefore particularly important to food scientists.\* In O/W emulsions we are concerned with phase transitions of emulsified fat, whereas in W/O emulsions we are concerned with phase transitions of emulsified water. In the food industry, we are primarily concerned with the crystallisation and melting of emulsified fats, because these transitions occur at temperatures that are commonly encountered during the production, storage, or handling of O/W emulsions, and because they usually have a pronounced influence on the bulk properties of food emulsions. In contrast, phase transitions of emulsified water are less likely to occur in foods because of the high degree of supercooling required to initiate crystallisation (Clausse, 1985).

The percentage of the total fat in a sample that is solidified at a particular temperature is known as the solid fat content (SFC). The SFC varies from 100% at low temperatures where the fat is completely solid to 0% at high temperatures where the fat is completely liquid. The precise nature of the SFC–temperature curve is an important consideration when selecting a fat for a particular food product. The shape of this curve depends on the composition of the fat, the thermal, and shear history of the sample, whether the sample is heated or cooled, the heating or cooling rate, the size of the emulsion droplets, and the type of emulsifier. The melting and crystallization behavior of emulsified substances can be quite different from that of the same substance in bulk (Dickinson and McClements, 1995). The crystallization of bulk fats is considered in Chapter 4, while the additional factors that influence the crystallization of emulsified fats are considered in Chapter 7. Experimental techniques that are used to provide information about the crystallization and melting of emulsion droplets are described in Chapter 11.

### 1.3.6 Droplet interactions

Many of the bulk physicochemical and sensory properties of food emulsions are strongly affected by the attractive and repulsive interactions acting between the droplets (Chapters 7–10). There are many different kinds of colloidal interactions that may operate in food emulsions, including van der Waals, electrostatic, steric, depletion, and hydrophobic interactions (Chapter 3). These interactions vary in their sign (attractive or repulsive), magnitude (strong to weak), and range (long to short). The overall characteristics of the droplet–droplet interactions in a particular food emulsion are determined by the relative contribution of the different kinds of colloidal interactions operating in that specific system, which depends on emulsion composition, microstructure, and environment. When the attractive forces dominate the droplets tend to associate with each other, but when the repulsive forces dominate the droplets tend to remain as individual entities (Chapter 3). The interactions between emulsion droplets can lead to large changes in the stability, rheology,

\* It should be noted that the continuous phase of an emulsion is also capable of melting or crystallizing which can have a profound influence on the overall properties. For example, the characteristic texture of ice cream is partly due to the presence of ice crystals in the aqueous continuous phase, whereas the rheology of butter and margarine is determined by the existence of a network of aggregated fat crystals in the oil continuous phase.

appearance, and flavor of food emulsions and so it is crucial to understand their physicochemical origin and characteristics. A brief overview of some of the analytical techniques that have recently been developed to provide information about droplet–droplet interactions is given in Chapter 11.

### 1.4 Hierarchy of emulsion properties

Scientists are becoming increasingly aware of the hierarchical nature of food emulsion properties (Figure 1.10). Ultimately, a food emulsion consists of an extremely complex mixture of many different kinds of molecules, for example, water, lipids, proteins, carbohydrates, surfactants, salts, flavors. These molecules vary in their chemical structure, polarity, reactivity, molecular mass, conformation, flexibility, and dynamics. The different types of molecules present in an emulsion interact with each other to form the oil, water, and interfacial phases, as well as any structural entities distributed within these phases, such as surfactant micelles, molecular aggregates, particle or polymer networks, air bubbles, fat crystals, or ice crystals. The physicochemical properties of the overall emulsion (e.g., optical properties, rheology, stability, and molecular partitioning) depend on the physicochemical properties of the individual oil, water, and interfacial phases, as well as the interactions that occur between these phases. The sensory properties of a food emulsion (e.g., appearance, texture, aroma, taste) depend on the direct or indirect interaction of the food emulsion and its components with the sensors in the human body, for example, light waves reflected from the emulsion reaching the eye, sound waves generated by the emulsion reaching the ear, flavor molecules released from the emulsion reaching

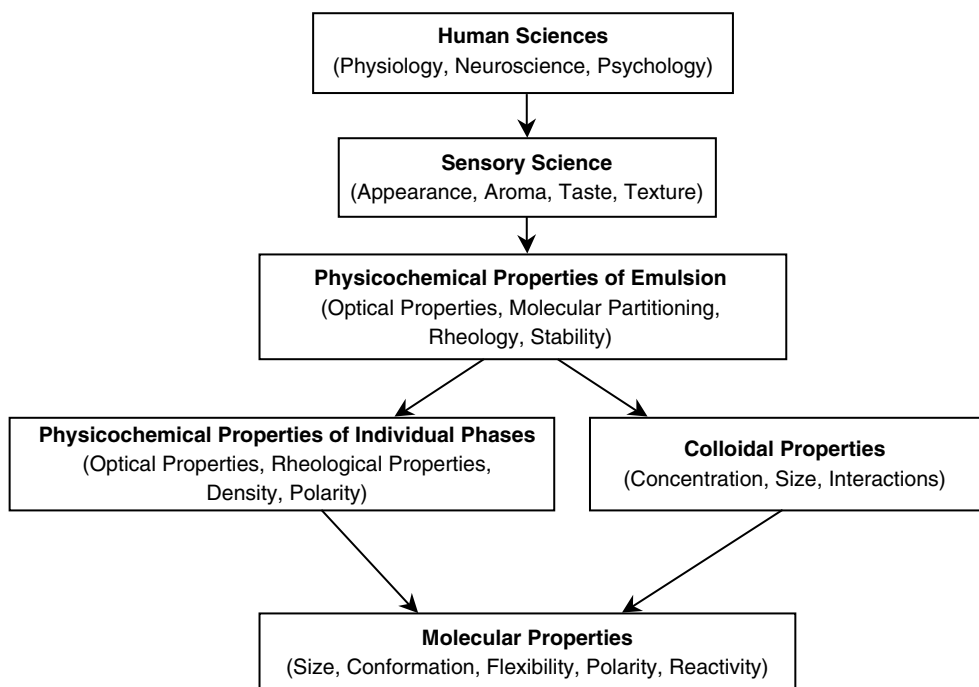


**Figure 1.10** The properties of emulsion-based food products can be understood at different hierarchical levels, ranging from molecular characteristics, to structural organization of molecules, to bulk physicochemical properties, to sensory properties, and ultimately to the interaction of the emulsion and its components with the human body.

receptors in the mouth and nose, forces and heat generated by the food interacting with tactile and temperature sensors in the hands and mouth. The way that a person responds to these sensory inputs depends on the physiology of the human sensory system, the way that the sensory information is processed, stored, and retrieved by the brain, and the way that this information is represented to consciousness. In addition, an individual's perception of a food product is strongly dependent on their background and experiences (e.g., culture, age, sex, ethnicity, social class). Hence, the quality or desirability of the same food product may be perceived differently by two different people or by the same person at different times. This brief discussion has highlighted the many different hierarchical levels involved in the study of food emulsions. A more complete understanding of the factors that determine the properties of emulsions depends on establishing the most important processes that operate at each hierarchical level, and then linking the processes that occur at different levels to one another. It should be noted that specialized analytical techniques and theoretical concepts are often required to study each hierarchical level, and so scientists with particular areas of expertise often focus their research programs on studying a particular level. For this reason, an integrated understanding of the physicochemical basis of the properties of food emulsions usually requires collaboration of scientists with different specializations, for example, physicists, physical chemists, analytical chemists, biochemists, polymer scientists, chemical engineers, sensory scientists, physiologists, psychologists, food scientists, and nutritionists. The integration of knowledge from different hierarchical levels of organization is an extremely ambitious and complicated task that will require many years of painstaking research. Nevertheless, the knowledge gained from such an endeavor will enable food manufacturers to design and produce higher quality foods in a more cost-effective and systematic fashion. For this reason, the connection among molecular, colloidal, bulk physicochemical, and sensory properties of food emulsions will be stressed throughout this book.

## *1.5 Understanding food emulsion properties*

Food emulsions are compositionally and structurally complex materials (Section 1.2.5). It is therefore particularly challenging to understand their properties at a fundamental scientific level. Nevertheless, appreciable progress has been made over the past few decades due to the coordinated efforts of scientists working in industry, academia, and government laboratories (Walstra, 2003b). The purpose of this section is to give a general overview of the factors that influence the topics and directions of research on food emulsions, and to highlight the general approaches that are used to provide information about food emulsion properties.

### *1.5.1 Factors influencing topics and directions of research*

As in other areas of science, progress in understanding the properties of food emulsions has not been uniform. Instead, certain aspects of the field have been the focus of intense study during a particular period, whereas others aspects have been largely ignored. A number of the most important factors that influence the choice of topics and directions of research on food emulsions are reviewed in this section.

#### *1.5.1.1 Relevance to industry and society*

Certain research topics are perceived as being of higher commercial value to the food industry or of greater relevance to government organizations at a particular time, and therefore attract greater financial and institutional support. The food industry usually supports research that improves manufacturing efficiency, reduces manufacturing costs,

or leads to the development of new or improved products. Government agencies usually support research that will improve the health or quality-of-life of its citizens, or that will increase the general efficiency or competitiveness of the food industry. Research scientists may find support for their research programs by working on topics that are already recognized as being of considerable commercial or societal value. Alternatively, research scientists may identify a research topic that has previously been neglected, but which they believe is of importance to industry or society. They then have to convince other scientists and funding agencies that the research topic has scientific merit and is of sufficient importance to warrant funding.

#### *1.5.1.2 Availability of scientific personnel with the appropriate expertise*

Certain topics are the focus of investigation because the research scientists working in the field have previously been trained in that particular area of expertise (e.g., they may have done graduate studies or postdoctoral research in a laboratory that specializes in this area). On the other hand, other topics are not studied because the scientists currently working in the field do not have the required expertise or conceptual framework to address them. This is particularly true in the study of food emulsions, which has grown rapidly to incorporate various aspects of many scientific disciplines, including mathematics, physics, chemistry, biology, engineering, sensory science, psychology, and physiology. This has meant that it is often difficult for individual scientists to make appreciable advances in knowledge when working in isolation.\* Instead, progress has become increasingly dependent on research being carried out by multidisciplinary teams consisting of scientists with different expertise, methodologies, and instrumentation. Indeed, the integration of knowledge from different disciplines is one of the dominant characteristics of many current research programs on food emulsions. Development of our understanding of food emulsion properties therefore depends on bringing together individuals with the diverse range of skills that can effectively work together as a team.

#### *1.5.1.3 Availability of appropriate theory and instrumentation*

Certain topics are amenable to study because analytical instrumentation is already available that can be used to probe the characteristics of the system that are of interest, and/or because appropriate physical theories are available to facilitate the design of experiments and the interpretation of measurements. On the other hand, other topics are not studied because they are too complicated to understand with the available analytical instrumentation or theoretical models. These topics may be of great industrial or societal importance, but knowledge of them cannot progress significantly until appropriate expertise, instrumentation, and theory is developed or adopted from another field. There are many examples of the rapid progress in the field of food emulsions resulting from the introduction of new theories or techniques. For example, the commercial availability of analytical instruments to rapidly and accurately measure the particle size distribution of emulsions meant that many experiments could be carried out that were not previously possible. A recent example of this phenomenon is the rapid development in our understanding of emulsion flavor that has occurred during the past decade (Chapter 9). A number of new analytical techniques became available that enabled researchers to measure the release of volatile components from foods on timescales relevant to mastication. This allowed researchers to design and perform experiments to systematically investigate the factors that influence flavor release in food emulsions, which in turn stimulated the development of physical theories to describe and predict flavor release. These theories made predictions that could be tested against

\* In reality, scientists never work in isolation since they always rely on the published work of earlier scientists.

experimental measurements and provided valuable new insights into the physicochemical and physiological basis of flavor release that were not possible earlier.

#### *1.5.1.4 Access to previous knowledge*

Another issue that has a strong influence on the topics and directions of research on food emulsions is accessibility to the knowledge accumulated by previous scientists working in similar or related areas. Developments in a particular field of scientific study are largely built on the experimental and theoretical work that has been done previously. A great deal of research has been carried out on food emulsions and much of this work has been published in scientific journals, conference proceedings, books, and online. It is therefore extremely important that researchers carry out extensive literature reviews of their field of interest, plus related fields, since this helps identify gaps in the current knowledge where research is needed, helps identify inconsistencies in previous studies, helps identify new techniques or theories that can be used, and helps avoid repetition of previous work. The number of scientific publications has increased enormously during the past few decades, which has made it increasingly difficult for scientists to be sure that they are thoroughly familiar with all of the previous research carried out in their field of interest. Nevertheless, advances in online information retrieval systems especially devoted to the scientific literature have certainly facilitated access to published research. Finally, it should be noted that a considerable amount of important research on food emulsions carried out by basic scientists working within food companies has not been published.

### *1.5.2 General approaches used to study food emulsions*

Our understanding of the factors that determine the properties of food emulsions normally progresses through a synthesis of observation, experimentation, and theory development. Some of the most important general approaches that have been employed by scientists to increase the knowledge of emulsion properties are presented below. An appreciation of the advantages and limitations of each of these approaches may help investigators design and interpret experiments. It should be stressed that there is no single unified approach to making scientific developments. Instead, scientists have to use their experience, creativity, and imagination to select the most appropriate approach for the particular system studied. In addition, the success of a particular research program largely depends on the motivation, persistence, and commitment of the individuals involved.

#### *1.5.2.1 Trial-and-error approach*

The trial-and-error approach is widely used in industry for solving manufacturing problems and for developing new and improved products and processes. In this approach, the investigator usually prepares a sample for study that has certain characteristics (e.g., composition or microstructure) and then subjects it to some form of processing treatment (e.g., storage, heating, chilling, freezing, stirring, pressure treatment). The properties of the sample are then measured and the investigator establishes whether the sample characteristics or the processing treatment lead to a final product with desirable characteristics. If the final product meets these requirements then the initial sample characteristics and/or processing treatments are selected, but if it does not meet these requirements, then the sample characteristics and/or processing treatments are changed and the procedure is repeated until a final product with suitable properties is obtained. The major advantage of the trial-and-error method is that it is sometimes possible to rapidly solve a problem or develop a product using the minimum of resources. For example, an investigator with some prior knowledge of a system may be able to rapidly select the optimum initial sample characteristics and processing treatments required to produce a desirable final

product. The major disadvantages of this method are that it may not be possible to solve the problem in a reasonable time (if the wrong input values are selected), it may not produce a solution that is robust, or it may not produce the optimum solution to the problem. If a more rigorous study was carried out, it might have been possible to identify a solution that was more efficient, more robust, or less expensive. In addition, the trial-and-error method is largely dependent on the accumulated expertise of the investigator and provides little insight into the basic physicochemical processes that govern the properties of food emulsions.

#### 1.5.2.2 *Black-box approach*

The black-box approach is a more systematic means of obtaining information about the system being studied, but it is also not concerned with providing information about the fundamental physicochemical processes occurring within the system. Instead, the system (the *black-box*) is subjected to one or more treatments (the *inputs*) and the change in one or more properties of the system in response to these treatments (the *outputs*) is measured. The investigator then reports the measured system properties for each of the various treatments and/or uses a statistical model to correlate the system properties to the treatments. To provide a concrete example of this approach, the system could be a protein-stabilized O/W emulsion, the treatment could be a change in temperature, and the measured property could be the emulsion viscosity. The investigator would prepare an emulsion, subject samples of it to different temperature treatments, measure the viscosities of each of the samples, and then report the change in emulsion viscosity with temperature. This approach is particularly useful for identifying the major factors that influence the properties of food emulsions and their components and in assessing their magnitude and relative importance. It is widely used as an initial screening procedure by investigators who are studying a system that has not been extensively studied before, since it enables them to rapidly develop an understanding of the dominant factors that influence its properties. In some situations, the black-box approach may be the only option available since the theoretical concepts or analytical techniques required to probe the internal operation of the system are not available. Nevertheless, the black-box approach has limited value when used improperly or when taken to extremes. For example, there are many examples of experiments on food emulsions that have been designed and analyzed primarily on the basis of sophisticated statistical models (such as surface response methodology), which have produced confusing and misleading results. Rather than using existing knowledge of the fundamental physicochemical properties of the system to design experiments or interpret data, investigators select (an often inappropriate) range of input and output variables based on some statistical model, and then find statistical correlations between the input and output variables. These statistical models can be very useful in establishing the relative importance of different factors, but the author believes that they should always be used extremely carefully and in combination with the physicochemical approach described below whenever possible. Indeed, if an investigator truly had no knowledge of the behavior of the system being studied, it would be difficult to select the type of input parameters to vary, the range of input parameters to select, and the material properties to measure. In practice, investigators usually have a fairly good *a priori* expectation of the factors that are likely to be important, which facilitates the selection of the most appropriate input and output variables to use.

#### 1.5.2.3 *Physicochemical approach*

The main disadvantages of the trial-and-error and black-box approaches is that they do not provide any direct understanding of the fundamental physicochemical processes that

occur within a system. Knowledge of these processes is usually desirable since it provides a deeper insight into the factors that determine the overall properties of the system, which greatly facilitates the identification of effective strategies for controlling the properties of the system, and can allow one to make predictions about how the system (or related systems) will behave under different conditions. For this reason, many researchers use a more fundamental “physicochemical approach” to investigating emulsion properties. This approach attempts to understand at a fundamental physicochemical level why a system behaves in precisely the way it does when it is subjected to a particular treatment. This approach can be used in two broad ways depending on the starting point. First, an investigator could start with some empirical observation or experimental result and then attempt to establish its physicochemical origin using a range of analytical techniques, physical concepts, and mathematical models. Second, an investigator could start with a conceptual or theoretical model and then use it to make predictions about how a real system should behave. These predictions could then be compared with experimental measurements made on a real system, and the investigator could determine how well the model describes the properties of the real system. If there are deviations between the theoretical predictions and experimental measurements, then the mathematical model could either be discarded or it could be modified to take them into account. By comparing how closely theoretical predictions and experimental measurements agree it is often possible to obtain quantitative insights into the physicochemical basis of food emulsion properties. In reality, these two different ways of using the physicochemical approach are closely related to each other and investigators often use a combination of both. The level of understanding that is achievable using the physicochemical approach is largely determined by the complexity of the system studied, the sophistication of the analytical instrumentation, and theoretical models available.

#### 1.5.2.4 *Reductionism–integrationist approach*

The reductionism–integrationist approach has proved to be an extremely powerful means of advancing our understanding of food emulsion properties. Food emulsions are extremely complex systems and many factors operate in concert to determine their overall properties. For this reason, experiments are usually carried out using simplified well-defined model systems that retain the essential features of the real system, but which ignore many of the secondary effects. For example, the emulsifying properties of proteins are often investigated by using an isolated individual protein, pure oil, and pure water (Dickinson, 1992). In reality, a protein ingredient used in the food industry consists of a mixture of different proteins, sugars, salts, fats, and minerals, and the oil and aqueous phases may contain a variety of different chemical constituents (Section 1.2.5). Nevertheless, by using a well-defined model system it is possible to elucidate the primary factors that influence the properties of proteins in emulsions in a more quantitative fashion. Once these primary factors have been established, it is possible to increase the complexity of the model by introducing additional variables and systematically examining their influence on the overall properties. This incremental approach eventually leads to a thorough understanding of the factors that determine the properties of actual food emulsions, and to the development of theories that can be used to describe and predict their behavior.

#### 1.5.2.5 *Open-minded approach*

Finally, another valuable means of advancing our understanding of food emulsions is to be receptive to the potential importance of *unexpected* results (Beveridge, 1950). If an experiment is designed that consistently produces an unexpected result, it is important to be aware that the result may be due to poor experimental design or that it may be due



to some interesting new phenomenon. Many of the most interesting discoveries in science are made by researchers who try to explain some result that did not correspond to their initial expectations. In these situations, it is usually important to carefully design further experiments that will provide evidence about the factors that influence the observed effect and about its physicochemical origin.

## 1.6 *Overview and philosophy*

It is impossible to cover every aspect of food emulsions in a book of this size. By necessity, one must be selective about the material presented and the style in which it is presented. Rather than reviewing the practical knowledge associated with each particular type of emulsion-based food product, I will focus primarily on the fundamental principles of emulsion science as applied to food systems because these principles are generally applicable to all types of food emulsions. Even so, I will use real food emulsions as examples where possible in order to emphasize the practical importance of the fundamental approach (particularly in Chapter 12). As mentioned earlier, we will pay particular attention to the relationship among molecular, colloidal, and bulk physicochemical properties of food emulsions, because we believe this approach leads to the most complete understanding of their behavior.

Throughout this book, it will be necessary to introduce a number of theories that have been developed to describe the properties of emulsions. Rather than concentrating on the mathematical derivation of these theories, we will highlight their physical significance and focus on their relevance to food scientists. A feeling for the major factors that determine the properties of food emulsions can often be gained by programming these theories onto a personal computer and systematically examining the role that each physical parameter in the equation plays.

Before ending this introductory chapter, we will give a brief overview of the subject matter of the remaining chapters in the book. In Chapters 2 and 3, I will review the various types of attractive and repulsive forces that can act on molecules and colloidal particles, and discuss how these interactions influence the organization of the molecules or particles within a system. In Chapter 4, I will review the major functional ingredients that are used in food emulsions (e.g., oil, water, emulsifiers, thickening agents, gelling agents), with particular emphasis on understanding the physicochemical basis of their functional properties. In Chapter 5, I will discuss the structure and characteristics of the interfacial region that separates bulk phases (e.g., oil and water) since this narrow region plays a crucial role in determining the overall properties of emulsions. In Chapter 6, I will discuss the physicochemical principles underlying emulsion formation and will review the various mechanical devices available for preparing emulsions for research and industrial applications. In Chapters 7–10, I will discuss the molecular–colloidal basis of the bulk physicochemical properties of emulsions, that is, stability, rheology, appearance, and flavor. In Chapter 11, I will discuss the most important analytical techniques that are used by scientists to provide information about the composition, microstructure, and physicochemical properties of food emulsions. Finally in Chapter 12, I will demonstrate the practical application of the principles of emulsion science by reviewing the formulation, formation, and physicochemical properties of three common types of food emulsions (i.e., dairy emulsions, beverages, and dressings).

## *chapter two*

---

# *Molecular characteristics*

## *2.1 Introduction*

Although food scientists have some control over the final properties of a product, they must work within the physical constraints set by nature, that is, the characteristics of the individual molecules\* and the type of interactions that occur between them. There is an increasing awareness within the food industry that the efficient production of foods with improved quality depends on a better understanding of the molecular basis of their bulk physicochemical and organoleptic properties (Eads, 1994; Baianu et al., 1995; Walstra, 2003a). The individual molecules within a food emulsion can interact with each other to form a variety of different structural entities (Figure 2.1). A molecule may be part of a bulk phase where it is surrounded by molecules of the same type, it may be part of a regular solution where it is surrounded by a mixture of molecules of the same and different type, it may be part of an electrolyte solution where it is surrounded by counterions and solvent molecules, it may accumulate at an interface between two phases, it may be part of a molecular cluster dispersed in a bulk phase, it may be part of a three-dimensional network that extends throughout the system, or it may form part of a complex biological structure (Israelachvili, 1992; Walstra, 2003a). The bulk physicochemical properties of food emulsions ultimately depend on the nature, properties, and interactions of the structural components formed by the molecules, for example, separate phases, interfaces, and particulates. The structural organization of a particular set of molecules is largely determined by the forces that act between them and the prevailing environmental conditions, for example, temperature and pressure. From a thermodynamic viewpoint, a certain arrangement of molecules may have the lowest free energy since it maximizes the number of favorable interactions, minimizes the number of unfavorable interactions, and maximizes the various entropy contributions. Nevertheless, foods are rarely in their most thermodynamically stable state, and therefore the structural organization of the molecules is often governed by kinetic factors that prevent them from reaching the arrangement with the lowest free energy (Section 1.2.1). For this reason, the structural organization of the molecules in foods is largely dependent on their previous history, that is, the temperatures, pressures, gravity, and applied mechanical forces experienced during their lifetime. To understand, predict, and control the behavior of food emulsions it is important to be aware of the origin and nature of the forces responsible for holding the molecules together, and how these forces lead to the various types of structures formed. Only then will it be possible to rationally create and stabilize foods that have internal structures that are known to be advantageous to food quality. The purpose of this chapter is to give a brief overview of the major types

\* The term “molecule” is used broadly to refer to molecular species, such as atoms, molecules, and ions.

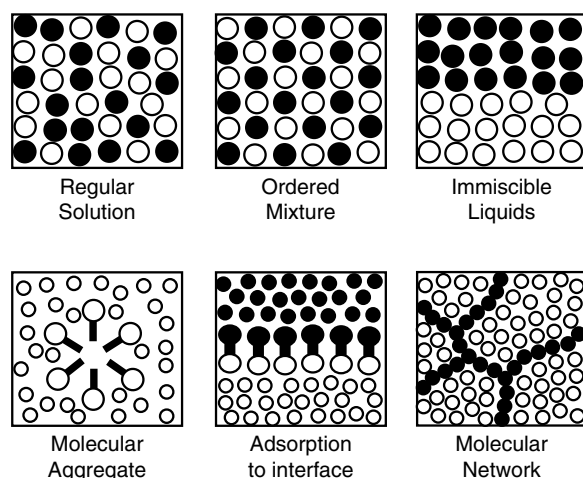


**Figure 2.1** The molecules in food emulsions may adopt a variety of different structural arrangements depending on the nature of their interactions with their neighbors.

of molecular forces and entropy effects important in materials, and to show how these characteristics influence the conformation and structural organization of molecules.

## 2.2 Forces of nature

There are four distinct types of forces of nature: strong nuclear interactions, weak nuclear interactions, electromagnetic interactions, and gravity (Israelachvili, 1992; Atkins, 1994). The strong and weak nuclear forces act over extremely short distances and are chiefly responsible for holding together subatomic particles in the nucleus. As nuclear rearrangements are not usually important in foods, these forces will not be considered further. Gravitational forces are relatively weak and act over large distances compared to other types of forces. Their strength is proportional to the product of the masses of the objects involved, and consequently they are insignificant at the molecular level because molecular masses are extremely small. Nevertheless, they do affect the behavior of food emulsions at the macroscopic level for example, sedimentation or creaming of droplets, the shape adopted by large droplets, meniscus formation, and capillary rise (Israelachvili, 1992). The dominant forces that act at the molecular level are all electromagnetic in origin, and can conveniently be divided into four types: covalent, electrostatic, van der Waals, and steric overlap (Israelachvili, 1992, Atkins, 1994, 2003; Walstra, 2003a). Despite acting over extremely short distances, often on the order of a few Angstroms or less, intermolecular forces are ultimately responsible for the bulk physicochemical and organoleptic properties of emulsions and other food materials.

## 2.3 Origin and nature of molecular interactions

### 2.3.1 Covalent interactions

Covalent bonds involve the sharing of outer-shell electrons between two or more atoms, so that the individual atoms lose their discrete nature (Karplus and Porter, 1970; Atkins, 1994). The number of electrons in the outer shell of an atom governs its *valency*, that is, the optimum number of covalent bonds it can form with other atoms. Covalent bonds may

be *saturated* or *unsaturated* depending on the number of electrons involved. Unsaturated bonds tend to be shorter, stronger, and more rigid than saturated bonds (Israelachvili, 1992; Atkins, 1994). The distribution of the electrons within a covalent bond determines its *polarity*. When the electrons are shared equally among the atoms the bond has a nonpolar character, but when the electrons are shared unequally the bond has a polar character. The polarity of a molecule depends on the symmetry of the various covalent bonds that it contains (see Section 2.3.2.). Covalent bonds are also characterized by their *directionality*, that is, their tendency to be directed at clearly defined angles relative to each other. The valency, saturation, polarity, strength, and directionality of covalent bonds determine the three-dimensional structure, flexibility, chemical reactivity, and physical interactions of molecules.

Chemical reactions involve the breaking and formation of covalent bonds (Atkins, 1994). The bulk physicochemical and organoleptic properties of food emulsions are altered by various types of chemical and biochemical reactions that occur during their production, storage, and consumption (Coultate, 1996; Fennema, 1996a; Fennema and Tannenbaum, 1996). Some of these reactions are beneficial to food quality, while others are detrimental. It is therefore important for food scientists to be aware of the various types of chemical reactions that occur in food emulsions, and to establish their influence on the overall properties of the system. The chemical reactions that occur in food emulsions are similar to those that occur in any other multicomponent heterogeneous food material, for example, oxidation of lipids and proteins, hydrolysis of proteins or polysaccharides, cross-linking of proteins, and Maillard reactions between reducing sugars and free amino groups (Damodaran, 1996; BeMiller and Whistler, 1996; Nawar, 1996). Nevertheless, the rates and pathways of these reactions are often influenced by the physical environment of the molecules involved, for example, whether they are located in the oil, water, or interfacial region (Wedzicha, 1988; Coupland and McClements, 1996; McClements and Decker, 2000).

Until fairly recently, emulsion scientists were principally concerned with understanding the physical changes that occur in food emulsions, rather than the chemical changes. Nevertheless, there is currently great interest in establishing the relationship between emulsion properties and the mechanisms of various chemical reactions that occur within them (Wedzicha et al., 1991; Coupland and McClements, 1996; Landy et al., 1996; Huang et al., 1997; McClements and Decker, 2001).

Despite the importance of chemical reactions on emulsion quality, it should be stressed that many of the most important changes in emulsion properties are a result of alterations in the spatial distribution of the molecules, rather than of alterations in their chemical structure, for example, creaming, flocculation, coalescence, Ostwald ripening, and phase inversion (Chapter 7). The spatial distribution of molecules is governed principally by their noncovalent (or physical) interactions with their neighbors, for example, electrostatic, van der Waals, and steric overlap. It is therefore particularly important to have a good understanding of the origin and nature of these interactions.

### 2.3.2 *Electrostatic interactions*

Electrostatic interactions occur between molecular species that possess a permanent electrical charge, such as ions and polar molecules (Murrell and Boucher, 1982; Reichardt, 1988; Rogers, 1989; Israelachvili, 1992; Norde, 2003). An ion is an atom or molecule that has either lost or gained one or more outer-shell electrons so that it obtains a permanent positive or negative charge (Atkins, 1994). A polar molecule has no net charge (i.e., as a whole the molecule is neutral), but it does have an electrical *dipole* because of an uneven distribution of the charges within it. Certain atoms are able to “pull” the electrons in the covalent bonds toward them more strongly than other atoms

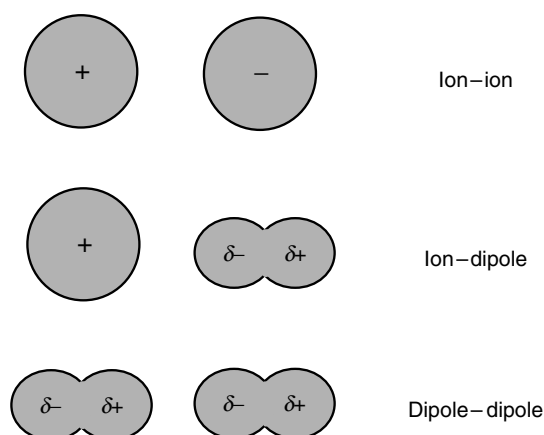


**Figure 2.2** Schematic representation of the most important types of intermolecular electrostatic interactions that arise between molecules.

(Atkins, 1994). As a consequence, they acquire a partial negative charge ( $\delta^-$ ), and the other atoms acquire a partial positive charge ( $\delta^+$ ). If the partial charges within a molecule are distributed symmetrically, they cancel each other and the molecule has no dipole (e.g.,  $\text{CCl}_4$ ), but if they are distributed asymmetrically the molecule will have a dipole (Israelachvili, 1992). For example, the chlorine atom in  $\text{HCl}$  pulls the electrons in the covalent bond more strongly than the hydrogen atom, and so a dipole is formed:  $\text{H}^{\delta+}\text{Cl}^{\delta-}$ . The strength of a dipole is characterized by the *dipole moment*  $\mu = ql$ , where  $l$  is the distance between two charges  $q^+$  and  $q^-$ . The greater the magnitude of the partial charges, or the further they are apart, the greater the dipole moment of a molecule.

The interaction between two molecular species is characterized by an *intermolecular pair potential*,  $w(s)$ , which is the energy required to bring two molecules from an infinite distance apart to a center-to-center separation  $s$  (Israelachvili, 1992). There are a number of different types of electrostatic interactions that can occur between permanently charged molecular species (ion-ion, ion-dipole, and dipole-dipole) (Figure 2.2), but they can all be described by a similar equation (Hiemenz and Rajagopalan, 1997):

$$w_E(s) = \frac{Q_1 Q_2}{4\pi\epsilon_0\epsilon_R s^n} \quad (2.1)$$

where  $Q_1$  and  $Q_2$  are the effective charges on the two species,  $\epsilon_0$  is the dielectric constant of a vacuum ( $8.85 \times 10^{-12} \text{ C}^2 \text{ J}^{-1} \text{ m}^{-1}$ ),  $\epsilon_R$  is the relative dielectric constant of the intervening medium,  $s$  is the center-to-center distance between the charges, and  $n$  is an integer that depends on the nature of the interaction. For ions, the value of  $Q$  is determined by their valency  $z$  and electrical charge  $e$  ( $1.602 \times 10^{-19} \text{ C}$ ), whereas for dipoles, it is determined by their dipole moment  $\mu$  and orientation (Table 2.1). Numerical calculations of the intermolecular pair potential for representative ion-ion, ion-dipole, and dipole-dipole interactions are illustrated in Figure 2.3a. It should be noted that Equation 2.1 is based on the assumption that the medium separating the two charged species is isotropic and homogeneous. In reality, the charged species are separated by one or more types of solvent molecules that have discrete sizes and physicochemical characteristics. When the separation between the charged species is relatively large compared to the size of the solvent molecules the assumption that the intervening medium is a continuum is a reasonably

**Table 2.1** Parameters Needed to Calculate the Interaction Pair Potential for Ion–Ion, Ion–Dipole, and Dipole–Dipole Electrostatic Interactions Using Equation 2.1 (see also Figure 2.3a). Here  $z$  is the Valence,  $\mu$  is the Dipole Moment,  $e$  is the Electronic Charge, and  $\phi$  is the Angle Between the Dipole Charges.

Interaction Type	Example	$Q_1 Q_2$	$n$
Ion–ion	$\text{Na}^+ \text{Cl}^-$	$(z_1 e)(z_2 e)$	1
Ion–dipole	$\text{Na}^+ \text{H}_2\text{O}$	$(z_1 e) \mu_2 \cos \phi$	2
Dipole–dipole	$\text{H}_2\text{O} \text{H}_2\text{O}$	$\mu_1 \mu_2 f(\phi)$	3

Source: From Hiemenz and Rajagopalan (1997).

good one. On the other hand, when the separation between the charged species is relatively small, this assumption breaks down and a more sophisticated analysis of the electrostatic interactions between the charged species is required. This analysis must take into account the size, shape, orientation, and interactions of all the molecules involved (Israelachvili, 1992).

Examination of Equation 2.1 and Figure 2.3a provides a number of valuable insights into the nature of intermolecular electrostatic interactions, and the factors that influence them:

1. The sign of the interaction may be either positive (repulsive) or negative (attractive) depending on the signs of charged molecules involved. If the charges have similar signs,  $w_E(s)$  is positive and the interaction is repulsive, but if they have opposite signs,  $w_E(s)$  is negative and the interaction is attractive.
2. The strength of the interaction depends on the magnitudes of the charges involved ( $Q_1$  and  $Q_2$ ). Thus, ion–ion interactions are stronger than ion–dipole interactions, which are in turn stronger than dipole–dipole interactions. In addition, the strength of interactions involving ions increases as their valency increases, whereas the strength of interactions involving polar species increases as their dipole moment increases.
3. The strength of the interaction increases as the center-to-center separation of the charged species decreases. Thus, interactions between small ions or molecules (which can get close together) are stronger than those between large ions or molecules of the same charge.
4. The strength of the interaction depends on the nature of the material separating the charges (via  $\epsilon_R$ ): the higher the relative dielectric constant, the weaker the interaction (Equation 2.1). Electrostatic interactions between two charged species in water ( $\epsilon_R = 80$ ) are therefore much weaker than those between the same species in oil ( $\epsilon_R = 2$ ). This phenomenon accounts for the much higher solubility of salts in water than in nonpolar solvents (Israelachvili, 1992).
5. The strength of the interaction depends on the orientation of any dipoles involved, being strongest when partial charges of opposite sign are brought close together. When the electrostatic interaction between a dipole and another charged species is much stronger than the thermal energy (Section 2.5), the dipole becomes permanently aligned so as to maximize the strength of the attraction. This alignment of dipoles is responsible for the high degree of structural organization of molecules in bulk water and the ordering of water molecules around ions in aqueous solutions (Chapter 4).
6. The range of the interaction depends on the nature of the charged molecular species involved, with ion–ion ( $1/s$ ) interactions being longer range than ion–dipole interactions ( $1/s^2$ ), which are in turn longer range than dipole–dipole interactions ( $1/s^3$ ).

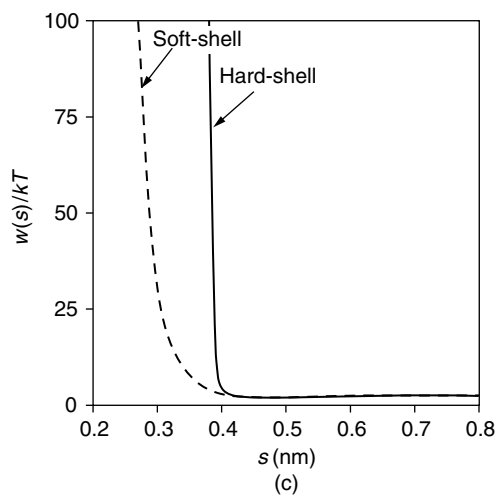
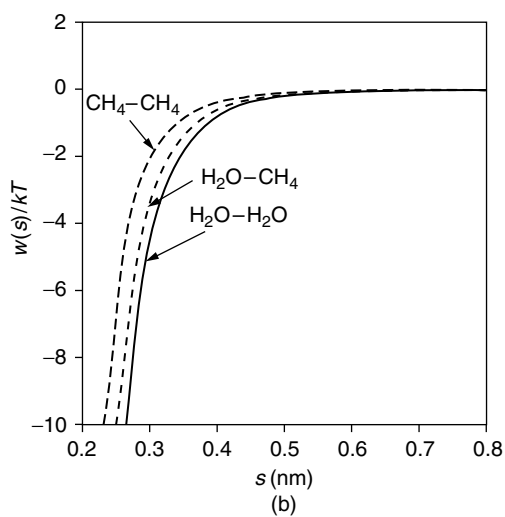
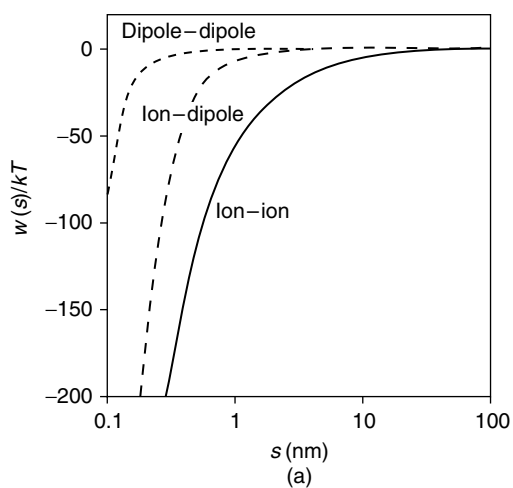


**Figure 2.3** Dependence of the intermolecular pair potential on intermolecular separation for (a) electrostatic, (b) van der Waals, and (c) steric overlap interactions.

**Table 2.2** Compilation of Molecular Properties of Some Common Liquids and Solutes Need to Calculate Intermolecular Interactions.

Molecule Type	$\sigma(\text{nm})$	$\alpha/4\pi\epsilon_0 (\times 10^{-30} \text{ m}^3)$	$\mu (D)^*$
<b>Molecular diameters, polarizabilities, and dipole moments</b>			
H <sub>2</sub> O	0.28	1.48	1.85
CH <sub>4</sub>	0.40	2.60	0
HCl	0.36	2.63	1.08
CH <sub>3</sub> Cl	0.43	4.56	1.87
CCl <sub>4</sub>	0.55	10.5	0
NH <sub>3</sub>	0.36	2.26	1.47
Methanol	0.42	3.2	1.69
Ethanol	— <sup>†</sup>	5.2	1.69
Acetone	— <sup>†</sup>	6.4	2.85
Benzene	0.53	10.4	0
<b>Static relative dielectric constants <math>\epsilon_R</math></b>			
Water	78.5	Chloroform	4.8
Ethylene glycol	40.7	Edible oils	2.5
Methanol	32.6	Carbon tetrachloride	2.2
Ethanol	24.3	Liquid paraffin	2.2
Acetone	20.7	Dodecane	2.0
Propanol	20.2	Hexane	1.9
Acetic acid	6.2	Air	1.0

Source: From Israelachvili (1992) and Buffler (1995).

\*D =  $3.336 \times 10^{-30}$  C m.

<sup>†</sup>Cannot be treated as spheres.

### 2.3.3 *van der Waals interactions*

van der Waals forces act between all types of molecular species, whether they are ionic, polar, or nonpolar (Israelachvili, 1992; Hiemenz and Rajagopalan, 1997; Norde, 2003). They are conveniently divided into three separate contributions, all of which rely on the polarization of molecules (Figure 2.4).

#### 2.3.3.1 *Dispersion forces*

These forces arise from the interaction between an instantaneous dipole and a dipole induced in a neighboring molecule by the presence of the instantaneous dipole. The electrons in a molecule are continually moving around the nucleus. At any given instant in time there is an uneven distribution of the negatively charged electrons around the positively charged nucleus, and so an *instantaneous* dipole is formed. This instantaneous dipole generates an electrical field that induces a dipole in a neighboring molecule. Consequently, there is an instantaneous attractive force between the two dipoles. On average, the attraction between the molecules is therefore finite, even though the average net charge on the molecules involved is zero.

#### 2.3.3.2 *Induction force*

These forces arise from the interaction between a permanent dipole and a dipole induced in a neighboring molecule by the presence of the permanent dipole\*. A permanent dipole

\* Ions may also induce dipoles in neighboring molecules, but this *ion polarization* interaction has a  $1/s^4$  dependence on intermolecular separation and is therefore not usually considered as a van der Waal interaction (Israelachvili, 1992).



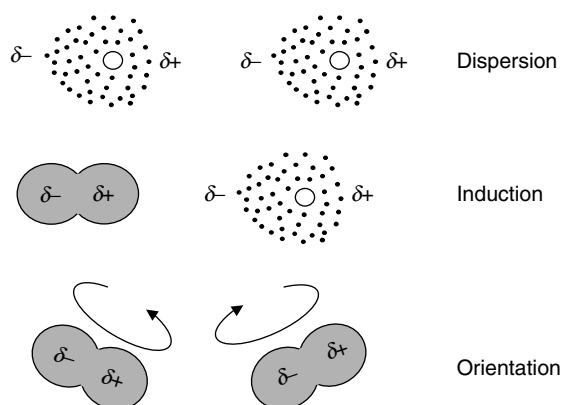


**Figure 2.4** Schematic representation of van der Waals intermolecular interactions which involve either the electronic or orientational polarization of molecules.

causes an alteration in the distribution of electrons of a neighboring molecule which leads to the formation of an induced dipole. The interaction between the permanent dipole and the induced dipole leads to an attractive force between the molecules.

### 2.3.3.3 Orientation forces

These forces arise from the interaction between two permanent dipoles that are continuously rotating. On average each individual rotating dipole has no net charge, but, there is still a weak attractive force between different dipoles because the movement of one dipole induces some correlation in the movement of a neighboring dipole. When the interaction between the two dipoles is strong enough to cause them to be permanently aligned, this contribution is replaced by the electrostatic dipole–dipole interaction described in the previous section.

As will be seen in the next chapter, an understanding of the origin of these three contributions to the van der Waals interaction has important consequences for predicting the stability of emulsion droplets to aggregation (Section 3.3).

The overall intermolecular pair potential due to van der Waals interactions is given by

$$w_{VDW}(s) = \frac{-(C_{disp} + C_{ind} + C_{orient})}{(4\pi\epsilon_0\epsilon_R)^2 s^6} \quad (2.2)$$

where  $C_{disp}$ ,  $C_{ind}$ , and  $C_{orient}$  are positive constants that depend on the dispersion, induction, and orientation contributions, respectively (Hiemenz and Rajagopalan, 1997). Their magnitude depends on the dipole moment (for permanent dipoles) and the polarizability (for induced dipoles) of the molecules involved in the interaction (Table 2.2). The polarizability is a measure of the strength of the dipole induced in a molecule when it is in the presence of an electrical field: the larger the polarizability the easier it is to induce a dipole in a molecule. For most biological molecules, the dominant contribution to the van der Waals interaction is the dispersion force, with the important exception of water where the major contribution is from the orientation force (Israelachvili, 1992). Examination of Equation 2.2 and Figure 2.3b provides some useful physical insights into the factors that influence the van der Waals interactions between two molecules:

1. The sign of the interaction is always negative (attractive) because the values of  $C_{disp}$ ,  $C_{ind}$ , and  $C_{orient}$  are always positive.

2. The strength of the interaction increases as the polarizability and dipole moment of the molecules involved increases.
3. The strength of the attraction decreases as the dielectric constant of the intervening medium increases, which highlights the electromagnetic origin of van der Waals interactions.
4. The range of the interaction is relatively short, decreasing rapidly with increasing intermolecular separation ( $1/s^6$ ).

Although van der Waals interactions act between all types of molecular species they are considerably weaker than electrostatic interactions (Figure 2.3 and Table 2.3). For this reason, they are most important in determining interactions between nonpolar molecules, where electrostatic interactions do not make a significant contribution. Indeed, the structure and physicochemical properties of organic liquids is largely governed by the van der Waals interactions between the molecules (Israelachvili, 1992).

### 2.3.4 Steric overlap interactions

When two atoms or molecules come so close together that their electron clouds overlap there is an extremely large repulsive force generated between them (Figure 2.3c). This steric overlap force is of a very short range and increases rapidly when the separation between the two molecules becomes less than the sum of their radii ( $\sigma = r_1 + r_2$ ). A number of empirical equations have been derived to describe the dependence of the steric overlap intermolecular pair potential,  $w_{\text{steric}}(s)$  on molecular separation (Israelachvili, 1992). The “hard-shell” model assumes that the repulsive interaction is zero when the separation is greater than  $\sigma$ , but infinitely large when it is less than  $\sigma$ :

$$w_{\text{steric}}(s) = \begin{cases} 0 & s \geq \sigma \\ \infty & s < \sigma \end{cases} \quad (2.3)$$

In reality, molecules are slightly compressible and so the increase in the steric overlap repulsion is not as dramatic as indicated by Equation 2.3. The slight compressibility of molecules is accounted for by a “soft-shell” model, such as the power-law model:

$$w_{\text{steric}}(s) = \left( \frac{\sigma}{s} \right)^{12} \quad (2.4)$$

At separations greater than  $\sigma$  the steric overlap repulsion is negligible, but at separations less than this value there is a steep increase in the interaction pair potential, which means that the molecules strongly repel one another. The strong repulsion that arises from steric overlap determines the effective size of atoms and molecules and how closely they can come together. It therefore has a strong influence on the packing of molecules in liquids and solids.

## 2.4 Overall intermolecular pair potential

We are now in a position to calculate the overall interaction between a pair of molecules. Assuming that no chemical reactions occur between the molecules, the overall intermolecular pair potential is the sum of the various physical interactions mentioned above:

$$w(s) = w_E(s) + w_{\text{VDV}}(s) + w_{\text{steric}}(s) \quad (2.5)$$

The magnitude of each of the individual contributions to the overall interaction potential is strongest at close separations and decreases as the molecules move apart. Nevertheless, the overall intermolecular pair potential has a more complex dependence on separation, which may be attractive at some separations and repulsive at others, because it is the sum of a number of interactions that each have different magnitudes, ranges, and signs.

To highlight some of the most important features of intermolecular interactions, it is useful to consider the interaction of a pair of spherical nonpolar molecules (i.e., no electrostatic interactions). The overall intermolecular pair potential for this type of system is given by an expression known as the Lennard–Jones potential (Bergethon and Simons, 1990; Baianu, 1992; Norde, 2003):

$$w(r) = \frac{-A}{s^6} + \frac{B}{s^{12}} \quad (2.6)$$

where the  $A$ -term represents the contribution from the van der Waals interactions (Equation 2.2) and the  $B$ -term represents the contribution from the steric overlap interaction (Equation 2.4). The dependence of the intermolecular pair potential on separation is illustrated in Figure 2.5. The van der Waals interactions are attractive at all separations, whereas the steric overlap interactions are repulsive. At large separations  $w(s)$  is so small that there is no effective interaction between the molecules. As the molecules are brought closer together the pair potential becomes increasingly attractive (negative) because the van der Waals interactions dominate. Eventually, the molecules get so close together that their electron clouds overlap and the pair potential becomes strongly repulsive (positive) because steric overlap interactions dominate. Consequently, there is a minimum in the overall intermolecular pair potential at some intermediate separation,  $s^*$ . Two molecules will tend to remain associated in this potential energy minimum in the absence of any disruptive influences (such as thermal energy or applied external forces), with a “bond length” of  $s^*$  and a “bond strength” of  $w(s^*)$ .

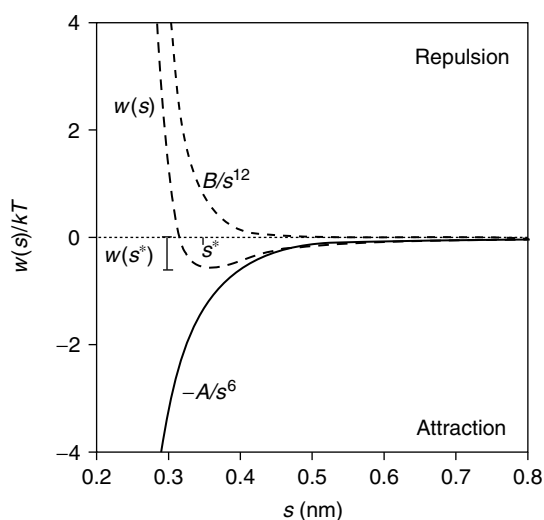


**Figure 2.5** Intermolecular pair potential for a pair of spherical nonpolar molecules. The curves were calculated assuming typical values for the constants:  $A = 10^{-77}$  J m<sup>6</sup> and  $B = 10^{-134}$  J m<sup>12</sup>.

**Table 2.3** Approximate Bond Strengths For Some of the Most Important Types of Molecular Interactions that Occur in Foods At Room Temperature.

Interaction Type	In Vacuum in Water			
	$w(s^*)$ (kJ mol <sup>-1</sup> )	$w(s^*)$ (RT)	$w(s^*)$ (kJ mol <sup>-1</sup> )	$w(s^*)$ (RT)
<b>Covalent bonds</b>				
C–O	340	140		
C–C	360	140		
C–H	430	170		
O–H	460	180		
C = C	600	240		
C $\equiv$ N	870	350		
<b>Electrostatic</b>				
Ion–ion				
Na <sup>+</sup> Cl <sup>-</sup>	500	200	6.3	2.5
Mg <sup>2+</sup> Cl <sup>-</sup>	1100	460	14.1	5.7
Al <sup>3+</sup> Cl <sup>-</sup>	1800	730	22.5	9.1
<b>Ion–dipole</b>				
Na <sup>+</sup> H <sub>2</sub> O	97	39	1.2	0.5
Mg <sup>2+</sup> H <sub>2</sub> O	255	103	3.2	1.3
Al <sup>3+</sup> H <sub>2</sub> O	445	180	5.6	2.3
<b>Dipole–dipole</b>				
H <sub>2</sub> OH <sub>2</sub> O	38	15	0.5	0.2
<b>Ion polarization</b>				
Na <sup>+</sup> CH <sub>4</sub>	24	10		
<b>van der Waals</b>				
CH <sub>4</sub> CH <sub>4</sub>	1.5	0.60		
C <sub>6</sub> H <sub>14</sub> C <sub>6</sub> H <sub>14</sub>	7.4	3.0		
C <sub>12</sub> H <sub>26</sub> C <sub>12</sub> H <sub>26</sub>	14.3	5.7		
C <sub>18</sub> H <sub>38</sub> C <sub>18</sub> H <sub>38</sub>	21.2	6.1		
CH <sub>4</sub> H <sub>2</sub> O	2.6	0.7		
H <sub>2</sub> OH <sub>2</sub> O	17.3	6.9		

*Note:* Dipole interactions were calculated assuming that the molecules were aligned to get maximum attraction. van der Waals forces were calculated from Israelachvili (1992) assuming that  $w(s^*)$  was approximately equal to the cohesive energy divided by 6.

The molecules in a substance are in continual motion (translational, rotational, and vibrational) because of their thermal energy,  $kT$  (Israelachvili, 1992; Atkins, 1994). The thermally induced movement of molecules has a disorganizing influence, which opposes the formation of intermolecular bonds. For this reason, the strength of intermolecular interactions is usually judged relative to the thermal energy:  $kT \approx 4.1 \times 10^{-24}$  kJ per bond or  $RT \approx 2.5$  kJ mol<sup>-1</sup>. If the bond strength is sufficiently greater than  $kT$  the molecules will remain together, but if the bond strength is sufficiently smaller than  $kT$  the molecules will tend to move apart. At intermediate bond strengths the molecules spend part of their time together and part of their time apart, that is, bonds are rapidly breaking and reforming.

The bond strengths of a number of important types of intermolecular interactions are summarized in Table 2.3. In a vacuum, the strength of these bonds decreases in the following order: ion–ion, covalent > ion–dipole > dipole–dipole > van der Waals. With the exception

of methane (a small nonpolar molecule), the bonds between the molecules shown in Table 2.3 are sufficiently strong (compared to the thermal energy) to hold them together in liquid or solid at room temperature. The strength of electrostatic and van der Waals interactions decreases appreciably when the molecules are surrounded by a solvent rather than a vacuum, especially when the solvent has a high dielectric constant (Israelachvili, 1992). When solute molecules are relatively large and sufficiently far apart (compared to the size of the solvent molecules), then the solvent can often be treated as a continuum with well-defined physicochemical properties (e.g., dielectric constant). On the other hand, when solute molecules are relatively small and in close proximity, it is usually necessary to take into account the dimensions, locations, and interactions of both the solute and solvent molecules on the overall interaction potential (see below).

It is often more convenient to describe the interaction between a pair of molecules in terms of *forces* rather than *potential energies* (Israelachvili, 1992). The force acting between two molecules can simply be calculated from the intermolecular pair potential using the following relationship:  $F(s) = -dw(s)/ds$ . The minimum in the potential energy curve therefore occurs at a separation where the net force acting between the molecules is zero, that is, the attractive and repulsive forces exactly balance. If the molecules move closer together they experience a repulsive force, and if they move further apart they experience an attractive force.

## 2.5 *Molecular structure and organization is determined by a balance of interaction energies and entropy effects*

In bulk materials, such as food emulsions, we are concerned with huge numbers of molecules, rather than a pair of isolated molecules in a vacuum. The overall structure and organization of molecules within a molecular ensemble depends on the interactions of each molecule with all of its neighbors (which may be similar or dissimilar types of molecules) and with various entropy effects (Murrell and Boucher, 1982; Murrell and Jenkins, 1994; Evans and Wennerstrom, 1994). One of the most powerful means of understanding the relationship between molecular structure, interactions, and organization in molecular ensembles is to use statistical thermodynamics (Sears and Salinger, 1975; Atkins, 1994). A molecular ensemble tends to organize itself so that the molecules are in an arrangement that minimizes the free energy of the system. The Gibbs free energy of a molecular ensemble is governed by both enthalpy and entropy contributions (Bergethon and Simons, 1990). The enthalpy contributions are determined by the molecular interaction energies discussed above, while the entropy contributions are determined by the tendency of a system to adopt its most disordered state. A variety of different types of entropy contributions are possible depending on the characteristics of the molecules involved and the nature of the system (Walstra, 2003a):

*Translational entropy:* The translational entropy is related to the number of different spatial positions that the molecules within a given volume can occupy. If the molecules are randomly distributed throughout the volume they have the highest translational entropy, but if they are organized in some way they have a lower translational entropy (e.g., by phase separating, adsorbing to a surface, forming clusters, or adopting a crystalline arrangement).

*Orientalional entropy:* The orientational entropy is related to the number of different positions (angles) that an anisometric molecule can adopt. If the molecules are free to rotate at any angle, then they have high orientational entropy, but if their rotation is restricted in one or more directions they have lower orientational entropy (e.g., due to adsorption to an interface).

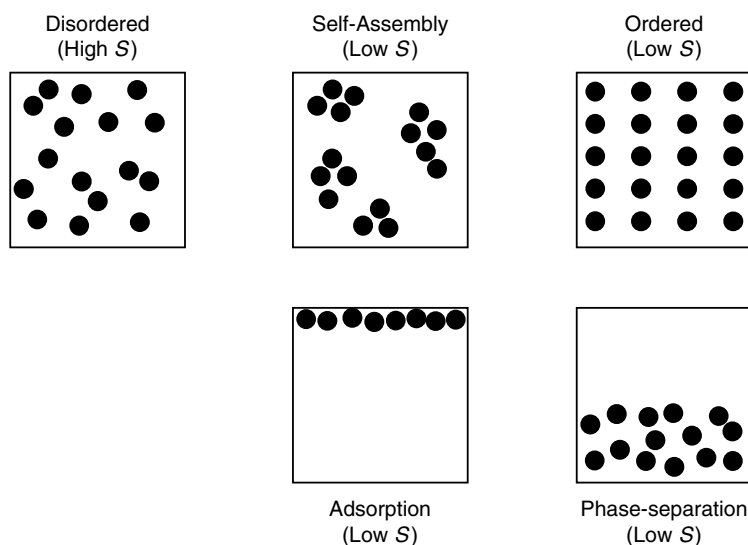


**Figure 2.6** Examples of physicochemical phenomenon that involve changes in the molecular organization of the system.

*Conformational entropy:* The conformational entropy is determined by the number of different conformations that a molecule can adopt. If a molecule can adopt many different conformations, then it has high entropy (e.g., a flexible random coil molecule), but if the number of conformations it can adopt is restricted then it has a low entropy (e.g., a globular or rod-like conformation).

*Mixing entropy:* The mixing entropy is determined by the number of different ways that two or more different kinds of molecules can adopt in a given volume. When the different kinds of molecules are randomly distributed throughout the volume the system has the highest entropy, but when one type of molecule is confined to one region and the other type of molecule is confined to another region then the system has a lower entropy.

There are many physicochemical processes that occur in food emulsions that involve one or more of the entropy changes mentioned previously, for example, mixing, self-association, binding, adsorption, solvent structuring, and denaturation. A number of these physicochemical processes will be encountered later in this book.

An understanding of the molecular basis for the organization of molecules within a particular system is usually obtained by comparing the strength of the molecular interactions and entropy contributions in that system to those in an appropriate *reference* system. Some examples of transitions between different spatial arrangements of molecules that are important in food emulsions are listed below (Figures 2.6 and 2.7):

- *Mixing:* Will a given collection of molecules form an intimate mixture of randomly dispersed molecules or will it phase separate?
- *Self-association:* Will solute molecules dispersed in a solvent exist as individual molecules or as molecular aggregates?
- *Ordering:* Will the molecules in a given volume arrange themselves into an ordered structure or will they be randomly distributed throughout the system?
- *Binding:* Will solute molecules dispersed in a biopolymer solution exist as unbound molecules or will they bind to the biopolymer molecules?

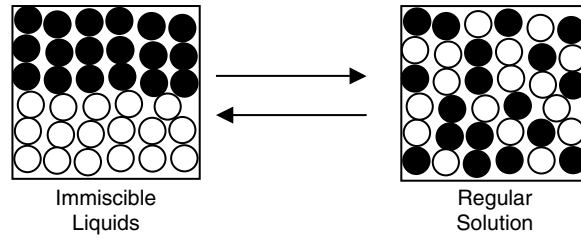


**Figure 2.7** System in which two types of molecules may be completely miscible or form a regular solution depending on the strength of the interactions between them and the entropy of mixing.

- *Adsorption*: Will solute molecules exist as individual molecules dispersed throughout the solvent or will they adsorb to a surface?
- *Conformation*: Will a biopolymer molecule dispersed in a solvent adopt a random coil or helix conformation?

In general, these different kinds of physiochemical process can be represented in terms of an equilibrium between two states with different molecular characteristics:

$$\text{State(1)} \leftrightarrow \text{State(2)} \quad (2.7)$$

The transition from one state to another is accompanied by a change in the free energy of the system:

$$\Delta G_{\text{tr}} = \Delta E_{\text{tr}} - T\Delta S_{\text{tr}} \quad (2.8)$$

where  $\Delta G_{\text{tr}}$ ,  $\Delta E_{\text{tr}}$ , and  $\Delta S_{\text{tr}}$  are the free energy, interaction energy, and entropy changes associated with the transition, respectively. If  $\Delta G_{\text{tr}}$  is negative, the transition is thermodynamically favorable; if  $\Delta G_{\text{tr}}$  is positive, the transition is thermodynamically unfavorable; and if  $\Delta G_{\text{tr}} \approx 0$ , the transition is thermodynamically neutral. The free energy change associated with a transition can often be related to the molecular characteristics of the system by using an appropriate physical model to calculate the change in interaction energies and entropy contributions that occur on going from one state to the other. The relative sign and magnitude of these contributions depend on the nature of the transition and on the type of molecules involved.

In general, the interaction energy ( $E$ ) of a particular arrangement of molecules can be determined by calculating the sum of all of the different types of interactions involved:

$$E = \sum_i n_i w_i \quad (2.9)$$

where  $n_i$  is the number of interactions of strength  $w_i$ . The change in interaction energies associated with a transition from State 1 to State 2 is then given by:

$$\Delta E = \sum_i n_{2,i} w_{2,i} - \sum_i n_{1,i} w_{1,i} \quad (2.10)$$

The entropy ( $S$ ) of a particular system can be calculated by the following expression (Atkins, 1994):

$$S = k_b \ln \Omega \quad (2.11)$$

where  $k_b$  is the Boltzmann constant and  $\Omega$  is the number of ways that the system can be arranged. The change in entropy associated with a transition can therefore be calculated from knowledge of the number of ways that the system can arrange itself in each different state:

$$\Delta S_{tr} = k_b (\ln \Omega_2 - \ln \Omega_1) \quad (2.12)$$

The above equations can be used to relate changes in the organization of molecular ensembles to changes in the molecular interactions and entropy contributions in the system. Nevertheless, it is often difficult to develop appropriate physical models that can be used to calculate changes in molecular interaction energies and entropy contributions for real systems, because of the lack of information about molecular interactions and structural organization. Despite this limitation, it is often useful to think of physicochemical processes in terms of the change in interaction energies and entropy contributions that occur due to a transition in their molecular structure or organization. In the following sections, we examine two physicochemical processes (mixing and conformational changes) in more detail to highlight the advantages of taking a molecular approach to understanding physicochemical phenomenon.

## 2.6 Thermodynamics of mixing

The use of molecular models for understanding the relationship between molecular organization, interaction energies, and entropy contributions is demonstrated by considering the thermodynamics of mixing of a simple system. Consider a hypothetical system that consists of a collection of two different types of equal-sized spherical molecules, A and B (Figure 2.7). The free energy change that occurs when these molecules are mixed is given by:

$$\Delta G_{mix} = \Delta E_{mix} - T\Delta S_{mix} \quad (2.13)$$

where  $\Delta E_{mix}$  and  $\Delta S_{mix}$  are the differences in the molecular interaction energy and entropy of the mixed and unmixed states, respectively. Practically, we may be interested in whether the resulting system consists of two immiscible liquids or as a simple mixture where the molecules are more or less intermingled (Figure 2.7). To a first approximation, thermodynamics tells us that if  $\Delta G_{mix}$  is highly positive, mixing is unfavorable and the molecules tend to exist as two separate phases (i.e., they are immiscible); if  $\Delta G_{mix}$  is highly negative, mixing is favorable and the molecules tend to be intermingled with each other (i.e., they are miscible); and if  $\Delta G_{mix} \approx 0$ , the molecules are partly miscible and partly immiscible. In practice, more complicated situations can occur depending on the relationship between  $\Delta G_{mix}$  and the composition of the system. For simplicity, we assume that if the two types of molecules do intermingle with each other they form a regular solution, that is, a completely random arrangement of the molecules (Figure 2.7b), rather than an ordered solution, in which the type A molecules are preferentially surrounded by type B molecules,



or vice versa. In practice, this means that the attractive forces between the two different types of molecules are not much stronger than the thermal energy of the system (Atkins, 1994; Evans and Wennerstrom, 1994). This argument is therefore only applicable to mixtures that contain nonpolar or slightly polar molecules, where strong ion-ion or ion-dipole interactions do not occur. Despite the simplicity of this model system, we can still gain considerable insight into the behavior of more complex systems that are relevant to food emulsions. In the following sections, we separately consider the contributions of the interaction energy and the entropy to the overall free energy change that occurs on mixing.

### 2.6.1 Potential energy change on mixing

An expression for  $\Delta E_{\text{mix}}$  can be derived by calculating the total interaction energy of the molecules before and after mixing (Israelachvili, 1992; Evans and Wennerstrom, 1994; Norde, 2003). For both the mixed and the unmixed system, the total interaction energy is determined by summing the contribution of each of the different types of bond:

$$E = n_{\text{AA}}w_{\text{AA}} + n_{\text{BB}}w_{\text{BB}} + n_{\text{AB}}w_{\text{AB}} \quad (2.14)$$

where  $n_{\text{AA}}$ ,  $n_{\text{BB}}$ , and  $n_{\text{AB}}$  are the total number of bonds, and  $w_{\text{AA}}$ ,  $w_{\text{BB}}$ , and  $w_{\text{AB}}$  are the intermolecular pair potentials at equilibrium separation, that correspond to interactions between A-A, B-B, and A-B molecules, respectively. The total number of each type of bond formed is calculated from the number of molecules present in the system, the coordination number of the individual molecules (i.e., the number of molecules in direct contact with them) and their spatial arrangement. For example, many of the A-A and B-B interactions that occur in the unmixed system are replaced by A-B interactions in the mixed system. The difference in the total interaction energy between the mixed and unmixed states is then calculated:  $\Delta E_{\text{mix}} = E_{\text{mix}} - E_{\text{unmixed}}$ . This type of analysis leads to the following equation (Evans and Wennerstrom, 1994).

$$\Delta E_{\text{mix}} = nX_{\text{A}}X_{\text{B}}w \quad (2.15)$$

where  $n$  is the total number of moles,  $w$  is the *effective interaction parameter*, and  $X_{\text{A}}$  and  $X_{\text{B}}$  ( $= 1 - X_{\text{A}}$ ) are the mole fractions of molecules of types A and B, respectively. The effective interaction parameter is a measure of the compatibility of the molecules in a mixture, and is related to the intermolecular pair potential between isolated molecules by the expression (Norde, 2003):

$$w = z \left( w_{\text{AB}} - \frac{1}{2} [w_{\text{AA}} + w_{\text{BB}}] \right) \quad (2.16)$$

where  $z$  is the coordination number of a molecule (i.e., the number of contacting neighbors). The effective interaction parameter determines whether the mixing of dissimilar molecules is energetically favorable ( $w$  negative), unfavorable ( $w$  positive), or indifferent ( $w = 0$ ). It should be stressed that even though there may be attractive forces between all the molecules involved (i.e.,  $w_{\text{AA}}$ ,  $w_{\text{BB}}$ , and  $w_{\text{AB}}$  may all be negative), the overall interaction potential can be either negative (favorable to mixing) or positive (unfavorable to mixing) depending on the *relative* magnitude of the interactions. If the strength of the interaction between two different types of molecules ( $w_{\text{AB}}$ ) is greater (more negative) than

the average strength between similar molecules ( $w_{AB} < [w_{AA} + w_{BB}]/2$ ), then  $w$  is negative, which favors the intermingling of the different types of molecules. On the other hand, if the strength of the interaction between two different types of molecules is weaker (less negative) than the average strength between similar molecules ( $w_{AB} > [w_{AA} + w_{BB}]/2$ ), then  $w$  is positive, which favors phase separation. If the strength of the interaction between different types of molecules is the same as the average strength between similar molecules ( $w_{AB} = [w_{AA} + w_{BB}]/2$ ), then the system has no preference for any particular arrangement of the molecules within the system. In summary, the change in the overall interaction energy may either favor or oppose mixing, depending on the relative magnitudes of the intermolecular pair potentials.

### 2.6.2 Entropy change on mixing

An expression for  $\Delta S_{\text{mix}}$  is obtained from simple statistical considerations (Israelachvili, 1992; Evans and Wennerstrom, 1994; Norde, 2003). The entropy of a system depends on the number of different ways the molecules can be arranged. For an immiscible system there is only one possible arrangement of the two different types of molecules (i.e., zero entropy), but for a regular solution there are a huge number of different possible arrangements (i.e., high entropy). A statistical analysis of this situation leads to the derivation of the following equation for the entropy of mixing (Atkins, 1994):

$$S_{\text{mix}} = -nR (X_A \ln X_A + X_B \ln X_B) \quad (2.17)$$

$\Delta S_{\text{mix}}$  is always positive because  $X_A$  and  $X_B$  are both between zero and one (so that the natural logarithm terms are negative), which reflects the fact that there is always an increase in entropy after mixing. For regular solutions, the entropy contribution ( $-T\Delta S_{\text{mix}}$ ) always decreases the free energy of mixing, that is, favors the intermingling of the molecules. It should be stressed that for more complex systems, there may be additional contributions to the entropy due to the presence of some order within the mixed state, for example, organization of solvent molecules around a solute molecule (Section 4.3).

### 2.6.3 Overall free energy change on mixing

For a regular solution, the free energy change on mixing depends on the combined contributions of the interaction energies and the entropy:

$$\Delta G_{\text{mix}} = n [X_A X_B w + RT(X_A \ln X_A + X_B \ln X_B)] \quad (2.18)$$

We are now in a position to investigate the relationship between the strength of the interactions between molecules and their structural organization within a bulk liquid. The dependence of the free energy of mixing on the effective interaction parameter and the composition of a system consisting of two different types of molecules is illustrated in Figure 2.8. The two liquids are completely miscible when the interactions between the dissimilar molecules are not too energetically unfavorable (i.e.,  $w < 2 RT$ ) because the entropy of mixing contribution dominates. This accounts for the miscibility of liquids in which the interactions between the different types of molecules are fairly similar, for example, two nonpolar oils. Two liquids are almost completely immiscible when the interactions between the dissimilar molecules are highly energetically unfavorable (i.e.,  $w > 4 RT$ ). This accounts for the immiscibility of oil and water, where the water molecules

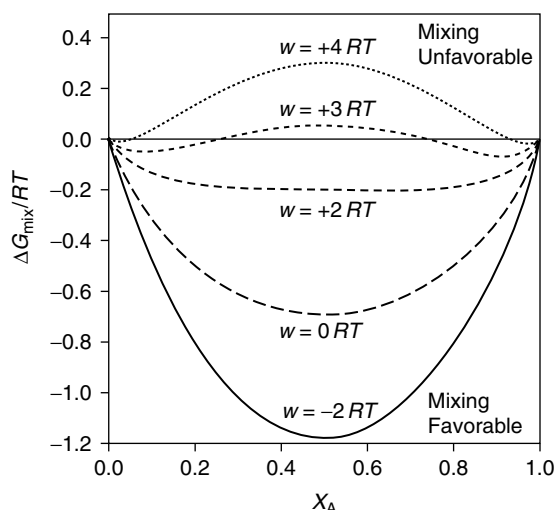


**Figure 2.8** Dependence of the free energy of mixing (calculated using Equation 2.18) on the composition and effective interaction parameter of a binary liquid. When  $\Delta G_{\text{mix}}$  is much less than  $-RT$  the system tends to be mixed, otherwise it will be partly or wholly immiscible.

can form strong hydrogen bonds with each other but not with oil molecules. Two liquids are partially miscible when the interactions between the dissimilar molecules are moderately unfavorable (i.e.,  $2 RT < w < 4 RT$ ). At these intermediate interaction strengths there are two minimum values in the  $\Delta G_{\text{mix}}$  versus  $X_A$  curve:  $X_{\text{AL}}$  and  $X_{\text{AH}}$ , which represent the lower and higher values, respectively (Figure 2.8). Under these circumstances, if the initial composition ( $X_{\text{AT}}$ ) of the overall system falls between these two minimum values, then the system separates into two phases, one with composition  $X_A = X_{\text{AL}}$  and the other with composition  $X_A = X_{\text{AH}}$ . The relative proportion of these two phases depends on the initial composition:  $\phi_{\text{AL}} = (X_{\text{AH}} - X_{\text{AT}})/(X_{\text{AH}} - X_{\text{AL}})$ ,  $\phi_{\text{AH}} = (1 - \phi_{\text{AL}})$ . The positions of  $X_{\text{AL}}$  and  $X_{\text{AH}}$  on the composition axis depend on the magnitude of the effective interaction parameter: the higher  $w$ , the smaller  $X_{\text{AL}}$  and the larger  $X_{\text{AH}}$  (Norde, 2003). Knowledge of the effective interaction parameter and composition of a system enables one to use the above equation for  $\Delta G_{\text{mix}}$  to construct a phase diagram that describes the conditions under which the molecular ensemble exists as an intimate mixture or as a phase separated system (Figure 2.9). The above approach therefore enables one to use thermodynamic considerations to relate bulk physicochemical properties of liquids (such as immiscibility) to molecular properties (such as the effective interaction parameter and the coordination number).

#### 2.6.4 Complications

The derivation of the equation for  $\Delta G_{\text{mix}}$  given above depends on making a number of simplifying assumptions about the properties of the system that are not normally valid in practice, for example, that the molecules are spherical, that they all have the same size and coordination number, and that there is no ordering of the molecules within the mixture (Israelachvili, 1992). It is possible to incorporate some of these features into the above theory, but a much more elaborate mathematical analysis is required. Food molecules come in all sorts of different sizes, shapes, and flexibilities, they may be nonpolar, polar, or amphiphilic, they may have one or more specific binding sites or they may have to be in a certain orientation before they can interact with their neighbors. In addition,

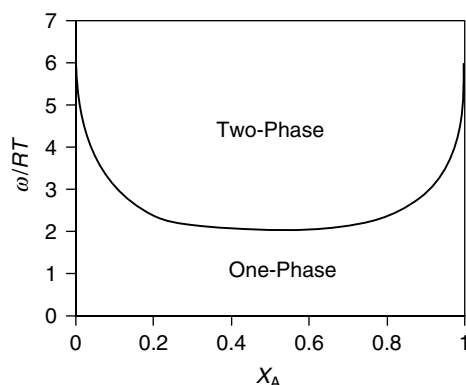


**Figure 2.9** Phase diagram describing the compositions and effective interaction parameters where the system exists as a one-phase (miscible) or two-phase (immiscible) system. This diagram was calculated using Equation 2.18 to find the minimum values in the  $\Delta G_{\text{mix}}$  vs.  $X_A$  graph.

a considerable degree of structural organization of the molecules within a solvent often occurs when a solute is introduced if the solute–solvent interactions are sufficiently strong. The variety of molecular characteristics exhibited by food molecules accounts for the great diversity of structures that are formed in food emulsions, such as bulk liquids, regular solutions, organized solutions, micelles, molecular networks, and immiscible liquids (Figure 2.1).

Another problem with the thermodynamic approach is that food systems are rarely at thermodynamic equilibrium because of the presence of various kinetic energy barriers that prevent the system from reaching its lowest free energy state. This approach cannot therefore tell us whether two liquids will exist as an emulsion or not, because an emulsion is a thermodynamically unstable system. Nevertheless, it can tell us whether two liquids are *capable* of forming an emulsion, that is, whether they are immiscible or miscible. Despite the obvious limitations of the simple thermodynamic approach, it does highlight some of the most important features of molecular organization, especially the importance of considering both interaction energies and entropy effects.

## 2.7 Molecular conformation

So far we have only considered the way that molecular interactions influence the spatial distribution of molecules in a system. Molecular interactions can also determine the three-dimensional conformation and flexibility of individual molecules (Lehninger et al., 1993; Atkins, 1994; Gelin, 1994; Norde, 2003; Walstra, 2003a). Small molecules, such as  $\text{H}_2\text{O}$  and  $\text{CH}_4$ , normally exist in a single conformation that is determined by the relatively strong covalent bonds that hold the atoms together (Karplus and Porter, 1970; Atkins, 1994). On the other hand, many larger molecules can exist in a number of different conformations because of the possibility of rotation around saturated covalent bonds, for example, proteins and polysaccharides (Bergethon and Simmons, 1990; Lehninger et al., 1993; Fennema, 1996a). A macromolecule will tend to adopt the conformation that has the lowest free energy under the prevailing environmental conditions (Alber, 1989). The conformational free energy of a molecule is determined by the various interaction energies and entropy contributions within the particular system (Dill, 1990). The molecular interactions may be between different parts of the same molecule (intramolecular) or between the molecule and its neighbors (intermolecular). Similarly, the entropy is determined by the number of

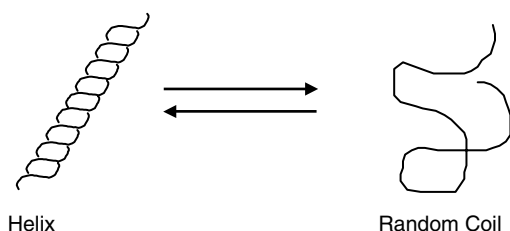


**Figure 2.10** The conformation of a molecule in solution is governed by a balance of interaction energies and entropic effects. A helical molecule unfolds when it is heated above a certain temperature because the random coil conformation is entropically more favorable than the helical conformation.

conformations that the molecule can adopt, as well as by any changes in the entropy caused by interactions with its neighbors, for example, restriction of their translational or rotational motion (Alber, 1989; Dill, 1990).

To highlight the importance of molecular interactions and entropy in determining the conformation of molecules in solution it is useful to examine a specific example. Consider a dilute aqueous solution containing hydrophilic biopolymer molecules that can exist in either a helical or a random coil conformation depending on the environmental conditions (Figure 2.10). Many types of food biopolymers are capable of undergoing this type of transformation, including the protein gelatin (Walstra, 1996b) and the polysaccharides xanthan, carrageenan, and alginate (BeMiller and Whistler, 1996). The free energy associated with the helix-to-coil transition between these two different conformations is given by:

$$\Delta G_{h \rightarrow c} = \Delta E_{h \rightarrow c} - T\Delta S_{h \rightarrow c} \quad (2.19)$$

where  $\Delta G_{h \rightarrow c}$ ,  $\Delta E_{h \rightarrow c}$ , and  $\Delta S_{h \rightarrow c}$  are the free energy, interaction energy, and entropy changes associated with the helix-to-coil transition. If  $\Delta G_{h \rightarrow c}$  is negative, the random coil conformation is favored; if  $\Delta G_{h \rightarrow c}$  is positive, the helix conformation is favored; and if  $\Delta G_{h \rightarrow c} \approx 0$ , the molecule spends part of its time in each of the conformations. In principle, a molecular interpretation of the free energy change associated with the helix-to-coil transition can be obtained by calculating the sum of the various intermolecular and intramolecular interaction energies in both the helix and coil states, and by calculating the number of different ways that all the molecules in the system (polymer and solvent) could arrange themselves in both the helix and coil states. In practice, this is extremely difficult to carry out because of the lack of information about the strength and number of all of the different kinds of interactions that occur in the system, and about the magnitude of the entropy effects. Nevertheless, a broad understanding of the relative importance of interaction energy and entropy contribution effects can be obtained. A helical conformation allows a molecule to maximize the number of energetically favorable intermolecular and intramolecular interactions, while minimizing the number of energetically unfavorable ones (Bergethon and Simmons, 1990). Nevertheless, it has a much lower entropy than the random coil state because the molecule can only exist in a single conformation, whereas in the random coil state the molecule can exist in a large number of different conformations. At low temperatures, the interaction energy term dominates the entropy term and so the molecule tends to exist as a helix, but as the temperature is raised the entropy term ( $-T\Delta S_{h \rightarrow c}$ ) becomes increasingly important until eventually it dominates and the molecule unfolds. The temperature at which the helix-to-coil transition takes place is referred to as the transition temperature,  $T_{h \rightarrow c}$ , which occurs when  $\Delta G_{h \rightarrow c} = 0$ . Similar arguments can be used to account for the unfolding of globular

proteins when they are heated above a particular temperature, although the relative contribution of the various types of interaction energies is different (Dickinson and McClements, 1995). It must be stressed that many food molecules are unable to adopt their thermodynamically most stable conformation because of the presence of various kinetic energy barriers (Section 1.2.1). When an energy barrier is much greater than the thermal energy of the system a molecule may be “trapped” in a metastable state indefinitely.

The flexibility of molecules in solution is also governed by both thermodynamic and kinetic factors. Thermodynamically, a flexible molecule must be able to exist in a large number of conformations that have fairly similar ( $\pm kT$ ) low free energies. Kinetically, the energy barriers that separate these energy states must be small compared to the thermal energy of the system. When both of these criteria are met, a molecule will rapidly move between a number of different configurations and therefore be highly flexible. If the free energy difference between the conformations is large compared to the thermal energy, the molecule will tend to exist predominantly in the minimum free energy state (unless it is locked into a metastable state by the presence of a large kinetic energy barrier).

Knowledge of the conformation and flexibility of a macromolecule under a particular set of environmental conditions is particularly important in understanding and predicting the behavior of many ingredients in food emulsions. The conformation and flexibility of a molecule determines its chemical reactivity, catalytic activity, intermolecular interactions, and functional properties, for example, solubility, dispersability, water-holding capacity, gelation, foaming, and emulsification (Damodaran, 1994, 1996, 1997; BeMiller and Whistler, 1996).

## 2.8 Compound interactions

When one consults the literature dealing with molecular interactions in foods and other biological systems, one often comes across the terms “hydrogen bonding” and “hydrophobic interactions” (Bergethon and Simons, 1990; Baianu, 1992; Fennema, 1996a; Paulaitis et al., 1996; Norde, 2003). In reality, these terms are a short-hand way of describing certain combinations of more fundamental interactions that occur between specific chemical groups commonly found in food molecules. Both of these *compound* interactions consist of contributions from various types of interaction energies (van der Waals, electrostatic, and steric overlap), as well as some entropy effects. It is useful to highlight the general features of hydrogen bonds and hydrophobic interactions in this section, before discussing their importance in determining the properties of individual food components later in Chapter 4. If one considers molecular organization in terms of compound interactions (rather than fundamental interactions), then it is usually difficult to divide the overall free energy term associated with a transition into  $\Delta E$  and  $\Delta S$  terms, since the compound interactions contain both interaction energy and entropy contributions. Nevertheless, it is often more convenient to group some of the entropy contributions with particular types of compound interactions (e.g., hydrophobic interactions), and consider the others separately (e.g., as translational, mixing, or conformational entropy contributions). The approach used to relate the free energy of mixing to the molecular interactions and entropy contributions can still be used (Section 2.5), but the effective interaction parameter is expressed in terms of interaction-free energies (e.g.,  $g_{AA}$ ,  $g_{BB}$ ,  $g_{AB}$ ) rather than just interaction energies (e.g.,  $w_{AA}$ ,  $w_{BB}$ ,  $w_{AB}$ ) (Norde, 2003).

### 2.8.1 Hydrogen bonds

Hydrogen bonds play a crucial role in determining the functional properties of many of the most important molecules present in food emulsions, including water, proteins, lipids,

carbohydrates, surfactants, and minerals (Chapter 4). They are formed between a lone pair of electrons on an electronegative atom (such as oxygen), and a hydrogen atom on a neighbouring group, that is,  $\text{O}-\text{H}^{\delta+} \dots \text{O}^{\delta-}$  (Bergethon and Simons, 1990; Lehniger et al., 1993; Norde, 2003). The major contribution to hydrogen bonds is electrostatic (dipole–dipole), but van der Waals forces and steric repulsion also make a significant contribution (Dill, 1990). Typically, they have bond strengths between 10 and 40 kJ mol<sup>-1</sup> and lengths of about 0.18 nm (Israelachvili, 1992). The actual strength of a particular hydrogen bond depends on the electronegativity and orientation of the donor and acceptor groups (Baker and Hubbard, 1984). Hydrogen bonds are stronger than most other examples of dipole–dipole interaction because hydrogen atoms have a strong tendency to become positively polarised and have a small radius. In fact, hydrogen bonds are so strong that they cause appreciable alignment of the molecules involved. The strength and directional character of hydrogen bonds are responsible for many of the unique properties of water (Chapter 4).

### 2.8.2 *Hydrophobic interactions*

Hydrophobic interactions also play a major role in determining the behaviour of many important ingredients in food emulsions, particularly lipids, surfactants, and proteins (Nakai and Li-Chan, 1988). They manifest themselves as a strong attractive force that acts between nonpolar groups separated by water (Ben-Naim, 1980; Tanford, 1980; Israelachvili, 1992; Norde, 2003). Nevertheless, the actual origin of hydrophobic interactions is the ability of water molecules to form relatively strong hydrogen bonds with their nearest neighbours, whereas nonpolar molecules can only form relatively weak van der Waals bonds (Israelachvili, 1992). When a nonpolar molecule is introduced into liquid water it causes the water molecules in its immediate vicinity to rearrange themselves which changes both the interaction energy and entropy of the system (Chapter 4). It turns out that these changes are thermodynamically unfavourable and so the system attempts to minimise contact between water and nonpolar groups, which appears as an attractive force between the nonpolar groups (Ben-Naim, 1980; Evans and Wennerstrom, 1994). It is this effect that is largely responsible for the immiscibility of oil and water, the adsorption of surfactant molecules to an interface, the aggregation of protein molecules and the formation of surfactant micelles, and it is therefore particularly important for food scientists to have a good understanding of its origin and the factors that influence it (Nakai and Li-Chan, 1988).

## 2.9 *Computer modeling of liquid properties*

Our understanding of the way that molecules organise themselves in a liquid can be greatly enhanced by the use of computer modelling techniques (Murrell and Jenkins, 1994; Gelin, 1994; Norde, 2003). Computer simulations of the relationship between molecular properties, structure, and organization have provided a number of valuable insights that are relevant to a better understanding of the behaviour of food emulsions, including the miscibility/immiscibility of liquids, the formation of surfactant micelles, the adsorption and displacement of emulsifiers at an interface, the transport of nonpolar molecules through an aqueous phase, the conformation and flexibility of biopolymers in solution, and the formation of gels (Esselink et al., 1994; Bergethon, 1998; Whittle and Dickinson, 1997; Dickinson, 2000, 2001; Dickinson and Krishna, 2001; Evilevitch et al., 2002; Ettelaie, 2003; Pugnaloni et al., 2003, 2004). An example of the power of computer simulation techniques for understanding molecular processes relevant to food emulsions is shown in Figure 2.11. The displacement of one type of molecule from an interface by another

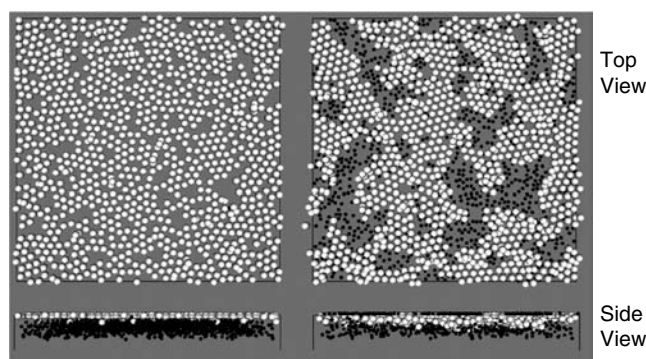


**Figure 2.11** Brownian dynamics simulation of the displacement of a gel-like adsorbed layer of bond-forming white spheres by more surface-active non-bond-forming small black spheres. (A) The displacer black spheres have been just introduced to the system beneath the interface. (B) The black spheres have partially displaced the gel-forming white spheres. The thickening of the displaced layer can be appreciated on the side-on profiles shown. (Kindly provided by Prof. Eric Dickinson and Dr. Luis Pugnali, University of Leeds, U.K.)

more surface-active type of molecule is simulated. This type of simulation can be used to provide insights into the molecular factors that influence the displacement of proteins from air–water or oil–water interfaces by surfactants or other proteins. The stability and physicochemical properties of emulsions are strongly influenced by interfacial properties, and so it is important to have a fundamental understanding of the factors that influence the type, concentration, interactions, and arrangement of surface-active molecules at interfaces (Chapters 5, 7–10).

The first step in a molecular simulation is to define the characteristics of the molecules involved (e.g., size, shape, flexibility, and polarity) and the nature of the intermolecular pair potentials that act between them (Gelin, 1994)\*. A collection of these molecules is arbitrarily distributed within a “box” that represents a certain region of space, and the change in the conformation and/or organisation of the molecules is then monitored as they are allowed to interact with each other. Depending on the simulation technique used, one can obtain information about the evolution of the structure with time and/or about the equilibrium structure of the molecular ensemble. The two most commonly used computer simulation techniques are the *Monte Carlo* approach and the *Molecular Dynamics* approach (Murrell and Boucher, 1982; Murrell and Jenkins, 1994).

### 2.9.1 Monte Carlo techniques

This technique is named after Monte Carlo, a town in the principality of Monaco (near southern France), which is famous for its gambling and casinos. The reason for this peculiar name is the fact that the movement of the molecules in the “box” is largely determined by a random selection process, just as the winner in a Roulette game is selected. Initially, one starts with an arbitrary arrangement of the molecules in the box. The overall interaction energy is then calculated from knowledge of the positions of all the molecules and their intermolecular pair potentials. One of the molecules is then randomly selected and moved to a new location and the overall interaction energy is recalculated. If the energy

\* It should be noted that it is usually necessary to make a number of simplifying assumptions about the properties and interactions of the molecules in order to create computer programs which can be solved in a reasonable time period.



decreases the move is definitely allowed, but if it increases the probability of the move being allowed depends on the magnitude of the energy change compared to the thermal energy. When the increase in energy is much greater than  $RT$  the move is highly unlikely and will probably be rejected, but if it is on the same order as  $RT$  it is much more likely to be accepted. This procedure is continued until there is no further change in the average interaction energy, which is taken to be the minimum potential energy state of the system. The free energy and entropy of the system are calculated by monitoring the fluctuations in the overall interaction energy after successive molecules have been moved once the system has reached equilibrium. The Monte Carlo technique therefore provides information about the *equilibrium* properties of a system, rather than about the evolution in its properties with time.

### 2.9.2 Molecular dynamics techniques

This technique is named after the fact that it relies on monitoring the movement of molecules with time. Initially, one starts with an arbitrary arrangement of the molecules in the "box." The computer then calculates the force that acts on each of the molecules as a result of its interactions with the surrounding molecules. Newton's equations of motion are then used to determine the direction and speed that each of the molecules move within a time interval that is short compared to the average time between molecular collisions (typically  $10^{-15}$  to  $10^{-14}$  sec). By carrying out the computation over a large number of successive time intervals it is possible to monitor the evolution of the system with time. The main limitation of this technique is that a huge number of computations have to be carried out in order to model events on time-scales relevant to pertinent physicochemical phenomena and using sufficient molecules to accurately represent these phenomena. Consequently, powerful computers and relatively long computation times are required to model even relatively simple molecular processes. Even so, as computer technology advances these computation times are decreasing, which enables researchers to model increasingly complex systems. A molecular dynamics simulation should lead to the same final state as a Monte Carlo simulation if it is allowed to proceed long enough to reach equilibrium. The free energy of the system is determined by the same method as for Monte Carlo simulations, that is, by taking into account the fraction of molecules that occupy each energy state once the system has reached equilibrium.

In practice, molecular dynamics simulations are more difficult to setup and take much longer to reach equilibrium than Monte Carlo simulations. For this reason, Monte Carlo simulations are more practical if a researcher is only interested in equilibrium properties, but molecular dynamic simulations are used when information about both the kinetics and thermodynamics of a system is required. Molecular dynamics techniques are particularly suitable for studying nonequilibrium processes, such as mass transport, fluid flow, adsorption kinetics, and solubilization processes (Dickinson and McClements, 1995). It is clear from the above discussion that each technique has its own advantages and disadvantages, and that both techniques can be used to provide useful insights into the molecular basis for some of the most important bulk physicochemical properties of food emulsions.

### 2.10 Measurement of molecular characteristics

Prediction of the organization of molecules using statistical thermodynamics or computer simulation techniques requires information about the total number and strength of the different kinds of bonds in the system, as well as of the spatial distribution of the molecules

within the system. Direct measurement of these molecular properties is usually extremely difficult because of their extremely small size, large number, and rapid movement. For this reason, most of the information that we have about molecular characteristics has to be inferred from more indirect measurements of the physicochemical properties of materials (Israelachvili, 1992):

- Measurements of the thermodynamic properties on gases, liquids, and solids (e.g., boiling points, heats of vaporization, lattice energies, ... Pressure-Volume-Temperature (PVT) data) provide information on short-range attraction between molecules.
- Measurements of the thermodynamic properties of solutions (e.g., solubility, miscibility, partitioning, phase diagrams, osmotic pressure) provide information about short-range solute-solute and solute-solvent interactions.
- Measurements of the bulk physicochemical properties of gases, liquids, and solids (e.g., density, compressibility, viscosity, diffusion, scattering, spectroscopy) provide information about short-range attractive and/or repulsive interactions between molecules.
- Measurements of adhesion forces holding solid surfaces together can provide information about short-range attractive interactions.
- Measurements of surface or interfacial properties (tensions or contact angles) can provide information about short-range liquid-liquid and solid-liquid interactions.

More recently a number of analytical methods have been developed to directly measure the forces acting between surfaces as a function of their separation, e.g., surface force apparatus, total internal reflection microscopy, atomic force microscopy, and osmotic pressure cells (Israelachvili, 1992). These techniques often provide the most detailed information about force-distance profiles for different kinds of molecular interactions.



## chapter three

---

# Colloidal interactions

### 3.1 Introduction

Food emulsions contain a variety of structural entities that have at least one dimension that falls within the colloidal size range (i.e., between a few nm and a few  $\mu\text{m}$ ), for example, molecular aggregates, micelles, emulsion droplets, fat crystals, ice crystals, and air cells (Dickinson and Stainsby, 1982; Dickinson, 1992; Friberg et al., 2004). The characteristics of these colloidal particles, and their interactions with each other, are responsible for many of the most important physicochemical and organoleptic properties of food emulsions. The ability of food scientists to understand, predict, and control the properties of food emulsions therefore depends on knowledge of the interactions that arise between colloidal particles. In this chapter, we examine the origin and nature of the most important types of colloidal interactions, while in later chapters we consider the relationship between these interactions and the stability, rheology, and appearance of food emulsions (Chapters 7–9).

The interaction between a pair of colloidal particles is the result of interactions between all of the molecules within them, as well as those within the intervening medium (Hunter, 1986; Israelachvili, 1992). For this reason, many of the interactions between colloidal particles appear at first sight to be similar to those between molecules, for example, van der Waals, electrostatic, and steric (Chapter 2). Nevertheless, the characteristics of these colloidal interactions are often different from their molecular counterparts, because of additional features that arise due to the relatively large size of colloidal particles and the relatively large number of different kinds of molecules involved. The major emphasis of this chapter will be on interactions between emulsion droplets, although the same principles can be applied to the various other types of colloidal particles that are commonly found in foods.

### 3.2 Colloidal interactions and droplet aggregation

Colloidal interactions govern whether emulsion droplets aggregate or remain as separate entities, as well as determining the characteristics of any aggregates formed, for example, their size, shape, porosity, and deformability (Dickinson, 1992; Bremer et al., 1993; Bijsterbosch et al., 1995; Walstra, 2003a). Many of the bulk physicochemical and organoleptic properties of food emulsions are determined by the degree of droplet aggregation and the characteristics of the aggregates (Chapters 7–9). It is therefore extremely important for food scientists to understand the relationship among colloidal interactions, droplet aggregation, and bulk properties.

In the previous chapter, the interaction between two isolated molecules was described in terms of an *intermolecular* pair potential. In a similar fashion, the interactions between two emulsion droplets can be described in terms of an *interdroplet* pair potential.

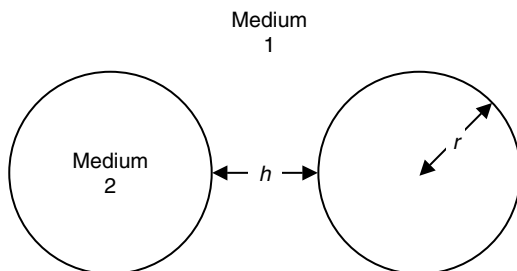


**Figure 3.1** Emulsion droplets of radius  $r$  separated by a surface-to-surface separation  $h$  through a liquid.

The interdroplet pair potential,  $w(h)$ , is the energy required to bring two emulsion droplets from an infinite distance apart to a surface-to-surface separation of  $h$  (Figure 3.1). Before examining specific types of interactions between emulsion droplets it is useful to examine the features of colloidal interactions in a more general fashion.

Consider a system that consists of two emulsion droplets of radius  $r$  at a surface-to-surface separation  $h$  (Figure 3.1). For convenience, we will assume that only two types of interactions occur between the droplets, one attractive and one repulsive:

$$w(h) = w_{\text{attractive}}(h) + w_{\text{repulsive}}(h) \quad (3.1)$$

The overall interaction between the droplets depends on the relative magnitude and range of the attractive and repulsive interactions. A number of different types of behavior can be distinguished depending on the nature of the interactions involved (Figure 3.2).

*Attractive interactions dominate at all separations.* If the attractive interactions are greater than the repulsive interactions at all separations, then the overall interaction is always attractive (Figure 3.2a), which means that the droplets will tend to aggregate (provided the strength of the interaction is greater than the disorganizing influence of the thermal energy).

*Repulsive interactions dominate at all separations.* If the repulsive interactions are greater than the attractive interactions at all separations, then the overall interaction is always repulsive (Figure 3.2b), which means that the droplets tend to remain as individual entities.

*Attractive interactions dominate at large separations, but repulsive interactions dominate at short separations.* At very large droplet separations there is no effective interaction between the droplets. As the droplets move closer together the attractive interaction initially dominates, but at closer separations the repulsive interaction dominates (Figure 3.2c). At some intermediate surface-to-surface separation there is a minimum in the interdroplet interaction potential ( $h_{\min}$ ). The depth of this minimum,  $w(h_{\min})$ , is a measure of the strength of the interaction between the droplets, while the position of the minimum,  $h_{\min}$ , corresponds to the most likely separation of the droplets. Droplets tend to aggregate when the strength of the interaction is large compared to the thermal energy ( $|w(h_{\min})| \gg kT$ ), remain as separate entities when the strength of the interaction is much smaller than the thermal energy ( $|w(h_{\min})| \approx 0$ ), and spend some time together and some time apart at intermediate interaction strengths. When droplets fall into a deep potential energy minimum they are said to be *strongly flocculated* or *coagulated* because a large amount of energy is required to pull them apart again. When they fall into a shallow minimum they are said to be *weakly flocculated* because they are fairly easy to pull apart. The fact that there is an extremely large repulsion between the droplets at close separations prevents them from coming close enough together to coalesce.

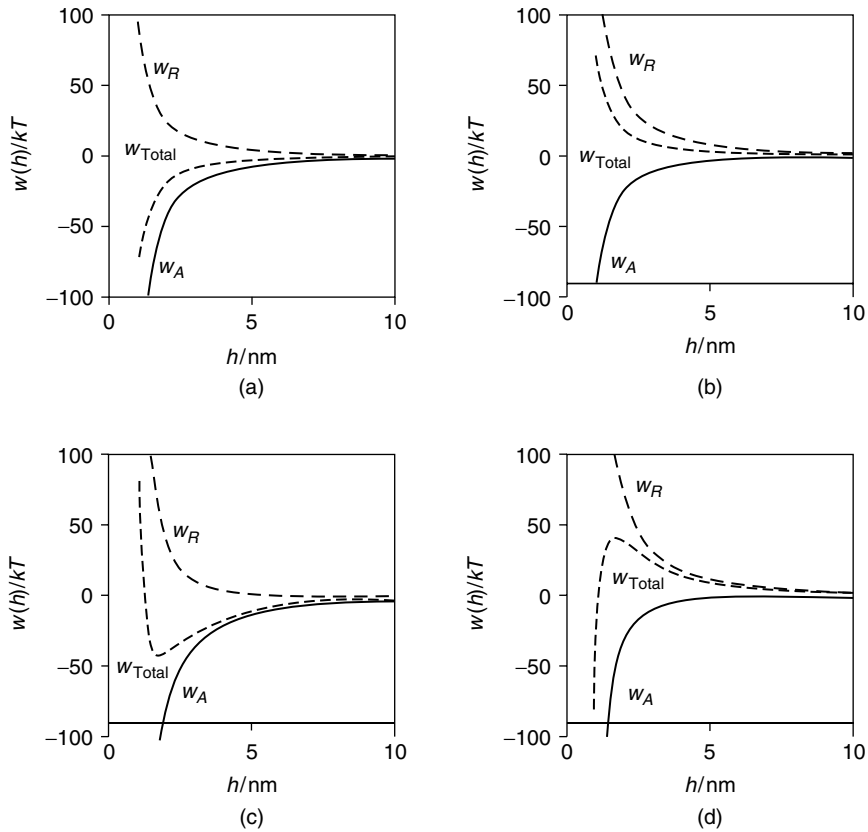


**Figure 3.2** The overall interaction of a pair of emulsion droplets depends on the relative magnitude and range of any attractive and repulsive interactions. The overall interaction may be attractive at some separations and repulsive at others.

*Repulsive interactions dominate at large separations, but attractive interactions dominate at short separations.* At very large droplet separations there is no effective interaction between the droplets. As the droplets move closer together the repulsive interaction initially dominates, but at closer separations the attractive interaction dominates (Figure 3.2d). At some intermediate surface-to-surface separation ( $h_{\max}$ ) there is an *energy barrier* that the droplets must overcome before they can move any closer together. If the height of this energy barrier is large compared to the thermal energy of the system ( $|w(h_{\max})| > 20kT$ ), the droplets are effectively prevented from coming close together and will therefore remain as separate entities (Friberg, 1997). If the height of the energy barrier is small compared to the thermal energy ( $|w(h_{\max})| < 5kT$ ), the droplets easily have enough thermal energy to “jump” over it, and they rapidly fall into the deep minimum that exists at close separations (Friberg, 1997). At intermediate values, the droplets still tend to aggregate but this process occurs slowly because only a fraction of droplet–droplet collisions has sufficient energy to “jump” over the energy barrier. The fact that there is an extremely strong attraction between the droplets at close separations is likely to cause them to coalesce, that is, merge together.

Despite the simplicity of the above model (Equation 3.1), we have already gained a number of valuable insights into the role that colloidal interactions play in determining whether emulsion droplets are likely to be unaggregated, flocculated, or coalesced.

In particular, the importance of the sign, magnitude, and range of the colloidal interactions has become apparent. As would be expected, the colloidal interactions that arise between the droplets in real food emulsions are much more complex than those considered above (Dickinson, 1992; Claesson et al., 2004). First, there are a number of different types of repulsive and attractive interactions that contribute to the overall interaction potential, each with a different sign, magnitude, and range. Second, food emulsions contain a huge number of droplets and other colloidal particles that have different sizes, shapes, and properties. Third, the liquid that surrounds the droplets may be compositionally complex, containing various types of ions and molecules. Droplet–droplet interactions in real food emulsions are therefore influenced by the presence of the neighboring droplets, as well as by the precise nature of the surrounding liquid. For these reasons, it is difficult to accurately account for colloidal interactions in real food emulsions because of the mathematical complexity of describing interactions among huge numbers of molecules, ions, and particles (Dickinson, 1992). Nevertheless, considerable insight into the factors that determine the properties of food emulsions can be obtained by examining the interaction between a pair of droplets. In addition, our progress toward understanding complex food systems depends on us first understanding the properties of simpler model systems. These model systems can then be incrementally increased in complexity and accuracy as advances are made in our knowledge.

In the following sections, the origin and nature of the major types of colloidal interactions that arise between emulsion droplets are reviewed. In Section 3.11, we then consider ways in which these individual interactions combine with each other to determine the overall interdroplet pair potential, and thus the stability of emulsion droplets to aggregation. Knowledge of the contribution that each of the individual colloidal interactions makes to the overall interaction is often of great practical importance, since it enables one to identify the most effective means of controlling the stability of a given system to droplet aggregation.

### 3.3 *van der Waals interactions*

#### 3.3.1 *Origin of van der Waals interactions*

*Intermolecular* van der Waals interactions operate between all of the different kinds of molecules in the dispersed and continuous phases of emulsions, which results in a net *colloidal* van der Waals interaction between the emulsion droplets (Hunter, 1986; Israelachvili, 1992; Hiemenz and Rajagopalan, 1997). Ultimately, the colloidal van der Waals interaction is a result of the orientation, induced, and dispersion contributions to the intermolecular van der Waals interaction discussed earlier (Section 2.3.3). An appreciation of these different contributions is important because it enables one to understand some of the physicochemical factors that influence the strength of colloidal van der Waals interactions between emulsion droplets, for example, retardation and electrostatic screening (see later).

#### 3.3.2 *Modeling van der Waals interactions*

The van der Waals interactions between macroscopic bodies can be calculated using two different mathematical approaches (Hunter, 1986; Derjaguin et al., 1987; Israelachvili, 1992; Hiemenz and Rajagopalan, 1997). In the *microscopic* approach, the van der Waals interaction between a pair of droplets is calculated by carrying out a pair-wise summation of the interaction energies of all the molecules in one of the droplets with all of the molecules in the other droplet. Calculations made using this approach rely on knowledge of the properties of the individual molecules, such as polarizabilities, dipole moments, and electronic energy levels. In the *macroscopic* approach, the droplets and surrounding medium are treated as continuous liquids that interact with each other because of the

fluctuating electromagnetic fields generated by the movement of the electrons within them. Calculations made using this approach rely on knowledge of the bulk physicochemical properties of the liquids, such as dielectric constants, refractive indices, and absorption frequencies. Under certain circumstances, both theoretical approaches give similar predictions of the van der Waals interaction between emulsion droplets. In general, however, the macroscopic approach is usually the most suitable for describing interactions between emulsion droplets because it automatically takes into account the effects of retardation and of the liquid surrounding the droplets (Hunter, 1986).

### 3.3.2.1 Interdroplet pair potential

The van der Waals interdroplet pair potential,  $w_{\text{VDW}}(h)$ , of two emulsion droplets of equal radius,  $r$ , separated by a surface-to-surface distance,  $h$ , is given by the following expression (Figure 3.1):

$$w_{\text{VDW}}(h) = -\frac{A_{212}}{6} \left[ \left( \frac{2r^2}{h^2 + 4rh} \right) + \left( \frac{2r^2}{h^2 + 4rh + 4r^2} \right) + \ln \left( \frac{h^2 + 4rh}{h^2 + 4rh + 4r^2} \right) \right] \quad (3.2)$$

where  $A_{212}$  is the *Hamaker function* for emulsion droplets (medium 2) separated by a liquid (medium 1). The value of the Hamaker function can be calculated using either the microscopic or macroscopic approaches mentioned above (Mahanty and Ninham, 1976). At close separations ( $h \ll r$ ), the above equation can be simplified considerably:

$$w_{\text{VDW}}(h) = -\frac{A_{212}r}{12h} \quad (3.3)$$

This equation indicates that van der Waals interactions between a pair of colloidal particles ( $w \propto 1/h$ ) are much longer range than those between a pair of molecules ( $w \propto 1/s^6$ ), which has important consequences for determining the stability of food emulsions. Equations for calculating the van der Waals interaction between spheres of unequal radius are given by Hiemenz and Rajagopalan (1997).

### 3.3.3.2 Hamaker function

In general, an accurate calculation of the Hamaker function of a pair of emulsion droplets is a complicated task (Mahanty and Ninham, 1976; Hunter, 1986; Israelachvili, 1992). Knowledge of the optical properties (dielectric permittivities) of the oil, water, and interfacial phases is required over a wide range of frequencies, and this information is not readily available for most substances (Hunter, 1986; Roth and Lenhoff, 1996). In addition, the full theory must be solved numerically using a digital computer (Pailthorpe and Russel, 1982). Nevertheless, approximate expressions for the Hamaker function have been derived, which can be calculated using data that can easily be found in the literature (Israelachvili, 1992):

$$A_{212} = A_{v=0} + A_{v>0} \quad (3.4)$$

where

$$A_{v=0} = \frac{3}{4} kT \sum_{s=1}^{\infty} \frac{1}{s^3} \left( \frac{\epsilon_1 - \epsilon_2}{\epsilon_1 + \epsilon_2} \right)^{2s} \quad \text{and} \quad A_{v>0} = \frac{3h\nu_e}{16\sqrt{2}} \frac{(n_1^2 - n_2^2)^2}{(n_1^2 + n_2^2)^{3/2}}$$



where  $\varepsilon$  is the static relative dielectric constant,  $n$  is the refractive index,  $\nu_e$  is the major electronic absorption frequency in the ultraviolet region of the electromagnetic spectrum (which is assumed to be equal for both phases),  $h$  is Planck's constant, and the subscripts 1 and 2 refer to the continuous phase and droplets, respectively. Equation 3.4 indicates that the Hamaker function of two similar droplets is always positive, which means that  $w_{VDW}(h)$  is always negative, so that the van der Waals interaction is always attractive. It should be noted, however, that the interaction between two colloidal particles containing different materials may be either attractive or repulsive, depending on the relative physical properties of the particles and intervening medium (Israelachvili, 1992; Milling et al., 1996).

In Equation 3.4, the Hamaker function is divided into two contributions: a zero-frequency component ( $A_{v=0}$ ) and a frequency-dependent component ( $A_{v>0}$ ). The overall interdroplet pair potential is therefore given by

$$w_{VDW}(h) = w_{v=0}(h) + w_{v>0}(h) \quad (3.5)$$

where  $w_{v=0}(h)$  and  $w_{v>0}(h)$  are determined by inserting the expressions for  $A_{v=0}$  and  $A_{v>0}$  into Equation 3.2 or 3.3. The zero-frequency component is due to *orientation* and *induction* contributions to the van der Waals interaction, whereas the frequency-dependent component is due to the *dispersion* contribution (Section 2.3.3). The separation of the Hamaker function into these two components is particularly useful for understanding the influence of electrostatic screening and retardation on van der Waals interactions (see below). The variation of  $w_{VDW}(h)$ ,  $w_{v=0}(h)$ , and  $w_{v>0}(h)$  with droplet separation for two oil droplets dispersed in water is shown in Figure 3.3.

For food emulsions, the Hamaker function is typically about  $0.56 \times 10^{-20}$  J ( $1.37kT$ ), with about 43% of this coming from the zero-frequency contribution and 57% from the frequency-dependent contribution. The physicochemical properties needed to calculate Hamaker functions for ingredients typically found in food emulsions are summarized in Table 3.1. In practice, the magnitude of the Hamaker function depends on droplet separation and is considerably overestimated by Equation 3.4 because of the effects of electrostatic screening, retardation, and interfacial layers (see below).

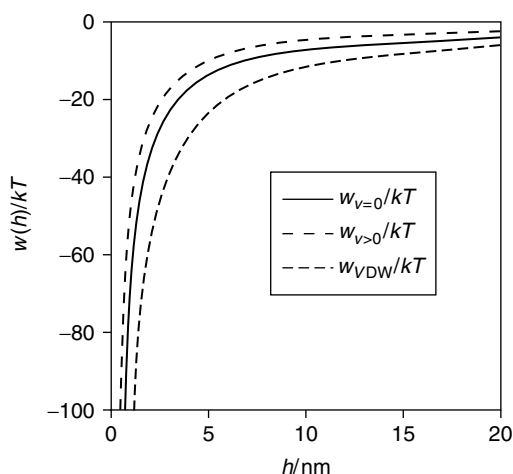


**Figure 3.3** Predicted dependence of the interaction potential on droplet separation for van der Waals interactions: total ( $w_{VDW}$ ); zero-frequency contribution ( $w_{v=0}$ ); frequency-dependent contribution ( $w_{v>0}$ ). See Table 3.1 for the physicochemical properties of the oil and water phases used in the calculations ( $r = 1 \mu m$ ).

**Table 3.1** Physicochemical Properties Needed to Calculate the Nonretarded Hamaker Function (Equation 3.4) for Some Materials Commonly Found in Food Emulsions.

Medium	Static Relative Dielectric Constant $\epsilon_R$	Refractive Index $n$	Absorption Frequency $\nu_e/10^{15} \text{ sec}^{-1}$
Water	80	1.333	3.0
Oil	2	1.433	2.9
Pure protein	5	1.56	2.9
$\frac{x}{100}\%$ protein in water	$5x + 80(1 - x)$	$1.56x + 1.333(1 - x)$	2.9
Pure Tween 20		1.468	2.9

Source: Data compiled from Israelachvili (1992), Wei et al. (1994), and Hato et al. (1996).

**3.3.3.2.1 Electrostatic screening effects.** The zero-frequency component of the Hamaker function ( $A_{v=0}$ ) is electrostatic in origin because it depends on interactions that involve permanent dipoles, that is, orientation and induction forces (Section 2.3.3). Consequently, this part of the van der Waals interaction is “screened” (reduced) when droplets are suspended in an electrolyte solution because of the accumulation of counterions around the droplets (Section 3.4). Electrostatic screening causes the zero-frequency component to decrease with increasing droplet separation, and with increasing electrolyte concentration (Manhanty and Ninham, 1976; Marra, 1986; Israelachvili, 1992; Mishchuk et al., 1995, 1996). At high electrolyte concentrations, the zero-frequency contribution decays rapidly with distance and makes a negligible contribution to the overall interaction energy at distances greater than a few  $\kappa^{-1}$  (Figure 3.4a), where  $\kappa^{-1}$  is the Debye screening length (see later). On the other hand, the frequency-dependent component ( $A_{v>0}$ ) is unaffected by electrostatic screening because the ions in the electrolyte solution are so large that they do not have time to move in response to the rapidly fluctuating dipoles (Israelachvili, 1992). Consequently, the van der Waals interaction may decrease by as much as 42% in oil-in-water emulsions at high ionic strength solutions because the zero-frequency component is completely screened. Equations for calculating the influence of electrostatic screening on van der Waals interactions have been developed (Israelachvili, 1992). To a first approximation, the influence of electrostatic screening on the zero-frequency contribution to the van der Waals interaction can be accounted for by replacing  $A_{v=0}$  with  $A_{v=0} \times e^{-2\kappa h}$  in the above equations (Israelachvili, 1992).

**3.3.3.2.2 Retardation.** The strength of the van der Waals interaction between emulsion droplets is reduced because of a phenomenon known as *retardation* (Israelachvili, 1992). The origin of retardation is the finite time taken for an electromagnetic field to travel from one droplet to another and back (Manhanty and Ninham, 1976). The frequency-dependent contribution to the van der Waals interaction ( $w_{v>0}$ ) is the result of a transient dipole in one droplet inducing a dipole in another droplet, which then interacts with the first dipole (Section 2.3.3). The strength of the resulting attractive force is reduced if the time taken for the electromagnetic field to travel between the droplets is comparable to the lifetime of a transient dipole, because then the orientation of the first dipole will have changed by the time the field from the second dipole arrives back (Israelachvili, 1992). This effect becomes appreciable at dipole separations greater than a few nanometers, and results in a decrease in the frequency-dependent ( $A_{v>0}$ ) contribution to the Hamaker function with droplet separation. The zero-frequency contribution ( $A_{v=0}$ ) is unaffected by retardation because it is electrostatic in origin (Manhanty and Ninham, 1976). Consequently, the contribution of the  $A_{v>0}$  term becomes increasingly small as the separation between the droplets increases, which leads to a decrease in the overall interaction potential

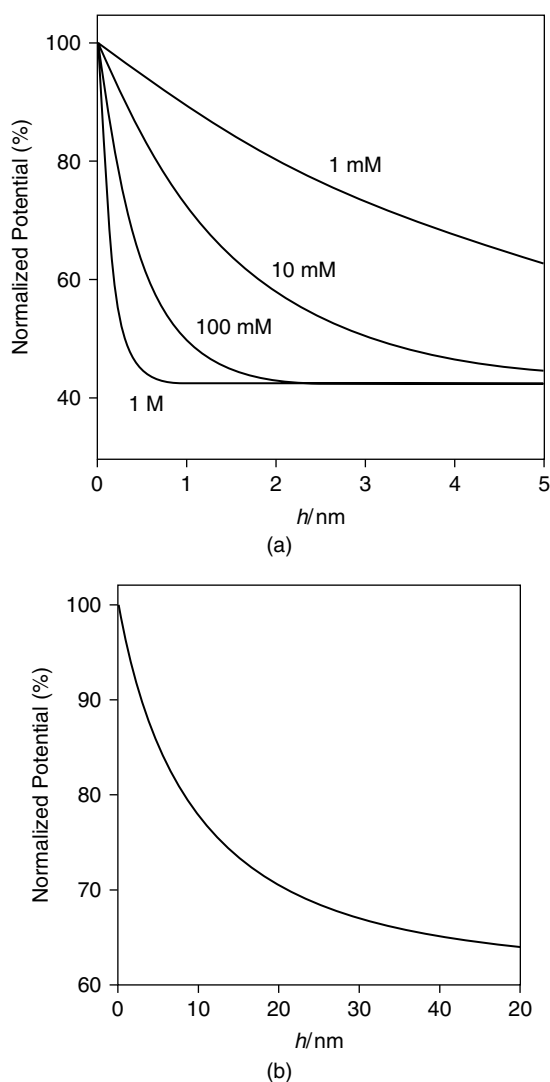


**Figure 3.4** Influence of (a) electrostatic screening and (b) retardation on the normalized van der Waals attraction between two oil droplets suspended in water. The normalized interaction potentials are reported as  $w(h)$  in the presence of the stipulated effect relative to  $w(h)$  in the absence of the effect expressed as a percentage. See Table 3.1 for the physicochemical properties of the phases used in the calculations.

(Figure 3.4b). Any accurate prediction of the van der Waals interaction between droplets should therefore include retardation effects. A number of authors have developed relatively simple correction functions that can be used to account for retardation effects (Schenkel and Kitchner, 1960; Gregory, 1969, 1981; Anandarajah and Chen, 1995; Chen and Anandarajah, 1996), although the most accurate method is to solve the full theory numerically (Mahanty and Ninham, 1976; Pailthorpe and Russel, 1982). To a first approximation, the influence of retardation on the frequency-dependent contribution to the van der Waals interaction can be accounted for by replacing  $A_{v>0}$  with  $A_{v>0} \times (1 + 0.11h)^{-1}$  in

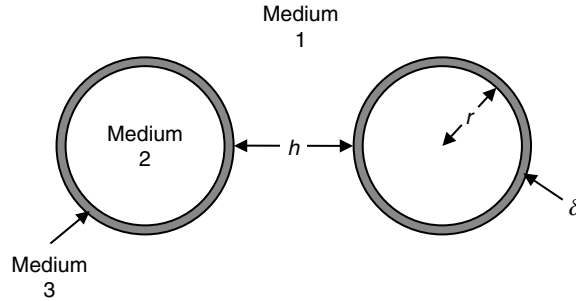


**Figure 3.5** The droplets in food emulsions are normally surrounded by an adsorbed emulsifier layer, which modifies their van der Waals interactions.

the above equations (Gregory, 1969). Thus, the retarded value of  $w_{v>0}(h)$  between two emulsion droplets at a separation of 20 nm is only about 30% of the nonretarded value.

**3.3.3.2.3 Influence of interfacial membranes.** So far we have assumed that the van der Waals interaction occurs between two homogeneous spheres separated by an intervening medium (Figure 3.1). In reality, emulsion droplets are normally surrounded by a thin layer of emulsifier molecules, and this interfacial layer has different physicochemical properties ( $\epsilon_r$ ,  $n$ , and  $v_e$ ) than either the oil or water phases (Figure 3.5). The molecules nearest the surface of a particle make the greatest contribution to the overall van der Waals interaction, and so the presence of an interfacial layer can have a large effect on the interactions between emulsion droplets, especially at close separations (Vold, 1961; Israelachvili, 1992; Parsegian, 1993).

The influence of an adsorbed layer on the van der Waals interactions between emulsion droplets has been considered by Vold (1961):

$$w_{\text{VDW}}(h) = -\frac{1}{12} \left[ A_{131} H\left(\frac{h}{2(r+\delta)}, 1\right) + A_{232} H\left(\frac{h+2\delta}{2r}, 1\right) + 2A_{132} H\left(\frac{h+\delta}{2r}, \frac{r+\delta}{r}\right) \right] \quad (3.6)$$

where the subscripts 1, 2, and 3 refer to the continuous phase, droplet, and emulsifier layer, respectively,  $h$  is the surface-to-surface separation between the *outer* regions of the adsorbed layers,  $\delta$  is the thickness of the adsorbed layer, and  $H(x, y)$  is a function given by

$$H(x, y) = \frac{y}{x^2 + xy + x} + \frac{y}{x^2 + xy + x + y} + 2 \ln \left( \frac{x^2 + xy + x}{x^2 + xy + x + y} \right)$$

The dependence of the (nonretarded and nonscreened) van der Waals interaction between two emulsion droplets on the thickness and composition of an interfacial layer consisting of a mixture of protein and water was calculated using Equation 3.6 and the physical properties listed in Table 3.1 (Figure 3.6). In the absence of the interfacial layer the attraction between the droplets was about  $-110kT$  at a separation of 1 nm. Figure 3.6 clearly indicates that the interfacial layer causes a significant alteration in the strength of the interactions between the droplets, leading to either an increase or decrease in the strength of the attraction depending on the concentration of protein in the interfacial membranes. At high protein concentrations (>60%) the attraction is greater than that between two bare emulsion droplets, whereas at low protein concentrations (<60%) it is smaller.

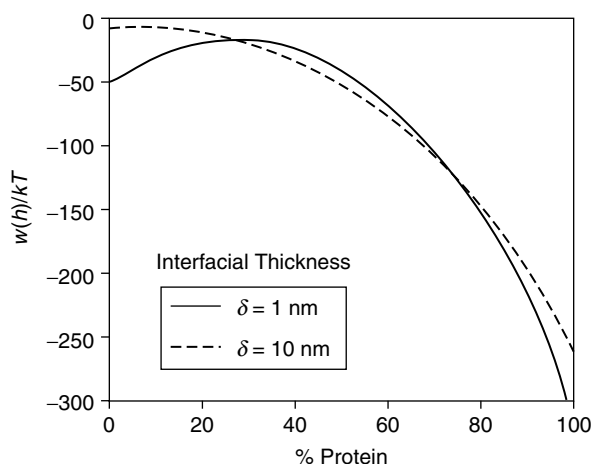


**Figure 3.6** Influence of the composition of an interfacial layer, consisting of water and protein, on the van der Waals interactions between emulsion droplets. The interdroplet pair potential is reported at an outer surface-to-surface separation of 1 nm for 1  $\mu$ m droplets. The physical properties of the oil, water, and interfacial layer used in the calculations are reported in Table 3.1.

### 3.3.3 General features of van der Waals interactions

1. The interaction between two oil droplets (or between two water droplets) is always attractive.
2. The strength of the interaction decreases with droplet separation, and the interaction is fairly long range ( $w \propto 1/h$ ).
3. The interaction becomes stronger as the droplet size increases.
4. The strength of the interaction depends on the physical properties of the droplets and the surrounding liquid (through the Hamaker function).
5. The strength of the interaction depends on the thickness and composition of the adsorbed emulsifier layer.
6. The strength of the interaction decreases as the concentration of electrolyte in an oil-in-water emulsion increases because of electrostatic screening.

van der Waals interactions act between all types of colloidal particles, and therefore they must always be considered when calculating the overall interaction potential between emulsion droplets (Israelachvili, 1992; Hiemenz and Rajagopalan, 1997). Nevertheless, it must be stressed that an accurate calculation of their magnitude and range is extremely difficult, because of the lack of physicochemical data required to perform the calculations, and because of the need to simultaneously account for the effects of screening, retardation, and interfacial layers (Hunter, 1986). The fact that van der Waals interactions are relatively strong and long range, and that they are always attractive, suggests that emulsion droplets would tend to associate with each other in the absence of any other interactions. In practice, many food emulsions are stable to droplet aggregation, which indicates the existence of repulsive interactions that are strong enough to overcome the van der Waals attraction. In the following sections, we discuss some of the most important types of these repulsive interactions, including electrostatic, steric, hydration, and thermal fluctuation interactions.

## 3.4 Electrostatic interactions

### 3.4.1 Origins of electrostatic interactions

The droplets in most food emulsions have an appreciable electrical charge (Section 5.4), and therefore electrostatic interactions may play an important role in determining their overall stability and physicochemical properties. The magnitude and sign of this charge depend on the type of emulsifier used to stabilize the emulsion, the concentration of the emulsifier at the interface, and the prevailing environmental conditions (e.g., pH, temperature, and ionic strength). All the droplets in an emulsion are usually stabilized by the same type of emulsifier and therefore have the same electrical charge. The electrostatic interaction between similarly charged droplets is repulsive, and so electrostatic interactions play a major role in preventing droplets from coming close enough together to aggregate.

The electrostatic interactions between emulsion droplets depend on the electrical characteristics of the droplet surfaces and the ionic composition of the surrounding aqueous phase (Hunter, 1986; Israelachvili, 1992; Hiemenz and Rajagopalan, 1997). The electrical properties of a surface are usually characterized by the surface charge density ( $\sigma$ ) and the electrical surface potential ( $\psi_0$ ). The surface charge density is the amount of electrical charge per unit surface area, whereas the surface potential is the free energy required to increase the surface charge density from zero to  $\sigma$  (Chapter 5). These values depend on the type and concentration of emulsifier present at a surface, as well as the nature of the electrolyte solution, for example, pH, ionic strength, and temperature. The important characteristics of the solution surrounding the droplets are the dielectric constant, concentration, and valency of the ions it contains (Evans and Wennerstrom, 1994).

### 3.4.2 Modeling electrostatic interactions

#### 3.4.2.1 Interdroplet pair potential

In food emulsions, we are usually interested in the strength of the electrostatic interactions between oil droplets dispersed in an aqueous continuous phase (Dickinson and Stainsby, 1982; Dickinson, 1992; Friberg, 1997; Claesson et al., 2004). An isolated charged droplet is surrounded by a cloud of counterions (Figure 3.7). When two similarly charged droplets approach each other their counterion clouds overlap and this gives rise to a repulsive interaction (Evans and Wennerstrom, 1994). The range of the electrostatic interaction is

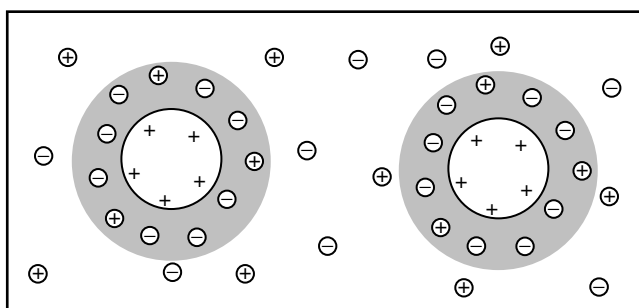


**Figure 3.7** Emulsion droplets can be considered to be surrounded by clouds of counterions, whose thickness is determined by the distance that has to be moved into the electrolyte solution before the charge of the counterions completely neutralizes the charge on the droplet surface. The thickness of this layer is therefore related to the Debye screening length.

primarily determined by the Debye screening length ( $\kappa^{-1}$ ), which is a measure of how far the electrical properties of the interface are sensed by counterions in the surrounding solution (Section 5.4):

$$\kappa^{-1} = \sqrt{\frac{\epsilon_0 \epsilon_R kT}{e^2 \sum n_{0i} z_i^2}} \quad (3.7)$$

where  $n_{0i}$  is the concentration of ionic species of type  $i$  in the bulk electrolyte solution (in molecules per cubic meter),  $z_i$  is their valancy,  $e$  is the elementary charge ( $1.602 \times 10^{-19}$  C),  $\epsilon_0$  is the dielectric constant of a vacuum, and  $\epsilon_R$  is the relative dielectric constant of the solution. For aqueous solutions at room temperatures,  $\kappa^{-1} \approx 0.304/\sqrt{I}$  nm, where  $I$  is the ionic strength expressed in moles per liter (Israelachvili, 1992).

The electrostatic repulsion between two similarly charged droplets can be divided into two contributions: (i) an *enthalpic* contribution associated with the change in the strength of the attractive and repulsive electrostatic interactions between the various charged species involved and (ii) an *entropic* contribution associated with the confinement of the counterions between the droplets to a smaller volume. The entropic contribution is strongly repulsive, whereas the enthalpic contribution is weakly attractive, and therefore the overall interaction is repulsive (Evans and Wennerstrom, 1994).

Mathematical models have been developed to relate the electrostatic interdroplet pair potential to the physical characteristics of the emulsion droplets and the intervening electrolyte solution (Hunter, 1986; Carnie et al., 1994; Okshima, 1994; Hiemenz and Rajagopalan, 1997). Analytical equations based on these models can be derived by making some simplifying assumptions (Sader et al., 1995). For example, if it is assumed that there is a relatively low surface potential ( $\psi_\delta < 25$  mV), and that the Debye screening length and surface-to-surface separation are much less than the droplet size (i.e.,  $\kappa^{-1} < r/10$  and  $h < r/10$ ), then fairly simple expressions for the electrostatic interdroplet pair potential between two similar droplets can be derived (Hunter, 1986). The equation that is applicable for a particular system depends on whether the interface can be treated as having constant potential or constant charge density when the droplets approach each other (see Section 3.4.2.2).

At constant surface potential:

$$w_{\text{electrostatic}}^w(h) = 2\pi\epsilon_0\epsilon_R r \psi_\delta^2 \ln(1 + \exp(-\kappa h)) \quad (3.8)$$

At constant surface charge:

$$w_{\text{electrostatic}}^\sigma(h) = -2\pi\epsilon_0\epsilon_R r \psi_\delta^2 \ln(1 - \exp(-\kappa h)) \quad (3.9)$$

The smallest droplets in most food emulsions are about 0.1  $\mu\text{m}$  in radius, which means that these equations are likely to be applicable at droplet separations less than about 10 nm, and at electrolyte concentrations greater than about 1 mM. Whether the electrostatic interaction between two droplets takes place under conditions of constant surface potential or constant surface charge depends on the ability of the surface groups to regulate their charge (Israelachvili, 1992; Reiner and Radke, 1993).

### 3.4.2.2 Factors influencing electrical characteristics of surfaces

**3.4.2.2.1 Charge regulation.** As two similarly charged emulsion droplets move closer together the interaction between them becomes increasingly repulsive (Figure 3.8). Certain systems are capable of reducing the magnitude of this increase by undergoing

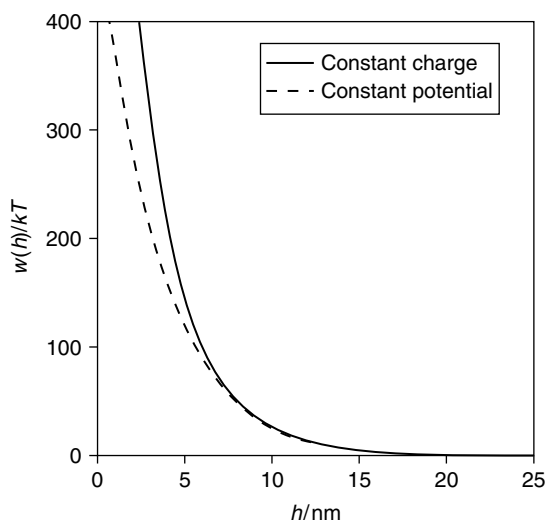


**Figure 3.8** Comparison of electrostatic interaction between a pair of emulsion droplets under conditions of constant surface charge and constant surface potential.

some form of reorganization of the molecular species present, which is referred to as *charge regulation* (Wei et al., 1993). For example, the surface charge may be regulated by adsorption–desorption of ionic emulsifiers (Yaminsky et al., 1996a,b) or by association–dissociation of charged groups (Hunter, 1986, 1989). Depending on the physical characteristics of a system, it is possible to discern three different situations that may occur when two droplets approach each other (Reiner and Radke, 1993):

1. *Constant surface charge.* As the droplets move closer together the number of charges per unit surface area remains constant, that is, no adsorption–desorption or association–dissociation of ions occurs. In this case, the electrostatic repulsion between the surfaces is at the maximum possible value because the surfaces are fully charged.
2. *Constant surface potential.* As the droplets move closer together the number of charges per unit surface area decreases so as to keep the surface potential constant, for example, by an adsorption–desorption or association–dissociation mechanism. In this case, the electrostatic repulsion between the surfaces is at the minimum possible value because the surface charge density is reduced as the droplets move closer together.
3. *Intermediate situation.* In reality, the electrostatic repulsion usually falls somewhere between the two extremes mentioned above because of charge regulation. The number of charges per unit surface area depends on the characteristics of the adsorption–desorption or association–dissociation mechanisms, for example, the surface activity of an ionic emulsifier or the pK value of an ionizable surface group. These processes take a finite time to occur, and therefore the surface charge density may also depend on the speed at which the droplets come together (Israelachvili, 1992; Israelachvili and Berman, 1995).

The variation of the interdroplet pair potential with separation is shown for two similarly charged droplets in Figure 3.8. There is a strong repulsive interaction between the droplets at close separations which decreases as the droplets move further apart. This repulsive



interaction is often sufficiently strong and long range to prevent droplets from aggregating. At relatively large droplet separations, Equations 3.8 and 3.9 give approximately the same predictions for the electrostatic interaction, but at closer separations the assumption of constant surface charge predicts a significantly higher repulsion than the assumption of constant surface potential (Figure 3.8). In practice, the interdroplet pair potential always lies somewhere between these two extremes and depends on the precise nature of the system.

**3.4.2.2.2 Ion binding.** The surface charge density of emulsion droplets is often influenced by adsorption of ionic substances present in the continuous or dispersed phases to the droplet surfaces, for example, ionic surfactants (e.g., phospholipids, fatty acids, or small molecule surfactants), multivalent mineral ions (e.g.,  $\text{Ca}^{2+}$ ,  $\text{Cu}^{2+}$ ,  $\text{Fe}^{3+}$ ), and charged biopolymers (e.g., proteins or polysaccharides). The primary driving force for the adsorption of these surface-active ions to charged surfaces is usually either hydrophobic or electrostatic attraction depending on ion type. The contribution of adsorbed ions to surface charge is governed mainly by the type and concentration of surface-active ions present in the system, and their relative affinities for the droplet surface. Depending on the nature of the ionic substances involved, ion adsorption can either decrease or increase the magnitude of the electrical charge, and under some circumstances it may even lead to charge reversal (Section 5.4).

**3.4.2.2.3 Ionic strength.** When the electrostatic interaction between a charged surface and the counterions is relatively weak, the surface charge density is simply related to the surface potential:  $\sigma = \epsilon_R \epsilon_0 \kappa \psi_\delta$  (Evans and Wennerstrom, 1994). This equation indicates that the electrical properties of a surface are altered by the presence of electrolyte in the aqueous phase, and has important consequences for the calculation of the electrostatic interdroplet pair potential. If the surface charge density remains constant when salt is added to the aqueous phase, then the surface potential decreases (because less energy is needed to bring a charge from infinity to the droplet surface through an electrolyte solution). Conversely, if the electrical potential remains constant as the salt concentration is increased, this means that the surface charge density must increase. In general, both  $\sigma$  and  $\psi_\delta$  tend to change simultaneously. In food emulsions, one can usually assume that the surface charge density is independent of ionic strength at low to moderate electrolyte concentrations for monovalent counterions and so one must take into account the variation of  $\psi_\delta$  with ionic strength when calculating the electrostatic repulsion between emulsion droplets (Kulmyrzaev et al., 2000a,b). For multivalent counterions, on binding usually occurs even at low ionic strength, thus altering  $\sigma$ .

**3.4.2.2.4 Heterogeneous charge distribution.** So far it has been assumed that the charge on the droplets is evenly spread out over the whole of the surface. In practice, droplets may have surfaces that have some regions that are negatively charged, some regions that are positively charged, and some regions that are neutral. The heterogeneous distribution of the charges on a droplet may influence their electrostatic interactions (Holt and Chan, 1997). Thus, two droplets (or molecules) that have no net charge may still be electrostatically attracted to each other if they have patches of positive and negative charge. Similarly, an electrically charged polymer may adsorb onto a droplet surface with the same net charge if the droplet surface has a heterogeneous distribution of positive and negative charges (Dickinson, 2003).

**3.4.2.3 Influence of ionic strength on magnitude and range of interactions.** The magnitude and range of the electrostatic repulsion between two droplets decreases as the ionic strength of the solution separating them increases because of electrostatic screening, that is, the accumulation of counterions around the surfaces (Figure 3.9). Electrostatic screening effects become more pronounced as the concentration and valency

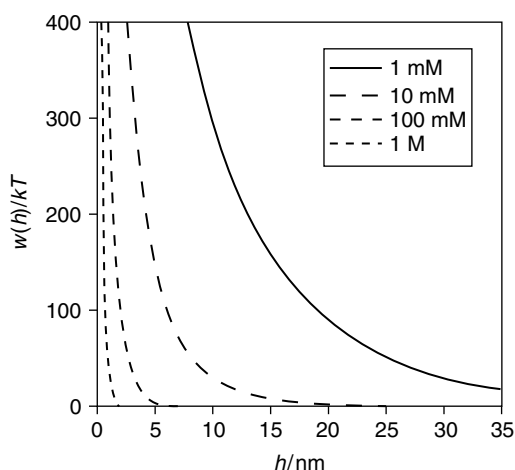


**Figure 3.9** Electrolyte reduces the magnitude and range of the electrostatic repulsion between emulsion droplets due to electrostatic screening.

of the counterions in the solution surrounding the emulsion droplets increases. The Debye screening length ( $\kappa^{-1}$ ) provides a good estimate of the influence of electrostatic screening effects on the range of electrostatic interactions, since it corresponds to the distance where the electrical potential falls to  $1/e$  of its value at droplet contact ( $h = 0$ ). Multivalent ions are much more effective at screening electrostatic interactions than monovalent ions (Equation 3.7). Consequently, much smaller concentrations of multivalent ions are required to promote emulsion instability (Hunter, 1986). This has important consequences for the texture and stability of many food emulsions, and explains the susceptibility of electrostatically stabilized emulsions to flocculation when the electrolyte concentration is increased above a critical level (Section 7.5).

#### 3.4.2.4 Influence of ion bridging on electrostatic interactions

Ion bridging is another type of colloidal interaction that involves electrostatic interactions (Ducker and Pashley, 1992; Dickinson, 2003). It occurs when a polyvalent ion simultaneously binds to the surface of two emulsion droplets that have an opposite charge to the ion (Figure 3.10). These polyvalent ions may be low molecular weight species, such as  $\text{Ca}^{2+}$ ,  $\text{Mg}^{2+}$ , or  $\text{Al}^{3+}$  (Dickinson et al., 1992; Agboola and Dalgleish, 1995, 1996a) or high molecular weight biopolymers, such as polysaccharides or proteins (Schmitt et al., 1998; Benichou et al., 2002; Dickinson, 2003). The tendency for ion bridging to occur depends on the strength of the electrostatic interaction linking the polyvalent ion to the droplets

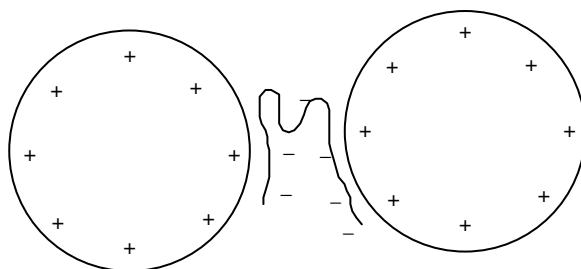


**Figure 3.10** Polyvalent ions are capable of forming ion bridges between emulsion droplets.

compared to the strength of the electrostatic repulsion between the similarly charged droplets. For this reason, large polyvalent species, such as ionic polysaccharides, are often particularly effective at forming ion bridges because they are able to act as a bridge between the droplets without allowing them to get too close together. The ability of polyvalent ions to form ion bridges is superimposed on their ability to modulate the electrostatic repulsion between droplets through ion binding and charge screening effects mentioned above.

### 3.4.3 *General characteristics of electrostatic interactions*

1. Electrostatic interactions may be either attractive or repulsive depending on the sign of the charges on the droplets. The interaction is repulsive when droplets have similar charges (which is usually the case), but is attractive when they have opposite charges.
2. The strength of the interaction decreases with droplet separation, and may be either long or short range depending on the ionic strength and dielectric constant of the electrolyte solution surrounding the droplets. The interaction becomes increasingly short range as the ionic strength increases because of electrostatic screening.
3. The strength of the interaction is proportional to the size of the emulsion droplets.
4. The strength of the interaction depends on the electrical characteristics of the droplet surfaces, that is, the number of emulsifier molecules adsorbed per unit surface area and the number of ionized groups per emulsifier molecule (which depends on the concentration of any potential determining ions in the aqueous phase, e.g.,  $H^+$  or  $OH^-$ ).
5. The interaction becomes more difficult to predict when charge regulation occurs (e.g., due to association–dissociation of ionizable groups or adsorption–desorption of ionic emulsifiers), especially at close droplet separations.
6. Ion binding and bridging effects have to be taken into account when polyvalent ions are involved. Ion binding may alter the surface charge density and surface potential of a droplet, whereas ion bridging may cause droplets to be linked together.

In this section, we have seen that under certain conditions repulsive electrostatic interactions may be relatively strong and long range compared to attractive van der Waals interactions (compare Figures 3.3 and 3.8). This suggests that they may be strong enough to prevent droplets from aggregating in certain systems. Indeed, it is widely recognized that electrostatic stabilization plays an important role in determining the aggregation of droplets in many food emulsions, and particularly those stabilized by proteins (Friberg, 1997; Dickinson and Stainsby, 1982; Dickinson, 1992; Demetriades and McClements, 1997a). It should also be recognized that electrostatic interactions influence various other properties of food emulsions, such as the partitioning of ingredients and the rates of chemical reactions (Chapters 7 and 9). The partitioning of ionized volatile flavor compounds between the headspace and bulk of emulsions is influenced by electrostatic interactions between flavor molecules and electrically charged interfaces (Guyot et al., 1996). The oxidation of lipids in food emulsions is often catalyzed by polyvalent ions, such as  $Fe^{3+}$ , that are normally present in the aqueous phase. The rate of iron-catalyzed lipid oxidation in oil-in-water emulsions has been shown to increase when the droplets have a negative charge because the  $Fe^{3+}$  catalyst and oil molecules are brought into close contact (Coupland and McClements, 1996; Mei et al., 1997; McClements and Decker, 2000). Knowledge of the factors that determine the magnitude and range of electrostatic interactions is therefore extremely important to food scientists for a variety of different reasons.

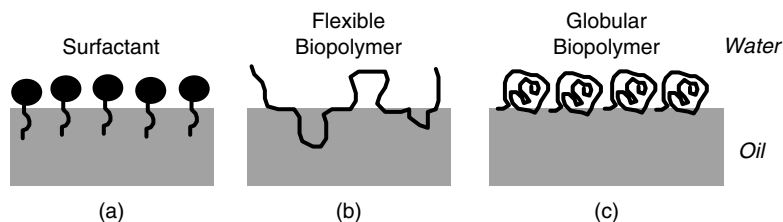


**Figure 3.11** Orientation of some emulsifiers at an oil–water interface: (a) small molecule surfactants, (b) flexible biopolymers, and (c) globular biopolymers.

## 3.5 Steric interactions

### 3.5.1 Origin of steric interactions

The droplets in most food emulsions are coated by a thin layer of emulsifier molecules, such as surfactants, phospholipids, proteins, or polysaccharides (Section 4.4). When two droplets approach each other sufficiently closely, then their emulsifier layers start to overlap and interact with each other. Steric interactions are a result of the intermingling and/or compression of the interfacial layers. At close droplet separations steric interactions are strongly repulsive and may therefore prevent emulsion droplets from aggregating. Nevertheless, the overall magnitude, sign, and range of steric interactions is strongly dependent on the characteristics of the interfacial layers (e.g., thickness, packing, rheology, and molecular interactions), and therefore depends on emulsifier type (Figure 3.11). An improved understanding of the relationship between the properties of the interfacial membranes formed by emulsifiers and the ability of emulsifiers to stabilize emulsion droplets against aggregation is particularly important for food scientists, since it would enable them to rationally select emulsifiers with optimum performance for each specific application.

### 3.5.2 Modeling steric interactions

#### 3.5.2.1 Interdroplet pair potential

As mentioned earlier, steric interactions arise when emulsion droplets get so close together that the interfacial layers overlap (Figure 3.12). This type of interaction can be conveniently divided into two contributions (Hunter, 1986; Hiemenz and Rajagopalan, 1997):

$$w_{\text{steric}}(h) = w_{\text{elastic}}(h) + w_{\text{mix}}(h) \quad (3.10)$$

The *elastic* contribution is due to the compression of the interfacial layers, whereas the *mixing* contribution is due to the intermingling of the emulsifier molecules within the interfacial layers (Figure 3.12).

#### 3.5.2.2 Mixing contribution

If it is assumed that the emulsifier molecules within the interfacial layers interpenetrate without the layers being compressed (Figure 3.12a), then the interaction is entirely due to mixing of the emulsifier molecules. The theories describing steric interactions are much less well developed than those describing electrostatic or van der Waals interactions, primarily because they are particularly sensitive to the precise structure, orientation, packing, and interactions of the emulsifier molecules within the interfacial membrane

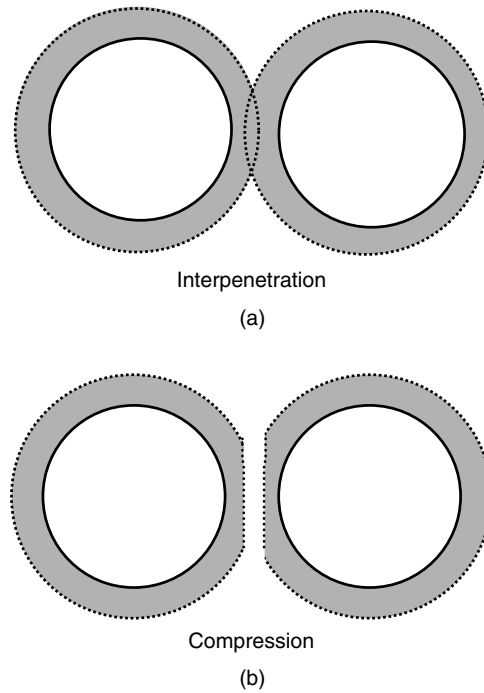


**Figure 3.12** Steric interactions between emulsion droplets can be divided into an *elastic* contribution which involves compression of the polymer layers and a *mixing* contribution which involves interpenetration of the polymer chains.

(Hunter, 1986; Claesson et al., 1995, 2004). These parameters vary from system to system and are difficult to account for theoretically or to measure experimentally. Mathematical theories have been developed for a number of simple well-defined systems, and it is informative to examine these because they provide some useful insights into more complex systems (Hunter, 1986). Consider a system that consists of polymeric emulsifier molecules that are permanently attached to the droplet surfaces, with a constant number of polymer chains per unit surface area. A mathematical analysis of the interactions that occur between the polymer chains when the interfacial layers approach each other leads to the following equation for the mixing contribution (Hunter, 1986):

$$w_{\text{mix}}(h) = 4\pi r k T m^2 N_A \frac{\bar{v}_p^2}{\bar{V}_s} \left( \frac{1}{2} - \chi \right) \left( 1 - \frac{1}{2} \frac{h}{\delta} \right)^2 \quad (3.11)$$

where  $m$  is the mass of polymer chains per unit area,  $\delta$  is the thickness of the adsorbed layer,  $N_A$  is Avogadro's number,  $\chi$  is the Flory–Huggins parameter,  $\bar{v}_p$  is the partial specific volume of the polymer chains, and  $\bar{V}_s$  is the molar volume of the solvent. The Flory–Huggins parameter depends on the relative magnitude of the solvent–solvent, solvent–segment, and segment–segment interactions, and is a measure of the *quality* of a solvent. It is related to the effective interaction parameter ( $w$ ) which was introduced in Chapter 2 to characterize the compatibility of molecules in mixtures:  $\chi = w/RT$ . In a good solvent ( $\chi < 1/2$ ), the polymer molecules prefer to be surrounded by solvent molecules. In a poor solvent ( $\chi > 1/2$ ), the polymer molecules prefer to be surrounded by each other. In an indifferent (theta) solvent ( $\chi = 1/2$ ), the polymer molecules have

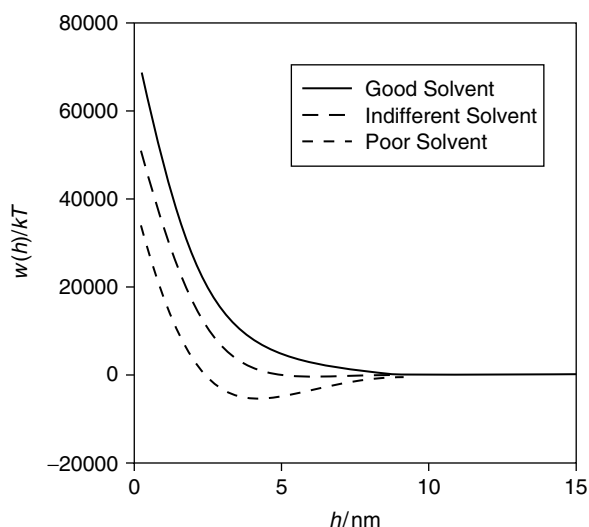


**Figure 3.13** Interdroplet pair potential due to steric polymeric interactions. At intermediate separations the steric polymeric interaction can be either attractive or repulsive depending on the quality of the solvent because of the mixing contribution, but at short separations it is strongly repulsive because of the elastic contribution.

no preference for either solvent or polymer molecules. In the original Flory–Huggins theory, it was assumed that  $\chi$  was entirely due to enthalpic contributions associated with the molecular interactions. In practice, it is more convenient to assume that  $\chi$  also contains entropic contributions since then interactions involving changes in the structural organization of the solvent can be accounted for, for example, hydrophobic interactions (Evans and Wennerstrom, 1994; Norde, 2003). Whether the mixing contribution is attractive or repulsive depends on the quality of the solvent (Figure 3.13). In a good solvent, the increase in concentration of polymer molecules in the interpenetration zone is thermodynamically unfavorable ( $w_{\text{mix}}$  positive), because it reduces the number of polymer–solvent contacts and therefore leads to a repulsive interaction between the droplets. Conversely, in a poor solvent it is thermodynamically favorable ( $w_{\text{mix}}$  negative), because it increases the number of polymer–polymer contacts and therefore leads to an attractive interaction between the droplets. In an indifferent solvent, the polymer molecules have no preference as to whether they are surrounded by solvent or by other polymer molecules and therefore the mixing contribution is zero. Thus, by altering solvent quality it is possible to change the mixing contribution from attractive to repulsive or vice versa. In food emulsions, this could be done by changing the solvent quality for the polymer chains, for example, by altering the temperature or adding alcohol to the aqueous phase.

### 3.5.2.3 Elastic contribution

If it is assumed that the interfacial layers surrounding the emulsion droplets are compressed without any interpenetration of the emulsifier molecules (Figure 3.12b), then the interaction is entirely elastic. When the interfacial layers are compressed a smaller volume is available to the emulsifier molecules and therefore their configurational entropy is reduced, which is thermodynamically unfavorable, and so this type of interaction is always repulsive ( $w_{\text{elastic}}$  positive).

For certain simple systems, the magnitude of the elastic contribution can be calculated from a statistical analysis of the number of configurations that the emulsifier molecules can adopt before and after the layers are compressed (Dickinson, 1992; Hiemenz and Rajagopalan, 1997; Quemada and Berli, 2002). Nevertheless, it is usually not possible to carry out such an analysis for most real systems because of the structural complexity of the interfacial layers. For these systems, it is often better to use semiempirical models to account for the elastic interaction. For example, a simple exponential model has recently been proposed to describe the steric repulsion between emulsion droplets stabilized by polymeric emulsifiers:  $w_{\text{elastic}}(h)/kT = A_E \exp(-\pi h/L)$ , where  $L$  is the polymer chain length and  $A_E$  is a parameter that depends on polymer chain length, chain packing, and droplet size (Quemada and Berli, 2002). An alternative semiempirical expression was developed by considering the force required to compress interfacial layers with specified rheologic characteristics (Jackel, 1964):

$$w_{\text{elastic}}(h) = 0.77E \left( \frac{1}{2}\delta - \frac{1}{2}h \right)^{5/2} (r + \delta), \quad (h < \delta) \quad (3.12)$$

$$w_{\text{elastic}}(h) = 0, \quad (h \geq \delta)$$

where  $E$  is the elastic modulus of the interfacial layer. This equation indicates that there is a negligible interaction between the droplets when the separation is greater than the thickness of one emulsifier layer ( $\delta$ ), but that there is a steep increase in the interaction energy when the droplets approach closer than this distance (Figure 3.13). As a first approximation, it may be possible to use measurements of the elastic modulus of macroscopic solutions and gels formed using emulsifier concentrations similar to those found in the interfacial region in Equation 3.12. Alternatively, the elastic modulus of an interfacial layer could be measured directly using various types of surface force apparatus (Claesson et al., 1995, 2004).

#### 3.5.2.4 Distance dependence of steric interactions

Steric interactions between emulsion droplets can be conveniently divided into three regimes, according to the separation of the surface of the bare droplets  $h$  relative to the thickness of the interfacial layers  $\delta$ :

1. *Zero interaction regime* ( $h \geq 2\delta$ ). At sufficiently large droplet separations, the interfacial layers do not overlap with each other and the steric interaction between the droplets is zero.
2. *Interpenetration regime* ( $\delta \leq h < 2\delta$ ). When the droplets are sufficiently close together for their interfacial layers to overlap with each other, so that the emulsifier molecules on different droplets can intermingle, but the interfacial layers are not significantly compressed, then the major contribution to the steric interaction is the mixing contribution ( $w_{\text{mix}}$ ). This contribution may be either repulsive (positive) or attractive (negative) depending on the solvent quality.
3. *Interpenetration and compression regime* ( $h < \delta$ ). When the droplets get so close together that the emulsifier layers start to compress each other the overall steric interaction is a combination of elastic and mixing contributions, although the strongly repulsive elastic component usually dominates, and so the overall interaction is repulsive.

It should be stressed that the length of the interpenetration and elastic regions actually depends on the precise nature of the emulsifier molecules within the interfacial layers

(Claesson et al., 1995, 2004). Flexible biopolymer molecules will have relatively large interpenetration regions, whereas compact globular proteins will have relatively small ones. Consequently, the choice of  $\delta$  as the distance where the elastic contribution first contributes to the interaction is rather arbitrary, and different values will be more appropriate for some systems. As mentioned earlier, the only way these values can accurately be established for a particular system is by measuring the force between two emulsifier-coated surfaces as they are brought closer together (Israelachvili, 1992; Claesson et al., 1995, 1996, 2004).

### 3.5.2.5 Optimum characteristics of steric stabilizers

To be effective at providing steric stabilization, an emulsifier must have certain physico-chemical characteristics (Hunter, 1986; Dickinson, 1992; Claesson et al., 2004). First, it must have some segments that bind strongly to the droplet surfaces (to anchor the emulsifier molecules to the surface) and other segments that protrude a significant distance into the surrounding liquid (to prevent the droplets coming close together). This means that the emulsifier must be amphiphilic, having some hydrophobic segments that protrude into the oil phase, and some hydrophilic segments that protrude into the aqueous phase (Figure 3.11). The binding to the interface must be strong enough to prevent the emulsifier from desorbing from the droplet surface as the droplets approach one another. Theoretical calculations suggest that a good polymeric stabilizer should have 10–20% of the molecule that adsorbs to the droplet surfaces, and 80–90% of the molecule that protrudes into the continuous phase (Claesson et al., 2004). Second, the continuous phase surrounding the droplets must be a sufficiently good solvent for the segments of the emulsifier molecules that protrude into it, so that the mixing contribution to the overall interaction energy is repulsive ( $w_{\text{mix}}$  positive). Third, the steric repulsive interaction must act over a distance that is comparable to the range of the attractive van der Waals interactions. Thus, emulsifiers that form thick interfacial layers (such as modified starch or gum arabic) are much more effective at stabilizing emulsions against flocculation than emulsifiers that form thin layers (such as globular proteins at their isoelectric point\*). Finally, the surface must be covered by a sufficiently high concentration of emulsifier. If too little of a polymeric emulsifier is present, a single emulsifier molecule may adsorb onto the surface of more than one emulsion droplet forming a bridge that causes the droplets to flocculate. In addition, some of the nonpolar regions will be exposed to the aqueous phase which leads to a hydrophobic attraction between the droplets (see Section 3.7). Many emulsifiers are charged, and therefore they stabilize emulsion droplets against aggregation through a combination of electrostatic and steric repulsion (Claesson et al., 1995, 2004).

### 3.5.3 General characteristics of steric interactions

1. Steric interactions are always strongly repulsive at short separations ( $h < \delta$ ), but may be either attractive or repulsive at intermediate separations ( $\delta < h < 2\delta$ ) depending on the quality of the solvent (Figure 3.13).
2. The range of steric interactions increases with the thickness of the adsorbed layer.
3. The strength of steric interactions increases with droplet size.
4. The strength of steric interactions depends on the precise molecular characteristics of the interfacial layer, for example, packing, flexibility, rheology, molecular interactions. Consequently, it varies considerably from system to system and is difficult to predict from first principles.

\* Thick biopolymer layers may also help stabilize droplets against aggregation by reducing the magnitude of the attractive van der Waals interaction (Section 3.3.6).



**Table 3.2** Comparison of the Advantages and Disadvantages of Polymeric and Electrostatic Stabilization Mechanisms in Food Emulsions.

Polymeric Steric Stabilization	Electrostatic Stabilization
Insensitive to pH	pH dependent—aggregation tends to occur when emulsifier loses charge
Insensitive to electrolyte	Aggregation tends to occur at high electrolyte concentrations (>CFC)
Large amounts of emulsifier needed to cover droplet surface	Small amounts of emulsifier needed to cover droplet surface
Weak flocculation (easily reversible)	Strong flocculation (often irreversible)
Good freeze–thaw stability	Poor freeze–thaw stability

Source: Adapted from Hunter (1986).

Steric interactions are one of the most common and important stabilizing mechanisms in food emulsions. Unlike electrostatic interactions, they occur in almost every type of food emulsion because most droplets are stabilized by a layer of adsorbed emulsifier molecules. Some food emulsions are stabilized almost entirely by steric stabilization, whereas others are mainly stabilized by a combination of steric and electrostatic stabilization. Food scientists must often decide the most appropriate emulsifier for a particular application, and so it is useful to compare the differences between steric and electrostatic stabilization (Table 3.2). The principal difference is their sensitivity to pH and ionic strength (Hunter, 1986). The electrostatic repulsion between emulsion droplets is dramatically decreased when the electrical charge on the droplet surfaces is reduced (e.g., by altering the pH) or screened (e.g., by increasing the concentration of electrolyte in the aqueous phase). In contrast, steric repulsion is fairly insensitive to both electrolyte concentration and pH.\* Another major difference is the fact that the electrostatic repulsion is usually weaker than the van der Waals attraction at short distances, whereas the steric stabilization is stronger (Hunter, 1986). This means that emulsions stabilized entirely by electrostatic repulsion are prone to coalescence when the droplets approach sufficiently closely, whereas emulsions stabilized by steric interactions may flocculate, but they are unlikely to coalesce because of the extremely strong short-range repulsion.

From a practical stand-point, another important difference is the fact that considerably more emulsifier is usually required to provide steric stabilization (because a thick interfacial layer is required) than to provide electrostatic stabilization. Thus, >5% modified starch is required to stabilize a 20 wt% oil-in-water emulsion containing 1  $\mu\text{m}$  droplets, whereas <0.5% whey-protein is required to stabilize the same system (Demetriades et al., 1997c; Chanamai and McClements, 2002). The amount of emulsifier required to prepare an emulsion is often an important financial consideration when formulating a food product.

## 3.6 Depletion interactions

### 3.6.1 Origin of depletion interactions

Many food emulsions contain small colloidal particles that are dispersed in the continuous phase that surrounds the droplets (Figure 3.14). These colloidal particles may be surfactant micelles

\* It should be stressed that the polymeric steric interaction may be effected by pH and ionic strength if the polymer molecules are charged, because this will alter the thickness of the interfacial layer and the interaction of the polymer chains.

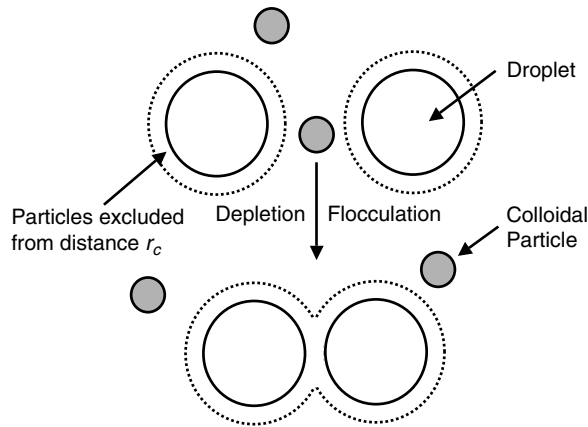


**Figure 3.14** An attractive depletion interaction arises between emulsion droplets when they are surrounded by small nonadsorbing colloidal particles.

formed when the free surfactant concentration exceeds some critical value (Bibette et al., 1990; Aronson, 1992; Bibette, 1991; McClements, 1994), individual polymer molecules (Sperry, 1982; Seebergh and Berg, 1994; Dickinson, 1994; Dickinson et al., 1995; Smith and Williams, 1995; Jenkins and Snowden, 1996) or aggregated polymers (Dickinson and Golding, 1997a,b). The presence of these colloidal particles causes an attractive interaction between the droplets that is often large enough to promote emulsion instability (McClements, 1994; Dickinson et al., 1996). The origin of this interaction is the exclusion of colloidal particles from a narrow region surrounding each droplet (Figure 3.14). This region extends a distance approximately equal to the radius of a colloidal particle away from the droplet surface. The concentration of colloidal particles in this *depletion zone* is effectively zero, while it is finite in the surrounding continuous phase. As a consequence, there is an osmotic potential difference that favors the movement of solvent molecules from the depletion zone into the bulk liquid, so as to dilute the colloidal particles and thus reduce the concentration gradient. The only way this process can be achieved is by two droplets aggregating and thereby reducing the volume of the depletion zone, which manifests itself as an attractive force between the droplets (Figure 3.14). Thus, there is an osmotic driving force that favors droplet aggregation, and which increases as the concentration of colloidal particles in the aqueous phase increases.

### 3.6.2 Modeling of depletion interactions

When the separation between two droplets is small compared to their size ( $h \ll r_d$ ), the interdroplet pair potential due to exclusion of the colloidal particles from the depletion zone is given by the following expression (Sperry, 1982):

$$w_{\text{depletion}}(h) = -\frac{2}{3}\pi r^3 P_{\text{OSM}} \left( 2 \left( 1 + \frac{r_c}{r} \right)^3 + \left( 1 + \frac{h}{2r} \right)^3 - 3 \left( 1 + \frac{r_c}{r} \right)^2 \left( 1 + \frac{h}{2r} \right) \right) \quad (3.13)$$

where  $P_{\text{OSM}}$  is the osmotic pressure arising from the exclusion of the colloidal particles,  $r$  is the radius of the emulsion droplets, and  $r_c$  is the radius of the colloidal particles. This equation is applicable for  $h < 2r_c$ , for higher droplet separations  $w_{\text{depletion}}(h) = 0$ . To a first

approximation, the osmotic pressure difference can be described by one of the following equivalent expressions (Hiemenz and Rajagopalan, 1997):

$$P_{\text{OSM}} = kTn_i(1 + 2n_i v) \quad (3.14a)$$

$$P_{\text{OSM}} = \frac{cRT}{M} \left( 1 + \frac{2N_A c v}{M} \right) \quad (3.14b)$$

$$P_{\text{OSM}} = \frac{cRT}{M} \left( 1 + \frac{2cR_v}{\rho_c} \right) \quad (3.14c)$$

where  $c$ ,  $M$ ,  $v$ ,  $n_i$ , and  $\rho_c$  are the concentration (in  $\text{kg m}^{-3}$ ), molecular weight (in  $\text{kg mol}^{-1}$ ), volume (in  $\text{m}^3$ ), number density (in  $\text{m}^{-3}$ ), and mass density (in  $\text{kg m}^{-3}$ ) of the colloidal particles, and  $N_A$  is Avogadro's number.\* The parameter,  $R_v$ , is called the *volume ratio* and is equal to the effective volume of a nonadsorbing colloidal particle divided by the actual volume of the constituent atoms added to the system (McClements, 2000). For compact spherical colloidal particles, such as solid spheres, surfactant micelles, or globular proteins,  $R_v \approx 1$ ; however, for asymmetrical solid particles or biopolymers that entrain large quantities of solvent as they rotate in solution,  $R_v \gg 1$  (Chapter 4). This phenomenon has important consequences for the ability of nonadsorbing colloidal particles to promote depletion flocculation in emulsions (see below).

The range of the depletion interactions is approximately equal to twice the radius of the nonadsorbed colloidal particles:  $2r_c$ . An estimate of the maximum strength of the attractive depletion interaction between two droplets can be obtained by calculating the interdroplet pair potential when the droplets are in contact (i.e.,  $h = 0$ ):

$$w_{\text{depletion}}(h = 0) = -2\pi r_c^2 P_{\text{OSM}} \left[ r + \frac{2}{3} r_c \right] \quad (3.15)$$

Theoretical predictions of the attractive depletion interactions between a pair of emulsion droplets are shown in Figure 3.15. The interaction potential is zero at droplet separations greater than the diameter ( $2r_c$ ) of the nonadsorbing colloidal particles and decreases to a finite negative value (given by Equation 3.15) when the droplets come into close contact. For nonadsorbing colloidal particles of constant molecular weight (or radius), the strength of the interaction increases with increasing particle concentration (Figure 3.15a). If it is assumed that an emulsion contains a constant mass concentration (wt%) of nonadsorbing colloidal particles that are compact spheres ( $R_v = 1$ ), then the range of the depletion attraction increases with increasing molecular weight of the particles, but the maximum strength of the interaction decreases with increasing  $M$  (Figure 3.15b). More complex behavior can be observed when the effective volume of the nonadsorbing colloidal particles is much greater than the actual volume of the added material (i.e.,  $R_v \gg 1$ ). For example, the attractive depletion interaction for an emulsion containing a constant mass concentration (wt%) of nonadsorbing colloidal particles that are assumed to be linear rigid rods is shown in Figure 3.15c. In this case, both the range and maximum strength of the depletion attraction increases with increasing molecular weight, since  $r_c \propto M$  and  $R_v \propto M^2$  (hence  $P_{\text{OSM}}$  can increase with increasing  $M$ , Equation 3.14c).

Depletion interactions rely on the colloidal particles not interacting strongly with the surface of the emulsion droplets. Otherwise, the bound particles would have to be displaced as the droplets moved closer together, which would require the input of energy and therefore be repulsive.

\* Equations 3.14a and 3.14b are applicable to non-adsorbing colloidal particles of any type. Equation 3.14c is most applicable for non-adsorbing polymers, where  $\rho_c$  is the mass density of the polymer backbone, rather than of the overall polymer and trapped liquid.

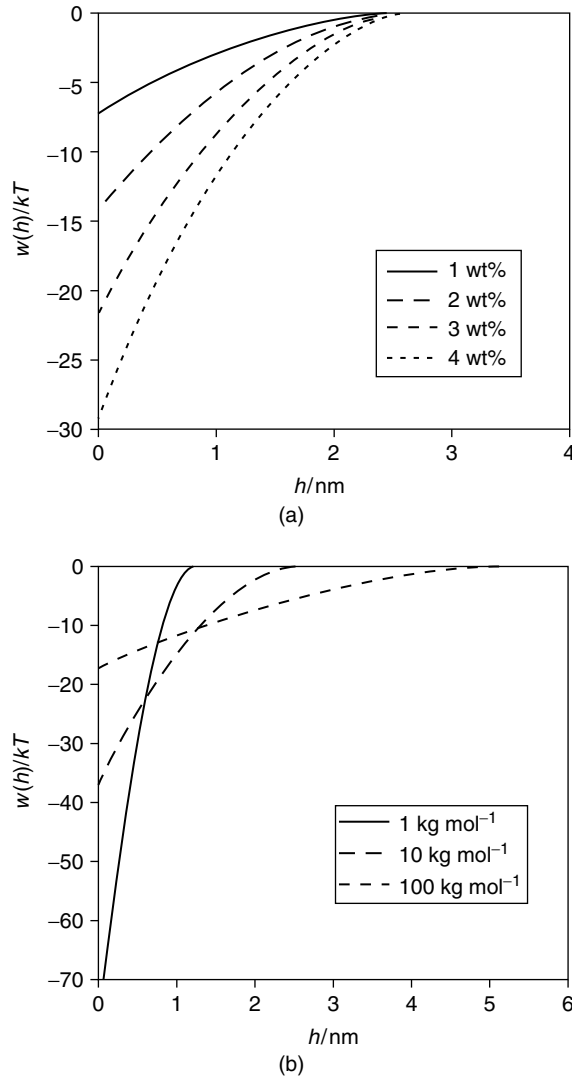


**Figure 3.15** (a) Influence of the concentration of the nonadsorbing colloidal particles (shown in wt% in the annotation box) on the attractive depletion interaction between emulsion droplets:  $r_d = 1\ \mu m$ ,  $r_c = 1.36\ nm$  ( $R_v = 1$ ). (b) Influence of the molecular weight of the nonadsorbing colloidal particles (shown in  $kg\ mol^{-1}$  in the annotation box) on the attractive depletion interaction between emulsion droplets:  $c = 5\ wt\%$ ,  $r_d = 1\ \mu m$ ,  $r_c = 0.63 - 2.9\ nm$ . It was assumed that the colloidal particles were dense spheres, so that  $r_c \propto M^{1/3}$  and  $R_v = 1$ . (c) Influence of the molecular weight of the nonadsorbing colloidal particles (shown in  $kg\ mol^{-1}$  in the annotation box) on the attractive depletion interaction between emulsion droplets:  $c = 5\ wt\%$ ,  $r_d = 1\ \mu m$ ,  $r_c = 2.8 - 14\ nm$  ( $R_v = 44 - 1,100$ ). It was assumed that the colloidal particles were linear rigid rods, so that  $r_c \propto M$  and  $R_v \propto M^2$ .

### 3.6.3 General characteristics of depletion interactions

1. The maximum strength of the depletion interaction increases as the size of the emulsion droplets increases.
2. The maximum strength of the depletion interaction increases as the concentration ( $n_i$  or  $c$ ) of nonadsorbing colloidal particles in the continuous phase increases (at constant  $M$  or  $r_c$ ).

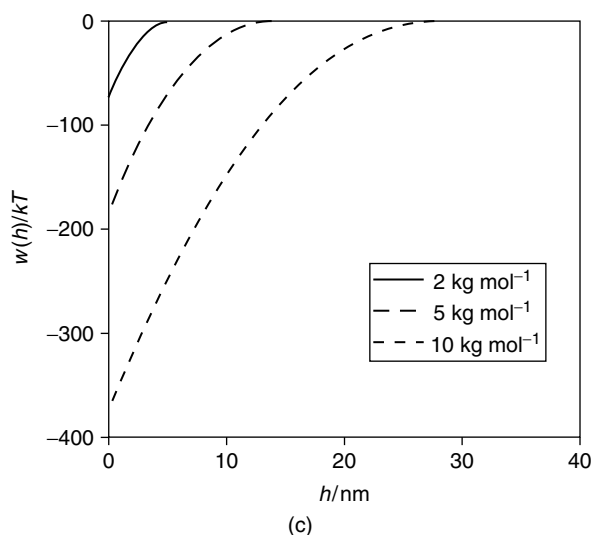


Figure 3.15 (Continued)

3. The maximum strength of the interaction may either decrease or increase with increasing molecular weight of the nonadsorbing colloidal particles at constant ( $n_i$  or  $c$ ) depending on their *volume ratio*,  $R_v$ .
4. The range of the depletion interaction ( $2r_c$ ) increases as the radius of the colloidal particles increases.

Equation 3.13 suggests that the strength of the depletion interaction is independent of pH and ionic strength. Nevertheless, these parameters may indirectly influence the depletion interaction by altering the effective size of the colloidal particles and the depletion zone. For example, changing the number of charges on a biopolymer molecule by altering the pH can either increase or decrease its effective size (Launay et al., 1986; Rha and Pradipasena, 1986). Increasing the number of similarly charged groups usually causes a biopolymer to become more extended because of electrostatic repulsion between the charged groups. On the other hand, decreasing the number of similarly charged groups or having a mixture of positively and negatively charged groups, usually causes a biopolymer to reduce its effective size. Altering the ionic strength of an aqueous solution also causes changes in the effective size of biopolymer molecules, for example, adding salt to a highly charged biopolymer molecule screens the electrostatic repulsion between charged groups and therefore causes a decrease in biopolymer size (Launay et al., 1986; Rha and Pradipasena, 1986). Thus, if the colloidal particles are ionic one would expect the strength of the depletion interaction to depend on pH and ionic strength, but if they are nonionic one would expect them to be fairly insensitive to these parameters (Demetriades and McClements, 1999). It should be noted that at high concentrations of free colloidal particles in the continuous phase one can actually have depletion stabilization (Hiemenz and Rajagopalan, 1997).

## 3.7 Hydrophobic interactions

### 3.7.1 Origin of hydrophobic interactions

Hydrophobic interactions are believed to play an important role in determining the stability and physicochemical properties of a number of food emulsions. For example, it has been proposed that this mechanism is responsible for promoting droplet flocculation

in heat-treated globular protein-stabilized emulsions (Monahan et al., 1996; Demetriades et al., 1997b; Kim et al., 2002a,b). Hydrophobic interactions are important when the surfaces of the droplets have some nonpolar character, either because they are not completely covered by emulsifier (e.g., during homogenization or at low emulsifier concentrations) or because the emulsifier has some hydrophobic regions exposed to the aqueous phase (e.g., denatured globular proteins).

There has been considerable debate about the physicochemical origin of the hydrophobic interactions that act between nonpolar surfaces separated by water (Attard, 2003). Experimental measurements of the forces between different kinds of hydrophobic surfaces have shown that the force–distance curves can be highly irreproducible and that they vary greatly from system to system (Christenson and Claesson, 2001). It appears that the various types of behavior observed in these experiments can be classified into two groups: (i) a long-range strong irreproducible attractive force; (ii) a short-range weaker reproducible attractive force (Christenson and Claesson, 2001; Attard, 2003). The long-range interaction has been attributed to the presence of “nanobubbles” that adhere to the nonpolar surfaces, whereas the short-range interaction has been attributed to a solvent structuring effect similar to the hydrophobic interaction for nonpolar molecules. The existence of stable nanobubbles on hydrophobic surfaces has been demonstrated by characteristic features of the measured force–distance curves and surface-imaging techniques (Attard, 2003). In the absence of nanobubbles only the short-range hydrophobic attraction is observed, but it should be noted that this attraction is still considerably stronger than the van der Waals attraction (Attard, 2003). The existence of nanobubbles on the surface of emulsion droplets in foods has not been demonstrated. Nevertheless, recent experiments suggest that nanobubbles may be present in hydrocarbon oil-in-water emulsions containing no emulsifier and that these nanobubbles may adversely influence emulsion stability (Pashley, 2003). The role of nondissolved air on the stability of food emulsions is clearly an interesting area of further research.

The molecular origin of the short-range hydrophobic attraction between droplets can be attributed to the ability of water molecules to form relatively strong hydrogen bonds with each other but not with nonpolar molecules (Section 4.3.3). Consequently, the interaction between nonpolar substances and water is thermodynamically unfavorable, which means that a system will attempt to minimize the contact area between these substances by causing them to associate (Tanford, 1980; Israelachvili, 1992; Israelachvili and Wennerstrom, 1996; Alaimo and Kumosinski, 1997). This process manifests itself as a relatively strong attractive force between hydrophobic substances dispersed in water, and is responsible for many important phenomenon that occur in food emulsions, such as protein conformation, micelle formation, adsorption of surfactants to interfaces, and the low water solubility of nonpolar compounds (Chapters 4 and 5).

### 3.7.2 Modeling hydrophobic interactions

Assuming that there are no nanobubbles adsorbed to the surface of emulsion droplets, then the hydrophobic interaction between emulsion droplets will only be due to the short-range interaction mentioned above. Under these circumstances, the interdroplet pair potential between two emulsion droplets with hydrophobic surfaces separated by water can be represented as an exponential decay (Israelachvili and Pashley, 1984; Pashley et al., 1985; Israelachvili, 1992; Skvarla, 2001):

$$w_{\text{hydrophobic}}(h) = -2\pi r \gamma_i \phi_H \lambda_0 e^{-h/\lambda_0} \quad (3.16)$$

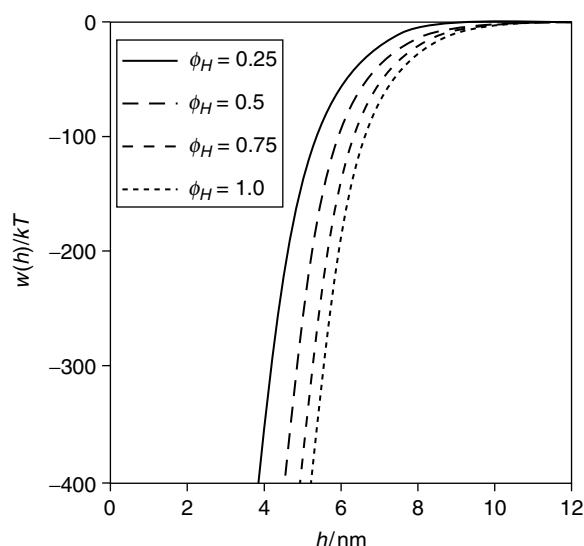


**Figure 3.16** An attractive hydrophobic interaction arises between emulsion droplets when their surfaces have some hydrophobic character, where  $\phi_H$  is approximately equal to the fraction of the droplet surface which is nonpolar.

where  $\gamma_i$  is the interfacial tension between the nonpolar groups and water (typically between 10 and 50 mJ m<sup>-2</sup> for food oils),  $\lambda_0$  is the decay length of the interaction (typically between 1 and 2 nm), and  $\phi_H$  is a measure of the surface hydrophobicity of the droplets. The surface hydrophobicity varies from 0 (for a fully polar surface) to 1 (for a fully nonpolar surface). Thus, the magnitude of the hydrophobic interaction increases as the surface hydrophobicity increases, that is,  $\phi_H$  tends toward unity (Figure 3.16). It should be noted that the above equation is probably a gross simplification and the actual short-range hydrophobic attraction will depend on the precise nature of the system involved. For example, experiments have shown that the hydrophobic interaction is not directly proportional to the number of nonpolar groups at a surface, because the alteration in water structure imposed by nonpolar groups is disrupted by the presence of any neighboring polar groups (Israelachvili, 1992). Thus, it is not possible to assume that  $\phi$  is simply equal to the fraction of nonpolar sites at a surface. As a consequence, it is difficult to accurately predict their magnitude from first principles. Measurements of the force versus distance profile of nonpolar surfaces have shown that the hydrophobic attraction is stronger than the van der Waals attraction up to relatively high surface separations (Israelachvili, 1992; Claesson et al., 2004).

When hydrophobic surfaces are covered by amphiphilic molecules, such as small molecule surfactants or biopolymers, the hydrophobic interaction between them is effectively screened and the overall attraction is mainly due to van der Waals interactions (Israelachvili, 1992). Nevertheless, hydrophobic interactions are likely to be significant when the surface has some hydrophobic character, for example, if the surface is not completely saturated with emulsifier molecules (Tcholakova et al., 2002), if it is bent to expose the oil molecules (Israelachvili, 1992), or if the emulsifier molecules have some hydrophobic regions exposed to the aqueous phase, for example, denatured adsorbed globular proteins (Demetriades et al., 1997b; Kim et al., 2002a,b).

### 3.7.3 General characteristics of hydrophobic interactions

Few studies have been carried out to systematically characterize the influence of environmental and solution conditions on the strength and range of hydrophobic interactions between emulsion droplets. Nevertheless, it is possible to gain some insight into the factors that would be expected to influence interdroplet hydrophobic interactions by examining the factors that influence the strength of intermolecular hydrophobic interactions. Intermolecular hydrophobic interactions become increasingly strong as the temperature is raised (Israelachvili, 1992). Thus, hydrophobic interactions between emulsion droplets should become more important at higher temperatures. Because the strength of hydrophobic interactions depends on the magnitude of the interfacial tension, any change in the properties of the solvent that increases the interfacial tension will increase the hydrophobic attraction or vice versa. The addition of small amounts of alcohol to the aqueous phase of an emulsion lowers  $\gamma$ , and therefore would be expected to reduce the hydrophobic attraction between nonpolar groups. Electrolytes that alter the structural arrangement of water molecules also influence the magnitude of the hydrophobic effect when they are present at sufficiently high concentrations (Christenson et al., 1990). Structure breakers tend to enhance hydrophobic interactions, whereas structure promoters tend to reduce them (Chapter 4). Variations in pH have little direct effect on the strength of hydrophobic interactions, unless there are accompanying alterations in the structure of the water or the interfacial tension (Israelachvili and Pashley, 1984).

## 3.8 Hydration interactions

### 3.8.1 Origin of hydration interactions

Hydration interactions arise from the structuring of water molecules around dipolar and ionic groups (in contrast to hydrophobic interactions which arise from structuring of water around nonpolar groups). Most food emulsifiers naturally have dipolar or ionic groups that are hydrated (e.g.,  $-\text{OH}$ ,  $-\text{COO}^-$ , and  $-\text{NH}_3^+$ ), and some are also capable of binding hydrated ions (e.g.,  $-\text{COO}^- + \text{Na}^+ \rightarrow -\text{COO}^- \text{Na}^+$ ). As two droplets approach each other, the bonds between the polar groups and the water molecules in their immediate vicinity must be disrupted, which results in a repulsive interaction (Besseling, 1997). The magnitude and range of the hydration interaction therefore depends on the number and strength of the bonds formed between the polar groups and the water molecules: the greater the degree of hydration, the more repulsive and long range the interaction (Israelachvili, 1992; Claesson et al., 2004; Norde, 2003).

### 3.8.2 Modeling hydration interactions

Just as with hydrophobic interactions, it is difficult to develop theoretical models to describe this type of interaction from first principles because of the complex nature of its origin and its dependence on the specific type of ions and polar groups present. Nevertheless, experimental measurements of the forces between two liquid surfaces have shown that hydration interactions are fairly short-range repulsive forces that decay exponentially with surface-to-surface separation (Claesson, 1987; Israelachvili, 1992):

$$w_{\text{hydration}}(h) = A r \lambda_0 e^{-h/\lambda_0} \quad (3.17)$$

where  $A$  is a constant that depends on the degree of hydration of the surface (typically between 3 and 30 mJ m<sup>-2</sup>) and  $\lambda_0$  is the characteristic decay length of the interaction



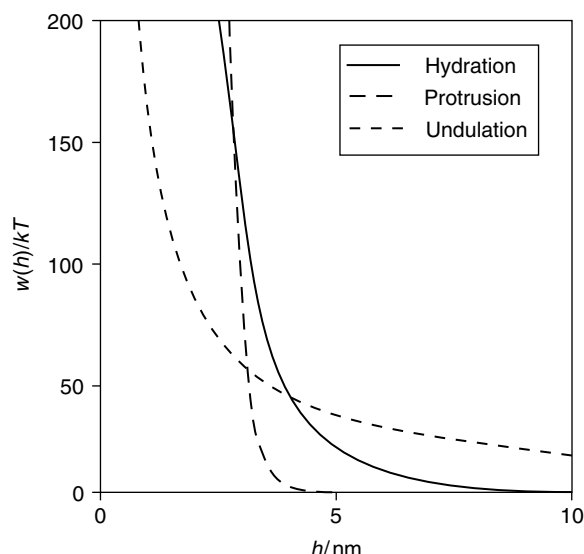


**Figure 3.17** Short-range repulsive interactions arise between emulsion droplets when they come into close contact due to hydration, protrusion, and undulation of interfacial layers.

(typically between 0.6 and 1.1 nm) (Israelachvili, 1992). The greater the degree of hydration of a surface group, the larger the values of  $A$  and  $\lambda_0$ . The hydration interaction is negligible at large droplet separations but becomes strongly repulsive when the droplets get closer than a certain separation (Figure 3.17). In practice, it is often difficult to isolate the contribution of the hydration forces from other short-range interactions that are associated with mobile interfacial layers at small separations (such as steric and thermal fluctuation interactions), and so there is still much controversy about their origin and nature. Nevertheless, it is widely accepted that they make an important contribution to the overall interaction energy in many systems.

Experimental measurements of the forces between extremely smooth solid surfaces separated by water reveal an oscillating force versus distance profile, rather than the smooth one predicted by the above equation (Israelachvili, 1992). The spacing between the peaks in this oscillating force curve is equal to the radius of water molecules, which suggests that energy needs to be supplied to expel each layer of water molecules. Nevertheless, these oscillations are not observed when the surfaces are relatively fluid or rough because the effects are averaged out, which would be the case for the surfaces of emulsion droplets.

### 3.8.3 General characteristics of hydration interactions

At high electrolyte concentrations, it is possible for ionic surface groups to specifically bind hydrated ions to their surfaces (Hunter, 1986, 1989; Miklavic and Ninham, 1990). Some of these ions have large amounts of water associated with them and can therefore provide strong repulsive hydration interactions. Specific binding depends on the radius and valency of the ion involved, because these parameters determine the degree of ion hydration. Ions that have small radii and high valencies tend to bind less strongly because they are surrounded by a relatively thick layer of tightly “bound” water molecules and some of these must be removed before the ion can be adsorbed (Israelachvili, 1992). As a general rule, the adsorbability of ions from water can be described by the lyotropic series:  $\Gamma^- > \text{Br}^- > \text{Cl}^- > \text{F}^-$  for monovalent anions and  $\text{K}^+ > \text{Na}^+ > \text{Li}^+$  for monovalent cations.

(in order of decreasing adsorbability). On the other hand, once an ion is bound to a surface the strength of the repulsive hydration interaction between the emulsion droplets increases with degree of ion hydration because more energy is needed to dehydrate the ion as the two droplets approach each other. Therefore, the ions that tend to adsorb the least strongly are also the ones that provide the greatest hydration repulsion when they do adsorb. Thus, it is possible to control the interaction between droplets by altering the type and concentration of ions present in the aqueous phase.

Hydration interactions are often strong enough to prevent droplets from aggregating (Israelachvili, 1992). Thus, oil-in-water emulsions that should contain enough electrolytes to cause droplet flocculation through electrostatic screening have been found to be stable because of specific binding of ions (Israelachvili, 1992). This effect is dependent on the pH of the aqueous phase because the electrolyte ions have to compete with the  $H^+$  or  $OH^-$  ions in the water (Miklavic and Ninham, 1990). For example, at relatively high pH and electrolyte concentrations ( $>10$  mM), it has been observed that  $Na^+$  ions can adsorb to negatively charged surface groups and prevent droplets from aggregating through hydration repulsion, but when the pH of the solution is decreased the droplets aggregate because the high concentration of  $H^+$  ions displace the  $Na^+$  ions from the droplet surface (Israelachvili, 1992). Nonionic emulsifiers are less sensitive to pH and ionic strength, and they do not usually bind highly hydrated ions. The magnitude of the hydration interaction decreases with increasing temperature because polar groups become progressively dehydrated as the temperature is raised (Israelachvili, 1992). In summary, the importance of hydration interactions in a particular system depends on the nature of the hydrophilic groups on the droplet surfaces, as well as on the type and concentration of ions present in the aqueous phase.

### 3.9 Thermal fluctuation interactions

#### 3.9.1 Origin of thermal fluctuation interactions

The interfacial region that separates the oil and aqueous phases of an emulsion is often highly dynamic (Israelachvili, 1992). In particular, interfaces that are comprised of small molecule surfactants tend to exhibit undulations because their bending energy is relatively small compared to the thermal energy of the system (Figure 3.18). In addition, the surfactant molecules may be continually twisting and turning, as well as moving in-and-out of the interfacial region. When two dynamic interfaces move close to each other they

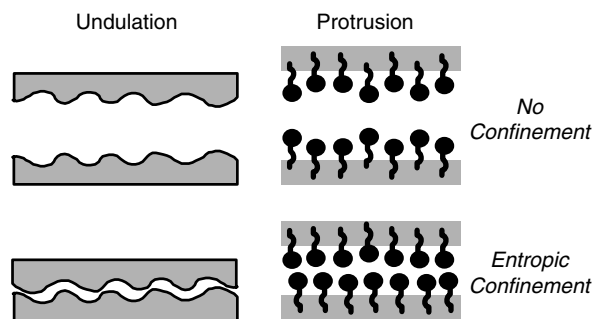


**Figure 3.18** Interfaces that are comprised of small molecule surfactants are susceptible to protrusion and undulation interactions.

experience a number of short-range repulsive *thermal fluctuation* interactions that are entropic in origin (Israelachvili, 1992). In emulsions the two most important of these are protrusion and undulation interactions.

### 3.9.2 Modeling thermal fluctuation interactions

Protrusion interactions are short-range repulsive interactions that arise when two surfaces are brought so close together that the movement of the surfactant molecules in-and-out of the interface of one droplet is restricted by the presence of another droplet, which is entropically unfavorable. The magnitude of this repulsive interaction depends on the distance that the surfactant molecules are able to protrude from the interface, which is governed by their molecular structure. The interdroplet pair potential due to protrusion interactions is given by the following expression (Israelachvili, 1992):

$$w_{\text{protrusion}}(h) \approx 3\pi\Gamma r k T \lambda_0 e^{-h/\lambda_0} \quad (3.18)$$

where  $\Gamma$  is the number of surfactant molecules (or head groups) per unit surface area and  $\lambda_0$  is the characteristic decay length of the interaction (typically between 0.07 and 0.6 nm), which depends on the distance the surfactant can protrude from the surface.

Undulation interactions are short-range repulsive interactions that arise when the wave-like undulations of the interfacial region surrounding one emulsion droplet is restricted by the presence of another emulsion droplet, which is entropically unfavorable. The magnitude and range of this repulsive interaction increases as the amplitude of the oscillations increases. The interdroplet pair potential due to undulation interactions is given by the following expression (Israelachvili, 1992):

$$w_{\text{undulation}}(h) \approx \frac{\pi r (kT)^2}{4k_b h} \quad (3.19)$$

where  $k_b$  is the bending modulus of the interfacial layer, which typically has values of between 0.2 and  $20 \times 10^{-20}$  J depending on the surfactant type. The magnitude of the bending modulus is related to the molecular geometry of the surfactant molecules (Section 4.1.1), and tends to be higher for surfactants that have two nonpolar chains, than those that have only one. Predictions of the protrusion and undulation interactions made using the above equations are shown in Figure 3.17.

### 3.9.3 General characteristics of fluctuation interactions

Thermal fluctuation interactions are much more important for small molecule surfactants that form fairly flexible interfacial layers, than for biopolymers that form fairly rigid interfacial layers. Both types of interactions tend to increase with temperature because the interfaces become more mobile. Nevertheless, this effect may be counteracted by increasing dehydration of any polar groups with increasing temperature. These interactions may play a significant role in stabilizing droplets against aggregation in emulsions stabilized by small molecule surfactants, particularly when they act in conjunction with other types of short-range repulsive interactions, such as steric or hydration interactions. The strength of this interaction is mainly governed by the structure and dynamics of the interfacial layer and therefore varies considerably from system to system (Israelachvili, 1992).

### 3.10 Nonequilibrium effects

So far, it has been assumed that the interactions between droplets occur under equilibrium conditions. In practice, the molecules and droplets in emulsions are in continual motion, which influences the colloidal interactions in a number of ways (Evans and Wennerstrom, 1994).

#### 3.10.1 Molecular rearrangements at the interface

The system may not have time to reach equilibrium when two droplets rapidly approach each other because molecular rearrangements take a finite time to occur, for example, adsorption–desorption of emulsifiers, ionization/deionization of charged groups, and conformational changes of biopolymers (Israelachvili, 1992; Israelachvili and Berman, 1995). As a consequence, the colloidal interactions between droplets may be significantly different from those observed under equilibrium conditions. These nonequilibrium effects depend on the precise nature of the system and are therefore difficult to account for theoretically.

#### 3.10.2 Hydrodynamic flow of continuous phase

The movement of a droplet causes an alteration in the flow profile of the intervening continuous phase, which can be “felt” by another droplet (Dukhin and Sjoblom, 1996; Walstra, 2003a). As two droplets move closer together, the continuous phase must be squeezed out from the narrow gap separating them against the friction of the droplet surfaces (Figure 3.19). This effect manifests itself as a decrease in the effective diffusion coefficient of the emulsion droplets,  $D(h) = D_0 G(h)$ , where  $D_0$  is the diffusion coefficient of a single droplet and  $G(h)$  is a correction factor that depends on surface-to-surface separation between the droplets (Hunter, 1986). Mathematical expressions for  $G(h)$  have been derived from a consideration of the forces that act on particles as they approach each other in a viscous liquid (Davis et al., 1989; Zhang and Davis, 1991; Dukhin and Sjoblom, 1996). For rigid spherical particles the hydrodynamic correction factor can be approximated by the following expression (Hunter, 1986):

$$G(h) = \frac{2h}{r} \frac{1 + (3h/2r)}{1 + (13h/2r) + (3h^2/r^2)} \quad (3.20)$$

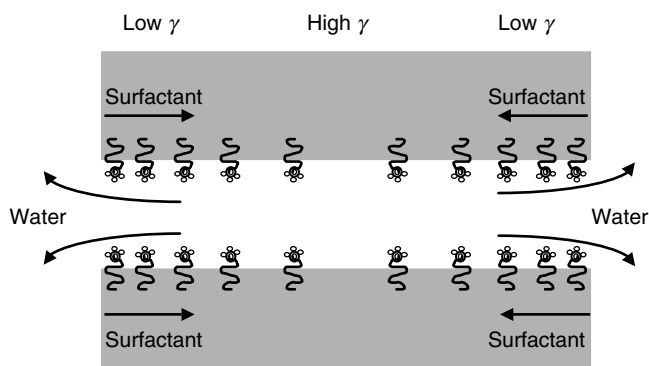


**Figure 3.19** Schematic representation of the Gibbs–Marangoni effect. As two emulsion droplets approach each other some of the intervening fluid separating them must flow out. The resulting viscous drag on the interfacial membrane may lead to a concentration gradient of emulsifier at the interface, which opposes fluid flow from between the droplets.

The value of  $G(h)$  varies from 0 when the particles are in close contact ( $h = 0$ ) to 1 when they are far apart and therefore have no influence on each other ( $h \rightarrow \infty$ ). Thus, as particles approach each other their speed gets progressively slower, and therefore they would not aggregate unless there was a sufficiently strong attractive colloidal interaction to overcome the repulsive hydrodynamic interaction. Equation 3.20 must be modified for emulsions to take into account the fact that there is less resistance to the movement of the continuous phase out of the gap between the droplets when their surfaces have some fluid-like characteristics (Davis et al., 1989; Zhang and Davis, 1991). Thus, the hydrodynamic resistance to the approach of fluid droplets is less than that for solid droplets. Hydrodynamic interactions are particularly important for determining the stability of droplets to flocculation and coalescence in emulsion systems (Chapter 7).

### 3.10.3 Gibbs–Marangoni effect

There may be an additional nonequilibrium contribution to the colloidal interactions between emulsion droplets due to the *Gibbs–Marangoni* effect (Walstra, 1993a, 1996b, 2003a). As two droplets approach each other, the liquid in the continuous phase is forced out of the narrow gap that separates them. As the liquid is squeezed out it drags some of the emulsifier molecules along the droplet surface, which leads to the formation of a region where the emulsifier concentration on the surfaces of the two emulsion droplets is lowered (Figure 3.19). This causes a surface tension gradient at the interface, which is thermodynamically unfavorable. The emulsifier molecules therefore have a tendency to flow toward the region of low emulsifier concentration and high interfacial tension, dragging some of the liquid in the surrounding continuous phase along with them. This motion of the continuous phase is in the opposite direction to the outward flow that occurs when it is squeezed from between the droplets, and therefore it opposes the movement of the droplets toward each other, and therefore increases their stability to close approach and coalescence. This effect is most important for emulsifiers that are relatively mobile at the oil–water interface, such as small molecule surfactants rather than surface-active biopolymers.

## 3.11 Total interaction potential

The overall interdroplet pair potential is the sum of the various attractive and repulsive contributions\*:

$$w_{\text{total}}(h) = w_{\text{VDW}}(h) + w_{\text{electrostatic}}(h) + w_{\text{steric}}(h) + w_{\text{depletion}}(h) + w_{\text{hydrophobic}}(h) + \dots \quad (3.21)$$

Not all of the interactions play an important role in every type of food emulsion, and it is often possible to identify two or three interactions that dominate the overall interaction. For this reason, it is informative to examine the characteristics of certain combinations of colloidal interaction that are particularly important in food emulsions. A summary of the characteristics of the various types of interactions is given in Table 3.3. In this section, the use of predicting the overall interdroplet pair potential as a function of droplet separation for understanding the behavior of food emulsions is demonstrated. We begin by considering a simple system, where only van der Waals attraction and steric repulsion operates, and then build up the complexity of the system by incorporating the effects of other important types of attractive and repulsive interactions. The physicochemical parameters used in the theoretical calculations are shown in figure captions.

\* In reality, it is not always appropriate to simply sum the contribution from all of the separate interactions because some of them are coupled (Ninham and Yaminsky, 1997). Nevertheless, this approach gives a good first approximation.

**Table 3.3** Summary of the Characteristics of the Various Types of Colloidal Interactions Between Emulsion Droplets\*.

Interaction Type	Sign	Strength	Range	Major Factors Affecting
van der Waals	A	S	LR	$\epsilon, n, I$
Electrostatic	R	W $\rightarrow$ S	SR $\rightarrow$ LR	$\psi_\delta, \sigma, \text{pH}, I$
Steric				
Elastic	R	S	SR	$\delta, E$
Mixing	A or R	W $\rightarrow$ S	SR	$\delta, w$
Depletion	A	W $\rightarrow$ S	SR	$\phi_c, r_c$
Hydrophobic	A	S	LR	$\phi_{\text{IP}}, T$
Hydration	R	S	SR $\rightarrow$ MR	$T$
Thermal fluctuation	R	S	SR $\rightarrow$ MR	$T$

\* The interactions are classified according to the following symbols: A = attractive, R = repulsive; S = strong, W = weak, SR = short range (<10 nm), MR = medium range (10–20 nm), and LR = long range (>20 nm). The major factors affecting the interactions are dielectric constant ( $\epsilon$ ), refractive index ( $n$ ), ionic strength ( $I$ ), surface potential ( $\psi_\delta$ ), surface charge density ( $\sigma$ ), thickness of interfacial layer ( $\delta$ ), elastic modulus of interfacial layer ( $E$ ), effective interaction parameter for emulsifier–solvent interactions ( $w$ ), and temperature ( $T$ ).

### 3.11.1 *van der Waals and steric*

The most basic model for describing the colloidal interactions between emulsion droplets is to consider that only van der Waals and steric interactions are important. van der Waals interactions always act between emulsion droplets and must therefore be taken into account. Similarly, the droplets in emulsions are nearly always stabilized by an interfacial layer of adsorbed emulsifier molecules and so steric interactions must also be taken into account. This type of model would be appropriate for describing the behavior of emulsion droplets stabilized by nonionic surfactants or uncharged biopolymers. It would also be appropriate for describing the behavior of emulsion droplets stabilized by charged surfactants or biopolymers at high salt concentrations where the electrostatic interactions are effectively screened.

The overall interdroplet pair potential for this simple model system is given by

$$w(h) = w_{\text{VDW}}(h) + w_{\text{steric}}(h) \quad (3.22)$$

The dependence of the overall interdroplet pair potential on droplet separation for emulsions with interfacial layers of different thickness are shown in Figure 3.20. It is assumed that the continuous phase is an indifferent quality solvent for the polymer, so that the mixing contribution to the polymeric steric interaction is zero (Section 3.5). At wide separations the overall interaction between the droplets is negligible. As the droplets move closer together, the attractive van der Waals interaction begins to dominate and so there is a net attraction between the droplets. However, once the droplets get so close together that their interfacial layers overlap then the repulsive steric interaction dominates and there is a net repulsion between the droplets. At a particular separation there is a minimum in the interdroplet pair potential, and this is the location where the droplets tend to reside. If the depth of this minimum is large compared to the thermal energy of the system the droplets remain aggregated, otherwise they move apart. The depth and position of the minimum depends on the thickness and properties of the interfacial layer surrounding the droplets. As the thickness of the adsorbed layer increases, the repulsive interaction between droplets becomes more significant at larger separations, and consequently the depth of the minima decreases. If the interfacial layer is sufficiently thick it may prevent the droplets from aggregating altogether, because the depth of the minimum

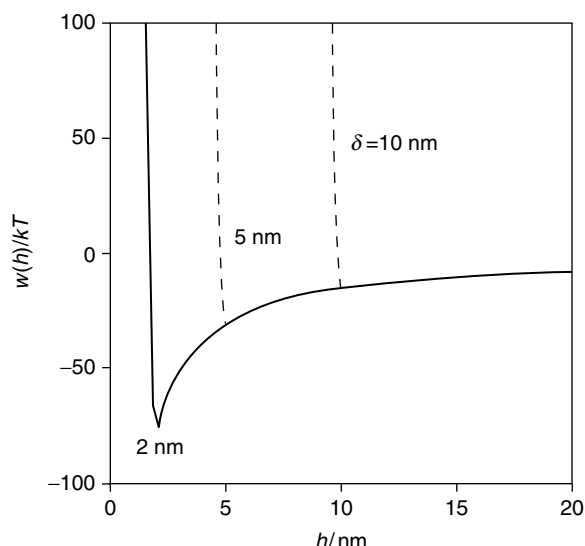


**Figure 3.20** Predicted interdroplet pair potentials for emulsions where only van der Waals and steric interactions are important. Predictions are carried out for oil-in-water emulsions with different thicknesses of adsorbed layers as stated in the annotation ( $r = 1 \mu\text{m}$ ,  $T = 25^\circ\text{C}$ ).

is relatively small compared to the thermal energy. This phenomenon accounts for the effectiveness of emulsifiers that form relatively thick interfacial layers (e.g., polysaccharides) at preventing droplet flocculation and coalescence in emulsions containing high salt concentrations, whereas emulsifiers that form relatively thin interfacial layers (e.g., globular proteins) can prevent coalescence but not flocculation (Chanamai and McClements, 2002). As mentioned in Section 3.3, the composition and thickness of the adsorbed layer may have an additional influence on the overall interaction potential due to its modification of the van der Waals interactions (which was not taken into account in the calculations carried out here).

### 3.11.2 *van der Waals, steric, and electrostatic*

The droplets in many food emulsions have an electric charge because of adsorption of surface-active ions or emulsifiers (Section 3.4). A more realistic model of the colloidal interactions between emulsion droplets is therefore obtained by considering van der Waals, steric, and electrostatic interactions:

$$w(h) = w_{\text{VDW}}(h) + w_{\text{steric}}(h) + w_{\text{electrostatic}}(h) \quad (3.23)$$

The dependence of the overall interdroplet pair potential on droplet separation for electrically charged droplets is shown in Figure 3.21. For simplicity of discussion, a more schematic representation of the general form of the interaction potential for this type of system is shown in Figure 3.22. When the two droplets are separated by a large distance there is no effective interaction between them. As they move closer together, then the van der Waals attraction dominates initially and there is a shallow minimum in the profile, which is referred to as the *secondary minimum*,  $w(h_{2\text{min}}^0)$ . When the depth of this minimum is large compared to the thermal energy ( $|w(h_{2\text{min}}^0)| \gg kT$ ) the droplets tend to be flocculated, but if it is small compared to the thermal energy, they tend to remain nonaggregated. At closer separations, the repulsive electrostatic interaction dominates and there is an

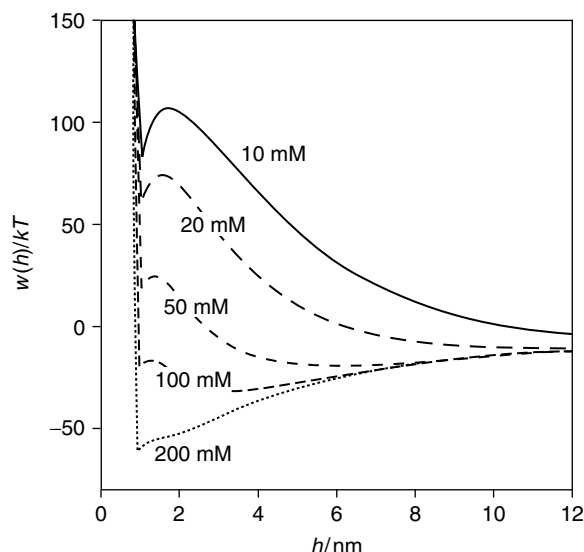


**Figure 3.21** Predicted interdroplet pair potentials for emulsions where only van der Waals, steric, and electrostatic interactions are important. Predictions are carried out for oil-in-water emulsions with different ionic strengths as stated in the annotation ( $r = 1\ \mu\text{m}$ ,  $\delta = 1\ \text{nm}$ ,  $T = 25^\circ\text{C}$ ,  $\psi_0 = 20\ \text{mV}$ ). The height of the energy barrier decreases as the ionic strength of the intervening medium increases because of electrostatic screening.

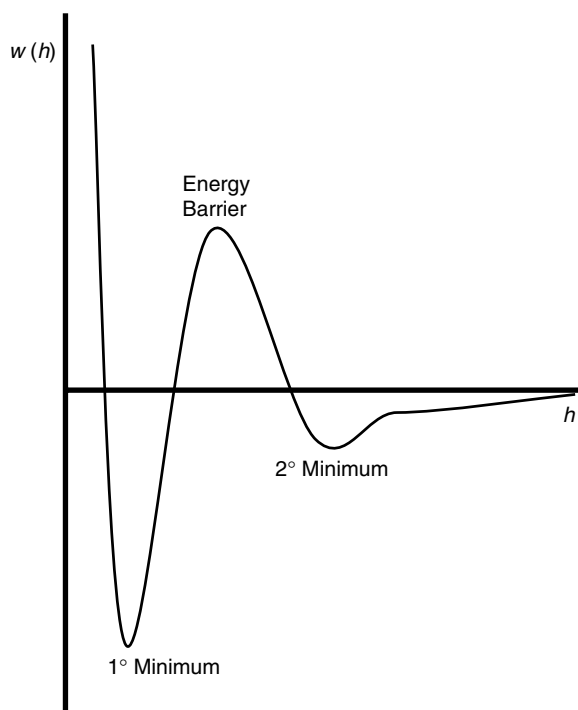


**Figure 3.22** Schematic representation of the overall interaction potential between a pair of electrically charged droplets covered by an interfacial membrane, assuming only van der Waals, steric, and electrostatic interactions are important. The depths of the primary and secondary minima and the height of the energy barrier determine the stability of the system to droplet aggregation.



energy barrier,  $w(h_{\max})$ , that must be overcome before the droplets can come any closer. At still closer separations, the attractive van der Waals interaction dominates the repulsive electrostatic interaction and there is a relatively deep *primary minimum*,  $w(h_{\min}^0)$ . If the energy barrier is sufficiently large compared to the thermal energy ( $|w(h_{\max})| > 20kT$ ), then it will effectively prevent the droplets from falling into the *primary minimum*. On the other hand, if it is relatively small compared to the thermal energy, then the droplets tend to fall into the primary minimum, which would lead to strong droplet aggregation. When the droplets get so close together that their interfacial membranes overlap, there is an extremely strong steric repulsion that dominates the other interactions. This short-range repulsive interaction should prevent the droplets from getting close enough together to coalesce.

There are a number of complicating factors that need to be taken into account when implementing the above approach. First, one must decide the location of the electrical charge in the system (e.g., at the oil droplet surfaces or at the outer edge of the interfacial membranes), since this will have a pronounced influence on the strength and range of the electrostatic interactions. Second, one may have to take into account the influence of electrostatic screening, retardation, and the interfacial membrane on the strength of the van der Waals interactions (Section 3.3). Third, one may have to take into account changes in the thickness or characteristics of the interfacial membrane if it consists of charged emulsifier molecules, since this will influence the strength and range of the steric interactions (Section 3.5). Despite these complicating factors, the above approach provides valuable insights into the factors that influence the stability of electrically charged emulsion droplets.

Electrostatically stabilized emulsions are particularly sensitive to the ionic strength and pH of the aqueous phase (Figure 3.21). At low electrolyte concentrations there may be a sufficiently high-energy barrier to prevent the droplets from coming close enough together to aggregate into the primary minimum. As the ion concentration is increased the screening of the electrostatic interaction becomes more effective (Section 3.4), which reduces the height of the energy barrier. Above a certain electrolyte concentration, often referred to as the *critical aggregation concentration* or CAC, the energy barrier is no longer high enough to prevent the droplets from falling into the deep primary minimum, and so the droplets tend to aggregate. This accounts for the susceptibility of many electrostatically stabilized food emulsions to droplet aggregation when salt is added to the aqueous phase (Hunt and Dalgleish, 1994, 1995; Demetriades et al., 1997a; Kim et al., 2002a,b; Keowmaneechai and McClements, 2002a). The electrical charge of many food emulsifiers is sensitive to the pH of the aqueous phase. For example, the droplet charge of protein-stabilized emulsions decreases as the pH tends toward the isoelectric point of the proteins, which reduces the magnitude of the electrostatic repulsion between the droplets. This accounts for the tendency of protein-stabilized emulsions to become flocculated when their pH is adjusted to the isoelectric point of the adsorbed proteins (Demetriades et al., 1997a). Nevertheless, the droplets are often stable to coalescence because of the presence of the short-range steric repulsion associated with the adsorbed protein layers.

It should be noted that the classical approach to describing the interactions between electrically charged particles is the *DLVO theory*, named after the four scientists who first proposed it: Derjaguin, Landau, Verwey, and Overbeek (Derjaguin et al., 1987; Derjaguin, 1989; Hiemenz and Rajagopalan, 1997). The DLVO theory does not take into account the steric repulsion that acts between droplets at close separations, and it is therefore not a particularly realistic model for describing the behavior of emulsion droplets coated by interfacial membranes. This theory predicts that the emulsion droplets would coalesce once they fell into the primary minimum because there would be no short-range repulsive force stopping them getting closer together.

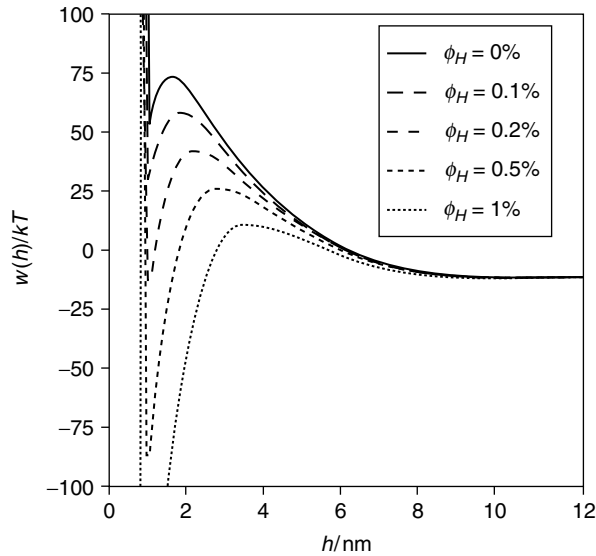


**Figure 3.23** Predicted interdroplet pair potentials for emulsions where van der Waals, steric, electrostatic, and hydrophobic interactions are important. Predictions are carried out for oil-in-water emulsions with different surface hydrophobicities as stated in the annotation box ( $r = 1 \mu\text{m}$ ,  $\delta = 1 \text{ nm}$ ,  $T = 25^\circ\text{C}$ ,  $\psi_0 = 20 \text{ mV}$ ,  $I = 20 \text{ mM}$ ). The height of the energy barrier decreases as the surface hydrophobicity increases because of the increase in the hydrophobic attraction.

### 3.11.3 *van der Waals, steric, electrostatic, and hydrophobic*

The droplet surfaces in many food emulsions acquire some hydrophobic character during their manufacture, storage, or consumption. A typical example is a whey-protein-stabilized emulsion that is subjected to a heat treatment (Monahan et al., 1996; Demetriades et al., 1997b; Kim et al., 2002a,b). Heating the emulsion above  $65^\circ\text{C}$  causes the protein molecules adsorbed to the oil–water interface to partially unfold and thus expose some of the nonpolar amino acids to the aqueous phase. The overall interdroplet pair potential for this type of system is given by

$$w(h) = w_{\text{VDW}}(h) + w_{\text{steric}}(h) + w_{\text{electrostatic}}(h) + w_{\text{hydrophobic}}(h) \quad (3.24)$$

The dependence of the overall interdroplet pair potential on droplet separation for droplets with different degrees of surface hydrophobicity is shown in Figure 3.23. As the hydrophobicity of the droplet surface increases, the hydrophobic attraction increases which causes a decrease in the height of the energy barrier. When the surface hydrophobicity is sufficiently large the energy barrier becomes so small that the droplets can aggregate into the primary minimum. This accounts for the experimental observation that whey-protein-stabilized emulsions become more susceptible to aggregation when they are heated above a temperature where the protein molecules unfold (Demetriades et al., 1997b).

### 3.11.4 *van der Waals, steric, electrostatic, and depletion*

Depletion interactions are important when the continuous phase of an emulsion contains a significant concentration of small colloidal particles, such as surfactant micelles or nonadsorbing biopolymers (Dickinson and McClements, 1995; Jenkins and Snowden, 1996).

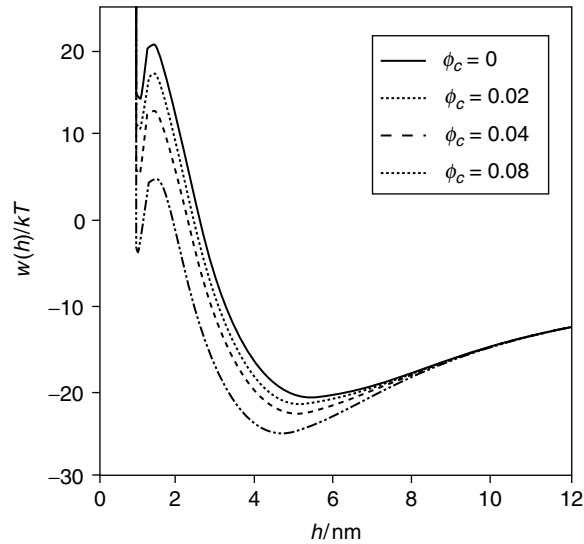


**Figure 3.24** Predicted interdroplet pair potentials for emulsions where van der Waals, steric, electrostatic, and depletion interactions are important. Predictions are carried out for oil-in-water emulsions containing different volume fractions of nonadsorbed colloidal particles dispersed in the continuous phase as stated in the annotation box ( $r = 1 \mu\text{m}$ ,  $\delta = 1 \text{ nm}$ ,  $r_c = 5 \text{ nm}$ ,  $T = 25^\circ\text{C}$ ,  $\psi_0 = 20 \text{ mV}$ ,  $I = 50 \text{ mM}$ ). The height of the energy barrier decreases as the concentration of colloidal particles increases because of the increase in the depletion attraction.

The interdroplet pair potential for a system in which depletion interactions are important is given by

$$w(h) = w_{\text{VDW}}(h) + w_{\text{steric}}(h) + w_{\text{electrostatic}}(h) + w_{\text{depletion}}(h) \quad (3.25)$$

The variation of the interdroplet pair potential with droplet separation for this type of system is shown in Figure 3.24. At low concentrations of colloidal particles the energy barrier is sufficiently large to prevent the droplets falling into the primary minimum. As the concentration of colloidal particles is increased the attraction between the droplets increases. A number of workers have shown that depletion interactions promote droplet flocculation in emulsions when the concentration of surfactant or biopolymer exceeds some critical concentration (Sperry, 1982; Aronson, 1991; McClements, 1994; Dickinson et al., 1995; Jenkins and Snowden, 1996).

### 3.12 Measurement of colloidal interactions

One of the major advances in recent years has been the development and usage of analytical instruments for accurately measuring the forces between macroscopic surfaces down to separations of a fraction of a nanometer (Israelachvili, 1992; Luckham and Costello, 1993; Claesson et al., 1996, 2004). A variety of different instruments have been developed for this purpose, including surface force apparatus, atomic force microscopy, light-lever instruments, and so on (Christenson and Claesson, 2001). Nevertheless, all of the instruments use some means of measuring the separation distance and force acting between two macroscopic surfaces as one of the surfaces is moved through the intervening liquid in a controlled fashion (Christenson and Claesson, 2001). The surfaces can be chemically or

physically modified to control their hydrophobicity, hydrophilicity, electrical charge, roughness, and thickness. In addition, it is possible to adsorb different types of emulsifiers onto the surfaces, and to vary the composition and properties of the liquid separating the surfaces. One drawback of these techniques for understanding the characteristics of particular types of interactions is that they only measure the overall interaction potential, and so it is necessary to design ways of disentangling the contributions from the various individual interactions. Nevertheless, the application of these techniques has led to considerable advances in our knowledge of the origin, sign, magnitude, and range of colloidal interactions, as well as providing a better understanding of the factors that influence these interactions (e.g., pH, temperature, ionic environment, solvent composition). Ultimately, the knowledge gained from application of these techniques will help food scientists to gain a better understanding of the factors that determine the stability of food emulsions.

### 3.13 *Prediction of colloidal interactions in food emulsions*

In this chapter, we have examined the origin, magnitude, and range of the most important types of attractive and repulsive interactions that can arise between emulsion droplets. In principle, it is possible to predict the likelihood that the droplets in an emulsion will be in an aggregated or a nonaggregated state using the theories given above. In practice, it is extremely difficult to make quantitative predictions about the properties of food emulsions for a number of reasons. First, food emulsions contain a huge number of different emulsion droplets (rather than just two) which interact with each other and with other components within the system, and it is difficult to quantify the overall nature of these interactions (Dickinson, 1992). Second, there is often a lack of information about the relevant physical parameters needed to carry out the calculations (Hunter, 1986). Third, certain simplifying expressions often have to be made in the theories in order to derive tractable expressions for the interaction energies, and these are not always justified (Ninham and Yaminsky, 1997). Fourth, food systems are not usually at thermodynamic equilibrium and so many of the above equations do not strictly apply (Israelachvili and Berman, 1995). Fifth, covalent interactions are important in some systems, and these are not taken into account in the above analysis (McClements et al., 1993d; Mohanan et al., 1996). Finally, food emulsions may be subjected to external forces that affect the interactions between the droplets, e.g., gravity, centrifugation, or mechanical agitation (Berli and Quemeda, 2002; Saether et al., 2004). Despite the limitations described above, an understanding of the various types of interactions that act between droplets gives food scientists a powerful tool for understanding and predicting the effects of ingredient formulations and processing conditions on the properties of many food products. It is often possible to predict the major factors that determine the stability of emulsions (*albeit* in a fairly qualitative fashion). Alternatively, in some systems it may be possible to experimentally measure the forces between surfaces using a force measurement technique (see Section 3.12) for a system that closely mimics the food system of interest. For example, it may be possible to coat the solid surfaces in the force measuring device with the same type of emulsifier as used in the food product and to use an aqueous solution with the same composition as found in the food product (e.g., pH, ionic composition). The force–distance curves could then be measured and the factors that influence them determined.



## *chapter four*

---

# *Emulsion ingredients*

### *4.1 Introduction*

Inspection of the labels of most commercially available food emulsions indicates that they contain a wide variety of different constituents, for example, oil, emulsifiers, thickening agents, gelling agents, buffering systems, preservatives, antioxidants, chelating agents, sweeteners, salts, colorants, flavors. Each of these constituents has its own unique molecular and functional characteristics. Ultimately, the physicochemical and organoleptic properties of a product depend on the type of constituents present, their physical location, and their interactions with each other. The efficient production of high-quality food emulsions therefore depends on knowledge of the contribution that each individual constituent makes to the overall properties, and how this contribution is influenced by the presence of the other constituents. One of the most important decisions that a food manufacturer must make during the design, formulation, and production of a food product is the selection of the most appropriate constituents for that particular product. Each ingredient must exhibit its desired functional properties within the food, while also being economically viable, convenient to use, of reliably high quality, compatible with other ingredients, readily available, and possibly “label friendly.”

It is possible to define the composition of an emulsion in a number of different ways: concentrations of specific atoms (e.g., H, C, O, N, Na, Mg, Cl); concentrations of specific molecules (e.g., water, sucrose, amylose,  $\beta$ -lactoglobulin); concentrations of general classes of molecules (e.g., proteins, lipids, carbohydrates, minerals); concentrations of composite ingredients (e.g., flour, milk, salt, egg); concentrations of functional ingredients (e.g., oil, water, emulsifiers, texture modifiers, buffering agents, preservatives). Food manufacturers are usually concerned with the concentration of composite or functional ingredients, because food components are normally purchased and used in this form. On the other hand, research scientists may be more interested in the concentrations of specific atoms, molecules, or molecular classes, depending on the purpose of their investigations. In this chapter, we will mainly categorize ingredients according to their functional roles within emulsions, since this seems to be the most logical and convenient means of discussing them.

The formulation of food products has traditionally been more of a craft than a science. Many of the foods that are familiar to us today are the result of a long and complex history of development. Consequently, there has often been a rather poor understanding of the role (or multiple roles) that each chemical constituent plays in determining their overall quality. The 20th century saw the development of large-scale industrial manufacturing operations where foods are mass produced. Mass production has led to the availability of a wide variety of low-cost foods that are quick and easy to prepare, and are therefore appealing to the modern consumer. Nevertheless, increasing reliance on mass production has meant that food manufacturers have had to develop a more thorough understanding

of the behavior of food ingredients before, during, and after processing (Hollingsworth, 1995). This knowledge is required for a number of reasons:

1. The properties of the ingredients entering a food factory often vary from batch-to-batch. Food manufacturers may reject poor quality ingredients or they may use their knowledge of the behavior of food ingredients under different conditions to adjust the food processing operations so that the final product has consistent properties.
2. Food manufacturers are often looking for cheaper alternatives to existing ingredients, for ingredients with improved functional properties, or for ingredients that are more "label friendly." An understanding of the role(s) that the original ingredient plays in a food will facilitate the rational selection of an alternative ingredient.
3. There is a growing trend toward improving the quality, variety, and convenience of processed foods (Sloan, 2003). Knowledge of ingredient properties enables food scientists to develop these foods in a more systematic and informed manner.
4. There is an increasing tendency toward removing or reducing the amounts of food constituents that have been associated with human health concerns (e.g., saturated fat, trans fatty acids, cholesterol, and salt) or the addition of food constituents that have been associated with maintaining or improving human health (e.g.,  $\omega$ -3 fatty acids, dietary fiber, and specific minerals). The removal of certain ingredients or the addition of new ingredients may cause significant changes in the taste, texture, or appearance of foods that consumers find undesirable (McClements and Demetriades, 1998; Malone et al., 2000, 2003a,b; Kilcast and Clegg, 2002). For example, many no-fat or low-fat products do not exhibit the desirable taste or textural characteristics of the full-fat products that they are designed to replace (O'Donnell, 1995; Kilcast and Clegg, 2002). Consequently, it is important to understand the role that each ingredient plays in determining the overall physicochemical and organoleptic properties of foods, so that this role can be mimicked by a healthier alternative ingredient.

This chapter provides an overview of the molecular, physicochemical, and functional characteristics of the major categories of functional ingredients present in food emulsions. Special emphasis is given to those ingredients that are particular to food emulsions, that is, emulsifiers and texture modifiers.

## 4.2 Fats and oils

Fats and oils are part of a group of compounds known as *lipids* (Gunstone and Norris, 1983; Weiss, 1983; Nawar, 1996; Gunstone and Padley, 1997; Akoh and Min, 2002; Larsson, 2004). By definition a lipid is a compound that is soluble in organic solvents, but insoluble or only sparingly soluble in water. This group of compounds contains a large number of different types of molecules, including acylglycerols, fatty acids, and phospholipids. Triacylglycerols are by far the most common lipid in foods, and it is this type of molecule that is usually referred to as a fat or oil. Edible fats and oils come from a variety of different sources including plants, seeds, nuts, animals, and fish (Sonntag, 1979a-c; Weiss, 1983; Nawar, 1996; Akoh and Min, 2002). By convention a *fat* is solid-like at room temperature, whereas *oil* is liquid, although these terms are often used interchangeably (Walstra, 1987). Because of their high natural abundance and their major importance in food emulsions, we will be mainly concerned with the properties of triacylglycerols in this section. Nevertheless, it should be mentioned that other types of lipids are more important in certain food emulsions, for example, the major lipid source in many beverage emulsions are flavor oils (Tan, 2004). The characteristics of flavor oils are discussed in more detail in the section on beverage emulsions (Chapter 12).

Fats and oils influence the nutritional, organoleptic, and physicochemical properties of food emulsions in a variety of ways. Lipids are a major source of energy and essential nutrients in the human diet; however, overconsumption of certain types of lipids (cholesterol, saturated fat, trans fatty acids) have been linked to human health concerns, such as obesity, cardiovascular disease, diabetes, and cancer (Chow, 1992; Smolin and Grosvenor, 1994; Gurr, 1997; Kritchevsky, 2002). Consequently, there has been a trend in the food industry to reduce the overall fat content of many traditional foods, as well as reducing the proportion of undesirable lipids within the fat phase (O'Donnell, 1995; Jones, 1996; Gurr, 1997). The challenge to the food scientist is to create a product that has the same desirable quality attributes as the original, but with a reduced fat content, which is often extremely difficult (Jones, 1996; McClements and Demetriades, 1998). On the other hand, underconsumption of certain types of polyunsaturated lipids has also been linked to various human health problems, such as heart disease, diabetes, cancer, and brain development (Gurr, 1997; Kritchevsky, 2002). Consequently, many food manufacturers are attempting to find effective strategies of incorporating these polyunsaturated lipids into foods, which is often problematic because of their poor oxidative stability (McClements and Decker, 2000).

The perceived flavor of a food emulsion is strongly influenced by the type and concentration of lipids present (Chapter 9). Lipids undergo a variety of chemical changes during the processing, storage, and handling of foods that generate products that can be either desirable or deleterious to their flavor profile (Nawar, 1996). Controlling these reactions requires knowledge of both lipid chemistry and emulsion science (Frankel, 1991; Frankel et al., 1994; Coupland and McClements, 1996; McClements and Decker, 2000). The flavor of food emulsions is also indirectly influenced by the presence of the lipid phase because flavor compounds can partition among the oil, water, and gaseous phases according to their polarities (Chapter 9). For this reason, the perceived aroma and taste of food emulsions are often strongly influenced by the type and concentration of lipids present. The lipid phase may also act as a solvent for various other important food components, including oil-soluble vitamins, antioxidants, preservatives, and essential oils. Reducing the lipid content of an emulsion can therefore have a profound influence on its flavor profile, stability, and nutritional content.

The characteristic appearance and rheology of food emulsions is largely a result of the immiscibility of oil and water, since this leads to a system where the droplets of one phase are dispersed in the other phase. Food emulsions usually appear turbid, cloudy, or opaque because the light passing through them is scattered by these droplets (McClements, 2002a,b). The intensity of the scattering depends on the concentration of droplets present, so that both the color and opacity of food emulsions are strongly influenced by their fat content (Chapter 10). The rheology of many food emulsions also depends on the fat content, since their overall viscosity increases with increasing droplet concentration, for example, creams, desserts, dressings, and mayonnaise (Chapter 8). The characteristic texture of some food emulsions is due to the ability of the oil phase to crystallize (Mulder and Walstra, 1974; Moran, 1994; Walstra, 2003a). The "spreadability" of water-in-oil (W/O) emulsions, such as margarines and butters, is determined by the formation of a three-dimensional network of aggregated fat crystals in the continuous phase which provides the product with mechanical rigidity (Moran, 1994; Flack, 1997). On the other hand, the creation of products such as ice cream and whipped cream depends on the controlled destabilization of partially crystalline oil droplets in oil-in-water (O/W) emulsions (Goff, 1997a-c). The tendency of a cream to thicken or "clot" when it is cooled below a certain temperature is due to the formation of fat crystals in the oil droplets, which causes them to aggregate (Boode, 1992). The melting of fat crystals in the mouth causes a cooling sensation that is an important sensory attribute of many fatty foods (Walstra, 1987).



The ability of food scientists to improve the quality of food emulsions therefore depends on an improved understanding of the multiple roles that fats and oils play in determining their properties.

### 4.2.1 Molecular structure and organization

Chemically, triacylglycerols are esters of a glycerol molecule and three fatty acid molecules (Figure 4.1). Each of the fatty acids may contain different numbers of carbon atoms, and may have different degrees of unsaturation and branching (Lawson, 1995; Nawar, 1996; Gunstone, 1997; Larsson, 2004). Nevertheless, most naturally occurring fatty acids have an even number of carbon atoms (usually less than 24) and are nonbranched. The fact that there are many different types of fatty acid molecules, and that these fatty acids can be located at different positions on the glycerol molecule, means that there are a huge number of possible triacylglycerol molecules present in foods. Indeed, edible fats and oils always contain a great many different types of triacylglycerol molecules, with the precise type and concentration depending on their origin (Weiss, 1983; Gunstone and Padley, 1997; Akoh and Min, 2002).

Triacylglycerol molecules have a “tuning-fork” structure, with the two fatty acids at the ends of the glycerol molecule pointing in one direction, and the fatty acid in the middle pointing in the opposite direction (Figure 4.1). Triacylglycerols are predominantly nonpolar molecules and so the most important types of molecular interactions with their neighbors are van der Waals attraction and steric overlap repulsion (Chapter 2). At a certain molecular separation there is a minimum in the intermolecular pair potential whose depth is a measure of the strength of the attractive interactions that hold the molecules together in the solid and liquid states (Section 2.4). Whether a triacylglycerol exists as a liquid or solid at a particular temperature depends on a balance between these attractive interactions and the disorganizing influence of the thermal energy (Section 4.2.3).

### 4.2.2 Bulk physicochemical properties

The bulk physicochemical properties of edible fats and oils depend on the molecular structure and interactions of the triacylglycerol molecules that they contain (Formo, 1979; Gunstone and Norris, 1983; Birker and Padley, 1987; Timms, 1991, 1995; Larsson, 2004). The strength of the attractive interactions between molecules and the effectiveness of their packing in a condensed phase determines their melting point, density, and rheology (Israelachvili, 1992). Triacylglycerols that contain branched or unsaturated fatty acids are not able to pack as closely together as those that contain linear saturated fatty acids, and so they have lower densities and higher compressibilities than saturated triacylglycerols (Walstra, 1987). The temperature at which a triacylglycerol melts also depends on the packing of the molecules: the more effective the packing the higher the melting point

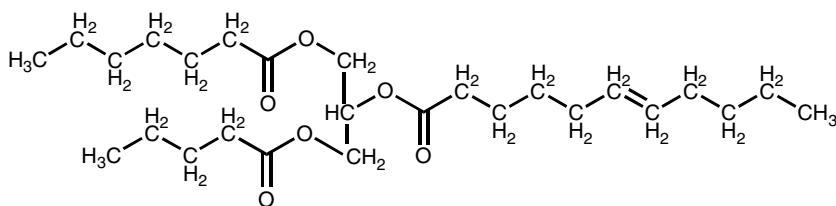


**Figure 4.1** Chemical structure of a triacylglycerol molecule, which is assembled from three fatty acids and a glycerol molecule.

**Table 4.1** Melting Points and Heats of Fusion of the Most Stable Polymorphic forms of Selected Triacylglycerol Molecules: L = Lauric Acid (C12:0); M = Myristic Acid (C14:0); P = Palmitic Acid (C16:0); S = Stearic Acid (C16:0); O = Oleic Acid (C18:1); Li = Linoleic (C18:2); and Ln = Linolenic (C18:3)

Triglyceride	Melting Point (°C)	$\Delta H_f$ (J g <sup>-1</sup> )
LLL	46	186
MMM	58	197
PPP	66	205
SSS	73	212
OOO	5	113
LiLiLi	-13	85
LnLnLn	-24	—
SOS	43	194
SOO	23	—

Source: Adapted from Walstra (2003a).

(Israelachvili, 1992; Walstra, 2003a). Thus, the melting points of triacylglycerols increase with increasing chain length; are higher for saturated than for unsaturated fatty acids; are higher for straight chained than branched fatty acids; and, are higher for triacylglycerols with a more symmetrical distribution of fatty acids on the glycerol molecule (Table 4.1). Triacylglycerol molecules have a relatively low dielectric constant because of their low polarity (Table 4.2). Knowledge of the dielectric constant of oils is important because it influences the range and magnitude of the colloidal interactions between droplets in emulsions, especially van der Waals and electrostatic interactions (Chapter 3).

Many of the bulk physicochemical properties of edible fats and oils have an important influence on the formation and stability of food emulsions. The creaming stability of emulsions depends on the density contrast between the oil and aqueous phases, and hence changes in the density of the oil phase may cause changes in the long-term stability of an emulsion (Section 7.3). The minimum size of droplets that can be produced by some homogenizers depends on the ratio of the viscosity of the dispersed phase to that of the continuous phase (Section 6.4.1). The viscosity of edible lipids decreases appreciably with temperature, and the precise nature of the viscosity–temperature profile depends on lipid type and composition (Coupland and McClements, 1997). Hence, the ability to produce an emulsion containing small droplets may depend on the nature of the oil used, as well

**Table 4.2.** Comparison of Some Bulk Physicochemical Properties of Liquid Oil (Triolein) and Water at 20°C

	Oil	Water
Molecular weight	885	18
Melting point(°C)	5	0
Density(kg m <sup>-3</sup> )	910	998
Compressibility	$5.03 \times 10^{-10}$	$4.55 \times 10^{-10}$
Viscosity(mPa s)	≈50	1.002
Thermal conductivity(W m <sup>-1</sup> K <sup>-1</sup> )	0.170	0.598
Specific heat capacity(J kg <sup>-1</sup> K <sup>-1</sup> )	1980	4182
Thermal expansion coefficient(°C <sup>-1</sup> )	$7.1 \times 10^{-4}$	$2.1 \times 10^{-4}$
Dielectric constant	3	80.2
Surface tension(mN m <sup>-1</sup> )	≈35	72.8
Refractive index	1.46	1.333

as on the homogenization conditions used in the emulsion preparation, for example, valve pressure, temperature. The interfacial tension of an oil–water interface may also influence the size of the droplets produced during homogenization, since droplet disruption usually becomes easier as the interfacial tension decreases (Section 6.4.1). The interfacial tension may also affect the long-term stability of emulsions by influencing the composition and properties of the interface formed. The interfacial tension of an oil depends on the polarity of the dominant lipid molecules present (e.g., triacylglycerols or terpenes), as well as on the presence of any minor surface-active components (e.g., free fatty acids, monoacylglycerols, diacylglycerols, or phospholipids). There can be significant variations in the interfacial tensions produced by oils depending on their origin and purity (Chanamai et al., 2002). Oil polarity may also influence the partitioning of functional constituents (such as flavors, antioxidants, preservatives, or colors) between the oil and aqueous phases, which may alter the physicochemical or sensory properties of the system. The strength and range of the colloidal interactions between the droplets in emulsions are determined by the dielectric constant and refractive index of the component phases (Chapter 3). The appearance of an emulsion depends on the scattering of light by the emulsion droplets and the absorption of light by any chromophoric materials present (Chapter 10), hence usage of oils of different refractive index or color may lead to differences in emulsion appearance. In summary, differences in the bulk physicochemical properties of oils can cause appreciable changes in the stability and properties of food emulsions.

The bulk physicochemical properties of many edible oils and fats are fairly similar (Coupland and McClements, 1997), and therefore the choice of oil type may not have a large influence on the overall properties of an emulsion. Nevertheless, some types of oil do have significantly different properties from the majority of other oils, which may appreciably influence their functional characteristics in emulsions. This may be particularly important when trying to replace one type of oil with another chemically-different type, for example, oil rich in monosaturated lipids with oil rich in polyunsaturated lipids, or a conventional oil with a fat substitute (Lindsay, 1996a). It should be noted that much of the research carried out to establish the colloidal basis of emulsion properties uses simple model systems containing highly purified oils with known chemical structures, for example, hydrocarbons. These model oils may facilitate the interpretation of experimental data, but one should be careful to ensure that conclusions drawn from these model systems apply to real food emulsions.

### 4.2.3 *Fat crystallization*

One of the most important characteristics of fats and oils is their ability to undergo solid–liquid phase transitions at temperatures that occur during the processing, storage, and handling of food emulsions (Walstra, 1987, 2003a; Timms, 1991, 1995; Gunstone and Padley, 1997; Lawler and Dimick, 2002). The texture, mouthfeel, stability, and appearance of many food emulsions depend on the physical state of the lipid phase (Moran, 1994). The conversion of milk into butter relies on the controlled destabilization of an O/W emulsion (milk) into a W/O emulsion (butter), which is initiated by the formation of crystals in the milk fat globules (Mulder and Walstra, 1974; Boode, 1992). The spreadability of the butter produced by this process is governed by the final concentration of fat crystals (Moran and Rajah, 1994). If the percentage of fat crystals is too high the product is firm and difficult to spread, and if it is too low the product is soft and tends to collapse under its own weight. The creation of food emulsions with desirable properties therefore depends on an understanding of the major factors that influence the crystallization and melting of lipids in foods (Birker and Padley, 1987).

The arrangement of triacylglycerol molecules in the solid and liquid state is shown schematically in Figure 4.2. The physical state of a triacylglycerol at a particular temperature

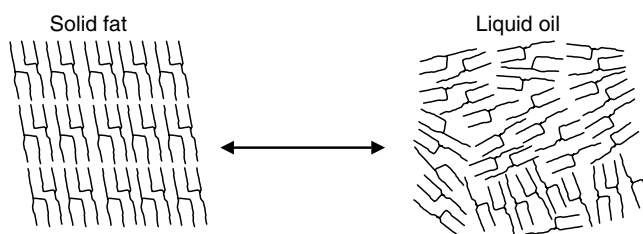


**Figure 4.2** The arrangement of triacylglycerols in the solid and liquid states depends on a balance between the organizing influence of the attractive interactions between the molecules and the disorganizing influence of the thermal energy.

depends on its free energy, which is made up of contributions from enthalpic and entropic terms:  $\Delta G_{S \rightarrow L} = \Delta H_{S \rightarrow L} - T\Delta S_{S \rightarrow L}$  (Atkins, 1994). The enthalpy term ( $\Delta H_{S \rightarrow L}$ ) represents the change in the overall strength of the molecular interactions between the triacylglycerols when they are converted from a solid to a liquid, whereas the entropy term ( $\Delta S_{S \rightarrow L}$ ) represents the change in the organization of the molecules that is brought about by the melting process. The strength of the bonds between the molecules is greater in the solid state than in the liquid state because the molecules are able to pack more efficiently, and so  $\Delta H_{S \rightarrow L}$  is positive, which favors the solid state. On the other hand, the entropy of the molecules in the liquid state is greater than that in the solid state, and therefore  $\Delta S_{S \rightarrow L}$  is positive, which favors the liquid state. At low temperatures, the enthalpy term dominates the entropy term ( $\Delta H_{S \rightarrow L} > T\Delta S_{S \rightarrow L}$ ), and therefore the solid state has the lowest free energy (Atkins, 1994; Walstra, 2003a). As the temperature increases, the entropic contribution becomes increasingly important. Above a certain temperature, known as the *melting point*, the entropy term dominates the enthalpy term ( $T\Delta S_{S \rightarrow L} > \Delta H_{S \rightarrow L}$ ) and so the liquid state has the lowest free energy. A material therefore changes from a solid to a liquid when its temperature is raised above the melting point. A solid-to-liquid transition (melting) is endothermic because energy must be added to the system to pull the molecules further apart. Conversely, a liquid-to-solid transition (crystallization) is exothermic because energy is released as the molecules come closer together.

The temperature dependence of the free energies of the solid and liquid states shows that below the melting point the solid state has the lowest free energy, but above it the liquid state has the lowest (Figure 4.3). Thermodynamics informs us whether or not a phase transition can occur, but it tells us nothing about the rate at which this process occurs or about the physical mechanism by which it is accomplished (Atkins, 1994). As will be seen below, an understanding of lipid phase transitions requires knowledge of both the thermodynamics and kinetics of the process. The crystallization of fats can be conveniently divided into three stages: supercooling, nucleation, and crystal formation (Boistelle, 1988; Mullin, 1993; Roos, 1995; Hartel, 2001; Mullin, 2001; Marangoni and Narine, 2002; Walstra, 2003a).

#### 4.2.3.1 Supercooling

Crystallization can only take place once a liquid phase is cooled below its melting point (Garside, 1987; Walstra, 1987, 2003a). Even so, a material may persist as a liquid below its melting point for a considerable time before any crystallization is observed (Skoda and van Tempel, 1963; Phipps, 1964; Mulder and Walstra, 1974). This is because of an activation energy that must be overcome before the liquid–solid phase transition can occur (Figure 4.4). If the magnitude of this activation energy is sufficiently high compared to the thermal energy of the system crystallization will not occur, even though the transition is thermodynamically favorable (Turnbull and Cormia, 1961). The system is then said to

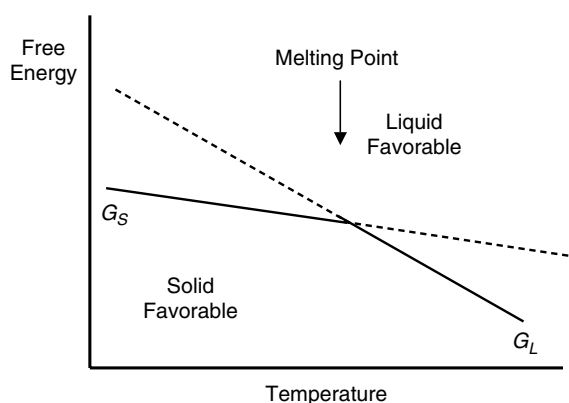


**Figure 4.3** Temperature dependence of the free energies of the solid and liquid states. At low temperatures the solid state is thermodynamically favorable, but above the melting point the liquid state is more favorable.

exist in a *metastable* state. The height of the activation energy depends on the ability of crystal nuclei to be formed in the liquid oil that are stable enough to grow into crystals (see Section 4.2.3.2.). The degree of supercooling of a liquid is defined as  $\Delta T = T - T_{mp}$ , where  $T$  is the temperature and  $T_{mp}$  is the melting point. The value of  $\Delta T$  at which crystallization is first observed depends on the chemical structure of the oil, the presence of any contaminating materials, the cooling rate, the microstructure of the oil (e.g., bulk vs. emulsified), and the application of external forces (Dickinson and McClements, 1995; Hartel, 2001). Pure oils containing no impurities can often be supercooled by more than 10°C before any crystallization is observed (Turnbull and Cormia, 1961; Dickinson et al., 1990; McClements et al., 1993a).

#### 4.2.3.2 Nucleation

Crystal growth can only occur after stable nuclei have been formed in a liquid. These nuclei are believed to be clusters of oil molecules that form small ordered crystallites, and are formed when a number of oil molecules collide and become associated with each other

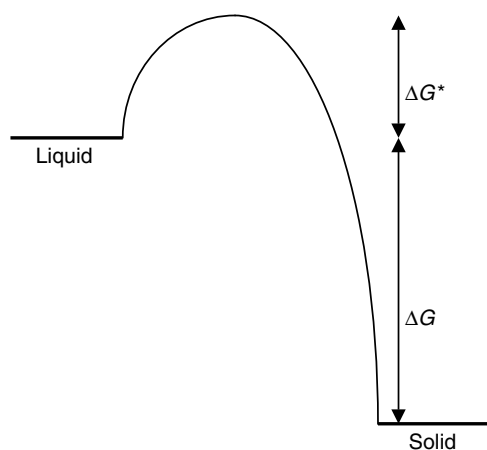


**Figure 4.4** When there is a sufficiently high activation energy between the solid and liquid states a liquid oil can persist in a metastable state below the melting point of a fat.

(Hernqvist, 1984; Hartel, 2001). There is a free energy change associated with the formation of one of these nuclei (Garside, 1987). Below the melting point, the bulk crystalline state is thermodynamically favorable, and so there is a decrease in free energy when some of the oil molecules in the liquid cluster together to form a nucleus. This negative free energy ( $\Delta G_V$ ) change is proportional to the volume of the nucleus formed. On the other hand, the formation of a nucleus leads to the creation of a new interface between the solid and liquid phases which requires an input of free energy to overcome the interfacial tension (Chapter 5). This positive free energy ( $\Delta G_S$ ) change is proportional to the surface area of the nucleus formed. The total free energy change associated with the formation of a nucleus is therefore a combination of a volume and a surface term (Hartel, 2001; Walstra, 2003a):

$$\Delta G = \Delta G_V + \Delta G_S = \frac{4}{3}\pi r^3 \frac{\Delta H_{\text{fus}} \Delta T}{T_{\text{mp}}} + 4\pi r^2 \gamma_i \quad (4.1)$$

where  $r$  is the radius of the nuclei,  $\Delta H_{\text{fus}}$  is the enthalpy change per unit volume associated with the liquid–solid transition (which is negative), and  $\gamma_i$  is the solid–liquid interfacial tension. The volume contribution becomes increasingly negative as the size of the nuclei increases, whereas the surface contribution becomes increasingly positive (Figure 4.5). The surface contribution dominates for small nuclei, while the volume term dominates for large nuclei. The overall free energy has a maximum value at a certain critical nucleus radius ( $r^*$ ):

$$\frac{d\Delta G}{dr} = 4\pi r^2 \frac{\Delta H_{\text{fus}} \Delta T}{T_{\text{mp}}} + 8\pi r \gamma_i = 0 \quad (4.2)$$

This equation can be rearranged to give an expression for the critical radius of the nucleus that must be achieved for crystallization to occur:

$$r^* = \frac{2\gamma_i T_{\text{mp}}}{\Delta H_{\text{fus}} \Delta T} \quad (4.3)$$

If a nucleus is formed that has a radius below this critical size it will tend to dissociate so as to reduce the free energy of the system. On the other hand, if a nucleus is formed that has a radius above this critical value it will tend to grow into a crystal. This equation

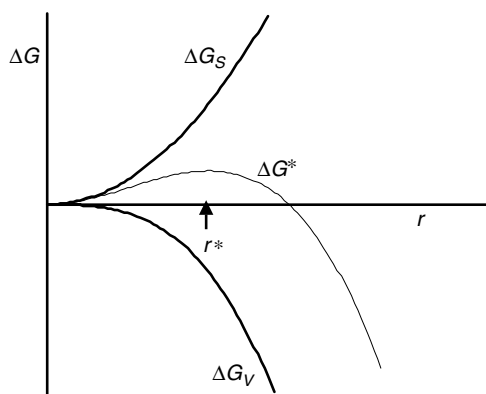


**Figure 4.5** The critical size of a nucleus required for crystal growth depends on a balance between the volume and surface contributions to the free energy of nuclei formation.

indicates that the critical size of nuclei required for crystal growth decreases as the degree of supercooling increases, which accounts for the increase in nucleation rate with decreasing temperature.

The rate at which nucleation occurs can be related to the activation energy  $\Delta G^*$  that must be overcome before a stable nuclei is formed (Boistelle, 1988):

$$J = A \exp(-\Delta G^*/kT) \quad (4.4)$$

where  $J$  is the nucleation rate, which is equal to the number of stable nuclei formed per second per unit volume of material,  $A$  is a preexponential factor,  $k$  is Boltzmann's constant, and  $T$  is the absolute temperature. The value of  $\Delta G^*$  is calculated by replacing  $r$  in Equation 4.1 with the critical radius given in Equation 4.3. The variation of the nucleation rate predicted by Equation 4.4 with the degree of supercooling ( $\Delta T$ ) is shown in Figure 4.6. The formation of stable nuclei is negligibly slow at temperatures just below the melting point, but increases dramatically when the liquid is cooled below a certain temperature,  $T^*$ . In reality, the nucleation rate increases with cooling up to a certain temperature, but then decreases on further cooling. This is because the increase in viscosity of the oil that occurs as the temperature is decreased slows down the diffusion of oil molecules toward the liquid–nucleus interface (Boistelle, 1988; Hartel, 2001). Consequently, there is a maximum in the nucleation rate at a particular temperature (Figure 4.6).

The type of nucleation described above occurs when there are no impurities present in the oil, and is usually referred to as *homogeneous nucleation* (Boistelle, 1988). If the liquid oil is in contact with foreign surfaces, such as the surfaces of dust particles, fat crystals, oil droplets, air bubbles, reverse micelles, or the vessel containing the oil, then nucleation can be induced at a higher temperature than expected for a pure system (Walstra, 1987, 2003a; McClements et al., 1993a; Hartel, 2001). Nucleation due to the presence of these foreign surfaces is referred to as *heterogeneous nucleation*, and can be divided into two types: primary and secondary (Boistelle, 1988; Hartel, 2001). Primary heterogeneous nucleation occurs when the foreign surfaces have a different chemical structure to that of the oil, whereas secondary heterogeneous nucleation occurs when the foreign surfaces are crystals with the same chemical structure as the liquid oil. Heterogeneous nucleation occurs when the impurities provide a surface where the formation of stable nuclei is more thermodynamically favorable than in the pure oil (Boistelle, 1988). As a result the degree

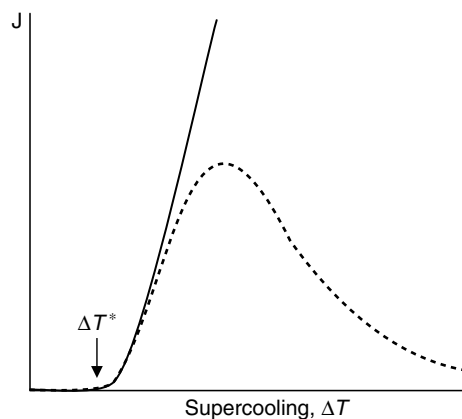


**Figure 4.6** Theoretically, the rate of the formation of stable nuclei increases with supercooling (solid line), but in practice, the nucleation rate decreases below a particular temperature because the diffusion of oil molecules is retarded by the increase in oil viscosity (broken line).

of supercooling required to initiate fat crystallization is reduced. On the other hand, certain types of impurities are capable of decreasing the nucleation rate of oils because they are incorporated into the surface of the growing nuclei and prevent any further oil molecules being incorporated (Hartel, 2001). Whether an impurity acts as a catalyst or an inhibitor of nucleation depends on its molecular structure and interactions with the nuclei (Boistelle, 1988; Garti and Yano, 2001). It should be noted that there is still considerable debate about the mathematical modeling of nucleation, since existing theories often give predictions of nucleation rates that are greatly different from experimental measurements (Walstra, 2003a). Nevertheless, the general form of the dependence of nucleation rates on temperature are predicted fairly well by existing theories.

#### 4.2.3.3 *Crystal growth*

Once stable nuclei have been formed, they grow into crystals by incorporating molecules from the liquid oil at the solid–liquid interface (Garside, 1987; Boistelle, 1988; Hartel, 2001; Walstra, 2003a). It should be noted that crystals have different faces, and each face may grow at an appreciably different rate, which partially accounts for the wide variety of different crystal shapes that can be formed by fats. The overall crystal growth rate depends on a number of factors, including mass transfer of the liquid molecules to the solid–liquid interface, mass transfer of noncrystallizing species away from the interface, incorporation of the liquid molecules into the crystal lattice, or removal of the heat generated by the crystallization process from the interface (Hartel, 2001). Any of these processes can be rate-limiting depending on the molecular characteristics of the system and the prevailing environmental conditions, for example, temperature profile and mechanical agitation. Consequently, a general theoretical model of crystal growth is difficult to construct. In crystallizing lipid systems, the incorporation of a molecule at the crystal surface is often rate-limiting at high temperatures, whereas the diffusion of a molecule to the solid–liquid interface is often rate-limiting at low temperatures. This is because the viscosity of the liquid oil increases as the temperature is lowered and so the diffusion of a molecule is retarded. The crystal growth rate therefore increases initially with supercooling, has a maximum rate at a certain temperature, and then decreases on further supercooling (Hartel, 2001). The dependence of the growth rate on temperature therefore shows a similar trend to the nucleation rate (Figure 4.6); however, the maximum rate of nuclei formation usually occurs at a different temperature to the maximum rate of crystal growth. Experimentally, it has been observed that the rate of crystal growth is proportional to the degree of supercooling, and inversely proportional to the viscosity of the melt (Timms, 1991).

A variety of mathematical theories have been developed to model the rate of crystal growth in crystallizing fats (Hartel, 2001). The most appropriate model for a specific situation depends on the rate-limiting step for that particular system under the prevailing environmental conditions, for example, mass transfer of the liquid molecules to the solid–liquid interface, mass transfer of noncrystallizing species away from the interface, incorporation of the liquid molecules into the crystal lattice, or removal of the heat generated by the crystallization process from the interface (Hartel, 2001).

It should be noted that once crystallization is complete, there may still be changes in crystal size and shape during storage due to postcrystallization processes, such as crystal aggregation or Ostwald ripening (Hartel, 2001; Walstra, 2003a). Crystal aggregation occurs when two or more crystals come together and form a larger crystal, whereas Ostwald ripening occurs when oil molecules migrate from smaller crystals to large crystals through the intervening medium. Aggregation and Ostwald ripening therefore both lead to an increase in the average size of the crystals present within a fat. Crystal growth during storage is often undesirable since it adversely affects the physicochemical and sensory properties of the final product (Walstra, 2003a).



#### 4.2.3.4 Crystal morphology

The morphology of the crystals formed depends on a number of internal factors (e.g., molecular structure, composition, packing, and interactions) and external factors (e.g., temperature–time profile, mechanical agitation, and impurities). In general, when a liquid oil is cooled rapidly to a temperature well below its melting point a large number of small crystals are formed, but when it is cooled slowly to a temperature just below its melting point a smaller number of larger crystals are formed (Moran, 1994; Timms, 1995; Hartel, 2001; Walstra, 2003a). This is because the nucleation rate increases more rapidly with decreasing temperature than the crystallization rate. Thus, rapid cooling produces many nuclei simultaneously that subsequently grow into small crystals, whereas slow cooling produces a smaller number of nuclei that have time to grow into larger crystals before further nuclei are formed. Crystal size has important implications for the rheology and organoleptic properties of many types of food emulsions. When crystals are too large they are perceived as being “grainy” or “sandy” in the mouth (Walstra, 1987, 2003a). The efficiency of molecular packing in crystals also depends on the cooling rate. If a fat is cooled slowly, or the degree of supercooling is small, then the molecules have sufficient time to be efficiently incorporated into a crystal (Walstra, 1987). At faster cooling rates, or higher degrees of supercooling, the molecules do not have sufficient time to pack efficiently before another molecule is incorporated. Thus, rapid cooling tends to produce crystals that contain more dislocations, and in which the molecules are less densely packed (Timms, 1991). The cooling rate therefore has an important impact on the morphology and functional properties of crystalline lipids in foods.

#### 4.2.3.5 Polymorphism

Triacylglycerols exhibit a phenomenon known as *polymorphism*, which is the ability of a material to exist in a number of crystalline structures with different molecular packing (Hauser, 1975; Garti and Sato, 1988; Sato, 1988; Hernqvist, 1990; Hartel, 2001; Walstra, 2003a; Larsson, 2004). The three most commonly occurring types of packing in triacylglycerols are hexagonal, orthorhombic, and triclinic which are usually designated as  $\alpha$ ,  $\beta'$ , and  $\beta$  polymorphic forms, respectively. The thermodynamic stability of the three forms decreases in the order:  $\beta > \beta' > \alpha$ . Even though the  $\beta$  form is the most thermodynamically stable, triacylglycerols often crystallize in one of the metastable states because they have a lower activation energy of nuclei formation (Figure 4.7). With time the crystals transform

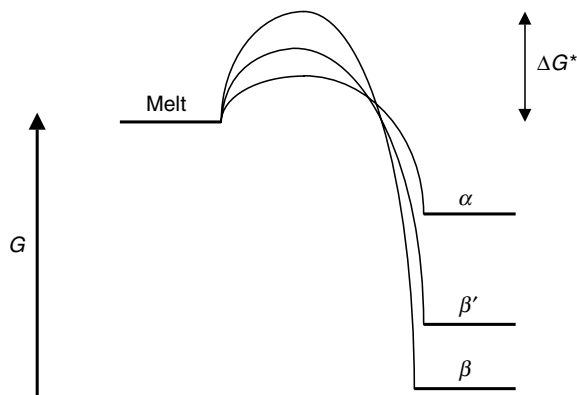


**Figure 4.7** The polymorphic state that is initially formed when an oil crystallizes depends on the relative magnitude of the activation energies associated with nuclei formation.

to the most stable state at a rate that depends on environmental conditions, such as temperature, pressure, and the presence of impurities (Timms, 1991). Polymorphic transitions often occur at a different rate in emulsified fats than in bulk fats (Walstra, 1987). In addition, the morphology and spatial arrangement of the crystals formed in emulsified fats is often different from those formed in bulk fats, which has been attributed to differences in heat transfer rates when crystallizing fats are surrounded by water rather than by oil and because of the physical limitations imposed by the droplet surfaces (Walstra, 2003a). Knowledge of the polymorphic form of the crystals in an emulsified fat is often important because it can impact the physicochemical and sensory properties of food emulsions.

#### 4.2.3.6 Crystallization of edible fats and oils

The melting point of a triacylglycerol depends on the chain length, branching, and degree of unsaturation of its constituent fatty acids, as well as their relative positions along the glycerol molecule (Table 4.1). Edible fats and oils contain a complex mixture of many different types of triacylglycerol molecules, each with a different melting point, and so they usually melt over a wide range of temperatures, rather than at a distinct temperature as would be the case for a pure triacylglycerol (Figure 4.8).

The melting profile of a fat is not simply the weighted sum of the melting profiles of its constituent triacylglycerols, because high melting point triacylglycerols are soluble in lower melting point ones (Timms, 1991). For example, in a 50:50 mixture of tristearin and triolein it is possible to dissolve 10% of solid tristearin in liquid triolein at 60°C (Walstra, 1987; Timms, 1995). The solubility of a solid component in a liquid component can be predicted assuming they have widely differing melting points (>20°C):

$$\ln x = \frac{\Delta H_{\text{fus}}}{R} \left[ \frac{1}{T_{\text{mp}}} - \frac{1}{T} \right] \quad (4.5)$$

Here  $x$  is the solubility, expressed as a mole fraction of the higher melting point component in the lower melting point component, and  $\Delta H_{\text{fus}}$  is the molar heat of fusion (Walstra, 1987).

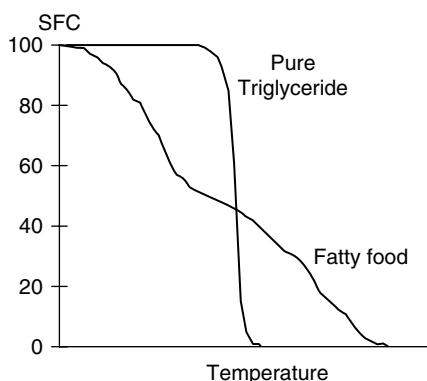


**Figure 4.8** Comparison of the melting profile of a pure triacylglycerol and a typical edible fat. The edible fat melts over a much wider range of temperatures because it consists of a mixture of many different pure triacylglycerol molecules each with different melting points.

The structure and physical properties of crystals produced by cooling a complex mixture of triacylglycerols is strongly influenced by the cooling rate and temperature (Moran, 1994; Hartel, 2001; Walstra, 2003a). If an oil is cooled rapidly all the triacylglycerols crystallize at approximately the same time and a *solid solution* is formed, which consists of homogeneous crystals in which the triacylglycerols are intimately mixed with each other (Walstra, 1987, 2003a). On the other hand, if the oil is cooled slowly the higher melting point triacylglycerols crystallize first, while the low melting point triacylglycerols crystallize later, and so *mixed crystals* are formed. These crystals are heterogeneous and consist of some regions that are rich in high melting point triacylglycerols and other regions that are depleted in these triacylglycerols. Whether a crystalline fat forms mixed crystals or a solid solution influences many of its physicochemical properties, such as density, compressibility, and melting profile (Walstra, 1987), which could have an important influence on the properties of a food emulsion.

Once a fat has crystallized, the individual crystals may aggregate to form a three-dimensional network that traps liquid oil through capillary forces (Moran, 1994). The interactions responsible for crystal aggregation in pure fats are primarily van der Waals interactions between the solid fat crystals, although "water bridges" between the crystals have also been proposed to play an important role (Moran, 1994). Once aggregation has occurred the fat crystals may partially fuse together which strengthens the crystal network (Timms, 1994, 1995; Walstra, 2003a). The system may also change over time due to the growth of larger crystals at the expense of smaller ones, that is, Ostwald ripening (Section 7.8).

#### 4.2.3.7 Fat crystallization in emulsions

The influence of fat crystallization on the bulk physicochemical properties of food emulsions depends on whether the fat forms the continuous phase or the dispersed phase. The characteristic stability and rheological properties of W/O emulsions, such as butter and margarine, are determined by the presence of a network of aggregated fat crystals within the continuous (oil) phase (Moran, 1994; Chrysam, 1996). The fat crystal network is responsible for preventing the water droplets from sedimenting under the influence of gravity, as well as determining the spreadability of the product. If there are too many fat crystals present the product is firm and difficult to spread, but when there are too few crystals present the product is soft and collapses under its own weight. Selection of a fat with the appropriate melting characteristics is therefore one of the most important aspects of margarine and spread production (Gunstone and Norris, 1983; Gunstone and Padley, 1997). The melting profile of natural fats can be optimized for specific applications by various physical or chemical methods, including blending, interesterification, fractionation, and hydrogenation (Birker and Padley, 1987; Gunstone and Padley, 1997).

Fat crystallization also has a pronounced influence on the physicochemical properties of many O/W emulsions, such as milk or salad cream (Mulder and Walstra, 1974; Boode, 1992). When the fat droplets are partially crystalline, a crystal from one droplet can penetrate into another droplet during a collision which causes the two droplets to stick together (Walstra, 1987; Boode, 1992; Dickinson and McClements, 1995). This phenomenon is known as *partial coalescence* and leads to a dramatic increase in the viscosity of an emulsion, as well as a decrease in the stability to creaming (Section 7.7). Extensive partial coalescence can eventually lead to phase inversion, that is, conversion of an O/W emulsion to a W/O emulsion (Mulder and Walstra, 1974). This process is one of the most important steps in the production of butters, margarines, and spreads (Moran and Rajah, 1994). Partial coalescence is also important in the production of ice cream and whipped creams, where an O/W emulsion is cooled to a temperature where the fat in the droplets partially crystallizes and is mechanically agitated to promote droplet collisions and aggregation

(Goff, 1997a–c). The aggregated droplets form a two-dimensional network around the air bubbles and a three-dimensional network in the continuous phase that contribute to the stability and texture of the product (Walstra, 2003a).

#### 4.2.4 Chemical changes

The type and concentration of molecules within the lipid phase can change with time due to chemical reactions. The two most important chemical changes that occur in edible fats and oils are lipolysis and oxidation (Sonntag, 1979b; Nawar, 1996). Lipolysis is the process where ester bonds of fats and oils are hydrolyzed by certain enzymes, or by a combination of heat and moisture. The result of lipolysis is the liberation of free fatty acids, which can be either detrimental or desirable to food quality. Lipolysis has deleterious effects on the quality of some food products because it leads to the generation of rancid off-flavors and off-odors (*hydrolytic rancidity*). In addition, free fatty acids are more surface-active than triacylglycerols and therefore accumulate preferentially at an oil–water or air–water interface, which increases their susceptibility to oxidation and may increase the tendency for emulsion droplets to coalesce (Coupland et al., 1996; Coupland and McClements, 1996). On the other hand, a limited amount of lipolysis is beneficial to the quality of some foods because it leads to the formation of desirable flavors and aromas, for example, cheese and yogurt (Nawar, 1996).

Many food emulsions contain polyunsaturated lipids that are highly susceptible to lipid oxidation. Indeed, lipid oxidation is one of the most serious causes of quality deterioration in many foods because it leads to the generation of undesirable off-flavors and off-odors (*oxidative rancidity*), as well as potentially toxic reaction products (Schultz, 1962; Simic et al., 1992; Nawar, 1996). In other foods, a limited amount of lipid oxidation is beneficial because it leads to the generation of a desirable flavor profile, for example, cheese. The term *lipid oxidation* describes an extremely complex series of chemical reactions that involves unsaturated lipids and oxygen (Halliwell and Gutteridge, 1991; Nawar, 1996). It has proved convenient to divide these reactions into three different types: initiation, propagation, and termination. Initiation occurs when a hydrogen atom is extracted from the methylene group ( $-\text{CH}=\text{CH}-$ ) of a polyunsaturated fatty acid, leading to the formation of a free radical ( $-\text{CH}=\text{C}^{\cdot}-$ ). This process can be started by a variety of different initiators that are present in foods, including naturally occurring lipid peroxides, transition metal ions, ultraviolet (UV) light, and enzymes (Nawar, 1996). It is worthwhile noting that many of these initiators are predominantly water soluble, which has important implications for the oxidation of emulsified oils, because the initiator must either travel through or interact across the interfacial membrane in order to come into contact with the oil (Coupland and McClements, 1996; McClements and Decker, 2000). Once a free radical has formed it reacts with oxygen to form a peroxy radical ( $-\text{CH}-\text{COO}^{\cdot}-$ ). These radicals are highly reactive and can extract hydrogen atoms from other unsaturated lipids and therefore propagate the oxidation reaction. Termination occurs when two radicals interact with each other to form a nonradical, and thus end their role as propagators of the reaction. During lipid oxidation a number of decomposition reactions occur simultaneously, which leads to the formation of a complex mixture of reaction products, including aldehydes, ketones, alcohols, and hydrocarbons (Nawar, 1996). Many of these products are volatile and therefore contribute to the characteristic odor associated with lipid oxidation. Some of the products are surface-active and would therefore accumulate at oil–water interfaces in emulsions, whereas others are water soluble and would therefore leach into the aqueous phase of emulsions (Coupland and McClements, 1996; McClements and Decker, 2000).

The growing trend of incorporating polyunsaturated lipids into food products in order to improve their nutritional profiles has meant that there has been a considerable research

effort to elucidate the relationship between emulsion properties and lipid oxidation (Frankel, 1991; Frankel et al., 1994; Coupland and McClements, 1996; McClements and Decker, 2000). Some of the work carried out in this area is discussed in the chapter on emulsion stability (Section 7.10).

#### 4.2.5 Selection of an appropriate lipid

A variety of edible fats and oils are available for usage in food emulsions, and the choice of the most appropriate type for a particular application depends on the nutritional, physicochemical, and sensory characteristics desired for that specific product. Some of the most important characteristics to consider when selecting a lipid source are briefly highlighted below.

##### 4.2.5.1 Nutritional profile

As mentioned earlier, there is a major trend in the food industry to decrease or increase the concentration of lipid components whose overconsumption (e.g., cholesterol, saturated fats, trans fatty acids) or underconsumption (e.g., polyunsaturated fats,  $\omega$ -3 fatty acids), respectively, has been linked to human health problems (Chow, 1992; Smolin and Grosvenor, 1994; Gurr, 1997; Kritchevsky, 2002). Many food manufacturers are therefore reformulating their products to replace existing oil sources with lipids with more healthful nutritional profiles (Jones, 1996). These more healthful lipids could be oils from different natural sources (e.g., fish oils), modified oils (e.g., chemically, physically, enzymatically, or genetically modified oils) or fat substitutes with low calorific values (e.g., Olestra<sup>TM</sup>). Nevertheless, changing the nutritional profile of an oil may also cause appreciable changes in its physicochemical and sensory properties (e.g., flavor profile, crystallization characteristics, and viscosity), which may adversely influence its functional properties within a specific product. For this reason, research is currently being carried out to produce emulsions containing oils with improved nutritional profiles, but which also maintain their desirable functional properties.

##### 4.2.5.2 Flavor profile

Triacylglycerols are relatively large molecules that have a low volatility and hence little inherent flavor. Nevertheless, different natural sources of edible fats and oils do have distinctive flavor profiles because of the characteristic volatile breakdown products and impurities that they contain, for example, compare the aromas of corn oil, olive oil, and fish oil. Oil from a specific natural source may therefore be selected for usage in a particular food product because it contributes to the overall flavor profile of the emulsion. The oil phase may also indirectly influence the flavor profile because of its ability to act as a solvent for volatile nonpolar molecules. The partitioning of flavor molecules among oil, water, and headspace regions and their release rate during mastication depends on factors such as the polarity, viscosity, and crystallinity of the lipid phase, which may vary from one source of oil to another (Chapter 9).

##### 4.2.5.3 Crystallization behavior

The suitability of edible fats and oils for many applications within food emulsions depends on their melting and crystallization temperatures, solid fat content (SFC)–temperature profile, crystal morphology, and polymorphic type. In some emulsions it is important that the fat does not crystallize during the lifetime of the product since this would lead to instability through partial coalescence. For example, it is important that the oils used to produce dressings do not crystallize (*cloud*) when exposed to refrigerator temperatures (Lopez, 1981; Hui, 1992). This can be achieved either by using oil sources that naturally

have low melting points, or by removing high melting fractions by selective crystallization (*winterization*) or by adding components that retard crystal formation, such as oil-soluble surfactants (Brandt, 1999). In other food emulsions the crystallization of the lipid phase is an integral part of their production and determines their desirable physicochemical and sensory attributes, for example, margarine, butter, whipped cream, ice cream. In these products it is usually important to select an oil that has a particular SFC versus temperature profile, and that forms crystals of the appropriate morphology and polymorphic form. A variety of analytical techniques are available to characterize the crystallization behavior of oils (Chapter 11). The desired crystallization characteristics can be obtained by selection of a natural oil with an appropriate triacylglycerol composition, or the triacylglycerol composition of the oil phase can be obtained by blending, fractionation, interesterification, or hydrogenation of oils (Nawar, 1996).

#### 4.2.5.4 *Oxidative stability*

Many edible fats and oils naturally contain significant quantities of polyunsaturated lipids, which are highly susceptible to lipid oxidation. Lipid oxidation leads to a reduction in the concentration of these health-promoting polyunsaturated lipids, as well as to the generation of volatile compounds that may cause an undesirable rancid flavor. Flavor oils also contain components that are susceptible to oxidative degradation reactions that lead to loss of desirable flavors and/or production of undesirable off-flavors. When selecting an oil for use in an emulsion-based food product it is often important to ensure that it has not undergone a significant amount of lipid oxidation prior to use, and that it will have good oxidative stability throughout the lifetime of the product. Analytical tests are available to assess the extent of lipid oxidation that has already occurred in an oil and to predict the susceptibility of oils to oxidation (Pike, 2003). The oxidative stability of an emulsion can be improved by using an oil source naturally low in polyunsaturated fats or by reducing the polyunsaturated fat content of a natural oil, for example, by partial hydrogenation\*. Nevertheless, many food manufacturers want to increase the concentration of polyunsaturated fats in food products because of their potential health benefits. For these products it is important to develop effective strategies for preventing or retarding lipid oxidation during the shelf life of the product (McClements and Decker, 2000).

#### 4.2.5.5 *Bulk physicochemical properties*

The type and concentration of molecules within an oil phase determine its bulk physicochemical properties, for example, viscosity, density, refractive index, dielectric constant, polarity, interfacial tension. These properties may have an appreciable influence on the formation, stability, and quality attributes of a food emulsion (Section 4.2.2). Hence, oils from different natural sources or that have been processed differently may behave differently when used in an emulsion. These differences may have to be taken into account when reformulating an emulsion to change the type of lipid used to make up the oil phase.

#### 4.2.5.6 *Oil quality*

In addition to the impurities mentioned above, the oils used to prepare emulsions may contain a variety of other impurities that adversely affect their suitability for particular applications, including off-flavors, pigments, phospholipids, and free fatty acids. For this reason, components that have a negative impact on emulsion quality are usually removed from oils prior to their usage in food products, for example, by deodorization, neutralization,

\* It should be noted that hydrogenation leads to the production of trans fatty acids, which have been linked to human health problems. Consequently, many food manufacturers are attempting to find means of reducing the trans-fatty acid content of foods.

degumming, and bleaching (Akoh and Min, 2002). A variety of analytical procedures are routinely used by food scientists to test the quality of an oil phase so as to ensure that it is suitable for usage in a product (Pike, 2003).

### 4.3 Water

Water plays an extremely important role in determining the bulk physicochemical and organoleptic properties of food emulsions. Its unique molecular and structural properties largely determine the solubility, conformation, and interactions of the other components present in aqueous solutions (Bergethon, 1998; Norde, 2003). It is therefore crucial for food scientists to understand the contribution that water makes to the overall properties of food emulsions.

#### 4.3.1 Molecular structure and organization

A water molecule is comprised of two hydrogen atoms covalently bonded to an oxygen atom (Figure 4.9). The oxygen atom is highly electronegative and pulls the electrons associated with the hydrogen atoms toward it (Fennema, 1996b; Norde, 2003). This leaves a partial positive charge ( $\delta^+$ ) on each of the hydrogen atoms, and a partial negative charge ( $\delta^-$ ) on each of the lone pairs of electrons on the oxygen atom. The tetrahedral arrangement of the partial charges on an individual water molecule means that it can form hydrogen bonds with four of its neighbors (Figure 4.9). A hydrogen bond is formed between a lone pair of electrons on the oxygen atom of one water molecule and a hydrogen atom on a neighboring water molecule, that is,  $\text{O}-\text{H}^{\delta+} \cdots \text{O}^{\delta-}$ . A hydrogen bond is actually a composite of more fundamental interactions, that is, dipole-dipole, van der Waals, steric, and partial charge transfer (Baker and Hubbard, 1984; Dill, 1990). The magnitude of the hydrogen bonds in water is typically between 13 and 25  $\text{kJ mol}^{-1}$  (5–10  $kT$ ), which is sufficiently strong to cause the water molecules to overcome the disorganizing influence of the thermal energy and become highly aligned with each other (Israelachvili, 1992). In order to maximize the number of hydrogen bonds formed, water molecules organize themselves into a three-dimensional

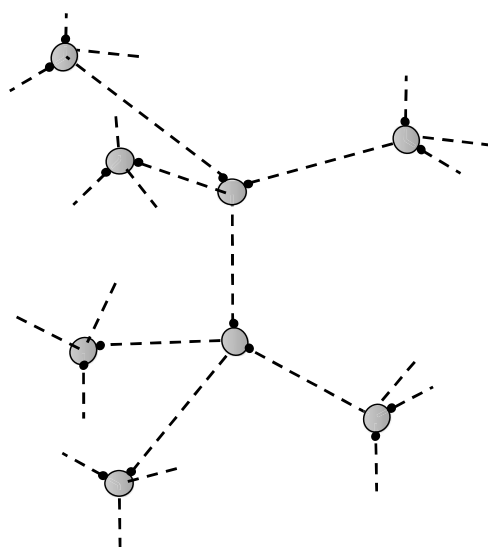


Figure 4.9 Molecular structure and tetrahedral organization of water molecules.

tetrahedral structure because this allows each water molecule to form hydrogen bonds with four of its nearest neighbors (Franks, 1972–1982; Fennema, 1996b). In the solid state, the number of hydrogen bonds formed per molecule is four. In the liquid state, the disorganizing influence of the thermal energy means that the number of hydrogen bonds per molecule is between 3 and 3.5 at room temperature, and decreases with increasing temperature. The three-dimensional tetrahedral structure of water in the liquid state is highly dynamic, with hydrogen bonds continually being broken and reformed as the water molecules move about. Water molecules that dissociate to form ions, such as  $\text{H}_3\text{O}^+$  and  $\text{OH}^-$ , do not fit into the normal tetrahedral structure of water, nevertheless, they have little effect on the overall structure and properties of water because their concentration is so low (Fennema, 1996b).

As well as forming hydrogen bonds with each other, water molecules are also capable of forming them with other polar molecules, such as organic acids, bases, proteins, and carbohydrates (Franks, 1972–1982). The strength of these interactions varies from 2–40 kJ mol<sup>-1</sup> (1–16 kT) depending on the electronegativity and orientation of the donor or acceptor groups (Baker and Hubbard, 1984). Many ions form relatively strong ion–dipole interactions with water molecules, which have a pronounced influence on the structure and physicochemical properties of water (Franks, 1975; Israelachvili, 1992; Fennema, 1996b). It is the ability of water molecules to form relatively strong bonds with each other and with other types of polar or ionic molecules that determines many of the characteristic properties of food emulsions.

#### 4.3.2 Bulk physicochemical properties

The bulk physicochemical properties of pure water are determined by the mass, dimensions, bond angles, charge distribution, and interactions of the water molecule (Fennema, 1996b; Norde, 2003). Water has a high dielectric constant because the uneven distribution of partial charges on the molecule means that it is easily polarized by an electric field (Hasted, 1972). It has a relatively high melting point, boiling point, enthalpy of vaporization, and surface tension, compared to other molecules of a similar size that also contain hydrogen (e.g.,  $\text{CH}_4$ ,  $\text{NH}_3$ ,  $\text{HF}$ , and  $\text{H}_2\text{S}$ ), because a greater amount of energy must be supplied to disrupt the strong hydrogen bonds holding the water molecules together in the condensed state (Israelachvili, 1992; Fennema, 1996b). The relatively low density of ice and liquid water is because the water molecules adopt a structure in which they are in direct contact with only four of their nearest neighbors, rather than forming a more close-packed structure (Franks, 1975; Fennema, 1996b). The relatively low viscosity of water is because of the highly dynamic nature of hydrogen bonds compared to the timescale of a rheology experiment. Even though energy is required to break the hydrogen bonds between water molecules as they move past each other, most of this energy is regained when they form new hydrogen bonds with their new neighbors.

The crystallization of water has a pronounced effect on the bulk physiochemical properties of food emulsions. The presence of ice crystals in the aqueous phase of an O/W emulsion, such as ice cream, contributes to the characteristic mouthfeel and texture of the product (Berger, 1997; Hartel, 2001; Walstra, 2003a). When these ice crystals grow too large a product is perceived as being “grainy” or “sandy,” which is commonly experienced when ice cream is melted and then refrozen (Berger, 1997). Many foods are designed to be freeze–thaw stable, that is, their quality should not be adversely affected once the product is frozen and then thawed (Partmann, 1975). Considerable care must be taken in the choice of ingredients and freezing–thawing conditions to create a food emulsion that is freeze–thaw stable. The basic principles of ice crystallization are similar to those described for fats and oils (Section 4.2.3.). Nevertheless, water does exhibit some



anomalous behavior because of its unique molecular properties, for example, it expands when it crystallizes, whereas most other substances contract (Fennema, 1996b). This is because the increased mobility of the water molecules in the liquid state means that they can get closer together, and so the density of the liquid state is actually greater than that of the solid state. Some of the most important bulk physicochemical properties of liquid water are compared with those of a liquid oil in Table 4.2. A more detailed discussion of the molecular basis of the physicochemical properties of water in relation to food quality is given by Fennema (1996b).

#### 4.3.3 *Influence of solutes on the organization of water molecules*

The aqueous phase of most food emulsions contains a variety of water-soluble constituents, including minerals, acids, bases, flavors, preservatives, vitamins, sugars, surfactants, proteins, and polysaccharides (Dickinson, 1992). The solubility, partitioning, volatility, conformation, and chemical reactivity of many of these food ingredients are determined by their interactions with water. It is therefore important for food scientists to understand the nature of solute–water interactions and their influence on the bulk physicochemical and organoleptic properties of food emulsions.

When a solute molecule is introduced into pure water, the normal structural organization and interactions of the water molecules are altered. This results in changes in the physicochemical properties of the water molecules that are affected by the presence of the solute, such as density, compressibility, melting point, boiling point, and mobility (Franks, 1975; Reichardt, 1988; Israelachvili, 1992; Murrell and Jenkins, 1994; Fennema, 1996b; Norde, 2003). The extent of these changes depends on the molecular characteristics of the solute, that is, its size, shape and polarity. The water molecules in the immediate vicinity of the solute experience the largest modification of their properties, and are often referred to as being “bound” to the solute (Reichardt, 1988; Murrell and Jenkins, 1994). In reality, these water molecules are not permanently bound to the solute, but rapidly exchange with the bulk water molecules, albeit with a reduced mobility (Franks, 1991; Fennema, 1996b). The mobility of “bound” water increases as the strength of the attractive interactions between it and the solute decreases, that is, non-polar–water > dipole–water > ion–water (Israelachvili, 1992). The amount of water “bound” to a solute can be defined as the number of water molecules whose properties are significantly altered by its presence. In practice, it is difficult to unambiguously define or stipulate the amount of “bound” water (Franks, 1991). First, the water molecules “bound” to a solute do not all have the same properties: the water molecules closest to the solute are more strongly influenced by its presence than those furthest away. Second, the physicochemical properties that are measured in order to determine the amount of “bound” water are each influenced to a different extent (e.g., density, compressibility, mobility, melting point). As a consequence, different analytical techniques often measure different amounts of “bound” water, depending on the physical principles on which they operate.

##### 4.3.3.1 *Interaction of water with ionic solutes*

Many of the solutes present in food emulsions are either ionic or are capable of being ionized, including salts, acids, bases, proteins, and polysaccharides (Fennema, 1996a). The degree of ionization of many of these solutes is governed by the pH of the aqueous solution, and so their interactions are particularly sensitive to pH. The ion–dipole interactions that occur between an ionic solute and a water molecule are usually stronger than the dipole–dipole interactions that occur between a pair of water molecules (Table 4.3). As a consequence, the water molecules in the immediate vicinity of an ion tend to orientate themselves so that their oppositely charged dipole faces the ion. Thus, a positively charged

**Table 4.3** Typical Water–Solute Interactions Found in Food Emulsions

Interaction Type	Typical Example	Interaction Strength Compared To Water–Water Hydrogen Bond
Water–ion	Free ions ( $\text{Na}^+$ , $\text{Cl}^-$ ) Ionic groups ( $-\text{CO}_2^-$ , $-\text{NH}_3^+$ )	Greater
Water–dipole	$-\text{C}=\text{O}$ , $-\text{NH}$ , $-\text{OH}$	Similar
Water–nonpolar	Alkyl group	Much smaller

Source: Adapted from Fennema (1996b).

ion causes the water molecules to align themselves so that a  $\delta^-$  group faces the ion, whereas the opposite is true for a negatively charged ion (Figure 4.10). The relatively strong nature of ion–dipole interactions means that the mobility of the water molecules near the surface of an ion is significantly less than that of bulk water (Reichardt, 1988; Fennema, 1996b; Robinson et al., 1996). The residence time of a water molecule in the vicinity of an ionic group is  $\approx 10^{-8}$  sec, whereas it is  $\approx 10^{-11}$  sec in bulk water (Fennema, 1996b). The influence of an ion on the mobility and alignment of the water molecules is greatest at its surface because the electric field is strongest there. As one moves away from the ion surface, the strength of the electric field diminishes, so that the ion–water interactions become progressively weaker. Thus, the water molecules become more mobile and are less likely to be aligned toward the ion. At a sufficiently large distance from the ion surface the water molecules are uninfluenced by its presence and have properties similar to those of bulk water (Franks, 1973; Reichardt, 1988). Alterations in the structural organization and interactions of water molecules in the vicinity of an ion cause significant changes in the physicochemical properties of water (Fennema, 1996b). The water that is “bound” to an ionic solute is less mobile, less compressible, more dense, has a lower freezing point, and has a higher boiling point than bulk water. Most ionic solutes have a high water solubility because the formation of many ion–dipole bonds in an aqueous solution helps to compensate for the loss of the strong ion–ion bonds in the crystals, which is coupled with the favorable entropy of mixing contribution (Chapter 2).

The number of water molecules whose mobility and structural organization is altered by the presence of an ion increases as the strength of its electric field increases (Norde, 2003). The strength of the electric field generated by an ion is determined by its charge divided by its radius (Israelachvili, 1992). Thus, ions that are small and/or multivalent generate strong electric fields that influence the properties of the water molecules up to

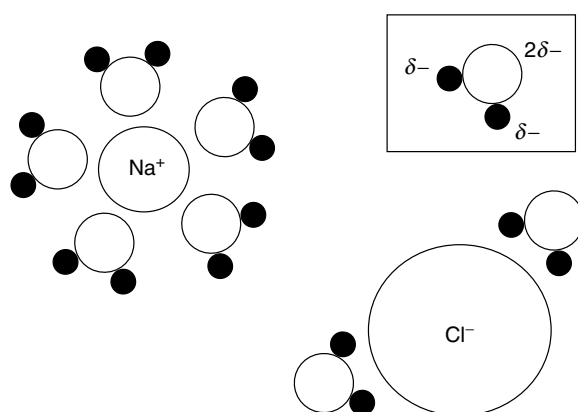


**Figure 4.10** Organization of water molecules around ions in aqueous solutions.

relatively large distances from their surface, for example,  $\text{Li}^+$ ,  $\text{Na}^+$ ,  $\text{H}_3\text{O}^+$ ,  $\text{Ca}^{2+}$ ,  $\text{Ba}^{2+}$ ,  $\text{Mg}^{2+}$ ,  $\text{Al}^{3+}$ , and  $\text{OH}^-$ . On the other hand, ions that are large and/or monovalent, generate relatively weak electrical fields, and therefore their influence extends a much shorter distance into the surrounding water, for example,  $\text{K}^+$ ,  $\text{Rb}^+$ ,  $\text{Cs}^+$ ,  $\text{NH}_4^+$ ,  $\text{Cl}^-$ ,  $\text{Br}^-$ , and  $\text{I}^-$ . The number of water molecules “bound” to an ion is usually referred to as the *hydration number*. Thus, the hydration number of small multivalent ions is usually larger than that of large monovalent ions.

When an ionic solute is added to pure water it disrupts the existing tetrahedral arrangement of the water molecules, but imposes a new order on the water molecules in its immediate vicinity (Norde, 2003). The overall structural organization of the water molecules in an aqueous solution can therefore either increase or decrease after a solute is added, depending on the amount of structure imposed on the water by the ion compared to that lost by disruption of the tetrahedral structure of bulk water (Collins and Washabaugh, 1985). If the structure imposed by the ion is greater than that lost by the bulk water, the overall structural organization of the water molecules is increased, and the solute is referred to as a *structure maker* (Figure 4.11). Ionic solutes that generate strong electric fields are structure makers, and the magnitude of their effect increases as the size of the ions decreases and/or their charge increases. If the structure imposed by an ion is not sufficiently large to compensate for that lost by disruption of the tetrahedral structure of bulk water, then the overall structural organization of the water molecules in the solution is decreased, and the solute is referred to as a *structure breaker* (Figure 4.11). Ionic solutes that generate weak electric fields are structure breakers, and the magnitude of their effect increases as their size increases or they become less charged (Israelachvili, 1992).

The influence of ionic solutes on the overall properties of water depends on their concentration (Israelachvili, 1992; Robinson et al., 1996). At low solute concentrations, the majority of water is not influenced by the presence of the ions and therefore has properties similar to that of bulk water. At intermediate solute concentrations some of the water molecules have properties similar to those of bulk water, whereas the rest have properties that are dominated by the presence of the ions. At high solute concentrations, all the water molecules are influenced by the presence of the solute molecules and therefore have properties that are appreciably different from those of bulk water. At relatively high salt

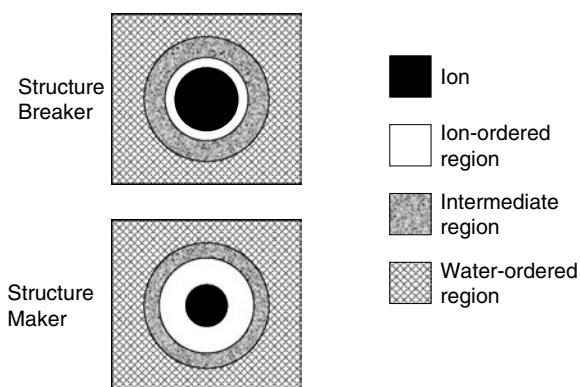


**Figure 4.11** Schematic representation of organization of water molecules around ionic solutes that act as either structure breakers or structure makers. The water molecules surrounding an ionic solute can be conceptually divided into three regions: (i) water molecules in the immediate vicinity of the solute that are highly organized; (ii) water molecules in the intermediate region between the solute-organized region and the bulk water region; and (iii) water molecules having the normal tetrahedral organization of bulk water.

concentrations, the solubility of biopolymer molecules in aqueous solutions generally decreases when the concentration of ionic solutes increases above a certain level, which is known as “salting-out,” because the solutes compete with the biopolymers for the limited amount of water that is available to hydrate them (Creighton, 1993). Ionic solutes may also influence the molecular conformation and association of biopolymers, and therefore their functional properties, by screening electrostatic interactions, by binding to oppositely charged groups, or by acting as salt bridges (Damodaran, 1996). Consequently, at relatively low salt concentrations, biopolymer solubility may either increase or decrease with increasing ionic strength depending on the precise nature of the interactions involved.

It is also useful to outline the various ways that ionic solutes can influence droplet–droplet interactions in O/W emulsions since this has a major impact on the stability and properties of these emulsions, especially those stabilized by ionic emulsifiers:

1. At relatively low concentrations (<10 mM), multivalent ions may bind to the surface of oppositely charged emulsion droplets, thereby decreasing the magnitude of their electrical charge ( $\zeta$ -potential) and reducing the strength of the electrostatic repulsion between them (Section 3.4). In addition, these ions may form salt bridges between charged emulsion droplets, thereby promoting droplet flocculation (Section 3.4).
2. At intermediate concentrations (<250 mM), ionic solutes screen electrostatic interactions (Section 3.4.) and screen the zero-frequency contribution to the van der Waals interaction (Section 3.3), thus altering the magnitude and range of the repulsive and attractive interactions between the droplets.
3. At relatively high concentrations (>500 mM), ionic (and other) solutes increase the attraction between emulsion droplets (and other types of colloidal particles) because of a steric exclusion effect (McClements, 2002c). Hydrated ions are significantly bigger than water molecules. Hence, there is a region surrounding the surface of an emulsion droplet where the water molecules can enter but the hydrated ions are excluded. This generates a solute concentration gradient between the solute-depleted region and the bulk aqueous solution, which is thermodynamically unfavorable and generates an attractive force between the emulsion droplets. This mechanism is similar to depletion flocculation, but has a much shorter range.
4. At relatively high concentrations (>500 mM), ionic solutes alter the structural organization of water, which influences the strength of hydrophobic interactions (Section 3.7). Structure breakers increase the hydrophobic attraction, whereas structure makers decrease the hydrophobic attraction.
5. Ionic solutes may cause changes in the conformation of biopolymer molecules adsorbed to the surface of emulsion droplets or dispersed in the continuous phase, which will alter the strength of the steric and depletion interactions between droplets (Sections 3.5 and 3.6).
6. The binding of hydrated ions to the surface of emulsion droplets may increase the hydration repulsion between the droplets (Section 3.8).

The fact that ions influence the interactions between emulsion droplets in so many different ways means that it is often difficult to accurately predict or quantify their effect on emulsion properties.

#### 4.3.3.2 Interaction of water with polar solutes

Many food constituents are noncharged molecules that are either entirely polar or contain polar regions, including alcohols, sugars, polyols, proteins, polysaccharides, and surfactants (Fennema, 1996a). Water is capable of participating in dipole–dipole interactions with the polar groups on these solutes (Franks, 1973, 1991; Norde, 2003). By far the most

important type of dipole–dipole interaction is between water and those solutes that have hydrogen bond donors (e.g.,  $-\text{O}-\text{H}^{\delta+}$ ) or acceptors (e.g.,  $\delta-\text{O}-$ ). The strength of hydrogen bonds between water and this type of polar solute is similar to that between two water molecules (Table 4.3). The addition of a polar solute to water therefore has much less influence on the mobility and organization of the water molecules in its immediate vicinity than does a similarly sized ionic solute (Fennema, 1996b). The influence of polar solutes on the properties of water is largely governed by the ease at which they can be accommodated into the existing tetrahedral structure of the water molecules. When a polar solute is of an appropriate size and shape, and has hydrogen bond acceptors and donors at positions where they can easily form bonds with the neighboring water molecules, it can fit into the tetrahedral structure (Brady and Ha, 1975; Galema and Hoiland, 1991; Franks, 1991; Schmidt et al., 1994). For this type of solute, there need be little change in the number of hydrogen bonds formed per water molecule or the overall structural organization of the water molecules. This type of solute therefore tends to be highly water-soluble because of the entropy of mixing (Chapter 2). If the solute molecule is not of an appropriate size and shape, or if its hydrogen bond donors and acceptors are not capable of aligning with those of neighboring water molecules, then it cannot easily fit into the tetrahedral structure of water. This causes a dislocation of the normal water structure surrounding the solute molecules, which is thermodynamically unfavorable. In addition, there may be a significant alteration in the physicochemical properties of the water molecules in the vicinity of the solute. For this reason, polar solutes that are less compatible with the tetrahedral structure of water tend to be less soluble than those that are compatible.

Just as with ionic solutes, the affect of polar solutes depends on their concentration. At low solute concentrations, most of the water has the same properties as bulk water, but at high concentrations a significant proportion of the water has properties that are altered by the presence of the solute. Nevertheless, it takes a greater concentration of a polar solute to cause the same affect as an ionic solute because of the greater strength of ion–water interactions compared to dipole–water interactions. At high solute concentrations there may also be a steric exclusion effect as mentioned in the previous section.

Interactions between polar groups and water determine a number of important properties of food components in emulsions. The hydration of the polar head groups of surfactant molecules is believed to be partly responsible for their stability to aggregation (Evans and Wennerstrom, 1994). When surfactants are heated, the head groups become progressively dehydrated, which eventually cause the molecules to aggregate (Section 4.5). These hydration forces also play an important role in preventing the aggregation of emulsion droplets stabilized by nonionic surfactants (Section 3.8). The three-dimensional conformation and interactions of proteins and polysaccharides is influenced by their ability to form intramolecular and intermolecular hydrogen bonds (Section 4.5). The solubility, partitioning, and volatility of polar solutes depend on their molecular compatibility with the surrounding solvent: the stronger the molecular interactions between a solute and its neighbors in a liquid, the greater its solubility and lower its volatility (Baker, 1987).

#### 4.3.3.3 *Interaction of water with nonpolar solutes: the hydrophobic effect*

The attraction between a water molecule and a nonpolar solute is much weaker than that between two water molecules, because nonpolar molecules are incapable of forming hydrogen bonds (Israelachvili, 1992; Evans and Wennerstrom, 1994; Norde, 2003). For this reason, when a nonpolar molecule is introduced into pure liquid water, the water molecules surrounding it change their orientation so that they can maximize the number of hydrogen bonds formed with neighboring water molecules (Figure 4.12). The structural rearrangement and alteration in the physicochemical properties of water molecules in the immediate

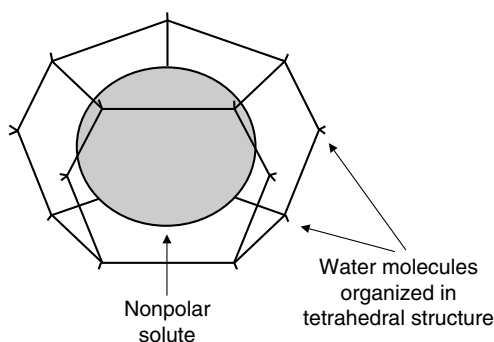


Figure 4.12 Schematic representation of the reorganization of water molecules near a nonpolar solute.

vicinity of a nonpolar solute is known as *hydrophobic hydration*. At relatively low temperatures, it is believed that a “cage-like” or clathrate structure of water molecules exists around a nonpolar solute, in which the water molecules involved have a coordination number of four, which is greater than that of the water molecules in the bulk phase (3–3.5) (Israelachvili, 1992). Despite gaining some order, the water molecules in the cage-like structures are still highly dynamic, having residence times of the order of  $10^{-11}$  sec (Evans and Wennerstrom, 1994). The alteration in the organization and interactions of water molecules surrounding a nonpolar solute has important implications for the solubility and interactions of nonpolar groups in water (Tanford, 1980; Israelachvili, 1992; Fennema, 1996b; Norde, 2003).

The behavior of nonpolar solutes in water can be understood by considering the transfer of a nonpolar molecule from an environment where it is surrounded by similar molecules to one where it is surrounded by water molecules (Tanford, 1980). When a nonpolar solute is transferred from a nonpolar solvent into water there are changes in both the enthalpy ( $\Delta H_{\text{transfer}}$ ) and entropy ( $T\Delta S_{\text{transfer}}$ ) of the system. The enthalpy change is related to the alteration in the overall strength of the molecular interactions, whereas the entropy change is related to the alteration in the structural organization of the solute and solvent molecules. The overall free energy change ( $\Delta G_{\text{transfer}}$ ) depends on the relative magnitude of these two contributions (Evans and Wennerstrom, 1994):

$$\Delta G_{\text{transfer}} = \Delta H_{\text{transfer}} - T\Delta S_{\text{transfer}} \quad (4.6)$$

The relative contribution of the enthalpic and entropic contributions to the free energy depends on temperature (Figure 4.13). An understanding of the temperature dependence of the free energy of transfer is important for food scientists because it governs the behavior of many food components during food processing, storage, and handling. At relatively low temperatures ( $<25^\circ\text{C}$ ), the number of hydrogen bonds formed by the water molecules in the cage-like structure surrounding the nonpolar solute is slightly higher than in bulk water and so  $\Delta H_{\text{transfer}}$  is negative (i.e., favors transfer). On the other hand, the water molecules in direct contact with the nonpolar solute are more ordered than those in bulk water and so the entropy term is positive (i.e., opposes transfer). Overall, the entropy term dominates and so the transfer of a nonpolar molecule into water is thermodynamically unfavorable (Tanford, 1980; Israelachvili, 1992).

As the temperature is raised the water molecules become more thermally agitated and so their organization within the cage-like structure is progressively lost, which has consequences for both the enthalpy and entropy contributions. First, some of the partial

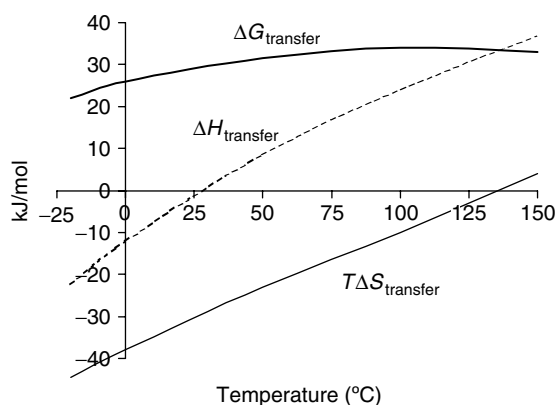


**Figure 4.13** Temperature dependence of the typical thermodynamics associated with the transfer of a nonpolar solute from a nonpolar liquid into water. Adapted from Creighton (1993).

charges on the water molecules face toward the nonpolar group and are therefore unable to form hydrogen bonds with the surrounding water molecules. Thus, the number of hydrogen bonds formed by the water molecules in the cage-like structure decrease with increasing temperature. At a certain temperature, the number of hydrogen bonds formed by the water molecules in the cage-like structure becomes less than that of bulk water. Below this temperature the enthalpy associated with transferring a nonpolar molecule into water is negative (exothermic) and so is favorable to transfer, but above this temperature it is positive (endothermic) and so is unfavorable to transfer (Tanford, 1980). The enthalpy term therefore makes an increasing contribution to opposing the transfer of nonpolar molecules into water as the temperature rises. Second, the increasing disorganization of the water molecules surrounding a nonpolar molecule as the temperature is raised means that the entropy difference between the water molecules in the cage-like structure and those in the bulk water is lessened. Thus, as the temperature is increased the contribution of the entropy term becomes progressively less important. In summary, at low temperatures the major contribution to the unfavorable free energy change associated with transfer of a nonpolar molecule into water is the entropy term, but at higher temperatures it is the enthalpy term (Creighton, 1993). Overall, the transfer of a nonpolar molecule from an organic solvent into water becomes increasingly thermodynamically unfavorable as the temperature is raised up to a certain temperature (around 100–150°C).

The free energy associated with transferring a nonpolar molecule from an environment where it is surrounded by similar molecules to one in which it is surrounded by water molecules has been shown to be a product of its surface area and the interfacial tension between the bulk nonpolar liquid and water that is,  $\Delta G = \gamma \Delta A$  (Tunon et al., 1992). An aqueous solution containing a nonpolar solute can decrease its free energy by reducing the unfavorable contact area between the nonpolar groups and water, which is known as the *hydrophobic effect*. The strong tendency for nonpolar molecules to associate with each other in aqueous solutions is a result of the attempt of the system to reduce the contact area between water and nonpolar regions and is known as the *hydrophobic interaction* (Section 3.7). The hydrophobic effect is responsible for many of the characteristic properties of food emulsions, including the aggregation of proteins, the formation of surfactant micelles, the adsorption of emulsifiers at oil–water and air–water interfaces, the aggregation of hydrophobic particles, and the immiscibility of oil and water.

The strength of the hydrophobic interaction between nonpolar substances in water is affected by the presence of ions in the aqueous phase separating them. Ions can either

increase or decrease the structural organization of water molecules in an aqueous solution, depending on whether they are structure makers or structure breakers (previous section). As one of the major driving forces for hydrophobic interactions is the difference in structural organization (entropy) between the water molecules in the immediate vicinity of the nonpolar solute and those in bulk water, then changes in the organization of the water molecules in bulk water alters its strength (Israelachvili, 1992). Structure makers decrease the magnitude of the hydrophobic interaction and therefore increase the water-solubility of nonpolar solutes because the difference in structural organization of water molecules in the bulk solution and in the immediate vicinity of a nonpolar solute is reduced, whereas structure breakers have the opposite effect. The strength of the hydrophobic interaction also depends on temperature, increasing as the temperature is raised up to a temperature somewhere above 100°C (Figure 4.13). The temperature dependence of the hydrophobic interaction has important implications for the functionality of many food constituents, since there may be appreciable changes in product temperature during the manufacture, storage, and usage of food emulsions.

#### 4.3.4 *Influence of solutes on the physicochemical properties of solutions*

Emulsion formation, stability, and properties are strongly influenced by the bulk physicochemical properties of the aqueous phase, for example, density, viscosity, refractive index, specific heat capacity, thermal conductivity, dielectric constant. For example, the ability to produce small emulsion droplets during homogenization depends on the viscosity and interfacial tension of the aqueous phase (Section 6.4.1). The creaming stability of O/W emulsions depends on the density and viscosity of the aqueous phase (Section 7.3). The flocculation and coalescence stability of emulsions depends on the strength of the attractive and repulsive interactions between the droplets, which is influenced by the ionic strength, dielectric constant, and refractive index of the aqueous phase (Chapter 3). The appearance of an emulsion is influenced by the contrast in refractive index between the oil and aqueous phases, since this determines the fraction of light scattered by the droplets (Section 10.5.2). The flavor of emulsions depends on the partitioning and release rate of flavor molecules in a food, which are influenced by the polarity and viscosity of the aqueous phase (Chapter 9). Knowledge of the bulk physicochemical properties of the aqueous phase is therefore important for predicting, understanding, and controlling the behavior of food emulsions.

The bulk physicochemical properties of an aqueous phase depend on the type, concentration, and interactions of the various solutes present. Solute may influence the bulk properties of water directly through their molecular interactions with the water molecules, or indirectly due to thermodynamic “colligative” effects (Atkins, 1994). For example, the presence of solutes in an aqueous solution causes a decrease in melting point, an increase in boiling point, and a decrease in water activity of aqueous solutions (Walstra, 2003a). Each solute type influences the bulk physicochemical properties of water in a different manner because of differences in its intrinsic molecular characteristics (e.g., size, shape, mass) and in its ability to alter the properties of the water molecules in its vicinity. The physicochemical properties of aqueous solutions containing different concentrations of many common solutes have been tabulated in the literature (e.g., CRC Handbook of Chemistry and Physics).

#### 4.3.5 *Selection of an appropriate aqueous phase*

From a scientific standpoint, water is usually considered to be a chemically distinct substance with the chemical formula  $H_2O$ . In practice, the “water” used in the commercial preparation of food emulsions normally contains significant concentrations of organic and inorganic contaminants that influence its physicochemical and sensory properties, for



example, acids, bases, minerals, microorganisms, off-flavors. Many of these contaminants can have an adverse affect on the quality of emulsion-based food products, and therefore they are often removed by treating the water prior to usage (Heath, 1978; Tan, 2004).

A variety of different solutes are often incorporated into the aqueous phase of food emulsions to control their physicochemical and sensory properties, including acids, bases, salts, buffers, sugars, emulsifiers, and biopolymers. The molecular and functional properties of the most important of these constituents are discussed elsewhere in this chapter. Each constituent plays one or more specific roles in determining the overall properties of a food emulsion, and these roles are often influenced by the presence of the other constituents. It is therefore important for food scientists to identify the role or multiple roles that each functional ingredient plays within a particular food emulsion, and to understand how these roles are influenced by the presence of other constituents. This knowledge will facilitate the rational selection of the optimum combination of ingredients required to produce the desired physicochemical and sensory properties of the final product.

## 4.4 Emulsifiers

The term “emulsifier” is used in this book to describe any surface-active substance that is capable of adsorbing to an oil–water interface and protecting emulsion droplets from aggregation (flocculation and/or coalescence). The most commonly used emulsifiers in the food industry are small-molecule surfactants, amphiphilic biopolymers, and surface-active particulate matter. These emulsifiers vary widely in their ability to form and stabilize emulsions depending on their molecular and physicochemical characteristics. Ideally, an emulsifier should rapidly adsorb to the oil–water interface during homogenization, reduce the interfacial tension by an appreciable amount, and prevent droplet coalescence from occurring during homogenization (Chapter 6). In addition, it is usually important that the emulsifier forms an interfacial membrane that prevents droplet aggregation (flocculation and/or coalescence) under the environmental conditions that the product experiences during manufacture, transport, storage, and usage (Chapter 7). In this section, we will review the major types of emulsifiers used in food products, and discuss some of the factors that should be considered in selecting an emulsifier for a particular application.

### 4.4.1 Surfactants

#### 4.4.1.1 Molecular characteristics

The term “surfactant” is used to refer to those relatively small surface-active molecules that consist of a hydrophilic “head” group, which has a high affinity for water, attached to a lipophilic “tail” group, which has a high affinity for oil (Myers, 1988; Hasenhuettl, 1997a; Lindman, 2001; Faergemand and Krog, 2003; Krog and Sparso, 2004). The principal role of surfactants in food emulsions is to improve emulsion formation and stability (Charalambous and Doxastakis, 1989; Hasenhuettl and Hartel, 1997; Stauffer, 1996, 1999). Nevertheless, they may also alter emulsion properties in a number of other ways, including forming surfactant micelles, interacting with biopolymers, or modifying the formation, growth, and structure of fat crystals (Bergentahl, 1997a; Bos et al., 1997; Deffenbaugh, 1997; Krog, 1997; Faergemand and Krog, 2003). A wide variety of surfactants are available for usage in food products, and a number of the most commonly used are listed in Table 4.4. These surfactants can be represented by the formula  $RX$ , where  $X$  represents the hydrophilic head and  $R$  the lipophilic tail (Dickinson and McClements, 1995). The characteristics of a particular surfactant depend on the nature of its head and tail groups. The head group may be anionic, cationic, zwitterionic, or nonionic (Myers, 1988; St Angelo, 1989; Zielinski, 1997), although most surfactants used in the food industry are mainly

**Table 4.4** Classes of Small Molecule Surfactants Commonly Used in Food Emulsions

Chemical Name	Abbreviation	EU Number	U.S. FDA	ADI (mg/kg)	Solubility
<b>Ionic</b>					
Lecithin		E 322	184.1400	NL	Oil/water
Fatty acid salts	FA	E 470	172.863	NL	Oil/water
Sodium stearyl lactylate	SSL	E 481	172.846	0–20	Water
Calcium stearyl lactylate	CSL	E 482	172.844	0–20	Oil
Citric acid esters of MG	CITREM	E 472c	172.832	NL	Water
Diacetyl tartaric acid esters of MG	DATEM	E 472e	184.1101	0–50	Water
<b>Nonionic</b>					
Monoglycerides	MG	E 471	184.1505	NL	Oil
Acetic Acid esters of MG	ACETEM	E 472a	172.828	NL	Oil
Lactic acid esters of MG	LACTEM	E 472b	172.852	NL	Oil
Succinic acid esters of MG	SMG	—	172.830	—	
Polyglycerol esters of FA	PGE	E 475	172.854	0–25	Water
Propylene glycol esters of FA	PGMS	E 477	172.856	0–25	Oil
Sucrose esters of FA		E 473	172.859	0–10	Oil/Water*
Sorbitan monostearate	SMS	E 491	172.842	0–25	Water
Sorbitan tristearate	STS	E 492	—	0–15	Oil
Polyoxyethylene (20) sorbitan monostearate	Polysorbate 60	E 435	172.836	0–25	Water
Polyoxyethylene (20) sorbitan tristearate	Polysorbate 65	E 436	172.838	0–25	Water
Polyoxyethylene (20) sorbitan monooleate	Polysorbate 80	E 433	172.840	0–25	Water

*Note:* The table includes their chemical name, abbreviation, acceptable daily intake (ADI), and solubility. NL = not limited.

\*The solubility of some classes of surfactants depends on the relative lengths of their hydrophilic and hydrophobic parts.

*Source:* Adapted from Krog (1997) and Faergemand and Krog (2003).

nonionic (e.g., monoglycerides [MG], Tweens, Polysorbates, Spans, ACETEM, LACTEM), anionic (e.g., fatty acid salts, stearyl lactylate salts, DATEM, CITREM), or zwitterionic\* (e.g., lecithin). The tail group usually consists of one or more hydrocarbon chains, having between 10 and 20 carbon atoms per chain (St Angelo, 1989; Bergensthal, 1997; Zielinski, 1997). Surfactant chains may be saturated or unsaturated, linear or branched, aliphatic and/or aromatic, but most food surfactants have either one or two linear aliphatic chains, which may be saturated or unsaturated (Stauffer, 1999). Each type of surfactant has functional properties that are determined by its unique molecular structure and the physicochemical environment that it operates within (Myers, 1988; Jonsson et al., 1998). In addition, surfactants vary considerably in their cost, usage levels, legal status, ingredient compatibility, and ease of usage (Krog, 1997; Stauffer, 1999; Faergemand and Krog, 2003).

\* A zwitterionic surfactant is one which has both positively and negatively charged groups on the same molecule.

Hence, there is no single surfactant that is suitable for every food application and so it is necessary to select the most appropriate surfactant for each particular product.

Food-grade surfactants are produced industrially by chemical processes using a variety of different raw materials, such as fats, oils, glycerol, organic acids, sugars, and polyols (Krog, 1997; Zielinski, 1997). Despite normally being called by a specific chemical name (Table 4.4), most commercial surfactants are actually highly complex mixtures of a number of different chemical species (Stauffer, 1999). This compositional heterogeneity can have a large impact on their functional properties in both laboratory studies of emulsion properties and in their usage as ingredients in food products (Walstra, 2003a). Consequently, it is often important to have analytical methods to determine the type and concentration of different chemical species present in a commercial surfactant (Hasenhuettl, 1997b). It should also be noted that surfactants are often used in combinations with other types of surfactants, rather than as individual components, since improved functional properties can often be obtained (Krog, 1997; Stauffer, 1999; Faergemand and Krog, 2003). Surfactant ingredients for usage in the food industry come in a variety of different forms, including liquids, pastes, solids, powders, and beads. The surfactant is usually suspended in the phase that it is most soluble in prior to homogenization, so that water-soluble surfactants are dispersed in the aqueous phase and oil-soluble surfactants are dispersed in the lipid phase. Even so, there are also many examples in the food industry where the surfactant is simply blended directly with the oil and aqueous phases. A variety of processing treatments may be required to ensure that the surfactant is adequately dispersed (e.g., shearing, heating), and these are usually stipulated by the ingredient supplier.

#### 4.4.1.2 *Physicochemical properties*

The various factors influencing the physicochemical properties of food and nonfood surfactants have been reviewed in detail elsewhere (Bergensstahl, 1997; Jonsson et al., 1998). This section will therefore only provide an overview of the most important functional properties of surfactants that are relevant to their application in food emulsions.

**4.4.1.2.1 *Molecular organization of surfactants in solution.*** At sufficiently low concentrations, surfactants exist as monomers in solution because the entropy of mixing overweighs the attractive forces operating between the surfactant molecules (Jonsson et al., 1998). Nevertheless, as their concentration is increased they can spontaneously aggregate into a variety of thermodynamically stable structures known as *association colloids*, for example, micelles, bilayers, vesicles, and reverse micelles (Figure 4.14). The primary driving force for the formation of these structures is the hydrophobic effect, which causes the system to adopt a molecular organization that minimises the unfavorable contact area between the nonpolar tails of the surfactant molecules and water (Evans and Wennerstrom, 1994; Heimenz and Rajagopalan, 1997). At still higher concentrations, surfactants may organize themselves into a variety of liquid crystalline structures, such as hexagonal, lamellar and reversed hexagonal phases (Jonsson et al., 1998; Hartel, 2001; Faergemand and Krog, 2003; Larsson, 2004). In addition, the surfactant solution may separate into a number of phases, with different compositions and molecular organizations. The molecular organization of surfactants in solutions depends mainly on the geometry and interactions of the surfactant molecules, the nature of the solvent, the solution composition, and the temperature (MacKay, 1987; Myers, 1988; Krog, 1997; Jonsson et al., 1998). The influence of solution and environmental conditions on the molecular organization of surfactants can be conveniently described by phase diagrams (Bergensstahl, 1997; Faergemand and Krog, 2003). Phase diagrams are usually determined empirically for a given surfactant system and allow one to determine the type, number, and composition of the phases formed under a given set of experimental conditions (Jonsson et al., 1998). The surfactant concentrations

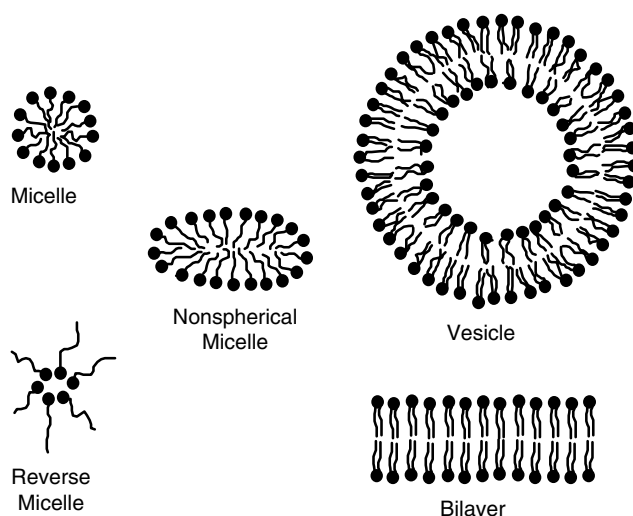


**Figure 4.14** Some typical structures formed due to the self-association of surfactant molecules at relatively low surfactant concentrations. At higher surfactant concentrations many different kinds of liquid crystalline phases may form.

normally used in food emulsions are insufficient to lead to the formation of liquid crystalline structures, although they are often high enough to lead to the formation of association colloids. In the remainder of this section we will focus on the properties of surfactant micelles, since these are the most common type of association colloid formed in food emulsions (Dickinson and McClements, 1995).

**4.4.1.2.2 Critical micelle concentration.** A surfactant forms micelles in an aqueous solution when its concentration exceeds some critical level, known as the *critical micelle concentration* or CMC (Myers, 1988; Lindman, 2001). Below the CMC, the surfactant molecules are dispersed predominantly as monomers, but once the CMC is exceeded, any additional surfactant molecules form micelles, and the monomer concentration remains fairly constant (Hiemenz and Rajagopalan, 1997). Micelles have highly dynamic structures because they are only held together by physical interactions that are relatively weak compared to the thermal energy of the system (Israelachvili, 1992). Despite the highly dynamic nature of their structure, surfactant micelles have a fairly well-defined average size and shape under a given set of environmental conditions (Israelachvili, 1992). Thus, when surfactant is added to a solution above the CMC the *number* of micelles tends to increase, rather than the size or shape of the individual micelles (although this may not be true at high surfactant concentrations). There is an abrupt change in the physicochemical properties of a surfactant solution when the CMC is exceeded, for example, surface tension, electrical conductivity, turbidity, and osmotic pressure (Rosen, 1978; Hiemenz and Rajagopalan, 1997; Jonsson et al., 1998). This is because the properties of surfactant molecules dispersed as monomers are different from those in micelles. For example, surfactant monomers are amphiphilic and have a high surface activity, whereas micelles have little surface activity because their surface is covered with hydrophilic head groups. Consequently, the surface tension of a solution decreases with increasing surfactant concentration below the CMC, but remains fairly constant above it (Section 5.7). The CMC of a surfactant solution depends on the chemical structure of the surfactant molecules, as well as on the solution composition and prevailing environmental conditions (Jonsson et al., 1998; Lindman, 2001). The CMC tends to decrease as the hydrophobicity of surfactant

molecules increases (e.g., by increasing the hydrocarbon tail length) or their hydrophilicity decreases (e.g., by decreasing the length of a nonionic head group or by exchanging an ionic head group for a nonionic one). For ionic surfactants, the CMC decreases appreciably with increasing ionic strength, since counterions screen the electrostatic repulsion between charged head groups, reducing the magnitude of this unfavorable contribution to micelle formation. The CMC is not usually strongly temperature-dependent over the temperature ranges normally found in foods (e.g., 0–100°C). For many commercial food-grade surfactants, the CMC does not occur at a well-defined concentration, but occurs over a range of concentrations, because the surfactant ingredient contains a mixture of components with different chain lengths, degrees of unsaturation, and head-group size (Walstra, 2003a).

**4.4.1.2.3 Krafft point.** It is usually necessary for a surfactant to be adequately dispersed in a solvent before it can exhibit its desired functional properties (Bergensstahl, 1997). For this reason, it is often necessary to heat surfactants that have a high melting point (usually ionic surfactants) above a critical temperature, known as the *Krafft point*, before they become soluble enough to function properly (Jonsson et al., 1998). The Krafft point occurs at the temperature where the solubility of the monomers equals the CMC of the surfactant (Figure 4.15). Below the Krafft point the solubility of the surfactant is low, but once the Krafft point is exceeded the surfactant solubility increases dramatically because micelles are much more soluble than monomers (Jonsson et al., 1998).

**4.4.1.2.4 Cloud point.** When a surfactant solution is heated above a certain temperature, known as the *cloud point*, it becomes turbid (Myers, 1988). This occurs because the hydrophilic head groups of the surfactant molecules become progressively dehydrated as the temperature is raised, which alters their molecular geometry and decreases the hydration repulsion between them (Israelachvili, 1992; Evans and Wennerstrom, 1994). Above a certain temperature, known as the *cloud point*, the micelles form aggregates that are large enough to scatter light and therefore make the solution appear turbid. As the temperature is increased further, the aggregates may grow so large that they sediment under the influence of gravity and form a separate phase that can be observed visually. The cloud point of nonionic surfactants tends to increase as the size of their hydrophilic

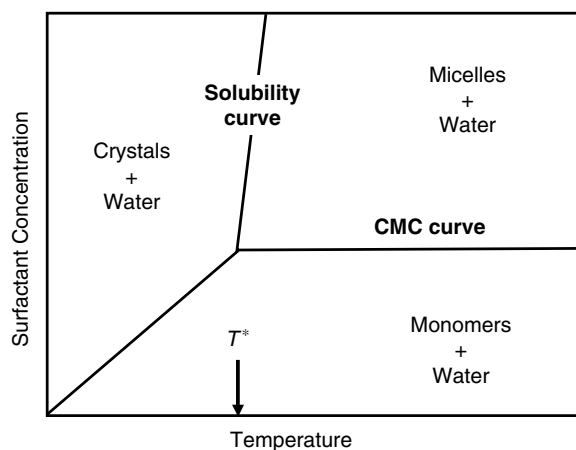


**Figure 4.15** Simplified phase diagram for a typical surfactant at relatively low surfactant concentrations. At higher surfactant concentrations many different kinds of liquid crystalline phases may form.

head group increases, and depends on the type and concentration of electrolytes present in aqueous solutions (Jonsson et al., 1998). Knowledge of the cloud point may be an important factor to consider when selecting a surfactant for a particular food emulsion application. The interfacial tension tends to decrease appreciably as the temperature is increased toward the cloud point of a surfactant, which means that droplets are easier to disrupt, but are also more prone to coalescence (Jonsson et al., 1998). Consequently, if an emulsion is going to receive some kind of thermal processing treatment it may be necessary to ensure that the cloud point of the surfactant used to stabilize the system is considerably higher than the maximum temperature experienced by the product. On the other hand, it may be advantageous to homogenize an emulsion at a temperature close to the cloud point of the surfactant since droplet disruption is facilitated and smaller droplet sizes can be achieved using the same input energy (Jonsson et al., 1998). The emulsion can then be cooled down to a temperature well below the cloud point to ensure that the droplets are stable to coalescence.

**4.4.1.2.5 Solubilization.** Nonpolar molecules, which are normally insoluble or only sparingly soluble in water, can be solubilized in an aqueous surfactant solution by incorporating them into micelles or other types of association colloids (Elworthy et al., 1968; Mukerjee, 1979; MacKay, 1987; Christian and Scamehorn, 1995). The resulting system is thermodynamically stable; however, it may take an appreciable time to reach equilibrium because of the time taken for molecules to diffuse through the system and because of the activation energy associated with transferring a nonpolar molecule from a bulk phase into a micelle (Dickinson and McClements, 1995; Kabalanov and Weers, 1996). Micelles containing solubilized materials are referred to as *swollen micelles* or *microemulsions*, whereas the material solubilized within the micelle is referred to as the *solubilize*. The ability of micellar solutions to solubilize nonpolar molecules has a number of potentially important applications in the food industry, including selective extraction of nonpolar molecules from oils, controlled ingredient release, incorporation of nonpolar substances into aqueous solutions, transport of nonpolar molecules across aqueous membranes, and modification of chemical reactions (Dickinson and McClements, 1995; Jonsson et al., 1998). There are three important factors that determine the functional properties of swollen micellar solutions: (i) the location of the solubilize within the micelles; (ii) the maximum amount of material that can be solubilized per unit mass of surfactant; and (iii) the solubilization rate. The concentration of surfactants in O/W emulsions is often high enough to form micelles in the aqueous phase. These micelles may be capable of solubilizing various kinds of nonpolar and amphiphilic molecules, including flavors, antioxidants, prooxidants, and preservatives, thereby altering their functional characteristics. Food manufacturers may therefore have to take into account the possibility that micelle solubilization may influence the bulk physicochemical and sensory properties of food emulsions.

**4.4.1.2.6 Surface activity and droplet stabilization.** Surfactant molecules adsorb to oil–water interfaces because they can adopt an orientation in which the hydrophilic part of the molecule is located in the water, while the hydrophobic part is located in the oil (St Angelo, 1989; Dickinson, 1992; Bergensthal, 1997). This minimizes the contact area between hydrophilic and hydrophobic regions, and therefore reduces the interfacial tension (Chapter 5). This reduction in interfacial tension is important during homogenization because it facilitates the further disruption of emulsion droplets, that is, less energy is needed to breakup a droplet when the interfacial tension is lowered (Section 6.4.1). Once adsorbed to the surface of a droplet the surfactant must provide a repulsive force that is strong enough to prevent the droplet from aggregating with its neighbors (Chapters 3 and 7). Ionic surfactants primarily provide stability by causing all of the emulsion droplets to have

the same electric charge and therefore electrostatically repelling each other (Section 3.4). Nonionic surfactants primarily provide stability by generating a number of short-range repulsive forces that prevent the droplets from coming too close together, such as steric, hydration, and thermal fluctuation interactions (Chapter 3). In addition, even oil droplets stabilized by nonionic surfactants often have an electrical charge and therefore electrostatic repulsion may also contribute to their stability (Pashley, 2003; Hsu and Nacu, 2003). Some surfactants form multilayers (rather than monolayers) at the surface of an emulsion droplet, which has been found to greatly enhance the stability of the droplets against aggregation (Frieberg and El Nokaly, 1983). In summary, surfactants must have three characteristics to be effective at enhancing the formation and stability of emulsions (Chapter 6). First, they must rapidly adsorb to the surface of the freshly formed emulsion droplets during homogenization. Second, they must reduce the interfacial tension by a significant amount. Third, they must form an interfacial layer that prevents the droplets from aggregating under the solution and environmental conditions pertaining to the emulsion.

The interfacial membranes formed by some surfactants (especially those containing saturated hydrocarbon chains) are capable of undergoing liquid–solid phase transitions on changes in temperature (Walstra, 2003a). Above a critical temperature ( $T_c$ ), the hydrocarbon chains have a relatively high molecular mobility and can be considered to be “fluid-like,” but below  $T_c$  the chains lose their molecular mobility, pack closely together, and can be considered to be more “solid-like.” The transition of the chain packing from fluid-like to solid-like usually causes an appreciable decrease in the interfacial tension, and may have important consequences for the functional properties of some emulsions.

It should be noted that the ability of surfactants to form micelles in the continuous phase of an emulsion can have a negative impact on emulsion stability, because they induce depletion flocculation or facilitate the transport of oil molecules between droplets (Dickinson and McClements, 1995). The ability of surfactants to regulate the depletion interactions between droplets can also have a pronounced influence on the rheological properties of emulsions (Chapter 8).

**4.4.1.2.7 Interaction with biopolymers.** Under certain circumstances, surfactant molecules bind to proteins and polysaccharides and the resulting surfactant–biopolymer complexes may have very different functional characteristics than either of the individual components (Goddard and Ananthapadmanabhan, 1993; Lindman et al., 1993; Nylander, 2004). These surfactant–biopolymer interactions can occur through a variety of different mechanisms, with the two most important being electrostatic and hydrophobic interactions (Caram-Lelham et al., 1997; Singh and Caram-Lelham, 1998; Singh and Nilsson, 1999). The number of surfactant molecules bound to a biopolymer, and whether the surfactant molecules bind as individual monomers or as micelle-like clusters, depends on the origin and nature of the interaction. The binding of surfactants to biopolymers can lead to large changes in the conformation, stability, and interactions of the biopolymer molecules. These changes can have a large influence on the bulk physicochemical properties of biopolymer solutions, such as appearance, rheology, and phase behavior (Goddard and Ananthapadmanabhan, 1993; Nylander, 2004). In addition, these interactions can lead to the formation of structures that may have novel functional properties, for example, for encapsulation and release.

When surfactant molecules are mixed with a solution of polymer molecules, they may exist in either a free or a bound state (Figure 4.16). In either of these states, the surfactant may exist as individual monomers or molecular clusters (e.g., micelles). The partitioning of surfactant molecules between these different molecular forms depends on the concentration and molecular characteristics of the biopolymer and surfactant (e.g., molecular weight, hydrophobicity, electrical charge, flexibility), as well as the prevailing solution and

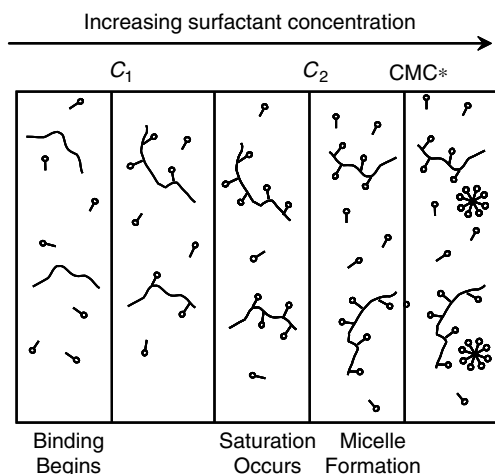


**Figure 4.16** Schematic representation of surfactant binding to biopolymers (assuming that the surfactants do not form micelle-like structures on binding, which is often the case):  $C_1$  is the surfactant concentration where binding begins;  $C_2$  is the surfactant concentration where the biopolymer becomes saturated with surfactant; and,  $CMC^*$  is the effective CMC of the surfactant in the presence of the biopolymer.

environmental conditions (e.g., temperature, pressure, pH, ionic strength, and external forces). A variety of different physicochemical mechanisms may either favor or oppose binding, for example, hydrophobic interactions, electrostatic interactions, configurational entropy, conformational entropy, and hydrogen bonding. In a system of a fixed biopolymer concentration and increasing amounts of surfactant, it is possible to define two critical surfactant concentrations: " $C_1$ " and " $C_2$ ."  $C_1$  is usually referred to as the *critical aggregation concentration* (CAC) and represents the onset concentration at which the interaction between the surfactant and the biopolymer first occurs. Above this concentration the surfactant molecules may either bind as monomers or as micelle-like clusters.  $C_2$  is the surfactant concentration at which the polymer becomes saturated with surfactant. Above this concentration, additional surfactant goes into the aqueous phase and forms monomers or micelles depending on whether or not the free surfactant concentration is below or above the CMC, respectively.  $C_1$  is generally well below the CMC of the surfactant and is only weakly dependent on the amount of polymer in solution. On the other hand,  $C_2$ , which represents the surfactant concentration at saturation of the polymer, is usually proportional to the polymer concentration.

Interactions between surfactants and polysaccharides are used in many types of food process to improve food properties. For example, surfactants (e.g., monoglycerides and stearyl lactylates) are often incorporated into starch-based products, such as breakfast cereals, pasta, and potato products, to improve their quality (Stauffer, 1999; Krog and Sparso, 2004). The surfactants form inclusion complexes with starch by inserting their hydrocarbon tails into helical coils formed by amylose or linear regions of amylopectin. These lipid–starch complexes are believed to improve the quality of starch-based products such as bread by increasing loaf volume, reducing crumb firmness, and delaying staling, mainly through their ability to retard the retrogradation of starch. The ability of surfactants to bind to starch depends on the molecular characteristics of the starch (e.g., chain length), as well as of the surfactants (e.g., head-group polarity, tail group length, and degree of unsaturation). Starch tends to bind more ionic than nonionic surfactant, and binds more saturated than unsaturated surfactants (Stauffer, 1999). Surfactants may also interact with a wide variety of other types of polysaccharides (e.g., cellulose, pectin, chitosan,



carrageenan), thereby altering their conformation, association and/or stability, which in turn leads to alterations in their functional properties, such as rheology, appearance, stability, and phase separation. Judicious usage of these interactions can be used to create food emulsions with novel properties or to develop encapsulation or delivery systems (Goddard and Ananthapadmanabhan, 1993).

Interactions between surfactants and proteins are also commonly used to improve processing operations or product properties (Nylander, 2004). These interactions may be either direct or indirect. Direct interactions involve binding of surfactants to proteins and can cause substantial changes in the conformation, stability, or interactions of protein molecules. Depending on the nature of the interaction, these changes may have either a beneficial or detrimental influence on the functional properties of proteins, for example, surface activity, foaming capacity, gelation, and solubility. Surfactants may also interact indirectly with proteins by either competing with them or displacing them from interfaces. For example, small-molecule surfactants are added to some emulsified food products to displace proteins from the surface of oil droplets, thereby facilitating the coalescence of the droplets during subsequent chilling and shearing operations, for example, ice cream and whipped cream (Friberg et al., 2004).

*4.4.1.2.8 Modification of fat crystallization.* Certain types of surfactants have been shown to be capable of modifying the nucleation and crystallization of lipids, which is used to control crystal formation in some food products (Stauffer, 1999). Surfactants have been shown to be capable of preventing clouding in salad oils by retarding the growth of fat crystals. The surfactants are believed to adsorb to the surface of any nuclei or small fat crystals formed in the oil, thereby inhibiting their further growth by preventing adsorption of additional lipid molecules. Surfactants have also been shown to inhibit undesirable polymorphic transitions of lipid crystals in chocolates, shortenings, and margarines.

#### *4.4.1.3 Surfactant classification schemes*

A number of classification schemes have been proposed to facilitate the rational selection of surfactants for particular applications. Classification schemes have been developed that are based on a surfactants solubility in oil and/or water (Bancroft's rule), its ratio of hydrophilic to lipophilic groups (hydrophile-lipophile balance [HLB] number), and its molecular geometry (Isrealachvili, 1992, 1994; Davis, 1994b; Bergensthal, 1997). Ultimately, all of these properties depend on the chemical structure of the surfactant, and so the different classification schemes are often closely related to each other.

*4.4.1.3.1 Bancroft's rule.* One of the first empirical rules developed to describe the type of emulsion that could be stabilized by a given surfactant was proposed by Bancroft (Davis, 1994b, Bergenstahl, 1997). Bancroft's rule states that the phase in which the surfactant is most soluble will form the continuous phase of an emulsion. Hence, a water-soluble surfactant should stabilize O/W emulsions, whereas an oil-soluble surfactant should stabilize W/O emulsions. It has recently been highlighted that the solubility should be determined by the total surfactant concentration (monomers + micelles) in a phase, not just the monomers (Binks, 1998). This rule works well for a wide range of surfactants, although there are a number of exceptions. For example, some amphiphilic molecules are highly soluble in either one phase or the other, but they do not form stable emulsions because they are not particularly surface-active or they do not protect droplets against aggregation. In summary, Bancroft's rule is a useful empirical method of determining the type of emulsion a surfactant will potentially stabilize (O/W or W/O); however, it provides little insight into the relationship between the molecular structure of a surfactant and the long-term stability of the emulsions formed.

**4.4.1.3.2 Hydrophile–lipophile balance (HLB).** The HLB concept is a semiempirical method that is widely used for classifying surfactants (Bergensstahl, 1997). The hydrophile–lipophile balance is described by a number that gives an indication of the relative affinity of a surfactant molecule for the oil and aqueous phases (Becher, 1983, 1985; Davis, 1994b). Each surfactant is assigned a HLB number according to its chemical structure. A molecule with a high HLB number has a high ratio of hydrophilic groups to lipophilic groups, and vice versa. The HLB number of a surfactant can be calculated from knowledge of the number and type of hydrophilic and lipophilic groups it contains, or it can be estimated from experimental measurements of its cloud point (Shinoda and Friberg, 1986). The HLB numbers of many surfactants have been tabulated in the literature (Shinoda and Kunieda, 1983; Becher, 1985, 1996). A widely used semiempirical method of calculating the HLB number of a surfactant is as follows (Davis, 1994b):

$$\text{HLB} = 7 + \Sigma(\text{hydrophilic group numbers}) - \Sigma(\text{lipophilic group numbers}) \quad (4.7)$$

Group numbers have been assigned to many different types of hydrophilic and lipophilic groups (Table 4.5). The sums of the group numbers of all the lipophilic groups and hydrophilic groups are substituted into the above equation and the HLB number is calculated. The HLB numbers of many food-grade surfactants have been calculated or determined experimentally (Table 4.6). Despite originally being developed as a semiempirical equation, Equation 4.7 has been shown to have a thermodynamic basis, with the sums corresponding to the free energy changes in the hydrophilic and lipophilic parts of the molecule when micelles are formed (Becher, 1985).

The HLB number of a surfactant gives a useful indication of its solubility in either the oil and/or water phases, and can be used to predict the type of emulsion that will be formed by a surfactant (Table 4.7). A surfactant with a low HLB number (3–6) is predominantly hydrophobic, dissolves preferentially in oil, stabilizes W/O emulsions, and forms reverse micelles in oil. A surfactant with a high HLB number (10–18) is predominantly hydrophilic, dissolves preferentially in water, stabilizes O/W emulsions, and forms micelles in water. A surfactant with an intermediate HLB number (7–9) has no particular preference for either oil or water, and is considered a good “wetting agent.” Molecules with HLB numbers below 3 (very hydrophobic) and above 18 (very hydrophilic) are often not particularly surface-active since they tend to accumulate preferentially in bulk oil or bulk water, rather than at an oil–water interface. Emulsion droplets are particularly prone to coalescence when they are stabilized by surfactants that have extreme or intermediate HLB numbers. At very high or low HLB numbers, a surfactant may have such a low

**Table 4.5** Selected HLB Group Numbers

Hydrophilic Group	Group Number	Lipophilic Group	Group Number
–SO <sub>4</sub> <sup>–</sup> Na <sup>+</sup>	38.7	–CH–	0.475
–COO <sup>–</sup> H <sup>+</sup>	21.2	–CH <sub>2</sub> –	0.475
Tertiary amine	9.4	–CH <sub>3</sub>	0.475
Sorbitan ester	6.8	–CH=	0.475
Glyceryl ester	5.25		
–COOH	2.1		
–OH	1.9		
–O–	1.3		
–(CH <sub>2</sub> –CH <sub>2</sub> –O)–	0.33		

Source: Adapted from Bergensstahl (1997), Friberg (1997), and Stauffer (1999).

**Table 4.6** Approximate HLB Numbers of Some Commonly Used Food Surfactants

Surfactant Name	HLB Number
Sodium lauryl sulfate	40
Sodium stearoyl lactylate	22
Potassium oleate	20
Sucrose monoester	20
Sodium oleate	18
Polyoxyethylene (20) sorbitan monopalmitate	15.6
Polyoxyethylene (20) sorbitan monooleate	15.0
Sucrose monolaurate	15.0
Polyoxyethylene (20) sorbitan monostearate	14.9
Decaglycerol monooleate	14
Decaglycerol monostearate	14
Ethoxylated monoglyceride	13
Decaglycerol dioleate	12
Polyoxyethylene (20) sorbitan tristearate	11
Polyoxyethylene (20) sorbitan trioleate	10.5
Hexaglycerol dioleate	9
Sorbitan monolaurate	8.6
DATEM	8
Soy lecithin	8
Decaglycerol hexaoleate	7
Triglycerol monostearate	7
Sorbitan monopalmitate	6.7
Glycerol monolaurate	5.2
Calcium stearoyl lactylate	5.1
Sucrose trimester	5
Sorbitan monostearate	4.7
Propylene glycol monolaurate	4.5
Sorbitan monooleate	4.3
Glycerol monostearate	3.8
Glycerol monooleate	3.4
Propylene glycol monostearate	3.4
Sorbitan tristearate	2.1
Sorbitan trioleate	1.8
Glycerol dioleate	1.8
ACETEM	1.5
Oleic acid	1.0

*Source:* Compiled from various sources.

surface activity that it does not accumulate appreciably at the droplet surface and therefore does not provide protection against coalescence. At intermediate HLB numbers (7–9), emulsions are unstable to coalescence because the interfacial tension is so low that very little free energy is required to disrupt the membrane. Empirical observations suggest that maximum emulsion stability is obtained for O/W emulsions using surfactants with a HLB number around 10–12, and for W/O emulsions around 3–5. This is because the surfactants are surface-active, but do not lower the interfacial tension so much that the droplets are easily disrupted. Under certain circumstances, it is possible to adjust the “effective” HLB number by using a combination of two or more surfactants with different HLB numbers (Becher, 1957; Stauffer, 1999). Surfactant blends are often used in the food industry to improve the overall functionality of surfactant systems in commercial products.

**Table 4.7** Comparison of Functional Attributes of Different General Classes of Emulsifiers

Chemical Name	Solubility	Emulsion Type	Usage Level (g/g <sub>oil</sub> )	pH Stability	Salt Stability	Temperature Stability
<b>Surfactants</b>						
Nonionic (low HLB)	Oil	W/O	~0.05	Good	Good	—
Nonionic (high HLB)	Water	O/W	~0.05	Good	Good	Poor at $T \sim \text{PIT}$
Ionic	Water	O/W	~0.05	Good	Poor at $I > \text{CFC}$	Poor at $T \sim \text{PIT}$
<b>Proteins</b>						
	Water	O/W	~0.05	Poor at IEP	Poor at $I > \text{CFC}$	Poor at $T > T_m$
<b>Polysaccharides</b>						
	Water	O/W	~1–1.5	Good	Good	Good

*Note:* It should be stressed that the behavior of a specific emulsifier may be different from these general characteristics, and the reader is referred to the text for additional information about the behavior of the different emulsifiers. The symbols in the table are PIT = phase inversion temperature;  $T_m$  = thermal denaturation temperature; IEP = isoelectric point;  $I$  = ionic strength; and CFC = critical flocculation concentration.

One of the major drawbacks of the HLB concept is that it does not take into account the fact that the functional properties of a surfactant molecule are altered significantly by changes in temperature or solution conditions (Davis, 1994b, Binks, 1998). Thus, a surfactant may be capable of stabilizing O/W emulsions at one temperature, but W/O emulsions at another temperature, even though it has exactly the same chemical structure. The HLB concept could be extended to include temperature effects by determining the group numbers as a function of temperature, although this would be a rather tedious and time-consuming task. Another limitation is that the optimum HLB number required for a surfactant to create a stable emulsion often depends on the oil type. Hence, the optimum “required” HLB number has to be empirically established for different kinds of oil.

**4.4.1.3.3 Molecular geometry and the phase inversion temperature (PIT).** The molecular geometry of a surfactant molecule can be described by a packing parameter,  $p$  (Israelachvili, 1992, 1994; Kabalanov and Wennerstrom, 1996):

$$p = \frac{v}{la_0} \quad (4.8)$$

where  $v$  and  $l$  are the volume and length of the hydrophobic tail, and  $a_0$  is the cross-sectional area of the hydrophilic head group (Figure 4.17). When surfactant molecules associate with each other, they tend to form monolayers that have a curvature that allows the most efficient packing of the molecules. At this *optimum curvature* the monolayer has its lowest free energy, and any deviation from this curvature requires the expenditure of free energy. The optimum curvature ( $H_0$ ) of a monolayer depends on the packing parameter of the surfactant: for  $p = 1$ , monolayers with zero curvature ( $H_0 = 0$ ) are preferred; for  $p < 1$ , the optimum curvature is convex ( $H_0 < 0$ ); and, for  $p > 1$  the optimum curvature is concave ( $H_0 > 0$ ) (Figure 4.17). Simple geometrical considerations indicate that spherical micelles are formed when  $p$  is less than 1/3, nonspherical micelles when  $p$  is between 1/3 and 1/2, and bilayers when  $p$  is between 1/2 and 1 (Israelachvili, 1992, 1994). Above a certain concentration bilayers join-up to form vesicles because energetically unfavorable end-effects can be eliminated. At values of  $p$  greater than 1 reverse micelles are formed, in which the hydrophilic head groups are located in the interior (away from the oil), and

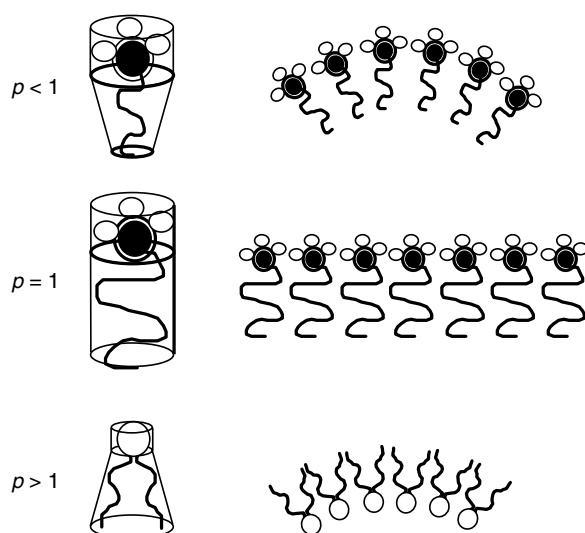


**Figure 4.17** The physicochemical properties of surfactants can be related to their molecular geometry.

the hydrophobic tail groups are located at the exterior (in contact with the oil) (Figure 4.14). The packing parameter therefore gives a useful indication of the type of association colloid that a surfactant molecule forms in solution.

The packing parameter is also useful because it accounts for the temperature dependence of the physicochemical properties of surfactant solutions and of emulsions (Kabalanov and Wennerstrom, 1996; Kabalanov, 1999). The temperature at which a surfactant solution converts from a micellar to a reverse-micellar system or an O/W emulsion changes to a W/O emulsion is known as the PIT (Shinoda and Kunieda, 1983; Shinoda and Friberg, 1986). Consider what happens when an emulsion that is stabilized by a surfactant is heated (Figure 4.18). At temperatures well below the PIT ( $\approx 20^{\circ}\text{C}$ ), the packing parameter is significantly less than unity, and so a system that consists of an O/W emulsion in equilibrium with a swollen micellar solution is favored. As the temperature is raised, the hydrophilic head groups of the surfactant molecules become progressively dehydrated, which causes  $p$  to increase toward unity. Thus, the emulsion droplets become more prone to coalescence and the swollen micelles grow in size. At the phase inversion temperature,  $p = 1$ , the emulsion breaks down because the droplets have an ultralow interfacial tension and therefore readily coalesce with each other (Aveyard et al., 1990; Kabalanov and Weers, 1996). The resulting system consists of excess oil and excess water (containing some surfactant monomers), separated by a third phase that contains surfactant molecules organized into bilayer structures. At temperatures sufficiently greater than the PIT ( $\approx 20^{\circ}\text{C}$ ), the packing parameter is much larger than unity, and the formation of a system that consists of a W/O emulsion in equilibrium with swollen reverse micelles is favored. A further increase in temperature leads to a decrease in the size of the reverse micelles and in the amount of water solubilized within them. The method of categorizing surfactant molecules according to their molecular geometry is now widely accepted as the most useful means of determining the type of emulsions they tend to stabilize (Kabalanov and Wennerstrom, 1996; Binks, 1998).

**4.4.1.3.4 Other factors.** The classification schemes mentioned above provide information about the type of emulsion that a surfactant tends to stabilize (i.e., O/W or W/O), but they do not provide much insight into the size of the droplets that are formed during

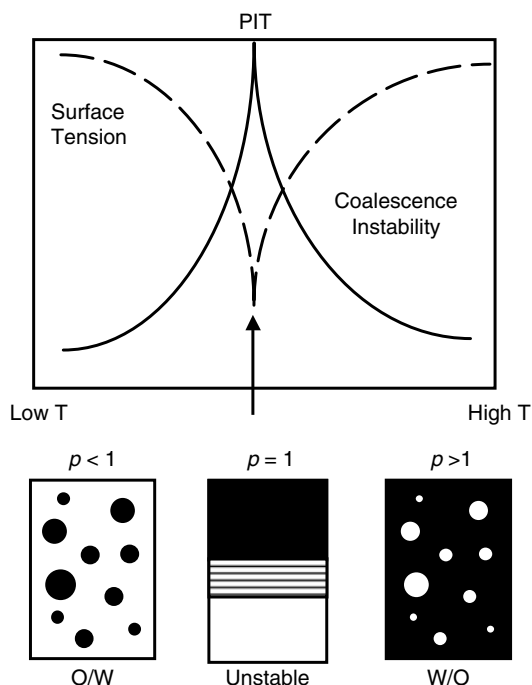


**Figure 4.18** The phase inversion temperature occurs when the optimum curvature of a surfactant monolayer is zero.

homogenization, the amount of surfactant required to form a stable emulsion, or the stability of the emulsion droplets once formed. In choosing a surfactant for a particular application these factors must also be considered. The speed at which a surfactant adsorbs to the surface of the emulsion droplets produced during homogenization determines the minimum droplet size that can be produced: the faster the adsorption rate, the smaller the size (Chapters 5 and 6). The amount of surfactant required to stabilize an emulsion depends on the total surface area of the droplets, the surface area covered per unit mass of surfactant, and the binding affinity for the interface (Chapters 5 and 6). The magnitude and range of the repulsive interactions generated by an interfacial surfactant layer, as well as its viscoelasticity, determine the stability of emulsion droplets to aggregation (Chapters 3 and 7).

#### 4.4.1.4 Common food-grade surfactants

The properties of a number of food-grade surfactants commonly used in the food industry are briefly discussed below and summarized in Tables 4.6 and 4.7. Water-soluble surfactants with relatively high HLB numbers (10–18) are normally used to stabilize O/W emulsions, such as beverages, dressings, deserts, and coffee whiteners. Nevertheless, they are also used to displace proteins from the surfaces of protein-stabilized fat droplets during the production of ice creams, whipped creams, and toppings (Krog, 1997; Faergemand and Krog, 2003; Krog and Sparso, 2004). Water-soluble surfactants may also bind to proteins or polysaccharides and modify their functional properties. Oil-soluble surfactants with relatively low HLB numbers (3–6) are often used to stabilize W/O emulsions, such as margarines and spreads. They are also used to inhibit fat crystallization in some O/W emulsions, since this improves the stability of the food product to refrigeration conditions, for example, dressings (Garti and Yano, 2001). Oil-soluble surfactants can also be used in

conjunction with water-soluble surfactants to facilitate protein displacement from fat droplets during the production of ice creams, whipped creams, and toppings (Faergemand and Krog, 2003). Surfactants with intermediate HLB numbers (6–9) have a poor solubility in both oil and water phases and are not particularly good emulsifiers when used in isolation. Nevertheless, their emulsification properties can be improved by using them in combination with other surfactants.

As mentioned earlier, most surfactants do not consist of an individual molecular species, but consist of a complex mixture of different types of molecular species. Some of the impurities in surfactant mixtures may adversely affect the physical or chemical stability of emulsions, for example, peroxides in nonionic surfactants can affect lipid oxidation (Nuchi et al., 2001). Hence, it may be necessary to ensure that a surfactant is of a reliable high purity and quality before it is used to prepare a product.

**4.4.1.4.1 Monoglycerides.** The term “monoglycerides” is commonly used to describe a series of surfactants produced by interesterification of fats or oils with glycerol (Faergemand and Krog, 2003). This procedure produces a complex mixture of monoacylglycerides, diacylglycerides, triacylglycerides, glycerol, and free fatty acids, which is often referred to as “monodiglycerides.” The monoacylglyceride fraction can be effectively separated (>90% purity) from the other fractions by molecular distillation to produce a more pure “distilled monoglyceride” ingredient. Distilled monoglycerides are available with hydrocarbon chains of differing lengths and degrees of unsaturation. Generally, monoglycerides are nonionic oil-soluble surfactants with relatively low HLB numbers (~2–5).

**4.4.1.4.2 Organic acid esters of monoglycerides.** Monoglycerides can be esterified with a variety of organic acids (e.g., acetic, citric, diacetyl tartaric, and lactic acids) to form surfactants with different functional properties (Faergemand and Krog, 2003). Organic acids can be esterified to either one or both of the free hydroxyl groups on the monoglycerides. The most common examples of this type of surfactant are acetylated monoglycerides (ACETEM), lactylated monoglycerides (LACTEM), diacetyl tartaric acid monoglycerides (DATEM), and citric acid esters of monoglycerides (CITREM). Each of these surfactants is available with hydrocarbon chains of differing lengths and degrees of unsaturation. ACETEM and LACTEM are nonionic oil-soluble surfactants with low HLB numbers, whereas DATEM and CITREM are anionic water-dispersible surfactants with intermediate or high HLB numbers.

**4.4.1.4.3 Polyol esters of fatty acids.** Surfactants with different functional characteristics can be produced by esterification of polyols with fatty acids (Faergemand and Krog, 2003). The type of polyol and fatty acids used to prepare the surfactant determine its functional characteristics. The polyols that are most commonly esterified with fatty acids are polyglycerol, propylene glycol, sorbitan, polyoxyethylene sorbitan, and sucrose. The fatty acids used to prepare these types of surfactants may vary in chain length (typically 12–18 carbon atoms) and degree of unsaturation. The solubility and functional properties of polyol esters of fatty acids depend on the relative sizes of the hydrophilic and lipophilic parts of the molecules. Surfactants with large polyol head groups tend to be water dispersible and have high HLB numbers (e.g., polyglycerol and polyoxyethylene sorbitan esters), whereas those with small polyol head groups tend to be oil soluble and have low HLB numbers (e.g., propylene glycol esters). The ratio of hydrophilic to lipophilic groups can be varied appreciably within some series of polyol esters of fatty acids by changing the size of the polyol group, which leads to both oil-soluble and water-dispersible surfactants being present in the same series, for example, sucrose esters. Sorbitan esters of fatty acids are one of the most commonly used oil-soluble nonionic surfactants, which are often

sold under the trade name "Span<sup>TM</sup>." On the other hand, polyoxyethylene sorbitan esters are one of the most commonly used water-dispersible nonionic surfactants, which are often sold under the trade names of "Polysorbate<sup>TM</sup>" or "Tween<sup>TM</sup>." These oil-soluble and water-soluble surfactants are often used in combination to improve the overall stability of emulsions.

**4.4.1.4.4 Stearoyl lactylate salts.** Surfactants can be produced by esterification of lactic acid with fatty acids in the presence of either sodium or calcium hydroxide (Faergemand and Krog, 2003). Sodium stearoyl lactylate (SSL) is an anionic water-dispersible surfactant with an intermediate HLB number, whereas calcium stearoyl lactylate (CSL) is an anionic oil-soluble surfactant with a low HLB number (Table 4.6). Commercial SSL ingredients often contain a significant fraction of free fatty acids, which limits their water solubility at pH values below 4 or 5 (Krog, 1997).

**4.4.1.4.5 Lecithin.** Lecithins are naturally occurring surface-active molecules that can be extracted from a variety of sources, including soybeans, rapeseed, and egg (Faergemand and Krog, 2003). Soy lecithin is the most widely used surfactant ingredient in the food industry since it can be economically extracted during the processing of crude soybean oil (Stauffer, 1999). The egg lecithin found in egg yolk is believed to play an important role in stabilizing mayonnaise and salad dressing, but it is too expensive to be extracted as a specialized surfactant ingredient (Stauffer, 1999). Natural lecithins contain a complex mixture of different types of phospholipids and other lipids, although they can be fractionated to form more pure ingredients that are enriched with particular fractions. The most common phospholipids in lecithin are phosphatidylcholin (PC), phosphatidyletanolamine (PE), and phosphatidylinositol (PI) (Faergemand and Krog, 2003). The hydrophilic head groups of these molecules are either anionic (PI) or zwitterionic (PC and PE), while the lipophilic tail groups consist of two fatty acids. Natural lecithin has intermediate solubility characteristics and HLB numbers (~8), which means that it is not particularly suitable for stabilizing either O/W or W/O emulsions when used in isolation, but it may be effective when used in combination with other surfactants. In addition, lecithin can be chemically or enzymatically hydrolyzed to break off one of the hydrocarbon tails to produce more hydrophilic surfactants that are capable of stabilizing O/W emulsions (Krog, 1997).

## 4.4.2 Amphiphilic biopolymers

### 4.4.2.1 Molecular characteristics

Proteins and polysaccharides are both naturally occurring polymers. Proteins are polymers of amino acids, whereas polysaccharides are polymers of monosaccharides (McGregor and Greenwood, 1980; Creighton, 1993; Lehninger et al., 1993; Damodaran, 1996; BeMiller and Whistler, 1996; Bergethon, 1998). The functional properties of food biopolymers (e.g., solubility, surface activity, thickening, and gelation) are ultimately determined by their molecular characteristics (e.g., molecular weight, conformation, flexibility, polarity, hydrophobicity, and interactions). These molecular characteristics are determined by the type, number, and sequence of the monomers that make up the polymer chain (Bergethon, 1998; Norde, 2003; Walstra, 2003a). Monomers vary according to their polarity (ionic, polar, nonpolar, or amphiphilic), physical dimensions, molecular interactions, and reactive groups (Creighton, 1993; Lehninger, et al., 1993). If a biopolymer contains only one type of monomer it is referred to as a homopolymer (e.g., amylose or cellulose), but if it contains different types of monomers it is referred to as a heteropolymer (e.g., gum arabic, pectin, and all proteins).



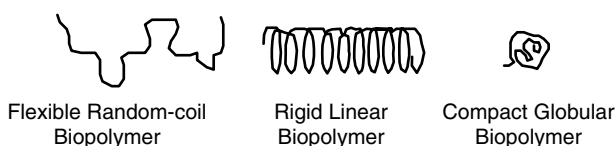


**Figure 4.19** Biopolymers can adopt a number of different conformations in solution depending on their molecular structure. These can be conveniently categorized as random coil, rod-like, and globular.

Both proteins and polysaccharides have covalent linkages between the monomers around which the polymer chain can rotate at certain well-defined angles. The fact that biopolymers contain relatively large numbers of monomers (typically between 20 and 20,000) and that rotation around the links in the chain is possible, means that they can potentially take up a huge number of different configurations in solution. In practice, biopolymers tend to adopt fairly well-defined conformations in an attempt to minimize the free energy of the system under the prevailing environmental conditions. This conformation is determined by a delicate balance of physicochemical phenomena, including hydrophobic interactions, electrostatic interactions, hydrogen bonding, van der Waals forces, and configurational entropy (Chapter 2). It should be stressed that most foods are actually nonequilibrium systems, and so a biopolymer may be trapped in a metastable state, because there is a large activation energy preventing it from reaching the most thermodynamically stable state. The configurations that biopolymer chains tend to adopt in aqueous solutions can be conveniently divided into three categories: globular, rod-like, or random coil (Figure 4.19). Globular biopolymers have fairly rigid compact structures, rod-like biopolymers have fairly rigid extended structures (often helical), and random-coil biopolymers have highly dynamic and flexible structures. Biopolymers can also be classified according to the degree of branching of the chain (Lehninger et al., 1993). Most proteins have linear chains, whereas polysaccharides can have either linear (e.g., amylose) or branched (e.g., amylopectin) chains. In practice, many biopolymers do not have exclusively one type of conformation, but have some regions that are random coil, some that are rod-like, and some that are globular. It should also be noted that biopolymers in solution may be present as individual molecules or they may be present as supramolecular structures where they are associated with one or more molecules of the same or different kind. Finally, it should be mentioned that biopolymers may undergo transitions from one conformation to another, or from one aggregation state to another, if their environment is altered, for example, pH, ionic strength, solvent composition, or temperature. The conformation and aggregation state of biopolymers play a major role in determining their functional attributes, and so it is usually important that food scientists are aware of the molecular characteristics of the biopolymers present in each particular food emulsion.

#### 4.4.2.2 Interfacial activity and emulsion stabilization

Usually, amphiphilic biopolymers must be fully dispersed and dissolved in an aqueous solution before they are capable of exhibiting their desirable emulsifying properties (Damodaran, 1996; McClements, 2002c). Solvation of biopolymer ingredients prior to homogenization is therefore an important step in the formation of many food emulsions. This process usually involves a number of stages, including dispersion, wetting, swelling, and dissolution. The effectiveness and rate of dissolution depends on many factors, including the nature of the ingredient (e.g., liquid, powder, or granules), biopolymer type and conformation, pH, ionic strength, temperature and composition of the aqueous

phase, as well as the application of shearing forces. Generally, factors that favor biopolymer–biopolymer interactions tend to oppose good dissolution, whereas factors that favor biopolymer–solvent interactions tend to promote good dissolution. These factors are primarily governed by the nature of the molecular interactions that dominate in the particular system, which depends strongly on biopolymer type and solvent composition. Discussions of the major factors that influence the dissolution of proteins and polysaccharides are given elsewhere (Brady, 1989; Dickinson and McClements, 1995; BeMiller and Whistler, 1996; Damodaran, 1996; McClements, 2002c).

After a biopolymer ingredient has been adequately dissolved in the aqueous phase it is important to ensure that the solution and environmental conditions (e.g., pH, ionic strength, temperature, and solvent composition) will not promote droplet aggregation during homogenization or after the emulsion is formed. For example, it is difficult to produce protein-stabilized emulsions at pH values close to the isoelectric point of the proteins or at high salt concentrations, because the electrostatic repulsion between the droplets is insufficient to prevent droplet aggregation once the emulsions are formed.

The interfacial activity of many biopolymers is due to the fact that they have both hydrophilic and lipophilic regions distributed along their backbones. For example, most proteins have significant numbers of exposed nonpolar amino acid side groups (Damodaran, 1996), whereas some polysaccharides have nonpolar side chains attached to their polar backbones (Dickinson, 2003). The major driving force for adsorption of these amphiphilic biopolymers to oil–water interfaces is therefore the hydrophobic effect. When the biopolymer is dispersed in an aqueous phase some of the nonpolar groups are in contact with water, which is thermodynamically unfavorable because of hydrophobic interactions (Section 4.3). When a biopolymer adsorbs to an interface it can adopt a conformation where the nonpolar groups are located in the oil phase (away from the water) and the hydrophilic groups are located in the aqueous phase (in contact with the water). Adsorption also reduces the contact area between the oil and water molecules at the oil–water interface, which lowers the interfacial tension (Chapter 5). Both of these factors favor the adsorption of amphiphilic biopolymers to oil–water interfaces. The conformation that a biopolymer adopts at an interface, and the physicochemical properties of the membrane formed, depend on its molecular structure and interactions (Das and Kinsella, 1990; Dickinson, 1992; Dalgleish, 1989, 1995, 1996a,b; Damodaran, 1996; Norde, 2003). Flexible random-coil biopolymers adopt an arrangement where the predominantly nonpolar segments protrude into the oil phase, the predominantly polar segments protrude into the aqueous phase, and the neutral regions lie flat against the interface (Figure 4.20). The membranes formed by these types of molecules tend to be relatively open, thick, and of low viscoelasticity. Globular biopolymers (usually proteins) adsorb to an interface so that the predominantly nonpolar regions on the surface of the molecule face the oil phase, while the predominantly polar regions face the aqueous phase, and so they tend to have a particular orientation at an interface (Figure 4.20). Once they have adsorbed to an interface, biopolymers often undergo structural rearrangements so that they can maximize the number of contacts between nonpolar groups and oil (Norde, 2003). Random-coil biopolymers are relatively flexible molecules and can therefore rearrange their structures fairly rapidly, whereas globular biopolymers are more rigid molecules and therefore rearrange more slowly. The unfolding of a globular protein at an interface often exposes amino acids that were originally located in the hydrophobic interior of the molecule, which can lead to enhanced interactions with neighboring protein molecules through hydrophobic attraction or disulfide bond formation (Dickinson and Matsumura, 1991; McClements et al., 1993d). Consequently, globular proteins tend to form relatively thin and compact membranes that have high viscoelasticities (Dickinson, 1992). This may account for the fact that membranes formed by globular proteins are more resistant to rupture than those formed by more random-coil proteins.

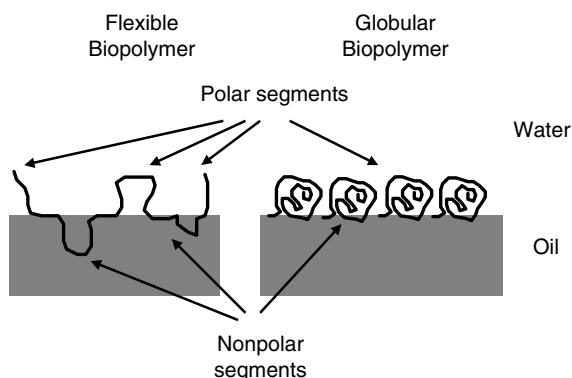


**Figure 4.20** The structure of the interfacial membrane depends on the molecular structure and interactions of the surface-active molecules.

To be effective emulsifiers, biopolymers must rapidly adsorb to the surface of the emulsion droplets created during homogenization, and then form an interfacial membrane that prevents the droplets from aggregating with one another (Chapter 6). The interfacial membranes formed by biopolymers can stabilize emulsion droplets against aggregation by a variety of different mechanisms, for example, steric, electrostatic, and hydration repulsion. The stabilizing mechanism that dominates in a particular system is largely determined by the characteristics of the interfacial membrane formed, for example, thickness, electrical charge, internal packing, exposed reactive groups. The dominant stabilizing mechanism operating in a particular emulsion determines the sensitivity of the system to droplet aggregation under different solution and environmental conditions, for example, pH, ionic strength, temperature, solvent quality. In the following sections, we will describe and compare the interfacial properties and emulsion stabilizing abilities of proteins and polysaccharides commonly used as food emulsifiers.

#### 4.4.2.3 Common biopolymer food emulsifiers

Many food emulsions are stabilized by surface-active biopolymers that adsorb to droplet surfaces and form protective membranes. Some of these functional biopolymers are integral components of more complex food ingredients used in food manufacture (e.g., milk, eggs, meat, fish, and flour), whereas others have been isolated from their normal environments and possibly modified before being sold as specialty ingredients (e.g., protein concentrates or isolates, hydrocolloid emulsifiers). In this section, we will focus primarily on those surface-active biopolymers that are sold as functional ingredients specifically designed for use as emulsifiers in foods. In addition, we will focus on the ability of biopolymers to create stable O/W emulsions, rather than on their interfacial activity, since the former is more relevant to their application as emulsifiers in the food industry. This point can be clearly illustrated by considering the interfacial characteristics of globular proteins near their isoelectric point. Globular proteins are capable of rapidly adsorbing to oil–water interfaces and forming thick viscoelastic membranes near their isoelectric points, but they will not form stable emulsions because the electrostatic repulsion between the droplets is insufficient to prevent droplet aggregation.

**4.4.2.3.1 Proteins.** The interfacial membranes formed by proteins are usually relatively thin and electrically charged, hence the major mechanism preventing droplet flocculation in protein-stabilized emulsions is electrostatic repulsion (Dickinson and

McClements, 1995; Claesson et al., 2004). Consequently, protein-stabilized emulsions are particularly sensitive to pH and ionic strength effects, and will tend to flocculate at pH values close to the isoelectric point of the adsorbed proteins and when the ionic strength exceeds a certain level. Emulsions stabilized by globular proteins are also particularly sensitive to thermal treatments, because these proteins unfold when the temperature exceeds a critical value exposing reactive nonpolar and sulfhydryl groups. These reactive groups increase the attractive interactions between droplets, which may lead to droplet flocculation. It should be noted that a number of methods have been developed to attempt to improve the emulsifying properties of protein ingredients, including limited hydrolysis to form peptides, modification of protein structure by chemical, physical, enzymatic, or genetic means, and blending of the proteins with other ingredients, although not all of these processes are currently legally allowed.

*Milk proteins.* Protein ingredients isolated from bovine milk are used as emulsifiers in a wide variety of emulsion-based food products, including beverages, frozen desserts, ice creams, sports supplements, infant formula, and salad dressings. Milk proteins can be conveniently divided into two major categories (Swaigood, 1996): caseins (~80 wt%) and whey proteins (~20 wt%). Casein and whey protein fractions can be separated from each other by causing the casein to precipitate from solution (the *curd*) and leaving the whey proteins in solution (the *whey*). Casein precipitation can be achieved by adjusting the pH close to the isoelectric point (~4.6) of the caseins or by adding an enzyme called *rennet* that cleaves the hydrophilic fraction of casein that is normally responsible for stabilizing casein micelles. If isoelectric precipitation is used the separated fractions are called “acid casein” and “acid whey,” whereas if enzyme precipitation is used the separated fractions are called “rennet casein” and “sweet whey.” The fractions separated using these two processes have different compositions, and therefore ingredients produced from them may have different functional properties. Curd formation is a critical step in the creation of cheese, and there are large quantities of whey remaining from this process that can be used to make functional whey protein ingredients. A variety of milk protein ingredients are available for usage as emulsifiers in foods, including whole milk, whey proteins, and caseins. These ingredients are usually sold in a powdered form, which is light cream to white in appearance and has a bland flavor. These powders are normally available in the form of protein concentrates (25–80% protein) or protein isolates (>90% protein). It should be noted that there are a relatively large number of different kinds of proteins in both casein and whey (see below), and that it is possible to fractionate these proteins into individual purified fractions. Purified fractions are normally too expensive to be used as emulsifying ingredients in the food industry, but they are frequently used in research studies because they facilitate the development of a more fundamental understanding of protein functionality in emulsions.

There are four main protein fractions in casein:  $\alpha_{s1}$  (~44%),  $\alpha_{s2}$  (~11%),  $\beta$  (~32%), and  $\kappa$  (~11%) (Swaigood, 1996; Oakenfull, et al., 1997). In general, these molecules have relatively random and flexible structures in solution, although they do have a limited amount of secondary and tertiary structure (Caessens, et al., 1999). The caseins also have some regions that are highly nonpolar and others that are highly charged, which plays a major role in determining their molecular and functional properties in foods (Dalglish, 1997b). In their natural state, the caseins tend to exist as complex molecular clusters called “micelles” that are typically between 50 and 250 nm in diameter and are partly held together by mineral ions (such as calcium phosphate). In commercial ingredients, caseins may also be present in a number of other sorts of molecular cluster depending on the way that the proteins were isolated, for example, sodium caseinate, calcium caseinate, acid casein, rennet casein (Dalglish, 1997b).

Caseinate-stabilized emulsions have been shown to be unstable to droplet flocculation at pH values (3.5–5.3) close to the protein's isoelectric point (Agboola and Dalgleish, 1996d) and at relatively high ionic strengths (Agboola and Dalgleish, 1996a; Dickinson and Davies, 1999; Schokker and Dalgleish, 2000; Srinivasan et al., 2000; Ye and Singh, 2001). Caseinate-stabilized emulsions tend to be more stable to heating than whey protein-stabilized emulsions, presumably because the relatively flexible casein molecules do not undergo appreciable heat-induced conformational changes like globular proteins do (Hunt and Dalgleish, 1995; Srinivasan et al., 2002). It should be noted that sufficiently high concentrations of nonadsorbed caseinate can promote emulsion instability through a depletion flocculation mechanism (Dickinson and Golding, 1997b; Srinivasan et al., 2002). The caseinate concentration where depletion flocculation occurs depends on the size of the nonadsorbed caseinate aggregates, which is governed by factors such as solution composition and environmental conditions (Dickinson and Golding, 1997b; Srinivasan et al., 2002).

Whey protein is also a complex mixture of different individual proteins, with the most common being  $\beta$ -lactoglobulin (~55%),  $\alpha$ -lactalbumin (~24%), serum albumin (~5%), and immunoglobulins (~15%) (Swaigood, 1996). Normally,  $\beta$ -lactoglobulin dominates the functional characteristics of whey proteins because of its relatively high concentration and unique physicochemical properties. Whey protein-stabilized emulsions tend to flocculate at pH values (~4–5.5) close to their isoelectric point (IEP ~5) (Demetriades et al., 1997a), at high salt concentrations (Agboola and Dalgleish, 1995; Hunt and Dalgleish, 1995; Demetriades et al., 1997a, Kulmyrzaev et al., 2000a,b), and on heating above the thermal denaturation temperature of the adsorbed proteins in the presence of salt (Monahan et al., 1996; Demetriades and McClements, 1998; Kim et al., 2002b). Users of whey protein emulsifiers in the food industry have reported that large variations in their functional properties can occur from batch-to-batch, which has been attributed to the presence of mineral impurities and partial denaturation of the proteins during their isolation. Preferential adsorption and competitive displacement of milk proteins with each other and with other types of emulsifiers have been widely studied (Corthaudon et al., 1991a–d; Dickinson, 1992, 2001; Dickinson and Iveson, 1993; Dalgleish, 1997a,b; Brun and Dalgleish, 1999).

*Meat and fish proteins.* Meat and fish contain a number of proteins that are surface-active and capable of stabilizing emulsions, for example, gelatin, myosin, actomyosin, sarcoplasmic proteins, and actin (Cofrades et al., 1996; Tornberg et al., 1997; Xiong, 1997). Many of these proteins play an important role in stabilizing meat emulsions, that is, products formed by blending or homogenizing fat, meat, and other ingredients. Emulsion stabilization is partly due to their ability to adsorb to the oil–water interface and partly due to their ability to increase the aqueous phase viscosity or to form a gel in the aqueous phase (Tornberg et al., 1997). Gelatin is one of the few proteins that have been isolated from meat and fish and sold commercially as a functional emulsifier ingredient. Gelatin is a relatively high molecular weight protein derived from animal collagen, for example, pig, cow, or fish. Gelatin is prepared by hydrolyzing collagen by boiling in the presence of acid (Type A gelatin) or alkaline (Type B gelatin). The IEP of Type A gelatin (~7–9) tends to be higher than that of Type B gelatin (~5). Gelatin exists as a random-coil molecule at relatively high temperatures, but undergoes a coil-helix transition on cooling below a critical temperature, which is about 10–25°C for pig and cow gelatin and about 0–5°C for fish gelatin (Leunberger, 1991). Gelatin has been shown to be surface-active and capable of acting as an emulsifier in O/W emulsions (Muller and Hermel, 1994; Lobo, 2002). Nevertheless, when used on its own gelatin often produces relatively large droplet sizes during homogenization (Dickinson and Lopez, 2001; Lobo, 2002), so that it has to be

hydrophobically modified by attachment of nonpolar side groups (Toledano and Magdassi, 1998) or used in conjunction with anionic surfactants to improve its effectiveness as an emulsifier (Muller and Hermel, 1994; Olijve et al., 2001). Research has been carried out to establish the ability of various other protein fractions of fish and meat muscle to act as emulsifiers (Galluzzo and Regenstien, 1978a,b, Huber and Regenstien, 1988; Tornberg et al., 1997; Huidobro et al., 1998). The ultimate objective of this work is to be able to convert waste products from fish and meat production into value-added functional ingredients for use as emulsifiers in foods. Nevertheless, there are currently few examples of functional ingredients derived from fish or meat products (other than gelatin) designed especially as emulsifiers.

*Egg proteins.* Both egg yolk and egg white contain a mixture of protein and non-protein components that are surface-active (Mine, 1998a,b, 2002; Anton et al., 2001; Azzam and Omari, 2002). Egg ingredients can be purchased in a variety of different forms for usage in food emulsions, including fresh egg yolks, frozen egg yolks, dried egg yolks, fresh whole eggs, frozen whole eggs, and dried whole eggs. Different egg ingredients are usually prepared using different processing treatments, which often influence their effectiveness at stabilizing emulsions (Paraskevopoulou et al., 1999; Anton et al., 2000a,b; Guerrero et al., 2000; Moros et al., 2002a,b). In the food industry, egg white is more commonly used for stabilizing foams, whereas egg yolk is more commonly used for stabilizing emulsions (Le Denmat et al., 2000; Anton et al., 2001; Mine, 2002; Moros et al., 2002a,b). Nevertheless, a number of studies have shown that egg white proteins can be used to stable O/W emulsions (Mine et al., 1991; Galazka et al., 2000). Egg yolk is widely used as an emulsifier in the production of mayonnaise, salad dressings, sauces, and cake batters (Mine, 1998a,b, 2002; Anton et al., 2001, 2002). The effectiveness of whole egg yolk and its individual constituents (plasma and granules) at forming O/W emulsions using a high-speed blender has been investigated (Mine, 1998a,b, 2002). Measurements of the mean particle diameter of the emulsions showed that plasma (mainly low density lipoprotein [LDL] and livetin) produced the smallest particles, followed by whole egg yolk, followed by granules (mainly high density lipoprotein [HDL] and phosvitin). Recently it has been demonstrated that LDL is the main contributor to the emulsifying properties of the plasma constituents (Mine, 2002; Martinet et al., 2003). The mean particle diameter of emulsions stabilized by egg yolk decreased from pH 3 to 9, suggesting that egg yolk was more efficient at forming emulsions at higher pH values. Studies of the ability of whole egg yolk, plasma, and granules to stabilize O/W emulsions prepared using a high-pressure valve homogenizer have also been carried out (Le Denmat et al., 1999, 2000). These researchers found that the main contributors to egg yolk functionality as an emulsion stabilizer were the plasma constituents, rather than the granules. Emulsions stabilized by egg yolk were found to be stable to droplet flocculation at pH 3 at relatively low salt concentrations (150 mM NaCl), but unstable to flocculation at pH 3 at high salt concentrations (550 mM NaCl), and at pH 7 (150 and 550 mM NaCl) (Anton et al., 2002). The instability of these emulsions was attributed to depletion, bridging, and electrostatic screening effects. It therefore seems that egg yolk is better at forming emulsions at high pH (Mine, 1998a,b), but stabilizing emulsions at low pH (Anton et al., 2002). Understanding the influence of pH and salt concentration on the stability of egg yolk stabilized emulsions is often complicated because these factors influence the solubility and structural organization of the protein molecules, as well as the interactions between the emulsion droplets (Anton and Gandemer, 1999). Like other globular proteins, the proteins in eggs will unfold and aggregate on heating above their thermal denaturation temperature, which influences the stability and rheological properties of emulsions (Le Denmet et al., 1999; Moros et al., 2002a,b). Emulsions stabilized by egg yolk have been shown to have poor

stability to freeze–thaw cycling (Mine, 1995). Preferential adsorption and competitive displacement of egg yolk proteins with each other and with other types of emulsifiers have been reviewed (Mine, 2002).

*Plant proteins.* Surface-active proteins can be extracted from a variety of plant sources, including legumes and cereals (Tornberg et al., 1997). A considerable amount of research has been carried out to establish the ability of these proteins to stabilize emulsions, and whether they could be made into commercially viable value-added ingredients for usage as emulsifiers in foods (Akintayo et al., 1998; Franco et al., 1998b; Wu et al., 1998; Webb et al., 2002). One of the most widely studied proteins extracted from a plant source is soy protein, which is commercially available as a protein concentrate or isolate (Molina et al., 2001; Floury et al., 2002; Khatib et al., 2002; Roesch and Corredig, 2002a,b; Hu et al., 2003; Saito et al., 2003). Soy protein ingredients are a complex mixture of many individual protein fractions with different molecular and functional characteristics, for example, 2S, 7S, 11S, and 15S fractions (Utsumi et al., 1997; Tornberg et al., 1997; Liu et al., 1999). In addition, each of these fractions contains a mixture of different protein subunits that also have different molecular and functional characteristics (Tornberg et al., 1997).

Previous studies have shown that soy proteins can decrease the interfacial tension between oil and water and therefore facilitate emulsion formation (Tornberg et al., 1997). Researchers have shown that it is possible to form stable O/W emulsions using soy proteins or their fractions as emulsifiers (Liu et al., 1999; Roesch and Corredig, 2002a,b). Nevertheless, compared to the other sources of proteins mentioned earlier, there have been far fewer systematic studies on the influence of environmental conditions (pH, ionic strength, and temperature) on the stability of soy protein-stabilized emulsions. Emulsions prepared using soy protein concentrates or isolates tend to be highly flocculated, possibly because of bridging of the relatively large soy protein aggregates between droplets (Tornberg et al., 1997). Consequently, soy proteins could be used to stabilize emulsions where droplet creaming is not usually a problem, for example, food products with relatively high droplet concentrations or high continuous phase viscosities. On the other hand, soy protein ingredients may be unsuitable for stabilizing relatively dilute emulsions where creaming would be accelerated by droplet flocculation. Nevertheless, researchers are examining methods of improving the emulsifying properties of soy proteins by fractionating them (Liu et al., 1999), by physically, chemically, enzymatically, or genetically modifying them (Tornberg et al., 1997; Molina et al., 2001; Floury et al., 2002) or by using them in combination with other ingredients (Aoki et al., 1994).

#### 4.4.2.3.2 Polysaccharides.

*Gum arabic.* Gum arabic is widely used as an emulsifier in the beverage industry to stabilize cloud and flavor emulsions (Tan, 2004). It is derived from the natural exudate of *Acacia senegal*, and consists of at least three high molecular weight biopolymer fractions. The surface-active fraction is believed to consist of branched arabinogalactan blocks attached to a polypeptide backbone (Phillips and Williams, 1995; Jayme et al., 1999; Dickinson, 2003). The hydrophobic polypeptide chain is believed to anchor the molecules to the droplet surface, while the hydrophilic arabinogalactan blocks extend into solution (Phillips and Williams, 1995; Islam et al., 1997). The interfacial membrane formed by gum arabic is believed to provide stability against droplet aggregation mainly through steric repulsion, but with some contribution from electrostatic repulsion also (Jayme et al., 1999; Chanamai and McClements, 2002). The influence of a variety of processing conditions on gum arabic functionality has been examined (Buffo et al., 2001, 2002; Buffo and Reineccius, 2002). For example, it has been shown that gum arabic stabilized emulsions remain stable to droplet

flocculation when exposed to a wide range of conditions, for example, pH (3–9), ionic strength (0–25 mM  $\text{CaCl}_2$ ), and thermal treatment (30–90°C) (Chanamai and McClements, 2002). Nevertheless, gum arabic has a relatively low affinity for oil–water interfaces compared to most other surface-active biopolymers, which means that it has to be used at relatively high concentrations to form stable emulsions. For example, as much as 20% gum arabic may be required to produce a stable 12 wt% O/W emulsion (Tse and Reineccius, 1995). For this reason, its application as an emulsifier is restricted to products that have relatively low droplet concentrations, for example, beverage emulsions. In addition, there have been frequent problems associated with obtaining a reliable source of consistently high quality gum arabic that has led many food scientists to investigate alternative sources of biopolymer emulsifiers for use in beverages (Kim et al., 1996; Tan, 1998, 2004; Garti, 1999). Gum arabic has a high water-solubility and a relatively low-solution viscosity compared to other gums, which facilitates its application as an emulsifier (Glicksman, 1983a–c).

*Modified starches.* Natural starches are hydrophilic molecules that have poor surface activity. Nevertheless, they can be made into effective emulsifiers by chemically attaching hydrophobic moieties along their backbones (Trubiano, 1995). These modified starches are widely used as emulsifiers in the beverage industry. One of the most commonly used modified starches is an octenyl succinate derivative of waxy-maize (Trubiano, 1995; Stauffer, 1999). It consists primarily of amylopectin that has been chemically modified to contain a side group that is anionic and nonpolar. These side groups anchor the molecule to the oil droplet surface, while the hydrophilic starch chains protrude into the aqueous phase and protect droplets against aggregation through steric repulsion. Because the dominant stabilizing mechanism is steric repulsion, emulsions stabilized by modified starch are resistant to changes in pH (3–9), ionic strength (0–25 mM  $\text{CaCl}_2$ ), and temperature (30–90°C) (Chanamai and McClements, 2002). Like gum arabic, modified starch has a relatively low interfacial activity (compared to proteins or surfactants), and so a large excess must be added to ensure that all the droplet surfaces are adequately coated. For example, it is recommended that about 12% modified starch is required to produce a stable 12 wt% O/W emulsion (Tse and Reineccius, 1995). Modified starches usually come in powdered or granular forms that are easily dispersible in cold water.

*Modified celluloses.* In its natural state cellulose is not usually suitable for usage as an emulsifier because it forms strong intermolecular hydrogen bonds, which make it insoluble in water. Nevertheless, it can be isolated and modified in a number of ways to produce food-grade ingredients that have interfacial activity and can be used as emulsifiers (Huang et al., 2001). The most commonly used surface-active cellulose derivatives are methyl cellulose (MC), hydroxypropyl cellulose (HPC), and methyl hydroxypropyl cellulose (MHPC). These ingredients are all nonionic polymers that are soluble in cold water, but tend to become insoluble when the solution is heated above a critical temperature (around 50–90°C). They have good stability to pH (2–11), salt, and freeze–thaw cycling, which may be beneficial in a number of food emulsion applications.

*Other polysaccharides.* A number of studies have shown that various other types of polysaccharides are capable of reducing oil–water interfacial tensions and forming stable emulsions, for example, galactomannans, pectin, chitosan (Garti and Reichman, 1993; Schmitt et al., 1998; Huang et al., 2001; Dickinson, 2003; Leroux et al., 2003). Nevertheless, there is still some debate about the molecular origin of their surface activity (e.g., nonpolar regions on the polysaccharide molecule itself, protein contaminants, or protein moieties bound to the polysaccharides), and about whether their ability to form stable emulsions is primarily due to their surface activity or the ability to thicken the aqueous phase (Dickinson, 2003).



**4.4.2.3.3 Protein–polysaccharide complexes.** Proteins tend to be better at producing small emulsion droplets when used at low concentrations than polysaccharides, whereas polysaccharides tend to be better at producing emulsions that are stable to a wider range of environmental conditions than proteins, for example, pH, ionic strength, temperature, freeze–thaw cycling (McClements, 2004). It may therefore be advantageous to combine the beneficial attributes of these two kinds of biopolymers to produce small emulsion droplets with good environmental stability. A number of researchers have shown that protein–polysaccharide complexes may have better emulsifying properties than either of the biopolymers used in isolation (Dickinson, 1993, 1995, 2003; Benichou et al., 2002b). These complexes may be held together either by physical or covalent interactions, and may be formed either before or after homogenization (McClements, 2004). Ingredients based on protein–polysaccharide interactions will have to be legally acceptable, economically viable, and show benefits over existing ingredients before they find widespread usage in the food industry. It should be noted that gum arabic is a naturally occurring protein–polysaccharide complex that is already widely used in the food industry as an emulsifier (Phillips and Williams, 1995, 2003).

#### 4.4.3 Selection of an appropriate emulsifier

In this section, we will discuss some schemes for classifying and comparing the effectiveness of different types of food emulsifiers, as well as some of the factors that should be considered when selecting an emulsifier for a particular application. As has been mentioned earlier an effective emulsifier should have the following general characteristics: (i) it should be capable of rapidly adsorbing to the surface of freshly formed droplets during homogenization; (ii) it should be capable of reducing the interfacial tension by a significant amount, and (iii) it should be capable of forming an interfacial membrane that is either resistant to rupture and/or provides a sufficiently strong repulsive interaction between the droplets. A number of food-grade constituents exhibit these general characteristics and can be used as emulsifiers, but they vary considerably in their ability to form and stabilize emulsions, as well as in their sensitivity to environmental conditions for example, pH, ionic strength, temperature, solvent composition (Table 4.7). It would therefore be useful to have a standardized means of assessing the relative efficiency of different types of emulsifiers for specific applications. Unfortunately, there has been little attempt to systematically compare the advantages and disadvantages of different emulsifiers under standardized conditions, so that it is currently difficult for food manufacturers to rationally select the most suitable ingredient for particular products. One of the purposes of this section is to highlight some criteria that could form the basis for such a comparison.

Food manufacturers usually measure and compare the functional properties of emulsifiers in terms of parameters that depend on the processing procedure and formulation of their actual food product, for example:

1. The minimum droplet size ( $d_{\min}$ ) that can be produced by a certain amount of emulsifier for a specified emulsion system using specified homogenization conditions.
2. The minimum amount of the emulsifier ( $c_{\min}$ ) required to produce a desired droplet size for a specified emulsion system using specified homogenization conditions.
3. The long-term stability (e.g., to creaming, flocculation, or coalescence) of a specified emulsion system produced by an emulsifier using specified homogenization conditions.

The characteristics of the specified emulsion system (e.g., oil type, oil concentration, aqueous phase composition) used to establish the efficiency of an emulsifier depends on

the food being produced, and will vary considerably from product-to-product. In addition, the specified homogenization conditions will also vary according to the type of homogenizer used (e.g., high-speed blender, high-pressure valve homogenizer, microfluidizer, or colloid mill) and the precise operating conditions (e.g., energy input, flow rate, temperature). The above approach is particularly suited for food manufacturers trying to determine the best emulsifier for usage in their specific product, but it is not particularly suited for development of a general classification scheme because of the wide variation in the composition and processing of different foods. This approach could be used to develop a more general classification scheme by stipulating standardized emulsion systems and homogenization conditions. The analytical methods developed to measure *emulsifier capacity* and *emulsion stability index* (Chapter 11) are attempts at developing emulsifier classification schemes based on this principle.

Colloid and interfacial scientists often characterize emulsifier properties in terms of quantitative physical parameters that can be measured using fundamental analytical instruments under well-defined environmental conditions:

1. *Surface load,  $\Gamma_{\text{sat}}$* : The surface load at saturation is the mass of emulsifier adsorbed per unit surface area of interface when the interface is saturated with emulsifier, and is usually expressed as  $\text{mg m}^{-2}$  (Chapters 5 and 11). The surface load provides a measure of the minimum amount of emulsifier required to produce an emulsion with a given surface area (or droplet size): the higher  $\Gamma$ , the greater the amount of emulsifier required to completely cover the same surface area.
2. *Maximum surface pressure,  $\pi_{\text{max}}$* : The maximum surface pressure is the interfacial tension of an oil–water interface in the absence of emulsifier minus the interfacial tension of the same interface when it is saturated with emulsifier (Chapter 5). It provides a measure of the ability of an emulsifier to decrease the oil–water interfacial tension, and thereby facilitate droplet disruption: the higher  $\pi_{\text{max}}$ , the lower the Laplace pressure, and the smaller the droplets that can be produced in a homogenizer at a fixed energy input, provided there is sufficient emulsifier present and that it adsorbs rapidly to the droplet surfaces (Chapter 6).
3. *Binding affinity,  $c_{1/2}$* : The binding affinity is a measure of how strongly an emulsifier adsorbs to an oil–water interface (Chapter 5). It can be expressed as the emulsifier concentration at which the surface pressure is half the maximum surface pressure. The stronger the binding affinity (the lower  $c_{1/2}$ ), the lower the concentration of emulsifier required to reach interfacial saturation.
4. *Adsorption kinetics,  $\tau_{\text{ads}}$* : Adsorption kinetics can be defined in terms of the average time required for an interface to become saturated with emulsifier (Chapter 5). It is important that this time be measured under conditions that adequately represent the highly dynamic conditions that occur in most homogenizers. In practice, it is difficult to establish an accurate measure of the adsorption kinetics of different emulsifiers under realistically dynamic conditions.
5. *Droplet aggregation stability*: The aggregation stability is a measure of the tendency for droplets to become aggregated (flocculated or coalesced) under a specified set of environmental conditions, for example, pH, ionic strength, temperature, shearing rate (Chapter 7). It can be expressed in a number of different ways, for example, the percentage of droplets that are flocculated or coalesced, the percentage of droplets larger than a specified size, or the percentage increase in the mean size of the particles in an emulsion due to droplet aggregation.

One of the major challenges of food scientists is to relate these more fundamental parameters to the more practical parameters mentioned above that are of interest to food manufacturers.

An attempt has been made to compare the relative efficiencies of different types of emulsifiers at stabilizing food emulsions (Table 4.7). This comparison shows that nonionic surfactants can be used at low levels, and provide good stability to droplet aggregation over a range of environmental conditions. Proteins can also be used at relatively low levels, but their ability to stabilize emulsions against droplet aggregation is strongly influenced by pH, ionic strength, and temperature. Emulsions stabilized by polysaccharides have much better stability to environmental conditions than proteins due to the fact that the predominant stabilizing mechanism is steric rather than electrostatic, but they usually have to be used at much higher levels.

The discussion above has highlighted the wide variety of emulsifiers available for use in food products. A food manufacturer must decide which of these emulsifiers is the most suitable for usage in each particular product. In addition to the physicochemical characteristics considered above, a food manufacturer must also consider a number of economic, legal, and marketing factors when selecting a suitable emulsifier. The most important of these are discussed at the end of this chapter (Section 4.7).

## 4.5 *Texture modifiers*

A number of ingredients commonly used in food emulsions are added because of their ability to modify the texture of the continuous phase (usually the aqueous phase of O/W emulsions). These ingredients can be conveniently divided into “thickening agents” and “gelling agents” depending on the molecular origin of their functional characteristics. For the purposes of this book I will consider thickening agents to be those ingredients whose functional characteristics are due to their highly extended molecular conformation in solution, whereas gelling agents are those ingredients whose functional characteristics are due to their ability to associate with each other through intermolecular cross-links (see below). Nevertheless, in practice there is often no clear distinction between these two different categories of texture modifiers, since thickening agents can form gels when used at sufficiently high concentrations and gelling agents can increase the viscosity of aqueous solutions (without forming gels) when used at sufficiently low concentrations. In addition, a particular type of biopolymer may act as a thickening agent under some conditions, but a gelling agent under other conditions, for example, at a different temperature, pH, or ionic strength. The major roles of texture modifiers in food emulsions are to provide the product with desirable textural and mouthfeel characteristics, and to improve emulsion stability by reducing the rate at which particulate matter moves, such as oil droplets, herbs, spices, cheese pieces, and air bubbles.

### 4.5.1 *Thickening agents*

The primary function of thickening agents in food emulsions is to increase the viscosity of the aqueous phase of O/W emulsions (Mitchell and Ledward, 1986; Imeson, 1997; Williams and Phillips, 2003). This viscosity enhancement modifies the texture and mouthfeel of food products (*thickening*), as well as reducing the rate at which particles sediment or cream (*stabilization*). Thickening agent ingredients are usually sold as powders or granules consisting of an individual type of biopolymer or a mixture of different types of biopolymers. The biopolymers found in thickening agents usually exist as highly hydrated and extended molecules or molecular aggregates in aqueous solutions. Their ability to increase the viscosity of a solution depends principally on their molecular weight, degree of branching, conformation, and flexibility (Launay et al., 1986; Rha and Pradipasena, 1986;

Cesero, 1994; Williams and Phillips, 2003). In this section, we consider the relationship between the molecular characteristics of biopolymers and their ability to act as thickening agents. Specific types of thickening agents commonly used in the food industry are outlined in Section 4.5.3.

#### 4.5.1.1 Effective volume of biopolymers in aqueous solutions

The effectiveness of a biopolymer at enhancing the viscosity of an aqueous solution is largely determined by its molecular structure (BeMiller and Whistler, 1996; Williams and Phillips, 2003). The effective volume of a biopolymer thickening agent in solution is considerably greater than the volume occupied by the atoms that make up the biopolymer chain because it sweeps out a large volume of solvent as it rapidly rotates due to Brownian motion (Figure 4.21). It is convenient to characterize this phenomenon in terms of a *volume ratio*,  $R_v$ :

$$R_v = \frac{V_E}{V_A} \approx \frac{4\pi r_g^3 \rho N_A}{3M} \quad (4.8)$$

where  $V_E$  is the “effective” volume of the biopolymer molecule in solution,  $V_A$  is the actual volume occupied by the biopolymer chain,  $r_g$  is the radius of gyration of the molecule,  $\rho$  is the density of the biopolymer chain,  $N_A$  is Avogadro’s number, and  $M$  is the molecular weight of the biopolymer.

#### 4.5.1.2 Relationship between biopolymer molecular structure and effective volume in solution

The effective volume of a biopolymer depends on its three-dimensional structure in solution (Figure 4.19). For molecules that form compact globular structures (such as many globular proteins) the actual volume of the molecule is close to its effective volume and therefore  $R_v \approx 1$ . The average end-to-end length ( $L$ ) of random-coil molecules is given by  $L \approx l\sqrt{n}$ , whereas for rigid rod-like molecules it is given by  $L \approx ln$ , where  $l$  is the length

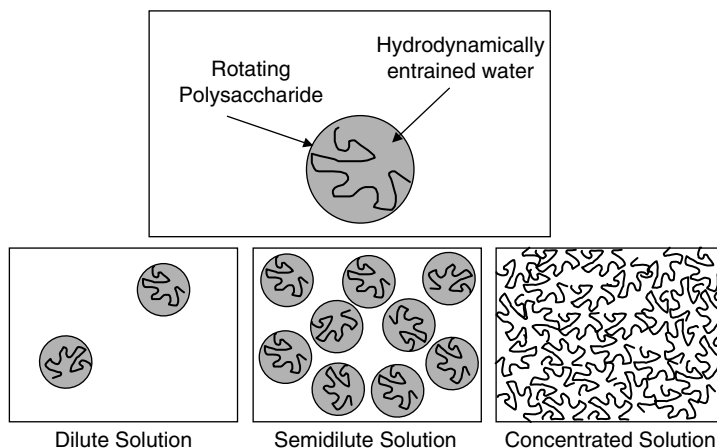


**Figure 4.21** Extended biopolymers sweep out a large volume of water as they rotate in solution and so they have a large effective volume fraction.

of the monomer unit and  $n$  is the number of monomers per molecule (Grosberg and Khokhlov, 1997). If we assume that the radius of gyration of the polysaccharide molecule is half the end-to-end length then we can obtain expressions for the effective volume of different types of molecules:

Globular biopolymers:

$$R_v \approx 1 \quad (4.9)$$

Random-coil biopolymers:

$$R_v \approx \frac{\pi n^{3/2} l^3 \rho N_A}{6M} \quad (4.10)$$

Rigid rod-like biopolymers:

$$R_v \approx \frac{\pi n^3 l^3 \rho N_A}{6M} \quad (4.11)$$

where  $M_0$  is the molecular weight of a monomer segment, and  $n = M/M_0$ . In practice, real biopolymers often have some regions that are compact, some that are rod-like, and some that are flexible and therefore they fall somewhere between these extremes (BeMiller and Whistler, 1996). Nevertheless, these equations give us some indication of the expected volume ratios of real biopolymers. For example, the molecular weight of polysaccharide segments is typically about 168 Da, and the length of a segment is typically about 0.47 nm (Voet and Voet, 1995). The molecular weights of polysaccharides used as thickening agents typically vary between 5 and 2000 kDa (BeMiller and Whistler, 1996; deMan, 1999). We would therefore expect volume ratios ranging from around unity to thousands of millions depending on the structure and molecular weight of the polysaccharide.

The above discussion indicates that biopolymers that have highly extended structures in solution have larger volume ratios than those that have compact structures. Thus,  $R_v$  tends to be higher for linear than for branched biopolymers with the same molecular weight, and tends to increase as the electrostatic repulsion between different segments on charged biopolymer molecules increase because this causes the molecule to become more extended (Walstra, 2003a).

#### 4.5.1.3 Viscosity enhancement by biopolymers in solution

The apparent viscosity ( $\eta$ ) of a colloidal dispersion containing spherical rigid particles suspended in an ideal liquid can be described over a wide range of particle concentrations using the following semiempirical equation (Liu and Masliyah, 1996):

$$\frac{\eta}{\eta_1} = \left(1 - \frac{\phi}{P}\right)^{[\eta]P} \quad (4.12)$$

where  $\eta_1$  is the viscosity of the continuous phase,  $[\eta]$  is the intrinsic viscosity =  $\lim_{\phi \rightarrow 0} \left(\frac{\eta/\eta_1 - 1}{\phi}\right)$ ,  $\phi$  is the volume fraction of the particles, and  $P$  is a packing parameter. The packing parameter is related to the volume fraction at which the particles become close packed, which depends on the applied shear stress and the polydispersity of the particles (Hunter, 1986). For rigid monodisperse spherical particles the following parameters have been determined experimentally:  $P = 0.57$  at low shear stresses,  $P = 0.68$  at high shear stresses, and  $[\eta] = 2.67$ .

To a first approximation the viscosity of a suspension of hydrated biopolymer molecules rotating in solution can be treated in a similar manner (McClements, 2000):

$$\frac{\eta}{\eta_1} \approx \left(1 - \frac{\phi_{\text{eff}}}{P}\right)^{-[\eta]P} \approx \left(1 - \frac{R_v c}{P\rho}\right)^{-[\eta]P} \quad (4.13)$$

where  $\phi_{\text{eff}}$  is the effective volume fraction of the biopolymer molecules in solution ( $= \phi R_v$ ),  $\phi$  is the actual volume fraction occupied by the biopolymer chains ( $= c/\rho$ ),  $c$  is the polysaccharide concentration (in  $\text{kg m}^{-3}$  of emulsion), and  $\rho$  is the density of the biopolymer chains (in  $\text{kg m}^{-3}$ ), which is approximately  $1600 \text{ kg m}^{-3}$  (Rahman, 1995). Theoretical predictions of viscosity versus biopolymer concentration for molecules with different volume ratios are shown in Figure 4.22. For convenience, it was assumed that the shear stresses applied to the emulsions were in the low shear regime so that  $P = 0.57$ . The viscosity increases dramatically when the biopolymer concentration exceeds a critical concentration, whose value decreases as the volume ratio increases.

In practice, Equation 4.13 only gives a very rough approximation of the viscosity of aqueous biopolymer solutions because the flexible biopolymer molecules cannot be treated as rigid spherical particles. The biopolymer molecules may become aligned with the shear field, interact with each other, or become entangled, thus changing their effective volume with shear stress. Nevertheless, the above equation does provide some useful insights into the relationship between the viscosity of polysaccharide solutions and the molecular structure of polysaccharide molecules.

The dependence of the rheology of an aqueous solution on biopolymer concentration can be divided into a number of different regions depending on the interaction between the molecules (Dickinson, 1992; Lapasin and Prici, 1995; Williams and Phillips, 2003). In the “dilute region” the biopolymer concentration is so low that the molecules (or molecular aggregates) do not interact with each other and can be treated as separate entities. As the concentration of biopolymer increases above some critical value,  $c^*$  ( $\approx P/R_v$ ), the viscosity of the solution increases rapidly because the spheres swept out by the biopolymers begin to interact with each other (Figure 4.22). This type of solution is known as a *semidilute* solution, because even though the molecules are interacting with one another, each individual

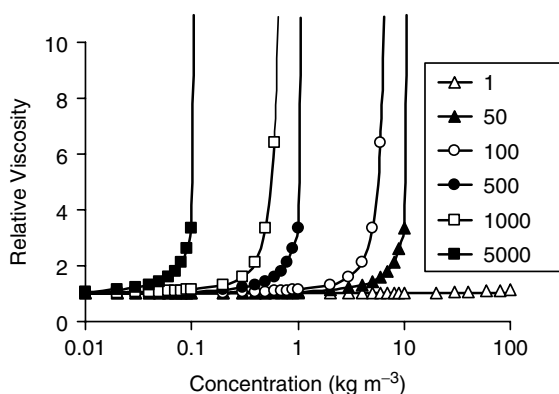


**Figure 4.22** Prediction of change in relative viscosity of aqueous biopolymer solutions with biopolymer concentration for different effective volume ratios,  $R_v$  (shown in box). The viscosity increases dramatically when the biopolymer molecules start to overlap with one another, which occurs at lower biopolymer concentrations for higher  $R_v$ .

biopolymer is still largely surrounded by solvent molecules. At still higher polymer concentrations, the molecules pack so close together that they become entangled with each other and the system has more gel-like characteristics. Biopolymers that are used to thicken the aqueous phase of emulsions are often used in the semidilute concentration range (Dickinson, 1992). A more detailed discussion of the influence of particle concentration on the rheology of colloidal dispersions is given in Chapter 8.

#### 4.5.1.4 Shear thinning in biopolymer solutions

Solutions containing extended biopolymers often exhibit strong shear-thinning behavior (pseudoplasticity), that is, their apparent viscosity decreases with increasing shear stress (Lapasin and Pricl, 1995; Williams and Phillips, 2003). The molecular origin of pseudoplasticity has been attributed to be the fact that applied shear stresses can cause disentanglement of biopolymers, alignment of biopolymers with the shear field, or disruption of weak physical interactions holding biopolymers together. Each of these molecular events has a characteristic relaxation time associated with it. At relatively low shear rates, there is insufficient time for these molecular phenomena to occur during the duration of the applied shear stress, and so the viscosity of the biopolymer solution is relatively high. As the shear rate is increased, these molecular relaxation phenomena occur on a similar timescale as the duration of the applied shear stresses, and so the viscosity begins to decrease. At sufficiently high shear rates, these molecular relaxation phenomena are completed within the experimental timescale so that the solution reaches a constant low viscosity. The viscosity of many biopolymer solutions therefore changes from a relatively constant high value at low shear rates, decreases at intermediate shear rates, and reaches a relatively constant low value at high shear rates (Figure 4.23). Some biopolymer solutions may even have a yield stress. If such a biopolymer solution experiences an applied stress that is below its yield stress it acts like an elastic solid, but when it experiences a stress that exceeds the yield stress it acts like a liquid (Chapter 8).

The characteristic rheological behavior of biopolymer solutions plays an important role in determining their functional properties in food emulsions. For example, a salad dressing must be able to flow when it is poured from a container, but must maintain its shape under its own weight after it has been poured onto a salad. The amount and type of biopolymer used must therefore be carefully selected so that it provides a low viscosity when the salad dressing is poured (high applied stress), but a high viscosity when the salad dressing is allowed to sit under its own weight (low applied stress). The viscosity

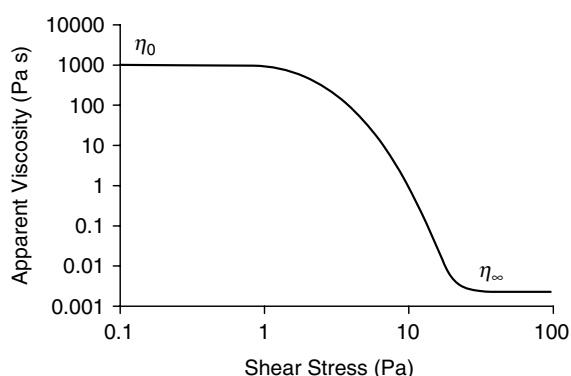


**Figure 4.23** Typical dependence of apparent shear viscosity on applied shear stress for a biopolymer thickening agent.

of biopolymer solutions is also related to the mouthfeel of a food product. Liquids that do not exhibit extensive shear-thinning behavior at the shear stresses experienced within the mouth are perceived as being “slimy.” On the other hand, a certain amount of viscosity is needed to contribute to the “creaminess” of a product. The shear-thinning behavior of biopolymer solutions is also important for determining the stability of food emulsions to creaming. As an oil droplet moves through an aqueous phase it only exerts a very small shear stress on the surrounding liquid. As a result of the shear-thinning behavior of the solution, it experiences a very high viscosity which greatly slows down the rate at which it creams\*.

Many biopolymer solutions also exhibit a shear-thinning behavior known as thixotropy that is, their apparent viscosity decreases with time when they are sheared at a constant rate. The molecular origin of thixotropy can also be attributed to the fact that applied shear stresses can cause disentanglement of biopolymers, alignment of biopolymers with the shear field, or disruption of weak physical interactions holding biopolymers together. Once the shearing stress is removed, the biopolymer molecules may be able to undergo molecular rearrangements that enable the biopolymers to become entangled, nonaligned, or associated with their neighbors again, and so the system regains its original structure and rheological properties. This type of system is said to be *reversible*, and the speed at which the structure is regained may be important for the practical application of a biopolymer in a food. If the molecular rearrangements are unable to take place once the stress is removed, or if they are only able to partially take place, then the system is said to be irreversible or partially reversible, respectively.

A food manufacturer must therefore select an appropriate biopolymer or combination of biopolymers to produce a final product that has a desirable mouthfeel, stability, and texture. Both proteins and polysaccharides can be used as thickening agents, but polysaccharides are usually preferred because they tend to have higher molecular weights and be more extended so that they can be used at much lower concentrations.

#### 4.5.2 Gelling Agents

Biopolymers are used as functional ingredients in many food emulsions because of their ability to cause the aqueous phase to gel, for example, yogurts, cheeses, deserts, egg, and meat products (Morris, 1986; Ledward, 1986; Clark and Lee-Tuffnell, 1986; Zeigler and Foegedding, 1990; Oakenfull et al., 1997; Williams and Phillips, 2003). Gel formation imparts desirable textural and sensory attributes, as well as preventing the droplets from creaming. A biopolymer gel consists of a three-dimensional network of aggregated or entangled biopolymers that entraps a large volume of water, giving the whole structure some “solid-like” characteristics.

The properties of biopolymer gels depend on the type, structure, and interactions of the molecules they contain (Dea, 1982; Zeigler and Foegedding, 1990; Oakenfull et al., 1997; Walstra, 2003a). Gels may be transparent or opaque, hard or soft, brittle or rubbery, homogeneous or heterogeneous, exhibit syneresis, or have good water-holding capacity. Gelation may be induced by a variety of different methods, including altering the temperature, pH, ionic strength or solvent quality, or by adding enzymes, denaturants or cross-linking agents. Biopolymers may be cross-linked to one another either by covalent and/or noncovalent bonds. The type of cross-links formed depends on the nature of the molecules involved, as well as the prevailing environmental conditions. Some common types of molecular interactions responsible for holding the molecules together in biopolymer gels are illustrated in Figure 4.24

\* It should be noted that biopolymers can actually promote creaming at certain concentrations because they cause depletion flocculation (Section 3.6).



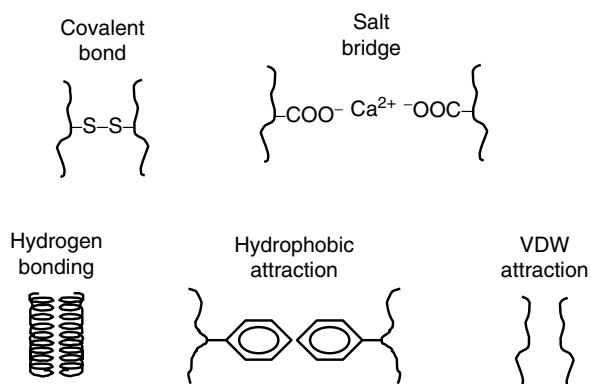


**Figure 4.24** Schematic representation of some common junction zones found in biopolymer gels.

It is sometimes convenient to distinguish between two different types of gels: particulate and filamentous (Figure 4.25). Particulate gels consist of a three-dimensional network of relatively large compact particles, which themselves are usually formed from numerous aggregated biopolymer molecules (Doi, 1993; Oakenfull et al., 1997; Foegeding et al., 2002). This type of gel tends to be formed when the individual biopolymer molecules are able to interact with their neighbors at any point on their surface. Particulate gels are optically opaque because the particles are large enough to strongly scatter light, and are prone to syneresis because the relatively large pore sizes between the particles mean that the water is not held tightly within the gel network by capillary forces. Common examples of particulate gels are those formed by heating aqueous solutions of globular proteins (e.g., whey, egg, or soy proteins) at pH values close to their isoelectric point or at high salt concentrations. Under these conditions, individual protein molecules aggregate with each other to form relatively large particles, and then these particles aggregate with each other to form the final gel network. Filamentous gels consist of thin filaments of individual or aggregated biopolymer molecules (Doi, 1993; Oakenfull et al., 1997; Ikeda et al., 2001; Morris et al., 2001). Filamentous gels tend to be optically transparent because the filaments are so thin that they do not scatter light significantly. They also tend to have good water-holding capacity because the small pore size of the gel network means that the water molecules are held tightly by capillary forces. Examples of filamentous gels are those formed by many hydrocolloids (e.g., gelatin, pectin, gellan, agar, alginates) and those formed by heating globular proteins at low ionic strengths and pH values sufficiently far

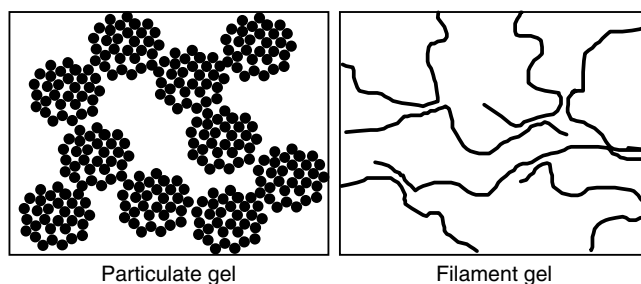


**Figure 4.25** Many food gels can be conveniently categorized as being either particulate or filamentous, depending on the structural organization of the molecules.

from the protein's isoelectric point. In hydrocolloid gels the filaments are individual molecules, but in globular protein gels the filaments are linear chains containing many protein molecules linked together (Doi, 1993; Morris et al., 2001; Najbar et al., 2003).

In some foods a gel is formed on heating (*heat-setting* gels), while in others it is formed on cooling (*cold-setting* gels) (Zeigler and Foegedding, 1990; Oakenfull et al., 1997; Williams and Phillips, 2003). Gels may also be either *thermoreversible* or *thermoirreversible*, depending on whether gelation is reversible or not. Gelatin is an example of a cold-setting thermoreversible gel: when a solution of gelatin molecules is cooled below a certain temperature a gel is formed, but when it is reheated the gel melts (Ledward, 1986). Egg white is an example of a heat-setting thermoirreversible gel: when egg white is heated above a certain temperature a characteristic white gel is formed, but when it is cooled back to room temperature it remains as a white gel, rather than reverting back into the relatively clear liquid from which it was formed (Zeigler and Foegedding, 1990; Doi, 1993; Oakenfull et al., 1997). Whether a gel is reversible or irreversible depends on the type of bonds holding the biopolymer molecules together, as well as any changes in the molecular structure and organization of the molecules during gelation. Biopolymer gels that are stabilized by noncovalent interactions, and which do not involve permanent changes in the structure of the individual molecules during the gelation processes, tend to be reversible. On the other hand, gels that are held together by covalent bonds, or which involve permanent changes in the structure of the individual molecules prior to gelation, tend to form irreversible gels.

The type of interactions holding the molecules together in gels varies from biopolymer to biopolymer (Figure 4.24), and plays a large role in determining the response of a gel to changes in its environment (Dea, 1982; Ledward, 1986; Morris, 1986; Zeigler and Foegedding, 1990; Nussinovitch, 1997; Oakenfull et al., 1997; Walstra, 2003a). Some proteins and polysaccharides form helical junction zones through extensive hydrogen bond formation (Table 4.8). This type of junction zone tends to form when a biopolymer solution is cooled and disrupted when it is heated, and is thus responsible for the formation of cold-setting reversible gels. Below the gelation temperature, hydrogen bonding favors junction zone formation between helices on different biopolymers, but above this temperature the configurational entropy favors a random-coil type structure and the junction zones are disrupted. Biopolymers with extensive nonpolar groups tend to associate via hydrophobic interactions, for example, caseins or denatured whey proteins. Electrostatic interactions play an important role in determining the gelation behavior of many biopolymers, and so gelation is particularly sensitive to the pH and ionic strength of solutions containing these biopolymers. For example, at pH values sufficiently far away from their isoelectric point, proteins may be prevented from gelling because of the strong electrostatic repulsion between the molecules; however, if the pH is adjusted near to the isoelectric point, or if salt is added, the proteins tend to aggregate and form a gel. The addition of multivalent ions, such as  $\text{Ca}^{2+}$ , can promote gelation of charged biopolymer molecules by forming salt bridges between anionic groups on molecules or by forming salt bridges between negatively charged helical regions. Proteins with thiol groups are capable of forming covalent linkages through thiol–disulfide interchanges, which help to strengthen and enhance the stability of gels. The tendency for a biopolymer to form a gel under certain conditions, and the physical properties of the gel formed, depend on a delicate balance of various kinds of biopolymer–biopolymer, biopolymer–solvent, and solvent–solvent interactions.

The properties of food emulsions that have a gelled aqueous phase are dependent on the nature of the interactions between the emulsifier adsorbed to the surface of the droplets and the biopolymer molecules in the gel network (McClements et al., 1993c; Dickinson et al., 1996; Walstra, 2003a). If there is a strong attractive interaction between the droplet

**Table 4.8** Summary of Molecular and Functional Properties of Thickening and Gelling Agents Commonly Used in Food Emulsions

Name	Structure	Solubility	Function	Aggregation Mechanism	Notes
<b>Carrageenan</b>					
$\kappa, \iota, \lambda$	Linear Anionic 200–400 kDa	Hot water Cold water	Thickening Gelling	Helix association Cold-set Thermoreversible	Not acid stable
<b>Agar</b>					
	Linear Nonionic* 80–140 kDa	Hot water	Thickening Gelling	Helix association Cold-set Thermoreversible*	
<b>Alginate</b>					
	Linear Anionic 32–200 kDa	Hot water Low $\text{Ca}^{2+}$	Thickening Gelling	$\text{Ca}^{2+}$ Cold-set Thermoreversible	Partly acid stable Multivalent ions should be added slowly
<b>Pectin</b>					
LM	Linear Anionic 5–150 kDa	Hot water Cold water (Low $\text{Ca}^{2+}$ )	Thickening Gelling	$\text{Ca}^{2+}$ Cold-set Thermoreversible	Acid stable, degrade on heating at pH >5
HM	Linear Anionic 5–150 kDa	Hot water Cold water (Low $\text{Ca}^{2+}$ )	Thickening Gelling	Acid + sugar Cold-set Thermoirreversible	Acid stable, degrade on heating at pH >5
<b>Seed gums</b>					
Guar gum	Linear Nonionic	Cold water Hot water	Thickening		Poor acid stab.
LBG	Linear Nonionic	Hot water	Thickening Gelling	Helix association Freeze-set Thermoirreversible	Poor acid stab.
<b>Xanthan</b>					
	Linear Anionic ~2500 kDa	Cold water Hot water	Thickening Gelling	Helix association Cold-set Thermoreversible	Acid, alkali, heat, and freeze-thaw stable

*(continued)*

**Table 4.8** Summary of Molecular and Functional Properties of Thickening and Gelling Agents Commonly Used in Food Emulsions (*Continued*)

Name	Structure	Solubility	Function	Aggregation Mechanism	Notes
<b>Gellan gum</b>					
	Linear Anionic	Hot water Cold water (Low divalent)	Thickening Gelling	Helix association + salt Cold setting Thermoreversible*	Poor acid stability Transparent gels *Gels formed in presence of multi-valent ions may be irreversible
<b>Starch</b>					
Native	Granules Nonionic	Hot water	Thickening Gelling	Granule swelling Heat-set Irreversible	Opaque
Modified	Linear/ branched Nonionic	Cold water Hot water	Thickening Gelling	Helix association Cold-set Reversible	A variety of modified starches are available for different applications
<b>Cellulose derivatives</b>					
MC MHPC	Linear Nonionic	Cold water	Thickening Gelling	Dehydration Heat-set Reversible $T_{gel} \sim 50-90^{\circ}\text{C}$	Acid and base Heating Freeze-thaw
HPC	Linear Nonionic	Cold water	Thickening	Precipitates $T_{ppt} \sim 40-45^{\circ}\text{C}$	Acid and base Heating Freeze-thaw
CMC	Linear Anionic		Thickening Gelling	Salt bridges	
MCC	Microcrystals	Insoluble	Thickening Gelling	Particle gel	Acid and base Heating Freeze-thaw
<b>Gelatin</b>					
	Linear Amphoteric Amphiphilic	Cold water	Thickening Gelling	Helix formation Cold-set Thermoreversible	Transparent gels

*(continued)*

**Table 4.8** Summary of Molecular and Functional Properties of Thickening and Gelling Agents Commonly Used in Food Emulsions (*Continued*)

Name	Structure	Solubility	Function	Aggregation Mechanism	Notes
<b>Casein</b>					
	Linear Amphoteric Amphiphilic	Cold water Warm water	Thickening Gelling	Rennet IEP precipitation Ca <sup>2+</sup> Alcohol	Opaque gels
<b>Globular proteins</b>					
	Linear Amphoteric Amphiphilic	Cold water Warm water	Thickening Gelling	Hydrophobic Heat-set Thermoirreversible	Transparent or opaque gels depending on pH and salt

*Note:* Biopolymers whose functional properties are influenced by Ca<sup>2+</sup> ions may also be influenced by the presence of other types of multivalent cations. It should be noted that many of the biopolymers mentioned below come in different forms that may have appreciably different functional properties than those mentioned here.

membrane and the gel network, then the network is reinforced and a strong gel is formed. On the other hand, if the emulsifier membrane does not interact favorably with the gel network then the droplets may disrupt the network and weaken the gel strength. The magnitude of this effect depends on the size of the emulsion droplets (McClements et al., 1993c). The larger the droplets compared to the pore size of the gel network, the greater the disruptive effect. Specific interactions between the proteins and surfactants may also influence the properties of the gels formed (Dickinson et al., 1996). For example, surfactants may bind to biopolymers and alter their thermal transition temperatures or their interactions with other molecules (Ananthapadmanabhan, 1993; Jones and Chapman, 1995; Kelley and McClements, 2003).

### 4.5.3 Commonly used texture modifiers

A variety of substances have the molecular characteristics required to make them suitable as thickening or gelling agents for use in food emulsions (Table 4.8). The most commonly used texture modifiers are biopolymers (polysaccharides and proteins) that are added to the aqueous phase of O/W emulsions\*. A brief overview of some of the biopolymers most commonly used as thickening agents in food emulsions is given in this section.

#### 4.5.3.1 Polysaccharides

**4.5.3.1.1 Carrageenans.** Carrageenans are natural hydrocolloids extracted from certain species of red seaweed (Piculell, 1995; Nussinovitch, 1997; Williams and Phillips, 2003). They are linear sulfated polysaccharides consisting of alternating  $\beta$ (1-3)- and  $\alpha$ (1-4)-linked galactose residues (Nussinovitch, 1997). There are three major types of carrageenan, which primarily differ in the number and position of sulfate ester groups on the galactose residues: kappa ( $\kappa$ ), iota ( $\iota$ ), and lambda ( $\lambda$ ). These differences in primary structure have a large influence on the functional characteristics of the different carrageenans, for example, solubility, thickening, gelation, environmental sensitivity, and ingredient

\* In W/O emulsions, such as margarine and butter, fat crystals play the role of texture modifiers by forming a three-dimensional network of aggregated crystals.

compatibility.  $\lambda$ -Carrageenan is commonly used as a thickening agent, whereas  $\kappa$ - and  $\iota$ -carrageenans are usually used as cold-setting reversible gelling agents. Carrageenan ingredients come in a variety of different forms with different functional attributes, for example, molecular weights, salts, blends. Typically, they are sold as salts (Na, K, Ca) and have number average molecular weights between 200 and 400 kDa (Nussinovitch, 1997).

Carrageenans usually have a random-coil conformation at relatively high temperatures, but undergo a helical-to-coil transition when they are cooled below a transition temperature ( $\sim 40$ – $70^\circ\text{C}$ ). The transition temperature depends on carrageenan structure, salt type and concentration, and the presence of sugars. In the presence of sufficiently high quantities of salt, helical regions of gelling carrageenans ( $\kappa$  and  $\iota$ ) can associate with each other to form hydrogen bonded junction zones that promote gel formation. Knowledge of the transition temperature is important when using carrageenans in foods since it determines the temperature above which they must be heated to adequately disperse and solubilize them in water, and the temperature they must be cooled below to form gels. Carrageenan is widely used in food emulsions such as milk shakes, ice creams, and deserts (Williams and Phillips, 2003).

Carrageenan is often used in blends with other polysaccharides (e.g., locust bean gum [LBG], konjac, or starch) to improve functional characteristics such as water-holding capacity, thickening, and gelation. Negatively charged carrageenan molecules may also interact with positively charged groups on proteins under certain circumstances, for example, pH, ionic strength, temperature. These interactions have been used to improve the stabilizing, thickening, gelling, and water-holding properties of various food products (Nussinovitch, 1997).

**4.5.3.1.2 Agars.** Agars are a group of natural hydrocolloids extracted from certain species of red seaweed (Stanley, 1995; Nussinovitch, 1997). They are linear polysaccharides consisting primarily of alternating  $\beta(1\text{-}3)$ - and  $\alpha(1\text{-}4)$ -linked galactose units. Different agars vary in the number and type of substituents (e.g., sulfate, pyruvate, urinate, or methoxyl) on the hydroxyl groups of the sugar residues and in the fraction of the  $\alpha(1\text{-}4)$ -linked galactose units that are present in the 3–6 anhydride form. Agar can be roughly divided into two fractions: agarose, a nonionic polysaccharide that gels; and, agaropectin, a slightly negatively charged polysaccharide that does not gel. The negatively charged fraction contains anionic substituents (usually sulfates) along its backbone. Commercial agars vary in the relative proportions of the nonionic and ionic fractions present. Typically, the mean weight average MW of agars is between 80 and 140 kDa, but they are usually highly polydisperse (Stanley, 1995). Agars usually require heating in aqueous solutions in order to adequately dissolve them. When the system is cooled it forms a viscous solution, which gels over time without the need for specific additives (e.g., multivalent ions or sugars). Agars are unusual in that their gelation temperatures on cooling ( $30$ – $40^\circ\text{C}$ ) are usually considerably below their melting temperatures on heating ( $85$ – $95^\circ\text{C}$ ). The gelation mechanism has been attributed to the transition of an appreciable part of the agar molecules from a random coil to a helical structure on cooling, and subsequent aggregation of the helical structures to form junction zones that are separated by fairly irregular flexible chain regions. Agars form thermoreversible cold-set gels.

**4.5.3.1.3 Alginates.** Alginates are natural hydrocolloids usually extracted from certain species of brown seaweed (Nussinovitch, 1997; Williams and Phillips, 2003). Alginates are linear copolymers of D-manuronic acid (M) and L-guluronic acids (G), which can be distributed as blocks of M, blocks of G, or blocks of alternating M and G residues. The M-blocks tend to have a flexible conformation, the G-blocks tend to have a relatively inflexible conformation, and the MG-blocks tend to have an intermediate flexibility between these two extremes. Alginates vary in their molecular weights (typically between

32 and 200 kDa) and in the proportions and distributions of the M and G groups along the chain, which lead to appreciable differences in their functional characteristics. The alginic acid extracted from brown seaweed is usually reacted with bases to produce sodium, potassium, calcium, or ammonium alginate salts. Alternatively, it can be reacted with propylene oxide to produce propylene glycol alginate (PGA), in which partial esterification of the carboxylic acid groups on the uronic acid residues occurs. The monovalent salts of alginate tend to have good water solubility, whereas alginic acid and multivalent salts of alginate tend to have fairly poor water solubility and form paste-like materials. Often special care is needed to adequately disperse and dissolve alginates when preparing them for use in food products (Nussinovitch, 1997). In the absence of multivalent ions, alginate tends to form viscous solutions since there is little intermolecular cross-linking, but in the presence of multivalent cations alginates tend to form cold-set thermoirreversible gels because the positively charged ions form electrostatic bridges between negatively charged polysaccharides (Williams and Phillips, 2003). The junction zones are believed to be between relatively stiff G-block regions on different alginate molecules. The gelation characteristics of a particular alginate are therefore strongly dependent on the number and length of the G-blocks.

Alginates have been used as thickening agents, gelling agents, and stabilizers in a variety of food emulsions (Moe et al., 1995; Nussinovitch, 1997). For example, they have been used as thickening agents in ice cream, soups, sauces, dressings, mayonnaise, and beverages and as gelling agents in desserts and whipped cream. Their functional attributes are primarily due to their texture modifying characteristics, but there may also be additional contributions arising from their interactions with other components, for example, other polysaccharides, proteins, fat droplets. PGA is widely used as a stabilizer and thickening agent in food emulsions, such as dressings and fruit beverages.

**4.5.3.1.4 Pectins.** Pectins are natural hydrocolloids found in the cell walls and intercellular regions of high plants (Voragen et al., 1995; Nussinovitch, 1997; Williams and Phillips, 2003). Most commercial pectins used in the food industry are extracted from citrus or apple pomace and sold as powders. The term "pectin" actually refers to a broad range of different molecular species. In general, pectin molecules tend to be comprised of "smooth" linear regions consisting of  $\alpha(1-4)$ -linked D-galacturonic acids separated by "hairy" branched regions consisting of various sugars. The galacturonic acid groups may be partly esterified by methyl groups and partly neutralized by bases. The fraction of esterified galacturonic groups is one of the main factors influencing the functional characteristics of commercial pectins. Pectins are usually classified as either high methoxyl (HM) or low methoxyl (LM) pectins depending on whether their degree of methylation (DM) is greater or less than 50%, respectively. HM pectins form gels under acidic conditions at high sugar contents, which is attributed to the reduction of electrostatic repulsion between the chains at low pH and the increased molecular attraction at high sugar contents. Gels formed by HM pectins are thermoirreversible cold-setting gels. The junction zones are believed to be hydrogen bonds and hydrophobic attraction between helical regions formed in the linear smooth regions of the molecules. LM pectins form gels in the presence of calcium, which is attributed to the ability of the positively charged calcium ions to form electrostatic bridges between the linear smooth regions of the negatively charged pectin molecules. Gels formed by LM pectins are thermoreversible cold-setting gels. The precise gelation characteristics of a particular pectin depend on its molecular structure (e.g., DE, amidation, molecular weight, branching) and the prevailing environmental conditions (e.g., pH, ionic strength, sugar content).

Pectins are water soluble, but usually have to be dispersed in warm water prior to use to ensure proper dissolution. Pectins are relatively stable to heating at low pH (3–5),

but may degrade at higher or lower pH values, with the effects being more pronounced the higher the DM (Voragen et al., 1995). Typically, the average molecular weight of pectins is between 50 and 150 kDa (Nussinovitch, 1997). The viscosity of pectin solutions depends on the concentration and type of pectin used, as well as solution conditions such as pH, ionic strength, and temperature. Typically, the pK value of the acid groups on pectin is around 3.5, so that it starts to lose its negative charge as the pH is lowered around and below this value. Pectins are used as stabilizers, thickening agents, and gelling agents in a variety of different food emulsions, for example, drinkable yogurts, dressings, mayonnaise, beverages, and ice cream.

**4.5.3.1.5 Seed gums (Galactomannans).** A number of polysaccharide texture modifiers are extracted from the seeds of various bushes, trees, and plants, for example, LBG, guar gum, and tara gum (Reid and Edwards, 1995; Nussinovitch, 1997; Williams and Phillips, 2003). These polysaccharides are primarily linear nonionic polysaccharides known as galactomannans (~10<sup>3</sup> kDa), which consist of  $\beta$ (1-4)-linked D-mannose residues with single  $\alpha$ -D-galactose residues linked to the main chain. One of the main differences between galactomannans from different sources is the degree of galactose substitution, with galactose-to-mannose ratios of 1:4.5 for LBG, 1:3 for tara gum, and 1:2 for guar gum. The galactose side chains tend to inhibit molecular associations and hence these variations in galactose content lead to differences in the functional properties of the different galactomannans, for example, solubility, thickening, and gelation. For example, guar gum can be dissolved in cold water, whereas LBG and tara gum require hot water for dissolution.

At ambient temperatures, galactomannans tend to exist as individual molecules in aqueous solutions because close intermolecular associations are inhibited by the presence of the galactose substituents. For this reason, seed gums are primarily used as thickening agents, rather than as gelling agents. Nevertheless, LBG has been shown to form irreversible gels on freezing, which has been attributed to self-association of nonsubstituted regions along the mannose backbone. Galactomannan solutions tend to be highly viscous, pseudoplastic, and thixotropic, and their rheological characteristics are not strongly influenced by pH or ionic strength because they are nonionic biopolymers. Galactomannans are sensitive to thermal degradation in acidic solutions (pH <4.5), which limits their application in some foods. Guar gum and LBG are widely used as thickening agents in food emulsions, such as dressings, mayonnaise, sauces, and deserts. It should be noted that their functional properties are often improved by using them in combination with other kinds of polysaccharide, for example, xanthan or carrageenan.

**4.5.3.1.6 Tree gum exudates.** A variety of polysaccharides can be extracted from the exudates of certain trees, for example, gum arabic, gum tragacanth, and gum karaya (Nussinovitch, 1997; Williams and Phillips, 2003). Gum arabic is the most widely used tree gum exudate in the food industry, but it is mainly used as an emulsifier in beverage emulsions (Section 4.4.2.3). Gum tragacanth is an exudate collected from the shrubs of the *Astragalus* species (Nussinovitch, 1997). It is a complex heterogeneous polysaccharide with a high molecular weight that has protein moieties attached. It contains a variety of different types of sugars and is acidic. It is used in foods to provide high viscosity and pseudoplastic properties. It has also been reported to be surface-active and capable of stabilizing emulsions. Gum tragacanth has good stability in acidic conditions, which makes it suitable for application in salad dressings and other low pH products.

**4.5.3.1.7 Xanthan gum.** Xanthan gum is the trivial name given to extracellular polysaccharides secreted by bacteria of the genus *Xanthomonas* (Morris, 1995a). Generally, the xanthan gum ingredients used in the food industry are relatively high molecular



weight polysaccharides that are produced commercially from *Xanthomonas campestris*. The primary structure of xanthan gum consists of a  $\beta$ -(1-4)-D-glucose backbone that is substituted with trisaccharide side chains at the C-3 positions of alternate glucose residues. The trisaccharide chains usually consist of mannose–glucuronic acid–mannose, with a relatively high proportion of the terminal mannose units containing either pyruvate or acetate residues (Nussinovitch, 1997). Consequently, the side chains of the xanthan molecules tend to have an appreciable negative charge. In aqueous solutions at relatively low temperatures, xanthan gum is believed to exist as stiff extended molecules with a largely helical structure, but at higher temperatures it exists as more random-coil molecules (Morris, 1995a). The helix-coil transition temperature is highly sensitive to ionic strength, and may range from 40 to >90°C (Nussinovitch, 1997). Under appropriate solution conditions, helical regions on different xanthan molecules may associate with each other, which may lead to the formation of a weak gel. Xanthan gum ingredients are readily soluble in both hot and cold water and are stable over a wide range of solution and environmental conditions, for example, pH, ionic strength, heating, freeze–thaw cycling, and mixing. Xanthan gum ingredients come in a range of molecular weights, typically around 10<sup>3</sup> kDa.

Xanthan gum forms highly viscous solutions at relatively low concentrations because it is a fairly stiff molecule that is highly extended in aqueous solutions. In addition, xanthan gum solutions exhibit pronounced reversible shear-thinning behavior, for example, the viscosity of a 0.5% solution has been shown to decrease by over three orders of magnitude from low to high applied shear rates (Morris, 1995a). At high salt concentrations, the rheology of xanthan gum solutions is relatively insensitive to temperature. The unique rheological characteristics of xanthan gum solutions are widely used in the formulation of food emulsions such as dressings, sauces, beverages, deserts, and cake batters (Williams and Phillips, 2003).

Xanthan can interact synergistically with a variety of other polysaccharides, leading to improved viscosity or gelation characteristics. In particular, xanthan gum is often used in food emulsions in conjunction with galactomannans, such as guar gum and LBG (Nussinovitch, 1997). The xanthan gum–galactomannan combination can be used to provide a rheological profile (viscosity vs. shear stress) that gives better emulsion stability, texture, and mouthfeel than xanthan gum alone. Xanthan gum also has a synergistic interaction with galactomannans, leading to the formation of thermoreversible gels.

**4.5.3.1.8 Gellan gum.** Gellan gum is an extracellular polysaccharide produced commercially as a fermentation product of the bacterium *Pseudomonas elodea*. It is a linear anionic heteropolysaccharide with a molecular weight of approximately 500 kDa (Nussinovitch, 1997). The linear chain consists of a repeating unit of four saccharides: glucose, glucuronic acid, glucose, and rhamnose. In nature there are approximately 1.5 substituents per repeating unit, comprising mainly of glycerate or acetate. These substituents hinder intermolecular association and therefore influence the gelling characteristics of gellan gums. Two forms of gellan gum are commonly produced commercially that have different functional properties: a low-acylated form that produces strong nonelastic brittle gels and a high-acylated form that produces soft elastic nonbrittle gels.

Gellan gums can be dissolved at ambient temperatures provided significant amounts of divalent ions are not present, otherwise they have to be heated. They give solutions that are highly viscous and pseudoplastic. The solution viscosity decreases steeply with increasing temperature due to a reversible helix-coil transition that occurs on heating (around 25–50°C). Gellan gums have good heat stability at neutral pH, but are susceptible to thermal degradation under acidic conditions. They form gels when cooled from high temperatures due to the formation of helical regions that can associate with each other

and form junction zones. Since they are electrically charged their thickening and gelling properties are highly sensitive to salt type and concentration. Divalent ions usually promote gelation by forming salt bridges between negatively charged helical regions. Gels formed in the presence of monovalent ions are usually thermoreversible, whereas those formed in the presence of multivalent ions may be thermoirreversible. A variety of gel characteristics can be achieved by altering the degree of esterification of the gellan gum and the mineral composition. Gellan gums can be used in food emulsions as thickening or gelling agents.

**4.5.3.1.9 Starch and its derivatives.** Starch is one of the most abundant naturally occurring polysaccharides, being found in the roots, stems, seeds, and fruits of all green leaf plants (BeMiller and Whistler, 1996). Its primary function in nature is to store energy. Starch is extracted from a wide variety of different sources with the most common being corn, potato, wheat, tapioca, and rice. There are two main fractions in starch: amylose and amylopectin (Zobel and Stephen, 1995). Amylose is essentially a linear chain (MW  $\sim 10^6$ ) of  $\alpha$ -D-(1-4)-linked glucose units, although there may be a limited number ( $< 0.5\%$ ) of  $\alpha$ -D-(1-6)-linked branches (BeMiller and Whistler, 1996). Amylopectin is a very large (MW =  $10^7 - 5 \times 10^8$ ) highly branched molecule also consisting primarily of  $\alpha$ -D-(1-4)-linked glucose units, but with a much higher fraction of ( $\sim 5\%$ ) of  $\alpha$ -D-(1-6)-linked branches (BeMiller and Whistler, 1996). Natural sources of starch vary appreciably in the ratio of amylose to amylopectin, which partially accounts for differences in their functional characteristics.

In nature, amylose and amylopectin are organized into complex biological structures within starch granules that consist of crystalline regions separated by amorphous regions (Zobel and Stephen, 1995). When aqueous solutions of starch granules are heated above a critical temperature they incorporate water and the crystalline regions are disrupted. The resultant swelling of the starch granule leads to an appreciable increase in solution viscosity (*gelatinization*). On further heating, a fraction of the starch leaches out of the granules and there is a subsequent decrease in viscosity. When the solution is cooled, linear regions of starch molecules associate with each other (*retrogradation*) and there may be an increase in viscosity or even gelation. The rheological characteristics of a particular native starch depend on the structural organization of the molecules within the starch granule, the ratio of amylose to amylopectin, the precise molecular characteristics of each of these fractions, the solution composition (e.g., pH, ionic strength, sugar content), and environmental factors (e.g., shearing, temperature, pressure). The gels formed by native starch often have limited application in the food industry, because they do not have the desired solubility, textural or stability characteristics. For this reason starches are often physically, chemically, or enzymatically modified to improve their functional properties, for example, pregelatinization, limited hydrolysis, addition of side groups (polar, ionic, or hydrophobic) or cross-linking (Wurzburg, 1995). Starch ingredients are currently available that are soluble in cold or hot water, that thicken or gel with or without heating, that exhibit a wide range of gelation characteristics (e.g., opacity, gel strength, water-holding capacity), and that have different stabilities to environmental conditions (e.g., heating, freezing, pH, ionic strength, shearing). These starches are used in a wide variety of different food emulsions as thickening agents, gelling agents, and stabilizers. For example, they are used in dressings, sauces, desserts, and beverages to provide desirable textural characteristics and to prevent gravitational separation of suspended matter.

**4.5.3.1.10 Cellulose and its derivatives.** Cellulose is the most abundant natural polysaccharide, being the major structural component of land plants (Coffey et al., 1995; Williams and Phillips, 2003). Cellulose is a linear polymer with a relatively high

molecular weight consisting of D-glucose units joined together by  $\text{D}\beta(1-4)$  linkages. In its natural state, cellulose is not usually suitable for usage as a texture modifier in processed foods because it forms strong intermolecular hydrogen bonds that make it insoluble in water. Nevertheless, it can be isolated and chemically modified in a number of ways to produce products that are useful as food ingredients. The most common cellulose derivatives used in foods are MC, carboxymethyl cellulose (CMC), HPC, and MHPC. These ingredients consist of cellulose molecules that have been chemically modified by adding substituents (M, CM, HP, or MHP) to the cellulose backbone. These substituents provide a steric hindrance that helps prevent strong intermolecular associations between cellulose backbones.

MC, MHPC, and HPC are all soluble in cold water, but tend to become insoluble when the solution is heated above a critical temperature (around 50–90°C). MC and MHPC both form reversible gels or highly viscous solutions on heating, whereas HPC just precipitates out of solution. The driving force for the aggregation of these cellulose derivatives at high temperatures has been attributed to the increase in hydrophobic attraction between the molecules, favoring cellulose–cellulose interactions (Williams and Phillips, 2003). MC, MHPC, and HPC are all nonionic polymers and therefore have good stability to pH and salt, as well as good compatibility with other ingredients. These products have been used as texture modifiers in a variety of food products, including dressings, sauces, creams, and deserts.

CMC, also known as cellulose gum, is an anionic linear polymer, which is manufactured by chemically attaching carboxymethyl groups to the backbone of native cellulose. It is normally sold in the form of either sodium or calcium salts, and is available in different molecular weights and degrees of substitution (DS). At a sufficiently high DS ( $> \sim 0.4$ ), CMC is readily soluble in water and forms viscous solutions. Because CMC is ionic, the viscosity of these solutions is sensitive to pH and ionic strength, as well as to the presence of other types of electrically charged molecules. CMC can form gels in the presence of multivalent ions due to electrostatic screening and bridging effects. CMC is an odorless and tasteless ingredient that is commonly used in foods and beverages to prevent gravitational separation of suspended particles and to create desirable textural attributes and mouthfeel, for example, deserts, dressings, sauces, bakery emulsions, and beverages (Nussinovitch, 1997).

Another commonly used cellulose-based product in the food industry is microcrystalline cellulose (MCC). This product is manufactured by treating native cellulose with hydrochloric acid to dissolve the amorphous regions leaving crystalline regions as colloidal sized particles (Coffey et al., 1995). MCC is water insoluble and so exists as small colloidal particles that are predominately dispersed in the aqueous phase. In aqueous solutions, MCC can form three-dimensional matrices of aggregated particles that form viscous solutions or gels depending on the concentration used. These solutions are pseudoplastic and thixotropic because the particle network breaks down on application of shear forces, but the viscosity or gel strength is regained once the shearing stress is removed. MCC functions over a wide range of temperatures, providing freeze–thaw and heat stability to many food products. This product is dispersible in water at relatively high pH ( $>3.8$ ), but may need addition of protective hydrocolloids to disperse it at lower pH values. MCC may also be advantageous in the formulation of low-fat products because it provides a creamy mouthfeel and opacity due to light scattering. MCC is used in a variety of food emulsions to improve emulsion stability and provide desirable textural attributes, including soups, sauces, meat products, dressings, and beverages.

#### 4.5.3.2 Proteins

**4.5.3.2.1 Gelatin.** Gelatin is a relatively high molecular weight protein derived from animal collagen, for example, pig, cow, or fish (Leunberger, 1991; Williams and Phillips, 2003). Gelatin is prepared by hydrolyzing collagen by boiling in the presence of

acid (Type A gelatin) or alkaline (Type B gelatin). The IEP of Type A gelatin (~ 7–9) tends to be higher than that of type B gelatin (~5). Type A gelatin is therefore quite unusual because it is positively charged over the entire pH range typically found in foods. Gelatin exists as a random-coil molecule at relatively high temperatures, but undergoes a coil-helix transition on cooling, which is at about 10–30°C for mammalian gelatin and at about 0–5°C for fish gelatin (Leunberger, 1991). Gelatin forms a thermoreversible cold-set gel on cooling below the coil-helix transition temperature due to formation of helical junction zones between segments of two or three gelatin molecules (Oakenfull et al., 1997). Gelatins are used in a number of emulsion-based food products as thickening agents and gelling agents, including deserts, beverages, soups, sauces, and dairy emulsions.

**4.5.3.2.2 Caseins.** As mentioned earlier, casein is a complex mixture of different proteins usually derived from bovine milk by acid or enzyme precipitation (Section 4.4.2.3). The ability of casein to act as a texture modifier is mainly determined by the ability of the casein molecules to associate with each other under suitable conditions. Caseins have significant fractions of nonpolar regions along their polypeptide chains, which favor self-association through hydrophobic interactions. They also have a relatively high amount of negatively charged phosphoserine residues, which favor self-association through electrostatic bridge formation by multivalent cations, such as  $\text{Ca}^{2+}$  (Oakenfull et al., 1997). More generally, the self-association of casein is strongly influenced by electrostatic interactions between the molecules and is therefore sensitive to pH and ionic strength. Casein molecules can be made to aggregate in a variety of ways to form viscous solutions or gels, for example, addition of ethanol, addition of rennet, addition of salts or pH adjustment to the isoelectric point (Dalgleish, 1997a,b; Oakenfull et al., 1997). Casein ingredients are available in a variety of different powdered forms for usage in food products, for example, whole casein or sodium, potassium, or calcium caseinate (Dalgleish, 1997a,b). Caseins are used in a wide variety of food emulsions as thickening and gelling agents, with the most important being yogurt.

**4.5.3.2.3 Globular proteins.** A number of texture modifiers used in food emulsions are based on the use of globular proteins extracted from a variety of sources, for example, whey, eggs, and soy (Doi, 1993; Damodaran, 1996; Oakenfull et al., 1997). These proteins tend to be fairly water soluble at ambient temperatures, providing the pH is sufficiently far from their isoelectric point. Nevertheless, they can thicken solutions or form gel when they are heated above a temperature where the globular proteins unfold (typically 60–80°C). Protein unfolding exposes reactive amino acid side groups that are normally buried in the globular proteins hydrophobic interior, such as nonpolar or sulfhydryl groups. Exposure of these groups promotes intermolecular interactions through hydrophobic attraction and disulfide bond formation. Gelation is particularly sensitive to the magnitude and range of the electrostatic interactions between protein molecules, so that gel characteristics are strongly dependent on pH and ionic strength. A range of different gel types can be produced by varying pH, ionic strength, and heating conditions, for example, brittle versus rubbery, strong versus weak, transparent versus opaque, good versus bad water-holding capacity. The heat-set gels formed by globular proteins tend to be irreversible, that is, when the gels are cooled they do not melt.

#### 4.5.3.3 Biopolymer blends

Biopolymers are often used in combination with other biopolymers, rather than in isolation, to form systems with novel structures and rheological properties (Grinberg and Tolstoguzov, 1996, 1997; Tolstoguzov, 1997; Schmitt et al., 1998; Benichou et al., 2002b; Lundin et al., 2003). When two different biopolymers are mixed together they may either form a one-phase or a two-phase system depending on the nature of the biopolymers involved, the solution

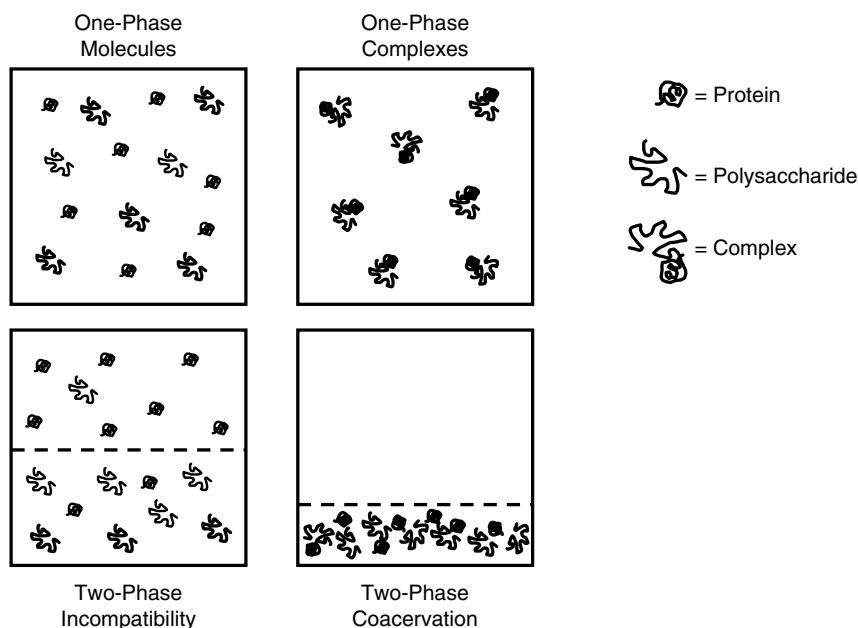


**Figure 4.26** Schematic representation of organization of biopolymer molecules in a mixed biopolymer system. The biopolymer solution may form one or two phases, containing aggregated or nonaggregated biopolymer molecules.

composition, and the prevailing environmental conditions (Figure 4.26). In a one-phase system, the two biopolymers can exist either as individual molecules or as soluble molecular complexes that are evenly distributed throughout the system, so that the solution composition is the same at every location. In a two-phase system, the solution separates into two distinct phases that have different biopolymer compositions. Phase separation can occur through two different physicochemical mechanisms: complex coacervation and thermodynamic incompatibility. In complex coacervation, the two biopolymers aggregate with each other due to relatively strong attractive interactions between them, for example, when they have opposite electrical charges. The resulting two-phase system consists of an insoluble phase that is rich in both biopolymers, and an aqueous phase that is depleted in both biopolymers (Figure 4.26). Thermodynamic incompatibility occurs when the free energy of mixing of the biopolymers is positive, which is common when biopolymers have different molecular conformations, dimensions, rigidities, or solvent affinities. This type of phase separation often occurs when one or both of the biopolymers are uncharged, or when both biopolymers have similar electrical charges. At sufficiently low biopolymer concentrations, the two biopolymers are intimately mixed and form a one-phase solution, but once the biopolymer concentration exceeds a certain level phase separation occurs and a two-phase solution is formed with one of the phases being rich in one type of biopolymer and depleted in the other type, and vice versa (Figure 4.26). The behavior of biopolymer blends under different solution and environmental conditions can be conveniently characterized in terms of phase diagrams (Tolstoguzov, 1997). These phase diagrams can often be used to optimize the biopolymer composition required to produce a solution with a particular microstructure and physicochemical properties.

Once a particular microstructure has been formed by phase separation of a mixed biopolymer solution it is often possible to trap the system in a kinetically stable state, and thus create novel food microstructures and rheological properties (Norton and Frith, 2001;

Lundin et al., 2003). For example, kinetic trapping can be achieved by changing solution or environmental conditions so that one or both of the phases thicken or gel, for example, by changing temperature, pH, ionic composition, or solvent quality. If this process is carried out in the presence of shear forces it is possible to produce a wide variety of different microstructures, for example, spheres, tear-drops, fibers (Tolstoguzov, 1997).

Different types of gel microstructures can be created using biopolymer blends by varying the nature of the biopolymers involved, the solution composition, and the prevailing environmental conditions, for example, interpenetrating networks comprised of different biopolymers, a single network that incorporates both types of biopolymers, or a "filled gel" consisting of regions rich in one biopolymer dispersed in regions rich in the other biopolymer. Each of these microstructures will have unique rheological and physicochemical properties, for example, gel strength, gelation rate, gelation temperature, water-holding capacity, and opacity. Many food scientists are currently attempting to understand the fundamental processes involved in the formation of structured biopolymer blends and in using these systems to create foods with novel or improved physicochemical and sensory properties (Bruin, 1999). In particular, mixed biopolymer systems appear to be an effective means of creating low-fat products with similar properties to high-fat products, for example, deserts, yogurts, dressings, and spreads (Norton and Frith, 2001).

#### 4.5.4 *Selection of an appropriate texture modifier*

There are a large number of different types of food ingredients that can be used by food manufacturers to modify the texture of their products. The choice of a particular type of ingredient or combination of ingredients depends on a number of physicochemical, legal, economic, and marketing factors (see Section 4.7). In this section, we will focus on the rheological and other physicochemical aspects influencing the selection of texture modifiers for use in food emulsions. Initially, a food manufacturer should stipulate the physicochemical and sensory properties that are desired for the particular product of interest. Some of the factors that might be considered are listed below:

1. Should the product be capable of passing through a homogenizer, flowing through a pipe, being stirred, or being packaged into a container during the manufacturing process?
2. Should the product be capable of pouring easily from a container during its usage by a consumer?
3. Are there special textural requirements that are desirable in the final product, for example, cling, spreadability, stirability?
4. Should the final product be a low-viscosity liquid, a highly viscous liquid, a paste, a gel, or a solid?
5. What kind of mouthfeel is desirable in the final product, for example, "watery," "creamy," "smooth," "thick?"
6. Is the texture modifier going to be used primarily to modify the texture of the product or to prevent gravitational separation of droplets or other particulate matter?
7. Should the texture modifier produce a transparent, translucent, or optically opaque solution?
8. Is it necessary for the texture modifier to have good freeze-thaw, thermal, or acid stability?
9. Should the desirable textural properties of the system only manifest themselves after the food has been processed in a certain way, for example, chilling, cooking?

After considering these factors, the manufacturer should establish certain measurable parameters that can be used to define the rheological (and other physicochemical) characteristics of the product, such as a viscosity versus shear stress profile, a yield stress, a modulus, a breaking stress or strain, a texture versus temperature profile (Chapter 8). The manufacture should then specify the optimum rheological characteristics desired for an acceptable product, which often involve correlating the results of rheological tests made on the product with sensory measurements made on the same product. Once the optimum rheological characteristics of the product have been specified, a food manufacturer can then experiment with different types and concentrations of texture modifiers within the food to determine the ingredient(s) that provides the desired functional characteristics.

## 4.6 *Other food additives*

Food emulsions also contain a variety of other ingredients that contribute to their stability, taste, texture, and appearance, such as acidulants, preservatives, flavorings, colorings, vitamins, minerals, and antioxidants (Heath, 1978; Lindsay, 1996a,b; Mathews, 1999; Tan, 2004). In this section, a brief overview of the most important of these food additives will be presented.

### 4.6.1 *pH control*

The pH of the aqueous phase plays an extremely important role in determining the physicochemical, microbiologic, and organoleptic properties of food emulsions (Lindsay, 1996b). The pH of the majority of food emulsions lies within the range 2.5 (e.g., beverage emulsions) to 7.5 (e.g., infant formulations). The pH of the aqueous phase can be adjusted by adding organic or inorganic acids or bases. The pH can be lowered by adding organic or inorganic acids, such as acetic, lactic, citric, malic, fumaric, succinic, or phosphoric acids. It can also be lowered by adding bacteria (*streptococci lactobacilli*) or enzymes ( $\delta$ -gluconolactone) to a food to promote biochemical reactions that lead to acid production. The pH can be increased by adding various types of organic and inorganic salts, such as phosphate, citrate, carbonate, bicarbonate, oxide, and hydroxide salts.

The pH of an aqueous solution can be stabilized at a particular value by using an appropriate buffering system. There may be some functional ingredients present within a food emulsion that were originally added for a different purpose, but which also have a significant buffering capacity, for example, proteins (Damodaran, 1996). Alternatively, specific ingredients can be added to emulsions as buffering agents, for example, weak organic or inorganic acids in combination with salts (Lindsay, 1996b). The type of buffering system used depends on the pH of the food. For example, the effective buffering ranges of some commonly used buffering systems are: pH 2.1–4.7 for citric acid–sodium citrate; pH 3.6–5.6 for acetic acid–sodium acetate; pH 2.0–3.0, 5.5–7.5 and 10–12 for the three ortho- and pyrophosphate anions (Lindsay, 1996b).

### 4.6.2 *Minerals*

Many minerals are essential for the maintenance of human health, as well as making an important contribution to the physicochemical and sensory properties of foods (Miller, 1996). The minerals in foods may exist in a variety of different forms, including free ions, complexes, and compounds, depending on their type and the environmental conditions, for example, pH, ionic strength, temperature, solution composition. The solubility of the minerals in the aqueous and oil phases can vary considerably depending on the form they exist in, which has important consequences for their functional properties in foods. For example, a chelated form of a mineral may act very differently than the nonchelated form.

It is therefore usually important for food manufacturers to control the form that the minerals are present in within a food.

There are currently deficiencies in the consumption of certain minerals that are essential for the maintenance of good health, for example, calcium, iron, selenium, and zinc. Consequently, many food manufacturers are fortifying their foods with these minerals. On the other hand, overconsumption of other minerals (e.g.,  $\text{Na}^+$ ) has been linked to adverse health effects, such as hypertension. For this reason, food manufacturers are developing effective strategies to reduce the levels or completely remove these types of minerals from foods. It should be noted that changing the mineral composition of food emulsions to improve their nutritional aspects may cause undesirable changes in their physicochemical and sensory properties.

High concentrations of minerals can have an adverse affect on the aggregation stability of O/W emulsions containing electrostatically stabilized droplets due to electrostatic screening and ion binding effects (Chapters 3 and 7). These effects can occur at relatively low mineral concentrations (<5 mM) when multivalent counterions are present, for example,  $\text{Ca}^{2+}$  in an emulsion containing negatively charged droplets. Certain mineral ions may also promote undesirable chemical reactions that lead to product deterioration, for example, iron and copper ions can promote lipid oxidation (McClements and Decker, 2000). In these systems, it is usually necessary to add chelating agents to sequester the mineral ions and prevent them from causing chemical instability. Certain types of minerals also influence the functional properties of other food ingredients. For example, the ability of many biopolymers to thicken or gel a solution is strongly dependent on the type and concentration of mineral ions present. Careful selection and control of the mineral ions present in food emulsions is therefore important when formulating a successful product.

#### 4.6.3 Sequestrants (chelating agents)

Chelating agents are often added to foods to sequester multivalent mineral ions (Lindsay, 1996b). Sequestering of mineral ions can have a number of beneficial functions in food emulsions, including improving the solubility of mineral ions, inhibiting lipid oxidation, retarding color or flavor loss, and preventing aggregation of charged droplets. Many of the most effective chelating agents currently used in food emulsions are synthetic, for example, ethylene diamine tetra acetate [EDTA], phosphoric acid, and polyphosphates (Reishce et al., 1998). Nevertheless, there is some concern about the use of synthetic chelating agents because they are believed to bind minerals so strongly that they may not be bioavailable and because consumers do not regard them as "label friendly." Natural chelating agents, such as citric acid, can be used to sequester minerals, but they tend to be less effective and have limited use in many foods because of their flavor, solubility, and/or requirement for acid environments. Research is therefore being carried out to identify alternative natural chelating agents that can be used in a wider range of food applications. A variety of proteins, protein hydrolysates, and polysaccharides have been shown to be effective at chelating transition metals (McClements and Decker, 2000). It is important to ensure that the chelating system chosen is effective under the solution conditions in the product (e.g., pH, ionic composition, temperature), and that it does not adversely affect the functional properties of other food ingredients.

#### 4.6.4 Antioxidants

The oxidation of lipids is one of the most important chemical reactions that occur in food emulsions that causes deterioration in product quality. Lipid oxidation can lead to the production of an off-flavor, loss of beneficial polyunsaturated lipids, and formation of



potentially toxic reaction products (McClements and Decker, 2000). "Lipid oxidation" is a general term that is used to describe a complex sequence of chemical changes that result from the interaction of lipids with oxygen active species (Nawar, 1996; Frankel, 1998; Akoh and Min, 2002). The precise mechanism of lipid oxidation in a particular food depends on the nature of the reactive species present and their physicochemical environment (Coupland and McClements, 1996a, McClements and Decker, 2000). Lipid oxidation can be conveniently divided into three distinct stages: initiation, propagation, and termination (Nawar, 1996; Frankel, 1998; Akoh and Min, 2002). One of the most effective means of retarding lipid oxidation in fatty foods is to incorporate antioxidants. Antioxidants work by a variety of different methods, including control of oxidation substrates (e.g., oxygen and lipids), control of prooxidants (e.g., reactive oxygen species and prooxidant metals), and inactivation of free radicals (Frankel, 1998). Antioxidants can be broadly divided into two categories depending on the mechanism by which they operate: primary antioxidants and secondary antioxidants.

Primary antioxidants retard lipid oxidation because they are capable of accepting free radicals, thereby retarding the initiation step or interrupting the propagation step (McClements and Decker, 2000). The effectiveness of these antioxidants depends on their chemical structure, solution conditions (pH, ionic strength, temperature), and physicochemical environment (oil, water, or interfacial region). Antioxidants that are effective at retarding lipid oxidation in bulk oils may not be as effective in emulsions due to differences in their location relative to lipid substrates or prooxidants (Frankel, 1998). Synthetic food additives, such as BHA, BHT, TBHQ, are common chain-breaking antioxidants used in food systems (Reische et al., 1998). These synthetic antioxidants are often highly effective at controlling lipid oxidation; however, consumer demand for all natural foods has prompted the food industry to look for more "label friendly" alternatives. For this reason a number of studies have been carried out to assess the effectiveness of natural chain-breaking antioxidants in bulk oils and emulsions, including tocopherols, fruit extracts, and plant extracts (Frankel, 1996; McClements and Decker, 2000).

Secondary antioxidants can retard lipid oxidation through a variety of mechanisms, including chelation of transition metals, replenishing of hydrogen to primary antioxidants, oxygen scavenging, and deactivation of reactive species (Reische et al., 1998). It should be noted that none of these mechanisms involve conversion of free radical species to more stable products. From the standpoint of O/W emulsions the most important type of secondary antioxidants are those that chelate transition metal ions (McClements and Decker, 2000). The presence of transition metals, such as iron or copper, in the aqueous phase of O/W emulsions has been shown to be a major factor in the promotion of lipid oxidation. The effectiveness of transition metals at promoting lipid oxidation increases dramatically when they are located near droplet surfaces because they are then in closer proximity to the lipid substrate. Consequently, any aqueous phase component that chelates transition metals and removes them from the vicinity of the droplet surface would be expected to retard lipid oxidation. A variety of synthetic and natural chelating agents are available as additives to prevent lipid oxidation in foods, for example, EDTA, phosphoric acid, polyphosphates, citric acid, other organic acids, proteins, and polysaccharides (Reische et al., 1998). The choice of a particular chelating agent depends on the specific food type.

There are a number of means of retarding oxidation of emulsified fat, which are not available for retarding oxidation of bulk fat. For example, lipid oxidation can be retarded in O/W emulsions by coating the oil droplets with a relatively thick interfacial membrane that is positively charged so that it prevents transition metal ions coming into close contact with the lipids inside the droplets (McClements and Decker, 2000). In practice, the most effective means of controlling lipid oxidation in emulsions is often to use a combination of different antioxidant strategies (Lindsay, 1996b; McClements and Decker, 2000).

#### 4.6.5 Antimicrobial agents

Chemical preservatives that have antimicrobial properties are added to many types of food emulsions to prevent spoilage during storage and to ensure their safety for human consumption (Lindsay, 1996b, Jay, 2000). The type of antimicrobial agent used in a particular food emulsion depends on the pH and thermal processing of the product, as well as its compatibility with the other ingredients present. Some common chemical antimicrobial agents and their effective pH ranges are acetic acid (pH 3.0–5.0), benzoic acid (pH 2.5–4.0), sorbic acid (pH 3.0–6.5), propionic acid (pH 2.5–5.0), sulfites (pH 2.5–5.0), and nitrites (pH 4.0–5.5). Due to growing consumer demands for “natural” food products, food manufacturers are increasingly trying to replace chemical preservatives with more “label friendly” antimicrobials extracted from natural sources, for example, herbs, spices, and plants. It should be stressed that in addition to the usage of antimicrobial additives, microbial growth in food emulsions is also inhibited using various other methods, for example, pH control, moisture control, thermal processing, nonthermal processing, chilling, and freezing (Jay, 2000).

#### 4.6.6 Flavors

The flavor of a food emulsion is one of the most important factors determining its overall quality (Chapter 9). A food manufacturer must therefore design each food product so that it has the desired characteristic flavor profile expected by consumers for that kind of product. A desirable flavor profile can be achieved by incorporating known concentrations of particular types of flavor molecules into a food (e.g., NaCl, sucrose, D-limonene, citric acid) or by using multicomponent ingredients that contain flavor molecules (e.g., lemon juice, herbs, spices, flavor oils, milk fat). Alternatively, the flavor profile might be generated or modified by ingredients that undergo chemical or biochemical reactions during food production, storage, or preparation, for example, lipid oxidation, browning reactions, or enzymatic reactions (Lindsay, 1996a, Jacobson, 1999).

A food manufacturer must decide the type and amount of flavoring components that must be incorporated into a food emulsion during the manufacturing process in order to produce a desirable flavor profile in the final food product. This is by no means a simple task, since the perceived flavor of a food emulsion is governed not only by the type and concentration of flavors present, but also by their partitioning and release rate, which depends on the composition and microstructure of the emulsion (Chapter 9). The most important factors that should be considered when selecting flavors for use in food emulsions are their partitioning between the oil, aqueous, interfacial, and headspace regions, and their rate of mass transport to the taste and odor receptors during consumption (Chapter 9). Due to the difficulty in predicting the flavor of a food emulsion from first principles, the creation of a final product with a desirable flavor profile often requires extensive formulation and reformulation of products after testing of their flavor profiles using analytical instruments and sensory tests.

Currently, there are trends within the food industry toward the usage of more natural flavors, and to reduce the concentration of certain sugars and salts. For example, natural sugar-based sweeteners, such as sucrose, high-fructose corn syrup, fruit juices, and honey, have traditionally been used to produce desirable flavor profiles in emulsions (Mathews, 1999); however, in many products these are being replaced with reduced calorie sweeteners based on polyhydric alcohols (mannitol, xylitol, and sorbitol) or nonnutritive sweeteners (e.g., aspartame, acesulfame K, saccharin, and sucralose) (Lindsay, 1996b). The food manufacturer should be aware that changing the level of sweeteners or salts in an emulsion may alter its overall physicochemical characteristics, so that the system has to be reformulated to produce a desirable product.

#### 4.6.7 Colorants

Appearance plays a major role in determining whether or not consumers will purchase a particular product, as well as their perception of the quality of the product once it is consumed (MacDougall, 2002a). The desired appearance for a particular product depends mainly on the product type and its description on the label. The overall appearance of an emulsion is determined by the amount of light it absorbs and scatters across the visible region of the electromagnetic spectrum (Chapter 10). For food emulsions, the most important elements of appearance are usually the color and the opacity. The opacity is mainly determined by particulate matter that scatters light, such as emulsion droplets, air bubbles, biopolymer aggregates, fat crystals, and ice crystals. The color is mainly determined by chromophoric materials that selectively absorb light in the wavelength range from 380 to 780 nm. Substances that can absorb electromagnetic energy in this region are usually referred to as dyes or pigments (Moss, 2002). A dye has been defined as a colored substance that is soluble in the medium in which it is dispersed, whereas a pigment is insoluble (Moss, 2002). The more general term “colorant” can be used to encompass both dyes and pigments. Substances that contribute to the color of an emulsion-based product may be naturally present in the other major ingredients used to formulate the product (e.g., oils, egg yolk) or they may be added as specific colorants. A wide variety of different natural and synthetic colorants are available to provide characteristic appearances to food emulsions, including fruit, vegetable, or plant extracts and FD&C colorants (Heath, 1978; Mathews, 1999; Francis, 1999). FD&C colorants are those synthetic food color additives approved by the United States Food and Drug Administration (FDA) for usage in foods, drugs, and cosmetics, for example, FD&C Red No. 40, FD&C Yellow No. 5, and FD&C Blue No. 1. Colorants may be either oil soluble or water soluble, which will determine the phase that they must be dispersed in during the production of emulsions. Many colorants undergo chemical degradation reactions that lead to a change or fading in color over time. Consequently, a manufacturer may have to develop effective strategies to prevent these undesirable changes, for example, by controlling light levels, oxygen content, pH, and storage temperatures or by adding preservatives. The overall appearance of an emulsion may also be controlled by adding particulate material that scatters light and therefore makes the product look cloudy or opaque, for example, titanium dioxide or particulated biopolymer aggregates. The type and concentration of colorants used in a product depends on the desired final appearance, as well as the composition and microstructure of the matrix. For example, a higher concentration of a colorant may be required to produce a certain color intensity in a high-fat O/W emulsion than in a low-fat version of the same product due to the greater amount of light scattering by the droplets (McClements, 2002a,b).

#### 4.6.8 Weighting agents

Weighting agents are often used in beverage emulsions to increase their creaming stability (Tan, 2004). The purpose of weighting agents is to reduce the density contrast between the oil droplets and the surrounding aqueous phase, thereby reducing the driving force for creaming (Tan, 2004). A variety of natural and synthetic weighting agents are available for usage in beverage emulsions. The most common are brominated vegetable oil (BVO), sucrose acetate isobutyrate (SAIB), dammar gum, and ester gum (Heath and Reineccius, 1986; Tan, 2004). Brominated vegetable oil is produced by addition of bromine molecules to unsaturated bonds on the fatty acid chains of the triacylglycerols in food oils, for example, corn oil, soybean oil, cotton seed oil, or olive oil. Ester gum is made by esterification of wood rosin with glycerol. Damar gum is a natural exudate obtained from the shrubs of the *Caesalpinaceae* and *Dipterocarpaceae* families. SAIB is made by the esterification

of sucrose with acetic and isobutyric anhydrides. Weighting agents are usually incorporated into the oil phase prior to homogenization. The density of the weighting agent determines how much of it is required to match the oil and aqueous phase densities: BVO = 1240 – 1330 kg m<sup>-3</sup>; SAIB = 1150 kg m<sup>-3</sup>; ester gum = 1080 kg m<sup>-3</sup>; and damar gum = 1060 kg m<sup>-3</sup>. Nevertheless, the type and amount of weighting agents that can be used in beverage emulsions is restricted by government and international regulations in many countries. For example, in the U.S. only 15 ppm BVO and 100 ppm ester gum can be present in the finished product (Tan, 2004). These relatively low levels mean that it is only possible to use weighting agents to improve the stability of O/W emulsions with very low droplet concentrations, typically <0.1 wt%, which practically limit their use to beverage emulsions.

#### 4.6.9 Fat replacers

Overconsumption of fatty foods is a major cause of obesity, which has been linked to major human health problems such as heart disease, diabetes, and cancer (American Heart Association). There has therefore been a considerable trend in the food industry toward the development of reduced fat, low-fat, or fat-free versions of traditional products (Jones et al., 1996; Ford et al., 2004). Fats play a variety of different roles in determining the overall appearance, texture, flavor, and stability of food emulsions (Chapters 7–10). Consequently, it is usually necessary to use a combination of fat replacement ingredients with different functional roles to replace the quality attributes lost when fat droplets are removed. Biopolymers, such as gums, starch, and proteins are often incorporated into reduced fat, light, low-fat, or fat-free products to provide some of these functional attributes (Clegg, 1996). In particular, insoluble biopolymer complexes that have similar particle sizes to oil droplets have been found to mimic many of the desirable quality attributes of the fat droplets in dressings, for example, Simplese™, which is a microparticulated whey protein ingredient (Singer, 1996). One of the hardest quality attributes to imitate when the fat is removed is the flavor profile, because the fat phase acts as a solvent for many characteristic flavors and controls their release rate during consumption (Ford et al., 2004). When the fat content is reduced the partitioning and release rate of flavor compounds is changed, which changes the overall flavor profile. In addition, the flavor profile may be changed due to interactions of the flavor molecules with proteins, polysaccharides, or surfactant micelles (Guichard, 2002). For these reasons, it is often necessary to supplement biopolymer fat replacers with other types of ingredients to obtain the desired flavor profile, such as surfactants or flavorings (Brandt, 1999).

An alternative method of reducing the fat content of emulsions is to replace a fraction or all of the conventional oil with nondigestible fat-like molecules (such as Olestra™, a sucrose fatty acid ester) or specially designed triacylglycerols with reduced caloric levels (such as Salatrim™ and Caprenin™). An ideal fat replacer should provide all of the quality attributes provided by conventional fat, while being safe to consume and significantly reducing the overall fat and calorie content. One of the advantages of this method is that the overall droplet concentration remains the same so that the physicochemical and sensory attributes of the product are fairly similar to those of a conventional product. To the author's knowledge these ingredients are not widely used in food emulsions because they are either not legally approved, do not have suitable physicochemical properties, or are not economically viable.

### 4.7 Factors influencing ingredient selection

As this chapter has shown there are a large number of different functional ingredients that can be used in food emulsions. Each of these ingredients has its own unique functional properties that contribute to the overall physicochemical and sensory properties

of the final product in a distinctive way. We have considered some of the physiochemical factors that food manufacturers should consider when selecting particular types of functional ingredients in previous sections. In this section, an overview of some of the other important factors that must be considered in choosing an ingredient for a particular application is given.

1. There are differences in the sensitivity of ingredients to solution composition and environmental conditions, for example, pH, ionic strength, temperature. The ingredients chosen must be capable of exhibiting their desired functional properties under the conditions that the product experiences during its production, storage, transport, and usage.
2. Certain ingredients can interact with other types of ingredients in ways that dramatically alter their functional attributes. These interactions may either be beneficial or detrimental to the overall properties of the system. It is therefore important to select a combination of ingredients that are compatible with one another.
3. There are often differences in supplier reliability, consistency from batch-to-batch, ease of handling, ease of usage, and shelf-life for each functional ingredient.
4. There are differences in the total amount and cost of ingredients required to provide the desired functional attributes to food emulsions.
5. There are legal limits, which vary from country to country, that specify the types and amounts of ingredients that can be used in particular foods.
6. There may be labeling and marketing requirements on the type of ingredients used. For example, consumers are becoming more interested in purchasing "all natural" products and therefore many food companies are examining the possibility of replacing synthetic ingredients with natural ones. In addition, it may be important to use an ingredient that is suitable for consumption by particular ethnic, religious, or social groups, for example, kosher, vegetarian, or vegan.

The food manufacturer must consider all of the above factors when selecting a combination of ingredients that are suitable for application in a particular product. Usually, it will not be possible to identify a series of ingredients that satisfies all of the desired characteristics, and it will be necessary to come to some compromise between functionality, cost, and labeling requirements.

## chapter five

---

# Interfacial properties and their characterization

### 5.1 Introduction

The interfacial region that separates the oil from the aqueous phase constitutes only a small fraction of the total volume of an emulsion (Table 1.1). Nevertheless, it has a major influence on the bulk physicochemical and sensory properties of food emulsions, including their formation, stability, rheology, and flavor (Chapters 6–9). Food scientists would like to know how interfacial characteristics (such as composition, structure, thickness, and rheology) impact emulsion properties, and how these interfacial characteristics depend on the type, concentration, and properties of the surface-active components in the system, so that they can rationally create emulsion-based foods with improved quality (Dickinson, 1992; Wilde, 2000).

An interface is a narrow region that separates two phases, which could be a gas and a liquid, a gas and a solid, two liquids, a liquid and a solid, or two solids (Walstra, 2003a). The two phases may consist of different kinds of molecules (e.g., oil and water) or different physical states of the same kind of molecule (e.g., liquid oil and solid fat). By convention, the region separating two condensed phases (solids or liquids) is referred to as an *interface*, while the region separating a condensed phase and a gas is called a *surface* (Everett, 1988). Nevertheless, the terms interface and surface are frequently used interchangeably, and in this chapter the term interface will often be used to cover both terms. A number of different types of surfaces and interfaces commonly occur in food emulsions, including oil–water (e.g., oil droplets in water), air–water (e.g., gas bubbles in water), ice–liquid water (e.g., ice crystals in water), and fat–oil (e.g., fat crystals in oil). In this chapter, we will mainly focus on the oil–water interface because it is present in all food emulsions. Nevertheless, we will consider various other types of surfaces and interfaces where appropriate, and it should be recognized that much of the discussion about oil–water interfaces is also applicable to other systems.

Initially, it is useful to provide a brief overview of the interfacial characteristics that are most important in determining the overall properties of food emulsions:

- *Interfacial composition.* The type and concentration of surface-active substances present at an interface strongly influence its free energy, structure, dimensions, electrical characteristics, and rheology, and therefore plays a major role in determining emulsion properties.
- *Interfacial structure.* The thickness and internal structure of the interfacial layer plays an important role in determining the magnitude and range of the colloidal forces acting between emulsion droplets (Chapter 3). For example, the range of

the steric repulsion between droplets increases as the thickness of the interfacial layer increases. (Section 3.5)

- *Interfacial electrical properties.* The electrical characteristics of the interface (e.g., surface charge density and surface potential) play an important role in determining the magnitude and range of the electrostatic interactions between emulsion droplets (Section 3.4), as well as influencing the adsorption of ions to emulsion droplet surfaces.
- *Interfacial energy.* The free energy stored in the interface, which is described by the surface or interfacial tension, determines the ease at which the interfacial area can be changed. This interfacial energy is important in emulsion formation, since it influences the amount of mechanical energy that must be input during homogenization to deform and break up droplets (Section 6.4.1). It is also important in determining the stability of some surfactant-stabilized emulsions to coalescence (Sections 4.4.1 and 7.6). Finally, measurements of the interfacial energy can be used to provide valuable information about interfacial composition, emulsifier adsorption kinetics, and interfacial rheology.
- *Interfacial rheology.* The rheological characteristics of an interface (e.g., dilational or shear rheology) are believed to influence the stability and physicochemical properties of some food emulsions, for example, droplet aggregation and creaming (Bos and van Vliet, 2001) and emulsion formation (Walstra and Smulder, 1998). In addition, measurements of the rheological characteristics of interfaces can be used to provide valuable information about the interactions of surface-active molecules within the interfacial layer.

In the remainder of this chapter, we consider the molecular characteristics of the interfacial region, thermodynamic relationships for describing its properties, the role that it plays in determining the bulk physicochemical properties of emulsions, and experimental techniques available for characterizing its properties.

## 5.2 General characteristics of interfaces

### 5.2.1 Interfaces separating two pure liquids

The interface that separates the oil and water phases is often assumed to be a planar surface of infinitesimal thickness (Figure 5.1a). This assumption is convenient for many purposes, but it ignores the highly dynamic nature of the interfacial region, as well as the structure and organization of the various types of molecules involved (Figure 5.1b). On the molecular level, the oil and water molecules intermingle with each other over distances of the order of a few molecular diameters (Everett, 1988; Evans and Wennerstrom, 1994; Jonsson et al., 1998). The composition of the system therefore varies smoothly across the interfacial region (Figure 5.1b), rather than changing abruptly (Figure 5.1a). The thickness and dynamics of the interfacial region depend on the relative magnitude of the interactions between the molecules involved (oil–oil, water–water, and oil–water): the more unfavorable the oil–water interactions, the thinner and more inflexible is the interface (Israelachvili, 1992; Evans and Wennerstrom, 1994).

Consider the various types of molecular interactions that operate in a two-phase system consisting of oil and water (Figure 5.2). The water molecules are capable of forming relatively strong hydrogen bonds with their neighbors in the bulk water phase, whereas the oil molecules are only capable of forming relatively weak van der Waals bonds with each other in the bulk oil phase. At the oil–water interface, oil molecules can only form relatively weak van der Waals bonds with water molecules, because they do not have polar groups that would enable them to form hydrogen bonds. Consequently, increasing

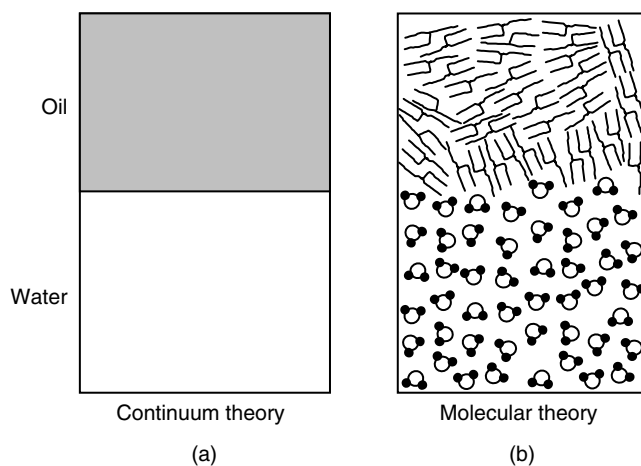


**Figure 5.1** Interfaces are often assumed to be planar surfaces of infinitesimally small thickness (a), but in reality they are highly dynamic and have a thickness that depends on the dimensions and interactions of the molecules (b).

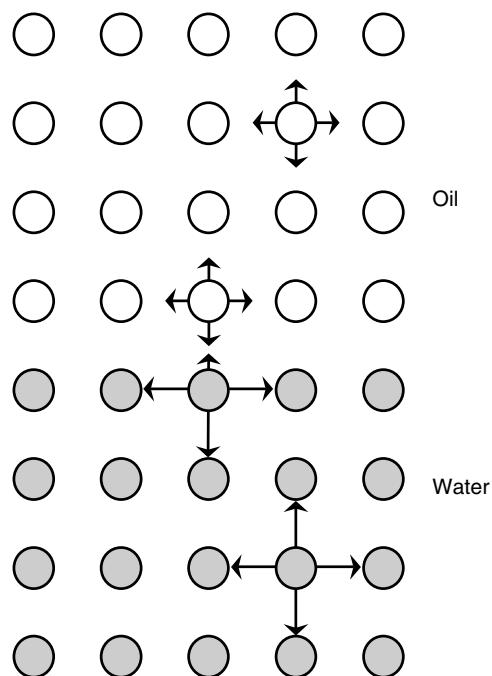


**Figure 5.2** The molecular origin of interfacial tension at a liquid-liquid interface is the imbalance of the attractive forces acting on the molecules at the interface. The length of the arrows is related to the strength of the attraction between molecules. Hence, water-water interactions are considerably stronger than oil-oil or oil-water interactions.



the number of interactions between oil and water molecules by increasing the interfacial area is unfavorable, because it involves replacing relatively strong water–water bonds with relatively weak water–oil bonds. In reality, one must take into account the structural organization (entropy) of the molecules at the interface, as well as their interaction energies (enthalpy), particularly because of the dominant role of the hydrophobic effect (Norde, 2003). In summary, the interaction of oil and water molecules at the interface is strongly thermodynamically unfavorable because of the hydrophobic effect (Section 4.3.3). It is therefore necessary to supply free energy to the system in order to increase the contact area between oil and water molecules. The amount of free energy that must be supplied is proportional to the increase in contact area between the oil and water molecules (Hiemenz and Rajagopalan, 1997):

$$\Delta G = \gamma_i \Delta A \quad (5.1)$$

where  $\Delta G$  is the free energy required to increase the contact area between the two immiscible liquids by  $\Delta A$  (at constant temperature and pressure) and  $\gamma_i$  is a constant of proportionality called the *interfacial tension*. If one of the phases is a gas, the interfacial tension is replaced by the *surface tension*,  $\gamma_s$ . Ultimately, the interfacial tension is determined by the magnitude of the imbalance of molecular interactions across an interface: the greater the imbalance of interactions, the greater the interfacial tension (Israelachvili, 1992; Evans and Wennerstrom, 1994). Conceptually, the interfacial tension can be thought of as a contractile force that manifests itself as a tendency for the system to minimize the contact area between the two phases. The interfacial tension can be expressed in units of energy per unit interfacial area ( $\text{J m}^{-2}$ ) or force per unit length of interface ( $\text{N m}^{-1}$ ). Selected values for the surface and interfacial tensions of some materials relevant to food scientists are presented in Table 5.1. For some simple systems, equations have been developed to relate the interfacial and surface tensions of materials to the number and magnitude of the various types of molecular interactions involved (Israelachvili, 1992; Norde, 2003).

Many of the most important macroscopic properties of food emulsions are governed by the imbalance of molecular forces at an interface, including the tendency for droplets to be spherical, the surface activity of emulsifiers, the nucleation and growth of ice and fat crystals, meniscus formation, and the rise of liquids in a capillary tube (Section 5.9).

**Table 5.1** Approximate Values at Ambient Temperature for Surface and Interfacial Tensions ( $\text{mJ m}^{-2}$ ) of Selected Materials Relevant to Food Scientists.

Substance	$\gamma_s$ (Against Air)	$\gamma_i$ (Against Water)	$\gamma_i$ (Against Oil)
Water	72	—	27.5
SDS solution*	37	—	—
Tween 20 solution*	—	—	26
Protein solution*	50	—	—
Gum Arabic solution*	—	—	43
40% sucrose solution	74	—	—
20% NaCl solution	82	—	—
<i>n</i> -Octane	22	—	—
<i>n</i> -Dodecane	25	—	—
<i>n</i> -Hexadecane	27	53.8	—
Triacylglycerol oil	35	30	—
Triacylglycerol crystal	—	31	4
Ethanol	22	0	—

\* Interfacial or surface tension at saturation coverage.

Source: Adapted from Jonsson et al. (1998) and Walstra (2003a).

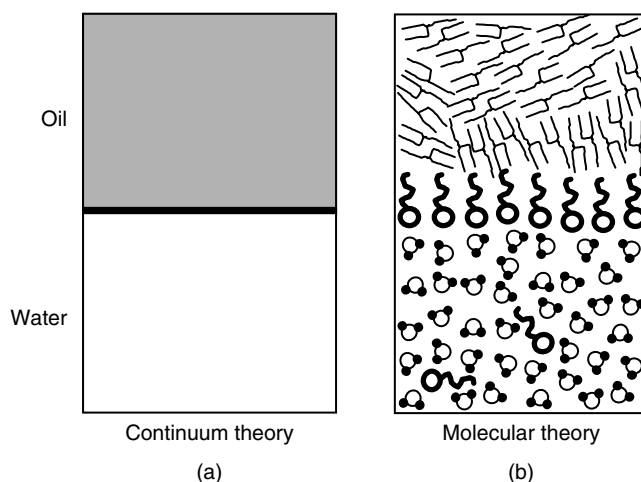


**Figure 5.3** Surface-active molecules accumulate in the interfacial region because this minimizes the free energy of the system.

### 5.2.2 Interfaces in the presence of solutes

So far, we have only considered the molecular characteristics of an interface that separates two pure liquids. In practice, food emulsions contain various types of surface-active solutes that accumulate at interfaces and alter their properties, for example, surfactants, phospholipids, proteins, polysaccharides, and alcohols (Dickinson and Stainsby, 1982; Dickinson, 1992; Krog, 1997; Stauffer, 1999). In this section, we focus on the molecular origins of solute adsorption to interfaces.

Consider a system that consists of an amphiphilic solute, an oil phase, and a water phase (Figure 5.3). The solute tends to accumulate at the interface separating the oil and water phases when the free energy of the adsorbed state is lower than that of the nonadsorbed state (Hiemenz and Rajagopalan, 1997). The difference in free energy between the adsorbed and nonadsorbed states,  $\Delta G_{\text{ads}}$ , is determined by changes in the interaction energies of the various molecules involved in the process, as well as by various entropy effects (Shaw, 1980; Hiemenz and Rajagopalan, 1997; Norde, 2003). The change in the interaction energies that occurs as a result of adsorption of a solute comes from two sources, one associated with the interface and the other with the solute itself. The hydrophobic effect makes a major contribution to both of these sources.\* First, when a solute adsorbs to an oil–water interface the number of unfavorable contacts between water molecules and oil are reduced. The direct contact between oil and water molecules is replaced by contacts between the nonpolar segments of the solute and oil, and between the polar segments of the solute and water (Israelachvili, 1992). Thermodynamically, these interactions are more favorable than the direct interactions between oil and water molecules. Second, surface-active solutes usually have both polar and nonpolar segments, and when they are dispersed in bulk water some of the nonpolar segments come into contact with water, which is thermodynamically unfavorable because of the hydrophobic effect. By adsorbing to an interface they are able to maximize the number of thermodynamically favorable interactions between the polar segments and water, while minimizing the number of unfavorable interactions between the nonpolar segments and water (Figure 5.3b).

\* It is assumed that the “interaction energy” includes both enthalpic and entropic contributions, so that hydrophobic interactions can be conveniently treated.

In addition to the hydrophobic effect, various other types of interaction energies may also contribute to the propensity of an amphiphilic solute to adsorb to an interface, including van der Waals, hydration, electrostatic, and steric interactions (Norde, 2003). The relative magnitude of these interactions, and whether they favor or oppose adsorption, depends on the type of solute involved, but these contributions are usually appreciably smaller than the hydrophobic effect.

There are also a number of entropic contributions that influence the tendency of solute molecules to adsorb to an interface (Norde, 2003):

1. *Configuration entropy.* When a molecule adsorbs to an interface it is confined to a region that is considerably smaller than the region it could potentially occupy in the bulk liquid. This reduction in the number of possible configurations that the molecule can adopt within the system leads to a decrease in entropy, which opposes adsorption.
2. *Orientation entropy.* When a molecule adsorbs to an interface its ability to adopt different three-dimensional orientations may be limited compared to when it is dispersed in the bulk liquid. This reduction in the number of possible orientations that the molecule can have leads to a decrease in entropy, which opposes adsorption.
3. *Conformation entropy.* When a polymeric molecule adsorbs to an interface the number of different conformations that it can adopt may either increase or decrease depending on the nature of the molecule. For example, the number of conformations adopted by flexible random-coil type biopolymers usually decreases after adsorption, whereas the number of conformations adopted by compact globular biopolymers usually increases (Norde, 2003). This contribution may therefore either decrease or increase the entropy, and so either oppose or favor adsorption, depending on whether the number of molecular conformations decreases or increases after adsorption.
4. *Interaction entropy.* The interaction entropy is primarily associated with changes in the organization of solvent molecules resulting from adsorption. The major contribution to the interaction entropy is the hydrophobic effect, which has already been included in the molecular interaction contribution discussed above. The number of highly ordered water molecules surrounding nonpolar groups decreases when an amphiphilic molecule adsorbs to an interface, which increases the entropy of the solvent molecules and favors adsorption. Nevertheless, there may also be other entropy contributions associated with changes in the organization of solvent molecules due to adsorption, for example, redistribution of counterions around charged groups (Norde, 2003).

The adsorption of a molecule to an interface will therefore only occur when the various favorable interaction energy and entropy contributions outweigh the unfavorable ones. If the adsorption free energy is highly negative (i.e.,  $\Delta G_{\text{ads}}/RT \ll 0$ ), then a molecule has a strong affinity for the surface and has a high surface activity. If the adsorption free energy is relatively small compared to the thermal energy (i.e.,  $\Delta G_{\text{ads}}/RT \approx 0$ ), then a molecule tends to be located mainly in the bulk liquid and has a low surface activity. If the adsorption free energy is highly positive (i.e.,  $\Delta G_{\text{ads}}/RT \gg 0$ ), then there is a deficit of solute in the interfacial region, which is referred to as *negative adsorption* (Shaw, 1980).

The change in free energy of a system that occurs when a surface-active solute is present manifests itself as a change in the interfacial (or surface) tension, that is, in the amount of free energy required to increase the interfacial (or surface) area between the water and oil (or air) phases by a unit amount. The interfacial tension is reduced in the presence of a surface-active solute because the thermodynamically unfavorable contacts between the oil and water phases are reduced: the higher the solute concentration at the interface, the

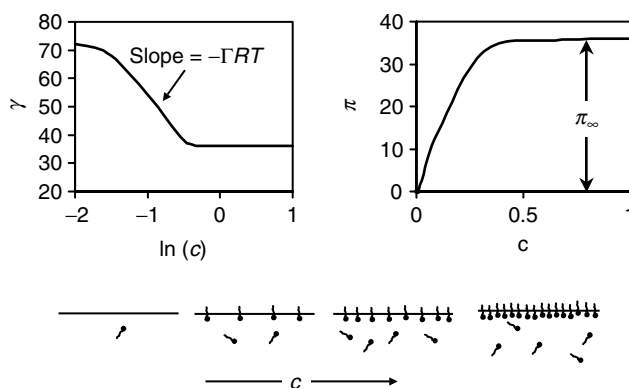


**Figure 5.4** The interfacial properties of an emulsifier can be conveniently characterized by plotting the interfacial tension or surface pressure as a function of emulsifier concentration in the bulk solution. As the bulk emulsifier concentration increases, the interfacial emulsifier concentration increases, which leads to a decrease in  $\gamma$  and an increase in  $\pi$  until the interface is saturated with emulsifier.

greater the reduction in interfacial tension. The reduction of the interfacial tension by the presence of a surface-active solute is referred to as the *surface pressure*:

$$\pi = \gamma_{o/w} - \gamma \quad (5.2)$$

where  $\gamma_{o/w}$  is the interfacial tension of a pure oil–water interface and  $\gamma$  is the interfacial tension in the presence of the surface-active solute (Hiemenz and Rajagopalan, 1997). Typical plots of the dependence of the interfacial tension and surface pressure on the concentration of a surface-active solute in the bulk solution are shown in Figure 5.4. As the solute concentration is increased the interfacial tension continues to fall from its value in the absence of solute ( $\gamma_{o/w}$ ), until it reaches a relatively constant level at high solute concentrations where the interface has become saturated with solute. In contrast, the surface pressure increases from zero in the absence of solute to a constant value ( $\pi_{\infty}$ ) at high solute concentrations where the interface has become saturated with solute. The value of  $\pi_{\infty}$  is a measure of how effectively the adsorbed solute molecules are able to minimize the thermodynamically unfavorable interactions between the oil and water phases at saturation. The higher the value of  $\pi_{\infty}$  for a particular interface, the better the solute is at minimizing thermodynamically unfavorable interactions at that interface.

The variation of surface tension with solute concentration for different types of molecules is shown in Figure 5.5. For a solute that has a high surface activity (i.e.,  $\Delta G_{\text{ads}}/RT \ll 0$ ), like sodium dodecyl sulfate (SDS), the surface tension decreases rapidly with increasing solute concentration then reaches a constant value when the surface is saturated. For a solute with a moderate surface activity, like methanol, the surface tension decreases more slowly with increasing solute concentration. For a solute with little or no surface activity (i.e.,  $\Delta G_{\text{ads}}/RT \approx 0$ ), like sucrose, there is little change in surface tension with increasing solute concentration. For a solute with a negative surface activity (i.e.,  $\Delta G_{\text{ads}}/RT > 0$ ), like NaCl, there is actually an increase in surface tension with increasing solute concentration. Thermodynamic equations for relating the interfacial concentration of a solute to its bulk concentration and surface activity are discussed in a later section.

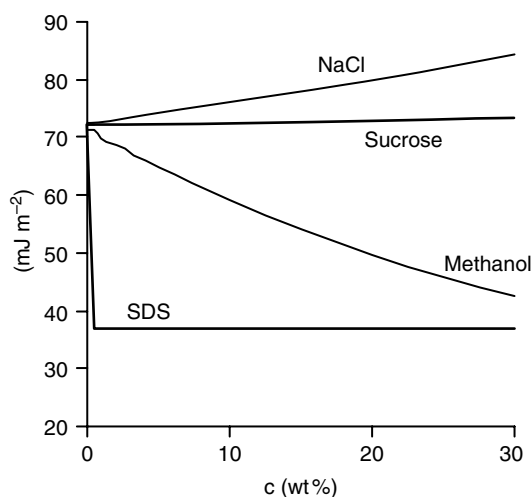


**Figure 5.5** Solutes have different surface tension vs. concentration profiles because of differences in their affinity for the surface.

### 5.3 Adsorption of solutes to interfaces

In the previous section, the molecular origin of the ability of solutes to adsorb to interfaces was highlighted. In this section, we introduce mathematical quantities and thermodynamic relationships that can be used to describe the adsorption of solutes to interfaces. As a whole, emulsions are thermodynamically unstable systems because of the unfavorable contact between oil and water molecules (Section 7.2.1). Nevertheless, their interfacial properties can often be described by thermodynamics because the adsorption–desorption of surface-active solutes occurs at a rate that is much faster than the timescale of the kinetic destabilization of the overall emulsion (Hunter, 1986).

#### 5.3.1 Definition of surface excess concentration

To define the concentration of solute that accumulates at an interface from a thermodynamic perspective it is convenient to assume that the interface is a smooth infinitesimally thin plane that separates two homogeneous liquids (Figure 5.1a). Initially, one has to decide precisely where this imaginary plane should be located in the system, as this location influences the value of the interfacial solute concentration (Hiemenz and Rajagopalan, 1997). In the following sections, the standard convention for assigning the location of the imaginary plane (the so-called *Gibbs dividing surface*) is introduced, and then the definition of the interfacial solute concentration (the so-called *surface excess concentration*) is given.

##### 5.3.1.1 Gas–liquid interface in the absence of solutes

For simplicity, consider a system that consists of liquid water in equilibrium with its vapor in the absence of any solutes (Figure 5.6). The volume fraction of water molecules in the liquid water is approximately unity, and decreases to approximately zero as one moves up through the interfacial region and into the vapor phase.

The imaginary plane interface could be located anywhere in the interfacial region indicated in Figure 5.6 (Hunter, 1986; Hiemenz and Rajagopalan, 1997). In practice, it is convenient to assume that the interface is located at a position where the excess concentration of the substance on one side of the interface is equal to the deficit concentration of the substance on the other side of the interface:  $c_{\text{excess}} = c_{\text{deficit}}$ . In this example, the *excess*

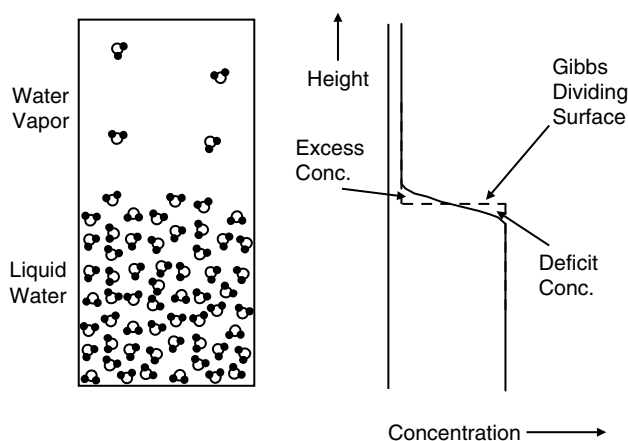


**Figure 5.6** From a thermodynamic standpoint, it is convenient to locate the interface (Gibbs dividing surface) separating a liquid and its vapor, where  $c_{\text{excess}} = c_{\text{deficit}}$ .

*concentration* corresponds to the amount of water above the interface that exceeds the quantity that would have been present if the concentration of water was the same as that in the bulk vapor phase right up to the interface. Similarly, the *deficit concentration* corresponds to the amount of water that is below the interface that is less than that which would have been present if the concentration of the water was the same as that in the bulk liquid phase right up to the interface. This location of the interface is known as the *Gibbs dividing surface*, after the scientist who first proposed this convention.

### 5.3.1.2 Gas-liquid interface in the presence of solutes

The concept of the Gibbs dividing surface is particularly useful for defining the amount of a surface-active solute that accumulates at an interface (Hunter, 1986). Consider a system that consists of a surfactant solution in contact with its vapor (Figure 5.7). The surface-active

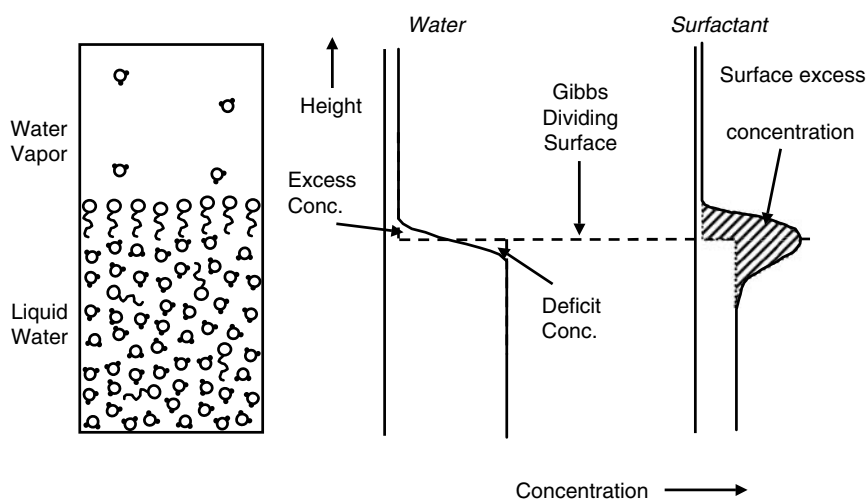


**Figure 5.7** When an emulsifier is present, the Gibbs dividing surface is conveniently located at the position, where  $c_{\text{excess}} = c_{\text{deficit}}$  for the liquid in which the emulsifier is most soluble, and the surface excess concentration is equal to the shaded region.

solute is distributed between the bulk aqueous phase, the vapor, and the interfacial region. The excess solute concentration at the surface ( $n_i$ ) corresponds to the total amount of solute present in the system minus that which would be present if the solute were not surface active, and equals the shaded area shown in Figure 5.7. The accumulation of solute molecules at an interface is characterized by a *surface excess concentration*,  $\Gamma$ , which is equal to the excess solute concentration divided by the surface area:  $\Gamma = n_i/A$ . Food emulsifiers typically have  $\Gamma$  values of a few  $\text{mg m}^{-2}$  (Dickinson, 1992; Dalgleish, 1996a). It is important to note that the solute molecules are not actually concentrated at the Gibbs dividing surface (which is infinitely thin), because of their finite size and the possibility of multilayer formation. Nevertheless, this approach is extremely convenient for thermodynamic descriptions of the properties of surfaces and interfaces (Hunter, 1986). The surface excess concentration is often identified with an experimentally measurable parameter called the *surface load*, which is the amount of emulsifier adsorbed to the surface of emulsion droplets per unit area of interface (Section 4.4.3).

### 5.3.1.3 Liquid–liquid interfaces

For an interface between pure oil and pure water the Gibbs dividing surface could either be positioned at the point where the excess and deficit concentrations of the oil or of the water were equal on either sides of the interface, which will in general be different (Tadros and Vincent, 1983). For convenience, it is usually assumed that the phase in which the surface-active solute is most soluble is the one used to decide the position of the Gibbs dividing surface. The surface excess concentration of a solute is then equal to that which is present in the system minus that which would be present if there were no accumulation at the interface (Hunter, 1986).

## 5.3.2 Relationship between adsorbed and bulk solute concentrations

Consider a system that consists of a solute solution in contact with a surface (Figure 5.3). There will be an equilibrium between the solute molecules adsorbed to the surface and those present in the bulk solution. As the solute concentration in the bulk liquid is increased, so does its concentration at the surface. The presence of solute molecules at the surface reduces the thermodynamically unfavorable contacts between air and water molecules, thereby reducing the surface tension (Norde, 2003). At a certain solute concentration, the surface tension reaches a constant value because the surface becomes saturated with solute molecules. It is useful to be able to mathematically describe the relationship between the adsorbed and free solute concentration, and to quantify how this relationship depends on the surface activity of the solute molecules. In this section, two different thermodynamic approaches that have been developed to describe this relationship are presented: the *Langmuir adsorption isotherm* and the *Gibbs adsorption isotherm* (Hunter, 1986; Hiemenz and Rajagopalan, 1997; Norde, 2003). These approaches are based on a thermodynamic analysis of the adsorption process, assuming that the adsorption–desorption of solutes at the surface is reversible, and that solute–solute interactions do not occur in the bulk solution or at the surface.

The *Langmuir adsorption isotherm* is useful for relating the amount of solute present at a surface to the concentration and surface activity of the solute in the bulk solution:

$$\theta = \frac{\Gamma}{\Gamma_{\infty}} = \frac{c/c_{1/2}}{1 + c/c_{1/2}} \quad (5.3)$$

where  $\theta$  is the fraction of adsorption sites that are occupied,  $\Gamma_{\infty}$  is the surface excess concentration when the surface is completely saturated with solute, and  $c_{1/2}$  is the solute

concentration in the bulk solution where  $\theta = 1/2$ . The equilibrium constant for adsorption ( $K = 1/c_{1/2}$ ) provides a good measure for the *surface activity* or *binding affinity* of an emulsifier: the greater  $1/c_{1/2}$  the higher the binding affinity. The surface activity of a molecule is related to the free energy of adsorption by the following equation:

$$K = \frac{1}{c_{1/2}} = \exp\left(-\frac{\Delta G_{\text{ads}}}{RT}\right) \quad (5.4)$$

where  $\Delta G_{\text{ads}}$  corresponds to the free energy change associated with exchanging a solvent molecule with a solute molecule at the surface. Thus, the more negative is the free energy change associated with solute adsorption ( $\Delta G_{\text{ads}}/RT$ ), the higher is the affinity of the solute for the surface. As mentioned earlier, the adsorption free energy has both enthalpy and entropy contributions. The enthalpy contributions are due to changes in the strength of the fundamental interaction energies associated with adsorption, for example, van der Waals, electrostatic, and steric (Chapter 2). The entropy contributions are due to differences in the number of ways the molecules can be arranged in the system in the nonadsorbed and adsorbed states, for example, configuration, orientation, conformation, and interaction entropies (Section 5.2). Attempts have been made in the literature to calculate the relative contributions of the various enthalpic and entropic contributions to  $\Delta G_{\text{ads}}$  for different kinds of emulsifiers (Norde, 2003). The magnitude of the enthalpy and entropy contributions to the overall free energy of adsorption can often be determined by measuring the temperature dependence of the surface-activity of the molecules (Norde, 2003).

Predictions made using the Langmuir adsorption equation for emulsifiers with low and high binding affinities are shown in Figure 5.8. The emulsifier concentration at the surface ( $\Gamma$ ) increases approximately linearly with increasing emulsifier concentration in the bulk solution ( $c$ ) at low emulsifier concentrations. At high emulsifier concentrations  $\Gamma/\Gamma_{\infty}$  tends toward unity, indicating saturation of the interface. In practice, there are often appreciable deviations between predictions made by the Langmuir equation and experimental measurements because the assumptions used in the derivation of the theory are not met for many real systems (Walstra, 2003a). Some important sources of deviation are: (i) surfactants may form micelles in solution so that their activity coefficient is very

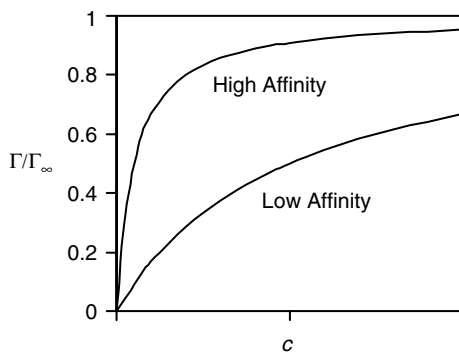


**Figure 5.8** Theoretical calculations of the dependence of the normalized surface excess concentration ( $\Gamma/\Gamma_{\infty}$ ) on emulsifier concentration in a bulk solution for two emulsifiers with different surface activities. The surface activity of a solute can be determined from a plot of surface excess concentration ( $\Gamma$ ) vs. surfactant concentration in the bulk solution ( $c$ ). The surface activity is defined as the concentration where  $\Gamma = 1/2\Gamma_{\infty}$  where  $\Gamma_{\infty}$  is the surface excess concentration when the interface is saturated with solute.



different from their concentration, (ii) emulsifiers may interact appreciably with each other at the surface so the binding sites cannot be treated as being independent, (iii) biopolymers unfold and interact at the interface so that the adsorption process cannot be considered to be reversible, (iv) solvent and emulsifier molecules have different sizes (Lucassen-Reynders, 1994; Norde, 2003; Walstra, 2003a). For this reason, a number of researchers have developed more sophisticated theories that take into account some of these effects (Wustneck et al., 1996; Fainerman et al., 1998, 2003; Prosser and Franses, 2001; Miller et al., 1998, 2000; Gurkov et al., 2003).

The *Gibbs adsorption isotherm* is useful for relating the amount of solute present at a surface ( $\Gamma$ ) to the surface tension (or surface pressure) and solute concentration in the bulk solution (which are both experimentally accessible):

$$\Gamma = -\frac{1}{pRT} \left( \frac{d\gamma}{d \ln(c)} \right) = \frac{1}{pRT} \left( \frac{d\pi}{d \ln(c)} \right) \quad (5.5)$$

where  $c$  is the concentration of solute in the aqueous phase,  $R$  is the gas constant,  $T$  is the absolute temperature, and  $p$  is a parameter that depends on solute type and solution conditions. For nonionic solutes,  $p = 1$ . For monovalent ionic solutes,  $p = 2$  at low ionic strengths,  $p = 1$  at high ionic strengths, and  $p = c/(c + c_E)$  at intermediate ionic strengths, where  $c_E$  is the concentration of monovalent electrolyte present in the aqueous solution (Norde, 2003). The parameter  $p$  takes into account the fact that there may be counterions closely associated with ionic solutes and that these ions can also accumulate at the interface (Hunter, 1986). The Gibbs adsorption isotherm can be used to determine the surface excess concentration of a solute from experimental measurements of the surface tension as a function of solute concentration, since  $\Gamma$  is related to the slope of a plot of  $\gamma$  (or  $\pi$ ) versus  $\ln(c)$  (Figure 5.4). The Gibbs adsorption isotherm can also be presented in the following form:

$$\pi = pRT \int_0^c \Gamma(c) d \ln c \quad (5.6)$$

This expression enables one to calculate the surface pressure (or tension) from knowledge of the relationship between the surface and bulk solute concentration. Equations for  $\Gamma(c)$  have been derived for various systems (Norde, 2003), for example, the Langmuir adsorption isotherm described above (Equation 5.3). Insertion of the Langmuir adsorption isotherm into the above equation and expressing the surface excess concentration in units of mass per unit area rather than moles per unit area gives

$$\pi = \left( \frac{pRT}{M} \right) \Gamma_{\infty} \ln \left( 1 + \frac{c}{c_{1/2}} \right) \quad (5.7)$$

This equation is only strictly applicable at low solute concentrations since it does not take into account solute–solute interactions in the bulk solution or at the interface. Nevertheless, it provides some valuable insights into the factors that influence the surface pressure. The surface pressure should increase as the emulsifier concentration increases ( $c$ ), the surface activity increases ( $1/c_{1/2}$ ), or the surface excess concentration ( $\Gamma_{\infty}$ ) at saturation increases.

Knowledge of  $\Gamma_{\infty}$  is important for formulating food emulsions because it determines the minimum amount of emulsifier that can be used to create an emulsion with a given size distribution (Section 6.6.1). The smaller the value of  $\Gamma_{\infty}$ , the greater the area of oil–water

interface that can be covered per gram of emulsifier, and therefore the smaller the size of droplets that can be effectively stabilized by the same amount of emulsifier. Plots of surface tension versus emulsifier concentration are also useful because they indicate the maximum surface pressure  $\pi_{\max}$  that can be achieved when the surface is saturated by an emulsifier, which has important consequences for the formation and stability of food emulsions (Chapters 6 and 7).

### 5.3.3 Stipulating interfacial properties of surface-active solutes

Overall, the interfacial characteristics of a surface-active solute can be described by plotting the surface excess concentration and surface pressure (or tension) versus surfactant concentration (Figure 5.4). The interfacial characteristics of a solute can then be conveniently described in terms of three thermodynamic parameters that can be determined from these curves:

- *Surface activity.* The surface activity ( $1/c_{1/2}$ ) of a solute is determined by the free energy change associated with adsorption of the solute from the bulk solution to the interface. It provides a quantitative measure of the affinity of a solute molecule for the interface: the higher  $1/c_{1/2}$ , the greater the surface activity.
- *Saturation surface pressure.* The surface pressure of the interface when it is saturated with solute molecules ( $\Pi_{\infty}$ ) is determined by how efficient the solute molecules are at minimizing the thermodynamically unfavorable contacts at the interface. It therefore depends on the packing of the solute molecules at the interface, as well as their interactions with the other molecules present there, for example, oil and water.
- *Saturation surface excess concentration.* The surface excess concentration at the interface when it is saturated with solute ( $\Gamma_{\infty}$ ) is determined by the mass of the individual solute molecules as well as how efficiently they can pack at the interface.

The above parameters are derived assuming that the adsorption–desorption process is reversible and that there are no solute–solute interactions in the bulk solution or at the interface. In practice, a thermodynamic interpretation of these parameters may therefore be invalid for many real systems because these assumptions are not met. Nevertheless, these parameters still provide a useful means of characterizing and comparing the interfacial properties of surface-active solutes in terms of experimentally measurable quantities.

The interfacial properties of a typical small molecule surfactant and a protein are compared in Figure 5.9. The protein has a much higher surface activity than the surfactant (lower  $c_{1/2}$ ), but the surfactant can lower the interfacial tension appreciably more at saturation than the protein. This means that proteins adsorb to interfaces at much lower bulk emulsifier concentrations than do surfactants, but that surfactants are effective at displacing proteins from interfaces at sufficiently high concentrations.

### 5.3.4 Adsorption kinetics

The rate at which an emulsifier adsorbs to an interface is one of the most important factors determining its efficacy as a food ingredient (Magdassi and Kamyshny, 1996; Walstra, 1996; Walstra and Smulders, 1998). The adsorption rate depends on the molecular characteristics of the emulsifier (e.g., size, flexibility, conformation, and interactions), the nature of the bulk liquid (e.g., viscosity, polarity), and the prevailing environmental conditions

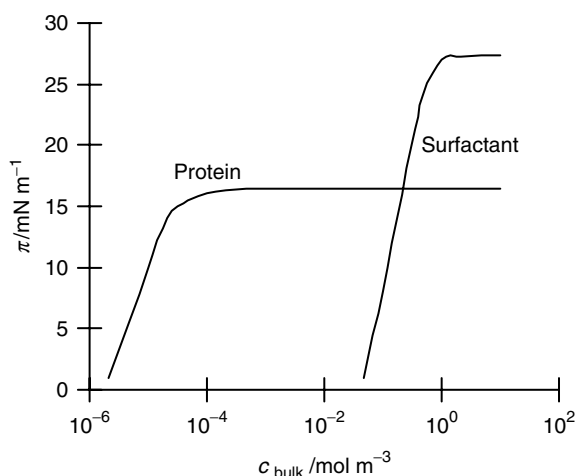


**Figure 5.9** Comparison of the affinity of amphiphilic biopolymers and small molecule surfactants for an oil–water interface. Biopolymers tend to have a higher surface activity and therefore saturate the interface at lower concentrations, but surfactants are usually more effective at minimizing unfavorable interactions at the interface and therefore have higher  $\pi_{\infty}$ .

(e.g., temperature and flow profile). It is often convenient to divide the adsorption process into two stages: (i) movement of the emulsifier molecules from the bulk liquid to the vicinity of the interface and (ii) attachment of the emulsifier molecules to the interface (Figure 5.10). In practice, emulsifier molecules are often in a dynamic equilibrium between the adsorbed and nonadsorbed states, and so we must also consider the rate at which emulsifier molecules leave the interface when calculating the net adsorption rate (Hunter, 1993; Magdassi and Kamyshny, 1996; Norde, 2003).

#### 5.3.4.1 Movement of molecules to the vicinity of an interface

In this section, we assume that an emulsifier molecule is adsorbed to an interface as soon as it encounters it, that is, there are no energy barriers that retard adsorption. In an isothermal quiescent liquid, emulsifier molecules move from a bulk liquid to an interface

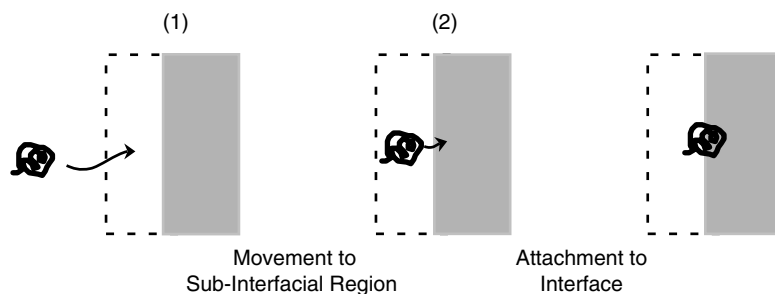


**Figure 5.10** The adsorption of a surface-active solute at an interface can be divided into a number of steps: (1) movement to the vicinity of the interface, (2) attachment to the interface. After attachment the emulsifier molecule may undergo conformational changes or interact with its neighbors, which would change its desorption rate.

by molecular diffusion with an initial adsorption rate given by (Tadros and Vincent, 1983; Magdassi and Kamyshny, 1996)

$$\frac{d\Gamma}{dt} = c \sqrt{\frac{D}{\pi t}} \quad (5.8)$$

where  $D$  is the translational diffusion coefficient of the emulsifier,  $\Gamma$  is the surface excess concentration,  $t$  is the time, and  $c$  is the concentration of emulsifier initially present in the bulk liquid (Norde, 2003). The variation of the surface excess concentration with time is obtained by integrating this equation with respect to time:

$$\Gamma(t) = 2c \sqrt{\frac{Dt}{\pi}} \quad (5.9)$$

Thus, a plot of the surface excess concentration versus  $\sqrt{t}$  should be a straight line that passes through the origin. This equation indicates that the accumulation of an emulsifier at an interface occurs more rapidly as the concentration of emulsifier in the bulk liquid increases or as the diffusion coefficient of the emulsifier increases. The diffusion coefficient increases as the size of molecules decrease, and one would therefore expect smaller molecules to adsorb more rapidly than larger ones. Experiments with proteins have shown that Equation 5.9 gives a good description of the early stages of adsorption to clean interfaces (Damodaran, 1990; Walstra, 1996). After the initial stages, the adsorption rate decreases because the interface becomes saturated with emulsifier molecules and therefore there are less sites available for the emulsifier to adsorb to (Figure 5.11). Mathematical models have been developed to describe the change in interfacial concentration with time at the later stages of adsorption (Norde, 2003). Models have been developed that take into account solute–solute interactions at the interface, the orientation of the solute molecules, and postadsorption conformational changes of solutes. In practice, the initial rate is often faster than that given by Equation 5.9 because of convection currents caused by temperature gradients within a liquid. Consequently, considerable care must be taken to ensure that the temperature within a sample is uniform when measuring diffusion-controlled adsorption processes.

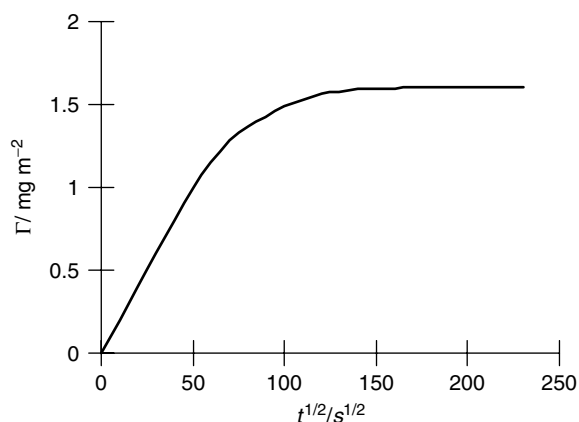


**Figure 5.11** Typical example of adsorption kinetics for a diffusion-controlled system. The surface excess concentration increases with time as emulsifier molecules accumulate at the interface.

The above equations do not apply during the homogenization of emulsions, because homogenization is a highly dynamic process and mass transport is governed mainly by convection rather than diffusion (Dickinson, 1992; Walstra, 1996). Under isotropic turbulent conditions the initial increase of the surface excess concentration with time is given by (Dukhin et al., 1995)

$$\Gamma(t) = Cr_d C \left( 1 + \frac{r_e}{r_d} \right)^3 t \quad (5.10)$$

where  $C$  is a constant that depends on the experimental conditions, and  $r_d$  and  $r_e$  are the radii of the droplet and emulsifier, respectively. This equation predicts that the adsorption rate increases as the concentration of emulsifier increases, the size of the emulsion droplets increases, or the size of the emulsifier molecules increases relative to the size of the droplets. This equation implies that when an emulsion is homogenized, the emulsifier molecules initially adsorb preferentially to the larger droplets, and that larger emulsifier molecules tend to adsorb more rapidly than smaller ones (which is the opposite to diffusion-controlled adsorption). This explains why large casein micelles adsorb faster than individual casein molecules during the homogenization of milk (Mulder and Walstra, 1974).

#### 5.3.4.2 Attachment of emulsifier molecules to interface

So far, we have assumed that as soon as an emulsifier molecule reaches an interface it is immediately adsorbed. In practice, there may be one or more energy barriers that must be overcome before a molecule adsorbs, and so only a fraction of the encounters between an emulsifier molecule and an interface lead to adsorption (Damodaran, 1990, 1996; Magdassi and Kamyshny, 1996; Norde, 2003). In these systems, adsorption kinetics may be governed by the height of the energy barrier, rather than by the rate at which the molecules reach the interface (Magdassi and Kamyshny, 1996).

There are a number of reasons that an energy barrier to adsorption may exist (Malmsten, 2003; Norde, 2003):

1. As an emulsifier molecule approaches an interface there may be various types of repulsive interactions between it and the emulsifier molecules already adsorbed to the interface, for example, electrostatic, steric, hydration, or thermal fluctuation (Chapter 3).
2. Some surface-active molecules will only be adsorbed if they are in a specific orientation when they encounter the interface. For example, it has been suggested that globular proteins that have hydrophobic patches on their surface must face toward an oil droplet during an encounter (Damodaran, 1990, 1996; Norde, 2003).
3. The ability of surfactant molecules to form micelles plays a major role in determining their adsorption kinetics (Dukhin et al., 1995; Stang et al., 1994; Karbstein and Schubert, 1995). Surfactant monomers are surface-active because they have a polar head group and a nonpolar tail, but micelles are not surface-active because their exterior is surrounded by hydrophilic head groups. The adsorption kinetics therefore depends on the concentration of monomers and micelles present, as well as the dynamics of micelle formation–disruption (Karbstein and Schubert, 1995; Kabalanov and Weers, 1996).

The adsorption of emulsifier molecules at a surface or interface can be measured using a variety of experimental methods (Couper, 1993; Kallay, et al., 1993; Dukhin et al., 1995;

Norde, 2003). The most commonly used is to measure the variation in surface or interfacial tension with time using a tensiometer (Section 5.7). A number of workers have also used radio-labeled emulsifier molecules to measure adsorption kinetics (Damodaran, 1990). A radioactivity detector is placed immediately above a water–air surface. The radio-labeled emulsifier is injected into the water and the increase in the radioactivity at the surface is recorded over time by the detector. The radioactivity is highly attenuated by the water, and so only those molecules that are close to the air–water surface are detected. A variety of other experimental methods that can detect changes in interfacial properties due to the adsorption of emulsifier molecules have also been used to monitor adsorption kinetics, including spectroscopy, scattering, and reflection of various forms of radiation and interfacial rheology (Sections 5.6–5.8).

## 5.4 *Electrical characteristics of interfaces*

### 5.4.1 *Origin of interfacial charge*

The droplets in most food emulsions have an appreciable electrical charge, and therefore electrostatic interactions may play an important role in determining their overall stability and physicochemical properties. Oil droplets in emulsifier free oil-in-water emulsions have been shown to have an electrical charge that depends on both pH and ionic strength (Marinova et al., 1996; Stachurski and Michalek, 1996; Pashley, 2003; Hsu and Nacu, 2003). For example, the  $\zeta$ -potential of sunflower oil droplets dispersed in aqueous solutions goes from positive at low pH (<5) to increasingly negative at higher pH (Hsu and Nacu, 2003). Similar trends have been observed for hydrocarbon droplets dispersed in water (Stachurski and Michalek, 1996; Pashley, 2003). The origin of this effect has been attributed to preferential adsorption of either  $\text{H}_3\text{O}^+$  (low pH) or  $\text{OH}^-$  (high pH) species from the water onto the droplet surfaces (Marinova et al., 1996; Hsu and Nacu, 2003). In addition, there may be surface-active ionic impurities present in many oils, such as free fatty acids. The droplets in food emulsions are normally stabilized by emulsifiers and so their electrical characteristics are largely determined by the characteristics of the interfacial layer of adsorbed emulsifier molecules. The emulsifiers used in foods may be anionic, cationic, or nonionic depending on their molecular characteristics and the prevailing environmental conditions (e.g., pH, ionic strength, temperature). Contrary to initial expectations, emulsion droplets stabilized by nonionic surfactants may have an appreciable electrical charge. For example, sunflower oil droplets stabilized by Tweens have been shown to have positive charges at low pH (<4) and negative charges at higher pH (Hsu and Nacu, 2003). Hence, they follow similar trends to bare oil droplets, but they tend to have more negative charges at the same pH, which causes their isoelectric points (IEPs) to shift to lower pH values. This phenomenon has been attributed to the preferential adsorption of  $\text{OH}^-$  ions to the hydrophilic head groups of the surfactants. The electrical properties of oil droplets stabilized by nonionic surfactants therefore seem to be dominated by the electrical characteristics of the bare droplets, but are modified somewhat by the presence of the interfacial layer of adsorbed surfactant molecules. Many types of commonly used food emulsifiers are either ionic or capable of being ionized, for example, proteins, polysaccharides, and surfactants (Section 4.4). All food proteins have acidic ( $-\text{COOH} + \text{COO}^- + \text{H}^+$ ) and basic ( $\text{NH}_2 + \text{H}^+ + \text{NH}_3^+$ ) groups whose degree of ionization depends on the pH and ionic strength of the surrounding aqueous phase (Charlambous and Doxastakis, 1989; Damadaron, 1996; Magdassi, 1996). Some surface-active polysaccharides, such as modified starch and gum arabic, also have acidic groups that may be ionized (BeMiller and Whistler, 1996; Stauffer, 1999). Ionic surfactants may be either positively or negatively charged depending on the nature of their hydrophilic head group (Linfield, 1976; Myers, 1988; Richmond, 1990; Jonsson et al., 1998).

The magnitude and sign of the electrical charge on an emulsion droplet therefore depend on the type of emulsifier used to stabilize it, the concentration of the emulsifier at the interface, and the prevailing environmental conditions (e.g., pH, temperature, and ionic strength). All the droplets in an emulsion are usually stabilized by the same type of emulsifier and therefore have the same electrical charge. The electrostatic interaction between similarly charged droplets is repulsive, and so electrostatic interactions play a major role in preventing droplets from coming close enough together to aggregate (Section 3.4).

The sign and magnitude of the electrical charge on emulsion droplets play an important role in determining the stability and physicochemical properties of food emulsions. For example, the electrical characteristics of the interface influence the magnitude and range of the colloidal interactions between emulsion droplets, as well as the tendency for various types of electrically charged molecules to accumulate at the droplet surfaces, for example, antioxidants, prooxidants, and flavors.

The electrical properties of an interface are usually characterized by the surface charge density ( $\sigma$ ) and the electrical surface potential ( $\psi_0$ ). The surface charge density is the amount of electrical charge per unit interfacial area, whereas the surface potential is the amount of free energy required to increase the surface charge density from zero to  $\sigma$ . The surface charge density is governed by the type and concentration of ionizable surface-active molecules adsorbed to the interface, as well as by the characteristics of the solution surrounding the interface (e.g., ion concentration, ion type, dielectric constant) and the prevailing environmental conditions (e.g., temperature).

The various kinds of ionic species present in food emulsions that influence the electrical properties of interfaces can be conveniently divided into three categories (Hunter, 1986, 1989):

*Potential determining ions (PDI).* This type of ion is responsible for the association–dissociation of charged groups, for example,  $-\text{COOH} \rightarrow \text{COO}^- + \text{H}^+$ . In food emulsions the most important PDIs are  $\text{H}^+$  and  $\text{OH}^-$ , because they govern the degree of ionization of acidic and basic groups on many proteins, polysaccharides, and phospholipids. The influence of PDIs on surface charge is therefore determined principally by the pH of the aqueous phase relative to the  $\text{pK}_a$  values of the ionisable surface groups.

*Indifferent electrolyte ions.* This type of ion accumulates around charged groups because of attractive electrostatic interactions, for example,  $\text{Na}^+$  ions may accumulate around a negatively charged  $-\text{COO}^-$  group. These ions reduce the strength of the electrical field around a charged group principally due to electrostatic screening, rather than by altering the surface charge density. Nevertheless, at sufficiently high ionic strengths some “indifferent” electrolyte ions may alter the degree of ionization of charged groups, either by altering their dissociation constants (i.e., their  $\text{pK}_a$  values) or by competing with  $\text{H}^+$  or  $\text{OH}^-$  ions (e.g.,  $-\text{COO}^- + \text{Na}^+ \rightarrow -\text{COO}^-\text{Na}^+$ ). The influence of indifferent electrolyte ions on surface charge is therefore determined principally by their effect on the ionic strength of the surrounding solution, and is usually characterized by the Debye screening length (see Section 5.4.2).

*Adsorbed ions.* The electrical characteristics of the interface can also be altered by adsorption of ions to the interface, which changes the surface charge density. In food emulsions, the most important types of adsorbed ions are ionic emulsifiers (e.g., many surfactants, proteins, and polysaccharides) and polyvalent ions (e.g., multivalent mineral ions and polyelectrolytes) (Chapter 4). The primary driving force for the adsorption of ionic emulsifiers to an interface is often the hydrophobic effect, whereas the major driving force for the adsorption of polyvalent ions is usually electrostatic attraction. The contribution of adsorbed ions to surface charge is governed mainly by their type and concentration in the overall system, and their relative affinities for the interface.

Food scientists are particularly interested in understanding the role that each of these different types of ion play in determining the overall properties and stability of food emulsions.

#### 5.4.2 Ion distribution near a charged interface

The development of mathematical models to describe the electrical properties of interfaces relies on an appreciation of the way that ions are organized close to charged surfaces (Norde, 2003). Consider a charged surface that is in contact with an electrolyte solution (Figure 5.12). Ions of opposite charge to the surface (*counterions*) are attracted toward it, whereas ions of similar charge (*coions*) are repelled from it. Nevertheless, the tendency for ions to be organized in the vicinity of a charged surface is opposed by the disorganizing influence of the thermal energy (Evans and Wennerstrom, 1994). Consequently, the concentration of counterions is greatest at the charged surface, and decreases as one moves away from the surface until it reaches the bulk counterion concentration, whereas the concentration of coions is smallest at the charged surface, and increases as one moves away from the surface until it reaches the bulk coion concentration (Figure 5.12). The concentration of counterions near a charged surface is always greater than the concentration of coions, and so a charged surface can be considered to be surrounded by a cloud of counterions. Nevertheless, the overall system must be electrically neutral, and so the charge on the surface must be completely balanced by the excess charge of the counterions in the electrolyte solution. The distribution of ions close to a charged surface is referred to as the *electrical double layer*, because it is convenient to assume that the system consists of two oppositely charged layers (Kitakara and Watanabe, 1984; Hunter, 1986, 1989; Heimenz and Rajagopalan, 1997). The first layer is the charged surface itself and the second layer is the neutralizing layer of counterions in the liquid in contact with the surface (Evans and Wennerstrom, 1994). The effective thickness of the second layer is determined

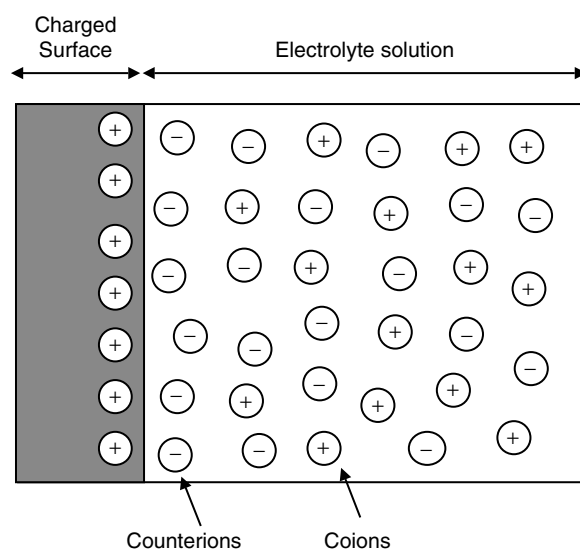


**Figure 5.12** The organization of ions near a charged surface is governed by two opposing tendencies: (i) electrostatic interactions, favor accumulation of counterions near an oppositely charged surface and (ii) thermal energy, which favors a random distribution of ions.



primarily by the ionic composition of the liquid, decreasing with increasing counterion valancy and concentration (see later).

It is possible to develop mathematical equations to predict the distribution of ions in the immediate vicinity of a charged surface from knowledge of the electrical characteristics of the surfaces and the properties of the solution in contact with it (Evans and Wennerstrom, 1994). The electrical properties of the surface are usually characterized in terms of the surface charge density ( $\sigma$ ) and electrical surface potential ( $\psi_0$ ), whereas the properties of the solution are usually characterized in terms of ion concentration, ion type, and dielectric constant (Evans and Wennerstrom, 1994). A mathematical relationship, known as the *Poisson–Boltzmann* equation, has been derived to relate the electrical potential in the vicinity of a charged surface to the concentration and type of ions present in the adjacent electrolyte solution (Evans and Wennerstrom, 1994):

$$\frac{d^2\psi(x)}{dx^2} = -\frac{e}{\epsilon_0\epsilon_R} \sum_i z_i n_{0i} \exp\left(\frac{-z_i e \psi(x)}{kT}\right) \quad (5.11)$$

where  $n_{0i}$  is the concentration of ionic species of type  $i$  in the bulk electrolyte solution (in molecules per cubic meter),  $z_i$  is their valancy,  $e$  is the elementary charge ( $1.602 \times 10^{-19}$  C),  $\epsilon_0$  is the dielectric constant of a vacuum,  $\epsilon_R$  is the relative dielectric constant of the solution, and  $\psi(x)$  is the electrical potential at a distance  $x$  from the charged surface. This equation is of central importance to emulsion science because it is the basis for the calculation of electrostatic interactions between emulsion droplets (Section 3.4). Nevertheless, its widespread application has been limited because it does not have an explicit analytical solution (Hunter, 1986). When accurate calculations are required it is necessary to solve the Poisson–Boltzmann numerically using a digital computer (Carnie et al., 1994). For certain systems, it is possible to derive much simpler analytical equations that can be used to calculate the electrical potential near a surface by making certain simplifying assumptions, for example, that the electrolyte ions are symmetrical (valancy 1:1, 2:2, and so on) or that the surface charge is not too high (Evans and Wennerstrom, 1994; Sader et al., 1995).

If it is assumed that the electrostatic attraction between the charged surface and the counterions is relatively weak compared to the thermal energy, that is,  $z_i e \psi_0 < kT$  (which means that  $\psi_0$  must be less than about 25 mV at room temperature in water), then a simple expression, known as the *Debye–Huckel* approximation, can be used to calculate the dependence of the electrical potential on distance from the surface (Hunter, 1986; Heimenz and Rajagopalan, 1997):

$$\psi(x) = \psi_0 \exp(-\kappa x) \quad (5.12)$$

This equation indicates that the electrical potential decreases exponentially with distance from the surface at a decay rate which is determined by the parameter,  $\kappa^{-1}$ , which is known as the *Debye screening length*. The Debye screening length is a measure of the “thickness” of the electrical double layer and it is related to the properties of the electrolyte solution by the following equation:

$$\kappa^{-1} = \sqrt{\frac{\epsilon_0 \epsilon_r kT}{e^2 \sum n_{0i} z_i^2}} \quad (5.13)$$

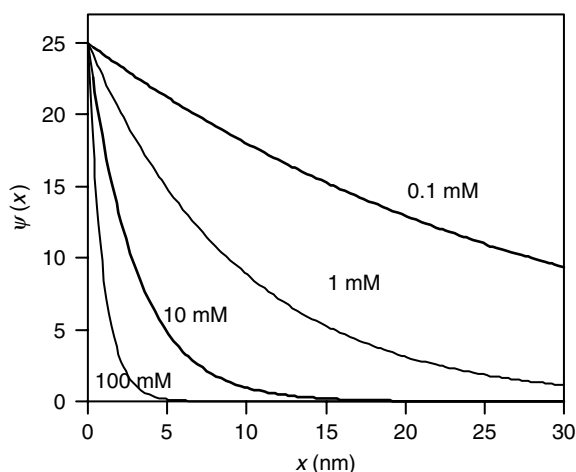


**Figure 5.13** Influence of ionic strength on the electric field near a charged surface. The electrical double layer shrinks as the electrolyte concentration increases or the ion valancy increases.

For aqueous solutions at room temperatures,  $\kappa^{-1} \sim 0.304 / \sqrt{I}$  nm, where  $I$  is the ionic strength expressed in moles per liter (Israelachvili, 1992). For example, the Debye screening lengths for NaCl solutions with different ionic strengths are: 0.3 nm for a 1 M solution, 0.96 nm for a 100 mM solution, 3 nm for a 10 mM solution, 9.6 nm for a 1 mM solution, and 30.4 for a 0.1 mM solution.

The Debye screening length is an extremely important characteristic of an electrolyte solution because it determines how rapidly the electrical potential decreases with distance from the surface. Physically,  $\kappa^{-1}$  corresponds to the distance from the charged surface where the electrical potential has fallen to  $1/e$  of its value at the surface. This distance is particularly sensitive to the concentration and valency of the ions in an electrolyte solution. As the ion concentration or valancy increases,  $\kappa^{-1}$  becomes smaller, and therefore the electrical potential decreases more rapidly with distance (Figure 5.13). The physical explanation for this phenomenon is that the neutralization of the surface charge occurs at shorter distances when the concentration of opposite charge in the surrounding solution increases.

It is often convenient to consider that a charged surface is surrounded by a "cloud" of counterions with a thickness equal to the Debye screening length, which depends strongly on the ion concentration and valency (Hunter, 1986; Evans and Wennerstrom, 1994). As will be seen in later chapters, the screening of electrostatic interactions by electrolytes has important consequences for the stability and rheology of many food emulsions because it can promote droplet flocculation (Chapters 7 and 8).

The Poisson–Boltzmann theory (and hence the Debye–Huckel approximation) assumes that an electrolyte solution is a continuum that contains ions which are infinitesimally small. It therefore allows ions to accumulate at an unrealistically large concentration near a charged surface (Kitakara and Watanabe, 1984; Evans and Wennerstrom, 1994). In reality, ions have a finite size and shape, and this limits the number that can be present in the first layer of molecules that are in direct contact with the surface (Derjaguin et al., 1987; Derjaguin, 1989; Israelachvili, 1992). This assumption is not particularly limiting for systems in which there is a weak interaction between the ions and the charged surface. Nevertheless, it becomes increasingly unrealistic as the strength of the electrostatic interactions between a charged surface and the surrounding ions increases relative to the thermal energy (Evans and Wennerstrom, 1994). In these cases, the Poisson–Boltzmann theory must be modified to take into account the finite size of the ions in the electrolyte

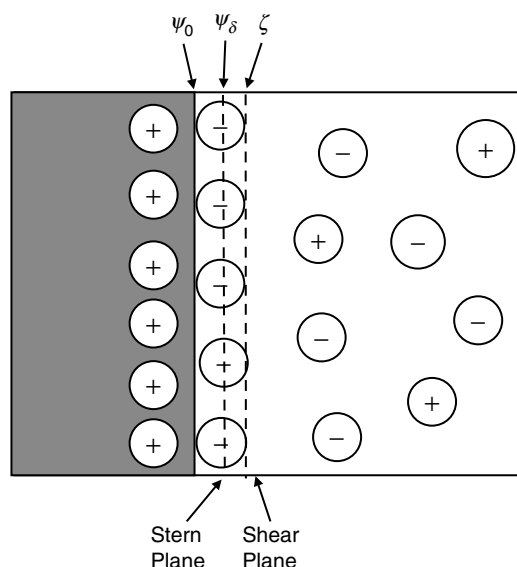


**Figure 5.14** When the electrostatic attraction between a charged surface and the surrounding counterions is relatively strong compared to the thermal energy, it is convenient to divide the electrolyte solution into an inner and an outer region.

solution. Conceptually, it is convenient to divide the distribution of counterions near a highly charged surface into two regions: an inner and an outer region (Figure 5.14).

*Inner region.* In the inner region, the attraction between the counterions and charged surface is relatively strong and therefore the counterions are relatively immobile, whereas in the outer region the attraction is much weaker and therefore the counterions are more mobile (Derjaguin, 1989; Evans and Wennerstrom, 1994; Norde, 2003). The thickness of the inner region,  $\delta$ , is approximately equal to the *radius* of the hydrated counterions, rather than their diameter, because the effective charge of an ion is located at its center (Heimenz and Rajagopalan, 1997). The inner region is sometimes referred to as the *Stern layer*, while the boundary between the inner and outer regions is referred to as the *Stern plane* (Figure 5.14). The electrical potential at the Stern plane ( $\psi_\delta$ ) is different from that at the surface ( $\psi_0$ ) because of the presence of the counterions in the Stern layer. For monovalent indifferent electrolyte counterions,  $\psi_\delta$  is less than  $\psi_0$ , because the surface charge is partly neutralized by the charge on the counterions (Figure 5.15a). The extent of this decrease depends on the number and packing of the counterions within the Stern plane (Derjaguin, 1989). The same behavior is observed for polyvalent counterions at low concentrations (such as multivalent mineral ions and polyelectrolytes), but at higher concentrations the surface may adsorb such a large number of oppositely charged multivalent counterions that its charge is actually reversed, so that  $\psi_\delta$  has an opposite sign to  $\psi_0$  (Figure 5.15b). If a charged surface adsorbs surface-active coions (e.g., ionic emulsifiers), it is even possible for  $\psi_\delta$  to be larger than  $\psi_0$  (Figure 5.15c). An increase in surface charge may occur when the hydrophobic attraction between the nonpolar tail of a surfactant and a surface is greater than any electrostatic repulsive interactions. In real food emulsions, there is usually a mixture of different types of ions present in the aqueous phase in contact with the charged surfaces, and these ions may all compete with each other at the surface. The magnitude of the electrical potential at the Stern plane therefore depends on the precise type and concentration of ions present in the system (Derjaguin, 1989).

A number of theories have been developed to take into account the effect of the finite size and limited packing of ions in the Stern layer on the relationship between  $\psi_\delta$  and  $\psi_0$ .

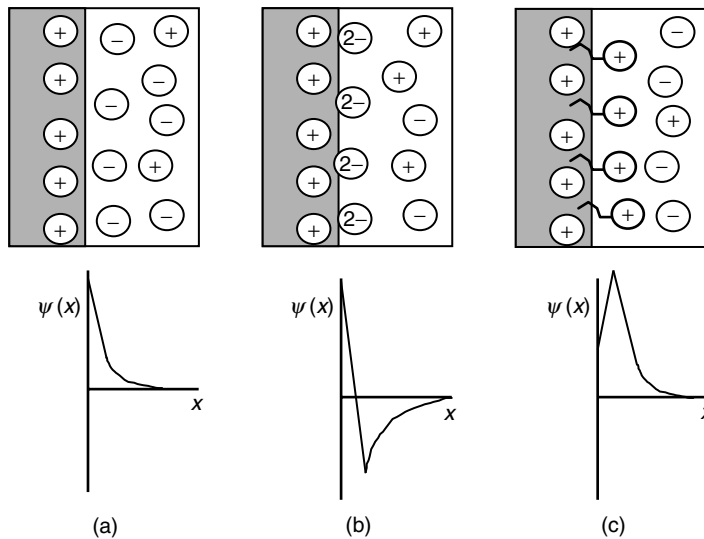


**Figure 5.15** The electrical potential at the Stern plane may be lower, higher, or a different sign to that at the bare surface depending on the strength of the interaction and the type of ions adsorbed.

One of the most widely used is the *Langmuir adsorption isotherm* mentioned earlier (Section 5.3), which assumes that there are only a finite number of binding sites at the surface, and that once these are filled the surface becomes saturated and cannot adsorb any more ions (Heimenz and Rajagopalan, 1997). In this case, the ion adsorption free energy is given by  $\Delta G_{\text{ads}} = -(ze\psi_{\delta} + \phi)$ . The  $ze\psi_{\delta}$  term is due to the electrostatic attraction between the ion and the surface, while the  $\phi$  term accounts for any specific binding effects. These specific binding effects could be due to hydrophobic interactions (e.g., when an emulsifier adsorbs) or due to chemical interactions (e.g.,  $-\text{COO}^{-} + \text{Na}^{+} \rightarrow -\text{COO}^{-}\text{Na}^{+}$ ). The fraction of surface sites that are occupied increases as the free energy of adsorption of an ion increases. The electrical potential at the Stern layer can be related to the electrical potential at the charged surface using the following equation (Heimenz and Rajagopalan, 1997):

$$\psi_{\delta} = \psi_0 - \frac{\delta \theta \sigma^{*}}{\epsilon_{\delta} \epsilon_0} \quad (5.14)$$

where  $\sigma^{*}$  is the surface charge density when the surface is completely saturated with ions,  $\delta$  is the thickness of the Stern layer,  $\theta$  is the fraction of ion binding sites that are occupied, and  $\epsilon_{\delta}$  is the relative dielectric constant of the Stern layer. This equation indicates that the difference between the potential at the surface and that at the Stern plane depends on the fraction of surface sites that are occupied. In principle, this equation can be used to calculate the change in the electrical potential of a surface due to ion adsorption. In practice, this equation is difficult to use because of a lack of knowledge about the values of  $\delta$ ,  $\phi$ , and  $\epsilon_{\delta}$  in the Stern layer (Derjaguin, 1989; Heimenz and Rajagopalan, 1997). These parameters are unique for every ion–surface combination and are difficult to measure experimentally. For this reason, it is usually more convenient to experimentally measure the electrical potential at the Stern plane, rather than attempting to predict it theoretically (Hunter, 1986).

Experiments have shown that  $\psi_{\delta}$  is closely related to the electrical potential at the *shear plane* (Hunter, 1986). When a liquid flows past a charged surface it “pulls” those counterions that are only weakly attached to the surface along with it, but leaves those

ions that are strongly attached in place, that is, those ions in the Stern plane. The shear plane is defined as the distance from the charged surface below which the counterions remain strongly attached and is approximately equal to the diameter of the hydrated ions (Figure 5.14). The electrical potential at the shear plane is referred to as the *zeta-potential* ( $\zeta$ ), and can be measured using various types of electrokinetic techniques (Section 11.6).

*Outer region.* In the outer region, the electrostatic interaction between the surface and the counterions is fairly weak (because the ions in the Stern layer partially screen the surface charge), and so the variation in electrical potential with distance can be described by replacing  $\psi_0$  with  $\psi_\delta$  in Equation 5.12:

$$\psi(x) = \psi_\delta \exp(-\kappa x) \quad (5.15)$$

where  $x$  is now taken to be the distance from the shear plane, rather than from the charged surface. The dependence of the electrical potential on distance from the shear plane can then be calculated once  $\psi_\delta$  is known. An appreciation of the factors that influence the distribution of ions near an electrically charged interface is important for understanding the interactions between charged emulsion droplets and the accumulation of ions near droplet surfaces.

### 5.4.3 Factors influencing interfacial electrical properties of emulsions

The most important factor influencing the sign and magnitude of the electrical charge on emulsion droplets is the type of emulsifier used to stabilize them (Section 5.4.1). Many types of commonly used food emulsifiers are either ionic or capable of being ionized, for example, proteins, polysaccharides, phospholipids, and surfactants (Section 4.4). The electrical characteristics of the interfaces formed by these emulsifiers depend on the number and type of ionizable groups present on the molecules. In particular, the pK values of the charged groups are particularly important for determining their extent of ionization at a particular pH. All food proteins have acidic (e.g.,  $-\text{COOH} \rightarrow \text{COO}^- + \text{H}^+$ ,  $\text{pK} \approx 4\text{--}5$ ;  $-\text{SH} \rightarrow \text{S}^- + \text{H}^+$ ,  $\text{pK} \approx 8.5$ ;  $-\text{OH} \rightarrow \text{O}^- + \text{H}^+$ ,  $\text{pK} \approx 10$ ) and basic (e.g.,  $-\text{C}_2\text{N}_2\text{H}_2 + \text{H}^+ \rightarrow -\text{C}_2\text{N}_2\text{H}_3^+$ ,  $\text{pK} \approx 8.5$ ;  $\text{NH}_2 + \text{H}^+ \rightarrow \text{NH}_3^+$ ,  $\text{pK} \approx 10\text{--}12$ ) groups whose degree of ionization depends on the pH and ionic strength of the surrounding aqueous phase (Charlambous and Doxastakis, 1989; Damadaron, 1996; Magdassi, 1996; Norde, 2003). Proteins are positively charged at pH values below their IEP, have no net charge at their IEP, and are negatively charged above their IEP. This has important consequences for the pH stability of protein-stabilized emulsions since the electrostatic repulsion between droplets is much smaller near the IEP than at higher or lower pH values (Chapter 3). Consequently, protein-stabilized emulsions usually exhibit a high degree of droplet flocculation at pH values near their IEPs (Section 7.5.1). Some surface-active polysaccharides, such as modified starch and gum arabic, also have acidic groups that may be ionized (BeMiller and Whistler, 1996; Stauffer, 1999). Ionic surfactants may be either positively or negatively charged depending on the nature of their hydrophilic head group (Linfield, 1976; Myers, 1988; Richmond, 1990; Jonsson et al., 1998), although most ionic surfactants used in foods are negatively charged (Krog and Sparso, 2004). As mentioned earlier, even droplets stabilized by nonionic surfactants may have an appreciable electrical charge (Section 5.4.1).

In addition to adsorption of charged emulsifiers, the surface charge density of emulsion droplets is also determined by adsorption of other types of ionic substances present in either the continuous and/or dispersed phases to the droplet surfaces, such as multivalent mineral ions (e.g.,  $\text{Ca}^{2+}$ ,  $\text{Cu}^{2+}$ ,  $\text{Fe}^{3+}$ ) or polyelectrolytes (e.g., proteins or polysaccharides). Adsorption of these ionic substances can alter the magnitude of the electrical charge on the emulsion droplets, change the sign of the charge on the droplets,

or act as bridges between charged droplets. The electrical potential (or  $\zeta$ -potential) of emulsion droplets is also reduced by the presence of indifferent ions that do not specifically bind to the droplet surface but increase the ionic strength of the surrounding liquid, for example, salts (Section 3.4).

#### 5.4.4 Characterization of interfacial electrical properties

A variety of analytical techniques are available for characterizing the electrical properties of interfaces. The electrical charge at an interface can often be determined by titrating PDI into the system and calculating the concentration of these ions that adsorb to the interface:  $\text{PDI}_{\text{adsorbed}} = \text{PDI}_{\text{total}} - \text{PDI}_{\text{free}}$  (Norde, 2003). For example, the PDIs for many food emulsifiers are  $\text{H}^+$  and  $\text{OH}^-$ , thus the concentration of adsorbed PDIs can be monitored by measuring the change in pH as the concentration of acid or base added to the system is changed. To determine the absolute interfacial charge using this technique it is necessary to define a reference point of known charge, which is usually taken to be the point of zero charge. The sign and magnitude of the electrical charge on an interface can also be determined using various electrokinetic techniques, for example, electroosmosis, electrophoresis, streaming potential, and streaming current (Norde, 2003). The particle electrophoresis technique is the most commonly used technique for characterizing the electrical properties of the droplet interfaces in emulsions. This technique measures the direction and velocity of particle movement in a well-defined electric field and then uses a mathematical model to determine the  $\zeta$ -potential of the particles (Section 11.6).

### 5.5 Interfacial composition and its characterization

#### 5.5.1 Factors influencing interfacial composition

Bulk physicochemical properties of emulsions, such as their ease of formation, stability, and texture, are governed by the nature of the interface, and therefore it is important for food scientists to understand the factors that determine the composition of the interfacial region (Dalgleish, 1996a). If an emulsion is prepared using a single type of emulsifier, then the interfacial membrane will be comprised of this emulsifier (Figure 5.16). Even so, the amount of emulsifier that adsorbs to the droplet surfaces (i.e.,

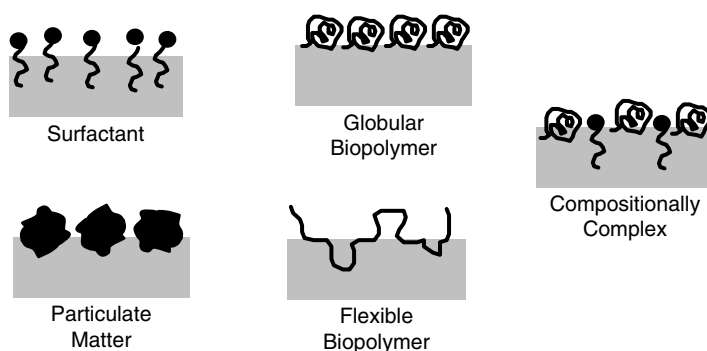


**Figure 5.16** The orientation and conformation of surface-active solutes at an interface is determined by their tendency to reduce the free energy of the system. The interfacial composition and structure depends on the type, concentration, and surface activity of the different surface-active molecules present in the system.

the surface load) may depend on a number of factors, including the initial emulsifier concentration, temperature, pH, ionic strength, and homogenization conditions. For example, the surface load increases as the initial emulsifier concentration in the aqueous phase increases for some globular protein-stabilized emulsions (Dalglish, 1996a; Rampon et al., 2003a,b). This phenomenon has been attributed to the fact that at high protein concentrations adsorption is relatively rapid, so that adsorbed protein molecules are unable to undergo extensive conformational changes and can therefore pack more efficiently (Cohen Stuart, 2003; Norde, 2003). The surface load may also increase at relatively high protein concentrations due to the formation of multiple layers of adsorbed proteins, rather than a single layer (Norde, 2003; Walstra, 2003a). The influence of temperature on the surface load depends on the emulsifier type and solution conditions (e.g., pH and ionic strength). The surface load of some globular proteins has been found to increase with temperature, presumably because the proteins partially unfold, which increases their surface hydrophobicity (Dickinson and Hong, 1994). The surface load of some protein-stabilized emulsions increase when the pH is adjusted toward the protein's IEP or when the salt concentration is increased, presumably because the electrostatic repulsion between adsorbed and nonadsorbed proteins is reduced (Dalglish, 1996a; Dalglish et al., 2002b).

Rather than containing a single type of surface-active substance, many food emulsions contain a mixture of different surface-active components, and so the interfacial membranes surrounding the droplets may be compositionally complex (Figure 5.16). In this case, the interfacial composition is determined by the concentrations of the various kinds of surface-active substances present, their relative affinity for the interface, the method used to prepare the emulsion, the solution conditions (e.g., temperature, pH, and ionic strength), and the history of the emulsion (e.g., the order in which the emulsifiers were added). Some of the most important factors influencing the interfacial composition of food emulsions containing a mixture of different emulsifiers are discussed below.

In a mixed emulsifier system, the interfacial composition depends on the relative adsorption rates of the different types of emulsifiers when the bulk solution is brought into contact with the interface, as well as on any subsequent changes that occur during storage (Dickinson, 1992). The relative adsorption rate of the emulsifiers depends on their molecular characteristics (e.g., size, shape, and polarity) and the flow profile within the bulk solution when it is brought into contact with the interface (e.g., static, laminar, or turbulent) (Section 5.3). For the case of food emulsions prepared by homogenization, the droplets will tend to be initially coated by those surface-active molecules that absorb to the interface most rapidly under turbulent conditions. Nevertheless, the interfacial composition may change during storage because some of the surface-active molecules that were initially present at the droplet surface are displaced by molecules in the bulk liquid that have a greater affinity for the surface. Alternatively, additional surface-active components may be added to the continuous phase of an emulsion after homogenization, and these may displace some of the original emulsifier molecules from the droplet surface. For example, small molecule surfactants are often added to ice cream premixes so as to displace the proteins from the surface of the milk fat globules prior to cooling and shearing (Goff et al., 1987; Goff, 1993). This causes the droplets to become more susceptible to partial coalescence, which leads to the formation of a network of aggregated droplets that stabilizes the air bubbles and gives the final product its characteristic texture and shelf life (Berger, 1997).

It is possible to relate the composition of an interface to the concentrations and surface activities of the emulsifier molecules present in a mixed emulsifier system by modifying

the Langmuir adsorption isotherm (Razumovsky and Damodaran, 2001):

$$\frac{\Gamma_1}{\Gamma_{1,\infty}} = \frac{c_1/c_{1,1/2}}{1 + c_1/c_{1,1/2} + c_2/c_{2,1/2}} \quad (5.16a)$$

$$\frac{\Gamma_2}{\Gamma_{2,\infty}} = \frac{c_2/c_{2,1/2}}{1 + c_1/c_{1,1/2} + c_2/c_{2,1/2}} \quad (5.16b)$$

where  $c_1$  and  $c_2$  are the concentrations of the two types of emulsifiers in the bulk solution,  $\Gamma_1$  and  $\Gamma_2$  are the surface excess concentrations of the emulsifiers at the interface,  $\Gamma_{1,\infty}$  and  $\Gamma_{2,\infty}$  are the surface excess concentrations at saturation, and  $c_{1,1/2}$  and  $c_{2,1/2}$  are the emulsifier concentrations where  $\Gamma_1/\Gamma_{1,\infty}$  and  $\Gamma_2/\Gamma_{2,\infty} = 1/2$ . This equation assumes that the solvent molecules and the two types of solute molecules all have the same dimensions (Lucassen-Reynders, 1994). These equations can be rearranged to give

$$\frac{\Gamma_1}{\Gamma_{\text{TOT}}} = \frac{c_1/c_{1,1/2}}{c_1/c_{1,1/2} + c_2/c_{2,1/2}} \quad (5.17a)$$

$$\frac{\Gamma_2}{\Gamma_{\text{TOT}}} = \frac{c_2/c_{2,1/2}}{c_1/c_{1,1/2} + c_2/c_{2,1/2}} \quad (5.17b)$$

Hence, the composition of the interface depends on the concentrations of the two different types of emulsifiers, as well as their relative affinities for the interface (i.e., their surface activities,  $1/c_{1/2}$ ). The change in interfacial composition when a more surface-active emulsifier ( $1/c_{1/2} = 1$ ) is added to a solution containing a fixed concentration of a less surface-active emulsifier ( $1/c_{1/2} = 2$ ) is shown in Figure 5.17. Initially, the interface is comprised entirely of type 1 emulsifier, but as the concentration of type 2 emulsifier is increased in

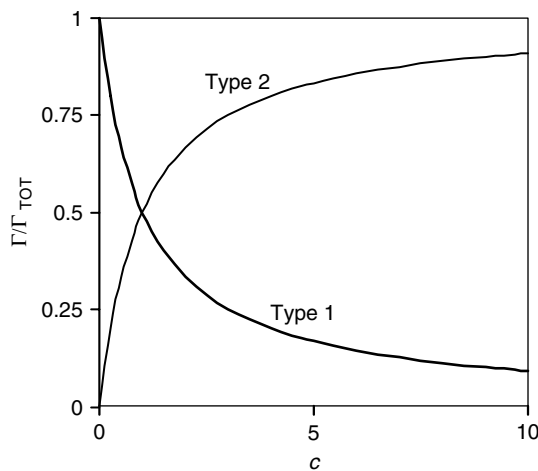


**Figure 5.17** Theoretical calculations of the dependence of interfacial composition on the composition of a bulk solution containing two different types of surface-active solutes (types 1 and 2). Initially, 2 wt% of type 1 molecule ( $1/c_{1/2} = 0.5$ ) is present in the bulk solution, then increasing amounts of type 2 molecule ( $1/c_{1/2} = 1$ ) are added to the bulk solution. The type 1 molecules are progressively displaced from the interface.



the bulk solution, then some of the type 1 emulsifier is displaced. In practice, the above approach usually has to be modified somewhat because the assumptions used in its derivation are not appropriate. For example, the solvent and two types of solutes may have different sizes, there may be interactions between the emulsifiers (either in the bulk solution and/or at the interfacial region) or the adsorption–desorption process may be irreversible due to conformational changes of one or both of the emulsifiers after adsorption (Lucassen–Reynders 1994; Norde, 2003).

It should be noted that the relative affinities of emulsifiers for an interface are influenced by solution and environmental conditions, such as temperature, pH, and ionic strength (Dickinson and Tanai, 1992; Hunt and Dalgleish, 1996; Dalgleish et al., 2002a,b). In addition, the phase in which a surfactant is most soluble also determines its effectiveness at displacing proteins from an interface. For example, water-soluble surfactants have been shown to be more effective at displacing proteins from the surface of oil droplets than oil-soluble surfactants (Dickinson et al., 1993c). The interfacial composition of an emulsion containing different types of emulsifiers may also depend on droplet size, since this determines the total amount of interfacial area available for the emulsifier molecules to adsorb to. If one of the emulsifiers is present at a relatively low concentration, then it may make up a substantial fraction of the interfacial membrane when the droplets are relatively large (small total surface area), but only a minor fraction when the droplets are relatively small (large total surface area) (Walstra, 1996a).

The displacement of emulsifier molecules from an interface may be retarded if they are capable of undergoing some form of conformational change that enables them to bind strongly to their neighbors. Some globular proteins become surface-denatured after adsorption to an interface because of the change in their molecular environment (Dickinson and Matsumura, 1991; McClements et al., 1993d; Kim et al., 2002a,b; Norde, 2003). When the proteins unfold they expose amino acids that are capable of forming disulfide bonds with their neighbors, and thus form an interfacial membrane that is partly stabilized by covalent bonds. This accounts for the experimental observation that the ease at which  $\beta$ -lactoglobulin can be displaced from the surface of oil droplets decreases as the emulsion ages (Dalgleish, 1996b). This effect is even more pronounced if an emulsion stabilized by globular proteins is heated above a temperature where the proteins are thermally denatured since the degree of covalent (disulfide) bond formation is then more extensive (McClements et al., 1993d; Dickinson and Hong, 1994, 1995a,b). It may then be extremely difficult to displace the aggregated protein molecules from the interface using small molecule surfactants, unless a chemical is added first to disrupt the covalent cross-links, for example, mercaptoethanol for disulfide bonds.

The above discussion has highlighted the wide variety of factors that can influence interfacial composition, such as emulsifier concentration, emulsifier type, solution conditions, temperature, and time. For this reason, a great deal of research is being carried out to establish the relative importance of each of these factors and on establishing the relationship between interfacial composition and the bulk physicochemical properties of food emulsions.

### 5.5.2 *Characterization of interfacial composition in emulsions*

A variety of analytical techniques are available for determining the composition of interfacial membranes; however, most of these are only suitable for making measurements at planar gas–liquid, liquid–liquid, or solid–liquid interfaces (Sections 5.6–5.8). In this section, we will focus primarily on those techniques that can be used to determine the interfacial composition of emulsions, but a few of the more commonly used techniques for analyzing planar interfaces will also be mentioned because they can provide valuable insights into the fundamental factors that influence interfacial composition.

The most commonly used method of obtaining information about interfacial composition in emulsions is to use the "depletion" technique (Dickinson, 1992; Dalgleish, 1996). An emulsion is prepared using a known concentration of emulsifier ( $c_{\text{Total}}$ ), and then the concentration of nonadsorbed emulsifier remaining in the continuous phase ( $c_{\text{NA}}$ ) after homogenization is determined using an appropriate analytical method, for example, a chemical, spectroscopic, electrophoretic, or chromatographic method. The concentration of adsorbed emulsifier is then deduced from the difference between the total emulsifier present and that which remains in the continuous phase:  $c_A = (c_{\text{Total}} - c_{\text{NA}})$ . The depletion method assumes that all of the "adsorbed" emulsifier is present at the oil–water interface. Some emulsifiers may have a significant solubility in the dispersed phase so that an appreciable fraction is present in the interior of the droplets rather than at the interface. In many food emulsions there may be more than one type of surface-active material present at the oil–water interface, so that it is important to determine the interfacial concentrations of the different species. This can also be achieved using the depletion method, but in this case it is necessary to use one or more analytical techniques to measure the concentration of the different kinds of surface-active species present in the total emulsion and in the continuous phase after homogenization. Chromatography and electrophoresis techniques are often used for this purpose, for example, SDS–polyacrylamide gel electrophoresis (PAGE) for proteins.

The depletion method is particularly suitable for determining the interfacial composition of emulsions that are prepared by the investigator, since then the initial concentration of the various surface-active species present in the system is known. If the interfacial composition of a preexisting emulsion needs to be determined and this emulsion was not prepared by the investigator, then a different method must be used because the initial concentration of surface-active species present in the system may not be known. In these cases, it is often possible to separate the droplets in an emulsion from the continuous phase by centrifugation or filtration. The droplets can then be collected and washed to remove any residual continuous phase. Washing can be achieved by dispersing the droplets in an appropriate buffer solution and then centrifuging or filtering them repeatedly. Once the droplets have been successfully separated from the continuous phase, a highly surface-active component can be added to the system to displace the original emulsifiers from the oil–water interfaces. In some cases, it may also be necessary to add an additional chemical component to breakdown any covalent bonds formed between adsorbed emulsifier molecules, for example, mercaptoethanol can be added to breakdown disulfide bonds between globular proteins and facilitate emulsifier displacement (Monahan et al., 1996). Once all the emulsifier molecules have been displaced from the droplet surfaces, the continuous phase containing the emulsifier could be separated from the droplets, and their concentration and identity could be established using appropriate analytical methods to analyze the continuous phase, for example, chromatography, electrophoresis, nuclear magnetic resonance (NMR), or mass spectrometry. Usually, it will be necessary to have a fairly good idea about the type of emulsifier molecules present in a system in order to select an appropriate analytical method to measure its concentration and identity.

Information about the nature of the emulsifier molecules present at the surface of an emulsion droplet can sometimes be obtained indirectly by measuring the change in droplet characteristics with solution or environmental conditions. For instance, the change in the electrical charge on the droplet surfaces could be determined as a function of pH, or the stability of droplets to flocculation could be measured as a function of pH, ionic strength, or temperature. Droplets stabilized by different types of emulsifiers behave differently when solution or environmental conditions are changed, hence it may be possible to obtain some insight into emulsifier type using this approach. For example, the  $\zeta$ -potential of the droplets in a protein-stabilized emulsion will go from positive to negative as the pH is

raised from below to above their IEP, whereas the electrical charge on the droplets in an ionic surfactant-stabilized emulsion may be relatively high and fairly insensitive to pH.

For some emulsions, it is possible to obtain information about the type and concentration of emulsifiers present at the droplet surfaces using instrumental methods. For example, it is often possible to infer the interfacial composition in emulsions from spectroscopy techniques that are sensitive to the molecular environment of emulsifier molecules, such as infrared, fluorescence, circular dichroism, and ultraviolet (UV)-visible spectroscopy (see Section 5.6).

## 5.6 *Interfacial structure*

### 5.6.1 *Factors influencing interfacial structure*

The structural organization of emulsifier molecules within the interfacial membranes surrounding emulsion droplets strongly influences the bulk physicochemical and sensory properties of many food emulsions. Interfaces are often treated as thin homogeneous layers of well-defined thickness, but in reality they are usually heterogeneous and structurally complex regions (Figure 5.16). Interfacial composition may vary both horizontally and vertically across the interface. For example, there is often a greater concentration of polymeric emulsifiers in the immediate vicinity of an interface where the polymers are densely packed, than at the outer edge of the interface where the polymers have a more flexible and open structure (Dickinson and McClements, 1995). In addition, there may be aggregation or phase separation of emulsifier molecules at an interface so that interfacial composition, thickness, and properties vary across the two-dimensional plane of the interface (Norde, 2003). A dramatic example of this kind of behavior has been observed at interfaces containing adsorbed proteins when small molecule surfactants are added to the bulk solution (Husband et al., 2001; Mackie et al., 2001, 2003). At relatively low surfactant concentrations, surfactant molecules adsorb to the interface and form small islands of surfactant located within the protein network. As the surfactant concentration is increased the size of the surfactant-rich regions expands, restricting the protein network to a smaller surface area. At relatively high surfactant concentrations, the protein region increases appreciably in thickness and eventually the protein molecules are completely displaced from the interface. The two-dimensional phase separation of the interface into a protein-rich and a surfactant-rich region can clearly be observed using various microscopy techniques (Figures 5.18 and 5.19). The structural evolution of the interfacial film depends on the type of protein that was initially present at the interface (Figure 5.19). For example, a nonionic surfactant forms fairly circular domains in  $\beta$ -casein films because there are only weak cross-links between the protein molecules and so the surfactants can easily push them aside. On the other hand, a nonionic surfactant forms irregular-shaped domains in  $\beta$ -lactoglobulin films because strong bond formation between protein molecules means that the film has to fracture before the surfactant domains can expand. Recent studies have shown that this type of two-dimensional phase separation also depends on the type of surfactant used to displace the adsorbed proteins (Gunning et al., 2004).

In addition to the structural characteristics mentioned above, there may also be appreciable changes in the conformation and interactions of emulsifier molecules after they are adsorbed to an interface, for example, surface or thermal denaturation of adsorbed globular proteins (Kim et al., 2002a,b, 2003; Norde, 2003). It is therefore important for food scientists to understand the factors that influence the structural organization of the surface-active molecules within interfacial membranes. The conformation and orientation of surface-active molecules adsorbed to an interface is governed by their attempt to reduce the free energy of the system (Evans and Wennerstrom, 1994; Cohen Stuart, 2003). Amphiphilic molecules

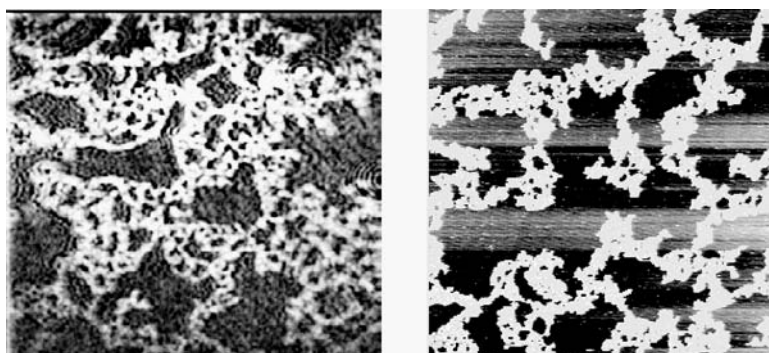


**Figure 5.18** BAM (left) and AFM (right) images of a planar interface consisting of a protein film ( $\beta$ -lactoglobulin) to which a nonionic surfactant (Tween 20) was added. The BAM image is  $300\ \mu\text{m} \times 260\ \mu\text{m}$ , while the AFM image is  $6\ \mu\text{m} \times 6\ \mu\text{m}$ . Pictures kindly supplied by Dr. Alan Mackie (Institute of Food Research, Norwich).

usually arrange themselves so that the maximum number of nonpolar groups is in contact with the oil phase, while the maximum number of polar groups is in contact with the aqueous phase, so as to reduce unfavorable hydrophobic interactions (Figure 5.16). For this reason, small molecule surfactants tend to have their polar head groups protruding into the aqueous phase, and their hydrocarbon tails protruding into the oil phase (Jonsson et al., 1998). Similarly, biopolymer molecules adsorb so that predominantly nonpolar segments are located within the oil phase, whereas predominantly polar segments are located within the water phase (Dickinson, 1992; Damodaran, 1996; Dalgleish, 1996a; Norde, 2003). For this reason, many biopolymer molecules often undergo structural rearrangements after adsorption to an interface so as to optimize the number of favorable interactions (Norde, 2003). In aqueous solution, globular proteins adopt a three-dimensional conformation in which the nonpolar amino acids are predominantly located

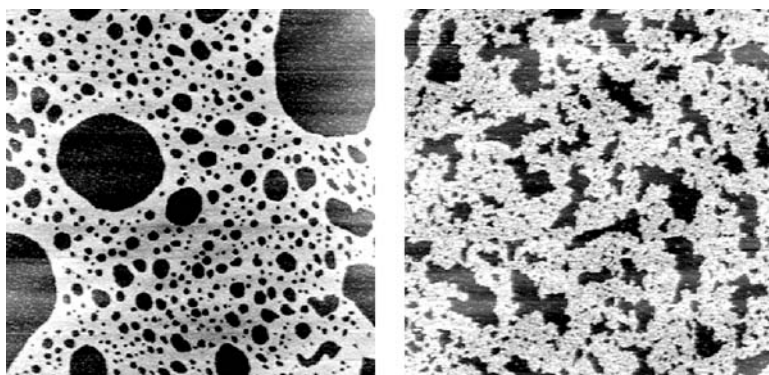


**Figure 5.19** AFM images of planar interfaces comprising of protein films (left =  $\beta$ -casein; right =  $\beta$ -lactoglobulin) to which a nonionic surfactant (Tween 20) has been added to displace the proteins. Both images are  $4\ \mu\text{m}$  across. The dark regions are surfactant and the lighter regions are protein. The surfactant forms fairly circular domains in the  $\beta$ -casein film because there are only weak interactions between the protein molecules. On the other hand, the surfactant forms irregular-shaped domains in the  $\beta$ -lactoglobulin films because there are strong interactions between the protein molecules so the film has to fracture before the domains can expand. Pictures kindly supplied by Mr. P. Gunning (Institute of Food Research, Norwich).

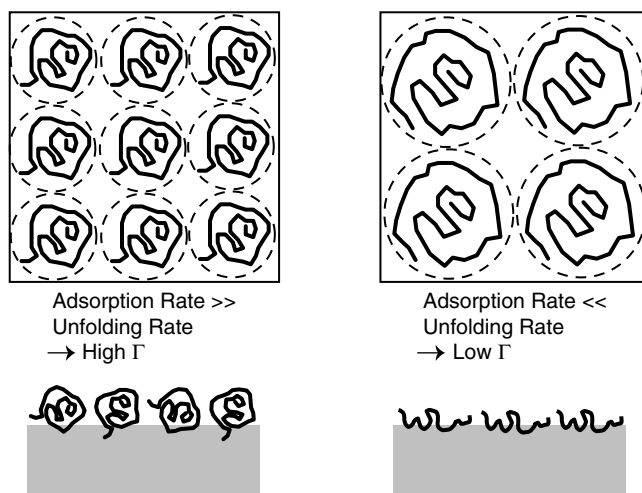


**Figure 5.20** For polymers that are able to undergo conformational changes at an interface, the surface excess concentration depends on the rate of the conformational changes compared to the adsorption rate. Relatively rapid adsorption gives less time for conformational changes and therefore leads to a more densely packed interface.

in the hydrophobic interior of the protein molecule so that they can avoid unfavorable hydrophobic interactions with the surrounding water molecules (Dill, 1990). When globular proteins adsorb to an oil–water interface they are no longer completely surrounded by water, and so the protein can reduce its free energy by altering its conformation so that more of the hydrophobic amino acids are located in the oil phase, and more of the polar amino acids are located in the water phase (Dalgleish, 1996a). The rate at which the conformation of a biopolymer changes at an oil–water interface depends on its molecular structure (Dickinson, 1992). Flexible random-coil molecules can rapidly alter their conformation, whereas rigid globular molecules change more slowly because of various kinetic constraints (Malmsten, 2003; Norde, 2003). Immediately after adsorption to an interface, a globular protein has a conformation that is similar to that in the bulk aqueous phase. With time it alters its conformation so that it can optimize the number of favorable interactions between the nonpolar amino acids and the oil molecules. An intermediate stage in this unfolding process is the exposure of some of the nonpolar amino acids to water, which is thermodynamically unfavorable because of the hydrophobic effect, and so there is an energy barrier that must be overcome before unfolding can occur (Norde, 2003). In this case, the rate of any conformational changes will depend on the height of the energy barriers compared to the thermal energy.

The conformation of biopolymer emulsifiers at an interface may also depend on when they arrive (Norde, 2003). Emulsifier molecules that arrive at the beginning of the adsorption process have a large surface area over which to spread, whereas those that arrive later have less room because of the presence of the other adsorbed emulsifier molecules. The final conformation of the biopolymer molecules may also depend on the adsorption rate compared to the rate of any conformational changes (Figure 5.20). If adsorption to the surface is faster than unfolding, then the surface excess concentration will be higher and the membrane will tend to be thicker (Cohen Stuart, 2003). On the other hand, if adsorption is slower than unfolding, then the surface excess concentration will be lower and the membrane will be thinner because significant spreading of the biopolymer molecules can occur. Finally, the

conformation of relatively flexible biopolymer emulsifiers may also depend on the strength of their attractive interactions with the interface, which can be described in terms of the *solvent quality* (Cohen Stuart, 2003). If the attraction between the monomers and the surface is extremely strong, then the biopolymer will tend to form a thicker interfacial membrane with tails and loops that extend further into the continuous phase. On the other hand, if the attraction between the monomers and surface is relatively weak, then the biopolymer will tend to form a thinner interfacial membrane with a higher proportion of trains and with loops and tails that do not extend as far into the continuous phase. This phenomenon occurs because when the attraction between the biopolymer and interface is relatively strong the monomers will tend to stick where they first encounter the interface and remain there, but when the attraction is relatively weak the biopolymer can undergo conformational changes after adsorption to maximize the number of favorable interactions with the interface.

The thickness and structural organization of biopolymer molecules within an interfacial membrane may be strongly dependent on pH, ionic strength, and temperature (Nino et al., 2003; Patino et al., 2003a,b). Electrostatic interactions involving biopolymer molecules depend on the sign, type, number, and distribution of the charged groups along the biopolymer chain. Many food biopolymers contain groups that change their degree of ionization in response to changes in pH, for example, carboxyl, amino, phosphate, sulphonate, and imidazole groups (Norde, 2003). An understanding of the influence of pH on interfacial structure depends on an appreciation of the change in the intramolecular and intermolecular electrostatic interactions involving adsorbed (and possibly nonadsorbed) molecules. At pH values where biopolymers have no net charge, the intramolecular electrostatic repulsion between similarly charged groups is usually reduced, and there may even be attraction between oppositely charged groups, and so the molecules tend to adopt a more compact interfacial structure (Sanchez et al., 2003). On the other hand, at pH values where the molecules have a high net charge there tends to be a strong electrostatic repulsion between different segments of the same biopolymer chain, which causes the molecules to adopt a more open structure. Similarly, intermolecular interactions between charged groups on different molecules also tend to favor a more dense interfacial membrane when the biopolymers have a low net charge (since there is less electrostatic repulsion between them), and a more open interfacial structure when the biopolymers have a high net charge (since there is a strong electrostatic repulsion between them). Finally, it should be noted that the thickness of the interfacial membrane may increase if the pH is adjusted to a value where adsorption of biopolymer molecules to the interface is promoted, for example, near the point of zero net charge.

Electrostatic interactions involving charged biopolymer molecules are also strongly influenced by ionic strength, and so the mineral content can have a pronounced influence of the structure of interfacial membranes. The range and magnitude of electrostatic interactions increases as the ionic strength decreases. Hence, the presence of salt will tend to decrease the thickness of interfacial membranes comprised of biopolymers with high charges by screening the electrostatic repulsion between different segments of the same molecule. On the other hand, the addition of salt may actually increase the thickness of interfacial membranes with no net charge if they contain a balance of positive and negative charges, because the salt screens the electrostatic attraction between the oppositely charged groups.

The thickness and structural organization of emulsifier molecules within an interfacial membrane may also depend on temperature, since temperature may influence solvent quality or the conformation and interactions of adsorbed molecules.

The thickness and structural organization of the emulsifier molecules within an interfacial membrane can have an important influence on the bulk physicochemical properties of food emulsions (Dalgleish, 1996a). The flocculation and coalescence stability of many protein-stabilized emulsions depends on the unfolding and interaction of the protein

molecules at the droplet surface. When globular proteins unfold they expose reactive amino acids that are capable of forming hydrophobic and disulfide bonds with their neighbors, thus generating a highly viscoelastic membrane that is resistant to coalescence (Dickinson and Matsumura, 1991; Dickinson, 1992). Conversely, if hydrophobic attraction and disulfide bond formation occurs between proteins adsorbed onto different droplets then extensive droplet flocculation can occur (McClements et al., 1993d; Kim et al., 2002a,b). The steric repulsion between emulsion droplets is strongly dependent on the thickness of the interfacial membrane (Section 3.5); hence any factor that changes the thickness of this membrane may have an important impact on the stability of droplets to aggregation.

The susceptibility of certain proteins to enzymatic hydrolysis depends on which side of the adsorbed molecule faces toward the droplet surface (Dalglish, 1996a,b). The susceptibility of surfactants with unsaturated hydrocarbon tails to lipid oxidation depends on whether their tails are orientated perpendicular or parallel to the droplet surface, the latter being more prone to oxidation by free radicals generated in the aqueous phase (Coupland and McClements, 1996).

### 5.6.2 Characterization of interfacial structure in emulsions

The impact of interfacial structure on emulsion properties means that it is important to have analytical techniques that can be used to measure interfacial thickness and the structural organization of emulsifier molecules within interfacial membranes (Dalglish, 1996). A number of the most important experimental techniques that are available to provide information about interfacial structure are listed in Table 5.2. Each of these techniques

**Table 5.2** Experimental Techniques to Characterize the Structural Properties of Interfaces.

Technique	Application
<b>Depletion Techniques</b>	
Non-adsorbed emulsifier measurement	Interfacial composition
<b>Scattering techniques</b>	
Light scattering	Thickness
Small angle x-ray scattering	Thickness, concentration profile
Neutron scattering	Thickness, concentration profile
<b>Reflection Techniques</b>	
Ellipsometry	Thickness, concentration profile
Neutron reflection	Thickness, concentration profile
<b>Techniques that Use Absorption of Electromagnetic Radiation</b>	
Infrared	Composition, conformational changes
Ultraviolet-visible	Composition, conformational changes
Fluorescence	Composition, conformational changes
Nuclear magnetic resonance	Composition, conformational changes
Circular dichroism	Secondary structure
<b>Biochemical Techniques</b>	
Enzyme hydrolysis	Orientation, conformation
Immunoassays	Orientation, conformation
<b>Microscopic Techniques</b>	
Atomic force microscopy	Interfacial topology
Electron microscopy	Interfacial structure and topology
Brewster angle microscopy	Two-dimensional organization of molecules

works on a different physical principle and is sensitive to a different aspect of the properties of an interface (Kallay et al., 1993). The majority of these techniques can only be used in fundamental studies of planar interfaces, although some of them can also be used to directly provide information about the properties of the interfaces in emulsions.

#### 5.6.2.1 Microscopy techniques

One of the most direct methods of obtaining information about the structural organization of molecules at an interface is to use microscopy (Kirby et al., 1995; Kalab et al., 1995; Smart et al., 1995). There have been rapid developments in many areas of microscopy during the past few decades that have led to the availability of a variety of powerful new analytical instruments for probing interfacial structure. Relatively large (>200 nm) changes in the structural organization of molecules at surfaces, such as the two-dimensional phase separation of protein–surfactant mixtures, can be observed by optical microscopy, for example, scanning near field optical microscopy, laser scanning confocal fluorescence, or Brewster angle microscopy (BAM) (Mackie et al., 2000; Gunning et al., 2001). Information about finer structural details can be obtained using electron microscopy or atomic force microscopy (AFM) (Mackie et al., 2001; Ying et al., 2003). AFM scans a small tip across the surface of a sample in order to construct a three-dimensional image of its surface. The major advantage of AFM is that little sample preparation is often needed, so that the structure of the interface is not adversely altered. A more detailed discussion of microscopy techniques is given in Chapter 11. The use of microscopy techniques for characterizing structural changes at interfaces is demonstrated in Figures 5.18 and 5.19, which show BAM and AFM images of the two-dimensional phase separation of protein–surfactant mixtures at a planar interface.

#### 5.6.2.2 Spectroscopy techniques

A number of spectroscopic techniques have been developed that rely on the absorption of electromagnetic radiation by the molecules at an interface, for example, infrared, UV, visible, fluorescence, and x-ray techniques (Kallay et al., 1993; Billsten et al., 2003; Hlady and Buijs, 2003). These techniques can either be used in a transmission mode, where the electromagnetic wave is propagated through the sample, or in a reflection mode, where the electromagnetic wave is reflected from the interface. In both cases, the absorption of the radiation by the wave is measured and correlated to some property of the molecules at the interface. The different techniques are sensitive to different characteristics of the molecules. Infrared and microwave techniques rely on characteristic molecular vibrations or rotations of different groups within a molecule, whereas UV–visible and fluorescence techniques rely on characteristic electronic transitions involving outer shell electrons (Penner, 1994a,b). These techniques have been used to determine the concentration of emulsifier molecules at an interface, to study adsorption kinetics, and to provide information about changes in molecular conformation (Kallay et al., 1993). When a molecule undergoes a conformational change the adsorption spectra is altered because of the change in the environment of the adsorbing groups. A number of these techniques have been adapted so that they can be used to analyze the structures of interfaces in emulsions. For example, Fourier transform infrared (FTIR) and front-face fluorescence spectroscopy (FFFS) have been used to provide information about changes in the conformation of globular proteins adsorbed to droplet surfaces in concentrated emulsions (Fang and Dalgleish, 1997, 1998; Green et al., 1999; Lefevre and Subirade, 2003; Rampon et al., 2003a–c).

Recently, a novel approach has been developed to monitor the properties of adsorbed protein emulsifiers in concentrated emulsions. In this approach, an emulsion



is made optically transparent by adding a solute to the aqueous phase so that its refractive index becomes the same as that of the oil phase (Husband et al., 2001). Because the resulting "refractive index matched emulsion" (RIME) is optically transparent it can be analyzed using standard spectroscopy techniques, such as fluorescence, FTIR, circular dichroism, or UV-visible spectrometry. It is therefore possible to use this approach to provide information about interfacial structure in concentrated emulsions. Nevertheless, there are concerns about the influence of the solutes added to the emulsions to increase the refractive index of the aqueous phase (e.g., glycerol, polyethylene glycol, or sucrose) on the structural properties of the proteins, since many solutes change protein conformation and aggregation at the high concentrations needed to create RIMES.

#### 5.6.2.3 Interference reflection techniques

A number of techniques have been developed that rely on the interference pattern produced by the reflection of a beam of light or subatomic particles from a thin interface (Malmsten, 2003; Lu, 2003; Ying et al., 2003). Ellipsometry relies on the reflection of a polarized light beam from a highly reflective planar surface (Azzam and Bashara, 1989; Malmsten et al., 1995; Malmsten, 2003). Initially, the phase and amplitude of the light beam reflected from the clean surface are measured. Emulsifier is then allowed to adsorb to the surface and the experiment is repeated. A mathematical analysis of the reflected wave provides information about the thickness and refractive index profile of the adsorbed layer. The refractive index profile can then be converted to a concentration profile. Recently, imaging ellipsometry techniques have been developed that enable one to scan the beam of light across a surface so that a two-dimensional image of the thickness and optical properties of an interface can be obtained (Ying et al., 2003). Information about interfacial composition can often be inferred from the optical properties.

BAM is another optical interference reflectance technique that has been used to provide information about the structural organization of surface-active molecules at planar interfaces. This technique has been used primarily to observe the two-dimensional organization of emulsifiers at planar surfaces and interfaces (Mackie et al., 2001; Patino et al., 2003a,b; Sanchez et al., 2003). This technique is based on the fact that there is no reflection of polarized light from a clean surface when the angle of incidence of the light is set at (or below) the Brewster angle. However, light is reflected when a relatively thin emulsifier layer (~2 nm) is present at the surface, providing that the refractive index of the layer is significantly different from the refractive index of the liquid below it. The reflected light can be used to form an image of the two-dimensional morphology of the layer (Figure 5.18). The BAM technique has recently been used to provide valuable information about the changes in interfacial structure that occur when small molecule surfactants displace proteins from surfaces or interfaces (Mackie et al., 2001). The two-dimensional phase separation of the interface into a protein-rich and a surfactant-rich region can clearly be observed using BAM (Figure 5.18).

Neutron reflection techniques work on a similar principle to optical reflection techniques, but they use a beam of neutrons, rather than a beam of light, to probe the interface (Dickinson et al., 1993a,b; Atkinson et al., 1995; Dickinson and McClements, 1995; Lu, 2003). The beam of neutrons is directed at an air-water or oil-water interface at an angle. The beam of neutrons reflected from the surface is analyzed and provides information about the thickness of the interface and the neutron refractive index profile, which can be related to the emulsifier concentration profile across the interface. These techniques have been widely used to study the characteristics of protein layers and the influence of pH and ionic strength on their properties.

#### 5.6.2.4 Scattering techniques

A number of analytical instruments based on scattering of radiation or subatomic particles are suitable for providing information about the structural organization of molecules adsorbed to interfaces, for example, optical, x-ray, or neutron scattering techniques. Analytical techniques based on the scattering of radiation or subatomic particles are most commonly used to provide information about interfacial thickness. They can therefore be used to compare the thickness of interfaces formed by different emulsifiers, or to study changes in interfacial thickness in response to alterations in environmental conditions, such as pH, ionic strength, or temperature. The application of these techniques has provided valuable insights into the structures formed by proteins at oil–water and air–water interfaces, which is useful for predicting the stability of emulsion droplets to flocculation or coalescence (Dalglish, 1996). An example of this approach is the use of light scattering (or some other particle sizing technique) to indirectly determine the thickness of the emulsifier layer surrounding colloidal particles. It is usually advantageous to use colloidal particles that are fairly monodisperse and that are stable to aggregation in the absence of emulsifier. The particle radius is then measured before and after addition of the emulsifier, and the difference in radius is taken to be equal to the thickness of the interfacial membrane.

#### 5.6.2.5 Langmuir trough measurements

Useful information about the structural organization of molecules at gas–liquid and liquid–liquid interfaces can be obtained using a Langmuir trough apparatus (Norde, 2003). A Langmuir trough consists of a container that holds the liquid(s) to be analyzed, a movable barrier that is capable of changing the area of the liquid–air interface, and a device for measuring the surface tension at the liquid–air interface, usually a Wilhelmy plate (Figure 5.21). The surface-active solute to be analyzed is either dissolved in the liquid or spread across the surface of the liquid depending on its solubility (Norde, 2003). The interfacial area is then decreased in a controlled fashion using a motor to drive the movable barrier, and the surface pressure ( $\pi$ ) is measured as a function of interfacial area ( $A$ ). The resulting  $\pi$ – $A$  plot depends on the interfacial characteristics of the individual solute molecules, as well as on the sign, magnitude, and range of solute–solute interactions

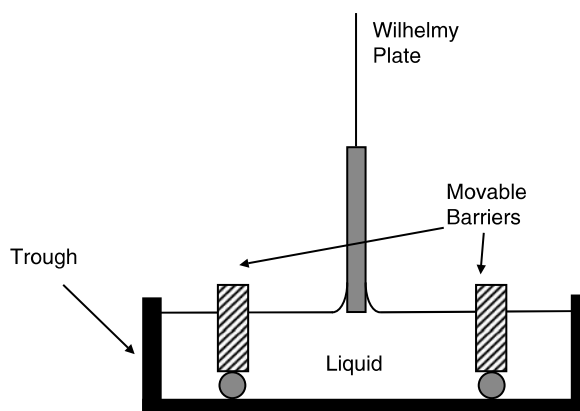


**Figure 5.21** Schematic diagram of Langmuir trough apparatus used to measure packing of solutes at interfaces, and interfacial dilational rheology, by measuring changes in surface pressure as a function of interfacial area.

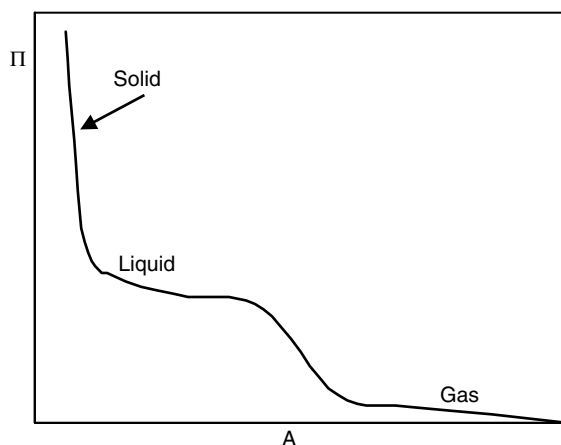


**Figure 5.22** Schematic representation of the change in surface pressure with interfacial area when the area is compressed. The  $\pi$ - $A$  profile can often be divided into a gas, liquid, and solid regime depending on the strength of the solute-solute interactions.

at the interface. A highly schematic  $\pi$ - $A$  plot is shown in Figure 5.22 for a model surface-active solute. It is convenient to divide the  $\pi$ - $A$  plot into different regimes depending on the strength of the solute-solute interactions. At high interfacial areas, the solute molecules are far apart and do not interact with each other, and therefore the surface pressure is mainly determined by the interfacial characteristics of the individual molecules. By analogy to three-dimensional systems this regime is usually called the "gas" phase because each solute molecule acts independently of its neighbors. As the interfacial area decreases, the interfacial concentration of the solute molecules increases, and solute-solute interactions begin to occur, which leads to an increase in the surface pressure. Even so, the solute molecules are still sufficiently far apart to be able to move freely past each other and so this regime is referred to as the "liquid" phase. When the interfacial area is decreased further the solute molecules become so closely packed together that there is a strong repulsive force between them, which leads to a steep increase in the surface pressure. This regime is usually referred to as the "solid" phase because the solute molecules are densely packed and have low mobility. The interfacial area where the surface pressure increases dramatically can provide valuable information about the packing of the surface-active molecules within the interfacial membrane at saturation, for example, the area per solute molecule. In practice,  $\pi$ - $A$  plots are often more complex than that shown in Figure 5.22 because of changes in the orientation of solute molecules or because of phase separation processes. The Langmuir trough can also be used in combination with various microscopy, reflection, and scattering techniques to provide information about changes in the structural organization of solute molecules as the interfacial area is changed, for example, BAM, fluorescence microscopy, neutron reflection, or x-ray scattering.

#### 5.6.2.6 Surface force measurements

The thickness of a layer of emulsifier molecules adsorbed to an interface can be determined by measuring the forces between two interfaces as they are brought into close contact (Claesson et al., 1995, 1996, 2004). There is usually a steep rise in the repulsive forces at close separations between the interfaces because of steric repulsion. The distance at which this rise is observed can be assumed to be the outer edge of the emulsifier layer.

By compressing the interfacial layer further some information about the packing of the adsorbed molecules can be obtained.

#### 5.6.2.7 Calorimetry techniques

Information about the conformation of proteins adsorbed to the surfaces of emulsion droplets has also been obtained using sensitive differential scanning calorimetry (DSC) techniques (Corredig and Dalgleish, 1995; Dalgleish, 1996; Fromell et al., 2003). The emulsion being analyzed is heated at a controlled rate and the amount of heat absorbed by the proteins when they undergo conformational changes is recorded by the DSC instrument. The temperature at which the conformation change occurs ( $T_{\text{transition}}$ ) and the amount of heat adsorbed by the protein during the transition ( $\Delta H_{\text{transition}}$ ) are determined. The values for the adsorbed protein are then compared with those for a solution containing a similar concentration of unadsorbed proteins. Experiments with oil-in-water emulsions containing adsorbed globular proteins, such as  $\alpha$ -lactalbumin, lysozyme, and  $\beta$ -lactoglobulin, have shown that there is a decrease in  $\Delta H_{\text{transition}}$  after adsorption, which suggests that they have undergone some degree of surface denaturation (Corredig and Dalgleish, 1995). After the proteins had been desorbed from the droplet surfaces it was observed that the denaturation of  $\beta$ -lactoglobulin was irreversible, but that of  $\alpha$ -lactalbumin and lysozyme was at least partially reversible. Flexible biopolymers that have little structure, such as casein, cannot be studied using this technique because they do not undergo any structural transitions that adsorb or release significant amounts of heat. It should be noted that the data from DSC experiments must be interpreted carefully because a reduction in  $\Delta H_{\text{transition}}$  may be because the protein has no secondary or tertiary structure or because the structure is so stable that it does not unfold at the same temperature as in water. In addition, the adsorption of a protein at an interface may also reduce  $\Delta H_{\text{transition}}$  because its thermodynamic environment has altered: in solution it is completely surrounded by water, but at an interface part of the molecule is in contact with a hydrophobic surface. Despite these limitations the DSC technique is a powerful tool for studying structural changes caused by adsorption, especially when used in conjunction with other techniques.

#### 5.6.2.8 Biochemical techniques

A number of biochemical techniques have also been developed to provide information about the structure and organization of biopolymer molecules at the surface of emulsion droplets (Dalgleish, 1996). The susceptibility of proteins to hydrolysis by specific enzymes can be used to identify the location of particular peptide bonds. When a protein is dissolved in an aqueous solution, the whole of its surface is usually accessible to enzyme hydrolysis, but when it is adsorbed to an interface it adopts a conformation where some of the amino acids are located close to the oil phase (and are therefore inaccessible to proteolysis), whereas others are exposed to the aqueous phase (and are therefore accessible to proteolysis). By comparing the bonds that are susceptible to enzyme hydrolysis and the rate at which hydrolysis occurs of the adsorbed and nonadsorbed proteins it is possible to obtain some idea about the orientation and conformation of the adsorbed proteins at the interface. This technique is more suitable for the study of flexible random-coil proteins, than for globular proteins, because the latter have compact structures which are not particularly accessible to enzyme hydrolysis in either the adsorbed or nonadsorbed states. Immunologic techniques can also be used to provide similar information. These techniques use the binding of antibodies to specific sites on a protein to provide information about its orientation at an interface or about any conformational changes that take place after adsorption.

## 5.7 Interfacial tension and its measurement

### 5.7.1 Factors influencing interfacial tension

Interfacial tension is a measure of the free energy required to increase the area of an interface by a unit amount, and is usually specified in units of  $\text{J m}^{-2}$  (or  $\text{N m}^{-1}$ ). The origin of the interfacial tension is the imbalance of molecular interactions between molecules located at the interface (Section 5.2). When a surface-active solute is present the interfacial tension is reduced because the solute can help minimize the thermodynamically unfavorable contacts between the different kinds of molecules at the interface. From a practical standpoint, the interfacial tension is important because it influences the droplet size produced by homogenization (Section 6.4.1), the stability of droplets to coalescence and Ostwald ripening (Sections 7.6 and 7.8), and the packing of large droplets in concentrated emulsions, such as mayonnaise and dressings (Section 12.4). In addition, the measurement of interfacial tension can provide valuable information about emulsifier and interfacial characteristics, such as surface excess concentration, surface activity, critical micelle concentration, adsorption rates, and interfacial rheology. Finally, the interfacial tension also influences many of the macroscopic properties of food materials, such as capillary rise, spreading, and wetting (Section 5.9).

### 5.7.2 Characterization of interfacial tension

The purpose of this section is to give an overview of some of the most important analytical instruments that have been developed to measure interfacial and surface tensions. By definition, surface tension is measured at a gas–fluid interface (e.g., air–water or air–oil), while interfacial tension is measured at a fluid–fluid interface (e.g., oil–water). These quantities are measured using analytical instruments called surface or interfacial tensiometers, respectively (Couper, 1993). A wide variety of different types of tensionmeters are available for providing information about the properties of surfaces and interfaces (Table 5.3). These instruments differ according to the physical principles on which they operate, their mechanical design, whether measurements are static or dynamic, and whether they are capable of measuring surface tension, interfacial tension, or both. “Static” measurements are carried out on surfaces or interfaces that are considered to be at

**Table 5.3** Summary of the Instruments used for Measuring Surface and Interfacial Tensions.

Surface Tension	Interfacial Tension
<b>Equilibrium</b>	
Du Nouy Ring	Du Nouy ring
Wilhelmy plate	Wilhelmy plate
Pendant drop	Pendant drop
Sessile drop	Sessile drop
Spinning drop	Spinning drop
Capillary rise	
<b>Dynamic</b>	
Maximum bubble pressure	Drop-volume
Oscillating jet	Pendant drop
Drop-volume	Spinning drop
Surface waves	

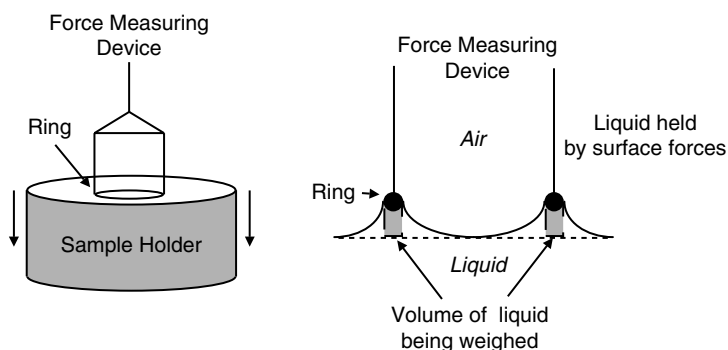


**Figure 5.23** Du Nouy ring method of determining the interfacial and surface tension of liquids. The force on the ring is measured as the vessel holding the liquid is lowered.

equilibrium, whereas "dynamic" measurements are carried out on surfaces or interfaces that are not at equilibrium.

#### 5.7.2.1 Du Nouy ring method

The Du Nouy ring method is commonly used to measure static surface and interfacial tensions of liquids (Couper, 1993; Hiemenz and Rajagopalan, 1997). The apparatus required to carry out this type of measurement consists of a vessel containing the liquid(s) to be analyzed and a ring that is attached to a sensitive force measuring device (Figure 5.23). The vessel is capable of being moved upward and downward in a controlled manner, while the position of the ring is kept constant. Initially, the vessel is positioned so that the ring is submerged just below the surface of the liquid being analyzed. It is then slowly lowered and the force exerted on the ring is recorded. As the surface of the liquid moves downward some of the liquid "clings" to the ring because of its surface tension (Figure 5.23). The weight of the liquid that clings to the ring is recorded by the force measuring device, and is related to the force that results from the surface tension.

The Du Nouy ring method is often used in a "detachment" mode. The vessel is lowered until the liquid clinging to the ring ruptures and the ring becomes detached from the liquid. The force exerted on the ring at detachment is approximately equal to the surface tension multiplied by the length of the ring perimeter:  $F = 4\pi R\gamma$ , where  $R$  is the radius of the ring. In practice, this force has to be corrected because the surface tension does not completely act in the vertical direction and because some of the liquid remains clinging to the ring after it has become detached.

$$F = 4\pi R\gamma\beta \quad (15.13)$$

where  $\beta$  is a correction factor that depends on the dimensions of the ring and the density of the liquid(s) involved. Values of  $\beta$  have been tabulated in the literature or can be calculated using semiempirical equations (Couper, 1993). One of the major problems associated with the Du Nouy ring method, as well as any other detachment method, is that serious errors may occur when it is used for measuring the surface tension of emulsifier solutions, rather than pure liquids. When a ring detaches from a liquid it leaves behind some fresh surface that is initially devoid of emulsifier. The measured surface tension therefore depends on the speed at which the emulsifier molecules move from the bulk liquid to the fresh surface during the detachment process. If an emulsifier adsorbs

rapidly compared to the detachment process, the surface tension measured by the detachment method will be the same as the equilibrium value, but if the emulsifier adsorbs relatively slowly the surface tension will be greater than the equilibrium value because the surface has a lower emulsifier concentration than expected.

The Du Nouy ring method can also be used to determine the interfacial tension between two liquids (Couper, 1993). In this case the ring is initially placed below the surface of the most dense liquid (usually water), and then the less dense liquid is poured on top (usually oil). The force acting on the ring is then measured as it is pulled up through the interface and into the oil phase. A similar equation can be used to determine the interfacial tension from the force exerted on the ring, but one has to take into account the densities of the oil and water phases and use a different correction factor. For two liquids that are partially immiscible with each other the interfacial tension may take an appreciable time to reach equilibrium because of the diffusion of water molecules into the oil phase and vice versa (Hunter, 1993).

The Du Nouy ring method can also be used to determine surface or interfacial tensions by continuously monitoring the force acting on the ring as the vessel containing the liquid is slowly lowered, rather than just measuring the detachment force. As the liquid is lowered the force initially increases, but at a certain position it reaches a maximum (when the surface tension acts vertically), before decreasing slightly prior to detachment. In this case the maximum force, rather than the detachment force, is used in the equations to calculate the surface or interfacial tension (Couper, 1993). This method has the advantage that it does not involve the rupture of the liquid, and therefore there are less problems associated with the kinetics of emulsifier adsorption during the detachment process.

For accurate measurements it is important that the bottom edge of the ring is kept parallel to the surface of the fluid, and that the contact angle between the liquid and the ring is close to zero. Rings are usually manufactured from platinum or platinum-iridium because these give contact angles that are approximately equal to zero. The Du Nouy ring method can be used to determine surface tensions to an accuracy of about  $0.1 \text{ mN m}^{-1}$  (Couper, 1993).

#### 5.7.2.2 *Wilhelmy plate method*

The Wilhelmy plate method is normally used to determine the static surface or interfacial tensions of liquids (Couper, 1993; Hiemenz and Rajagopalan, 1997). Nevertheless, it can also be used to monitor adsorption kinetics provided that the accumulation of the emulsifier at the surface is slow compared to the measurement time, for example, for dilute protein solutions (Dickinson, 1992). The apparatus consists of a vessel that contains the liquid to be analyzed and a plate, which is attached to a sensitive force measuring device (Figure 5.24). The vessel is capable of being moved upward and downward, while the plate remains stationary. The vessel is positioned so that the liquid just comes into contact with the plate, that is, the bottom of the plate is parallel to the surface of the bulk liquid. Some of the liquid "climbs" up the edges of the plate because this reduces the thermodynamically unfavorable contact area between the plate and the air. The amount of liquid that moves up the plate depends on its surface tension and density. If the force measuring device is zeroed prior to bringing the plate into contact with the liquid (to take into account the mass of the plate), then the force recorded by the device is equal to the weight of liquid clinging to the plate. This weight is balanced by the vertical component of the surface tension multiplied by the length of the plate perimeter:

$$F = 2(l + L) \gamma \cos \theta \quad (5.14)$$

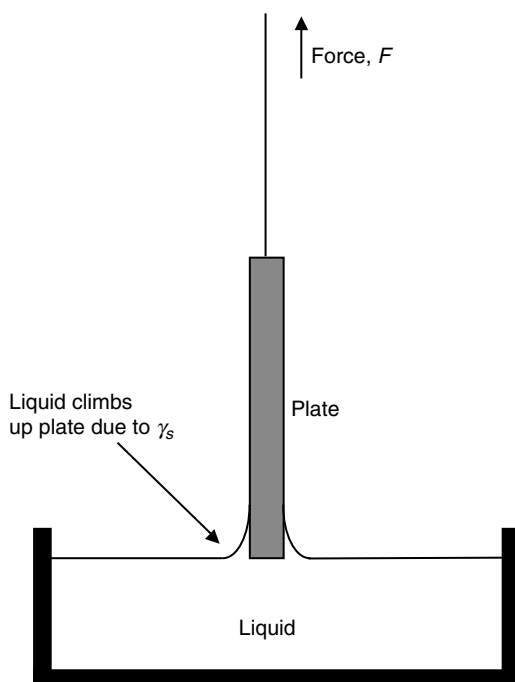


**Figure 5.24** Wilhelmy plate method of determining the interfacial and surface tension of liquids. The force on the plate is measured as the vessel holding the liquid is lowered.

where  $l$  and  $L$  are the length and thickness of the plate and  $\theta$  is the contact angle. Thus, the surface tension of a liquid can be determined by measuring the force exerted on the plate. Plates are often constructed of materials that give a contact angle close to zero, such as platinum or platinum/iridium, as this facilitates the analysis ( $\cos \theta = 1$ ). The Wilhelmy plate can also be used to determine the interfacial tension between two liquids (Hiemenz and Rajagopalan, 1997). In this case, the plate is positioned so that its bottom edge is parallel to the interface between the two bulk liquids, and the force measuring device is zeroed when the plate is located in the less dense liquid (usually oil). A major advantage of the Wilhelmy plate method over the Du Nouy ring method is that it does not rely on the disruption of the liquid surface, and therefore is less prone to errors associated with the adsorption kinetics of emulsifiers (see earlier).

The Wilhelmy plate method is widely used to study the adsorption kinetics of proteins (Dickinson, 1992). It can be used for this purpose because their adsorption rate is much slower than the time required to carry out a surface tension measurement. The plate is positioned at the surface of the liquid at the beginning of the experiment, and then the force required to keep it at this position is recorded as a function of time. The Wilhelmy plate method is usually unsuitable for studying the adsorption kinetics of small molecule surfactants because they adsorb too rapidly to be followed using this technique. For accurate measurements it is important that the bottom of the plate is kept parallel to the liquid surface, and that the contact angle is either known or close to zero. Accuracies of about  $0.05 \text{ mN m}^{-1}$  have been reported using this technique (Couper, 1993).

### 5.7.2.3 Sessile and pendant drop methods

The sessile and pendant drop methods can be used to determine the static surface and interfacial tensions of liquids (Hunter, 1986; Couper, 1993). The shape of a liquid droplet



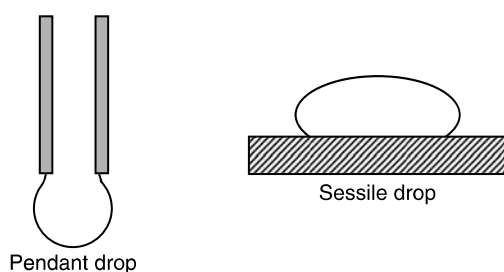


**Figure 5.25** Sessile drop and pendant drop methods of determining the interfacial and surface tension of liquids. The shape of the drops is recorded and analyzed mathematically.

depends on a balance between the gravitational and surface forces. Surface forces favor a spherical droplet because this shape minimizes the contact area between the liquid and its surroundings. On the other hand, gravitational forces tend to cause droplets to become flattened (if they are resting on a solid surface) or elongated (if they are hanging on a solid surface or from a capillary tip). A flattened drop is usually referred to as a "sessile" drop, whereas a hanging one is referred to as a "pendant" drop (Figure 5.25). The equilibrium shape that is adopted by a droplet is determined by its volume, density, and surface or interfacial tension.

The surface or interfacial tension is determined by measuring the shape of a drop using an optical microscope, often in conjunction with an image analysis program, and mathematical equations that describe the equilibrium shape (Couper, 1993). This technique can be used to determine surface or interfacial tensions as low as  $10^{-4} \text{ mN m}^{-1}$ , and can also be used to simultaneously determine the contact angle. The accuracy of this technique has been reported to be about 0.01% (Couper, 1993). Recently, powerful analytical instruments based on this principle have been developed that combine interfacial tension measurements with interfacial rheology measurements (see Section 5.8.2).

#### 5.7.2.4 Drop-volume method

The drop-volume method is used to measure surface and interfacial tensions of liquids by a detachment method. The liquid to be analyzed is pumped through the tip of a vertical capillary tube whose tip protrudes into air or an immiscible liquid (Figure 5.26). A droplet detaches itself from the tip of the capillary tube when the separation force (due to gravity) is balanced by the adhesion force (due to surface or interfacial tension). To measure surface tension the tip should point downward into air, whereas to measure interfacial tension the tip may point either upward or downward depending on the relative densities of the two liquids being analyzed. If the liquid in the tip has a higher density than the surrounding medium, the opening of the tip faces down and the drop moves downward once it becomes detached. On the other hand, if the liquid in the tip has a lower density, then the tip faces up and the drop moves upward when it becomes detached.

The surface or interfacial tension can be related to the volume of the detached droplet by analyzing the forces that act on it just prior to detachment (Couper, 1993):

$$\gamma = \frac{V_{\text{DROP}} \Delta \rho g}{\pi d} \quad (5.18)$$

where  $d$  is the diameter of the tip,  $\Delta \rho$  is the density difference between the liquid being analyzed and the surrounding liquid,  $V_{\text{DROP}}$  is the volume of the droplet, and  $g$  is the

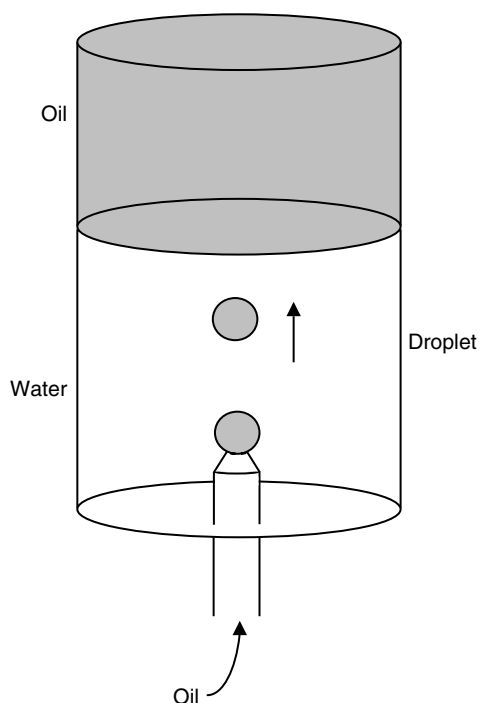


**Figure 5.26** Drop-volume method of determining the interfacial and surface tension of liquids.

gravitational constant. The volume of the droplets can be determined using a graduated syringe or by weighing them using a sensitive balance (once the liquid density is known).

As with other detachment methods, the surface area of the droplet expands rapidly during the detachment process, and therefore the method is unsuitable for analyzing liquids that contain emulsifiers whose adsorption time is comparable to the detachment time. To obtain reliable results it is normal practice to bring the droplet slowly to the detachment process. The accuracy of this technique has been reported to be better than  $0.1 \text{ mN m}^{-1}$  (Couper, 1993).

#### 5.7.2.5 Spinning drop method

The spinning drop method is used to measure static interfacial tensions of liquids (Couper, 1993). It was designed to characterize liquids that have particularly low interfacial tensions, that is, between  $10^{-6}$  and  $5 \text{ mN m}^{-1}$ . Most food emulsions have interfacial tensions that are above this range, and so this technique is not widely used in the food industry for studying oil–water interfaces, though it is being used to study the very low interfacial tensions between phase separated biopolymer solutions (Scholten et al., 2002). This technique may also be useful for some fundamental studies and therefore its operating principles are briefly outlined below.

A drop of oil (or water) is injected into a glass capillary tube that is filled with a more dense liquid (usually water). When the tube is made to spin at a particular angular frequency,  $\omega$  the droplet becomes elongated along its axis of rotation so as to reduce its rotational kinetic energy (Figure 5.27). The elongation of the droplet causes an increase in its surface area, and is therefore opposed by the interfacial tension. Consequently, the equilibrium shape of the droplet at a particular angular frequency depends on the

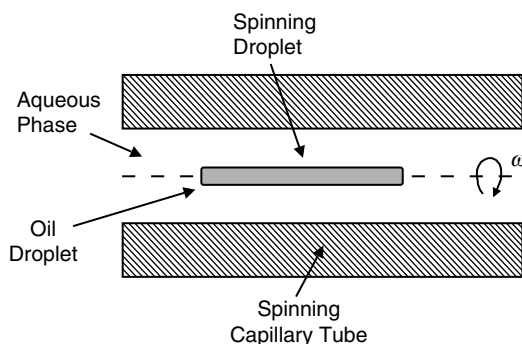


Figure 5.27 Spinning drop method of determining the interfacial tension of liquids.

interfacial tension. The shape of the elongated droplet is measured using optical microscopy, and the interfacial tension is then calculated using the following equation:

$$\gamma = kr^3\omega^2\Delta\rho \quad (5.19)$$

where  $k$  is an instrument constant that can be determined using liquids of known interfacial tension,  $r$  is the radius of the elongated droplet, and  $\Delta\rho$  is the difference in density between the oil (or water) and the surrounding liquid. This equation is applicable when the droplet becomes so elongated that it adopts an almost cylindrical shape. More sophisticated equations are needed when the shape of the droplet does not change so dramatically (Couper, 1993).

#### 5.7.2.6 Maximum bubble pressure method

The maximum bubble pressure method is used to measure the static or dynamic surface tensions of liquids (Couper, 1993). The apparatus required to carry out this type of measurement consists of a vertical capillary tube whose tip is immersed below the surface of the liquid being analyzed (Figure 5.28). Gas is pumped into the tube which causes an

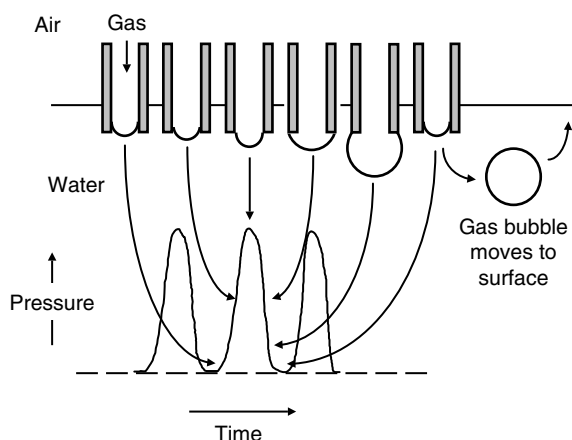


Figure 5.28 Maximum bubble pressure method of determining the surface tension of liquids.

increase in the pressure and results in the formation of a bubble at the end of the tip. The build-up of pressure in the tube is monitored using a pressure sensor inside the instrument. As the bubble grows the pressure increases until it reaches a maximum when the bubble becomes hemispherical and the surface tension acts in a completely vertical direction. Any further bubble growth beyond this point causes a decrease in the pressure. Eventually, the bubble formed breaks away from the tip and moves to the surface of the liquid, then another bubble begins to form and the whole process is repeated. The maximum bubble pressure can be related to the surface tension using suitable mathematical equations (Couper, 1993).

The maximum bubble pressure method can be used to measure the static surface tension of pure liquids at any bubble frequency. It can also be used to monitor the dynamic surface tension of emulsifier solutions by varying the bubble frequency. The age of the gas-liquid interface is approximately half the time interval between detachment of successive bubbles, and can be varied by changing the flow rate of the gas. It is therefore possible to monitor adsorption kinetics of emulsifiers by monitoring the surface tension as a function of bubble frequency. The dynamic surface tension decreases as the bubble frequency increases because there is less time for the emulsifier molecules to move to the surface of the droplets. The variation in the dynamic surface tension with bubble frequency therefore gives an indication of the speed at which emulsifier molecules are adsorbed to the surface. This information is important to food manufacturers because the adsorption rate of emulsifiers determines the size of the droplets produced during homogenization: the faster the rate, the smaller the droplet size (Chapter 6). Nevertheless, it should be pointed out that the maximum bubble pressure method can only be used to measure dynamic surface tensions down to about 50 ms, whereas many surfactants have faster adsorption rates than this. More rapid techniques are therefore needed to study these systems, such as the oscillating jet, capillary wave, and punctured membrane methods described elsewhere (Couper, 1993; Stang et al., 1994).

One of the major advantages of the maximum bubble method is that it can be used to analyze optically opaque liquids because it is not necessary to visually observe the bubbles. In addition, it is not necessary to know the contact angle of the liquid because the maximum pressure occurs when the surface tension acts in a completely vertical direction.

## 5.8 Interfacial rheology

### 5.8.1 Factors influencing interfacial rheology

The rheological properties of the interfacial membrane influence the formation, stability, and texture of many food emulsions and therefore it is important to establish the factors that influence interfacial rheology (Bos and van Vliet, 2001). Interfacial rheology has been defined as the "study of the mechanical and flow properties of adsorbed layers at fluid interfaces" (Murray and Dickinson, 1996). When an emulsion is subjected to mechanical agitation, the surfaces of the droplets experience a number of different types of deformations as a result of the stresses acting on them (Walstra, 2003a). Stresses may cause different regions of the interface to move past each other, without altering the overall surface area, which is known as *interfacial shear deformation*. Alternatively, they may cause the surface area to expand or contract (like a balloon when it is inflated or deflated), which is known as *interfacial dilational deformation*. An interface may have solid-like characteristics that are described by an *interfacial elastic constant* or fluid-like characteristics that are described by an *interfacial viscosity*. In practice, most interfaces have partly "solid-like" and partly "fluid-like" characteristics and therefore exhibit viscoelastic behavior.

**Table 5.4** Rheological Characteristics of Interfaces.

	Viscosity	Elasticity
Shear deformation	$\tau_i = \eta_i \dot{\sigma}_i$	$\tau_i = G_i \sigma_i$
Dilatational deformation	$d\gamma_i = \varepsilon_i \frac{dA}{A}$	$d\gamma_i = \kappa_i A \frac{d\gamma}{dA}$

It is convenient to assume that an interface is infinitesimally thin so that it can be treated as a two-dimensional plane, because its rheological characteristics can then be described using the two-dimensional analogs of the relationships used to characterize bulk materials (Chapter 8). A number of the most important rheological characteristics of interfaces are summarized in Table 5.4, where  $\tau_i$  is the interfacial shear stress,  $\sigma_i$  is the interfacial shear strain,  $\eta_i$  is the interfacial shear viscosity,  $G_i$  is the interfacial shear modulus,  $\varepsilon_i$  is the interfacial dilatational elasticity,  $\kappa_i$  is the interfacial dilatational viscosity,  $A$  is the surface area, and  $\gamma$  is the surface or interfacial tension. In general,  $G_i (= G_i' + iG_i'')$  and  $\varepsilon_i (= \varepsilon_i' + i\varepsilon_i'')$  are frequency-dependent complex numbers, whose real part is related to the storage modulus and whose imaginary part is related to the loss modulus. For a predominantly elastic material  $G_i'/G_i''$  or  $\varepsilon_i'/\varepsilon_i'' > 1$ , whereas for a predominantly fluid material  $G_i'/G_i''$  or  $\varepsilon_i'/\varepsilon_i'' < 1$ . The frequency dependence of the shear and elastic modulus depend on the time taken for any molecular rearrangements to occur in the interface relative to the time that the deforming stress is applied.

Generally, those emulsifiers that tend to undergo extensive intermingling or cross-linking at an interface will tend to form a membrane that has a high interfacial viscosity or elastic modulus, such as globular proteins and some polysaccharides. On the other hand, emulsifiers that do not strongly intermingle or cross-link will tend to form interfacial membranes with relatively low viscosities or elastic modulus, for example, small molecule surfactants and casein. The interfacial rheology is therefore strongly governed by factors that alter the nature and strength of the interactions between the molecules adsorbed to the interface, for example, emulsifier concentration, temperature, pH, and ionic strength. For example, the interfacial rheology of globular proteins tends to increase over time due to conformational changes that lead to interfacial aggregation.

## 5.8.2 Characterization of interfacial rheology

### 5.8.2.1 Measurement of interfacial shear rheology

A variety of experimental methods have been developed to measure the shear rheology of surfaces and interfaces (Murray and Dickinson, 1996). One of the most commonly used methods is analogous to the concentric cylinder technique used to measure the shear properties of bulk materials (Chapter 8). The sample to be analyzed is placed in a temperature-controlled vessel, and a thin disk is placed in the plane of the interface that separates the two phases, for example, water-and-air or oil-and-water (Figure 5.29). The vessel is then rotated and the torque on the disk is measured. The sample can be analyzed in a number of different ways depending on whether it is solid-like, liquid-like, or viscoelastic. For liquid-like interfaces, the shear viscosity is determined by measuring the torque on the disk as the vessel is rotated continuously. For solid-like interfaces, the shear modulus is determined by measuring the torque on the disk after the vessel has been moved to a fixed angle. For viscoelastic interfaces, the complex shear modulus is usually determined by measuring the torque continuously as the vessel is made to oscillate backward and forward at a certain frequency and angle.

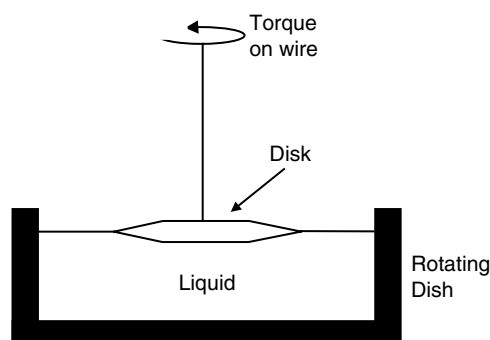
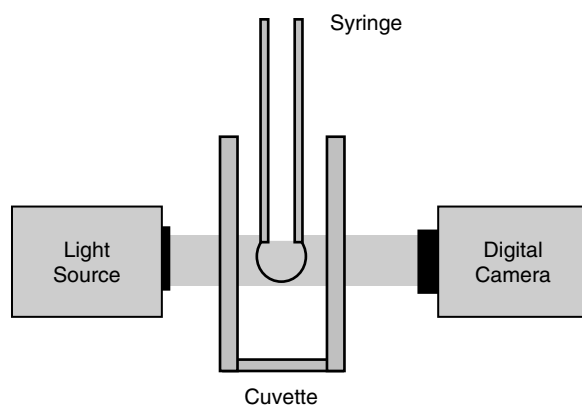


Figure 5.29 Experimental technique for measuring interfacial shear rheology.

The interfacial shear viscosity or elasticity of surfactant membranes is usually several orders of magnitude less than that of biopolymer membranes because biopolymer molecules often become entangled or interact with each other through various covalent or physical forces. The rheology of emulsions depends on the concentration, size, and interactions of the droplets that they contain. Similarly, the rheology of interfaces depends on the concentration, size, and interactions of the adsorbed emulsifier molecules that they contain. Interfacial shear rheology measurements are particularly useful for providing information about adsorption kinetics, competitive adsorption, and the structure and interactions of molecules at an interface, especially when they are used in conjunction with experimental techniques that provide information about the concentration of the emulsifier molecules at the interface, for example, interfacial tension or radioactive labeling techniques. The concentration of emulsifier molecules at an interface often reaches a constant value after a particular time, while the shear modulus or viscosity continues to increase because of interactions between the adsorbed molecules (Dickinson, 1992; Norde, 2003).

#### 5.8.2.2 Measurement of interfacial dilational rheology

One of the most convenient methods of characterizing both the interfacial tension and the interfacial dilational rheology of liquid–gas and liquid–liquid interfaces is to use the oscillating drop method (Benjamins et al., 1996; Benjamin and Lucassen-Reynders, 1998). Sophisticated analytical instruments based on this principal have recently become commercially available and are being widely used to provide valuable insights into the factors that influence interfacial rheology. One of the fluids is placed into a syringe that is attached to a capillary tube, while the other fluid is poured into a temperature-controlled cuvette (Figure 5.30). A light source and digital camera are used to record the shape of the droplet formed at the tip of the capillary tube when it is dipped into the cuvette. The interfacial tension is determined by analyzing the shape of the drop using a suitable mathematical model (Figure 5.30). The interfacial dilational rheology is determined by measuring the change in interfacial tension ( $\gamma$ ) and interfacial area ( $A$ ) of the droplet when its volume is increased or decreased in a controlled manner by applying a pressure to the liquid in the capillary tube via a piston:  $\varepsilon = d\gamma/d \ln A$ . The change in droplet volume can be carried out in a step-wise fashion or periodically (usually sinusoidally). If a sinusoidal wave is used, then the complex viscoelastic modulus of the interfacial membrane can be determined at a particular frequency:  $\varepsilon^* = \varepsilon' + i\varepsilon''$  where  $\varepsilon'$  is the storage modulus and  $\varepsilon''$  is the loss modulus. The frequency of the sinusoidal wave applied to the fluid in the capillary tube can be varied, which can provide useful information about the timescale of molecular rearrangements occurring at the interface. This type of instrument can be used to monitor



**Figure 5.30** Oscillating drop technique for measuring the tension and dilational rheology of surfaces and interfaces.

changes in interfacial rheology with solution composition, time, or temperature. The oscillating drop method is being widely used to study the characteristics of interfacial membranes formed by emulsifiers relevant to food systems, and to establish the factors that affect these characteristics (Benjamins et al., 1996; Benjamin and Lucassen-Reynders, 1998; Puff et al., 1998).

A variety of other analytical techniques are also available for measuring interfacial dilational rheology, for example, trough and over-flowing cylinder methods (Murray and Dickinson, 1996; Miller et al., 1997; Lucassen-Reynders and Benjamins, 1999). Trough methods measure the surface or interfacial tension of a liquid using a Wilhelmy plate as the interfacial area is varied by changing the distance between two solid barriers that confine the liquid (Figure 5.21). In some instruments it is possible to vary the distance between the barriers in a sinusoidal fashion so that the complex dilational modulus can be determined (Lucassen-Reynders and Benjamins, 1999). The over-flowing cylinder method can also be used to measure the dynamic dilational rheology of surfaces or interfaces (van Kalsbeek and Prins, 1999). A Wilhelmy plate is used to measure the surface or interfacial tension of a liquid as it is continuously pumped into a cylinder so that it overflows at the edges. The dilational viscosity is measured as a function of the surface age by altering the rate at which the liquid is pumped into the cylinder.

The interfacial dilational rheology of liquids can also be determined by capillary wave methods (Noskov et al., 2003). In these methods a laser beam reflected from the surface of a liquid is used to determine the amplitude and wavelength of the surface waves, which can then be related to the dilational modulus or viscosity of the surface using an appropriate theory. These surface waves are believed to play an important role in the coalescence of emulsion droplets (Section 7.6), and therefore this technique may provide information that has direct practical importance to food scientists.

It should be noted that the dilational rheology of an interface is often influenced by the adsorption kinetics of emulsifiers (Murray and Dickinson, 1996). When a surface undergoes a dilational expansion the concentration of emulsifier per unit area decreases and therefore its surface tension increases, which is thermodynamically unfavorable. The dilational elasticity or viscosity is a measure of this resistance of the surface to dilation (Table 5.4). When there are emulsifier molecules present in the surrounding liquid they may be adsorbed to the surface during dilation and thereby reduce the surface tension. The dilational rheology therefore depends on the rate at which emulsifier molecules are

adsorbed to a surface relative to the rate at which the interfacial area is changed, which is determined by emulsifier concentration, molecular structure, and the prevailing environmental conditions (Section 5.3). The faster the molecules adsorb to the freshly formed interface, the lower is the resistance to dilation, and therefore the lower is the dilational modulus or viscosity. When an interface undergoes dilational compression some of the emulsifier molecules may leave the interface to reduce the resulting strain, and therefore the desorption rate may also influence the rheological characteristics of an interface.

## 5.9 Practical implications of interfacial phenomena

In this section, we consider a number of the important practical implications of interfacial properties for bulk liquids and emulsions.

### 5.9.1 Properties of curved interfaces

The majority of surfaces or interfaces found in food emulsions are curved, rather than planar. The curvature of an interface alters its characteristics in a number of ways. The interfacial tension tends to cause an emulsion droplet to shrink in volume so as to reduce the unfavorable contact area between the oil and water phases (Hunter, 1986; Everett, 1988; Jonsson et al., 1998). As the droplet shrinks there is an increase in its internal pressure because of the compression of the water molecules. Eventually, an equilibrium is reached where the inward stress due to the interfacial tension is balanced by the outward stress associated with compressing the bonds between the liquid molecules inside the droplet.\* At equilibrium, the pressure within the droplet is larger than that outside, and can be related to the interfacial tension and radius of the droplets using the *Young–Laplace equation* (Adamson, 1990):

$$\Delta p = \frac{2\gamma}{r} \quad (5.20)$$

This equation indicates that the pressure difference across the interface of an emulsion droplet increases as the interfacial tension increases or the size of the droplet decreases. The properties of a material depend on the pressure exerted on it, and so the properties of a material within a droplet are different from those of the same material in bulk (Atkins, 1993). This effect is usually negligible for liquids and solids that are contained within particles that have radii greater than a few micrometers, but it does become significant for smaller particles (Hunter, 1986). For example, the solubility of a substance in a liquid surrounding it increases as the radius of the spherical particle containing the substance decreases (Dickinson, 1992; Atkins, 1993):

$$\frac{S}{S^*} = \exp\left(\frac{2\gamma v}{rRT}\right) \quad (5.21)$$

where  $S$  is the solubility of the substance when it is contained within a spherical particle of radius  $r$ ,  $S^*$  is the solubility of the same substance when it is contained within a spherical particle of infinite radius (i.e., the solubility of the bulk substance), and  $v$  is the molar volume of the substance. For a typical food oil contained within a droplet surrounded by water ( $v = 10^{-3} \text{ m}^3 \text{ mol}^{-1}$ ,  $\gamma = 10 \text{ mJ m}^{-2}$ ), the value of  $S/S^*$  is 2.24, 1.08, 1.01, and 1.00 for

\* The shrinkage of a droplet due to the interfacial tension is usually negligibly small, because liquids have a very low compressibility.



oil droplets with radii of 0.01, 0.1, 1, and 10  $\mu\text{m}$ , respectively. The dependence of the solubility of substances on the size of the particles that they are contained within has important implications for the stability of emulsion droplets, fat crystals, and ice crystals in many foods because of Ostwald ripening, that is, the growth of larger particles at the expense of smaller ones due to diffusion of the substance contained within the particles through the intervening medium (Section 7.8).

So far, it has been assumed that the interfacial tension of a droplet is independent of its radius. Experimental work has indicated that this assumption is valid for oil droplets, even down to sizes where they only contain a few molecules, but that it is invalid for water droplets below a few nanometers because of the disruption of long range hydrogen bonds (Israelachvili, 1992). It should also be noted that the droplets in emulsions are usually covered with a layer of emulsifier molecules, which will alter the interfacial tension and the mass transfer rate of molecules across the interface.

### 5.9.2 Contact angles and wetting

In food systems, we are often interested in the ability of a liquid to spread over or “wet” the surface of another material. In some situations, it is desirable for a liquid to spread over a surface (e.g., when coating a food with an edible film), while in other situations it is important that a liquid does not spread (e.g., when designing waterproof packaging). When a drop of liquid is placed on the surface of a material it may behave in a number of ways, depending on the nature of the interactions between the various types of molecules present. The two extremes of behavior that are observed experimentally are outlined below (Figure 5.31):

1. *Poor wetting.* The liquid gathers up into a lens, rather than spreading across the surface of a material.
2. *Good wetting.* The liquid spreads over the surface of the material to form a thin film.

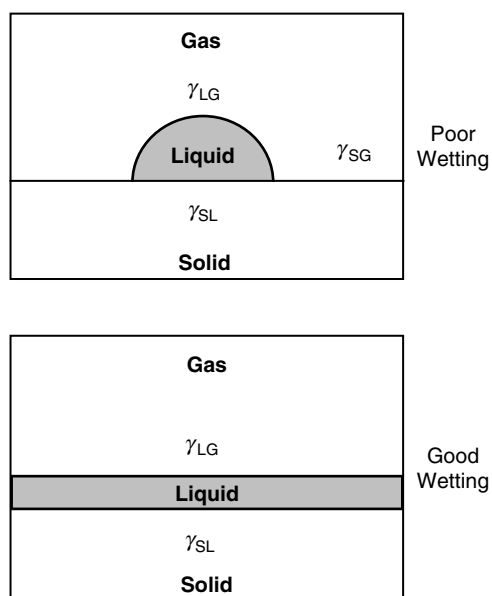


**Figure 5.31** The wetting of a surface by a liquid depends on a delicate balance of molecular interactions among solid, liquid, and gas phases.

The situation that occurs in practice depends on the relative magnitude of the interactions between the various types of molecules involved, that is, solid–liquid, solid–gas, and liquid–gas. A system tends to organize itself so that it can maximize the number of thermodynamically favorable interactions and minimize the number of thermodynamically unfavorable interactions between the molecules. Consider what may happen when a drop of liquid is placed on a solid surface (Figure 5.31). If the liquid remained as a lens there would be three different interfaces: solid–liquid, solid–gas, and liquid–gas, each with its own interfacial or surface tension. If the liquid spread over the surface there would be a decrease in the area of the solid–gas interface, but an increase in the areas of both the liquid–gas and solid–liquid interfaces. The tendency for a liquid to spread therefore depends on the magnitude of the solid–gas interactions ( $\gamma_{SG}$ ) compared to the magnitude of the solid–liquid and liquid–gas interactions that replace it ( $\gamma_{SL} + \gamma_{LG}$ ). This situation is conveniently described by a *spreading coefficient*, which is defined as (Hunter, 1993; Norde, 2003):

$$S = \gamma_{SG} - (\gamma_{SL} + \gamma_{LG}) \quad (5.22)$$

If the interfacial tension of the solid–gas interface is greater than the sum of the interfacial tensions associated with the solid–liquid and liquid–gas interfaces ( $\gamma_{SG} > \gamma_{SL} + \gamma_{LG}$ ), then  $S$  is positive and the liquid tends to spread over the surface to reduce the thermodynamically unfavorable contact area between the solid and the gas. On the other hand, if the interfacial tension associated with the solid–gas interface is less than the sum of the interfacial tensions associated with the solid–liquid and liquid–gas interfaces ( $\gamma_{SG} < \gamma_{SL} + \gamma_{LG}$ ), then  $S$  is negative and the liquid tends to form a lens.

The shape of a droplet on a solid surface can be predicted by carrying out an equilibrium force balance at the point on the surface where the solid, liquid, and gas meet (Figure 5.32) using the Young–Dupré equation (Hiemenz and Rajagopalan, 1997; Norde, 2003):

$$\gamma_{SG} = \gamma_{SL} + \gamma_{LG} \cos \theta \quad (5.23)$$

so that

$$\cos \theta = \frac{\gamma_{SG} - \gamma_{SL}}{\gamma_{LG}} \quad (5.24)$$

here  $\theta$  is known as the contact angle, which is the angle of a tangent drawn at the point where the liquid contacts the surface (Figure 5.32). The shape of a droplet on a surface can

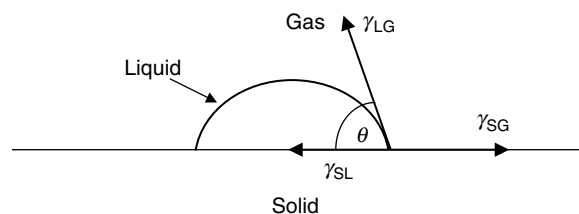


Figure 5.32 Force balance of a droplet at a solid–gas interface.

therefore be predicted from knowledge of the contact angle: the smaller the  $\theta$ , the greater the tendency for the liquid to spread over the surface. The Young–Dupré equation contains two parameters that cannot be determined independently ( $\gamma_{SG}$  and  $\gamma_{SL}$ ). This equation is therefore only useful when it is used in combination with another equation that allows one to estimate one of the unknown terms (Norde, 2003).

So far we have only considered the situation where a liquid spreads over a solid surface, but similar equations can be used to consider other three component systems, such as a liquid spreading over the surface of another liquid (e.g., oil, water, and air), or of a solid particle at an interface between two other liquids (e.g., a fat crystal at an oil–water interface). The latter case is important when considering the nucleation and location of fat crystals in oil droplets, and has a pronounced influence on the stability and rheology of many important food emulsions, including milk, cream, butter, and whipped cream (Walstra, 1987, 2003a; Boode, 1992; Goff, 1997a–c; Goff and Hartel, 2003).

The above equations assume that the materials involved are completely insoluble in each other, so that the values of  $\gamma_{SG}$ ,  $\gamma_{SL}$ , and  $\gamma_{LG}$  (or the equivalent terms for other three component systems), are the same as those for pure systems. If the materials are partially miscible then the interfacial tensions will change over time until equilibrium is reached (Hunter, 1993). The solubility of one component in another generally leads to a decrease in the interfacial tension. This means that the shape that a droplet adopts on a surface may change with time, for example, a spread liquid may gather into a lens or vice versa, depending on the magnitude of the changes in the various surface or interfacial tensions (Norde, 2003). When surface-active solutes are present in the system there will be changes in the relative magnitudes of the various surface and interfacial tensions, which may drastically alter the ability of a liquid to spread over or wet a surface.

The contact angle of a liquid can conveniently be measured using a microscope, which is often attached to a computer with video image analysis software (Hunter, 1986). A droplet of the liquid to be analyzed is placed on a surface and its shape is recorded via the microscope. The contact angle is determined by analyzing the shape of the droplet using an appropriate theoretical model (Hiemenz and Rajagopalan, 1997). There are a number of important practical considerations that must be taken into account in order to perform accurate contact angle measurements, including the effects of surface roughness, surface heterogeneity, and adsorption of vapor or surfactants to the solid surface (Norde, 2003). The advantages and disadvantages of a variety of other techniques available for measuring contact angles have been considered elsewhere (Hunter, 1986).

The concepts of a contact angle and a spreading coefficient are useful for explaining a number of important phenomena that occur in food emulsions. The contact angle determines the distance that a fat crystal protrudes from the surface of a droplet into the surrounding water (Boode, 1992; Walstra, 2003a), and whether nucleation occurs within the interior of a droplet or at the oil–water interface (Dickinson and McClements, 1995). It also determines the amount of liquid that is drawn into a capillary tube and the shape of the meniscus at the top of the liquid (Hunter, 1986; Hiemenz and Rajagopalan, 1997). The contact angle also determines the effectiveness of particulate matter at stabilizing emulsion droplets against aggregation, since it determines how far these particles protrude out of the droplets, that is, pickering stabilization (Norde, 2003; Walstra, 2003a). Knowledge of the contact angle is also often required in order to make an accurate measurement of the surface or interfacial tension of a liquid (Couper, 1993). Finally, measurement of the contact angle of a water droplet placed on a surface can be used to quantify the surface hydrophobicity of that surface (Norde, 2003).

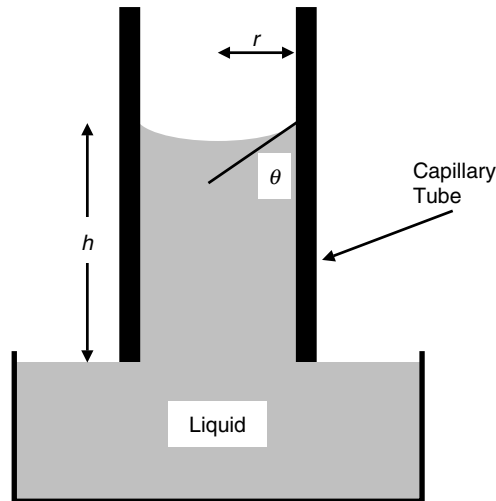


Figure 5.33 The rise of a liquid up a capillary tube is a result of its surface tension.

### 5.9.3 Capillary rise and meniscus formation

The surface tension of a liquid governs the rise of liquids in capillary tubes and the formation of menisci (curved surfaces) at the top of liquids (Hunter, 1986; Hiemenz and Rajagopalan, 1997). When a glass capillary tube is dipped into a beaker of water the liquid climbs up the tube and forms a curved surface (Figure 5.33). The origin of this phenomenon is the imbalance of intermolecular forces at the various surfaces and interfaces in the system (Evans and Wennerstrom, 1994). When water climbs up the capillary tube some of the air–glass contact area is replaced by water–glass contact area, while the air–water contact area remains fairly constant. This occurs because the imbalance of molecular interactions between glass and air is much greater than that between glass and water. Consequently, the system attempts to maximize the glass–water contacts and minimize the glass–air contacts, by having the liquid climb up the inner surface of the capillary tube. This process is opposed by the downward gravitational pull of the liquid. When the liquid has climbed to a certain height, the surface energy it gains by optimizing the number of favorable water–glass interactions is exactly balanced by the potential energy that must be expended to raise the mass of water up the tube (Hiemenz and Rajagopalan, 1997). A mathematical analysis of this equilibrium leads to the derivation of the following equation:

$$\gamma = \frac{\Delta \rho g h r}{2 \cos \theta} \quad (5.25)$$

where  $g$  is the gravitational constant,  $h$  is the height that the meniscus rises above the level of the water,  $r$  is the radius of the capillary tube,  $\Delta \rho$  is the difference in density between the water and the air, and  $\theta$  is the contact angle (Figure 5.33). When a capillary tube is made from a solid material that is completely wetted by the fluid into which it is dipped (e.g.,  $\theta = 0^\circ$ ,  $\cos \theta = 1$ ), then the fluid moves upward, for example, glass and water. On the other hand, when a capillary tube is made from a solid material that is poorly wetted by the fluid into which it is dipped (e.g.,  $\theta = 180^\circ$ ,  $\cos \theta = -1$ ), then the fluid will move downward, for example, glass and mercury.

The above equation indicates that the surface tension can be estimated from a measurement of the height that a liquid rises up a capillary tube and the contact angle: the greater the surface tension, the higher the liquid rises up the tube. This is one of the oldest and simplest methods of determining the surface tension of pure liquids, but it has a number of problems that limit its application to emulsifier solutions (Couper, 1993). For these systems, it is better to use the surface and interfacial tension measuring devices described earlier in this chapter.

Capillary forces are responsible for the entrapment of water in biopolymer networks and oil in fat crystal networks. When the gaps between the network are small, the capillary force is strong enough to hold relatively large volumes of liquid, but when the gaps exceed a certain size the capillary forces are no longer strong enough and syneresis or "oiling-off" occurs. Knowledge of the origin of capillary forces is therefore important for understanding the relationship between the microstructure of foods and many of their quality attributes.

#### 5.9.4 *Interfacial phenomenon in food emulsions*

We conclude this chapter by briefly outlining some of the most important practical implications of interfacial phenomena for food emulsions. One of the most striking features of food emulsions when observed under a microscope is the sphericity of the droplets. Droplets tend to be spherical because this shape minimizes the thermodynamically unfavorable contact area between oil and water molecules, which is described by the Laplace equation (see earlier). Droplets become nonspherical when they experience an external force that is large enough to overcome the Laplace pressure, for example, gravity, centrifugal forces, or mechanical agitation. The magnitude of the force needed to deform a droplet decreases as their interfacial tension decreases or their radius increases. This accounts for the ease at which the relatively large droplets in highly concentrated emulsions, such as mayonnaise, are deformed into polygons (Dickinson and Stainsby, 1982).

The thermodynamic driving force for coalescence and "oiling-off" is the interfacial tension between the oil and water phases caused by the imbalance of molecular interactions across an oil–water interface (Section 7.2). On the other hand, the ability of the interfacial membrane to resist rupture or to prevent droplets from coming close together is responsible for their kinetic stability (Sections 7.4–7.6). The reason that surface-active molecules adsorb to an air–fluid or oil–water interface is because of their ability to reduce the surface or interfacial tension (Section 5.2.2). The tendency of a liquid to spread over the surface of another material or to remain as a lens depends on the relative magnitude of the interfacial and surface tensions between the different types of substances involved (Section 5.9.2).

The formation of stable nuclei in a liquid is governed by the interfacial tension between the crystal and the melt (Section 4.2.3). The larger the interfacial tension between the solid and liquid phases, the greater the degree of supercooling required to produce stable nuclei. The interfacial tension also determines whether an impurity is capable of promoting heterogeneous nucleation.

The solubility of a substance increases as the size of the particle containing it decreases (Section 5.9.1). If a suspension contains particles (emulsion droplets, fat crystals, ice crystals, or air bubbles) of different sizes there is a greater concentration of the substance dissolved in the region immediately surrounding the smaller particles than that surrounding the larger particles. Consequently, there is a concentration gradient that causes material to move from the smaller particles to the large particles (Walstra, 2003a). With time this process manifests itself as a growth of the large particles at the expense of the smaller

ones, which is referred to as Ostwald ripening (Section 7.8). This process is responsible for the growth in size of emulsion droplets, fat crystals, ice crystals, and air bubbles in food emulsions, which often has a detrimental effect on the quality of a food. For example, the growth of ice crystals in ice cream causes the product to be perceived as "gritty" (Berger, 1997). It should be clear from this chapter, that even though the interfacial region only comprises a small fraction of the total volume of an emulsion it plays an extremely important role in determining their bulk physicochemical properties.



## *chapter six*

---

# *Emulsion formation*

### *6.1 Introduction*

Fresh milk is an example of a naturally occurring emulsion that can be consumed directly by human beings (Swaigood, 1996). In practice, however, most milk is subjected to a number of processing operations prior to consumption in order to ensure its safety, to extend its shelf life, and to create new products (Robinson, 1993, 1994; Walstra, 1999). Processing operations, such as homogenization, pasteurization, whipping, chilling, freezing, churning, enzyme treatment, and aging are responsible for the wide range of properties exhibited by dairy products, for example, homogenized milk, cream, ice cream, butter, and cheese (Section 12.2). Unlike dairy products, most other food emulsions are manufactured by combining raw materials that are not normally found together in nature (Dickinson and Stainsby, 1982; Dickinson, 1991; Stauffer, 1999; Friberg et al., 2004). For example, a salad dressing may be prepared using water, proteins from milk, oil from soybeans, vinegar from apples, and polysaccharides from seaweed. The physicochemical and sensory properties of a particular food emulsion depend on the type and concentration of ingredients that it contains, as well as the method used to create it. To improve the quality of existing products, develop new products, and reduce production costs it is important for food manufacturers to have a thorough understanding of the physical processes that take place during emulsion formation. This chapter discusses the physical principles of emulsion formation, the various techniques available for creating emulsions, and the factors that affect the efficiency of emulsion formation. It should be mentioned that this chapter focuses on mechanical methods of producing emulsions, rather than on chemical or spontaneous emulsification methods (Vincent et al., 1998), since these latter methods are rarely used in the food industry.

### *6.2 Overview of homogenization*

The formation of an emulsion may involve a single step or a number of consecutive steps, depending on the nature of the starting material and the method used to create it. Prior to converting separate oil and aqueous phases into an emulsion it is often necessary to disperse the various functional ingredients into the phase in which they are most soluble. Oil-soluble ingredients, such as lipophilic vitamins, colors, antioxidants, and surfactants are mixed with oil, while water-soluble ingredients, such as hydrophilic proteins, polysaccharides, sugars, salts, buffers, vitamins, colors, antioxidants, and surfactants are mixed with water. Having said this, in some situations it is more convenient to incorporate powdered functional ingredients directly into an oil–water mixture, regardless of the phase in which they are most soluble, since this helps prevent clumping and facilitates dispersion during subsequent mixing and homogenization processes. Certain types of powdered ingredients are often mixed together in the powder form before adding to the mixing vessel. High-speed mixing



is often required to prevent clumping of ingredients and to stop them sticking to the sides of the vessel. Some functional ingredients require a heat treatment after incorporation into the system since this promotes some kind of conformational change that facilitates dispersion and dissolution (e.g., heating above a helix-to-coil transition temperature of a polysaccharide). On the other hand, it is important not to overheat other ingredients because this adversely affects their functionality (e.g., heating above the thermal denaturation temperature of a globular protein). The intensity and duration of the mixing process depends on the time required to solvate and uniformly distribute the ingredients. Adequate solvation is important for the functionality of a number of food components, for example, the emulsifying properties of proteins are often improved by allowing them to hydrate in water for a few minutes or hours prior to homogenization (Kinsella and Whitehead, 1989). If the lipid phase contains any crystalline material it is necessary to warm it to a temperature where all the fat melts prior to homogenization, otherwise it is difficult, if not impossible, to create a stable emulsion (Mulder and Walstra, 1974; Phipps, 1985). On the other hand, excessive heating of thermally labile lipids may have an adverse affect on product quality (e.g., oxidation of polyunsaturated lipids). Most ingredient suppliers provide instructions on the optimum conditions required to disperse ingredients during emulsion formation, for example, mixing, solvent, and temperature requirements.

The process of converting two immiscible liquids into an emulsion is known as *homogenization*, and a mechanical device designed to carry out this process is called a *homogenizer* (Loncin and Mercer, 1979; Walstra, 1993b; Schubert and Karbstein, 1994; Walstra and Smulders, 1998). Depending on the nature of the starting material it is convenient to divide homogenization into two categories. The creation of an emulsion directly from two separate liquids will be defined as *primary* homogenization, whereas the reduction in size of the droplets in an already existing emulsion will be defined as *secondary* homogenization (Figure 6.1). The creation of a particular type of food emulsion may involve the use of either of these types of homogenization, or a combination of them. For example, the preparation of a salad dressing at home in the kitchen is usually carried out by direct homogenization of the aqueous and oil phases using a fork, whisk, or blender, and is therefore an example of primary homogenization, whereas homogenized milk is manufactured by reducing the size of preexisting fat globules in raw milk, and so is an example of secondary homogenization. In many food processing operations and laboratory studies it is more efficient to prepare an emulsion using two steps. The separate oil and water phases are converted to a coarse emulsion that contains fairly large droplets using one type of homogenizer (e.g., a high-speed blender), and then the size of the droplets is reduced using another type of

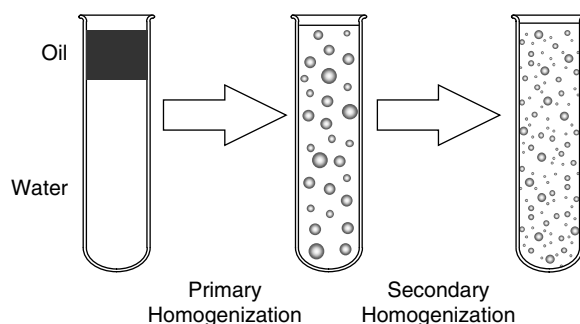


**Figure 6.1** Homogenization can be conveniently divided into two categories: primary and secondary homogenization. Primary homogenization is the conversion of two bulk liquids into an emulsion, whereas secondary homogenization is the reduction in size of the droplets in an existing emulsion.

homogenizer (e.g., a high-pressure valve homogenizer). Many of the same physical processes occur during primary and secondary homogenization (e.g., mixing, droplet disruption, and droplet coalescence), and so there is no clear distinction between them.

Emulsions that have undergone secondary homogenization usually contain smaller droplets than those that have undergone primary homogenization, although this is not always the case. Some homogenizers are capable of producing emulsions with small droplet sizes directly from the separate oil and water phases, for example, high-intensity ultrasound, microfluidizers, or membrane homogenizers (see Section 6.5).

The physical processes that occur during homogenization can be highlighted by considering the formation of an emulsion from pure oil and pure water. When the two liquids are placed in a container they tend to adopt their thermodynamically most stable state, which consists of a layer of oil on top of a layer of water (Figure 6.1). This arrangement is adopted because it minimizes the contact area between the two immiscible liquids, and because oil has a lower density than water (Section 7.2). To create an emulsion it is necessary to supply energy in order to disrupt and intermingle the oil and water phases, which is usually achieved by mechanical agitation (Walstra, 1993b; Walstra and Smulder, 1998; Schubert et al., 2003). The type of emulsion formed in the absence of an emulsifier depends primarily on the initial concentration of the two liquids: at high oil concentrations a water-in-oil emulsion tends to be formed, but at low oil concentrations an oil-in-water emulsion tends to be formed\*. In this example, we assume that the oil concentration is so low that an oil-in-water emulsion is formed. Mechanical agitation can be applied in a variety of different ways (Section 6.5), the simplest being to vigorously shake the oil and water together in a sealed container. Immediately after shaking an emulsion is formed that appears optically opaque because light is scattered by the emulsion droplets (Chapter 10). The oil droplets formed during the application of the mechanical agitation are constantly moving around and frequently collide and coalesce with neighboring droplets. As this process continues the large droplets formed move to the top of the container due to gravity and merge together to form a separate layer. As a consequence, the system reverts back to its initial state—a layer of oil sitting on top of a layer of water (Figure 6.1). The thermodynamic driving forces for this process are the hydrophobic effect, which favors the minimization of the contact area between the oil and water, and gravity, which favors the upward movement of the oil (Section 7.2).

To form an emulsion that is (kinetically) stable for a reasonable period of time one must prevent the droplets from merging together after they have been formed (Walstra, 1983, 1993b; Walstra and Smulder, 1998). This is normally achieved by having a sufficiently high concentration of *emulsifier* present during the homogenization process. The emulsifier adsorbs to the surface of the droplets during homogenization forming a protective membrane that prevents the droplets from coming close enough together to coalesce. The size of the droplets produced during homogenization depends on two processes: (i) the initial generation of droplets of small size, and, (ii) the rapid stabilization of these droplets against coalescence once they are formed (Section 6.4).

Many of the bulk physicochemical and organoleptic properties of food emulsions depend on the size of the droplets they contain, including their stability, texture, taste, and appearance (Chapters 7–10). One of the major objectives of homogenization is therefore to create an emulsion in which the majority of droplets fall within an optimum size range, which has previously been established by the food manufacturer to produce a product with the desired quality attributes. It is therefore important for food scientists to appreciate the major factors that determine the size of the droplets produced during homogenization.

This brief introduction to homogenization has highlighted some of the most important aspects of emulsion formation, including the necessity to mechanically agitate the system,

\* In the presence of an emulsifier the type of emulsion formed is governed mainly by the properties of the emulsifier, that is the HLB number and optimum curvature (Chapter 4).

the competing processes of droplet formation and droplet coalescence, and the role of the emulsifier. These topics will be considered in more detail in the rest of the chapter.

### 6.3 Flow profiles in homogenizers

The rates of droplet disruption, droplet coalescence, and emulsifier adsorption within a particular homogenizer depend on the flow profile that the fluids experience (Schubert, 1997; Walstra and Smulders, 1998). For this reason, we begin by providing a brief outline of the major types of flow profile that emulsions can experience within homogenizers used to prepare food emulsions (Walstra, 2003a):

1. *Laminar flow.* At relatively low flow rates, fluid flow tends to be regular, smooth, and well-defined.
2. *Turbulent flow.* At relatively high flow rates, fluid flow tends to be irregular, chaotic, and ill-defined due to the formation of eddies within the fluid.
3. *Cavitation flow.* In the presence of highly fluctuating pressure variations within a fluid the flow profile is extremely complex because of the formation of small cavities that violently implode and generate shock waves.

A more detailed explanation of these flow profiles can be found elsewhere (Walstra, 1993, 2003a; Walstra and Smulders, 1998; Canselier et al., 2002). In practice, the flow regime within a homogenizer is often a combination of two or more of these different flow types. The tendency for laminar or turbulent flow to occur depends on the balance of viscous (frictional) and inertial forces acting on the fluid, which is normally characterized by the Reynolds number:

$$Re = \frac{\text{inertial forces}}{\text{viscous forces}} = \frac{L\bar{v}\rho_c}{\eta_c} \quad (6.1)$$

where  $L$  is some characteristic length of the system (e.g., the diameter of a pipe or a droplet),  $\bar{v}$  is the average fluid flow velocity,  $\rho_c$  is the density of the fluid, and  $\eta_c$  is the viscosity of the fluid. When the viscous forces generated within a fluid dominate the inertial forces (low  $Re$ ) the flow profile is laminar; however, when the Reynolds number in the fluid exceeds some critical value ( $Re_{Cr}$ ), the flow goes from laminar to turbulent and inertial forces dominate. For the flow of a Newtonian fluid through a cylindrical pipe ( $L = D$ , the diameter of the pipe),  $Re_{Cr}[\text{fluid}] = 2300$ . For the flow of a Newtonian fluid around a spherical droplet ( $L = d$ , the diameter of the droplet,  $\bar{v} = v$ , the velocity of the droplet relative to the fluid),  $Re_{Cr}[\text{drop}] = 1$ .

Based on the above definitions of the Reynolds number for fluids and droplets, it is useful to distinguish different flow regimes responsible for droplet disruption in homogenizers that use laminar or turbulent flow profiles, depending on the type of fluid flow they experience and the type of forces mainly responsible for droplet disruption (Walstra and Smulders, 1998):

1. *Laminar-viscous (LV) regime.* The dominant flow profile in the fluid is laminar ( $Re[\text{fluid}] < Re_{Cr}[\text{fluid}]$ ), and viscous forces are predominantly responsible for droplet disruption ( $Re[\text{drop}] < Re_{Cr}[\text{drop}]$ ).
2. *Turbulent-viscous (TV) regime.* The dominant flow profile in the fluid is turbulent ( $Re[\text{fluid}] > Re_{Cr}[\text{fluid}]$ ), and viscous forces are predominantly responsible for droplet disruption ( $Re[\text{drop}] < Re_{Cr}[\text{drop}]$ ).
3. *Turbulent-inertial (TI) regime.* The dominant flow profile in the fluid is turbulent ( $Re[\text{fluid}] > Re_{Cr}[\text{fluid}]$ ), and inertial forces are predominantly responsible for droplet disruption ( $Re[\text{drop}] > Re_{Cr}[\text{drop}]$ ).

The viscous forces acting on the droplets are due to the flow of fluid parallel to the surface of the droplets, whereas the inertial forces are due to local pressure fluctuations in the fluid and tend to act perpendicular to the surface of the droplets (Walstra and Smulder, 1998). The flow regime responsible for droplet disruption depends on the type of homogenizer used to create the emulsion (Table 6.1), as well as the physicochemical characteristics of the fluid (e.g., density and viscosity) (Table 6.2).

## 6.4 Physical principles of emulsion formation

As mentioned earlier, the size of the droplets produced by a homogenizer depends on a balance between two opposing physical processes: *droplet disruption* and *droplet coalescence* (Figure 6.2). A better understanding of the factors that influence these processes would help food manufacturers to select the most appropriate ingredients and homogenization conditions required to produce a particular food product. An overview of droplet disruption, droplet coalescence, and the role of the emulsifier in these processes is given in this section. The reader is referred elsewhere for more thorough discussions of the physicochemical basis of emulsion formation (Walstra, 1993b, 2003a; Walstra and Smulders, 1998; Schubert et al., 2003).

### 6.4.1 Droplet disruption

The precise nature of the physical processes that occur during emulsion formation depends on the type of homogenizer used, since this determines the type of flow profile that the droplets experience (Table 6.1). Nevertheless, there are some common aspects of droplet disruption that apply to most types of homogenizers. The initial stages of primary homogenization involve the breakup and intermingling of the bulk oil and aqueous phases so that fairly large droplets of one of the liquids become dispersed throughout the other liquid (Walstra, 1983, 1993b). The later stages of primary homogenization, and the whole of secondary homogenization, involve the disruption of larger droplets into smaller ones. It is therefore particularly important to understand the nature of the forces that are responsible for the disruption of droplets during homogenization. Whether or not a droplet breaks up is determined by a balance between *interfacial forces* that tend to hold the droplets together and *disruptive forces* generated within the homogenizer that tend to pull them apart (Walstra, 1983, 1993b; Walstra and Smulders, 1998).

#### 6.4.1.1 Interfacial forces

An emulsion droplet tends to be spherical because this shape minimizes the thermodynamically unfavorable contact area between the oil and aqueous phases (Section 5.9.1). Changing the shape of a droplet, or breaking it up into a number of smaller droplets, increases this contact area and therefore requires an input of free energy. The interfacial force responsible for keeping a droplet in a spherical shape is characterized by the *Laplace pressure* ( $\Delta P_L$ ), which acts across the oil–water interface toward the center of the droplet so that there is a larger pressure inside the droplet than outside of it:

$$\Delta P_L = \frac{4\gamma}{d} \quad (6.2)$$

Here  $\gamma$  is the interfacial tension between oil and water, and  $d$  is the droplet diameter. To deform and disrupt a droplet during homogenization it is necessary to apply an external force that is significantly larger than the interfacial force (Walstra, 1983, 1996b, 2003a). Equation 6.2 indicates that the pressure required to disrupt a droplet increases as the interfacial tension increases or as the droplet size decreases. It also indicates that intense pressure

Table 6.1 Comparison of the Attributes of Different Types of Homogenizers Used to Prepare Food Emulsions.

Homogenizer Type	Throughput	Dominant Flow Regime	Energy Density (Jm <sup>-3</sup> )	Relative Energy Efficiency	Minimum Droplet Size	Sample Viscosity
High-speed mixer Colloid mill	Batch or continuous	TI, TV, LV	Low-high	Low	2 µm	Low to medium
	Continuous	LV (TV)	Low-high 10 <sup>3</sup> to 10 <sup>8</sup>	Intermediate	1 µm	Medium to high
High-pressure homogenizer	Continuous	TI, TV (CI) LV*	Medium-high 10 <sup>6</sup> to 10 <sup>8</sup>	High	0.1 µm	Low to medium
	Batch or continuous	CI	Medium-high 10 <sup>6</sup> to 10 <sup>8</sup>	Low	0.1 µm	Low to medium
Ultrasonic jet homogenizer	Continuous	CI	Medium-high 10 <sup>6</sup> to 10 <sup>8</sup>	High	1 µm	Low to medium
	Continuous	TI, TV	Medium-high 10 <sup>6</sup> to 2 × 10 <sup>8</sup>	High	<0.1 µm	Low to medium
Membrane processing	Batch or continuous	Injection	Low-medium <10 <sup>3</sup> to 10 <sup>8</sup>	Very high	0.3 µm	Low to medium

Source: Adapted from Walstra (1993), Schubert (1997), and Walstra and Smulder (1998).

Note: Symbols: TI = turbulent-inertial, TV = turbulent-viscous, LV = laminar-viscous, and CI = cavitational.

\*In a high-pressure homogenizer the dominant droplet disruption mechanism is highly dependent on the nature of the homogenization nozzle, and may be either turbulent or laminar elongational (Schubert, 1997).

**Table 6.2** Equations for Calculating the Stresses, Mean Particle Diameters, Adsorption Times, Deformation Times, and Collision Times for Droplets in Emulsions Under Laminar and Turbulent Flow Conditions.

Regime	Laminar-Viscous (LV)	Turbulent-Viscous (TV)	Turbulent-Inertial (TI)
$Re$ , flow	$< \sim 1000$	$> \sim 2000$	$> \sim 2000$
$Re$ , droplet	$< 1$	$< 1$	$> 1$
Stress acting on droplets	$\eta_c G$	$(\epsilon \eta_c)^{1/2}$	$(\epsilon^2 d^2 \rho_c)^{1/3}$
Mean diameter ( $d$ )	$\frac{2\gamma We_{Cr}}{\eta_c G}$	$\frac{\gamma}{(\epsilon \eta_c)^{1/2}}$	$\left( \frac{\gamma^3}{\epsilon^2 \rho_c} \right)^{1/5}$
Collision time ( $\tau_{COL}$ )	$\frac{\pi}{8G\phi}$	—	$\frac{1}{15\phi} \left( \frac{d^2 \rho_c}{\epsilon} \right)^{1/3}$
Adsorption time ( $\tau_{ABS}$ )	$\frac{6\pi\Gamma}{dm_c G}$	$\frac{6\pi\Gamma \eta_c^{1/2}}{dm_c \epsilon^{1/2}}$	$\frac{\Gamma}{m_c} \left( \frac{\rho_c}{d\epsilon} \right)^{1/3}$
Deformation time ( $\tau_{DEF}$ )	$\frac{\eta_D}{\eta_c G}$	$\frac{\eta_D}{(\eta_c \epsilon)^{1/2}}$	$\frac{\eta_D}{(\epsilon^2 d^2 \rho)^{1/3}}$
Duration of disruptive forces ( $\tau_{DIS}$ )	$\frac{1}{G}$	$\frac{\eta_c^{1/2}}{\epsilon^{1/2}}$	$\frac{1}{2} \left( \frac{\rho \gamma^2}{\epsilon^3} \right)^{1/5}$

Source: Adapted from Walstra (1983, 1993a) and Walstra and Smulder (1998).

Note:  $\Gamma$  = excess surface concentration,  $G$  = shear rate,  $\epsilon$  = power density,  $\rho_c$  = continuous phase density,  $\eta_c$  and  $\eta_D$  = viscosities of continuous and dispersed phases,  $d$  = droplet diameter,  $\phi$  = dispersed phase volume fraction,  $\gamma$  = interfacial tension, and  $m_c$  = emulsifier concentration ( $\text{mol m}^{-3}$ ).

gradients must be generated within a homogenizer in order to overcome the interfacial forces holding the emulsion droplets together. For example, the Laplace pressure of a 1  $\mu\text{m}$  diameter droplet with an interfacial tension of 0.01  $\text{Nm}^{-1}$  is about 40 kPa, which corresponds to a pressure gradient of  $\Delta P_L/d \approx 40 \times 10^9 \text{ Pa m}^{-1}$  across the droplet. These large pressure gradients cannot be achieved using simple mixers or blenders, instead specially designed homogenizers are normally required to produce emulsions with small droplets (Section 6.5).

#### 6.4.1.2 Disruptive forces

The nature of the disruptive forces that act on a droplet during homogenization depends on the flow conditions it experiences (i.e., laminar, turbulent, or cavitation), and therefore on the type of homogenizer used (Phipps, 1985; Walstra, 1993, 2003a; Schubert, 1997; Walstra and Smulders, 1998). The dominant flow regimes prevailing in some commonly used homogenizers are summarized in Table 6.1. For a droplet to be broken up during homogenization, the disruptive forces must exceed the interfacial forces and their duration must be longer than the time required for droplet deformation (Stone, 1994; Karbstein and Schubert, 1995a,b). The relative magnitude of disruptive and interfacial forces is conveniently characterized by the Weber number ( $We$  = disruptive forces/interfacial forces) (Walstra, 1983). Droplets tend to be disrupted when the Weber number exceeds some critical value (around unity), which depends on the physical characteristics of the oil and aqueous phases. The relative duration of disruptive forces ( $\tau_{DIS}$ ) and droplet deformation ( $\tau_{DEF}$ ) is conveniently characterized by the ratio  $\tau_{DIS}/\tau_{DEF}$ . Droplets tend to be disrupted when the duration of the applied disruptive forces is longer than the time required for the droplet to become deformed, that is,  $\tau_{DIS}/\tau_{DEF} > 1$ . Approximate expressions for the duration of the disruptive

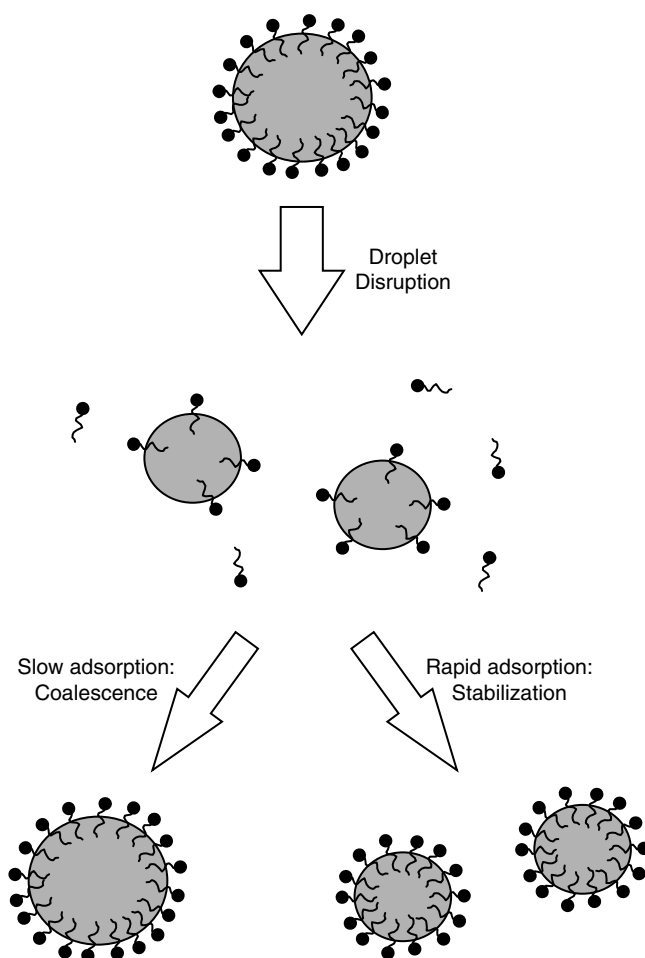


**Figure 6.2** The size of the droplets produced during homogenization depends on the balance between the time for an emulsifier to adsorb to the surface of a droplet ( $\tau_{\text{ADS}}$ ) and the time between droplet–droplet collisions ( $\tau_{\text{COL}}$ ).

forces and the droplet deformation time under different flow regimes are summarized in Table 6.2. These expressions can be used to predict whether droplets will be disrupted in a particular flow regime (Walstra, 1993b; Walstra and Smulders, 1998).

The flow profile of an emulsion within a homogenizer is usually extremely complex and is difficult to model mathematically (Phipps, 1985; Walstra and Smulder, 1998). For this reason it is not easy to accurately calculate the disruptive forces that a droplet experiences during homogenization. Nevertheless, it is possible to gain considerable insight into the factors that affect homogenization by considering droplet disruption under simpler flow conditions that approximate those occurring in actual homogenizers, that is, laminar, turbulent, or cavitation flow conditions (Gopal, 1968; Walstra, 1983, 1993b; Williams et al., 1997; Walstra and Smulder, 1998; Schubert et al., 2003).

*Laminar flow conditions.* As mentioned earlier, this type of flow profile is predominant at low flow rates (i.e., low Reynold numbers), where the fluid moves in a regular and well-defined pattern (Gopal, 1968; Curle and Davies, 1968; Walstra, 1993b). Different types of laminar flow profiles are possible, depending on the direction and velocity at which different regions within the fluid move relative to one another, for example, simple shear,

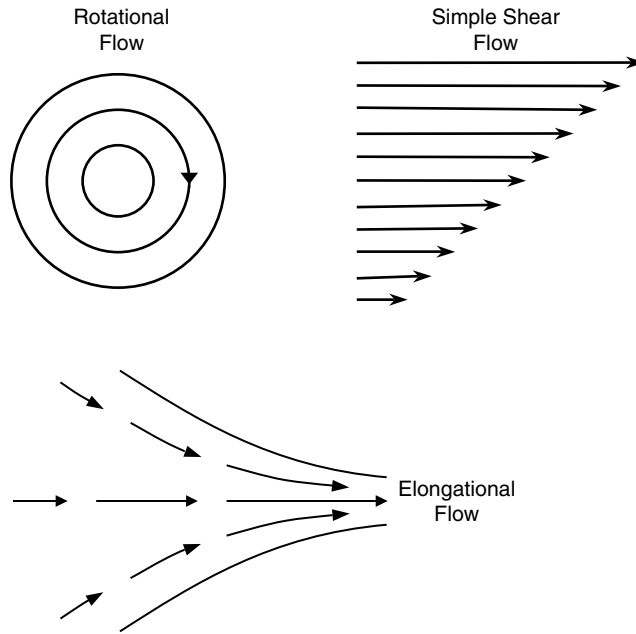


**Figure 6.3** Examples of some types of laminar flow that may occur in fluids at relatively low Reynolds number.

rotational, and elongational flow (Figure 6.3). For convenience, we will mainly consider droplet disruption under simple shear flow conditions in order to highlight some of the most important factors that influence this process. Nevertheless, it should be stressed that simple shear flow is rarely the dominant droplet disruption mechanism in commercial homogenizers, instead, it is usually elongational or turbulent flow (Schubert, 1997). In the presence of a simple shear field a droplet experiences a combination of normal and tangential stresses (Loncin and Merson, 1979). These stresses cause the droplet to rotate and become elongated, as well as causing the liquid within the droplet to circulate (Figure 6.4). At sufficiently high shear rates the droplet becomes so elongated that it is broken up into a number of smaller droplets (Stone, 1994; Williams et al., 1997). The manner in which the droplets breakup depends on the ratio of the viscosities of the droplet and continuous phase ( $\eta_D/\eta_C$ ). Experiments in which droplets were photographed under different flow conditions have shown that at low values of  $\eta_D/\eta_C$  the droplets break up at their edges, at intermediate values they break up near their middle, and at high values they may not break up at all, because there is insufficient time for the droplets to deform during the application of the disruptive forces (Gopal, 1968; Williams et al., 1997).

The disruptive forces that a droplet experiences during simple shear flow are determined by the shear stress ( $G\eta_C$ ) that acts on the droplet, and so the Weber number is given by (Walstra, 1993b)\*:

$$We = \frac{\text{shear forces}}{\text{interfacial forces}} = \frac{G\eta_C d}{2\gamma} \quad (6.3)$$

\* The reason that a factor of 4 appears in Equation 6.2, while a factor of 2 appears in Equation 6.3, is because only half of the applied shear force goes to deforming the droplet, the remainder causes the droplet to rotate and is therefore not responsible for droplet disruption.



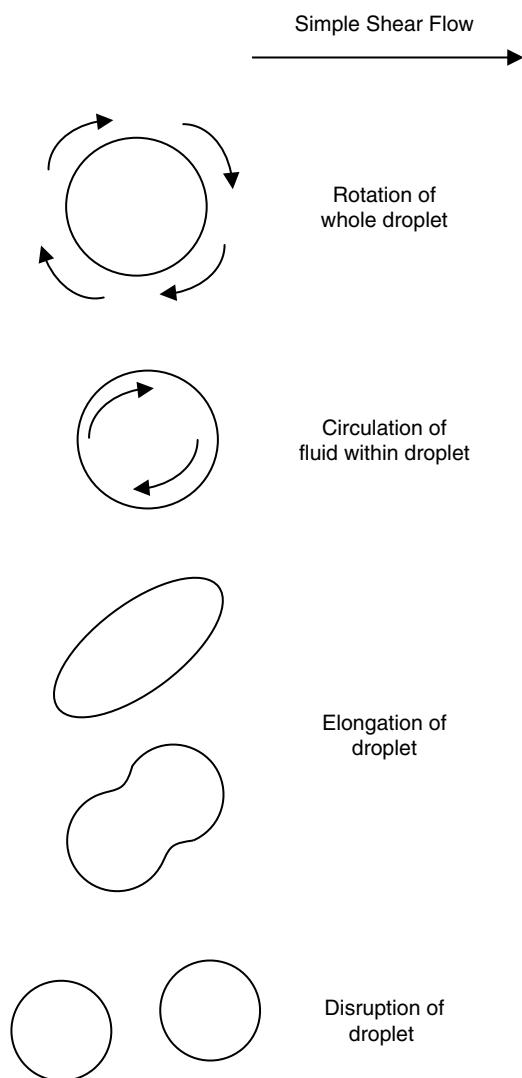


**Figure 6.4** In the presence of a simple shear flow droplets may rotate and become elongated. In addition, the fluid inside of them may circulate around the center of the droplet.

Here  $G$  is the shear rate and  $\eta_c$  is the viscosity of the continuous phase. For a given system, it is possible to define a critical Weber number,  $We_{cr}$ , which is the value of  $We$  where the droplets are just stable to disruption. If an emulsion has a Weber number above this critical value (i.e., high shear rates or large droplets), then the droplets will be broken up, otherwise they will remain intact (Figure 6.5). The critical Weber number of an emulsion in the absence of emulsifier depends principally on the ratio of the viscosities of the dispersed and continuous phases (Janssen et al., 1994; Karbstein and Schubert, 1995a; Williams et al., 1997).  $We_{cr}$  has a minimum value when  $\eta_D/\eta_c$  is between 0.1 and 1, and increases significantly as the viscosity ratio decreases below 0.05 or increases above 5 (Figure 6.5). The behavior of droplets during the disruption process has been widely studied and is now well understood (Bentley and Leal, 1986; Stone, 1994; Janssen et al., 1994; Walstra and Schubert, 1998). Droplets are resistant to breakup at low viscosity ratios ( $<0.05$ ) because they are able to become extremely elongated before any disruption occurs. They are resistant to

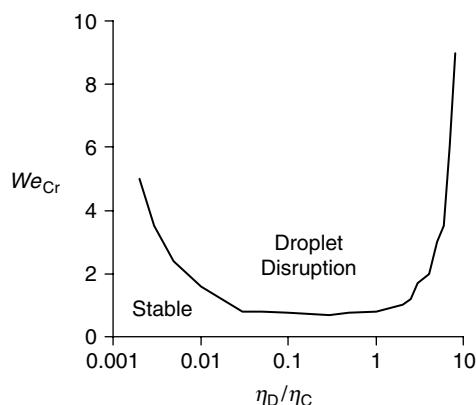


**Figure 6.5** Dependence of the critical Weber number on the viscosity of the dispersed and continuous phases under simple shear flow conditions. (Adapted from Schubert and Armbruster, 1992.)

breakup at high viscosity ratios ( $>5$ ) because they do not have sufficient time to become deformed before the flow field causes them to rotate to a new orientation and therefore alter the distribution of disruptive stresses acting on them. At intermediate viscosity ratios, the droplets tend to form a dumbbell shape just prior to breaking up.

In practice, droplet disruption under laminar flow conditions often occurs by a combination of both viscous and elongational contributions (Walstra and Smulder, 1998). Under these conditions there is reduced droplet rotation, reduced circulation of fluid within the droplet, and an increase in the effective viscosity of the fluid. Consequently, elongational flow exerts a higher stress on droplets than simple shear flow and is therefore more effective at breaking up droplets. In addition, the dependence of the critical Weber number on  $\eta_D/\eta_C$  is much less when there is a significant elongational flow component, there being a gradual decrease in  $We_{Cr}$  from 1 to 0.1 as  $\eta_D/\eta_C$  goes from  $10^{-4}$  to  $10^2$  (Walstra and Smulder, 1998).

In the presence of emulsifiers, such as small molecule surfactants or proteins, the behavior of droplets in flow fields has been found to be different from that in the absence of emulsifiers, which has been primarily attributed to their influence on the rheology of the interfacial membrane (Lucassen-Reynders and Kuipers, 1992; Janssen et al., 1994; Williams et al., 1997). Droplets are more difficult to disrupt than would be expected from their equilibrium interfacial tension, because the emulsifier imparts rheological properties to the droplet interface that increase its resistance to tangential stresses. These rheological properties may be due to the formation of interfacial tension gradients caused by movement of surfactant molecules across the interface, that is, the Gibbs–Marangoni effect (Walstra and Smulders, 1998). Alternatively, they may be due to the intrinsic dilational and shear rheology of the interfacial membrane, for example, many proteins and polysaccharides form highly viscoelastic membranes (Bos and van Vliet, 2001).

A food manufacturer usually wants to produce an emulsion that contains a majority of droplets below some specified size, and so it is important to establish the factors that determine the size of the droplets produced during homogenization. For simple shear flow the following relationship gives a good description of the maximum size of droplets that can persist in an emulsion during homogenization under steady-state conditions (Walstra, 1983, 1993b; Walstra and Smulder, 1998):

$$d_{\max} = \frac{2\gamma We_{Cr}}{G\eta_C} \quad (6.4)$$

Any droplets larger than  $d_{\max}$  will be disrupted, whereas any smaller droplets will remain intact. This equation indicates that the size of the droplets produced during homogenization decreases as the interfacial tension  $\gamma$  decreases, as the shear rate increases, or as the viscosity of the continuous phase increases. It also indicates that a higher shear rate is required to decrease the droplet size when the viscosity of the continuous phase is low. It is for this reason that homogenizers that rely principally on simple shear flow conditions, such as colloid mills with smooth disks, are not suitable for generating emulsions with small droplet sizes when the continuous phase has a low viscosity (Walstra, 1983). For this type of system it is better to use homogenizers that use elongational, turbulent, or cavitation flow to break up the droplets, for example, high-pressure valve, microfluidizer, or high-intensity ultrasonic homogenizers.

*Turbulent flow conditions.* Turbulence occurs when the flow rate of a fluid exceeds some critical value, which is determined by the Reynolds number (Curle and Davies, 1968; Walstra, 1983, 1993b; Phipps, 1985; Walstra and Smulders, 1998). Turbulence is characterized by rapid and chaotic fluctuations in the velocity of the fluid with time and location. The disruption of droplets under turbulent flow conditions is caused by the extremely large shear and pressure gradients associated with the eddies generated in the fluid (Walstra, 1993b). An eddy is a region within a fluid where there is a close correlation between the fluid velocity of the different elements (Curle and Davies, 1968). There is normally a range of different sized eddies formed within a liquid during turbulence. The shear and pressure gradients associated with these eddies increase as their size decrease (Walstra, 1983). As a consequence, large eddies are believed to be relatively ineffective at disrupting emulsion droplets. Very small eddies are also believed to be ineffective at breaking up droplets because they generate such high shear stresses that most of their energy is dissipated through viscous losses, rather than through droplet disruption. For these reasons, intermediate sized eddies are thought to be largely responsible for droplet disruption under turbulent flow conditions (Walstra, 1983, 1993b). When a droplet is in the vicinity of one of these intermediate sized eddies it is deformed and disrupted because of the large shear gradient acting across it (Gopal, 1968).

As mentioned earlier, the turbulent flow conditions can be divided into two categories depending on whether the droplets are primarily disrupted by viscous or inertial forces, that is, the TV (turbulent-viscous) and TI (turbulent-inertial) regimes.

For turbulent conditions the Weber number is given by (Karbstein and Schubert, 1995a)

$$We = \frac{\text{turbulent forces}}{\text{interfacial forces}} \quad (6.5)$$

Mathematical expressions have been derived for the disruptive forces acting on droplets under the TV and TI regimes, hence it is possible to calculate the Weber number under turbulent conditions (Walstra and Smulder, 1998). These equations have been used to predict the maximum size of droplets that can persist during homogenization once a steady state has been reached:

$$\text{For TV: } d_{\max} = \frac{\gamma}{(\epsilon \eta_c)^{1/2}} \quad (6.6a)$$

$$\text{For TI: } d_{\max} = \left( \frac{\gamma^3}{\epsilon^2 \rho_c} \right)^{1/5} \quad (6.6b)$$

For emulsions created using a homogenizer that operates under turbulent conditions, the droplet size should decrease as the power density increases and the interfacial tension decreases, which has been observed in practice (Walstra and Smulders, 1998). In addition, the droplet size should decrease with increasing fluid viscosity under TV conditions, or decreasing fluid density under TI conditions.

A number of experimental studies have shown that the viscosities of the dispersed and continuous phases influence the maximum droplet size that can persist during homogenization under turbulent (TI) conditions, there being a minimum in  $d_{\max}$  when  $\eta_D/\eta_C$  is between 0.1 and 5 (Braginsky and Belevetskaya, 1996). The dependence of the droplet size produced during homogenization on the viscosity ratio under turbulent flow conditions is therefore similar in form to that produced under laminar flow conditions (Figure 6.5). It is therefore possible to reduce the size of the droplets produced during homogenization by ensuring that the viscosity ratio falls within the optimum range for droplet breakup ( $0.1 < \eta_D/\eta_C < 5$ ), which could be achieved by varying the temperature, changing the oil type, or adding thickening agents to the aqueous phase. The viscosity may also influence the droplet size if it is large enough to suppress turbulence. For example, an increase in viscosity due to the presence of thickening agents or high concentrations of droplets may be sufficient to prevent turbulent flow conditions and therefore lead to inefficient homogenization (Walstra, 1993b).

An emulsion does not normally remain in a homogenizer long enough for steady-state conditions to be attained, and so the above equations are not strictly applicable. In practice, the size of the droplets in an emulsion decreases as the length of time they spend in the disruption zone of a homogenizer increases, until eventually a constant value is reached (Karbstein and Schubert, 1995a). This is because droplets take a finite time to be deformed, and so the turbulent forces must act over a period that is sufficiently longer than this time if all the droplets are to be effectively disrupted (Walstra, 1993b). The deformation time is proportional to the viscosity of a droplet and therefore the more viscous the disperse phase the less likely is droplet breakup within a specified time (Table 6.2). Emulsions produced under turbulent flow conditions are always polydisperse because of the distribution of eddy sizes in the fluid. In fact, the statistical theories used to derive the above equations indicate that droplets formed under turbulent conditions should follow a log-normal distribution, which is often observed in practice (Gopal, 1968; Walstra and Smulder, 1998).

*Cavitation flow conditions.* Cavitation occurs in fluids that are subjected to rapid changes in pressure, and is particularly important in ultrasonic and high-pressure valve homogenizers (Gopal, 1968; Phipps, 1985; Canselier et al., 2002). A fluid contracts when the pressure acting on it increases, and expands when the pressure decreases. When the instantaneous pressure that a fluid experiences falls below some critical value a cavity is formed (Lickiss and McGrath, 1996). As the fluid continues to expand the cavity grows and some of the surrounding liquid evaporates and moves into it. During a subsequent compression the cavity catastrophically collapses generating an intense shock wave that propagates into the surrounding fluid and causes any droplet in its immediate vicinity to be deformed and disrupted. Extremely high temperatures and pressures are associated with these shock waves, but they are of very short duration and highly localized, so that limited damage is usually caused to the vessel containing the fluid. Nevertheless, over time cavitation effects are known to cause significant damage to the surfaces of high-pressure valve homogenizers and ultrasonic transducers, which become "pitted" (Gopal, 1968; Phipps, 1985). Cavitation only occurs in fluids when the intensity of the fluctuating pressure field exceeds a critical value, known as the *cavitation threshold*. This threshold is high in pure liquids, but is reduced when cavitation nuclei, such as gas bubbles or impurities are present. The cavitation threshold also depends on the frequency of the pressure fluctuations, decreasing with decreasing frequency (Gopal, 1968).

#### 6.4.1.3 *The role of the emulsifier in droplet disruption*

The ease at which a droplet can be disrupted during homogenization increases as the interfacial tension decreases (Equation 6.2). Thus, it should be possible to produce droplets with smaller sizes by homogenizing in the presence of an emulsifier that reduces the interfacial tension (Walstra, 1993b). For example, adding an emulsifier that decreases the interfacial tension from 50 to 5 mN m<sup>-1</sup> should decrease the size of the droplets produced under laminar flow conditions by an order of magnitude (Schubert and Armburster, 1995). Nevertheless, there are a number of other factors that also determine the effectiveness of emulsifiers at reducing the droplet size. First, the rate at which an emulsifier adsorbs to the surface of the droplets during homogenization must be considered (Walstra, 1983). Immediately after their formation droplets have a low concentration of emulsifier adsorbed to their surface, and are therefore more difficult to disrupt because of the relatively high interfacial tension. With time a greater amount of emulsifier accumulates at the surface, which decreases the interfacial tension and therefore facilitates droplet disruption. Thus, the quicker the emulsifier adsorbs to the surface of the droplets during homogenization the smaller the droplets produced. Second, the ability of emulsifiers to enhance the interfacial rheology of emulsion droplets hampers the breakup of droplets, which leads to larger droplets sizes than those expected from the equilibrium interfacial tension (Lucassen-Reynders and Kuipers, 1992; Janssen et al., 1994; Williams et al., 1997). These two effects partly account for the poor correlation between droplet size and equilibrium interfacial tension reported in the literature (Walstra, 1983).

#### 6.4.1.4 *Role of nonideal fluid behavior on droplet disruption*

The equations given above are only strictly applicable to homogenization of ideal (Newtonian) liquids (Chapter 8). In practice, many liquids used in the food industry exhibit nonideal behavior, which can have a pronounced influence on the efficiency of droplet disruption, and therefore on the size of the droplets produced during homogenization (Walstra, 1983, 1993b). Many biopolymers used to thicken or stabilize emulsions exhibit pronounced shear thinning behavior (Section 4.5.1). As a consequence, the viscosity used in the above equations should be that which the droplet experiences at the shear rates that occur during homogenization, rather than that which is measured in a viscometer at low shear rates. In addition, biopolymers may be capable of suppressing the formation of eddies, which may reduce the efficiency of homogenization carried out under turbulent flow conditions (Walstra, 1993b).

### 6.4.2 *Droplet coalescence*

Emulsions are highly dynamic systems in which the droplets continuously move around and frequently collide with each other, for example, due to Brownian motion, gravity, or mechanical agitation (Section 7.5.1). Droplet–droplet collisions are particularly rapid during homogenization because of the intense mechanical agitation of the emulsion. If droplets are not protected by a sufficiently strong interfacial membrane they tend to coalesce with one another during a collision (Walstra, 1993b). Immediately after the disruption of an emulsion droplet there is insufficient emulsifier present to completely cover the newly formed surface, and therefore the new droplets are more likely to coalesce with their neighbors during a collision. To prevent coalescence it is necessary to form a sufficiently concentrated emulsifier membrane around the droplets before they have time to collide with their neighbors (Figure 6.2). The size of the droplets produced during homogenization therefore depends on the time taken for the emulsifier to be adsorbed to the surface of the droplets ( $\tau_{\text{Ads}}$ ) relative to the time between droplet–droplet collisions ( $\tau_{\text{COL}}$ ). These times depend on the flow profile that the droplets experience, as well as the nature of the

emulsifier used. Estimates of the adsorption and collision times have been established for laminar and turbulent flow conditions (Table 6.2).

The equations given in Table 6.2 are only strictly applicable to dilute emulsions, even so, they do give some useful insights into the factors that influence homogenization. Ideally, a food manufacturer wants to minimize droplet coalescence during homogenization by ensuring that  $\tau_{\text{ADS}}/\tau_{\text{COL}} \ll 1$ . The following expression has been shown to be applicable for both laminar and turbulent flow regimes (Walstra, 2003a):

$$\frac{\tau_{\text{ADS}}}{\tau_{\text{COL}}} \approx \frac{6\pi\Gamma\phi}{dm_c} \quad (6.7)$$

Thus, coalescence within a homogenizer should decrease as the disperse phase volume fraction ( $\phi$ ) decreases, the diameter of the droplets ( $d$ ) increases, the excess surface concentration ( $\Gamma$ ) decreases, and the concentration of emulsifier ( $m_c$ ) increases.

The importance of emulsifier adsorption kinetics on the size of the droplets produced during homogenization has been demonstrated experimentally (Schubert, 1993). Under the same homogenization conditions, it has been shown that emulsifiers that adsorb rapidly produce smaller droplet sizes than those that adsorb more slowly. Most food emulsifiers do not adsorb rapidly enough to completely prevent droplet coalescence, and so the droplet size achieved during homogenization is greater than that which is theoretically possible (Stang et al., 1994).

In addition to the factors already mentioned, the tendency for droplets to coalesce during (or shortly after) homogenization depends on the effectiveness of the interfacial membrane to resist coalescence during a droplet–droplet encounter. The resistance of an interfacial membrane to coalescence depends on the concentration of emulsifier molecules present, as well as their structural and physicochemical properties, for example, dimensions, electrical charge, packing, and interactions (Chapters 4 and 7). Information about the rate of coalescence within a homogenizer can be obtained using a variety of methods. A number of methods that have been proved particularly useful are briefly discussed below.

In the first method, an emulsion is recirculated through a homogenizer at a fixed operating pressure until a constant droplet size distribution is obtained where droplet coalescence is balanced by droplet disruption (Mohan and Narsimhan, 1997; Narsimhan and Goel, 2001). The operating pressure is then reduced to a new value and the change in droplet size distribution with homogenization time (or number of passes) is monitored. The droplet size increases with homogenization time due to droplet coalescence until a new (larger) steady-state value is reached where droplet coalescence is again balanced by droplet disruption. The faster the coalescence rate within the homogenizer, the faster the increase in droplet size.

In the second method, an oil-in-water emulsion is prepared that contains a hydrophobic fluorescent probe in a fraction of the droplets, but no probe in the remainder of the droplets (Lobo, 2002; Lobo et al., 2002). This “mixed emulsion” is prepared by combining an emulsion that contains no probe with an emulsion that contains some probe, with all other aspects of the emulsions being similar, for example, droplet size distribution, oil type, emulsifier type. The fluorescent probe is chosen so that the fluorescent emission spectrum depends on the local probe concentration in the oil phase, for example, due to formation of dimers that have a different spectrum than monomers. Coalescence during homogenization causes the dispersed phases of different droplets to be mixed, thereby reducing the local probe concentration and changing the fluorescence spectrum. Measurement of the change in fluorescence spectrum with time provides information about the coalescence rate.

In the third method, a “mixed emulsion” is prepared by combining two oil-in-water emulsions that contain different colored oil-soluble dyes within the droplets (e.g., blue and yellow), but are similar in other aspects (Schubert et al., 2003). The mixed emulsion is then homogenized by recirculating it through a homogenizer at a fixed operating pressure and the change in droplet composition with homogenization time (or number of passes) is monitored by measuring the change in the color of the droplets using optical microscopy. As homogenization proceeds, the droplets coalesce with each other and their contents are mixed, which results in a decrease in the fraction of droplets with the initial dye colors (yellow and blue) and an increase in the fraction of droplets of mixed color (green).

In the fourth method, a “mixed emulsion” is prepared by combining two oil-in-water emulsions that contain different oil types (e.g., hexadecane and 1-bromo-hexadecane or hexadecane and octadecane), but are otherwise similar. The mixed emulsion is then homogenized by recirculating it through a homogenizer at a fixed operating pressure and the change in droplet composition due to coalescence is monitored with homogenization time (or number of passes). The change in droplet composition with time is determined by measuring some physical property of the system that depends on oil composition, for example, refractive index (Tainse et al., 1996) or melting point (Elwell et al., 2003).

The above methods can be used to quantify the factors that influence droplet coalescence within a homogenizer. For protein-stabilized emulsions in a high-pressure valve homogenizer, the coalescence rate was found to be higher for higher homogenization pressures, larger drop sizes, higher dispersed phase volume fractions, pH values closer to the isoelectric point, and high ionic strengths (Mohan and Narsimhan, 1997). For emulsions stabilized by ionic surfactants prepared using a high-pressure valve homogenizer, the coalescence rate was found to be higher for higher homogenization pressures, for lower surfactant concentrations, and to depend on dispersed phase volume fraction and ionic strength (Tainse et al., 1996; Narsimhan and Goel, 2001; Lobo and Svereika, 2003). Coalescence rates of oil-in-water emulsions stabilized by different kinds of emulsifier have also been compared, for example, in high-pressure valve homogenizers, the coalescence rate was higher for whey protein than for sodium caseinate stabilized droplets (Mohan and Narsimhan, 1997), was higher for egg yolk than for Tween stabilized droplets (Schubert et al., 2003) and was higher for Tween 20 than for caseinate stabilized droplets (Elwell et al., 2003).

#### 6.4.3 *The role of the emulsifier*

The above discussion has highlighted two of the most important functions of emulsifiers during the homogenization process:

1. They decrease the interfacial tension between the oil and water phases, thereby reducing the amount of free energy required to deform and disrupt the droplets.
2. They form a protective coating around the droplets that prevents them from coalescing with each other.

The size of the droplets produced during homogenization therefore depends on a number of different characteristics of an emulsifier: (a) the ratio of emulsifier to dispersed phase—there must be sufficient emulsifier present to completely cover the surfaces of the droplets formed, (b) the time required for the emulsifier to move from the bulk phase to the droplet surface—the faster the adsorption time, the smaller the droplet size, (c) the probability that an emulsifier molecule will be adsorbed to the surface of a droplet during an encounter between it and the droplet—the greater the adsorption efficiency, the smaller the droplet size, (d) the amount that the emulsifier reduces the interfacial tension—the

greater the amount, the smaller the droplet size, (e) the extent to which the emulsifier alters the dynamic interfacial rheology—the greater the resistance to deformation, the more difficult is droplet disruption (larger size) and the less likely is droplet coalescence (smaller size), and (f) the effectiveness of the emulsifier membrane at protecting the droplets against coalescence—the better the protection, the smaller the droplet size.

## 6.5 Homogenization devices

A number of different types of homogenization devices have been developed to produce food emulsions. Each of these devices has its own advantages and disadvantages, and range of materials where it is most suitably applied. The choice of a particular homogenizer depends on whether the emulsion is being made in a factory or in a laboratory, the equipment available, the volume of material to be homogenized, the desired throughput, the nature of the starting materials, the desired droplet size distribution, the required physicochemical properties of the final product, and the cost of purchasing and running the equipment. The most important types of homogenizers used in the food industry or by food scientists working in research laboratories are discussed below. The general characteristics of these different homogenizers are compared in Table 6.1.

### 6.5.1 High-speed mixers

High-speed mixers are the most commonly used method for directly homogenizing oil and aqueous phases in the food industry (Loncin and Merson, 1979; Brennan et al., 1981; Fellows, 2000). In a batch process, the oil, water, and other ingredients to be homogenized are placed in a suitable vessel (Figure 6.6), which may contain as small as a few cm<sup>3</sup> (for laboratory use) or as large as several m<sup>3</sup> (for industrial use) of liquid. The components are then agitated by a mixing head that rotates at high speed (typically up to 3600 r min<sup>-1</sup>). The various ingredients may all be added at the beginning of the process or they may be

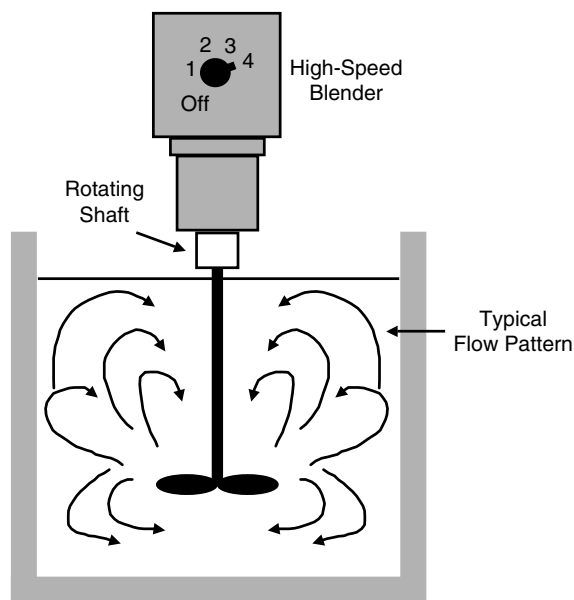


**Figure 6.6** High-speed mixers are often used in the food industry to directly homogenize oil and aqueous phases.



added sequentially to improve dispersion and/or reduce homogenization times. The rapid rotation of the mixing head generates a combination of longitudinal, rotational, and radial velocity gradients in the liquids, which disrupts the interfaces between the oil and water, causes the liquids to become intermingled, and breaks the larger droplets into smaller ones (Fellows, 1988). Efficient homogenization is achieved when the horizontal and vertical flow profiles distribute the liquids evenly throughout the vessel, which can be facilitated by having baffles fixed to the inside walls of the vessel (Gopal, 1968). The design of the mixing head also determines the efficiency of the homogenization process, and a number of different types are available for different situations, for example, blades, propellers, and turbines (Fellows, 1988). Specially designed mixing heads are often used to generate more intense and evenly distributed disruptive forces, so as to create smaller droplets, reduce homogenization times, and/or ensure more uniform mixing. The homogenization efficiency can also be increased by using countercurrent mixing devices, where the container rotates in one direction and the mixing head rotates in another. For industrial purposes, many high-speed mixing devices are available that are capable of in-line (rather than batch) operation so that products can be produced continuously. Typical throughputs for in-line devices range from a few liters to a few hundred liters hour<sup>-1</sup>. Blending generally leads to a slight increase in the temperature of an emulsion because some of the mechanical energy is converted into heat due to viscous dissipation. If any of the ingredients in the emulsion are sensitive to heat it may be necessary to control the temperature of the vessel during homogenization. High-speed mixers are particularly useful for preparing emulsions with low or intermediate viscosities (Table 6.1). The droplet size usually decreases as the homogenization time or the rotation speed of the mixing head is increased, until a lower limit is achieved which depends on the nature and concentration of the ingredients used and the power density of the mixer. Typically, the droplets produced by a high-speed mixer range between 2 and 10  $\mu\text{m}$  in diameter. Industrial mixers are often designed to avoid excessive incorporation of air bubbles during homogenization, because this can have an adverse affect on the processing and properties of many emulsion-based food products. As well as being used to create coarse food emulsions, high-speed mixers are commonly used to ensure effective dispersion and dissolution of ingredients, particularly powdered ingredients.

### 6.5.2 Colloid mills

Colloid mills are widely used in the food industry to homogenize medium and high-viscosity liquids (Loncin and Merson, 1979; Walstra, 1983; Fellows, 1988; Schubert, 1997). A variety of different designs of colloid mill are commercially available, but they all operate on fairly similar physical principles (Figure 6.7). A colloid mill usually contains two disks: a *rotor* (a rotating disk) and a *stator* (a static disk). The liquids to be homogenized are usually fed into the center of the colloid mill in the form of a coarse emulsion, rather than as separate oil and aqueous phases, because the device is much more efficient at reducing the size of the droplets in a preexisting emulsion (secondary homogenization), than at homogenizing two separate phases (primary homogenization). The coarse emulsion is usually prepared directly from the oil, water, and other ingredients using a high-speed mixer. The rapid rotation of the rotor generates a shear stress in the gap that causes the larger droplets to be broken down into smaller ones, and generates a centrifugal force that causes the fluid to move from the center to the periphery of the disks where it is either collected or passed through a pipe to another unit-operation. The intensity of the shear stresses can be altered by varying the thickness of the gap between the rotor and stator (typically from 50 to 1000  $\mu\text{m}$ ), varying the rotation speed (typically from 1000 to 20,000 r min<sup>-1</sup>), or by using disks that have roughened surfaces or interlocking teeth (Gopal, 1968; Schubert, 1997). When the surfaces of the rotor and stator are smooth the dominant droplet disruption

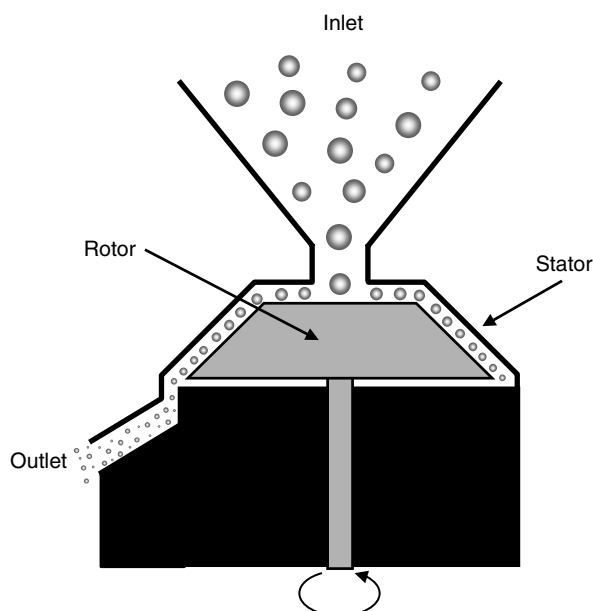


**Figure 6.7** Colloid mills are mainly used in the food industry to homogenize intermediate and high-viscosity materials.

mechanism is laminar shear flow, but when the surfaces are roughened or toothed it is turbulence (Schubert, 1997). Droplet disruption can also be enhanced by increasing the length of time the emulsion spends in the colloid mill, either by decreasing the flow rate or by passing the emulsion through the device a number of times. Typically, the flow rate can be varied between 4 and 20,000 l h<sup>-1</sup>. It should be noted that many of the factors that increase the effectiveness of droplet disruption also increase the manufacturing costs (by increasing energy costs or reducing product throughput). Food manufacturers must therefore select the rotation speed, gap thickness, rotor/stator type, and throughput that give the best compromise between droplet size and manufacturing costs. It is usually necessary to have some form of cooling device as part of a colloid mill in order to offset the increase in temperature caused by viscous dissipation losses. Colloid mills are more suitable for homogenizing intermediate and high-viscosity fluids (such as peanut butter, fish, or meat pastes) than high-pressure valve or ultrasonic homogenizers (Table 6.1). Typically, they can be used to produce emulsions with droplet diameters between 1 and 5  $\mu\text{m}$ .

### 6.5.3 High-pressure valve homogenizers

High-pressure valve homogenizers are probably the most common methods of producing fine emulsions in the food industry (Lees and Pandolfe, 1986; Stang et al., 2001). Like colloid mills, they are more effective at reducing the size of the droplets in a preexisting emulsion, than at creating an emulsion directly from two separate liquids (Pandolfe, 1991, 1995). A coarse emulsion is usually produced using a high-speed mixer and is then fed directly into the input of the high-pressure valve homogenizer. The homogenizer has a pump that pulls the coarse emulsion into a chamber on its backstroke and then forces it through a narrow valve at the end of the chamber on its forward stroke (Figure 6.8). As the coarse emulsion passes through the valve it experiences a combination of intense disruptive forces that cause the larger droplets to be broken down to smaller ones (Phipps, 1985). The actual flow regime that is responsible for disrupting the droplets in a particular high-pressure valve homogenizer

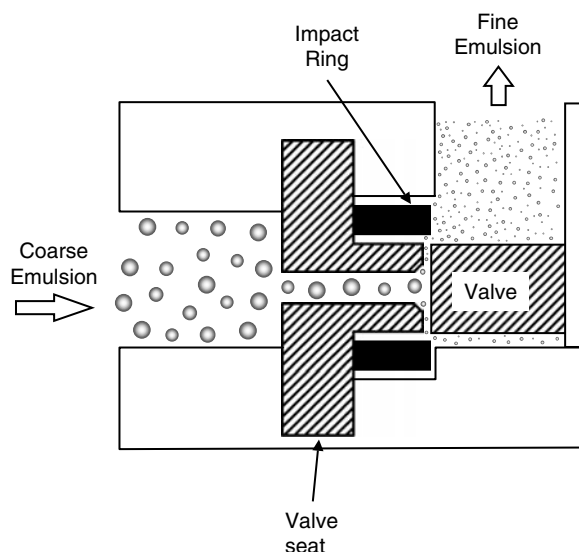


**Figure 6.8** High-pressure valve homogenizers are used to produce emulsions with fine droplet sizes.

depends on the characteristics of the material being homogenized (e.g., viscosity), the size of the homogenizer (e.g., bench-top or production), and the design of the homogenization nozzle (Walstra and Smulder, 1998; Stang et al., 2001). Different types of nozzles have been designed to increase the efficiency of droplet disruption for different kinds of applications, for example, standard, microfluidizer\*, jet disperser, or orifice valve (Schubert et al., 2003). The dominant droplet disruption mechanism tends to be *inertial forces* in turbulent flow for standard nozzle and microfluidizer nozzles, and *shear forces* in laminar elongational flow for jet disperser and orifice valves (Stang et al., 2001). Most commercial homogenizers use spring-loaded standard valves so that the gap through which the emulsion passes can be varied (typically between 15 and 300  $\mu\text{m}$ ). Decreasing the gap size increases the pressure drop across the valve, which causes a greater degree of droplet disruption and smaller droplets to be produced. On the other hand, decreasing the gap size increases the energy input required to form an emulsion, thereby increasing manufacturing costs. The throughputs of industrial homogenizers typically vary between 100 and 20,000  $\text{l h}^{-1}$ , while homogenization pressures vary between 3 and 20 MPa.

Experiments have shown that there is an approximately linear relationship between the logarithm of the homogenization pressure ( $P$ ) and the logarithm of the droplet diameter ( $d$ ), that is,  $\log d \propto \log P$  (Walstra, 1983; Phipps, 1985; Walstra and Smulder, 1998; Stang et al., 2001). The constant of proportionality depends on the dominant flow regime inside the homogenizer, which in turn depends on the dimensions of the homogenizer, the dominant droplet disruption mechanism, and the fluid viscosity (Walstra and Smulder, 1998; Stand et al., 2001). For a large homogenizer and a low fluid viscosity, the flow regime is predominantly TI and  $d \propto P^{-0.6}$ . For a large homogenizer and a high fluid viscosity, the flow regime is predominantly TV and  $d \propto P^{-0.75}$ . For small homogenizers, like those used in many laboratory studies, the flow regime may even be LV and  $d \propto P^{-1.0}$ . In addition, the efficiency of droplet disruption also depends on the dimensions of the homogenizer because of the different times that the emulsion spends in the region where droplet disruption actually occurs. In large homogenizers, the droplets may experience many more disruption events

\* Microfluidizer homogenizers are discussed in more detail in a later section.

than in a small homogenizer operating at the same pressure, and therefore droplet disruption is more efficient. These differences in the dominant flow profiles present within homogenizers of different dimensions have to be taken into account when one wants to scale-up from laboratory experiments to actual production (Walstra and Smulder, 1998).

Some commercial devices use a “two-stage” homogenization process, in which the emulsion is forced through two consecutive valves. The first valve is at high pressure and is responsible for breaking up the droplets, while the second valve is set at a lower pressure and is mainly responsible for disrupting any “flocs” that are formed during the first stage (Phipps, 1985).

High-pressure valve homogenizers can be used to produce a wide variety of different food products, although they are most suitable for low and intermediate viscosity materials, particularly when a small droplet size is required. If the oil and aqueous phases have been blended prior to homogenization, it is often possible to create an emulsion with submicron particles using a single pass through the homogenizer (Pandolfe, 1995). If very fine emulsion droplets are required it is usually necessary to pass the emulsion through the homogenizer a number of times. Emulsion droplets with diameters as low as  $0.1\text{ }\mu\text{m}$  can be produced using this method, provided there is sufficient emulsifier present to completely cover the oil–water interface formed and that the emulsifier adsorbs rapidly enough to prevent droplet coalescence.

The temperature rise in a high-pressure valve homogenizer is often fairly small, but it can become appreciable if the emulsion is recirculated or particularly high pressures are used. In these cases it may be necessary to keep the emulsion cool by using a water-jacketed homogenization chamber. In other circumstances it may be necessary to keep the homogenizer warm during the homogenization process, for example, to prevent crystallization of a lipid phase (Schubert et al., 2003).

#### 6.5.4 Ultrasonic homogenizers

Ultrasonic homogenizers have been used for many years to produce emulsions (McCarthy, 1964; Gopal, 1968; Abismail et al., 1999; Canselier et al., 2002). This type of homogenizer uses high-intensity ultrasonic waves that generate intense shear and pressure gradients within a material that disrupt the droplets mainly due to cavitation and turbulent effects (Section 6.4.). A number of methods are available for generating high-intensity ultrasonic waves, but only two are commonly used in industry: piezoelectric transducers and liquid jet generators (Gopal, 1968; Canselier et al., 2002).

Piezoelectric transducers are used in the bench-top ultrasonic homogenizers that are found in many research laboratories (Figure 6.9a). They are ideal for preparing small volumes of emulsion (a few  $\text{cm}^3$  to a few  $100\text{ cm}^3$ ), which is an important consideration in research laboratories because the chemicals used are often expensive. An ultrasonic transducer consists of a piezoelectric crystal contained within a protective metal casing, which is usually tapered at the end. A high-intensity electrical wave is applied to the transducer, which causes the piezoelectric crystal inside it to rapidly oscillate and generate an ultrasonic wave. The ultrasonic wave is directed toward the tip of the transducer where it radiates into the surrounding liquids and generates intense pressure and shear gradients (mainly due to cavitation effects) that cause the liquids to be broken up into smaller fragments and intermingled with one another. The fact that the ultrasonic energy is focused on a small volume of the sample near the tip of the ultrasonic transducer means that it is important to have good agitation in the sample container. In small vessels this is achieved by the fluid flow induced by the ultrasonic field itself, but in large vessels it is often necessary to have additional agitation to ensure effective mixing and homogenization of all of the sample. To create a stable emulsion it is usually necessary to irradiate a sample

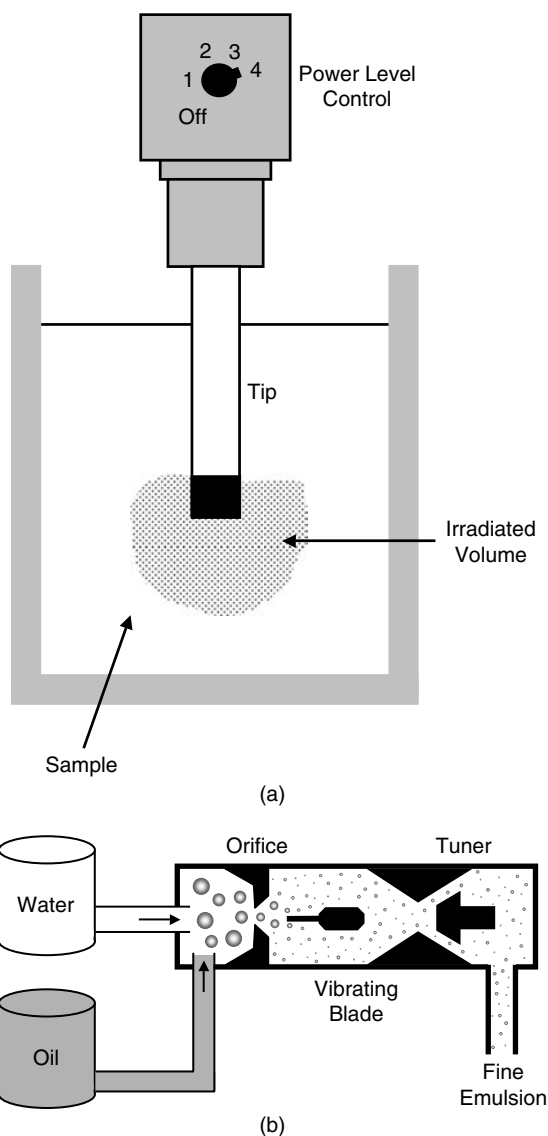


**Figure 6.9** Ultrasonic probe (a) and jet homogenizers (b) are commonly used in the food industry for the production of emulsions. These devices work principally by generating intensity disruptive forces through a cavitation mechanism.

with ultrasound for periods ranging from a few seconds to a few minutes. Continuous application of ultrasound to a sample can cause appreciable heating, and so it is often advantageous to apply the ultrasound in a number of short bursts. Traditionally, piezoelectric type homogenizers were used for batch preparation of emulsions, but in-line flow-through versions have also been developed (Canselier et al., 2002; Schubert et al., 2003). It should be noted that prolonged exposure of certain food components to high-intensity ultrasound can promote degradation, for example, oxidation of lipids, depolymerization of polysaccharides, or denaturation of proteins.

Ultrasonic jet homogenizers are used mainly for the industrial preparation of food emulsions (Figure 6.9b). A stream of fluid is made to impinge on a sharp edged blade that

causes the blade to rapidly vibrate, thus generating an intense ultrasonic field that breaks up any droplets in its immediate vicinity due to a combination of cavitation, shear, and turbulence (Gopal, 1968; Canselier et al., 2002). The major advantages of this device are that it can be used for the continuous production of emulsions, it can generate very small droplets, and it is usually more energy efficient than high-pressure valve homogenizers, that is, less energy is required to produce droplets of the same size (Schubert et al., 2003). Even so, the vibrating blade is prone to erosion because of the high-intensity ultrasonic field that means that it has to be replaced frequently. Fluid flow rates between 1 and 500,000  $\text{lh}^{-1}$  are possible using this technique.

The principle factors determining the efficiency of ultrasonic homogenizers are the intensity, duration and frequency of the ultrasonic waves (Gopal, 1968; Behrend et al., 2000). Below a frequency of about 18 kHz ultrasonic waves become audible and are therefore objectionable to users. In principle, emulsions can be formed using ultrasonic waves with frequencies as high as 5 MHz, but the homogenization efficiency decreases with increasing frequency (Canselier et al., 2002). For these reasons most commercial devices use ultrasonic waves with frequencies between 20 and 50 kHz. The size of the droplets produced during homogenization can be decreased by either increasing the intensity of the ultrasonic radiation or the length of time it is applied (Abismail et al., 1999; Canselier et al., 2002). A linear relationship between the logarithm of the mean droplet diameter and the logarithm of the energy input has been observed for continuous flow ultrasonic homogenizers, with a constant of proportionality of  $-0.4$  (Walstra, 1983). The efficiency of ultrasonic homogenization depends on the viscosity of the component phases (Behrend et al., 2000).

#### 6.5.5 Microfluidization

Microfluidization is a technique that is capable of efficiently creating emulsions with extremely small droplet sizes, using either primary or secondary homogenization (Dickinson and Stainsby, 1988; Strawbridge et al., 1995; Keane et al., 2000). This type of homogenizer usually consists of a fluid inlet, some kind of pumping device, and an interaction chamber containing two channels through which the fluids are made to flow and interact with each other (Figure 6.10). Fluids are introduced into the homogenizer, accelerated to a high velocity within the channels using the pumping device, and then made to simultaneously impinge with each other on a solid surface. Intense disruptive forces are generated when the fluids collide with each other, which cause the fluids to intermingle, and the droplets to be disrupted. A microfluidizer can be used to reduce the size of the droplets in a preexisting emulsion by directing portions of the coarse emulsion to flow through different channels (Figure 6.10a). Alternatively, the technique can be used to create emulsions directly from the individual oil and aqueous phases (Dickinson and Stainsby, 1988). In this case, an oil phase is directed down one channel and an aqueous phase is directed down the other channel (Figure 6.10b). Extremely small emulsion droplets can be produced by passing an emulsion through a microfluidizer a number of times or by increasing the pressure used to accelerate the fluids through the channels (Strawbridge et al., 1995). A variety of different channel types have been designed to increase the efficiency of droplet disruption, for example, straight or zig-zag channels. Microfluidizers are available for small-scale laboratory applications and for full-scale production applications. The minimum volumes that can be produced using laboratory-scale microfluidizers are around 10 ml, which is convenient for preparation of emulsions using ingredients that are costly or scarce. Operating pressures up to 275 MPa and throughputs up to 12,000  $\text{lh}^{-1}$  can be achieved using industrial microfluidizers. Similar maximum operating pressures can be achieved using laboratory models, which account for their ability to produce very small droplets, that is,  $<0.1 \mu\text{m}$ .

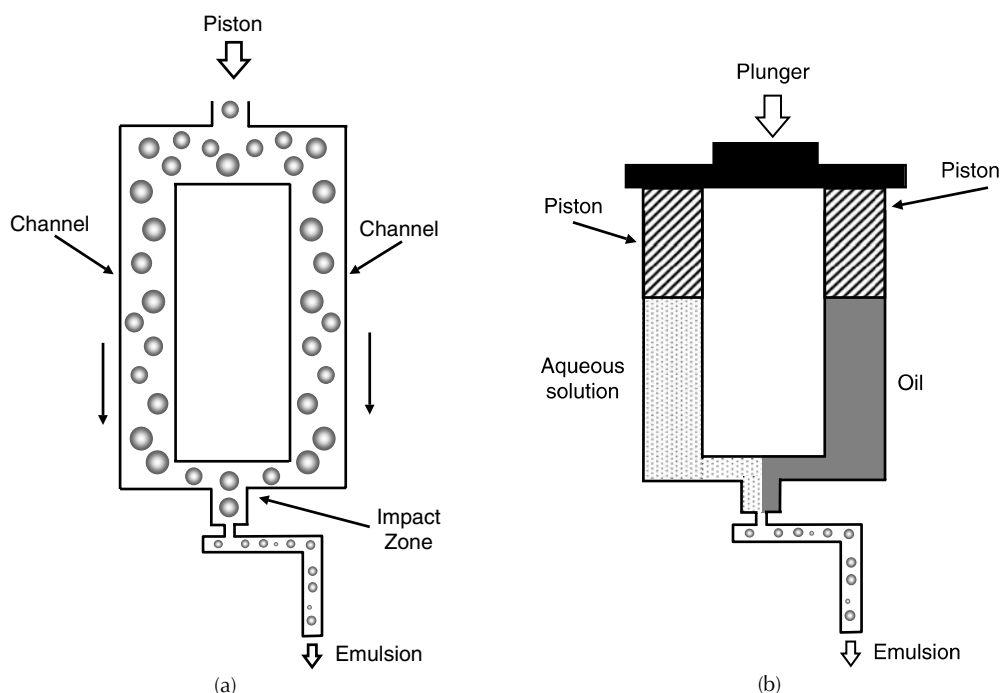


**Figure 6.10** In a microfluidizer the fluids are brought together at a high velocity that causes intermingling and droplet disruption. Microfluidizers can be used to reduce the droplet size in an existing emulsion (a) or to produce an emulsion from separate oil and water phases (b).

### 6.5.6 Membrane and microchannel homogenizers

In a membrane homogenizer, an emulsion is formed by forcing one immiscible liquid (the disperse phase) into another immiscible liquid (the continuous phase) through a solid membrane that contains small pores (Figure 6.11). The size of the droplets formed depends on the diameter of the pores in the membrane, the dynamic interfacial tension between the oil and water phases, the transmembrane pressure, and the flow of the continuous phase across the membrane (Kandori, 1995; Suzuki et al., 1996; Schröder et al., 1998; Schröder and Schubert, 1999; Vladisavljevic and Schubert, 2003a,b). Membranes can be manufactured with different mean pore diameters so that emulsions with different mean droplet sizes can be produced (Kandori, 1995). Ideally, the membrane should contain pores with similar diameters as this would lead to the production of fairly monodisperse droplets, but in practice there is often a distribution of pore sizes, which means that the droplets produced are usually more or less polydisperse. The membrane must be sufficiently strong so that it is not broken by the pressures applied to the fluids during homogenization. The polarity of the membrane is also important, as it determines the type of emulsions that can be produced (Suzuki et al., 1999). Hydrophobic membranes are needed to produce water-in-oil emulsions, whereas hydrophilic membranes are needed to produce oil-in-water emulsions. The membrane technique can be used as either a batch or a continuous process (Kandori, 1995). In the batch process, droplets are formed by forcing the dispersed phase through a cylindrical membrane that is dipped into a vessel containing the continuous phase (Figure 6.11). In the continuous process, the homogenizer consists of a cylindrical membrane through which the continuous phase flows, which is located within a tube through which the dispersed phase flows. The dispersed phase is pressurized so that

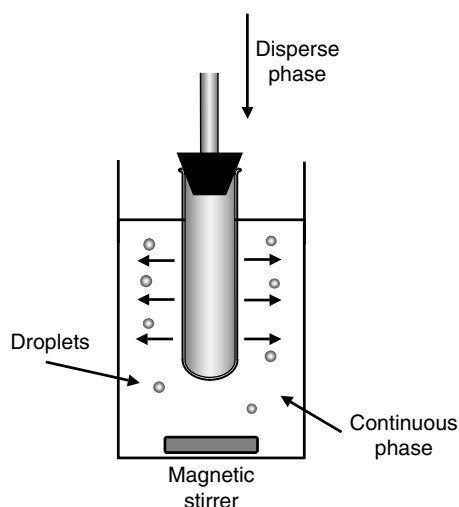


**Figure 6.11** Batch version of a membrane homogenizer. The disperse phase is forced into the continuous phase through small pores in a solid membrane.

it is forced through the membrane, where it forms small droplets in the continuous phase. More recently it has been found that membrane homogenizers can also be used to effectively reduce the size of droplets in preexisting coarse emulsions, for example, those prepared by high-speed blending. The major advantages of this approach are that higher transmembrane fluxes can be achieved and emulsions with higher droplet concentrations can more easily be produced.

Microchannel homogenizers work on a fairly similar principle to membrane homogenizers, except that the disperse phase is forced through microchannels with well-defined geometries and the droplets detach due to a Laplace instability mechanism (Schubert and Lambrich, 2003). This technique has proved to be particularly useful for producing droplets with very narrow particle size distributions (Kawakatsu et al., 1997; Kobayashi et al., 2003).

An increasing number of applications for membrane and microchannel homogenizers are being identified, and instruments based on these principles can now be purchased commercially for preparing emulsions in the laboratory (Kandori, 1995; Schröder and Schubert, 1999; Nakashima et al., 2000). These instruments can be used to produce oil-in-water, water-in-oil, and multiple emulsions, by selecting a material with an appropriate polarity to make the membranes or microchannels from (Schroder and Schubert, 1999; Suzuki et al., 1999; Kawakatsu et al., 2001; Christov et al., 2002; Sugiura et al., 2004). The major advantages of this type of homogenizer are the ability to produce emulsions with narrow droplet size distributions and the fact that they are highly energy efficient because much less energy is lost due to viscous dissipation (Vladisavljevic and Schubert, 2003a,b). Emulsions with mean droplet diameters as low as 0.3  $\mu\text{m}$  can be produced using these homogenizers.

### 6.5.7 Homogenization efficiency

The energy efficiency of a homogenizer ( $\epsilon_H$ ) can be calculated by comparing the minimum amount of energy theoretically required to form an emulsion ( $E_{\min}$ ), with the actual amount of energy that is expended during homogenization ( $E_V$ ):

$$\epsilon_H = \frac{E_{\min}}{E_V} \times 100 \quad (6.8)$$



The minimum amount of energy required to form an emulsion is equal to the free energy needed to increase the interfacial area between the oil and water phases:  $E_{\min} = \Delta A \gamma$ , where  $\Delta A$  is the increase in interfacial area (per unit volume of emulsion) and  $\gamma$  is the interfacial tension. For a typical oil-in-water emulsion,  $E_{\min}$  has a value of about  $3 \text{ kJ m}^{-3}$ , assuming that  $\phi = 0.1$ ,  $r = 1 \text{ }\mu\text{m}$ , and  $\gamma = 10 \text{ mN m}^{-1}$  (Walstra, 1983). The actual amount of energy required to form an emulsion depends on the type of homogenizer used and the operating conditions. For a high-pressure valve homogenizer,  $E_v$  is typically about  $10,000 \text{ kJ m}^{-3}$ , and so the homogenization efficiency is less than 0.1% (Walstra, 1983). The reason that homogenization is such an inefficient process is because the disruption of small droplets requires the generation of extremely high-pressure gradients. These pressure gradients must be large enough to overcome the Laplace pressure gradient ( $\approx 2\gamma/r^2$ ), which is about  $2 \times 10^{10} \text{ Pa m}^{-1}$  for a  $1 \text{ }\mu\text{m}$  emulsion droplet. The pressure gradient due to shear forces acting across a droplet is given by  $G\eta_c/r$ , which indicates that the shear rate must exceed about  $2 \times 10^7 \text{ sec}^{-1}$  in order to disrupt the droplets. The movement of liquids at such high shear rates leads to large amounts of energy dissipation because of frictional losses. The conversion of mechanical work into heat also accounts for the increase in temperature observed during homogenization.

The total amount of energy supplied to an emulsion during the homogenization process is often referred to as the energy density, which has been defined as the energy input per unit volume of emulsion, or the power input per unit volume flow rate of emulsion (Schubert et al., 2003). In general, the energy density is given by the following relation (Walstra and Smulder, 1998):

$$E_v = \int P_v(t) dt$$

where  $P_v$  is the net power density and  $t$  is the duration of the emulsification procedure. Droplet disruption only occurs when  $P_v$  exceeds some critical value, which depends on the Laplace pressure of the droplets. If the net power density is below this in any region within the homogenizer, then droplet disruption will not occur and the energy is wasted. The values of  $E_v$  or  $P_v$  used in the above equation depend on the type of homogenizer used to create the emulsion (Walstra and Smulder, 1998; Canselier et al., 2002; Schubert et al., 2003). For most of the major types of homogenizers used in the food industry theoretical or semiempirical relationships are available to calculate the energy density (Schubert, 1997; Canselier et al., 2002; Schubert et al., 2003). For example, in a high-pressure valve homogenizer, the energy density is equal to the operating pressure:  $E_v = P$ . Alternatively, an estimation of the net energy consumption of a homogenizer can be determined by measuring the increase in temperature of the emulsion during homogenization (since >99.9% of the energy is lost as heat) or by measuring the electrical power requirements of the homogenizer (Walstra and Smulder, 1998; Abismail et al., 1999).

A number of methods of improving the energy efficiency of homogenizers have been suggested (Walstra and Smulder, 1998):

- Homogenization efficiency is normally improved by increasing the net power intensity and decreasing the duration of the emulsification process. This can be achieved by increasing the fluid volume where droplet disruption occurs efficiently relative to that where droplet disruption is inefficient.
- Homogenization efficiency can often be improved by increasing the disperse phase volume fraction of the emulsion, then diluting it to the desired droplet concentration afterward. This approach is effective because most of the energy lost during homogenization is due to friction, which is proportional to the overall emulsion volume. Experiments have shown that the same droplet diameter can often be achieved by

a homogenizer if the ratio of emulsifier to disperse phase and the homogenization conditions are kept constant. Hence, increasing the disperse phase volume fraction reduces the overall frictional losses required to produce the same droplet size.

- Homogenization efficiency can be improved by increasing the emulsifier concentration, since this leads to a greater decrease in interfacial tension and faster emulsifier adsorption, thereby facilitating droplet disruption and retarding droplet coalescence.
- Homogenization efficiency can often be improved by using a combination of different homogenizers, or by using the same homogenizer at increasing intensities. This approach is based on the principle that different kinds of flow regime are more or less efficient at disrupting different sized droplets. For example, homogenizing using a high-speed blender and then a high-pressure valve homogenizer is more energy efficient than using either technique alone.

### 6.5.8 Comparison of homogenizers

The choice of a homogenizer for a particular application depends on a number of factors, including the desired droplet size distribution, the volume of sample to be homogenized, the desired throughput, the energy consumption, the physicochemical properties of the component phases and the final product, the equipment available, the initial costs, and the running costs (Karbstein and Schubert, 1995; Schubert, 1997). After choosing the most suitable type of homogenizer, one must select the optimum operating conditions for that particular device, such as flow rate, pressure, gap thickness, temperature, homogenization time, and rotation speed (Karbstein and Schubert, 1995). Some of the most important differences between homogenizers are briefly discussed below:

#### 6.5.8.1 Energy densities and efficiency

A plot of the mean droplet size produced by a homogenizer as a function of the energy density is one of the most convenient means of establishing its effectiveness and efficiency at creating emulsions with small droplets (Figure 6.12). Homogenizers vary considerably

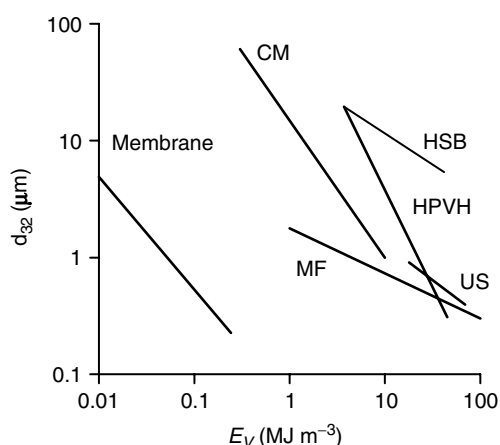


**Figure 6.12** Comparison of homogenization characteristics of different mechanical homogenizers—variation of mean droplet size with energy input: HPVH = high-pressure valve homogenizer; CM = colloid mill; US = ultrasonic homogenizer; HSB = high-speed blender; MF = microfluidizer. In practice, the precise relationship for a given device depends on the specific characteristics of the emulsion and homogenizer. (Adapted from Walstra, 1983 and Schubert et al., 2003.)

in the range of energy densities that they are capable of generating, and in the efficiency of these energy levels at disrupting emulsion droplets (Figure 6.12). High-speed mixers and colloid mills are only suitable for preparing emulsions with relatively large droplet sizes ( $r > 1 \mu\text{m}$ ), whereas the other major types of homogenizers can be used to prepare submicron droplets.

#### 6.5.8.2 *Primary versus secondary homogenization*

Some homogenizers can be used to convert separate oil and aqueous phases directly into an emulsion (primary homogenization), whereas others can only be used to reduce the size of the droplets in a preexisting emulsion (secondary homogenization). High-speed mixers, membrane homogenizers, ultrasonic homogenizers, and some forms of microfluidizer can be used for primary homogenization, whereas high-pressure valve homogenizers and colloid mills are most suitable for secondary homogenization.

#### 6.5.8.3 *Product rheology*

Another important difference between homogenizers is the rheological characteristics of the materials that they can handle during the homogenization process. Some high-speed mixers and colloid mills can be used to homogenize highly viscous fluids, whereas most other types of homogenizers are only suitable for low and/or intermediate viscosity fluids.

#### 6.5.8.4 *Product volume or throughput*

For industrial applications one usually wants to produce the largest volume of material in the shortest amount of time. Most of the homogenizers mentioned in this chapter are capable of high volume throughputs, either in a batch or continuous operation mode, although there are significant differences in their maximum capacities. In particular, membrane and microchannel homogenizers usually have appreciably lower maximum flow rates than the other major types of homogenizers. In research and development applications, one often needs to prepare small volumes of emulsion because the ingredients are relatively expensive. In these situations it is often possible to use scaled-down versions of industrial equipment or to use small-scale instruments specifically designed for laboratory usage. Ultrasonic transducers are widely available in many laboratories to produce small volumes of emulsions, but one has to be careful that the high-intensity levels used do not promote degradation reactions, such as protein denaturation, lipid oxidation, or polysaccharide depolymerization.

#### 6.5.8.5 *Droplet distribution characteristics*

There are appreciable differences in the distribution of droplet sizes that can be produced by different kinds of homogenizer. Some homogenizers are capable of generating narrow droplet size distributions (e.g., membrane and microchannel homogenizers), whereas others are only capable of generating rather broad distributions (e.g., high-speed mixers, high-pressure valve homogenizers, colloid mills, microfluidizers, and ultrasonic homogenizers) (Walstra and Smulders, 1998; Schubert et al., 2003; Vladislavjevic et al., 2004). The use of membrane or microchannel homogenizers may be particularly useful in situations where narrow droplet size distributions are important, for example, in fundamental studies of the relationship between droplet characteristics and emulsion properties.

#### 6.5.8.6 *Selecting and purchasing an homogenizer*

The selection of an appropriate homogenizer for a particular application usually involves close cooperation between the food processor and the manufacturer of the equipment. The food processor must first specify the desired throughput, pressure, temperature, particle size, hygiene requirements, and properties of the sample. The equipment manufacturer will then be able to recommend a piece of equipment that is most suitable for the

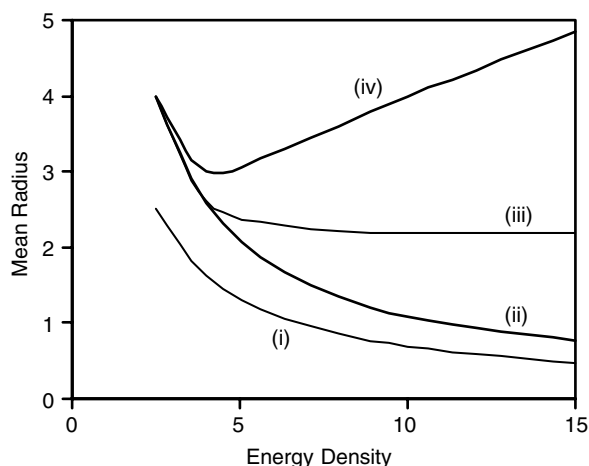


**Figure 6.13** Schematic representation of change in mean droplet size with increasing energy intensity during homogenization for different situations: (i) excess emulsifier and rapid adsorption of emulsifier to interface; (ii) excess emulsifier and slow adsorption of emulsifier to interface; (iii) insufficient emulsifier to completely cover the high surface area associated with the formation of small droplets at high energy intensities; and (iv) loss of emulsifier efficiency at high energy intensities, for example, due to denaturation.

specific product, for example, size, valve design, flow rates, and construction materials. It is good practice for food processors to test a number of homogenizers from different manufacturers under conditions that approximate those that will be used in the factory prior to making a purchase.

## 6.6 Factors that influence droplet size

The size of the droplets produced during homogenization is important because it determines the stability, appearance, texture, and taste of the final product (Chapters 7–10). To create a product with specific properties it is therefore necessary to ensure that the majority of the droplets fall within some preestablished size range. For this reason, it is important for food scientists to be aware of the major factors that influence the size of the droplets produced by homogenizers.

### 6.6.1 Emulsifier type and concentration

For a fixed concentration of oil, water, and emulsifier there is a maximum interfacial area that can be completely covered by the emulsifier. As homogenization proceeds the size of the droplets decreases and the interfacial area increases (Figure 6.13). Once the droplets fall below a certain size there may be insufficient emulsifier present to completely cover their surface and so they tend to coalesce with their neighbors. The minimum size of stable droplets that can be theoretically produced during homogenization (assuming monodisperse droplets\*) is therefore governed by the type and concentration of emulsifier present:

$$r_{\min} = \frac{3\Gamma_{\text{sat}}\phi}{c_s} = \frac{3\Gamma_{\text{sat}}\phi}{c'_s(1-\phi)} \quad (6.9)$$

\* For a polydisperse emulsion the radius used in Equation 6.9 should be the volume–surface mean radius (Chapter 1).

where  $\Gamma_{\text{sat}}$  is the excess surface concentration of the emulsifier at saturation (in  $\text{kgm}^{-2}$ ),  $\phi$  is the disperse phase volume fraction,  $c_s$  is the concentration of emulsifier in the emulsion (in  $\text{kgm}^{-3}$ ), and  $c'_s$  is the concentration of emulsifier in the continuous phase (in  $\text{kgm}^{-3}$ ). This equation indicates that the minimum droplet size can be decreased by increasing the emulsifier concentration, decreasing the droplet concentration, or using an emulsifier with a smaller  $\Gamma_{\text{sat}}$ . For a 10 vol% ( $\phi = 0.1$ ) oil-in-water emulsion containing 1% ( $\sim 10 \text{ kgm}^{-3}$ ) of emulsifier the minimum droplet radius is about 60 nm (assuming  $\Gamma_{\text{sat}} = 2 \times 10^{-6} \text{ kgm}^{-2}$ ). In practice, there are a number of factors that mean that the droplet size produced during homogenization is greater than the theoretical minimum.

In order to attain the theoretical minimum droplet size, a homogenizer must be capable of generating a pressure gradient that is large enough to disrupt any droplets that are greater than  $r_{\text{min}}$ , that is,  $>2\gamma/r_{\text{min}}^2$  (Section 6.5). Some types of homogenizers are not capable of generating such high-pressure gradients and are therefore unsuitable for producing emulsions with small droplet sizes, even though there may be sufficient emulsifier present (Walstra, 1983). The emulsion must also spend sufficient time within the homogenization zone for all of the droplets to be completely disrupted. If an emulsion passes through a homogenizer too rapidly or if there is an uneven distribution of disruptive energy within the homogenization zone, then some of the droplets may not be disrupted (Walstra and Smulder, 1998).

Even if a homogenizer is capable of producing small droplets, the emulsifier molecules must adsorb rapidly enough to form a protective interfacial layer around the droplets that prevents them from coalescing with their neighbors. The emulsifier also influences the droplet size by reducing the interfacial tension between the oil and aqueous phases, thereby facilitating droplet disruption. Consequently, the more rapid an emulsifier adsorbs, and the greater the reduction of the interfacial tension, the smaller the droplets that can be produced at a certain homogenizer energy input.

Many different types of emulsifiers can be used in the food industry, and each of these exhibits different characteristics during homogenization, for example, the speed at which they adsorb, the maximum reduction in interfacial tension, and the effectiveness of the interfacial membrane at preventing droplet coalescence. Factors that influence the adsorption kinetics of emulsifiers, and their effectiveness at reducing interfacial tension, were discussed in Chapter 5, while factors that affect the stability of droplets against coalescence will be covered in Chapter 7. A food manufacturer must select the most appropriate emulsifier for each type of food product, taking into account their performance during homogenization, solution conditions, cost, availability, legal status, ability to provide long-term stability, and the desired physicochemical properties of the product. Some of the different kinds of behavior that could be observed during homogenization are illustrated in Figure 6.13.

In summary, the influence of emulsifier concentration on droplet size can be divided into two regions (Tcholakova et al., 2002, 2003):

1. *Insufficient emulsifier.* When the emulsifier concentration is limiting (i.e., there is insufficient emulsifier present to cover all of the droplet surface area created by the homogenizer), then the droplet size is governed primarily by the emulsifier concentration, rather than the energy input of the homogenizer. The surface load of the emulsifier remains relatively constant in this regime and is close to the value of the excess surface concentration of the emulsifier at saturation ( $\Gamma_{\text{SAT}}$ ). Under these conditions the mean droplet size produced by homogenization is given by Equation 6.9.
2. *Excess emulsifier.* When the emulsifier concentration is in excess (i.e., there is more emulsifier present than is required to completely cover all of the droplet surface area created by the homogenizer), then the droplet size is relatively independent of emulsifier concentration and depends primarily on the energy input of the homogenizer. Under these circumstances the mean droplet diameter that can be produced

depends on the flow conditions prevalent in the homogenizer (see next section). If the emulsifier does not form multiple layers at the interface then the surface load of the emulsifier will remain relatively constant in this regime ( $\Gamma \approx \Gamma_{\text{SAT}}$ ). Alternatively, if the emulsifier is capable of forming multiple layers at the interface then the surface load may increase as the overall concentration of emulsifier in the system is increased ( $\Gamma > \Gamma_{\text{SAT}}$ ). This latter affect has been observed for globular proteins, such as whey proteins, where the surface load increases up to a certain level as the overall emulsifier concentration is increased (Tcholakova et al., 2002, 2003).

### 6.6.2 Energy input

The size of the droplets in an emulsion can be reduced by increasing the intensity or duration of disruptive energy supplied during homogenization (as long as there is sufficient emulsifier to cover the surfaces of the droplets formed). The range of energy inputs that can be achieved by a given homogenization device, and the effectiveness of this energy at disrupting the droplets, depends on the type of homogenizer used (Figure 6.12). The energy input can be increased in a number of different ways depending on the nature of the homogenizer. In a high-speed mixer the energy input can be enhanced by increasing the rotation speed or the length of time that the sample is blended. In a high-pressure valve homogenizer it can be enhanced by increasing the homogenization pressure or recirculating the emulsion through the device. In a colloid mill it can be enhanced by using a narrower gap between the stator and rotator, increasing the rotation speed, by using disks with roughened surfaces, or by passing the emulsion through the device a number of times. In an ultrasonic homogenizer the energy input can be enhanced by increasing the intensity of the ultrasonic wave or by sonicating for a longer time. In a microfluidizer the energy input can be enhanced by increasing the velocity at which the liquids are brought into contact with each other or by recirculating the emulsion. In a membrane homogenizer the energy input can be enhanced by increasing the pressure at which the liquid is forced through the membrane or the flow rate of the continuous phase across the membrane. Under a given set of homogenization conditions (energy intensity, emulsion composition, temperature) there is a certain size below which the emulsion droplets cannot be reduced with repeated homogenization, and therefore homogenizing the system any longer would be inefficient.

Increasing the energy input usually leads to an increase in manufacturing costs and therefore a food manufacturer must establish the optimum compromise between droplet size, time, and cost. The energy input required to produce an emulsion containing droplets of a given size depends on the energy efficiency of the homogenizer used (Walstra, 1983).

Under most circumstances there is a decrease in droplet size as the energy input is increased. Nevertheless, there may be occasions when increasing the energy actually leads to an increase in droplet size because the effectiveness of the emulsifier is reduced by excessive heating or exposure to high pressures. This could be particularly important for protein-stabilized emulsions, because the molecular structure and functional properties of some proteins are particularly sensitive to changes in their environmental conditions. For example, globular proteins, such as  $\beta$ -lactoglobulin, are known to unfold and aggregate when they are heated above a certain temperature, which reduces their ability to stabilize emulsions (Section 4.4.2).

### 6.6.3 Properties of component phases

The composition and physicochemical properties of both the oil and aqueous phases influence the size of the droplets produced during homogenization (Phipps, 1985; Walstra

and Smulder, 1998). Variations in the type of oil or aqueous phase will alter the viscosity ratio,  $\eta_D/\eta_C$ , which determines the minimum size that can be produced under steady-state conditions (Section 6.4). Different oils have different interfacial tensions when placed in contact with water because they have different molecular structures or because they contain different amounts of surface-active impurities, such as free fatty acids, monoacylglycerols, or diacylglycerols. These surface-active lipid components tend to accumulate at the oil–water interface and lower the interfacial tension thus lowering the amount of energy required to disrupt a droplet.

The aqueous phase of an emulsion may contain a wide variety of components, including minerals, acids, bases, biopolymers, sugars, alcohols, and gas bubbles. Many of these components will alter the size of the droplets produced during homogenization because of their influence on rheology, interfacial tension, coalescence stability, or adsorption kinetics. For example, the presence of low concentrations of short-chain alcohols in the aqueous phase of an emulsion reduces the size of the droplets produced during homogenization because of the reduction in interfacial tension (Banks and Muir, 1988). The presence of biopolymers in an aqueous phase has been shown to increase the droplet size produced during homogenization due to their ability to suppress the formation of small eddies during turbulence (Walstra, 1983). Protein-stabilized emulsions cannot be produced close to the isoelectric point of a protein or at high electrolyte concentrations because the proteins are susceptible to aggregation. A knowledge of the composition of both the oil and aqueous phases of an emulsion and the role that each component plays during homogenization is therefore important when optimizing the size of the droplets produced by a homogenizer.

Some studies have shown that the smallest droplet size that can be achieved using a high-pressure valve homogenizer increases as the disperse phase volume fraction increases (Phipps, 1985). There are a number of possible reasons for this (i) increasing the viscosity of an emulsion may suppress the formation of eddies responsible for breaking up droplets, (ii) if the emulsifier concentration is kept constant there may be insufficient present to completely cover the droplets, and (iii) the rate of droplet coalescence is increased. On the other hand, other studies have shown that there is little change in the mean droplet diameter with increasing disperse phase volume fraction, providing the ratio of emulsifier to disperse phase is kept constant and there is sufficient emulsifier present to cover all of the droplets formed (Schubert et al., 2003).

### 6.6.4 Temperature

Temperature influences the size of the droplets produced during homogenization in a number of ways. The viscosity of both the oil and aqueous phases is temperature dependent, and therefore the minimum droplet size that can be produced may be altered because of a variation in the viscosity ratio,  $\eta_D/\eta_C$  (Section 6.4). Usually the viscosity of oils decreases more rapidly with increasing temperature than the viscosity of water, hence  $\eta_D/\eta_C$  for an oil-in-water emulsion would tend to decrease, thereby facilitating droplet disruption at higher temperatures. Heating an emulsion usually causes a slight reduction in the interfacial tension between the oil and water phases that would be expected to facilitate the production of small droplets (Section 6.4). Certain types of emulsifiers lose their ability to stabilize emulsion droplets against flocculation and aggregation when they are heated above a certain temperature. For example, when small molecule surfactants are heated close to their phase inversion temperature they are no longer effective at preventing droplet coalescence\*, or when globular proteins are heated above a critical temperature they unfold and aggregate

\* It should be noted that droplet disruption is highly efficient near the surfactant PIT, so that it is often possible to efficiently homogenize an emulsion at this temperature to produce small droplets, then rapidly cool it to a lower temperature to reduce coalescence.

(Section 4.4.2). Alterations in temperature also influence the competitive adsorption of surface-active components, thereby altering interfacial composition, which may in turn alter the physicochemical properties of emulsions (Dickinson and Hong, 1994).

The temperature is also important because it determines the physical state of the lipid phase (Section 4.2.3). It is practically impossible to homogenize a fat that is either completely or substantially solid because it will not flow through a homogenizer or because a huge amount of energy is required to break up the fat crystals into small particles. There are also problems associated with the homogenization of oils that contain even small amounts of fat crystals because of partial coalescence (Section 7.7). The crystals from one droplet penetrate into another droplet leading to the formation of a "clump." Extensive clump formation leads to the generation of large particles and to a dramatic increase in the viscosity that would cause a homogenizer to become blocked. For this reason it is usually necessary to warm a sample prior to homogenization to ensure that the lipid phase is completely liquid. For example, milk fat is usually heated to about 40°C to melt all the fat crystals prior to homogenization (Phipps, 1985).

## 6.7 Demulsification

Demulsification is the process whereby an emulsion is converted into separate oil and aqueous phases from which it was comprised, and is therefore the opposite process to homogenization (Lissant, 1983; Menon and Wasan, 1985; Hunter, 1989). There are a number of technologic processes in the food industry where demulsification is important, for example, oil recovery or the separation of lipid and aqueous phases. Demulsification is also important in research and development because it is often necessary to divide an emulsion into separate oil and aqueous phases so that their composition or properties can be characterized. For example, the oil phase must often be extracted from an emulsion in order to determine the extent of lipid oxidation (Coupland et al., 1996) or to measure the partition coefficient of a food additive (Huang et al., 1997). Demulsification is achieved by causing the droplets to come into close contact with each other and then to coalesce. As this process continues it eventually leads to the complete separation of the oil and aqueous phases. Knowledge of the physical principles of demulsification requires an understanding of the factors that determine the stability of emulsions to flocculation and coalescence (Chapter 7).

A variety of different types of emulsifiers are used in the food industry to stabilize droplets against flocculation and coalescence (Section 4.4). Each type of emulsifier relies on different physicochemical mechanisms to prevent droplet aggregation, including electrostatic, steric, hydration, and thermal fluctuation interactions (Chapter 3). The selection of the most appropriate demulsification technique for a given emulsion therefore depends on knowledge of the type of emulsifier used to stabilize the system and of the mechanisms by which it provides stability. In the following sections, we begin by considering demulsification methods appropriate for specific types of emulsifiers, and then we consider more general methods suitable for most types of emulsifiers.

### 6.7.1 Nonionic surfactants

Nonionic surfactants usually stabilize emulsion droplets against aggregation through a combination of steric, hydration, and thermal fluctuation interactions (Chapter 3). Nevertheless, the interfacial membranes formed by nonionic surfactants are often unstable to rupture when the droplets are brought into close contact. Demulsification can therefore be achieved by altering the properties of an emulsion so that the droplets come into close contact for prolonged periods. This can often be achieved by heating an emulsion so that the polar head groups of the surfactant molecules become dehydrated, because this reduces



the hydration repulsion between the droplets and allows them to come closer together. In addition, the optimum curvature of the surfactant monolayer tends toward zero as the size of the head group decreases, which increases the likelihood of coalescence (Section 4.4.1). This demulsification technique cannot be used for some emulsions stabilized by nonionic surfactants because the phase inversion temperature is much greater than 100°C, or because heating may cause degradation or loss of one of the components being analyzed. In these cases, it is necessary to induce demulsification using alternative methods.

The addition of medium chain alcohols has also been found to be effective at promoting demulsification in some systems (Menon and Wasan, 1985). There are two possible explanations for this behavior: (i) the alcohol displaces some of the surfactant molecules from the interface and forms an interfacial membrane that provides little protection against droplet aggregation and (ii) the alcohol molecules are able to get between the tails of the surfactant molecules at the interface, thereby causing the optimum curvature of the interface to tend toward zero and increasing the likelihood of droplet coalescence (Section 4.4.1). In some emulsions, it is possible to promote droplet coalescence by adding a strong acid that cleaves the head groups of the surfactants from their tails so that the polar head group moves into the aqueous phase and the nonpolar tail moves into the droplet, thereby providing little protection against droplet coalescence.

### 6.7.2 *Ionic surfactants*

Ionic surfactants stabilize droplets against coalescence principally by electrostatic repulsion (Section 3.4). Like nonionic surfactants, the membranes formed by ionic surfactants are not particularly resistant to rupture once the droplets are brought into close contact (Evans and Wennerstrom, 1994). The most effective method of inducing droplet coalescence in these systems is therefore to reduce the magnitude of the electrostatic repulsion between the droplets (Menon and Wasan, 1985). This can be achieved by adding electrolyte to the aqueous phase of the emulsion so as to screen the electrostatic interactions. Sufficient electrolyte must be added so that the energy barrier between the droplets decreases below a critical level (~20 kT) (Section 3.11.2). This process can most easily be achieved using multivalent ions, because they are more effective at screening electrostatic interactions at low concentrations than monovalent ions. In addition, the addition of electrolyte may cause the optimum curvature of ionic surfactants to tend toward zero thereby promoting droplet coalescence (Section 4.4.1). Alternatively, the pH may be altered so that the surfactant loses its charge, which depends on the dissociation constant of the ionizable groups. Electromechanical methods can also be used to promote demulsification. An electric field is applied across an emulsion that causes the charged droplets to move toward the oppositely charged electrode. A semipermeable membrane is placed across the path of the droplets that captures the droplets but allows the continuous phase to pass through. The droplets are therefore forced against the membrane until their membranes are ruptured and they coalesce.

### 6.7.3 *Biopolymer emulsifiers*

Biopolymers principally stabilize droplets against coalescence through a combination of electrostatic and polymeric steric interactions. In addition, they tend to form thick viscoelastic membranes that are highly resistant to rupture. There are two different strategies that can be used to induce droplet coalescence in this type of system:

1. The biopolymer can be digested by strong acids, bases, or enzymes so that it is broken into small fragments that are either not surface active or do not form a sufficiently strong membrane.

2. The biopolymers are displaced from the interface by small molecule surfactants and then the droplets are destabilized using one of the methods described in the previous sections. Some proteins are capable of forming an interfacial membrane in which the molecules are covalently bound to each other through disulfide bonds. In order to displace these proteins it may be necessary to cleave the disulfide bonds prior to displacing the proteins, for example, by adding mercaptoethanol.

The Gerber and Babcock methods of determining the total fat content of milk are examples of the first of these strategies, while the detergent method is an example of the second (Pike, 2003).

#### 6.7.4 General methods of demulsification

A variety of physical techniques are available that can be used to promote demulsification in most types of emulsions. In all of the demulsification processes mentioned above, the separation of the oil phase from the aqueous phase can be facilitated by centrifuging the emulsion after the coalescence process has been initiated. In some emulsions, it is also possible to separate the phases directly by centrifugation at high speeds, without the need for any pretreatment (Menon and Wasan, 1985; van Aken, 2004). Centrifugation forces the droplets to one end of the container, which causes their interfacial membranes to become ruptured and therefore leads to phase separation.

Demulsification can also be achieved using various types of filtration devices (Menon and Wasan, 1985). The emulsion is passed through a filter that adsorbs emulsion droplets. When a number of these adsorbed droplets come into close contact they merge together to form a single large droplet that is released back into the aqueous phase. As the emulsion passes through the filter this process continues until eventually the oil and water phases are completely separated from each another.

Finally, freeze-thaw cycling is a particularly efficient method of promoting droplet coalescence and oiling-off in many types of emulsions. The emulsion is cooled to a temperature where the water freezes, and is then cooled back to room temperature. This process can be repeated a number of times to improve its effectiveness.

#### 6.7.5 Selection of most appropriate demulsification technique

As well as depending on the type of emulsifier present, the choice of an appropriate demulsification technique also depends on the sensitivity of the other components in the system to the separation process. For example, if one is monitoring lipid oxidation or trying to determine the concentration of an oil-soluble volatile component it is inadvisable to use a demulsification technique that requires excessive heating. On the other hand, if the sample contains a lipid phase that is crystalline it is usually necessary to warm the sample to a temperature where all the fat melts prior to carrying out the demulsification procedure.

### 6.8 Future developments

Homogenization is an extremely important step in the production of emulsion-based food products. The efficiency of this process has a large impact on the bulk physicochemical and sensory properties of the final product. This chapter has reviewed the progress that has already been made in identifying the factors that influence homogenization. Nevertheless, a great deal of research is still required before we can fully understand this process because of the inherent complexity of the physicochemical processes involved. The existing

theories need to be extended to give a more realistic description of emulsion formation in commercial homogenization devices. In addition, systematic experiments using well characterized emulsions and homogenization devices need to be carried out. Our understanding of this area will also be advanced due to the valuable insights provided by computer simulations. Computer models have been developed to predict the size distribution of droplets produced in homogenizers (Lachaise et al., 1996). These models can take into account the competition between droplet disruption and droplet coalescence mechanisms, as well as the influence of emulsifier adsorption kinetics on these processes. In addition, the development and refinement of novel methods of creating emulsions (such as membrane and microchannel homogenizers) are likely to continue, which may lead to the introduction of more efficient methods of creating emulsions in the laboratory or factory.

Before finishing this chapter it is important to mention that homogenization is only one step in the formation of a food emulsion. A number of other processing operations usually come before or after homogenization, including chilling, freezing, pasteurization, drying, mixing, churning, and whipping. The quality of the final product is determined by the affect that each of these processing operations has on the properties of the food. Homogenization efficiency may be influenced by the effectiveness of any of the preceding processing operations, and it may alter the effectiveness of any of the following processing operations. Thus it is important to establish the interrelationship between the various food processing operations on the final properties of a product.

## chapter seven

---

# Emulsion stability

### 7.1 Introduction

The term “emulsion stability” refers to the ability of an emulsion to resist changes in its properties over time: the more stable the emulsion, the more slowly its properties change. An emulsion may become unstable due to a number of different types of physical and chemical processes.\* Physical instability results in an alteration in the spatial distribution or structural organization of the molecules, whereas chemical instability results in an alteration in the kind of molecules present. Creaming, flocculation, coalescence, partial coalescence, phase inversion, and Ostwald ripening are examples of physical instability (Dickinson and Stainsby, 1982; Dickinson, 1992; Walstra, 1996a, 2003a), whereas oxidation and hydrolysis are common examples of chemical instability (Fennema, 1996; McClements and Decker, 2000). The development of an effective strategy to prevent undesirable changes in the properties of a particular food emulsion depends on the dominant physicochemical mechanism(s) responsible for the changes. In practice, two or more of these mechanisms may operate in concert. It is therefore important for food scientists to identify the relative importance of each mechanism, the relationship between them, and the factors that influence them, so that effective means of controlling the stability and physicochemical properties of emulsions can be established.

The length of time that an emulsion must remain stable depends on the nature of the food product (Dickinson, 1992). Some food emulsions are formed as intermediate steps during a manufacturing process, and therefore only need to remain stable for a few seconds, minutes, or hours (e.g., cake batter, ice cream mix, and margarine premix), whereas others must remain stable for days, months, or even years prior to consumption (e.g., mayonnaise, salad dressings, and cream liqueurs). On the other hand, the production of some foods involves a controlled *destablization* of an emulsion during the manufacturing process, for example, margarine, butter, whipped cream, and ice cream (Mulder and Walstra, 1974; Boode, 1992; Chrysam, 1996; Goff, 1997a–c, 2002, 2003; Walstra, 1999; Goff and Hartel, 2003). One of the major objectives of emulsion scientists working in the food industry is to establish the specific factors that determine the stability of each particular type of food emulsion, as well as to elucidate general principles that can be used to predict the behavior of food products or processes. In practice, it is very difficult to quantitatively predict the stability of food emulsions from first principles because of their compositional and structural complexity. Nevertheless, an appreciation of the origin and nature of the various destabilization mechanisms is still an invaluable tool for controlling and improving emulsion stability. Because of the difficulties in theoretically predicting emulsion

\* It should be noted that the properties of emulsions may also change with time due to microbiological changes, for example, the growth of specific types of bacteria or mould.

stability, food scientists often rely on the use of analytical techniques to experimentally monitor changes in emulsion properties over time. By using a combination of theoretical understanding and experimental measurements food manufacturers are able to predict the influence of different ingredients, processing operations, and storage conditions on the stability and properties of food emulsions.

The rate at which an emulsion breaks down, and the mechanism by which this process occurs, depends on its composition and microstructure, as well as on the environmental conditions it experiences during its lifetime, for example, temperature variations, mechanical agitation, and storage conditions. In this chapter, we examine the physicochemical basis of each of the major destabilization mechanisms responsible for change in food emulsion properties, as well as discussing the major factors that influence them, methods of controlling them, and experimental techniques for monitoring them. This information is particularly useful for food manufacturers who need to formulate emulsions with enhanced shelf life or to promote emulsion instability in a controlled fashion.

## 7.2 Thermodynamic and kinetic stability of emulsions

When we consider the “stability” of an emulsion it is extremely important to distinguish between its *thermodynamic stability* and its *kinetic stability* (Dickinson, 1992). Thermodynamics tells us whether a given process will occur or not, whereas kinetics tells us the rate at which it will proceed if it does occur (Atkins, 1994). All food emulsions are thermodynamically unstable systems and will eventually break down if they are left long enough. For this reason, it is differences in kinetic stability that are largely responsible for the diverse range of physicochemical and sensory properties exhibited by different food emulsions.

### 7.2.1 Thermodynamic stability

The thermodynamic instability of an emulsion is readily demonstrated if one agitates a sealed vessel containing pure oil and pure water, and then observes the change in the appearance of the system with time. The optically opaque emulsion that is initially formed by agitation breaks down over time until a layer of oil is observed on top of a layer of water (Figure 6.1).

The origin of this thermodynamic instability can be illustrated by comparing the free energy of a system consisting of an oil and an aqueous phase before and after emulsification (Hunter, 1989). To simplify this analysis we will initially assume that the oil and water have similar densities so that no creaming or sedimentation occurs. As a consequence, the final state consists of a single large droplet suspended in the continuous phase (Figure 7.1), rather than a layer of oil on top of a layer of water (Figure 6.1). In its initial state, prior to emulsification, the free energy is given by

$$G^i = G_O^i + G_W^i + G_I^i - TS_{\text{config}}^i \quad (7.1)$$

and in its final state, after emulsification, it is given by

$$G^f = G_O^f + G_W^f + G_I^f - TS_{\text{config}}^f \quad (7.2)$$

where  $G_O$ ,  $G_W$ , and  $G_I$  are the free energies of the oil phase, water phase, and the oil–water interface, respectively,  $T$  is the absolute temperature, and  $S$  is the configurational entropy

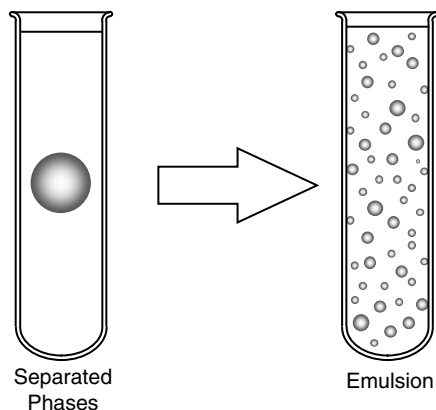


**Figure 7.1** The formation of an emulsion is thermodynamically unfavorable because of the increase in surface area between the oil and water phases.

of the droplets in the system. The superscripts  $i$  and  $f$  refer to the initial and final states of the system. The free energies of the bulk oil and water phases remain constant before and after homogenization:  $G_O^i = G_O^f$  and  $G_W^i = G_W^f$ , and so the difference in free energy between the initial and final states is given by (Hunter, 1989)

$$\Delta G_{\text{formation}} = G^f - G^i = G_I^f - G_I^i - (TS_{\text{config}}^f - TS_{\text{config}}^i) = \Delta G_I - T \Delta S_{\text{config}} \quad (7.3)$$

By definition the difference in interfacial free energy between the initial and final states ( $\Delta G_I$ ) is equal to the increase in contact area between the oil and water phases ( $\Delta A$ ) multiplied by the interfacial tension ( $\gamma$ ):  $\Delta G_I = \gamma \Delta A$ . Hence,

$$\Delta G_{\text{formation}} = \gamma \Delta A - T \Delta S_{\text{config}} \quad (7.4)$$

The change in interfacial free energy ( $\gamma \Delta A$ ) is always positive, because the contact area increases after homogenization, and therefore it opposes emulsion formation. On the other hand, the configurational entropy term ( $-T \Delta S_{\text{config}}$ ) is always negative, because the number of arrangements accessible to the droplets in the emulsified state is much greater than in the nonemulsified state, and therefore it favors emulsion formation. An expression for the configurational entropy can be derived from a statistical analysis of the number of configurations emulsion droplets can adopt in the initial and final states (Hunter, 1989):

$$\Delta S_{\text{config}} = -\frac{nk}{\phi} (\phi \ln \phi + (1 - \phi) \ln(1 - \phi)) \quad (7.5)$$

where  $k$  is Boltzmann's constant,  $n$  is the number of droplets in the emulsion, and  $\phi$  is the disperse phase volume fraction. In most food emulsions, the configurational entropy is much smaller than the interfacial free energy and can be ignored (Hunter, 1989). As an example, consider a 10 vol% oil-in-water (O/W) emulsion containing 1  $\mu\text{m}$  droplets ( $\gamma = 0.01 \text{ N m}^{-1}$ ). The interfacial free energy term ( $\gamma \Delta A$ ) is about  $3 \text{ kJ m}^{-3}$  of emulsion, whereas the configurational entropy ( $T \Delta S$ ) term is about  $3 \times 10^{-7} \text{ kJ m}^{-3}$ .

The overall free energy change associated with the creation of a food emulsion can therefore be represented by the following expression:

$$\Delta G_{\text{formation}} = \gamma \Delta A \quad (7.6)$$

Thus, the formation of a food emulsion is always thermodynamically unfavorable, because of the increase in interfacial area after emulsification. It should be noted that the configurational entropy term can dominate the interfacial free energy term in emulsions in which the interfacial tension is extremely small, and that these systems are therefore thermodynamically stable (Hunter, 1989). This type of thermodynamically stable system is usually referred to as a *microemulsion*, to distinguish it from thermodynamically unstable (macro)emulsions.

In practice, the oil and water phases normally have different densities, and so it is necessary to include a free energy term that accounts for gravitational effects, that is, the tendency for the liquid with the lowest density to move to the top of the emulsion. This term contributes to the thermodynamic instability of emulsions and accounts for the observed creaming or sedimentation of droplets (Section 7.3).

### 7.2.2 Kinetic stability

The free energy change associated with emulsion formation determines whether an emulsion is thermodynamically stable or not, but it does not give any indication of the rate at which the properties of an emulsion change with time, the type of changes that occur, or the physical mechanism(s) responsible for these changes. Information about the time dependence of emulsion stability is particularly important to food scientists who need to create food products that retain their desirable properties for a sufficiently long time under a variety of different environmental conditions. For this reason, food scientists are usually more interested in the *kinetic stability* of emulsions than in their thermodynamic stability.

The importance of kinetic effects can be highlighted by comparing the long-term stability of emulsions with the same composition but with different droplet sizes. An emulsion that contains small droplets usually has a longer shelf life (greater kinetic stability) than one that contains large droplets, even though it is more thermodynamically unstable (because it has a larger interfacial area,  $\Delta A$ ).

Despite the fact that food emulsions exist in a thermodynamically unstable state many of them remain kinetically stable (*metastable*) for months or even years. What is the origin of this kinetic stability? Conceptually, the kinetic stability of an emulsion can be attributed to an activation energy,  $\Delta G^*$ , which must be overcome before the emulsion can reach its most thermodynamically favorable state (Figure 7.2). An emulsion that is kinetically stable has to have an activation energy that is significantly larger than the thermal energy of the system ( $kT$ ). For most emulsions, an activation energy of about  $20 kT$  is sufficient to provide long-term stability (Friberg, 1997). In reality, emulsions have a number of different metastable states, and each of these has its own activation energy. Thus, an emulsion may move from one metastable state to another before finally reaching the most thermodynamically stable state. A change from one of these metastable states to another may be sufficient to have a deleterious effect on food quality.

The kinetic stability of emulsions can only be understood with reference to their dynamic nature. The droplets in an emulsion are in a continual state of motion and frequently collide into one another, due to their Brownian motion, gravity, or applied external forces. Whether droplets move apart, remain loosely associated with each other or fuse together after a collision depends on the nature of the interactions between them. The kinetic stability of emulsions is therefore largely determined by the dynamics and

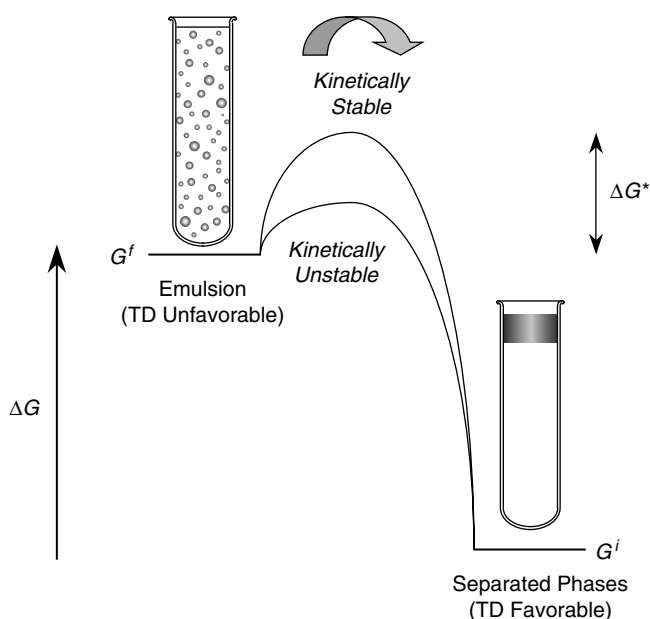


**Figure 7.2** Emulsions are thermodynamically unstable systems, but may exist in a metastable state, and therefore be kinetically stable.

interactions of the droplets they contain. Consequently, a great deal of this chapter will be concerned with the nature of the interactions between droplets and the factors that determine droplet movement in emulsions.

Earlier it was mentioned that if pure oil and pure water are agitated together a temporary emulsion is formed that rapidly reverts back to its individual components (Section 6.2). This is because there is a very low activation energy between the emulsified and unemulsified states. To create an emulsion that is kinetically stable for a reasonably long period of time it is necessary to have either an emulsifier or a texture modifier present that produces an activation energy that is sufficiently large to prevent instability. An emulsifier adsorbs to the surface of freshly formed droplets and forms a protective membrane that prevents them from merging together, while a texture modifier increases the viscosity of the continuous phase or forms a gel so that droplets collide less frequently with one another (Section 4.4 and 4.5). The role of emulsifiers and texture modifiers on emulsion stability will therefore be another common theme of this chapter.

### 7.3 Gravitational separation

In general, the droplets in an emulsion have a different density to that of the liquid that surrounds them, and so a net gravitational force acts on them (Dickinson and Stainsby, 1982; Hunter, 1989; Dickinson, 1992; Walstra, 1996a,b; Robins and Hibberd, 1998; Robins, 2000). If the droplets have a lower density than the surrounding liquid they have a tendency to move upward, which is referred to as *creaming* (Figure 7.3). Conversely, if they have a higher density than the surrounding liquid they tend to move downward, which is referred to as *sedimentation*. The densities of most edible oils (in their liquid state) are lower than that of water, and so there is a tendency for oil to accumulate at the top of an emulsion and water at the bottom. Thus, droplets in an O/W emulsion tend to cream, whereas those in a water-in-oil (W/O) emulsion tend to sediment.



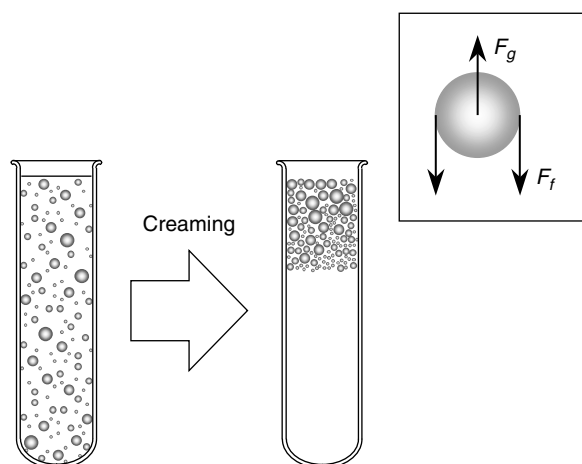


**Figure 7.3** Food emulsions are prone to creaming because of the density difference between the oil and water phases. Inset: the forces acting on an emulsion droplet.

Gravitational separation is usually regarded as having an adverse affect on the quality of food emulsions. A consumer expects to see a product that appears homogeneous, and therefore the separation of an emulsion into an optically opaque droplet-rich layer and a less opaque droplet-depleted layer is undesirable. The textural attributes of a product are also adversely affected by gravitational separation, because the droplet-rich layer tends to be more viscous than expected, whereas the droplet-depleted layer tends to be less viscous. The taste and mouthfeel of a portion of food therefore depend on the location from which it was taken from the emulsion. A sample selected from the top of an O/W emulsion that has undergone creaming will seem too “rich” because of the high fat content, whereas a sample selected from the bottom will seem too “watery” because of the low fat content. Gravitational separation is also a problem because it causes droplets to come into close contact for extended periods which can lead to enhanced flocculation or coalescence, and eventually to oiling off—the formation of a layer of pure oil on top of the emulsion. When a food manufacturer is designing an emulsion-based product it is therefore important to control the rate at which gravitational separation occurs.

Each food product is unique, containing different types of ingredients and experiencing different environmental conditions during its processing, storage, and consumption. As a consequence, the optimum method of controlling gravitational separation varies from product to product. In this section, we consider the most important factors that influence gravitational separation, as well as strategies for controlling it.

### 7.3.1 Physical basis of gravitational separation

#### 7.3.1.1 Stokes' law

The rate at which an isolated rigid spherical particle creams in an ideal liquid is determined by the balance of forces that acts on it (Figure 7.3 inset). When a particle has a lower density than the surrounding liquid an upward gravitational force acts on it (Hunter, 1989; Hiemenz and Rajagopalan, 1997):

$$F_g = -\frac{4}{3}\pi r^3(\rho_2 - \rho_1)g \quad (7.7)$$

where  $r$  is the radius of the particle,  $g$  is the acceleration due to gravity,  $\rho$  is the density, and the subscripts 1 and 2 refer to the continuous and dispersed phases, respectively. As the particle moves upward through the surrounding liquid it experiences a hydrodynamic frictional force that acts in the opposite direction and therefore retards its motion:

$$F_f = 6\pi\eta_1rv \quad (7.8)$$

where  $v$  is the creaming velocity and  $\eta$  is the shear viscosity. The particle rapidly reaches a constant velocity, where the upward force due to gravity balances the downward force due to friction, that is,  $F_g = F_f$ . By combining Equations 7.7 and 7.8, we obtain the Stokes' law equation for the creaming rate of an isolated spherical particle in a liquid:

$$v_{\text{Stokes}} = -\frac{2gr^2(\rho_2 - \rho_1)}{9\eta_1} \quad (7.9)$$

The sign of  $v_{\text{Stokes}}$  determines whether the droplet moves upward (+) or downward (-). To a first approximation, the stability of a food emulsion to creaming can be estimated using Equation 7.9. For example, an oil droplet ( $\rho_2 = 910 \text{ kg m}^{-3}$ ) with a radius of  $1 \text{ }\mu\text{m}$  suspended in water ( $\eta_1 = 1 \text{ mPa sec}$ ,  $\rho_1 = 1000 \text{ kg m}^{-3}$ ) will cream at a rate of about  $17 \text{ mm}$  per day. Thus, one would not expect an emulsion containing droplets of this size to have a particularly long shelf life. As a useful rule of thumb, an emulsion in which the calculated creaming rate is less than about  $1 \text{ mm}$  per day can be considered to be stable toward creaming (Dickinson, 1992).

In the rest of this section we shall mainly consider creaming, rather than sedimentation, because it is more common in food systems. Nevertheless, the same physical principles are important in both cases, and the methods of controlling them are similar. In the initial stages of creaming the droplets move upward and a droplet-depleted layer is observed at the bottom of the container (Figure 7.4). When the droplets reach the top of the emulsion they cannot move upward any further and so they pack together to form a "creamed layer." The final thickness of the creamed layer depends on the initial droplet concentration in the emulsion and the effectiveness of the droplet packing. Droplets may

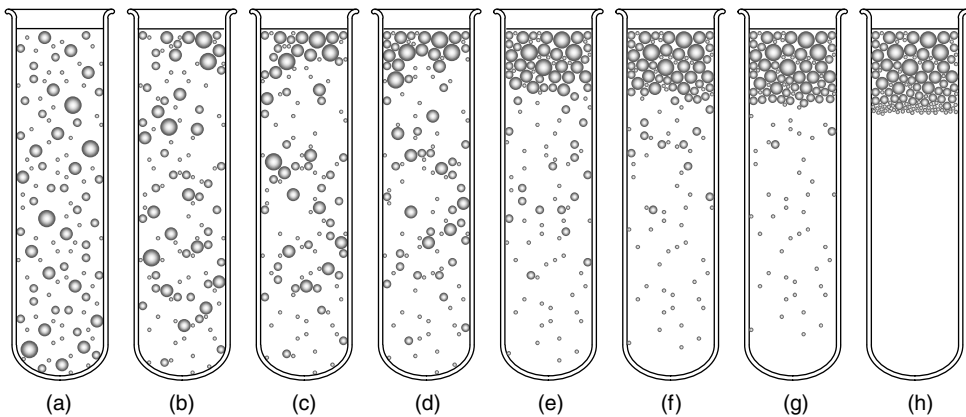


**Figure 7.4** Schematic representation of the time dependence of droplet creaming in oil-in-water emulsions. Droplets move upward until they cannot move any further and then form a "creamed" layer. Larger droplets tend to move upward faster than smaller ones.

pack tightly or loosely depending on their polydispersity and the nature of the interactions between them. Tightly packed droplets tend to form a relatively thin creamed layer, whereas loosely packed droplets form a relatively thick creamed layer. Many of the factors that determine the packing of droplets in a creamed layer also determine the structure of flocs (see Section 7.5.3). The droplets in a creamed emulsion can often be redispersed by mild agitation, providing that they are not too strongly attracted to each other or that coalescence has not occurred.

### 7.3.1.2 Deviations from Stokes' law

Stokes' law can only be strictly used to calculate the velocity of an isolated rigid spherical particle suspended in an ideal liquid of infinite extent (Dickinson, 1992; Hiemenz and Rajagopalan, 1997). In practice, there are often large deviations between the creaming velocity predicted by Stokes' law and experimental measurements of creaming in food emulsions, because many of the assumptions used in deriving Equation 7.9 are invalid. Some of the most important factors that alter the creaming rate in food emulsions are considered below.

**7.3.1.2.1 Droplet fluidity.** Stokes' equation assumes that there is no slip at the interface between the droplet and the surrounding fluid, which is only strictly true for solid particles. The liquid within a droplet can move when a force is applied to the droplet's surface, thus the frictional force that opposes the movement of a droplet is reduced, which causes an increase in the creaming velocity (Dickinson and Stainsby, 1982):

$$v = v_{\text{Stokes}} \frac{3(\eta_2 + \eta_1)}{3\eta_2 + 2\eta_1} \quad (7.10)$$

This expression reduces to Stokes' equation when the viscosity of the droplet is much greater than that of the continuous phase ( $\eta_2 \gg \eta_1$ ). Conversely, when the viscosity of the droplet is much less than that of the continuous phase ( $\eta_2 \ll \eta_1$ ), the creaming rate is 1.5 times faster than that predicted by Equation 7.9. In practice, the droplets in most food emulsions can be considered to act like rigid spheres because they are surrounded by a viscoelastic interfacial layer that prevents the fluid within them from moving (Walstra, 1996a, 2003a).

**7.3.1.2.2 Nondilute systems.** The creaming velocity of droplets in concentrated emulsions is less than that in dilute emulsions because of hydrodynamic interactions between the droplets (Hunter, 1989; Walstra, 1996b). As an emulsion droplet moves upward due to gravity, an equal volume of continuous phase must move downward to compensate. Thus, there is a net flow of continuous phase downward, which opposes the upward movement of the droplets, and therefore decreases the creaming velocity. In fairly dilute emulsions (i.e. <2% droplets) the creaming velocity of spherical particles has been derived mathematically from a consideration of fluid hydrodynamics (Hunter, 1989):

$$v = v_{\text{Stokes}} (1 - 6.55\phi) \quad (7.11)$$

In more concentrated emulsions, a number of other types of hydrodynamic interactions also reduce the creaming velocity of the droplets. These hydrodynamic effects can be partly accounted for by using a value for the viscosity of a concentrated emulsion in Equation 7.9, rather than that of the continuous phase (see Chapter 8).

A semiempirical equation that has been found to give relatively good predictions of the creaming behavior of concentrated emulsions has been developed (Hunter, 1989):

$$v = v_{\text{Stokes}} \left( 1 - \frac{\phi}{\phi_c} \right)^{k\phi_c} \quad (7.12)$$

Here  $\phi_c$  and  $k$  are parameters that depend on the nature of the emulsion. Normally,  $\phi_c$  is taken to be the volume fraction at which the spherical particles become closely packed (Hunter, 1986). For monodisperse latex suspensions the following values have been determined experimentally:  $k = 5.4$  and  $\phi_c = 0.585$ . Nevertheless, different values have been found to be appropriate for quasi-monodisperse O/W emulsions stabilized by an anionic surfactant, that is,  $k = 8$  and  $\phi_c = 0.585$  (Chanamai and McClements, 2000b,c). The  $k$  and  $\phi_c$  parameters can therefore be thought of as semiempirical quantities, whose precise value for a particular system needs to be determined experimentally. The above equation predicts that the creaming velocity decreases as the droplet concentration increases, until creaming is completely inhibited once a critical disperse phase volume fraction ( $\phi_c$ ) has been exceeded (Figure 7.5).

In general, the value of  $\phi_c$  used in the above equation depends on the packing of the droplets within an emulsion, which is governed by their polydispersity and colloidal interactions. Polydisperse droplets are able to fill the available space more effectively than monodisperse droplets because the small droplets can fit into the gaps between the larger ones, hence  $\phi_c$  tends to be higher for polydisperse than for monodisperse emulsions (Das and Ghosh, 1990). When the droplets are strongly attracted to each other they can form a particle gel network at relatively low droplet concentrations, which severely restricts droplet movement at lower  $\phi$  values (Figure 7.6). On the other hand, when the droplets are strongly repelled from each other their effective size increases, which also severely restricts droplet movement at lower  $\phi$  values. In the case of strong droplet attraction or repulsion the above equation must therefore be modified (see later).

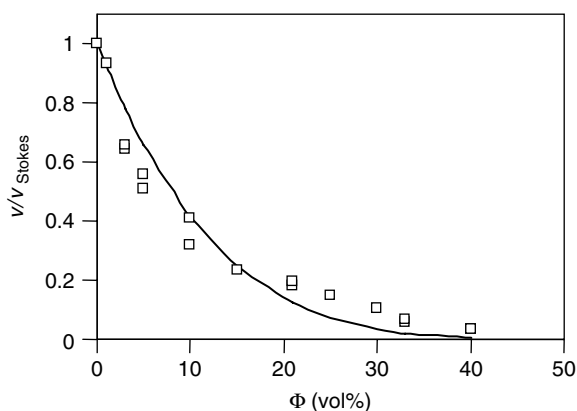


**Figure 7.5** Comparison of measured (points) and predicted (line) relative creaming rates as a function of disperse phase volume fraction for quasi-monodisperse oil-in-water emulsions (Chanamai and McClements, 2000c). The predicted values were calculated using Equation 7.12 with  $\phi_c = 0.585$  (58.5%) and  $k = 8$ . Creaming is effectively retarded when the emulsion droplets become close packed.

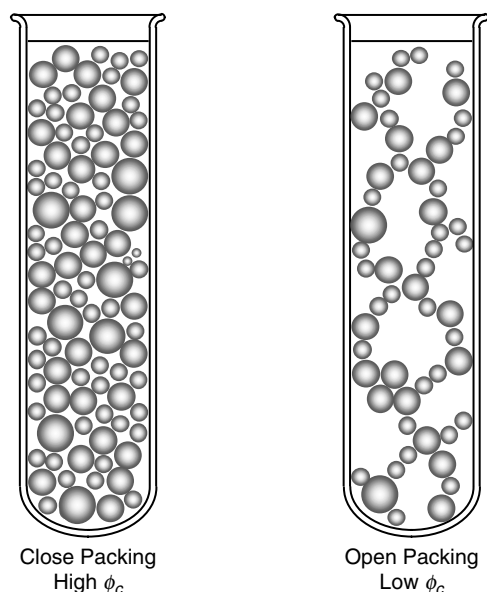


**Figure 7.6** Creaming is prevented when the disperse phase volume fraction exceeds a critical value ( $\phi_c$ ) where the droplets become so closely packed that they cannot easily move past each other. This critical value occurs at lower disperse phase volume fractions when the droplets are flocculated.

**7.3.1.2.3 Polydispersity.** Food emulsions normally contain a range of different droplet sizes and the larger droplets tend to cream more rapidly than the smaller droplets, so that there is a distribution of creaming rates within an emulsion (Figure 7.4). Larger droplets tend to cream faster than smaller ones, which leads to an accumulation of larger droplets at the top of an emulsion (Pinfield et al., 1997). Thus, there is both a droplet concentration profile and a droplet size profile in the vertical direction within an emulsion. As the larger droplets move upward more rapidly they collide with smaller droplets (Melik and Fogler, 1988; Dukhin and Sjoblom, 1996). If the droplets aggregate after a collision they will cream at a faster rate than either of the isolated droplets. Detailed information about the evolution of the droplet concentration and size profiles within an emulsion can be obtained by using computer simulations that take into account polydispersity (Davis, 1996; Tory, 1996; Pinfield et al., 1997). For many purposes, it is only necessary to have an average creaming velocity, which can usually be estimated by using a mean droplet radius ( $r_{54}$ ) in the Stokes' equation (Dickinson, 1992; Walstra, 1996b; Binks, 1998; Walstra, 2003a).

**7.3.1.2.4 Droplet flocculation.** In many food emulsions the droplets aggregate to form flocs (Section 7.5). The size and structure of the flocs within an emulsion has a large influence on the rate at which the droplets cream (Bremer, 1992; Bremer et al., 1993; Walstra, 1996b; Pinfield et al., 1997; Chanamai and McClements, 2000b). At low or intermediate droplet concentrations, where flocs do not substantially interact with one another, flocculation tends to increase the creaming velocity because the flocs have a larger effective size than the individual droplets (which more than compensates for the fact that the density difference between the flocs and the surrounding liquid is reduced). In concentrated emulsions, flocculation retards creaming because a three-dimensional network of aggregated flocs is formed that prevents the individual droplets from moving (Figure 7.6). The droplet concentration at which creaming is prevented depends primarily on the internal structure of the flocs formed. A network can form at lower disperse phase volume fractions

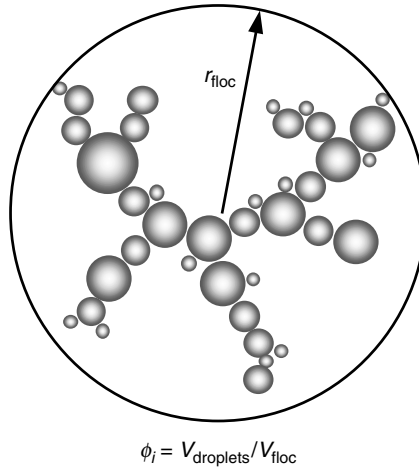


**Figure 7.7** A floc can be considered to consist of a spherical particle with a particular radius ( $r_{\text{floc}}$ ) and internal packing ( $\phi_i$ ).

when the droplets in a floc are more openly packed, and therefore creaming is prevented at lower droplet concentrations (Figure 7.6). Openly packed flocs tend to form when there is a strong attraction between the droplets (Section 7.5.3.).

Mathematical models can be derived to predict the creaming rate of a flocculated emulsion if one assumes that the flocs are spherical and do not break down during creaming (Chanamai and McClements, 2000b). For example, Stokes' law can be used to predict the creaming velocity of the flocs in a dilute emulsion (where floc–floc interactions are negligible) by replacing the characteristics of the individual droplets ( $r$ ,  $\rho_2$ ) by those of the flocs ( $r_{\text{floc}}$ ,  $\rho_{\text{floc}}$ ):

$$v_{\text{floc}} = -\frac{2gr_{\text{floc}}^2(\rho_{\text{floc}} - \rho_1)}{9\eta_1} \quad (7.13)$$

The radius ( $r_{\text{floc}}$ ) and density ( $\rho_{\text{floc}}$ ) of flocs depend on the number of droplets per floc ( $n$ ) and the internal packing ( $\phi_i$ ) of the droplets within the flocs (Figure 7.7). If it is assumed that the flocs are spherical, then their internal packing is given by the expression:  $\phi_i = V_{\text{droplets}}/V_{\text{floc}}$ , where  $V_{\text{droplets}}$  is the volume of the droplets within the floc ( $=n4\pi r^3/3$ ) and  $V_{\text{floc}}$  is the volume of the floc ( $=4\pi r_{\text{floc}}^3/3$ ). The expressions for  $V_{\text{droplets}}$  and  $V_{\text{floc}}$  can be inserted into the expression for  $\phi_i$  to give the following equation:

$$r_{\text{floc}} = r \cdot 3 \sqrt{\frac{n}{\phi_i}} \quad (7.14)$$

where  $\phi_i$  is independent of the floc size. For random close packing of hard spheres  $\phi_i \approx 0.63$  (Quemada and Berli, 2002). This equation indicates that the floc size should increase as the number of droplets within it increases or as the packing becomes more open. The density of the flocs can also be calculated from knowledge of the packing of the droplets within them:

$$\rho_{\text{floc}} = \phi_i \rho_2 + (1 - \phi_i) \rho_1 \quad (7.15)$$

Flocculation increases the effective size of the particles within the emulsion (which enhances creaming), while decreasing the density contrast between the particles and the surrounding fluid (which retards creaming). The overall influence of flocculation on the creaming velocity can be conveniently characterized by a creaming instability ratio:  $v_{\text{floc}}/v_{\text{Stokes}}$ . For dilute emulsions this ratio can be calculated using Stokes' law (Equation 7.9) and the density of the flocs (Equation 7.15):

$$\frac{v_{\text{floc}}}{v_{\text{Stokes}}} = \frac{r_{\text{floc}}^2 \phi_i}{r^2} \quad (7.16)$$

As expected this equation predicts that the creaming rate should increase as the size of the flocs increases or as the droplets become more densely packed within the flocs.

In a concentrated flocculated suspension the creaming velocity is reduced because of hydrodynamic interactions between the particles and can be described by the same semiempirical equation as used for concentrated nonflocculated suspensions by replacing  $v$  with  $v_{\text{floc}}$  and  $\phi$  with  $\phi_{\text{floc}} (= \phi_i)$ :

$$v_{\text{floc},\phi} = v_{\text{floc}} \left( 1 - \frac{\phi}{\phi_c \phi_i} \right)^{k\phi_c} = v_{\text{Stokes}} \frac{r_{\text{floc}}^2 \phi_i}{r^2} \left( 1 - \frac{\phi}{\phi_c \phi_i} \right)^{k\phi_c} \quad (7.17)$$

Here the values of  $\phi_c$  and  $k$  have the same meanings (and approximately the same numerical values) as in nonflocculated emulsions, that is,  $\phi_c \sim 0.585$  and  $k \sim 5.4$ . This equation can be used to predict the influence of floc size and internal packing on their creaming velocity (Figure 7.8). In dilute emulsions ( $\phi \rightarrow 0$ ), the normalized creaming velocity ( $v_{\text{floc},\phi}/v_{\text{Stokes}}$ ) increases with increasing floc radius (higher  $r_{\text{floc}}$ ) and internal packing (higher  $\phi_i$ ). For concentrated emulsions, the normalized creaming velocity decreases more rapidly with increasing droplet concentration as the internal packing decreases (Figure 7.8a). These predictions confirm experimental observations that droplet flocculation promotes creaming in dilute emulsions because of the increase in particle size, but may retard it in concentrated emulsions

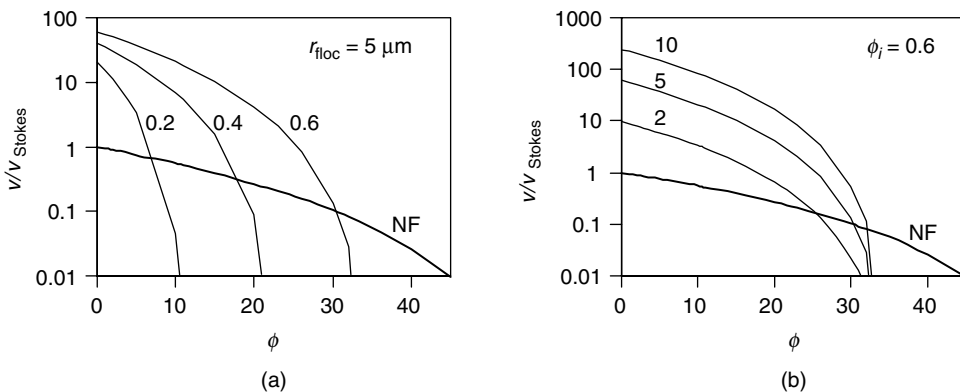


**Figure 7.8** Predicted influence of floc radius and internal packing on normalized creaming velocity of oil-in-water emulsions with different disperse phase volume fractions. The curves in figure A represent flocs with different internal packing ( $\phi_i = 0.2, 0.4, 0.6$ ) but the same radius ( $r_{\text{floc}} = 5 \mu\text{m}$ ). The curves in figure B represent flocs with the same internal packing ( $\phi_i = 0.6$ ) but different radius ( $r_{\text{floc}} = 2, 5, \text{ or } 10 \mu\text{m}$ ). NF represents nonflocculated emulsions.

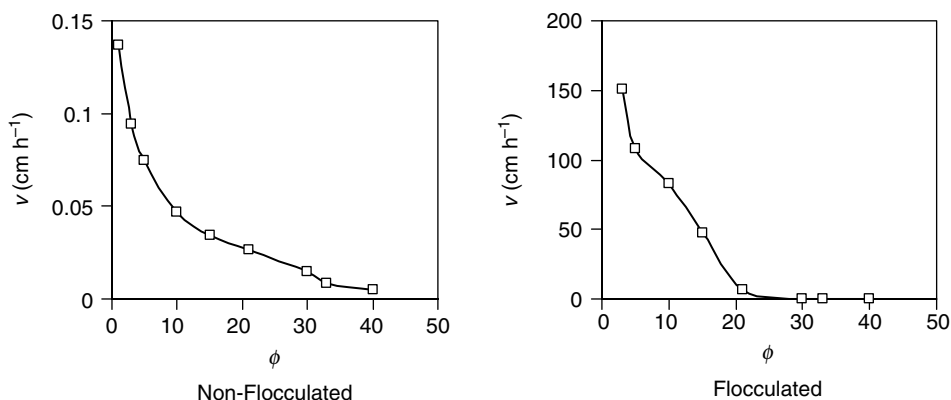


**Figure 7.9** Dependence of creaming velocities on droplet concentration for *n*-hexadecane oil-in-water emulsions containing monodisperse droplets ( $r = 0.86 \mu\text{m}$ ) stabilized by SDS. The emulsions were either nonflocculated (7 mM SDS) or flocculated (80 mM SDS) depending on the concentration of free SDS micelles added to promote depletion flocculation (Chanamai and McClements, 2000b). Note the difference in scales on the two graphs.

because of the formation of a network of aggregated droplets that extends throughout the emulsion volume (Chanamai and McClements, 2002b). Experimental measurements of the creaming velocity in nonflocculated and flocculated quasi-monodisperse O/W emulsions largely confirm the predictions of the above theories (Figure 7.9).

**7.3.1.2.5 Non-Newtonian rheology of continuous phase.** The continuous phase of many food emulsions is non-Newtonian, that is, the viscosity depends on shear stress or has some elastic characteristics (Chapter 8). As a consequence, it is important to consider the most appropriate apparent viscosity to use in the Stokes' equation (van Vliet and Walstra, 1989; Walstra, 1996b, 2003a). Biopolymers, such as modified starches or gums, are often added to O/W emulsions to increase the viscosity of the aqueous phase (Section 4.5). Many of these biopolymer solutions exhibit pronounced shear-thinning behavior, having a high viscosity at low shear rates that decreases dramatically as the shear rate is increased (Section 4.5.1). This property is important because it means that the droplets are prevented from creaming, but that the food emulsion still flows easily when poured from a container (Dickinson, 1992). Creaming usually occurs when an emulsion is at rest, and therefore it is important to know the apparent viscosity that a droplet experiences as it moves through the continuous phase under these conditions. The shear stress acting on a droplet undergoing gravitational separation is  $\tau \approx 2\Delta\rho gr$ , which is typically between  $10^{-4}$  and  $10^{-2}$  Pa for food emulsions (Walstra, 2003a). Solutions of thickening agents have extremely high apparent shear viscosities at these relatively low shear stresses, and hence the droplets will tend to cream extremely slowly (Walstra, 1996b).

Some aqueous biopolymer solutions have a yield stress ( $\tau_B$ ), below which the solution acts like an elastic solid, and above which it acts like a viscous fluid (van Vliet and Walstra, 1989). In these systems droplet creaming is effectively eliminated when the yield stress of the solution is larger than the stress exerted by a droplet as it moves through the continuous phase, that is,  $\tau_B \geq |2\Delta\rho gr|$  (Walstra, 2003a). Typically, a value of about 10 mPa is required to prevent emulsion droplets of a few micrometers from creaming, which is often exceeded in practice. Similar behavior is observed in W/O emulsions containing a network of aggregated fat crystals when it has a sufficiently high yield stress to prevent the water droplets from undergoing sedimentation.



The above discussion highlights the importance of carefully defining the rheological properties of the continuous phase. For this reason, it is good practice to measure the viscosity of the continuous phase over the range of shear rates that an emulsion droplet is likely to experience during processing, storage, and handling, which may be as wide as  $10^{-7}$  to  $10^3 \text{ sec}^{-1}$  (Dickinson, 1992).

**7.3.1.2.6 Electrical charge.** Charged emulsion droplets tend to move more slowly than uncharged droplets for a number of reasons (Dickinson and Stainsby, 1982; Walstra, 1986b; Hiemenz and Rajagopalan, 1997). First, repulsive electrostatic interactions between similarly charged droplets mean that they cannot get as close together as uncharged droplets. Thus, as a droplet moves upward there is a greater chance that its neighbors will be caught in the downward flow of the continuous phase. Second, the cloud of counterions surrounding a droplet moves less slowly than the droplet itself, which causes an imbalance in the electrical charge that opposes the movement of the droplet. Third, if the electrostatic repulsive interactions between droplets are sufficiently strong and long range then the droplets may be prevented from moving because of the substantial increase in the effective volume fraction of the droplets.

**7.3.1.2.7 Fat crystallization.** Many food emulsions contain a lipid phase that is either partly or wholly crystalline (Mulder and Walstra, 1974; Boode, 1992; Dickinson and McClements, 1995). In O/W emulsions, the crystallization of the lipid phase affects the overall creaming rate because solid fat ( $\rho \approx 1200 \text{ kg m}^{-3}$ ) has a higher density than liquid oil ( $\rho \approx 910 \text{ kg m}^{-3}$ ). The density of a droplet containing partially crystallized oil is given by  $\rho_{\text{droplet}} = \phi_{\text{SFC}}\rho_{\text{solid}} + (1 - \phi_{\text{SFC}})\rho_{\text{liquid}}$ , where  $\phi_{\text{SFC}}$  is the volume fraction of solid fat (relative to the total fat). At a solid fat content (SFC) of about 30% an oil droplet has a similar density as water and will therefore neither cream nor sediment. At lower SFCs the droplets cream, and at higher SFCs they sediment. This accounts for the more rapid creaming of milk fat globules at  $40^\circ\text{C}$  (where they are completely liquid) than at  $20^\circ\text{C}$  (where they are partially solid) (Mayhill and Newstead, 1992).

As mentioned above, crystallization of the fat in a W/O emulsion may lead to the formation of a three-dimensional network of aggregated fat crystals that prevents the water droplets from sedimenting, for example, in butter and margarine (Dickinson and Stainsby, 1982). In these systems there is a critical SFC necessary for the formation of a network, which depends on the morphology of the fat crystals (Walstra, 1987, 2003a). The importance of network formation is illustrated by the effect of heating on the stability of margarine. When margarine is heated above a temperature where most of the fat crystals melt, the network breaks down and the water droplets sediment, leading to the separation of the oil and aqueous phases.

**7.3.1.2.8 Adsorbed layer.** The presence of a layer of adsorbed emulsifier molecules at the surface of an emulsion droplet affects the creaming rate in a number of ways (Tan, 2004). First, it increases the effective size of the emulsion droplet, and therefore the creaming rate is increased by a factor of  $(1 + \delta/r)^2$ , where  $\delta$  is the thickness of the adsorbed layer. Typically, the thickness of an adsorbed layer is between 2 and 10 nm, and therefore this effect is only significant for very small emulsion droplets ( $<0.1 \mu\text{m}$ ). Second, the adsorbed layer may alter the effective density of the dispersed phase,  $\rho_2$  (Tan, 2004). The effective density of the dispersed phase when the droplets are surrounded by an adsorbed layer can be calculated using the following relationship, assuming that the thickness of the adsorbed layer is much smaller than the radius of the droplets ( $\delta \ll r$ ):

$$\rho_2 = \frac{\rho_{\text{droplet}} + 3(\delta/r)\rho_{\text{layer}}}{1 + 3(\delta/r)} \quad (7.18)$$

The density of the emulsifier layer is usually greater than that of either the continuous or dispersed phases, and therefore the adsorption of emulsifier increases the effective density of the dispersed phase (Tan, 2004). The density of large droplets ( $r \gg \delta$ ) is approximately the same as that of the bulk dispersed phase, but that of smaller droplets may be altered significantly. It is therefore possible to retard creaming by using a surface-active biopolymer that forms a relatively thick and dense interfacial layer. This mechanism may be important in slowing down creaming in beverage emulsions, since the droplet size is relatively small and the interfacial layers are relatively thick (Tan, 2004).

**7.3.1.2.9 Brownian motion.** Another major limitation of Stokes' equation is that it ignores the effects of Brownian motion on the creaming velocity of emulsion droplets (Pinfield et al., 1994; Walstra, 1996b; Hiemenz and Rajagopalan, 1997). Gravity favors the accumulation of droplets at either the top (creaming) or bottom (sedimentation) of an emulsion. On the other hand, Brownian motion favors the random distribution of droplets throughout the whole of the emulsion because this maximizes the configurational entropy of the system. The equilibrium distribution of droplets in an emulsion that is susceptible to both creaming and Brownian motion is given by the following equation (ignoring the finite size of the droplets) (Walstra, 1996b):

$$\phi(h) = \phi_0 \exp\left(\frac{-4\pi r^3 \Delta\rho g h}{3kT}\right) \quad (7.19)$$

where  $\phi(h)$  is the concentration of the droplets at a distance  $h$  below the top of the emulsion, and  $\phi_0$  is the concentration of the droplets at the top of the emulsion. If  $\phi(h) = \phi_0$ , then the droplets are evenly dispersed between the two locations (i.e., Brownian motion completely dominates), but if  $\phi(h) \ll \phi_0$ , the droplets tend to accumulate at the top of the emulsion (i.e., creaming dominates). Predictions of the dependence of  $\phi(h)/\phi_0$  on emulsion height ( $h$ ) for typical food emulsions ( $\Delta\rho = 100 \text{ kg m}^{-3}$ ) are shown in Figure 7.10. These predictions suggest that Brownian motion may play a role on the creaming behavior of emulsions when the droplet radius is less than about  $0.1 \mu\text{m}$ , and that the accumulation of droplets at the top of an emulsion due to creaming should be almost completely retarded when the droplet radii is less than about  $10 \text{ nm}$ .

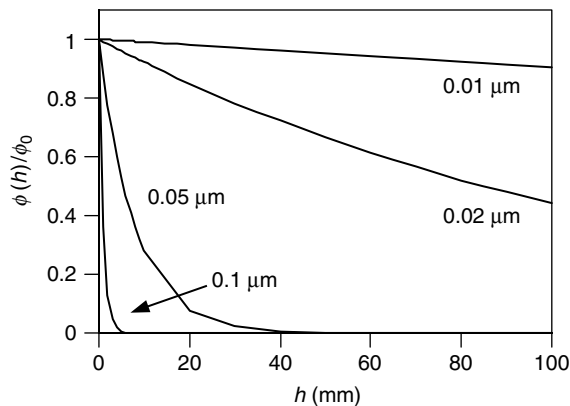


**Figure 7.10** Predicted influence of Brownian motion on the distribution of oil droplets in model oil-in-water emulsions with different droplet sizes ( $\Delta\rho = 100 \text{ kg m}^{-3}$ )

**7.3.1.2.10 Complexity of creaming.** The above discussion has highlighted the many factors that need to be considered when predicting the rate at which droplets cream in emulsions. In some situations, it is possible to combine two or more of the factors mentioned above into a simple analytical equation. However, it may be difficult to accurately model the creaming behavior of an emulsion if a large number of factors operate simultaneously. In these situations, the most comprehensive method of predicting gravitational separation in emulsions is to use computer simulations (Pinfield et al., 1994, 1997; Tory, 1996).

### 7.3.2 Methods of controlling gravitational separation

The discussion of the physical basis of gravitational separation in the previous section has highlighted a number of ways of retarding its progress in food emulsions.

#### 7.3.2.1 Minimize density difference

The driving force for gravitational separation is the density difference between the droplets and the surrounding liquid:  $\Delta\rho = \rho_2 - \rho_1$ . It is therefore possible to prevent gravitational separation by “matching” the densities of the oil and aqueous phases (Tan, 2004). Most naturally occurring triacylglycerol-based edible oils have fairly similar densities ( $\approx 910 \text{ kg m}^{-3}$ ) and therefore food manufacturers have limited flexibility in preventing creaming by changing the type of oil used in their product.\* Nevertheless, a number of alternative strategies have been developed that enable food manufacturers to match the densities of the dispersed and continuous phases more closely.

Density matching can be achieved by mixing oil-soluble or oil-dispersible “weighting agents” that have a higher density than water with the oil phase prior to homogenization, so that the overall density of the oil droplets becomes similar to that of the aqueous phase (Stauffer, 1999; Tan, 2004). Different types of weighting agents are available to food manufacturers, including brominated vegetable oil (BVO), ester gum (EG), damar gum (DG), and sucrose acetate isobutyrate (SAIB). BVO is made by bromination of vegetable oil ( $\rho \approx 1330 \text{ kg m}^{-3}$ ). EG is made by esterification of wood rosin with glycerol ( $\rho \approx 1080 \text{ kg m}^{-3}$ ). DG is a natural exudate obtained from the shrubs of the Caesalpinaceae and Dipterocarpaceae families ( $\rho \approx 1050\text{--}1080 \text{ kg m}^{-3}$ ). SAIB is made by the esterification of sucrose with acetic and isobutyric anhydrides ( $\rho \approx 1146 \text{ kg m}^{-3}$ ). Because of the differences in their densities, different amounts of the weighting agents are required to completely match the density of the oil phase to that of the aqueous phase, with their effectiveness at density matching decreasing in the following order: BVO > SAIB > EG > DG (Chanamai and McClements, 2000a). Weighting agents also vary in their legal status and maximum permissible usage level in different countries, as well as in their cost and ease of use.

The influence of adding a weighting agent (BVO) to the oil phase of an O/W emulsion is demonstrated in Figure 7.11. At low BVO concentrations, the density of the droplets is less than that of the aqueous phase and creaming occurs. At high BVO concentrations, the density of the droplets is greater than that of the aqueous phase and sedimentation occurs. At a certain BVO concentration ( $\sim 25\%$ ) the density of the droplets equals that of the aqueous phase and gravitational separation is completely suppressed.

If the droplets in an O/W emulsion are sufficiently small, it may be possible to prevent gravitational separation by using an emulsifier that forms a relatively thick and dense interfacial layer, because this decreases the density difference between the oil droplets and

\* It should be noted that the flavor oils used in beverage emulsions usually have appreciably lower densities than triacylglycerol oils (Section 12.3).

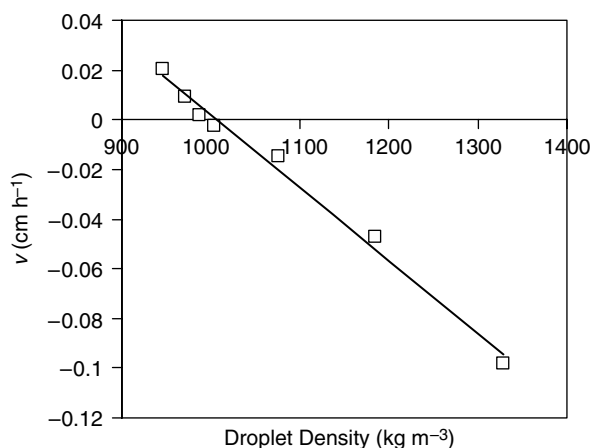


**Figure 7.11** Influence of droplet density on the creaming velocity of 1 wt% oil-in-water emulsions containing different ratios of soybean oil to BVO (0–100%) at 25°C. When  $\rho_2 < \rho_1$ , creaming occurs, when  $\rho_2 > \rho_1$  sedimentation occurs, and when  $\rho_2 = \rho_1$  no droplet movement occurs. Densities of pure liquids: aqueous phase = 1000.4  $\text{kg m}^{-3}$ ; soybean oil = 911.1  $\text{kg m}^{-3}$ ; BVO = 1329.5  $\text{kg m}^{-3}$ .

the surrounding liquid (Section 7.3.1). This mechanism has been proposed to be important in beverage O/W emulsions where the droplet size is relatively low and the thickness of the interfacial membrane is relatively thick (Tan, 2004).

In some emulsions it is possible to control the degree of gravitational separation by varying the SFC of the lipid phase. As mentioned in Section 7.3.1, an oil droplet with a SFC of about 30% has a similar density to water and will therefore be stable to gravitational separation. The SFC of a droplet could be controlled by altering the composition of the lipid phase or by controlling the temperature (Dickinson and McClements, 1995). In practice, this procedure is unsuitable for many food emulsions because partially crystalline droplets are susceptible to partial coalescence, which severely reduces their stability (Section 7.7).

### 7.3.2.2 Reduce droplet size

Stokes' law indicates that the velocity at which a droplet moves is proportional to the square of its radius (Equation 7.9). The stability of an emulsion to gravitational separation can therefore be enhanced by reducing the size of the droplets it contains. Homogenization of raw milk is one of the most familiar examples of the retardation of creaming in a food emulsion by droplet size reduction (Swaisgood, 1996). A food manufacturer generally aims to reduce the size of the droplets in an emulsion below some critical radius that is known to be small enough to prevent them from creaming during the lifetime of the product. In practice, homogenization leads to the formation of emulsions that contain a range of different sizes, and the largest droplets are most susceptible to gravitational separation. For this reason, a food manufacturer usually specifies the minimum percentage of droplets that can be above the critical droplet radius without leading to a significant decrease in perceived product quality. For example, cream liqueurs are usually designed so that less than 3% of the droplets have radii greater than 0.2  $\mu\text{m}$  (Dickinson, 1992). Even though a small fraction of the droplets are greater than this size, and therefore susceptible to creaming, this does not cause a major problem because the presence of the droplet-rich creamed layer at the top of the emulsion is obscured by the opacity produced by the smaller droplets remaining in the bulk of the emulsion that do not cream appreciably.

The creaming stability can also be improved by preventing any changes in the system that lead to an increase in the droplet size, such as flocculation, coalescence, or Ostwald ripening (see later).

#### 7.3.2.3 *Modify continuous phase rheology*

Increasing the viscosity of the liquid surrounding a droplet,  $\eta_l$ , decreases the velocity at which the droplet moves (Equation 7.9). Thus, the stability of an emulsion to gravitational separation can be enhanced by increasing the viscosity of the continuous phase, for example, by adding a thickening agent (Section 4.5). Gravitational separation may be completely retarded if the continuous phase contains a three-dimensional network of aggregated molecules or particles that traps the droplets and prevents them from moving. Thus, the droplets in O/W emulsions can be completely stabilized against creaming by using biopolymers that form a gel in the aqueous phase (Section 4.5), while the droplets in W/O emulsions can be completely stabilized against sedimentation by ensuring there is a network of aggregated fat crystals in the oil phase (van Vliet and Walstra, 1989).

#### 7.3.2.4 *Increase droplet concentration*

The rate of gravitational separation can be retarded by increasing the droplet concentration. At a sufficiently high disperse phase volume fraction the droplets are prevented from moving because they are so closely packed together (Figure 7.6). It is for this reason that the droplets in mayonnaise, which has a high disperse phase volume fraction, are more stable to creaming than those in salad dressings, which have a lower disperse phase volume fraction. Nevertheless, it should be mentioned that it is often not practically feasible to alter the droplet concentration, and therefore one of the alternative methods of preventing creaming should be used. It may be possible to increase the effective volume fraction of the droplets in an emulsion, without increasing the overall fat content, by using water-in-oil-in-water (W/O/W) emulsions, rather than conventional O/W emulsions (Dickinson and McClements, 1995; Benichou et al., 2002a).

#### 7.3.2.5 *Alter degree of droplet flocculation*

The rate of gravitational separation can be controlled by altering the degree of flocculation of the droplets in an emulsion. In dilute emulsions, flocculation causes enhanced gravitational separation because it increases the effective size of the particles. To improve the stability of these systems, it is important to ensure that the droplets are prevented from flocculating (Section 7.5). In concentrated emulsions, flocculation reduces the rate of gravitational separation because the droplets are prevented from moving past one another (Figure 7.6). The critical disperse phase volume fraction at which separation is prevented depends on the structural organization of the droplets within the flocs (Section 7.5.3.). The stability of concentrated emulsions may therefore be enhanced by altering the nature of the colloidal interactions between the droplets and therefore the structure of the flocs formed.

### 7.3.3 *Experimental characterization of gravitational separation*

To theoretically predict the rate at which gravitational separation occurs in an emulsion it is necessary to have information about the densities of the dispersed and continuous phases, the droplet size distribution, and the rheological properties of the continuous phase. The density of the liquids can be measured using a variety of techniques, including density bottles, hydrometers, and oscillating U-tube density meters (Pomeranz and Meloan, 1994; Nielsen, 2003). The droplet size distribution can be measured by microscopy,

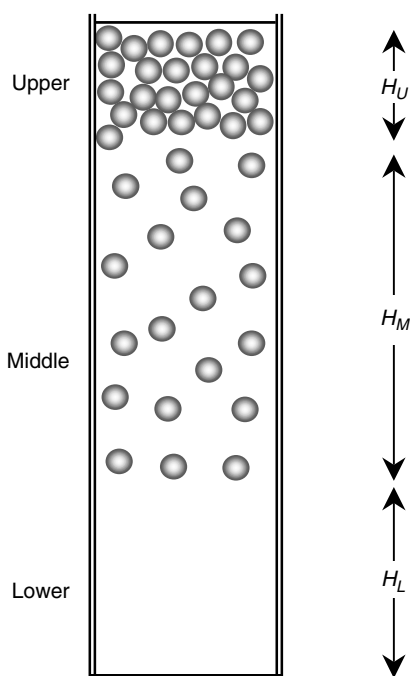


**Figure 7.12** Different layers are often observed in an emulsion undergoing creaming: (i) an upper “cream” layer ( $\phi > \phi_{\text{initial}}$ ); (ii) a middle layer ( $\phi = \phi_{\text{initial}}$ ); (iii) a lower “serum” layer ( $\phi < \phi_{\text{initial}}$ ).

light scattering, electrical pulse counting, or ultrasonic methods (Section 11.3). The rheological properties of the continuous phase can be characterized using various types of viscometers and dynamic shear rheometers (Section 8.3). In principle, it is possible to predict the long-term stability of a food emulsion from knowledge of these physicochemical properties and a suitable mathematical model. In practice, this approach has limited use because the mathematical models are not currently sophisticated enough to take into account the inherent complexity of most food emulsions. For this reason, it is often more appropriate to directly measure the gravitational separation of the droplets in an emulsion.

The simplest method of monitoring gravitational separation is to place an emulsion in a transparent test tube, leave it for a certain length of time, and then measure the height of the interfaces between the different layers formed (Figure 7.12). For example, in O/W emulsions it is often possible to visually discern a lower droplet-depleted “serum” layer ( $\phi < \phi_{\text{initial}}$ ), an intermediate “emulsion” layer ( $\phi = \phi_{\text{initial}}$ ), and a droplet-rich “creamed” upper layer ( $\phi > \phi_{\text{initial}}$ ). This procedure can often be accelerated by centrifuging an emulsion at a fixed speed for a certain length of time (Smith and Mitchell, 1976; Sherman, 1995). Nevertheless, the use of accelerated creaming tests as a means of predicting the long-term stability of emulsions to gravitational separation should be treated with caution because the factors that determine droplet movement in a gravitational field may be different from those that are important in a centrifugal field. For example, the continuous phase may have a yield stress that is exceeded in a centrifuge, but which would never be exceeded under normal storage conditions. The two major problems associated with determining the extent of creaming visually are: (i) it is only possible to obtain information about the location of the boundaries between the different layers, rather than about the full vertical concentration profile of the droplets, and (ii) in some systems it is difficult to clearly locate

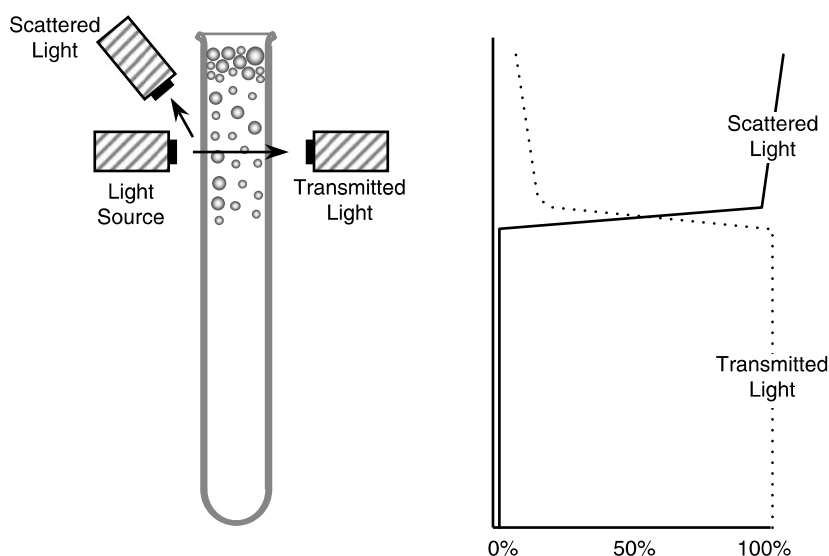


**Figure 7.13** Light scattering device for monitoring creaming or sedimentation of droplets in emulsions. The light source and detectors scan vertically up the emulsion and record the intensity of transmitted and scattered light.

the boundaries between the different layers because the boundaries are diffuse or the layers are optically opaque.

A more sophisticated method of monitoring gravitational separation is to use light scattering (Davis, 1996; Chanamai and McClements, 2000a). An emulsion is placed in a vertical glass tube and a monochromatic beam of near infrared light is directed through it (Figure 7.13). The percentage of transmitted and/or scattered light is measured as a function of emulsion height using one or two detectors by scanning the light beam up and down the sample using a stepper motor. The variation of droplet concentration with emulsion height can sometimes be deduced from the percentage of transmitted and/or scattered light using a suitable theory or calibration curve. Nevertheless, it is often difficult to quantify the actual droplet concentration versus height profile within emulsions because the intensities of the scattered and transmitted light do not change appreciably with changes in  $\phi$  at high droplet concentrations and are also dependent on droplet radius (Chantrapornchai et al., 1999a,b). In principle, this technique could be used to measure both the size and concentration of the droplets at any height by measuring the angular dependence of the intensity of the scattered light. This technique is finding increasing use for the characterization of gravitational separation in food emulsions due to the fact that fully automated analytical instruments based on this principle have recently become commercially available. The major disadvantages of this technique are that it is unsuitable for monitoring gravitational separation in some concentrated emulsions, and it is difficult to accurately determine the full profile of droplet concentration versus emulsion height.

Traditionally, the kinetics of gravitational separation was monitored in concentrated emulsions by physically removing sections of an emulsion from different heights and then analyzing the concentration of droplets in each section, for example, by measuring the density or by evaporating the water (Pal, 1994). These techniques cause the destruction of the sample being analyzed and cannot therefore be used to monitor creaming in the same sample as a function of time. Instead a large number of similar samples have to be prepared and each one analyzed at a different time. Recently, a number of nondestructive

analytical methods have been developed to monitor gravitational separation in concentrated emulsions without disturbing the sample, for example, electrical conductivity, ultrasound, and nuclear magnetic resonance (NMR) (Chapter 11). Information about gravitational separation can be obtained by inserting electrodes into an emulsion and measuring the change in electrical conductivity across them at different heights and times. Using a suitable theoretical model the electrical conductivity at a particular emulsion height can be converted into a droplet concentration. The ultrasonic device is very similar to the light scattering technique described above, except that it is based on the propagation of ultrasonic waves through an emulsion, rather than electromagnetic waves. An ultrasonic transducer is scanned vertically up and down an emulsion, which enables one to determine the droplet concentration (and sometimes droplet size) as a function of emulsion height. NMR imaging techniques, which are based on differences in the response of oil and water to the application of a radio frequency pulse, have also been used to monitor gravitational separation in emulsions. These techniques enable one to obtain a three-dimensional image of the droplet concentration (and sometimes droplet size) within a concentrated emulsion without the need for dilution, but they are expensive to purchase and require highly skilled operators, which has limited their application.

#### 7.4 *General features of droplet aggregation*

The droplets in emulsions are in continual motion because of the effects of thermal energy, gravity, or applied mechanical forces, and as they move about they frequently collide with their neighbors (Lips et al., 1993; Dukhin and Sjoblom, 1996). After a collision, emulsion droplets may either move apart or remain aggregated, depending on the relative magnitude of the attractive and repulsive interactions between them (Chapter 3). Droplets aggregate when there is a minimum in the interdroplet pair potential that is sufficiently deep and accessible to the droplets. The two major types of aggregations in food emulsions are flocculation and coalescence (Dickinson and Stainsby, 1982; Dickinson, 1992; Walstra, 1996a,b; 2003a; Saether et al., 2004). Flocculation is the process whereby two or more droplets come together to form an aggregate in which the droplets retain their individual integrity, whereas coalescence is the process whereby two or more droplets merge together to form a single larger droplet. In this section, we consider some of the more general features of droplet aggregation, while in the following sections we discuss droplet flocculation and coalescence separately in order to highlight the most important factors that influence them in food emulsions.

Consider a system that initially consists of a number of nonaggregated spherical particles dispersed in a liquid. Over time, the particles may either remain as individual entities or they may associate with their neighbors. Droplet association may take the form of flocculation or coalescence, where flocculation may either be reversible (weak flocculation) or irreversible (strong flocculation or coagulation). As an emulsion scientist one is interested in predicting the evolution of the particle size distribution of the system. In particular, one would like to know the change in the concentration of the different types of particles present in the system with time, that is, individual particles, particles present in weak or strong flocs (dimers, trimers, and so on), and particles that have become coalesced (dimers, trimers, and so on). Considerable progress has been made in developing mathematical models to describe the kinetics of droplet aggregation in colloidal systems (Saether et al., 2004). In general, the aggregation kinetics depends on the mechanism responsible for particle-particle encounters, the hydrodynamic and colloidal interactions acting between the particles, and the susceptibility of the thin film separating the particles to become ruptured. Some of the most important physiochemical mechanisms that influence the rate of particle aggregation in emulsions are identified in Figure 7.14. The relative



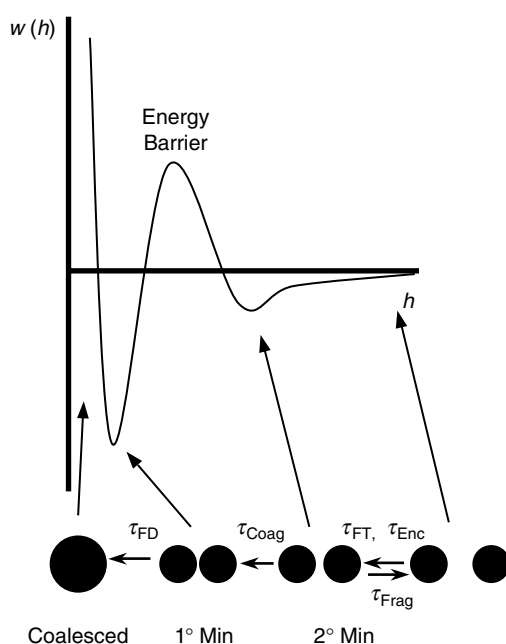


**Figure 7.14** Droplet aggregation involves a number of physiochemical processes, including droplet approach, film thinning, thin film formation, and thin film rupture. These processes are strongly dependent on the colloidal and hydrodynamic interactions between the droplets. The overall aggregation rate and the type of aggregation that occurs depend on which of these processes are rate limiting.

importance of these processes on droplet aggregation is briefly discussed below assuming that the colloidal interactions in the system are similar to those shown in Figure 7.14, that is, a secondary minimum, an energy barrier, a deep primary minimum, and a strong short-range repulsion.

#### 7.4.1 Droplet–droplet encounters

The first prerequisite for droplet aggregation to occur is that the droplets move toward each other and come into close proximity. The rate at which droplets encounter each other is largely determined by the dominant mechanism responsible for droplet movement in the emulsion, for example, Brownian motion, gravity, applied shear. A droplet encounter time ( $\tau_{Enc}$ ) can be defined, which provides a measure of the average time between droplet collisions.

#### 7.4.2 Film thinning

When the droplets come into close proximity a relatively thin film of continuous phase is formed between them and this fluid must be squeezed out before the droplets can get any closer. This process generates a hydrodynamic resistance to droplet approach because of the friction associated with fluid flow out of the thin film (Ivanov et al., 1999). In addition, there may be various attractive and repulsive colloidal interactions between the droplets with different signs, magnitudes, and ranges, which will also alter the rate at which droplets approach each other. A characteristic film thinning time ( $\tau_{FT}$ ) can be defined,

whose magnitude depends on the nature of the colloidal and hydrodynamic interactions acting between the droplets.

### 7.4.3 Thin film formation

The film of continuous phase separating the droplets will continue to thin up to a certain value, after which a number of events may occur depending on the nature of the colloidal and hydrodynamic interactions in the system (Ivanov et al., 1999; Petsev, 2000; Dukhin et al., 2001; Mishchuk et al., 2002). The droplets may move apart (no aggregation), remain in a secondary minimum (weak flocculation), remain in a primary minimum (coagulation), or move closer together and coalesce (Figure 7.14).

- *No aggregation.* If the secondary minimum is shallow, and there is a high energy barrier, then the droplets will tend to move apart immediately after a collision.
- *Weak flocculation.* If the secondary minimum is fairly deep, and there is a high energy barrier, then the droplets will tend to weakly flocculate with a relatively thick film of continuous phase (but still only a few nm) separating the droplets. The fragmentation time ( $\tau_{\text{Frag}}$ ) is a measure of the average time that droplets spend in the secondary minimum before moving apart. This time increases as the depth of the secondary minimum increases.
- *Coagulation (strong flocculation).* If the energy barrier is relatively low, but there is a strong short-range repulsion, then the droplets may fall into the primary minimum and be strongly flocculated with a relatively thin film of continuous phase between the droplets. Droplets may move directly into the primary minimum immediately following a droplet–droplet encounter, or (more usually) they may jump over the energy barrier after they have been present in a secondary minimum for some time. In the latter case, the coagulation time ( $\tau_{\text{Coag}}$ ) is a measure of the average time that droplets take to move from the secondary minimum into the primary minimum. The coagulation time increases as the height of the energy barrier increases.

### 7.4.4 Film rupture

Droplet coalescence occurs if the thin film of fluid (the continuous phase) separating the droplets is ruptured and the fluids within the droplets (the dispersed phase) merge together (Kabalinov, 1998; van Aken, 2004). If there is no strong short-range repulsion between the droplets, then they will tend to rapidly coalesce after falling into the primary minimum because there is nothing preventing them from getting close together. In this case, the rate of droplet coalescence is largely determined by the probability that the droplets obtain sufficient energy to jump over the primary energy barrier. In the presence of a high short-range repulsion, the droplets should be stable to coalescence. Nevertheless, droplet coalescence is often observed in real systems even though a short-range repulsive force does exist, which is due to the rupture of the thin film separating the droplets. Film rupture can occur through a variety of different mechanisms depending on the nature of any emulsifiers present at the droplet interfaces (see later). The rate of droplet coalescence depends on the film disruption time ( $\tau_{\text{FD}}$ ), which is the average time required for a rupture to appear in a film.

The goal of theoreticians is to derive mathematical expressions for each of the characteristic times associated with these different physical events, since mathematical models can then be developed to predict the change in the number of the different types of particles (nonaggregated, flocculated, and coalesced droplets) in a system with time (Saether et al., 2004).

The relative magnitude of these different characteristic times determines whether the system remains stable, undergoes flocculation, or undergoes coalescence.

## 7.5 Flocculation

As mentioned earlier, flocculation is the process whereby two or more droplets associate with each other, but maintain their individual integrities. Droplet flocculation may be either advantageous or detrimental to emulsion quality depending on the nature of the food product. Flocculation accelerates the rate of gravitational separation in dilute emulsions, which is usually undesirable because it reduces their shelf life (Luyten et al., 1993; Tan, 2004). It also causes a pronounced increase of emulsion viscosity, and may even lead to the formation of a gel (Demetriades et al., 1997a,b). Some food products are expected to have a low viscosity and therefore flocculation is detrimental. In other products, a controlled amount of flocculation may be advantageous because it leads to the creation of a more desirable texture. Improvements in the quality of emulsion-based food products therefore depend on a better understanding of the factors that determine the degree of floc formation, the structure of the flocs formed, the strength of the bonds holding the droplets together within the flocs, and the rate at which flocculation proceeds. In addition, it is important to understand the effect that flocculation has on the bulk physicochemical and sensory properties of emulsions, for example, shelf life, texture, taste, and appearance (Chapters 8–10).

### 7.5.1 Physical basis of flocculation

In general, mathematical models can be derived to account for the change in the number of nonfloculated, flocculated, and coalesced particles in an emulsion with time (Saether et al., 2004). In this section, we present a relatively simple model to describe droplet flocculation in colloidal dispersions containing monodisperse spherical particles. As flocculation proceeds there is a decrease in the total number of particles (monomers + aggregates) in an emulsion, which can be described by the following equation (Evans and Wennerstrom, 1994):

$$\frac{dn_T}{dt} = -\frac{1}{2}FE \quad (7.20)$$

where  $dn_T/dt$  is the flocculation rate,  $n_T$  is the total number of particles per unit volume,  $t$  is the time,  $F$  is the collision frequency, and  $E$  is the collision efficiency. A factor of  $1/2$  appears in the equation because a collision between *two* particles leads to a reduction of *one* in the total number of particles present. Equation 7.20 indicates that the rate at which flocculation proceeds depends on two factors: the frequency of collisions between the droplets and the fraction of collisions that leads to aggregation.

#### 7.5.1.1 Collision frequency

The collision frequency is the total number of droplet encounters per unit time per unit volume of emulsion. Any factor that increases the collision frequency increases the flocculation rate (provided that it does not also decrease the collision efficiency). Collisions between droplets occur as a result of their movement, which may be induced by Brownian motion, gravitational separation, or applied mechanical forces.

**7.5.1.1.1 Collisions due to Brownian motion.** In quiescent systems, the collisions between droplets are mainly a result of their Brownian motion. By considering the diffusion

of particles in a dilute suspension, von Smoluchowski was able to derive the following expression for the collision frequency (Hiemenz and Rajagopalan, 1997):

$$F_B = 16\pi D_0 r n^2 \quad (7.21)$$

where  $F_B$  is the collision frequency due to Brownian motion ( $\text{m}^3 \text{sec}^{-1}$ ),  $D_0$  is the diffusion coefficient of a single particle ( $\text{m}^2 \text{sec}^{-1}$ ),  $n$  is the number of particles per unit volume ( $\text{m}^{-3}$ ), and  $r$  is the droplet radius (m). For rigid spherical particles,  $D_0 = kT/6\pi\eta_1 r$ , where  $\eta_1$  is the viscosity of the continuous phase,  $k$  is Boltzmann constant, and  $T$  is the absolute temperature. Hence,

$$F_B = k_B n^2 = \frac{8kTn^2}{3\eta_1} = \frac{3kT\phi^2}{2\eta_1\pi^2 r^6} \quad (7.22)$$

where  $k_B$  is a second-order rate constant ( $\text{m}^3 \text{sec}^{-1}$ ) and  $\phi$  is the disperse phase volume fraction. For particles dispersed in water at room temperature the collision frequency is  $\approx 0.64 \times 10^{18} \phi^2 / r^6$  ( $\text{m}^3 \text{sec}^{-1}$ ), when the radius is expressed in micrometers. Equation 7.22 indicates that the frequency of collisions between droplets can be reduced by decreasing their volume fraction, increasing their size, or increasing the viscosity of the continuous phase. If it is assumed that every collision between two particles leads to aggregation, and that the rate constant is independent of aggregate size, then the flocculation rate is given by:  $dn_T/dt = -1/2F_B$ , which can be integrated to give the following expression for the change in the total number of particles with time (Evans and Wennestrom, 1994):

$$n_T = \frac{n_0}{1 + (1/2)k_B n_0 t} \quad (7.23)$$

where  $n_0$  is the initial number of particles per unit volume. The time taken to reduce the number of droplets in an emulsion by half can be calculated from the above equation:

$$\tau_{1/2} = \frac{2}{k_B n_0} = \frac{3\eta_1}{4kTn_0} = \left( \frac{\pi\eta_1}{kT} \right) \frac{r^3}{\phi_0} \quad (7.24)$$

For a system where the particles are suspended in water at room temperature,  $\tau_{1/2} \approx r^3 / \phi_0$  sec when  $r$  is expressed in micrometers. Thus, an O/W emulsion with  $\phi = 0.1$  and  $r = 1 \mu\text{m}$  would have a half-life of about 10 sec, which is on the same order as the existence of an emulsion prepared by shaking oil and water together in the absence of a texture modifier or emulsifier. It is also possible to derive an equation to describe the change in the number of dimers, trimers, and other aggregates with time (Evans and Wennerstrom, 1994):

$$n_k = n_0 \left( \frac{t}{\tau_{1/2}} \right)^{k-1} \left( 1 + \frac{t}{\tau_{1/2}} \right)^{-k-1} \quad (7.25)$$

where  $n_k$  is the number of aggregates per unit volume containing  $k$  particles. The predicted variation in the total concentration of particles and of the concentration of monomers ( $k = 1$ ), dimers ( $k = 2$ ), and trimers ( $k = 3$ ) with time is shown in Figure 7.15. As would be expected

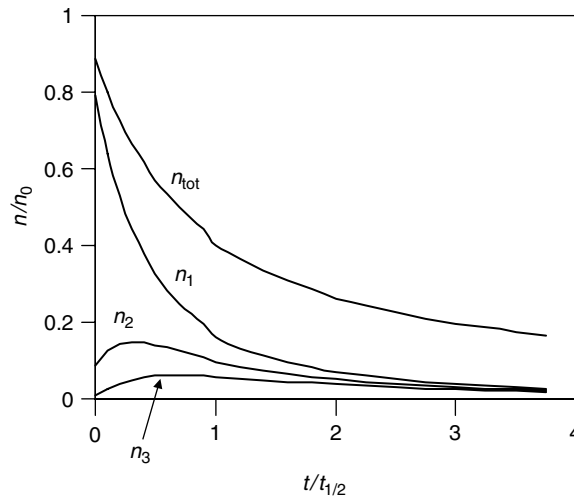


**Figure 7.15** Dependence of the concentration of the total number of particles ( $n_t$ ), monomers ( $n_1$ ), dimers ( $n_2$ ), and trimers ( $n_3$ ) on time  $t/\tau_{1/2}$ . The number of monomers decreases with time, whereas the number of aggregates initially increases and then decreases.

the total number of particles and the number of monomers decrease progressively with time as flocculation proceeds, while the number of dimers, trimers, and other aggregates initially increase with time and then decrease as they interact with other particles and form larger aggregates.

The above equations are only applicable to dilute suspensions containing identical spherical particles suspended in an ideal liquid (Vanapalli and Coupland, 2004). Many of the assumptions used in their derivation are not valid for actual food emulsions, which may be concentrated, polydisperse, and have nonideal continuous phases. In addition, the properties of the flocs cannot be assumed to be the same as those of the monomers, and therefore the above theory has to be modified to take into account the dimensions, structure, and hydrodynamic behavior of the flocs (Bremer, 1992; Walstra, 1996b).

**7.5.1.1.2 Collisions due to gravitational separation.** In polydisperse emulsions, droplet-droplet encounters can occur because of the different creaming (or sedimentation) rates of the differently sized droplets. Large droplets move more quickly than smaller ones and therefore they collide with them as they move upward (or downward). The collision frequency for gravitationally induced flocculation is given by (Melik and Fogler, 1988; Zhang and Davis, 1991):

$$F_G = \pi(v_2 - v_1)(r_1 + r_2)^2 n_1 n_2 \quad (7.26)$$

$$F_G = k_G n_1 n_2 = \frac{g \Delta \rho \phi_1 \phi_2}{8 \pi \eta_1} \left[ \frac{(r_2^2 - r_1^2)(r_1 + r_2)^2}{r_1^3 r_2^3} \right] \quad (7.27)$$

where  $F_G$  is the collision frequency due to gravitational separation,  $v_i$  is the Stokes' creaming velocity of a particle with radius  $r_i$ , and  $\Delta \rho$  is the density difference between the droplets and the surrounding liquid. This equation indicates that the collision frequency increases as the difference between the creaming velocities of the particles increases.

The rate of gravitationally induced flocculation can therefore be retarded by ensuring that the droplet size distribution is not too wide, decreasing the density difference between the oil and aqueous phases, decreasing the droplet concentration, or increasing the viscosity of the continuous phase. Equation 7.27 would have to be modified before it could be applied to systems that do not obey Stokes' law (Section 7.3). In addition, it does not take into account the fact that the droplets reach a position at the top or bottom of an emulsion where they cannot move any further and are therefore forced to encounter each other.

**7.5.1.1.3 Collisions due to applied shear forces.** Food emulsions are often subjected to various kinds of shear flow during their production, storage, and transport. Consequently, it is important to appreciate the effect that shearing has on their stability to flocculation. In a system subjected to Couette flow, the collision frequency is given by (Dickinson, 1992; Walstra, 1996b; Vanapalli and Coupland, 2004):

$$F_s = k_s n^2 = \frac{16}{3} Gr^3 n^2 = \left( \frac{3G}{\pi^2} \right) \frac{\phi^2}{r^3} \quad (7.28)$$

where  $F_s$  is the collision frequency due to shear. Thus, the frequency of shear-induced collisions can be retarded by decreasing the shear rate, increasing the droplet size, or decreasing the disperse phase volume fraction. It should be noted that the collision frequency is independent of the viscosity of the continuous phase.

**7.5.1.1.4 Relative importance of different collision mechanisms.** In general, each of the above mechanisms may contribute to the droplet collision frequency in an emulsion. In practice, one or other of the mechanisms usually dominates, depending on the composition and microstructure of the product, as well as the prevailing environmental conditions. To effectively control the collision frequency it is necessary to establish the mechanism that is the most important in the particular system being studied. It is convenient to use the collision frequency due to Brownian motion as a reference value, since this process occurs in most fluid emulsions. The ratio of the shear-to-Brownian motion collision frequencies ( $F_s/F_B$ ) and the gravitational-to-Brownian motion collision frequencies ( $F_G/F_B$ ) are plotted as a function of shear rate ( $G$ ) and particle size ratio ( $=r_2/r_1$ ), respectively, in Figure 7.16

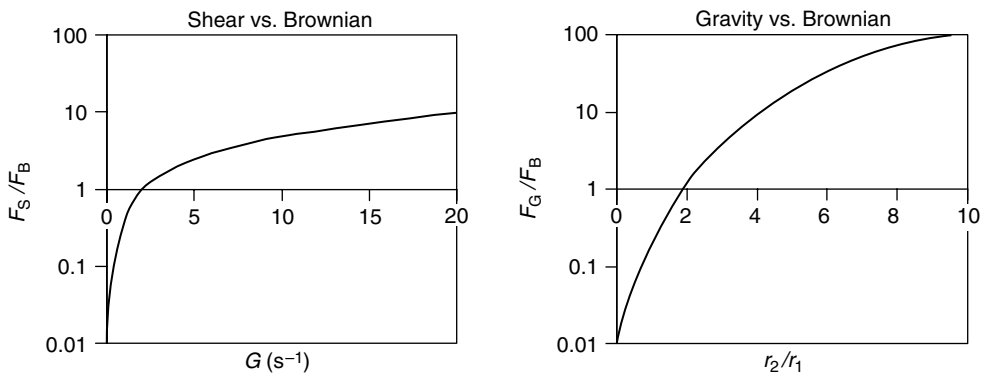


**Figure 7.16** Relative importance of the different collision mechanisms for typical food emulsions ( $\Delta\rho = 90 \text{ kg m}^{-3}$ ,  $r = 1 \text{ }\mu\text{m}$ ,  $\phi = 0.1$ ). (A) Shear-induced collisions become increasingly important as the shear rate is increased. (B) Gravitationally induced collisions become increasingly important as the ratio of droplet sizes increases or the viscosity of the continuous phase decreases.

for a typical O/W emulsion. At low shear rates ( $G < 2 \text{ sec}^{-1}$ ), collisions due to Brownian motion dominate, but at high shear rates those due to mechanical agitation of the system dominate. Gravitationally induced collisions dominate those due to Brownian motion when the particle size ratio exceeds about 2, and thus it is likely to be most important in emulsions that have a broad particle size distribution.

### 7.5.1.2 Collision efficiency

If every encounter between two droplets led to aggregation then emulsions would not remain stable long enough to be practically useful. To prevent droplets from flocculating during a collision it is necessary to have a sufficiently high repulsive energy barrier to stop them from coming too close together (Chapter 3). The height of this energy barrier determines the likelihood that a collision will lead to flocculation, that is, the collision efficiency. The collision efficiency,  $E$ , has a value between 0 (no flocculation) and 1 (every collision leads to flocculation),\* and depends on the hydrodynamic and colloidal interactions between the droplets. The flocculation rate therefore depends on the precise nature of the interactions between the emulsion droplets (Ivanov et al., 1999). For collisions induced by Brownian motion (Dukhin and Sjoblom, 1996; Walstra, 1996b):

$$-\frac{dn_B}{dt} = \frac{4kTn^2E_B}{3\eta_1} \quad (7.29)$$

$$E_B = \left( 2 \int_2^\infty \frac{\exp[w(s)/kT]}{s^2 G(s)} ds \right)^{-1} \quad (7.30)$$

where  $s$  is the dimensionless center-to-center distance between the droplets ( $s = [2r + h]/r$ ),  $r$  is the droplet radius, and  $h$  is the surface-to-surface separation. Colloidal interactions are accounted for by the  $w(s)$  term, and hydrodynamic interactions by the  $G(s)$  term (Chapter 3). When there are no colloidal interactions between the droplets ( $w(s) = 0$ ) and no hydrodynamic interactions ( $G(s) = 1$ ), Equation 7.24 becomes equivalent to that derived by Smoluchowski (Equations 7.20 and 7.22). The stability of an emulsion to aggregation is governed primarily by the maximum height of the energy barrier,  $w_{\max}(s)$ , rather than by its width (Friberg, 1997). To enhance the stability of an emulsion against flocculation it is necessary to have an energy barrier that is large enough to prevent the droplets from coming close together. The half-lives of emulsions with different height energy barriers have been estimated (Friberg, 1997), and are shown in Table 7.1. An energy barrier of

**Table 7.1** Approximate Flocculation Half-lives for Electrostatically Stabilized Emulsions with Different Energy Barriers.

$w(h_{\max})/kT$	Half-life
0	0.6 sec
1	1 sec
5	30 sec
10	1.2 h
15	23 h
20	3 years
50	$3 \times 10^{13}$ years

Source: Adapted from Friberg (1997).

\* In practice,  $E$  can have a value which is somewhat higher than 1 because droplet collisions are accelerated when there is a strong attraction between the droplets.

about  $20kT$  is usually sufficient to provide good long-term stability to emulsions. Expressions for the efficiency of shear and gravitationally induced collisions also depend on colloidal and hydrodynamic interactions, and have been derived for some simple systems (Zhang and Davis, 1991; Rother et al., 1997; Chin et al., 1998; Wilson et al., 2000; Mousa et al., 2001).

### 7.5.1.3 Overall droplet growth rate

To a first approximation, the increase in mean particle diameter with time in an emulsion due to flocculation can be calculated by assuming that at any given time the particles formed are monodisperse and have an “effective” particle diameter given by

$$d(t) = \sqrt[3]{\frac{6\phi}{\pi n_T(t)}} \quad (7.31)$$

The change in effective particle diameter with time can then be calculated by substituting this expression in the equation for the change in the total number of particles with time given above:

$$d^3 = d_0^3 + \frac{3}{\pi} \phi F_B E t \quad (7.32)$$

where  $d_0$  and  $d$  are the mean particle diameters at time zero and  $t$ , respectively. This equation indicates that there should be a linear increase in the cube of the mean particle diameter with time, and that the growth rate should increase with increasing droplet concentration, collision frequency, and collision efficiency. In practice, although the mean size of the particles in a flocculating emulsion may increase steadily with time (Figure 7.17a), the growth of the particles is not usually uniform throughout the size distribution (Figure 7.17b). Often, a fraction of the droplets become flocculated while the rest remain nonflocculated so that a bimodal particle size distribution is observed (Figure 7.17). More complex mathematical models are required to predict the change in the full particle size distribution with time.

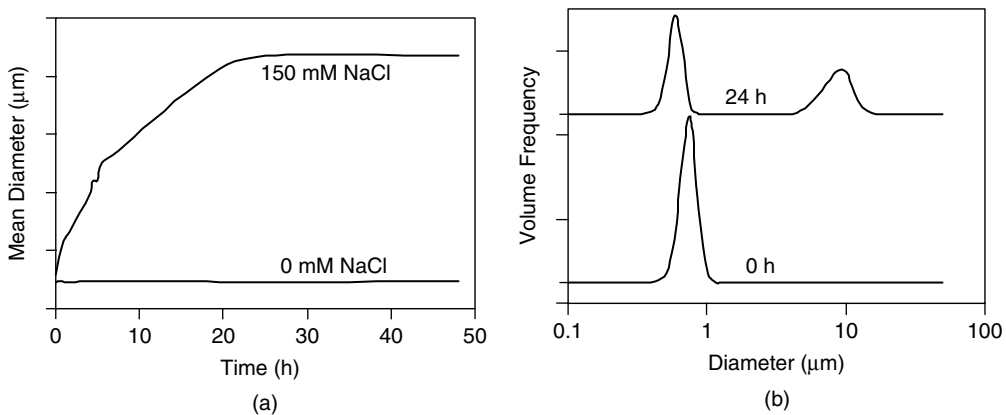


**Figure 7.17** Evolution of mean particle diameter and particle size distribution of 5 wt% *n*-hexadecane oil-in-water emulsions (1 wt%  $\beta$ -lactoglobulin; pH 7.0; 0 or 150 mM NaCl) during storage at 30°C. (a) Mean particle diameter for 0 and 150 mM NaCl; (b) particle size distribution for 150 mM NaCl after 0 and 24 h storage. The droplet size increases because of flocculation induced by surface denaturation of adsorbed globular proteins (Kim et al., 2002a).



## 7.5.2 Methods of controlling flocculation

Knowledge of the physical basis of droplet flocculation facilitates the development of effective strategies of controlling it in food emulsions. These strategies can be conveniently divided into those that influence the collision frequency and those that influence the collision efficiency.

### 7.5.2.1 Collision frequency

The flocculation rate can be controlled by manipulating the collision frequency of the droplets. The most effective means of achieving this depends on the dominant collision mechanism in the emulsion, that is, Brownian motion, gravity, or mechanical agitation. The rate at which droplets encounter each other in an unstirred emulsion can be reduced by increasing the viscosity of the continuous phase (Equation 7.22). Flocculation may be completely retarded if the continuous phase contains a three-dimensional network of aggregated molecules or particles that prevents the droplets from moving, for example, a biopolymer gel or a fat crystalline network. The collision frequency increases when an emulsion is subjected to sufficiently high shear rates (Equation 7.28), and therefore it may be important to ensure that a product is protected from mechanical agitation during its storage and transport in order to avoid flocculation. The collision frequency increases as the droplet concentration increases or the droplet size decreases, with the precise nature of this dependence being determined by the type of collision mechanism that dominates. The rate of collisions due to gravitational separation depends on the relative velocities of the particles in an emulsion, and therefore decreases as the density difference between the droplet and surrounding liquid decreases or as the viscosity of the continuous phase increases (Equation 7.27).

### 7.5.2.2 Collision efficiency.

The most effective means of controlling the rate and extent of flocculation in an emulsion is to regulate the colloidal interactions between the droplets. Flocculation can be prevented by designing an emulsion in which the repulsive interactions between the droplets are significantly greater than the attractive interactions. A wide variety of different types of colloidal interactions can act between the droplets in an emulsion, for example, van der Waals, steric, electrostatic, hydrophobic, and depletion (Chapter 3). Which of these is important in a given system depends on the type of ingredients present, the microstructure of the emulsion, and the prevailing environmental conditions. To control flocculation in a particular system it is necessary to identify the most important types of colloidal interactions.

**7.5.2.2.1 Electrostatic interactions.** Many O/W emulsions used in the food industry are (at least partly) stabilized against flocculation by using electrically charged emulsifiers that generate an electrostatic repulsion between the droplets, for example, ionic surfactants, proteins, or polysaccharides (Section 4.4). The flocculation stability of electrostatically stabilized O/W emulsions depends mainly on the electrical properties of the emulsion droplets ( $\psi_0$  and  $\sigma$ ), and the pH and ionic strength of the surrounding aqueous phase (Section 3.11.2). The number, position, sign, and dissociation constants of the ionizable groups on adsorbed emulsifier molecules determine the electrical behavior of emulsion droplets under different environmental conditions. For each type of food product it is therefore necessary to select an emulsifier with appropriate electrical characteristics.

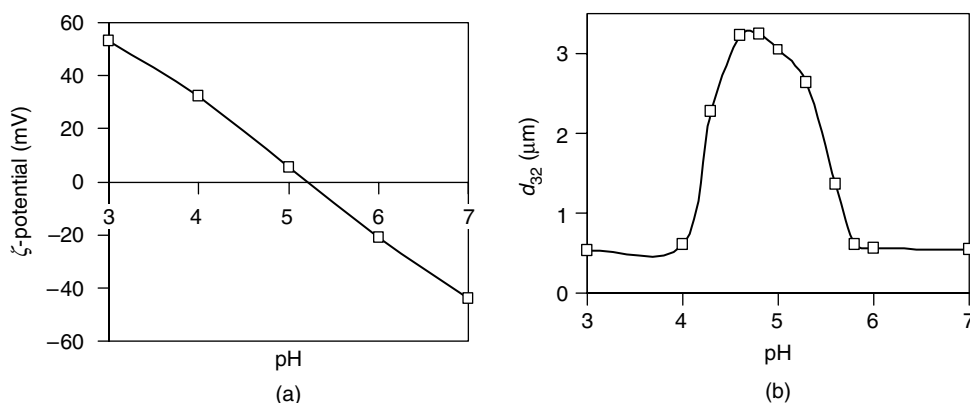


**Figure 7.18** Influence of pH on the  $\zeta$ -potential and flocculation stability of corn oil-in-water emulsions stabilized by whey-protein isolate. Extensive flocculation is observed near to the isoelectric point of the proteins (pH  $\sim$  5) because the electrostatic repulsion is no longer sufficiently strong to prevent droplet aggregation.

Hydrogen ions are potential determining ions for many food emulsifiers (e.g.,  $\text{COOH} \rightarrow \text{COO}^- + \text{H}^+$  or  $\text{NH}_3 + \text{H}^+ \rightarrow \text{NH}_4^+$ ), and therefore the sign and magnitude of the electrical charge on emulsion droplets is determined principally by the pH of the surrounding solution (Section 3.4). In protein-stabilized emulsions the electrical charge on the droplets goes from positive at low pH, to zero at the isoelectric point, to negative at high pH (Figure 7.18A). This change in droplet charge has a large impact on the stability of protein-stabilized emulsions to droplet flocculation (Figure 7.18B). At pH values sufficiently above or below the isoelectric point of the proteins, the droplet charge is large enough to prevent flocculation because of the relatively strong electrostatic repulsion between the droplets. At pH values near to the isoelectric point (IEP  $\pm$  2), the net charge on the proteins is relatively low and the electrostatic repulsion between the droplets is no longer sufficiently strong to prevent flocculation. Droplet flocculation leads to a pronounced increase in the viscosity of an emulsion, as well as a decrease in creaming stability, and therefore has important implications for food quality (Demetriades et al., 1997a; Agboola and Dalgleish, 1996a,d; Kulmyrzaev et al., 2000a,b).

The ionic strength of an aqueous solution depends on the concentration and valency of the ions it contains (Section 5.4.2). As the ionic strength is increased the electrostatic repulsion between droplets is progressively screened, until eventually it is no longer strong enough to prevent flocculation (Section 3.11.2). The minimum amount of electrolyte required to cause flocculation is known as the *critical flocculation concentration* or CFC. The CFC decreases as the surface potential of the emulsion droplets decreases and as the valency of the counterions increases. It has been shown that  $\text{CFC} \propto \psi_0^4/z^2$  (where  $\psi_0$  is the surface potential and  $z$  is the counterion valency) for droplets with relatively low surface potentials, that is,  $\psi_0 < 25$  mV (Hunter, 1986). These low surface potentials are found in many food emulsions that are susceptible to flocculation. Under certain conditions,  $\psi_0$  is inversely proportional to the valency of the counterions, so that  $\text{CFC} \propto 1/z^6$ , which is known as the Schultz–Hardy rule (Hunter, 1986). This relationship indicates that a much lower concentration of a multivalent ion is required to cause flocculation, than a monovalent ion, for example, 64 times less of a divalent counterion should be required than a monovalent counterion. The Schultz–Hardy rule can be derived from the DLVO theory by assuming that the CFC occurs when the potential energy barrier, which normally prevents droplets from aggregating, falls to a value of zero due to the addition of salt.

Consequently, when two droplets collide with each other they immediately aggregate into the primary minimum. In practice, significant droplet flocculation occurs when the potential energy barrier is slightly higher than zero, and therefore the Schultz–Hardy rule is expected to slightly overestimate the CFC (Hunter, 1986).

The ability of ions to promote droplet flocculation in emulsions also depends on whether they are indifferent ions or specifically bound ions (Section 5.4). Monovalent counterions (e.g.,  $K^+$ ,  $Na^+$ , and  $Cl^-$ ) tend to be indifferent ions that screen electrostatic interactions, but do not alter the surface charge density or isoelectric point of electrically charged emulsion droplets by binding to the droplet surfaces (Kulmyrzaev and Schubert, 2004). On the other hand, multivalent counterions (e.g.,  $Ca^{2+}$ ,  $Cu^{2+}$ ,  $Fe^{2+}$ ,  $Fe^{3+}$ ,  $Al^{3+}$ , and  $SO_4^{2-}$ ) may bind to the surface of emulsion droplets, thereby altering the surface charge density and isoelectric point of the droplets, as well as screening the electrostatic interactions (Mei et al., 1998a; Silvestre et al., 1999; Kulmyrzaev et al., 2000a). Specifically adsorbed mineral ions usually decrease the surface charge density on droplets by an amount that depends on their valency and concentration, but they may also cause charge reversal if present at sufficiently high concentrations (Kippax et al., 1998). In addition to their influence on surface charge specifically adsorbed ions are often highly hydrated and therefore increase the short-range hydration repulsion between droplets (Ivanov et al., 1999). In general, multivalent counterions tend to be much more effective at reducing the flocculation stability of electrostatically stabilized emulsions than monovalent counterions.

The influence of monovalent and divalent counterions on the stability of protein-stabilized O/W emulsions is illustrated in Figure 7.19. In this system, the proteins are negatively charged, so that the counterions are  $K^+$  and  $Ca^{2+}$ . Appreciable droplet flocculation was observed in the emulsions when the counterion concentration exceeded about 250–300 mM  $K^+$  or 3–4 mM  $Ca^{2+}$ . These results are in accordance with the Schultz–Hardy rule and highlight the much greater effectiveness of multivalent ions at promoting droplet flocculation in emulsions stabilized by electrostatic repulsion.

The flocculation stability of emulsions containing electrically charged droplets can be controlled in a variety of ways depending on the system. To prevent flocculation it is necessary to ensure that the droplets have a sufficiently high surface potential under the existing solution conditions (which often requires that the pH be controlled) and that the electrolyte concentration is below the CFC for the specific kinds of minerals present in the aqueous phase and the prevailing pH. In some foods it is necessary to have relatively high concentrations of multivalent mineral ions present for nutritional purposes, for

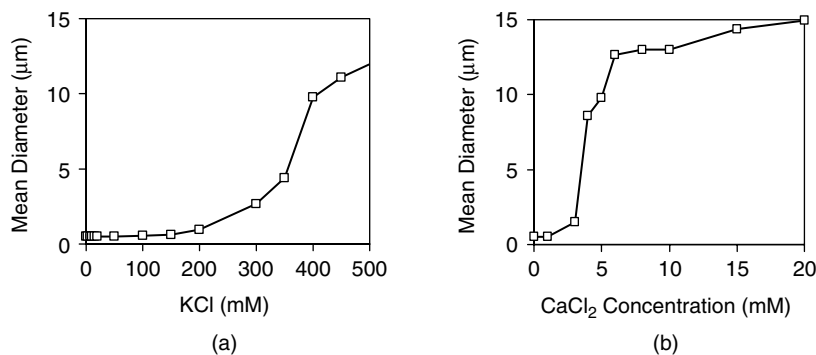


**Figure 7.19** Influence of mineral ion concentration on droplet flocculation in 20 wt% corn oil-in-water emulsions stabilized by whey-protein isolate (1 wt% WPI, pH 7.0). At this pH, the protein-stabilized droplets have a negative charge, so that  $Ca^{2+}$  counterions are more effective at promoting flocculation than  $K^+$  counterions. (Keowmaneechai and McClements, 2002a)

example, mineral-fortified emulsions used in infant, elderly, and athlete formulations. The potential negative impact of multivalent ions on emulsion stability can be reduced in a number of ways: (i) using an emulsifier that provides stability through a nonelectrostatic mechanism, for example, steric repulsion; (ii) ensuring that multivalent ions are excluded from the formulation, for example, by using purified water or other ingredients; (iii) by adding ingredients that sequester multivalent ions, for example, ethylene diamine tetra acetate (EDTA), citrate, or polyphosphates (Keowmaneechai and McClements, 2002b).

**7.5.2.2.2 Steric interactions.** Many food emulsifiers prevent droplet flocculation through steric repulsion, for example, some polysaccharides and nonionic surfactants (Chapters 3 and 4). This repulsion must be sufficiently strong and long range to overcome any attractive interactions (Section 3.11.1). Sterically stabilized emulsions are usually much less sensitive to variations in pH and ionic strength than electrostatically stabilized emulsions (Hunter, 1986). Nevertheless, they can become unstable to flocculation under certain conditions. If the composition of the continuous phase or the temperature is altered so that polymer–polymer interactions become more favorable than solvent–solvent/solvent–polymer interactions, then the mixing contribution to the steric interaction becomes attractive and may promote droplet flocculation (Section 3.5). A sterically stabilized emulsion may also become unstable if the thickness of the interfacial membrane is reduced (Section 3.11.1), which could occur if the polymeric segments on the emulsifier were chemically or biochemically cleaved (e.g., by acid or enzyme hydrolysis), if the continuous phase became a poor solvent for the polymer segments, or if electrostatic repulsive interactions between molecules within a charged biopolymer membrane were screened. Short-range hydration forces make an important contribution to the flocculation stability of many sterically stabilized emulsions (Israelachvili, 1992; Evans and Wennerstrom, 1994). In these systems, droplet flocculation may occur when the emulsion is heated, because emulsifier head groups are progressively dehydrated with increasing temperature (Israelachvili, 1992; Aveyard et al., 1990).

**7.5.2.2.3 Biopolymer bridging.** Many types of biopolymers promote flocculation by forming bridges between two or more droplets (Lips et al., 1991; Dickinson, 2003). Biopolymers may adsorb either directly to the bare surfaces of the droplets or to the adsorbed emulsifier molecules that form the interfacial membrane (Walstra, 1996b, 2003a; Dickinson, 2003). To be able to bind to the droplets there must be a sufficiently strong attractive interaction between segments of the biopolymer and the droplet surface. The most common types of interactions that operate in food emulsions are hydrophobic and electrostatic (Dickinson, 1989, 1992, 2003).

When a biopolymer has a number of nonpolar residues along its backbone some of them may associate with hydrophobic patches on one droplet, while others associate with hydrophobic patches on another droplet. This type of bridging flocculation tends to occur when a biopolymer is used as an emulsifier and there is an insufficient quantity present to completely cover the oil–water interface formed during homogenization (Walstra, 1996b). Bridging may occur either during the homogenization process or after it is complete, for example, when a biopolymer is only weakly associated with a droplet then some of its segments can desorb and become strongly attached to a neighboring droplet. This type of bridging flocculation can usually be prevented by ensuring there is a sufficiently high concentration of biopolymer present in the continuous phase prior to homogenization (Dickinson and Euston, 1991; Dickinson, 1992, 2003; Stoll and Buffle, 1996).

Bridging flocculation can also occur when a biopolymer in the continuous phase has an electrical charge that is opposite to that of the droplets (Pal, 1996; Dickinson, 2003). In this case, bridging flocculation can be avoided by ensuring the droplets and biopolymer

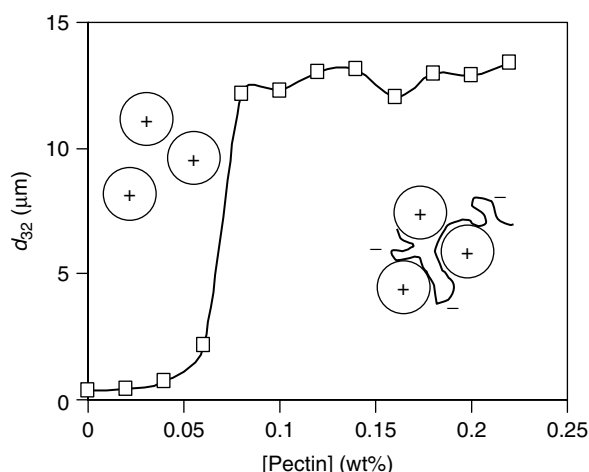


**Figure 7.20** Influence of pectin concentration on droplet flocculation in 5 wt% corn oil-in-water emulsions stabilized by  $\beta$ -lactoglobulin (pH 3.0). At this pH, the protein-stabilized droplets have a positive charge and the pectin has a negative charge, which leads to charge neutralization and bridging flocculation (Moreau et al., 2003).

have similar charges, or that either the droplets or biopolymer are uncharged. An example of this type of bridging flocculation is shown in Figure 7.20, which shows the change in mean particle size with pectin concentration for protein-stabilized emulsions. In this case, the emulsion droplets are positively charged and the negatively charged pectin molecules act as bridges that hold two or more droplets together into flocs. At sufficiently high biopolymer concentrations the flocs may not form (or can easily be disrupted) because there is sufficient biopolymer present to completely cover all of the droplet surfaces, and so a single biopolymer does not link more than one droplet (Dickinson, 2003).

**7.5.2.2.3 Hydrophobic interactions.** This type of interaction is important in emulsions that contain droplets that have nonpolar regions exposed to the aqueous phase. Their role in influencing the stability of food emulsions has largely been ignored, probably because of the lack of theories to describe them and of experimental techniques to quantify them. Even so, it has been proposed that hydrophobic interactions are responsible for the influence of surface denaturation and thermal denaturation of adsorbed proteins on the flocculation stability of O/W emulsions stabilized by globular proteins (McClements et al., 1993d; Hunt and Dalgleish, 1995; Demetriades et al., 1997b; Kim et al., 2002a,b).

At room temperature,  $\beta$ -lactoglobulin-stabilized emulsions (pH 7, 0 mM NaCl) are stable to flocculation because of the relatively strong electrostatic repulsion between the droplets (Kim et al., 2002a,b). Nevertheless, they become unstable to droplet flocculation when a sufficiently high level of salt is present in the continuous phase (Figure 7.21). At relatively low temperatures (<65°C), droplet flocculation has been attributed to surface denaturation of the proteins after adsorption. Surface denaturation occurs because of differences in the molecular environment of proteins in the nonadsorbed state (where they are surrounded by water) and the adsorbed state (where they are surrounded by water on one side and oil on the other). Consequently, the proteins undergo conformational changes after adsorption do maximize the number of favorable interactions and minimize the number of unfavorable interactions in their new environment. It is been proposed that the conformational changes resulting from surface denaturation lead to an increased exposure of nonpolar and sulfhydryl containing amino acids to the aqueous phase, which

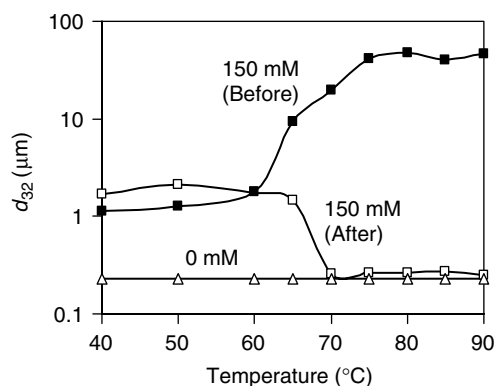


**Figure 7.21** Influence of temperature and salt on the flocculation stability of *n*-hexadecane oil-in-water emulsions stabilized by  $\beta$ -lactoglobulin (pH 7; 0 or 150 mM NaCl). Flocculation may occur due to surface or thermal denaturation of adsorbed proteins depending on holding temperatures, salt content, and whether salt is added before or after heating (Kim et al., 2002b).

promotes droplet aggregation through increased hydrophobic attraction and disulfide bond formation between proteins adsorbed to different droplets.

When  $\beta$ -lactoglobulin-stabilized emulsions are heated above the thermal denaturation temperature of the adsorbed globular proteins ( $\sim 70^\circ\text{C}$ ) in the presence of salt (150 mM NaCl), protein unfolding becomes much more extensive, which leads to an increase in the extent of droplet flocculation (Figure 7.21). Nevertheless, it is interesting to note that very little droplet flocculation is observed when a  $\beta$ -lactoglobulin-stabilized emulsion is heated above the thermal denaturation temperature in the absence of salt, and then salt is added after the emulsion has been cooled to room temperature (Figure 7.21). These results suggest that interactions between proteins adsorbed onto different droplets are favored when the droplets are in close proximity during heating (i.e., high salt), but that interactions between proteins adsorbed onto the same droplets are favored when droplets are not in close proximity during heating (i.e., low salt). This knowledge may provide a useful practical method of reducing the susceptibility of globular protein-stabilized emulsions to droplet flocculation during heat processing.

Hydrophobic interactions are also likely to be important in emulsions in which there is not enough emulsifier present to completely saturate the surfaces of the droplets (Dickinson, 2003). This may occur when there is insufficient emulsifier present in an emulsion prior to homogenization or when an emulsion is diluted so much that some of the emulsifier desorbs from the droplet surfaces.

Flocculation due to hydrophobic interactions can be avoided by ensuring that there is sufficient emulsifier present to completely cover the droplet surfaces or by selecting an emulsifier that does not undergo detrimental conformational changes that increase the surface hydrophobicity at the temperatures used during processing, storage, or handling.

**7.5.2.2.4 Depletion interactions.** The presence of nonadsorbing colloidal particles, such as biopolymers or surfactant micelles, in the continuous phase of an emulsion causes an increase in the attractive force between the droplets due to an osmotic effect associated with the exclusion of colloidal particles from a narrow region surrounding each droplet (Section 3.6). This attractive force increases as the concentration of colloidal particles increases, until eventually it may become large enough to overcome the repulsive interactions between the droplets and cause them to flocculate (Aronson, 1992; Jenkins and Snowdon, 1996). This type of droplet aggregation is usually referred to as *depletion*

*flocculation* (Walstra, 1996a,b). A wide variety of different biopolymers and surfactants have been shown to be capable of inducing depletion flocculation when added in sufficiently high concentrations, including surfactants [Tween 20, sodium dodecyl sulfate (SDS)], polysaccharides (xanthan gum, gum arabic, modified starch, maltodextrin, pectin, carrageenan), and proteins (whey and caseinate) (Dickinson et al., 1993a,d; Dickinson and Golding, 1997a,b; Dickinson et al., 1997, 2003; Chanamai and McClements, 2001). The lowest concentration required to cause depletion flocculation is referred to as the CFC by analogy to the CFC used to characterize the effect of salt on the stability of electrostatically stabilized emulsions. The CFC decreases as the size of the emulsion droplets increases and the effective volume fraction of the colloidal particles increases (McClements, 2000). The flocculation rate initially increases as the concentration of nonadsorbing colloidal particles is increased because of the enhanced attraction between the droplets, that is, a higher *collision efficiency*. However, once the concentration of colloidal particles exceeds a certain concentration the flocculation rate often decreases because the viscosity of the continuous phase increases so much that the movement of the droplets is severely retarded, that is, a lower *collision frequency*.

The influence of depletion flocculation on the creaming stability of O/W emulsions containing different concentrations of a nonadsorbing uncharged biopolymer (maltodextrin) is illustrated in Figure 7.22. In the absence of biopolymer, the emulsions are stable to creaming over a 1 week period. However, once the biopolymer concentration in the continuous phase of the emulsions exceeds the CFC, then the net attraction between the droplets is sufficiently large to cause them to flocculate. The increase in mean particle size brought about by droplet flocculation initially leads to rapid creaming. However, at higher biopolymer concentrations the creaming rate is decreased, even though there is still a strong depletion attraction between the droplets, because the movement of the droplets is restricted due to the large increase in continuous phase viscosity. The CFC is strongly dependent on the molecular weight of the biopolymer molecules, decreasing as the molecular weight of maltodextrin increases (Figure 7.22). This can be attributed to the fact that the effective volume ( $R_v$ ) of the maltodextrin molecules increases as their molecular weight increases, hence they are more effective at promoting depletion flocculation (McClements, 2000).

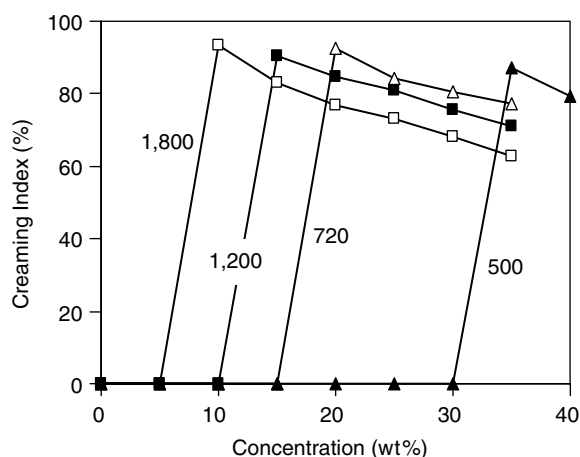


**Figure 7.22** Influence of maltodextrin concentration on the creaming stability of 5% corn oil-in-water emulsions. Depletion flocculation was observed above the critical flocculation concentration, which depended on the molecular weight of the maltodextrin (shown next to curves, in Da).

For ionic colloidal particles, such as ionic surfactants or charged biopolymers, the CFC is expected to be strongly dependent on electrolyte concentration because of its ability to screen electrostatic interactions, thereby reducing the effective volume of the colloidal particles. Studies of nonionic surfactant-stabilized O/W emulsions containing a nonadsorbed biopolymer (dextran sulfate), have shown that the CFC increases as the salt concentration increases because the effective volume of the ionic biopolymer is reduced by electrostatic screening effects (Demetriades and McClements, 1999). In general, any change in solution conditions that alters the effective volume of the nonadsorbed colloidal particles will influence the CFC, for example, temperature, ionic strength, solvent quality (Dickinson and Golding, 1997b; Srinivasan et al., 2002). It should be stressed that when an emulsion that undergoes depletion flocculation is diluted for particle sizing measurements (e.g., light scattering or electrical pulse counting), the flocs usually break down since the concentration of nonadsorbed colloid particles falls below the CFC, that is, depletion flocculation is usually weak and reversible.

**7.5.2.2.5 Hydrodynamic interactions.** The efficiency of the collisions between droplets is also determined by the strength of the hydrodynamic interactions between them (Davis et al., 1989; Dukhin and Sjoblom, 1996). As two droplets approach each other, a repulsion arises because of the resistance associated with the flow of the continuous phase from the thin gap between them. The magnitude of this resistance decreases as the droplet surfaces become more mobile, leading to an increase in the collision efficiency (Section 3.10.2). On the other hand, the collision efficiency may be reduced when the droplet surfaces are stabilized by small molecule surfactants because of the Gibbs–Marangoni effect (Section 3.10.3).

**7.5.2.2.6 Covalent interactions.** The droplets in flocs may also be held together by covalent interactions. For example, disulfide bond formation between protein molecules adsorbed onto different emulsion droplets has been proposed to account for the stability of flocs formed by surface and thermal denaturation of globular proteins (McClements et al., 1993d; Monahan et al., 1996; Kim et al., 2000a,b). Covalent bonds are relatively short-range interactions and therefore droplets have to be in close proximity in order for this type of interaction to occur. This accounts for the fact that when  $\beta$ -lactoglobulin-stabilized emulsions are heated above the thermal denaturation temperature of the adsorbed proteins in the presence of salt (small droplet separation) extensive interdroplet disulfide bond formation occurs, but when they are heated to the same temperature in the absence of salt (large droplet separation) only intradroplet disulfide bonds are formed. Consequently, extensive droplet flocculation is observed when  $\beta$ -lactoglobulin-stabilized emulsions are heated in the presence of salt (150 mM NaCl), but little droplet flocculation is observed when the same emulsions are heated in the absence of salt and then the same amount of salt is added after the emulsions are cooled to room temperature (Kim et al., 2002b).

### 7.5.3 Structure and properties of flocculated emulsions

The appearance, taste, texture, and stability of emulsions is strongly influenced by the characteristics of any flocs formed, for example, their number, size, flexibility, and packing (Walstra, 1993, 2003a). The structure and properties of flocs are mainly determined by the nature of the colloidal and hydrodynamic interactions between the droplets, but they also depend on the mechanism responsible for the droplet collisions, that is, Brownian motion, gravity, or mechanical agitation (Bremer, 1992; Evans and Wennerstrom, 1994). Valuable insights into the relationship between these parameters and floc characteristics have been obtained from a combination of computer simulations and experimental measurements.



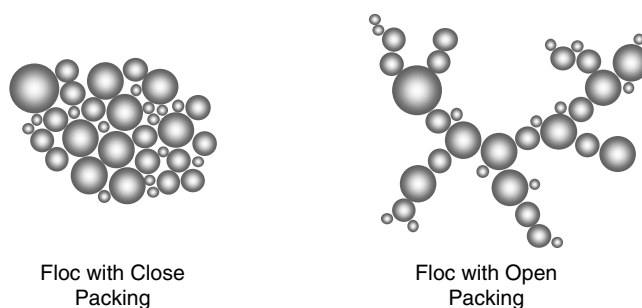


**Figure 7.23** Schematic representation of different types of floc structures. The internal structure of flocs tends to be more open (lower  $\phi_i$ ) when the attractive forces between the droplets are stronger.

#### 7.5.3.1 Influence of colloidal interactions on floc structure

When the attraction between the droplets is relatively strong compared to the thermal energy, the flocs formed tend to have open structures in which each droplet is only linked to two or three of its neighbors (Figure 7.23). This type of open structure is formed because the droplets “stick” firmly together at the point where they first come into contact and are unable to undergo any subsequent structural rearrangements (Bremer, 1992). As a consequence, a droplet that encounters a floc cannot move very far into its interior before becoming attached to another droplet. This type of floc is characterized by a tenuous structure that traps large amounts of continuous phase within it. The volume fraction of particles within such a floc may be as low as 0.13, depending on its size and the strength of the interactions (Dickinson, 1992). When the attraction between the droplets is relatively weak compared to the thermal energy, the droplets do not always stick together after a collision and they may be able to roll around each other after sticking together. Thus, a droplet that encounters a floc is able to penetrate closer to its center and flocs are able to undergo structural rearrangements, which means that the droplets can pack more closely together (Bijsterbosch et al., 1995). This type of floc is characterized by a more compact structure that traps less of the continuous phase. The volume fraction of the particles in this type of floc may be as high as 0.63, which is close to the value for random packing of monodisperse particles (Dickinson, 1992).

#### 7.5.3.2 Use of fractal geometry to describe floc structure

Fractal geometry has proven to be a valuable tool for characterizing the structural organization of droplets in flocs (Bremer, 1992; Peleg, 1993; Walstra, 1993a, 2003a). Fractal geometry is applicable to systems that exhibit a phenomenon known as self-similarity, that is, have structures that appear self-similar when observed at different levels of magnification (Figure 7.24). There are no truly fractal objects in nature because all real objects have a definite upper and lower size. Nevertheless, many natural objects do show self-similarity over a number of levels of magnification and can therefore be described by fractal geometry (Peleg, 1993). Despite their extremely complex structures, these fractal objects can be described by a single parameter,  $D$ , known as the fractal dimension.

The concept of a fractal dimension is best illustrated by considering the two-dimensional fractal flocs model shown in Figure 7.24. The floc with the “string-of-beads” type structure has a fractal dimension of one ( $D = 1$ ), because increasing the level of magnification by a factor of  $X$  changes the number of particles per floc by a factor of  $X^1$ , that is,  $N \propto X^1$ . The floc that contains the array of closely packed particles has a fractal dimension

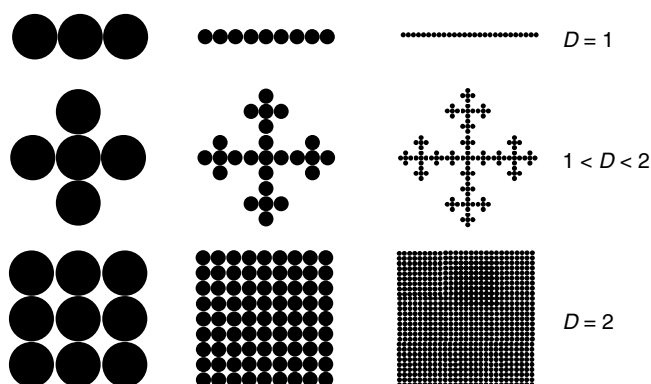


Figure 7.24 Two-dimensional structures that illustrate the concept of self-similar (fractal) flocs.

of two ( $D = 2$ ), because increasing the level of magnification by a factor of  $X$  changes the number of particles per floc by a factor of  $X^2$ , that is,  $N \propto X^2$ . These are the two extreme values of the fractal dimension of a two-dimensional structure. There are many other types of flocs that have self-similar structures with intermediate fractal dimensions (Figure 7.24). The number of particles in these flocs is described by the relationship:  $N \propto X^D$ , where the fractal dimension  $D$  has a noninteger value between 1 and 2. The closer the value is to one, the more tenuous is the floc structure, and the closer it is to two, the more compact. The number of particles in a fractal floc is given by the relationship:  $N = (R/r)^D$ .

In nature, flocs are three-dimensional structures and so  $D$  ranges from 1 to 3: the higher the fractal dimension, the more compact the floc structure (Peleg, 1993). The volume fraction of droplets in a three-dimensional floc is given by (Bremer, 1992; Walstra, 2003a):

$$\phi_F = \left( \frac{R}{r} \right)^{D-3} \quad (7.33)$$

This equation indicates that the internal packing of a floc becomes more open as the floc size increases at the same fractal dimension, that is,  $\phi_F$  decreases as  $R$  increases (because  $D < 3$ ). One of the major factors influencing the fractal dimension is whether the reaction is diffusion-limited (every collision leads to aggregation,  $E \rightarrow 1$ ) or reaction-limited (only a fraction of collisions leads to aggregation,  $E < 1$ ). For diffusion-limited aggregation, the fractal dimension is usually around 1.7–1.75, but for reaction-limited aggregation it may be appreciably higher (up to 2.4) (Walstra, 2003a). Thus, the flocs formed by diffusion-limited aggregation tend to have more open structures than those formed by reaction-limited aggregation. The fractal dimension of flocs can be determined using a variety of experimental techniques, including rheometry, light scattering, and microscopy (Bremer, 1992). Thus, it is possible to quantify the influence of different parameters on the structure of the flocs formed, for example, pH, ionic strength, and temperature.

It should be mentioned that fractal flocs are only kinetically stable structures (Evans and Wennerstrom, 1994). When there is a strong attraction between the droplets the most thermodynamically stable arrangement would be one in which the droplets formed a closely packed structure, as this would maximize the number of favorable attractive interactions. It is because there is a large activation energy associated with the rearrangement of droplets within a floc that means that it retains its fractal structure. If the external stresses acting on the flocs are sufficiently larger than the forces holding the droplets together, then the flocs may change from a fractal to a nonfractal structure, for example,

Brownian motion, mechanical agitation, gravity, or centrifugal forces. Nevertheless, if the rearrangements only occur over a short distance, then the overall system may still have a fractal structure, but the primary units are then clusters of droplets rather than individual droplets (Walstra, 2003a). In this case, the radius of the clusters, rather than that of the individual droplets, should be used in Equation 7.33. It should also be stressed that not all types of aggregation mechanisms lead to the formation of flocs with fractal structures (Walstra, 2003a).

### 7.5.3.3 Influence of floc structure on emulsion properties

The structure and properties of flocs has a pronounced affect on the stability and rheological properties of emulsions. An emulsion containing flocculated droplets has a higher viscosity than one containing the same concentration of nonflocculated droplets (Section 8.4.7). This is because the effective volume fraction of a floc is greater than the sum of the volume fractions of the individual droplets due to the presence of the continuous phase trapped within it (Quemada and Berli, 2002). The apparent viscosity of emulsions usually increases as the floc structure becomes more tenuous for the same reason (Walstra, 2003a). Emulsions that contain flocculated droplets tend to exhibit pronounced shear thinning behavior, that is, the viscosity decreases as the shear rate or shear time increases (Section 8.4.7). Shear thinning occurs for two reasons: (i) the flocs are deformed and become aligned with the shear field, which decreases their resistance to flow, and (ii) the flocs are disrupted by the shear forces, which decreases their effective volume fraction (Figure 7.25) (Bujannenez and Dickinson, 1994; Bower et al., 1997, 1999). The ease with which the flocs in an emulsion are deformed and disrupted decreases as the number and strength of the attractive interactions between the droplets increases (Uriev, 1994; Pal, 1996; Berli et al., 2002; Quemada and Berli, 2002). Thus, one would expect that a higher shear stress would be required to disrupt flocs in emulsions containing droplets that are strongly bound to each another, than one in which they are only weakly bound. Once the shearing forces are removed from an emulsion, the bonds between the droplets may reform. The rate at which this process occurs and the type of structures formed often has an important influence on the quality of food emulsions.

In some cases, shearing an emulsion can actually promote droplet flocculation because the efficiency and frequency of collisions between the droplets is increased (Spicer and Pratsanis, 1996). Thus, an emulsion that is stable under quiescent conditions may become

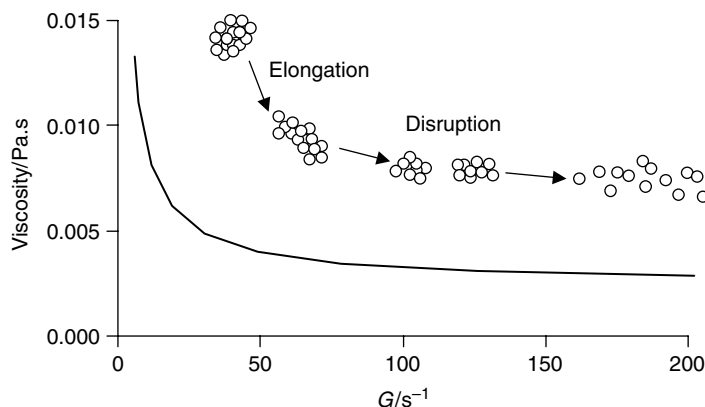


**Figure 7.25** Schematic diagram of events that occur during the shearing of a flocculated emulsion and their effect on emulsion viscosity. Flocs become increasingly deformed and disrupted with increasing shear stress, which leads to a decrease in emulsion viscosity.

flocculated when it is subjected to shear forces (Dalglish, 1997a). This type of emulsion initially shows shear thickening behavior because the formation of flocs leads to an increase in viscosity, but at higher shear rates these flocs may become deformed and disrupted, which leads to a decrease in viscosity (Pal, 1996). Emulsions may therefore exhibit complex rheological behavior depending on the nature of the colloidal interactions between the droplets.

At sufficiently high disperse phase volume fractions, flocculation leads to the formation of a three-dimensional network of aggregated droplets that extends throughout the emulsion (Bijsterbosch et al., 1995; Manoj et al., 1998a,b; Blijdenstein et al., 2003b; Berli et al., 2003). This type of system is referred to as a particle gel, and can be characterized by a yield stress that must be exceeded before the emulsion will flow (Pal, 1992, 1996; Tadros, 1996; Quemada and Berli, 2002). The value of the yield stress increases as the disperse phase volume fraction increases and as the strength of the attractive forces between the droplets increases (Pal, 1996). The minimum disperse phase volume fraction required to form a particle gel decreases as the structure of the flocs become more tenuous (i.e.,  $D \rightarrow 1$ ) because this type of structure is able to fill the available space more effectively (Figure 7.6). Thus, two emulsions may have exactly the same disperse phase volume fractions yet one could be a low viscosity liquid and the other a viscoelastic gel depending on the nature of the colloidal interactions between the droplets.

Flocculation also affects the stability of emulsions to creaming. In dilute emulsions, flocculation increases the creaming rate because the effective size of the particles in the emulsion is increased, which more than compensates for the decrease in  $\Delta\rho$  (Equation 7.16). In concentrated emulsions, the droplets are usually prevented from creaming because the formation of a three-dimensional network of aggregated droplets prevents them from moving (Figure 7.6).

#### 7.5.4 Experimental measurement of flocculation

A wide variety of experimental techniques have been developed to monitor both the extent and the rate of flocculation in emulsions. The most direct method is to observe the emulsion through an optical or electron microscope (Section 11.3.1). The association of droplets with one another can be determined subjectively by eye or more quantitatively by transferring an image of the emulsion to a computer and using image analysis techniques (Jokela et al., 1990; Mikula, 1992; Brooker, 1995). The major drawback of most microscopic techniques is that the delicate structure of the flocs may be disturbed by the procedures used to prepare the samples for observation. In addition, in concentrated emulsions it is often difficult to determine whether two droplets are flocculated or just in close proximity.

Flocculation can be monitored indirectly by measuring the change in the particle size distribution with time using a particle sizing instrument, for example, light scattering, ultrasonic spectrometry, NMR, or electrical pulse counting (Section 11.3). These instruments often provide a fairly qualitative indication of the extent of flocculation in an emulsion, because of a lack of suitable mathematical models to convert the experimental measurements into physical characteristics of the flocs, for example, internal packing, bond strength, dimensions. For example, light scattering techniques usually assume that the particles in an emulsion are isolated homogeneous spheres, whereas flocs are inhomogeneous and nonspherical aggregates that contain many individual droplets, and therefore the theories normally used to interpret light scattering data are no longer valid.

In many systems it is important to determine whether the increase in droplet size is caused by flocculation, coalescence, or Ostwald ripening. The simplest method of achieving this is to alter the emulsion in a way that would be expected to break down any flocs

that are present. If there are no flocs present, the particle size will not change after the alteration, but if there are flocs present there will be a decrease in the particle size. A variety of methods are available for breaking down flocs: (i) altering solvent conditions, such as pH, ionic strength, polarity, or temperature; (ii) applying mechanical agitation, such as stirring or sonication; and (iii) adding a more surface-active agent, such as a small molecule surfactant, which displaces the original emulsifier from the droplet interface and which does not cause flocculation itself. The choice of a suitable method depends on the nature of the emulsion, and in particular on the type of emulsifier used to stabilize the system. In emulsions where the interfacial membrane consists of proteins that are held together by extensive intermolecular disulfide bonds it may be necessary to use a combination of mercaptoethanol (to break the disulfide bonds) and a small molecule surfactant (to displace the proteins and stabilize the droplets).

As with microscopy, the preparation of samples for analysis using particle sizing instruments often disturbs the structures of the flocs. For example, emulsions often have to be diluted before they can be analyzed, which can cause disruption of the flocs, particularly when there is only a weak attraction between the droplets. In addition, it is important to carry out dilution using a solvent that has similar properties to the continuous phase in which the droplets were originally dispersed (e.g., ionic strength, pH, and temperature), otherwise the floc structure may be altered. The dispersion of droplets by stirring may also cause some of the flocs to break down, particularly when they are only held together by weak attractive forces. Many of these problems can be overcome using modern particle sizing techniques based on ultrasonics, electroacoustics, NMR, or dielectric spectrometry, because these instruments can be used to analyze concentrated emulsions without the need for any sample preparation (Section 11.3).

As mentioned previously, flocculation causes an increase in the viscosity of an emulsion, and may eventually lead to the formation of a particle gel. As a consequence, flocculation can often be monitored by measuring the change in viscosity or shear modulus of an emulsion (Grover and Bike, 1995; Tadros, 1996; Pal, 1996; Manoj et al., 1998b). An indication of the strength of the attractive forces between flocculated droplets can be obtained from measurements of the viscosity or shear modulus versus shear stress (Pal, 1996; Quemada and Berli, 2002). As the shear stress is increased the flocs become deformed and disrupted so that the viscosity or shear modulus decreases. The stronger the attractive forces between the flocculated droplets, the higher the shear stress needed to disrupt them. Another indirect measurement of the degree of flocculation in an emulsion is to determine the rate at which droplets cream or sediment (Luyten et al., 1993; Basaran et al., 1998; Manoj et al., 1998a; Chanamai and McClements, 2001). As mentioned earlier, flocculation may either increase or decrease the creaming rate depending on the droplet concentration and the structure of the flocs formed. Experimental methods that can be used to monitor creaming and sedimentation were discussed in Section 7.3.3.

## 7.6 Coalescence

Coalescence is the process whereby two or more liquid droplets merge together to form a single larger droplet (Figure 7.26). It is the principal mechanism by which an emulsion moves toward its most thermodynamically stable state because it involves a decrease in the contact area between the oil and water phases (Section 7.2). Coalescence causes emulsion droplets to cream or sediment more rapidly because of the increase in their size (Section 7.3). In O/W emulsions, coalescence eventually leads to the formation of a layer of oil on top of the material, which is referred to as *oiling off*. In W/O emulsions, it leads to the accumulation of water at the bottom of the material. An understanding of the factors

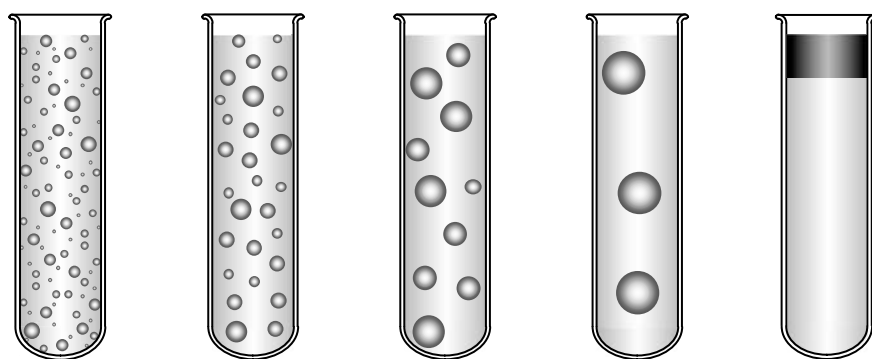


**Figure 7.26** Droplet coalescence leads to a growth in the mean droplet diameter and may eventually lead to complete separation of the oil and aqueous phases.

that influence coalescence is therefore important to food manufacturers attempting to create products with extended shelf lives.

### 7.6.1 *Physical basis of coalescence*

Coalescence is the result of the liquid within two or more emulsion droplets coming into molecular contact (Evans and Wennerstrom, 1994; Kabalnov and Wennerstrom, 1996; Kabalnov, 1998; Walstra, 1996a,b, 2003a). This process can only occur when droplets are in close proximity and the thin film of material separating them is ruptured.\* The fact that the droplets must be in close contact means that coalescence is much more dependent on short-range forces and the precise molecular details of a system, than either gravitational separation or flocculation. The rate at which coalescence proceeds and the physical mechanism by which it occurs are therefore highly dependent on the nature of the emulsifier used to stabilize the system. For this reason, our knowledge of coalescence is much less well developed than that of the other major forms of emulsion instability. Even so, a combination of theoretical and experimental studies has led to a fairly good understanding of the major factors that influence coalescence in some important systems. In general, the susceptibility of droplets to coalescence is determined by the physical mechanism responsible for droplet encounters (e.g., Brownian motion, simple shear, turbulence, gravity), the nature of the forces that act on and between the droplets (i.e., colloidal and hydrodynamic forces), and the resistance of the thin film of material separating the droplets to rupture (see above).

#### 7.6.1.1 *Physical and molecular processes associated with coalescence*

The most important physical and molecular processes that must occur in order for two droplets to coalesce were discussed earlier, that is, droplet encounters, film thinning, film formation, and film rupture (Figure 7.14, Section 7.4). In this section, we focus on some additional factors that are particularly important for determining the stability of droplets to coalescence.

**7.6.1.1.1 Droplet deformation.** In certain systems, emulsion droplets become deformed as they approach each other, which has a pronounced influence on their stability to coalescence (Walstra, 2003a). When the film separating the droplets has thinned to a

\* This material consists of the continuous phase, plus any interfacial membranes surrounding the droplets.

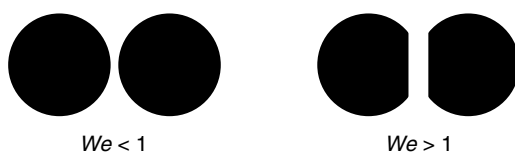


**Figure 7.27** Under certain circumstances emulsion droplets become deformed, for example, large diameter, low interfacial tension, high external stresses. The increase in contact area between flattened droplets has a large impact on coalescence stability.

certain level the surfaces of the droplets become flattened (Figure 7.27). Droplet flattening occurs when the external forces acting on the droplets exceed the internal forces responsible for holding the droplets in a spherical shape (Ivanov et al., 1999; Walstra, 2003a). The internal forces are a result of the Laplace pressure (as well as the resistance of the interfacial membranes to deformation), whereas the external forces may have a variety of origins, including colloidal, hydrodynamic, mechanical, and gravitational forces. The tendency for droplets to become deformed can be described by a Weber number (Walstra, 2003a):

$$We = \frac{\sigma_{\text{EXT}} r^2}{2\gamma h} \quad (7.34)$$

where  $\sigma_{\text{EXT}}$  is the external force,  $r$  is the droplet radius,  $\gamma$  is the interfacial tension, and  $h$  is the surface-to-surface separation. For  $We < 1$  the droplets will tend to remain spherical, but for  $We > 1$  they will tend to be deformed and a flat film is formed between them (Figure 7.27). Expressions for the Weber number for different kinds of external stresses have been given elsewhere (Walstra, 2003a). Calculations using these expressions show that relatively small emulsion droplets ( $r < 1 \mu\text{m}$ ) with interfacial tensions similar to those found in foods tend to remain spherical (unless they are centrifuged at relatively high speeds), but relatively large droplets ( $r > 10 \mu\text{m}$ ) or droplets with low interfacial tensions are often appreciably deformed by the colloidal, hydrodynamic, gravitational, or mechanical forces in the system (Petsev, 1998; Walstra, 2003a). Theoretical and experimental studies have shown that the overall coalescence rate of an emulsion is strongly dependent on the propensity for droplets to become deformed (Petsev, 1998; Ivanov et al., 1999). It is therefore important to take this factor into account when considering droplet coalescence in food emulsions containing relatively large droplets.

**7.6.1.1.2 Film rupture.** Theoretical predictions of the hydrodynamic and colloidal interactions between emulsion droplets often suggest that certain emulsions should be stable to coalescence. For example, if there is a sufficiently high energy barrier or short-range repulsion between the droplets the emulsions should remain indefinitely stable to coalescence. Alternatively, if the droplet surfaces are immobile, then hydrodynamic theory suggests that the droplets should not coalesce because the velocity of film thinning is proportional to the droplet separation ( $V \propto h$ ). Hence, the velocity of film thinning approaches zero as  $h$  approaches zero, so that the droplets should never actually contact each other. Nevertheless, coalescence is often observed experimentally in systems with these characteristics, which suggests that some other mechanism must be involved in initiating droplet coalescence. The tendency for coalescence to occur depends on the

tendency for the thin film of liquid separating the droplet surfaces to rupture. In general, the kinetics of film rupture can be described by the following expression (Walstra, 2003a):

$$f_{\text{FR}} = f_0 \exp\left(-\frac{\Delta G_{\text{FR}}}{k_B T}\right) \quad (7.35)$$

where  $f_{\text{FR}}$  is the frequency of film rupture per unit area ( $\text{m}^{-2} \text{sec}^{-1}$ ),  $f_0$  is the natural frequency ( $\text{m}^{-2} \text{sec}^{-1}$ ), and  $\Delta G_{\text{FR}}$  is the free energy change associated with causing a rupture in the film (e.g., a hole). Typically, the natural frequency of film rupture is around  $10^{30} \text{m}^{-2} \text{sec}^{-1}$  (Kabalnov, 1998). In general, the free energy penalty associated with film rupture depends on many factors including the interfacial tension, hole size, film thickness, colloidal interactions, and mechanical properties of the interfaces (Kabalnov, 1998). An expression for  $\Delta G_{\text{FR}}$  is given below for a simple model system where film rupture is attributed to hole formation (see Section 7.6.1.2). If droplet coalescence occurs when emulsion droplets are in prolonged contact, then film disruption is likely to be the rate-limiting step for droplet coalescence.

#### 7.6.1.2 Mechanisms of film rupture

Before coalescence can occur it is necessary for the thin film separating the droplets to be ruptured. A number of mechanisms have been proposed to account for the rupture of this thin film (Deminier et al., 1998; Kabalnov, 1998; van Aken, 2004). The relative importance of these different mechanisms is largely determined by the characteristics of the continuous phase separating the droplets (e.g., thickness, viscosity, and interfacial tension), and the interfacial membranes surrounding the droplets (e.g., thickness, dilational modulus, shear modulus, and colloidal interactions). In the absence of emulsifier at the droplet surfaces, the following mechanisms could lead to film disruption and coalescence:

- *Capillary wave formation.* Capillary waves form spontaneously in thin films because of the thermal motion of the system (Figure 7.28). If the amplitude of the thermal fluctuations exceeds approximately half the film thickness, a point will be created where the fluids in the different droplets come into molecular contact with each other, which leads to the formation of a hole through which the dispersed phases

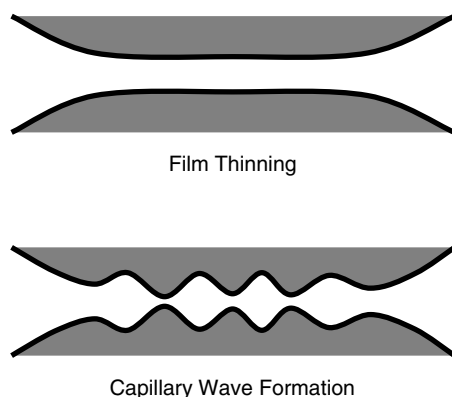


**Figure 7.28** As two droplets approach each other a thin film of continuous phase is formed between them. Once droplets get closer than a critical distance they may spontaneously merge because thermal fluctuations in the thin film generate capillary waves that promote hole formation.



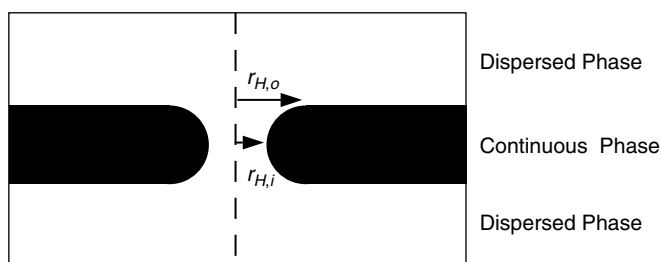


**Figure 7.29** A hole may spontaneously form in the thin film separating emulsion droplets leading to coalescence.

can flow. Capillary waves are damped by repulsive interactions among droplets, high interfacial tensions, and high interfacial mechanical rigidity (Kabalanov, 1998; Walstra, 2003a). In practice, it is believed they are principally responsible for film disruption in systems where the interfacial tensions are extremely low or where there are no repulsive interactions between droplets.

- *Spontaneous hole formation.* Small holes may form spontaneously in a thin film because of the thermal motion of the system (Figure 7.29). If the size of these holes is below some critical value they tend to shrink and collapse, but if it is above this value they tend to grow and film rupture occurs (Kabalanov, 1998).

In most food emulsions, the droplets are surrounded by a layer of emulsifier molecules and there may be mechanical stresses applied to the system. The above mechanisms may also promote film disruption in these systems (Kabalanov, 1998), but additional factors should also be considered (van Aken et al., 2003; van Aken, 2004).

- *Insufficient emulsifier.* If there is insufficient emulsifier present in a system to completely cover all of the oil–water interfaces present, then there will be gaps in the interfacial membranes surrounding the droplets. Coalescence could then occur if two gaps on different droplets came into close proximity, for example, due to spontaneous hole or capillary wave formation. This type of coalescence is likely to be most important during homogenization where new surfaces are continually being created by the intense forces generated within a homogenizer.
- *Film stretching.* If a sufficiently large stress is applied parallel to an interface that is covered with emulsifier, then some of the emulsifier molecules may be dragged along the interface, leaving some regions where there is an excess of emulsifier and other regions where there is a depletion of emulsifier. Coalescence could then occur if two emulsifier-depleted regions on different droplets came into close proximity during a droplet–droplet encounter. This process is only likely to be important if the adsorption of the emulsifier is relatively slow compared to the duration of the applied stresses and droplet encounter frequency, otherwise emulsifier would have time to adsorb to the droplet surfaces and cover the gaps. Film stretching is likely to be important in emulsions that are subjected to intense mechanical stresses, especially if the droplets are in close proximity, for example, in flocculated or concentrated emulsions.
- *Film tearing.* If a sufficiently large stress is applied parallel to an interface that is comprised of a highly cohesive layer of emulsifier molecules, then it may cause the interfacial membrane to tear, leaving exposed emulsifier-depleted patches that promote coalescence (van Aken, 2004). This mechanism is likely to be important in

systems where the interfacial membranes are highly cohesive (e.g., protein membranes with extensive cross-linking), particularly under high applied mechanical stresses, for example, shearing, homogenization, centrifugation. It is likely to be less important in dilute, nonfloculated, and quiescent emulsions because the forces generated in these systems are not strong enough to tear the interfacial membranes.

### 7.6.1.3 Hole formation

In this section, we focus on the spontaneous formation of a hole in the thin layer of material separating two emulsion droplets. Hole formation involves overcoming a free energy penalty associated with creating a hole in the thin layer (Kabalnov, 1998). A physical model, known as the *de Vries* theory, has been developed to calculate the magnitude of the free energy change associated with the formation of a hole in a thin film. Hole formation involves two contributions that cause changes in the contact area between the oil and water phases: (i) there is an increase in contact area inside the film due to hole formation; (ii) there is a decrease in contact area at the planar edges of the film due to hole formation (Figure 7.29). The first contribution dominates for small holes, while the second contribution dominates for large holes. Since increasing the contact area between the oil and water phases is thermodynamically unfavorable, there is an increase in free energy associated with hole formation for small holes, but a decrease for large holes. A geometrical analysis of hole formation has led to the following approximate expression for the overall free energy change associated with hole formation (Kabalanov, 1998):

$$\Delta G_H = -2\pi\gamma[r_H^2 - (\pi - 2)r_H h - (\pi - 3)h^2] \quad (7.36)$$

where  $\gamma$  is the interfacial tension,  $r_H$  is the hole radius, and  $h$  is the film thickness. Calculations of the free energy associated with hole formation versus the hole radius are shown in Figure 7.30. Initially, there is an increase in free energy with increasing hole size, until a maximum value ( $\Delta G_H^*$ ) is reached at a critical hole radius ( $r_H^*$ ), after which there is a decrease in free energy with further increase in hole size. The critical hole radius occurs at 57% of the film thickness (Kabalnov, 1998). If a hole is spontaneously formed that is below the critical hole radius ( $r_H < r_H^*$ ), then the hole will tend to collapse, but if a hole

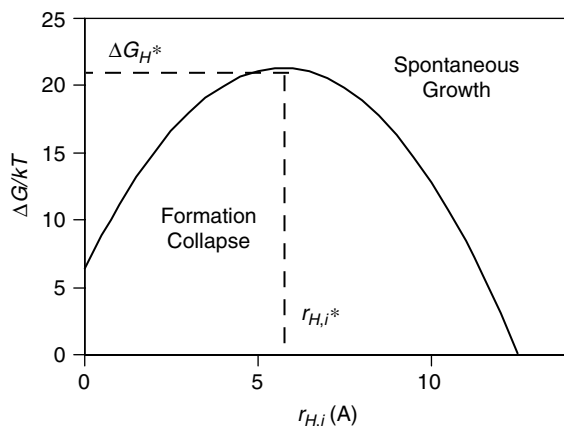


**Figure 7.30** There is a free energy change ( $\Delta G_H$ ) associated with hole formation that determines the frequency of film rupture. Holes only grow once they exceed a critical size ( $r_H^*$ ), otherwise they shrink and disappear.

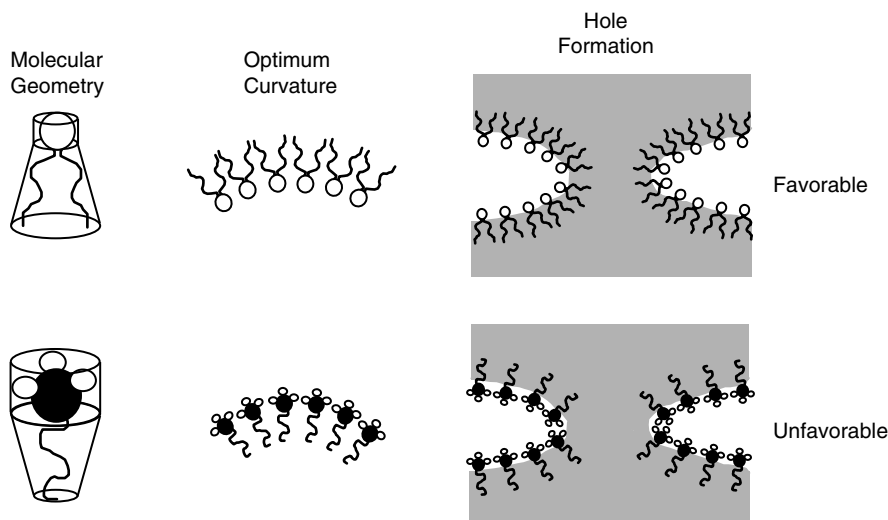


**Figure 7.31** Coalescence occurs more rapidly when the optimum curvature of a surfactant is similar to that of the edge of the hole formed in the thin film. Thus, coalescence is more favorable in oil-in-water emulsions when the surfactant tail group cross-sectional area is greater than that of the head group.

is spontaneously formed that is above the critical hole radius ( $r_H > r_H^*$ ), then the hole will expand, the film will rupture, and coalescence will occur.

The propensity for hole formation to occur is strongly influenced by the presence of emulsifiers at the oil–water interfaces (Kabalnov, 1998). First, emulsifiers decrease the interfacial tension, thereby reducing the free energy associated with altering the contact area between the oil and water phases when a hole is formed. Second, there are additional contributions to hole formation associated with the rheology of the interfacial membranes, for example, the bending energy and dilational modulus (Binks, 1998; Kabalnov, 1998; Ivanov et al., 1999). For example, the formation of a hole in the thin film that separates the droplets depends on the development of a highly curved edge (Figure 7.31). If the curvature of the edge is close to the optimum curvature of the emulsifier membrane ( $H_0 \approx H_{\text{edge}}$ ), then the formation of the hole is thermodynamically favorable. On the other hand, if the optimum curvature of the emulsifier is opposite to that of the edge, then the formation of a hole is thermodynamically unfavorable, and free energy will need to be expended to bend the interface to the correct curvature. The dependence of hole formation on the optimum curvature of a membrane means that coalescence is related to the molecular geometry of the emulsifier molecules (Section 4.4.1). The relationship between the molecular geometry and coalescence stability of O/W and W/O emulsions is highlighted in Figure 7.31. When two oil droplets are separated by a thin film of water (as in an O/W emulsion), then hole formation will be much more likely for a surfactant with a large packing parameter ( $p > 1$ ), than a surfactant with a small packing parameter ( $p < 1$ ). In summary, the coalescence rate tends to increase as the interfacial tension and/or rigidity of the interfacial membranes formed by the adsorbed emulsifier molecules decrease.

#### 7.6.1.4 Rate-limiting step for coalescence

The above discussion of the physicochemical processes that may occur when droplets approach each other suggests that droplet coalescence can be divided into different categories depending on the rate-limiting step.

**7.6.1.4.1 Coalescence immediately after a collision.** In this situation, coalescence occurs immediately after two or more droplets encounter each other during a collision. This type of coalescence is likely to dominate in emulsions where the droplets are free to move around and collide with each other, and there is no deep secondary minimum, high energy barrier, or strong short-range repulsion. Droplets will tend to exist as individual droplets or as coalesced droplets, without substantial flocculation occurring. The rate at which this type of coalescence occurs is governed by many of the same factors as flocculation, that is, the collision frequency and efficiency (Section 7.5.1). The collision frequency is determined by the dominant mechanism responsible for droplet movement for example, Brownian motion, gravity, or applied mechanical forces (Section 7.5.1.1). The collision efficiency is determined by the probability that the droplets can jump over the energy barrier. If the energy barrier is small, then the coalescence collision efficiency is high ( $E_c \rightarrow 1$ ), which may occur when there is no emulsifier present and no electrostatic repulsion between the droplets. If the energy barrier is relatively large, the collision efficiency may be extremely low ( $E_c \rightarrow 0$ ), which is likely to occur in the presence of an emulsifier or if the droplets have an appreciable electrical charge. This type of coalescence is only likely to be significant in systems in which there is insufficient emulsifier present to completely saturate the droplet surfaces or during homogenization where emulsifiers may not have sufficient time to cover the droplet surfaces before a droplet–droplet collision occurs (Chapter 6). It may also be important in emulsions that are subjected to high shear forces, because the impact forces that act on the droplets as the result of a collision may then be sufficient to cause the droplets to jump over the primary minimum. This type of coalescence depends on the collision frequency and therefore follows second-order kinetics (Walstra, 2003a).

**7.6.1.4.2 Coalescence from the secondary minimum.** In this situation, coalescence occurs after the emulsion droplets have been trapped in the secondary minimum for a certain period, that is, the droplets are already in fairly close proximity. The rate of coalescence depends on how quickly the droplets can move from the secondary to the primary minimum over the energy barrier, which is governed primarily by the height of the energy barrier (Petsev, 2000). This type of coalescence is likely to be important in emulsions in which there is a relatively deep secondary minimum, and no strong short-range repulsion to prevent the droplets from coalescing once they have moved into the primary minimum. The rate-limiting step for this type of coalescence is the average time taken for the droplets to move from the secondary to primary minimum,  $\tau_{2 \rightarrow 1^0}$ . This type of process has first-order kinetics (Walstra, 2003a).

**7.6.1.4.3 Coalescence from the primary minimum.** In this situation, coalescence occurs spontaneously after the droplets have been in contact for a prolonged period in the primary minimum. This type of coalescence is likely to be important in systems in which there is a relatively strong short-range repulsion between the droplets, which prevents them from coalescing immediately after moving over the energy barrier and into the primary minimum. The rate-limiting step for this type of coalescence is the average time taken for film rupture to occur, that is,  $\tau_{FR}$ . This type of process has first-order kinetics (Walstra, 2003a; Saether et al., 2004). This mechanism is likely to be the most important in food systems, because they usually have an interfacial membrane that generates very strong short-range repulsion between the droplets.

Coalescence from the primary or secondary minimum occurs when the droplets are in close proximity for extended periods, and is therefore particularly important in emulsions that have high droplet concentrations, that contain flocculated droplets, or that contain droplets that have accumulated at the top (or bottom) of the sample due to

creaming (or sedimentation). In these situations it is no longer convenient to describe the rate at which coalescence occurs in terms of a collision frequency and efficiency, because the droplets are already in contact with each other. Instead, it is more useful to characterize these types of coalescence in terms of a *coalescence time*, that is, the length of time the droplets remain in contact before coalescence occurs. In practice, all of the droplets in an emulsion do not usually coalesce after the same time, and therefore it is more appropriate to define an average coalescence time or to stipulate a range of times over which the majority of the droplets coalesce.

#### 7.6.1.5 Modeling droplet growth due to coalescence

The most appropriate mathematical model to describe coalescence in a particular system depends on the physicochemical phenomenon that is the rate-limiting step for coalescence in that particular system, for example, droplet encounters, movement from secondary to primary minimum, or film rupture. In most food emulsions, it is likely that film rupture is the rate-limiting step because of the relatively strong short-range repulsion generated by the emulsifiers. An approximate expression for the change in the mean droplet size with time in an emulsion due to coalescence has been derived assuming that the droplets are densely packed together and film rupture is a random process (Kabalnov, 1998):

$$\frac{1}{d^2} = \frac{1}{d_0^2} - \frac{Z}{3}ft \quad (7.37)$$

where,  $d$  is the droplet diameter after time  $t$ ,  $d_0$  is the initial droplet diameter,  $Z$  is the number of neighbors in contact with each droplet ( $\sim 6$ ), and  $f$  is the frequency of film rupture. This equation can be used to estimate the time required for complete coalescence to occur (i.e.,  $d \rightarrow \infty$ ):  $\tau \approx 1/(2d_0^2f)$ , assuming  $Z = 6$ . Thus, the coalescence time decreases with increasing initial droplet size and rupture frequency. In general, the above equation has to be modified to take into account the fact that the droplets are not densely packed together, that is, the contact area between droplets is often only a relatively small fraction of their overall surface areas. If it is assumed that the droplets remain spherical during coalescence, and that the thickness of the thin film remains constant, then the following expression can be derived for the change in droplet diameter with time based on the approach described by Kabalnov (1998):

$$\frac{1}{d} = \frac{1}{d_0} - \frac{Z}{12}f\pi h^*t \quad (7.38)$$

where  $h^*$  is the film thickness, which is taken to be the surface-to-surface droplet separation at the primary minimum. This equation can also be used to predict the time for complete coalescence to occur (i.e.,  $d \rightarrow \infty$ ):  $\tau \approx 1/(d_0fh^*)$ , assuming  $Z = 6$ . Coalescence should therefore occur more rapidly with increasing initial droplet size, rupture frequency, and film thickness (although it should be noted that the rupture frequency decreases with film thickness).

The above equations suggest that the mean droplet size increases steadily with time during coalescence, but they give no indication of the expected change in the droplet size distribution with time. Experimental studies of coalescence in concentrated O/W emulsions stabilized by small molecule surfactants have shown that coalescence may proceed by either a homogeneous or a heterogeneous process depending on the system composition and environmental conditions (Demiñiere et al., 1998). In the homogeneous process all the droplets in the emulsion grow uniformly throughout the different regions of the

system, but in the heterogeneous process a few of the droplets grow very rapidly, while the rest remain approximately the same size as in the original system. Homogeneous coalescence therefore tends to lead to the formation of monomodal droplet size distributions with the peak moving upward with time, whereas heterogeneous coalescence tends to lead to the formation of bimodal droplet size distributions with the fraction of droplets in the larger peak growing with time. Heterogeneous coalescence may lead to extensive "oiling-off," where an oil layer is formed on top of the emulsion. More sophisticated physical models than the ones discussed above are therefore required to model the change in the particle size distribution with time due to coalescence.

Finally, it should be noted that if the rate-limiting step for coalescence is droplet encounters, rather than film rupture, then the equations developed for droplet flocculation can be used to predict the change in mean particle size with time.

## 7.6.2 *Methods of controlling coalescence*

The rate at which coalescence occurs is strongly dependent on the colloidal and hydrodynamic interactions between the droplets, as well as the physicochemical properties of the interfacial membranes that surround the droplets. As a consequence, the most appropriate method of controlling coalescence is highly dependent on the type of emulsifier used to stabilize the system, as well as the prevailing environmental conditions. Even so, it is possible to give some general advice about the most effective methods of avoiding coalescence. These methods can be conveniently divided into two categories: those that prevent droplet contact and those that prevent rupture of the interfacial membranes surrounding the droplets.

### 7.6.2.1 *Prevention of droplet contact*

The coalescence rate can be decreased by reducing the length of time that droplets are in close contact. The droplet contact time can be reduced in a number of different ways, including: (i) decreasing their collision frequency; (ii) ensuring that they do not flocculate; (iii) preventing them from forming a concentrated layer at the top (or bottom) of an emulsion due to creaming (or sedimentation); and (iv) ensuring that the droplet concentration in the emulsion is not so high that the droplets become close packed.

Even when the droplets are in contact with each other for extended periods (e.g., in flocs, creamed layers, or concentrated emulsions), then they can still be prevented from coalescing by ensuring that they do not get too close. The probability of coalescence occurring increases as the thickness of the layer of continuous phase separating them decreases, because thermal fluctuations may then become large enough to form a hole that extends from one droplet to another. The thickness of this layer is determined principally by the magnitude and range of the various attractive and repulsive forces that act between the droplets (Chapter 3). The coalescence stability can therefore be enhanced by ensuring there is a sufficiently large repulsive interaction to prevent the droplets from coming into close contact. This can be achieved in a number of ways, including varying the emulsifier type, pH, ionic strength, or temperature.

### 7.6.2.2 *Prevention of rupture of interfacial membranes*

The rupture of the thin film between the droplets depends on changes in its shape caused by thermal energy or applied mechanical forces (Evans and Wennerstrom, 1994; Kavalnov, 1998; Deminiere et al., 1998; van Aken, 2004). The magnitude of these changes is governed by the interfacial tension and rheology of the membrane (Israelachvili, 1992; Evans and Wennerstrom, 1994). The lower the interfacial tension or rheology the more mobile is the interface and therefore the more likely a hole will form that leads to film rupture.

Consequently, coalescence becomes less likely as the interfacial tension or the viscoelasticity of the membrane increases (Dickinson, 1992). The thickness of the interfacial membranes around the droplets is also likely to influence the coalescence stability of emulsions. Droplets with thicker membranes would be expected to provide the greatest stability because they are less likely to be ruptured and they provide a greater steric repulsion between the droplets. For small molecule surfactants, it is important to select an emulsifier that has an optimum curvature that does not favor coalescence (Section 7.6.1.3).

The likelihood of a hole forming somewhere in a thin film increases as its overall area increases. Consequently, the larger the contact area between two droplets, the greater the coalescence rate. The coalescence rate therefore increases as the size of the droplets in an emulsion increases, or when the droplets become flattened against one another. Droplet flattening tends to occur in highly concentrated emulsions, in creamed layers, or when emulsions are subjected to external forces (Dickinson and Stainsby, 1982; Walstra, 1996b, 2003a). Large droplets are more prone to flattening than smaller droplets because the interfacial forces that tend to keep them in a spherical shape are lower (Section 6.4.1). Large droplets are also more prone to collision-induced coalescence because the impact forces generated during a collision are greater, and the magnitude of the attractive forces between the droplets is larger. On the other hand, increasing the size of the droplets decreases the frequency of the encounters between droplets, which may be the dominant effect in emulsions where the rate-limiting step is the collision frequency.

Emulsion droplets stabilized by relatively thick cohesive interfacial membranes (e.g., proteins and polysaccharides) are relatively resistant to coalescence under quiescent conditions, but may become unstable when mechanical forces are applied to the system (e.g., intense stirring, homogenization, or centrifugation), especially in concentrated systems (van Aken, 2004). This instability has been attributed to stretching and tearing of the interfacial membranes surrounding the droplets, which leads to the exposure of emulsifier-depleted regions on the droplet surfaces.

### 7.6.3 Factors affecting coalescence

#### 7.6.3.1 Emulsifier type

Protein emulsifiers have been found to be extremely effective at providing protection against coalescence, especially under quiescent conditions (Dickinson, 1992; van Aken and Zoet, 2000; van Aken, 2002, 2004). The main reason for this is that proteins are capable of producing emulsions with small droplet sizes, they provide strong repulsive forces between droplets (due to a combination of electrostatic and steric interactions), the interfacial tension is relatively high, and they form membranes that are highly resistant to rupture. Emulsion droplets stabilized by polysaccharides are also highly stable to coalescence for the same reasons. Partially hydrolyzed proteins are less effective at preventing coalescence because they tend to form thinner, less viscoelastic interfacial layers that are easier to rupture (Euston et al., 2001; van der Ven et al., 2001).

Extensive coalescence has been observed in protein-stabilized emulsions when they are subjected to mechanical stresses, such as shear, elongational, or turbulent flow (Dickinson, 1997; Dickinson and Davies, 1999; Mohan and Narsimhan, 1997; van Aken, 2002). Mechanical stresses may cause the adsorbed proteins to undergo extensive clumping at the droplet surfaces. Clump formation may lead to exposure of oil regions in the interfacial membranes that promotes droplet coalescence. Alternatively, strong intermolecular interactions between proteins adsorbed onto different droplets may lead to “tearing” of the interfacial membranes when the emulsions are exposed to mechanical stresses and the droplets are separated. Presumably, this tearing process would lead to the formation of

oil patches in the interfacial membrane that were temporarily not covered by protein, thereby making the system susceptible to coalescence.

Coalescence of emulsions stabilized by small molecule surfactants is largely governed by their ability to keep droplets apart, rather than the resistance of the droplet membrane to rupture. Nonionic surfactants, such as the Tweens, do this by having polymeric hydrophilic head groups that provide a large steric overlap and hydration repulsion (Section 3.5). Ionic surfactants, such as SDS and fatty acids, achieve this mainly through electrostatic repulsion (Section 3.4). Nevertheless, this electrostatic repulsion is only appreciable when the aqueous phase has a low ionic strength. At high ionic strengths, the electrostatic repulsion is screened by the counterions, so that the droplets come close together, and are prone to coalescence, because the membrane is easily disrupted due to its low interfacial viscosity and interfacial tension.

### 7.6.3.2 *Influence of environmental conditions*

Food manufacturers often need to create emulsions with extended shelf lives and so it is important for them to understand the influence of various types of processing and storage conditions on droplet coalescence. As mentioned above, emulsions stabilized by milk proteins are fairly stable to coalescence under quiescent conditions, provided that the droplets are completely liquid (Das and Kinsella, 1990; van Aken, 2004). However, droplet coalescence may occur when the droplets are subjected to shear forces or brought into close contact for extended periods, for example, in a creamed layer or concentrated emulsion (Dickinson and Williams, 1994; van Aken, 2004). The presence of small amounts of low-molecular weight surfactants in the aqueous phase greatly enhances the tendency of emulsion droplets to coalesce during shearing (Chen and Dickinson, 1993; Dickinson et al., 1993b; Lips et al., 1993). The stability of emulsions to shear forces therefore depends on the structure and properties of the adsorbed interfacial layer (Dickinson et al., 1993b). Centrifugation of an emulsion may also lead to extensive coalescence because the droplets are forced together into a compact droplet-rich layer with sufficient force to flatten the droplets and disrupt the membranes (Dickinson and Stainsby, 1982; van Aken, 2002, 2004).

When an O/W emulsion is frozen only part of the water is initially crystallized and the oil droplets are forced into the remaining liquid region (Sherman, 1968a; Berger, 1997; Dickinson and Stainsby, 1982; Hartel, 2001). The ionic strength of this region is increased significantly because of the concentration of salts and other components. The combination of forcing the droplets into a more confined space and of altering the solvent conditions is often sufficient to disrupt the droplet membranes and promote coalescence once an emulsion is thawed (Berger, 1997). In addition, the oil droplets may crystallize during the freezing process, which can lead to emulsion instability through partial coalescence (Section 7.7). Under certain circumstances, freezing can cause cold denaturation of proteins, which may lead to a reduction in their functionality (Walstra, 2003a). Finally, freezing of the water phase may lead to dehydration of the emulsifier molecules adsorbed to the surface of the droplets, which promotes droplet–droplet interactions. There are many factors that contribute to the instability of emulsions during freezing and thawing, and the development of freeze–thaw stable emulsions still remains a major challenge to food scientists.

Coalescence may also be promoted when an emulsion is dried into a powder, because drying may disrupt the integrity of the interfacial layer surrounding the droplets, for example, during freeze or spray drying (Young et al., 1993a,b), which leads to coalescence once the emulsion is reconstituted. The coalescence stability can often be improved by adding relatively high concentrations of protein or carbohydrates to the system prior to drying (Young et al., 1993a,b). These molecules form a thick interfacial membrane around the droplets that is less prone to disruption during the dehydration process.



The coalescence of droplets in an emulsion may also be influenced by various chemical or biochemical changes that occur over time. Lipid oxidation leads to the development of surface-active reaction products that may be capable of displacing emulsifier molecules from the droplet surface and thereby promoting coalescence (Coupland and McClements, 1996). Extensive enzymatic hydrolysis of proteins or polysaccharides could cause an interfacial layer to be disrupted (Euston et al., 2001), again promoting droplet coalescence. An understanding of the various chemical and biochemical factors that determine coalescence is therefore essential in creating emulsions with extended shelf lives or that can be broken down under specific conditions.

#### 7.6.3.3 *Influence of impurities and surfaces*

In many food emulsions, droplet coalescence is promoted by the presence of impurities and surfaces, for example, gas bubbles, solid particles, crystals, surfaces (van Aken, 2004). For example, coalescence can be promoted when the droplets are in close proximity to a fluid or solid surface, provided the dispersed phase is capable of wetting the surface (i.e., the contact angle is lower than 90°). This type of coalescence is believed to be important in aerated O/W emulsions, where the oil droplets become coalesced when they spread around air bubbles, for example, in whipped cream. Surface-induced droplet coalescence may also be promoted when emulsion droplets are confined between thin moving surfaces, for example, in a colloid mill during homogenization or in the mouth during mastication (van Aken, 2004). Finally, droplet coalescence may be promoted by the presence of solid particles or crystals due to their ability to disrupt the thin film separating the droplets, especially during shearing, for example, fat, ice, sugar, or salt crystals.

#### 7.6.4 *Measurement of droplet coalescence*

Experimental characterization of coalescence can be carried out using a variety of analytical techniques, many of which are similar to those used to monitor flocculation (Section 7.5.4). The most direct approach is to observe droplet coalescence using an optical microscope (Mikula, 1992). An emulsion is placed on a microscope slide and the change in the droplet size distribution is measured as a function of time, by counting the individual droplets manually or by using a computer with image processing software. It is possible to observe individual coalescence events using a sufficiently rapid camera, but these events are often so improbable in food emulsions that they are difficult to follow directly (Dickinson, 1992; Walstra, 1996b). The change in droplet size of an emulsion during storage can also be measured using other forms of microscopy, such as confocal laser scanning or electron microscopy (Section 11.3.1).

An alternative microscopic method involves the observation of the coalescence of single emulsion droplets at a planar oil–water interface (Dickinson et al., 1988). An oil droplet is released from a capillary tube into an aqueous phase and moves upward to the oil–water interface due to gravity (Figure 7.32). The time taken for the droplet to merge with the interface after it has arrived there is determined by observing it using an optical microscope. The results from this type of experiment demonstrate that there are two stages to droplet coalescence: (i) a lag phase corresponding to film thinning, where the droplet remains at the interface but no coalescence occurs, and (ii) a coalescence phase, where the membrane spontaneously ruptures and the droplets merge with the bulk liquid. Droplets exhibit a spectrum of coalescence times because membrane rupture is a chance process. Consequently, there is an approximately exponential decrease in the number of noncoalesced droplets remaining at the interface with time after the lag phase. The major disadvantages of this technique are that only droplets above about 1  $\mu\text{m}$  can be observed, and that coalescence often occurs so slowly that it is impractical to monitor it continuously using



**Figure 7.32** Microscopic technique for monitoring coalescence of single droplets at a planar oil–water interface. The time taken for a droplet to merge with the interface is determined microscopically.

a microscope. To detect coalescence over a reasonably short period, it is necessary to have relatively low concentrations of emulsifier at the surfaces of the droplets, which is unrealistic because the droplets in food emulsions are nearly always saturated with emulsifier.

Droplet coalescence can also be monitored by measuring the time dependence of the droplet size distribution using an instrumental particle sizing technique, such as light scattering, electrical pulse counting, ultrasonic spectrometry, or NMR (Section 11.3). These instruments are fully automated and provide a measurement of the size of a large number of droplets in only a few minutes. Nevertheless, it is important to establish whether the increase in droplet size is due to coalescence, flocculation, or Ostwald ripening. Coalescence can be distinguished from flocculation by measuring the droplet size distribution in an emulsion, then changing the environmental conditions so that any flocs are broken down and remeasuring the droplet size distribution (Section 7.5.4). If no flocs are present the average droplet size remains constant, but if there are flocs present it decreases. Coalescence is more difficult to distinguish from Ostwald ripening because they both involve an increase in the average size of the individual droplets with time.

As mentioned earlier, studies of coalescence can take a considerable time to complete because of the very slow rate of the coalescence process. Coalescence studies can be accelerated by applying a centrifugal force to an emulsion so that the droplets are forced together: the more resistant the membrane to disruption, the higher the centrifugation force it can tolerate or the longer the time it will last at a particular speed before membrane disruption is observed (Smith and Mitchell, 1976; Sherman, 1995; van Aken, 2002). The extent of coalescence is determined by measuring the change in the particle size distribution or the extent of oiling off (Kabalnov, 1998; Deminiere et al., 1998). Alternatively, coalescence can be accelerated by subjecting the emulsions to high shear forces and measuring the shear rate at which coalescence is first observed, or the length of time that the emulsion must be sheared at a constant shear rate before coalescence is observed (Dickinson and Williams, 1995). Nevertheless, these accelerated coalescence tests may not always give a good indication of the long-term stability of an emulsion. For example, chemical or biochemical changes may occur in an emulsion that is stored for a long period that eventually lead to coalescence, but they may not be detected in an accelerated coalescence test. Alternatively, there may a critical force that is required to cause membrane rupture that is exceeded in a centrifuge or shearing device, but which would never be

exceeded under normal storage conditions. As a consequence, one must use these accelerated coalescence tests with caution.

The rate of coalescence can also be measured in emulsions where there is no net change in droplet size with time, for example, when droplet breakup and disruption rates balance each other during homogenization (Section 6.4.2). In general, these methods involve creating an emulsion that initially contains a mixture of droplets with different internal compositions, then measuring the redistribution of the dispersed phase components with time after mechanical stresses have been applied to the emulsions. For example, an O/W emulsion may be created that has a fraction of oil droplets containing a yellow oil-soluble dye and the other fraction containing a blue oil-soluble dye (Schubert et al., 2003). If the droplets coalesce with each other then their contents are mixed, which results in a decrease in the fraction of droplets with the initial dye colors (yellow and blue) and an increase in the fraction of droplets of mixed color (green).

## 7.7 Partial coalescence

Partial coalescence occurs when two or more partly crystalline oil droplets come into contact and form an irregularly shaped aggregate (Figure 7.33). The aggregate partly retains the shape of the droplets from which it was formed because the mechanical strength

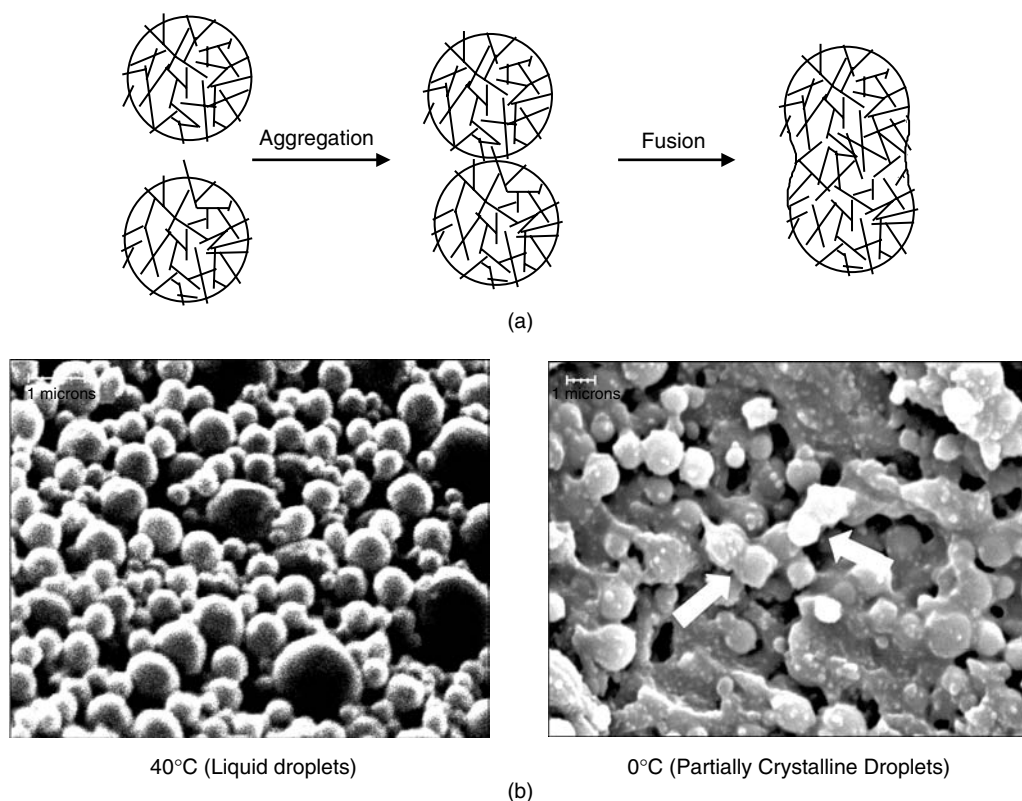


**Figure 7.33** Partial coalescence occurs when a crystal from one partially crystalline oil droplet penetrates into the liquid portion of another partially crystalline oil droplet. (a) Schematic representation of partial coalescence. (b). Cryo-SEM images of 40 wt% Tween 20 stabilized emulsion quench cooled from either 40°C (liquid droplets) or 0°C (partially crystalline droplets). Irregular fat aggregates are formed in the latter case due to partial coalescence. Scale bar is 1  $\mu\text{m}$ . SEM images kindly supplied by Prof. John Coupland (Pennsylvania State University).

of the fat crystal network within the droplets prevents them from completely merging together (Boode, 1992; Dickinson and McClements, 1995; Walstra, 1996b, 2003a; Coupland, 2002). The partially crystalline oil droplets may encounter each other during a collision within a bulk aqueous medium or they may encounter each other after adsorption to the surfaces of air bubbles formed during shearing. Partial coalescence is particularly important in dairy products, because milk fat globules are partly crystalline over a fairly wide range of temperatures (Mulder and Walstra, 1974; Walstra and van Beresteyn, 1975; Buchheim and Dejmek, 1997; Berger, 1997; Walstra, 1999, 2003a). The application of shear forces or temperature cycling to cream containing partly crystalline milk fat globules can cause partial coalescence, which leads to a marked increase in viscosity (*thickening*) and subsequent phase separation (van Boekel and Walstra, 1981; Boode et al., 1991; Boode, 1992; Vanapalli and Coupland, 2001). Partial coalescence is an essential process in the production of ice cream, whipped toppings, butter, and margarine (Dickinson and Stainsby, 1982; Barford and Krog, 1987; Barford et al., 1991; Moran, 1994; Goff, 1997a–c, 1999, 2002, 2003). O/W emulsions are cooled to a temperature where the droplets are partly crystalline and a shear force is applied, which leads to droplet aggregation via partial coalescence (Mulder and Walstra, 1974). In butter and margarine aggregation results in phase inversion (Moran, 1994), whereas in ice cream and whipped cream the aggregated fat droplets form a network that surrounds the air cells and extends throughout the aqueous phase, thus providing the necessary mechanical strength required to produce good stability and texture (Barford et al., 1987; Goff, 1993; 1997a–c; Goff and Hartel, 2003).

### 7.7.1 Physical basis of partial coalescence

Partial coalescence is initiated when a solid fat crystal from one droplet penetrates into the liquid oil portion of another droplet (Boode, 1992; Boode and Walstra, 1993a,b; Boode et al., 1993; Walstra, 1996b, 2003a). Normally, the fat crystal would be surrounded by the aqueous phase, but when it penetrates into another droplet it is surrounded by liquid oil. This causes the droplets to remain aggregated because it is thermodynamically more favorable for a fat crystal to be surrounded by oil molecules than by water molecules, that is, the fat crystal is wetted better by liquid oil than by water. Over time the droplets merge more closely together because this reduces the surface area of oil exposed to water (Figure 7.33). Hence, the junction holding the droplets together often becomes stronger and more difficult to break after aging of the emulsion (Walstra, 2003a).

Partial coalescence may occur immediately after two droplets come into contact with each other, or it may occur after the droplets have been in contact for an extended period (Boode, 1992). The partially crystalline droplets may encounter each other in the bulk aqueous phase or after adsorption to the surface of an air bubble formed by agitating the systems. Partial coalescence is affected by many of the same factors that influence normal coalescence, including contact time, collision frequency, droplet separation, colloidal and hydrodynamic interactions, interfacial tension, and membrane viscoelasticity (Section 7.6). Nevertheless, there are also a number of additional factors that are unique to partial coalescence, the most important being the fact that the oil phase is crystalline (Boode and Walstra, 1993a,b; Walstra, 1996b, 2003a).

The  $\phi_{\text{SFC}}$  is the percentage of fat that is crystalline at a particular temperature, varying from 0% for a completely liquid oil to 100% for a completely solid fat. Partial coalescence only occurs in emulsions that contain partly crystalline droplets, because a solid fat crystal from one droplet must penetrate into the liquid oil region of another droplet (Boode and Walstra, 1993a,b; Walstra, 2003a). If the droplets were completely liquid they would undergo normal coalescence, and if they were completely solid they would undergo flocculation rather than partial coalescence because the rigid droplets are not able to merge

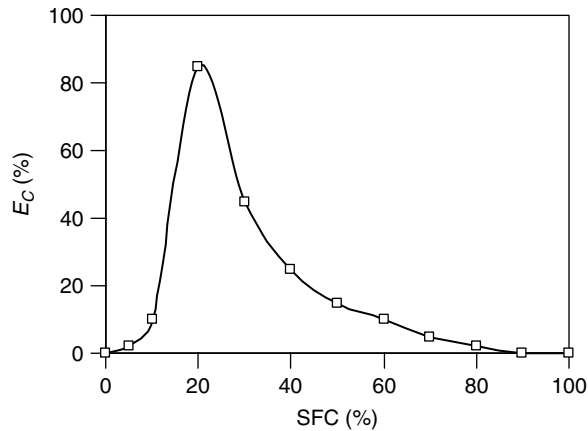


**Figure 7.34** Schematic diagram of the influence of droplet solid fat content on the rate of partial coalescence in oil-in-water emulsions. A maximum rate is usually observed at an intermediate solid fat content.

together. Increasing the  $\phi_{\text{SFC}}$  from 0% causes an initial increase in the partial coalescence rate until a maximum value is reached, after which the partial coalescence rate decreases (Boode and Walstra, 1993a,b). Consequently, there is a certain  $\phi_{\text{SFC}}$  at which the maximum rate of partial coalescence occurs (Figure 7.34). The SFC at which this maximum rate occurs depends on the morphology and location of the crystals within the droplets, as well as the magnitude of the applied shear field (Boode, 1992; Boode and Walstra, 1993a,b; Walstra, 2003a).

The dimensions and location of the fat crystals within an emulsion droplet play an important role in determining its susceptibility to partial coalescence (Darling, 1982; Campbell, 1989; Walstra, 2003a). The further a fat crystal protrudes into the aqueous phase, the more likely it is to penetrate another droplet and therefore cause partial coalescence (Darling, 1982; Walstra, 1996b). The different types of partially crystalline fat globules commonly observed in milk are represented in Figure 7.35 (Walstra, 1967). Milk fat usually crystallizes as small platelets that appear needle shaped when observed by polarized light microscopy (Walstra, 1967; Boode, 1992). These crystals may be evenly distributed within the interior of the droplet (type N), located exclusively at the oil–water interface (type L) or a combination of the two (type M). The type of crystals formed depends on whether

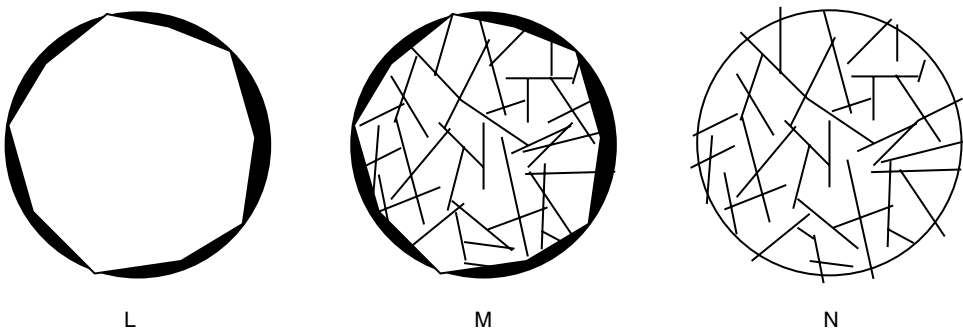


**Figure 7.35** Typical distributions of fat crystals found in milk fat globules.

the nucleation is homogeneous, surface heterogeneous, or volume heterogeneous, as well as the cooling conditions (Dickinson and McClements, 1995; Walstra, 2003a).

It is possible to alter the distribution of fat crystals within an emulsion droplet after they have been formed by carefully cycling the temperature (Boode et al., 1991; Boode, 1992). When milk is cooled rapidly, there is a tendency for the fat crystals within the droplets to be fairly evenly distributed (type N). Thermodynamically, it is actually more favorable for these crystals to be located at the oil–water interface rather than in the interior of the droplets, but their movement to the interface is restricted because they are trapped within the fat crystal network. If the emulsion is heated to a temperature where most (but not all) of the crystals melt, the crystal network is broken down, and the remaining crystals move to the interface unhindered by the crystal network. When the emulsion is cooled these crystals act as nucleation sites and crystal growth is restricted to the droplet surface. Thus, L-type droplets are formed with large crystals located at the oil–water interface. This phenomenon is believed to be responsible for the increase in the rate of partial coalescence that occurs during temperature cycling of O/W emulsions (Boode et al., 1991). The crystals at the interface in L-type droplets are larger and protrude further into the aqueous phase and are therefore more likely to cause partial coalescence (Boode, 1992).

In other types of food emulsions there may be different crystal structures within the droplets than those shown in Figure 7.35. The crystal structure formed will depend on factors such as the chemical structure of the fat, the cooling rate, temperature cycling, the application of shear forces, droplet size distribution, the type of emulsifier used to stabilize the emulsion droplets, and the presence of any impurities that can poison or catalyze crystal growth. Further work is needed to elucidate the relationship between the morphology and location of crystals within emulsion droplets and their propensity to undergo partial coalescence.

### 7.7.2 *Methods of controlling partial coalescence*

The various factors that influence partial coalescence in O/W emulsions have recently been reviewed by Walstra (2003a). The major factors are the disperse phase volume fraction, mechanical agitation, crystal morphology, contact angle, colloidal interactions, and interfacial structure. In this section, we use this knowledge to highlight methods of controlling partial coalescence in O/W emulsions.

#### 7.7.2.1 *Prevention of close contact*

Partial coalescence is more likely to occur in emulsions that contain droplets that remain in contact for extended periods, that is, flocculated emulsions, concentrated emulsions, and creamed layers (Walstra, 2003a). For example, experiments have shown that partial coalescence occurs more rapidly when oil droplets are located in a creamed layer than when they are freely suspended in the aqueous phase (Boode, 1992). This is because the contact time is greater and the interdroplet separation is reduced. In emulsions containing freely suspended droplets, the rate of partial coalescence is proportional to the frequency of encounters between emulsion droplets. Thus, anything that increases the collision frequency will increase the rate of partial coalescence (provided it does not also reduce the collision efficiency). The precise nature of these effects depends on whether the droplet collisions are induced by Brownian motion, shear, or gravity (van Boekel and Walstra, 1981; Boode et al., 1991). In general, the collision frequency is proportional to the square of the disperse phase volume fraction (Section 7.5.1). Experiments with O/W emulsions have shown that the partial coalescence rate is roughly proportional to  $\phi^2$  up to oil concentrations around 20%, after which it increases more rapidly than expected (Walstra, 2003a).

O/W emulsions that are stable to partial coalescence under quiescent conditions are often prone to it when they are subjected to mechanical agitation. A number of physicochemical

mechanisms may contribute to the increased rate of partial coalescence during shearing of emulsions. First, shearing increases the collision frequency. Second, shearing may increase the collision efficiency because a crystal protruding from one droplet is more likely to penetrate into another droplet when the droplets “roll over” each other in a shear field (Walstra, 2003a). Finally, a high shear stress may force droplets closer together, thus allowing fat crystals to penetrate through the interfacial membranes surrounding the droplets more effectively. Partial coalescence is usually more rapid when emulsions are subjected to turbulent flow conditions than laminar flow conditions (Walstra, 2003a).

Partial coalescence can only occur when droplets get so close together that a fat crystal from one droplet protrudes into another droplet. Thus, any droplet–droplet interaction that prevents droplets from coming into close contact should decrease the rate of partial coalescence, for example, electrostatic, steric, hydration, and hydrodynamic repulsion. On the other hand, any droplet–droplet interaction that causes the droplets to come into close contact should increase the rate of partial coalescence, for example, van der Waals, hydrophobic, depletion, shear, centrifugal, and gravitational forces.

The size of the droplets in an emulsion affects partial coalescence in a number of ways. The efficiency of partial coalescence can increase with droplet size because there is a greater probability of their being a crystal present in the contact zone between the droplets (Boode, 1992; Walstra, 2003a). On the other hand, increasing the droplet size decreases their collision frequency, which can lead to a decrease in partial coalescence with increasing size (McClements et al., 1994). The influence of droplet size is therefore quite complex and depends on the rate-limiting step in the partial coalescence process.

#### 7.7.2.2 *Prevention of interfacial membrane disruption*

Emulsifiers that form thicker and more viscoelastic films at the oil–water interface are more resistant to penetration by fat crystals and so provide greater stability to partial coalescence (Walstra, 2003a). Consequently, the rate of partial coalescence is less for droplets stabilized by proteins than for those stabilized by small molecule surfactants (Palanuwech and Coupland, 2003). The chemical structure of the emulsifier molecules at the interface of the emulsion droplets has an important impact on the stability of a number of foods. The presence of phospholipids in dairy emulsions has been observed to decrease their stability to thickening under the influence of shear forces, which has been attributed to the displacement of protein molecules from the oil–water interface by the more surface-active phospholipids, leading to the formation of an emulsifier film that is more susceptible to penetration by fat crystals (Boode, 1992). When an ice cream mix or dairy whipped topping is aged in the presence of small molecule surfactants prior to cooling and shearing the resulting product has improved texture and better stability (Goff, 1997a–d; Goff and Hartel, 2003). This is because emulsifiers displace the milk proteins from the oil–water interface and so enhance the tendency for partial coalescence to occur during subsequent cooling and shearing. For these reasons small molecule surfactants are often added to ice creams and dairy toppings to improve their physical characteristics. van Boekel and Walstra (1981) calculated that only about one in a million encounters between droplets leads to partial coalescence. This suggests that the rate-limiting step of partial coalescence is the penetration of the emulsifier film by a crystal and subsequent nucleation, rather than the collision frequency.

#### 7.7.2.3 *Control of crystal concentration, structure, and location*

The degree of partial coalescence in an emulsion can be regulated by controlling the concentration, structure, and location of the fat crystals within the droplets. The most effective method of preventing partial coalescence is to ensure that all the droplets are

either completely liquid or completely solid. This can be achieved by carefully controlling the temperature of the emulsion so that it is above or below some critical level. If it is not possible to alter the temperature, then the SFC could be controlled by selecting a fat with a different melting profile (Moran, 1994). The susceptibility of an emulsion to partial coalescence also depends on the morphology and the precise location of the fat crystals within the emulsion droplets. The greater the number of crystals that protrude from a droplet and the further that they protrude, the more effective is partial coalescence. At low SFCs the crystals often do not penetrate very far into the aqueous phase, but once a critical SFC is reached a network of aggregated crystals is formed, which tends to increase the likelihood that crystals will protrude out of the droplets (Walstra, 2003a). Thus, two emulsions with the same SFC may have very different stabilities because of differences in crystal structure. The number and morphology of crystals in droplets can be controlled by varying the cooling rate at which they are formed, by selecting an appropriate fat source, or by adding components that modify fat nucleation and crystal growth rates (Sato, 1988; Awad and Sato, 2001, 2002; Awad et al., 2001).

### 7.7.3 *Experimental characterization of partial coalescence*

A variety of experimental techniques have been used to monitor the susceptibility of food emulsions to partial coalescence (Dickinson and McClements, 1995; Hartel, 2001). The physical state of fats can be monitored using experimental techniques that use differences in the physicochemical properties of the solid and liquid phases (e.g., density, compressibility, birefringence, molecular mobility, or packing) or changes associated with the solid-liquid phase transition (e.g., absorption or release of heat). The physicochemical properties that are of most interest to food scientists are: (i) the final melting point of the fat, (ii) the variation of the SFC with temperature, (iii) the morphology, interactions, and location of the crystals within the droplets, (iv) the packing of the fat molecules within the crystals, and (v) the influence of droplet crystallization on the overall stability and physicochemical properties of the emulsion.

The variation of the SFC with temperature can be measured using a variety of techniques, including density measurements, differential scanning calorimetry, NMR, ultrasonic velocity measurements, and electron spin resonance (Dickinson and McClements, 1995; Hartel, 2001). The technique used in a particular experiment depends on the equipment available, the information required, and the nature of the sample being tested. The position of fat crystals relative to an oil-water interface depends on the relative magnitude of the oil-water, oil-crystal, and crystal-water interfacial tensions, and is characterized by the contact angle (Darling, 1982; Campbell, 1989; Walstra, 2003a). Darling (1982) has described a technique that can be used to measure the contact angle between liquid oil, solid fat, and aqueous phases.

Two fats can have exactly the same SFC but very different physical characteristics because of differences in the crystal habit and spatial distribution of the crystals. The location of crystals within a system, and their crystal habit can be studied by polarized light microscopy (Boode, 1992; Kellens et al., 1992) or electron microscopy (Soderberg et al., 1989) depending on the size of the crystals. The packing of the molecules in the crystals can be determined by techniques that use the scattering or adsorption of radiation (Hartel, 2001). X-ray diffraction and small angle neutron scattering have been used to determine the long and short spacings of the molecules in fat crystals (Hernqvist, 1990; Cebula et al., 1992; Hartel, 2001). Infrared and Raman spectroscopy have been used to obtain information about molecular packing via its affect on the vibration of certain chemical groups in fat molecules (Chapman, 1965). Each polymorphic form has a unique spectrum that can be used to identify it. The polymorphic form of fat crystals can also be



identified by measuring the temperature at which phase transitions occur and the amount of heat absorbed/released using differential scanning calorimetry (DSC) (Hartel, 2001). Recently, techniques have been developed that combine different analytical techniques to simultaneously monitor changes in SFC and polymorphism in emulsions, for example, DSC, ultrasonics, and x-ray diffraction (Awad and Sato, 2001, 2002).

Partial coalescence leads to an increase in the size of the particles in an emulsion, which can be followed by microscopic, light scattering, electrical pulse counting, or ultrasonic techniques (Section 11.3). In addition, partial coalescence may lead to extensive oiling-off, which can be monitored by visual observation or by spectrometry (Palanuwech et al., 2003).

Ultimately, a food scientist is interested in the influence of droplet crystallization on the bulk physicochemical properties of a food emulsion, such as its appearance, stability, and texture. Partial coalescence also causes an increase in emulsion viscosity, and may eventually lead to the formation of a three-dimensional network of aggregated droplets, so that it can be monitored by measuring the increase in viscosity or shear modulus, either as a function of time or temperature (Boode, 1992; Boode and Walstra, 1993a,b; Walstra, 2003a). The stability of emulsion droplets to creaming or sedimentation is also influenced by partial coalescence, which can be followed by the techniques described in Section 7.3.

## 7.8 Ostwald ripening

Ostwald ripening is the process whereby large droplets grow at the expense of smaller ones because of mass transport of dispersed phase from one droplet to another through the intervening continuous phase (Figure 7.36) (Kabalnov and Shchukin, 1992; Taylor, 1995; Weers, 1998). It is negligible in most food emulsions because the mutual solubility's of triacylglycerols and water are so low that the mass transport rate is insignificant (Dickinson and Stainsby, 1982; Weers, 1998). Nevertheless, it is important in O/W emulsions that contain more water-soluble lipids, for example, flavor oils (Ray et al., 1983; Buffo and Reineccius, 2001), or when the aqueous phase contains alcohol, for example,

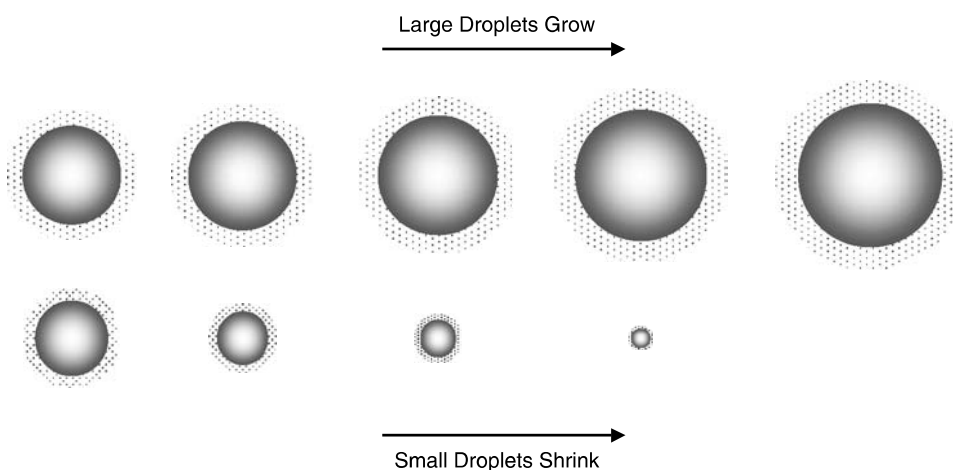


**Figure 7.36** Ostwald ripening involves the growth of large droplets at the expense of smaller ones due to diffusion of dispersed phase through the continuous phase. The driving force for this process is the fact that the solubility of a substance within a droplet in the continuous phase surrounding it increases with decreasing droplet radius.

cream liqueurs (Agboola and Dalgleish, 1996c; Dickinson and Golding, 1998; Weers, 1998; Dickinson et al., 1999). In this type of system the food manufacturer may have to consider methods for retarding the rate of Ostwald ripening.

### 7.8.1 Physical basis of Ostwald ripening

Ostwald ripening occurs because the solubility of the material in a spherical droplet increases as the size of the droplet decreases, which is described by the Kelvin equation (Heimenz and Rajagopalan, 1997):

$$S(r) = S(\infty) \exp\left(\frac{2\gamma V_m}{RT r}\right) = S(\infty) \exp\left(\frac{\alpha}{r}\right) \quad (7.39)$$

Here  $V_m$  is the molar volume of the solute,  $\gamma$  is the interfacial tension,  $S(\infty)$  is the solubility of the solute in the continuous phase for a droplet with infinite curvature (a planar interface),  $S(r)$  is the solubility of the solute when contained in a spherical droplet of radius  $r$ , and  $\alpha (=2\gamma V_m/RT)$  is a characteristic length scale. In this section, the term “solute” is used to describe the material contained within the droplets, that is, the dispersed phase of an emulsion. The increase in solubility with decreasing droplet size means that there is a higher concentration of solute around a small droplet than around a larger one (Figure 7.36). The solute molecules therefore move from the smaller droplets to the larger droplets because of this concentration gradient. This process causes the smaller droplets to shrink, and the larger droplets to grow, leading to an overall net increase in the mean droplet size with time. In general, Ostwald ripening can be divided into two periods (Figure 7.37). In the initial non-steady-state period, the emulsion has a droplet size distribution that is mainly determined by the homogenization conditions. As Ostwald ripening proceeds the shape of the droplet size distribution evolves toward a particular mathematical form, which is determined by the physicochemical processes associated with droplet shrinkage and growth (Weers, 1998). In the steady-state period, the droplet size distribution maintains a time-independent form, and only shifts up the particle size axis during aging (Figure 7.37).

Once steady state has been achieved, there is a time-dependent critical radius ( $r_c$ ), below which the droplets shrink and disappear, and above which they grow at the expense of smaller ones (Weers, 1998). This critical radius is approximately equal to the number mean radius of the droplets ( $r_c = r_{10}$ ), which increases with time according to the following

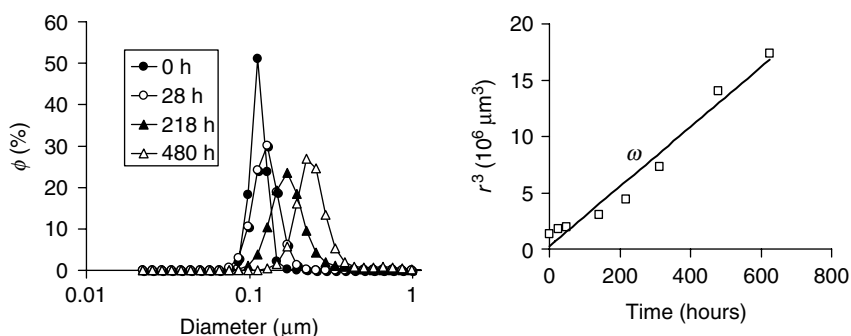


**Figure 7.37** Time dependence of the droplet size distribution and the cube of the mean droplet size for 5 wt% *n*-tetradecane oil-in-water emulsions stabilized by a nonionic surfactant undergoing Ostwald ripening (Weiss et al., 2000).

equations, which have been derived from the Lifshitz–Slezov–Wagner (LSW) theory (Kabalnov and Shchukin, 1992):

$$\frac{d\langle r \rangle^3}{dt} = \frac{4}{9} \alpha S(\infty) D \quad (7.40)$$

$$r^3 - r_0^3 = \omega t = \frac{4}{9} \alpha S(\infty) D t \quad (7.41)$$

where  $D$  is the translation diffusion coefficient of the solute through the continuous phase. These equations indicate that the cube of the mean particle size should increase linearly with time, and that the rate of this process increases as the equilibrium solubility of the solute molecules in the continuous phase increases.

Experiments have shown that the droplet size distribution does tend to adopt a time-independent form during Ostwald ripening, but that the shape of the distribution is slightly different from that predicted from the LSW theory (Weers, 1998). In addition, numerous experiments have shown that the cube of the mean particle size increases linearly with time, and that the Ostwald ripening rate is proportional to the solubility of the disperse phase in the continuous phase (Weers, 1998). Nevertheless, experimentally determined values of the Ostwald ripening rate in O/W emulsions (in the absence of micelle solubilization effects) have been found to be about two to three times higher than that predicted by the LSW theory, which has been attributed to the Brownian motion of the oil droplets (Weers, 1998). In the presence of micelle solubilization effects, the measured Ostwald ripening rates may be much greater than those predicted by the LSW theory. The time dependence of the droplet size distribution and mean droplet diameter for a model O/W emulsion stabilized by a nonionic surfactant is shown in Figure 7.37.

The above equations assume that the emulsion is dilute, whereas most food emulsions are concentrated, and so the growth or shrinkage of a droplet cannot be considered to be independent of its neighbors. Thus, the growth rate must be modified by a correction factor that takes into account the spatial distribution of the droplets (Kabalnov and Shchukin, 1992). For concentrated emulsions, the Ostwald ripening rate is higher than predicted by the above equations by a factor  $F$ , which increases from 1 to  $\sim 2.3$  as the droplet concentration increases from 0 to 30% (Weers, 1998).

The above equations also assume that the rate-limiting step is the diffusion of the solute molecules through the continuous phase. Most food emulsions contain droplets that are surrounded by interfacial membranes and in some instances these membranes may retard the diffusion of solute molecules in or out of the droplets. Under these circumstances the above equation must be modified to take into account the diffusion of solute molecules across the interfacial membrane (Kabalnov and Shchukin, 1992):

$$\frac{d\langle r \rangle^3}{dt} = \frac{3}{4\pi} \left( \frac{S_m - S_c}{R_m + R_c} \right) \quad (7.42)$$

where  $S_m$  and  $S_c$  are the solubilities of the solute in the membrane and continuous phase, and  $R_m$  and  $R_c$  are the diffusion resistances of the membrane and continuous phase:

$$R_m = \frac{1}{4\pi r D_m} \quad \text{and} \quad R_c = \frac{\delta C_{m,\infty}}{4\pi r^2 D_c C_{c,\infty}} \quad (7.43)$$

Here  $\delta$  is the thickness of the droplet membrane,  $C_{i,\infty}$  is the solubility of the solute in the specified phase, and the subscripts  $m$  and  $c$  refer to the properties of the membrane and the continuous phase, respectively. When the diffusion of the solute molecules through the interfacial membrane is limiting, the growth rate of the droplet size is proportional to  $r^2$  rather than  $r^3$  (Kabalnov and Shchukin, 1992).

## 7.8.2 Methods of controlling Ostwald ripening

The various factors that influence Ostwald ripening in emulsions have been reviewed in detail previously, for example, droplet size, solute solubility, interfacial tension, interfacial diffusion, droplet composition (Kabalnov and Shchukin, 1992; Weers, 1998). Knowledge of these factors can be used to control the rate of Ostwald ripening in emulsions.

### 7.8.2.1 Droplet size distribution

Ostwald ripening proceeds more rapidly when the average size of the droplets in an emulsion decreases, because the solubility of the dispersed phase increases with decreasing droplet radius (Walstra, 2003a). Hence, the droplet size increases more rapidly in emulsions containing small droplets than large droplets. The initial rate also increases as the width of the particle size distribution increases (Kabalnov and Shchukin, 1992). Ostwald ripening can therefore be retarded by ensuring that an emulsion has a narrow droplet size distribution, and that the droplets are fairly big. Nevertheless, there may be other problems associated with having relatively large droplets in an emulsion, such as accelerated creaming, flocculation, or coalescence.

### 7.8.2.2 Solubility

The greater the equilibrium solubility of the dispersed phase in the continuous phase, the faster the rate of Ostwald ripening (Equation 7.40). Ostwald ripening is therefore extremely slow in O/W emulsions containing lipids that are sparingly soluble in water (e.g., triacylglycerols), but may occur at an appreciable rate in emulsions containing lipids that are smaller and/or more polar (e.g., flavor oils) (Dickinson and Stainsby, 1988; Buffo and Reineccius, 2001). Certain substances are capable of increasing the water solubility of lipids in water, and are therefore able to enhance the Ostwald ripening rate, for example, alcohols or surfactant micelles (McClements and Dungan, 1993; McClements et al., 1994b; Coupland et al., 1997; Agboola and Dalgleish, 1996d; Dickinson and Golding, 1998; Dickinson et al., 1999; Weiss et al., 2000). Ostwald ripening could therefore be retarded by excluding these substances from the emulsion, or by using lipids with a low-water solubility.

### 7.8.2.3 Interfacial membrane

The rate of Ostwald ripening increases as the interfacial tension increases (Equation 7.40). Consequently, it is possible to retard its progress by using an emulsifier that is highly effective at reducing the interfacial tension (Kabalnov et al., 1995; Weers, 1998). The mass transport of molecules from one droplet to another depends on the rate at which the molecules diffuse across the interfacial membrane (Kabalnov and Shchukin, 1992). It may therefore be possible to retard Ostwald ripening by decreasing the diffusion coefficient of the dispersed phase in the membrane, or by increasing the thickness of the membrane. Little work has been carried out in this area; however, it may prove to be a useful means of controlling the stability of some food emulsions. Finally, the resistance to deformation of the interfacial membranes surrounding droplets may also be able to reduce the Ostwald ripening rate. The shrinkage or growth of droplets stabilized by biopolymers (proteins or polysaccharides) that form cohesive interfacial membranes may be retarded because of the mechanical resistance of the membranes to changes in their area (Weers, 1998). For example,

it has been shown that cross-linking the proteins in the interfacial membranes surrounding droplets in protein-stabilized O/W emulsions may be able to provide some limited improvement in emulsion stability to Ostwald ripening (Dickinson et al., 1999).

#### 7.8.2.4 Droplet composition

The Ostwald ripening rate is particularly sensitive to the composition of emulsion droplets that contain a mixture of components with different solubilities in the continuous phase (Kabalnov and Shchukin, 1992; Dickinson and McClements, 1995; Arlauskas and Weers, 1996; Weers, 1998; Sadtler et al., 2002). Consider an O/W emulsion that contains droplets comprised of two different types of oil-soluble components:  $M_{\text{Low}}$  has a low-water solubility and  $M_{\text{High}}$  has a high-water solubility. The diffusion of  $M_{\text{High}}$  molecules from the small to the large droplets occurs more rapidly than the  $M_{\text{Low}}$  molecules. Consequently, there is a greater percentage of  $M_{\text{High}}$  in the larger droplets than in the smaller droplets. Differences in the composition of emulsion droplets are thermodynamically unfavorable because of the entropy of mixing: it is entropically more favorable to have the two oils distributed evenly throughout all of the droplets, rather than concentrated in particular droplets. Consequently, there is a thermodynamic driving force that operates in opposition to the Ostwald ripening effect. The change in droplet size distribution with time then depends on the concentration and solubility of the two components within the oil droplets. The following stability criterion has been derived to predict the different types of behavior possible (Weers, 1998):

$$X_{\text{Low}} > \frac{2\alpha_{\text{High}}}{3d_0} \quad (7.44)$$

where  $X_{\text{Low}}$  is the initial mole fraction of the low-solubility component present within the overall disperse phase,  $\alpha_{\text{High}} (=2\gamma V_m/RT)$  is the characteristic length scale of the high-solubility component, and  $d_0$  is the initial mean droplet diameter of the emulsion. If the above stability criterion is met and  $M_{\text{Low}}$  is completely insoluble in the continuous phase, then the driving force for Ostwald ripening (differences in droplet size) is exactly compensated for by the driving force for the entropy of mixing (differences in droplet composition) and the size and composition of the droplets remain constant (Kabalnov and Shchukin, 1992). If the above stability criterion is met and  $M_{\text{Low}}$  has some solubility in the continuous phase, then Ostwald ripening will occur, but with an overall Ostwald ripening rate given by the following equation (Weers, 1998):

$$\omega_{\text{mix}} = \left( \frac{\phi_{\text{Low}}}{\omega_{\text{Low}}} + \frac{\phi_{\text{High}}}{\omega_{\text{High}}} \right)^{-1} \quad (7.45)$$

where  $\phi$  and  $\omega$  are the volume fraction and Ostwald ripening rates of the pure substances. This equation predicts that the presence of the low-solubility component will slow down the overall Ostwald ripening rate. Nevertheless, the general characteristics of the ripening process are similar to those of pure oils, that is,  $d^3$  increases linearly with time, and the shape of the droplet size distribution is time invariant. If there is an insufficient amount of the low-solubility component in the emulsion droplets, then a bimodal droplet size distribution develops over time (Weers, 1998).

It may therefore be possible to control the rate of Ostwald ripening in some O/W food emulsions by using an oil phase that contains a mixture of lipids with different water solubilities. Similar improvements in stability to Ostwald ripening can be obtained in W/O emulsions (such as margarine or butter) by including water-soluble components that have a low solubility in the lipid continuous phase, for example, salts (Walstra, 2003a).

Finally, it should be noted that a similar phenomenon to Ostwald ripening may occur in emulsions that is called *composition* ripening (Weers, 1998). If an emulsion contains droplets that have different internal compositions, then there is a thermodynamic driving force (entropy of mixing) that favors the exchange of the disperse phase material between the droplets until they all have similar compositions. This process can be achieved by diffusion of oil molecules through the continuous phase separating the droplets. Composition ripening may be a useful practical means of introducing an oil-soluble component into the droplets of a preexisting O/W emulsion. An emulsion of the oil-soluble component could be prepared and then mixed with the preexisting emulsion. Provided the oil-soluble component has sufficient solubility in the aqueous phase, then it will be incorporated into all of the droplets given sufficient time.

### 7.8.3 Experimental characterization of Ostwald ripening

Methods of monitoring Ostwald ripening are fairly similar to those used to monitor droplet coalescence, that is, techniques that measure changes in droplet size distribution with time (Section 7.6.4). If the droplets are sufficiently large ( $>1\ \mu\text{m}$ ) then optical microscopy can be used (Kabalnov and Shchukin, 1992), otherwise, instrumental particle sizing techniques, such as light scattering, electrical pulse counting, or ultrasonics can be used (Section 11.3). Nevertheless, it is often difficult to directly distinguish between coalescence and Ostwald ripening using these particle sizing techniques because both instability mechanisms lead to an increase in the average size of the droplets over time. It is sometimes possible to distinguish between coalescence and Ostwald ripening by measuring the change in particle size distribution with time and by examining the factors that influence the rate of droplet growth.

## 7.9 Phase inversion

Phase inversion is the process whereby a system changes from an O/W emulsion to a W/O emulsion or vice versa (Figure 7.38). Phase inversion is an essential step in the manufacture of a number of important food products, including butter and margarine (Mulder and Walstra, 1974; Dickinson and Stainsby, 1982; Moran, 1994; Goff et al., 1997a–c). In other foods, phase inversion is undesirable because it has an adverse effect on their

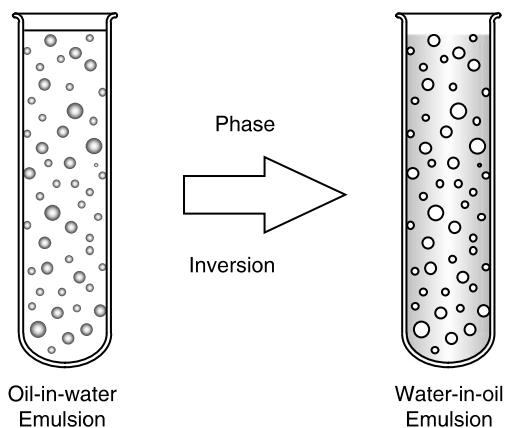


**Figure 7.38** Phase inversion involves the conversion of an oil-in-water emulsion to a water-in-oil emulsion or vice versa.

appearance, texture, stability, and taste. In these products, a food manufacturer wants to avoid the occurrence of phase inversion.

### 7.9.1 *Physical basis of phase inversion*

Phase inversion is usually triggered by some alteration in the composition or environmental conditions of an emulsion, for example, disperse phase volume fraction, emulsifier type, emulsifier concentration, solvent conditions, temperature, or mechanical agitation (Shinoda and Friberg, 1986; Dickinson, 1992; Campbell et al., 1996; Brooks et al., 1998). Only certain types of emulsions are capable of undergoing phase inversion, rather than being completely broken down into their component phases. These emulsions are capable of existing in a kinetically stable state both before and after the phase inversion has taken place. It is usually necessary to agitate an emulsion during the phase inversion process, otherwise it will separate into its component phases.

The physicochemical basis of phase inversion is believed to be extremely complex, involving aspects of flocculation, coalescence, partial coalescence, and emulsion formation (Brooks, 1998). At the point where phase inversion occurs, which is often referred to as the "balance point," the system may contain regions of O/W emulsion, W/O emulsion, multiple emulsion, and bicontinuous phases. Phase inversion in food emulsions can be conveniently divided into two different categories according to its origin.

#### 7.9.1.1 *Surfactant-induced phase inversion*

Surfactant-induced phase inversion occurs in emulsions that are stabilized by small molecule surfactants and may be of a "transitional" or a "catastrophic" type depending on the physicochemical mechanism involved (Binks, 1998). Transitional phase inversion is caused by changes in the molecular geometry of the surfactant molecules in response to alterations in solution or environmental conditions, for example, temperature, ionic strength, or effective hydrophile-lipophile balance (HLB) number (Shinoda and Friberg, 1986; Salager, 1988; Evans and Wennerstrom, 1994). For example, an emulsion stabilized by a nonionic surfactant undergoes a transition from an O/W emulsion, to a bicontinuous system, to a W/O emulsion on heating because of the progressive dehydration of the head groups (Lehnert et al., 1994; Binks, 1998). This process is characterized by a phase inversion temperature (PIT), which is governed by the molecular geometry of the surfactant molecules (Davis, 1994b). An O/W emulsion stabilized by an ionic surfactant exhibits a similar kind of behavior when the concentration of electrolyte in the aqueous phase is increased (Salager, 1988; Binks, 1993, 1998). Increasing the ionic strength causes the system to undergo a transition from an O/W emulsion, to a bicontinuous system, to a W/O emulsion, because the electrical charge on the surfactant head groups is progressively screened by the counter ions (Section 4.4.1). Phase inversions may also be induced by changing the effective HLB number of the surfactants by mixing surfactants together (Binks, 1998). A surfactant stabilized emulsion may switch from a W/O emulsion at a low HLB number, to a bicontinuous system at intermediate HLB, to an O/W emulsion at high HLB number. In general, the tendency for this type of phase inversion to occur is determined by the packing parameter ( $p$ ) of the surfactant (Section 4.4.1), with  $p < 1$  favoring an O/W emulsion,  $p \approx 1$  favoring a bicontinuous system, and  $p > 1$  favoring a W/O emulsion.

Catastrophic phase inversion usually occurs when the disperse phase volume fraction is increased above a critical level (Binks, 1998; Brooks et al., 1998). As the droplet concentration is gradually increased, there is suddenly a dramatic change in the system characteristics. The point where phase inversion occurs also depends on the intensity of agitation and the rate at which the disperse phase is added to the emulsion.

Transitional phase inversions are usually reversible, whereas catastrophic phase inversions are usually irreversible (Binks, 1998). For example, when a transitional phase inversion is induced in an O/W emulsion by increasing its temperature above the PIT, the emulsion will usually revert back into an O/W emulsion when it is cooled back below the PIT. Nevertheless, it is often necessary to continuously agitate the system during this process, or else it will separate into the individual oil and water phases. In addition, there is often an effect that is analogous to that of supercooling, that is, the temperature at which the phase inversion occurs on heating is different from that on cooling (Dickinson, 1992; Vaessen and Stein, 1995). This is because there is an activation energy that must be overcome before a system can be transformed from one state to another.

#### 7.9.1.2 *Fat crystallization-induced phase inversion*

When an O/W emulsion containing completely liquid droplets is cooled to a temperature where the droplets are partly crystalline and then sheared it may undergo a phase inversion to a W/O emulsion (Mulder and Walstra, 1974; Dickinson and Stainsby, 1982; Walstra, 2003a). The principle cause of this type of phase inversion is partial coalescence of the droplets, which leads to the formation of a continuous fat crystal network that traps water droplets within it. This is one of the principal manufacturing steps in the production of margarine and butter (Dickinson and Stainsby, 1982). When the emulsion is heated to a temperature where the fat crystals melt the emulsion breaks down because the water droplets are released and sediment to the bottom of the sample where they coalesce with other water droplets. This is clearly seen when one melts margarine or butter and then cools it back to the original temperature: the system before and after heating are very different. This type of phase inversion depends mainly on the crystallization of the fat and on the resistance of the droplets to partial coalescence (see Section 7.7).

### 7.9.2 *Methods of controlling phase inversion*

The propensity for phase inversion to occur in an emulsion can be controlled in a number of ways.

#### 7.9.2.1 *Disperse phase volume fraction*

If the dispersed phase volume fraction of an emulsion is increased, while all the other experimental variables are kept constant (e.g., emulsifier type, emulsifier concentration, temperature, shearing rate), then a critical volume fraction ( $\phi_{cp}$ ) may be reached where the system either undergoes a catastrophic phase inversion or completely breaks down so that the excess dispersed phase forms a layer on top of the emulsion. There is usually a range of volume fractions over which an emulsion can exist as either a W/O emulsion or as an O/W emulsion (Dickinson, 1992). Within this region the emulsion can be converted from one state to another by altering some external property, such as the temperature or shear rate. From geometrical packing considerations it has been estimated that this range extends from  $1 - \phi_{cp} < \phi < \phi_{cp}$ , where  $\phi_{cp}$  refers to the volume fraction when the droplets are packed closely together without being distorted. In practice, factors other than simple geometric considerations will influence this range, including the fact that the droplets can become deformed and the chemical structure of the emulsifier used. Catastrophic phase inversion can therefore be prevented by ensuring that the droplet concentration is kept below  $\phi_{cp}$  ( $\sim 0.6$ ).

#### 7.9.2.2 *Emulsifier type and concentration*

The most important factor determining the susceptibility of an emulsion to surfactant-induced transitional phase inversion is the molecular geometry of the surfactant used to stabilize the droplets (Evans and Wennerstrom, 1994; Binks, 1998). Surfactant-stabilized



emulsions undergo a phase inversion when some change in the environmental conditions causes the optimum curvature of the surfactant monolayer to tend toward zero (or  $p \rightarrow 1$ ), for example, temperature, ionic strength, or the presence of a cosurfactant. These types of surfactants usually have an intermediate HLB number or are electrically charged. Alternatively, mixtures of two different types of surfactants can be used, one to stabilize the O/W emulsion and the other the W/O emulsion. The point at which phase inversion occurs is then sensitive to the ratio of the surfactants used (Dickinson, 1992). Emulsions stabilized by proteins do not exhibit this type of phase inversion because proteins are incapable of stabilizing W/O emulsions. The total concentration of emulsifier present in the system is also important because there must be a sufficient quantity present to cover all of the droplets formed in both the O/W and W/O states on either side of the phase inversion.

The emulsifier type and concentration is also important in determining the stability of emulsions to fat crystallization-induced phase inversion. Emulsifiers that form thick viscoelastic membranes are more likely to protect an emulsion from this type of phase inversion because they retard partial coalescence (Section 7.7). It is therefore extremely important to select an emulsifier that exhibits the appropriate behavior over the experimental conditions that a food emulsion experiences during its lifetime.

#### 7.9.2.3 *Mechanical agitation*

It is often necessary to subject an emulsion to a high shearing force to induce phase inversion in the region where it can possibly exist as either an O/W or W/O emulsion. The higher the shearing force the more likely that phase inversion is to occur. In addition, if the shearing force were not applied then the system may just undergo phase separation into the individual oil and water phases, rather than being transformed into a phase-inverted emulsion.

#### 7.9.2.4 *Temperature*

Increasing or decreasing the temperature of emulsions is one of the most important means of inducing phase inversion. The mechanism by which this process occurs depends on whether the phase inversion is induced by surfactant changes or crystallization. Cooling an O/W emulsion to a temperature where the oil partly crystallizes and shearing causes fat crystallization-induced phase inversion. On the other hand, heating an O/W emulsion stabilized by a surfactant may cause surfactant-induced phase inversion above the PIT.

Fat crystallization-induced phase inversion is the most important type in the food industry because it is an essential step in the manufacture of butter and margarine (Dickinson and Stainsby, 1982). Surfactant-induced phase inversion may be important in emulsions stabilized by nonionic surfactants that must be heated to high temperatures, for example, for pasteurization, sterilization, or cooking. In these systems, it is important for the food manufacturer to ensure that the PIT of the emulsifier is above the highest temperature that the emulsion will experience during processing, storage, and handling.

### 7.9.3 *Characterization of phase inversion*

Phase inversion can be monitored using a variety of experimental techniques (Lehnert et al., 1994). When an emulsion changes from the O/W to the W/O emulsion type or vice versa, there is usually a significant change in emulsion viscosity. This is because the viscosity of an emulsion is governed principally by the viscosity of the continuous phase (which is different for oil and water) and the disperse phase volume fraction (which may also be altered) (Chapter 8). An O/W emulsion has an aqueous continuous phase and so its electrical conductivity is much greater than that of a W/O emulsion (Lehnert et al., 1994;

Keikens et al., 1997). Thus, there is a dramatic reduction in the electrical conductivity of an O/W emulsion when phase inversion occurs (Allouche et al., 2003). Information about the process of phase inversion may also be obtained by monitoring the emulsion under a microscope (Pacek et al., 1994) or by measuring the change in droplet size using a particle sizing technique (Section 11.3). Measurements of the temperature dependence of the interfacial tension between the oil and water phases can also be used to predict the likelihood that phase inversion will occur in an emulsion (Shinoda and Friberg, 1986; Lehnert et al., 1994).

## 7.10 *Chemical and biochemical stability*

The majority of this chapter has been concerned with the physical instability of food emulsions, rather than with their chemical instability. This is largely because emulsion scientists have historically focused mainly on the physical aspects of food emulsions. Nevertheless, there are many types of chemical or biochemical reactions that can have adverse effects on the quality of food emulsions, for example, lipid oxidation, biopolymer hydrolysis, flavor or color degradation (Fennema, 1996a). For this reason there has been a growing interest in the influence of various chemical and biochemical reactions on the stability of food emulsions in recent years.

One of the most common forms of instability in foods that contain fats is lipid oxidation (St. Angelo, 1992; Nawar, 1996; McClements and Decker, 2000). Lipid oxidation leads to the development of undesirable "off-flavors" (rancidity) and potentially toxic reaction products. In addition, it may also promote the physical instability of some emulsions (Coupland and McClements, 1996; McClements and Decker, 2000). For example, many of the reaction products generated during lipid oxidation are surface active, and may therefore be able to interact with the interfacial membrane surrounding the droplets in such a way as to lead to droplet coalescence. The importance of lipid oxidation in food emulsions has led to a considerable amount of research being carried out in this area over the past few years (Frankel, 1991; Coupland and McClements, 1996; McClements and Decker, 2000; Jacobsen et al., 2001a). The main emphasis of this work is to develop effective strategies for retarding lipid oxidation in emulsions by incorporating antioxidants, controlling storage conditions, or engineering droplet interfacial properties. It should also be noted that lipid oxidation may promote oxidation of adsorbed or nonadsorbed proteins in an emulsion, and that this may alter their nutritional and functional properties (Rampon et al., 2001). Chemical degradation of flavor and color molecules in beverage emulsions are briefly considered in Section 12.3.

There is also an increasing interest in the influence of biochemical reactions on the properties of food emulsions (Dalgleish, 1996a, 2004). A number of studies have recently been carried out to determine the influence of enzyme hydrolysis on the stability and physicochemical properties of food emulsions (Agboola and Dalgleish, 1996b,c; Euston et al., 2001; van der Ven et al., 2001). These studies have shown that the properties of food emulsions can be altered appreciably when the adsorbed proteins are cleaved by enzyme hydrolysis. A number of studies have also shown that globular proteins become denatured after they have been adsorbed to the surface of an emulsion droplet, and that they remain in this state after they are desorbed (Corredig and Dalgleish, 1995; de Roos and Walstra, 1996; Fang and Dalgleish, 1997, 1998). This has important implications for the action of many enzymes in food emulsions. The activity of an enzyme may be completely lost when it is adsorbed to the surface of the droplets in an emulsion, and therefore any biochemical reactions catalyzed by it will cease (de Roos and Walstra, 1996).

Given the obvious importance for food quality, it seems likely that there will be an increasing emphasis on the influence of biochemical and chemical reactions on the stability of food emulsions in the future.



## chapter eight

---

# Emulsion rheology

### 8.1 Introduction

*Rheology* is the science that is concerned with the deformation and flow of matter (Macosko, 1994). Most rheological tests involve applying a specific force to a material and measuring the resulting flow and/or deformation of the material (Whorlow, 1992). The rheological properties of a material are then established by analyzing the relationship between the applied force and the resultant flow or deformation. Knowledge of the rheological properties of food emulsions is important for a variety of reasons (Sherman, 1968a–c, 1970, 1982; Dickinson and Stainsby, 1982; Race, 1991; Shoemaker et al., 1992; Rao et al., 1995; Rao, 1995; Dickinson, 1998; McKenna and Lyng, 2003). The efficiency of droplet disruption in a homogenizer depends on the viscosity of the individual components, as well as on the overall rheology of the product (Sections 6.4 and 6.6). The shelf life of many food emulsions depends on the rheological characteristics of the component phases, for example, the creaming of oil droplets in oil-in-water emulsions is strongly dependent on the viscosity of the aqueous phase (Section 7.3). Information about the rheology of food emulsions is used by food engineers to design processing operations that depend on the way that the product flows, for example, flow through a pipe, stirring in a mixer, passage through a heat-exchanger, packaging into containers (McKenna and Lyng, 2003). Many of the sensory attributes of food emulsions are directly related to their rheological properties, for example, creaminess, thickness, smoothness, spreadability, pourability, flowability, brittleness, and hardness (Chapter 9). A food manufacturer must therefore be able to design and consistently produce a product that has the desirable rheological properties expected by the consumer. Finally, rheological measurements are frequently used by food scientists as an analytical tool to provide fundamental insights about the structural organization and interactions of the components within emulsions, for example, measurements of viscosity versus shear rate can be used to provide information about the strength of the colloidal interactions between droplets (Hunter, 1993; Tadros, 1994; Quemada and Berli, 2002). The purpose of this chapter is to present the general principles of rheology, to discuss the relationship between the rheological characteristics of food emulsions and their colloidal properties, and to provide an overview of analytical instruments commonly used to characterize the rheological properties of food emulsions.

Food emulsions are compositionally and structurally complex materials that can exhibit a wide range of different rheological behaviors, ranging from low viscosity fluids (e.g., milk and fruit juice beverages), to viscoelastic gels (e.g., yogurt and deserts), to fairly hard solids (e.g., refrigerated margarine and butter). Food scientists aim to develop theories that can be used to describe and predict the rheological behavior of this diverse group of products, as well as experimental techniques that can be used to quantify their textural

properties. Despite the diversity of rheological behavior exhibited by food emulsions it is often possible to characterize their rheology in terms of a few simple models: the *ideal solid*, the *ideal liquid*, and the *ideal plastic* (Tung and Paulson, 1995; Rao, 1999; Daubert and Foegeding, 2003). More complex systems can then be described by combining two or more of these simple models. In the following sections the concepts of the ideal solid, ideal liquid, and ideal plastic are introduced, as well as some of the deviations from these models that are commonly observed in food emulsions.

## 8.2 Rheological properties of materials

### 8.2.1 Solids

In our everyday lives we come across solid materials that exhibit quite different rheological characteristics, for example, the resistance of the material to an applied force (soft vs. hard) or the amount of deformation or force required to cause the material to fracture (brittle vs. tough). Despite this range of different behavior it is possible to characterize the rheological properties of many solid foods in terms of a few simple concepts.

#### 8.2.1.1 Ideal elastic solids

An ideal elastic solid is often referred to as a *Hookean solid* after Robert Hooke, the scientist who first described this type of behavior (Whorlow, 1992; Macosko, 1994; Rao et al., 1995). Hooke observed experimentally that there is a linear relationship between the deformation of a solid material and the magnitude of the force applied to it, provided the deformation is not too large (Figure 8.1). He also observed that when the force was removed from the material it returned back to its original length. In general, the force per unit area (or *stress*)

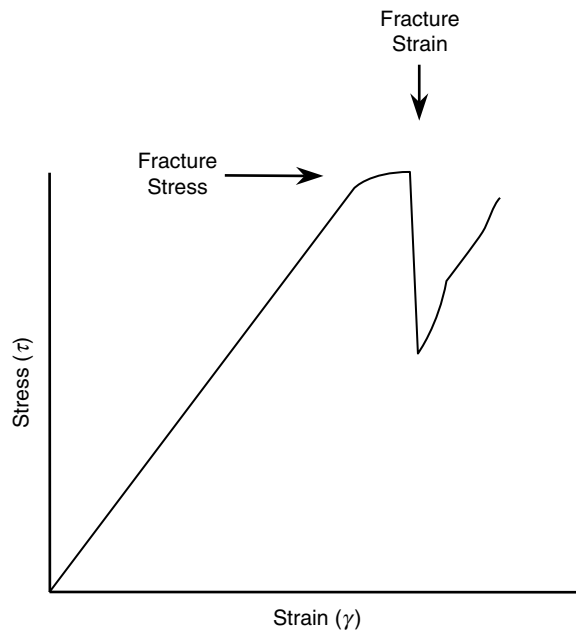


**Figure 8.1** At small deformations there is a linear relationship between the applied stress and the resultant strain for an ideal elastic (Hookean) solid. At higher deformations the stress is no longer linearly related to strain and the material will eventually fracture.

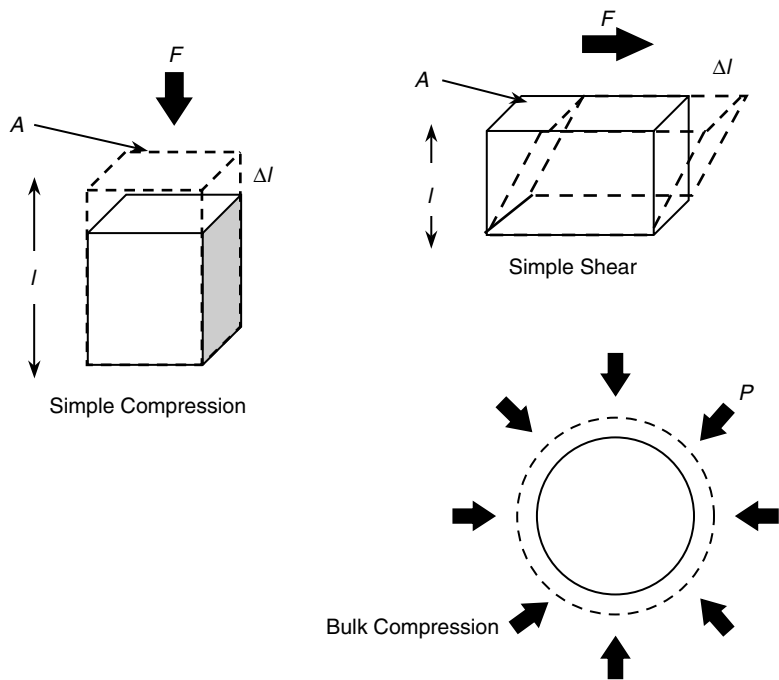


**Figure 8.2** An elastic solid can be deformed in a number of different ways depending on the nature of the applied stress. Here  $F$  is force,  $A$  is area,  $l$  is initial length,  $\Delta l$  is change in Length and  $P$  is pressure.

acting on the material is proportional to the relative deformation (or *strain*) of the material. Hooke’s law can therefore be summarized by the following statement:

stress ( $\tau$ ) = constant ( $E$ )  $\times$  strain ( $\gamma$ )

(8.1)

A stress can be applied to a material in a number of different ways, including simple shear, simple compression (or elongation), and bulk compression (or expansion) (Figure 8.2). Equation 8.1 is applicable to each of these situations, but the values of the stress, strain, and constant used depend on the nature of the deformation (Table 8.1). In addition, the strain can also be defined in a number of different ways depending on the way that the length of the material is expressed (Walstra, 2003a). For example, in a compression experiment, the

**Table 8.1** rheological Parameters for Different Types of Deformations of Elastic Solids.

Deformation	Stress	Strain	Elastic Modulus
Simple shear	$\tau = \frac{F}{A}$	$\gamma = \frac{\Delta l}{l} = \tan \phi$	$G = \frac{\tau}{\gamma} = \frac{F}{A \tan \phi}$
Simple compression	$\tau = \frac{F}{A}$	$\gamma = \frac{\Delta l}{l}$	$Y = \frac{\tau}{\gamma} = \frac{Fl}{A \Delta l}$
Bulk compression	$\tau = \frac{F}{A} = P$	$\gamma = \frac{\Delta V}{V}$	$K = \frac{\tau}{\gamma} = \frac{PV}{\Delta V}$

*Note:*  $G$  is the shear modulus,  $Y$  is the Young’s modulus,  $K$  is the bulk modulus,  $P$  is the pressure, and the other symbols are defined in Figure 8.2.

*Cauchy* or *engineering* strain is defined as the change in material length ( $\Delta l = l - l_0$ ) divided by the original material length ( $l_0$ ):  $\gamma_E = \Delta l / l_0$ . Alternatively, the *Hencky* or *natural* strain is defined as the change in material length divided by the length at the time of measurement:  $\gamma_H = |\ln(l/l_0)|$ . It has been reported that the Hencky strain is more appropriate than the Cauchy strain for large material deformations (Daubert and Foegeding, 2003; Walstra, 2003a). Similarly, the stress can be defined as being equal to the applied force divided by the original cross-sectional area of a material (*engineering stress*), or as the applied force divided by the cross-sectional area of the material at the time of measurement (*natural stress*). These values may be appreciably different if the cross-sectional area of a material changes during deformation, and it is advisable to use the natural stress rather than the engineering stress, particularly for large material deformations (Walstra, 2003a).

The equations given in Table 8.1 assume that the material is homogeneous and isotropic, that is, its properties are the same in all directions. To characterize the rheological constants of an ideal elastic solid it is therefore necessary to measure the change in its dimensions when a force of known magnitude is applied.

The elastic behavior of a solid is related to the intermolecular forces that hold the molecules (or other structural units) together. When a stress is applied to a material the bonds between the molecules are compressed or expanded and therefore they store energy. When the stress is removed, the bonds give up this energy and the material returns to its original shape. The elastic modulus of an ideal elastic solid is therefore related to the strength of the interactions between the molecules within it and the number of interactions per unit area of material. In reality, the elastic modulus of a solid may also depend on the internal structure of a solid, for example, if there are any cracks or dislocations present.

#### 8.2.1.2 Nonideal elastic solids

Hooke's law is only strictly applicable to elastic materials at relatively low strains, and therefore many fundamental rheological studies of solid foods are carried out using very small material deformations ( $<1\%$ ). Nevertheless, the rheological behavior of foods at large deformations is often more relevant to their actual use, for example, spreadability, slicing, or mastication (van Vliet, 1995; Walstra, 2003a). For this reason it is also important to characterize the rheological behavior of solids at large deformations. At strains just above the region where the Hooke's law is obeyed the stress is no longer proportional to the strain, and therefore an *apparent modulus* is defined, which is equal to the stress/strain at a particular value of the strain. It is therefore important to stipulate the strain (or stress) that an apparent modulus of a material is measured when reporting rheological data made on nonideal solids. In this range of deformations, the material still returns to its original shape once the force is removed, even though it does not obey Hooke's law. Above a certain deformation; however, a solid may not return back to its original shape after the applied stress is removed, because it either fractures or flows. A material that breaks at low strains is referred to as being *brittle*, whereas a material that flows is referred to as being *plastic* or *viscoelastic* depending on the nature of the flow (see later). The stress at which a material fractures is referred to as the *fracture stress* ( $\tau_{Fr}$ ), whereas the strain at which it fractures is referred to as the *fracture strain* ( $\gamma_{Fr}$ ) (Walstra, 2003a). A material usually fractures or flows when the forces holding the structural units (e.g., atoms, molecules, particles) together in the material are exceeded. This often begins at regions where the bonds holding the material together are relatively weak, for example, a crack or dislocation. Knowledge of the fracture stress or fracture strain of a material is often a useful indication of its ability to be broken up during mastication, cut with a knife, or ruptured during storage and transport.

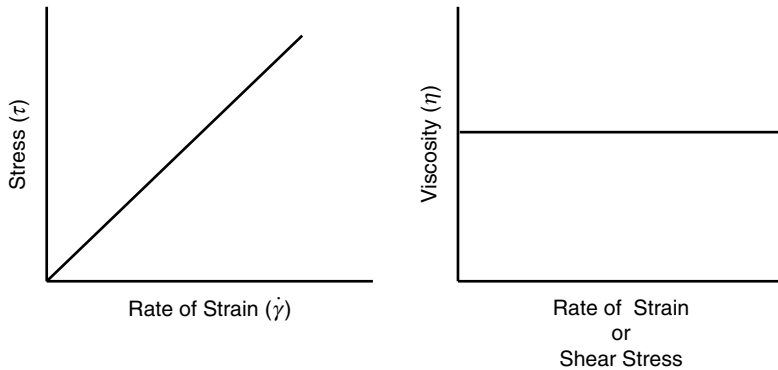


**Figure 8.3** Stress is proportional to *rate* of strain for an ideal (Newtonian) liquid, and the viscosity is independent of the applied rate of strain (or shear stress).

### 8.2.2 Liquids

Liquid food emulsions also exhibit a wide range of rheological properties. Some have low viscosities and flow easily, like milk, while others are highly viscous, like double cream. Even so, it is often possible to characterize their rheological properties using a few simple concepts.

#### 8.2.2.1 Ideal liquids

The ideal liquid is often referred to as a *Newtonian* liquid, after Isaac Newton, the scientist who first described its behavior (Whorlow, 1992; Macosko, 1994; Rao, 1995). When a shear stress is applied to an ideal liquid it continues to flow as long as the stress is applied (Figure 8.3). Once the applied stress is removed, the liquid will continue to flow until the kinetic energy stored within it is dissipated as heat due to friction. In this case, there is no elastic recovery of the material once the applied stress is removed, that is, it does not return to its original shape.

The viscosity of a liquid is a measure of its resistance to flow: the higher the viscosity, the greater the resistance (Macosko, 1994). The concept of viscosity can be understood by considering a liquid that is contained between two parallel plates (Figure 8.4). The bottom plate is at rest, while the top plate moves in the  $x$  direction with a constant velocity,  $v$ .

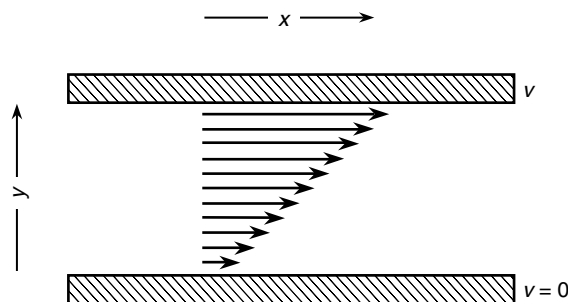


**Figure 8.4** The viscosity of a liquid can be envisaged as arising from the friction generated by thin layers of liquid as they slide across each other: the greater the friction, the higher the energy dissipation, and the greater the viscosity.



It is assumed that the liquid between the plates consists of a series of infinitesimally thin layers. The liquid layers in direct contact with the bottom and top plates are assumed to “stick” to them, so that they have velocities of 0 and  $v$ , respectively. The intervening liquid layers slide over each other with velocities that range between 0 and  $v$ , the actual value being given by  $dy(dv/dy)$ , where  $dy$  is the distance from the bottom plate and  $dv/dy$  is the velocity gradient between the plates. The shear stress applied to the fluid is equal to the shear force divided by the area over which it acts ( $\tau = F/A$ ). The rate of strain is given by the change in displacement of the layers per unit time:  $d\gamma/dt$  (or  $\dot{\gamma}$ ) =  $dv/dy$ . For an ideal liquid, the shear stress is proportional to the rate of strain (Figure 8.3):

$$\tau = \eta \dot{\gamma} \quad (8.2)$$

where the constant of proportionality,  $\eta$ , is called the *viscosity*. The viscosity arises from the friction between the “layers” of liquid as they slide past one another (Macosko, 1994). The lower the viscosity of a liquid, the less resistance between the liquid layers, and therefore the smaller the force required to cause the top plate to move with a given velocity, or the faster the top plate moves when a given force is applied. The ideal viscous fluid differs from the ideal elastic solid because the shear stress is proportional to the *rate* of strain (Figure 8.3), rather than the strain (Figure 8.1). It should be noted that the value of a fluid's viscosity actually depends on the type of flow profile that it exhibits, for example, simple shear flow ( $\eta_{ss}$  or  $\eta$ ) or elongational flow ( $\eta_{el}$ ) (Walstra, 2003a). The elongational viscosity is always higher than the shear viscosity:  $\eta_{el} = Tr \times \eta$ , where the Trouton ratio ( $Tr$ ) depends on the precise nature of the elongational flow (Walstra, 2003a). Most rheometers used to characterize food emulsions use shear flow conditions and therefore measure the shear viscosity, but some do use fully or partly elongational flow conditions.

The units of shear stress ( $\tau$ ) are  $\text{N m}^{-2}$  (or Pa), and those of shear rate ( $\dot{\gamma}$ ) are  $\text{sec}^{-1}$  thus the viscosity ( $\eta$ ) has units of  $\text{N sec m}^{-2}$  (or Pa sec) in the SI system. Viscosity can also be expressed in the older cgs units of Poise, where  $1 \text{ Pa sec} = 10 \text{ P}$ . Thus, the viscosity of water at room temperature is around  $1 \text{ mPa sec}$ ,  $0.001 \text{ Pa sec}$ ,  $0.01 \text{ P}$ , or  $1 \text{ Centipoise (cP)}$ , depending on the units used.

Ideally, a Newtonian liquid should be incompressible (its volume does not change when a force is applied to it), isotropic (its properties are the same in all directions), and structureless (it is homogeneous). Although many liquid foods do not strictly meet these criteria, their rheological behavior can still be described excellently by Equation 8.2, for example, milk, sugar solutions, brine, and honey. Nevertheless, there are many others that exhibit nonideal liquid behavior and so their properties cannot be described by Equation 8.2.

The type of flow depicted in Figure 8.4 occurs at low applied shear rates and is known as *laminar flow*, because the liquid travels in a well-defined laminar pattern. At higher shear rates, eddies form in the liquid and the flow pattern is much more complex (Walstra, 2003a). This type of flow is referred to as *turbulent* and it is much more difficult to mathematically relate the shear stress to the shear rate under these conditions. For this reason, instruments that measure the viscosity of liquids are designed to avoid nonlaminar flow.

### 8.2.2.2 Nonideal liquids

Nonideal rheological behavior may manifest itself in a variety of different ways in liquids, for example, the viscosity of a liquid may depend on the *shear rate* and/or the *time* over which the shear stress is applied, or the fluid may exhibit some elastic as well as viscous

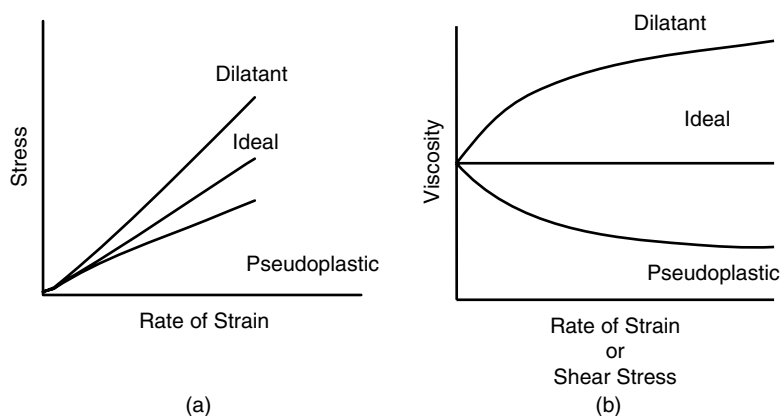


**Figure 8.5** Comparison of the viscosity of ideal and nonideal liquids: (a) Shear stress vs. rate of shear strain; (b) Apparent viscosity vs. rate of shear strain (or shear stress).

properties (Macosko, 1994; Tung and Paulson, 1995; Walstra, 2003a). Plastic and viscoelastic materials, which have some elastic characteristics, are considered in later sections.

**8.2.2.2.1 Shear-rate dependent nonideal liquids.** In an ideal liquid, the viscosity is independent of shear rate and of the length of time that the liquid is sheared, that is, the ratio of the shear stress to the shear rate does not depend on shear rate or time (Figure 8.5). In practice, many food emulsions have viscosities that do depend on the shear rate and the length of time that the system is sheared (Dickinson, 1992, 1998). In this section, we examine emulsions in which the viscosity depends on shear rate, but is independent of the shearing time (Dickinson, 1992). In the following section, we examine emulsions in which the viscosity depends on both the shear rate and shearing time.

The viscosity of an emulsion may either increase or decrease as the shear rate is increased, rather than staying constant as for a Newtonian liquid (Figure 8.5). In these systems the viscosity at a particular shear rate is referred to as the *apparent* viscosity (Walstra, 2003a). The dependence of the apparent viscosity on shear rate means that it is crucial to stipulate the shear rate used to carry out the measurements when reporting data. The choice of shear rate to use when measuring the apparent viscosity of a nonideal liquid is a particularly important consideration when carrying out rheological measurements that are supposed to mimic some process that occurs in a food naturally, for example, flow through a pipe, stirring, or mixing in a vessel, pouring from a bottle, creaming of an individual emulsion droplet, or mastication of a food (Table 8.2).

**Table 8.2** Typical Rates of Shear Strain Observed in Some Common Processes Relevant to Food Emulsions.

Process	Shear Rate ( $\text{sec}^{-1}$ )
Pumping	$10^0$ to $10^3$
Mixing and stirring	$10^1$ to $10^3$
Chewing and swallowing	$10^1$ to $10^2$
Pouring	$10^{-2}$ to $10^2$
Droplet creaming	$10^{-6}$ to $10^{-3}$

Source: Adapted from Vanapalli and Coupland (2004).

A laboratory test should use a shear rate that is as close as possible to that which the food experiences in practice.

The two most common types of shear-rate dependent nonideal liquids are:

1. *Pseudoplastic fluids*. Pseudoplastic flow is the most common type of nonideal behavior exhibited by food emulsions. It manifests itself as a *decrease* in the apparent viscosity of a fluid as the shear rate is increased, and is therefore often referred to as *shear thinning* (Figure 8.5). Pseudoplasticity may occur for a variety of reasons in food emulsions, for example, the spatial distribution of the particles may be altered by the shear field, nonspherical particles may become aligned with the flow field, solvent molecules bound to the particles may be removed, or flocs may be deformed and disrupted (Hunter, 1993; Mewis and Macosko, 1994; Newstein et al., 1999).
2. *Dilatant fluids*. Dilatant behavior is much less common than pseudoplastic behavior. It manifests itself as an increase in the apparent viscosity as the shear rate is increased, and is therefore often referred to as *shear thickening* (Figure 8.5). Dilatancy can be observed in concentrated emulsions or suspensions where the particles are packed tightly together (Hunter, 1989). At intermediate shear rates the particles form two-dimension “sheets” that slide over each other relatively easily, but at higher shear rates these sheets are disrupted and so the viscosity increases (Pal, 1996). Shear thickening may also occur when the particles in an emulsion become flocculated because of an increased collision frequency (Section 7.5); however, this process usually leads to time-dependent behavior and so will be considered in the following section.

Liquids that exhibit pseudoplastic behavior often have a viscosity versus shear stress profile similar to that shown in Figure 8.6. The viscosity decreases from a constant value at low shear stresses ( $\eta_0$ ) to another constant value at high shear stresses ( $\eta_\infty$ ). A number of mathematical equations have been developed to describe the rheological behavior of shear-rate dependent nonideal liquids. The major difference is the range of shear stresses

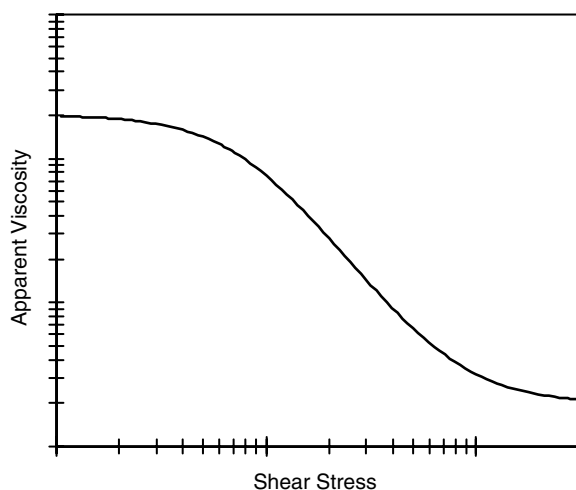


**Figure 8.6** Typical apparent viscosity vs. shear stress profile for a shear-thinning (pseudoplastic) material. The apparent viscosity decreases from a constant value ( $\eta_0$ ) at low shear rates to another constant value ( $\eta_\infty$ ) at high shear rates (Predicted using Meter model).

over which they are applicable. The “Meter” model can be used to describe the dependence of the apparent viscosity on shear stress across the whole shear stress range (Hunter, 1989):

$$\eta = \eta_{\infty} + \frac{\eta_0 - \eta_{\infty}}{1 + (\tau/\tau_i)^n} \quad (8.3)$$

where  $\tau_i$  is the shear stress where the viscosity is mid-way between the low and high shear rate limits ( $= \frac{1}{2} [\eta_0 + \eta_{\infty}]$ ), and  $n$  is the power index. The rheological properties of this type of system can therefore be characterized by four parameters:  $\eta_0$ ,  $\eta_{\infty}$ ,  $\tau_i$ , and  $n$ . Recently, equations similar to Equation 8.3 have been developed to relate the shear-dependence of the apparent viscosity to the strength of the attractive interactions acting between the droplets in flocculated emulsions (see later). The dependence of the apparent viscosity on shear rate can be described using a similar equation by replacing  $\tau/\tau_i$  with  $\dot{\gamma}/\dot{\gamma}_i$ .

If measurements are only carried out at shear rates that are sufficiently less than the high shear rate plateau, then the rheology can be described by the *Ellis* model (Hunter, 1993):

$$\eta = \frac{\eta_0}{1 + (\tau/\tau_i)^n} \quad (8.4)$$

If measurements are only carried out at intermediate shear rates (i.e., above the low shear plateau and below the high shear plateau), then the viscosity can often be described by a simple *power-law* model (Hunter, 1993):

$$\eta = A(d\gamma/dt)^{B-1} \quad (8.5)$$

The constants  $A$  and  $B$  are usually referred to as the *consistency index* and the *power index*, respectively (Dickinson, 1992). For an ideal liquid  $B = 1$ , for an emulsion that exhibits shear thinning  $B < 1$ , and for an emulsion that exhibits shear thickening  $B > 1$ . Equation 8.5 is easy to use since it only contains two unknown parameters that can simply be obtained from a plot of  $\log(\eta)$  versus  $\log(\dot{\gamma})$ . Nevertheless, these equations should only be used after it has been proven experimentally that the relationship between  $\log(\tau)$  and  $\log(d\gamma/dt)$  is linear over the shear stresses or shear rates used. In addition, the power-law model is only applicable over a relatively narrow shear stress range.

**8.2.2.2.2 Time-dependent nonideal liquids.** The apparent viscosity of the fluids described in the previous section depended on the shear rate (or shear stress), but not on the length of time that the shear stress was applied. There are many food emulsions whose apparent viscosity either increases or decreases with time during the application of shear. In some cases this change is reversible and the fluid will recover its original rheological characteristics if it is allowed to stand for a sufficiently long period. In other cases, the change brought about by shearing the sample is irreversible, and the sample will not recover its original characteristics.

An appreciation of the time-dependency of the flow properties of food emulsions is of great practical importance in the food industry. The duration of pumping or mixing operations, for instance, must be carefully controlled so that the food sample has an apparent viscosity that is suitable for the next processing operation. If a food is mixed or pumped for too long it may become too thick or too runny and thus lose its desirable rheological properties.

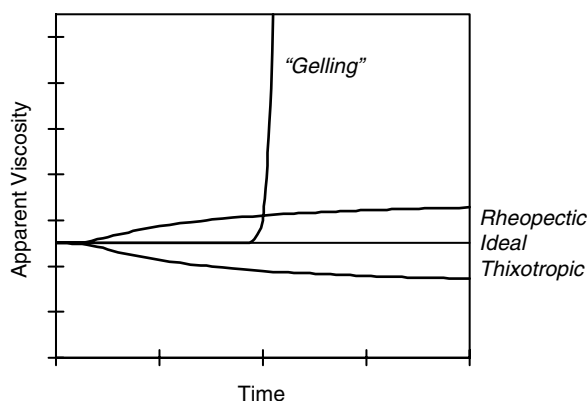


**Figure 8.7** Comparison of the apparent viscosity vs. time profiles of ideal and time-dependent nonideal liquids. The viscosity may increase or decrease to a constant value with time. Alternatively, it may increase steeply due to network formation after a particular time.

The dependence of a liquid rheology on time is usually associated with some kind of relaxation process (Hunter, 1993; Mewis and Macosko, 1994). When an external force is applied to a system that is initially at equilibrium the material takes a certain length of time to reach the new equilibrium condition, which is characterized by a relaxation time,  $\tau_R$ . When the measurement time is of the same order as the relaxation time it is possible to observe changes in the properties of the system with time. Thus, the rheological properties of an emulsion depend on the timescale of the experiment. Time-dependent nonideal fluids are classified into two different categories:

1. *Thixotropic behavior.* A thixotropic fluid is one in which the apparent viscosity *decreases* with time when the fluid is subjected to a constant shear rate (Figure 8.7). Emulsions that exhibit this type of behavior often contain particles (e.g., droplets, crystals, or biopolymers) that are aggregated by weak forces. Shearing of the material causes the aggregated particles to be progressively deformed and disrupted, which decreases the resistance to flow and therefore causes a reduction in the apparent viscosity over time. If the relaxation time associated with the disruption of the flocs is shorter than the measurement time then the apparent viscosity will be observed to tend to a constant final value. This value may correspond to the point where the rate of structure disruption is equal to the rate of structure reformation, or where there is no more structure to be broken down. In pseudoplastic liquids, the break down of the aggregated particles occurs so rapidly that the system almost immediately attains its new equilibrium position, and so it appears as though the apparent viscosity is independent of time.
2. *Rheoplectic.* A rheoplectic fluid is one in which the apparent viscosity *increases* with time when the fluid is subjected to a constant shear rate (Figure 8.7). One of the most common reasons for this type of behavior is that shearing increases both the frequency and efficiency of collisions between droplets, which leads to enhanced aggregation (Section 7.5.1), and consequently to an increase in the apparent viscosity over time.

The rheological properties of some liquids are irreversible, that is, once the shear stress is removed the system does not fully regain its original rheology. Liquids that exhibit this type of permanent change in their properties are called *rheodestructive*. This type of behavior

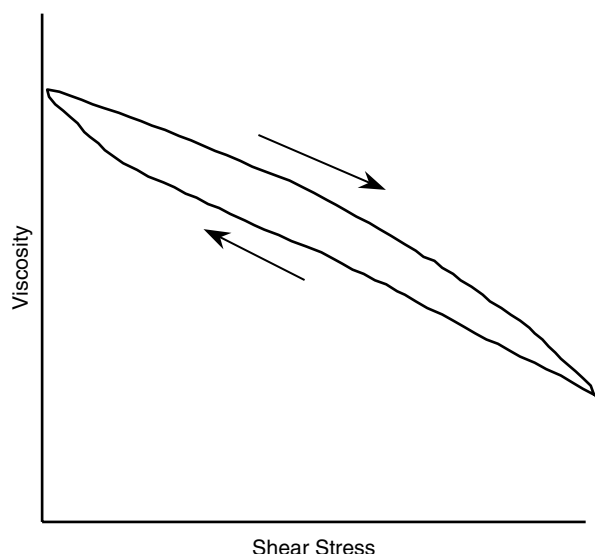


**Figure 8.8** A typical apparent viscosity vs. shear stress hysteresis curve for a liquid whose viscosity depends on the length of time that it is sheared for.

might occur when flocs are disrupted by an intense shear stress and are unable to reform when the shear stress is removed. On the other hand, the rheological properties of other liquids are partially or fully reversible, that is, once the shear stress is removed the system eventually regains some or all of its original rheology. In this case, the recovery time is often an important characteristic of the liquid.

The rheological properties of time-dependent nonideal liquids can be characterized by measuring the change in their apparent viscosity with time during application of a constant shear stress. Alternatively, the apparent viscosity of the liquid can be measured when the shear rate is increased from zero to a certain value, and then decreased back to zero again (Figure 8.8). When there is a significant structural relaxation in a system the upward curve is different from the downward curve and one obtains a *hysteresis loop*. The area within the loop depends on the degree of relaxation that occurs and the rate at which the shear stress is altered. The slower the shear stress is altered, the more time the system has to reach its equilibrium value and therefore the smaller the area within the hysteresis loop. By carrying out measurements as a function of the rate at which the shear stress is increased it is possible to obtain information about the relaxation time.

Information about the time required for a liquid to recover its rheological properties after an applied shear stress has been removed can be obtained by measuring the rheology after the liquid has been left to stand for a certain period in the absence of shear. By varying the time between the applied shear and the rheological measurements it is possible to obtain some information about how quickly the system recovers its original rheological properties.

### 8.2.3 *Plastics*

A number of food emulsions exhibit rheological behavior known as *plasticity*, for example, mayonnaise, margarine, butter, and certain spreads (Sherman, 1968a, 1970; Tung and Paulson, 1995). A plastic material has elastic properties below a certain applied stress, known as the *yield stress* but flows like a fluid when this stress is exceeded.

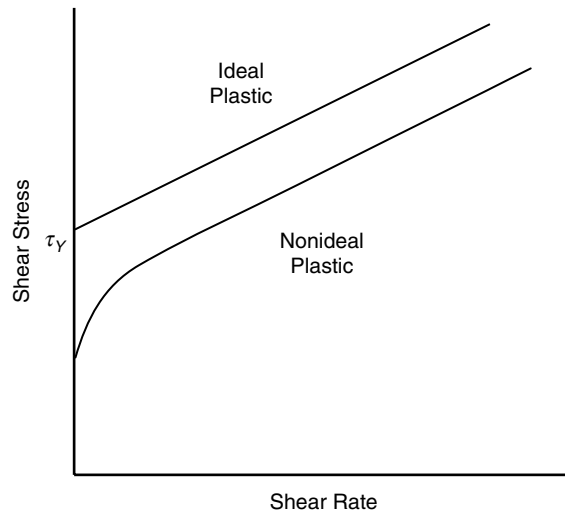


Figure 8.9 Rheological behavior of an ideal (Bingham) plastic and a nonideal plastic.

#### 8.2.3.1 Ideal plastics

The ideal plastic material is referred to as a *Bingham plastic* after the scientist who first proposed this type of rheological behavior (Sherman, 1970). Two equations are needed to describe the rheological behavior of a Bingham plastic, one below the yield stress and one above it:

$$\tau = G\gamma \quad (\text{for } \tau < \tau_Y) \quad (8.6)$$

$$\tau - \tau_0 = \eta\dot{\gamma} \quad (\text{for } \tau \geq \tau_Y) \quad (8.7)$$

where  $G$  is the shear modulus,  $\eta$  is the viscosity, and  $\tau_Y$  is the yield stress. The rheological properties of an ideal plastic are shown in Figure 8.9.

Foods that exhibit plastic behavior usually consist of a network of aggregated molecules or particles dispersed in a liquid matrix (Clark, 1987; Edwards et al., 1987; Tung and Paulson, 1995; Walstra, 2003a). For example, margarine and butter consist of a network of tiny fat crystals dispersed in a liquid oil phase (Moran, 1994). Below a certain applied stress there is a small deformation of the sample, but the weak bonds between the crystals are not disrupted. When the applied stress exceeds the yield stress, the weak bonds are broken and the crystals slide past one another leading to flow of the sample. Once the force is removed the flow stops. A similar type of behavior can be observed in emulsions containing three-dimensional networks of aggregated droplets.

#### 8.2.3.2 Nonideal plastics

Above the yield stress the fluid flow may exhibit non-Newtonian behavior similar to that described earlier for liquids, for example, pseudoplastic, dilatant, thixotropic, or rheopectic. The material may also exhibit nonideal elastic behavior below the yield stress, for example, the yield point may not be sharply defined, instead, the stress may increase dramatically, but not instantaneously, as the shear rate is increased (Figure 8.9). This would occur if the material did not begin to flow at a particular stress, but there was a gradual break down of the network structure over a range of applied stresses (Sherman, 1968a).

### 8.2.4 Viscoelastic materials

Many food emulsions are not pure liquids or pure solids, but have rheological properties that are partly viscous and partly elastic (Sherman, 1968a, 1970; Dickinson, 1992; Walstra, 2003a). Plastic materials exhibit elastic behavior below a certain value of the applied stress, and viscous behavior above this value. In contrast, viscoelastic materials exhibit both viscous and elastic behaviors simultaneously. In an ideal elastic solid, all the mechanical energy applied to the material is stored in the deformed bonds, and is returned to mechanical energy once the force is removed, that is, there is no loss of mechanical energy. On the other hand, in an ideal liquid, all of the mechanical energy applied to the material is dissipated due to friction, that is, the mechanical energy is converted to heat. In a viscoelastic material, part of the energy is stored as mechanical energy within the material, and part of the energy is dissipated as heat. For this reason, when a force is applied to a *viscoelastic* material it does not instantaneously adopt its new dimensions nor does it instantaneously return back to its original nondeformed state when the force is removed (as an ideal elastic material would). In addition, the material may even remain permanently deformed once the force is removed. The rheological properties of a viscoelastic material are characterized by a complex elastic modulus,  $E^*$ , which is comprised of an elastic and a viscous contribution:

$$E^* = E' + iE'' \quad (8.8)$$

Here  $E'$  is known as the *storage* modulus and  $E''$  as the *loss* modulus. Two types of experimental tests are commonly used to characterize the rheological properties of viscoelastic materials: one based on *transient* measurements, and the other on *dynamic* measurements (Whorlow, 1992). Both types of tests can be carried out by the application of simple shear, simple compression, or bulk compression to the material being analyzed. Simple shear tests are the most commonly used to analyze food emulsions and so only these will be considered here. Nevertheless, the same basic principles are also relevant to other kinds of applied stresses.

#### 8.2.4.1 Transient tests

In a transient experiment, either a constant stress is applied to a material and the resulting strain is measured as a function of time (*creep*), or a material is deformed to a constant strain and the stress required to keep the material at this strain is measured as a function of time (*stress relaxation*):

*Creep.* In a creep experiment a constant stress is applied to a material and then the change in its dimensions with time is monitored, which results in a strain versus time curve (Sherman, 1968a, 1970). The data are usually expressed in terms of a parameter called the *compliance*,  $J$ , which is equal to the ratio of the strain to the applied stress (and is therefore the reciprocal of the modulus). The compliance is proportional to the strain, but it is a better parameter to use to characterize the rheological properties of the material because it takes into account the magnitude of the applied stress. The time dependence of the compliance of a material can also be measured when the stress is removed, which is referred to as a *creep recovery* experiment. A typical compliance versus time curve for a viscoelastic material is shown in Figure 8.10. This curve can be divided into three regions (Sherman, 1968a):

1. A region of instantaneous elastic deformation in which the bonds between the particles are stretched elastically. In this region the material acts like an elastic solid with a compliance ( $J_0$ ) given by the ratio of the strain to the applied stress.



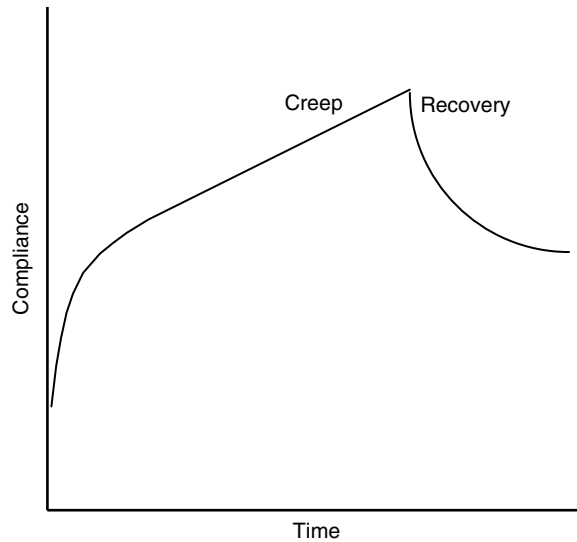


**Figure 8.10** A typical compliance vs. time curve for a viscoelastic material, such as ice cream.

2. A region of retarded elastic compliance in which some bonds are breaking and some are reforming. In this region the material has viscoelastic properties and its compliance is given by  $J_R = J_M(1 - \exp(-t/\tau_M))$ , where  $J_M$  and  $\tau_M$  are the mean compliance and retardation time.
3. A region of Newtonian compliance,  $J_N$ , when the bonds are disrupted and do not reform so that the material only flows:  $J_N = t/\eta_N$ .

The total creep compliance of the system is therefore given by:

$$J(t) = J_0 + J_R(t) + J_N(t) = J_0 + J_M(1 - \exp(-t/\tau_M)) + t/\eta_N \quad (8.9)$$

This type of material is usually referred to as a *viscoelastic liquid*, because it continues to flow for as long as the stress is applied. Some materials exhibit a different type of behavior and are referred to as *viscoelastic solids*. When a constant stress is applied to a viscoelastic solid the creep compliance increases up to a finite equilibrium value ( $J_E$ ) at long times, rather than increasing continuously. When the force is removed the compliance returns to zero, unlike a *viscoelastic liquid*, which does not return to its initial shape once the force is removed.

**Stress relaxation.** Instead of applying a constant force and measuring the change in the strain with time, it is also possible to apply a constant strain and measure the stress required to keep the material at this strain as a function of time. This type of experiment is referred to as *stress relaxation*. The same type of information can be obtained from creep and stress relaxation experiments, and the method used largely depends on the type of rheological instrument available.

#### 8.2.4.2 Dynamic tests

The usage of dynamic tests to characterize the rheological properties of viscoelastic materials has become routine in many laboratories due to the commercial availability of sophisticated dynamic rheometers. In a dynamic experiment, a sinusoidal stress is applied to a material and the resulting sinusoidal strain is measured, or vice versa (Tung and Paulson,

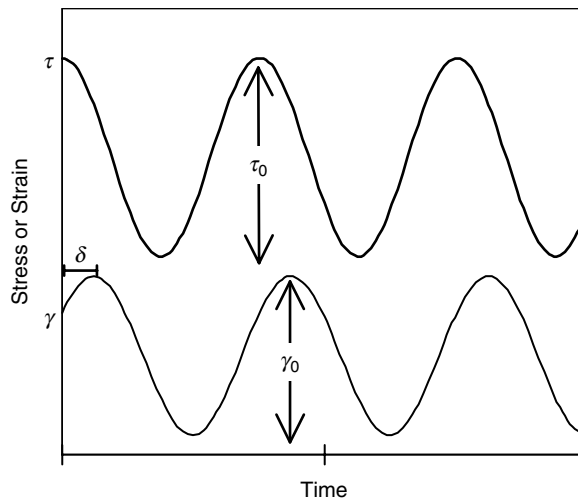


**Figure 8.11** The rheological properties of a viscoelastic material can be determined by measuring the relationship between an applied sinusoidal stress and the resultant sinusoidal strain (or vice versa).

1995; Liu and Masliyah, 1996). In this section, we will only consider the case where a stress is applied to the sample and the resultant strain is measured. The applied stress is characterized by its maximum amplitude ( $\tau_0$ ) and its angular frequency ( $\omega$ ). The resulting strain has the same frequency as the applied stress, but its phase is different because of relaxation mechanisms associated with the material, which cause viscous dissipation of some of the applied mechanical energy (Whorlow, 1992). Information about the viscoelastic properties of the material can therefore be obtained by measuring the maximum amplitude ( $\gamma_0$ ) and phase shift ( $\delta$ ) of the strain (Figure 8.11). The amplitude of the applied stress used in this type of test is usually chosen to be sufficiently small that the material is in the *linear viscoelastic region*, that is, the stress is proportional to the strain, and the properties of the material are not affected by the experiment (van Vliet, 1995; Liu and Masliyah, 1996).

If the applied stress varies sinusoidally with time then (Whorlow, 1992):

$$\tau = \tau_0 \cos(\omega t) \quad (8.10)$$

and the resulting harmonic strain is

$$\gamma = \gamma_0 \cos(\omega t - \delta) \quad (8.11)$$

The compliance of the material is therefore given by

$$J(t) = \frac{\gamma}{\tau} = \frac{\gamma_0}{\tau_0} (\cos \delta \cos \omega t + \sin \delta \sin \omega t) \quad (8.12)$$

or

$$J(t) = J' \cos \omega t + J'' \sin \omega t \quad (8.13)$$

where  $J' (= \gamma_0 \cos \delta / \tau_0)$  is known as the *storage compliance*, which is the in-phase component of the compliance, and  $J'' (= \gamma_0 \sin \delta / \tau_0)$  is known as the *loss compliance*, which is the 90°

out-of-phase component of the compliance. The in-phase component of the compliance is determined by the elastic properties of the material, whereas the 90° out-of-phase component is determined by the viscous properties. This is because the stress is proportional to the strain ( $\tau \propto \gamma$ ) for elastic materials, whereas it is proportional to the *rate* of strain ( $\tau \propto d\gamma/dt$ ) for viscous materials (Macosko, 1994).

The dynamic rheological properties of a material can therefore be characterized by measuring the frequency-dependence of the applied stress and the resulting strain, and then plotting a graph of  $J'$  and  $J''$  versus frequency. Alternatively, the data are often presented in terms of the magnitude of the complex compliance ( $J^* = J' - iJ''$ ) and the phase angle:

$$|J^*| = \sqrt{J'^2 + J''^2} \quad (8.14)$$

$$\delta = \tan^{-1}\left(\frac{J''}{J'}\right) \quad (8.15)$$

The phase angle of a material provides a useful insight into its viscoelastic properties:  $\delta = 0^\circ$  for a perfectly elastic solid;  $\delta = 90^\circ$  for a perfectly viscous fluid; and,  $0 < \delta < 90^\circ$  for a viscoelastic material. The more elastic a material (at a particular frequency), the smaller the phase angle, and the lower the amount of energy dissipated per cycle. Gels are often defined as having phase angles less than  $45^\circ$ , but this value actually depends on the measurement frequency, and so it is also important to specify the frequency when reporting gelation times or gelation temperatures determined using this definition. In addition, measurements of the rheological properties of viscoelastic materials as a function of frequency can provide valuable information about relaxation times associated with structural changes within the material.

It is often more convenient to express the rheological properties of a viscoelastic material in terms of its modulus, rather than its compliance (Whorlow, 1992). The complex, storage, and loss moduli of a material can be calculated from the measured compliances using the following relationships:

$$G^* = G' + iG'' \quad G' = \frac{J'}{J'^2 + J''^2} \quad G'' = \frac{J''}{J'^2 + J''^2} \quad (8.16)$$

Sophisticated analytical instruments are available to measure the dynamic rheological properties of viscoelastic materials, and usage of these techniques is providing valuable insights into the factors that influence the rheology of food emulsions.

### 8.3 Measurement of rheological properties

Food emulsions can exhibit a wide range of different types of rheological behavior, including, liquid, solid, plastic, and viscoelastic (Dickinson and Stainsby, 1982; Dickinson, 1992; McClements, 2003). Consequently, a variety of instrumental methods have been developed to characterize their rheological properties. Instruments vary according to the type of deformation that they apply to the sample (e.g., shear, compression, elongation, or some combination), the rheological properties that they can measure (e.g., shear modulus, viscosity, viscoelasticity), the nature of the samples that they can test (e.g., liquids, solids, gels), their cost, their sensitivity, the range of accessible shear stresses or strains, the ability to scan temperature or not, their ease of operation and data processing, and their ability to make off-line or in-line measurements (Whorlow, 1992; Steffe, 1996; Rao, 1999; Roberts, 2003).

In many industrial applications it is necessary to have instruments that make measurements that are rapid, low-cost, simple to carry out and reproducible, rather than giving absolute fundamental data (Sherman, 1970; Rao, 1995, 1999). Thus, simple empirical measurement techniques are often used in quality assurance laboratories, rather than the more sophisticated and expensive instruments used in research and development laboratories. The information obtained from these empirical instruments is often difficult to relate to the fundamental rheological constants of a material because the applied stresses and strains are not easily measured or defined. Rather than having a simple elongation, shear or compression, different types of forces may be applied simultaneously. For example, when a blade cuts through a meat product, both shear and compression forces are applied simultaneously, and the sample is deformed beyond the limit where Hooke's law is applicable. To compare data from different laboratories it is necessary to carefully follow standardized test procedures. These procedures may define experimental parameters such as the design of the device used, the magnitude of the applied force or deformation, the speed of the probe, the length of time the force is applied for, the measurement temperature, and the sample dimensions and preparation procedure.

For food scientists involved in research and development it is usually necessary to use instruments that provide information about the fundamental rheological constants of the material being tested, for example,  $\eta$ ,  $G'$ ,  $G''$  (Steffe, 1996; Rao, 1999). These instruments are designed to apply well-defined stresses and strains to a material in a controlled manner so that stress-strain relationships can be measured and interpreted using available mathematical models. Rheological properties determined using these techniques can be compared with measurements reported by researchers in the literature or made by colleagues working in other laboratories with different instruments. In addition, measured fundamental rheological properties can be compared with theoretical predictions made by mathematical models developed to relate the structure and composition of materials to their fundamental rheological properties (Larson, 1999; Walstra, 2003a).

It is convenient to categorize rheological instruments according to whether they use simple compression (or elongation) or shear forces\* (Steffe, 1996; Rao, 1999).

### 8.3.1 Simple compression and elongation

This type of test is most frequently carried out on solid or semisolid foods that are capable of supporting their own weight, for example, food gels, butter, margarine, and frozen ice cream (Rao et al., 1995; Bourne, 1997). Measurements are often carried out using instruments referred to generally as *Universal Testing Machines*. The solid sample to be analyzed is placed between a fixed plate and a moving probe (Figure 8.12). The probe can have many different designs depending on the type of information required, including a flat plate, a blade, a cylindrical spike, and even a set of teeth!

The probe can be moved vertically, either upward or downward, at a controlled speed. Either the probe or the plate contains a pressure sensor that measures the force exerted on the sample when it is deformed by the probe. The instrument also records the distance that the probe moves through the sample. The stress and strain experienced by a material can therefore be calculated from knowledge of its dimensions, and the force and deformation recorded by the instrument. Often it is necessary to measure the change in the dimensions during the compression (or elongation) test so as to calculate the true stress.

\* At present few commercial instruments use bulk compression tests to analyze the rheology of food emulsions, although information about the bulk modulus of emulsions can be obtained by combining ultrasonic and density measurements.

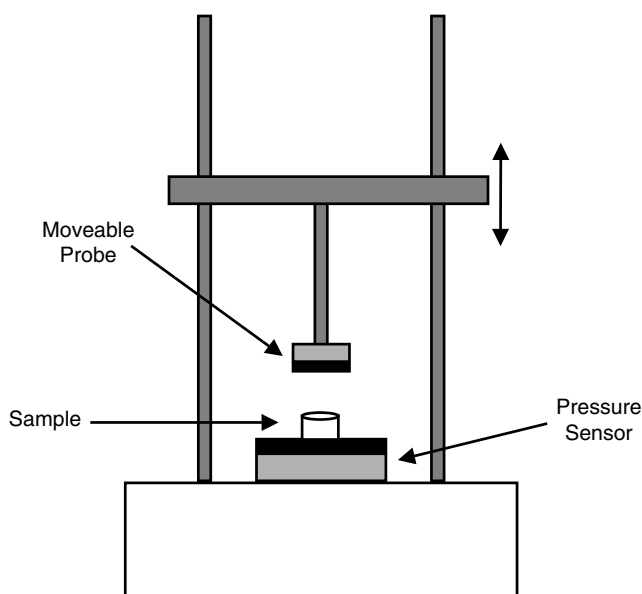


**Figure 8.12** Universal Testing Machine that can be used to measure the rheological properties of materials using compression or elongation tests.

Some of the common tests carried out using Universal Testing Machines are the following:

1. *Stress–strain curve.* The stress on a sample is measured as a function of strain as it is compressed at a fixed rate (Figure 8.1). The resulting stress–strain curve is used to characterize the rheological properties of the material being tested. The slope of stress versus strain at relatively small deformations is often a straight line, with a gradient equal to the elastic modulus (Table 8.1). At intermediate deformations the stress may no longer be proportional to the strain and some flow may occur, so that when the stress is removed the sample does not return to its original shape. At larger deformations the sample may rupture and the fracture stress, strain, and modulus can be determined. The operator must decide the distance and speed at which the probe will move through the sample. For viscoelastic materials, the shape of the upward and downward curves may be different, and depends on the speed at which the probe moves. This type of test is used commonly to test solid samples and gels, such as margarine, butters, spreads, and desserts.
2. *Repeated deformation.* The sample to be analyzed is placed between the plate and the probe, and then the probe is lowered and raised a number of times at a fixed speed so that the sample experiences a number of compression cycles (Rao et al., 1995). An ideal elastic solid would show the same stress–strain curve for each cycle; however, the properties of many materials are altered by compression (e.g., due to fracture or flow), and therefore successive compression cycles give different stress–strain curves. Analysis of the stress–strain relationship over a number of cycles is often used to calculate a variety of empirical parameters that are believed to be related to the sensory texture of foods, such as hardness, fracturability, cohesiveness, springiness (Bourne, 1997). This type of test is often used to give some indication of the processes that occur when a food is chewed in the mouth, that is, the breakdown of food structure.

3. *Transient experiments.* A material is placed between the plate and the probe, is then compressed to a known deformation and the relaxation of the stress with time is measured (stress relaxation). Alternatively, a constant stress is applied to the sample and the variation of the strain is measured over time (creep). This type of experiment is particularly useful for characterizing the rheological properties of viscoelastic food emulsions (see Section 8.2.4).

By using different fixtures the same type of instrument can be used to carry out elongation experiments. A sample is clamped at both ends, and then the upper clamp is moved upward at a controlled speed and the force required to elongate the sample is measured by the pressure sensor as a function of sample deformation. Again the elastic modulus and fracture properties of the material can be determined by analyzing the resulting stress–strain relationship. Universal Testing Machines can also be adapted to perform various other types of experiments, for example, such as bending, slicing, or forcing a material through an orifice.

A number of more sophisticated instruments, based on dynamic rheological measurements, have been developed to characterize the rheological properties of solids, plastics, and viscoelastic materials (Wunderlich, 1990; Whorlow, 1992; Rao, 1999). As well as carrying out the standard compression measurements mentioned above, they can also be used to carry out dynamic compression measurements on viscoelastic materials. The sample to be analyzed is placed between a plate and a probe and an oscillatory compression stress of known amplitude and frequency is applied to it. The amplitude and phase of the resulting strain are measured, and converted into a storage and loss modulus using suitable equations (Section 8.2.4.2.). The amplitude of the applied stress must be small enough to be in the linear viscoelastic region of the material. These instruments are relatively expensive to purchase, and are therefore used mainly by research laboratories in large food companies, government institutions and Universities. Nevertheless they are extremely powerful tools for carrying out fundamental studies of food emulsions. The rheological properties of a sample can be measured as a function of storage time or temperature, and thus processes such as gelation, aggregation, crystallization, melting, and glass transitions can be monitored. The measurement frequency can also be varied, which provides valuable information about relaxation processes occurring within a sample.

Some complications can arise when carrying out simple compression experiments. There may be friction between the compressing plates and the sample which can lead to the generation of shear as well as compression forces (Whorlow, 1992). For this reason it is often necessary to lubricate the sample with oil to reduce the effects of friction. In addition, the cross-sectional area of the sample may change during the course of the experiment, which would have to be taken into account when converting the measured forces into stresses (Walstra, 2003a). Finally, for viscoelastic materials, some stress relaxation may occur during the compression or expansion, so that the results depend on the rate of sample deformation.

An interesting adaptation of compression testing, called *squeezing flow viscometry*, has been developed for the rheological testing of liquids and semisolid foods (Campanella and Peleg, 2002). This technique is based on compressing a sample between two parallel plates and measuring the resulting force–height relationship. A variety of different measurement protocols are possible for analyzing different kinds of samples. The squeezing flow viscometry technique has potential advantages over many of the conventional methods used to measure the rheological properties of liquids because it can minimize problems associated with slip at the sample-measurement cell boundary, and reduce structural disruption caused by insertion of a sample into a narrow measurement cell (Damrau and Peleg, 1997).

### 8.3.2 Shear measurements

Instruments that use shear measurements are used to characterize the rheological properties of liquids, viscoelastic materials, plastics, and solids (Whorlow, 1992; Steffe, 1996; Rao, 1995, 1999). The type of instrument and test method used in a particular situation depends on the physicochemical characteristics of the sample being analyzed, as well as on the kind of information required. Some instruments can be used to characterize the rheological properties of both solids and liquids, whereas others can only be used for either solids or liquids. Certain types of viscometers are capable of measuring the viscosity of fluids over a wide range of shear rates and can therefore be used to analyze both ideal and nonideal liquids, whereas in others the shear rate cannot be controlled and so they are only suitable for analyzing ideal liquids. A number of instruments can be used to characterize the rheological behavior of viscoelastic materials using both transient and dynamic tests, whereas others can only use either one or the other type of test. To make accurate and reliable measurements it is important to select the most appropriate instrument and test method, and to be aware of possible sources of experimental error.

#### 8.3.2.1 Capillary viscometers

The simplest and most commonly used capillary viscometer is called the *Ostwald viscometer* (Hunter, 1986; Whorlow, 1992; Rao, 1999). This device usually consists of a glass U-tube into which the sample to be analyzed is poured. The whole arrangement is placed in a thermostated water-bath to reach the measurement temperature (Figure 8.13). The viscosity of the liquid is measured by sucking it into one arm of the tube using a slight vacuum and then measuring the time taken for a fixed volume of it to flow back through a capillary

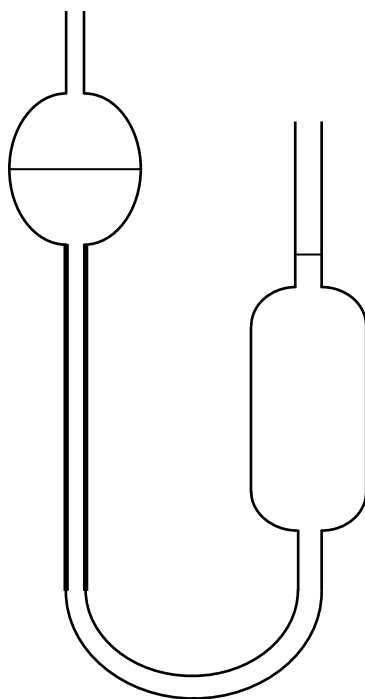


Figure 8.13 Capillary viscometer used to measure the viscosity of liquids.

of fixed radius and length. The time taken to travel through the capillary is related to the viscosity by the following equation:

$$t = C \frac{\eta}{\rho} \quad (8.17)$$

where  $\rho$  is the density of the fluid,  $t$  is the measured flow time, and  $C$  is a constant that depends on the precise size and dimensions of the U-tube. The higher the viscosity of the fluid, the longer it takes to flow through the tube. The simplest method for determining the viscosity of a liquid is to measure its flow time and compare it with that of a liquid of known viscosity, such as distilled water:

$$\eta_s = \left( \frac{t_s}{t_0} \frac{\rho_s}{\rho_0} \right) \eta_0 \quad (8.18)$$

where the subscripts  $s$  and  $0$  refer to the sample being analyzed and the reference fluid, respectively. This type of viscometer is used principally to measure the viscosity of Newtonian liquids. It is normally unsuitable for analyzing non-Newtonian liquids because the sample does not experience a uniform and controllable shear rate (Hunter, 1986). Nevertheless, some limited information on the flow behavior of non-Newtonian liquids can be obtained by carrying out measurements using U-tubes with capillaries of different diameters (McKenna and Lyng, 2003). It may also be necessary to use U-tubes with different diameters to analyze liquids with different viscosities: the larger the diameter, the higher the viscosity of the sample that can be analyzed. In more modern U-tube instruments the fluid is made to flow through the tube by applying an external pressure to it, rather than relying on its hydrostatic pressure (McKenna and Lyng, 2003). This external pressure can be applied using a piston or compressed gas.

### 8.3.2.2 Mechanical viscometers and dynamic rheometers

A number of mechanical rheological instruments have been designed to measure the shear properties of liquids, viscoelastic materials, plastics, and solids (Whorlow, 1992; Macosko, 1994; McKenna and Lyng, 2003). These instruments are usually computer controlled and can often carry out sophisticated rheological tests as a function of time, temperature, shear rate, or oscillation frequency. Basically, the sample to be analyzed is placed in a thermostated measurement cell (Figure 8.14), where it is subjected to a controlled shear stress (or strain). The resulting strain (or stress) is measured by the instrument, and so the rheological properties of the sample can be determined from the stress–strain relationship. The type of rheological test carried out depends on whether the sample is liquid, solid, or viscoelastic. The instruments can be divided into two different types: *constant stress* instruments that apply a constant torque to the sample and measure the resultant *strain* or *rate of strain*, and *constant strain* instruments that apply a constant *strain* or *rate of strain* and measure the torque generated in the sample. For convenience, we will only discuss constant stress instruments below, although both types of instruments are commonly used in the food industry. In addition, with many of the modern instruments it is possible to make a constant stress instrument operate like a constant strain instrument, and vice versa.



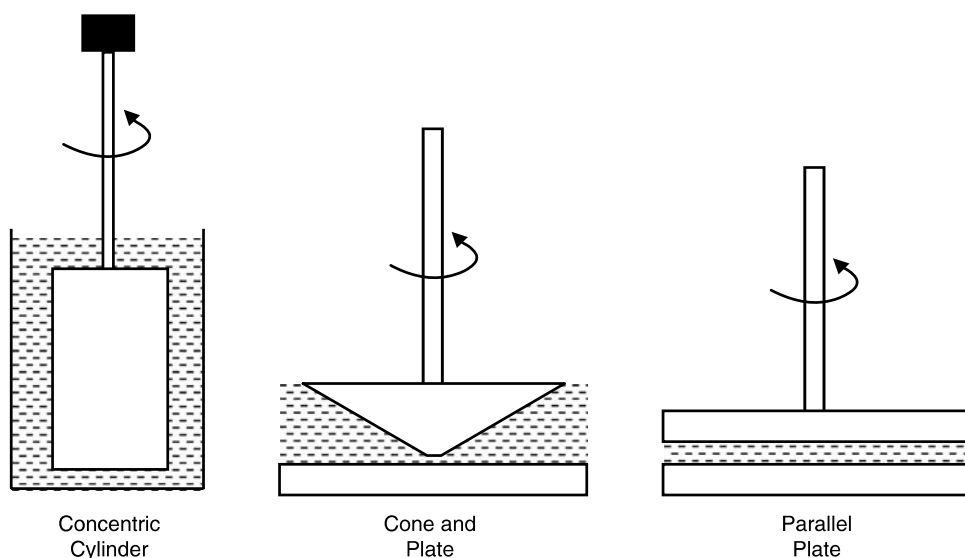


**Figure 8.14** Different types of measurement cells commonly used with dynamic shear rheometers and viscometers.

A number of different types of measurement cells can be used to contain the sample during an experiment (Pal et al., 1992; McKenna and Lyng, 2003):

1. *Concentric cylinder.* The sample is placed in the narrow gap between two concentric cylinders (Figure 8.14). Normally, the inner cylinder (the *bob*) is driven at a constant *torque* (angular force) and the resultant *strain* (angular deflection) or *rate of strain* (speed at which the cylinder rotates) is measured, depending on whether one is analyzing a predominantly solid or liquid sample.\* For a solid, the angular deflection of the inner cylinder from its rest position is an indication of its elasticity: the larger the deflection, the smaller the shear modulus. For a liquid, the speed at which the inner cylinder rotates is governed by the viscosity of the fluid between the plates: the faster it spins at a given torque, the lower the viscosity of the liquid being analyzed. The torque can be varied in a controlled manner so that the (apparent) elastic modulus or viscosity can be measured as a function of shear stress. This instrument can be used for measuring the viscosity of Newtonian liquids, the apparent viscosity of non-Newtonian liquids, the viscoelasticity of semisolids, and the elasticity of solids. In some instruments the outer cylinder rotates and the inner cylinder remains fixed, but the principles of the measurements are the same.
2. *Parallel plate.* In this type of measurement cell the sample is placed between two parallel plates (Figure 8.14). The lower plate is stationary, while the upper one can rotate. A constant *torque* is applied to the upper plate, and the resultant *strain* or *rate of strain* is measured, depending on whether one is analyzing a predominantly solid or liquid sample. The main problem with this type of experimental arrangement is that the shear strain varies across the sample: the shear strain in the middle of the sample being less than that at the edges. The parallel plate arrangement is therefore only suitable for analyzing samples that have rheological properties that are independent of shear rate, and it is therefore unsuitable for analyzing nonideal liquids or solids.

\* In some instruments, the outer cylinder rotates and the torque on the inner cylinder is measured.

3. *Cone and plate.* This is essentially the same design as the parallel plate measurement cell, except that the upper plate is replaced by a cone (Figure 8.14). The cone has a slight angle that is designed to ensure that a more uniform shear stress acts across the sample. The cone-and-plate arrangement can therefore be used to analyze nonideal materials.
4. *Vane.* A vane consists of a multibladed bob that is placed in a sample and then rotated around its axis (Parker and Vigouroux, 2003). This method is finding increasing usage for characterizing semisolid food emulsions because it overcomes many of the problems associated with conventional measurement geometries, such as disruption of sample structure during insertion into the device and wall slip.

Often the rheological properties of samples are measured either as a function of storage time at a fixed temperature or as the temperature is varied in a controlled manner.

### 8.3.2.3 Possible sources of experimental error

It should be noted that the rheological characterization of emulsion-based products using shear viscometers and rheometers does present a number of specific challenges (Sherman, 1970; Hunter, 1989; Pal et al., 1992; Steffe, 1996; Larson, 1999). This section highlights a number of possible sources of experimental error that should be avoided or taken into account when carrying out rheology measurements on food emulsions. Mewis and Macosko (1994) discuss other sources of error that are common to all types of rheology measurements.

**8.3.2.3.1 Rheometer gap effects.** The gap between the cylinders or plates should be at least 20 times greater than the diameter of the droplets, so that the emulsion appears as a homogeneous material within the device (Pal et al., 1992). On the other hand, the gap must be narrow enough to ensure a fairly uniform shear stress across the whole of the sample.

**8.3.2.3.2 Wall-slip effects.** A phenomenon known as wall slip may occur within a viscometer or rheometer, which can cause serious errors in rheological measurements if not properly taken into account (Sherman, 1970; Franco et al., 1998a; Sanchez et al., 2001). It is normally assumed that the liquid in direct contact with the surfaces of the measurement cell moves with them at the same velocity (Hunter, 1986). This assumption is usually valid for simple liquids because the small molecules are caught within the surface irregularities on the walls and are therefore dragged along with them. For an emulsion, this assumption may not hold because the droplets or flocs are greater in size than the surface irregularities. Under these circumstances, phase separation occurs at the cylinder surface and a thin layer of continuous phase acts as a lubricant so that slip occurs. The instrument response is then determined mainly by the properties of this thin layer of liquid, rather than by the bulk of the material being tested. Wall-slip effects can be minimized by roughening the surfaces of measurement cells or by using a range of different gap widths (Hunter, 1986; Pal et al., 1992; Franco et al., 1998a; Sanchez et al., 2001; Barnes and Nguyen, 2001). Alternatively, different measurement geometries or rheological techniques can be used to overcome this effect, such as the vane geometry (Parker and Vigouroux, 2003) or squeezing flow techniques (Campanella and Peleg, 2002; Estellé et al., 2003).

**8.3.2.3.3 Sample history.** The rheological properties of many food emulsions depend strongly on their thermal and shear history, and so this must be carefully controlled in order to obtain reproducible measurements (Franco et al., 1998a). For example, the viscosity of many flocculated food emulsions decreases substantially on shearing due to disruption of particle flocs, and the recovery of the original viscosity takes a certain length of time to achieve after the shear stress is removed. For these systems, it is extremely important to establish a consistent thermal and shear sample history prior to starting any rheological measurements. For example, it may be necessary to place an emulsion in a thermostated measurement cell,

then apply a fixed shear stress for a constant time, then allow it to sit for a fixed time, and then begin the rheological measurements. The objectives of this process are to break down and reform the structure of the emulsion in a reproducible and consistent manner.

**8.3.2.3.4 Gravitation separation.** Many emulsions are susceptible to creaming or sedimentation during the course of an experiment, which causes the vertical distribution of droplets in the emulsion to become inhomogeneous (Mewis and Macosko, 1994). For example, in emulsions where the droplet density is less than the density of the surrounding liquid, creaming leads to the formation of a droplet-rich layer at the top of the emulsion and a droplet-depleted layer at the bottom (Section 7.3). The separation of an emulsion into a creamed and a serum layer should be avoided because the rheological characteristics of a separated emulsion may be appreciably different from those of a homogeneous emulsion. The importance of this effect depends on the geometry of the measurement cell. In a concentric cylinder measurement cell, the formation of a viscoelastic or plastic creamed layer may dominate the rheology of the whole emulsion because the shear stress is applied to the sides of the emulsion. On the other hand, in a cone-and-plate or parallel plate rheometer, the formation of a viscoelastic or plastic creamed layer may have a different effect because the shear stress is applied to the top and bottom of the emulsions. An approximate criterion that has been proposed to ensure that gravitational separation effects do not greatly affect measurements, is that the droplets should move less than 10% of the emulsion height in the rheometer during the course of a measurement (Mewis and Macosko, 1994):

$$t_{10\%h} = \frac{0.45h\eta_1}{gr^2(\rho_2 - \rho_1)} \quad (8.19)$$

where  $h$  is the height of the emulsion in the rheometer,  $\rho_2$  is the density of the droplets,  $\rho_1$  is the density of the continuous phase,  $\eta_1$  is the viscosity of the continuous phase,  $g$  is the acceleration due to gravity, and  $r$  is the droplet radius. For a typical oil-in-water emulsion without thickening or gelling agent in the aqueous phase inside a typical concentric cylinder measurement cell ( $\eta_1 = 1$  m Pa sec;  $\Delta\rho = 80$  kg m<sup>-3</sup>,  $h = 50$  mm):  $t_{10\%h} \sim 470/r^2$  min, when  $r$  is expressed in micrometers. Thus, for 1  $\mu$ m droplets the sample will be stable for almost 8 h, but for 10  $\mu$ m droplets the sample will only be stable for about 5 min.

**8.3.2.3.5 Hydrodynamic instabilities.** Hydrodynamic instabilities occur in fluids at sufficiently high flow rates which generate secondary flows that interfere with the rheological measurements, for example, inertial effects (Larson, 1999). These effects can be observed in concentric cylinder type rheometers at high shear rates, particularly for low viscosity fluids, where it appears that the shear viscosity increases with increasing shear rate.

### 8.3.3 Empirical techniques

Many of the rheological instruments mentioned above are unsuitable for widespread application in the food industry because the instrumentation is too expensive, highly skilled operators are required, or measurements take too long to carry out (Sherman, 1970; Rao et al., 1995). For this reason a large number of empirical techniques have been developed by food scientists that provide simple and rapid determinations of the rheological properties of a sample (McKenna and Lyng, 2003). Many of these empirical techniques have become widely accepted for analyzing specific food types. Typical examples may be penetrometers to measure the hardness of butters, margarines, and spreads (Sherman, 1970), devices for measuring the time taken for liquids to flow through a funnel (Liu and Masliyah, 1996), or devices that measure the time it takes for a spherical ball to fall through a sample contained within a glass

tube (Becher, 1957; Steffe, 1996). It is difficult to analyze the data from these devices using fundamental rheological concepts because it is difficult to define the stresses and strains involved. Nevertheless, these devices are extremely useful where rapid empirical information is more important than fundamental understanding.

## 8.4 Rheological properties of emulsions

Food emulsions exhibit a wide range of different rheological properties, ranging from low viscosity liquids to fairly rigid solids. The rheological behavior of a particular food depends on the type and concentration of ingredients that it contains, as well as on the processing and storage conditions it has experienced. In this section, the relationship between the rheological properties of emulsions and their composition and microstructure is discussed. We begin by considering the rheology of dilute suspensions of non-interacting rigid spheres, because the theory describing the properties of this type of system is well established (Hunter, 1986; Mewis and Macosko, 1994; Hiemenz and Rajagopalan, 1997). Nevertheless, many food emulsions are concentrated and contain nonrigid, nonspherical, and/or interacting droplets (Dickinson, 1992). The theoretical understanding of these types of systems is less well developed, although appreciable progress has been made and this will be discussed in the following sections.

One of the major factors influencing the rheological properties of colloidal dispersions is the packing of the particles within the system (Quemada and Berli, 2002). It is therefore useful to begin with a general discussion of the influence of particle packing on the rheology for a colloidal dispersion containing rigid spherical particles that do not interact through long-range colloidal interactions (Figure 8.15):

1. *Dilute systems* ( $\phi < 0.05$ ): The particles are sufficiently far apart that they do not interact with each other and their movement is only determined by Brownian forces. The emulsion is a fluid with a relatively low viscosity that is dominated by the viscosity of the continuous phase.

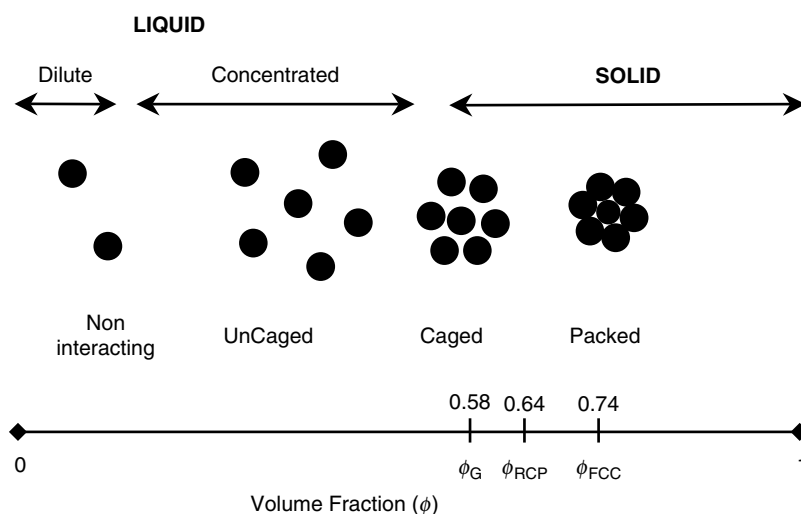


**Figure 8.15** The rheological behavior of colloidal dispersions containing rigid spheres in the absence of long-range interactions is strongly dependent on the disperse phase volume fraction of the particles (Adapted from Berli and Quemada, 2002).

2. *Concentrated systems* ( $0.05 < \phi < 0.49$ ): The particles interact appreciably with each other through hydrodynamic interactions and particle collisions, which hinders their movement. The emulsion is still fluid with a viscosity that becomes increasingly high as the particle concentration increases.
3. *Partially "crystalline" systems* ( $0.49 < \phi < 0.54$ ): Over this concentration range the particles separate into two distinct phases: a "crystalline" phase consisting of closely packed particles, and a "fluid" phase consisting of mobile loosely packed particles.
3. *Glassy systems* ( $0.58 < \phi < 0.64$ ): The movement of the particles is severely restricted because of the close proximity of their neighbors, and the particles can be considered to be trapped in "cages," where they can vibrate but cannot easily move past one another. This type of emulsion can exhibit both solid-like and fluid-like behaviors, acting like a solid at low shear stresses and a fluid once a critical yield stress has been exceeded and the particles can move past one another.
1. *"Crystalline" systems* ( $\phi > 0.64$ ): The particles are packed so closely together that they can no longer undergo either vibrational or translational motion. Random close packing occurs at  $\phi = 0.64$ , and more densely packed structures occur at higher particle concentrations where other types of crystalline structures are adopted, for example, face-centered cubic packing occurs at  $\phi = 0.74$ . This type of colloidal dispersion behaves like an elastic solid.

The critical volume fractions given above are generally different for real food emulsions because the particles are fluid and therefore deformable, and because various types of attractive and repulsive colloidal forces act between the droplets. In the following sections some of the theoretical models that have been developed to describe the rheological properties of emulsions in different concentration limits will be discussed.

#### 8.4.1 Dilute suspensions of rigid spherical particles

The viscosity of a liquid increases on the addition of rigid spherical particles because the particles disturb the normal flow of the fluid causing greater energy dissipation due to friction (Hunter, 1986; Mewis and Macosko, 1994). Einstein derived an analytical equation to relate the viscosity of a suspension of rigid spheres to its composition:

$$\eta = \eta_1(1 + 2.5\phi) \quad (8.20)$$

where  $\eta_1$  is the viscosity of the liquid surrounding the droplets and  $\phi$  is the dispersed phase volume fraction. This equation assumes that the liquid is Newtonian, the particles are rigid and spherical, that there are no particle–particle interactions, that there is no slip at the particle–fluid interface, and that particle motion effects are unimportant. The Einstein equation predicts that the viscosity of a dilute suspension of spherical particles increases linearly with particle volume fraction (Figure 8.16), and is independent of particle size and shear rate. The Einstein equation gives excellent agreement with experimental measurements for suspensions that conform to the above criteria, often up to particle concentrations of about 5% (i.e.,  $\phi < 0.05$ ).

It is convenient to define a parameter known as the *intrinsic viscosity* of a colloidal suspension  $[\eta]$  (Hiemenz and Rajagopalan, 1997):

$$[\eta] = \lim_{\phi \rightarrow 0} [(\eta - \eta_1)/\phi\eta_1] \quad (8.21)$$

Thus, for dilute emulsions:

$$\eta = \eta_1(1 + [\eta]\phi) \quad (8.22)$$

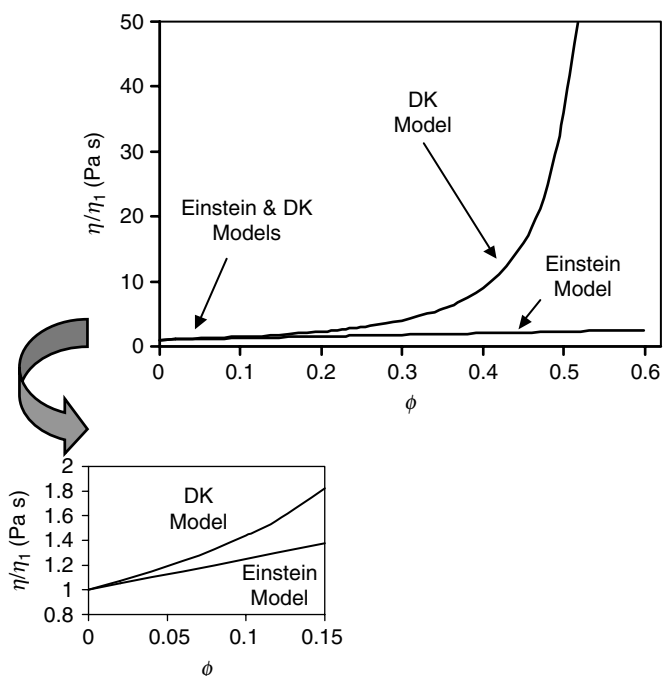


**Figure 8.16** The viscosity of colloidal dispersions increases with increasing disperse phase volume fraction. The Einstein model is appropriate for describing the rheological behavior at relatively low particle concentrations (see inset), but other models must be used at higher concentrations.

For rigid spherical particles, the intrinsic viscosity tends to 2.5 as the volume fraction tends to zero (Walstra, 2003a). For nonspherical particles or for particles that swell due to the adsorption of solvent the intrinsic viscosity is larger than 2.5 (Hiemenz and Rajagopalan, 1997), while for fluid particles it may be smaller (see below). Measurements of  $[\eta]$  can therefore provide valuable information about the shape or degree of solvation of macromolecules and colloidal particles in solution.

#### 8.4.2 Dilute suspensions of fluid spherical particles

Food emulsions usually contain fluid, rather than solid particles. In the presence of a flow field, the inner liquid (dispersed phase) within a droplet may circulate because it is dragged along by the outer liquid (continuous phase) that flows past the droplet (Sherman, 1968a; Dickinson and Stainsby, 1982). Consequently, the difference in velocity between the liquids on either side of the droplet interface is less than that for a solid particle, which means that less energy is lost due to friction and therefore the viscosity of the suspension is lower. The greater the viscosity of the fluid within a droplet, the more it acts like a rigid sphere, and therefore the higher the viscosity of the suspension.

The viscosity of a suspension of noninteracting spherical droplets is given by (Tadros, 1994; Larson, 1999)

$$\eta = \eta_1 \left( 1 + \left[ \frac{\eta_1 + 2.5\eta_2}{\eta_1 + \eta_2} \right] \phi \right) \quad (8.23)$$

where  $\eta_2$  is the viscosity of the liquid in the droplets. For droplets containing relatively high viscosity liquids ( $\eta_2/\eta_1 \gg 1$ ), the intrinsic viscosity tends to 2.5, and therefore this equation tends to that derived by Einstein (Equation 8.20). For droplets containing relatively low viscosity fluids ( $\eta_2/\eta_1 \ll 1$ ), such as air bubbles, the intrinsic viscosity tends to unity, and so the suspension viscosity is given by:  $\eta = \eta_1(1 + \phi)$ . One would therefore expect the viscosity of oil-in-water or water-in-oil emulsions to be somewhere between these two extremes, depending on the viscosities of the dispersed and continuous phases. In practice, the droplets in most food emulsions are coated by a layer of emulsifier molecules that form a viscoelastic membrane. This membrane retards the transmittance of the tangential stress from the continuous phase into the droplet, and therefore hinders the flow of the fluid within the droplet (Pal et al., 1992; Tadros, 1994; Walstra, 2003a). This may be due to the inherent viscoelasticity of the interfacial membrane (e.g., proteins or polysaccharides) (Dickinson, 2001) or due to the Gibbs–Marangoni effect (e.g., surfactants) (Walstra and Smulders, 1998). For this reason, most food emulsions contain droplets that act like rigid spheres, and so their viscosities can be described by the Einstein equation at sufficiently low droplet concentrations.

At sufficiently high flow rates, the hydrodynamic forces acting on the droplets can become so large that they overcome the interfacial forces holding the droplets together and cause the droplets to become deformed and eventually disrupted (Section 6.4). Nevertheless, the shear rates required to cause droplet disruption are usually so high that the flow profile may no longer be simple shear flow, and so it may not be possible to make accurate measurements of the shear viscosity under these conditions. Nevertheless, knowledge of the viscosity of fluids at high shear rates is important for engineers who design mixers and homogenizers.

### 8.4.3 Dilute suspensions of rigid nonspherical particles

Many of the particles in food emulsions may have nonspherical shapes, for example, flocculated droplets, partially crystalline droplets, fat crystals, ice crystals, or biopolymer molecules (Dickinson, 1992). Consequently, it is important to appreciate the effects of particle shape on suspension viscosity. The shape of many particles can be approximated as prolate spheroids (rod-like) or oblate spheroids (disk-like). A spheroid is characterized by its axis ratio  $r_p = a/b$ , where  $a$  is the major axis and  $b$  is the minor axis (Figure 8.17). For a sphere,  $a = b$ , for a prolate spheroid  $a > b$ , and for an oblate spheroid  $a < b$ . The flow profile of a fluid around a nonspherical particle causes a greater degree of energy dissipation than that around a spherical particle, which leads to an increase in viscosity (Hunter, 1986; Mewis and Macosko, 1994; Hiemenz and Rajagopalan, 1997). The magnitude of this

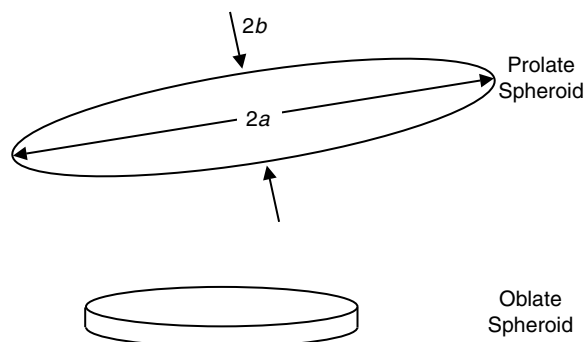


Figure 8.17 Examples of oblate and prolate spheroids.

effect depends on the rotation and orientation of the spheroid particle. For example, the viscosity of a rod-like particle is much lower when it is aligned parallel to the fluid flow, rather than perpendicular, because the parallel orientation offers less resistance to flow.

The orientation of a spheroid particle in a flow field is governed by a balance between the hydrodynamic forces that act on it and its rotational Brownian motion (Mewis and Macosko, 1994). The hydrodynamic forces favor the alignment of the particle along the direction of the flow field, because this reduces the energy dissipation. On the other hand, the alignment of the particles is opposed by their *rotational* Brownian motion, which favors the complete randomization of their orientations. The relative importance of the hydrodynamic and Brownian forces is expressed in terms of a dimensionless number, known as the Peclet number,  $Pe$ . For simple shear flow (Mewis and Macosko, 1994; Larson, 1999):

$$Pe = \frac{\dot{\gamma}}{D_R} \quad (8.24)$$

where  $\dot{\gamma}$  is the shear rate and  $D_R$  is the *rotational* Brownian diffusion coefficient, which depends on particle shape:

$$D_R = \frac{kT}{8\pi\eta r^3} \quad \text{for rigid spheres} \quad (8.25)$$

$$D_R = \frac{3kT}{32\pi\eta b^3} \quad \text{for circular disks} \quad (8.26)$$

$$D_R = \frac{3kT}{8\pi\eta r^3} (\ln 2r_p - 0.5) \quad \text{for long thin rods} \quad (8.27)$$

When the Peclet number is much less than unity ( $Pe \ll 1$ ), the rotational Brownian motion dominates, and the particles tend to rotate freely in the liquid. This type of behavior is observed when the particles are small, the shear rate is low, and/or the viscosity of the surrounding fluid is low. When the Peclet number is much greater than unity ( $Pe \gg 1$ ), the hydrodynamic forces dominate, and the particles become aligned with the flow field (Figure 8.18b). This type of behavior is observed when the particles are large, the shear rate is high, and/or the viscosity of the surrounding liquid is high.

The viscosity of a suspension of dilute nonspherical particles therefore depends on the shear rate. At low shear rates (i.e.,  $Pe \ll 1$ ), the viscosity has a constant high value. As the shear rate is increased the hydrodynamic forces become more important and so the particles become orientated with the flow field, which causes a reduction in the viscosity. At high shear rates (i.e.,  $Pe \gg 1$ ), the hydrodynamic forces dominate and the particle remains aligned with the shear field and therefore the viscosity has a constant low value (Figure 8.18b). Thus dilute suspensions of nonspherical particles exhibit shear-thinning behavior. The shear rate at which the viscosity starts to decrease depends on the size and shape of the particles, as well as the viscosity of the surrounding liquid. Mathematical formulae similar to Equation 8.3 have been developed to calculate the influence of shear rate on the viscosity of suspensions of nonspherical particles, but these usually have to be solved numerically. Nevertheless, explicit expressions are available for systems containing very small or very large particles (Hiemenz and Rajagopalan, 1997; Larson, 1999).



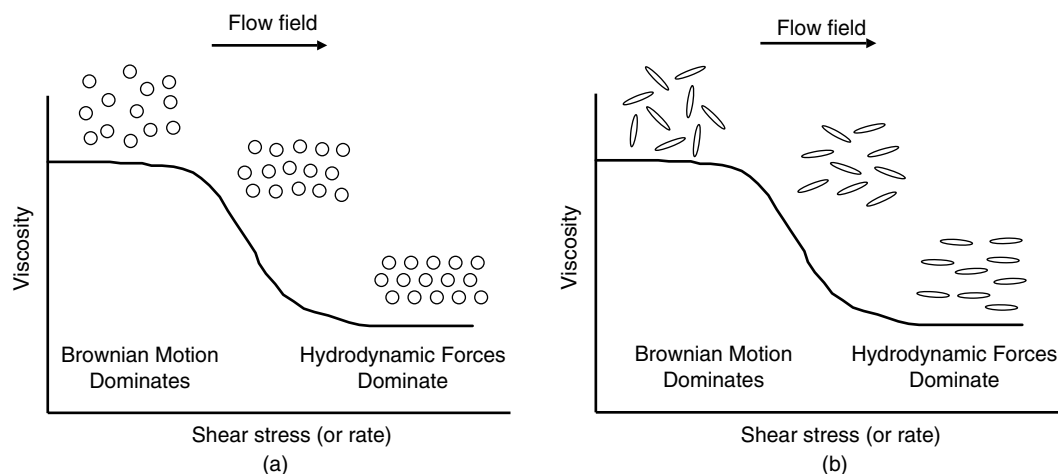


**Figure 8.18** Schematic representation of various factors that cause shear-thinning behavior in colloidal dispersions: (a) spatial ordering of particles; (b) directional alignment of nonspherical particles. The randomizing influence of Brownian motion dominates at low shear stresses, but the organizing influence of shear forces dominate at high shear stresses. At higher applied shear stresses other types of behavior can be observed, e.g., shear thickening.

#### 8.4.4 Dilute suspensions of flocculated particles

When the attractive forces between the droplets dominate the repulsive forces, and are sufficiently greater than the thermal energy of the system, then droplets can aggregate into either a primary minimum or a secondary minimum (Chapter 3). The rheological properties of many food emulsions are dominated by the fact that the droplets are flocculated, and so it is important to understand the factors that determine the rheological characteristics of these systems. It is often convenient to categorize systems as being either strongly flocculated ( $w_{\text{attractive}} > 20kT$ ) or weakly flocculated ( $1kT < w_{\text{attractive}} < 20kT$ ) depending on the strength of the attraction between the droplets within the flocs (Liu and Masliyah, 1996). The structures of flocs containing weakly flocculated droplets are particularly sensitive to the applied shear stress, whereas those containing strongly flocculated droplets are not.

Dilute suspensions of flocculated droplets consist of flocs that are so far apart that they do not interact with each other through colloidal or hydrodynamic forces. An emulsion containing flocculated droplets has a higher viscosity than an emulsion containing the same number of isolated droplets because the flocs trap some of the continuous phase within their structure and therefore have a higher *effective* volume fraction than the actual volume fraction of the individual droplets (Liu and Masliyah, 1996; Quemada and Berli, 2002). In addition, the flocs may rotate in solution because of their rotational Brownian motion, sweeping out an additional amount of the continuous phase, and thus increasing their *effective* volume fraction even further.

Suspensions of flocculated particles tend to exhibit pronounced shear-thinning behavior (Quemada and Berli, 2002) (Figure 8.19). At low shear rates, the hydrodynamic forces are not large enough to disrupt the bonds holding the particles together and so the flocs act like particles with a fixed size and shape, resulting in a constant viscosity. As the shear rate is increased, the hydrodynamic forces become large enough to cause flocs to become deformed and eventually disrupted. The deformation of the flocs results in them becoming elongated and aligned with the shear field, which results in a reduction in the viscosity. The disruption of the flocs decreases their effective volume fraction and therefore also

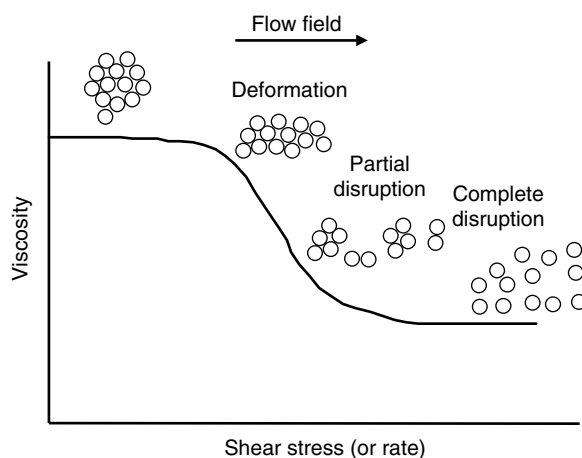


**Figure 8.19** An emulsion containing flocculated droplets exhibits shear-thinning behavior because the flocs are progressively aligned, deformed and disrupted in the shear field.

contributes to a decrease in the suspension viscosity. The viscosity reaches a constant value at high shear rates, either because all of the flocs are completely disrupted so that only individual droplets remain, or because the number of flocculated droplets remains constant since the rate of floc formation is equal to that of floc disruption (Campanella et al., 1995).

Depending on the nature of the interdroplet pair potential (Section 3.11), it is also possible to observe shear thickening due to particle flocculation under the influence of the shear field (de Vries, 1963). Some emulsions contain droplets that are not flocculated under quiescent conditions because there is a sufficiently high energy barrier to prevent the droplets from falling into a primary minimum; however, when a shear stress is applied to the emulsions the frequency of collisions and the impact force between the droplets increases, which can cause the droplets to gain sufficient energy to “jump” over the energy barrier and become flocculated, therefore leading to shear thickening.

Quite complicated behavior can therefore be observed in some emulsions (Pal et al., 1992; Liu and Masliyah, 1996; Larson, 1999). For example, an emulsion that contains droplets which are weakly flocculated in a secondary minimum exhibits shear thinning at fairly low shear rates, but shows shear thickening when the shear rate exceeds some critical level where the droplets have sufficient energy to “jump” over the energy barrier and fall into the primary minimum. The value of this critical shear rate increases as the height of the energy barrier increases. Knowledge of the interdroplet pair potential is therefore extremely useful for understanding and predicting the rheological behavior of flocculated food emulsions.

The size, shape, and structure of flocs largely determine the rheological behavior of dilute suspensions of flocculated particles (Dickinson and Stainsby, 1982; Liu and Masliyah, 1996; Quemada and Berli, 2002). Flocs formed by the aggregation of emulsion droplets may have structures that are fractal (Section 7.5.3). The effective volume fraction ( $\phi_{\text{eff}}$ ) of a fractal floc is related to the size of the floc and the fractal dimension by the following expression (Bremer, 1992; Walstra, 2003a):

$$\phi_{\text{eff}} = \frac{\phi}{\phi_i} = \phi \left( \frac{R}{r} \right)^{3-D} \quad (8.28)$$

where  $r$  is the droplet radius,  $R$  is the floc radius,  $\phi_i$  is the internal packing of the droplets within the floc, and  $D$  is between 1 (open packing) and 3 (close packing). The viscosity of a dilute emulsion containing fractal flocs can therefore be established by substituting this expression into the Einstein equation:

$$\eta = \eta_1(1 + [\eta]\phi_{\text{eff}}) = \eta_1(1 + [\eta]\phi(R/r)^{3-D}) \quad (8.29)$$

This equation gives a useful insight into the relationship between the rheology and micro-structure of flocculated emulsions. Flocs with fairly open structures (i.e., lower  $D$ ) have higher viscosities than those with compact structures because they have higher effective volume fractions (Equation 8.29). As mentioned earlier, the viscosity decreases with increasing shear rate partly because of disruption of the flocs, that is, a decrease in  $R$ . The shear stress at which the viscosity decreases depends on the magnitude of the forces holding the droplets together within a floc. The greater the strength of the forces, the larger the shear rate required to deform and disrupt the flocs. Thus, the dependence of the viscosity of an emulsion on shear stress can be used to provide valuable information about the strength of the bonds holding the droplets together (Sherman, 1970; Dickinson and Stainsby, 1982; Hunter, 1989; Quemada and Berli, 2002).

#### 8.4.5 Concentrated suspensions of nonflocculated particles in the absence of long-range colloidal interactions

When the concentration of particles in a suspension exceeds a few percent the particles begin to interact with each other through a combination of hydrodynamic and colloidal interactions, and this alters the viscosity of the system (Hunter, 1986; Mewis and Macosko, 1994; Tadros, 1994; Larson, 1999). In this section, we examine the viscosity of concentrated suspensions in the absence of long-range colloidal interactions between the particles, that is, it is assumed that the particles act like hard spheres. The more complicated situation of suspensions in which long-range colloidal interactions are important is treated in the following section. Hydrodynamic interactions are the result of the relative motion of neighboring particles, and are important in all types of nondilute suspensions (Larson, 1999).

At low concentrations, hydrodynamic interactions are mainly between pairs of particles, but as the concentration increases three or more particles may be involved (Pal, 2000a,b, 2001). As the concentration increases the measured viscosity becomes larger than that predicted by the Einstein equation because these additional hydrodynamic interactions lead to a greater degree of energy dissipation (Figure 8.16). The Einstein equation can be extended to account for the effects of these interactions by including additional volume fraction terms (Pal et al., 1992):

$$\eta = \eta_1(1 + a\phi + b\phi^2 + c\phi^3 + \dots) \quad (8.30)$$

The value of the constants,  $a$ ,  $b$ ,  $c$ , and so on, can either be determined experimentally or calculated theoretically. For a suspension of rigid spherical particles the value of  $a$  is 2.5, so that this equation tends to the Einstein equation at low volume fractions. A rigorous theoretical treatment of the interactions between pairs of droplets has established that  $b = 6.2$  for rigid spherical particles (Hunter, 1986). It is extremely difficult to theoretically calculate the value of higher order terms because of the complexity of the mathematical treatment of interactions between three or more particles (Pal, 2000a,b, 2001). In addition, each successive constant only extends the applicability of the equation to a slightly higher

volume fraction. For this reason, it has proved to be more convenient to adopt a semiempirical approach to the development of equations that describe the viscosity of concentrated suspensions. One of the most widely used equations was derived by Dougherty and Krieger and is applicable across the whole volume fraction range (Hunter, 1986; Mewis and Macosko, 1994):

$$\frac{\eta}{\eta_1} = \left(1 - \frac{\phi}{\phi_c}\right)^{-[\eta]\phi_c} \quad (8.31)$$

where  $\phi_c$  is a *packing parameter* that is related to the volume fraction at which the spheres become close packed, and  $[\eta]$  is the intrinsic viscosity. Typically, the value of  $\phi_c$  is between 0.6 and 0.7 for spheres that do not interact via long-range colloidal interactions, but it may be considerably lower for suspensions in which there are strong long-range attractive or repulsive interactions between the droplets (see following sections). The intrinsic viscosity is 2.5 for spherical particles, but may be much larger for nonspherical, swollen, or aggregated particles (Hiemenz and Rajagopalan, 1997). Predictions of the increase in the viscosity of a colloidal suspension with increasing particle volume fraction made using the Dougherty–Krieger equation are shown in Figure 8.16. An equation with a similar form as the Dougherty–Krieger equation is also widely used to describe the viscosity of concentrated colloidal dispersions, but the exponent  $-[\eta]\phi_c$  is replaced by  $-2$ . This value is fairly close to the value that would be obtained if typical values for  $[\eta]$  ( $= 2.5$ ) and  $\phi_c$  ( $= 0.7$ ) were inserted into the above expression, that is,  $-[\eta]\phi_c = -1.75$ . This and other models developed to describe the viscosity of concentrated emulsions have been reviewed elsewhere (Tadros, 1994, 1996; Quemada and Berli, 2002).

The viscosity of concentrated suspensions often exhibits shear-thinning behavior due to Brownian motion effects (Pal et al., 1992; Mewis and Macosko, 1994; Liu and Masliyah, 1996). We have already mentioned that shear thinning occurs when the shear stress is large enough to overcome the rotational Brownian motion of nonspherical particles (see above). Shear thinning can also occur because of the translational Brownian motion of particles (Figure 8.18a). At low shear stresses, the particles have a three-dimensional isotropic and random distribution because of their Brownian motion (Hunter, 1993; Larson, 1999). As the shear stress increases, and there is a balance of Brownian and hydrodynamic forces, the particles become more ordered along the flow lines to form “strings” or “layers” of particles that offer less resistance to the fluid flow and therefore cause a decrease in the suspension viscosity (Phung et al., 1996). These strings are believed to pack into a hexagonal pattern (Brady, 2001). At higher shear stresses, hydrodynamic forces dominate and the colloidal particles form clusters, which leads to pronounced shear-thickening behavior (Phung et al., 1996; Brady, 2001; Maranzano and Wagner, 2001; Shapley et al., 2003).

The decrease in viscosity with increasing shear stress in the intermediate region can be described by the following equation:

$$\eta = \eta_\infty + \frac{\eta_0 - \eta_\infty}{1 + (\tau/\tau_i)} \quad (8.32)$$

where  $\tau_i$  is a critical shear stress that is related to the size of the droplets:  $\tau_i = kT/\beta r^3$ , and  $\beta$  is a dimensionless constant with a value of about 0.431 (Hunter, 1989). The value of  $\tau_i$  is a characteristic of a particular system that describes the relative importance of the *translational* Brownian motion and hydrodynamic shear forces. When  $\tau \ll \tau_i$ , Brownian motion dominates and the particles have a random distribution, but when  $\tau \gg \tau_i$ , the

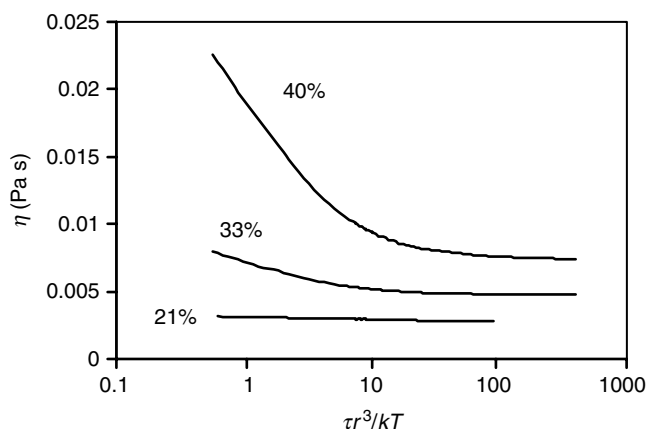


**Figure 8.20** Dependence of apparent viscosity on droplet concentration (vol%) and normalized shear rate ( $\tau r^3/kT$ ) for monodisperse *n*-hexadecane oil-in-water emulsions stabilized by SDS (Chanamai and McClements, 2000c).

shear forces dominate and the particles become organized into “strings” or “layers” along the lines of the shear field, which causes less energy dissipation. This equation indicates that the viscosity decreases from a constant value at low shear stresses ( $\eta_0$ ) to another constant value at high shear stresses ( $\eta_\infty$ ). The viscosity can decrease by as much as 30% from its low shear rate value, with the actual amount depending on the disperse phase volume fraction (Hunter, 1989). The shear rate at which the viscosity starts to decrease from its  $\eta_0$  value is highly dependent on the particle size. For large particles,  $\tau_i$  is often so low that it is not possible to observe any shear-thinning behavior, but for smaller particles shear-thinning behavior may be observed at the shear rates typically used in a rheological experiment. The influence of this effect on the shear-thinning behavior of nonfloculated emulsions is shown in Figure 8.20, which shows data derived from measurements on monodisperse oil-in-water emulsions with two different droplet diameters (Chanamai and McClements, 2000c). The emulsion viscosity is virtually independent of shear stress at low droplet concentrations (<20%), but shows distinct shear-thinning behavior at higher droplet concentrations.

The Dougherty–Krieger equation can still be used to describe the dependence of the suspension viscosity on disperse phase volume fraction, but the value of  $\phi_c$  used in the equation is shear rate dependent. This is because droplets can pack more efficiently at higher shear rates and therefore  $\phi_c$  increases with shear rate (Hunter, 1989; Quemada and Berli, 2002).

#### 8.4.6 Suspensions of nonfloculated particles with repulsive interactions

Most food emulsions contain droplets that have various types of colloidal interactions acting between them, for example, van der Waals, electrostatic, steric, hydrophobic, depletion, and so on (Chapter 3). The precise nature of these interactions has a dramatic influence on the rheology of particulate suspensions. For example, two emulsions with the same droplet concentration could have rheological properties ranging from a low viscosity Newtonian liquid to a highly viscoelastic material, depending on the nature of the colloidal interactions. In this section, we consider suspensions containing isolated spherical particles with repulsive interactions. In the following section, we will consider

the rheological properties of emulsions where attractive interactions dominate between droplets leading to flocculation.

The major types of droplet repulsions in most food emulsions are due to electrostatic and steric interactions (Chapter 3). These repulsive interactions prevent the droplets from coming into close contact when they collide with each other, and therefore increase the effective volume fraction of the droplets (Tadros, 1994; Mewis and Macosko, 1994; Larson, 1999):

$$\phi_{\text{eff}} = \phi \left( 1 + \frac{\delta}{r} \right)^3 \quad (8.33)$$

where  $\delta$  is equal to half the distance of closest separation between the two droplets.

For steric stabilization  $\delta$  is approximately equal to the thickness of the adsorbed layer (Tadros, 1994). For electrostatically stabilized particles  $\delta$  is related to the Debye screening length  $\kappa^{-1}$  (Larson, 1999), and can be described by the following equation at low shear stresses (Mewis and Macosko, 1994):

$$\delta = \kappa^{-1} \ln \left( \frac{\alpha}{\ln(\alpha/(\ln \alpha))} \right) \quad (8.34)$$

where  $\alpha = 4\pi\epsilon_0\epsilon_R\psi_0r^2\kappa \exp(2r\kappa)/kT$ ,  $\epsilon_0$  is the dielectric permittivity of a vacuum,  $\epsilon_R$  is the relative dielectric permittivity of the continuous phase,  $\psi_0$  is the electrical potential at the droplet surface,  $r$  is the radius,  $\kappa^{-1}$  is the Debye screening length,  $k$  is Boltzmann's constant, and  $T$  is the absolute temperature. For electrically charged oil droplets, the distance of closest contact therefore decreases as the surface charge decreases or as the ionic strength of the aqueous phase increases.

It is convenient to categorize droplets with repulsive interactions as being either "hard" particles or "soft" particles (Liu and Masliyah, 1996). A hard particle is incompressible and so its effective size is independent of shear rate or droplet concentration. On the other hand, a soft particle is compressible and so its effective size may be reduced at high shear rates or droplet concentrations. Sterically stabilized droplets with dense interfacial layers are usually considered to act like hard particles because the layer is relatively incompressible, whereas electrostatically stabilized droplets or sterically stabilized droplets with open interfacial layers are usually considered to act like soft particles because the layer is compressible.

Two approaches can be taken to mathematically describe the viscosity of concentrated colloidal dispersions containing particles with repulsive interactions using the Dougherty–Krieger equation. In the first approach, the actual volume fraction of the particles ( $\phi$ ) normally used in the Dougherty–Krieger equation is replaced by the effective volume fraction of the particles ( $\phi_{\text{eff}}$ ). For hard particles the value of  $\phi_c$  is taken to be the same as for noninteracting particles, but for soft particles the value of  $\phi_c$  is increased because the particles may be compressed at higher volume fractions and therefore pack more efficiently. As a consequence the viscosity of an emulsion containing soft particles is lower than one containing hard particles at the same *effective* volume fraction. In the second approach, the value of  $\phi_c$  normally used in the Dougherty–Krieger equation is treated as an adjustable parameter ( $\phi_c^*$ ) that is determined experimentally. In this case,  $\phi_c^*$  decreases with an increase in particle–particle repulsion because the particles become close packed at lower actual particle volume fractions.

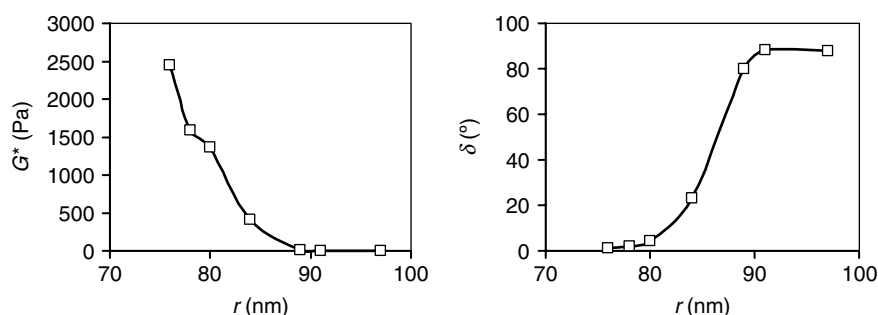


**Figure 8.21** Dependence of complex shear modulus ( $G^*$ ) and phase angle ( $\delta$ ) on droplet radius for  $n$ -octadecane oil-in-water emulsions stabilized by SDS (Weiss and McClements, 2000).

Above the maximum packing volume fraction, the colloidal dispersions behave as viscoelastic or plastic materials that can be characterized in terms of their dynamic shear modulus or their elastic modulus, yield stress, and plastic viscosity (Weiss and McClements, 2000). The modulus of these particle gels normally increases with decreasing droplet size, increasing droplet concentration, and increasing strength and range of the repulsive interactions. A variety of theories have been developed to relate the rheological characteristics of this type of particle gel to their colloidal characteristics (Buscall et al., 1982; Goodwin and Ottewill, 1991; Quemeda and Berli, 2002).

The influence of repulsive interactions on the rheology of emulsions depends on the magnitude of  $\delta$  relative to the size of the particles. For relatively large particles (i.e.,  $\delta \ll r$ ), this effect is negligible, but for small droplets or droplets with thick layers around them (i.e.,  $\delta \approx r$ ), this effect can significantly increase the viscosity of a suspension (Tadros, 1994). This effect is demonstrated in Figure 8.21, which shows the dependence of the apparent shear modulus and phase angle of oil-in-water emulsions containing electrically charged droplets on droplet size (Weiss and McClements, 2000). When the droplets are small the electrical double layers overlap with each other and the emulsion has solid-like characteristics (high  $G^*$  and low  $\delta$ ), but when the droplets are relatively large the electrical double layers do not overlap substantially and the emulsion has liquid-like characteristics ( $G^* \approx 0$  and  $\delta \approx 90^\circ$ ).

The rheological properties of electrostatically stabilized systems containing small emulsion droplets are particularly sensitive to pH and salt concentration. The viscosity normally decreases initially with increasing salt concentration because screening of the charges decreases  $\delta$ . Above a certain salt concentration, the interactions between the droplets would become attractive, rather than repulsive, and therefore flocculation will occur causing an increase in emulsion viscosity with salt. The rheological properties of electrostatically stabilized emulsions are therefore particularly sensitive to the pH, salt concentration, and type of ions present.

#### 8.4.7 Concentrated suspensions with attractive interactions: flocculated systems

In concentrated flocculated emulsions, the flocs are close enough to interact with each other, through hydrodynamic interactions, colloidal interactions, or entanglement. To a first approximation, the viscosity of flocculated emulsions can be described using the same approach as used for nonflocculated emulsions by assuming that the particles are flocs, rather than individual droplets. The Dougherty–Krieger equation (or equivalent equations) can then be modified by using the *effective* volume fraction of the flocs

( $\phi_{\text{eff}} = \phi/\phi_i$ ), rather than the actual volume fraction of the individual droplets in the equations:

$$\frac{\eta}{\eta_1} = \left(1 - \frac{\phi_{\text{eff}}}{\phi_c}\right)^{-[\eta]\phi_c} = \left(1 - \frac{\phi}{\phi_c \phi_i}\right)^{-[\eta]\phi_c} = \left(1 - \frac{\phi}{\phi_{c,\text{eff}}}\right)^{-[\eta]\phi_c} \quad (8.35)$$

where  $\phi_c$  is the packing parameter for a suspension of spherical particles ( $\approx 0.6$ – $0.7$ ),  $\phi_i$  is the volume fraction of droplets within the flocs ( $\approx 0.2$ – $1$ ),  $\phi_{c,\text{eff}} (= \phi_c \phi_i)$  is the *effective* packing parameter for a suspension of flocculated droplets, and  $[\eta]$  is the intrinsic viscosity ( $\approx 2.5$ ). The following, slightly simpler, alternative expressions have also been used to describe the apparent viscosity of concentrated flocculated emulsions (Quemada and Berli, 2002):

$$\frac{\eta}{\eta_1} = \left(1 - \frac{\phi_{\text{eff}}}{\phi_c}\right)^{-2} = \left(1 - \frac{\phi}{\phi_c \phi_i}\right)^{-2} = \left(1 - \frac{\phi}{\phi_{c,\text{eff}}}\right)^{-2} \quad (8.36)$$

The above equations demonstrate that at a fixed actual droplet volume fraction, the emulsion viscosity increases as the internal packing of the droplets within the flocs decreases (lower  $\phi_i$ ) because the effective volume fraction of the particles then increases (Figure 8.22). In practice the value of  $\phi_i$  depends on the magnitude of the applied shear stress, since shear forces can breakdown the flocs (Quemada and Berli, 2002). The dependence of the apparent shear viscosity of weakly flocculated emulsions on shear stress has been related to the strength and range of the colloidal interactions between the droplets (Quemada and Berli, 2002):

$$\eta(\tau) = \eta_\infty \left( \frac{1 + \tau/\tau_i}{\Re + \tau/\tau_i} \right)^2 \quad (8.37)$$

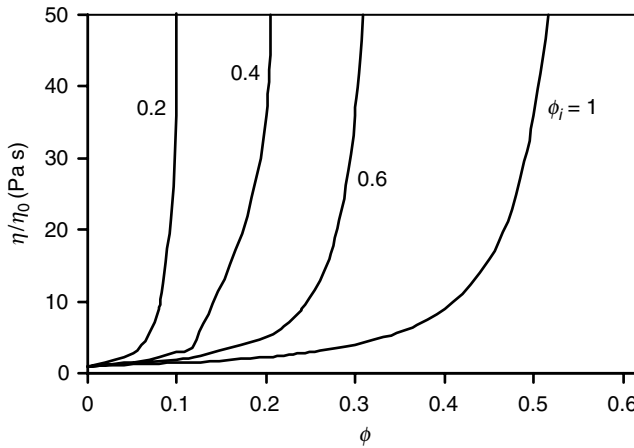


**Figure 8.22** Calculations of the influence of internal packing of the droplets within flocs ( $\phi_i$ ) on the emulsion viscosity vs. disperse phase volume fraction dependence. The more open the packing, the lower the droplet concentration where a steep increase in viscosity is observed.



where the rheological index  $\mathfrak{R}$  is given by the following expression for emulsions in which the droplet concentration is either below or above the effective packing parameter:

$$\mathfrak{R} = \left( \frac{1 - \phi/\phi_c\phi_{i,0}}{1 - \phi/\phi_c\phi_{i,\infty}} \right) = \begin{cases} \sqrt{\eta_\infty/\eta_0} ; \phi < \phi_c\phi_{i,0} \\ -\tau_y/\tau_i ; \phi \geq \phi_c\phi_{i,0} \end{cases} \quad (8.38)$$

Here  $\phi_{i,0}$  and  $\phi_{i,\infty}$  are the volume fractions of droplets within the flocs at low and high shear stress,  $\tau_i$  is the critical shear stress, and  $\tau_y$  is the yield stress. The values of the viscosity at low and high shear stress extremes,  $\eta_0$  and  $\eta_\infty$ , can be calculated by inserting the values of  $\phi_{i,0}$  and  $\phi_{i,\infty}$  into Equation 8.35 or 8.36.

At droplet concentrations below the effective packing fraction ( $\phi < \phi_{c,eff} (= \phi_c\phi_{i,0})$ ) the emulsions exhibit fluid-like characteristics, but above the effective packing fraction they only flow once the applied stress exceeds the yield stress. In the absence of droplet flocculation, the critical shear stress is given by  $\tau_i = kT/r^3$ . In the presence of droplet flocculation, the critical shear stress depends on the magnitude of the attractive or repulsive interactions between the droplets (Quemada and Berli, 2002). For example, in the presence of a weakly attractive interaction between the droplets the critical shear stress is given by

$$\tau_i = \frac{kT}{r^3} \left( 1 + \frac{U_{\min}}{kT} \right) \quad (8.39)$$

where  $U_{\min}$  is the strength of the attractive interaction between the droplets, that is, the magnitude of the interaction potential at the droplet separation where the interaction potential is a minimum:  $|w(h_{\min})|$ . Theoretical predictions of the influence of the attractive force between emulsion droplets on their shear-thinning behavior are shown in Figures 8.23 and 8.24. When the droplet concentration is below the effective packing fraction the apparent viscosity decreases from a constant value at low shear stresses to another constant value at high shear stresses. The critical shear stress where extensive shear thinning starts increases as the strength of the attraction between the droplets increases (Figure 8.23). When the droplet concentration is above the effective packing fraction, no flow is observed at applied shear

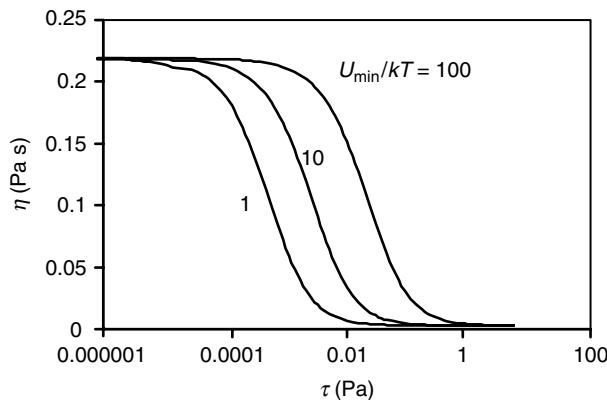


**Figure 8.23** Calculations of the influence of the attractive interaction strength ( $U_{\min}$ ) on the shear stress dependence of the apparent viscosity of oil-in-water emulsions below the effective packing parameter. It was assumed that:  $\phi = 0.2$ ,  $\phi_{c,0} = 0.225$ ,  $\phi_{c,\infty} = 0.585$ ,  $r = 1 \mu\text{m}$ ,  $\eta_0 = 1 \text{ mPa s}$ .

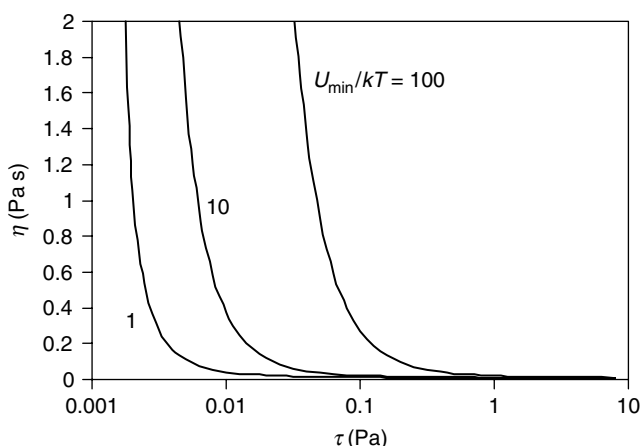


**Figure 8.24** Calculations of the influence of the attractive interaction strength ( $U_{\min}$ ) on the shear stress dependence of the apparent viscosity of oil-in-water emulsions above the effective packing parameter. It was assumed that:  $\phi = 0.4$ ,  $\phi_{c,\infty} = 0.585$ ,  $r = 1 \mu\text{m}$ ,  $\eta_0 = 1 \text{ mPa s}$ ,  $\tau_y = 0.001 \text{ Pa}$ .

stresses below the yield stress but extensive shear thinning is observed once the yield stress is exceeded, with the viscosity depending on the strength of the attraction between the droplets (Figure 8.24). The above equations can be used to estimate the strength of the attraction between droplets in weakly flocculated emulsions from measurements of their apparent viscosity versus shear stress (Quemada and Berli, 2002).

When the droplet concentration exceeds the effective packing fraction a three-dimensional network of aggregated droplets is formed with solid-like characteristics (Sherman, 1970; Goodwin and Ottewill, 1991; Pal, 1996). The more open the structure of the droplets within the flocs, the lower the value of the actual droplet volume fraction where the network is formed. Network formation causes a suspension of particles to exhibit plastic and/or viscoelastic characteristics (Pal, 1996; Quemada and Berli, 2002). The network of aggregated droplets acts like a solid at low shear stresses because the applied forces are not sufficient to overcome the forces holding the droplets together. Once a critical shear stress is exceeded, the bonds between the droplets are disrupted and so the droplets can flow past one another. If some of the bonds are capable of reforming during the shearing process, then the emulsion will exhibit viscoelastic behavior (Sherman, 1968). At higher shear stresses, the rate of bond disruption greatly exceeds that of bond formation and the emulsion acts like a liquid. Consequently, a suspension containing a three-dimensional network of aggregated particles often has a yield stress, below which it acts like an elastic solid and above which it acts like a liquid. Above the yield stress, the suspension often exhibits strong shear-thinning behavior as more and more flocs are deformed and disrupted. The magnitude of the yield stress depends on the strength of the attractive forces holding the particles together: the greater the attractive forces, the greater the yield stress (Pal, 1996). The rheology of the system is also sensitive to the structural organization of the droplets, e.g., whether they are loosely or densely packed, and the number of bonds per droplet (Bremer, 1992; Bremer et al., 1993; Pal, 1996; Narine and Marangoni, 1999; Marangoni and Narine, 1999; Larson, 1999; Marangoni, 2000).

A variety of theoretical and computational models have been developed to describe the rheological characteristics of particle networks (Papenhuijzen, 1972; Shi et al., 1990; Bremer et al., 1993; van Vliet, 1995; Lodge and Heyes, 1999; Larson, 1999; Dickinson, 2000). These models attempt to relate the bulk rheological properties of particle networks (elastic

modulus, shear modulus, yield stress, viscosity) to the structural organization of the particles within the network and the strength of the attractive forces between the particles. The main differences between the models are the simplifying assumptions made about the structural organization of the particles and the nature of the colloidal interactions acting between the particles.

#### 8.4.8 *Emulsions with semisolid continuous phases*

A number of food emulsions consist of droplets dispersed in a continuous phase that is gelled, e.g., a fat crystalline or biopolymer network (Sherman, 1970; Dickinson and Stainsby, 1982; Dickinson, 1992; Moran, 1994; Walstra, 2003a). Butter and margarine consist of water droplets suspended in a liquid oil phase that contains a three-dimensional network of aggregated fat crystals. Many meat products, deserts, and sauces consist of oil droplets suspended in an aqueous phase of aggregated biopolymer molecules. The rheology of these systems is usually dominated by the properties of the continuous phase, and therefore their properties can be described using theories developed for networks of aggregated fat crystals or biopolymer molecules (Clark, 1987; Walstra, 2003a). Nevertheless, in some systems the presence of the emulsion droplets does play a significant role in determining the overall rheological behavior (see below).

It is important that spreadable products, such as butter, margarine, and low-fat spreads, retain their shape when they are removed from the refrigerator, but that they spread easily when a knife is applied (Sherman, 1970; Moran, 1994). These products must therefore be designed so that they exhibit plastic properties, that is, they have a yield stress below which they are elastic and above which they are viscous (Walstra, 2003a). The plastic behavior of this type of product is usually attributed to the presence of a three-dimensional network of aggregated fat crystals. Low shear stresses are not sufficiently large to disrupt the bonds which hold the aggregated crystals together, and so the product exhibits solid-like behavior. Above the yield stress, the applied shear stress is sufficiently large to cause the bonds to be disrupted, so that the fat crystals flow over each other and the product exhibits viscous-like behavior. After the stress is removed the bonds between the fat crystals reform over time and therefore the product regains its elastic behavior. The creation of a product with the desired rheological characteristics involves careful selection and blending of various food oils, as well as control of the cooling and shearing conditions used during the manufacture of the product (Hartel, 2001; Walstra, 2003a). To the author's knowledge, little systematic research has been carried out to establish the influence of the characteristics of the water droplets on the rheological properties of these products, e.g., particle size distribution, emulsifier type, and disperse phase volume fraction.

Research has been carried out to determine the influence of oil droplets on the rheology of filled gels (Yost and Kinsella, 1993; McClements et al., 1993e; Dickinson and Hong, 1995b; Dickinson and Yamamoto, 1996). For example, filled gels have been created by heating oil-in-water emulsions that contain a significant amount of whey protein in the continuous phase above a temperature where the proteins unfold and form a three-dimensional network of aggregated molecules. The oil droplets can either act as *structure promoters* or *structure breakers* depending on the nature of their interaction with the gel network. When the droplets are stabilized by dairy proteins, the attractive interactions between the adsorbed proteins and those in the network reinforce the network and increase the gel strength. Conversely, when the droplets are stabilized by small molecule surfactants (that do not interact strongly with the protein network) the presence of the droplets tends to weaken the network and decrease the gel strength. Quite complex rheological behavior can be observed in emulsions containing mixtures of proteins and small molecule surfactants (Dickinson and Hong, 1995b; Dickinson and Yamamoto, 1996). The shear modulus

of filled gels containing protein-stabilized oil droplets increases dramatically when a small amount of surfactant is added to the system, but decreases at higher surfactant values. The incorporation of surfactants into filled gels may therefore prove to be an effective means of controlling their rheological properties.

The influence of the emulsion droplets on the rheology of filled gels also depends on their size relative to the pore size of the gel network (McClements et al., 1993e; Yost and Kinsella, 1993). If the droplets are larger than the pore size, they tend to disrupt the network and decrease the gel strength, but if they are smaller than the pore size they are easily accommodated into the network without disrupting it.

## 8.5 Computer simulation of emulsion rheology

Recent advances in the computer simulation of the rheological properties of emulsions and other colloidal dispersions have provided scientists with a powerful new tool that complements laboratory experiments and analytical theories (Boek et al., 1997; Bergholtz, 2001; Brady, 2001). The most commonly used simulation method for describing the properties of emulsions and suspensions is Stokesian Dynamics (Phung et al., 1996). In this approach it is assumed that the colloidal particles are suspended in a continuum, which is characterized by a certain density and viscosity. The increase in viscosity of the system due to the presence of the colloidal particles is then calculated. The motions of the particles in the suspension are calculated from knowledge of the forces acting on them. These forces include (i) Brownian motion due to thermal fluctuations of the solvent, (ii) colloidal interactions (e.g., van der Waals, electrostatic, steric, depletion, and so on), and (iii) hydrodynamic interactions (i.e., short-range lubrication forces and long-range many body interactions). Computer simulation models can be used to predict the behavior of solid particles, fluid particles, nonspherical particles, and polydisperse systems (Brady, 2001). For systems with well-defined colloidal interactions (e.g., approximate hard-sphere systems), predictions of the rheology of colloidal dispersions made using Stokesian Dynamics are in excellent agreement with experimental measurements (Brady, 2001). Computer simulations can be used to systematically probe the relationship between colloidal properties (such as droplet size, concentration, and interactions) and bulk rheological properties (such as apparent viscosity and shear modulus).

Computer simulations carried out on colloidal dispersions containing monodisperse hard spheres have shown that the microstructure and rheology of the system change with increasing applied shear stress in simple shear flow conditions (Phung et al., 1996; Foss and Brady, 2000):

- *Low Peclet numbers.*\* At low  $Pe$  numbers, Brownian motion dominates and the colloidal particles are randomly distributed within the colloidal dispersion. Hence, the viscosity of the colloidal dispersion has a relatively high plateau value.
- *Intermediate Peclet numbers.* At intermediate  $Pe$  numbers, the organization of the particles in the colloidal dispersion progressively changes from a more random structure to a more organized structure because the shear forces start becoming of the same magnitude and then dominate the Brownian motion forces. Hence, the colloidal dispersion exhibits shear-thinning behavior in this regime because there is less resistance to fluid flow when the colloidal particles become more organized (see below).

\* As mentioned earlier, the Peclet number is a measure of the magnitude of the applied shear forces relative to the magnitude of the Brownian motion forces.

- *High Peclet numbers.* At high  $Pe$  numbers, shear forces completely dominate Brownian motion forces and the colloidal particles become organized into “strings” along the flow direction and these strings align themselves into hexagonal-like structures. The formation of these strings leads to an appreciable reduction in the resistance of the system to flow, which results in a pronounced reduction in the viscosity of the colloidal dispersion.
- *Very high Peclet numbers.* At sufficiently high  $Pe$  numbers, the colloidal particles become paired together after a collision due to short-range hydrodynamic lubrication forces. These particles then rotate together as a pair, which prevents the formation of particle strings and an organized layered structure. As a result, the resistance of the system to flow increases, which leads to pronounced shear-thickening behavior at high shear stresses.

These computer simulations agree with experimental measurements of the rheological properties of colloidal dispersions that approximate hard-sphere systems (Brady, 2001). Simulations made on colloidal dispersions containing rigid hard-sphere monodisperse particles are not a particularly accurate model for food emulsions that contain fluid soft-sphere polydisperse droplets. Nevertheless, they provide extremely valuable insights into the relationship between particle characteristics, emulsion microstructure, and bulk rheology. In addition, as mathematical theories, programming procedures, and computing power improve it is becoming possible to incorporate some of these factors into the simulations, e.g., fluid droplets, nonspherical droplets, polydispersity, and colloidal interactions (Brady, 2001). The continued usage of these simulation techniques in the food industry should facilitate the design of laboratory experiments and the interpretation of experimental data.

## 8.6 Major factors influencing emulsion rheology

In this section, the major factors influencing the rheological properties of food emulsions are briefly discussed.

### 8.6.1 Disperse phase volume fraction

The viscosity of a nonfloculated emulsion increases with disperse phase volume fraction (Figure 8.16) because the presence of the droplets increases the energy dissipation associated with fluid flow (Mewis and Macosko, 1994; Larson, 1999). At low droplet concentrations the viscosity increases linearly with  $\phi$  (Equation 8.20), but at higher droplet concentrations the viscosity increase is steeper (Equations 8.30 and 8.31). Above a critical disperse phase volume fraction,  $\phi_c$ , the droplets are packed so closely together that they cannot easily flow past each other. Above this droplet concentration the emulsion viscosity increases steeply and the emulsion gains gel-like properties, e.g., elasticity, viscoelasticity, plasticity. The precise nature of the dependence of the viscosity on volume fraction is mainly determined by the nature of the colloidal interactions between the droplets. For example, when there is a relatively strong repulsion or attraction between the droplets, their *effective* volume fraction may be much greater than their *actual* volume fraction, which leads to a large increase in emulsion viscosity (Section 8.4). Food products whose rheological characteristics are not dominated by the effects of strong colloidal interactions, thickening or gelling agents can be used to illustrate the influence of droplet volume fraction on emulsion viscosity. Full fat milk ( $\phi \sim 0.04$ ) is a fairly low viscosity fluid, heavy cream ( $\phi \sim 0.36$ ) is a fairly high viscosity fluid, and mayonnaise ( $\phi \sim 0.80$ ) is a viscoelastic gel. In principle, it is therefore possible for food manufacturers to control the rheology of food emulsions by varying their disperse

phase volume fraction. In practice, this is rarely feasible because of constraints associated with ingredient cost, nutritional attributes, flavor, or shelf life. Consequently, it is more common for food manufacturers to modify emulsion rheology using alternative methods, e.g., by adding thickening or gelling agents (see below).

### 8.6.2 Rheology of component phases

Theoretically, the viscosity of a fluid emulsion is directly proportional to the viscosity of the continuous phase (Equations 8.20, 8.30, and 8.31). Consequently, any alteration in the rheology of the continuous phase will have a corresponding influence on the rheology of the whole emulsion. For food emulsions with droplet concentrations below the maximum packing fraction ( $\phi_c$ ), the most effective means of modifying their rheology is to add thickening or gelling agents. It is for this reason that polysaccharides and proteins are often incorporated into the aqueous phase of food emulsions to modify their texture or improve their creaming stability, e.g., beverages, salad dressings, sauces, dips, and desserts (Pettit et al., 1995; Pal, 1996; Ford et al., 2004). The functional attributes of various thickening and gelling agents were discussed in Section 4.5. Similarly, the rheology of water-in-oil emulsions, such as margarine or butter, is largely determined by the rheological characteristics of the fat crystal network present in the oil phase (Moran, 1994; Buchheim and Dejmek, 1997). Hence, the overall rheology of these products is usually manipulated by altering the structure, concentration, or interactions of the fat crystals, e.g., by altering the temperature, history, or composition of the fat phase.

The presence of emulsion droplets can still have a significant impact on the overall texture of emulsions whose rheology is dominated by that of the continuous phase. For example, the rheology of many salad dressing products is largely determined by the presence of biopolymers in the aqueous phase (Dickinson, 1992, 1998). These biopolymers act as thickening agents that give the salad dressings high viscosities, shear-thinning behavior, and stability against droplet creaming. Nevertheless, many biopolymers promote the formation of a three-dimensional network of aggregated droplets due to their ability to promote depletion flocculation (Dickinson, 1998; McClements, 1999). This droplet network has been shown to significantly modify the overall rheological characteristics of model salad dressing products (Manoj et al., 1998a,b; Dickinson, 1998). For example, the formation of a network of aggregated droplets tends to increase the viscosity and the extent of shear thinning in oil-in-water emulsions containing nonadsorbed biopolymers in the aqueous phase (Dickinson, 1998). Biopolymers that promote droplet aggregation through a bridging mechanism may also have a pronounced influence on emulsion rheology (Dickinson, 1998, 2003).

Another example of the influence of droplets on the rheology of emulsions whose properties are dominated by the rheology of the continuous phase is provided by the filled whey protein gels mentioned earlier (McClements et al., 1993e; Dickinson and Hong, 1995; Dickinson and Yamamoto, 1996). Oil droplets can act as either structure *promoters* or structure *breakers* depending on whether their interfacial membranes are incorporated into the gel network or not.

The rheology of the dispersed phase has a minor influence on the rheology of most fluid food emulsions because the droplets are covered by a viscoelastic membrane that makes them behave similarly to rigid spheres (Tadros, 1994; Walstra, 1996a, 2003a); however, in concentrated oil-in-water emulsions, such as mayonnaise, the rheology of the droplets can play an important role. In these systems, the droplets may deform on the application of a stress and therefore an emulsion containing fluid droplets would be expected to have a lower resistance to deformation than a suspension containing rigid particles.

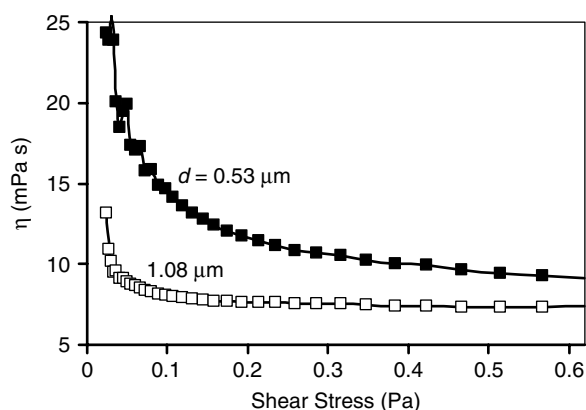


**Figure 8.25** Shear-thinning behavior of monodisperse 40 vol% *n*-hexadecane oil-in-water emulsions with different droplet diameters.

### 8.6.3 Droplet size

The influence of the droplet size and the droplet size distribution on the rheology of an emulsion depends on the disperse phase volume fraction and the nature of the colloidal interactions. In the absence of appreciable colloidal interactions, droplet size alters emulsion rheology because of its influence on the relative importance of Brownian motion and shear stress effects (Mewis and Macosko, 1994). This effect is only appreciable in emulsions with relatively high droplet concentrations, that is,  $\phi > 0.45$  (Pal et al., 1992; Pal, 1996; Dickinson, 1998). Nevertheless, if there are appreciable long-range repulsive interactions between droplets this type of shear-thinning effect can occur at lower droplet concentrations (Chanamai and McClements, 2000c). For example, Figure 8.25 shows that there is strong shear-thinning behavior in monodisperse oil-in-water emulsions containing 40 vol% electrically charged droplets, and that the apparent viscosity is appreciably larger for droplets with diameters of 0.53  $\mu\text{m}$  than for droplets with diameters of 1.08  $\mu\text{m}$  at the same shear stress. The influence of droplet size on emulsion viscosity becomes less important at higher shear stresses because shear forces then dominate Brownian motion effects (Figure 8.18a).

The mean droplet size and degree of polydispersity has a particularly significant influence on the rheology of highly concentrated emulsions, close to or above the effective packing parameter (Liu and Masliyah, 1996; Pal, 1996). In emulsions containing nonfloculated droplets the maximum packing parameter ( $\phi_c$ ) depends on the polydispersity. Droplets are able to pack more efficiently when they are polydisperse and therefore the viscosity of a concentrated polydisperse emulsion is less than that of a monodisperse emulsion with the same droplet volume fraction. It is partly because of this fact that it is possible to make mayonnaise products that have droplet concentrations above the theoretical maximum packing parameter of monodisperse droplets. In addition, the relatively large droplets in mayonnaise can become deformed, which also facilitates high packing.

### 8.6.4 Colloidal interactions

The nature of the colloidal interactions between the droplets in an emulsion is one of the most important factors determining its rheological behavior. When the interactions are long-range and repulsive, the effective volume fraction of the dispersed phase may be significantly greater than its actual volume fraction ( $\phi_{\text{eff}} = \phi(1 + \delta/r)^3$ ), and so the emulsion viscosity increases (Section 8.4.6). When the interactions between the droplets are sufficiently attractive,

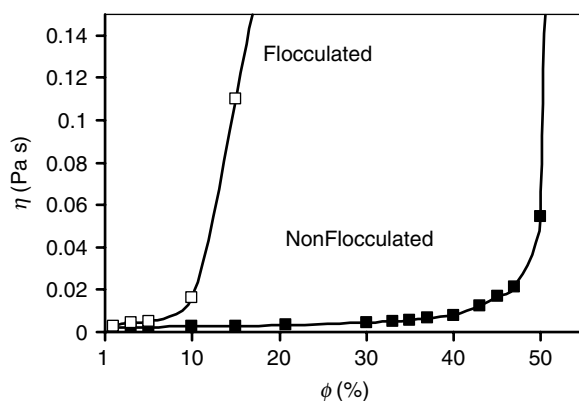


**Figure 8.26** Dependence of the apparent viscosity on droplet volume fraction for flocculated (SDS = 80 mM) and nonflocculated (SDS = 7 mM) monodisperse *n*-hexadecane oil-in-water emulsions (shear stress = 0.1 Pa). The emulsions contained 0.86  $\mu\text{m}$  diameter droplets. Droplet flocculation was induced by adding excess SDS micelles into the continuous phase.

the effective volume fraction of the dispersed phase is increased due to droplet flocculation, which also results in an increase in emulsion viscosity (Section 8.4.7). The rheological properties of an emulsion therefore depend on the relative magnitude and range of the attractive (mainly van der Waals, hydrophobic, and depletion) and repulsive (mainly electrostatic, steric, and thermal fluctuation) interactions between the droplets (Chapter 3). Manipulation of the colloidal interactions between droplets can therefore be used to effectively control the rheological properties of food emulsions. The viscosity of oil-in-water emulsions can be increased appreciably by promoting droplet flocculation (Dickinson, 1998). Droplet flocculation can be achieved in a variety of different ways depending on the nature of the system involved. For example, droplet flocculation can be induced by adding biopolymers to increase the depletion attraction (Dickinson and Golding, 1997a,b; Manoj et al., 1998a,b; Tuinier and de Kruif, 1999), by adding biopolymers to cause bridging flocculation (Dickinson, 1998), by altering the pH or ionic strength to reduce electrostatic repulsion (Hunt and Dalgleish, 1994; Demetriades et al., 1997), and by heating globular protein-stabilized emulsions to increase the hydrophobic attraction and disulfide interactions (Demetriades and McClements, 1998; Kim et al., 2002b). The influence of droplet flocculation on the viscosity of monodisperse oil-in-water emulsions is clearly shown in Figure 8.26. The droplets in the flocculated emulsion were made to flocculate by adding surfactant micelles (SDS) to the continuous phase to promote depletion flocculation. The emulsion containing flocculated droplets has a higher viscosity than the emulsion containing nonflocculated droplets at low droplet concentrations, and exhibited stronger shear-thinning behavior. In addition, the droplet volume fraction at which the emulsion viscosity increased sharply was considerably reduced when the emulsion droplets were flocculated (Figure 8.26). The reasons for the change in emulsion rheology caused by droplet flocculation were discussed in Section 8.4.7.

### 8.6.5 Droplet charge

Many food emulsions contain droplets that have an electrical charge due to the adsorption of ionizable surface-active components, such as ionic surfactants, proteins, or polysaccharides (Chapters 3 and 5). The charge on a droplet can influence the rheological properties of an emulsion in a number of ways. First, droplet charge influences emulsion rheology due to the *primary electroviscous effect* (Pal, 1996; Larson, 1999; Rubio-Hernandez et al., 2004). As a



charged droplet moves through a fluid, the cloud of counterions surrounding it becomes distorted. This causes an attraction between the charge on the droplet and that associated with the cloud of counterions that lags slightly behind it. This attraction opposes the movement of the droplets and therefore increases the emulsion viscosity because more energy is needed to cause the droplets to move at the same rate as uncharged droplets. Mathematical analysis of this phenomenon has shown that the *primary electroviscous effect* is fairly small in most colloidal dispersions (Hiemenz and Rajagopalan, 1997), particularly at the relatively high salt levels present in most food emulsions. Second, the droplet charge influences the emulsion rheology through the *secondary electroviscous effect*, which accounts for the fact that electrically charged emulsion droplets cannot approach as closely together as can uncharged droplets due to electrostatic repulsion (Hiemenz and Rajagopalan, 1997). Consequently, the effective diameter of the droplets is increased, which leads to an increase in emulsion viscosity and a decrease in the droplet volume fraction where the viscosity increases steeply. Secondary electroviscous effects can have a pronounced impact on the rheology of emulsions when the Debye screening length is of the same order of magnitude as the droplet radius, that is,  $\kappa^{-1} \sim r$ . Dickinson (1998) has shown that the viscosity of oil-in-water emulsions stabilized by an anionic surfactant (SDS) are considerably larger than those stabilized by a nonionic surfactant (Tween 20) at high droplet volume fractions because of this effect. The secondary electroviscous effect has a dramatic effect on the rheological properties of emulsions near the maximum packing volume fraction. Figure 8.21 shows the droplet size dependence of the dynamic shear rheology ( $G^*$  and  $\delta$ ) of 25 wt% octadecane oil-in-water emulsions containing negatively charged droplets (Weiss and McClements, 2000). When the droplet radius was below 80 nm the emulsions had solid-like characteristics ( $\delta \sim 0^\circ$ ) and a yield stress, but when the radius was above 90 nm the emulsions had fluid-like characteristics ( $\delta \sim 90^\circ$ ). This dramatic change in emulsion rheology occurred because the effective volume fraction of the droplets increased as the droplet radius decreased, and so the maximum packing volume fraction was exceeded below a particular droplet radius. Third, the droplet charge may influence emulsion rheology through the *tertiary electroviscous effect* (Hiemenz and Rajagopalan, 1997), which accounts for the fact that the thickness of adsorbed layers may change with the ionic environment (pH, ionic strength). This effect will have the biggest impact on the rheology of emulsions stabilized by relatively thick layers of charged biopolymers, e.g., some proteins and polysaccharides. As the pH or ionic strength of the aqueous phase is altered the electrostatic interactions between the biopolymer chains adsorbed to the interface change, which may lead to either an increase or decrease in the thickness of the adsorbed layer. Finally, it should be noted that one of the most dramatic influences of droplet charge on emulsion rheology occurs in electrostatically stabilized systems. If the pH or the ionic strength of the aqueous phase is altered so that the electrostatic repulsion between the droplets is no longer sufficient to overcome the attractive interactions, the droplets will flocculate. Droplet flocculation causes an appreciable increase in emulsion viscosity and causes the emulsion to become strongly shear thinning (see earlier).

## 8.7 Future Trends

Over the past few years, there has been a growing emphasis on understanding the colloidal basis of the rheology of food emulsions, rather than just treating them as a “black box” whose properties can be characterized in terms of certain rheological parameters. Researchers are attempting to quantitatively relate the rheological properties of food emulsions to the characteristics, interactions, and spatial distribution of the droplets they contain. A wide variety of analytical, mathematical, and computational techniques are being developed and used to achieve this objective. Powerful commercial instruments are widely available to quantify the colloidal characteristics of both dilute and concentrated emulsions, e.g., droplet size,

concentration, and electrical charge (Hunter, 1998; Meyers, 2000; Hills et al., 2001). Theoretical, computational, and experimental work is providing a much better understanding of the various types of colloidal interactions that operate between emulsion droplets (Bergenstahl and Claesson, 1997; Claesson et al., 2001). The cost, sensitivity, and range of commercial rheometers are continually improving. In addition, more sophisticated rheological instruments with novel measurement capabilities are being developed and marketed that will certainly lead to further insights into the colloidal basis of the bulk rheology of emulsions, e.g., the capability of measuring normal forces or of measuring the elongational viscosity. Researchers have also become more aware of the possible problems associated with obtaining accurate measurements using these instruments (e.g., wall-slip effects and sample disruption during introduction into the instrument), and are developing effective strategies to overcome these problems (e.g., roughened cell surfaces, vane geometry, squeezing flow).

New rheometers are also being developed that will enable researchers to measure changes in the structure of emulsions as they are being sheared or compressed, e.g., rheo-optics (Mewis et al., 1998), rheoacoustics (Chanamai et al., 2000d), and rheo-NMR techniques (Sinton et al., 1994; McCarthy and Kerr, 1998). Traditional microscopic techniques are being refined so that they can be used to characterize the microstructure of delicate materials, such as emulsions (Dickinson, 1995). In addition, new microscopic technologies are being developed to characterize the organization of molecules at an interface (Patino and Nino, 1999; Plucknett et al., 2001; Morris et al., 2001). Advances in our understanding of the relationship between emulsion rheology and colloidal characteristics are also being made through development of more comprehensive physical theories (Bremer et al., 1993; Larson, 1999; Marangoni, 2000) and the usage of powerful computational techniques (Lodge and Heyes, 1999; Dickinson, 2000; Whittle and Dickinson, 1997, 2001). The application of these new concepts and tools will eventually lead to a much better understanding of the colloidal basis of emulsion rheology. This knowledge will enable food manufacturers to design foods in a more rational fashion, which should eventually lead to improvements in product quality and reductions in manufacturing costs.

Most of the fundamental research carried out on establishing the colloidal basis of emulsion rheology has so far focused on fairly simple model systems. Nevertheless, most real food emulsions are highly complex multicomponent and heterogeneous systems. More systematic research is therefore required to understand the factors that influence the rheology of these more complex systems. The best approach is to start by understanding the rheology of relatively simple model systems, and then incrementally build up the complexity of these models until they resemble actual food systems.

Finally, although significant progress is being made toward relating the sensory perception of emulsion mouthfeel and texture to their rheology and microstructure, more systematic work is still needed. Many previous studies have focused on establishing statistical correlations between descriptors of sensory attributes (e.g., *creaminess*, *thickness*, *coating*) and rheological parameters (e.g., apparent viscosity, yield stress, flow index, or shear modulus) measured on bulk emulsions. This work is certainly important and relevant, but a deeper understanding of the basis of the perceived textural qualities of food emulsions will require work at the physicochemical, physiologic, and psychologic levels. For example, precisely how does the flow of an aqueous solution containing biopolymers or oil droplets across the tongue and inside of the mouth lead to the sensory perception of "creaminess?" This kind of knowledge would help us understand how droplet concentration, size, and interactions influenced the sensory perception of food emulsions, which would facilitate the development of healthful foods that retained their desirable sensory attributes but contained lower fat contents. This approach will require the collaboration of scientists with expertise in a wide range of different disciplines, including food science, physical chemistry, colloid science, rheology, sensory testing, biology, physiology, and neuropsychology.



## chapter nine

---

# Emulsion flavor

### 9.1 Introduction

The overall perceived flavor of a food is due to sensory inputs to the brain resulting from the interactions of volatile and nonvolatile food components with odor, taste, trigeminal, and tactile receptors in the nose and mouth before, during, and after mastication (Bell, 1996; Taylor, 1996, 1998; Duran and Costell, 1999; Smith and Margolskee, 2001). Flavor is one of the most important factors determining the perceived quality of foods (Roberts and Taylor, 2000a,b; Gilbert and Firestein, 2002). Consumers expect that each type of food product will have its own particular characteristic flavor profile. For example, a yogurt might be expected to have a “creamy” “strawberry” flavor, a fruit beverage to have a “tangy” “orangey” flavor, and a cooking sauce to have a “rich” “buttery” flavor. A food manufacturer must therefore ensure that the flavor profile of a product is desirable and that it conforms to consumer expectations for that kind of product. A flavor profile may be achieved by incorporating known concentrations of particular types of flavor molecules into a food (e.g., NaCl, sucrose, D-limonene, citric acid) or by using multicomponent ingredients that contain flavor molecules (e.g., lemon juice, herbs, spices, flavor oils, milk fat). Alternatively, the flavor profile of a food might be generated by ingredients that undergo chemical or biochemical reactions during food production, storage, or preparation, for example, lipid oxidation, browning reactions, or enzymatic reactions (Lindsay, 1996; Jacobsen, 1999; van Ruth et al., 1999a,b; van Ruth and Roozen, 2000). A food manufacturer may therefore wish to know the type and amount of flavoring components that must be incorporated into a food during the manufacturing process in order to produce a desirable flavor profile in the final food product. On the other hand, a food manufacturer may want to know how to avoid the production of an off-flavor within a food during manufacture, storage, or usage.

The rational design of foods with desirable flavor profiles depends on an understanding of the relationship between the types and concentrations of flavoring substances present and the final flavor perceived by consumers (Pothakamury and Barbosa-Canovas, 1995). Nevertheless, a quantitative understanding of this relationship is extremely difficult because of the complexity of the physicochemical, physiological, and psychological processes involved.

#### 9.1.1 Physicochemical processes

The flavor of a food is not simply determined by the type and concentration of flavor molecules present, but also by their ability to reach the appropriate sensory receptors in the nose and mouth (Taylor and Linforth, 1996; Larson and Larson, 1997). The time dependence of the concentration of a particular flavor at a receptor depends on its initial concentration, its initial location within the food, and its ability to move from this location to the receptor. The overall flavor profile therefore depends on the partitioning and mass transport of the

various flavor molecules in the different regions within a food, for example, headspace, oil, water, interface. Flavor partitioning and mass transport in emulsions depend on the molecular characteristics of the flavor molecules (e.g., size, polarity, electrical charge), their interactions with other food components (e.g., binding, solubilization), the characteristics of the emulsion (e.g., disperse phase volume fraction, droplet size distribution, interfacial properties), and the physicochemical properties of the component phases (e.g., polarity, rheology, physical state).

### 9.1.2 *Physiological processes*

Once the flavor molecules have reached the receptors they may interact with them through a variety of physicochemical mechanisms to produce electrochemical signals that are transmitted to the brain via the nervous system (Labows and Cagan, 1993; Bell, 1996; Smith and St. John, 1999). The *odor* of a food is the result of interactions of certain volatile components with taste receptors in the nose (olfactory epithelium), whereas the *taste* of a food is due to interactions of certain nonvolatile components with receptors in the mouth (Taylor, 1996, 1998; Duran and Costell, 1999; Gilbertson et al., 2000; Smith and Margolskee, 2001; Blake, 2002). The *mouthfeel* of a food is primarily the result of interactions between the food and nonspecific receptors within the taste buds that are sensitive to tactile stimuli (Smith and Margolskee, 2001). In certain foods there is also a contribution to overall flavor from a “pain” sensation, which is caused by interactions of certain food components with *trigeminal* receptors in the nose and mouth. A great deal of research is currently being carried out to identify the molecular basis of flavor–receptor interactions, for example, how the signals are generated, transported, and represented in the brain (Duran and Costell, 1999; Smith and Margolskee, 2001; Margolskee, 2002).

### 9.1.3 *Psychological processes*

Sensory perception, expectations, and eating habits vary from individual to individual, depending on their age, sex, culture, and previous experiences, so that the same food may be perceived as tasting differently by two individuals or by a single individual at different times (Prescott, 1999; Ratey, 2001). Understanding the role of psychological factors on food flavor is therefore extremely difficult.

### 9.1.4 *General aspects*

This chapter focuses primarily on the physicochemical aspects of flavor partitioning and release in foods, because these are the most relevant topics to emulsion science. Physiological and psychological aspects of food flavor are considered to be beyond the scope of this book. In addition, the various legal, economic, and marketing constraints that must be considered when selecting flavoring substances for use in foods will not be treated in this chapter for example, ingredient safety, cost, and perceived “healthfulness.”

Given the large number of factors that can contribute to food flavor it is extremely difficult to accurately predict the flavor of a final product from knowledge of its composition and physicochemical characteristics. For this reason, the formulation of food flavors is often the result of art and craft, rather than the application of fundamental scientific principles. Even so, a more rigorous scientific approach to this topic would have great benefits for the food industry because it would enable manufacturers to design foods in a more rational, systematic, and cost-effective manner. Thus, even though it may not be possible to precisely predict the flavor profile of a final product from knowledge of its overall composition and structure, it may be possible to identify the major factors that influence the flavor profile and thus find the most effective strategies for improving its flavor.

The intention of this chapter is to provide a general overview of the basic physicochemical principles of flavor partitioning and release in food emulsions, rather than to discuss the

factors that determine the flavor characteristics of specific types of food emulsions. Nevertheless, the application of these basic principles to specific food emulsions should enable food scientists to improve their flavor profiles in a more rational and systematic fashion. In particular, this chapter will focus on the role of flavor molecule characteristics (e.g., partition coefficients, mass transport coefficients) and emulsion properties (e.g., droplet concentration, droplet size distribution, interfacial characteristics) on flavor partitioning and release.

One area that should benefit particularly from an improved understanding of the influence of emulsion composition and microstructure on food flavor is the development of healthy alternatives to conventional foods, for example, reduced fat, low fat, or fat-free foods (McClements and Demetriades, 1998). Many of these healthy alternatives have not gained widespread consumer acceptance because the removal of a particular component compromised the flavor profile, for example, when the fat is removed from a yogurt it loses its “creamy” taste (Brauss et al., 1999). By rationally understanding how flavor distribution and release are affected by the various components within a food it should become possible to manipulate the concentration of flavors and other components to produce healthy alternatives to conventional foods with improved flavor profiles.

## 9.2 Flavor partitioning

The perception of a flavor molecule depends on its precise location within a food emulsion. Nonvolatile molecules responsible for taste are perceived more intensely when they are present in an aqueous phase than in an oil phase (McNulty, 1987; Kinsella, 1989; Smith and Margolskee, 2001). Volatile molecules responsible for aroma can only be detected by the nose after they have been released into the vapor phase above an emulsion (Overbosch et al., 1991; Taylor and Linfoth, 1996; Taylor, 1996). The aroma molecules may be transported directly into the nose by sniffing a food, or they may be released from a food during mastication and carried into the nose retronasally (Harrison, 1998; de Roos, 2000). Certain flavor molecules may associate with the interfacial membrane surrounding emulsion droplets, which alters their concentration in the vapor and aqueous phases (Wedzicha, 1988; Guichard, 2002). A better understanding of the factors that determine the partitioning of flavor molecules within emulsions would therefore facilitate the rational development of foods with improved flavor profiles (Taylor, 1998).

An emulsion system can be conveniently divided into four phases between which the flavor molecules distribute themselves: the interior of the droplets; the continuous phase; the oil–water interfacial region; and the vapor phase above the emulsion.\* The relative concentration of the flavor molecules in each of these regions depends on their molecular structure and the properties of each of the phases (Baker, 1987; Bakker, 1995; de Roos, 2000). In this section, we start by examining flavor partitioning in some simple model systems and then move on to some more complicated and realistic model systems. It should be stressed, that most of the physical principles of flavor partitioning in emulsions are also applicable to the partitioning of other types of food ingredients, such as antioxidants, colors, preservatives, or vitamins (Wedzicha, 1988; Coupland and McClements, 1996; Huang et al., 1997; McClements and Decker, 2000).

### 9.2.1 Partitioning between a homogeneous liquid and a vapor

The simplest situation to consider is the partitioning of a flavor between a homogeneous liquid and the vapor above it (Figure 9.1). At thermodynamic equilibrium the flavor distributes itself between the liquid and vapor according to the equilibrium partition

\* Flavors could also be present at the air-emulsion interface, but the surface area of this region is usually so small that the amount of flavor involved is negligible.

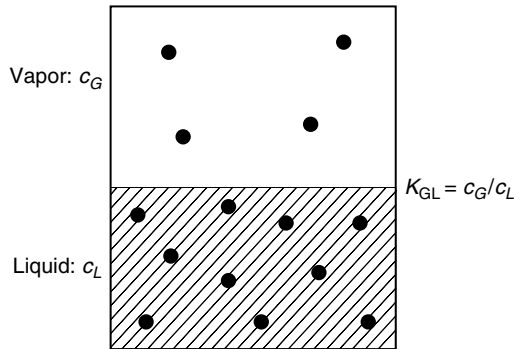


**Figure 9.1** Flavor molecules distribute themselves between a bulk liquid and its vapor phase according to their equilibrium partition coefficient ( $K_{GL} = c_G/c_L$ ).

coefficient (Wedzicha, 1988; Taylor, 1998):

$$K_{GL} = \frac{a_G}{a_L} \quad (9.1)$$

where  $a_G$  and  $a_L$  are the activity coefficients of the flavor in the gas and liquid phases, respectively. The concentration of flavors in foods is usually very low and so the activity coefficients can be replaced by concentrations, since interactions between flavor molecules are usually insignificant (Wedzicha, 1988; Overbosch et al., 1991):

$$K_{GL} = \frac{c_G}{c_L} \quad (9.2)$$

where  $c_G$  and  $c_L$  are the concentrations of the flavor in the gas and liquid phases, respectively. From a practical standpoint, it is convenient to represent the partitioning of a flavor as the mass fraction of the total amount of flavor in the system that is present in the vapor phase:

$$\Phi_m = \frac{1}{1 + V_L / (V_G K_{GL})} \quad (9.3)$$

where  $V_G$  and  $V_L$  are the volumes of the gas and liquid phases, respectively.

The magnitude of the gas–liquid partition coefficient depends on the relative strength of the interactions between the flavor molecules and their surroundings in the gas and liquid phases (Tinoco et al., 1985; Israelachvili, 1992):

$$K_{GL} = \exp\left(-\frac{\Delta G_{GL}}{RT}\right) \quad (9.4)$$

where  $\Delta G_{GL}$  is the difference in free energy per mole of the flavor in the gas and liquid phases. This free energy term depends on the change in molecular interactions and configurational entropy that occur when a flavor molecule moves from the vapor phase into the liquid phase:  $\Delta G_{GL} = \Delta G_{int} - T \Delta S_{config}$  (Israelachvili, 1992). The configurational entropy favors the random distribution of the flavor molecules throughout the whole volume of the system, rather than their confinement to just the liquid phase, and therefore it always

**Table 9.1** Equilibrium Partition Coefficients of Some Common Flavors in Oil and Water at 25°C.

Compound	Air–Water $K_{\text{GW}}$	Air–Oil $K_{\text{GO}}$	Oil–Water $K_{\text{OW}}$
<i>Aldehydes</i>			
Acetaldehyde	$2.7 \times 10^{-3}$		
Propanal	$3.0 \times 10^{-3}$		
Butanal	$4.7 \times 10^{-3}$	$2.3 \times 10^{-3}$	2.0
Pentanal	$6.0 \times 10^{-3}$	$1.0 \times 10^{-3}$	6.0
Hexanal	$8.7 \times 10^{-3}$	$0.35 \times 10^{-3}$	25
Heptanal	$11 \times 10^{-3}$	$0.10 \times 10^{-3}$	110
Octanal	$21 \times 10^{-3}$	$0.04 \times 10^{-3}$	530
Nonanal	$30 \times 10^{-3}$		
<i>Ketones</i>			
Butan-2-one	$1.9 \times 10^{-3}$	$1.9 \times 10^{-3}$	1.0
Pent-2-one	$2.6 \times 10^{-3}$		
Heptan-2-one	$5.9 \times 10^{-3}$	$1.03 \times 10^{-3}$	5.7
Oct-2-one	$7.7 \times 10^{-3}$		
Nonan-2-one	$15 \times 10^{-3}$		
Undecan-2-one	$26 \times 10^{-3}$		
<i>Alcohols</i>			
Methanol	$0.18 \times 10^{-3}$		
Ethanol	$0.21 \times 10^{-3}$	$10 \times 10^{-3}$	0.021
Propanol	$0.28 \times 10^{-3}$		
Butanol	$0.35 \times 10^{-3}$	$0.57 \times 10^{-3}$	0.65
Pentanol	$0.53 \times 10^{-3}$		
Hexanol	$0.63 \times 10^{-3}$	$0.36 \times 10^{-3}$	1.8
Heptanol	$0.77 \times 10^{-3}$		
Octanol	$0.99 \times 10^{-3}$	$0.09 \times 10^{-3}$	11

Source: Data compiled from Buttery et al. (1969, 1971, 1973) and Overbosch et al. (1991).

favors volatilization. The change in free energy associated with the molecular interactions is determined by the formation of solvent–flavor bonds ( $\approx zg_{\text{SF}}$ ) and the disruption of solvent–solvent bonds ( $\approx 1/2zg_{\text{SS}}$ ), which occurs when a flavor molecule moves from the vapor into the solvent.\* Here,  $z$  is the coordination number of the flavor molecules, and  $g_{\text{SS}}$  and  $g_{\text{SF}}$  are the solvent–solvent and solvent–flavor molecular interaction free energies (Chapter 2). The change in the interaction free energy associated with transferring a molecule from the vapor phase to the liquid phase therefore depends on the relative strength of both the solvent–solvent and solvent–flavor interactions:  $\Delta G_{\text{int}} \approx zn(g_{\text{SF}} - 1/2g_{\text{SS}})$ , where  $n$  is the number of moles of flavor molecules (Israelachvili, 1992). The change in the molecular interaction free energy normally opposes flavor volatilization because the flavor molecules can form relatively strong attractive interactions with their neighbors in the solvent (e.g., through van der Waals or electrostatic attraction), but not when they are in the gas phase. Even so, the magnitude of  $\Delta G_{\text{int}}$  depends on the molecular characteristics of both the flavor and solvent molecules (e.g., molecular weight, charge, hydrophobicity).

As mentioned above, the molecular characteristics of flavor molecules largely determine their partition between the liquid and gas phases (Table 9.1). When a nonpolar flavor molecule

\* This simple analysis assumes that the sizes of the solvent and flavor molecules are approximately equal. In addition, the molecular interactions are expressed as free energies ( $g$ ) rather than pair potentials ( $w$ ) because this enables one to more conveniently account for hydrophobic interactions (Norde, 2003).



is dispersed in a nonpolar solvent, so that only van der Waals forces make a significant contribution to the interaction energy contribution, there is a decrease in volatility with increasing molecular weight (Buttery et al., 1973). This is because the number of favorable attractive interactions between the flavor molecules and the solvent molecules increases as the molecular weight of the flavor molecules increases (Israelachvili, 1992), and because the configurational entropy contribution decreases as the molecular weight increases (Atkins, 1994). On the other hand, when a nonpolar flavor molecule is dispersed in a polar solvent there is a decrease in volatility with increasing molecular weight (Buttery et al., 1969; Buttery et al., 1971; Bomben et al., 1973; Franzen and Kinsella, 1975). Nonpolar flavors are less volatile in nonpolar solvents than in polar solvents (Buttery et al., 1973; Bakker, 1995), because a number of relatively strong hydrogen bonds between the solvent molecules have to be replaced by relatively weak van der Waals bonds when a nonpolar molecule is introduced into a polar solvent, which is thermodynamically unfavorable because of the hydrophobic effect (Israelachvili, 1992). In addition, polar flavors are less volatile in polar solvents than in nonpolar solvents (Table 9.1), because the hydrogen bonds that form in polar solvents are more strongly attractive than the van der Waals bonds that form in nonpolar solvents.

### 9.2.2 Influence of flavor ionization

A number of water-soluble flavors have chemical groups that are capable of undergoing proton association–dissociation as a result of changes in pH (e.g.,  $-\text{COOH} \rightarrow -\text{COO}^- + \text{H}^+$  or  $-\text{NH}_3^+ \rightarrow -\text{NH}_2 + \text{H}^+$ ). The volatility and flavor characteristics of the different ionic forms of a molecule are different because of changes in their molecular interactions with the solvent (Baldwin et al., 1973; Wedzicha, 1988; Guyot et al., 1996; de Roos, 2000). For example, the ionized form of a flavor is less volatile in an aqueous solution than the nonionized form because it can form strong ion–dipole interactions with the surrounding water molecules, whereas the nonionized form can only form weaker dipole–dipole interactions. It is therefore important to take into account the effect of ionization on the partitioning of flavor molecules. The concentration of a specific ionic form at a certain pH can be determined using the Henderson–Hasselbach equation:  $\text{pH} = \text{p}K_a - \log(c_{\text{Acid}}/c_{\text{Base}})$ , where  $\text{p}K_a = -\log(K_a)$  and  $K_a$  is the dissociation constant of the acidic group (Atkins, 1994).

The volatility of the ionized form of a flavor is usually much lower than that of the nonionized form, and so the concentration of the flavor in the vapor phase is determined principally by the amount of nonionized flavor ( $c_{L,N}$ ) present in the liquid phase:  $c_{L,N} = c_L(1 + 10^{\text{pH}-\text{p}K_a})^{-1}$ . The partition coefficient is therefore given by

$$K_{\text{GL}} = \frac{c_G}{c_{L,N}} = \frac{c_G(1 + 10^{\text{pH}-\text{p}K_a})}{c_L} \quad (9.5)$$

In practice, it is more convenient to define an *effective* partition coefficient, which is equal to the concentration of the flavor in the vapor phase relative to the *total* amount of flavor in the liquid phase ( $c_L = c_{L,I} + c_{L,N}$ ), where  $c_{L,I}$  is the concentration of the ionized form of the flavor:

$$K_{\text{GL}}^e = \frac{c_G}{c_L} = \frac{K_{\text{GL}}}{(1 + 10^{\text{pH}-\text{p}K_a})} \quad (9.6)$$

When the pH of the aqueous solution is well below the  $\text{p}K_a$  value of the acid group, the flavor molecule is almost exclusively in the nonionized form ( $K_{\text{GL}}^e = K_{\text{GL}}$ ), and so the flavor

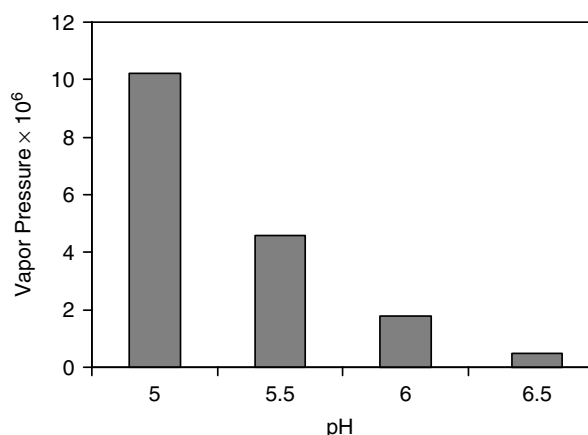


**Figure 9.2** Influence of pH on volatility of hexanoic acid in 5% oil-in-water emulsions at 25°C. Adapted from Figure 1 in de Roos (2000).

in the vapor phase is at its most intense. As the pH is raised toward the  $pK_a$  value of the acid group, the fraction of flavor molecules in the nonionized form decreases ( $K_{GL}^e < K_{GL}$ ), and so the flavor in the vapor phase becomes less intense (Figure 9.2).

It should be stressed that the ionization of a flavor molecule may also influence the partition coefficient because it alters its interactions with other charged molecules within the aqueous phase. For example, there may be attractive electrostatic interactions between an ionized flavor molecule and an oppositely charged biopolymer, which leads to flavor binding (Guichard, 2002), and therefore a reduction of its concentration in the vapor phase (Section 9.2.3).

### 9.2.3 Influence of flavor binding on partitioning

Many proteins and carbohydrates are capable of binding flavor molecules, thereby altering flavor partitioning and perceived flavor of foods (Franzen and Kinsella, 1975; Bakker, 1995; O'Neill, 1996; Hansen and Booker, 1996; Hau et al., 1996; Lubbers et al., 1998; Andriot et al., 1999; Delarue and Giampaoli, 2000; Reiners et al., 2000; Goubet et al., 2001; Guichard, 2002; Semenova et al., 2002; van Ruth and Villeneuve, 2002). This alteration is often detrimental to food quality because it changes the characteristic flavor profile, but it can also be beneficial when the bound molecules are off-flavors. A flavor chemist must therefore take binding effects into account when formulating the flavor of a particular product.

The equilibrium partition coefficient of a flavor in the presence of a biopolymer that can bind it is given by

$$K_{GL} = \frac{c_G}{c_{L,F}} \quad (9.7)$$

where  $c_{L,F}$  is the concentration of free (unbound) flavor present in the liquid. The concentration of free flavor depends on the nature of the binding between the flavor and biopolymer, for example, binding constants and stoichiometry (Overbosch et al., 1991). Binding may be the result of covalent bond formation or physical interactions, such as electrostatic, hydrophobic, van der Waals, or hydrogen bonds (Chapter 2). It may take place at specific

sites on the surface of a biopolymer molecule or nonspecifically at any location on the surface. It may be reversible or irreversible.

Assuming that the binding interaction is a reversible first-order reaction, the extent of flavor binding to a biopolymer can be conveniently characterized by an *equilibrium binding constant*,  $K_b$  (Harrison and Hills, 1997a):

$$K_b = \frac{c_{L,B}}{c_{L,F}c_b} \quad (9.8)$$

where  $c_b$  is the concentration of the biopolymer,  $c_{L,F}$  and  $c_{L,B}$  are the concentrations of free and bound flavor in the liquid phase ( $c_L = c_{L,F} + c_{L,B}$ ) and  $c_L$  is the total concentration of flavor in the liquid phase. The overall degree of flavor binding is conveniently characterized in terms of a *binding parameter* ( $B = K_b c_b$ ), which takes into account both the strength of the binding constant and the concentration of biopolymer present. The stronger the binding between the flavor and a biopolymer, the greater the value of  $K_b$  or  $B$ .

It is convenient to define an *effective* partition coefficient, which relates the concentration of flavor in the gas phase to the total amount of flavor in the liquid phase (Overbosch et al., 1991; Harrison and Hill, 1997b; Harrison et al., 1997):

$$K_{GL}^e = \frac{c_G}{c_L} = \frac{K_{GL}}{1 + K_b c_b} = \frac{K_{GL}}{1 + B} \quad (9.9)$$

This equation indicates that the concentration of flavor in the vapor phase is not influenced by the biopolymer when the binding is relatively weak ( $B \ll 1$ ), but that there is a large reduction in the flavor concentration in the vapor phase when the binding is relatively strong ( $B > 1$ ). It also indicates that the equilibrium headspace flavor concentration should decrease with increasing biopolymer concentration when the binding interaction is relatively strong.

Binding constants are frequently measured experimentally by equilibrium dialysis (van Holde, 1971). A biopolymer solution is placed inside a semipermeable dialysis bag, which is then suspended in a solution of the flavor molecules. The large biopolymer molecules are restricted to the inside of the dialysis bag, while the small flavor molecules can move through it. After the system has reached equilibrium, the amount of flavor bound to the biopolymer molecules is determined by measuring the concentration of flavor in the bag above that which would be expected in the absence of biopolymer (van Holde, 1971). An alternative technique which is also widely used to measure flavor binding is headspace analysis (Chaintreau et al., 1995; Doyen et al., 2001; Guichard, 2002). In this technique, the partition coefficient is determined by measuring the equilibrium concentration of volatiles in the headspace above a solution. By measuring the partition coefficient at different biopolymer concentrations it is possible to determine the flavor–biopolymer binding constant. A variety of other analytical techniques can also be used to determine the thermodynamic binding isotherms of flavors to biopolymers and other molecules in aqueous solutions, such as fluorescence spectroscopy (Dufour and Haertle, 1990; Muresan et al., 2001), nuclear magnetic resonance (Jung et al., 2002; Jung and Ebeler, 2003), ultrasonic velocimetry (Nikitina and Nikitin, 1990), isothermal titration calorimetry (Kelley and McClements, 2003), and chromatography (Guichard, 2002). Information about the nature of the molecular interactions and about the structural characteristics of the binding sites can be obtained using advanced spectroscopy techniques, such as nuclear magnetic resonance (NMR) (Lubke et al., 2002), electronic paramagnetic

spectroscopy (Goubet et al., 2000), and infrared spectroscopy (Lubke et al., 2000). It should be noted that the extent of binding depends on the conformation of the biopolymer molecule (Fares et al., 1998).

#### 9.2.4 Influence of surfactant micelles on partitioning

Surfactants are normally used to stabilize emulsions against aggregation by providing a protective membrane around the droplets (Chapter 7). Nevertheless, there is often enough free surfactant present in the dispersed and/or continuous phases to form micelles or reverse micelles (Section 4.4). Micelles may solubilize nonpolar molecules in their hydrophobic interior, thereby increasing the affinity of nonpolar flavors for the aqueous phase (Horike and Akahoshi, 1996; Suratkhar and Mahapatra, 2000). They may also solubilize amphiphilic molecules between hydrophilic surfactant head groups (Suratkhar and Mahapatra, 2000). Similarly, reverse micelles in an oil phase are capable of solubilizing certain kinds of polar and amphiphilic molecules within their structures (Jonsson et al., 1998). The presence of micelles and/or reverse micelles in a pure liquid or in an emulsion may therefore alter the distribution of flavor molecules among the oil phase, aqueous phase, and headspace regions, thereby altering the perceived flavor of the system.

The partitioning of flavor compounds between a surfactant solution and the gas above it can be described by the following equation:

$$\frac{1}{K_{GL}} = \frac{\phi_M}{K_{GM}} + \frac{\phi_C}{K_{GC}} \quad (9.10)$$

where  $\phi_M$  is the volume fraction of the micelles,  $\phi_C$  is the volume fraction of the continuous phase surrounding the micelles ( $\phi_M + \phi_C = 1$ ),  $K_{GM}$  ( $= c_G/c_M$ ) is the gas-micelle partition coefficient, and  $K_{GC}$  ( $= c_G/c_C$ ) is the gas-continuous phase partition coefficient. It is difficult to directly measure the partitioning of a flavor between gas and micelles, and so it is more convenient to rewrite the above equation in the following form:

$$K_{GL} = \frac{K_{GC}}{1 + \phi_M(K_{MC} - 1)} \quad (9.11)$$

where  $K_{MC}$  ( $= c_M/c_C$ ) is the partition coefficient of the flavor molecules between the micelles and the continuous phase. Equation 9.11 indicates that the higher the affinity of the flavor molecules for the micelles ( $K_{MC} \gg 1$ ), the smaller the headspace flavor concentration. Experimental measurements have shown that surfactant micelles are capable of reducing the headspace concentration of flavor molecules above aqueous solutions (Horike and Akahoshi, 1996; Suratkhar and Mahapatra, 2000).

#### 9.2.5 Partitioning in emulsions in the absence of an interfacial membrane

In an ideal "emulsion," consisting of two immiscible liquids in the absence of an emulsifier, we must consider the partitioning of the flavor amongst the dispersed, continuous, and vapor phases (Figure 9.3). We therefore have to define three different partition coefficients:

$$K_{DC} = \frac{c_D}{c_C}, \quad K_{GC} = \frac{c_G}{c_C}, \quad K_{GD} = \frac{c_G}{c_D} \quad (9.12)$$

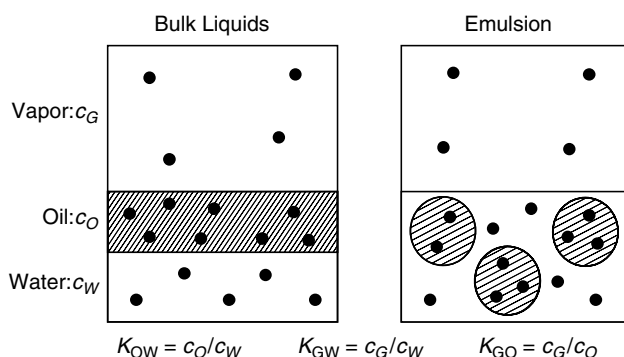


**Figure 9.3** In a two liquid system the flavor molecules partition themselves among the oil, water, and vapor phases according to the equilibrium partition coefficients.

where  $K$  is the partition coefficient,  $c$  is the concentration, and the subscripts  $D$ ,  $C$ , and  $G$  refer to the dispersed, continuous, and gas phases, respectively. In foods the dispersed and continuous phases are usually oil and water. The distribution of flavor molecules between these two phases is therefore characterized by an oil–water partition coefficient ( $K_{OW}$ ), with  $K_{OW} < 1$  for predominantly polar flavor molecules and  $K_{OW} > 1$  for predominantly nonpolar flavor molecules. The value of  $K_{OW}$  for a particular type of flavor molecule depends to some extent on the nature of the oil phase (e.g., polarity) and the aqueous phase (e.g., composition). More generally, the relative polarity of flavor molecules can be ranked according to their  $\log P$  values, where  $P$  is the octanol–water partition coefficient at a specified temperature (Taylor, 1998).  $\log P$  is positive for hydrophobic flavors and negative for hydrophilic flavors. The partitioning of flavor molecules between oil and water phases depends on the relative strength of their molecular interactions with their surroundings in the two phases (Israelachvili, 1992). Hence, nonpolar molecules tend to favor the oil phase, while polar molecules tend to favor the water phase.

The partition coefficient of a flavor molecule between an emulsion and vapor phase is given by (Overbosch et al., 1991):

$$\frac{1}{K_{GE}} = \frac{\phi_D}{K_{GD}} + \frac{\phi_C}{K_{GC}} \quad (9.13)$$

where  $\phi_D + \phi_C = 1$ . Thus, the partition coefficient between an emulsion and its vapor can be predicted from knowledge of  $K_{GD}$  and  $K_{GC}$ . Experiments with flavor compounds dispersed in oil-in-water emulsions have shown that this equation gives a good description of the behavior of emulsions, provided that the flavor does not interact with the interface or any free emulsifier in the aqueous phase (Guyot et al., 1996).

Predictions of the mass fraction of flavor in the water and headspace phases of oil-in-water emulsions with the same overall flavor concentration but different disperse phase volume fractions are shown in Figure 9.4. For nonpolar flavors ( $K_{OW} > 1$ ), the water and headspace flavor concentration decreases with increasing oil content. The sharpness of this decrease increases as the flavor molecules become more hydrophobic, so that even a small increase in droplet concentration in a dilute oil-in-water emulsion could cause a large decrease in water and headspace flavor concentration for a highly nonpolar flavor ( $K_{OW} \gg 1$ ). For polar flavors ( $K_{OW} < 1$ ), the headspace flavor concentration increases slightly and the water flavor concentration decreases slightly with increasing  $\phi$  at relatively low oil contents, but the changes occur more sharply at higher oil contents (Figure 9.4).

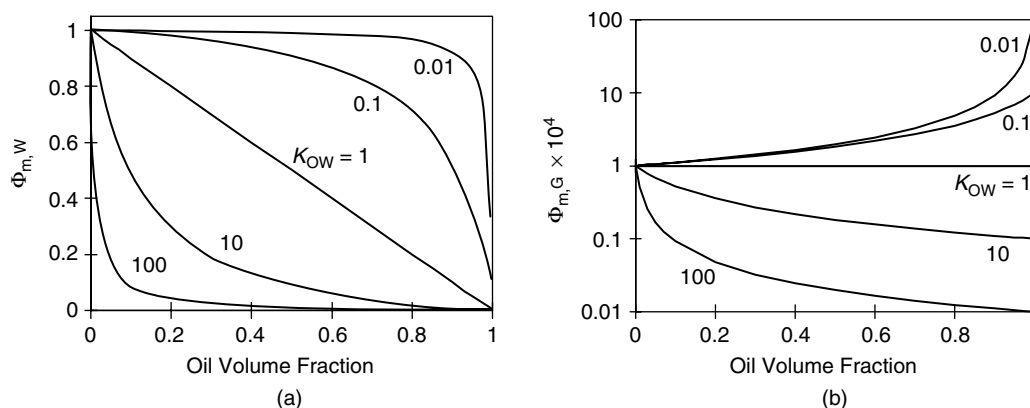


**Figure 9.4** (a) Influence of disperse phase volume fraction and oil–water partition coefficient on the aqueous phase concentration of flavor molecules in an oil-in-water emulsion ( $K_{GC} = 0.01$ ,  $V_G = 10 \text{ cm}^3$ ,  $V_E = 100 \text{ cm}^3$ ). (b) Influence of disperse phase volume fraction and oil–water partition coefficient on the headspace concentration of flavor molecules in an oil-in-water emulsion ( $K_{GC} = 0.01$ ,  $V_G = 10 \text{ cm}^3$ ,  $V_E = 100 \text{ cm}^3$ ).

The steepness of the changes at high oil contents increases as the flavor molecules become more hydrophilic. Practically, this means that the volatile nonpolar flavors in relatively dilute oil-in-water emulsions become more odorous as the fat content is decreased, whereas the volatile polar flavors remain relatively unchanged (Guyot et al., 1996; Jo and Ahn, 1999; Miettinen et al., 2002). This has important consequences when deciding the type and concentration of flavors to use in low fat analogs of existing emulsion-based food products (McClements and Demetriades, 1998).

One possible limitation of Equation 9.13 is that it does not take into account the droplet size. The assumption that the partitioning of additives is independent of particle size is likely to be valid for emulsions that contain fairly large droplets (i.e.,  $d > 0.1 \text{ }\mu\text{m}$ ), because the influence of the curvature of a droplet on the solubility of the material within it is not significant (Hunter, 1986). However, when the droplet diameter falls below a critical size, there is a significant increase in the solubility of the material within it because of the increased Laplace pressure (Adamson, 1990). Thus, one might expect the flavor concentration in the continuous phase and in the vapor phase to increase as the size of the droplets in an emulsion decreased below this critical value. In practice, few food emulsions have droplets this small, so that this effect is unlikely to be appreciable.

## 9.2.6 Partitioning in emulsions in the presence of an interfacial membrane

Even though the interfacial region constitutes only a small fraction of the total volume of an emulsion, it can have a pronounced influence on the partitioning of surface-active molecules, especially when they are present at low concentrations, which is usually the case for food flavors. The influence of the interfacial membrane can be highlighted by a simple calculation of the amount of a surface-active additive that can associate with it (Wedzicha, 1988). Assume that the additive occupies an interfacial area of  $1 \text{ m}^2 \text{ mg}^{-1}$ , which is typical of many surface-active components (Dickinson, 1992). The interfacial area per unit volume of an emulsion is given by the following relationship:  $A_s = 6\phi/d_{32}$ , where  $d_{32}$  is the volume-surface mean diameter (McClements and Dungan, 1993). If we assume that the additive is present in  $100 \text{ cm}^3$  of an emulsion with a disperse phase volume fraction of 0.1 and a mean droplet diameter of  $1 \text{ }\mu\text{m}$ , then the total interfacial area of the droplets is  $60 \text{ m}^2$ . It would therefore

take about 60 mg of additive to completely saturate the interface, which corresponds to a concentration of approximately 0.1 wt%. Many flavors are used at concentrations that are considerably less than this value, and therefore their ability to accumulate at an interface has a large influence on their partitioning within an emulsion.

The accumulation of a flavor at an interface reduces its concentration in the oil, water, and gaseous phases, by an amount that depends on the interfacial area, the flavor concentration, and the affinity of the flavor for the interface (Jacobsen et al., 1999).

### 9.2.6.1 Reversible binding

When the binding between the flavor and the interface is reversible, we can define a number of additional partition coefficients:

$$K_{ID} = \frac{c_I}{c_D}, \quad K_{IC} = \frac{c_I}{c_C}, \quad K_{IG} = \frac{c_I}{c_G} \quad (9.14)$$

where  $c_i$  represents the concentration of flavor molecules present within the interfacial membranes. In this case, the partition coefficient between the gas and the emulsion is given by

$$\frac{1}{K_{GE}} = \frac{\phi_D}{K_{GD}} + \frac{\phi_C}{K_{GC}} + \frac{\phi_I}{K_{GI}} \quad (9.15)$$

In practice, it is difficult to directly measure the partition coefficient between the gas and interfacial region ( $K_{GI}$ ), and so it is better to express the equation in terms of properties that are simpler to measure: that is,  $K_{GI} = K_{GC}/K_{IC}$ . In addition, the properties of the interface are usually better expressed in terms of the interfacial area, rather than the volume fraction. Equation 9.15 can therefore be expressed in the following manner:

$$\frac{1}{K_{GE}} = \frac{\phi_D}{K_{GD}} + \frac{\phi_C}{K_{GC}} + \frac{A_s K_{IC}^*}{K_{GC}} \quad (9.16)$$

where  $K_{IC}^* = \Gamma_I/c_C$  is the partition coefficient between the interface and the continuous phase and  $\Gamma_I$  is the mass of the flavor per unit interfacial area. Thus, the partition coefficient of an emulsion ( $K_{GE}$ ) can be predicted from experimental measurements that are all relatively simple to carry out, that is,  $K_{GC}$ ,  $K_{GD}$ , and  $K_{IC}$  or  $K_{IC}^*$ . This equation assumes that the concentration of flavor at the interface is well below the saturation level. Once the interfacial region becomes saturated with flavor, the remainder will be distributed between the bulk phases.

The influence of the interface on the volatility of a surface-active flavor molecule is shown in Figure 9.5. As the size of the droplets in the emulsion is decreased, the interfacial area increases, and therefore a greater amount of flavor associates with the interface, thereby reducing its volatility. Nevertheless, it should be stated that this type of behavior is only likely to be observed when there is no free emulsifier in the aqueous phase, either as individual molecules or micelles. In practice, there is often free emulsifier in the aqueous phase, for example, biopolymers that can bind flavors or surfactant micelles that can solubilize flavors (Charles et al., 2000a,b). In these systems the flavor volatility is more likely to depend on the total concentration of emulsifier in the system, rather than on the droplet size. Another factor that should be considered in emulsions containing very small droplets is that the concentration of a flavor in the continuous and gas phases may increase with decreasing droplet size because of the influence of the droplet curvature on solubility (Section 9.2.5).

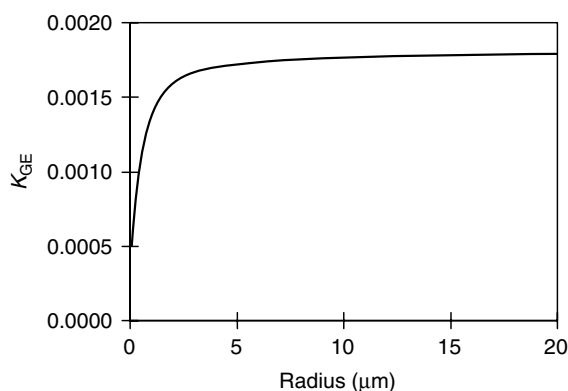


**Figure 9.5** Influence of droplet size on the volatility of surface-active flavor molecules that associate with an interfacial membrane ( $K_{GD} = 0.001$ ,  $K_{GC} = 0.002$ ,  $K_{IC} = 10^{-6}$ ,  $\phi = 0.1$ ,  $V_G = 10 \text{ cm}^3$ ,  $V_E = 100 \text{ cm}^3$ ). This calculation assumes that the flavors do not interact with nonadsorbed emulsifier molecules.

### 9.2.6.2 Irreversible binding

When the binding of a flavor to the interface is irreversible (e.g., due to a covalent interaction between the flavor and an adsorbed emulsifier molecule), then its concentration in the vapor phase is only determined by the amount of free flavor in the emulsion ( $K_{GE} = c_G/c_{E,F}$ ). Under these circumstances, it is usually more convenient to use an *effective* partition coefficient, which is equal to the concentration of flavor in the vapor phase relative to the *total* amount of flavor in the emulsion ( $K_{GE}^e = c_G/c_E$ ):

$$\frac{1}{K_{GE}^e} = \left( \frac{c_E}{c_E - A_s \Gamma_I} \right) \left( \frac{\phi_D}{K_{GD}} + \frac{\phi_C}{K_{GC}} \right) \quad (9.17)$$

where  $\Gamma_I$  is now the amount of flavor that is irreversibly bound to the interface per unit surface area. If the flavor does not interact with the interface, and the interfacial region has a negligible volume, then this equation reduces to Equation 9.13, but if the flavor irreversibly binds to the interface its concentration in the vapor phase is reduced.

Studies using oil-in-water emulsions containing different types of flavor compounds have indicated that amphiphilic flavors, such as butyric acid, bind strongly to the interface of a droplet and thus reduce the partition coefficient  $K_{GE}^e$  (Guyot et al., 1996). Nevertheless, a great deal of systematic research is still needed to determine the factors that influence the volatility of different flavor compounds in food emulsions (Guichard, 2000). Special emphasis should be made on establishing the molecular basis of this process so that predictions about the flavor profile of a food can be made from knowledge of its composition and the type of flavor components present. This type of information could then be used by flavor chemists to formulate foods with specific flavor profiles.

## 9.3 Flavor release

### 9.3.1 Overview of physicochemical process of flavor release

Flavor release is the process whereby flavor molecules move from a food to the flavor receptors in the mouth and nose (McNulty, 1987; Overbosch et al., 1991; Harrison, 2000).



An appreciation of the relative merits of the different mathematical models developed to describe flavor release from emulsions depends on knowledge of the physicochemical processes occurring (de Roos, 2000). When a food emulsion is in a closed environment, the flavor molecules are initially distributed among the oil, water, interfacial, and headspace regions according to their equilibrium partition coefficients (Section 9.2). The flavor of a food emulsion can therefore be perceived prior to placing it in one's mouth by "sniffing" the headspace. In this process the volatile flavor molecules leave the emulsion, enter the nostrils, and interact with the flavor receptors in the nose.

After the emulsion is placed in the mouth, it is diluted with saliva, which disturbs the equilibrium flavor concentrations and acts as a driving force for the mass-transport processes that lead to flavor release (de Roos, 2000). Flavor molecules initially present in the aqueous phase of the emulsion move through the emulsion-saliva mixture until they reach the taste receptors inside the mouth or they reach the surface of the emulsion-saliva mixture, where they are released into the headspace above the emulsion (Harrison, 1998, 2000). Flavor molecules present within oil droplets must first move through the interior of the droplets, across the interfacial membrane and into the aqueous phase before these processes can occur. The volatile flavor molecules in the headspace are carried retronasally from the mouth through the air passages and into the nasal cavity (Buettner et al., 2002). Once the volatile flavor molecules reach the nasal cavity they are adsorbed onto the surface of a mucus membrane, which they must travel across before they can reach the flavor receptors (Harrison, 2000; Buettner et al., 2002). It should be noted that different flavor molecules are released from foods at different rates, hence the perceived flavor of a food changes significantly during mastication (de Roos, 2000).

In practice, the physicochemical processes mentioned above are complicated by a variety of different factors (Land, 1996; Harrison et al., 1997; Harrison and Hills, 1997a,b; Harrison, 1998, 2000; de Roos, 2000). The temperature of the emulsion may change during mastication, which can lead to phase changes (e.g., melting, crystallization, biopolymer unfolding) and/or changes in the physicochemical properties of the components (e.g., partition coefficients, viscosities). The food is also subjected to complex mechanical forces during mastication, which may cause fragmentation, breakdown, and mixing of the emulsion. Dilution of the emulsion with saliva changes the composition, physicochemical properties, and pH of the system. In addition, the gas phase above the emulsion is periodically being mixed and transferred away from the mouth due to mastication and breathing, and the emulsion is periodically being removed from the mouth due to swallowing.

Despite the complexity of the above processes, considerable progress has been made in modeling flavor release from emulsions over the past few years, and many of these factors have now been included into mathematical models (de Roos, 2000). In this section, we examine some of the mathematical models that have been developed to describe the release of both nonvolatile and volatile flavor components from foods. The major differences between these models are the assumptions that are made in their derivation, for example, the nature of the mass transfer process, the nature of the rate-limiting step, or the geometry of the system (de Roos, 2000).

### 9.3.2 *Release of nonvolatile compounds (taste)*

Ideally, one would like to know the time dependence of the concentration of the various flavor molecules released from a food at the taste receptors within the mouth. In practice, it is difficult to measure flavor concentrations at the site of the taste receptors, and so flavor release is often characterized in terms of the maximum amount of flavor that can potentially be released from a food into the aqueous phase and the kinetics of this release process.

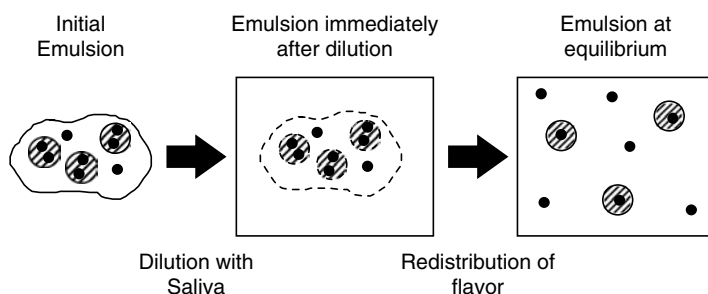


**Figure 9.6** The flavor in a food is initially distributed according to the partition coefficients. When it is diluted with saliva in the mouth the equilibrium is upset, and flavor is released from the droplets.

### 9.3.2.1 Maximum amount of flavor released

A relatively simple model, based on the equilibrium partitioning of flavor molecules between oil and water, has been used to describe the theoretical maximum amount of flavor that can be released from an oil-in-water emulsion when it is placed in the mouth and diluted with saliva (McNulty, 1987). The model assumes that the food is initially at equilibrium, so that the distribution of the flavor between the droplets and continuous phase is given by the equilibrium partition coefficient ( $K_{OW}$ ). When the food is placed in the mouth it is diluted by saliva (Figure 9.6). Immediately after dilution the concentration of flavor in the aqueous phase is reduced and there is a thermodynamic driving force that favors the release of flavor from the droplets until the equilibrium flavor distribution specific to  $K_{OW}$  is restored.

The potential for flavor release on emulsion dilution can be characterized by the ratio of the flavor in the aqueous phase once equilibrium has been reestablished, to that immediately after dilution (when the system is not at equilibrium):

$$E_F = \frac{c_{We}}{c_{Wd}} = \frac{[\phi(K_{OW} - 1) + 1](DF - \phi)}{[\phi(K_{OW} - 1) + DF](1 - \phi)} \quad (9.18)$$

where  $DF$  is the dilution factor of the emulsion ( $= V_f/V_i$ ),  $V_i$  and  $V_f$  are the emulsion volume before and after dilution,  $\phi$  is the disperse phase volume fraction of the initial emulsion,  $c_{Wd}$  is the concentration of flavor in the aqueous phase immediately after dilution, and  $c_{We}$  is the concentration in the aqueous phase once equilibrium has been reestablished. The higher the value of  $E_F$ , the greater the potential for flavor release. Despite its simplicity, this model can be used to make some valuable predictions about the factors that determine flavor release from foods (McNulty, 1987), for example, the extent of flavor release on dilution increases as either  $\phi$  or  $K_{OW}$  increases. One of the major limitations of this model is that it makes the assumption that the flavor distribution reaches equilibrium during mastication. In addition, it provides no information about the rate at which flavor molecules are released from droplets and move to taste receptors.

### 9.3.2.2 Kinetics of flavor release

The taste of an emulsion depends on the rate at which the flavor molecules move from the food to the receptors on the tongue and inside of the mouth. The flavor molecules in an emulsion are distributed between the oil and aqueous phases. Nevertheless, it has been postulated that taste perception is principally a result of those molecules present in the water phase (McNulty, 1987), because the flavor must cross an aqueous membrane before

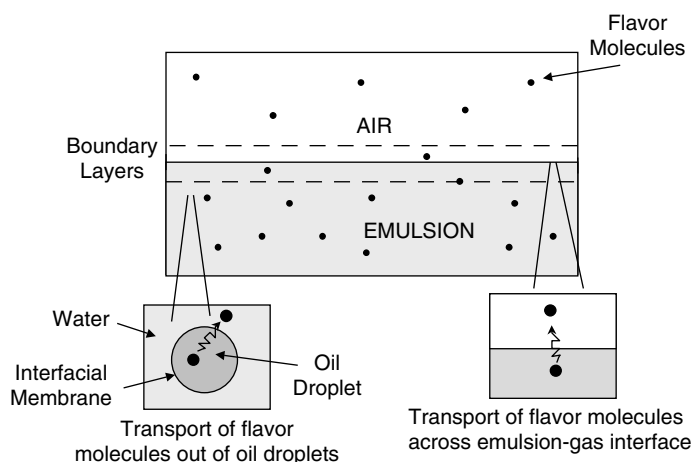


**Figure 9.7** Schematic diagram of the physicochemical processes occurring during flavor release from an oil-in-water emulsion during mastication.

reaching the taste receptors (Taylor, 1996; Smith and Margolskee, 2001). An indication of the kinetics of flavor release can therefore be obtained from knowledge of the time dependence of the flavor concentration in the aqueous phase (rather than at specific taste receptors). In this section, we will principally be concerned with flavor release from oil-in-water emulsions because it is believed that water-in-oil emulsions, such as butter or margarine, break down to oil-in-water emulsions in the mouth before significant flavor release occurs (Bakker and Mela, 1996).

When an oil-in-water emulsion is diluted with saliva some of the flavor molecules in the droplets move into the aqueous phase (Figure 9.7). A mathematical theory, known as the Crank model, has been developed to describe the rate at which a solute is released from a spherical droplet surrounded by an infinite volume of a well-stirred liquid (Crank, 1975; Lian, 2000):

$$\frac{M_t}{M_0} = 1 - \sum_{n=0}^{\infty} \frac{6}{\pi^2 n^2} \exp \left[ -\frac{D\pi^2 n^2}{K_{DC} r^2} t \right] \quad (9.19)$$

where  $M_t$  is the total amount of solute that has diffused out of the sphere by time  $t$ ,  $M_0$  is the initial amount of solute in the sphere,  $D$  is the translational diffusion coefficient of the flavor within the droplet,  $r$  is the droplet radius, and  $n$  is an integer. This equation assumes that the concentration of solute (flavor) in the aqueous phase is initially zero, and therefore this equation is only strictly applicable to systems with high  $K_{DC}$  values or emulsions that are diluted with high concentrations of saliva. The equation above involves calculating an infinite series of terms, which makes it difficult to apply in practice. Flavor release can be more easily modeled using the following equation, which gives predictions that are in close agreement with the Crank model (Lian, 2000):

$$\frac{M_t}{M_0} = 1 - \exp \left[ -\frac{1.2D\pi^2}{K_{DC} r^2} t \right] \quad (9.20)$$

The Crank model provides some useful insights into the factors that influence the rate of flavor release from oil droplets. Predictions of the influence of droplet radius on flavor

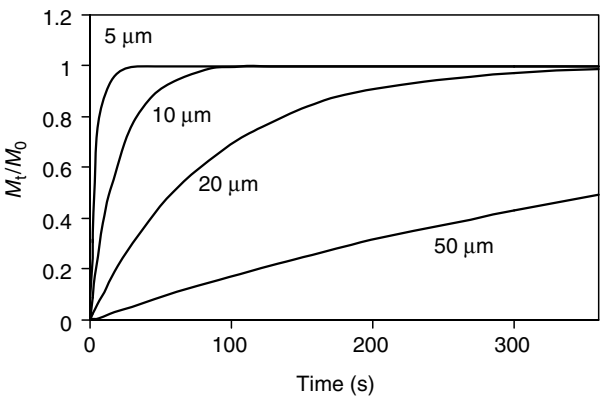


**Figure 9.8** Kinetics of flavor release from spherical droplets suspended in a liquid. The release rate was predicted using the Crank model for different sized oil droplets assuming the diffusion coefficient within the droplets was  $D = 4 \times 10^{-10} \text{ m sec}^{-1}$ .

release from oil droplets suspended in water made using the Crank model are shown in Figure 9.8. There is a rapid initial increase in the amount of flavor released from the droplets into the aqueous phase, followed by a more gradual increase at longer times as the flavor concentrations in the oil and aqueous phases approach the equilibrium values. The release rate increases as the size of the droplets decreases, because the flavor molecules have a shorter distance to diffuse.

A convenient measure of the rate of flavor release is the time required for half of the total flavor to diffuse out of the droplets,  $t_{1/2}$ , which is given by the following approximate expression for the Crank model (Lian, 2000):

$$t_{1/2} = \frac{0.0585r^2K_{DC}}{D} \tag{9.21}$$

The variation of  $t_{1/2}$  with oil droplet radius and equilibrium partition coefficient of the flavor molecules ( $K_{DC} = K_{OW}$ ) is shown in Table 9.2. The time for half of the flavor molecules contained in the droplets to be released is strongly dependent on the equilibrium partition coefficient, with  $t_{1/2}$  increasing with increasing flavor hydrophobicity, that is, increasing  $K_{OW}$ .

**Table 9.2** Influence of Droplet Radius and Oil–Water Partition Coefficient on the Time Taken for Half of the Flavor Molecules to Diffuse Out of Spherical Droplets Predicted Using the Crank Model.

$r(\mu\text{m})$	$K_{OW} = 1$	$K_{OW} = 10$	$K_{OW} = 100$	$K_{OW} = 1000$
$t_{1/2} \text{ (sec)}$				
0.1	$1.46 \times 10^{-6}$	$1.46 \times 10^{-5}$	$1.46 \times 10^{-4}$	$1.46 \times 10^{-3}$
0.2	$5.84 \times 10^{-6}$	$5.84 \times 10^{-5}$	$5.84 \times 10^{-4}$	$5.84 \times 10^{-3}$
0.5	$3.65 \times 10^{-5}$	$3.65 \times 10^{-4}$	$3.65 \times 10^{-3}$	$3.65 \times 10^{-2}$
1	$1.46 \times 10^{-4}$	$1.46 \times 10^{-3}$	$1.46 \times 10^{-2}$	$1.46 \times 10^{-1}$
2	$5.84 \times 10^{-4}$	$5.84 \times 10^{-3}$	$5.84 \times 10^{-2}$	$5.84 \times 10^{-1}$
5	$3.65 \times 10^{-3}$	$3.65 \times 10^{-2}$	$3.65 \times 10^{-1}$	3.65
10	$1.46 \times 10^{-2}$	$1.46 \times 10^{-1}$	1.46	14.6
20	$5.84 \times 10^{-2}$	$5.84 \times 10^{-1}$	5.84	58.4
50	$3.65 \times 10^{-1}$	3.65	36.5	365
100	1.46	14.6	146	1460

For relatively polar flavor molecules ( $K_{OW} \leq 1$ ), flavor release occurs extremely rapidly ( $t_{1/2} < 5$  sec) in emulsions containing droplets with radii less than about 100  $\mu\text{m}$ , hence one would not expect diffusion of this type of flavor molecule out of the emulsion droplets to be limiting. In addition, the flavor of polar flavor molecules is mainly due to their aqueous phase concentration, rather than their concentration in the oil phase. On the other hand, for relatively nonpolar molecules ( $K_{OW} \gg 1$ ), flavor release may occur quite slowly from relatively large droplets. For example,  $t_{1/2}$  is approximately 1.5 and 15 sec for  $K_{OW} = 100$  and 1000, respectively, in emulsions containing 10  $\mu\text{m}$  radius droplets. Diffusion of flavor molecules out of emulsion droplets may therefore become rate limiting in systems with relatively high  $K_{OW}$  and large droplet radius. In summary, it seems that the movement of flavor molecules from oil droplets into an aqueous phase will not be the rate-limiting step in flavor release providing the emulsion is well agitated and the droplets are relatively small, but may become rate limiting if the droplets are relatively large and the flavor molecules are highly nonpolar.

The Crank model for flavor release from emulsion droplets assumes that the rate-limiting step is the transport of flavor molecules through the droplets, that is, that there is no external resistance to mass transport from the surrounding continuous phase (Lian, 2000). Other models have been developed on the assumption that the rate-limiting step is the mass transport of the flavor in the continuous phase away from the droplet surface, for example, the Sherwood correlation (Lian, 2000). Recently, a more general model has been developed based on interfacial mass transfer theory that takes both of these limits into account (Lian, 2000). This theory can be used to provide a more detailed analysis of the influence of equilibrium partition coefficients, droplet size, diffusion coefficients, and fluid flow rates on flavor release within the mouth.

The droplets in food emulsions are normally coated by an interfacial membrane. It is possible that this membrane may act as a barrier to the mass transport of flavor molecules out of the emulsion droplets (Harvey et al., 1995). A number of experimental studies suggest that interfacial membranes formed from globular proteins may slow down diffusion of certain types of flavor molecules (Harvey et al., 1995; Landy et al., 1998; Rogacheva et al., 1999; Seuvre et al., 2002). Nevertheless, more theoretical and experimental work is needed to confirm this hypothesis. If mass transport of flavor across the interfacial membrane surrounding the droplets is rate limiting then it may be possible to design membranes to control the rate of flavor release. These systems may provide food manufacturers with a means of creating low fat food products with similar flavor release profiles as higher fat foods.

Another important factor that influences the rate of flavor release in many emulsion-based food systems is the breakup of the product within the mouth during mastication (Lian, 2000; Malone et al., 2000). For example, mastication of a gelled product containing emulsion droplets (e.g., a desert) leads to the production of relatively large gel particles, with each one containing an appreciable number of emulsion droplets (Gwartney et al., 2000). It has been shown experimentally that flavor (diacetyl and  $\delta$ -decalactone) release occurs more rapidly from emulsion gels containing low droplet concentrations (2.5% oil) when the food breaks down rapidly into small gel pieces during mastication, than when it breaks down into larger gel pieces (Gwartney et al., 2000). This was probably because the flavor molecules had a shorter distance to diffuse through the smaller pieces into the saliva than through the larger pieces (Malone et al., 2000; Malone and Appelqvist, 2003). Recently, interfacial mass transfer theories have been developed to predict the influence of gel particle size and oil droplet concentration on flavor release from gel particles containing emulsion droplets (Lian, 2000). These theories are similar to the ones described above for flavor release from emulsion droplets, except that it is assumed that the flavor is released from a spherical gel particle that can be characterized by an effective diffusion

coefficient ( $D_{ep}$ ) and an effective particle–fluid partition coefficient ( $K_{pf}$ ). The value of these effective parameters depends on the concentration of droplets within the gel particles, the oil–water partition coefficient, and the diffusion coefficients of the flavor molecules in the oil and aqueous phases. Theoretical predictions and experimental measurements show that the rate of flavor release from gelled emulsions with constant oil concentrations decreases as the size of the gel particles increases (Malone et al., 2000; Lian, 2000). This method of encapsulating oil droplets in gel particles has been proposed as an effective means of creating low fat emulsions with similar flavor release profiles as higher fat emulsions (Malone et al., 2000; Malone and Appelqvist, 2003).

### 9.3.3 Release of volatile compounds (aroma)

The release of volatile compounds from a food emulsion involves the mass transfer of the compounds from the emulsion to the vapor phase, and then into the nose where they can interact with the flavor receptors located within the nasal cavity (Overbosch et al., 1991; Harrison, 2000; de Roos, 2000). The aroma molecules may reach the nose directly by sniffing (orthonasally) a food prior to mastication or indirectly by being transported from the mouth to the nose via the connecting airways during mastication (retronasally). Mathematical models have been developed to describe both of these processes (de Roos, 2000). In this section, we will focus on the models developed to describe flavor release during mastication.

To a first approximation the aroma profile of a food can be characterized by the change in concentration of volatile flavor molecules within the headspace above an emulsion with time (Harrison and Hills, 1997a). Nevertheless, it should be noted that flavor molecules are selectively adsorbed by and differentially transported across the mucus membranes that line the airways and nasal cavity, which may mean that the time dependence of the flavor profile in the vapor phase does not precisely correspond to that at the flavor receptors within the nose (Harrison, 2000; Buettner et al., 2002).

#### 9.3.3.1 Flavor release from homogeneous liquids

One of the most comprehensive mathematical models developed to describe flavor release from liquids is derived from *penetration theory* (Harrison, 1998, 2000). This theory is based on the assumption that the rate-limiting step for flavor release is mass transport of the flavor molecules across the liquid–gas interface. It also assumes that the liquid is agitated so that mass transport of flavor molecules across the liquid–gas interface occurs through a combination of molecular diffusion and eddy diffusion. Agitation causes a small volume element (an *eddy*) of the liquid to move from within the bulk of the liquid to the liquid–gas interface. During the finite time that the volume element spends at the interface flavor molecules are transported into the gas phase due to molecular diffusion. The volume element then moves away from the interface where it is remixed with the bulk liquid. When a liquid is in contact with a fixed volume of gas, then the change in concentration of flavor molecules in the headspace above the liquid with time is given by the following equation:

$$c_G(t) = c_G(\infty) \left[ 1 - \exp\left(-\frac{\gamma A h_D t}{v_L}\right) \right] \quad (9.22)$$

where

$$\gamma = \left[ \frac{v_L}{K_{GL} v_G} + 1 \right] \quad \text{and} \quad c_G(\infty) = \frac{K_{GL} c_L(0) v_L}{K_{GL} v_G + v_L}$$

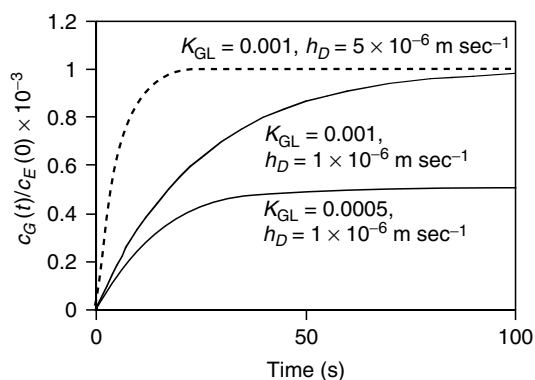


**Figure 9.9** Prediction of flavor release from homogeneous liquid assuming different gas–liquid partition coefficients ( $K_{GL}$ ) and mass transfer coefficients through the liquid ( $h_D$ ).

here  $c_G(t)$  is the concentration of flavor in the gas phase at time  $t$ ,  $c_G(\infty)$  is the concentration of the flavor in the gas phase when the system has reached equilibrium,  $c_L(0)$  is the initial concentration of flavor in the liquid,  $A$  is the liquid–gas surface area,  $h_D$  is the mass transfer coefficient in the liquid,  $v_L$  is the volume of the liquid, and  $v_G$  is the volume of gas in the headspace above the liquid. The predicted influence of  $K_{GL}$  and  $h_D$  on the rate of flavor release from homogeneous liquids is shown in Figure 9.9. The rate of flavor release is independent of  $K_{GL}$  at short times, but increases as the flavor compounds become more volatile ( $K_{GL}$  increases) at longer times. As would be expected, the flavor release rate decreases as the flavor molecules move more slowly through the liquid ( $h_D$  decreases).

A measure of the rate of flavor release can be obtained by calculating the time for the headspace concentration of flavor molecules to reach half the final equilibrium value using the above equations:

$$t_{1/2} = \frac{v_L \ln 2}{\gamma A h_D} = \frac{\ln 2}{A h_D (1/K_{GL} V_G + 1/V_L)} \quad (9.23)$$

The predicted dependence of  $t_{1/2}$  on the volatility ( $K_{GL}$ ) and mass transfer coefficient ( $h_D$ ) of the flavor molecules in the liquid is shown in Figure 9.10. As the volatility of the flavor molecule increases or their mass transfer coefficient through the liquid decreases, the rate of flavor release decreases, that is,  $t_{1/2}$  increases.

In summary, the penetration theory predicts that the rate of flavor release from a good solvent ( $K_{GL}$  low) is much slower than the rate from a poor solvent ( $K_{GL}$  high). Thus, a nonpolar flavor will be released more slowly from a nonpolar solvent than a polar solvent and vice versa. This accounts for the fact that the ranking of the release rates of flavors from water is opposite to that from oil (Overbosch et al., 1991). It also indicates that anything that decreases the diffusion coefficient of the flavor molecules in the liquid should decrease the release rate, for example, increasing the viscosity of the liquid or the size of the flavor molecules.

In reality, the gas above a liquid food does not maintain a fixed volume within the mouth during the mastication process, since there is gas flow due to respiration and swallowing (Thomson, 1986; Harrison and Hills, 1997b). When the flavor is constantly swept away from the surface of the food, the concentration gradient of flavor at the surface is increased and so the rate of flavor loss is more rapid than under nonflow conditions.

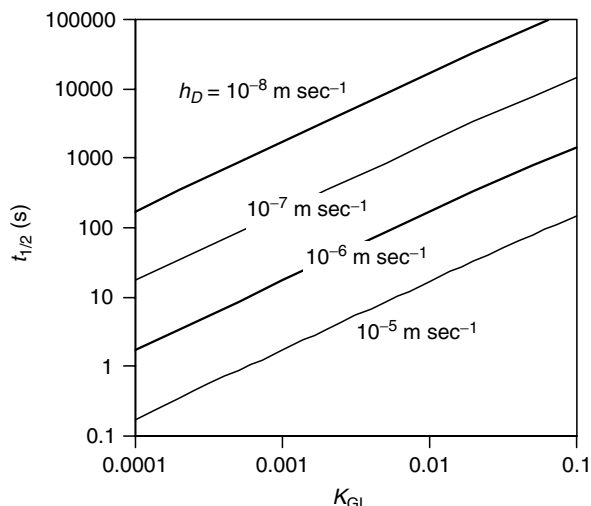


**Figure 9.10** Dependence of the time for the headspace concentration of flavor molecules to reach half the final equilibrium value ( $t_{1/2}$ ) on the gas-liquid partition coefficient ( $K_{GL}$ ) and mass transfer coefficient ( $h_D$ ) of flavor molecules in a liquid.

The penetration theory has been extended to include the influence of gas flow on flavor release from liquids (Harrison and Hills, 1997b; Harrison, 1998):

$$c_G(t) = \frac{Ah_D c_L(0)}{v_G} \left[ \frac{\exp(-s_+ t) - \exp(-s_- t)}{s_+ - s_-} \right]$$

$$s_{\pm} = \frac{\alpha}{2} \pm \frac{\sqrt{\alpha^2 - 4\beta}}{2} \quad (9.24)$$

$$\alpha = \frac{Q}{v_G} + \frac{Ah_D}{v_G K_{GL}} + \frac{Ah_D}{v_L} \quad \beta = \frac{QAh_D}{v_G v_L}$$

Here,  $Q$  is the gas flow rate. This equation reduces to Equation 9.22 when there is no gas flow, that is,  $Q = 0$ . Penetration theory provides valuable insights into the physicochemical factors that influence flavor release from homogeneous liquids, for example, initial flavor concentration in the fluid, gas-fluid partition coefficients, and mass transfer coefficients. The variation of the headspace concentration with time calculated using penetration theory (Equation 9.24) for flavor release from a liquid in the presence of gas flow is shown in Figure 9.11. There is a rapid initial increase in flavor concentration in the headspace until a maximum value is reached. The headspace concentration then decreases with time as flavor molecules are depleted from the emulsion. It is convenient to characterize this kind of dynamic flavor release profile in terms of a maximum intensity ( $I_{MAX}$ ) and the time required to reach the maximum intensity ( $t_{MAX}$ ). An equation for  $t_{MAX}$  can be derived from Equation 9.24 by finding the point where  $dc_G(t)/dt = 0$  (Harrison and Hills, 1997b):

$$t_{MAX} = \frac{1}{s_- - s_+} \ln \left( \frac{s_-}{s_+} \right) \quad (9.25)$$



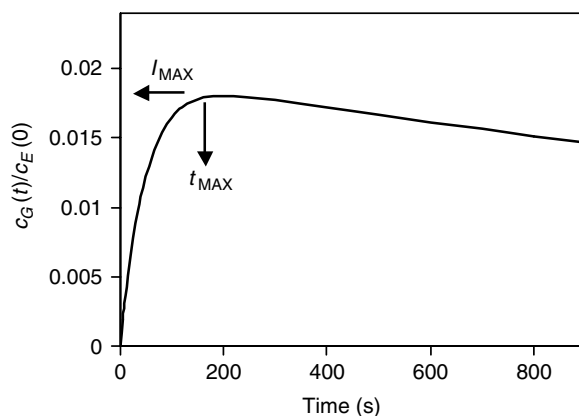


**Figure 9.11** Predicted variation of the headspace concentration of a flavor molecule with time calculated using penetration theory for flavor release from a liquid in the presence of gas flow (Harrison and Hills, 1997b).

The value of the maximum flavor intensity can then be determined by inserting this time into Equation 9.24,  $I_{\text{MAX}} = c_G(t_{\text{MAX}})$ . Theoretical predictions have shown that  $t_{\text{MAX}}$  becomes shorter with increasing gas flow rate and increasing mass transfer coefficient (Harrison and Hills, 1997b). They have also shown that  $I_{\text{MAX}}$  is proportional to the initial concentration of flavor in the liquid, and decreases with increasing gas flow rate. A concerted research effort is currently being devoted to correlating the values of  $I_{\text{MAX}}$  and  $t_{\text{MAX}}$  determined using analytical techniques to similar values determined by time-intensity sensory analysis (Moore et al., 2000; Hollowood et al., 2000).

Recently, the penetration model has been extended to include a variety of other physicochemical processes that occur during mastication, such as breathing, saliva flow, and breakup of solid food into pieces (Harrison and Hills, 1997b; Harrison et al., 1998; Harrison, 1998, 2000). The penetration theory is only one mathematical approach that can be used to describe flavor release from liquids. Other theories have been developed assuming that the flavor transport through the various phases is either due to diffusion or convection (Overbosch et al., 1991; Banavara et al., 2002). A completely different approach is to use quantitative structure property relationships (QSPR) to statistically correlate some measurable parameter (such as  $I_{\text{MAX}}$  or  $t_{\text{MAX}}$ ) to the physicochemical properties of the flavor molecules involved (such as molecular weight, octanol–water partition coefficient, or vapor pressure) (Taylor and Linforth, 2001; Linforth et al., 2000). In the QSPR approach the liquid is treated as a “black box” since none of the physicochemical processes involved in flavor release are explicitly considered. Consequently, new correlations must be established for each new system, which is the main limitation of this approach.

### 9.3.3.2 Influence of ingredient interactions

A number of ingredients commonly found in food emulsions are capable of decreasing the rate of flavor release because of their ability to bind flavors, solubilize flavors, or retard the mass transfer of flavors, for example, proteins, carbohydrates, and surfactant micelles (Overbosch et al., 1991; Guichard, 2002). The penetration theory described in the previous section has been extended to take into account the effect of reversible binding of flavor molecules to biopolymers (or other flavor binders) on flavor release from liquids (Harrison and Hills, 1997b). If it is assumed that the interaction between the flavor molecule and

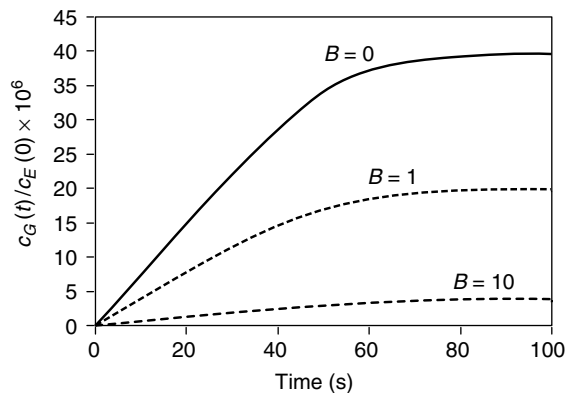


**Figure 9.12** Predicted variation of the headspace concentration of a flavor molecule with time calculated using penetration theory for flavor release from a liquid containing different substances that can bind the flavors, as characterized by the parameter  $B$  (Harrison and Hills, 1997b).

biopolymer is in equilibrium, then the penetration theory predicts the rate of flavor release to be:

$$c_G(t) = \frac{c_L(0)(K_{GL} + v_G/v_L)}{(1 + K_b c_b)} \left[ 1 - \exp \left( - \frac{A h_D}{v_G} \left( \frac{1}{K_{GL}} + \frac{v_G}{v_L} \frac{1}{1 + K_b c_b} \right) t \right) \right] \quad (9.26)$$

where  $K_b$  and  $c_b$  are the binding constant and concentration of the biopolymer, respectively (see Equation 9.8). The above equation provides valuable insights into the physicochemical properties that influence flavor release in the presence of biopolymers (Harrison and Hills, 1997b). As would be expected, the amount of flavor released and the rate of flavor released from a liquid into the headspace is reduced when the biopolymer concentration or binding constant increases (i.e.,  $B = K_b c_b$  increases) because there is a smaller fraction of free flavor available for release (Figure 9.12). The above model is based on release of flavor into the headspace in the absence of gas and saliva flow. The penetration model has been extended to take into account the influence of breathing and saliva flow on flavor release from liquids containing biopolymers that bind flavors (Harrison, 1998).

The release rate may also be reduced because of the ability of certain food ingredients to retard the movement of flavor molecules to the surface of the liquid, which may be due to an enhanced viscosity or due to structural hindrance (Kokini, 1987; Harrison and Hills, 1997a,b; Harrison, 1998; Nahon et al., 2000). The translational diffusion coefficient of a molecule is inversely proportional to the viscosity of the surrounding liquid, and so increasing the viscosity of the liquid will decrease the rate of flavor release because the diffusion of the flavor molecules is reduced. Nevertheless, it is important to be aware that the microscopic viscosity experienced by a small molecular moving through a solution may be very different to the macroscopic viscosity of the bulk solution (Nahon et al., 2000; Walstra, 2003a). For example, sugar molecules move through xanthan solutions at almost the same rate as they move through pure water, even though the macroscopic viscosity of the xanthan solutions (measured at low shear rates) is many orders of magnitude greater than that of water, because the pores between the biopolymer network are much greater than the size of the sugar molecule (Basaran et al., 1998). Even so, highly concentrated or aggregated biopolymer networks may provide a physical barrier through which flavor molecules cannot directly pass, so that they have to take a tortuous path through the

network which increases the time taken for them to reach the surface (Walstra, 2003a). The penetration theory involves both molecular and eddy diffusion and the molecules and eddies may experience different solution viscosities depending on their size and rate of movement. It is for this reason that it is often difficult to calculate the mass transfer coefficient used in the penetration theory from first principles (Harrison, 1998). If flavor molecules are reversibly associated with surfactant micelles their release rate will depend on the diffusion coefficient of the micelles, as well as the kinetics of micelle breakdown (Section 4.4.1).

Highly volatile flavors (high  $K_{GL}$ ) are most affected by viscosity or structural hindrance effects because the rate-limiting step in their release from a food is the movement through the liquid, rather than the movement away from the liquid surface (Overbosch et al., 1991). On the other hand, low volatile flavors (low  $K_{GL}$ ) are affected less, because the rate-limiting step in their release is the movement away from the liquid surface, rather than through the liquid (Roberts et al., 1996).

A great deal of research has been carried out to establish the relative importance of binding and retarded mass transfer mechanisms for various systems (Hau et al., 1996; Guichard, 1996; Roberts et al., 1996). In some systems it has been suggested that rheology is the most important factor because the rate of flavor release decreased as the viscosity of a biopolymer solution or the strength of a biopolymer gel increased (Baines and Morris, 1989; Carr et al., 1996). In other systems it has been suggested that flavor binding is more important in reducing the flavor release rate (Guichard, 1996). In practice, it is likely that both flavor binding and restricted mass transport mechanisms will play an important role in reducing flavor release rates in many foods (Bakker et al., 1998; Guichard, 1996, 2002). Nevertheless, more systematic research is needed to establish the precise role of biopolymers and other ingredients in retarding flavor release in real food systems. The influence of ingredient interactions on release rates has important consequences for the formulation of many food products. For example, it may be necessary to incorporate more flavor into a food to achieve the same flavor intensity when the biopolymer concentration is increased, or it may be possible to add a biopolymer that binds an off-flavor.

### 9.3.3.3 Flavor release from emulsions

The penetration theory described above has also been used to model the rate of flavor release from emulsions (Harrison and Hills, 1997b; Harrison et al., 1997; Harrison, 1998). This theory is based on the assumption that the rate-limiting step for flavor release is the transfer of volatiles across the emulsion–gas boundary, and that the partitioning of flavor molecules between the oil and aqueous phases is extremely rapid compared to the transport across the emulsion–gas boundary. An estimate of the rate-limiting step for flavor release can be obtained by comparing the release times for movement of flavor molecules across the liquid–air interface (Figure 9.10), with the release times for movement of flavor molecules out of the droplets (Table 9.2). The physicochemical process with the longer release time ( $t_{1/2}$ ) for a particular system (e.g.,  $K_{GL}$ ,  $K_{OW}$ ,  $h_D$ ,  $r$ ) will be the rate-limiting step. Under most circumstances the rate-limiting step is the movement of flavor molecules across the liquid–gas interface. However, for highly nonpolar flavors ( $K_{OW} \geq 100$ ), the rate-limiting step may be diffusion of flavor molecules out of the droplets, provided that the droplets are relatively large ( $r \geq 5 \mu\text{m}$ ), the volatility of the flavors is relatively low ( $K_{GL} \leq 0.01$ ), and the mass transfer coefficient of the flavor through the liquid is relatively fast ( $h_D \geq 10^{-6} \text{ m sec}^{-1}$ ). It therefore appears that for most practical situations the penetration theory should provide a good estimate of the flavor release rate from emulsions.

The same equations (based on penetration theory) can be used to describe the kinetics of flavor release from emulsions as were used to describe flavor release from homogeneous liquids (Section 9.3.3.1), except that the physical characteristics of the homogeneous

liquids ( $h_D$ ,  $K_{GL}$ ) are replaced with equivalent values for the emulsion ( $h_D(\phi, r)$ ,  $K_{GE}$ ). The values of the mass transport coefficient and the gas–liquid equilibrium partition coefficient for an emulsion depend on its composition and microstructure, as well as the physicochemical characteristics of the component phases, for example, polarity, viscosity (Harrison and Hills, 1997). The following expressions have been given for these parameters for simple oil-in-water emulsions (Harrison, 1998):

$$K_{GE} = \frac{K_{GC}}{1 + (K_{DC} - 1)\phi} \quad (9.27)$$

$$h_D(\phi, r) = h_D(0) \exp \left[ -1.57 \times 10^{-6} \frac{\phi}{r} \right] \quad (9.28)$$

here  $h_D(0)$  is the mass transfer coefficient of a particular flavor molecule through the continuous phase. Typically,  $h_D(0)$  has a value around  $2.5 \times 10^{-6} \text{ m sec}^{-1}$  (Harrison, 1998). In practice, the value of  $h_D(\phi, r)$  depends on the precise nature of the emulsion system, and often has to be determined experimentally. The influence of disperse phase volume fraction on the time dependence of the flavor concentration in a headspace with gas flow above model oil-in-water emulsions is shown in Figure 9.13. In this example, the flavor molecules are assumed to be relatively nonpolar and volatile ( $K_{OW} = 10$ ;  $K_{GW} = 1 \times 10^{-3}$ ). Initially, the concentration of flavor in the headspace increases rapidly until a maximum value is reached ( $I_{MAX} = c_G(t_{MAX})$ ) at time  $t_{MAX}$ , after which there is a slight decrease in the headspace flavor concentration due to the overall loss of flavor from the emulsion. As the oil concentration in the emulsions increases, there is a decrease in the maximum flavor intensity reached, but the time to reach the maximum intensity does not change appreciably (Figure 9.13). The predicted dependence of  $I_{MAX}$  and  $t_{MAX}$  on droplet concentration for oil-in-water emulsions containing model polar ( $K_{OW} = 0.1$ ) and nonpolar ( $K_{OW} = 10$ ) flavor molecules assumed to have the same volatility in water ( $K_{GW} = 1 \times 10^{-3}$ ) is shown in Figure 9.14. For the nonpolar flavor there is a rapid decrease in the maximum flavor

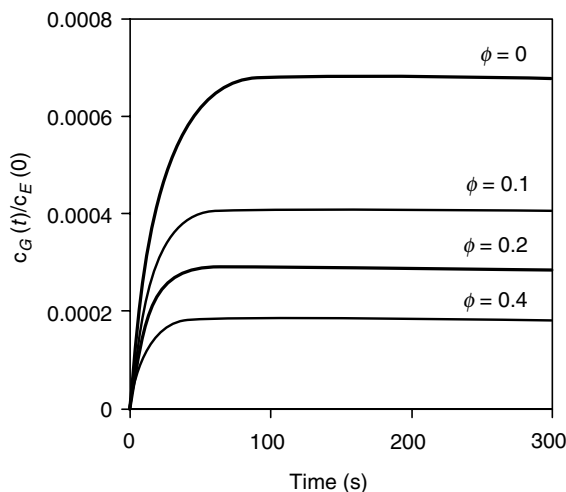


**Figure 9.13** Predicted influence of droplet concentration on flavor release from oil-in-water emulsion containing model nonpolar ( $K_{OW} = 10$ ,  $K_{GW} = 0.001$ ) flavor molecules.

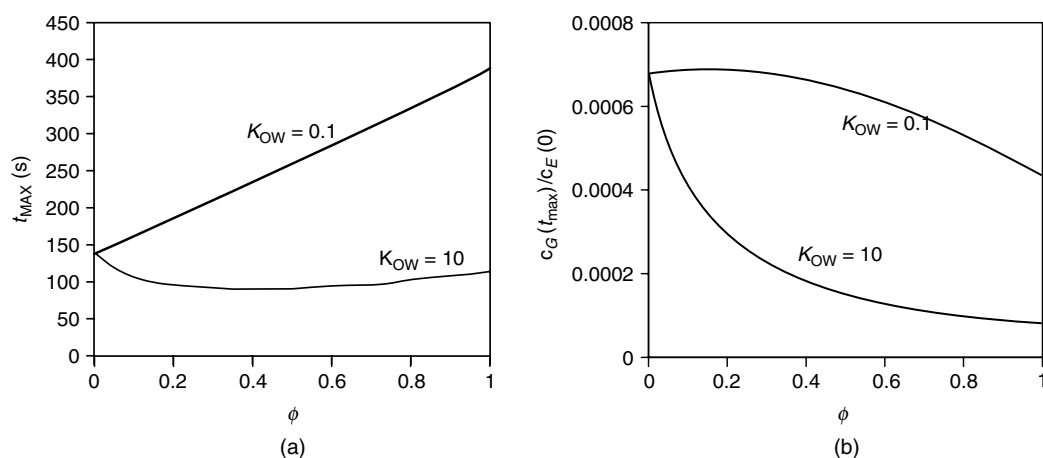


**Figure 9.14** Predicted influence of disperse phase volume fraction on (a) release time ( $t_{MAX}$ ) and (b) maximum flavor intensity ( $c_G(t_{MAX})$ ) for oil-in-water emulsions containing model polar ( $K_{OW} = 0.1$ ,  $K_{CW} = 0.001$ ) and nonpolar ( $K_{OW} = 10$ ,  $K_{CW} = 0.001$ ) flavor molecules predicted using penetration theory. The other parameters used in the model were:  $r = 1 \mu\text{m}$ ,  $h_D(0) = 2.5 \times 10^{-6} \text{ m sec}^{-1}$ ,  $V_G = 35 \text{ cm}^3$ ,  $V_E = 5 \text{ cm}^3$ ,  $A = 4.5 \text{ cm}^2$ , and  $Q = 30 \text{ ml min}^{-1}$ .

intensity as the oil concentration is increased from 0 to 30%, followed by a slower decrease at higher oil concentrations (Figure 9.14b). For the polar flavor the maximum flavor intensity only decreases appreciably at relatively high oil concentrations (>70%). The time to reach the maximum intensity is relatively insensitive to droplet concentration for the nonpolar flavor, but increases appreciably with increasing  $\phi$  for the polar flavor (Figure 9.14a). This obviously has important consequences for the development of reduced fat foods with similar profiles as full fat analogs. The above theory has recently been extended to take into account the effects of dilution of an emulsion by saliva within the mouth (Harrison, 1998).

The penetration theory provides many useful insights into the factors that determine flavor release in emulsions (Harrison and Hills, 1997b; Harrison, 1998):

- Initial rates of flavor release in the headspace above an emulsion decrease with increasing oil concentration, decreasing mass transfer coefficient (and hence increasing emulsion viscosity), and decreasing emulsion-headspace contact area.
- The maximum flavor concentration ( $I_{MAX}$ ) attained in the headspace is proportional to the initial flavor concentration in the emulsion, and decreases with increasing gas and saliva flow rates. The value of  $I_{MAX}$  also depends on the oil-water partition coefficient ( $K_{OW}$ ), decreasing as the flavor molecules become more nonpolar. The value of  $I_{MAX}$  usually decreases with increasing fat content, but in some situations it may increase depending on the precise values of  $K_{OW}$  and  $K_{CW}$  (Harrison and Hills, 1997b).
- The time to reach the maximum flavor concentration ( $t_{MAX}$ ) decreases with increasing gas and saliva flow rates, with the effect being more pronounced for nonpolar flavors (Harrison and Hills, 1997b). The penetration theory predicts that  $t_{MAX}$  usually decreases (faster release) with decreasing oil concentration and increasing droplet size (Harrison and Hills, 1997b), because mass transport of flavor molecules through the emulsion is hindered due to the resulting increase in emulsion viscosity (Harrison et al., 1997).

It should be noted that different flavor molecules have different partition coefficients and mass transport coefficients, so that they will be released at different times and intensities depending on emulsion composition and microstructure, as well as mastication conditions (gas flow, saliva flow, product breakup). The balance of a flavor profile may therefore change considerably over time, which will alter the flavor perceived by a consumer.

The above equations predict that the release rate from an oil-in-water emulsion will be different to that from a water-in-oil emulsion with the same composition, because of the differences in the value of  $h_D(0)$  used to calculate  $h_D(\phi, r)$  for the oil and water phases. Some studies have shown that the release rate is faster from oil-in-water emulsions than from water-in-oil emulsions, which would be expected because flavor molecules should travel faster through water than oil (Overbosch et al., 1991; Bakker and Mela, 1996). Nevertheless, other studies have indicated that the taste perception of oil-in-water and water-in-oil emulsions of the same composition is approximately the same (Barylko-Pikielna et al., 1994; Brossard et al., 1996). This may be because water-in-oil emulsions rapidly break down to oil-in-water emulsions during mastication (Bakker and Mela, 1996).

## 9.4 Emulsion mouthfeel

The term "mouthfeel" describes a variety of tactile sensations that are experienced within the mouth during food mastication, such as "creamy," "thick," "thin," "rich," "smooth," "slimy," and "watery." As such, it plays a major role in determining the perceived quality of many emulsion-based food products (Mela et al., 1994; Malone et al., 2003a,b). Mouthfeel is mainly the result of interactions between the contents of the mouth during mastication (food and saliva) and receptors within the mouth that respond to tactile stimuli (Smith and Margolskee, 2001). A fundamental understanding of the relationship between the mouthfeel of food products and their composition and microstructure is difficult because of the complexity of the physicochemical, physiological, and psychological processes involved (Malone et al., 2003a,b). After a food is ingested, it undergoes a variety of compositional, structural, and rheological modifications within the mouth prior to being swallowed because of temperature changes, dilution with saliva, and exposure to compressive, shearing, and tensile forces. The perceived mouthfeel of a food product is believed to be primarily determined by a combination of colloidal, bulk rheological, and thin-film rheological behavior (Malone et al., 2003a; van Aken, 2004). Nevertheless, visual and auditory cues may also contribute to the perceived mouthfeel of a product, for example, the appearance of a food or the sound it makes during mastication.

The mouthfeel of food emulsions has been shown to be strongly influenced by the type, concentration, and interactions of the colloidal particles and macromolecules present (Roland et al., 1999; Frost et al., 2001; Clegg et al., 2003; Kilcast and Clegg, 2002; Wendin and Hall, 2001). The perceived "fattiness," "creaminess," and "thickness" of oil-in-water emulsions has been found to increase as the droplet concentration increases (Mela et al., 1994; Moore et al., 1998; Wendin and Hall, 2001; Kilcast and Clegg, 2002). The creaminess of oil-in-water emulsions was also found to depend on droplet size, which was partly attributed to the associated change in emulsion viscosity (Mela et al., 1994; Clegg et al., 2003; Terpestra et al., 2003). Creaminess has also been found to depend on the type of emulsifier used to stabilize the droplets, possibly due to differences in their impact on droplet flocculation and emulsion viscosity (Moore et al., 1998). Previous studies indicate that there is a strong correlation between perceived creaminess and emulsion viscosity; however, these studies also suggest that other factors that depend on droplet characteristics are important (Moore et al., 1998;

Wendin and Hall, 2001). Products with reduced fat contents may contain “fat-replacers” that are designed to provide a mouthfeel similar to that of the conventional full fat product. These fat replacers are often designed to have characteristics that are similar to the emulsion droplets in conventional products. For example, spherical particles (0.1–20  $\mu\text{m}$ ) have been formed using biopolymer aggregates made from proteins and/or polysaccharides to mimic emulsion droplets (Leverbre et al., 1993). Another contribution to mouthfeel that may be important during consumption of some food emulsions is the cooling sensation associated with melting of emulsified fat in the mouth due to the endothermic enthalpy change associated with fat crystal melting (Walstra, 1987). Recently, it has been shown that the breakdown of fat droplets within the mouth and the ability of the released fat to coat the tongue may also play an important role in determining the mouthfeel of emulsions (van Aken, 2004).

Biopolymers, such as polysaccharides or proteins, are often added to food emulsions as stabilizers or texture modifiers (Dickinson and Stainsby, 1982; Mitchell and Ledward, 1986; Dickinson, 1992, 2003; Phillips and Williams, 1995, 2003). The type and concentration of biopolymers present, as well as their interactions with each other, influences the microstructure, thin-film rheology, and bulk rheology of emulsions (Dickinson, 1992; Grotenhuis et al., 2000; Malone et al., 2003a). The perceived mouthfeel of food emulsions is normally changed by the presence of biopolymers that influence their microstructure and texture (Pettitt et al., 1995; Wendin et al., 1997a,b, 1999). The relationship between the rheological properties of aqueous biopolymer solutions and their perceived mouthfeel has been reviewed (Morris, 1995b). It has been shown that there is a strong correlation between the perceived “thickness,” “stickiness,” and “sliminess” of polysaccharide solutions and their shear viscosity or modulus measured under shear conditions representative of those in the mouth (Morris, 1995b; Malone et al., 2003a). In general, the shear rates experienced by foods within the mouth depend on the foods’ unique rheological characteristics, and may vary from 5 to 50  $\text{sec}^{-1}$ . As a simple rule of thumb, it has been suggested that shear rates of 10  $\text{sec}^{-1}$  for large-deformation shear viscosity measurements or 50  $\text{rad sec}^{-1}$  for small-deformation dynamic shear modulus measurements give a reasonable representation of mouth conditions. It has been suggested, that the small-deformation measurements often give a better correlation to initial perceived mouthfeel because they do not cause appreciable breakdown of the food microstructure. Polysaccharides have also been shown to reduce the perceived “flavor intensity” of flavored aqueous solutions, which has been attributed to their ability to suppress the mixing of the food within the mouth.

The ability of biopolymers to alter emulsion rheological characteristics may also influence the way that an emulsion coats the surface of the mouth during mastication (Michalski et al., 1998; Malone et al., 2003a). Biopolymers may also influence the force required to deform and disrupt gelled emulsions into smaller fragments within the mouth (Gwartney et al., 2000; Malone et al., 2000).

At present our understanding of the physicochemical basis of the mouthfeel of food emulsions is still rather limited. It is clear that more systematic research is needed to establish the influence of emulsion characteristics, such as droplet size, droplet concentration, droplet-droplet interactions, oil type, and aqueous phase composition, on the mouthfeel of food emulsions. Such studies will require a combination of sensory analysis and instrumental measurements of the properties of emulsions with various compositions and microstructures. Some of the major factors that need to be studied in more detail have recently been identified: (1) the initial rheology and mechanical properties of the food being consumed; (2) the changes in food properties during mastication; (3) the influence of food microstructure and composition on flavor partitioning and release; (4) the physiology of the mouth; and (5); food-mouth interactions (Malone et al., 2003a; van Aken, 2004).

## 9.5 Measurement of emulsion flavor

Major advances have been made in the experimental characterization of the flavor of food emulsions during the past few years, especially in the development of analytical techniques that simulate the complex processes that occur during mastication, such as breathing, chewing, and saliva flow (Marsili, 1997; Odake et al., 1998, 2000; Steinhart et al., 2000; Taylor and Linforth, 2000). In this section, analytical techniques that can be used to measure equilibrium partition coefficients and flavor release kinetics in emulsions are reviewed.

### 9.5.1 Analysis of volatile flavor compounds

Aroma is the result of interactions between receptors in the nose and volatile flavor molecules released from the food into the gaseous phase above the food. Information about food aroma is therefore usually obtained by analyzing the type and concentration of volatile flavor compounds in the headspace above a food (Franzen and Kinsella, 1975; O'Neil, 1996; Landy et al., 1996; Guyot et al., 1996; Steinhart et al., 2000; Stephan et al., 2000). Headspace analysis can be carried out using a variety of different methods depending on the information required and the sophistication of the instrumentation used, including equilibrium, kinetic, and *in vivo* analysis methods (Taylor and Linforth, 2000; Steinhart et al., 2000; Stephan et al., 2000; van Ruth, 2001; van Ruth and O'Connor, 2001a,b; Dattatreya et al., 2002; Rabe et al., 2002, 2003).

#### 9.5.1.1 Equilibrium measurements

Static headspace analysis is primarily used to determine the equilibrium partition coefficient of a flavor compound between a liquid and the headspace above it. The liquid to be analyzed is placed in a sealed container that is stored under conditions of constant temperature and pressure. Samples of the gas phase are removed from the headspace using a syringe (or other device) that is inserted through the lid of the sealed container, and the concentration of flavor is measured, usually by gas chromatography (GC) or high performance liquid chromatography (HPLC). Information about the type of flavor molecules present in the headspace can be determined after they have been separated by GC or HPLC, either by comparing the retention times of the chromatogram peaks with known standards or by analyzing each of the peaks using an analytical technique that provides information about chemical structure, for example, NMR or mass spectrometry. The concentration of volatile flavors in many foods is too low to be detected directly by conventional chromatography techniques, and therefore it is necessary to preconcentrate the samples prior to analysis (Taylor and Linforth, 2000). This can be achieved by collecting the volatiles on adsorbent materials or solid-phase microextraction (SPME) fibers (Adams et al., 2001; Fabre et al., 2002; Jung and Ebeler, 2003; Roberts et al., 2003). The concentrated volatiles are then desorbed from these materials and analyzed using conventional chromatography methods. Another way of increasing the amount of volatile flavor molecules collected from a sample is to store it for a certain length of time (to allow the flavor molecules to move into the headspace) and then rapidly remove all the headspace gasses by flushing an inert gas through the collection chamber. This method is based on the principle that the removal of headspace gases from the sample cell is much faster than the movement of flavor molecules from the emulsion into the headspace. Potential problems that need to be considered when measuring partition coefficients of flavor molecules by headspace analysis have been discussed (Taylor, 1998).

General information about the overall flavor profile above a food can be obtained using analytical instruments called "electronic noses." These devices were developed to simulate the response of human sensory receptors to food flavor (Linforth, 2000;



Steinhart et al., 2000; Stephan et al., 2000; Miettinen et al., 2002). Electronic noses consist of an array of different sensors that generate electronic signals when they interact with flavors that the human nose is sensitive to. Each individual sensor responds to many different kinds of flavor molecules, but the intensity of the signal produced depends on molecular type, as well as molecular concentration. The pattern of signal intensities produced by the different sensors within an electronic nose provides a means of discriminating samples based on differences in their flavor profiles. Electronic noses are therefore suitable for comparing the flavor profiles of different samples, rather than for providing quantitative data about flavor concentrations or qualitative data about the type of flavor molecules present in a food (Hodgins, 1997).

#### 9.5.1.2 Kinetic measurements

Headspace analysis can also be carried out by analyzing samples of headspace over time to monitor the kinetics of flavor release from a sample stored in a measurement cell (Taylor et al., 2000; Harvey et al., 2000; Dattatreya et al., 2002). Special measurement cells have been developed to mimic the influence of saliva dilution, temperature, and shearing on flavor release into the headspace (Roberts and Acree, 1995). The same analytical procedures can then be used to determine the type and concentration of flavor compounds in the headspace as is used in the equilibrium analysis methods described above, for example, chromatography, mass spectrometry, NMR, electronic nose. Nevertheless, the concentrations of volatiles collected for analysis in dynamic methods are usually smaller than for static methods since the samples are collected over a shorter time period, and therefore the use of preconcentration techniques is often more important (Taylor and Linforth, 2000). Recently, analytical techniques have been developed that enable real-time measurement of changes in flavor profile with time (Taylor and Linforth, 2000; Harvey et al., 2000; Malone et al., 2000). In these techniques the headspace is continuously collected and fed to a specially designed mass spectrometer for analysis of the type and concentration of flavor molecules present.

Measurement of the time dependence of flavor release is believed to provide a more accurate representation of the sensory perception of foods, since human perception systems have evolved to be more sensitive to detecting changes in flavor rather than to detecting absolute values (Dijksterhuis and Piggot, 2000).

#### 9.5.1.3 In vivo headspace analysis

There has been considerable progress in the development of analytical instruments that can measure the change in flavor profiles of foods during mastication by human beings (Taylor and Linforth, 2000; Harvey et al., 2000). The basic requirements for successful development of this type of technique have recently been discussed, for example, sensitivity, specificity, speed, and design of instrument-human interface (Taylor and Linforth, 2000). Application of these *in vivo* methods is providing important new insights into the factors that influence the flavor profiles of food emulsions during consumption (Malone et al., 2000). In these instruments, the gas phase is normally collected from the nose of a human subject before, during, and after food mastication by attaching a collection tube to one of the nostrils. As with kinetic methods, aliquots of gas phase can be collected periodically for later analysis or the gas phase can be analyzed continuously using specially designed mass spectrometers (Taylor and Linforth, 2000). *In vivo* methods provide a more accurate representation of the complex processes occurring during food consumption than conventional kinetic methods (Grab and Geffler, 2000). Application of these techniques have shown that different flavor molecules are released at different times, depending on their physicochemical characteristics, the structure and composition of the

food matrix, and the mastication conditions (Taylor and Linforth, 2000; Harvey et al., 2000; Malone et al., 2000). There is considerable emphasis in the field of flavor research on correlating the results of *in vivo* headspace analysis with sensory time-intensity measurements (Malone et al., 2000).

### 9.5.2 Analysis of nonvolatile flavor compounds

The taste of a food is usually determined by specific types of nonvolatile molecules present in the saliva during mastication. Analytical characterization of food taste is therefore usually based on measurements of the type and concentration of nonvolatile flavors present in aqueous solutions. In emulsions, the taste molecules partition between the oil and aqueous phases, and therefore analytical characterization of food taste in these systems often involves measurements of the oil–water partition coefficients and oil-to-water release rates of flavor molecules. A variety of analytical methods have been developed to provide this kind of information.

#### 9.5.2.1 Equilibrium measurements

The equilibrium partition coefficient of a flavor between a bulk oil and bulk water phase can be determined by measuring the concentration of flavor in the two phases after the system has been left long enough to attain equilibrium (McNulty, 1987; Guyot et al., 1996; Huang et al., 1997). The flavor is usually added to one of the liquids first, and then the water phase is poured into the container and the oil phase is poured on top (Figure 9.15). The container is sealed and stored in a temperature-controlled environment until equilibrium is achieved, which can be a considerable period (a few hours, days, or weeks), although this time can be shortened by mild agitation of the sample. The concentration of flavor molecules in the oil and water phases is then measured. The method used to determine flavor type and concentration depends on the nature of the flavor molecule. The most commonly used techniques are spectrophotometry, chromatography, mass spectrometry, radio-labeling, and electrophoresis. As with headspace analysis the type of flavor molecules present in a liquid can be determined using NMR or mass spectrometry once the flavor molecules have been separated by electrophoresis or chromatography techniques. In some systems it is possible to analyze the solutions directly, whereas in others it is necessary to extract the flavors first using appropriate solvents.

The partition coefficient of flavors in emulsions can be determined using a similar procedure. A flavor component can be added to either the bulk oil or bulk aqueous phase prior to homogenization (providing it is not lost during emulsion preparation) or it can

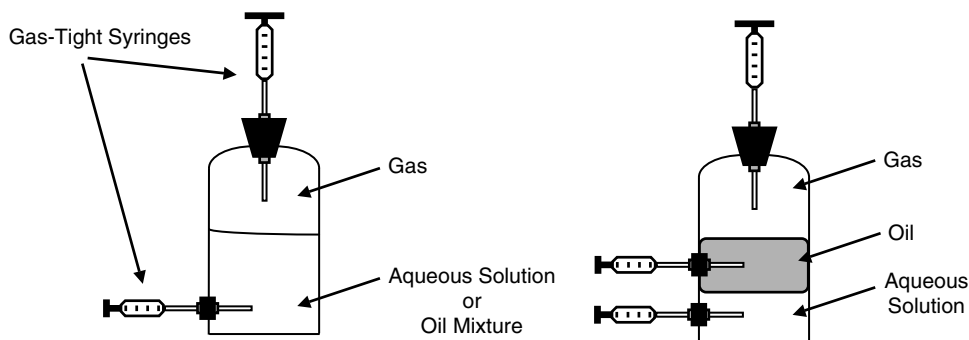


**Figure 9.15** Diagram of stirred diffusion cells used to measure the kinetics of flavor release in liquids and emulsions.

be added to the continuous phase of a preformed emulsion. The emulsion to be analyzed is then placed into a container, which is filled to the top and sealed to prevent flavor partitioning into the vapor phase. It is then stored in a temperature-controlled environment until it reaches equilibrium. Equilibrium is attained much more rapidly in an emulsion than in a nonemulsified system because flavor molecules only have to diffuse a relatively short distance through the droplets. The emulsion is centrifuged or filtered to separate the droplets from the continuous phase, and then a sample of the continuous phase is removed for analysis of the flavor concentration. The partition coefficient can then be determined from knowledge of the flavor concentration in the continuous phase and in the whole emulsion:  $K_{DC} = c_D/c_C = (c_{\text{total}} - c_C)/c_C$ . Alternatively, an emulsion containing flavor molecules can be placed in a dialysis cell (or bag) with a membrane that allows flavor molecules to freely pass through, but not emulsion droplets. The system is then allowed to come to equilibrium and the concentration of flavor molecules outside the dialysis cell is measured. The equilibrium partition coefficient could then be determined from this information and knowledge of the total flavor and droplet concentration in the emulsion. One important limitation of these techniques is that they cannot distinguish between flavor that is contained within the droplets and that which is associated with the interfacial membrane.

#### 9.5.2.2 Kinetic measurements

Flavor release occurs under the dynamic conditions present within the mouth (Land, 1996), and so a number of workers have developed analytical techniques that attempt to mimic these conditions. Stirred diffusion cells for monitoring the mass transport of flavor compounds between an oil and aqueous phase under shear conditions have been developed (McNulty and Karel, 1973; Rogacheva et al., 1999). The flavor compound is initially dissolved in either the oil or aqueous phases. A known volume of the aqueous phase is then poured into the vessel, and a known volume of oil is poured on top. The oil and aqueous phase are sheared separately using a pair of stirrers, and samples are extracted periodically using syringes that protrude into each of the liquids (Figure 9.15). These samples are then analyzed to determine the concentration of the flavor within them. The liquids are stirred at a rate that ensures a uniform flavor distribution, without significantly disturbing the air–water or oil–water interfaces. By carrying out the measurements over a function of time it is possible to determine the kinetics of flavor transport between the oil and water phases.

A similar system can be used to study the movement of flavor from a solution or emulsion to the vapor phase above it. The liquid to be analyzed is placed in a sealed vessel and stirred at a constant rate (often designed to simulate shear rates occurring during mastication). A syringe is used to withdraw samples from the headspace above the liquid as a function of time. Alternatively, a continuous flow of gas can be passed across the stirred liquid and the concentration of flavor within it determined by chromatography (Roberts and Acree, 1995, 1996; Parker and Marin, 2000). Thus, it is possible to simulate the agitation of the food within the mouth, as well as the flow of the gas across the food during manufacture.

#### 9.5.2.3 In vivo analysis

As mentioned earlier, there has been considerable progress in the development of *in vivo* analytical instruments to measure changes in flavor profiles with time during food mastication by human beings (Taylor and Linfoth, 2000; Harvey et al., 2000). *In vivo* methods of measuring the release of nonvolatile flavor molecules from foods during mastication have recently been described (Davidson et al., 1999, 2000; Hollowood et al., 2002). Samples

of saliva are periodically collected from the tongue of a human subject during mastication of a food and then analyzed using conventional methods. Alternatively, "chew-and-spit" techniques or in-mouth sensors can be used to provide information about the change in the type and concentration of flavor molecules with time (Davidson et al., 2000). Good correlations have been found between analytical measurements of the evolution of the concentration of certain taste molecules within the mouth during mastication and time-intensity sensory studies carried out on similar systems (Davidson et al., 2000).

### 9.5.3 Sensory analysis

The ultimate test of the flavor profile of a food product is its acceptance by consumers. Analytical tests carried out in a laboratory help to identify the most important factors that determine flavor, but they cannot model the extreme complexity of the human sensory system. For this reason, sensory analysis by human subjects is still one of the most important methods of assessing the overall flavor profile of food samples (Buttery et al., 1973; Williams, 1986; Barylko-Pikielna et al., 1994; Guyot et al., 1996; Dijksterhuis and Piggot, 2000; Piggot et al., 1998; Piggot, 2000). Sensory methods can be conveniently divided into two categories: discriminant methods and descriptive methods (Stone and Sidel, 1993; Piggot et al., 1998; Murray et al., 2001). In discriminant methods panelists are requested to identify whether there is a sensory difference in specified properties between two or more food samples. In descriptive methods the panelists are requested to assess and rank specified properties of food samples based on previously established sensory descriptors. Sensory analysis can also be categorized according to whether a trained or nontrained panel is used to carry out the evaluation (Lindsay, 1996a; Piggot et al., 1998). In some situations the sensory evaluation is carried out by specialists that have previously been trained to recognize particular flavors, or to detect slight differences in flavor profiles. In other situations, sensory evaluation is carried out using relatively large panels of untrained individuals that are representative of the general population or some specified segment of the general population, and the resulting data is statistically analyzed to ascertain significant differences between samples. Traditionally, sensory analysis involved a panelist giving an overall impression of some prespecified characteristic of a food sample after smelling or tasting. It is now widely recognized that the perceived flavor of a food changes with time before, during, and after mastication (Taylor and Linfoth, 2000). For this reason, a number of dynamic sensory analysis methods have been developed (Dijksterhuis and Piggot, 2000). For example, in "time-intensity" analysis a panelist is asked to rank the intensity of some flavor characteristic over time. Usually, the flavor intensity starts from a low value, reaches some maximum value during mastication, and then fades away (Harvey et al., 2000). Rather than report the full intensity versus time profile, it is often convenient to report the time-intensity flavor profile in terms of a small number of parameters that are more amenable to statistical or mathematical analysis (Moore et al., 2000). For this reason, the time-intensity profile is often characterized in terms of parameters such as the onset time ( $t_{\text{onset}}$ ), time to reach maximum intensity ( $t_{\text{MAX}}$ ), total duration ( $t_{\text{DUR}}$ ), maximum intensity ( $I_{\text{MAX}}$ ), area under the curve (AUC), and rate of release ( $M_{\text{release}}$ ) (Gwartney et al., 2000; Moore et al., 2000). Alternatively, the full flavor intensity versus time profile can be fitted using an appropriate mathematical model, and then the flavor release profile can be described by a small number of mathematical parameters (Janestad et al., 2000).

Despite the importance of sensory methods for assessing the flavor profiles of food emulsions, they do have a number of important limitations. Sensory analysis is often time-consuming and expensive to carry out, and individuals vary widely in their evaluation of food flavor (Piggot et al., 1998). For this reason, there is considerable emphasis on the

development of quantitative analytical procedures that correlate well with the results of sensory analysis (Taylor and Linforth, 2000). A number of studies have shown good correlation between the results of certain instrumental methods of measuring flavor profiles and sensory tests on emulsions (Guyot et al., 1996; Moore et al., 2000; Malone et al., 2000). Nevertheless, the goodness of the correlation depends on the type of analytical procedure used to determine the flavor profile and how well it models the complicated events that occur during the mastication and consumption of foods (Haahr et al., 2000).

## 9.6 Overview of factors influencing emulsion flavor

In this section, the major factors that influence the partitioning and release of flavors from food emulsions are summarized. In particular, the factors that influence the concentration of flavor molecules in the aqueous phase and in the headspace of an emulsion are focused on because it is these concentrations that determine the perceived taste and aroma of food emulsions.

### 9.6.1 Disperse phase volume fraction

The equilibrium concentration of nonvolatile flavor compounds in the aqueous phase of an emulsion depends primarily on the oil–water partition coefficient of the flavor molecules:

$$\Phi_{m,W} = \left( 1 + \frac{\phi K_{OW}}{1 - \phi} \right)^{-1} \quad (9.29)$$

where  $\Phi_{m,W}$  is the mass fraction of flavor molecules in the aqueous phase ( $= m_W/m_E$ ),  $m_W$  is the mass of flavor in the aqueous phase,  $m_E$  is the mass of flavor in the emulsion,  $\phi$  is the volume fraction of the oil phase, and  $K_{OW}$  is the oil–water partition coefficient. Knowledge of  $\Phi_W$  is important because the initial concentration of flavor molecules in the aqueous phase of an emulsion influences the taste intensity of a food immediately after it is placed in the mouth (McNulty, 1987). The aqueous phase concentration of highly polar flavors ( $K_{OW} \ll 1$ ) is relatively independent of fat content up to relatively high values, after which it decreases rapidly (Figure 9.4a). The aqueous phase concentration of highly nonpolar flavors ( $K_{OW} \gg 1$ ) decreases rapidly as the fat content increases until it reaches a relatively low constant level at higher fat contents (Figure 9.4a). The aqueous phase concentration of flavor molecules of intermediate polarity ( $K_{OW} \approx 1$ ) gradually decreases as the fat content increases. These calculations indicate that emulsion fat content can have a major impact on the initial concentration of nonvolatile flavor molecules present in the aqueous phase of an emulsion. Hence, one would expect that for certain types of flavors human beings would experience different initial taste intensities depending on the fat content of a product, which has important implications for the development of reduced fat food products (Malone et al., 2000).

The influence of  $\phi$  on the concentration of volatile flavor molecules in the headspace above an emulsion also depends on the polarity of the flavor molecules, that is, their oil–water partition coefficient. For an emulsion in equilibrium with the gas phase in the headspace above it:

$$\Phi_{m,G} = \left( 1 + \frac{V_E}{V_G} \left( \frac{\phi K_{OW} + (1 - \phi)}{K_{GW}} \right) \right)^{-1} \quad (9.30)$$

where  $\Phi_{m,G}$  is the mass fraction of flavor in the gas phase ( $= m_G/m_E$ ),  $m_G$  is the mass of flavor in the headspace,  $m_E$  is the mass of flavor in the emulsion,  $K_{GW}$  is the gas–water partition coefficient, and  $V_E$  and  $V_G$  are the volumes of the emulsion and gas phases, respectively.

The equilibrium concentration of a nonpolar flavor molecule ( $K_{OW} > 1$ ) in the headspace above an oil–water emulsion decreases as the oil concentration increases (Figure 9.4b). The magnitude of this effect increases as the hydrophobicity of the nonpolar flavor molecules increases, that is,  $K_{OW}$  increases. For highly nonpolar molecules ( $K_{OW} \gg 1$ ), the decrease in headspace flavor concentration occurs extremely steeply when the oil concentration is increased from 0 to a fraction of a percent. These predictions are supported by sensory and analytical measurements on oil-in-water emulsions containing nonpolar flavors (Schirle-Keller et al., 1994; Guyot et al., 1996; Jo and Ahn, 1999; Miettinen et al., 2002; Carey et al., 2002; van Ruth et al., 2002a,b; Roberts et al., 2003). Conversely, the equilibrium concentration of a polar flavor molecule ( $K_{OW} < 1$ ) in the headspace above an oil–water emulsion increases slightly as the oil concentration increases up to a certain fat content, after which it increases more dramatically (Figure 9.4b). The magnitude of this effect increases with the polarity of the flavor molecules. These predictions are supported by sensory and analytical measurements on oil-in-water emulsions containing polar flavors (Guyot et al., 1996; Jo and Ahn, 1999; Miettinen et al., 2002). The equilibrium headspace concentration of flavor molecules of intermediate polarity ( $K_{OW} \approx 1$ ) is relatively independent of the oil concentration. Good agreement between theoretical calculations of the equilibrium headspace concentrations above emulsions and experimental measurements have been found, provided that there are no components in the emulsions that bind flavors significantly (Guyot et al., 1996; Roberts et al., 2003). This change in flavor profile with droplet concentration has important consequences for the formulation of reduced fat emulsions. Reducing the fat content of an oil-in-water emulsion below a particular level may significantly alter the perceived flavor profile due to an increase in the concentration of nonpolar flavors in the aqueous phase and headspace. On the other hand, reducing the fat content of a water-in-oil emulsion below a particular level may alter the flavor profile by appreciably increasing the concentration of polar flavors in the aqueous phase, while reducing the concentration in the headspace.

The influence of disperse phase volume fraction on the rate of flavor release from emulsions has been the subject of a number of theoretical and experimental studies. When an emulsion is diluted with an aqueous phase (e.g., water, buffer, or saliva) the equilibrium distribution of flavor molecules among the oil, water, and gas phases is disturbed, which is the thermodynamic driving force for flavor release (McNulty, 1987; de Roos, 2000). Consequently, there is a change in the concentration of nonvolatile flavor molecules in the aqueous phase (taste) and headspace (aroma) with time.

Theoretical predictions, supported by experimental results on model systems, indicate that the *rate* of flavor release from oil-in-water emulsions into the headspace decreases as the fat content increases, and that this effect is more dramatic for nonpolar than for polar molecules (Harrison et al., 1997b; Malone et al., 2000; van Ruth et al., 2002a,c). For example, the influence of fat content on the change in perceived intensity of a nonpolar flavor (heptan-2-one,  $K_{OW} = 72$ ) with time for model oil-in-water emulsions determined by time-intensity sensory analysis is shown in Figure 9.16. These results were supported by analytical measurements of flavor concentrations in gas samples taken from panelist's nostrils during mastication (Malone et al., 2000). Similar findings have been obtained using more realistic models of actual food emulsions. For example, analytical and sensory measurements on model yogurt systems have shown that low fat yogurts (0.2%) released nonpolar volatiles more quickly and with a higher intensity than higher fat yogurts (3.5 or 10%) (Brauss et al., 1999). On the other hand, fat content had little influence on the

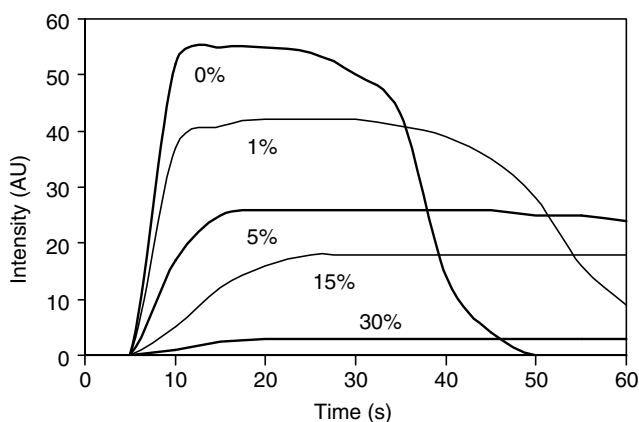


**Figure 9.16** Influence of fat content on the change in perceived intensity of a nonpolar flavor (heptan-2-one,  $K_{OW} = 72$ ) with time for model oil-in-water emulsions determined by time-intensity sensory analysis. Adapted from Malone et al. (2000).

maximum intensity ( $I_{MAX}$ ) or the time to reach maximum intensity ( $t_{max}$ ) for polar volatiles because these molecules were already largely present in the aqueous phase (Brauss et al., 1999). Similarly time-intensity sensory measurements of the aroma of oil-in-water emulsions have shown that  $I_{MAX}$  decreases appreciably with increasing fat content for the nonpolar flavor limonene, but that  $I_{MAX}$  is relatively independent of fat content for the more polar flavor vanillin (Mialon and Ebeler, 1997). In summary, fat content has a much greater impact on  $I_{MAX}$  for nonpolar than for polar flavor molecules, but there is only a relatively small impact of fat content on  $t_{max}$  for both nonpolar and polar flavors (Brauss et al., 1999; Malone et al., 2000).

### 9.6.2 Droplet size

Intuitively, one might not expect droplet size to have a significant impact on equilibrium flavor concentrations in emulsions, since the equations presented to predict these concentrations in the aqueous phase and headspace do not depend on emulsion microstructure (Section 9.2). Nevertheless, there are a number of ways that the droplet size could influence the equilibrium distribution of flavor molecules within an emulsion. First, the vapor pressure of a material contained within a droplet increases as the size of the droplet decreases (Adamson, 1990), which would increase the equilibrium headspace concentration. Nevertheless, this effect only becomes appreciable for relatively small droplets ( $d < 100$  nm), and therefore is unlikely to be significant in most food emulsions. Second, droplet size may have an indirect influence on flavor distribution in emulsions due to changes in the total emulsifier concentration or in the relative distribution of emulsifiers between adsorbed and nonadsorbed states. A lower concentration of emulsifier is often used to produce emulsions with larger droplet sizes since there is less surface area to cover. If an emulsifier is capable of binding or solubilizing flavor molecules, then a change in the total emulsifier concentration will change the flavor profile. In emulsions containing a constant total emulsifier concentration, the fraction of emulsifier molecules adsorbed to the droplet interfaces increases as the droplet surface area increases (droplet size decreases). If an emulsifier can bind or solubilize flavor molecules, and the extent of this interaction is different for the adsorbed and nonadsorbed states, then the flavor distribution within an emulsion may be altered by a change in droplet size. For example, adsorption of globular proteins to droplet

interfaces induces changes in their molecular structure, which can alter their flavor binding capacity (Charles et al., 2000a).

A number of experimental studies have found that equilibrium concentrations of flavors in the headspace above oil-in-water emulsions with constant emulsifier concentrations are relatively independent of droplet size (Landy et al., 1996; Carey et al., 2002). Presumably, in these studies the flavor molecules either did not interact with the emulsifiers or flavor binding was similar in the adsorbed and nonadsorbed states of the emulsifier. On the other hand, other studies have shown that the headspace flavor concentration depends on droplet size, presumably because flavor–emulsifier interactions were important (Matsubara and Texter, 1986; Texter et al., 1987; Wedzicha, 1988; Miettinen et al., 2002; van Ruth et al., 2002a,b).

The theoretical models developed to describe flavor release from emulsions are usually based on the assumption that the rate-limiting step is either the mass transport of flavor molecules across the emulsion–gas interface or the diffusion of flavor molecules out of the droplets (Section 9.3). An estimation of which of these two mechanisms is likely to be rate limiting for a particular emulsion can be determined by dividing the half-time for flavor diffusion out of an emulsion droplet,  $t_{1/2}(\text{droplet})$  (Equation 9.21) by the half-time for flavor release at the emulsion–air interface,  $t_{1/2}(\text{interface})$  (Equation 9.23):

$$\text{Ratio} = \frac{t_{1/2}(\text{droplet})}{t_{1/2}(\text{interface})} = \frac{0.0585r^2K_{\text{DC}}}{D} \times \frac{Ah_D(1/K_{\text{GE}}V_G + 1/V_L)}{\ln 2} \quad (9.31)$$

If this ratio is greater than unity flavor release will be limited by diffusion of flavor molecules out of the droplets, but if it is less than unity flavor release will be limited by mass transport of flavor molecules across the emulsion–air interface. By assuming that the mass transport through the emulsion is not strongly influenced by droplet size (i.e.,  $h_D$  equals the value in the continuous phase), a critical droplet radius ( $r_{\text{critical}}$ ) can be calculated by setting the ratio in Equation 9.31 to unity. The influence of the oil–water ( $K_{\text{OW}}$ ) and air–water ( $K_{\text{GW}}$ ) partition coefficients on  $r_{\text{critical}}$  were calculated for a range of values typical for flavors in food emulsions (Figure 9.17). The rate-limiting step is flavor diffusion out of the droplets for  $r > r_{\text{critical}}$ , and mass transport of flavor molecules across the emulsion–gas

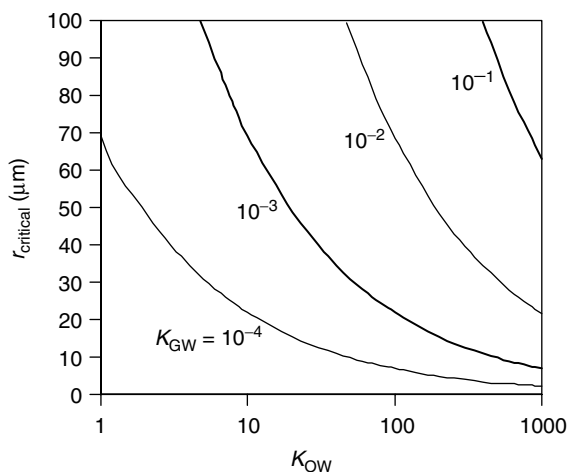


**Figure 9.17** Influence of oil–water ( $K_{\text{OW}}$ ) and air–water ( $K_{\text{GW}}$ ) partition coefficients on  $r_{\text{critical}}$  calculated for a range of values typical for flavors in food emulsions.



interface for  $r < r_{\text{critical}}$ . For relatively polar and volatile flavor molecules,  $r_{\text{critical}}$  is appreciably greater than the droplet radii found in most food emulsions (i.e.,  $> 10 \mu\text{m}$ ). Hence, mass transport across the emulsion–gas interface would be expected to be rate limiting in these systems. Under these circumstances, theory predicts that the rate of flavor release should increase with increasing droplet size since  $h_D$  increases with  $r$  (Equation 9.28). For highly nonpolar flavors with relatively low volatilities the critical radius approaches the droplet radii found in some food emulsions (i.e.,  $2\text{--}10 \mu\text{m}$ ). In these systems, flavor release could be limited by diffusion of flavor molecules out of the oil droplets. Under these circumstances, theory predicts that the flavor release rate should decrease with increasing droplet size since it takes longer for flavor molecules to diffuse out of the droplets (Equation 9.21). The influence of droplet size on the flavor release rate of an emulsion will therefore depend on the precise nature of the system.

In salad dressings ( $d = 20\text{--}86 \mu\text{m}$ ) and model oil-in-water emulsions ( $d = 7$  or  $15 \mu\text{m}$ ) containing relatively large emulsion droplets, it was observed that the release of nonpolar flavor molecules into the headspace decreased with increasing droplet size (Charles et al., 2000a,b). This was presumably because diffusion of the flavor molecules out of the oil droplets was the rate-limiting step for flavor release in these systems. In contrast, the release of polar flavors from the same emulsions and the release of nonpolar flavors from oil-in-water emulsions containing relatively small droplets ( $d < 1.1 \mu\text{m}$ ) occurred more rapidly when the droplet size was increased (Charles et al., 2000b; van Ruth et al., 2002a). This was presumably because diffusion of the flavor molecules across the emulsion–gas interface was the rate-limiting step for flavor release in these systems.

### 9.6.3 Interfacial characteristics

The chemistry, thickness, structure, and charge of the interfacial membrane surrounding the droplets may influence the equilibrium flavor distribution within an emulsion. Some flavor molecules are capable of binding to emulsifier molecules, for example, through physical or covalent interactions (Guichard, 2002). The change in molecular environment of a protein after adsorption to a droplet surface may change the characteristics of any flavor binding sites (Charles et al., 2000a; Seuvre et al., 2000). For example, the flavor binding site may be directed toward the oil phase, rather than exposed to the aqueous phase, which may alter the accessibility of the flavor molecule. Alternatively, a globular protein may undergo a conformational change that alters the physicochemical characteristics of the binding sites. Experimental studies have shown that flavor binding by proteins in oil–water systems is influenced by the characteristics of the flavor molecules and the structure of the system (Seuvre et al., 2000). For example, 2-nonanone was bound less strongly by  $\beta$ -lactoglobulin in an emulsified oil–water system than in a nonemulsified oil–water system, whereas isoamyl acetate was unaffected by system structure (Seuvre et al., 2000). Electrically charged flavor molecules, such as ionized acids, may be attracted to oppositely charged emulsion droplets due to electrostatic interactions, which lead to flavor binding and a reduction of the flavor concentration in the aqueous and vapor phases (Guichard, 2002).

A number of studies have suggested that interfacial membranes consisting of adsorbed proteins may form a barrier to flavor transfer across an oil–water interface (Harvey et al., 1995; Druax and Voilley, 1997; Landy et al., 1998; Rogadcheva et al., 1999; Seuvre et al., 2002). Nevertheless, reductions in mass transfer rates could also be because proteins bind some of the flavor molecules and reduce the concentration gradient at the oil–water interface thus slowing down flavor release (Carey et al., 2002). If the protein does act as a barrier to flavor release then the resistance of the interfacial membrane to mass transfer processes will depend on its thickness and internal structure. It may therefore be possible

to control the release rate of certain flavors from oil-in-water emulsions by varying the type of emulsifier used to stabilize the droplets. Alternatively, it may be possible to manipulate the mass transport properties of a particular emulsifier membrane (e.g., a globular protein) by controlling environmental conditions, such as temperature, pH, or ionic strength, which are known to change the thickness, rheology, or packing of emulsifier molecules in the membrane (Chapters 4 and 5). Nevertheless, further systematic studies are required on well-characterized model systems to conclusively establish the physicochemical basis of the effects of interfacial membranes on flavor release rates.

#### 9.6.4 Oil phase characteristics

The nature of the oil phase in an emulsion could potentially alter the flavor profile through a variety of different physicochemical phenomenon, including oil polarity, oil viscosity, and fat crystallization. The equilibrium concentration of flavor molecules in the aqueous phase and headspace of an emulsion is largely determined by the oil–water partition coefficient ( $K_{OW}$ ), which depends on oil polarity. Oils vary significantly in their polarity, depending on the type and structure of their molecular constituents, hence the equilibrium partitioning of flavors in emulsions depends on oil type (Landy et al., 1998; Seurve et al., 2000). From an experimental point of view, it is therefore important to use model oils with polarities similar to real oils when carrying out equilibrium partitioning or flavor release studies. For example, hydrocarbons that are often used as model oils in studies of emulsions are considerably more nonpolar than many real food oils, for example, triacylglycerols or flavor oils (Wedzicha, 1988). The results of studies with these systems may therefore not be truly representative of real systems.

Oils may also contain surface-active materials that form reverse micelles or other association colloids (e.g., fatty acids, phospholipids, and other polar lipids), which can solubilize water, amphiphilic, and polar molecules into the oil phase (Jonsson et al., 1998). The presence of these surface-active materials may therefore alter the equilibrium distribution of flavor molecules within an emulsion. One would expect that the  $K_{OW}$  values of more polar flavor molecules would be increased in the presence of reverse micelles in the oil phase, which would reduce their concentration in the aqueous phase and headspace.

The physical state of the droplets in an emulsion also influences the distribution and release of flavor molecules since flavor molecules cannot easily penetrate into the solid state (McNulty and Karel, 1973; Guichard, 2002). The concentration of flavor components in the aqueous phase of an emulsion would be expected to be higher if the fat phase was partly crystallized because there would be a smaller amount of liquid oil available for the flavor molecules to partition into (Roberts et al., 2003). An increase in solid fat content (SFC) would therefore be expected to have a similar effect as a decrease in overall fat content in emulsions containing liquid droplets. The influence of the SFC of lipid droplets on flavor release from milk-based emulsions has recently been examined (Roberts et al., 2003). The droplet SFC was varied in two ways: (1) carrying out the experiments at different temperatures; (2) using oils with different degrees of crystallization at the same temperature. These experiments indicated that the headspace concentration of nonpolar volatile flavors increased as the SFC increased, but that there was little change in the concentration of polar volatile flavors with SFC. The thermal history of the samples was also found to have an influence on the headspace flavor concentration above emulsions containing partially crystalline droplets (Roberts et al., 2003). When nonpolar flavors were added to an emulsion at a temperature where the oil phase was predominantly liquid (25°C), then the emulsion was cooled to a temperature where the droplets were partially crystalline (10°C), the flavor concentration in the headspace was less than when the flavors were directly added to the emulsion at the lower temperature (10°C). It was postulated

that this phenomenon occurred because the flavors became physically entrapped within the oil droplets when they crystallized, so that they were not released as efficiently. In another study, no significant difference was observed between the headspace concentrations of flavors measured at room temperature in emulsions containing either tricaprylin (m.p. 4°C) or trilaurin (m.p. 47°C); however, the authors did not state whether the flavor was added before or after the emulsion droplets were crystallized (Carey et al., 2002).

The viscosity of the oil phase would be expected to influence the diffusion of nonpolar flavor molecules from within the droplets. In emulsions where the rate-limiting step to flavor release was mass transport of flavor molecules through the droplets (e.g., emulsions containing large droplets and highly nonpolar flavors), then the flavor release rate would be expected to decrease with increasing oil viscosity. To the author's knowledge, the influence of oil phase viscosity on flavor release from oil-in-water emulsions has not previously been studied experimentally.

### 9.6.5 Aqueous phase characteristics

The addition of sugars, salts, acids, or bases to the aqueous phase of an emulsion will obviously have a direct effect on its perceived sweetness, saltiness, sourness, and bitterness. Nevertheless, the presence of high concentrations of these water-soluble compounds may also influence the flavor of emulsions indirectly by changing the equilibrium partition coefficients of the other flavor molecules present or by altering the kinetics of mass transfer processes. The equilibrium concentration of flavor molecules in the aqueous phase and headspace of an emulsion is largely determined by the oil-water partition coefficient ( $K_{OW}$ ). The addition of water-soluble compounds to the aqueous phase may alter  $K_{OW}$  of flavor molecules because it changes the free energy associated with transferring them from the oil to the aqueous phase. Water-soluble compounds, such as sugars or salts, may either increase or decrease  $K_{OW}$  (Friel et al., 2000; Nahon et al., 2000), depending on whether they decrease or increase the transfer free energy, respectively. Sugars have also been shown to influence the rate of flavor release from aqueous solutions by altering the equilibrium partition coefficient and by decreasing the mass transport coefficient through the emulsion (due to increasing its viscosity) (Nahon et al., 2000). Adjustment of the pH of an aqueous solution by addition of acids or alkalis may also change the flavor profile of an emulsion by changing the ionization of flavor molecules (Section 9.2).

The equilibrium partition coefficient of flavor molecules may also be affected by binding of flavors to biopolymers (proteins, polysaccharides) or solubilization of flavors in surfactant micelles (Guichard, 2002). If an aqueous phase constituent strongly binds a flavor molecule, then there is an increase in the overall flavor concentration in the aqueous phase, a decrease in the oil phase, and a decrease in the headspace. Selective binding of a flavor molecule therefore alters the flavor profile of a food by altering the equilibrium distribution of flavor compounds (Overbosch et al., 1991; Harrison and Hills, 1997a). Flavor binding also alters the rate at which flavors are released from emulsions, with the amount of flavor released and the release rate decreasing with increasing binding constant and biopolymer concentration (Harrison and Hills, 1997a; Harrison, 1998; Andriot et al., 2000). Flavor binding may occur through a variety of physical (e.g., electrostatic, hydrogen bonding, hydrophobic) and/or chemical (e.g., covalent bond formation) interactions between flavor molecules and biopolymers.

Previous studies have shown that many categories of flavor molecules, such as alkanes, aldehydes, and ketones, bind to different types of proteins, for example, casein,  $\beta$ -lactoglobulin, bovine serum albumin, soy protein, and gelatin (Langourieux and Crouzet, 1995; O'Neil, 1996; Hansen and Booker, 1996; Boudaud and Dumont, 1996; Bakker et al., 1998; Jouenne and Crouzet, 2000a,b; Li et al., 2000; Guichard and Langourieux, 2000;

Guichard, 2002). These proteins have little flavor themselves, but can cause significant changes in the flavor profile of an emulsion by binding either desirable or undesirable flavors. The extent of flavor binding depends on the molecular structure of the flavor and protein molecules. Nonpolar flavors are believed to bind to nonpolar patches on the surfaces of proteins through hydrophobic attraction (Guichard and Langourieux, 2000). An increase in binding of flavors to  $\beta$ -lactoglobulin has been observed in the presence of urea or on heating, because these treatments cause partial unfolding of the proteins, which increases their surface hydrophobicity (O'Neil, 1996). Flavors may also bind to polysaccharides, such as starch, dextrans, and pectins, but in this case the molecular interactions involved are more likely to be van der Waals, electrostatic, or hydrogen bonds (Hau et al., 1996; Braudo et al., 2000; Guichard and Etievant, 1998; Arvisenet et al., 2002). Certain types of polysaccharides bind flavor molecules by forming helical complexes around them (Heinemann et al., 2001). In some systems binding may be irreversible due to specific chemical reactions between biopolymer and flavor molecules (Adams et al., 2001).

Biopolymers, particularly random-coil proteins and polysaccharides, may greatly increase the viscosity of aqueous solutions (Section 4.5). These biopolymers have been shown to decrease the rate of flavor release from aqueous solutions and emulsions, which has been attributed to their ability to decrease the convective mixing of flavor components in the mouth (Morris, 1995b). This reduces the presence of freshly formed surfaces with relatively high flavor concentrations, thereby reducing the rate of flavor release. The reduction is not usually due to the reduction in the diffusion of small flavor molecules through the polymer network (Morris, 1995b).

## 9.7 *Concluding remarks and future directions*

The overall perceived flavor of a food emulsion is the result of a mixture of taste, aroma, and mouthfeel contributions. A quantitative understanding of the physicochemical basis of emulsion flavor is complicated by the fact that flavor release during mastication is a highly dynamic and complex process that may involve changes in the temperature, structure, composition, and physical state of the food within the mouth over time. The molecules responsible for food flavor move to receptors in the mouth and nose during mastication. The time-intensity profile of flavors at these receptors depends on the initial concentration of flavor molecules in the food, their partitioning between the various phases within the emulsion, their binding interactions with other food components, and their mass transport from their initial location within the emulsion to the taste receptors. Despite the complexities of the physicochemical processes involved in flavor release from food emulsions, considerable progress has been made, largely due to the development of theories to model flavor release and sophisticated analytical and sensory techniques for detecting and characterizing food flavors, especially under conditions that mimic mastication. An improved understanding of the physicochemical basis of flavor release in food emulsions will facilitate the rational design and creation of foods with improved flavors. In particular, this knowledge should aid in the production of better-tasting healthy alternatives to conventional foods, such as reduced fat, low fat, or fat-free foods. The importance of this approach has recently been demonstrated by researchers who have used an understanding of the influence of microstructure on mass transport processes in emulsions to design low fat foods with similar flavor release profiles as high fat foods (Malone et al., 2000).

Understanding the physicochemical, physiological, and psychological basis of food flavor is an extremely active research area, with many research articles and books being

published in the past few years. A number of areas that would be particularly fruitful for future work on food emulsions are listed below:

- Development of more physically realistic mathematical theories for modeling flavor partitioning and release in food emulsions is necessary. These models should take into account flavor binding, mass transport through the various phases in the emulsion (e.g., oil, water, interface) and through the different regions of the human body (e.g., saliva, mouth, nasal cavity), and dynamic changes in the system (e.g., temperature, composition, structure, state, forces). It is important that these theories are rigorously tested using experiments on well-defined model systems to ascertain their range of applicability and their limitations.
- Development, refinement, and application of analytical techniques and experimental protocol for measuring flavor release, especially under conditions that mimic the dynamic physicochemical processes occurring during mastication.
- Systematic studies of the influence of droplet characteristics (e.g., particle size distribution, disperse phase volume fraction, droplet–droplet interactions, droplet physical state, interfacial properties) on flavor partitioning, flavor release, and perceived sensory flavor.
- Systematic studies of the influence of specific food components on the partitioning, release, and sensory characteristics of specific flavors is required, with special emphasis on establishing the molecular basis for these effects. In particular, it is still necessary to conclusively determine the relative importance of flavor binding and retarded diffusion effects of various biopolymers on flavor release.
- Tabulation of partition coefficients of major flavor components for oil–water, air–water, and air–oil systems under standardized conditions (e.g., temperature, pressure, pH, ionic strength) is needed. In addition, a consistent and systematic means of characterizing flavor binding interactions with other ingredients is required (e.g., determine binding constants and stoichiometry under standardized conditions).
- Development of novel flavor release technologies for use in low fat food products. These techniques could be based on engineering of interfacial properties (Rogatcheva et al., 1999; Seuvre et al., 2002), use of multiple emulsions (Dickinson et al., 1994), usage of particulated emulsion gels (Malone et al., 2000), or flavor encapsulation in biopolymer complexes (Burova et al., 1999).
- Systematic studies of the complex changes in food structure that occur during mastication, and of the interactions between specific food components and the mouth. In particular, experiments aimed at establishing the link between sensory perception and the physicochemical and structural properties of foods is required.

## *chapter ten*

---

# *Appearance*

### *10.1 Introduction*

The first impression that a consumer usually has of a food emulsion is a result of its appearance (Francis and Clydesdale, 1975; Manley, 1993; Hutchings, 1999). Consequently, appearance plays an important role in determining whether or not consumers will purchase a particular product, as well as their perception of the quality once the product is consumed (MacDougall, 2002a). A number of different characteristics contribute to the overall appearance of a food emulsion, including its surface gloss, opacity, color, and homogeneity (Hutchings, 1999). These characteristics are the result of interactions between light waves and the emulsion (McClements, 2002a,b). The light that is incident on an emulsion may be reflected, transmitted, scattered, absorbed, and refracted before being detected by the human eye (Francis and Clydesdale, 1975; Farinato and Rowell, 1983; Francis, 1995; Hutchins, 1999). A better understanding of the relationship between the appearance of emulsions and their composition and microstructure will aid in the design of foods with improved quality. This chapter highlights some of the most important factors that contribute to the overall appearance of emulsions. As with previous chapters, it focuses on establishing the physicochemical basis of emulsion color, rather than on describing the factors that contribute to the appearance of particular types of food emulsions, such as the type and concentration of specific pigments present. Reviews of the chemistry of natural and synthetic colorants commonly used in foods, and of the molecular structures that cause these substances to appear colored are given elsewhere (Francis, 2002; Moss, 2002; Nielsen et al., 2002).

The appearance of a material is determined by a combination of factors, including the characteristics of the light source, detector, and material (Judd and Wyszecki, 1963; Billmeyer and Saltzman, 1981; Wyszecki and Stiles, 1982; Joshi, 2000). A change in the characteristics of any of these three factors alters the perceived appearance of the material. The light source generates the electromagnetic radiation that the material interacts with before the radiation reaches the human eye. A change in the spectral power distribution of a light source (i.e., the intensity vs. wavelength spectrum of the electromagnetic radiation it generates) will therefore cause a change in the perceived color of a material. Thus, a material appears differently when it is illuminated by a white light than when it is illuminated by a red light, even though the material and the observer have not changed. The most common light source is the “daylight” produced by the sun, which contains radiation with energies ranging across the whole visible spectrum (around 400–700 nm). At night or inside a building, artificial light is a more important light source. Materials reflect, absorb, transmit, and scatter the electromagnetic radiation that impinges on them depending on their geometry, composition, and microstructure. Certain wavelengths of

light are more strongly affected by these processes than others, which lead to the observed differences in color, opacity, and gloss of materials. The sensitivity and specificity of the detector (human eye or instrumental device) to different wavelengths and intensities of light also influence the appearance of a material. Finally, the relative location of the light source, material, and detector may also influence the final appearance of a material. In this chapter we will focus primarily on the influence of the composition and microstructure of emulsions on their overall appearance. Even so, it must be stressed that the same emulsion will appear differently when observed using different light sources or detectors.

## 10.2 General aspects of optical properties of materials

The purpose of this section is to introduce some of the most important factors that influence the optical properties of materials in general. This information will facilitate an understanding of the factors that determine the optical properties of food emulsions described in later sections.

### 10.2.1 Interaction of light with matter

#### 10.2.1.1 Transmission, reflection, and refraction

When an electromagnetic wave is incident on a boundary between two homogeneous nonabsorbing materials it is partly reflected and partly transmitted (Figure 10.1). The relative importance of these processes is determined by the refractive indices of the two materials, the surface topography, and the angle at which the light meets the surface (Hutchins, 1999).

The reflection of an electromagnetic wave from a surface may be either *specular* or *diffuse* (Figure 10.2). Specular reflectance occurs from optically smooth surfaces and is characterized by the fact that the angle of reflection is equal to the angle of incidence ( $\phi_{\text{reflection}} = \phi_{\text{incidence}}$ ). Diffuse reflectance occurs from optically rough surfaces and is characterized by the fact that the incident light is reflected over many different angles

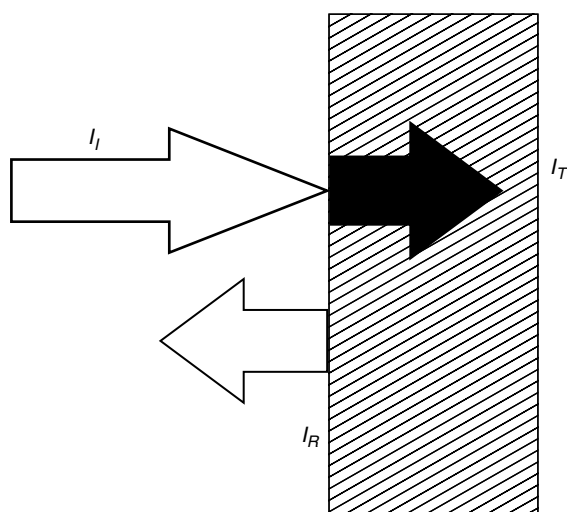


**Figure 10.1** When a light wave encounters a planar boundary between two materials it is partly reflected and partly transmitted. The relative proportions of reflected and transmitted light depend on the difference in refractive index between the two materials.

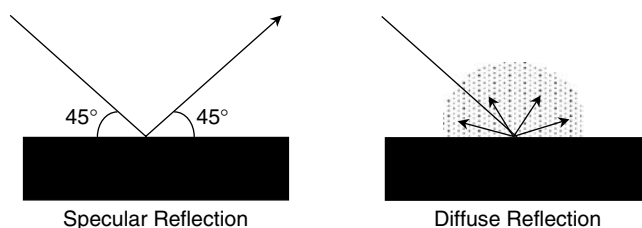


**Figure 10.2** Comparison of complete specular and diffuse reflectance. In practice, reflectance from real objects is usually a combination of both types of reflectance.

(Figure 10.2). Diffuse reflectance is the major form of reflection from the surface of concentrated emulsions, because of multiple scattering effects from the large number of droplets present (McClements, 2002a,b).

The fraction of light reflected from a smooth plane boundary separating two materials when the angle of incidence is perpendicular to the boundary is given by the reflection coefficient,  $R$ :

$$R = \left( \frac{m-1}{m+1} \right)^2 \quad (10.1)$$

where  $m$  is the *relative refractive index* ( $= n_2/n_1$ ), and  $n_1$  and  $n_2$  are the refractive indices of the two materials (Hutchins, 1999). This equation highlights the fact that the fraction of light reflected from the surface increases as the difference in refractive index between the two materials increases: about 0.1% of light is reflected from an interface between oil ( $n_o = 1.43$ ) and water ( $n_w = 1.33$ ), while about 2% is reflected from an interface between water and air ( $n_a = 1$ ). These reflection coefficients may seem small, but the total amount of energy reflected from a concentrated emulsion becomes appreciable because a light wave encounters a huge number of different droplets and is reflected from each one of them.

When a light wave encounters a planar material at an angle, part of the wave is reflected at an angle equal to that of the incident wave, while the rest is refracted (transmitted) at an angle that is determined by the relative refractive indices of the two materials and the angle of incidence:  $\sin(\phi_{\text{refraction}}) = \sin(\phi_{\text{incidence}})/m$  (Hutchins, 1999). It should be noted that if a light wave traveling through a transparent medium encounters another transparent medium with a lower refractive index, then refraction does not occur once the angle of incidence exceeds a critical angle. This critical angle depends on the refractive index of the two media, and is approximately  $49^\circ$  for a water–air boundary. Above the critical angle, all of the light is reflected and therefore refraction no longer occurs. This phenomenon is the basis of Brewster Angle Microscopy, which is commonly used to study the structural organization of molecules adsorbed to interfaces (Section 11.3.1).

### 10.2.1.2 Light absorption

Absorption is the process whereby a photon of electromagnetic energy is transferred to an atom or molecule (Atkins, 1994; Penner, 1994a; Pomeranz and Meloan, 1994). The primary cause of absorption of electromagnetic radiation in the visible region is the transition of outer-shell electrons from lower to higher electronic energy levels (Moss, 2002). A photon is only absorbed when it has an energy that exactly corresponds to the difference between the energy levels involved in the transition, that is,  $\Delta E = h\nu = hc/\lambda$ , where  $h$  is Planck's constant,  $\nu$  is the frequency of the electromagnetic wave,  $c$  is the velocity of the electromagnetic wave, and  $\lambda$  is the wavelength.



The visible region consists of electromagnetic radiation with wavelengths between 380 and 750 nm, which corresponds to energies between 120 and 230 kJ mol<sup>-1</sup> in water (Penner, 1994a). Substances that can absorb electromagnetic energy in this region are usually referred to as dyes or pigments (Moss, 2002). A dye is defined as a colored substance that is soluble in the medium in which it is dispersed, whereas a pigment is insoluble (Moss, 2002). The more general term "colorant" can be used to encompass both dyes and pigments. Most colorants in foods have chemical structures containing resonance structures in which the electrons are shared over a number of bonds, for example, conjugated unsaturated bonds, aromatic ring structures, or electron donating/withdrawing groups (Hutchins, 1999; Moss, 2002). Food colorants have different colors because variations in their chemical structure lead to differences in their ability to selectively adsorb radiation in different regions of the visible spectrum. The relationship between the chemical structure of food colorants and their absorption spectra has been reviewed (Moss, 2002). Food colorants can be classified according to their origin (natural, nature-identical, or synthetic) or chemical structure (i.e., isoprenoid derivatives, tetrapyrrol derivatives, benopyran derivatives, artifacts, and others) (Moss, 2002).

Absorption causes a reduction in the intensity of a light wave as it passes through a material, which can be described by the following equation (Penner, 1994b; Pomeranz and Meloan, 1994):

$$T = \frac{I_T}{I_0} \quad (10.2)$$

where  $T$  is the *transmittance*,  $I_T$  is the intensity of the light that travels directly through the sample, and  $I_0$  is the intensity of the incident wave. In practice,  $I_T$  may also be reduced because of reflections from the surfaces of the measurement cell that is used to contain the sample, and due to absorption by the solvent and measurement cell (Penner, 1994b). These losses can be taken into account by comparing  $I_T$  with the intensity of a wave that has traveled through a reference cell (usually containing pure solvent), rather than with  $I_0$ :

$$T = \frac{I_T}{I_{0,R}} \quad (10.3)$$

where,  $I_{0,R}$  is the intensity of the light that has traveled directly through the reference cell. The transmittance of a substance decreases exponentially with increasing colorant concentration or sample length (Pomeranz and Meloan, 1994). For this reason, it is often more convenient to express the absorption of light in terms of an *absorbance* ( $A$ ) because this is proportional to colorant concentration and sample length:

$$A = -\log \frac{I_T}{I_{0,R}} = \alpha cl \quad (10.4)$$

where  $\alpha$  is a constant of proportionality known as the *absorptivity*,  $c$  is the colorant concentration, and  $l$  is the sample path length. The linear relationship between absorbance and concentration holds over the colorant concentrations used in most food emulsions. The color intensity of a particular colorant therefore depends on its concentration and absorptivity.

The appearance of an emulsion to the human eye is determined by the interactions between it and electromagnetic radiation in the visible region (Francis and Clydesdale,

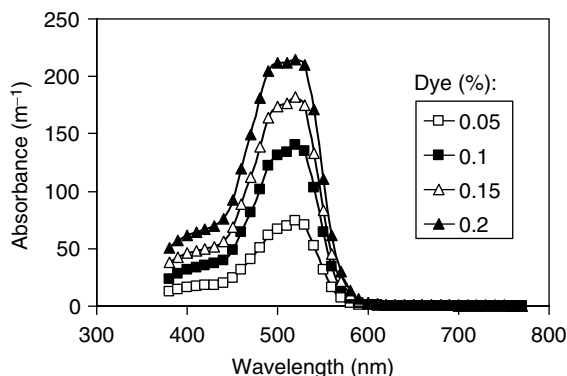


**Figure 10.3** Absorption spectrum of aqueous solutions containing different concentrations of a red food dye (FD&C red #3 and red #40). The solution appears red because light is primarily absorbed at all wavelengths (400–605 nm) except those corresponding to red (605–700 nm).

1975; Hutchins, 1999). It is therefore important to measure the absorbance over the whole range of visible wavelengths (390–750 nm). A plot of absorbance versus wavelength is referred to as an *absorption spectrum* (Figure 10.3). An absorption peak occurs at a wavelength that depends on the difference between the energy levels of the electronic transitions in the colorants ( $\lambda = ch/\Delta E$ ). Absorption peaks are fairly broad in the visible region because transitions occur between the different vibrational and rotational energy levels within the electronic energy levels, and because of interactions between neighboring molecules (Penner, 1994b). Different molecules have different electronic outer-shell structures and hence different visible absorption spectra. The color of an emulsion therefore depends on the absorption spectra and concentration of the various chromophoric molecules contained within it.

### 10.2.1.3 Light scattering

Scattering is the process whereby a wave that is incident on a particle is directed into directions that are different from that of the incident wave (Farinato and Rowell, 1983; Bohren and Huffman, 1983; Hiemenz and Rajagopalan, 1997). The extent of light scattering by an emulsion is primarily determined by the droplet concentration, the relationship between the droplet size and the wavelength, and the difference in refractive index between the droplets and the surrounding liquid (Bohren and Huffman, 1983; McClements, 2002a,b).

The scattering of light from an emulsion droplet can be characterized by a scattering pattern, which describes the angular dependence of the intensity of scattered light ( $I(\theta)$  vs.  $\theta$ ) (Farinato and Rowell, 1983). The scattering pattern is strongly dependent on the size of the droplets relative to the wavelength of light (Figure 10.4). For low ratios ( $r/\lambda < 0.1$ ), the light is scattered fairly evenly in all directions and can be described by Rayleigh theory (Hutchins, 1999):

$$I = \frac{8\pi^4 r^6}{d^2 \lambda^4} \left( \frac{m^2 - 1}{m^2 + 2} \right)^2 (1 + \cos 2\theta) \quad (10.5)$$

where  $r$  is droplet radius,  $\lambda$  is the wavelength of light,  $d$  is the distance from the droplet to the detector,  $m$  is the relative refractive index, and  $\theta$  is the scattering angle. When the droplet size is similar to the wavelength ( $r/\lambda = 1$ ), the scattering pattern becomes much

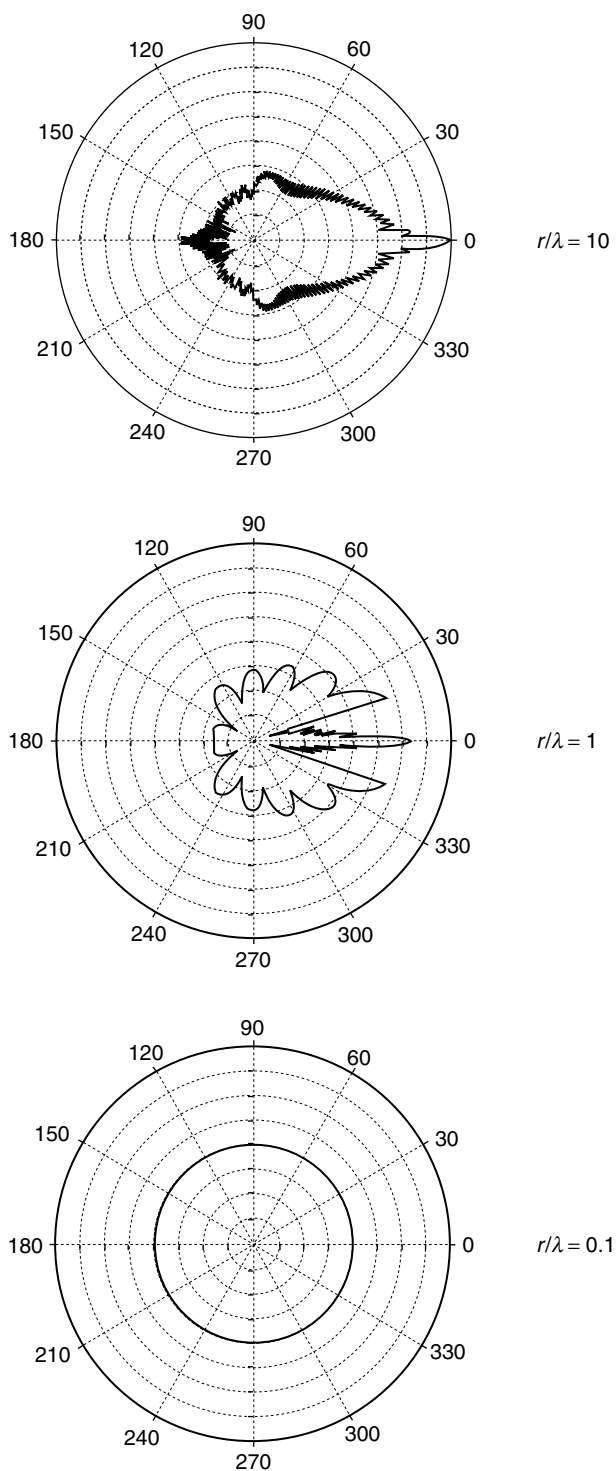


**Figure 10.4** Scattering patterns for droplets in the long, intermediate, and short wavelength regimes calculated using Mie theory.

more complex because of interference effects, that is, due to constructive or destructive interference of the waves interacting with different parts of the same droplet. As the droplet size increases relative to the wavelength ( $r/\lambda > 10$ ), more of the light wave is scattered into the forward direction (Figure 10.4). The more mathematically rigorous Mie theory is required to describe the light scattering behavior of these intermediate and large sized droplets (Bohren and Huffman, 1983).

As the particle size increases the scattering efficiency per unit volume of scatterers (integrated over all angles) increases to a maximum value (at  $r \approx \lambda/8$ ) and then decreases again (Hutchings, 1999). Practically, this means that for a fixed particle volume fraction the appearance of a colloidal dispersion goes from transparent to opaque to transparent again as the particle size is increased from  $r \ll \lambda$  to  $r \gg \lambda$ .

The scattering characteristics of an emulsion are strongly influenced by the concentration of droplets present (Figure 10.5). In highly dilute emulsions a light wave only encounters a single droplet before exiting the emulsion, which is referred to as “single scattering” (Bohren and Huffman, 1983). In more concentrated emulsions a light wave scattered by one droplet may encounter another droplet and be scattered again, which is referred to as “multiple scattering” (Bailey and Cannell, 1994). At sufficiently high droplet concentrations multiple scattering may become so extensive that the photons in the light wave travel through the emulsion by a diffusion process (Vargas and Niklasson, 1997a,b; Vargas, 1999, 2000, 2002). A variety of mathematical theories have been developed to relate the scattering characteristics of colloidal dispersions to the scattering characteristics and location of the individual particles. Single scattering theories are based on the assumption that the overall scattering characteristics of an emulsion can be found by simply summing the scattering contributions from all of the individual droplets present (Bohren and Huffman, 1983). Theories have also been developed to describe multiple scattering and diffusion of light through concentrated colloidal dispersions, although these are more complicated because it is necessary to include the multiply scattered waves in the overall waves that encounter a particle (Swanson and Billard, 2000; Vargas, 1999, 2002). It should be noted that when the droplets are relatively close to each other (i.e., less than a few droplet diameters), they can no longer be considered to scatter light independently of each other (Billmeyer and Richards, 1973). Under these circumstances it is not possible to calculate the scattering characteristics of an emulsion by combining the scattering characteristics of the individual particles.

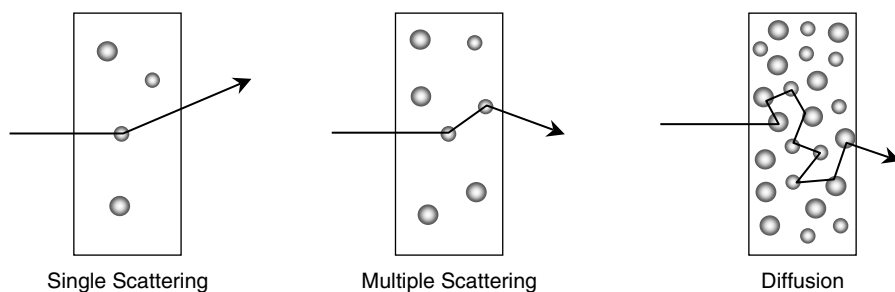


**Figure 10.5** Schematic representation of the passage of a light wave through emulsions of varying droplet concentration.

The reduction in the intensity of the light transmitted through an emulsion due to scattering by the droplets can be described by the following equation:

$$T = \frac{I_T}{I_{0,R}} = \exp(-\tau l) \quad (10.6)$$

where  $\tau$  is the turbidity. The turbidity of an emulsion depends on the size and concentration of the droplets present (see below). Indeed, measurements of the turbidity of dilute emulsions versus wavelength can be used to determine droplet sizes (Section 11.3.2).

The scattering of light waves by droplets mainly determines the turbidity, opacity, cloudiness, or lightness of an emulsion, which are desirable features of many types of food emulsions (Hernandez and Baker, 1991; Hernandez et al., 1991). For example, low concentrations of oil droplets consisting of vegetable or flavor oils are used to provide a turbid appearance to many types of fruit beverages, which gives them a natural looking character and appeal (Dickinson, 1994; Tan, 2004).

### 10.2.2 Human vision

The appearance of a food product is determined by the light waves that leave the light source, impinge on the material, and then enter the eye (Hutchins, 1999). The light waves enter the eye through the lens and are then focused onto the retina, which consists of numerous light-sensitive photoreceptors called “rods” and “cones.” The cones operate in normal or bright light and are responsible for color vision, whereas the rods operate in low light and are not capable of discriminating colors (Hutchins, 2002a; Ratey, 2001). At intermediate light levels there is a gradual change from one type of response to the other (Hutchins, 2002a). It is proposed that there are three types of cones, with each one being sensitive to different portions of the visible spectrum: red (long wavelength), green (medium wavelength), and blue (short wavelength) (MacDougall, 2002b). The spectral sensitivity of each type of cone has been established experimentally by color-matching experiments (Hutchins, 1999). There are slight differences between different human individuals, although most human beings have quite similar responses that can be defined in terms of a “standard observer” (Francis, 1995, 1999). When light waves impinge on the photoreceptors they act as transducers that generate electrochemical signals that are transmitted to the brain via the optic nerves (Hutchins, 2002b). The color of an object is determined by the relative magnitude of the signals from the red, green, and blue cones. The lightness or darkness of an object is determined by the overall intensity of the light waves reaching the photoreceptors, that is, the number of photons arriving at the photoreceptors per unit time. Considerable progress has recently been made in establishing the physiological processes involved in transduction of light waves into electrochemical signals at the photoreceptors, and in elucidating the pathways that these signals take along the optic nerves to the different regions in the brain responsible for vision (Ratey, 2001). Nevertheless, the process is extremely complicated and there are many psychological factors that also influence an individual’s perception of an object’s appearance (Hutchins, 2002a).

### 10.2.3 Quantitative description of appearance

It is notoriously difficult for human beings to quantitatively describe the appearance of objects due to the huge number of different possible colors, variations in the illuminating environment, and differences in the perception, psychology, vocabulary, and descriptive powers of individuals. Hence, two people observing the same object may describe its color differently. Consequently, there has been considerable effort in the development of reliable

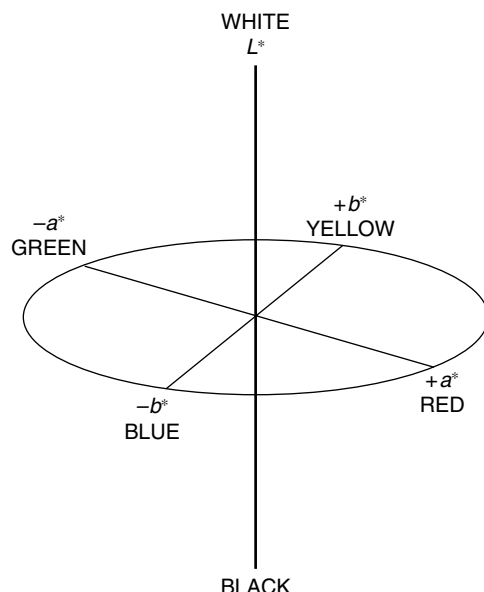


**Figure 10.6** The color of a substance can be represented in three-dimensional space using the  $L^*a^*b^*$  tristimulus coordinate system.

instrumental methods for objectively quantifying color and of standardized protocols for reporting colors. A variety of standardized methods have been developed to describe the color of objects based on the *tristimulus coordinates* concept, that is, the color of a material can be fully characterized by three mathematical parameters. One of the most widely used systems is the CIELAB system developed by the Commission International de l'Eclairage (CIE), which specifies the color of a material in terms of three coordinates:  $L^*$ ,  $a^*$ , and  $b^*$  (Judd and Wyszecki, 1963; Wyszecki and Stiles, 1982; Hutchins, 1999). The advantage of using a coordinate system is that the color of an object can be described in terms of just three mathematical variables. It is then possible to determine whether an object meets some predefined quality criteria in a quantitative manner. A graphical representation of the  $L^*a^*b^*$  tristimulus coordinate system is shown in Figure 10.6. In this color space,  $L^*$  represents the lightness and  $a^*$  and  $b^*$  are color coordinates: where  $+a^*$  is the red direction,  $-a^*$  is the green direction,  $+b^*$  is the yellow direction,  $-b^*$  is the blue direction, low  $L^*$  is dark, and high  $L^*$  is light (Wyszecki and Stiles, 1982). A variety of other tristimulus coordinate systems have been developed to describe the colors of objects and so it is important to define precisely which system was used when presenting experimental data (Hutchings, 1999). It is also important to specify the nature of the standardized light source (daylight, incandescent light, or fluorescent light) and standardized observer ( $2^\circ$  or  $10^\circ$ ).

### 10.3 Mathematical modeling of emulsion color

Before presenting mathematical models that can be used to predict the color of dilute and concentrated emulsions it is useful to give an overview of the physical processes that occur when a light wave encounters an emulsion. When a beam of white light is incident on the outer surface of an emulsion some of the light is transmitted into it and some of the light is reflected from it (Kortum, 1969; Frei and MacNeil, 1973; Frei et al., 1975). The relative proportions of transmitted and reflected light depend on the geometry, composition, and microstructure of the emulsion, as well as the nature of the container that holds

it (Kerker, 1969; Kortum, 1969; Bohren and Huffman, 1983). That part of the light that is transmitted into the emulsion travels through the continuous phase and interacts with the droplets. Any chromophoric substances present in either the continuous or dispersed phases will cause some of the light waves to be absorbed, by an amount that depends on the concentration and absorbance spectrum of the various colorants, the wavelength of the light used and the distance the wave travels through. Some wavelengths are absorbed more strongly than others so that the color of the light emerging from the emulsion is no longer white. For example, if light was absorbed strongly at wavelengths corresponding to orange-to-violet (400–605 nm), then the light emerging from an emulsion would appear red (605–700 nm). When a light wave that enters an emulsion encounters a droplet, part of the wave is transmitted and part of the wave is scattered (van de Hulst, 1957; Kerker, 1969). The fraction of the wave that is scattered and the direction that the scattered wave travels depends on the refractive index of the droplets and continuous phase, as well as on the size of the droplets relative to the wavelength of light (Bohren and Huffman, 1983). A light wave is only scattered by a single droplet when it propagates through a dilute emulsion (single scattering), but it is scattered by many droplets when it propagates through a concentrated emulsion (multiple scattering) (Figure 10.5). In a highly concentrated emulsion, a significant fraction of the incident light may travel back to the surface of an emulsion through multiple scattering events and emerge as diffusely reflected light (Kortum, 1969). The overall appearance of an emulsion is therefore determined by a combination of light scattering and absorption phenomena. Scattering is largely responsible for the turbidity, opacity, or lightness of an emulsion, whereas absorption is largely responsible for the chromaticness (*blueness, greenness, redness*, and so on).

As explained earlier, it is useful to be able to quantify emulsion color in terms of tristimulus coordinates because of the difficulty that human beings have in objectively specifying the precise color of objects (Hunter and Harold, 1987). In this section, we describe a theoretical approach that can be used to relate the tristimulus coordinates of emulsions to their composition and microstructure (McClements, 2002a,b). The various steps involved in this approach are shown schematically in Figure 10.7 for both dilute and concentrated emulsions. In this approach, it is assumed that the color of dilute emulsions is determined mainly by the light that is transmitted through them, whereas the color of concentrated emulsions is determined mainly by the light that is reflected from their surface. In practice, many food emulsions fall somewhere between these two extremes and their appearance is the result of both reflected and transmitted light.

### 10.3.1 Calculation of scattering characteristics of emulsion droplets

The first step in calculating the color of an emulsion is to calculate the scattering efficiency\* ( $Q_s$ ) and the asymmetry factor ( $g$ ) of the droplets over the visible wavelength range (380–780 nm) (Figure 10.8). The scattering efficiency is a measure of the fraction of the incident energy that is removed from the forward beam by scattering, whereas the asymmetry factor is a measure of the angular distribution of the energy scattered by a droplet (Kerker, 1969). Mathematically, the scattering efficiency is the ratio of the scattering cross section to the geometrical cross section, whereas the asymmetry factor is the average cosine of the scattering angle (Bohren and Huffman, 1983). As  $g$  tends toward unity, the scattered light is directed more and more in the forward direction (Figure 10.4). These two parameters

\* In systems where the absorption coefficient of an emulsion is comparable to or larger than the scattering coefficient it is not possible to uncouple absorption and scattering phenomenon (as assumed in this work). Under these circumstances one should use the extinction efficiency  $Q_{\text{ext}}$  rather than the scattering efficiency  $Q_s$ .

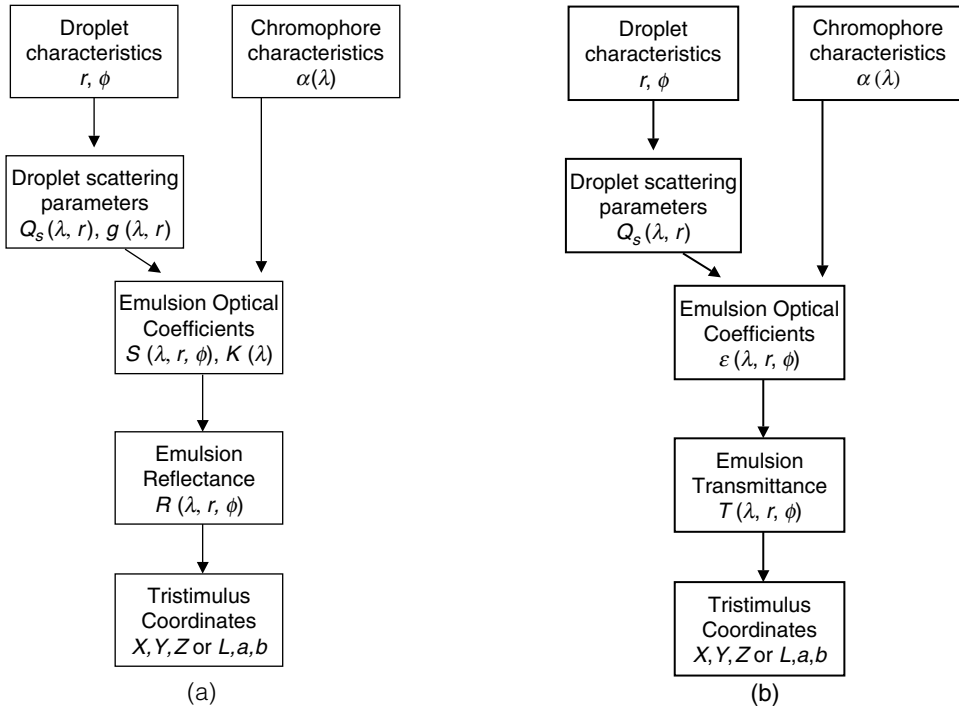


**Figure 10.7** Schematic representation of the theoretical calculation of the color of (a) concentrated emulsions from their reflectance spectrum and (b) dilute emulsions from their transmission spectrum.

can be calculated for droplets of arbitrary size using Mie theory (Dave, 1969; Wickansingham, 1973):

$$Q_s = \frac{2}{x^2} \sum_{n=1}^{\infty} (2n+1) [ |a_n|^2 + |b_n|^2 ] \quad (10.7)$$

$$g = \frac{4}{x^2 Q_s} \sum_{n=1}^{\infty} \left\{ \frac{n(n+2)}{n+1} [f(a_n, b_n)] + \frac{2n+1}{n(n+1)} [f'(a_n, b_n)] \right\} \quad (10.8)$$

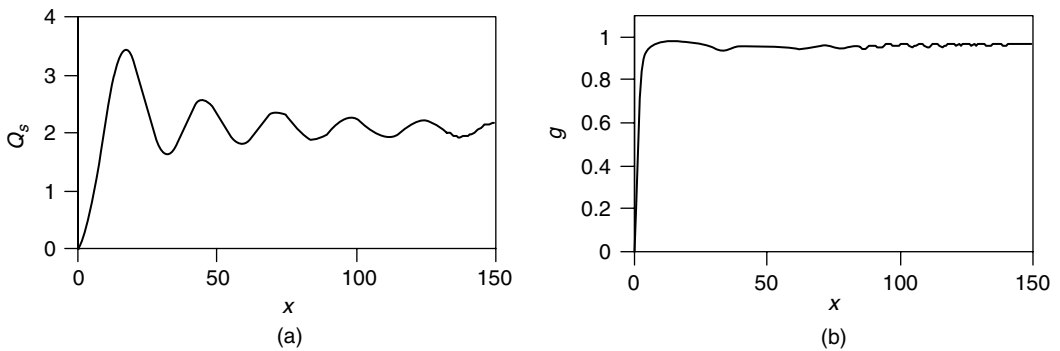


**Figure 10.8** Dependence of scattering characteristics of emulsion droplets ( $Q_s$  and  $g$ ) on the size parameter ( $x$ ) for 1  $\mu\text{m}$  radius oil droplets ( $n_2 = 1.43$ ) dispersed in water ( $n_1 = 1.33$ ).



where  $x = 2\pi r n_1 / \lambda$ ,  $r$  is the droplet radius,  $\lambda$  is the wavelength,  $m$  is the ratio of the complex refractive index of the droplets to that of the surrounding medium ( $= [n_2 - ik_2] / [n_1 - ik_1]$ ),  $n_1$  and  $n_2$  are the refractive indices of the continuous phase and dispersed phase,  $k_1$  and  $k_2$  are the absorptive indices of the continuous phase and dispersed phase,  $f[a, b]$  and  $f'[a, b]$  are functions of  $a$  and  $b$ , and  $a$  and  $b$  are coefficients that depend on  $x$  and  $m$ . Recurrence relations are available in the literature for calculating the  $a$  and  $b$  coefficients (Wickramasinghe, 1973; Bohren and Huffman, 1983). Under certain conditions it is possible to use approximations for the above expressions. For example, for small particles the *Rayleigh-Gans-Debye* theory can be used, or for particles with  $m$  close to unity the *anomalous diffraction* theory can be used (Kerker, 1969). Nevertheless, with the widespread availability of sophisticated mathematical software and rapid digital computers there is little reason for using these approximations rather than the full Mie theory. Indeed, computer programs are commercially available for calculating  $Q_s$  and  $g$  as a function of relative refractive index, wavelength, and droplet size (Michel, 2004). Numerical calculations of the dependence of  $Q_s$  and  $g$  on  $x$  are shown in Figure 10.8 for a typical oil-in-water emulsion. These calculations indicate that the extent of light scattering by emulsion droplets depends on their size relative to the wavelength of light. The main limitation of the Mie theory is that it does not take into account mutual polarization effects that become important when the droplets are in close proximity, that is, highly concentrated or flocculated emulsions (Kerker, 1969).

### 10.3.2 Calculation of spectral transmittance or reflectance of emulsions

The second step in calculating the color of an emulsion is to determine the spectral transmittance (for dilute emulsions) or spectral reflectance (for concentrated emulsions).

#### 10.3.2.1 Dilute emulsions

In terms of its optical properties, an emulsion can be defined as being “dilute” when a light wave that propagates through it only encounters a single droplet before emerging, that is, no multiple scattering occurs (Kerker, 1969). In this section, we assume that the appearance of a dilute emulsion is determined by the light transmitted through it. In practice, the color of a dilute emulsion perceived by an individual is a combination of reflected, scattered, and transmitted light, which is more difficult to quantify mathematically. Even so, transmission measurements on dilute emulsions are extremely valuable for instrumentally quantifying their color. The fraction of light transmitted through a dilute emulsion depends on the scattering of light by the droplets and the absorption of light by any colorants. The overall amount of light transmitted through an emulsion can therefore be characterized by the extinction coefficient,  $\varepsilon$ , which depends on the turbidity ( $\tau$ ) and the absorption coefficient ( $\alpha$ ):

$$T = \frac{I_T}{I_{0,R}} = \exp(-\varepsilon x) \quad (10.9)$$

$$\varepsilon = \tau + \alpha \quad (10.10)$$

where  $T$  is the transmittance,  $I_T$  is the intensity of light transmitted through a sample cell containing an emulsion,  $I_{0,R}$  is the intensity of light that has traveled through a reference cell containing the continuous phase of an emulsion in the absence of droplets and colorants, and  $x$  is the emulsion path length.

The absorption coefficient spectrum,  $\alpha(\lambda)$ , of the colorants in an emulsion normally has to be determined experimentally. The emulsion may contain chromophoric species in both the oil and aqueous phases. To determine the overall absorption spectrum of an

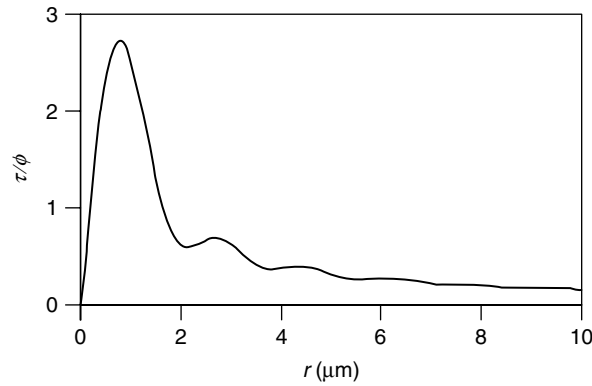


**Figure 10.9** Theoretical prediction of the influence of droplet radius on the turbidity of dilute oil-in-water emulsions ( $n_1 = 1.33$ ,  $n_2 = 1.43$ ,  $\lambda = 400$  nm).

emulsion it may therefore be necessary to measure the absorption spectra of the oil and aqueous phases separately:  $\alpha_E(\lambda) = \phi \alpha_D(\lambda) + (1 - \phi) \alpha_C(\lambda)$ , where the subscripts  $E$ ,  $D$ , and  $C$  refer to the emulsion, dispersed phase, and continuous phase, respectively, and  $\phi$  is the dispersed phase volume fraction. The turbidity of an emulsion can be calculated from the scattering characteristics of its droplets (Kerker, 1969):

$$\tau = \frac{3\phi Q_s}{4r} \quad (10.11)$$

The transmission spectrum,  $T(\lambda)$ , of a dilute emulsion can therefore be calculated from the droplet size and concentration and the measured absorption spectrum by combining Equations 10.7 and 10.11. The predicted dependence of the turbidity of dilute emulsions on droplet size for a single wavelength (400 nm) is shown in Figure 10.9. The turbidity is greatest at intermediate particle sizes, where the radius of the droplets is approximately similar to that of the wavelength. The wavelength of light varies from 0.3 to 0.7  $\mu\text{m}$ , and therefore emulsions containing droplets of this size would be expected to be the most turbid.

### 10.3.2.2 Concentrated emulsions

In this section, we assume that a “concentrated” emulsion is one in which the light waves propagate entirely by diffusion (Mudgett and Richards, 1971; Vargas, 2002), but the droplets are not close enough together for mutual polarization effects to be significant (Kerker, 1969). Most concentrated emulsions are optically opaque, and therefore their color is determined by the reflection of light waves from (or near to) their surface, rather than by the transmission of light waves through them. The spectral reflectance of an optically opaque emulsion can be related to its scattering and absorption characteristics using Kubelka–Munk theory (Kortum, 1969):

$$R = 1 + \frac{K}{S} - \sqrt{\frac{K}{S} \left[ \frac{K}{S} + 2 \right]} \quad (10.12)$$

where  $K$  and  $S$  are the absorption and scattering coefficients of the emulsion, respectively. Note that  $R$ ,  $K$ , and  $S$  are all wavelength dependent. The Kubelka–Munk theory is based on a two-flux solution of the radiative transfer theory, which mathematically describes the

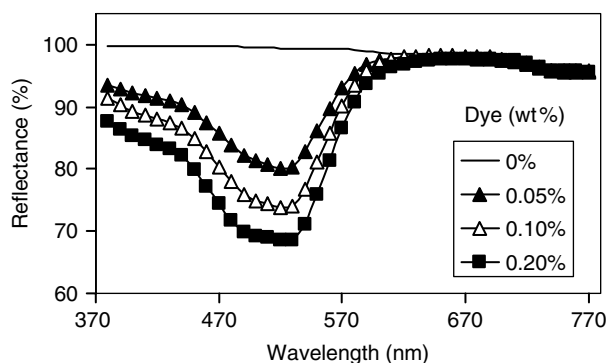


**Figure 10.10** Theoretical predictions of the influence of red dye concentration (shown in the annotation box) on the reflectance spectra of 10 wt% oil-in-water emulsions ( $\phi = 0.1$ ,  $r = 0.15 \mu\text{m}$ ).

propagation of light waves through media that both scatter and absorb radiation (Mudgett and Richards, 1971). The  $K$  and  $S$  coefficients can be related to the scattering and absorption characteristics of emulsion components using the following equations, which were established by empirically comparing the predictions made using the two-flux radiative transfer theory to those made using a more exact many-flux theory (Mudgett and Richards, 1971):

$$K = 2\alpha_E \quad (10.13)$$

$$S = \frac{3}{4}\pi r^2 Q_s [1 - g] - \frac{1}{4}\alpha_E \quad (10.14)$$

Predictions of the wavelength dependence of the spectral reflectance of relatively concentrated emulsions ( $\phi = 0.1$ ,  $r = 0.15 \mu\text{m}$ ) with different red dye concentrations are shown in Figure 10.10. In the absence of dye, emulsions appear “whitish” because the spectral reflectance does not change appreciably over the entire wavelength range. In the presence of dye, there are troughs in the reflectance spectra that correspond to the peaks in the absorption spectra of the red dye (Figure 10.3). These troughs become deeper as the dye concentration increases because more light is selectively absorbed by the dye molecules at these wavelengths.

As mentioned earlier, the above equations are based on the assumption that the propagation of light through an emulsion is entirely diffuse. In practice, light may pass through a material by both diffuse and nondiffuse processes and therefore the equations must be modified. These modifications become increasingly important as the droplet concentration or scattering efficiency decreases (Mudgett and Richards, 1971; Hapke, 1993). The above equations are also invalid at high droplet concentrations because of mutual polarization effects, that is, the polarization field of one droplet may interfere with that of another droplet (Kerker, 1969). This effect usually occurs when the droplets are closer than a few diameters to each other, for example in highly concentrated or flocculated systems. Another limitation of the above theory is that it assumes that the reflection occurs from a boundary between pure continuous phase and a semiinfinite emulsion (Kottrum, 1969). In reality, an emulsion is usually contained in an optically transparent container (e.g., a plastic, glass or quartz bottle or cuvette) and so the reflection occurs from an air–wall–emulsion–wall arrangement. Methods of taking into account the influence of the optical measurement arrangement on emulsion color are described in a later section. Other limitations of the Kubelka–Munk theory and methods of overcoming them have been described elsewhere (Hapke, 1993; Hutchings, 1999).

### 10.3.3 Relationship of tristimulus coordinates to spectral reflectance and transmittance

The third step in the theoretical prediction of emulsion color is to calculate the tristimulus coordinates from the spectral transmittance (dilute emulsions) or spectral reflectance (concentrated emulsions) (Figure 10.7). The  $X$ ,  $Y$ ,  $Z$  tristimulus coordinates are related to the spectral reflectance by the following equations (Wyszecki and Stiles, 1982):

$$X = k \sum_{380 \text{ nm}}^{770 \text{ nm}} S(\lambda) \bar{x}(\lambda) R(\lambda) \quad (10.15)$$

$$Y = k \sum_{380 \text{ nm}}^{770 \text{ nm}} S(\lambda) \bar{y}(\lambda) R(\lambda) \quad (10.16)$$

$$Z = k \sum_{380 \text{ nm}}^{770 \text{ nm}} S(\lambda) \bar{z}(\lambda) R(\lambda) \quad (10.17)$$

$$k = \frac{100}{\sum_{380 \text{ nm}}^{770 \text{ nm}} S(\lambda) \bar{y}(\lambda)} \quad (10.18)$$

where  $S(\lambda)$  is the spectral distribution of the standard illuminant at wavelength  $\lambda$ ,  $\bar{x}(\lambda)$ ,  $\bar{y}(\lambda)$ , and  $\bar{z}(\lambda)$  are the human response functions of the CIE color system, and  $R(\lambda)$  is the spectral reflectance of the material. These human response functions were determined by the CIE by measuring the sensitivity of the different light-sensitive receptors. The above equations highlight the fact that the appearance of an emulsion depends on the nature of the light source ( $S(\lambda)$ ), the observer ( $\bar{x}(\lambda)$ ,  $\bar{y}(\lambda)$ ,  $\bar{z}(\lambda)$ ) and the material ( $T(\lambda)$  or  $R(\lambda)$ ). It is particularly important to use values of  $S(\lambda)$  that are applicable to the light source used in an experiment when comparing theoretically and experimentally determined tristimulus coordinates. The same approach can be used to calculate the  $X$ ,  $Y$ ,  $Z$  values of a dilute emulsion, but in this case the transmittance spectrum,  $T(\lambda)$ , rather than the reflectance spectrum,  $R(\lambda)$ , is used in Equations 10.15–10.18.

The  $X$ ,  $Y$ , and  $Z$  coordinates are not easily interpreted in terms that are used by human beings to describe color (Hunter and Harold, 1987). Consequently, a variety of other color scales have been developed that use coordinates that are more closely related to quantities associated with human perception of color, for example,  $L^*a^*b^*$ ,  $L^*C^*h$ , Hunter-Lab,  $Yxy$ , Munsell (Wyszecki and Stiles, 1982; Hutchins, 1999). One of the most widely used is the CIE 1976  $L^*a^*b^*$  color scale mentioned in an earlier section, which is calculated from the  $X$ ,  $Y$ ,  $Z$  values using published formulas (Wyszecki and Stiles, 1982):

$$L^* = 116 \sqrt[3]{Y/Y_n} - 16 \quad (10.19)$$

$$a^* = 500 \left[ \sqrt[3]{X/X_n} - \sqrt[3]{Y/Y_n} \right] \quad (10.20)$$

$$b^* = 200 \left[ \sqrt[3]{Y/Y_n} - \sqrt[3]{Z/Z_n} \right] \quad (10.21)$$

These equations are only applicable when  $X/X_n$ ,  $Y/Y_n$ , or  $Z/Z_n$  are greater than 0.01, and must be corrected otherwise (Hunter and Harold, 1987). The  $X_n$ ,  $Y_n$ , and  $Z_n$  values are calculated using Equations 10.19–10.21, but with  $R(\lambda)$  for concentrated emulsions) or  $T(\lambda)$  (for dilute emulsions) equal to unity. The above equations enable one to calculate the tristimulus coordinates of an emulsion based on knowledge of its spectral reflectance or transmittance.

### 10.3.4 Influence of polydispersity

The theory described above assumes that the droplets in the emulsion are all of the same size, that is, they are monodisperse. In reality, emulsions normally contain a range of different droplet sizes and the light waves are scattered differently by the droplets in each size class (Bohren and Huffman, 1983). In this section, we show how polydispersity can be incorporated into the equations for calculating the transmission and reflection coefficients of emulsions. For dilute emulsions, the turbidity given by Equation 10.11 should be replaced by the following expression:

$$\tau = \frac{3}{4} \sum_{i=1}^N \frac{\phi_i Q_{s,i}}{r_i} \quad (10.22)$$

where  $\phi_i$ ,  $r_i$ , and  $Q_{s,i}$  are the volume fraction, radius, and scattering efficiency of the droplets in the  $i$ th size class, and  $N$  is the total number of size classes. The transmittance spectrum and tristimulus coordinates can then be calculated as described above. For concentrated emulsions, the scattering coefficient given by Equation 10.14 should be replaced with the following expression:

$$S = \frac{3}{4} \left[ \pi \sum_{i=1}^N r_i^2 Q_{s,i} [1 - g_i] \right] - \frac{1}{4} \alpha_E \quad (10.23)$$

where  $\Sigma_{s,i}$  and  $g_i$  are the scattering cross section and asymmetry factor of the droplets in the  $i$ th size class. The reflectance spectrum and tristimulus coordinates can then be calculated as described above. When an emulsion contains a range of different droplet sizes the undulations in the optical properties (e.g.,  $Q_s$ ) with droplet radius that are observed in a monodisperse emulsion are smoothed out (Kerker, 1969). Incidentally, Equations 10.22 and 10.23 can also be used to calculate the transmission and reflection spectra of emulsions containing droplets consisting of different types of materials.

### 10.3.5 Numerical calculations of emulsion color

The light scattering theory described above enables one to predict the influence of composition and microstructure on the optical properties of food emulsions (McClements, 2002a,b). The theory could be used to optimize product color without having to carry out time-consuming and laborious experiments. In this section, the light scattering theory is used to investigate some of the major factors that influence the color of concentrated oil-in-water emulsions: droplet concentration; droplet radius; refractive index ratio; dye concentration. It is assumed that the emulsion contains a red dye and that light reflection occurs from a planar boundary between pure continuous phase and the emulsion (Figure 10.11), that is, the influence of the optical measurement system is ignored (see later). Numerical calculations of the color of dilute emulsions have been carried out and compared with experimental measurements in a previous publication (Chanamai and McClements, 2001).

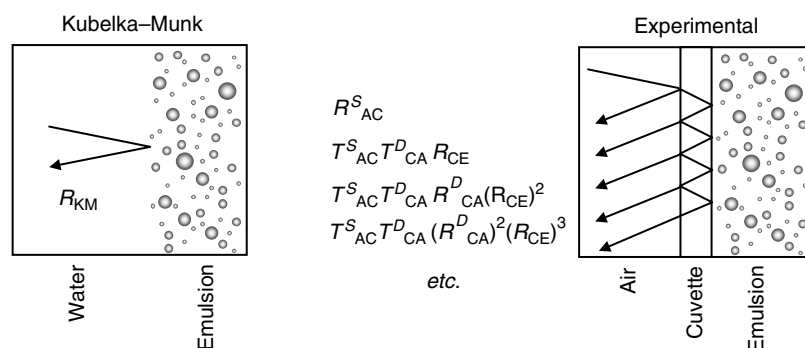


**Figure 10.11** Comparison of reflection from a planar continuous phase–emulsion boundary (assumed in Kubelka–Munk theory) with reflection from an air–wall–emulsion interface (experimental situation).

In these examples, emulsion color is represented by lightness ( $L^*$ ) and chroma ( $C = (a^{*2} + b^{*2})^{1/2}$ ), where  $L^*$  is a measure of lightness/darkness and  $C$  is a measure of color intensity. The influence of droplet concentration ( $\phi = 0 - 0.2$ ) and droplet radius ( $r = 0.1 - 10 \mu\text{m}$ ) on the color of monodisperse oil-in-water emulsions ( $n_1 = 1.33$ ,  $n_2 = 1.43$ ) was calculated (Figures 10.12 and 10.13). The dependence of the color coordinates on droplet concentration for emulsions with the same droplet radius ( $r = 0.1, 1$ , or  $10 \mu\text{m}$ ) is shown in Figure 10.12. Emulsion lightness ( $L^*$ ) increased with increasing droplet concentration because more light was multiply scattered backward by the droplets. The lightness increased steeply as the droplet volume fraction increased from 0 to 0.05, and then increased less steeply at higher droplet concentrations (Figure 10.12a). This has important consequences for the development of emulsion-based products with reduced droplet concentrations (e.g., low fat salad dressings). When the droplet concentration is decreased below a certain level the product appearance changes dramatically, which may have an adverse impact on perceived quality. The chromaticness of the emulsions decreased with increasing droplet concentration. From a sensory perspective, this means that the color of the emulsions becomes more faded in appearance as the droplet concentration is increased (Chantrapornchai et al., 1998, 1999a,b).

The dependence of emulsion color on droplet concentration is strongly affected by droplet size (Figure 10.12). The  $L^*$  value increased and the chromaticness decreased as the

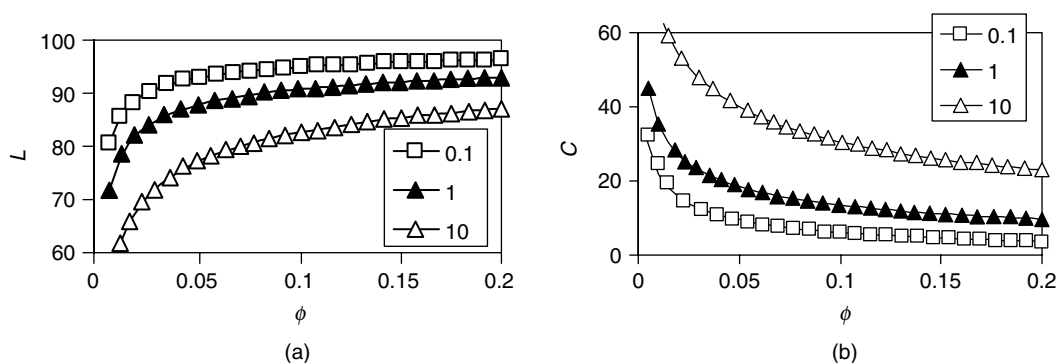


**Figure 10.12** Theoretical prediction of the influence of droplet concentration on the color coordinates of oil-in-water emulsions ( $n_1 = 1.33$ ,  $n_2 = 1.43$ ) containing different droplet radii (see annotation box), but the same dye concentration ( $c_{\text{dye}} = 0.002 \text{ wt\% red dye}$ ).

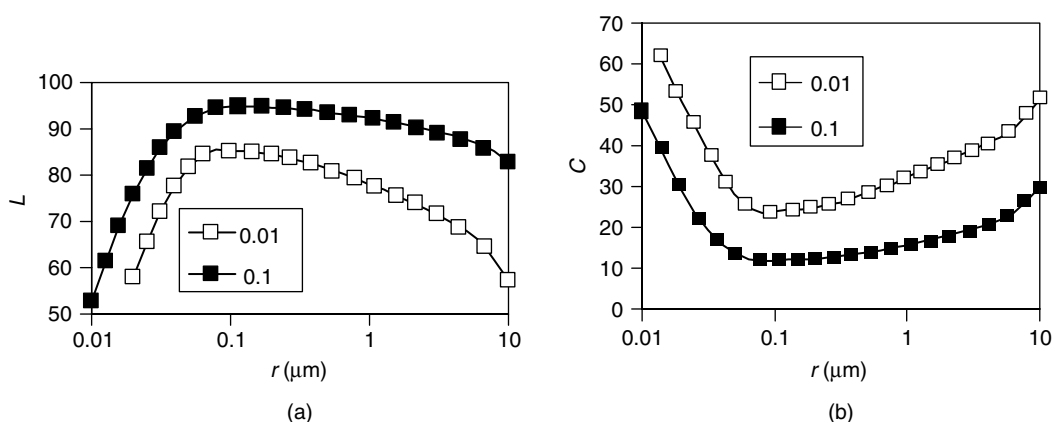


**Figure 10.13** Theoretical prediction of the influence of droplet radius on the color coordinates of 1 vol% ( $\phi = 0.01$ ) and 10 vol% ( $\phi = 0.1$ ) oil-in-water emulsions ( $n_1 = 1.33$ ,  $n_2 = 1.43$ ) with the same red dye concentration ( $c_{\text{dye}} = 0.002$  wt%).

droplet radius decreased from 10 to 0.1  $\mu\text{m}$ . The full dependence of the color coordinates on droplet radius is shown in Figure 10.13 for emulsions with the same droplet concentration ( $\phi = 0.01$  and 0.1). The lightness has a maximum value in emulsions containing 0.1  $\mu\text{m}$  radius droplets, and decreases for smaller or larger droplet sizes. In contrast, the turbidity of dilute emulsions containing the same kind of aqueous and oil phases has a maximum value for droplets around 1.3  $\mu\text{m}$  radius (Chanamai and McClements, 2001). The differences in the dependence of lightness and turbidity on radius can be attributed to the fact that the turbidity only depends on the fraction of light removed from the forward beam by scattering (i.e.,  $Q_s$ —Equation 10.11), whereas the lightness also depends on the direction that the light is scattered (i.e.,  $Q_s$  and  $g$ —Equations 10.11–10.14). As the droplet radius increases, more of the light is scattered in the forward direction ( $g \rightarrow 1$ , Figure 10.8), and therefore a smaller fraction of light is scattered backward and detected as diffusely reflected light. As expected, the chroma of the emulsions exhibits a minimum value at the droplet size where the lightness exhibits its maximum value.

The influence of refractive index on the color of emulsions is shown in Figure 10.14. These calculations were carried out assuming that the droplet radius ( $r = 1$   $\mu\text{m}$ ), droplet

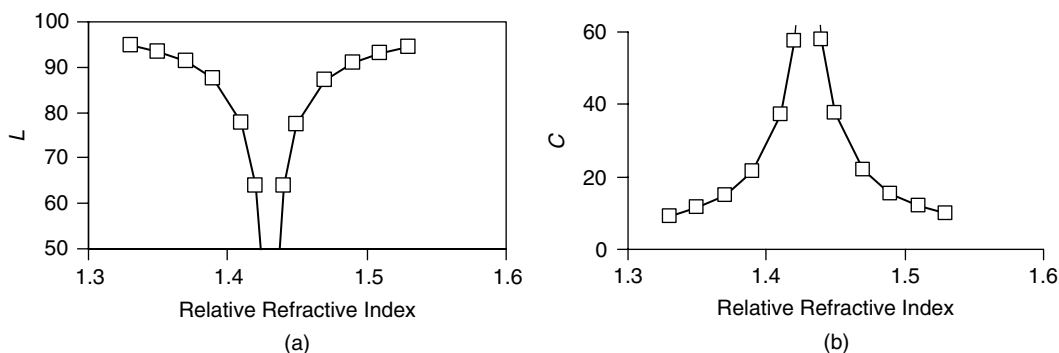


**Figure 10.14** Theoretical prediction of the influence of refractive index ratio ( $n_2/n_1$ ) on the color coordinates of oil-in-water emulsions ( $n_2 = 1.43$ ) containing the same red dye concentration ( $c_{\text{dye}} = 0.002$  wt%), droplet concentration ( $\phi = 0.1$ ), and droplet radius ( $r = 1$   $\mu\text{m}$ ).

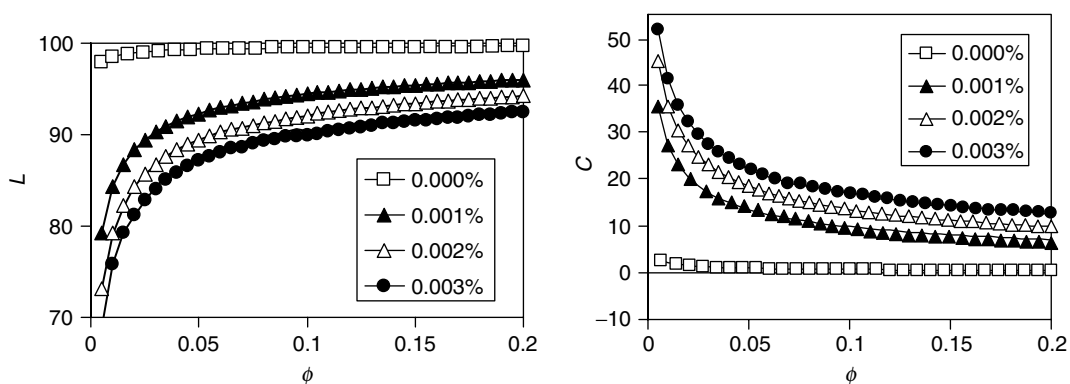


**Figure 10.15** Theoretical prediction of the influence of droplet concentration on the color coordinates of 10 vol% oil-in-water emulsions ( $n_1 = 1.33$ ,  $n_2 = 1.43$ ) containing different dye concentrations (see annotation box), but the same droplet radius ( $r = 1 \mu\text{m}$ ).

concentration ( $\phi = 0.1$ ), and refractive index of the droplets ( $n_2 = 1.43$ ) remained constant, but the refractive index of the continuous phase varied ( $n_1 = 1.33 - 1.53$ ). In practice, this kind of situation could be achieved by adding a water-soluble solute to the aqueous phase of an oil-in-water emulsion, for example, salt, sugar, or polyol (Weiss and Liao, 2000; Chantrapornchai et al., 2001b). The lightness decreased and the chroma increased as the refractive index of the droplets tended toward that of the continuous phase (Figure 10.14). This is because the scattering efficiency of the droplets decreases as the refractive index ratio ( $n_2/n_1$ ) tends toward unity (Kerker, 1969), consequently a smaller fraction of light is scattered in the backward direction. The influence of dye concentration on the color of emulsions is shown in Figure 10.15. Emulsion lightness decreased with increasing red dye concentration because the dye molecules absorbed light and therefore less light was reflected back from the emulsions. As would be expected, the presence of dye had a pronounced influence on the color intensity (chroma) of the emulsions.

The numerical calculations shown in Figures 10.12–10.15 demonstrate the usefulness of light scattering theory as a means of establishing the major factors that determine the color of concentrated oil-in-water emulsions. Changes in emulsion color resulting from alterations in composition or microstructure can be rapidly determined using a personal computer, rather than having to carry out time-consuming, costly, and laborious experiments. As will be shown in the following sections, there is excellent qualitative agreement between predictions of the light scattering theory and experimental measurements, but the quantitative agreement is not as good because of the influence of the optical measurement system on emulsion color.

### 10.3.6 Influence of measurement cell

To quantitatively compare the color of emulsions predicted by light scattering theory to the color of emulsions measured by an analytical instrument it is necessary to account for the nature of the optical measurement system. As mentioned previously, the light scattering theory assumes that the light waves are reflected from a planar boundary between a continuous phase and an emulsion, whereas in reality the reflection occurs at an air–wall–emulsion–wall arrangement (Figure 10.11). Experiments have shown that the reflectance of light from a microheterogeneous material is reduced appreciably when it is covered by a smooth layer of an optically transparent material (Chatfield, 1962). This reduction is a result of the reverberations of light waves within the layer of covering



material: each time a light wave encounters the emulsion it is partly transmitted and absorbed (Figure 10.11). It is therefore necessary to develop methods of correcting the light scattering theory so that it takes into account the influence of the optical measurement system. Three methods of carrying out this correction procedure are outlined below:

- *Theoretical approach.* The first method involves theoretically accounting for the influence of the optical measurement system on the fraction of light reflected from a concentrated emulsion (McClements et al., 1998). This approach uses mathematical equations to calculate the fraction of light that is reflected or transmitted at the various boundaries within the optical measurement system. The main advantage of this method is that it can be used without having to carry out any experiments. The color of an emulsion can be predicted from its composition and microstructure, provided information about the optical measurement system is known, for example, the refractive index of the material making up the measurement cell and the angle of incidence of the light beam. Nevertheless, the agreement between the predictions of the mathematical model and experimental measurements are not always in close agreement because of difficulties in fully modeling the complex processes involved (McClements et al., 1998).
- *Semiempirical calibration approach.* The second method involves establishing an empirical relationship between the theoretically predicted reflection coefficient ( $R_p$ ) and the experimentally measured reflection coefficient ( $R_M$ ) using a series of emulsions containing a wide range of droplet sizes, droplet concentrations, and dye concentrations (Chantrapornchai et al., 1998). The main disadvantage of this approach is that a large number of calibration experiments have to be carried out for each optical measurement system using emulsions of known composition and microstructure. Nevertheless, the empirical calibration approach seems to be the most successful for obtaining good quantitative agreement between theory and experiment.
- *Optical system approach.* Another method of improving the agreement between theory and experiment is to use an optical measurement system that corresponds more closely to the assumptions made in the light scattering theory (Figure 10.11). Ideally, the emulsion should be contained in an optically transparent container with parallel walls that is constructed from a material with the same refractive index as the continuous phase of the emulsion. In addition, the sample container, optical source, and optical detector should be placed within a fluid that also has the same refractive index as the emulsion continuous phase. The reflection of the light beam will then occur from a boundary between a material with the same refractive index as the emulsion continuous phase and the emulsion itself, as assumed in the theory. This approach would be expected to greatly improve the agreement between the theory and experiment; however, it may still be necessary to apply some empirical correction to improve the agreement further because of the practical difficulty in finding materials with appropriate refractive indices.

## 10.4 Measurement of emulsion color

A variety of different approaches have been developed to quantify the color of materials (Hutchins, 1999). Originally, the color of a material was quantified by a human subject who compared its color with a series of colored tiles or cards and determined the one that gave the best color match (MacDougall, 2002b). The tiles or cards were then replaced by specially designed optical instruments that could produce a wide range of different colors by combining light from three different colored light sources: red, green, and blue (Francis, 1999). The intensities of the red, green, and blue light sources were then adjusted until

they produced a color that matched that of the material being analyzed, and the material color was specified in terms of these three light intensities. These traditional color-matching techniques have now been largely replaced by modern photoelectric colorimeters, which can be classified into two groups according to their operating principles: spectrophotometric and trichromatic colorimeters (MacDougall, 2002b; Joshi, 2000, 2002). These colorimeters come in a variety of different formats depending on the nature of the application, for example, bench-top, hand-held, and on-line instruments. Many of these instruments also come with a variety of different optical measurement arrangements that are suitable for analyzing different types of materials: liquids, semisolids or solids; transparent, translucent, or opaque materials (Hutchins, 1999; Joshi, 2002). Most modern instruments automatically calculate and report the tristimulus coordinates of a material in terms of a user-specified color space system, for example, XYZ, CIELAB, or Hunter-Lab coordinates.

### 10.4.1 Spectrophotometric colorimeters

The color of emulsions can often be determined using ultraviolet (UV)–visible spectrophotometers that measure the transmission and/or reflection of light from objects as a function of wavelength in the visible region (Clydesdale, 1975; Francis and Clydesdale, 1975; Hutchins, 1999). These instruments usually consist of a light source, a wavelength selector, a sample holder, and a light detector (Figure 10.16).

#### 10.4.1.1 Transmission spectrophotometry

A beam of white light, which contains electromagnetic radiation across the whole of the visible spectrum, is passed through a wavelength selector that isolates radiation of a specific wavelength (Figure 10.16a). This monochromatic wave is then passed through a measurement cell that contains the sample and the intensity of the transmitted wave is measured using a light detector. By comparing the intensity of the light transmitted by the sample with that transmitted by a reference material (e.g., distilled water) it is possible to determine the transmittance of the sample (Equation 10.9). A transmittance spectrum is obtained by carrying out this procedure across the whole range of wavelengths in the visible region. Transmission measurements can only be carried out on emulsions that allow a significant amount of light to pass through them. Practically, this means that they can only be used on relatively dilute emulsions, for example, droplet concentrations <0.1 wt%

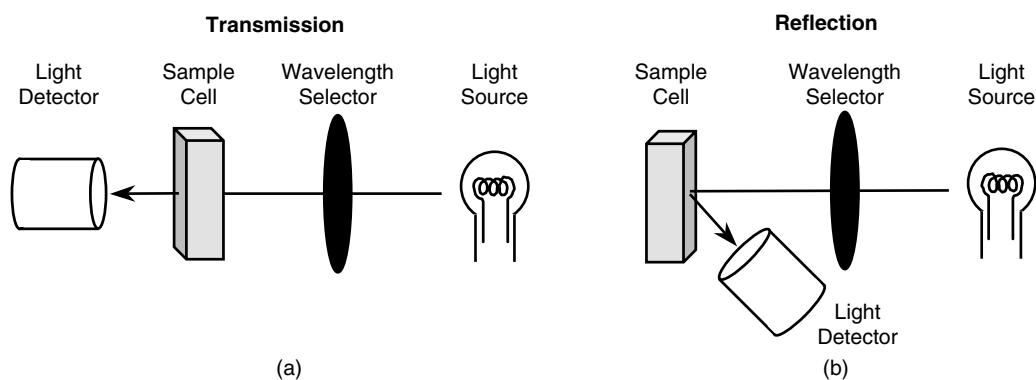


**Figure 10.16** Examples of transmission and reflection spectrophotometers that can be used to measure the color of food emulsions.

for a typical food emulsion. Nevertheless, it should be noted that transmission measurements can be made on considerably more concentrated emulsions provided that the refractive index of the droplets is close to that of the continuous phase, that is, the refractive index ratio is close to unity (Husband et al., 2001).

#### 10.4.1.2 Reflection spectrophotometry

In these instruments the intensity of light reflected from the surface of a sample is measured (Figure 10.16b). The reflectance,  $R$ , of a material is defined as the ratio of the intensity of the light reflected from the sample ( $I_s$ ), to the intensity of the light reflected from a reference material of known reflectance ( $I_R$ ):  $R = I_s/I_R$ . The reference material is usually chosen to be a white plate that reflects the vast majority of light incident on it at all wavelengths. The optical arrangement used to carry out the measurement depends on whether the reflection from the sample is specular or diffuse (Figure 10.17). For specular reflection, the intensity of the reflected light is measured at an angle of  $90^\circ$  to the incident wave, whereas for diffuse reflection the light intensity must be measured at other angles. The most commonly used optical arrangements for characterizing the color of diffusely reflecting samples are the "45/0" and "0/45" geometries for flat surfaces and the "diffuse/0" and "near 0/diffuse" geometries for integrating spheres (Figure 10.17). In the *45/0 geometry* a sample is illuminated with a light beam at an angle of  $45^\circ$  to its surface and the intensity of the reflected wave is measured perpendicular to the sample surface (Figure 10.17). In the *0/45 geometry* a sample is illuminated by a light beam directed perpendicular to its surface and the intensity of the reflected wave is measured at an angle of  $45^\circ$  to the sample surface. In both of these methods the specular reflectance is not detected since it is reflected at an appreciably different angle from that of the detector. In the *diffuse/0 geometry* the incident light beam is directed to the inside of an integrating sphere where it is diffusely reflected.

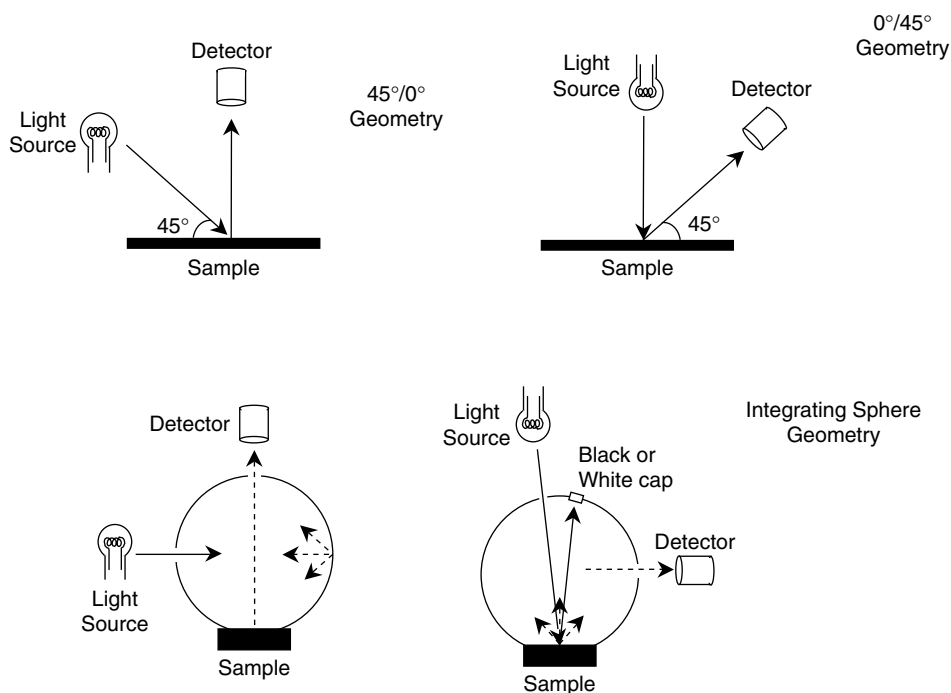


**Figure 10.17** Different measurement cells available to quantify the color of diffusely reflecting materials.

The intensity of the radiation that is diffusely reflected at an angle perpendicular to the surface of the material is then measured. In the *near 0/diffuse geometry* a light beam is directed onto the sample at an angle of about  $8^\circ$ , where it is diffusely reflected. The diffusely reflected radiation bounces from the inner surfaces of the integrating sphere and the intensity of the reflected signal is measured at a specific angle. Any specularly reflected light can be included or excluded from the detected signal by placing a white or black cap, respectively, at a reflection angle of  $8^\circ$ . Whether the specularly reflected light is included or excluded from an analysis depends on the nature of the material analyzed and the type of information required. For any of the above optical geometries, a reflectance spectrum is obtained by measuring the intensity of the reflected light across the whole range of wavelengths in the visible region. The instrument uses a grating or filter arrangement to select specific wavelengths for analysis.

The transmittance and reflectance spectra obtained from a sample can themselves be used to characterize the relative magnitudes of the absorption and scattering of light by an emulsion as a function of wavelength. Alternatively, the color of a product can be specified in terms of trichromatic coordinates by analyzing the spectra using appropriate mathematical transformation functions, as described above (Section 10.3). Most modern spectrophotometric colorimeters automatically report the color of a material in terms of its tristimulus coordinates, for example,  $L^*$ ,  $a^*$ ,  $b^*$  values. Possible sources of errors when analyzing food materials using this type of colorimeter have been discussed in the literature (MacDougall, 2002b; Joshi, 2002).

#### 10.4.2 Trichromatic colorimeters

Trichromatic colorimeters are designed to measure the color of materials in a manner that is analogous to the way that the human eye sees objects, that is, they have detectors that measure the intensity of the “red,” “green,” and “blue” components of light in a manner that mimics the photoreceptors on the human retina (Francis and Clydesdale, 1975; Hutchins, 1999; Francis, 1995, 1999); however, colorimeters use a consistent well-defined light source and have a carefully controlled optical arrangement (light source sample detector) so that the results are reproducible and quantifiable.

A simple colorimeter consists of a light source, a sample cell containing the material to be analyzed, a set of three filters (red, green, and blue), and a photocell to determine the light intensity (Figure 10.18). As mentioned above the three filters are designed to duplicate the response of the human eye (Francis, 1999). The intensity of a light beam is

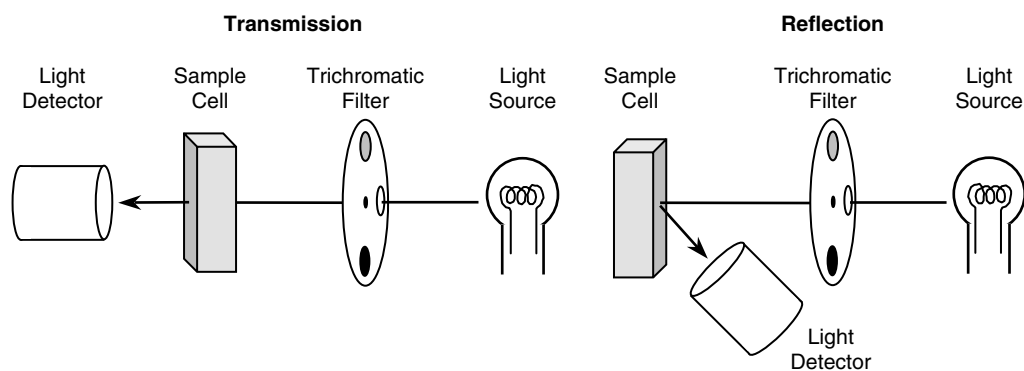


**Figure 10.18** Schematic diagram of simple trichromatic colorimeters that can be used to measure the color of food emulsions in either transmission or reflection mode.

measured after it has interacted with the sample and passed through one of the color filters. This procedure is then repeated for the other two filters, and the sample is characterized in terms of tristimulus coordinates related to the intensities of light waves passing through the red, green, and blue filters. Like spectrophotometers, colorimeters are capable of making either transmission or reflectance measurements, and similar optical arrangements are available for measuring specular and diffuse reflectance from samples. Reflectance measurements are most suitable for determining the color of concentrated emulsions, while transmission measurements are more suitable for characterizing dilute emulsions. Possible sources of errors when analyzing food materials using this type of colorimeter have been discussed in the literature (MacDougall, 2002b; Joshi, 2002).

### 10.4.3 *Light scattering*

Light scattering techniques are used principally to determine the size distribution of the droplets in an emulsion (Section 11.3). Knowledge of the droplet size distribution enables one to predict the influence of the droplets on light scattering, and therefore on the turbidity of an emulsion (Hernandez and Baker, 1991; Dickinson, 1994). Alternatively, the experimentally determined scattering pattern—the intensity of scattered light versus scattering angle—can be used directly to describe the scattering characteristics of the emulsion droplets (Figure 10.4).

The scattering of light from dilute emulsions is sometimes characterized by a device known as a Nephelometer (Hernandez et al., 1991). This device measures the intensity of light that is scattered at an angle of  $90^\circ$  to the incident beam. The intensity of light scattered by a sample is compared with that scattered by a standard material of known scattering characteristics, for example, formazin (Hernandez et al., 1991). Because small droplets scatter light more strongly at wide angles than large droplets, the Nephelometer is more sensitive to the presence of small droplets than are turbidity measurements. Nephelometers can be used to provide information about the “haze” or “cloudiness” of products such as beverages.

### 10.4.4 *Sensory analysis*

Ultimately, the appearance of an emulsion must be acceptable to the consumer and therefore it is important to carry out sensory tests (Hutchins, 1999). Sensory methods can be conveniently divided into two categories: discriminant methods and descriptive methods (Piggot, 1988; Piggot et al., 1998). In discriminant methods panelists are requested to identify whether there is a sensory difference in specified properties between two or more food samples. In descriptive methods the panelists are requested to assess and rank specified properties of food samples based on previously established sensory descriptors. Sensory analysis can also be categorized according to whether a trained or nontrained panel is used to carry out the evaluation (Hutchins, 1999). Sensory tests must be carried out in a room where the light source is carefully controlled to obtain reproducible measurements that correspond to the conditions a person might experience when consuming the product (Francis and Clydesdale, 1975; Hutchins, 1999).

## 10.5 *Major factors influencing emulsion color*

A number of systematic experimental studies have recently been carried out to determine the influence of composition and microstructure on the color of emulsions (Chantrapornchai et al., 1998, 1999a,b, 2001a,b; McClements et al., 1998; Chanamai and McClements, 2001). These measurements are in excellent qualitative agreement with predictions made using

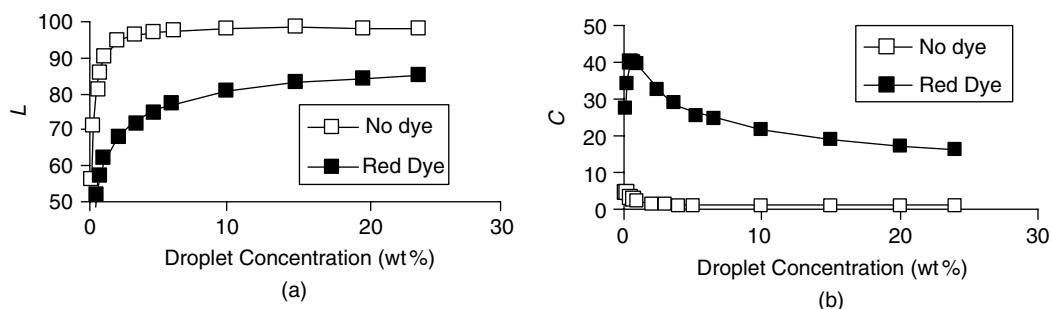


**Figure 10.19** Influence of droplet concentration on the lightness ( $L$ ) and chroma ( $C$ ) of *n*-hexadecane oil-in-water emulsions ( $r \sim 0.15 \mu\text{m}$ ) in the presence and absence of a red dye (Chantrapornchai et al., 1999b).

the light scattering theory mentioned in Section 10.3; however, the quantitative agreement is not so good, mainly because of problems associated with accounting for the optical measurement system.

### 10.5.1 Droplet concentration and size

Experimental measurements of the influence of droplet concentration and size on the color of oil-in-water emulsions have been carried out (Chantrapornchai et al., 1998, 1999a,b). These studies have shown that emulsion lightness increased steeply as the droplet concentration was increased from 0 to 5 wt%, after which it changed less dramatically (Figure 10.19a), as predicted by the theory (Figure 10.12). The intensity of the emulsion color ( $C$ ) tends to fade with increasing droplet concentration, except at low droplet concentrations (0–1 wt%) in dyed emulsions where there is initially an increase in  $C$  (Figure 10.19b). This initial increase has been attributed to the influence of multiple scattering on the effective pathlength that the light waves travel through the emulsion before being reflected back to the detector (Chantrapornchai et al., 1999b). Experiments with polydisperse *n*-hexadecane oil-in-water emulsions have shown that emulsion lightness has a maximum value and emulsion chroma has a minimum value for droplets with radii around  $0.1 \mu\text{m}$ , and that  $L^*$  decreased and  $C$  increased as the droplet radius was increased from  $0.1$  to  $15 \mu\text{m}$  (Figure 10.20), which is in qualitative agreement with theory (Figure 10.13). The increase in emulsion lightness and decrease in emulsion chroma with increasing droplet concentration

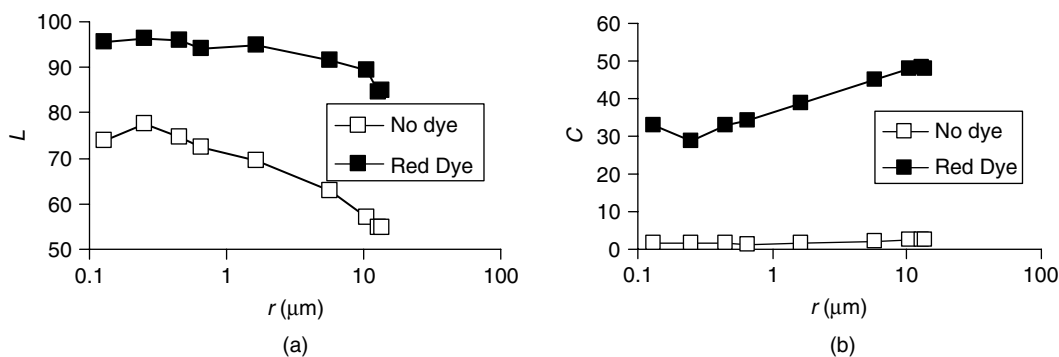


**Figure 10.20** Influence of droplet radius on the lightness ( $L$ ) and chroma ( $C$ ) of 9.6 wt% *n*-hexadecane oil-in-water emulsions in the presence and absence of a red dye (Chantrapornchai et al., 1999b).

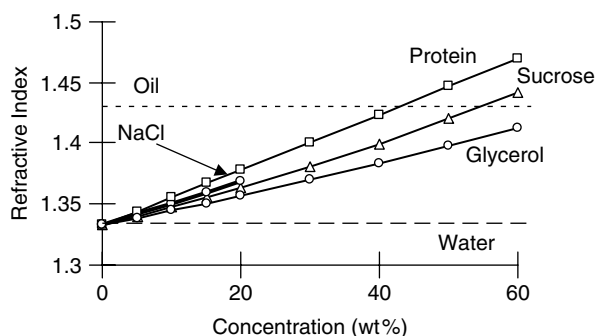


**Figure 10.21** The refractive index of aqueous solutions increases when the solute concentration (salt, sugar, protein, polyol) increases.

(from 0 to 20 wt%) and decreasing droplet radius (from 15 to 0.1  $\mu\text{m}$ ) was confirmed by sensory analysis for emulsions containing blue dye (Chantrapornchai et al., 1998). The size of the particles in oil-in-water emulsions may change appreciably over time due to coalescence, Ostwald ripening, or flocculation (Chapter 7), which would be expected to alter their color. The color of oil-in-water emulsions has been shown to change appreciably over time due to droplet growth caused by Ostwald ripening (Weiss and McClements, 2000). On the other hand, little change in emulsion color was observed when the droplets ( $r = 0.18 \mu\text{m}$ ) in soybean oil-in-water emulsions were flocculated by either a depletion or an electrostatic screening mechanism (Chantrapornchai et al., 2001a). This suggests that emulsion color is more sensitive to changes in particle size caused by the growth of individual droplets, rather than by the formation of flocs.

### 10.5.2 Relative refractive index of droplets

Experimental measurements of the influence of refractive index ratio ( $= n_2/n_1$ ) on the color of oil-in-water emulsions have also been carried out (Weiss and Liao, 2000; Benichou et al., 2001; Chantrapornchai et al., 2001b). The refractive index ratio can be varied by adding water-soluble solutes (such as polyols or sugars) to the aqueous phase to increase its refractive index (Figure 10.21). For example, the influence of refractive index ratio on emulsion color has been studied using *n*-hexadecane oil-in-water emulsions ( $r = 0.15 \mu\text{m}$ ,  $n_2 = 1.43$ ) with different amounts of glycerol added to the continuous phase to vary its refractive index from 1.33 to 1.53 (Chantrapornchai et al., 2001b). As expected from theory (Figure 10.14), emulsion lightness was high when the refractive index of the droplets was either much smaller or much greater than the refractive index of the continuous phase, but decreased as the refractive index ratio tended toward unity (Figure 10.22). In the region where  $n_2 \approx n_1$ ; however, the lightness of the emulsions depended strongly on whether the plate behind the emulsions was black or white because some of the light propagated through the emulsion and was reflected from the back plate. This highlights the practical difficulty of measuring the color of emulsions using reflectance techniques when the overall scattering by the droplets is weak. In these systems, it is often better to use transmission measurements to quantify emulsion color.

### 10.5.3 Colorant type and concentration

Experimental measurements of the influence of dye type and concentration on the color of oil-in-water emulsions have also been carried out (Chantrapornchai et al., 1999a). The reflectance spectra of *n*-hexadecane oil-in-water emulsions with the same mean droplet

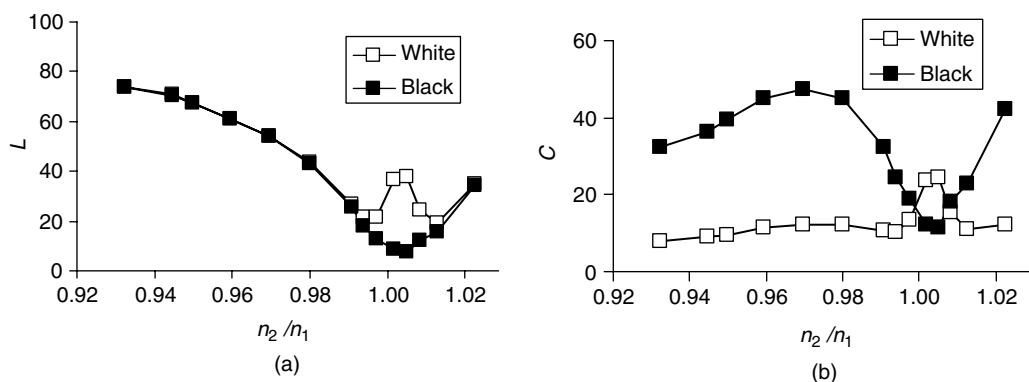


**Figure 10.22** Influence of relative refractive index ( $n_2/n_1$ ) on the lightness ( $L$ ) and chroma ( $C$ ) of 4 wt% *n*-hexadecane oil-in-water emulsions in the presence of a red dye (Chantrapornchai et al., 2001b). The refractive index of the aqueous phase was varied by adding glycerol. Measurements were made against either a white or black background.

diameter (0.3  $\mu\text{m}$ ), droplet concentration (9.6 wt%), and dye concentration (0.1 wt%), but different dye types (red, green, or blue) are shown in Figure 10.23. For each dye, the troughs in the reflectance spectra of the emulsions corresponded to peaks in the absorption spectra of the dye solutions. The red dye had a single broad reflectance trough at 380–600 nm, the green dye had two fairly deep troughs at 380–500 and 500–670 nm, and the blue dye had a small trough at 380–440 nm and a deep trough at 500–670 nm. The troughs in the reflectance spectra occur because energy is selectively absorbed by the chromophores in the dyes at these wavelengths. The color of a concentrated emulsion is therefore a result of the selective absorption of the incident white light that is reflected from its surface. For example, the red emulsion appears “red” because violet-to-yellow light (380–590 nm) is absorbed, leaving predominantly orange-to-red light (590–760 nm) in the reflected beam. As predicted by the light scattering theory, the addition of dyes to emulsions has been shown to decrease their lightness because less light is reflected back to the detector, and increase their chroma because more light is selectively adsorbed (Chantrapornchai et al. 1998, 1999a,b).

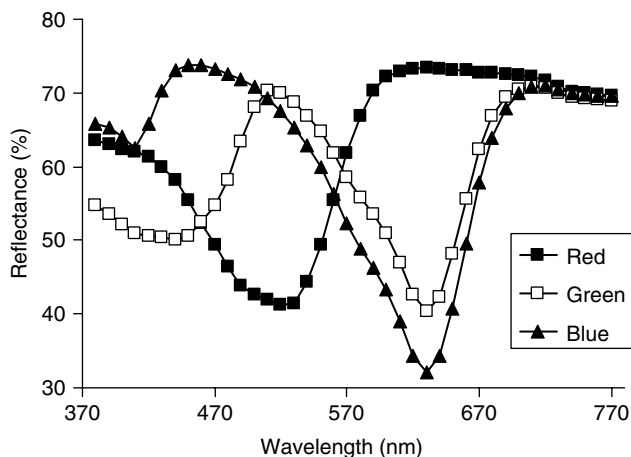


**Figure 10.23** Experimental measurements of the reflectance of 9.6 wt% *n*-hexadecane oil-in-water emulsions ( $r = 0.15 \mu\text{m}$ ) containing different dye types (Chantrapornchai et al., 1999).



### 10.5.4 *Factors affecting color of real food emulsions*

The influence of droplet and colorant characteristics on emulsion color determined in studies using model oil-in-water emulsions are supported by measurements made on real food systems. For example, it has been shown that the visual perception of coffee “creaminess” increases with increasing milk concentration due to the greater scattering by the fat globules and protein aggregates within milk (Hutchins, 1999). In instrumental and sensory studies, it has been shown that the lightness of milk increases as the concentration of fat droplets (Phillips et al., 1995) or particulate fat substitutes increases (Phillips and Barbano, 1997) due to increased light scattering effects. The same studies showed that the color intensity of the food emulsions decreased as their lightness increased. The perceived cloudiness of fruit beverages increases as the concentration of clouding agents is increased due to the greater amount of light scattering by the oil droplets within them (Hernandez and Baker, 1991; Hernandez et al., 1991; Tan, 2004). It should be noted that the perceived color intensity of a dilute food emulsion may initially increase with increasing droplet concentration and then decrease once a certain droplet concentration is exceeded due to multiple scattering effects (Chantrapornchai et al., 1999; Hutchins, 1999).

The color of skim milk appears different when measured in reflection or transmission mode because of light scattering by the casein micelles (Hutchins, 1999). The casein micelles scatter light more strongly in the blue region of the visible spectrum. Skim milk appears bluish when viewed in reflection mode because a greater fraction of blue light is scattered back to the eye, and reddish when viewed in transmission mode because blue light is selectively filtered out of the transmitted light. Skim milk can be made to have a more creamy appearance by adding particles that scatter light across the whole of the wavelength spectrum, for example, protein aggregates, fat droplets, or titanium dioxide (Phillips et al., 1995; Phillips and Barbano, 1997).

A variety of studies have shown that the lightness decreases and the color intensity increases as the concentration of chromophoric material in a food emulsion increases. For example, the color strength increases and the creamy appearance decreases as the concentration of coffee solids used to prepare coffee drinks is increased (Hutchins, 1999). Similarly, the color intensity of orange juice increases as the concentration of added colorant increases.

Finally, it should be noted that many food emulsions do not have a completely uniform appearance, which may be either desirable or undesirable. For example, an emulsion may contain particles that are large enough to be resolved by the human eye ( $>0.1$  mm), for example, air bubbles, spices, herbs. Alternatively, the droplets in a food emulsion may move to either the top (creaming) or bottom (sedimentation) of a container during storage, leading to a distinct creamed layer and serum layer. This type of phase separation may be undesirable so that the food manufacturer must develop strategies to prevent emulsion instability due to gravitational separation (Section 7.3).

## 10.6 *Concluding remarks and future directions*

Appearance is one of the most important criteria that consumers use to judge the desirability, quality, and safety of food products. Until fairly recently there was a rather poor understanding of the physicochemical basis of food emulsion appearance. Nevertheless, considerable advances have been made in the past few years on developing a quantitative understanding of the factors that determine emulsion appearance. The overall perceived appearance of a food emulsion is the result of its interactions with light waves for example, transmission, reflection, absorption, and scattering. Mathematical models have

been developed based on light scattering theory that enable one to predict the influence of droplet concentration, droplet size, dye concentration, and dye adsorption characteristics on the color of both dilute and concentrated emulsions. The usage of these models would enable food scientists to design emulsions with desirable appearances in a more rational and systematic fashion. Nevertheless, further work is still required to mathematically account for the influence of the optical measurement system on the predicted appearance of emulsions.



## *chapter eleven*

---

# *Characterization of emulsion properties*

### *11.1 Introduction*

The efficient production of high-quality emulsion-based food products depends on understanding the relationship between their bulk physicochemical characteristics and their colloidal properties, as well as on the successful implementation of this knowledge in industrial practice. Advances in these areas rely on the availability of analytical techniques and methodologies to provide information about the molecular, colloidal, physicochemical, and sensory properties of food emulsions and their components (Gaonkar, 1995). Analytical techniques are needed for research and development purposes to elucidate at a fundamental level the key factors that determine the overall physicochemical and sensory properties of food emulsions, such as stability, texture, flavor, and appearance (Chapters 7–10). They are also needed in food production factories to monitor foods before, during, and after production so as to ensure that their properties conform to predefined quality criteria (Nielsen, 2003).

In this chapter, analytical techniques and methodologies that have been developed specifically to characterize the properties of the droplets in food emulsions will be described, for example, emulsifier efficiency, disperse phase volume fraction, droplet size distribution, droplet crystallinity, and droplet charge. In previous chapters, experimental methods for characterizing molecular properties (Chapter 2), colloidal interactions (Chapter 3), interfacial properties (Chapter 5), emulsion stability (Chapter 7), emulsion rheology (Chapter 8), emulsion flavor (Chapter 9), and emulsion appearance (Chapter 10) were reviewed. Analytical techniques for measuring chemical, enzymatic, and microbiological properties of emulsions will not be considered here.

### *11.2 Testing emulsifier effectiveness*

One of the most important decisions a food manufacturer must make when developing an emulsion-based food product is to select the most appropriate emulsifier (Charalambous and Doxastakis, 1989; Dickinson, 1992; Hasenhuettl, 1997; Stauffer, 1999; Krog and Sparso, 2004). A huge number of emulsifiers are available as food ingredients, and each has its own unique characteristics and optimum range of applications (Hasenhuettl and Hartel, 1997; Krog and Sparso, 2004). The effectiveness of an emulsifier for a particular application is governed by a number of characteristics, including the minimum amount required to produce a stable emulsion, its ability to produce small droplets during homogenization, and its ability to prevent droplets from aggregating over time (Section 4.4). These characteristics depend on

the food in which the emulsifier is present and the prevailing environmental conditions, for example, pH, ionic strength, ion type, oil type, ingredient interactions, temperature, and mechanical agitation (Sherman, 1995). For this reason, it is difficult to accurately predict the behavior of an emulsifier from knowledge of its chemical structure alone (although some broad predictions about its functional properties are usually possible). Instead, it is often better to test the efficiency of an emulsifier under conditions that are similar to those found in the actual food product in which it is going to be used (Sherman, 1995).

Two relatively simple empirical procedures used to test emulsifier efficiency are discussed in this section: emulsifying capacity (EC) and emulsion stability index (ESI). More sophisticated analytical techniques and procedures that have been developed for characterizing the interfacial characteristics of emulsifiers are discussed in Chapter 5, for example, surface activity, saturation surface pressures, excess surface concentration, critical micelle concentrations, adsorption kinetics, and interfacial rheology.

### 11.2.1 *Emulsifying capacity*

It is often important for a food manufacturer to know the minimum amount of an emulsifier that can be used to create a stable emulsion. The EC of a water-soluble emulsifier is defined as the maximum amount of oil that can be dispersed in an aqueous solution containing a specific amount of the emulsifier without the emulsion breaking down or inverting into a water-in-oil emulsion (Sherman, 1995). Experimentally, it is usually determined by placing an aqueous emulsifier solution into a vessel and continuously agitating using a high speed mixer as small volumes of oil are titrated into the vessel (Swift et al., 1961; Das and Kinsella, 1990).<sup>\*</sup> The end-point of the titration occurs when the emulsion breaks down or inverts, which can be determined by optical, rheological, or electrical conductivity measurements. The greater the volume of oil that can be incorporated into the emulsion before it breaks down, the higher the EC of the emulsifier. Although this test is widely used to characterize emulsifiers, it has a number of drawbacks that limit its application as a standard procedure (Sherman, 1995; Dalgleish, 1996a,b, 2004). The main problem with the technique is that the amount of emulsifier required to stabilize an emulsion depends on the oil–water interfacial area, rather than on the oil concentration, and so the EC depends on the size of the droplets produced during agitation. As a consequence, the results are particularly sensitive to the type of blender and blending conditions used in the test. In addition, the results of the test have also been found to depend on the rate at which the oil is titrated into the vessel, the method used to determine the endpoint, the initial emulsifier concentration, and the measurement temperature (Sherman, 1995). The EC should therefore be regarded as a qualitative index, which depends on the specific conditions used to carry out the test. Nevertheless, it is useful for comparing the efficiency of different emulsifiers under the same experimental conditions.

A more reliable means of estimating the minimum amount of emulsifier required to form an emulsion is to measure the surface load ( $\Gamma_s$ ), which corresponds to the mass of emulsifier required to cover a unit area of droplet surface (Dickinson, 1992). A stable emulsion is prepared by homogenizing known amounts of oil, water, and emulsifier. The mass of emulsifier adsorbed to the surface of the droplets per unit volume of emulsion ( $C_a/\text{kg m}^{-3}$ ) is equal to the initial emulsifier concentration minus that remaining in the aqueous phase after homogenization (which is determined by centrifuging and/or filtering the emulsion to remove the droplets and then analyzing the emulsifier concentration in the serum). The total droplet surface area covered by the adsorbed emulsifier is given

<sup>\*</sup> The EC of an oil-soluble emulsifier can be determined in the same way, except that the water is titrated into the oil phase.

by  $S = 6\phi V_e/d_{32}$ , where  $V_e$  is the emulsion volume and  $d_{32}$  is the volume–surface mean droplet diameter. Thus, the surface load can be calculated as

$$\Gamma_s = \frac{C_a V_e}{S} = \frac{C_a d_{32}}{6\phi} \quad (11.1)$$

Typically, the value of  $\Gamma_s$  for food emulsifiers is around a few  $\text{mg m}^{-2}$ . Knowledge of the surface load enables one to calculate the minimum amount of emulsifier required to prepare an emulsion containing droplets of a given size and concentration. In practice, an excess of emulsifier is usually needed because it does not all adsorb to the surface of the droplets during homogenization due to the finite time taken for an emulsifier to reach the oil–water interface and because there is an equilibrium between the emulsifier at the droplet surface and that in the continuous phase (Hunt and Dalgleish, 1994; Dalgleish, 1996a,b). In addition, the surface load is often dependent on environmental conditions, such as pH, ionic strength, temperature, and protein concentration (Dickinson, 1992; Hunt and Dalgleish, 1994; Dalgleish, 1996a,b, 2004).

### 11.2.2 Emulsion stability index

Another measure of an emulsifier's effectiveness for a particular application is its ability to produce emulsions that remain stable to droplet aggregation. This is usually achieved by measuring the change in particle size of an emulsion after storage for a specified length of time or after exposure to some environmental stress (e.g., heating, freezing, stirring). The smaller the increase in particle size, the better is the emulsifier at stabilizing the system. Attempts have been made to define a single parameter that can be used to compare the effectiveness of different emulsifiers at stabilizing emulsion droplets against aggregation. One parameter that has been widely used by researchers in the food industry is called the ESI (Pearce and Kinsella, 1978; Reddy and Fogler, 1981; Pandolf and Masucci, 1984). Originally, the ESI was determined from measurements of the turbidity of a dilute emulsion carried out using an UV–visible spectrophotometer:

$$\text{ESI} = \frac{\tau(0)t}{\tau(t) - \tau(0)} \quad (11.2)$$

where  $\tau(0)$  is the initial turbidity of the emulsion and  $\tau(t)$  is the turbidity measured at time  $t$  (Qi et al., 1997; Kim et al., 2003). In this definition, the ESI would be equivalent to the reciprocal of the slope of a plot of emulsion turbidity versus time normalized with respect to the initial emulsion turbidity (assuming that the turbidity changed linearly with time). This relatively simple approach should be treated with caution because there is not a simple mathematical relationship between emulsion turbidity and particle size, particularly in the region where the particle radius is approximately equal to the wavelength of light used (Chapter 10). Indeed, the emulsion turbidity may either increase or decrease with increasing particle size, depending on the initial particle size. A more suitable expression for the ESI, based on particle size measurements, is given below:

$$\text{ESI} = \frac{d(0)t}{d(t) - d(0)} \quad (11.3)$$

where  $d(0)$  is the initial mean droplet diameter of the emulsion and  $d(t)$  is the mean droplet diameter measured at time  $t$ . The major advantage of this method is that the mean droplet

**Table 11.1** Predicted Relationship Between the Expected Lifetime of an Emulsion and the Emulsion Stability Index.

Stability Time*	ESI (min)
1 min	0.1
1 h	$6.0 \times 10^2$
1 day	$1.4 \times 10^4$
1 week	$1.0 \times 10^5$
1 month	$4.0 \times 10^5$
1 year	$5.3 \times 10^6$

\* The stability time is assumed to be the time taken for the mean droplet diameter to increase by 10%.

diameter can be determined using analytical instruments specifically designed for particle size analysis (such as light scattering, electrical pulse counting, or ultrasonic spectroscopy) rather than on turbidity measurements. In this definition, the ESI would be equivalent to the reciprocal of the slope of a plot of mean droplet diameter versus time normalized with respect to the initial mean droplet diameter (assuming that the droplet diameter changed linearly with time). The ESI goes from an infinitely high value for a completely stable system to a finite value for a highly unstable system. Numerically, the ESI is equal to the time required for the mean particle diameter to double in size. The relationship between ESI and the expected lifetime of an emulsion is shown in Table 11.1. It is also possible to define an emulsion instability index (EII), which increases as the effectiveness of an emulsifier at preventing droplet aggregation decreases, for example,  $EII = (d(t) - d(0))/d(0)t$ , which is the slope of a plot of particle diameter versus time normalized with respect to the initial particle diameter.

It should be noted that there are a number of potential practical problems associated with any method used to define an emulsion stability (or instability) index for comparing the effectiveness of different emulsifiers:

1. The growth in particle size within an emulsion may occur through a number of different mechanisms (e.g., flocculation, coalescence, or Ostwald ripening). It is often important to establish which of these mechanisms is dominant in a particular system, e.g., by using the methods described in Chapter 7.
2. The mean particle size does not usually increase linearly with time, so that the value of the ESI may depend on the time that the measurements were carried out. It is therefore important to use a standardized incubation time when comparing emulsifier effectiveness, for example, 24 h or 1 week.
3. The particle size distribution may change from monomodal (single-peaked) to multimodal (multi-peaked) with time. In some situations knowledge of the change in the full particle size distribution with time is more important than knowledge of the time dependence of the mean particle size. In addition, the ESI will depend strongly on the type of mean particle size used to represent the full particle size distribution in a multimodal system, for example,  $d_{10}$ ,  $d_{32}$ , or  $d_{43}$  (Section 1.3.2).
4. The particle growth rate usually depends on initial droplet size, droplet concentration, and continuous phase rheology. These parameters may vary from system-to-system and therefore it is usually important to use standardized conditions when comparing the effectiveness of different emulsifiers at stabilizing emulsions against droplet aggregation.
5. Particle growth may occur naturally at a relatively slow rate, and therefore it is difficult to assess the long-term stability of an emulsion from measurements made

soon after the emulsion is prepared. This problem can sometimes be overcome by accelerating the rate of droplet aggregation in an emulsion, for example, by centrifugation (Das and Kinsella, 1990; van Aken, 2004) or shearing (Dickinson and Williams, 1994). The ESI may then be determined from measurements of the mean droplet diameter made before and after an emulsion is stressed using well-defined conditions. Nevertheless, one must be aware that the value determined in an accelerated test does not always give a good representation of that determined in a long-term storage test.

At present, there is no evidence that a single parameter, such as the ESI, can be used to quantitatively compare the effectiveness of emulsifiers when measurements are carried out in different emulsion systems under different conditions. For this reason, emulsifier effectiveness at stabilizing droplets against aggregation is often demonstrated by reporting the measured mean particle diameters or full particle size distributions, rather than as a calculated ESI. Nevertheless, the ESI is useful when one is comparing a series of emulsifiers under standardized conditions, or when one is examining the influence of specific changes in solution or environmental conditions on the functionality of a particular emulsifier (with all other conditions being standardized).

## 11.3 Microstructure and droplet size distribution

### 11.3.1 Microscopy

The unaided human eye can resolve objects that are greater than 0.1 mm (100  $\mu\text{m}$ ) apart (Aguilera and Stanley, 1990). Many of the structural components in food emulsions are smaller than this lower limit and so cannot be observed directly by eye, for example, emulsion droplets, surfactant micelles, fat crystals, gas bubbles, and protein aggregates (Dickinson, 1992). Our normal senses must therefore be augmented by microscopic techniques that enable us to observe tiny objects (Vaughan, 1979; Aguilera and Stanley, 1990; Kalab et al., 1995; Smart et al., 1995). A number of these techniques are available to provide information about the structure, dimensions, and organization of the components within food emulsions, for example, optical microscopy, electron microscopy, and atomic force microscopy (AFM) (Caldwell et al., 1992; Stanley et al., 1993; Kirby et al., 1995; Kalab et al., 1995; Smart et al., 1995; Morris et al., 1999). These techniques have the ability to provide information about structurally complex systems in the form of "images" that are relatively easy to comprehend by human beings (Kirby et al., 1995). Each microscopic technique works on different physicochemical principles and can be used to examine different levels and types of structural organization. Nevertheless, any type of microscopy must have three qualities if it is going to be used to examine the structure of small objects: resolution, magnification, and contrast (Aguilera and Stanley, 1990). *Resolution* is the ability to distinguish between two objects that are close together. *Magnification* is the number of times that the image is greater than the object being examined. *Contrast* determines how well an object can be distinguished from its background.

#### 11.3.1.1 Conventional optical microscopy

Although the optical microscope was developed centuries ago, it is still one of the most valuable tools for observing the microstructure of emulsions (Vaughan, 1979; Mikula, 1992; Hunter, 1986, 1993; Flint, 1994). An optical microscope contains a series of lenses that direct light through the specimen and magnify the resulting image (Figure 11.1). The resolution of an optical microscope is determined by the wavelength of light used and the mechanical design of the instrument (Murphy, 2001). The theoretical limit of resolution of an optical



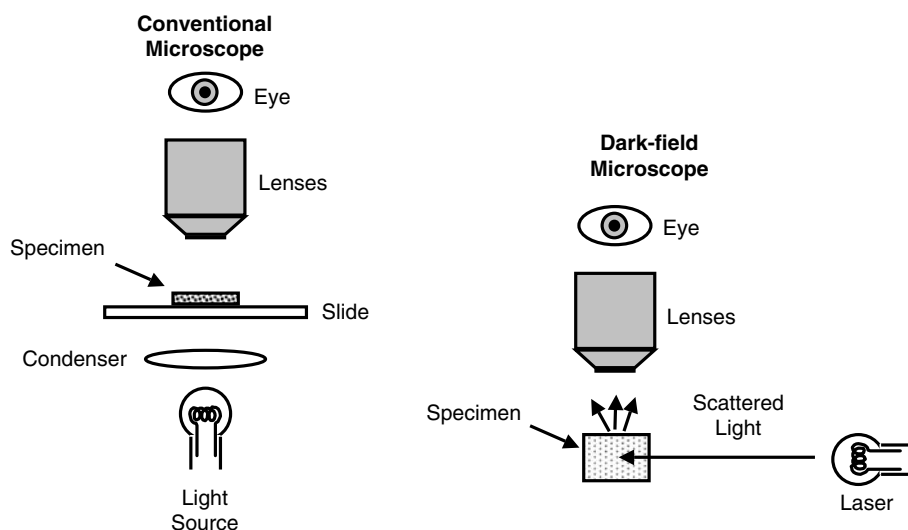


**Figure 11.1** Comparison of conventional bright-field and dark-field microscopes that can be used to observe emulsion microstructure.

microscope is about  $0.2\ \mu\text{m}$ , but in practice it is difficult to obtain reliable measurements below about  $1\ \mu\text{m}$  (Hunter, 1993). This is because of technical difficulties associated with the design and manufacture of the optical components with the microscope and because the Brownian motion of small particles causes images to appear blurred. The optical microscope therefore has limited application to many food emulsions because they contain structures with sizes below the lower limit of resolution. Nevertheless, it can provide valuable information about the size distribution of droplets in emulsions that contain larger droplets, and can often be used to distinguish between flocculation and coalescence (Mikula, 1992), which is sometimes difficult using instrumental particle sizing techniques based on light scattering, electrical pulse counting, or ultrasonic spectroscopy (see later). Images of flocculated and nonflocculated emulsions obtained by conventional optical microscopy are shown in Figure 11.2. These emulsions contained relatively small droplets

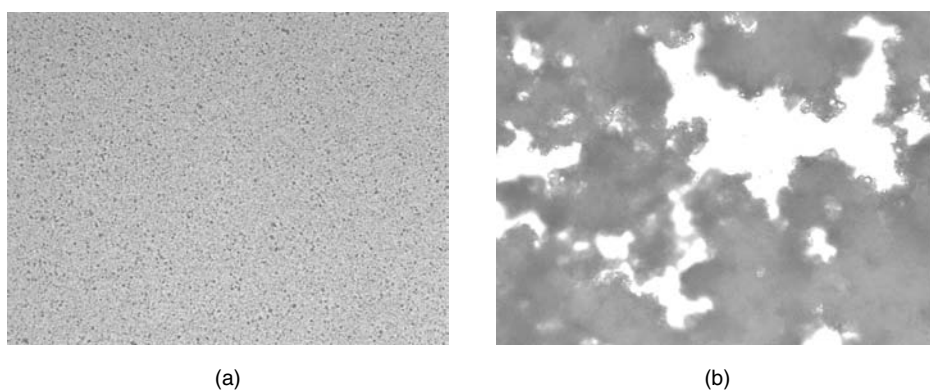


**Figure 11.2** Micrographs of (a) nonflocculated and (b) flocculated oil-in-water emulsions containing small droplets obtained using optical microscopy.

( $d < 1 \mu\text{m}$ ) so it was difficult to distinguish the individual droplets in the nonfloculated emulsion, but the effects of droplet aggregation are clearly seen in the floculated emulsion. A clear example of the use of optical microscopy for studying emulsions with relatively large droplets ( $d > 1 \mu\text{m}$ ) is shown in Figure 11.1.

The natural contrast between the major components in food emulsions is often fairly poor (because they have similar refractive indices or colors), which makes it difficult to reliably distinguish them from each other using conventional bright-field optical microscopy. For this reason, the technique has been modified in a number of ways to enhance the contrast, improve the image quality, and provide more detailed information about the composition and microstructure of emulsions (Flint, 1994; Murphy, 2001). Various types of chemical stains are available that bind to particular components within an emulsion (e.g., the proteins, polysaccharides, or lipids) or preferentially partition into either the oil phase or the aqueous phase (Gurr, 1961; Green, 1991). Specific structural features within an emulsion can therefore be highlighted by judicious selection of stains (Smart et al., 1995). Nevertheless, these stains must be used with caution because their application can alter the structures being examined. In addition, they are often difficult to incorporate into concentrated or semisolid emulsions.

The contrast between different components can be improved without using chemical stains by modifying the design of the optical microscope, for example, by using *phase contrast* or *differential interference contrast* microscopy (Aguilera and Stanley, 1990; Murphy, 2001). These techniques improve contrast by using special lenses that convert small differences in refractive index into differences in light intensity.

The structure of optically anisotropic food components, such as fat crystals, starch granules, and muscle fibers, can be studied using *polarization* light microscopy (Aguilera and Stanley, 1990). Microscopes used for polarization light microscopy are equipped with a polarizer positioned in the optical path before the specimen, and an analyzer positioned in the optical path after the specimen. The analyzer is simply another polarizer that can be rotated. Image contrast is the result of the ability of plane-polarized light to interact with optically anisotropic (birefringent) regions within a specimen (which therefore appear bright), but not isotropic regions (which therefore appear dark). This technique is particularly useful for monitoring phase transitions of fat, and to determine the location and morphology of fat crystals in emulsion droplets (Walstra, 1967; Boode, 1992).

The characteristics of particles with dimensions less than a micrometer can be observed by dark-field illumination using an instrument known as an ultramicroscope (Shaw, 1980; Farinato and Rowell, 1983; Hunter, 1986). A beam of light is passed through the specimen at a right angle to the eyepiece (Figure 11.1). In the absence of any particles the specimen appears completely black, but when there are particles present they scatter light and the image appears as a series of bright spots against a black background. This technique can be used to detect particles as small as 10 nm; however, the particles appear as blurred spots, rather than as well-defined images whose size can be measured directly. The particle size is inferred from the brightness of the spots or from measurements of their Brownian motion. The ultramicroscope can also be used to determine the number of particles in a given volume, or to monitor the motion of particles in an electric field (Section 11.6).

Certain food components either fluoresce naturally or can be made to fluoresce by adding fluorescent dyes that bind to them (Aguilera and Stanley, 1990; Kalab et al., 1995; Herman and Tanke, 1998; Murphy, 2001). Fluorescent materials adsorb electromagnetic radiation at one wavelength and emit it at a higher wavelength (Skoog et al., 1994). A conventional bright-field optical microscope can be modified to act as a fluorescence microscope by adding two filters (or other suitable wavelength selectors). One filter is placed before the light enters the sample and produces a monochromatic *excitation* beam. The other filter is placed after the light beam has passed through the sample and produces

a monochromatic *emission* beam. A variety of fluorescent dyes (fluorophores) are available that bind to specific components within a food (e.g., proteins, fats, or carbohydrates) or that are more soluble in one phase than another (e.g., oil vs. water) (Larison, 1992). Fluorescence microscopes often use an ultraviolet light source to illuminate the specimen (which is therefore invisible to the human eye), whereas the light emitted by the fluorescent components within a specimen is in the visible part of the electromagnetic spectrum, and so they appear as bright objects against a black background. Fluorescence microscopy is a very sensitive technique that is particularly useful for studying structures that are present at such small concentrations that they cannot be observed using conventional optical microscopy. In addition, it can be used to highlight particular structures within an emulsion by selecting fluorescent dyes that specifically bind to them.

One of the major drawbacks of optical microscopy is the possibility that sample preparation alters the structure of the specimen being analyzed (Aguilera and Stanley, 1990; Kalab et al., 1995). Sample preparation may be a simple procedure, such as spreading an emulsion across a slide, or a more complex procedure such as fixing, embedding, slicing, and staining a sample (Flint, 1994; Smart et al., 1995). Even a procedure as simple as spreading a specimen across a slide may alter its structural properties, and should therefore be carried out carefully and reproducibly. Other disadvantages of optical microscopy are that measurements are often time-consuming and subjective, it is often necessary to analyze a large number of different regions within a sample to obtain statistically reliable data, and it is limited to studying structures greater than about 1  $\mu\text{m}$  (Mikula, 1992). Most modern optical microscopes now have the capability of being linked to personal computers that can rapidly store and analyze digital images, and thus enhance their ease of operation (Murphy, 2001). Another interesting development is the ability to combine optical microscopy with other types of analytical measurement techniques so as to obtain additional information about emulsion properties, for example, changes in the microstructure of a sample can be observed as it is subjected to mechanical forces. These rheo-optic techniques have been used to provide information about the breakdown of flocculated droplets in shear fields (Wagner, 1998; Verly et al., 2003; van der Linden et al., 2003) and the strength of the forces acting between droplets in concentrated emulsions (Brujic et al., 2003a,b).

#### 11.3.1.2 *Laser scanning confocal microscopy*

Laser scanning confocal microscopy (LSCM) can provide extremely valuable information about the microstructure of food emulsions (Blonk and Aalst, 1993; Brooker, 1995; Smart et al., 1995; Vodovotz et al., 1996). This technique provides higher clarity images than conventional optical microscopy, and often allows the generation of three-dimensional images of structures without the need to physically section the specimen. The LSCM focuses an extremely narrow laser beam at a particular point in the specimen being analyzed and a detector measures the intensity of the resulting signal (Figure 11.3). A two-dimensional image is obtained by carrying out measurements at different points in the  $x$ - $y$  plane, either by moving the specimen (and keeping the laser beam stationary) or by moving the laser beam (and keeping the specimen stationary). An image is generated by combining the measurements from each individual point. Three-dimensional images are obtained by focusing the laser beam at different vertical depths ( $z$ -plane) into the specimen and then scanning in the horizontal direction ( $x$ - $y$  plane). Observation of the microstructure of multicomponent systems is often facilitated by using the natural fluorescence of certain components or by using fluorescent dyes that bind selectively to specific components (e.g., proteins, fats, or carbohydrates) or that are more soluble in one phase than another (e.g., oil vs. water) (Larison, 1992). The LSCM technique suffers from some of the same problems as conventional optical microscopy, but it has a better resolution and sensitivity, and the sample preparation is often less severe.

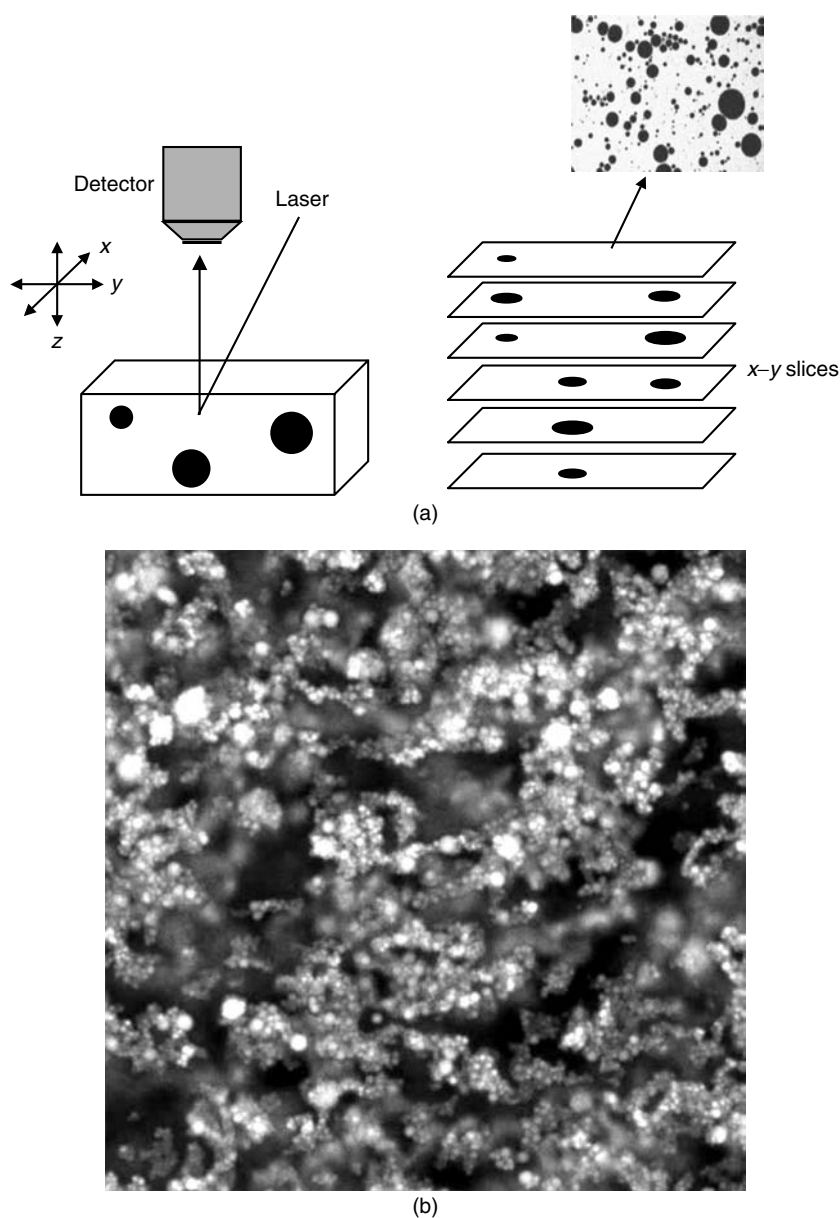


**Figure 11.3** Laser scanning confocal microscopy. (a) A laser beam is scanned across a particular  $x$ - $y$  plane within a sample. By combining successive  $x$ - $y$  planes it is possible to create a three-dimensional image of an emulsion. (b) Confocal image of a flocculated oil-in-water emulsion—image size 275  $\mu\text{m}$  across. Image kindly supplied by Dr. Peter Wilde (Institute of Food Research, Norwich).

The LSCM technique has proved to be an extremely powerful method of studying the structures of food emulsions and their components. It has been used to determine the size, concentration, and organization of droplets in oil-in-water emulsions (Jokela et al., 1990; Dickinson et al., 2003), to examine the microstructure of butter, margarines, and low fat spreads (Blonk and van Aalst, 1993; van Dalen, 2002), to monitor creaming of droplets (Brakenhoff et al., 1988), to follow changes in interfacial composition on emulsion droplets

(Heertje et al., 1996), to study phase separation of water-in-water emulsions (Plucknett et al., 2001), and to monitor the structural organization and interactions of droplets in concentrated emulsions (Bruijic et al., 2003a,b). The use of the LSCM technique is demonstrated in Figure 11.3b, which shows an image of a flocculated oil-in-water emulsion.

#### 11.3.1.3 *Electron microscopy*

Electron microscopy is widely used to examine the microstructure of food emulsions, particularly those that contain structural components that are smaller than the lower limit of resolution of optical microscopes (ca.  $< 1 \mu\text{m}$ ), for example, protein aggregates, small emulsion droplets, fat or ice crystals, micelles, and interfacial membranes (Chang et al., 1972; Tung and Jones, 1981; Aguilera and Stanley, 1990; Heertje and Paques, 1995; Munoz and Mikula, 1997). It can be used to provide information about the concentration, dimensions, and spatial distribution of structural entities within a specimen, providing that the specimen's microstructure is not significantly altered by the sample preparation (Heertje and Paques, 1995). With suitable sample preparation electron microscopy can be used to analyze both oil-in-water and water-in-oil emulsions that are either liquid or solid. Electron microscopes are fairly large pieces of equipment, which are relatively expensive to purchase and maintain (Smart et al., 1995). For this reason, they tend to be available only at fairly large research laboratories or food companies.

Electron microscopes use electron beams, rather than light beams, to provide information about the structure of materials (Aguilera and Stanley, 1990; Heertje and Paques, 1995). These beams are directed through the microscope using a series of magnetic fields, rather than optical lenses. Electron beams have much smaller wavelengths than light and so they can be used to examine much smaller objects. In principle, the smallest size that can be resolved is about 0.2 nm, but in practice it is usually about 1 nm due to limitations in the stability and performance of the magnetic lenses. Two types of electron microscope are commonly used to examine the structure of food systems: transmission electron microscopy (TEM) and scanning electron microscopy (SEM). Traditionally, it was necessary to keep electron microscopes under high vacuum because electrons are easily scattered by atoms or molecules in a gas, and this would cause deterioration in image quality. This meant that specimens usually had to undergo extensive preparation procedures (e.g., fixation, dehydration) so as to ensure that they were free of all volatile components that could evaporate, for example, water and organic molecules. Nevertheless, environmental SEM instruments are now available that are capable of obtaining images of materials in a gaseous environment, and so there are far fewer problems associated with artifact generation during sample preparation (Smart et al., 1995; Donald, 2003; Stokes, 2001, 2003).

**11.3.1.3.1 *Transmission electron microscopy.*** A cloud of electrons, produced by a tungsten cathode, is accelerated through a small aperture in a positively charged plate to form an electron beam (Figure 11.4). This beam is focused and directed through the specimen by a series of magnetic lenses. Part of the electron beam is either adsorbed or scattered by the specimen, while the rest is transmitted. The beam of transmitted electrons is magnified by a magnetic lens and then projected onto a screen to create an image of the specimen. The fraction of electrons transmitted by a substance depends on its electron density: the lower the electron density, the greater the fraction of electrons transmitted and the darker is the image. Components with different electron densities therefore appear as regions of different intensity on the image. Images are typically 100 to 500,000 times larger than the portion of specimen being examined, which means that structures as small as 0.4 nm can be observed (Hunter, 1993).

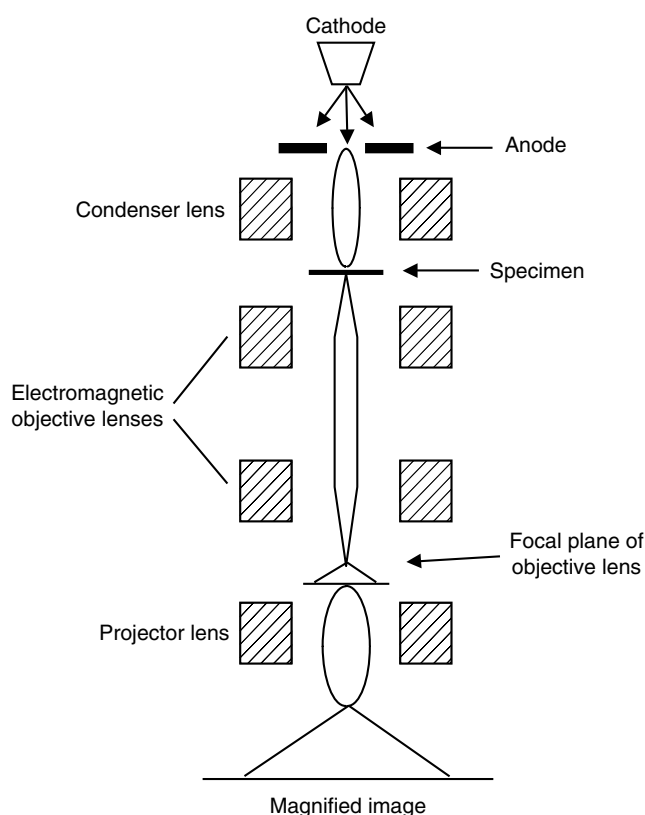


**Figure 11.4** Schematic diagram of a transmission electron microscopy. An electron beam is directed through the sample and the intensity of the transmitted beam is measured.

Electrons are highly attenuated by most materials and therefore specimens must be extremely thin in order to allow enough of the electron beam through to be detected (Aguilera and Stanley, 1990; Heertje and Paques, 1995; Wang, 2003). Specimens used in electron microscopy are therefore much thinner ( $\sim 0.05\text{--}0.1\ \mu\text{m}$ ) than those used in light microscopy ( $\sim 1\ \mu\text{m}$  to a few mm). The difference in electron densities of food components is naturally quite small, and therefore it is difficult to differentiate them. For this reason, the density contrast between components is usually enhanced by selectively staining the sample with various heavy metal salts (which have high electron densities), such as lead, tungsten, or uranium. These salts bind selectively to specific components, which enables them to be distinguished from the rest of the sample. The metal salts may bind to the component itself (positive staining) or to the surrounding material (negative staining). In *positive staining* a dark specimen is seen against a light background, whereas in *negative staining* an illuminated specimen is seen against a dark background. The need to use very thin dehydrated specimens that often require staining means that sample preparation is considerably more time consuming and cumbersome than for other forms of microscopy, and may lead to appreciable image artifacts.

The information produced by TEM is usually in the form of a two-dimensional image that represents a thin slice of the specimen (Figure 11.5b). Nevertheless, it is possible to obtain some insight about the three-dimensional structure of a sample using a technique

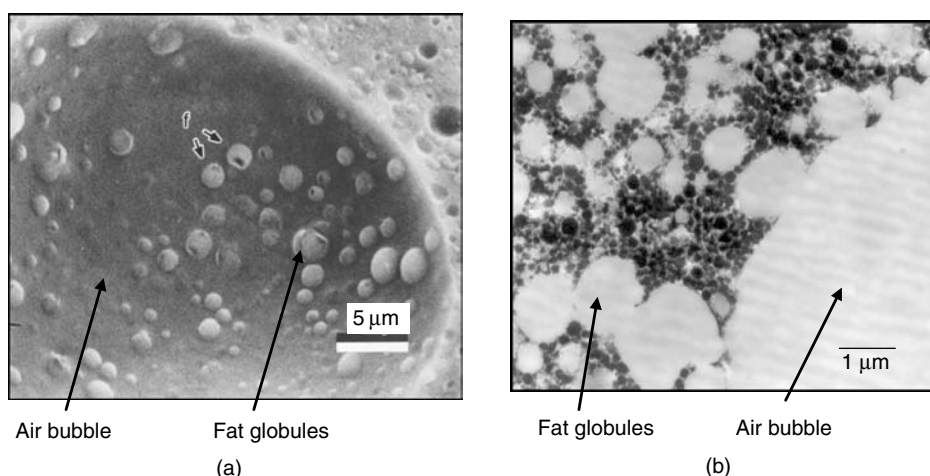


**Figure 11.5** Comparison of electron micrographs of ice cream produced by (a) SEM and (b) TEM. TEM normally produces a two-dimensional image of a thin slice of specimen, whereas SEM produces a more three-dimensional looking image of the topography of a specimen. This micrograph shows large air bubbles in ice cream with fat globules that are either adsorbed to the air–water interface or present as a three-dimensional network of aggregated droplets in the aqueous continuous phase. Micrographs were kindly supplied by Prof. Douglas Goff of the University of Guelph.

called *metal shadowing* (Figure 11.6). A vapor of a heavy metal, such as platinum, is sprayed onto the surface of a sample at an angle (Hunter, 1993). The sample is then dissolved away using a strong acid, which leaves a metal replica of the sample. When a beam of electrons is transmitted through the metal replica the “shadows” formed by the specimen are observed as illuminated regions that have characteristic patterns from which the topography of the specimen can be deduced.

**11.3.1.3.2 Scanning electron microscopy.** SEM is commonly used to provide images of the surface topography of specimens (Heertje and Paques, 1995). It relies on the measurement of secondary electrons generated by a specimen when it is bombarded by an electron beam, rather than the electrons that have traveled directly through the specimen. A focused electron beam is directed at a particular point on the surface of a specimen. Some of the energy associated with the electron beam is absorbed by the material and causes it to generate secondary electrons, which leave the surface of the sample and are recorded by a detector. An image of the specimen is obtained by scanning the electron beam in an  $x$ – $y$  direction over its surface and recording the number of electrons generated at each location. Because the intensity at each position depends on the angle between the

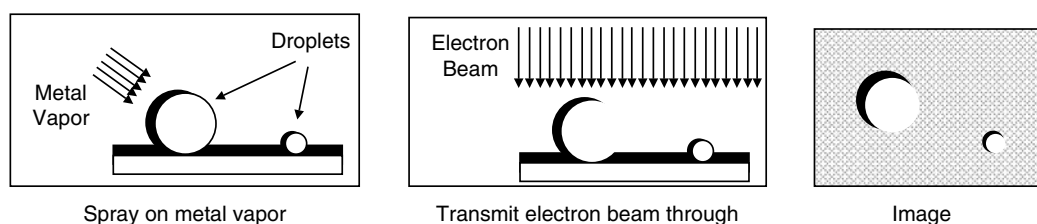


**Figure 11.6** TEM can be used to obtain images of the surface topography of a specimen using a technique known as *metal shadowing*.

electron beam and the surface the electron micrograph has a three-dimensional appearance (Figure 11.5a).

Sample preparation for SEM is considerably easier and tends to produce fewer artifacts than sample preparation for TEM. Because an image is produced by secondary electrons generated at the surface of a specimen, rather than by an electron beam that travels through a specimen, it is not necessary to use ultrathin samples. Even so, the specimens used in conventional SEM often have to be cut, fractured, fixed, and dehydrated, which may alter their structures. Nevertheless, many of these problems have been overcome with the introduction of environmental SEM (Donald, 2003; Stokes, 2003). The resolving power of SEM is about 3–4 nm, which is an order of magnitude worse than TEM, but about two or three orders of magnitude better than optical microscopy. Another major advantage of SEM over optical microscopy is the large *depth of field*, which means that images of relatively large structures are all in-focus (Hunter, 1993).

Electron microscopy is widely used by food scientists to determine the size of emulsion droplets, the dimensions and structure of flocs, the surface morphology of droplets and air bubbles, the size, shape, and location of fat crystals, and the microstructure of three-dimensional networks of aggregated biopolymers (Chang et al., 1972; Kalab, 1981; Tung and Jones, 1981; Hermansson, 1988; Aguilera and Stanley, 1990; Lee and Morr, 1992; Heertje and Paques, 1995; Bucheim and Dejmek, 1997; Goff et al., 1999). TEM and SEM electron micrographs of ice cream are compared in Figure 11.5. TEM gives a two-dimensional cross-section of the sample, whereas SEM gives a more three-dimensional image. Traditionally, one of the major limitations of electron microscopy has been the difficulty in preparing samples without altering their structure. In addition, the use of high energy electron beams often caused changes in the structure of delicate specimens. Many of these problems are being overcome due to recent advances in the design of electron microscopes and sample preparation techniques (Smart et al., 1995). In particular, the introduction of environmental SEM, which can image emulsions in their natural state without the need of extensive sample preparation, is proving to be a particularly powerful means of providing images of emulsions (Stokes et al., 1998; Mathews and Donald, 2002). Recently, it has been shown that environmental SEM techniques can be used to monitor the changes in microstructure of heterogeneous materials when they are subjected to mechanical forces (Stokes, 2001; Rizzieri et al., 2003). Application of these techniques to emulsion-based systems should provide new insights into the relationship between rheology and microstructure.

#### 11.3.1.4 Atomic force microscopy

Atomic force microscopy has the ability to provide information about structure at the atomic and molecular level, and is therefore complementary to the other forms of microscopy mentioned above (Miles and McMaster, 1995; Santos and Castanho, 2004). Commercial instruments based on this technology are widely available and are finding increasing usage in the food industry (Kirby et al., 1995). Application of AFM to food emulsions has provided valuable information about the microstructure and organization of the various structural entities present within them (Gunning et al., 2004).

The AFM creates an image by scanning a tiny probe (similar to the stylus of a record player, but only a few micrometers in size), across the surface of the specimen being analyzed (Figure 11.7). When the probe is held extremely close to the surface of a material it experiences a repulsive force, which causes the cantilever to which it is attached to be bent away from the surface. The extent of the bending is measured using an extremely sensitive optical system. By measuring the deflection of the probe as it is moved over the surface of the material it is possible to obtain an image of its structure. In practice, it is more common to measure the force required to keep the deflection of the probe constant,



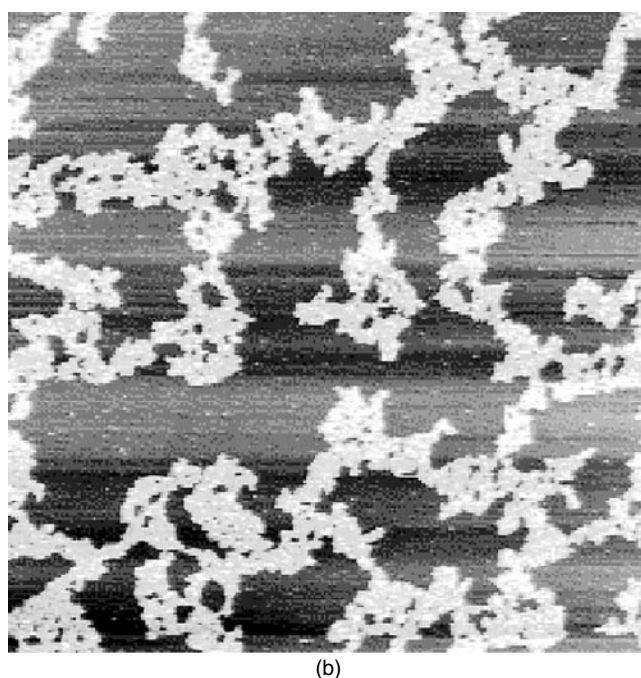
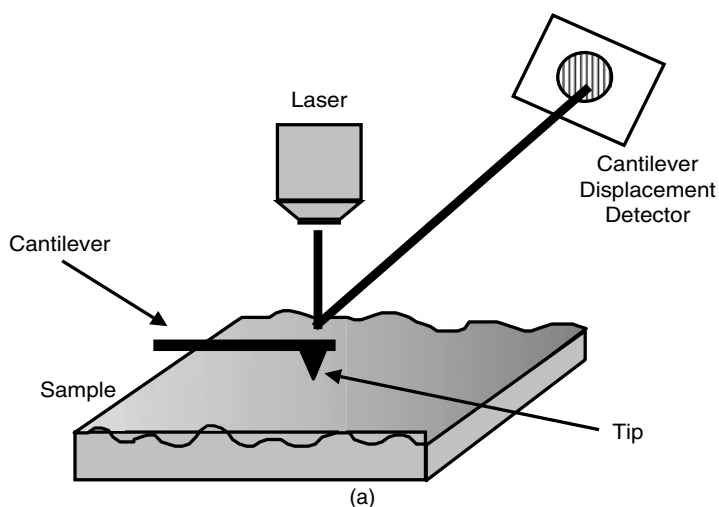


**Figure 11.7** Atomic force microscopy. (a) A probe attached to a cantilever arm is scanned over the surface of a specimen and its displacement is measured using an accurate laser detection system. The deflection of the cantilever required to maintain the probe at the same location relative to the specimen surface is measured, which generates an image of the specimen. (b) AFM image of a planar interface comprising of a  $\beta$ -lactoglobulin film to which a nonionic surfactant (Tween 20) was added—image is  $6\ \mu\text{m} \times 6\ \mu\text{m}$  across. Picture kindly supplied by Dr. Alan Mackie (Institute of Food Research, Norwich).

as this reduces the possible damage caused by a probe as it moves across the surface of a sample. The resolution of AFM depends principally on the size and shape of the probe and the accuracy to which it can be positioned relative to the sample. Traditionally, samples to be analyzed needed to be dissolved in a suitable solvent and then dried on to the surface

of an extremely flat plate such as mica. Modern commercial instruments typically enable lateral resolution of structures on the order of nanometers and vertical resolutions on the order of tenths of nanometers. They have also been designed to minimize the damage to specimens associated with sample preparation and analysis, and can be used to analyze wet samples. Multifunctional scanning probe microscopes are available that can be used to measure characteristics, such as surface topography, elasticity, friction, and adhesion.

Atomic force measurements have been used to observe the structure of individual and aggregated polysaccharide and protein molecules, for example, xanthan, pectin, acetan, starch, collagen, myosin, and bovine serum albumin (Miles and McMaster, 1995; Kirby et al., 1995). This type of study is useful for examining the relationship between the structure and interactions of biopolymer molecules and the type of gels they form. AFM has also been used to study the molecular organization of emulsifiers at planar oil–water and air–water interfaces (Kirby et al., 1995; Mackie et al., 2000). AFM techniques have been developed that are capable of quantifying the magnitude and range of colloidal interactions between emulsion droplets (Claesson et al., 1996; Gunning et al., 2004). An example of the use of AFM for observing the microstructure of planar interfaces is demonstrated in Figure 11.7b, which shows the two-dimensional separation that occurs when a small molecule surfactant is adsorbed to a protein film.

### 11.3.2 Static light scattering

#### 11.3.2.1 Principles

Particle size analysis instruments that use static light scattering (also called laser diffraction) are based on the principle that a beam of light directed through an emulsion is scattered by the droplets in a well-defined manner (Farinato and Rowell, 1983; Hunter, 1986; Hiemenz and Rajagopalan, 1997). A measurement of the extent of light scattering by an emulsion can be used to determine the particle size distribution and concentration by using a mathematical model to relate the measured data to the particle characteristics. Analytical instruments based on this principle have been commercially available for many years, and are widely used in the food industry for research, development, and quality control purposes. Many of these instruments are fully automated, easy to use, and provide information about the full particle size distribution of an emulsion within a few minutes. A variety of different instruments are available that use static light scattering. One of the main differences between these techniques is the angle (or range of angles) at which the intensity of the light waves that have interacted with the emulsion are detected (Hiemenz and Rajagopalan, 1997). Some instruments only measure the intensity of light that has traveled directly through the emulsion (mainly non-scattered light), whereas others measure the intensity of light that has been scattered by the emulsion droplets. Intensity measurements may be carried out at a fixed angle (e.g.,  $\theta = 0, 45, 90$ , or  $180^\circ$ ) or over a range of angles, and they may be carried out at a fixed wavelength or over a range of wavelengths depending on the design of the instrument. The size of the particles that an instrument is sensitive to depends on the range of wavelengths used, with low-angle measurements being more sensitive to large droplets, and wide-angle measurements being more sensitive to smaller droplets.

The interaction of an electromagnetic wave with an emulsion is characterized by a *scattering pattern*, which is the angular dependence of the intensity of the light emerging from the emulsion,  $I(\Phi)$  (Figure 11.8). The size and concentration of droplets in an emulsion is ascertained from the scattering pattern using a suitable theory (Farinato and Rowell, 1983). Theories that relate light scattering data to droplet size distributions are based on a mathematical analysis of the propagation of an electromagnetic wave through an ensemble of particles. A number of theories are available,

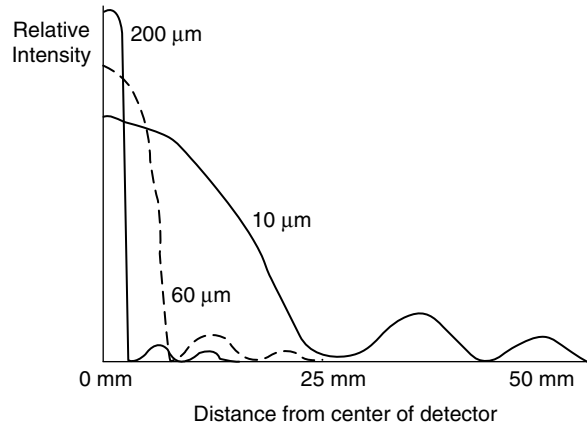


**Figure 11.8** The scattering pattern from an emulsion is characterized by measuring the intensity of the scattered light,  $I(\Phi)$ , as a function of angle  $\Phi$  between the incident and scattered beams. Droplet size distributions can be determined by analyzing these curves using a suitable light scattering theory.

which vary according to their mathematical complexity and the type of systems they can be applied to (van de Hulst, 1957; Kerker, 1969; Bohren and Huffman, 1983). The interaction between light waves and emulsion droplets can be conveniently divided into three regimes, according to the relationship between the droplet radius ( $r$ ) and the wavelength ( $\lambda$ ):

1. Long-wavelength regime ( $r < \lambda/20$ )
2. Intermediate-wavelength regime ( $\lambda/20 < r < 20\lambda$ )
3. Short-wavelength regime ( $r > 20\lambda$ )

The scattering pattern associated with each of these regimes is distinctly different (Figure 11.9, Figure 10.4).

**11.3.2.1.1 Long-wavelength regime.** The simplest equation for relating the characteristics of the particles in a suspension to the scattering pattern produced when a monochromatic light beam passes through it was derived by Lord Raleigh over a century ago

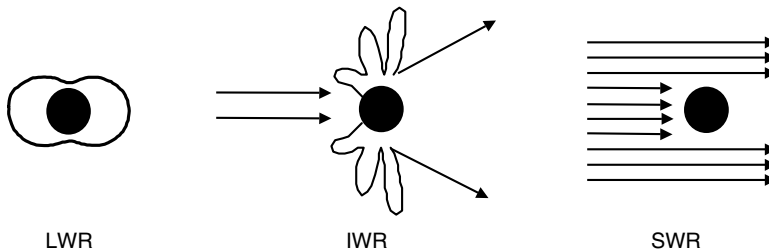


**Figure 11.9** Schematic representation of different scattering patterns for droplets in the long-, intermediate-, and short-wavelength regimes (See also Figure 10.4).

and is applicable in the long-wavelength regime (Sherman, 1968):

$$\frac{I(\Phi)}{I_i} = \frac{6\pi^3 \phi r^3}{\lambda^4 R^2} \frac{(n_2^2 - n_1^2)^2}{(n_2^2 + 2n_1^2)^2} (1 + \cos^2 \Phi) \quad (11.4)$$

where  $I_i$  is the initial intensity of the light beam in the surrounding medium,  $\phi$ , is the disperse phase volume fraction,  $R$  is the distance between the detector and the scattering droplet, and  $n_1$  and  $n_2$  are the refractive indices of the continuous phase and droplets, respectively. This equation cannot be used to interpret the scattering patterns of most food emulsions because the size of the droplets (typically between 0.1 and 100  $\mu\text{m}$ ) is of the same order or larger than the wavelength of light used (typically between 0.2 and 1  $\mu\text{m}$ ). Nevertheless, it can be applied to suspensions that contain smaller particles, such as surfactant micelles or protein molecules (Hiemenz and Rajagopalan, 1997). The Raleigh equation also provides some useful insights into the factors that influence the scattering profile of emulsions. It indicates that the degree of scattering from an emulsion is linearly related to the droplet concentration, and increases as the refractive indices of the materials become more dissimilar.

**11.3.2.1.2 Intermediate-wavelength regime.** As mentioned earlier, most food emulsions contain droplets that are in the intermediate-wavelength regime. The scattering profile in this regime is extremely complex because light scattered from different parts of the same droplet are out of phase and therefore constructively and destructively interfere with one another (Hiemenz and Rajagopalan, 1997). For the same reason, the mathematical relationship between the scattering pattern and the particle size is much more complex. A mathematician called *Mie* developed a theory that can be used to interpret the scattering patterns of dilute emulsions containing spherical droplets of any size (van de Hulst, 1957; Kerker, 1969). The Mie theory is fairly complicated, but it can be solved rapidly using modern computers. This theory gives excellent agreement with experimental measurements, and is used by most commercial particle sizing instruments. It should be pointed out that the Mie theory assumes that the light waves are only scattered by a single particle, and so it is only strictly applicable to dilute emulsions. In more concentrated emulsions, a light beam scattered by one droplet may subsequently interact with another droplet, and this alters the scattering pattern (Ma et al., 1990). For this reason, emulsions must be diluted prior to analysis to a concentration where multiple scattering effects are negligible, that is,  $\phi < 0.05\%$ .

**11.3.2.1.3 Short-wavelength regime.** When the wavelength of light is much smaller than the particle diameter, the droplet size distribution can be determined directly by optical microscopy (Section 11.3.1).

### 11.3.2.2 Measurement techniques

**11.3.2.2.1 Angular scattering methods.** Most modern particle sizing instruments that are based on static light scattering, measure the angular dependence of the scattered light. The sample to be analyzed is diluted to an appropriate concentration and then placed in a transparent measurement cell (Figure 11.10). A monochromatic light beam is generated by a laser (e.g., helium–neon,  $\lambda = 632.8 \text{ nm}$ ) and directed through the measurement cell where it is scattered by the emulsion droplets. The intensity of the scattered light is measured as a function of scattering angle using an array of photosensitive detectors located around the sample or by using a single photosensitive detector that can be moved around the sample. The scattering pattern recorded by the detector(s) is sent to a computer

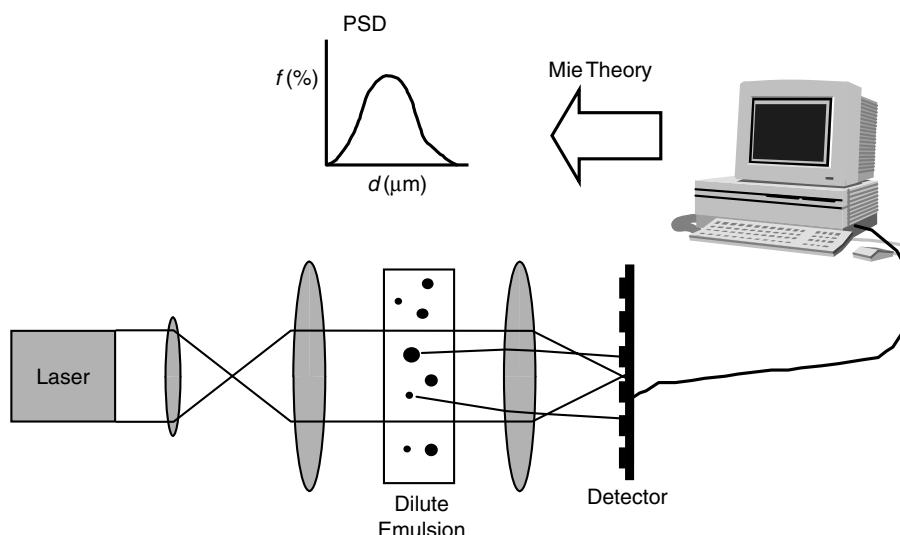


**Figure 11.10** Design for a particle sizing instrument that uses low-angle laser light scattering. A laser beam is passed through a dilute emulsion contained within an optically transparent measurement cell. The intensity of scattered light at different scattering angles is then measured using a series of detectors, and a suitable theory is used to convert the scattering pattern into a particle size distribution.

where it is stored and analyzed. Generally, the scattering angle is inversely related to the particle size, so that the scattering pattern of an emulsion contains information about the particle size distribution. The particle size distribution that gives the best fit between the experimental measurements of  $I(\Phi)$  versus  $\Phi$  and those predicted by the Mie theory is calculated. This calculation requires knowledge of the (complex) refractive index of both the particles and surrounding liquid at the wavelength of the laser used, which has to be entered by the user. The resulting data are presented as a table or graph of droplet concentration versus droplet size (Section 1.3.2). Most modern particle sizing instruments are fully automated and once the emulsion sample has been placed in the instrument the measurement procedure only takes a few minutes to complete. Before analyzing a sample, the instrument is usually *blanked* by measuring the scattering profile from the continuous phase in the absence of emulsion droplets. This scattering pattern is then subtracted from that of the emulsion to eliminate extraneous scattering from background sources other than the droplets, for example, dust or optical imperfections.

The range of droplet radii that can be detected using this type of experimental arrangement depends on the range of angles over which the instrument measures the intensity (Hiemenz and Rajagopalan, 1997). Most particle sizing instruments routinely used in the food industry detect the intensity of light scattered by emulsion droplets at relatively low angles, and are therefore sensitive to relatively large droplets. These instruments are often referred to as *low-angle laser light scattering* instruments, and can be used to analyze droplets with radii in the range of 0.1–1000  $\mu\text{m}$ . A number of instrument manufacturers have extended this particle size range by including optical arrangements that are sensitive to droplets with radii as small as 0.01  $\mu\text{m}$ , for example, by using more than one laser and measuring the intensity of the backscattered light. Particle sizing instruments based on static light scattering can also be purchased that can measure the intensity of scattered light over a much wider range of angles. These

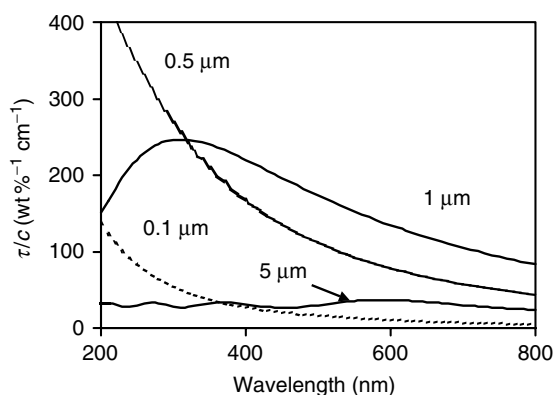


**Figure 11.11** Turbidity vs. wavelength spectra for emulsions with different droplets sizes. Droplet size distributions can be determined by analyzing these curves using a suitable light scattering theory.

*wide-angle laser light scattering* instruments can be used to determine the size of much smaller particles than low-angle laser light scattering instruments, for example, molecules or particles with radii less than a nanometer.

**11.3.2.2.2 Spectroturbidimetric methods.** These techniques measure the turbidity of a dilute emulsion as a function of wavelength (Walstra, 1968; Pearce and Kinsella, 1978; Reddy and Fogler, 1981; Pandolf and Masucci, 1984). The turbidity,  $\tau$ , is determined by comparing the intensity of light that has traveled directly through an emulsion ( $I$ ), with that which has traveled directly through the pure continuous phase ( $I_i$ ):  $\tau = -\ln(I/I_i)/L$ , where  $L$  is the sample path length. The greater the scattering of light by an emulsion, the lower the intensity of the transmitted wave, and therefore the larger the turbidity. The turbidity of a dilute emulsion is linearly related to the disperse phase volume fraction, and so turbidity measurements can be used to determine  $\phi$  if the droplet size remains constant. The dependence of the turbidity on wavelength for emulsions with different droplet sizes is shown in Figure 11.11. Analysis of these curves using an appropriate mathematical model can be used to provide information about the droplet size distribution.

The emulsion to be analyzed is placed in a cuvette and its turbidity is measured over a range of wavelengths (typically between 200 and 1000 nm). The droplet size distribution is then determined by finding the best fit between the experimental measurements of turbidity versus wavelength, and those predicted by the Mie theory. The spectroturbidimetric technique can be carried out using the UV–visible spectrophotometers found in most research laboratories, which may circumnavigate the need to purchase one of the expensive commercial light scattering instruments mentioned above. Nevertheless, some samples adsorb light strongly in the UV–visible region, which interferes with the interpretation of the turbidity spectra. In addition, the refractive indices of the disperse and continuous phases must be known and these vary with wavelength (Walstra, 1968).

**11.3.2.2.3 Reflectance methods.** An alternative method of determining the droplet size of emulsions is to measure the light reflected back from an emulsion ( $\Phi = 180^\circ$ ). The intensity of backscattered light is related to the size of the droplets in an emulsion (Lloyd, 1959; Sherman, 1968; McClements, 2002a,b). This technique has been used much less frequently than the spectroturbidimetric or angular scattering techniques, but may prove useful for the study of concentrated emulsions that are opaque to light.

### 11.3.2.3 Applications

The principal application of static light scattering techniques in the food industry is to determine droplet size distributions of emulsions (McClements, 1998, 2001). Knowledge of the initial particle size distribution of an emulsion is useful for predicting its long-term stability to creaming, flocculation, coalescence, and Ostwald ripening (Chapter 7). On the other hand, measurements of the time dependence of the particle size distribution can be used to monitor the kinetics of these destabilization processes (Chapter 7). Static light scattering instruments are widely used in research and development laboratories to investigate the influence of droplet size on physicochemical properties, such as stability, appearance, flavor, and rheology. They are also used in quality control laboratories to ensure that a product meets the predetermined specifications for droplet size, for example, to ensure that the mean droplet radius is below a specified value or that a specified fraction of droplets is below a particular droplet radius. Nevertheless, it should be noted that these techniques are unsuitable for *in situ* analysis of food emulsions that are optically opaque or solid-like (e.g., salad dressings, mayonnaise, butter, margarine, and ice cream) because of problems associated with transmitting light through the sample or introducing the sample into the measurement cell.

To obtain reliable data from a commercial light scattering instrument it is important to operate it properly and to be aware of (and eliminate if necessary) any potential sources of error (McClements, 2001). Errors may come from a variety of different sources, including the sample itself, the operation of the mechanical and optical components of the instrument, and the mathematical model used to convert the measured data into a particle size distribution. Some of the most important potential sources of error in static light scattering measurements are discussed below:

**11.3.2.3.1 Sample errors.** Commercial static light scattering instruments are designed to analyze dilute emulsions where only single scattering of the light waves occurs. Concentrated emulsions must therefore be diluted and made homogeneous prior to analysis to avoid multiple scattering effects. One must be aware that dilution and stirring of emulsions may cause appreciable alterations in particle size distribution, particularly in emulsions containing flocculated droplets. When emulsion dilution is necessary prior to analysis, it is usually important to carry it out using a buffer solution that has the same properties as the continuous phase of the original emulsion, for example, pH and ionic strength.

**11.3.2.3.2 Mathematical model errors.** Mathematical models derived from light scattering theory are used to convert light scattering measurements into particle size distributions. Generally, these models are based on the assumptions that the scattering particles are spherical, homogeneous, and noninteracting. To solve these mathematical models it is necessary to input information about the real and imaginary parts of the refractive indices of both the continuous and dispersed phases of an emulsion at the operating wavelength(s) of the light source. This type of optical information is often available for the relatively simple model emulsions used in research laboratories, but it may not be available for many real food emulsions, which are both structurally and compositionally complex. The mathematical model used to interpret light scattering data is fairly complex, and it is usually necessary for commercial instruments to make some *a priori* assumption about the shape of the particle size distribution in order to solve the theory in a reasonable time. These assumptions may not always be valid and may lead to errors under certain circumstances. One must be especially careful when using light scattering instruments to determine the particle size distribution of flocculated emulsions. In flocculated emulsions,

the droplets aggregate into heterogeneous “particles” that have an ill-defined refractive index and shape. Consequently, the particle size distribution determined by light scattering gives only an approximate indication of the true size of the flocs. In addition, emulsions often have to be diluted (to eliminate multiple scattering effects) and stirred (to ensure they are homogeneous) prior to measurement. Dilution and stirring are likely to disrupt any weakly flocculated droplets, but leave strongly flocculated droplets intact. For these reasons, commercial light scattering techniques can only give a qualitative indication of the extent of droplet flocculation.

*11.3.2.3.3 Instrumental errors.* The optical and mechanical design of each commercial light scattering instrument is often different, for example, the characteristics of the optical cell, the number, position, and sensitivity of the light detectors, and the way that the emulsion is introduced, agitated, and circulated in the optical cell. These differences can mean that the same emulsion can be analyzed using instruments from different manufacturers (or even from the same manufacturer) and quite large variations in the measured droplet size distributions can be observed, even though they should be identical (Coupland and McClements, 2001). For this reason, commercial light scattering instruments are often more useful for following qualitative changes, rather than giving absolute values. Finally, it is important to ensure that the instrument is operating correctly prior to use, for example, that the optical cell is clean, and that no air bubbles are being introduced into the sample that might interfere with the measurements.

### 11.3.3 *Dynamic light scattering and diffusing wave spectroscopy*

#### 11.3.3.1 *Principles*

Dynamic light scattering techniques are based on measurements of the translational diffusion coefficient ( $D$ ) of droplets determined by analyzing the interaction between a laser beam and an emulsion (Hunter, 1986; Horne, 1995). In a dilute emulsion, where there are no particle–particle interactions, the size of the droplets can be calculated using the Stokes–Einstein equation:

$$r = \frac{kT}{6\pi\eta_1 D} \quad (11.5)$$

where  $\eta_1$  is the viscosity of the continuous phase. Analytical instruments based on conventional dynamic light scattering [photon correlation spectroscopy (PCS) and Doppler shift spectroscopy (DSS)] are primarily designed to analyze emulsions where the laser beam only undergoes single scattering before reaching the detector (Horne, 1995). On the other hand, those based on diffusing wave spectroscopy (DWS) are designed to analyze concentrated emulsions where the laser beam undergoes extensive multiple scattering and propagates through the system by diffusion before reaching the detector (Pine et al., 1988, 1990). As well as determining droplet size, dynamic light scattering techniques can also be used to monitor phenomenon that alter the translational diffusion coefficient of droplets moving through colloidal dispersions, for example, droplet aggregation or network formation.

#### 11.3.3.2 *Measurement techniques*

A number of experimental techniques have been developed to measure the size of colloidal particles based on measurements of their translational diffusion coefficient (Hunter, 1993). The two most commonly used methods in commercial instruments are PCS and DSS.



**11.3.3.2.1 Photon correlation spectroscopy.** When a laser beam is directed through an ensemble of particles a scattering pattern is produced that is a result of the interaction between the electromagnetic waves and the particles (Horne, 1995). The precise nature of this scattering pattern depends on the relative position of the particles in the measurement cell. If the scattering pattern is observed over very short time intervals ( $\approx \mu\text{sec}$ ) one notices that there are slight variations in its intensity with time, which are caused by the change in the relative position of the particles due to their Brownian motion. The frequency of these fluctuations depends on the speed at which the particles move, and hence on their size. The change in the scattering pattern is monitored using a detector that measures the intensity of the photons,  $I(t)$ , which arrive at a particular scattering angle (or range of scattering angles) with time. If there is little change in the position of the particles within a specified time interval,  $\tau$ , the scattering pattern remains fairly constant and  $I(t) \approx I(t + \tau)$ . On the other hand, if the particles move an appreciable distance within the time interval the scattering pattern is altered significantly and  $I(t) \neq I(t + \tau)$ . The correlation between the scattering patterns measured at different times can be expressed mathematically by an intensity *autocorrelation function* (Horne, 1995):

$$C(\tau) = \frac{1}{N} \sum_{i=1}^N I(t_i)I(t_i + \tau) \quad (11.6)$$

where  $N$  is the number of times this procedure is carried out, which is typically of the order of  $10^5$  to  $10^6$ . As the time interval  $\tau$  between which the two scattering patterns are compared is increased, the autocorrelation function decreases from a high value, where the scattering patterns are highly correlated, to a constant low value when all correlation between the scattering patterns is lost (Figure 11.12). For a monodisperse emulsion, the autocorrelation function decays exponentially with a relaxation time  $\tau_c$ :  $C(\tau) = \exp(-\tau/\tau_c)$ . This relaxation time is related to the translational diffusion coefficient of the particles:  $D = (2Q^2\tau_c)^{-1}$ , where  $Q$  is the scattering vector, which describes the strength of the interaction between the light wave and the particles (Horne, 1995):

$$Q = \frac{4\pi n}{\lambda} \sin \frac{\theta}{2} \quad (11.7)$$

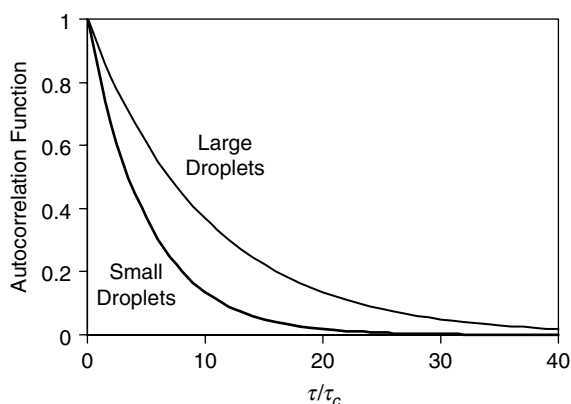


**Figure 11.12** Schematic representation of the decay of the autocorrelation function with time interval due to Brownian motion of the particles measured by photon correlation spectroscopy. The decay occurs more rapidly for small particles because they move faster in the measurement time interval.

here  $n$  is the refractive index of the medium,  $\lambda$  is the wavelength of light, and  $\theta$  is the scattering angle. Thus, by measuring the decay of the autocorrelation function with time at a certain angle it is possible to determine  $\tau_c$ , from which the diffusion coefficient can be calculated, and hence the particle size can be determined from the Stokes–Einstein equation (Equation 11.5).

PCS is suitable for accurate determination of particle size in suspensions that are monodisperse or that have a narrow size distribution. It is less reliable for suspensions with broad size distributions because of difficulties associated with interpreting the more complex autocorrelation decay curves (Horne, 1995).

**11.3.3.2.2 Doppler shift spectroscopy.** When a laser beam is scattered from a moving particle it experiences a shift in frequency, known as a Doppler shift (Trainer et al., 1992; Horne, 1995). The frequency of the scattered wave increases slightly when the particle moves toward the laser beam, and decreases slightly when it moves away. Consequently, there is a symmetrical distribution of Doppler shifts around the original frequency of the laser beam. The magnitude of the Doppler shift increases with particle velocity, and hence with decreasing particle size. Consequently, there is a broad distribution of Doppler shifts in a polydisperse suspension that contains particles moving at different velocities (Figure 11.13). The particle size distribution is determined by analyzing this Doppler shift spectrum. Two types of measurement techniques are commonly used in DSS: homodyne and heterodyne. Homodyne techniques determine the Doppler shifts by making use of the interference of light scattered from one particle with that scattered from all the other particles, whereas heterodyne techniques determine frequency shifts by comparing the frequency of the light scattered from the particles with a reference beam of fixed frequency (Trainer et al., 1992). The heterodyne technique is capable of analyzing suspensions with much higher particle concentrations than is possible using the homodyne technique and so only it will be considered here.

A typical experimental arrangement for making Doppler shift measurements is shown in Figure 11.14. A laser beam is propagated along an optical waveguide that is immersed

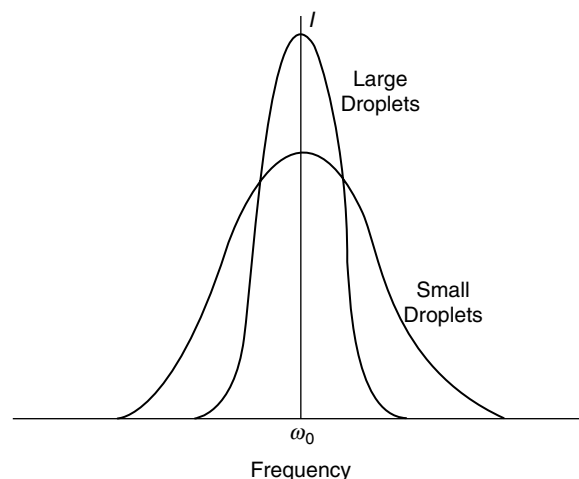


**Figure 11.13** Doppler shift spectroscopy measures the frequency shift that occurs when a light wave is scattered by a moving particle. The distribution of frequency shifts can be related to the particle size distribution using suitable theories, since small particles move more rapidly and therefore cause a greater frequency shift.

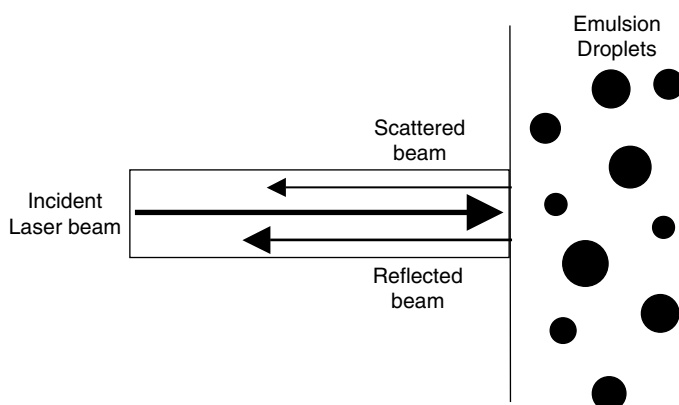


**Figure 11.14** Experimental technique for measuring the Doppler shift of particles based on the heterodyne measurement technique.

in the sample being analyzed. Part of the laser beam is reflected from the end of the waveguide and returns to the detector, where it is used as a reference beam because its frequency is not Doppler shifted. The remainder of the laser beam propagates into the sample, and part of it is scattered back up the waveguide by the particles in its immediate vicinity ( $\sim 100\ \mu\text{m}$  pathlength). This backscattered light is frequency shifted by an amount that depends on the velocity of the particles. The difference in frequency between the reflected and scattered waves is equivalent to the Doppler shift.

The variation of the power  $P(\omega)$  of the scattered waves with angular frequency ( $\omega$ ) has the form of a Lorentzian function:

$$P(\omega) = I_0 \langle I_s \rangle \frac{\omega_0}{\omega^2 + \omega_0^2} \quad (11.8)$$

where  $I_0$  and  $\langle I_s \rangle$  are the reference and scattered light intensities, and  $\omega_0$  is a characteristic frequency that is related to the scattering efficiency and diffusion coefficient of the particles:  $\omega_0 = DQ^2$ . Particle size is determined by measuring the variation of  $P(\omega)$  with  $\omega$ , and then finding the value of the diffusion coefficient that gives the best fit between the measured spectra and that predicted by the above equation. For polydisperse systems it is necessary to take into account that there is a distribution of particle sizes. The calculation of particle size requires that the analyst inputs the refractive indices of the continuous and dispersed phases, the viscosity of the continuous phase, and the measurement temperature. Because the path length of the light beam in the sample is so small (about  $100\ \mu\text{m}$ ) it is possible to analyze much more concentrated emulsions (up to 40%) than with static light scattering or PCS techniques (Trainer et al., 1992), although some form of correction factor usually has to be applied to take into account the influence of droplet interactions on the diffusion coefficient (Horne, 1995). Commercial instruments are available that are easy to use and that can analyze an emulsion in a few minutes.

**11.3.3.2.3 Diffusing wave spectroscopy.** Diffusing wave spectroscopy is a type of dynamic light scattering that is suitable for studying relatively concentrated colloidal dispersions, rather than dilute ones (Pine et al., 1988, 1990; Weitz et al., 1992, 1993; Larson, 1999). Traditional dynamic light scattering is used to study colloidal dispersions where only single scattering events occur. On the other hand, DWS is used to study colloidal dispersions

that are sufficiently concentrated that the light waves are scattered many times before they exit the sample. Extensive multiple scattering means that the light waves move through the system in a random-walk fashion, which can be modeled mathematically as a diffusion process. Like dynamic light scattering, DWS is based on measurements of the intensity autocorrelation function of a colloidal dispersion as a function of time, resulting from temporal fluctuations of scattered light caused by particle mobility (ten Grotenhuis et al., 2000; Blijdenstein et al., 2003a). The movement of a particle in a colloidal dispersion is usually the result of Brownian motion or convection processes. A mathematical analysis of the autocorrelation function enables one to determine the *mean square displacement* ( $\langle \Delta r^2(t) \rangle$ ) of the colloidal particles, which is a measure of their mobility. Measurements can either be carried out in a transmission or a reflection mode using this technique.

#### 11.3.3.3 Applications

Dynamic light scattering techniques are particularly useful for measuring the size of particles that are below the lower detection limit of static light scattering techniques, for example, small emulsion droplets, protein aggregates, and surfactant micelles (Hallet, 1994; Dalgleish and Hallet, 1995; Horne, 1995; Dalgleish et al., 1997). Commercial instruments based on this principle are typically capable of analyzing particles with diameters between 3 nm and 3  $\mu$ m. One of the major limitations of these dynamic light scattering techniques is that they assume that the viscosity of the aqueous phase is Newtonian, which is not the case for many food emulsions, especially those that contain thickening agents.

As well as determining particle sizes, dynamic light scattering techniques can also be used to monitor the flocculation of particles in suspensions because aggregation causes them to move more slowly (Dalgleish and Hallet, 1995). It can also be used to determine the thickness of adsorbed layers of emulsifier on spherical particles (Dalgleish and Hallet, 1995). The radius of the spherical particles is measured in the absence of emulsifier (providing they are stable to aggregation) and then in the presence of emulsifier. The difference in radius is equal to the thickness of the adsorbed layer, although this value may also include the presence of any solvent molecules associated with the emulsifier. Alternatively, the change in particle radius can be monitored when a substance is added that causes the interfacial membrane to be degraded and/or displaced, which also provides some measure of the dimensions of the interfacial membrane.

PCS is restricted to the analysis of fairly dilute suspensions of particles ( $\phi < 0.1\%$ ), so as to avoid multiple scattering events and to transmit sufficient intensity of light waves through the system to be detected. DSS can be used to analyze much more concentrated emulsions (up to 40 wt%) because the path length of the light beam in the sample is so small (Trainer et al., 1992; Horne, 1995). DWS can also be used to study emulsions that are concentrated because it relies on extensive multiple scattering of the light waves. This technique has been used to provide valuable information about physicochemical phenomena that influence the mobility of emulsion droplets, for example, particle size, particle-particle interactions, flocculation, or changes in continuous phase rheology (Hemar and Horne, 1999; Grotenhuis et al., 2000; Harden and Viasnoff, 2001; Blijdenstein et al., 2003a; Hemar et al., 2003; Nicolas et al., 2003).

#### 11.3.4 Electrical pulse counting

Electrical pulse counting techniques (also called electrozone sensing or Coulter counter techniques) are based on measurements of changes in electrical conductivity when a dilute emulsion is pulled through a small hole (Lines, 1994; McClements, 2001). The emulsion to be analyzed is placed in a beaker that has two electrodes dipping into it (Figure 11.15). One of the electrodes is contained in a glass tube that has a small hole in it, through which the

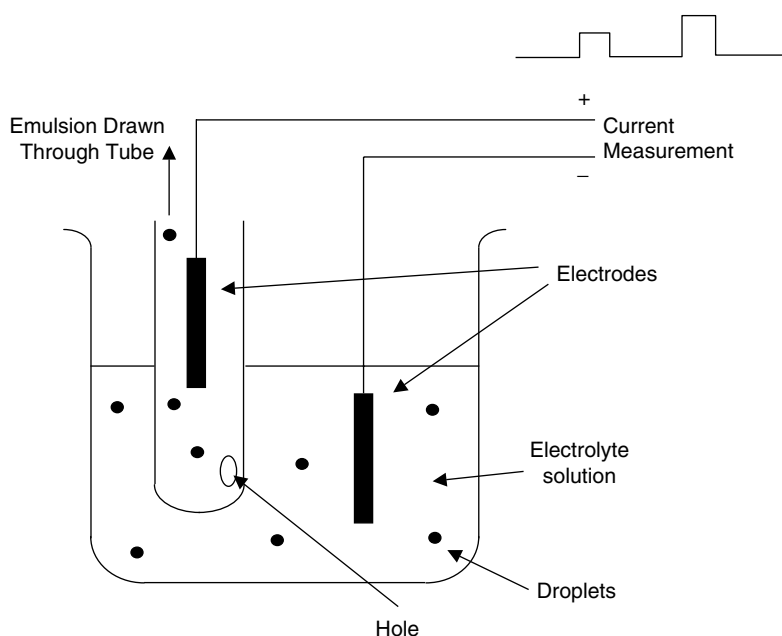


**Figure 11.15** Electrical pulse counter suitable for determining emulsion droplet size distributions. The momentary decrease in current is measured when an oil droplet passes through a small hole in a glass tube. The number of pulses per unit volume provides information about droplet concentration, while the area under a pulse provides information about droplet size.

emulsion is sucked. When an oil droplet passes through the hole it causes a decrease in the current between the electrodes because oil has a much lower electrical conductivity than water. Each time a droplet passes through the hole, the instrument records a decrease in current, which it converts into an electrical pulse. The instrument controls the volume of liquid that passes through the hole and so the droplet concentration can be determined by counting the number of electrical pulses in a known volume. When the droplets are small compared to the diameter of the hole, the droplet size is simply related to the height of the pulses:  $d^3 = kP$ , where  $d$  is the droplet diameter,  $P$  is the pulse height, and  $k$  is an instrument constant that is determined by recording the pulse height of a standard suspension of monodisperse particles of known diameter. Electrical pulse counting techniques are capable of determining the size distribution of particles with diameters between 0.4 and 1200  $\mu\text{m}$  (Hunter, 1986; Mikula, 1992; Lines, 1994), and are therefore suitable for analyzing most food emulsions. To cover this whole range it is necessary to use glass tubes with different sized apertures. Typically, droplets between 2 and 60% of the diameter of the aperture can be reliably analyzed. Thus, a tube with an aperture of 16  $\mu\text{m}$  can be used to analyze droplets with diameters between 0.3 and 10  $\mu\text{m}$ . If an emulsion contains a wide range of droplet sizes it may be necessary to use a number of glass tubes with different aperture sizes to determine the full droplet size distribution. Instruments based on this principle have been commercially available for many years and are widely used in the food industry.

There are a number of practical problems associated with this technique that may limit its application to certain systems (Lines, 1994). First, it is necessary to dilute an emulsion considerably before analysis so that only one particle passes through the hole at a time, otherwise a pair of particles would be counted as a single larger particle. As mentioned earlier, dilution of an emulsion may alter the structure of any flocs present, especially when the attraction between the droplets is small. Second, the emulsion droplets must be

suspended in an electrolyte solution (typically 5 wt% salt) to ensure that the electrical conductivity of the aqueous phase is sufficiently large to obtain accurate measurements. The presence of an electrolyte alters the nature of the colloidal interactions between charged droplets, which may change the extent of flocculation from that which was present in the original sample. Third, any weakly flocculated droplets may be disrupted by the shear forces generated by the flocs as they pass through the small hole. Fourth, if an emulsion contains a wide droplet size distribution it is necessary to use a number of glass tubes with different aperture sizes to cover the full size distribution. Fifth, if there is a large density contrast between the dispersed and continuous phase the emulsions droplets may cream or sediment before they have time to be pulled through the aperture. Sixth, it is not possible to analyze emulsions that contain relatively small droplets ( $d < 0.4 \mu\text{m}$ ). Despite these limitations, electrical pulse counting is usually considered to be more reliable and accurate than light scattering in emulsions where it is applicable.

### 11.3.5 Sedimentation techniques

#### 11.3.5.1 Principles

Techniques based on this principle obtain information about the particle size of an emulsion by measuring the velocity at which droplets sediment (or cream) in a gravitational or centrifugal field. Sedimentation techniques can be used to determine the size distribution of particles between 1 nm and 1 mm, although a number of different types of instruments have to be used to cover the whole of this range (Hunter, 1986, 1993).

#### 11.3.5.2 Measurement techniques

**11.3.5.2.1 Gravitational sedimentation.** The terminal velocity of an isolated rigid spherical particle suspended in a Newtonian liquid moving entirely due to gravitational forces is given by Stokes' equation:

$$v = \frac{2(\rho_2 - \rho_1)gr^2}{9\eta_1} \quad (11.9)$$

where  $\rho_2$  is the density of the droplets,  $\rho_1$  and  $\eta_1$  are the density and viscosity of the continuous phase,  $g$  is the acceleration due to gravity, and  $r$  is the droplet radius. The droplet size can therefore be determined by measuring the velocity at which particles move through the liquid once the densities of both phases and the viscosity of the continuous phase are known. The concentration of the droplets at a particular position can be monitored using a variety of experimental methods, including visual observation, optical microscopy, light scattering, nuclear magnetic resonance (NMR), ultrasound, x-ray adsorption, and electrical measurements (Mikula, 1992; Pal, 1994; Dickinson and McClements, 1995). Commercial instruments are available based on this principle that can determine droplet diameters in the range 0.1–300  $\mu\text{m}$ . It should be noted that the Stokes' equation cannot be used to reliably estimate droplets of radius less than about 0.1  $\mu\text{m}$  because of Brownian motion effects (Walstra, 2003a).

**11.3.5.2.2 Centrifugal Sedimentation.** When an emulsion is placed in a centrifuge and rotated rapidly, it is subjected to a centrifugal force that causes the droplets to move inward when they have a lower density than the surrounding liquid (e.g., oil-in-water emulsions) or outward when they have a higher density (e.g., water-in-oil emulsions). The velocity ( $v(x)$ ) that the droplets move through the surrounding liquid depends on their size, as well as on the angular velocity ( $\omega$ ) at which the tube is centrifuged and their distance from the center of the rotor ( $x$ ). The droplet motion can be conveniently characterized

by a *sedimentation coefficient*, which is independent of the angular velocity and location of the droplets (Thomas et al., 1991; Hunter, 1993):

$$S = \frac{v(x)}{\omega^2 x} \quad (11.10)$$

The radius of an isolated spherical particle in a fluid is related to the sedimentation coefficient by the following equation:

$$r = \sqrt{\frac{9\eta_1 S}{2(\rho_2 - \rho_1)}} \quad (11.11)$$

Droplet sizes can therefore be determined by measuring their sedimentation coefficient within a known centrifugal field. The sedimentation coefficient is related to the distance of the droplets from the rotor center:  $S = [\ln(x_2/x_1)]/[\omega^2(t_2 - t_1)]$ , where  $x$  is the position of the particle at time  $t$  (Hunter, 1993; Hiemenz and Rajagopalan, 1997). For monodisperse systems,  $S$  (and therefore  $r$ ) can simply be determined by measuring the time required for droplets to move from one position ( $x_1$ ) to another position ( $x_2$ ). For a polydisperse system, the full particle size distribution can be determined by measuring the amount of material that passes a specific value of  $x$  with time (Middleberg et al., 1990). The concentration of droplets at a particular position can be determined using a variety of methods, including optical microscopy, light scattering, and x-ray adsorption. Commercial instruments are available based on this principle that can determine droplet diameters in the range 0.01–30  $\mu\text{m}$ . These instruments are known by a variety of names, including sedimentation field flow fractionation and photosedimentation.

### 11.3.5.3 Applications

Traditionally, techniques based on gravitational or centrifugal separation have not been widely used in the food industry for particle size analysis. Nevertheless, they are likely to find more widespread use with the introduction of commercial instruments based on this principle that are capable of analyzing droplets with a wide range of different particle sizes. One major advantage of these methods is that it is often possible to fractionate the droplets in an emulsion into different size classes, and then carry out further analysis of the droplets in each size class. This may be important in systems where the composition of the droplets depends on their particle size, or when there is more than one type of particle in the system (Weers, 1998).

## 11.3.6 Ultrasonic spectrometry

### 11.3.6.1 Principles

Ultrasonic spectrometry uses interactions between ultrasonic waves and emulsions to obtain information about particle size distribution and concentration (McClements, 1991, 1996; Dukhin and Goetz, 1996; Povey, 1995, 1997; Dukhin et al., 2000; Coupland and McClements, 2004). This technique can be used to measure the size of droplets with radii between 10 nm and 1000  $\mu\text{m}$ . Particle sizing instruments based on ultrasonic spectrometry are available commercially, and are finding increasing use within the food industry. These instruments have some important advantages over many traditional particle sizing technologies because they can often be used to analyze emulsions that are concentrated and optically opaque, without the need for any sample preparation.

As an ultrasonic wave propagates through an emulsion its velocity and attenuation are altered due to its interaction with the droplets. These interactions may take a number of different forms: (i) some of the wave is *scattered* into directions that are different from that of the incident wave; (ii) some of the ultrasonic energy is converted into heat due to various *absorption* mechanisms (e.g., thermal conduction and viscous drag); and (iii) there is interference between waves that travel through the droplets, waves that travel through the surrounding medium, and waves that are scattered. The relative importance of these different mechanisms depends on the thermophysical properties of the component phases, the frequency of the ultrasonic wave, and the concentration and size of the droplets.

As with light scattering, the scattering of ultrasound by a droplet can be divided into three regimes according to the relationship between the particle size and the wavelength of the radiation: (i) the long-wavelength regime ( $r < \lambda/20$ ), (ii) the intermediate-wavelength regime ( $\lambda/20 < r < 20\lambda$ ), and (iii) the short-wavelength regime ( $r > 20\lambda$ ). The wavelength of ultrasound (10  $\mu\text{m}$  to 10 mm) is much greater than that of light (0.2–1  $\mu\text{m}$ ), and so ultrasonic measurements are usually made in the long-wavelength regime, whereas light scattering measurements are often made in the intermediate-wavelength regime.

In the long-wavelength regime, the ultrasonic properties of fairly dilute emulsions ( $\phi < 15\%$ ) can be related to their physicochemical characteristics using the following equation:

$$\left(\frac{K}{k_1}\right)^2 = \left(1 - \frac{3\phi i A_0}{k_1^3 r^3}\right) \left(1 - \frac{9\phi i A_1}{k_1^3 r^3}\right) \quad (11.12)$$

where  $K$  is the complex propagation constant of the emulsion ( $= \omega/c_e + i\alpha_e$ ),  $k_1$  is the complex propagation constant of the continuous phase ( $= \omega/c_1 + i\alpha_1$ ),  $\omega$  is the angular frequency,  $c$  is the ultrasonic velocity,  $\alpha$  is the attenuation coefficient,  $i = \sqrt{-1}$ , and  $r$  is the droplet radius. The  $A_0$  and  $A_1$  terms are the monopole and dipole scattering coefficients of the individual droplets, which depend on the adiabatic compressibility, density, specific heat capacity, thermal conductivity, cubical expansivity, and viscosity of the component phases, as well as on the frequency of the ultrasonic waves and the droplet size (Epstein and Carhart, 1953). The above equation can be used to relate the ultrasonic velocity and attenuation coefficient of an emulsion to the droplet size and concentration, once the thermophysical properties of the component phases are known, since  $c_e = \omega/\text{Re}(K_e)$  and  $\alpha_e = \text{Im}(K_e)$ . Most commercial particle sizing instruments based on ultrasonic spectrometry use more sophisticated mathematical models to relate the measured ultrasonic parameters to the droplet characteristics than the relatively simple one mentioned above. These models are applicable in the long-, intermediate-, and short-wavelength regimes, and often take into account multiple scattering and other particle interaction effects (McClements, 1996; McClements et al., 1998).

The dependence of the ultrasonic velocity and attenuation coefficient of an emulsion in the long-wavelength regime on droplet size and concentration is shown in Figure 11.16. The ultrasonic velocity increases with droplet size, while the attenuation multiplied by wavelength ( $\alpha\lambda$ ) has a maximum value at an intermediate droplet size. It is this dependence of the ultrasonic properties of an emulsion on droplet size that enables ultrasound to be used as a particle sizing technology. An emulsion is analyzed by measuring its ultrasonic velocity and/or attenuation as a function of frequency, and then finding the droplet size and concentration that give the best fit between the experimental data and the theory. For polydisperse emulsions the equation has to be modified to take into account the droplet size distribution (McClements, 1991, 1996). One of the major limitations of the ultrasonic technique is the fact that a great deal of information about the thermophysical properties of the component phases is needed to interpret the measurements, and these



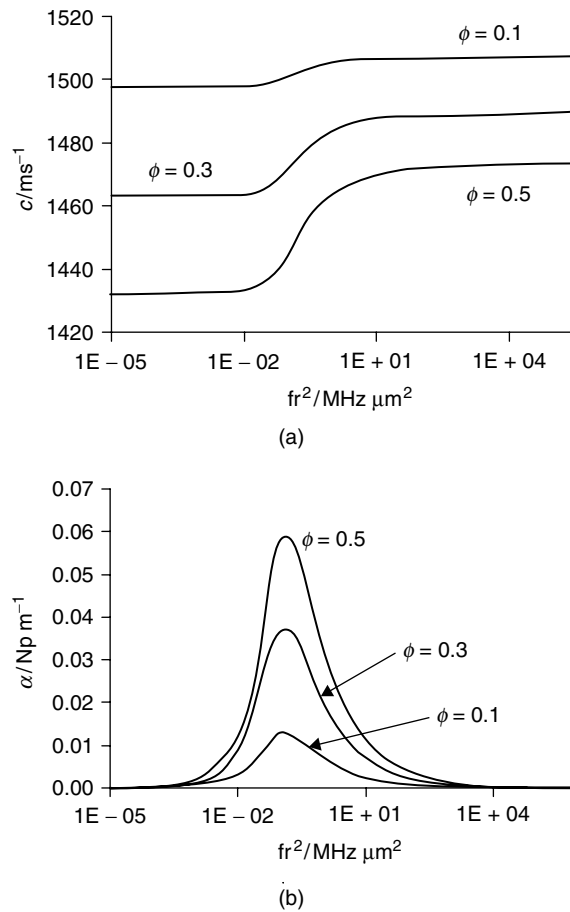


**Figure 11.16** Dependence of the ultrasonic properties of an emulsion on its droplet size and disperse phase volume fraction in the long-wavelength regime: (a) ultrasonic velocity; (b) ultrasonic attenuation coefficient.

data are often not readily available in the literature (Coupland and McClements, 2001, 2004). In addition, for droplet concentrations greater than about 15% it is necessary to extend the above equation to take into account interactions between the droplets (Hemar et al., 1997; McClements et al., 1999). The mathematical models used to convert measured ultrasonic attenuation or velocity spectra into particle size distributions and concentrations in most commercially available ultrasonic particle size analyzers do take into account certain types of particle interaction effects. Nevertheless, it should be noted that some important effects are often ignored and that this can lead to erroneous results (McClements et al., 1998, 1999).

#### 11.3.6.2 Measurement techniques

The ultrasonic properties of materials can be measured using a number of different experimental arrangements, for example, pulsed or continuous wave techniques (McClements, 1996). The major difference between them is the form in which the ultrasonic energy is applied to the sample and the experimental configuration used to carry out the measurements. Some commercial particle sizing instruments based on ultrasonic spectrometry use pulsed ultrasound, whereas others use continuous wave ultrasound.

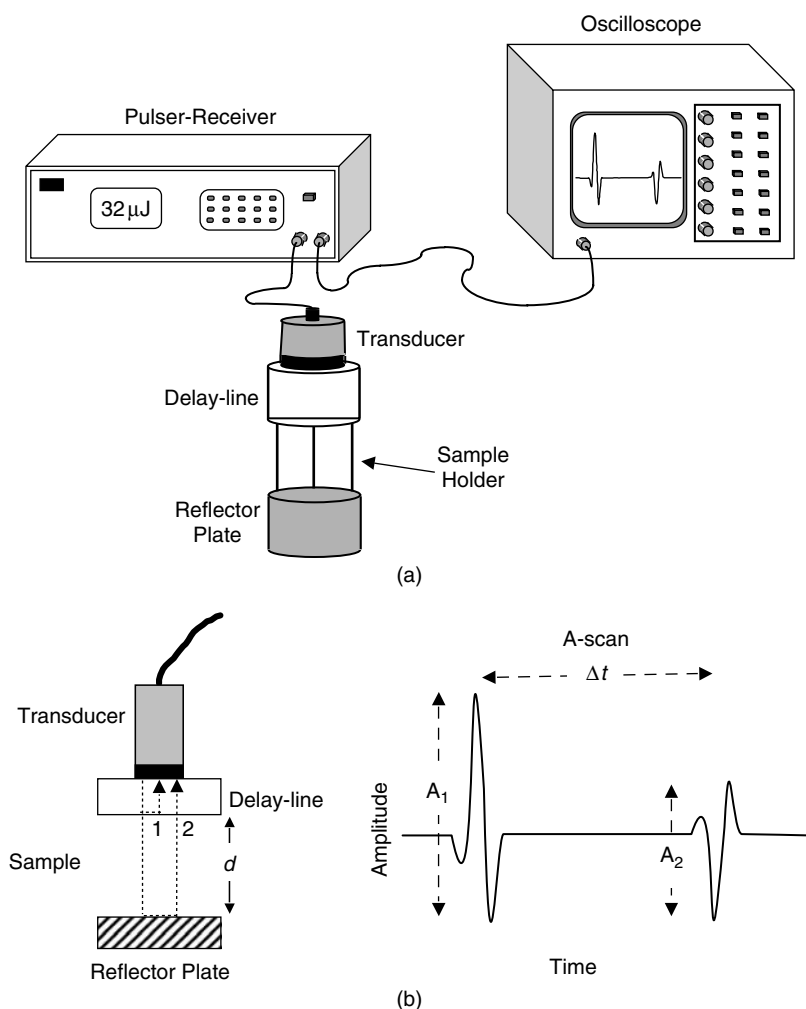


**Figure 11.17** Example of an ultrasonic pulse-echo technique that can be used to measure the ultrasonic velocity and attenuation coefficient of emulsions.

The principles of pulsed ultrasonic techniques can be demonstrated by considering the “pulse-echo” technique (Figure 11.17). The sample to be analyzed is contained within a thermostated measurement cell that has an ultrasonic transducer fixed to one side. An electrical pulse is applied to the transducer, which stimulates it to generate a pulse of ultrasound that is directed into the sample. This pulse travels across the sample, is reflected from the back wall of the measurement cell, travels back through the sample, and is then detected by the same transducer (Figure 11.17). The ultrasonic pulse received by the transducer is converted back into an electrical pulse which is digitized and saved for analysis.

The ultrasonic velocity and attenuation coefficient of a sample are determined by measuring the time-of-flight ( $t$ ) and amplitude ( $A$ ) of the ultrasonic pulse that has traveled through it. The ultrasonic velocity is equal to the distance traveled by the pulse ( $2d$ ) divided by its time-of-flight:  $c = 2d/t$ . The attenuation coefficient is calculated by comparing the amplitude of a pulse that has traveled through the sample, with that of a pulse that has traveled through a material whose attenuation coefficient is known:  $\alpha_2 = \alpha_1 - \ln(A_2/A_1)/2d$ , where the subscripts 1 and 2 refer to the properties of the reference material and the material being tested, respectively. To determine the droplet size distribution of an emulsion it is necessary to

measure the frequency dependence of its ultrasonic properties, which can be achieved using either tone-burst or broadband pulsed techniques (McClements, 1996). The “through-transmission” technique is another pulsed ultrasound technique commonly used to analyze emulsions (McClements, 1996). This technique is similar to the pulse-echo technique except that separate transducers are used to generate and receive the ultrasonic pulse.

Interferometric techniques use continuous waves, rather than pulsed waves, to measure the ultrasonic properties of materials (O'Driscoll et al., 2003). The continuous waves are made to reflect backward and forward between two parallel barriers, leading to the formation of a constructive and destructive interference pattern. By measuring the change in intensity of the ultrasonic signal when either the distance between the barriers is altered or the frequency of the ultrasonic waves is varied it is possible to determine the ultrasonic velocity and attenuation coefficient of the sample. As with pulsed techniques it is necessary to measure the frequency dependence of the ultrasonic properties of an emulsion in order to determine its particle size distribution.

### 11.3.6.3 Applications

Ultrasound has major advantages over many other particle sizing technologies because it can be used to measure droplet size distributions in concentrated and optically opaque emulsions *in situ*. In addition, it can be used as an on-line sensor for monitoring the characteristics of food emulsions during processing, which gives food manufacturers much greater control over the quality of the final product. The possibility of using ultrasound to measure particle sizes in real foods has been demonstrated for casein micelles in milk, milk fat globules, salad dressings, and salad creams (Coupland and McClements, 2004).

The two major disadvantages of the ultrasonic technique are the large amount of thermophysical data required to interpret the measurements, and the fact that small air bubbles can interfere with the signal from the emulsion droplets (McClements, 1991, 1996; Coupland and McClements, 2004). In addition, it is important to use an appropriate theory to interpret ultrasonic spectra obtained from an emulsion. If an emulsion is highly concentrated or flocculated, then the traditional ultrasonic scattering theory has to be extended to take into account various types of particle–particle interactions, for example, thermal overlap, viscous overlap, and aggregate scattering effects (McClements et al., 1998, 1999; Chanamai et al., 1999; 2000d; Herrmann and McClements, 1999).

### 11.3.7 Nuclear magnetic resonance

Instrumental techniques based on NMR usually use interactions between radio waves and the nuclei of hydrogen atoms to obtain information about the properties of materials.\* NMR techniques based on the *restricted diffusion* of molecules within emulsion droplets, have been developed to measure the droplet size distribution of emulsions (Balinov et al., 2004). These techniques are sensitive to particle sizes between 0.2 and 100  $\mu\text{m}$  (Dickinson and McClements, 1995).

The principles of the technique are fairly complex, and have been described in detail elsewhere (Soderman and Balinov, 1996; van Duynhoven et al., 2002; Balinov et al., 2004). Basically, the sample to be analyzed is placed in a static magnetic field gradient and a series of radio frequency pulses is applied to it. These pulses cause some of the hydrogen nuclei in the sample to be excited to higher energy levels, which leads to the generation of a detectable NMR signal. The amplitude of this signal depends on the movement of the nuclei in the sample: the further the nuclei move during the experiment, the greater

\* NMR techniques can also be used to study the nuclei of certain other isotopes, but these are not widely used for particle sizing.

the reduction in the amplitude. A measurement of the signal amplitude can therefore be used to study molecular motion.

In a bulk liquid, the distance that a molecule can move in a certain time is governed by its translational diffusion coefficient,  $x_{\text{rms}} = \sqrt{2Dt}$ . When a liquid is contained within an emulsion droplet of diameter  $d$  its diffusion may be restricted because of the presence of the interfacial droplet boundary. If the movement of a molecule in a droplet is observed over relatively short times ( $t \ll d^2/2D$ ) the diffusion is unrestricted, but if it is observed over longer times the diffusion is restricted because the molecule cannot move further than the diameter of the droplet. By measuring the attenuation of the NMR signal at different times it is possible to identify when the diffusion becomes restricted, and thus estimate the droplet size. Because this technique relies on the movement of molecules within droplets, it is independent of droplet flocculation (Lee et al., 1998).

NMR restricted diffusion measurements have been used to determine the droplet size distribution of a variety of oil-in-water and water-in-oil emulsions, including model systems, margarine, cream, and cheese (Callaghan et al., 1983; van den Enden et al., 1990; Li et al., 1992; Soderman et al., 1992; Lee et al., 1998; Marciani et al., 2001; Van Dalen, 2002; Hollingsworth and Johns, 2003; Rousseau et al., 2003). NMR imaging techniques based on the same principle have also been used to measure the droplet size distribution in different regions within an emulsion, for example, within a cream layer (McDonald et al., 1999). The NMR technique is particularly useful at determining the actual size of the individual droplets in flocculated emulsions (rather than the floc size), because the restricted diffusion of the molecules within the droplets is not influenced by the flocculation process (Lee et al., 1998). The technique has been used to monitor droplet growth in emulsions due to droplet coalescence and Ostwald ripening (Lee et al., 1998; Hedin and Furo., 2001). Finally, NMR restricted diffusion measurements carried out on the continuous phase of emulsions have been used to provide information about the structural organization of the droplets within an emulsion (Hills et al., 2000). Like ultrasonic spectrometry, it is nondestructive and can be used to analyze emulsions that are concentrated and optically opaque (Dickinson and McClements., 1995; Balinov et al., 2004). NMR instruments are commercially available that have been designed to measure droplet size distributions of emulsions, and these instruments are likely to find increasing use in the food industry.

### 11.3.8 Neutron scattering

Neutron scattering techniques use interactions between a beam of neutrons and an emulsion to determine the droplet size distribution (Dickinson and Stainsby, 1982; Eastoe, 1995; Reynolds et al., 2000). They can also be used to provide information about the thickness of interfacial layers and the spatial distribution of droplets in emulsions (Hone et al., 2002). This technique has a couple of special features that make it particularly suitable for studying food emulsions (Eastoe, 1995). First, the scattering of neutrons from emulsion droplets is very weak and therefore multiple scattering effects are not appreciable, which means that concentrated emulsions can be analyzed without dilution. Second, the scattering of neutrons from heterogeneous materials depends on the "contrast" between the different components, which can be manipulated by the experimenter. Thus, it is possible to selectively highlight specific structural features within an emulsion (see below). Despite its ability to generate information that is difficult to obtain using other techniques, the application of neutron scattering to food emulsions is limited because a nuclear reactor is needed to generate the neutron beam. There are only a small number of neutron scattering facilities in the world that are generally accessible, and beam time is rather limited and must be scheduled many months in advance of the proposed experiment (Stothart, 1995).

In many respects, the measurement principle of neutron scattering is similar to that of static light scattering, except that a beam of neutrons is used instead of light. The sample to be analyzed is placed into a cuvette that is inserted between a source of neutrons and a neutron detector (Stothart, 1995). A beam of neutrons is passed through the emulsion and the intensity of the scattered neutrons is measured as a function of scattering angle (and/or wavelength). Information about the properties of the emulsion is then obtained by interpreting the resulting spectrum using an appropriate neutron scattering theory (Eastoe, 1995).

Each type of atomic nuclei scatters neutrons to a different extent, which is characterized by a "scattering cross-section" (Lovsey, 1984). The scattering of neutrons from a heterogeneous material, such as an emulsion, depends on the contrast between the scattering cross-sections of the different components: the greater the contrast, the more intense the scattering. One of the most important attributes of neutron scattering is the ability to alter the scattering cross-section of molecules that contain hydrogen atoms, for example, water, proteins, fats, and carbohydrates (Eastoe, 1995; Stothart, 1995). Normal hydrogen ( $^1\text{H}$ ) and deuterium ( $^2\text{H}$ ) have significantly different scattering cross-sections, and so by varying the  $^1\text{H}$ : $^2\text{H}$  ratio of a particular type of molecule it is possible to increase or decrease its contrast with respect to the other components in an emulsion. As a consequence, it is possible to emphasize specific structural components within an emulsion, for example, droplets, interfacial membrane, or continuous phase components.

Consider an oil-in-water emulsion that consists of oil droplets covered by an interfacial layer that are suspended in an aqueous phase (Figure 11.18). By altering the ratio of water to deuterated water in the aqueous phase it is possible to match the aqueous phase to either the interfacial layer, or to the oil within the droplets. Alternatively, the interfacial layer could be matched to the droplet by partial deuteration of either the oil or emulsifier molecules. Thus, it is possible to obtain information about the dimensions of the interfacial layer alone, the oil droplet alone, or the droplet + interfacial layer.

Neutron scattering measurements have been used to monitor changes in droplet size distribution in emulsions due to destabilization mechanisms, for example, Ostwald ripening (Egelhaaf et al., 1999). An interesting recent application of neutron scattering to a food emulsion was for the determination of the size of the droplets in "Pastis," an aniseed-based alcoholic beverage popular in the south of France and elsewhere (Grillo, 2003). When the optically transparent alcoholic beverage is diluted with water it turns a cloudy white color because of the formation of micron-sized oil (anethol) droplets. Neutron scattering has also been used to quantify the partitioning of surfactant molecules between emulsion droplet surfaces and the surrounding continuous phase (Staples et al., 2000).

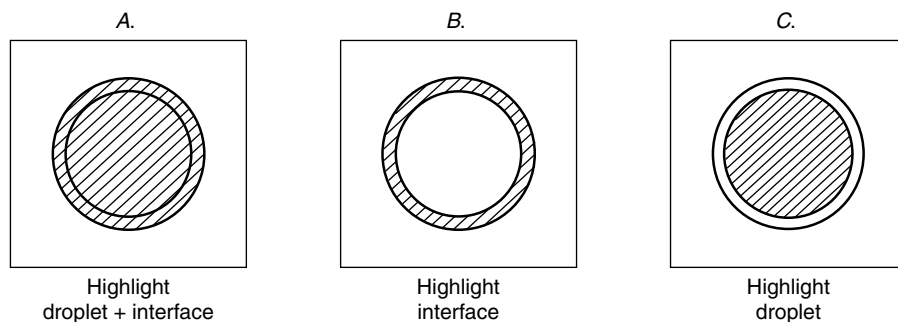


**Figure 11.18** Concept of contrast matching of emulsions in neutron scattering experiments. The droplet, interfacial membrane, or both can be highlighted.

### 11.3.9 Dielectric spectroscopy

This technique depends on the dielectric response of an emulsion during the application of an electromagnetic wave (Clausse, 1983; Asami, 1995; Sjoblom et al., 1996). The possibility of using dielectric spectroscopy to determine the droplet size distribution of concentrated emulsions has been demonstrated (Garrouch et al., 1996). The dielectric permittivity of an emulsion is measured over a wide range of electromagnetic frequencies and the resulting spectra are analyzed using a suitable theory to determine the droplet size distribution. The major limitation of this technique is that it can only be used to determine droplet size distributions in emulsions containing charged particles. Even so, it can be used to simultaneously measure the zeta ( $\zeta$ ) potential and droplet size distribution, and it can be used to analyze emulsions that are concentrated and optically opaque without the need for any sample dilution. It may therefore have some important applications in the food industry. Nevertheless, dielectric spectroscopy is still in its infancy and a lot more research is still required before the technique becomes more widely accepted and used.

### 11.3.10 Electroacoustics

Electroacoustic techniques use a combination of electrical and acoustic phenomenon to determine both the size distribution and  $\zeta$ -potential of emulsion droplets (O'Brien et al., 1995; Carasso et al., 1995; Dukhin and Goetz, 1996; Dukhin et al., 2000). The underlying principle of these techniques is described in more detail in the section on  $\zeta$ -potential measurements (Section 11.6.2). Particle sizing instruments based on the electroacoustic principle are commercially available and are capable of analyzing droplets with sizes between 0.1 and 10  $\mu\text{m}$  (Hunter, 1998a,b). This particle size range has been extended in some commercial instruments (10 nm to 1000  $\mu\text{m}$ ) by combining the electroacoustic technology with ultrasonic spectrometry (Dukhin et al., 2000; Hsu and Nacu, 2003). Instruments based on electroacoustics are capable of analyzing emulsions with high droplet concentrations (<50%) without any sample dilution (Dukhin et al., 2000; Kong et al., 2001c; O'Brien et al., 2003). These techniques have been used to measure particle size distributions in a wide variety of different oil-in-water and water-in-oil emulsions, including model systems and food products (Isaacs et al., 1990; Hunter, 1998a,b; Dukhin et al., 2000; Djerdjev et al., 2003; Kong et al., 2001a–c, 2003). Nevertheless, there are some limitations of the electroacoustic technique for certain applications. For example, the droplets must have an electrical charge, there must be a significant density contrast between the droplets and the surrounding liquid, and the viscosity of the continuous phase must be known at the measurement frequency (which is not always the same as that measured in a conventional viscometer).

## 11.4 Disperse phase volume fraction

### 11.4.1 Proximate analysis

The concentration of droplets in an emulsion can be determined using many of the proximate analysis methods developed to determine the composition of foods (Pomeranz and Meloan, 1994; Nielsen, 2003). A variety of *solvent extraction* techniques are available for measuring fat content, for example, continuous, semicontinuous, and discontinuous methods (Pal, 1994; Min and Boff, 2003). The sample to be analyzed is usually dried, ground, and mixed with a nonpolar organic solvent that extracts the oil. The solvent is then physically separated from the remainder of the food, and the oil content is determined by evaporating the solvent and weighing the residual oil. The lipid content of oil-in-water

emulsions can also be determined using *nonsolvent extraction techniques* developed to measure the fat content of dairy emulsions. In the *Gerber* and *Babcock* methods, an emulsion is placed in a specially designed bottle and then mixed with sulfuric acid, which digests the interfacial membrane surrounding the droplets and thus causes coalescence (Min and Boff, 2003). The bottle is centrifuged to facilitate the separation of the oil and aqueous phases, and the percentage of oil in the emulsion is determined from the calibrated neck of the bottle. A similar procedure is involved in the *Detergent* method, except that a surfactant is added to promote droplet coalescence, rather than sulfuric acid. In some circumstances it is important to know the types of lipids present in a food emulsion, as well as the overall fat content. Information about lipid type can be obtained using a number of different analytical techniques, including physical, chemical, chromatographic, and spectroscopy methods (Pike, 2003).

The water content of an emulsion can also be determined using a variety of proximate analysis techniques (Pomeranz and Meloan, 1994; Bradley, 2003). The simplest of these involves weighing an emulsion before and after the water has been evaporated, which may be achieved by conventional oven, vacuum oven, microwave oven, or infrared light. The moisture content of food emulsions could also be determined by distillation procedures. The emulsion is placed in a specially designed flask that has a calibrated sidearm. An organic solvent is mixed with the emulsion, and the flask is heated to cause the water to evaporate and collect in the sidearm. This procedure is continued until all of the water has evaporated and then its volume is determined from the calibrations on the sidearm. The water content of emulsions containing relatively low moisture contents can be conveniently determined using chemical methods, such as the Karl-Fischer titration.

Many of these techniques are labor intensive, time-consuming, and destructive, and so are unsuitable for rapid quality assurance tests. For this reason, analytical instruments based on physical or spectroscopic methods are becoming increasingly popular for rapid and nondestructive analysis of food composition, for example, electrical, density, infrared, and x-ray techniques (Pike, 2003; Bradley, 2003,). Infrared techniques are particularly powerful because they are capable of simultaneously determining the concentration of fat, water, protein, and carbohydrate in a food once they have been properly calibrated (Wilson, 1995; Wehling, 2003).

## 11.4.2 Density measurements

### 11.4.2.1 Principles

One of the simplest methods of determining the disperse phase volume fraction of an emulsion is to measure its density (Pal, 1994). The density of an emulsion ( $\rho_e$ ) is related to the densities of the continuous ( $\rho_1$ ) and dispersed phases ( $\rho_2$ ):  $\rho_e = \phi\rho_2 + (1 - \phi)\rho_1$ . The disperse phase volume fraction of an emulsion can therefore be determined by measuring its density, and knowing the density of the oil and aqueous phases:

$$\phi = \frac{\rho_e - \rho_1}{\rho_2 - \rho_1} \quad (11.13)$$

The densities of the dispersed and continuous phases in a food emulsion are appreciably different, being about  $900 \text{ kg m}^{-3}$  for liquid oils and about  $1000 \text{ kg m}^{-3}$  for aqueous phases. It is relatively simple to measure the density of an emulsion to better than  $0.2 \text{ kg m}^{-3}$ , and so the dispersed phase volume fraction can be determined to better than 0.002 (0.2 vol%) using this technique. The fact that the density of liquid oils is lower than that of water means that the density of an emulsion usually decreases with increasing oil content (Figure 11.19).

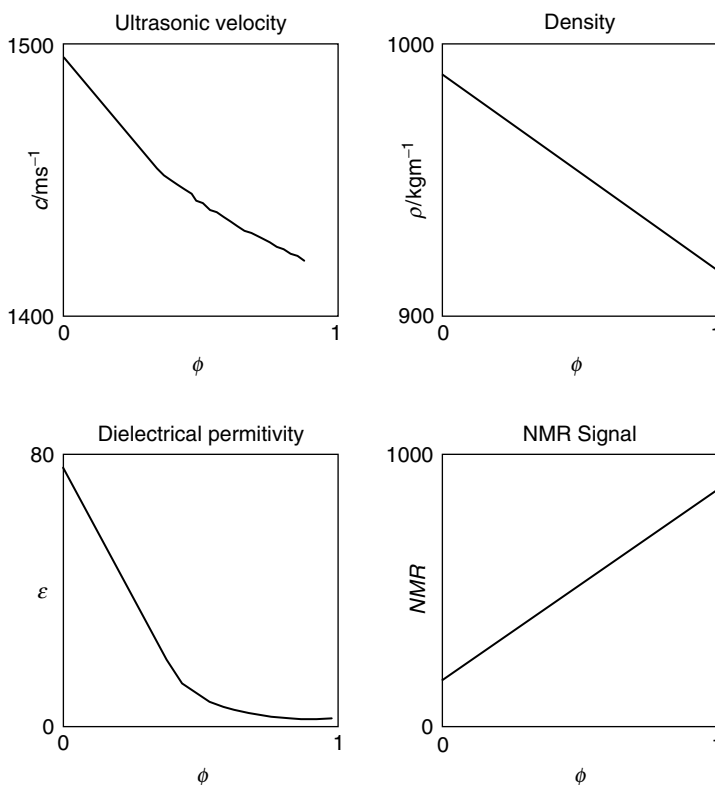


**Figure 11.19** Dependence of various physicochemical properties of oil-in-water emulsions on their disperse phase volume fraction.

#### 11.4.2.2 Measurement Techniques

**11.4.2.2.1 Density bottles.** A liquid sample is poured into a glass bottle of known mass and volume (Pomeran and Meloan, 1994). The bottle and liquid are allowed to equilibrate to the measurement temperature and then weighed using an accurate balance. The mass of emulsion ( $m_{\text{emulsion}}$ ) required to completely fill the container at a given temperature is measured. The internal volume of the container is determined by measuring the mass of distilled water, a material whose density is known accurately, it takes to fill the bottle ( $V_{\text{bottle}} = m_{\text{water}}/\rho_{\text{water}}$ ). Thus, the density of the emulsion can be determined:  $\rho_{\text{emulsion}} = m_{\text{emulsion}}/V_{\text{bottle}}$ . The density of an emulsion is particularly sensitive to temperature, and so it is important to carefully control the temperature when accurate measurements are required. It is also important to ensure that the container is clean and dry prior to weighing, and that it contains no gas bubbles. Gas bubbles reduce the volume of liquid in the bottle without contributing to the mass, and therefore lead to an underestimate of the sample density.

**11.4.2.2.2 Hydrometers.** Several methods for measuring the density of liquids are based on Archimedes principle, which states that the upward buoyant force exerted on a body immersed in a liquid is equal to the weight of the displaced liquid (Pomeran and Meloan, 1994; Bradley, 2003). This principle is used in *hydrometers*, which are graduated hollow glass bodies that float on the liquid to be tested. The depth that the hydrometer sinks into a liquid depends on the density of the liquid. The hydrometer sinks to a point



where the mass of the displaced liquid is equal to the mass of the hydrometer. Thus, the depth to which a hydrometer sinks increases as the density of the liquid decreases. The density of a liquid is usually read directly from graduated calibrations on the neck of the hydrometer. Hydrometers are less accurate than density bottles, but much more rapid and convenient to use.

**11.4.2.2.3 Oscillating U-tubes.** The density of fluids can be measured rapidly and accurately using an instrument called an *oscillating U-tube densitometer* (Pal, 1994). The sample to be analyzed is placed in a glass U-tube, which is forced to oscillate sinusoidally by the application of an alternating mechanical force. The resonant frequency of the U-tube is related to its overall mass, and therefore depends on the density of the material contained within it. The density of a fluid is determined by measuring the resonant frequency of the U-tube and relating it to the density using an appropriate mathematical equation. The instrument must be calibrated with two fluids of accurately known density (usually distilled water and air). Density can be measured to better than  $0.1 \text{ kg m}^{-3}$  in a few minutes using this technique. Recently, on-line versions of this technique have been developed for monitoring the density of fluids during processing. A small portion of a fluid flowing through a pipe is directed through an oscillating U-tube and its density is measured before being redirected into the main flow. Despite being capable of rapid and precise measurements, one must be careful when using oscillating U-tubes to determine the density of emulsions because the density of particulate suspensions depends on the measurement frequency. Thus, the density determined in an oscillating U-tube may not agree with that determined under static conditions, for example, using a density bottle.

### 11.4.2.3 Applications

An accurate measurement of emulsion density can be carried out using inexpensive equipment that is available in many laboratories. The technique is nondestructive and can be used to analyze emulsions that are concentrated and optically opaque. One possible problem of the technique is that the physical state of the emulsion constituents may influence the accuracy of a measurement. For example, the density of solid fat is greater than that of liquid oil, and therefore the density of an emulsion depends on the solid fat content, as well as the total fat content. In these situations, it is necessary to heat the emulsion to a temperature where it is known that all of the fat crystals have melted and then measure its density. The technique may also have limited application in multicomponent emulsions where the composition (and therefore density) of the aqueous phase changes considerably, for example, proteins, carbohydrates, and minerals all cause an appreciable increase in the density of the aqueous phase.

## 11.4.3 Electrical conductivity

### 11.4.3.1 Principles

The disperse phase volume fraction of an emulsion can be conveniently determined by measuring its electrical conductivity,  $\epsilon$  (Clausse, 1983; Robin et al., 1994; Asami, 1995). The electrical conductivity of water is much higher than that of oil, and so there is a decrease in  $\epsilon$  as the oil content of an emulsion increases (Figure 11.19). In dilute emulsions, the disperse phase volume fraction is related to the electrical conductivity by the following equation (Clausse, 1983):

$$\phi = \left( \frac{\epsilon_e - \epsilon_1}{\epsilon_e + 2\epsilon_1} \right) \left( \frac{\epsilon_2 + 2\epsilon_1}{\epsilon_2 - \epsilon_1} \right) \quad (11.14)$$

where the subscripts 1, 2, and  $e$  refer to the continuous phase, dispersed phase, and emulsion, respectively. More complex expressions have been derived to relate the disperse phase volume fraction of concentrated emulsions to their electrical properties.

#### 11.4.3.2 *Measurement techniques*

The electrical conductivity of an emulsion can simply be determined using a conductivity cell (Siano, 1998). This cell consists of a couple of electrodes that are connected to electrical circuitry that is capable of measuring the electrical conductivity of the sample contained between the electrodes. The electrical conductivity of an aqueous phase depends on the concentration of electrolytes present, and so it is important to properly characterize the electrical properties of the component phases.

#### 11.4.3.3 *Applications*

The electrical conductivity technique can be used to determine the disperse phase volume fraction of concentrated and optically opaque emulsions without the need of any sample preparation. Measurements are independent of the size of the emulsion droplets, which is an advantage when the droplet size distribution is unknown (Robin et al., 1994). The electrical conductivity of an emulsion is dependent on the physical state of its constituents, and therefore it may be necessary to heat an emulsion to a temperature where all of the crystals have melted before making a measurement. The electrical conductivity is also sensitive to the ionic strength of the aqueous phase, and therefore it is necessary to take this into account when carrying out the analysis (Skodvin et al., 1994).

### 11.4.4 *Alternative techniques*

The disperse phase volume fraction can be measured using many of the techniques used to determine droplet size distributions (Section 11.3). Light scattering and electrical pulse counting techniques can be used to determine disperse phase volume fractions in dilute emulsions ( $\phi < 0.1\%$ ), whereas DSS, DWS, ultrasonic, electroacoustic, dielectric, neutron scattering, and NMR techniques can be used to analyze much more concentrated emulsions. All of these techniques rely on their being a measurable change in some physicochemical property of an emulsion as its droplet concentration increases, for example, the intensity of scattered or transmitted light; the attenuation or velocity of an ultrasonic wave; the amplitude or decay time of an NMR signal (Figure 11.19). Some of these techniques can be used to simultaneously determine the droplet size distribution and disperse phase volume fraction, whereas others can be used to determine  $\phi$  independently of knowledge of the droplet size. The disperse phase volume fraction of food emulsions can also be determined using physical and spectroscopic methods developed for general analysis of food composition, for example, x-rays or infrared (Bradley, 2003; Min and Boff, 2003).

## 11.5 *Droplet crystallinity*

### 11.5.1 *Dilatometry*

#### 11.5.1.1 *Principles*

Dilatometry has been used for many years to monitor the crystallinity of both dispersed and continuous phases of emulsions (Turnbull and Cormia, 1961; Skoda and van den Tempel, 1963; Phipps, 1964). The technique is based on measurements of the density change that occurs when a material melts or crystallizes. The density of the solid state of a material is usually greater than that of the liquid state because the molecules are able

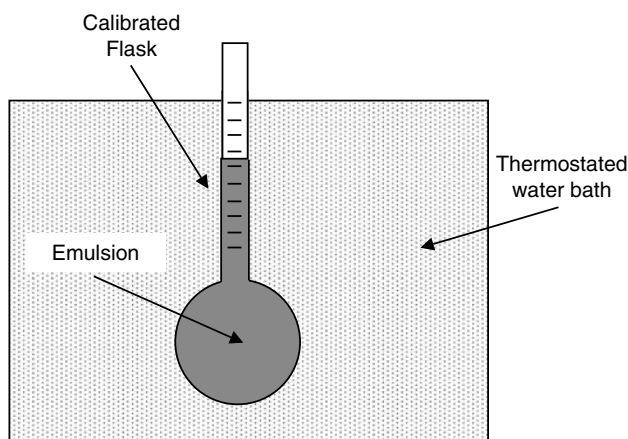


**Figure 11.20** Schematic diagram of a simple dilatometer used for monitoring phase transitions of materials.

to pack more efficiently.\* Consequently, there is a decrease in the density of a material when it melts and an increase when it crystallizes. The fraction of crystalline droplets in an emulsion can therefore be determined using the following equation:

$$\phi_c = \frac{\rho_e - \rho_{eL}}{\rho_{eS} - \rho_{eL}} \quad (11.15)$$

where  $\rho_e$  is the density of an emulsion containing partially crystalline droplets, and  $\rho_{eL}$  and  $\rho_{eS}$  are the densities of the same emulsion when the droplets are either completely liquid or completely solid, respectively. The values of  $\rho_{eL}$  and  $\rho_{eS}$  are usually determined by extrapolating density measurements from higher and lower temperatures into the region where the droplets are partially crystalline.

#### 11.5.1.2 Measurement techniques

In principle, dilatometry can be carried out using any experimental technique that is capable of measuring density (see Section 11.4). In practice, dilatometry is often performed using a specially designed piece of apparatus (Figure 11.20). A known mass of sample is placed into a glass bulb that is connected to a calibrated capillary tube. A liquid, such as mercury or colored water, is poured into the capillary tube above the fat. The change in volume of the sample when it crystallizes or melts is then determined by observing the change in height of the liquid in the capillary tube. These measurements can either be carried out as the temperature of the sample is varied in a controlled way, or as the sample is held at a constant temperature over time (Turnbull and Cormia, 1961). The data can be presented as a volume change or as a density change, depending on which is the most convenient.

#### 11.5.1.3 Applications

The temperature dependence of the density of an oil-in-water emulsion containing droplets that undergo a phase transition is shown in Figure 11.21. When the emulsion is heated from a temperature where the droplets are initially completely solid there is a sharp decrease in density when the droplets begin to melt. Conversely, when an emulsion is cooled from a

\* With the important exception of water near its freezing point.

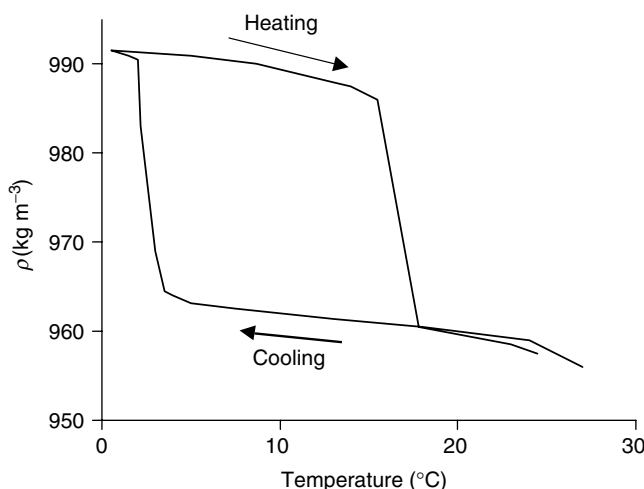


**Figure 11.21** Temperature dependence of the density of a hexadecane oil-in-water emulsion. For food oils, melting and crystallization normally occur over a wider range of temperatures than shown here.

temperature where the droplets are initially completely liquid there is a sharp increase in density when the droplets begin to crystallize. The crystallization temperature is considerably lower than the melting temperature because of supercooling effects (Section 4.2.3). In food emulsions, oil droplets normally melt over a much wider temperature range than that shown for a pure oil in Figure 11.21 because they contain a mixture of different triacylglycerols, each with its own melting point.

## 11.5.2 Nuclear magnetic resonance

### 11.5.2.1 Principles

Nuclear magnetic resonance has been used to measure the solid content of food emulsions for many years (Walstra and van Beresteyn, 1975, van Boekel, 1981; Dickinson and McClements, 1995). NMR instruments are capable of rapidly analyzing emulsions that are concentrated and optically opaque, without the need for any sample preparation. For this reason, they have largely replaced the more cumbersome and time-consuming dilatometry method in laboratories that can afford the relatively high initial cost of an NMR instrument. The NMR technique uses interactions between radio waves and the nuclei of hydrogen atoms to obtain information about the solid content of a material. The fundamental principles of this application have been described elsewhere (Dickinson and McClements, 1995), and so only a simplified description of the technique will be given here. Basically, a radio frequency pulse is applied to an emulsion, which causes some of the hydrogen nuclei to move into an excited state leading to the generation of a detectable NMR signal. The frequency, amplitude and decay time of this signal depends on the ratio of solid-to-liquid material in the sample. Thus, by analyzing the characteristics of the NMR signal it is possible to obtain information about the solid content of the material.

### 11.5.2.2 Measurement techniques

A variety of NMR instruments are commercially available that can be used to measure the solid content of emulsions. These instruments vary in their operating principles, the types of information they are capable of providing, and their cost. The more sophisticated instruments can measure a large number of different physicochemical characteristics of emulsions, but

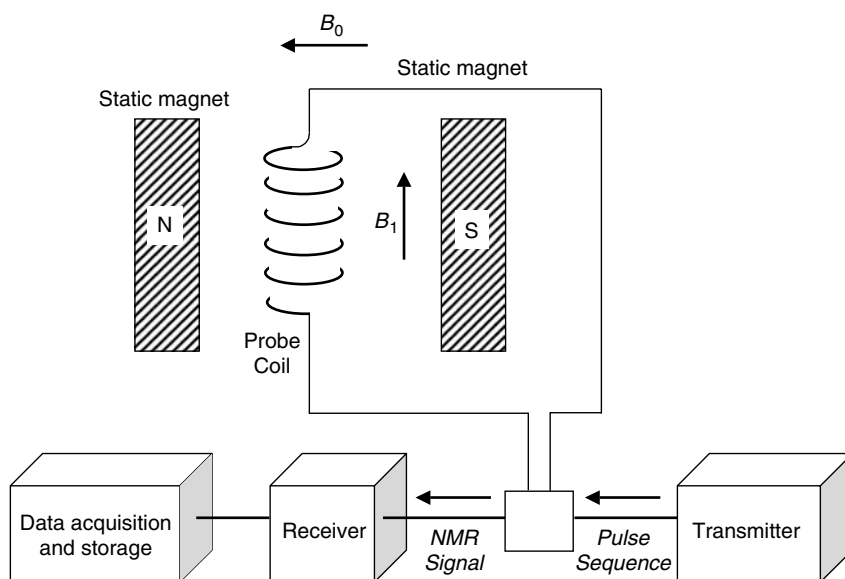


**Figure 11.22** Example of an experimental arrangement for making NMR measurements of the solid content of emulsions.

they are often very expensive and require highly trained operators, so their application is restricted to a small number of research laboratories. A number of less sophisticated instruments are available that have a more limited range of applications, but which are considerably less expensive and easier to use. These instruments are the most widely used to determine the solid content of foods and therefore only they will be considered here.

A typical pulsed NMR instrument consists of a *static magnet*, a *probe coil*, *electronics* to generate and receive electromagnetic pulses, and a *computer* to regulate the measurement procedure and to analyze and store the data (Figure 11.22). Nuclei in the sample are excited to a higher energy level by applying a radio frequency pulse via the probe coil, and the excited nuclei are detected by the same coil once the radio frequency pulse is removed. The detected signal is digitized by a digital-to-analog converter and stored in the computer for data analysis. The solid content is determined by analyzing the decay rate of the detected signal after the application of the radio frequency pulse.

The decay of the NMR signal is much more rapid for a solid than a liquid (Figure 11.23). Consequently, the solid and liquid phases in a sample can be differentiated by measuring the decay of the NMR signal with time. Immediately after the radio frequency pulse is switched off, the NMR signal ( $S_0$ ) is proportional to the total number of nuclei in the liquid and solid phases. After a certain time, the contribution from the solid phase has completely decayed, and the signal ( $S_t$ ) is then proportional to the number of nuclei in the liquid phase. Assuming that the NMR signal per gram of the solid and liquid phases is similar, the solid content can simply be determined:  $\phi_c = (S_0 - S_t)/S_0$ . In practice, it is not possible to measure the signal at zero time because the NMR receiver takes a short time to recover after the radio frequency pulse is applied. Consequently, it is necessary to use a correction factor that accounts for the slight decay of the signal before the first measurement is made. The solid content can also be determined by only making measurements of the signal from the liquid phase, since  $S_t$  is proportional to the mass of liquid phase present,  $M_L$ . The mass of liquid in a sample is deduced by measuring  $S_t$  and using a previously prepared calibration curve of  $M_L$  versus  $S_t$ . If the total mass of the

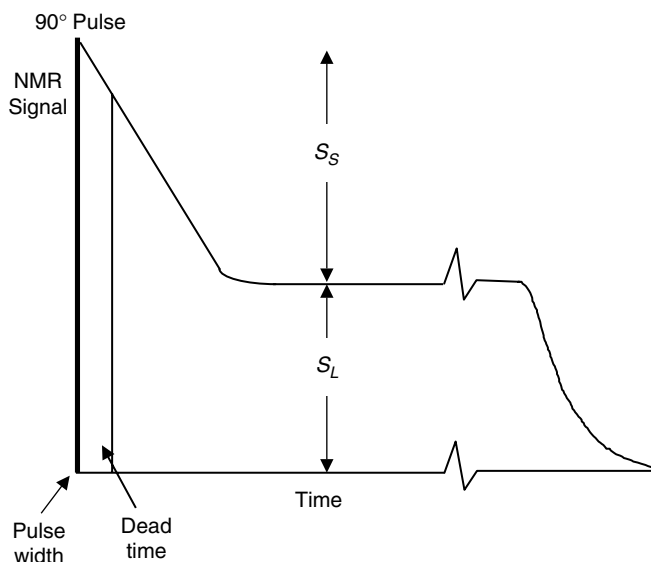


**Figure 11.23** Decay of NMR signal after the application of an NMR pulse is much more rapid for solid than liquid fat.

sample analyzed,  $M_T$  is known, then  $\phi_c = (M_T - M_L)/M_T$ . The solid content can also be determined by measuring  $S_t$  for a partially crystalline sample, and then heating it to a temperature where all of the solid phase melts and measuring it again:  $\phi_c = (S'_t - S_t)/S'_t$ , where the prime refers to the measurement at the higher temperature. This value has to be corrected to take into account the temperature dependence of the NMR signal of the liquid phase.

### 11.5.2.3 Applications

Nuclear magnetic resonance has been used to determine the extent of droplet crystallization in emulsions in a number of fundamental studies and commercial products (Walstra and van Beresteyn, 1975; Waddington, 1980; van Boekel, 1981; Dickinson and McClements, 1995; Le Botlan et al., 2000). Bench top instruments are available that are extremely simple and rapid to use. A tube containing the sample is placed in the NMR instrument and the solid content is given out in a few minutes or less. The technique is therefore particularly useful for quality control purposes where many samples have to be rapidly analyzed. Attempts have been made to develop on-line versions of these NMR instruments, but their application is limited because the sample cannot be analyzed within a metal pipe because of its distorting influence on the magnetic field. An additional limitation is that the technique cannot be used to accurately determine the solid contents when the degree of crystallization is small (<5%).

Before leaving this section it should be noted that there are a variety of other NMR techniques that can also be used to determine droplet solid contents (Dickinson and McClements, 1995; Yan et al., 1996; Divakar, 1998). The most powerful of these is *NMR imaging*, which can be used to determine the solid content at any location within a material, so that it is possible to obtain a three-dimensional image of the droplet crystallinity (Simoneau et al., 1991, 1993; Yan et al., 1996). These imaging techniques provide food scientists with an extremely powerful method of monitoring and predicting the long-term stability of food emulsions. Nevertheless, these techniques are extremely expensive and

require highly skilled operators, and so are currently only available to a small number of research laboratories.

### 11.5.3 Thermal analysis

#### 11.5.3.1 Principles

Differential scanning calorimetry (DSC) and differential thermal analysis (DTA) are two thermal analysis techniques that can be used to monitor melting and crystallization of emulsion droplets (Walstra and van Berysteyn, 1975; McClements et al., 1993a; Clausse, 1998; Palanuwech and Coupland, 2003). These techniques are based on measurements of the heat released or adsorbed by a sample when it is subjected to a controlled temperature program. A material tends to release heat when it crystallizes and absorb heat when it melts. The major difference between the two techniques is the method used to measure the heat adsorbed or released by the sample.

#### 11.5.3.2 Measurement techniques

**11.5.3.2.1 Differential scanning calorimetry.** DSC records the *energy* necessary to establish a zero temperature difference between a sample and a reference material that are either heated or cooled at a controlled rate (Schenz, 2003). Thermocouples constantly measure the temperature of each pan and two heaters below the pans supply heat to one or other of the pans so that they both have exactly the same temperature (Figure 11.24).

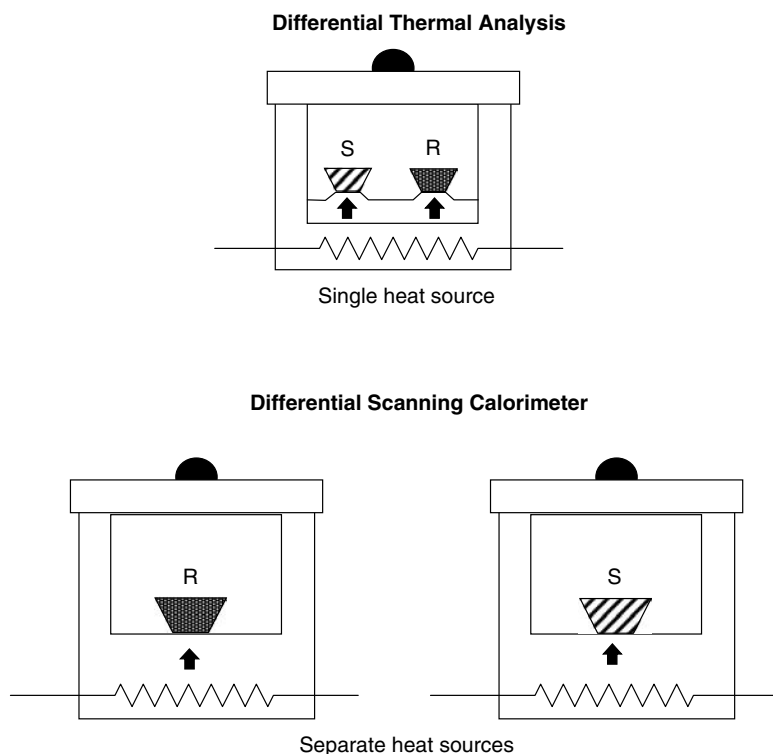


**Figure 11.24** DTA and DSC instruments provide information about phase transitions in emulsions by measuring the heat released or adsorbed when the sample is subjected to a controlled temperature program.

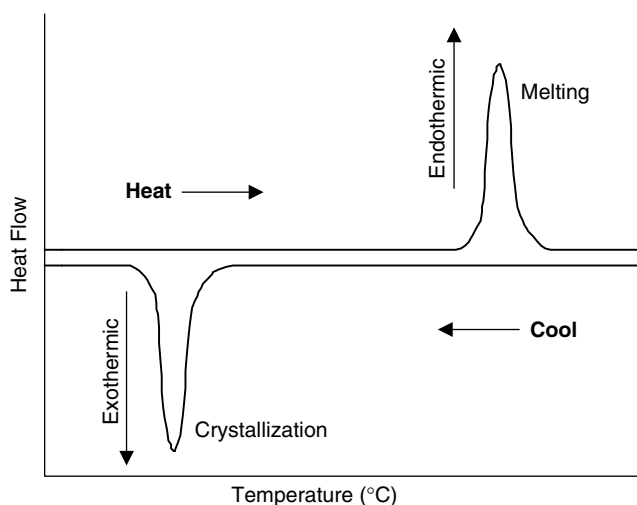


**Figure 11.25** Thermal analysis of the melting and crystallization of oil droplets in an oil-in-water emulsion using calorimetry.

If a sample were to undergo a phase transition it would either absorb or release heat. To keep the temperature of the two pans the same an equivalent amount of energy must be supplied to either the test or reference cells. Special electrical circuitry is used to determine the amount of energy needed to keep the two sample pans at the same temperature. DSC data are therefore reported as the rate of energy absorption ( $Q$ ) by the sample relative to the reference material as a function of temperature (Figure 11.25).

**11.5.3.2.2 Differential thermal analysis.** DTA records the difference in *temperature* between a substance and a reference material when they are heated or cooled at a controlled rate (Schenz, 2003). A DTA instrument consists of two sample holders that are contained within an environment whose temperature can be varied in a controlled fashion (Figure 11.24). A few milligrams of sample are accurately weighed into a small aluminum pan and placed into one of the sample holders. A reference, usually an empty aluminum pan or a pan containing a material that does not undergo a phase transition over the temperature range studied, is placed into the other sample holder. The sample and reference pans are then heated or cooled together at a controlled rate. The difference in temperature,  $\Delta T$ , between the two pans is recorded by thermocouples located below each of the pans. The output from the instrument is therefore a plot of  $\Delta T$  versus  $T$ . If the sample *absorbs* heat (an endothermic process) then it will have a slightly *lower* temperature than the reference, but if it *releases* heat (an exothermic process) it will have a slightly *higher* temperature. Thus, measurements of the difference in temperature between the sample and reference pans can be used to provide information about physical and chemical changes that occur in the sample.

### 11.5.3.3 Applications

Thermal analysis can be used to determine the temperature range of a phase transition, as well as the amount of material involved in a phase transition (Figure 11.25). When an emulsion containing solid droplets is heated above the melting point of the dispersed phase the droplets melt and an endothermic peak is observed. The melting temperature can therefore be ascertained by measuring the position of the peak. The area under the peak is proportional to the amount of material that undergoes the phase transition:  $A = k \Delta H_f m$ ,



where  $\Delta H_f$  is the heat of fusion per gram,  $m$  is the mass of material undergoing the phase transition in grams, and  $k$  is a constant that depends on the instrumental settings used to make the measurement. The value of  $k$  is determined by measuring the peak areas of a series of samples of known mass and heat of fusion. Thus, the mass of material that melts can be determined by measuring the peak area. When an emulsion containing liquid droplets is cooled an exothermic peak is observed when the droplets crystallize. The crystallization temperature and the amount of material that has crystallized can be determined in the same way as for the melting curve. As mentioned earlier, the droplets tend to crystallize at a much lower temperature than they melt because of supercooling effects (Section 4.2.3). In addition, the melting range of edible fats is much wider than that shown in Figure 11.25 because they contain a mixture of triacylglycerols, each with a different melting point.

Thermal analysis has been used to monitor the influence of oil type, emulsifier type, cooling rates, catalytic impurities, polymorphic changes, and droplet size on the nucleation and crystallization of droplets in oil-in-water emulsions (McClements et al., 1993a; Dickinson and McClements, 1995; Clausse, 1998; Vanapalli et al., 2002a,b). It has also been used to study the factors that influence the melting and crystallization of water droplets in water-in-oil emulsions (Clausse, 1985, 1998), and to study phase transitions in the continuous phase of emulsions (Palanuwech and Coupland, 2003). DSC techniques have also been used to monitor changes in emulsion droplet composition brought about by compositional ripening processes, since the melting/crystallization behavior of a material is strongly correlated to its composition (Dickinson and McClements, 1995; Clausse, 1998; Clausse et al., 2002). Thermal analysis has proved particularly useful for monitoring the stability of emulsion droplets to coalescence when either the fat and/or water phases crystallizes (Vanapalli et al., 2002a,b; Palanuwech and Coupland, 2003).

## 11.5.4 Ultrasonics

### 11.5.4.1 Principles

The ultrasonic properties of a material change significantly when it melts or crystallizes, and so ultrasound can be used to monitor phase transitions in emulsions (Dickinson et al., 1990, 1991; McClements, 1991, 1997; Coupland and McClements, 2004). The temperature dependence of the ultrasonic velocity of an oil-in-water emulsion in which the droplets crystallize is shown in Figure 11.26. When an emulsion is cooled from a temperature where the droplets are initially liquid to a temperature where the droplets begin to crystallize there is a steep increase in ultrasonic velocity, because the ultrasonic velocity is larger in solid fat than in liquid oil. Conversely, when an emulsion is cooled from a temperature where the droplets are initially solid to a temperature where the droplets begin to melt there is a steep decrease in ultrasonic velocity. The droplets crystallize at a temperature that is much lower than the melting point of the bulk oil because of supercooling effects (Section 4.2.3).

To a first approximation, the fraction of crystalline material ( $\phi_c$ ) in an emulsion can be determined using the following equation (Dickinson et al., 1991):

$$\phi_c = \left( \frac{1}{c_e^2} - \frac{1}{c_{eL}^2} \right) \left( \frac{1}{c_{eS}^2} - \frac{1}{c_{eL}^2} \right)^{-1} \quad (11.16)$$

where  $c_{eL}$  and  $c_{eS}$  are the ultrasonic velocities in the emulsion if all the droplets were either completely liquid or completely solid, respectively. These values are determined

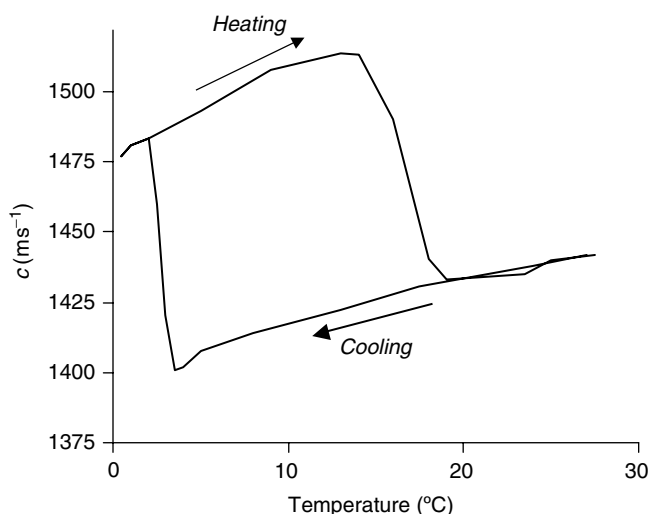


**Figure 11.26** Crystallization and melting of oil droplets in an emulsion can be monitored by ultrasonic velocity measurements.

by extrapolating measurements from higher and lower temperatures into the region where the fat is partially crystalline, or by using ultrasonic scattering theory to calculate their values (Dickinson et al., 1991).

#### 11.5.4.2 Measurement techniques

The ultrasonic properties of an emulsion can be measured using the same techniques as used for determining the droplet size distribution by ultrasonic spectrometry (Section 11.3.6). The measurements are usually carried out in one of two ways: isothermal or temperature scanning. In an isothermal experiment the temperature of the emulsion is kept constant and the change in the ultrasonic velocity is measured as a function of time. In a temperature scanning experiment the ultrasonic velocity is measured as the temperature is increased or decreased at a controlled rate.

#### 11.5.4.3 Applications

The solid contents determined using ultrasound are in good agreement with those determined using traditional techniques such as dilatometry (Hussin and Povey, 1984) and NMR (McClements and Povey, 1987; Singh et al., 2002). Ultrasound has been used to monitor phase transitions in nonfood oil-in-water emulsions (McClements et al., 1991; Dickinson et al., 1990), triglyceride oil-in-water and water-in-oil emulsions (McClements, 1989; Coupland et al., 1993; Hodate et al., 1997; Kashchiev et al., 1998; Awad et al., 2001; Awad and Sato, 2001, 2002), margarine and butter (McClements, 1989), shortening and meat (Miles et al., 1985), and various triglyceride/oil mixtures (McClements and Povey, 1988; Singh et al., 2002).

It should be noted that in some systems large increases in the attenuation coefficient and appreciable velocity dispersion have been observed during melting and crystallization because of a relaxation mechanism associated with the solid-liquid phase equilibrium (McClements et al., 1993f). The ultrasonic wave causes periodic fluctuations in the temperature and pressure of the material that perturb the phase equilibrium. When a significant

proportion of the material is at equilibrium a large amount of ultrasonic energy is absorbed due to this process. This effect depends on the ultrasonic frequency, the relaxation time for the phase equilibrium, and the amount of material undergoing phase equilibrium, and can cause large deviations in both the ultrasonic velocity and attenuation coefficient. In systems where this phenomenon is important it is not possible to use Equation 11.16 to interpret the data. Nevertheless, it may be possible to use ultrasound to obtain valuable information about the dynamics of the phase equilibrium.

## 11.6 Droplet charge

### 11.6.1 Particle electrophoresis

In this technique, a sample of the emulsion to be analyzed is placed into a measurement cell and a static electrical field  $E$  is applied across it via a pair of electrodes (Figure 11.27). This causes any charged emulsion droplets to move toward the oppositely charged electrode (Hunter, 1986, 1993). The sign of the charge on the emulsion droplets can therefore be deduced from the direction that they move. When an electrical field is applied across an emulsion the droplets accelerate until they reach a constant velocity,  $v$ , where the electrical pulling force is exactly balanced by the viscous drag force exerted by the surrounding liquid. This velocity depends on the size and charge of the emulsion droplets, and its measurement can therefore be used to provide information about these parameters. Experimentally, particle velocity is determined by measuring the distance that they move in a known time, or the time taken for them to move a known distance. Droplet motion can be monitored using a number of different experimental methods. The movement of relatively large particles ( $>1\ \mu\text{m}$ ) can be monitored by optical microscopy or static light scattering, whereas the movement of smaller particles can be monitored by an ultramicroscope, static light scattering, or dynamic light scattering.

Mathematical expressions have been derived to relate the movement of a droplet in an electric field to its electrical charge ( $\zeta$ -potential) (Hunter, 1986). These expressions are based on a theoretical consideration of the forces that act on a particle when it has reached constant velocity, that is, the electrical pulling force is balanced by the viscous drag force. The mathematical theory that describes this process depends on the droplet size and charge, the thickness of the Debye layer, the viscosity of the surrounding liquid, and the strength of the applied electric field. The general solution of this theory leads to a complicated expression

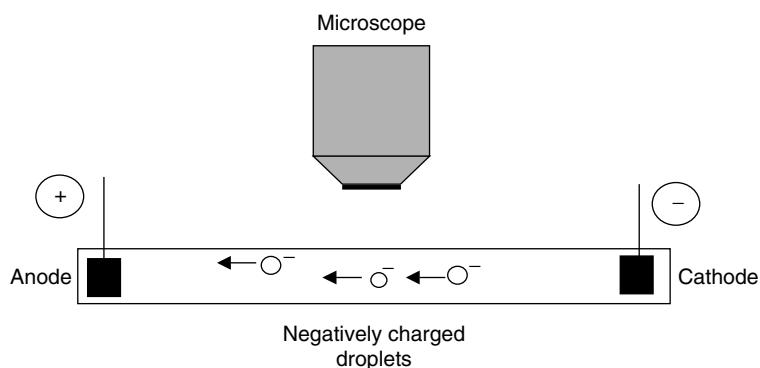


**Figure 11.27** Example of an electrophoretic mobility cell that can be used to measure the  $\zeta$ -potential of emulsion droplets.

that relates all of these parameters. Nevertheless, under certain experimental circumstances, it is possible to derive simpler expressions:

$$\xi = \frac{3\eta u}{2\epsilon_0\epsilon_R}, \quad \kappa r \ll 1 \quad (11.17)$$

$$\xi = \frac{\eta u}{\epsilon_0\epsilon_R}, \quad \kappa r \gg 1 \quad (11.18)$$

where  $\eta$  is the viscosity of the surrounding liquid,  $u$  is the electrophoretic mobility (= particle velocity divided by electric field strength),  $\epsilon_0$  is the dielectric constant of a vacuum, and  $\epsilon_R$  is the relative dielectric constant of the material. In practice, the latter equation is the most applicable to emulsions, because the droplet size is usually much greater than the Debye length,  $\kappa^{-1}$ . In some systems the droplet size is comparable to the Debye length and so is necessary to solve the full theory, rather than use one of the above expressions.

In commercial instruments, the particle velocity is often determined automatically using sophisticated light scattering techniques (Hunter, 1986). For example, two coherent beams of light are made to intersect with each other at a particular position within a measurement cell so that they form an interference pattern that consists of regions of low and high light intensity. The charged emulsion droplets are made to move through the interference pattern by applying an electrical field across the cell. As the droplets move across the interference pattern they scatter light in the bright regions, but not in the dark regions. The faster a droplet moves through the interference pattern, the greater the frequency of the intensity fluctuations. By measuring and analyzing the frequency of these fluctuations it is possible to determine the particle velocity, which can then be mathematically related to the  $\zeta$ -potential. The sign of the charge on the particles is ascertained from the direction that they move in the electric field. It should be noted that some colloidal dispersions contain different kinds of particles with different electrical charges. Many early  $\zeta$ -potential instruments were only capable of measuring some ensemble average of the droplet charge that represented the whole system, whereas many modern instruments are capable of determining the charges of the different types of particles.

Many of the commercial instruments available for measuring the  $\zeta$ -potential of emulsion droplets combine particle electrophoresis measurements with dynamic light scattering measurements so that both the droplet charge and the droplet size distribution (from a few nm to a few  $\mu\text{m}$ ) can be determined using the same instrument. These instruments are particularly powerful tools for predicting the stability and bulk physicochemical properties of food emulsions. A measurement of the influence of pH, ionic strength, or solution composition on the  $\zeta$ -potential of the droplets in an emulsion often provides valuable insights into the major factors that determine the stability of the system. For example, the influence of pH on the  $\zeta$ -potential of a protein ( $\beta$ -lactoglobulin) stabilized emulsion is shown in Figure 11.28. The droplet  $\zeta$ -potential moves from positive at low pH, to zero at the protein isoelectric point (IEP  $\approx 5$ ), to negative at high pH. The magnitude of the droplet charge is relatively low around the IEP and so the emulsion is particularly sensitive to flocculation because the electrostatic repulsion between the droplets is no longer sufficiently strong to overcome the attractive van der Waals interactions (Section 7.5).

Finally, it should be stressed that one must be particularly careful when using particle electrophoresis measurements carried out on diluted emulsions to estimate the  $\zeta$ -potential of the droplets in concentrated emulsions. Emulsion dilution can cause a significant alteration in the  $\zeta$ -potential of emulsion droplets due to the change in pH, ionic strength, and/or composition of the solution surrounding the droplets. Ideally, one should therefore

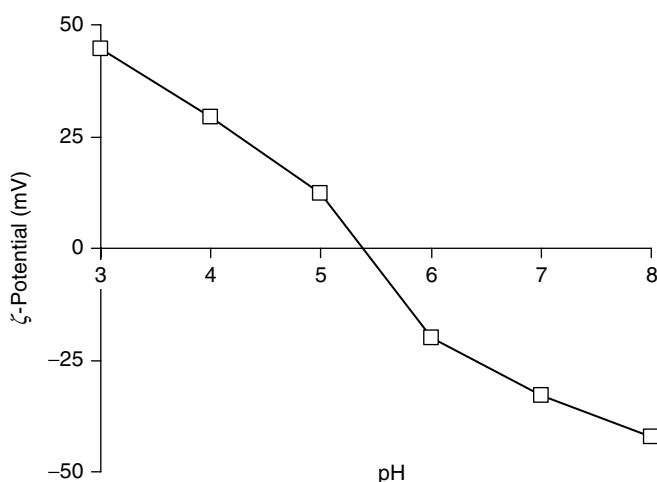


**Figure 11.28** Dependence of the  $\zeta$ -potential of a dilute  $\beta$ -lactoglobulin stabilized oil-in-water emulsion on pH measured using a particle electrophoresis instrument.

dilute an emulsion with its own continuous phase in order to minimize changes in droplet charge. Practically, this can often be achieved by centrifuging an emulsion and collecting the serum phase to use as an emulsion dilutant. Otherwise, one should ensure that the pH and ionic strength of the diluting fluid is similar to that of the continuous phase of the original emulsion. Often it is important to know the surface charge density ( $\sigma$ ) of the emulsion droplets, rather than only the  $\zeta$ -potential. For example, changes in the surface charge density can be used to monitor binding of counterions to emulsion droplets (Kulmyrzaev et al., 2000a,b; Kulmyrzaev and Schubert, 2004). The surface charge density can be calculated from the  $\zeta$ -potential when the ionic strength of the solution surrounding the droplets is known (Hunter, 1986). For example,  $\xi = \sigma / \epsilon_R \epsilon_0 \kappa$ , when the electrostatic attraction between the counterions and the droplet surface is relatively weak (Chapters 3 and 5). Thus, if one wants to estimate the surface charge density of the emulsion droplets from  $\zeta$ -potential measurements one must know or control the ionic strength of the continuous phase.

### 11.6.2 Electroacoustics

Analytical instruments based on electroacoustics are commercially available for measuring the size, concentration, and  $\zeta$ -potential of droplets in emulsions and other colloidal dispersions (Hunter, 1993; O'Brien et al., 1994; Carasso et al., 1995; Dukhin and Goetz, 1996; Kong et al., 2001a-c). Electroacoustic measurements can be carried out in one of two ways: (i) electrosonic amplitude (ESA)—an electric signal is applied to an emulsion and the resulting acoustic signal generated by the oscillating particles is recorded; (ii) colloid vibration potential (CVP)—an acoustic signal is applied to an emulsion and the resulting electric signal generated by the oscillating particles is recorded.

In the ESA method the sample to be analyzed is placed in a measurement cell and an alternating electrical field is applied across it via a pair of electrodes. This causes any charged droplets to rapidly move backward and forward in response to the electrical field (Figure 11.29). An oscillating droplet generates a pressure wave, with the same frequency as the alternating electric field, which emanates from it and can be detected by an ultrasonic transducer. The amplitude of the signal received by the transducer is known as the ESA

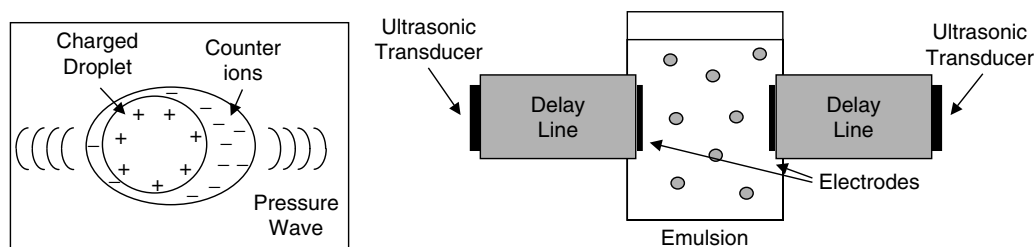


**Figure 11.29** Principles of the electroacoustic technique. In the ESA technique an oscillating electric signal is applied to an emulsion and the resulting acoustic signal generated by the oscillating droplets is recorded.

and is proportional to the dynamic mobility,  $\mu_d$ , of the particles in the suspension. The dynamic mobility of the particles is related to their  $\zeta$ -potential and size:

$$\mu_d = \left( \frac{\varepsilon_0 \varepsilon_R \xi}{\eta} \right) G \left( \frac{\omega r^2 \rho}{\eta} \right) \quad (11.19)$$

here  $\varepsilon_R$  is the relative permittivity of the continuous phase,  $\xi$  is the  $\zeta$ -potential,  $\omega$  is the angular frequency,  $r$  is the droplet radius, and  $\eta$  and  $\rho$  are the viscosity and density of the continuous phase, respectively.  $G$  is a function that varies from 1 at low frequencies to 0 at high frequencies. The frequency dependence of  $G$  is associated with the phase lag between the alternating electrical field and the oscillating pressure wave generated by the particles, which arises because of their inertia. At low frequencies, the particles move in-phase with the electric field, and so the dynamic mobility is equal to the static mobility:  $\mu_d = \varepsilon_0 \varepsilon_R \xi / \eta$  (i.e.,  $G = 1$ ). At extremely high frequencies, the electric field alternates so quickly that the particles have no time to respond and therefore remain stationary. Under these circumstances no ultrasonic pressure wave is generated by the particles (i.e.,  $G = 0$ ). The transition from the low to high frequency regions occurs at a characteristic relaxation frequency  $\omega_R$ , which is related to the size of the particles, decreasing as the size (inertia) of the particles increases. By measuring the frequency dependence of the dynamic mobility it is therefore possible to determine the droplet size. By measuring the dynamic mobility at low frequencies (where it is independent of droplet size) it is possible to determine the  $\zeta$ -potential.

In the CVP method an ultrasonic wave is applied to an emulsion, which causes the droplets to oscillate backward and forward due to the density difference between themselves and the surrounding medium. An oscillating charged particle generates an alternating electric field that can be detected using suitable electrodes. The amplitude of the signal received by the electrodes is called the CVP and it can also be used to determine the size and  $\zeta$ -potential of the emulsion droplets. The major advantage of electroacoustic techniques is that they can be applied to concentrated emulsions ( $\phi \leq 50\%$ ) without the need of any sample dilution. Nevertheless, they can only be used to analyze emulsion droplets that are charged and that have a significant density difference to the surrounding liquid, and therefore they have limited application for some food systems.

The use of electroacoustics for measuring the  $\zeta$ -potential of droplets in concentrated emulsions is illustrated in Figure 11.30. When calcium ions are added to a 20% oil-in-water emulsion stabilized by lecithin they “bind” to the surface of the negatively charged droplets and reduce the  $\zeta$ -potential. Above a certain concentration, they actually cause the sign of the droplet charge to become reversed. At calcium concentrations where the

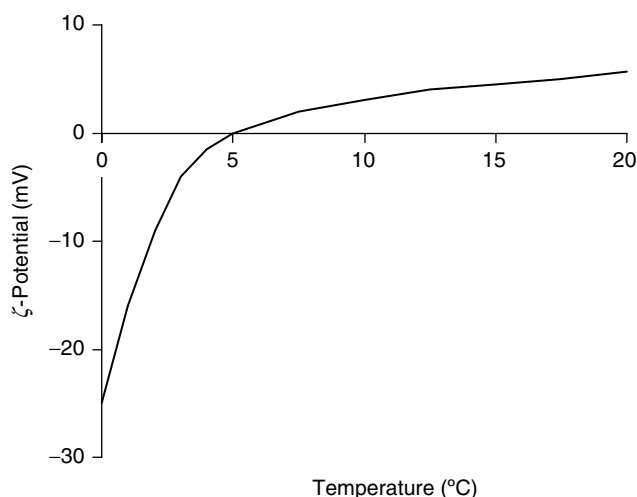


**Figure 11.30** Dependence of the  $\zeta$ -potential of a 20% oil-in-water emulsion on the calcium concentration measured using an electroacoustic technique (Data taken from Colloidal Dynamics Pty Ltd., Application Note 203, Matec Applied Sciences, Hopkinton, MA).

$\zeta$ -potential is low, the electrostatic repulsion between droplets is relatively small, which leads to droplet flocculation (Chapters 3 and 7).

## 11.7 Droplet interactions

The sign, magnitude, and range of the colloidal interactions that operate between the droplets in emulsions largely determine the stability and physicochemical properties of the overall system (Chapters 3 and 7). It is therefore important for researchers to have information about the dominant colloidal interactions operating in a particular emulsion system, and to have knowledge of the factors that influence these interactions. At present there are no commercially available analytical instruments specifically designed to provide information about droplet interactions. Nevertheless, a number of techniques have recently been developed that can be used to provide direct or indirect information about droplet–droplet interactions. Information about the interactions between emulsion droplets can often be inferred from measurements of the force–distance profiles measured between macroscopic surfaces, for example, using surface force apparatus or thin-film studies (Section 3.12). Some of the methods that have been developed to provide information about interactions between actual emulsion droplets are listed below:

1. *Emulsion stability studies.* Sometimes it is possible to estimate the magnitude of certain kinds of droplet–droplet interactions from emulsion stability studies. For example, the minimum amount of salt required to promote droplet flocculation in an electrostatically stabilized emulsion can provide indirect information about the strength of the attractive interactions, for example, van der Waals (Montagne et al., 2003).
2. *Rheology.* Interpretation of measurements of the apparent viscosity of emulsions versus applied shear stress using a suitable mathematical model can provide information about the attractive forces acting between droplets in flocculated emulsions (Quemada and Berli, 2002; Berli et al., 2002).

3. *Atomic force microscopy.* Droplet–droplet interactions can be characterized by directly measuring force versus distance profiles between a droplet attached to a cantilever and a droplet attached to a solid support using AFM (Mulvaney et al., 1996; Gunning et al., 2004).
4. *Magnetic chaining.* When an external magnetic field is applied to an emulsion containing monodisperse paramagnetic oil droplets a magnetic dipole is induced in the droplets, which causes them to align into linear chains parallel to the magnetic field (Dimitrova and Leal-Calderon, 1999). The equilibrium separation of the droplets in these chains occurs at the position where the repulsive colloidal forces equal the attractive magnetic force (which can be calculated using theoretical models). The magnitude of the magnetic force can be varied in a controlled manner by varying the strength of the applied magnetic field. The resulting change in the separation between the droplets in the linear chains can be determined using light scattering techniques. Hence, it is possible to obtain a force versus separation profile that characterizes the droplet–droplet interactions in the system.

Further development of these methods, as well as the introduction of new methods, will provide food scientists with powerful tools for predicting the long-term stability of food emulsions and to systematically elucidate the factors that influence emulsion properties.





## *chapter twelve*

---

# *Food emulsions in practice*

### *12.1 Introduction*

The majority of this book has focused on a discussion of the basic physicochemical principles of emulsion science. In this final chapter, the importance of understanding these principles for improving food emulsion properties is demonstrated through a discussion of a selected number of actual food products that exist as emulsions: dairy emulsions, beverage emulsions, and dressings. These products were chosen because their bulk physicochemical characteristics are governed primarily by the presence of the emulsion droplets, so that their properties can easily be understood in terms of the principles explained in previous chapters.

### *12.2 Milk and cream*

Milk is one of the few food products that exist naturally as an emulsion (Harper and Hall, 1976; Walstra and Jenness, 1984; Jensen, 1995; Bucheim and Dejmek, 1997; Walstra, 1999). In its natural state milk is an oil-in-water (O/W) emulsion that consists of milk fat globules suspended in an aqueous phase that contains a complex mixture of proteins, sugars, and salts. The primary function of milk in nature is to serve as a nutrient delivery system for the infants of mammals. It therefore contains a complex mixture of nutrients vital for the growing infant, for example, proteins, lipids, minerals, and vitamins (Jensen, 1995; Swaisgood, 1996). In modern societies, milk is rarely consumed in its natural state and usually undergoes some form of processing prior to consumption, for example, separation, homogenization, pasteurization, sterilization. Milk may also be processed to create a wide variety of commonly used food products, such as cream, ice cream, yogurt, cheese, and butter (Walstra, 1999).

#### *12.2.1 Composition*

Milk composition varies depending on the mammalian species, genetic variations within a species, age, lactation stage, diet, habitat, climate, storage conditions, and so on (Jensen, 1995; Bucheim and Dejmek, 1997; Walstra, 1999). Nevertheless, the concentrations of the major components in bovine milk tend to fall into certain well-defined ranges. The average composition of bovine milk from Western cattle is given in Table 12.1.

##### *12.2.1.1 Dispersed phase*

The dispersed phase of raw bovine milk typically makes up about 4.1 wt% of the total mass and is comprised predominantly of lipids (Jensen, 1995). The overall lipid fraction of bovine milk consists of about 96–98% triacylglycerols, with the remainder being diacylglycerols,

**Table 12.1** Average Composition of Bovine Milk.

Component	Percentage
Water	86.6
Lactose	5.0
Fat	4.1
Protein	3.6
Ash	0.7

Source: Adapted from Swaisgood (1996).

phospholipids, sterols, free fatty acids, and monoacylglycerols (Swaisgood, 1996). These components are present either in the interior of the droplets or at the oil–water interface depending on their concentration and polarity. Milk fat has an extremely complex triacylglycerol composition, with hundreds of different types identified (Jensen, 1995). The most commonly occurring fatty acids in the triacylglycerol fraction are either saturated (e.g., 14:0, 16:0, and 18:0) or monounsaturated (e.g., 18:1). Milk fat also contains a significant proportion of short-chain saturated fatty acids (e.g., 4:0–12:0). The wide range of melting points exhibited by the different triacylglycerols present in milk means that milk fat melts over a broad range of temperatures, typically from  $-40$  to  $+40^{\circ}\text{C}$  (Bucheim and Dejmek, 1997; Walstra, 1999). The melting and crystallization behavior of milk fat is strongly influenced by emulsification. Emulsified milk fat can be supercooled to a much lower temperature than bulk milk fat because the heterogeneous nuclei normally responsible for initiating nucleation are distributed across such a huge number of isolated droplets (Walstra, 1999). The crystallization of emulsified milk fat promotes emulsion instability in some products due to partial coalescence, for example, creams, whereas in other products it is an essential step in their production, for example, ice cream or whipped cream (Goff, 1997a–c, 2000; Goff et al., 1999). The fat globules also serve as solvents for the oil-soluble vitamins found in milk, such as vitamins A, D, and E (Swaisgood, 1996).

#### 12.2.1.2 Interfacial membrane

The native milk fat globule membrane in raw milk is comprised predominantly of phospholipids and proteins, although various other types of polar lipids and glycoproteins are also present, for example, diacylglycerols, monoacylglycerols, and free fatty acids (Swaisgood, 1996; Bucheim and Dejmek, 1997; Walstra, 1999). The membrane is typically between 8 and 10 nm in thickness (Walstra, 1999). The composition and structure of the native milk fat globule membrane may be changed significantly during processing or storage due to physical rearrangements or chemical reactions of the various protein and lipid components present (Jensen, 1995). When milk is homogenized there is an approximately five- to ten-fold increase in the specific surface area of oil exposed to the aqueous phase. This additional interface is covered predominantly by proteins adsorbed from the aqueous phase, that is, casein and whey proteins (Walstra, 1999). Typically, there is about  $10\text{ mg m}^{-2}$  proteins adsorbed to the droplet surfaces after homogenization, with the vast majority ( $\sim 95\%$ ) being caseins. Electron microscopy studies indicate that this relatively high protein load is due to the adsorption of casein micelles to the droplet surfaces (Bucheim and Dejmek, 1997). The reason for this phenomenon has been attributed to the fact that relatively large particles (such as casein micelles) are adsorbed to droplets surfaces in preference to smaller particles (such as individual whey protein or casein molecules) under the turbulent flow conditions prevailing during homogenization (Walstra, 1993b). This phenomenon can clearly be seen when homogenized O/W emulsions containing casein micelles are viewed by electron microscopy (Figure 12.1). Regions of the droplet

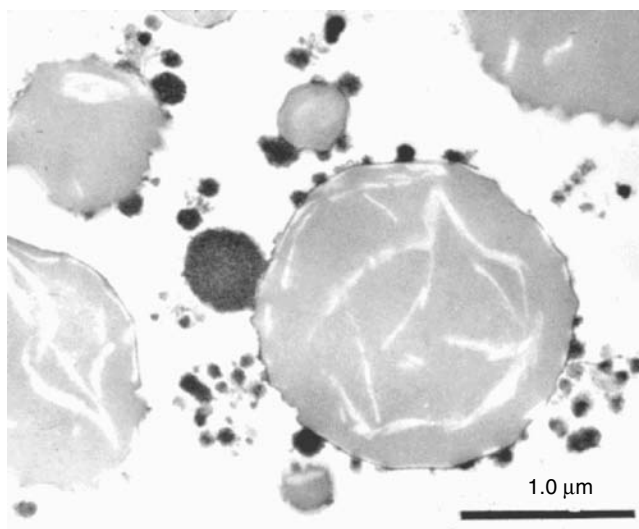


**Figure 12.1** Example of preferential adsorption of casein micelles to fat droplet surfaces. TEM micrograph of homogenized ice cream mix kindly supplied by Prof. Douglas Goff (University of Guelph, Canada).

surface that are covered predominantly by casein micelles tend to have a grainy appearance, whereas those covered by individual casein or whey protein molecules tend to have a smooth appearance (Sharma et al., 1996a,b, Bucheim and Dejmek, 1997; Goff et al., 1999). The composition and structure of the interfacial membrane in homogenized milk may change considerably during storage and processing because of molecular rearrangements or chemical reactions of adsorbed proteins, and because of competitive adsorption between different protein fractions in the aqueous phase and at the interface (Jensen, 1995; Bucheim and Dejmek, 1997). Interfacial properties may also be altered due to the addition of surface-active materials that can adsorb to the membrane and displace the proteins, such as the small molecule surfactants often added to ice cream and whipped dairy products (Goff, 1997a–d, 2000). An example of this phenomenon is shown in Figure 12.2, which shows the

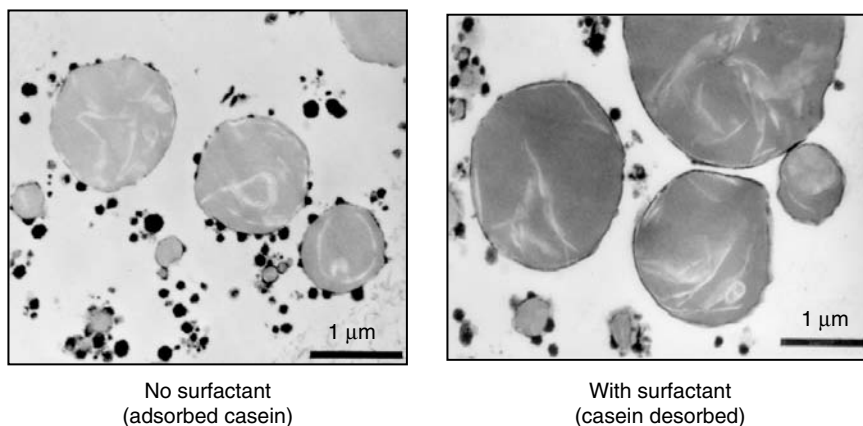


**Figure 12.2** Example of displacement of casein micelles from fat droplet surfaces by addition of a small molecule surfactant. TEM micrograph of homogenized ice cream mix kindly supplied by Prof. Douglas Goff (University of Guelph, Canada).

change in interfacial microstructure when a small molecule surfactant is added to an O/W emulsion that originally had casein micelles adsorbed to the oil droplet surfaces.

### 12.2.1.3 Continuous phase

The continuous phase of raw milk is compositionally complex, consisting primarily of a mixture of proteins, sugars, minerals, and water-soluble vitamins (Swaigood, 1996; Walstra, 1999). Typically, the aqueous phase is slightly acidic, having a pH value between 6.5 and 6.7 at ambient temperature. The proteins can be divided into two major fractions depending on their molecular structure and pH-solubility characteristics: the caseins (~80%) and the whey proteins (~20%). The caseins have predominantly flexible random coil structures and are relatively insoluble at their isoelectric points (IEP  $\approx$  4.6), for example,  $\alpha_{s1}$ -casein,  $\alpha_{s2}$ -casein,  $\beta$ -casein, and  $\kappa$ -casein. The whey proteins have compact globular structures and are relatively soluble at their isoelectric points (IEP  $\approx$  5.2), for example,  $\beta$ -lactoglobulin ( $\beta$ -La),  $\alpha$ -lactalbumin ( $\alpha$ -La), bovine serum albumin (BSA), and immunoglobulins (Ig). The whey proteins tend to unfold when heated above 60–80°C, which can lead to extensive protein aggregation (provided the electrostatic repulsion between the molecules is not too high). The caseins are stable to aggregation during thermal processing when heated in isolation, but may form insoluble complexes when heated in the presence of the whey proteins (Corredig and Dalgleish, 1996, 1999; Anema and Li, 2003a,b). In raw milk, the whey proteins tend to exist as monomers or dimers, whereas the caseins cluster into molecular aggregates referred to as “casein micelles.” These micelles vary in radius from 10s to 100s of nanometers, and are responsible for the turbid appearance of skim milk because of their ability to scatter light (Walstra, 1999). Casein micelles are held together by a combination of hydrophobic attraction and salt bridges involving multivalent ions, including calcium, magnesium, phosphate, and citrate (Walstra, 1999).

The aqueous phase also contains a variety of organic and inorganic minerals, such as chlorides, phosphates, citrates, and bicarbonates of sodium, potassium, chloride, and magnesium (Swaigood, 1996). These minerals may be present as free ions or ion complexes. In particular, many of the multivalent minerals are incorporated within the casein micelles. If they were in their free ion state, they would promote droplet flocculation by reducing the  $\zeta$ -potential on the droplets and screening electrostatic interactions (Keowmanachai and McClements, 2002a,b).

The predominant carbohydrate in milk is lactose, which is a disaccharide comprised of glucose and galactose (Swaigood, 1996). Lactose has a relatively low water solubility and may form crystals in dairy products, such as ice cream and condensed milk, which gives these products a grainy texture (McGee, 1984; Hartel, 2001). There may also be a number of minor carbohydrate constituents present, such as glucose, galactose, and some oligosaccharides.

### 12.2.2 Microstructure

Bovine milk is an O/W emulsion consisting of milk fat droplets dispersed in an aqueous continuous phase (Walstra, 1999). The fat droplets in raw milk typically range between 0.1 and 10  $\mu\text{m}$  in radius and typically have a mean radius ( $r_{32}$ ) between 1 and 2  $\mu\text{m}$  (Bucheim and Dejmek, 1997; Walstra, 1999). After homogenization, the fat droplets typically range between 0.05 and 0.5  $\mu\text{m}$  in radius and have a mean radius ( $r_{32}$ ) of about 0.25  $\mu\text{m}$  (Bucheim and Dejmek, 1997). As mentioned earlier, the interfacial membranes surrounding fat droplets in homogenized milk are typically between 8 and 10 nm thick, containing about 10 mg  $\text{m}^{-2}$  protein, with the vast majority (~95%) of these being caseins (Walstra, 1999). This relatively high protein load is due to the adsorption of significant quantities of casein micelles to the droplet surfaces during homogenization (Bucheim and

Dejmek, 1997). As mentioned above, the regions of the droplet surface covered by casein micelles tend to have a grainy appearance when viewed by electron microscopy, whereas those covered by individual casein or whey protein molecules tend to have a smooth appearance (Sharma et al., 1996a,b, Bucheim and Dejmek, 1997). The tendency for the droplets to aggregate in milk products depends on their composition, thermal history, and mechanical history. Droplet flocculation may be induced by adjusting the pH, adding minerals, heating, cooling, or shearing (Walstra, 1999).

### 12.2.3 Production

Raw bovine milk is produced naturally by cows (Jensen, 1995; Swaisgood, 1996). The lipid phase, aqueous phase, and milk fat globule membrane are synthesized in different regions of the mammary gland prior to being brought together and released through the udder. Milk is seldom consumed in a raw state because of physical, chemical, biochemical, and microbiologic deterioration processes. The relatively large droplet size in raw milk means that it is highly susceptible to creaming. Raw milk contains bacteria and enzymes that tend to lead to a fairly rapid deterioration in product quality and safety. Milk products therefore receive a variety of processing treatments prior to commercial distribution to ensure that they are safe to consume and maintain a high standard of quality (Walstra, 1999).

The creaming stability of raw milk is greatly improved by reducing the mean droplet size by homogenization. The most commonly used mechanical device for producing homogenized milk is the high-pressure valve homogenizer (Walstra, 1999), although other devices may also be used, for example, ultrasonic homogenizers or microfluidizers (Strawbridge et al., 1995). Typically, the mean droplet radius is reduced from around 2 to 0.2  $\mu\text{m}$  by homogenization, which should lead to a decrease in the creaming velocity of around 100-fold (Section 7.3).

After homogenization milk is usually thermally processed (pasteurized) to destroy disease-causing and spoilage microorganisms and to inactivate undesirable enzymes (Walstra, 1999). The extent of microbial destruction depends on the temperature and holding time used in the pasteurization process, with higher temperatures and longer times destroying more microorganisms. Nevertheless, excessive thermal processing reduces milk quality since it causes thermal denaturation of whey proteins, protein aggregation, generation of off-flavors and off-colors, and loss of nutritional quality. The minimum thermal processing conditions required to effectively inactivate harmful microorganisms depend on the precise nature of the product, and are highly regulated by national and international organizations. Commonly used combinations of temperature and holding time for milk are 72°C for 16 sec (high-temperature short time, HTST) and 63°C for 30 min (low-temperature long time, LTLT). The shelf life of milk can be extended considerably (to a few months) by using more severe thermal treatments to kill all of the bacteria and their spores, for example, ultrapasteurization or ultrahigh temperature (UHT) processing. Typical temperature–time combinations used by the dairy industry for milk sterilization are 30 min at 110°C, 30 sec at 130°C, or 1 sec at 145°C (Walstra, 1999). After pasteurization the product is rapidly cooled to refrigeration temperatures to retard the growth of any remaining microorganisms.

Fluid dairy products with higher fat contents can be produced by evaporation of some of the water phase or by collecting the cream layer after centrifugation (Walstra, 1999). Evaporated milks are produced by evaporating nearly 60% of the water from whole milk under vacuum. The resulting product is then homogenized and sterilized. This type of milk has a yellowish color and a characteristic “cooked” flavor because of chemical reactions associated with the sterilization process. Cream and skim milk are produced by

**Table 12.2** Typical Fat Contents and Solids-Nonfat Contents of Milk and Cream Products.

Product	Fat (%)	SNF (%)
Skim milk	<0.5	>8.25
Low fat milk	1.0	>8.25
Reduced fat milk	2.0	>8.25
Whole milk	>3.25	>8.25
Evaporated milk	>6.5	>16.5
Half-and-half	10.5–18	7.75
Light cream	18–30	7.2
Light whipping cream	30–36	–
Heavy cream	36–40	5.55

Source: Assembled from various sources.

separating the fat globules from the aqueous phase using gravitational separation or centrifugation. The fat globules have a lower density than the surrounding aqueous phase and therefore move upward in the presence of gravity or an applied centrifugal field (Section 7.3). Milk and cream products with varying fat contents can then be produced by blending different ratios of skim milk and cream (Table 12.2). Some creams are legally permitted to contain additional milk solids, emulsifiers, stabilizers, flavorings and various other ingredients. All cream products are pasteurized or ultrapasteurized after production.

## 12.2.4 Physicochemical properties

### 12.2.4.1 Stability

Raw milk is highly unstable to creaming because of the relatively large diameter of the milk fat globules and the appreciable density difference between the oil and aqueous phases ( $\sim 80 \text{ kg m}^{-3}$  at refrigeration temperatures). An observable amount of creaming can usually be observed in raw milk in a few hours or days. In cooled raw milk, the rate of creaming may be accelerated even further because of the presence of an immunoglobulin–lipoprotein complex (cryoglobulin) that can form bridges between milk fat globules, thereby promoting droplet flocculation (Walstra, 1999). At temperatures where the milk fat is partially crystalline (e.g.,  $0\text{--}10^\circ\text{C}$ ), the droplets in raw milk are susceptible to partial coalescence, especially when the milk is sheared. The extent of droplet aggregation depends on the type, size, and location of the fat crystals within the fat droplets, which is largely determined by the composition of the milk fat and the thermal history of the milk, for example, cooling rate and previous holding temperatures (Walstra, 1999). Raw milk is usually fairly stable to thermal processing, even though the milk fat globule membrane does undergo some changes (Bucheim and Djemek, 1997).

Homogenized milk is susceptible to many of the same forms of instability as raw milk, plus some additional factors. The mean droplet radius in homogenized milk ( $\sim 0.2\text{--}0.3 \mu\text{m}$ ) is about 5–10 times smaller than that in raw milk ( $\sim 1\text{--}2 \mu\text{m}$ ). Consequently, homogenized milk has a much improved stability to creaming (approximately 50- to 100-fold). If the concentration of proteins present in the aqueous phase of raw milk is insufficient to completely cover all of the surface area produced during homogenization, the droplets may aggregate through a bridging flocculation mechanism. This kind of droplet aggregation can often be avoided by using a two-stage high-pressure valve homogenizer, where the first stage is responsible for reducing the size of the fat globules and the second stage is designed to disrupt any flocs formed through the bridging mechanism (Walstra, 1999).

A rationalization of the influence of environmental conditions on the stability of homogenized milk can be gained by considering that it consists primarily of casein-stabilized droplets surrounded by an aqueous phase containing casein and whey proteins. For example, droplet flocculation can be induced by decreasing the pH toward the isoelectric point of the casein (pH 4.6), adding mineral ions to screen the electrostatic interactions between the droplets (e.g., sodium, potassium, or calcium ions), heating to a temperature where the  $\beta$ -lactoglobulin unfolds and forms complexes with the caseins that can cross-link the droplets, or addition of rennet to cleave the adsorbed casein and reduce the thickness and charge of the interfacial membrane.

#### 12.2.4.2 Rheology

Milk has a low viscosity because of its low disperse phase volume fraction ( $\phi = 0.041$ ) and the low viscosity of its continuous phase, as would be expected from the Einstein equation:  $\eta = \eta_0(1 + 2.5\phi)$  (Section 8.4). Nevertheless, the viscosity of milk may increase appreciably if the droplets and/or nonadsorbed protein molecules aggregate to form flocs because this increases the effective volume fraction of the particles. Aggregation could be induced by adjusting the pH to the isoelectric point of the proteins, adding high concentrations of mineral ions to screen electrostatic interactions, heating to promote bridging flocculation, or cooling and shearing to promote partial coalescence. The viscosity of milks and creams increases as their fat content increases as would be expected for typical O/W emulsions (Section 8.4). The most dramatic increase occurs between 30 and 40% milk fat because the droplets begin to become close packed. This accounts for the high viscosity of heavy creams that have fat contents greater than 40%.

#### 12.2.4.3 Appearance

The turbid appearance of skim milk is a result of light scattering by colloidal casein micelles. The color of skim milk is also influenced by the presence of the casein micelles. Casein micelles scatter light more strongly in the blue region of the visible spectrum than in the red region, so that skim milk appears different when viewed in reflection or transmission modes (Hutchins, 1999). Skim milk appears bluish when viewed in reflection mode because a greater fraction of blue light is scattered back to the eye, and reddish when viewed in transmission mode because blue light is selectively filtered out of the transmitted light. The lightness of milk increases as the fat content increases, particularly in the concentration range from 0 to 4 wt%, due to the scattering of light by the fat globules (Section 10.5.1). Skim milk can also be made to have a more creamy appearance by adding sufficient quantities of nonfat particles that scatter light, for example, protein aggregates or titanium dioxide particles (Phillips et al., 1995; Phillips and Barbano, 1997). Milk also contains a number of constituents that absorb light, such as carotene and riboflavin, which contribute to its color.

#### 12.2.4.4 Flavor

The flavor of milk is rather bland, and hence any slight changes are easily detected by consumers (McGee, 1984; Parliament and McGorin, 2000). A detrimental flavor profile may occur in milk as a result of consumption of foodstuffs containing off-flavors by the cow. Alternatively, off-flavors may be generated within milk due to chemical or biochemical reactions promoted by light, oxygen, heat, enzymes, or microbial activity (Parliament and McGorin, 2000). To avoid the formation of off-flavors, milk producers must therefore carefully control feeding, collection, storage, processing, and distribution conditions (Walstra, 1999). The complex chemical composition of milk means that its overall flavor is the result of contributions from many different components. The major contributions



to milk flavor are the slightly sweet taste from lactose, the slightly salty taste from minerals, and the characteristic milky odors produced by volatile short-chain fatty acids and sulfur compounds (McGee, 1984). These odors are often produced through autooxidation of lipids or proteins. Full fat milk and cream have a rich smooth mouthfeel, which is largely lost when the fat droplets are removed to create skim milk.

### 12.2.5 Dairy products

Milk and cream are used as the basis for the creation of a wide variety of common food products, including whipped cream, ice cream, yogurt, cheese, and butter (Walstra, 1999). A brief overview of some of these products is given in this section, with special emphasis being given to the emulsion science aspects.

#### 12.2.5.1 Whipped cream

Whipped cream is formed by beating air into cream at relatively low temperatures (Barford, 1995; Goff, 1997). It consists of air bubbles dispersed in a structurally complex lipid–aqueous medium. During the whipping process air bubbles are formed that are stabilized by a combination of adsorbed proteins and aggregated fat globules. Adsorbed globular proteins are believed to undergo surface denaturation, which leads to the formation of a viscoelastic membrane around the air bubbles. Whipping the cream when it is relatively cool (0–7°C) leads to partial coalescence of the fat globules, which form a fairly rigid network around the air bubbles and throughout the medium separating the air bubbles. The network of aggregated fat globules therefore provides stability and texture to the final product. Sometimes biopolymers, such as gums or gelatin, are added to whipping cream to improve its whipping properties by increasing the viscosity of the aqueous phase, thereby slowing down the movement of air bubbles. The addition of sugars to whipping cream can be either detrimental or advantageous to foam quality (Damodaran, 1996). If the sugars are added prior to whipping, the foam volume and stability may be adversely affected because the sugars stabilize the globular structure of the whey proteins, thereby retarding protein surface denaturation and aggregation and reducing the tendency for a viscoelastic protein membrane to form around the air bubbles. On the other hand, if the sugars are added after whipping the foam stability is often improved because they increase the viscosity of the aqueous phase and therefore retard the movement of the air bubbles.

#### 12.2.5.2 Butter

Butter is a water-in-oil emulsion, typically comprising 80% milk fat, 18% water, and 2% milk solids, that is formed from cream by carrying out a controlled phase inversion (Dickinson and Stainsby, 1982; Flack, 1997; Walstra, 1999). The cream used in butter production is separated from whole milk and is then usually pasteurized. The cream is then cooled to a temperature where the droplets are partially crystalline (typically 12–18°C), then mechanically agitated (*churned*). The physicochemical phenomenon responsible for phase inversion of the cream is similar to that responsible for providing the stability and texture to whipped creams, but more dramatic. When the partially crystalline fat globules collide with each other during the churning process they undergo partial coalescence, which leads to the formation of clumps of aggregated fat globules (Sections 7.7 and 7.9). The presence of air bubbles incorporated into the cream during the churning process facilitates this process by causing the fat globules to be disrupted and spread out around their surface. The clumps grow progressively larger during the churning process and aggregate with one another, until eventually phase inversion occurs. At the end of churning the system consists of water droplets, air bubbles, and some intact fat globules suspended

in a fat crystal network. The texture and stability of butter at a particular temperature depend largely on the solid fat content, and the morphology and size of the fat crystals within the network, which in turn depend on the composition of the butter fat and the thermal and shear history of the product (Flack, 1997; Hartel, 2001).

### 12.2.5.3 Ice cream

Ice cream is a structurally complex colloidal food system consisting of air bubbles ( $\sim 50\text{--}80\ \mu\text{m}$ ), ice crystals ( $\sim 30\text{--}50\ \mu\text{m}$ ), and fat globules ( $\sim 1\ \mu\text{m}$ ) dispersed in a fluid aqueous phase that contains freeze-concentrated sugars, minerals, and proteins (Goff, 1997a–d, 2000, 2002; Goff et al., 1999; Goff and Hartel, 2003; Marshall et al., 2003). If it is not produced or stored correctly ice cream may also contain lactose crystals, which give it an undesirable grainy texture. A schematic representation of the microstructure of ice cream is shown in Figure 12.3. Legal regulations specify the types and amounts of constituents that can be present in ice cream, such as milk fat, milk solids, air, stabilizers, and emulsifiers. Nevertheless, ice creams still vary considerably in flavor, appearance, texture, and shelf life depending on the precise nature of the ingredients, processing operations, and storage conditions used.

An ice cream mix is prepared by blending together milk or cream, sweetening agents, flavorings, and various other ingredients (e.g., stabilizers and emulsifiers). The mix is then usually pasteurized, homogenized, and cooled. It is then aged at refrigerator temperatures ( $0\text{--}5^\circ\text{C}$ ) for a few hours to allow the fat to partially crystallize and the water-soluble ingredients to fully hydrate. Small molecule surfactants are often added to the ice cream mix prior to aging because they displace proteins from fat globule surfaces, which facilitates partial coalescence of the fat globules during the subsequent freezing/agitation process.

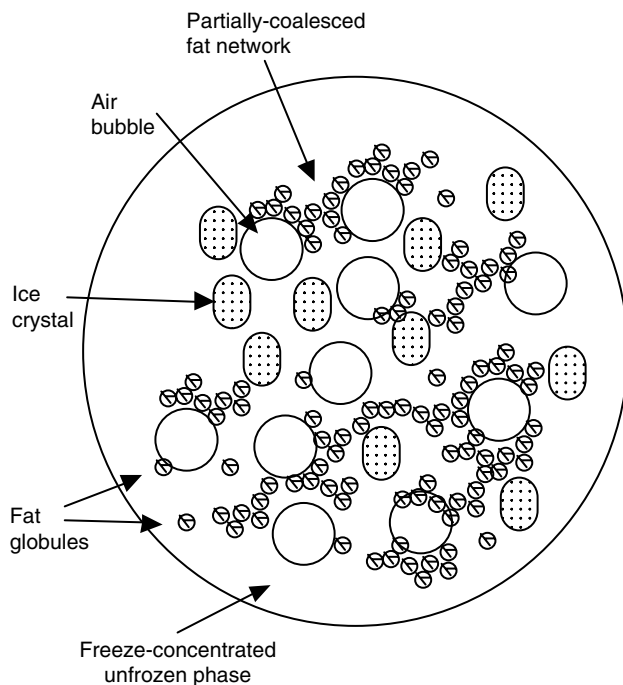


**Figure 12.3** Schematic representation of the microstructure of ice cream, which contains air bubbles, fat globules, ice crystals, and freeze-concentrated aqueous phase. The fat globules form a three-dimensional network within the aqueous phase and around the air bubbles. Diagram kindly supplied by Prof. Douglas Goff (University of Guelph, Canada).

After aging, the ice cream mix is cooled to a temperature appreciably below the normal freezing point of water, which causes a fraction of the water to crystallize. The remainder of the water remains in a liquid state because of the depression in its freezing point caused by the presence of the freeze-concentrated dissolved solids. The texture and mouthfeel of the final product are strongly influenced by the nature of the ice crystals formed during the freezing process (Hartel, 2001). Slow cooling tends to lead to the formation of a small number of relatively large ice crystals, which gives the final product a grainy texture and icy mouthfeel. Rapid cooling combined with mechanical agitation leads to the formation of a large number of evenly distributed and relatively small ice crystals, which impart a smooth texture and creamy mouthfeel. The fact that an appreciable fraction of the water does not crystallize also means that the ice cream is not too hard to consume. Air bubbles are formed and incorporated into the ice cream mix during the freezing process, which also contribute to the formation of ice creams with softer and lighter textures. Cooling and mechanical agitation also causes the fat globules to undergo partial coalescence and form an aggregated network that surrounds the air bubbles and extends throughout the aqueous phase, which provides additional stability and texture to the product (Figure 12.3). After the freezing stage particulate flavoring matter can be incorporated into the relatively soft ice cream, such as nuts, fruits, chocolate, chips, and so on. Soft-serve ice creams are usually used directly after the freezing process, whereas hard-frozen ice creams undergo an additional hardening step. In this step, the product is packaged and stored at freezing temperatures ( $-30$  to  $-40^{\circ}\text{C}$ ) in the absence of mechanical agitation, which causes a greater fraction of the water to crystallize and increases the mechanical strength of the product. Once the ice cream has been produced it should be stored at refrigerator temperatures (typically  $-23$  to  $-18^{\circ}\text{C}$ ) to maintain its desirable appearance and texture. It is important to avoid excessive freeze-thaw cycling as this will lead to the formation of large ice crystals and possibly lactose crystals that give the product an undesirable grainy texture. Polysaccharide stabilizers are often incorporated into ice cream mix to retard the formation of large ice crystals during storage, as well as to provide a more desirable body and texture to the final product (Goff, 1993; Marshall et al., 2003).

#### 12.2.5.4 Yogurt

Many yogurts can be considered to be O/W emulsions consisting of milk fat globules suspended in a viscoplastic aqueous phase (Robinson, 1993; Tamime and Robinson, 1999; Tamime, 2003). The aqueous phase contains a three-dimensional network of aggregated casein and whey proteins, which gives yogurt its characteristic textural attributes. Yogurt is primarily formed from milk and/or cream, but a variety of other ingredients may also be present, including sweeteners (e.g., sugar, aspartame), flavorings (e.g., vanilla, coffee, banana, strawberry), and other ingredients (e.g., stabilizers, fruits, preserves). A yogurt mix, formed by blending the various ingredients together, is pasteurized at a temperature that inactivates pathogenic and spoilage organisms as well as causing thermal denaturation of globular whey proteins, for example,  $85^{\circ}\text{C}$  for 30 min or  $95^{\circ}\text{C}$  for 10 min. The denatured whey proteins form a complex with the caseins that results in a finer structure and firmer texture in the final product. The yogurt mix is then homogenized and cooled to a temperature of about  $43^{\circ}\text{C}$ , lactic acid producing bacteria (typically *Lactobacillus bulgaricus* and *Streptococcus thermophilus*) are added and the system is aged for a few hours. The bacteria use the lactose in the milk as an energy source and produce lactic acid as a waste product. Consequently, the pH of the aqueous phase decreases from 6.7 to 4.5, which leads to extensive aggregation of the proteins because casein molecules are released from casein micelles and because the final pH is close to the isoelectric point of the dairy proteins so electrostatic repulsion no longer prevents them from coming into close proximity. Protein aggregation leads to the formation of a three-dimensional gel network that extends

throughout the yogurt and gives the product its characteristic textural properties. After a certain period the product is cooled to refrigerator temperatures, which retards the activity of the bacteria. Yogurt is stored at refrigeration temperatures (5°C) to slow down physical, chemical, and microbiologic degradation. The flavor of yogurt depends largely on the presence of added flavoring substances, the fat content, and the nature of the fermentation process used. One of the major challenges of the modern yogurt industry is to produce nonfat or low fat yogurts that have similar sensory characteristics as their full fat counterparts. When the fat is removed the appearance of the yogurt becomes less light, and the flavor profile may be adversely altered. The lightness of reduced fat yogurts can be increased by adding nonfat particulate matter that scatters light (Yazici and Akgun, 2004), whereas the flavor profile can be improved by encapsulating the fat globules in gel particles to slow down flavor release (Harvey et al., 2000).

#### 12.2.5.5 Cheese

Cheese is an example of an O/W emulsion consisting of milk fat globules suspended in a semisolid aqueous phase (Fox, 1993; Fox and McSweeney, 1998; Fox et al., 2000). There are a huge number of different types of cheeses consumed internationally, that vary in their texture, appearance, taste, and shelf life. Nevertheless, the majority of the cheeses are produced by a fairly similar production method.

Initially, lactic acid producing bacteria and rennet are added to warm milk. The bacteria convert lactose in the milk to lactic acid, which reduces the pH of the aqueous phase to the optimum value for efficient function of the rennet enzyme. This enzyme cleaves  $\kappa$ -casein at the Phe(105)-Met(106) linkage in the peptide chain, which splits the molecule into a highly charged hydrophilic portion (casein macropeptide) and a relatively hydrophobic portion (para- $\kappa$ -casein).  $\kappa$ -Casein forms an integral part within the structure of casein micelles, and its hydrophilic portion is believed to help prevent casein micelles from aggregating. Once this part is removed by the action of the rennet the casein micelles rapidly coagulate to form a "curd" that entraps most of the fat globules, leaving an aqueous phase, known as the "whey" that contains lactose, whey proteins, water-soluble vitamins, and minerals. After aging, the majority of the whey is drained from the curd. The curds are then usually cut, pressed, cooked, and salted, which causes the matrix of aggregated proteins to shrink and facilitates further removal of the whey. Traditionally, the whey was regarded as a waste product, but it is now used by the dairy industry to produce a variety of value-added functional ingredients, including whey protein concentrates and whey protein isolates. Once most of the whey has been removed from the curd it is aged (*ripened*) under carefully controlled storage conditions (temperature and humidity). During the ripening process microbial enzymes breakdown lipids and proteins into a multitude of different taste and aromas molecules (e.g., fatty acids, fatty acid reaction products, peptides, and amino acids) that give the cheese its characteristic flavor. In addition, the proteins undergo chemical and physical interactions with each other that alter the textural characteristics of the product.

Each type of cheese has its own unique physicochemical and sensory characteristics due to differences in the type of milk or cream used (fat content, pasteurization, homogenization), bacteria or molds added, and storage conditions used during ripening, in addition to various other refinements of the general process. Microstructural investigations of cheeses show that they usually consist of fat globules entrapped in a three-dimensional network of aggregated proteins (Fox et al., 2000). If nonhomogenized milk is used to prepare the cheese, the fat globules do not tend to interact with the protein network, but if homogenized milk is used the fat globules interact with the network because they are mainly covered by proteins themselves. Fat globules may therefore make a major contribution to the texture of many cheeses. For example, when cheddar cheese is heated above

the melting temperature of the fat droplets there is an irreversible collapse of its structure and liquid oil is expressed.

## 12.3 Beverage emulsions

In general, the term “beverage emulsion” refers to any O/W emulsion that can be drunk, for example, tea, coffee, milk, infant formula, sports drinks, fruit drinks, and colas (Mathews, 1999). In this chapter, the term is used more narrowly to refer to nondairy and noncarbonated beverages that are drunk cold (i.e., fruit and cola drinks) because this category of products has common compositions and physicochemical characteristics (Tan, 1998, 2004). This type of product can be conveniently divided into two categories: *beverage flavor emulsions*, which are used to provide a combination of flavor, cloudiness, and color to finished products; *beverage cloud emulsions*, which are used primarily to give cloudiness to finished products (Heath and Reineccius, 1986; Tan, 2004). Beverage emulsions are usually prepared in a relatively concentrated form (10–30 wt% oil), as this facilitates their transport and storage. The finished product (<0.1 wt% oil) is then prepared by diluting the concentrated emulsion with an aqueous solution. The beverage concentrate is often manufactured in one factory and shipped to another production facility for dilution. The formulation and production of beverage emulsions that have prolonged shelf lives requires a thorough understanding of the factors that determine their physicochemical properties. The beverage industry is facing new challenges in product formulation as it introduces beverages with new flavors and appearances, and introduces health-promoting beverages fortified with vitamins, minerals, or other nutraceuticals (Mathews, 1999). This chapter provides a brief overview of the composition, microstructure, and physicochemical properties of beverage emulsions, focusing on their colloidal aspects. An appreciation of the information provided in this chapter should facilitate the rational design and creation of beverage emulsion products with improved or novel properties.

### 12.3.1 Composition

#### 12.3.1.1 Dispersed phase

Beverage emulsions are O/W emulsions hence the dispersed phase consists principally of oil and various other components that are either partially or totally insoluble in the aqueous phase, for example, flavors, antioxidants, and weighting agents (Tan, 2004). The type of oil present within the droplets depends mainly on whether the beverage emulsion is of the “cloud” or “flavor” type. The droplets in cloud emulsions are comprised primarily of nonflavor oils (e.g., vegetable oils or terpene oils), whereas the droplets in flavor emulsions are comprised of flavor oils (e.g., citrus oils) or mixtures of flavor oils and nonflavor oils. Nonflavor oils do not contribute directly to the flavor profile of beverage emulsions, and are used mainly because of their ability to form oil droplets that scatter light. The most commonly used flavor oils are citrus oils, such as orange, lemon, lime, and grapefruit (Heath, 1978; Tan, 2004). These oils are highly complex substances that contain a variety of different kinds of molecules, with different molecular weights, structures, and polarities. Citrus oils are primarily comprised of hydrocarbon terpenes (monoterpenes and sesquiterpenes) that have little odor or taste themselves (Tan, 2004). Nevertheless, citrus oils also contain many oxygenated terpenoids that do contribute to the overall flavor profile, for example, alcohols, ketones, acids, and esters (Shaw, 1986; Rouseff and Naim, 2000). Many flavor oils contain components that have a limited amount of water solubility. As a result beverage emulsions containing these oils are more susceptible to Ostwald ripening than emulsions containing conventional oils (Buffo and Reineccius, 2001). Some of the components in flavor oils are susceptible to chemical degradation

(e.g., cyclization or oxidation) and therefore it may be necessary to carefully control environmental conditions (pH, temperature, light, minerals) or incorporate preservatives to improve their stability (Freeburg et al., 1994; Mathews, 1999; Rouseff and Naim, 2000). Another problem with flavor oils is that their density ( $\sim 845\text{--}890\text{ kg m}^{-3}$ ) is relatively low compared to that of the aqueous phase ( $\sim 1000\text{--}1050\text{ kg m}^{-3}$ ), which means that O/W emulsions prepared entirely from these oils would be unstable to creaming (see later). It is for this reason that weighting agents are normally incorporated into the oil phase.

The purpose of weighting agents is to reduce the density contrast between the oil droplets and the surrounding aqueous phase, thereby reducing the driving force for creaming (Tan, 2004). A variety of natural and synthetic weighting agents are available for usage in beverage emulsions. The most commonly used are brominated vegetable oil (BVO), sucrose acetate isobutyrate (SAIB), dammar gum, and ester gum (Heath and Reineccius, 1986; Tan, 2004). Brominated vegetable oil is produced by addition of bromine to unsaturated bonds on the triacylglycerols found in food oils, for example, corn oil, soybean oil, cotton seed oil, or olive oil. Ester gum is made by esterification of wood rosin with glycerol. Damar gum is a natural exudate obtained from the shrubs of the *Caesalpinaceae* and *Dipterocarpaceae* families. SAIB is made by the esterification of sucrose with acetic and isobutyric anhydrides. The weighting agent is incorporated into the oil phase prior to homogenization. The density of the weighting agent determines how much of it is required to match the oil and aqueous phase densities: BVO =  $1240\text{--}1330\text{ kg m}^{-3}$ ; SAIB =  $1150\text{ kg m}^{-3}$ ; ester gum =  $1080\text{ kg m}^{-3}$ ; damar gum =  $1060\text{ kg m}^{-3}$ . Nevertheless, the type and amount of weighting agents that can be used in beverage emulsions is restricted by government and international regulations in many countries. For example, in the U.S. only 15 ppm BVO and 100 ppm ester gum can be present in the finished product (Tan, 2004). This means that it is often not possible to identically match the density of the oil phase and the aqueous phase using a single type of weighting agent.

The relationship between droplet density and droplet concentration for a finished beverage product containing 15 ppm BVO is shown in Figure 12.4. These calculations were carried out assuming that the oil droplets consisted of a mixture of brominated vegetable oil and regular vegetable oil, assuming,  $\rho_{\text{BVO}} = 1300\text{ kg m}^{-3}$ ,  $\rho_{\text{VO}} = 920\text{ kg m}^{-3}$ ,

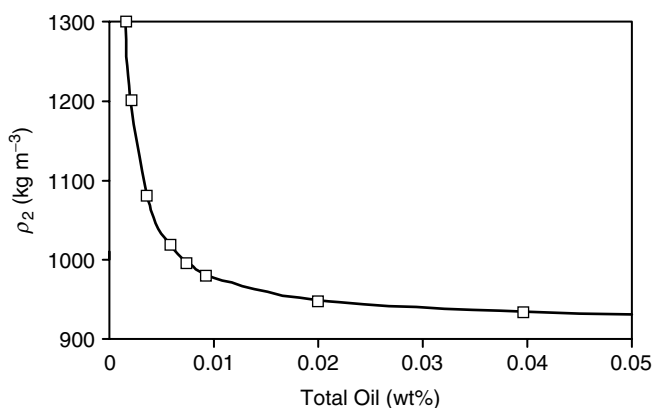


**Figure 12.4** Calculated dependence of oil droplet density in O/W emulsions containing the legal maximum of BVO (15 ppm) on total oil concentration. Droplet creaming is prevented when the density of the droplets equals that of the aqueous phase ( $\rho_1 \approx 1010\text{ kg m}^{-3}$  for a soda drink). This figure shows that creaming can only be effectively retarded in dilute emulsions ( $<0.01\text{ wt\%}$  oil). It was assumed that the densities of the vegetable oil and brominated vegetable oils in the droplets were  $\rho_{\text{VO}} = 900\text{ kg m}^{-3}$ ,  $\rho_{\text{BVO}} = 1300\text{ kg m}^{-3}$ .

and  $\rho_{\text{aqueous}} = 1010 \text{ kg m}^{-3}$ . Only at relatively low droplet concentrations ( $<0.006 \text{ wt\%}$ ) is it possible to completely match the density of the oil droplets to that of the aqueous phase using the legal limit of BVO. To improve creaming stability it would therefore be beneficial to use as low a droplet concentration as possible, while maintaining the other desirable attributes of the product, such as appearance and flavor. In addition to the weighting agents mentioned above, the beverage industry is currently evaluating the effectiveness of a number of other types (Tan, 2004).

#### 12.3.1.2 Interfacial membrane

The composition and structure of the interfacial membrane in beverage emulsions is largely determined by the type of emulsifiers used to stabilize the system. The most widely used emulsifiers currently in beverage emulsions are the amphiphilic polysaccharides gum arabic and modified starch (Ray et al., 1995; Kim et al., 1996; McNamee et al., 1998; Trubiano, 1995; Garti, 1999). The molecular and functional characteristics of these emulsifiers were described in Section 4.4.2. Traditionally, gum arabic was the most commonly used emulsifier because of its high water solubility, low solution viscosity, and good ability to form a protective membrane around emulsion droplets (Glicksman, 1983). Nevertheless, there have been many problems associated with its usage within the beverage industry because of variations in its quality from batch-to-batch. These variations have been associated to the natural variability of the plant species it is extracted from, as well as the nature of the extraction, processing and storage conditions (Buffo et al., 2001). Consequently, research has been carried out to identify alternative sources of emulsifiers for use in beverage emulsions (Kim et al., 1996; Tan, 1998, 2004; Garti, 1999). Hydrophobically modified starches have proved to be one of the most promising replacements for gum arabic (Trubiano, 1995). Typically, a starch is chemically modified to contain nonpolar side groups containing typically between 5 and 18 carbon atoms (Stauffer, 1999). These side groups anchor the molecule to the droplet surface, while the hydrophilic starch chains protrude into the aqueous phase and protect droplets against aggregation through steric repulsion. Modified starches tend to be mildly anionic in aqueous solutions and have surface activities similar to those of gum arabic (Tse, 1990). One of the main advantages of modified starch is that it is much less susceptible to batch-to-batch variations in emulsifier efficiency than gum arabic (Tan, 2004). It can also be dissolved in cold water, has little intrinsic flavor, has good stability to pH and temperature variations, and can often be used at lower levels than gum arabic.

Gum arabic and modified starch have relatively low surface activities (compared to proteins or surfactants), and so a large excess must be added to ensure that all the droplet surfaces are adequately coated (Phillips and Williams, 1995, 2003). For example, as much as 20% gum arabic or 12% modified starch may be required to produce a stable 12.5 wt% O/W emulsion (Tse and Reineccius, 1995). As a result there is a large excess of nonabsorbed polysaccharide in the aqueous phase of emulsions prepared from them (Tan, 1998; Garti, 1999). Under certain circumstances these nonabsorbed biopolymers have been shown to promote droplet flocculation through a depletion mechanism (Chanamai and McClements, 2001). The major stabilizing mechanism of these biopolymer emulsifiers is believed to be steric repulsion because they form relatively thick interfacial membranes; however, electrostatic repulsion may also play a role since both gum arabic and modified starches have a significant negative charge (Chanamai and McClements, 2002). O/W emulsions stabilized by gum arabic or modified starches have been shown to have good stability to variations in pH (3–9), calcium concentration (0–25 mM), and temperature (30–90°C) (Chanamai and McClements, 2002).

Due to the relatively large amounts of gum arabic and modified starch required to form stable emulsions a variety of other emulsifiers have been proposed as potential substitutes, such as proteins, other surface-active polysaccharides, and small molecule surfactants (Edris, 1998; Kim et al., 1996, Tan, 1998; 2004; Garti, 1999; Chanamai and McClements, 2002).

Nevertheless, protein-stabilized oil droplets are more sensitive to environmental conditions (pH, ionic strength, temperature) than polysaccharides, and small molecule surfactants may have problems associated with flavors or user-friendly labeling.

#### 12.3.1.3 *Continuous phase*

The major component in the continuous phase of beverage emulsions is water, which typically makes up between 60 and 95% (Tan, 1998, 2004). The long-term physical and chemical stability of beverage emulsions is strongly dependent on the usage of good quality water. For this reason water is usually treated to remove minerals, undesirable taste and odor molecules, colloidal matter, and microorganisms prior to usage in the production of beverage emulsions (Heath, 1978; Tan, 2004).

Some beverage emulsions contain biopolymer thickening agents to provide desirable body, mouthfeel, and textural properties, as well as slowing down the gravitational separation of oil droplets or other suspended matter (Tan, 2004). A variety of thickening agents have been specially formulated for usage in beverage emulsions, including modified starches, xanthan, pectin, guar gum, alginates, carageenans, and carboxymethylcelluloses. These thickening agents are available in a wide variety of different forms (single biopolymers, biopolymer blends, molecular weights, charges, and so on) with different functional attributes (viscosity enhancement, environmental sensitivity, dispersibility, ingredient compatibility).

Beverage emulsions also contain a variety of other water-soluble ingredients that contribute to their stability, taste, texture, and appearance, such as acidulants, preservatives, flavorings, colorings, vitamins, minerals, and antioxidants (Heath, 1978; Mathews, 1999; Tan, 2004). The pH of many beverage emulsions is around 2.5–4.5 and therefore they must contain acidulants, such as citric, malic, tartaric, phosphoric, or lactic acids. These acids contribute to the flavor profile, help prevent microbial growth, and may retard oxidation reactions by chelating multivalent cations. Preservatives, such as benzoic acid or sodium benzoate, are usually added to beverage emulsions to prevent microbial growth. A wide variety of different natural and synthetic colorants are added to beverage emulsions to provide their characteristic appearances, for example, fruit, vegetable, or plant extracts, FD&C colorants (Heath, 1978; Francis, 1999; Mathews, 1999). Many of these colorants may undergo chemical degradation reactions in beverages that lead to color fading over time. Various natural (e.g., sucrose, high-fructose corn syrup, fruit juices, honey) and/or artificial (e.g., aspartame, sucralose, and saccharin) sweeteners are added to beverage emulsions to produce a desirable flavor profile (Mathews, 1999).

When formulating a beverage emulsion it is important to ensure that all of the ingredients are compatible with each other, and that they will remain stable during the expected lifetime of the product (Mathews, 1999). The types of ingredients selected for a particular beverage product are also governed by various legal, economic, and marketing considerations.

#### 12.3.2 *Microstructure*

The finished product is a dilute O/W emulsion consisting of oil droplets dispersed in an aqueous medium. The droplets in beverage emulsions are usually so small that they cannot be properly observed by optical microscopy because their size is close to the limit of resolution of the microscope and because they move rapidly due to Brownian motion. Electron microscopy can be used to provide information about the droplet size distribution of beverage emulsions, but this technique is expensive, time-consuming, and laborious to use, not widely available, and the sample preparation used may alter the microstructure (Tan, 2004). For this reason, the microstructure of beverage emulsions is usually determined indirectly using particle sizing instruments, such as laser diffraction or electrical pulse counting (Section 11.3). In a stable beverage emulsion the droplets should be isolated, but in an unstable system the



droplets may be flocculated. Usually, a beverage emulsion manufacturer will establish some particle size distribution criteria to assess the efficiency of the homogenization process and to predict the long-term stability of the final product. For example, it may be stipulated that the majority of oil droplets must be below a certain particle diameter for a product to be acceptable, for example, 90 vol% of droplets below a diameter of 0.5  $\mu\text{m}$ . The thickness and structure of the interfacial membrane will depend on the type of emulsifier used to stabilize the system. For example, small molecule surfactants or globular proteins tend to form relatively thin compact membranes, whereas polysaccharides tend to form relatively thick open membranes.

### 12.3.3 *Production*

Beverage emulsions are usually prepared using a two-step process: a beverage emulsion concentrate (10–30 wt% oil) is prepared, which is diluted extensively to create the finished product (<0.1 wt% oil) (Tan, 2004). The emulsion is stored and transported in a concentrated form to reduce costs associated with having large quantities of water present.

#### 12.3.2.1 *Beverage emulsion concentrate*

Initially, all of the aqueous phase components are usually mixed together and all of the oil phase components are mixed together. The separate oil and aqueous phases may then have to be heated and mechanically agitated to facilitate dissolution and dispersion of the various ingredients present. Once the oil and aqueous phases have been prepared they are blended together using a high-speed mixer to form a coarse emulsion, which is then homogenized using a high-pressure valve homogenizer to form a fine emulsion. Homogenization may be carried out using either a one- or two-stage homogenizer, and the emulsion is often passed through the homogenizer more than once to ensure that the droplet size is small enough to prevent creaming. After homogenization the emulsion is pasteurized to reduce the microbial load, and then stored or transported to the place where it will be used.

#### 12.3.2.2 *Finished product*

The finished product is created by diluting the beverage emulsion concentrate with aqueous phase containing acidulants, colors, flavors, preservatives, and so on. Typically, the concentrate is diluted 500–1000 times to produce a final droplet concentration less than 0.1 wt%. The final product is often homogenized again to ensure that the nonpolar colors, flavors, and preservatives are incorporated into the oil droplets. The product is then packaged into a bottle, carton, pouch, or other suitable container either before or after thermal processing to ensure microbial stability.

### 12.3.4 *Physicochemical properties*

#### 12.3.4.1 *Stability*

The appearance, flavor, and mouthfeel of a beverage emulsion largely determine its quality. It is important that the desirable physicochemical and sensory attributes of a product are retained up to the time that it is consumed. Nevertheless, products often experience variations in their composition, temperature, and mechanical stress during production, transport, storage, and consumption that adversely affect their stability. A better understanding of the factors that influence the stability of beverage emulsions would enable manufacturers to develop products with enhanced quality and shelf lives. A number of studies have examined the influence of emulsifier characteristics (Dickinson et al., 1989; Ray et al., 1995; Kim et al., 1996; McNamee et al., 1998; Garti, 1999), oil composition (Freeburg et al., 1994), weighting agents (Trubiano, 1995; Tan, 1998; 2004), temperature (Tse and Reineccius, 1995; Chanamai and McClements, 2002), pH, and ionic strength (Jayme et al., 1999; Chanamai and McClements, 2002) on the stability of beverage emulsions and beverage emulsion analogs.

The most common instability mechanisms observed in beverage emulsions are “ringing” and “oiling-off” (Trubiano, 1995; Tan, 1997, 1998). Ringing is the formation of a whitish “ring” around the neck of the container, while “oiling-off” is the formation of a shiny oil slick on top of the product. Ringing and oiling-off are the results of a variety of physico-chemical mechanisms that occur within the beverage emulsion, including gravitational separation, flocculation, coalescence, and Ostwald ripening (Chapter 7). The driving force for ringing is the fact that the oil phase has a lower density than the aqueous phase so that the droplets are susceptible to creaming. A variety of methods have been employed by the beverage industry to slow down creaming in beverage emulsions (Tan, 2004). The physical basis of these methods can be understood by referring to Stokes equation, which describes the creaming velocity of an isolated sphere through a fluid (Section 7.3.1):

- *Reduction of density contrast.* Stokes law predicts that the creaming velocity of a droplet is proportional to the density difference between the droplet and surrounding liquid. The density of typical flavor and food oils (845–920 kg m<sup>-3</sup>) is appreciably smaller than the density of the aqueous phases of beverage emulsions (1000–1050 kg m<sup>-3</sup>). Hence, the oil droplets will tend to move upward due to gravity. For this reason, beverage manufacturers usually add weighting agents to increase the density of the oil phase, for example, BVO, SAIB, damar gum, or ester gum (Tan, 2004). Nevertheless, it is often not possible to completely match the densities of the oil and aqueous phases because of legal limitations on the maximum amount of weighting agent that can be used. The effective density of an oil droplet may also be increased somewhat by the presence of a thick densely-packed interfacial membrane, since the density of the adsorbed layer is usually greater than that of water. This effect is only significant for relatively small droplets where the interfacial membrane comprises a significant fraction of the total effective volume of the droplet (Section 7.3).
- *Reduction of particle size.* Stokes law predicts that the creaming velocity of a droplet is proportional to its radius squared. The stability of a beverage emulsion to creaming can therefore be greatly increased by ensuring that the majority of droplets are below some critical size, typically around 0.3 μm in diameter. Beverage manufacturers therefore usually ensure that the homogenization process produces an emulsion with the majority of droplets below some prescribed critical size. In addition, the emulsion is usually formulated to avoid processes that lead to an increase in particle size during storage, for example, flocculation, coalescence, or Ostwald ripening (Tan, 2004). Nevertheless, one must be careful not to make the droplets too small or they will become less efficient at scattering light and the emulsion will lose its desirable cloudy appearance (Chapter 10).
- *Increased aqueous phase viscosity.* Stokes law predicts that the velocity at which a droplet moves upward due to gravity is inversely proportional to the viscosity of the surrounding fluid. The creaming stability may therefore be improved by increasing the viscosity of the continuous phase. The viscosity of the continuous phase increases with increasing sugar concentration, but the decrease in creaming velocity associated with this phenomenon is off-set by the increase in creaming velocity caused by the increase in density contrast between the oil and aqueous phase (Chanamai and McClements, 2000a). Thickening agents, such as hydrocolloids, may be added to the aqueous phase in relatively low concentrations to substantially increase its viscosity (Tan, 2004). Nevertheless, one must be careful not to induce depletion or bridging flocculation (Section 7.5) or to adversely affect the desirable flow characteristics or mouthfeel of the final product (Chapters 8 and 9).

The stability of the droplets in beverage emulsions to droplet flocculation and coalescence is believed to be primarily due to steric repulsion between the droplets, since O/W emulsions stabilized by gum arabic and modified starch have been found to be insensitive to pH and mineral content (Chanamai and McClements, 2002). Nevertheless, some studies have suggested that electrostatic repulsion may also make some contribution to beverage emulsion stability, since stability is sensitive to mineral content (Jayme et al., 1999; Buffo et al., 2001). It has been postulated that the stability of the oil droplets in beverage emulsions to aggregation may depend on the strength of the interaction between the emulsifier and the droplet surface, which depends on oil polarity and impurities. Gum arabic and modified starch do not adsorb strongly to oil–water interfaces, as demonstrated by their interfacial tension versus concentration profiles (Chanamai et al., 2002). They may therefore be desorbed from a droplet interface that is highly polar or from a droplet that contains surface-active impurities that can compete with the hydrophobic portions of the polysaccharides for the interface. This may explain some of the instabilities seen in beverage emulsions stabilized by these emulsifiers (Buffo and Reineccius, 2001; Buffo et al., 2001).

#### 12.3.4.2 *Texture*

The rheology of diluted beverage emulsions is largely determined by the rheological characteristics of the aqueous phase, because the droplet concentration is extremely low (Tan, 2004). Hence, the rheology is mainly determined by the concentration of any thickening agents and sugars present. On the other hand, the rheology of concentrated beverage emulsions is strongly influenced by both the droplet concentration and the rheological characteristics of the aqueous phase (Buffo and Reineccius, 2002). From a practical standpoint, it is important to have a beverage concentrate that has as low a moisture content as possible to reduce shipping and storage costs, but that is not so viscous that it cannot be easily used. Rheological characteristics of beverage concentrates that give the best compromise between low moisture content and handling can be achieved by selecting an appropriate droplet and stabilizer concentration.

#### 12.3.4.3 *Flavor*

The desired flavor profile for a particular beverage emulsion product depends on its type and label description, for example, orange, lemon, strawberry, cola, “tangy,” “fresh,” “creamy,” and so on (Heath, 1978; Shaw, 1986; Heath and Reineccius, 1986; Mathews, 1999). The overall flavor profile of a product is determined by the contribution of many different ingredients, including acids, sweeteners, oil-soluble flavors present within the droplets, water-soluble flavors dispersed in the aqueous phase, and volatile flavors in the headspace (Deibler and Acree, 2000; Mathews, 1999; Brandt, 2002). The equilibrium distribution and release rate of flavors also depend on the presence of nonflavoring compounds, for example, due to flavor binding to polysaccharides or proteins, or due to partitioning of flavors between oil, aqueous or interfacial phases (Guichard, 2002). The product manufacturer must therefore manipulate the type and concentration of the various flavoring and nonflavoring ingredients present to obtain the desired flavor profile (Chapter 9). Nevertheless, the flavor profile may change over time because some flavoring compounds are susceptible to chemical degradation (e.g., oxidation, hydrolysis, or polymerization) during storage or processing, which leads to loss of the original flavor profile and/or formation of undesirable off-flavors (Heath and Reineccius, 1986; Freeburg et al., 1994; Kuznetsova et al., 1996; Iwanami et al., 1997; Carlotti et al., 1999; Mathews, 1999; Rouseff and Naim, 2000). To avoid or minimize these changes it is often important to add preservatives (e.g., antioxidants, chelating agents), control product composition (e.g., oxygen, acidity, mineral content, biopolymer content), and control storage conditions (e.g., light exposure, temperature fluctuations).

(Heath, 1978; Mathews, 1999; Rouseff and Naim, 2000). The mouthfeel of beverage emulsions is largely determined by the presence of particulate matter (e.g., oil droplets or fruit pulp), sugars, and thickening agents (Mathews, 1999).

#### 12.3.4.4 Appearance

The overall appearance of beverage emulsions is determined principally by scattering of light by the emulsion droplets, and selective absorption of light by any colorants (Francis, 1999). The precise appearance therefore depends primarily on the droplet characteristics (size, concentration, refractive index) and the colorant characteristics (type and concentration). Finished beverage products usually have slightly turbid or “cloudy” appearances because the concentration of oil droplets present is relatively low (typically <0.1 wt%). The turbidity of beverage emulsions increases with increasing droplet concentration, and depends on droplet radius, having a maximum value of around 0.5  $\mu\text{m}$  (Hernandez and Baker, 1991; Hernandez et al., 1991). A variety of different natural and synthetic colorants are approved for use in beverage emulsions (Francis, 1999). The combination of colorants used in a particular beverage emulsion depends on consumer expectations arising from the name given on the product label, for example, orange juice (cloudy orange), cranberry juice (clear red), and lime juice (clear green). The appearance of a beverage emulsion may change during storage due to alterations in the droplet or colorant characteristics. Droplet aggregation (flocculation or coalescence) or Ostwald ripening will change the size of the particles present, which alters their light scattering profiles, and therefore the emulsion turbidity or lightness (Chapter 10). The turbidity of a beverage emulsion may also be reduced if some of the oil droplets cream to the top of the product during storage. Many of the natural and synthetic colorants used in beverage emulsions are susceptible to chemical degradation during storage (Francis, 1999). The chemical degradation of colors can be controlled using many of the same methods as used for controlling degradation of flavors, for example, adding preservatives, controlling product composition, and controlling storage conditions.

## 12.4 Dressings

A wide variety of dressings are used on salads and in other foods to enhance their palatability and desirability, for example, mayonnaise, salad, French, Italian, Russian, Blue Cheese, Ranch, and Thousand Island dressings (Ford et al., 2004). The market for this type of product is growing as more exotic flavors and ingredients are introduced and more healthful versions are developed (Brandt, 1999). Most of these dressings are either O/W emulsions or fat-free products designed to mimic the physicochemical properties of O/W emulsions (Ford et al., 2004). The fat content of dressings varies from zero to more than 80% (Table 12.3). Detailed information about the production, testing and regulations pertaining to dressings and sauces can be found in the publications of the *Association of Dressings and Sauces* (Atlanta, Georgia). In general, dressings are sold either as prefabricated O/W emulsions or as separate oil and aqueous phases that are mixed together immediately prior to consumption. Only the former type of dressing will be considered in this chapter.

Dressings can be classified as either “spoonable” or “pourable” depending on their composition and rheological characteristics (Ford et al., 2004). Spoonable products tend to have a high fat content and exhibit strong plastic-like behavior so that they must be removed from their container with a spoon (or other suitable object), whereas pourable dressings tend to have a lower fat content and flow when poured from a bottle or other container. There are standards of identity within the U.S. governing the composition and properties of a number of types of dressings, including mayonnaise, salad dressing, and French dressing. These standards specify the type and amount of certain components that

**Table 12.3** Typical Fat Contents of Mayonnaise and Dressings.

Product	Fat Content (%)
Regular mayonnaise	~75
Reduced fat mayonnaise	~50
Light mayonnaise	~25
Low fat mayonnaise	~20
Fat-free mayonnaise	~0
Regular dressings	30–60
Reduced fat dressings	22–45
Light dressings	15–30
Low fat dressings	5–10
Fat-free dressings	~0

Source: Adapted from Association for Dressings and Sauces (2002).

a food must contain in order to be given a particular name (Nielsen, 2003). For example, in the U.S. the regulations specify that mayonnaise should contain >65% vegetable oil, >2.5% acetic or citric acid, egg-containing ingredients, and may contain various other specified optional ingredients, for example, salts, sugars, spices, and sequestrants (Code of Federal Regulations, 2002, Title 21, Volume 2, Part 169.140).

The development of more “healthy” versions of traditional dressings has been stimulated by increasing consumer awareness of the overconsumption of certain food components (e.g., cholesterol and saturated fats) and the underconsumption of others (e.g.,  $\omega$ -3 fatty acids) (Nettleton, 1995; Deis, 1997; Brandt, 1999). This has led to the popularity of “reduced fat,” “light,” “low fat,” or “fat-free” versions of traditional products, as well as the introduction of products fortified with health-promoting lipids, such as  $\omega$ -3 fatty acids, plant stanol esters, or plant sterol esters (Brandt, 1999). There are government regulations in many countries regarding the level of fat a product must contain in order to be given one of these names on its label (Nielsen, 2003). There has also been a trend toward the introduction of dressings containing more exotic flavors and ingredients (Brandt, 1999). In addition, there has been a push toward the creation of more “clean” labels by replacing synthetic ingredients (such as polysorbates) with more natural ones (such as dairy proteins) (Ford et al., 2004). The development of these new products has created fresh challenges for emulsion scientists working in the dressings industry, for example, how to incorporate these new ingredients without detrimentally influencing the physical or chemical stability of the system.

## 12.4.1 Composition

### 12.4.1.1 Dispersed phase

The droplets in dressings consist primarily of edible oils, but they may also contain oil-soluble components, such as flavors, antioxidants, and vitamins. A wide variety of different types of oils have traditionally been used in dressings, including soybean, cottonseed, corn, canola, olive, sesame, safflower, and sunflower oils (Hui, 1992). It is important that these “salad oils” do not crystallize (*cloud*) when exposed to refrigerator temperatures (e.g., 0°C for 5.5 h), presumably so that they do not promote emulsion instability through partial coalescence (Lopez, 1981; Hui, 1992). This can be achieved by using oils with low melting points, by removing high melting fractions by selective crystallization (*winterization*), or by adding components that retard crystal formation, such as polyglycerol esters of fatty acids (Brandt, 1999). Oils may also be processed prior to use to remove components that have a negative impact on color, flavor, or stability, for example, refining, deodorization,

and bleaching (Akoh and Min, 2002). More recently the food industry has developed and marketed dressings using various other types of oils in response to the consumer's desire for a more healthful diet, for example, plant sterol esters and oils containing  $\omega$ -3 fatty acids (Brandt, 1999).

As mentioned earlier, one of the major trends in the food industry is to reduce the fat content of dressings, which has led to the popularity of "reduced fat," "light," "low fat," or "fat-free" versions of traditional products (Table 12.3). The total fat content of dressings can be reduced by replacing the fat droplets with other nonfat ingredients that are designed to provide similar overall quality attributes (Ford et al., 2004). As we have seen in previous chapters, fat droplets play a variety of different roles in determining the overall appearance, texture, flavor, and stability of O/W emulsions (Chapters 7–10). Consequently, it is usually necessary to use a combination of nonfat ingredients with different functional roles to replace the quality attributes lost when fat droplets are removed. Biopolymers, such as gums, starch, and proteins are often incorporated into fat-reduced products to provide some of these functional attributes (Clegg, 1996). In particular, insoluble biopolymer complexes that have similar particle sizes to oil droplets have been found to mimic many of the desirable quality attributes of the fat droplets in dressings, for example, Simplese™, which is a microparticulated whey protein ingredient (Singer, 1996). One of the hardest quality attributes to imitate when the fat is removed is the flavor profile. This is because the fat phase acts as a solvent for many characteristic nonpolar flavors and controls their release rate during consumption (Ford et al., 2004). When the fat content is reduced the partitioning and release rate of flavor compounds is changed, which changes the flavor profile (Chapter 9). In addition, flavors may bind to certain types of proteins and polysaccharides, which also changes the flavor profile (Guichard, 2002). For these reasons, it is often necessary to supplement biopolymer fat replacers with other types of ingredients to obtain the desired flavor profile, such as surfactants or flavorings (Brandt, 1999).

An alternative method of reducing the fat content of dressings is to replace a fraction or all of the conventional oil with nondigestible fat-like molecules (such as Olestra™, a sucrose fatty acid ester) or specially designed triacylglycerols with reduced caloric levels (such as Salatrim™ and Caprenin™). An ideal fat replacer should provide all of the quality attributes provided by conventional fat, while being safe to consume and significantly reducing the overall fat and calorie content. One of the advantages of this method is that the overall droplet concentration remains the same, so that the physicochemical and sensory attributes of the product are fairly similar to those of a conventional product. To the author's knowledge these ingredients are not currently used in dressings because they are either not legally approved or they do not have suitable physicochemical properties. Even so, research is being carried out to determine their suitability for application in these products.

Another trend has been to replace traditional oils with more health-promoting oils, such as polyunsaturated lipids, which have been claimed to help reduce incidences of heart disease and cancer, as well as promoting brain development (Watkins and German, 2002; Kritchevsky, 2002). One of the main problems associated with incorporating polyunsaturated lipids into foods is their high susceptibility to oxidation (McClements and Decker, 2000). For example, mayonnaise containing fish oils, which are a good source of  $\omega$ -3 fatty acids, are particularly prone to lipid oxidation (Jacobsen et al., 1998, 1999a,b). A variety of strategies have therefore been developed to retard lipid oxidation in this type of product, for example, incorporating antioxidants, adding chelating agents to sequester iron, reducing the oxygen concentration, minimizing exposure to heat and light, avoiding contamination by prooxidants, and controlling interfacial properties (McClements and Decker, 2000). Dressings are also being marketed that contain plant sterol esters and plant

stanol esters, which have been claimed to reduce the risk of coronary heart disease by lowering blood cholesterol levels (Brandt, 1999).

#### 12.4.1.2 *Continuous phase*

The continuous phase of dressings consists of a variety of soluble and insoluble components dispersed in water. Depending on the product, the soluble fraction may contain acids, salts, sweeteners, colorants, flavors, antioxidants, chelating agents, and biopolymers, while the insoluble fraction may contain herbs, spices, starch granules, egg yolk granules, cheese fragments, and so on (Ford et al., 2004). The presence and characteristics of this type of particulate matter can usually be determined by optical or electron microscopy.

A wide variety of different thickening agents are used in dressings, with the majority being either natural or chemically modified polysaccharides, such as xanthan, starch, modified starch, cellulose gum, cellulose gel, carrageenans, alginates, locust bean gum, gum arabic, pectin, and guar gum. These components usually have extended molecular structures that increase the viscosity of the continuous phase, and thereby contribute desirable texture and mouthfeel to the emulsion (Stephan, 1995; Nussinovitch, 1997). The high viscosity of the aqueous phase also slows down the movement of oil droplets and other particular matter, which improves the shelf life of the product. The presence of these nonadsorbed biopolymers may also promote depletion flocculation of the oil droplets in dressings, which leads to the formation of a network of aggregated droplets that provides desirable textural attributes to the final product (Manoj et al., 1998a,b). Thickening agents are usually used alone or in combinations with each other to create desirable textural, mouthfeel and stability characteristics. The level of thickening agent required depends on the desired texture of the final product. If one is trying to produce a highly viscous product similar to a spoonable dressing or mayonnaise, then the lower the fat content the higher the level of thickening agent required to produce the same texture (Frank, 2000). From a practical viewpoint, it is important that thickening agents are used that are capable of withstanding the acidic conditions of the aqueous phase of dressings.

Chelating agents, such as ethylene diamine tetra acetate (EDTA), are often incorporated into dressings to sequester iron (a lipid oxidation catalyst), thereby slowing down the rate of lipid oxidation in the product (McClements and Decker, 2000). Lipid oxidation may also be retarded by adding antioxidants that will partition into the oil, interfacial region, or aqueous phases depending on their polarity (Jacobsen et al., 1999a,b). Sugars, salts, acids, and flavorings all contribute to the desirable taste and aroma of a product. Acids, such as acetic acid, lactic acid, citric acid, or phosphoric acid, are used to control the pH of the aqueous phase between 2.5 and 4.5, which helps prevent microbial growth. In addition, many of these acids are also capable of chelating iron, which slows down lipid oxidation (Jacobsen et al., 2001b, McClements and Decker, 2000). Many dressings contain preservatives and antimicrobials to extend their shelf life, such as benzoic acid, sodium benzoate, potassium benzoate, sorbic acid, and potassium sorbate.

#### 12.4.1.3 *Interfacial membrane*

The composition, structure, and properties of the interfacial membrane that surrounds the oil droplets in a dressing depend mainly on the type of surface-active substances present in the system (Ford et al., 2004). A variety of different classes of emulsifiers and other surface-active substances may be adsorbed to the droplet interfaces in dressings, including small molecule surfactants (e.g., polysorbates), phospholipids (usually from egg yolk or milk), proteins (usually from egg or milk), chemically modified polysaccharides (e.g., modified starch or propylene glycol alginate), and particulate matter

(e.g., from spices, mustard, starch, or egg yolk). These surface-active components may be added as specific emulsifier ingredients (e.g., whey protein concentrate) or they may be present in other more complex ingredients (e.g., whole milk or egg yolk). The emulsifiers used in dressings must be capable of functioning under acidic conditions, must be of consistent quality from batch-to-batch, and must be compatible with the other components present.

In most dressing products the primary role of the emulsifier is to prevent droplet coalescence, rather than droplet flocculation. Usually, droplet flocculation is a problem because it leads to an increase in the effective size of the particles, which promotes creaming instability (Section 7.5); however, this process is not usually important in dressings because the high disperse phase volume fraction or high viscosity of the aqueous phase severely restricts the movement of the droplets. To prevent droplet coalescence the interfacial membrane must be capable of generating a sufficiently strong repulsive force between the droplets that prevents them from coming into close proximity and/or it must have rheological characteristics that make it resistance to rupture (Chapter 7). Different types of emulsifiers perform these functions in different ways depending on their molecular structure, interactions, and properties.

In this section, we primarily focus on the characteristics of the interfacial membranes of mayonnaise and salad dressings because these products have been most widely studied and their interfacial composition is largely determined by the type of ingredients specified in governmental regulations. Mayonnaise and salad dressing are mainly stabilized by surface-active components in eggs, that is, proteins, phospholipids, and lecithin–protein particulate complexes (Mine, 1998a,b, Anton et al., 2000a,b, Le Denmat et al., 2000). These components are capable of forming interfacial membranes that are resistant to rupture and that are capable of generating strong repulsive interactions between the droplets. Egg ingredients can be purchased in a variety of different forms for usage in dressings, including liquid egg yolks, frozen egg yolks, dried egg yolks, liquid whole eggs, frozen whole eggs, and dried whole eggs. Different egg ingredients are usually prepared using different processing treatments, which influences their effectiveness at stabilizing mayonnaise (Paraskevopoulou et al., 1999; Guerrero et al., 2000; Moros et al., 2002a,b). Microscopy studies indicate that other kinds of particulate matter may also be adsorbed to the oil droplet surfaces in mayonnaise and salad dressings, such as mustard, spice, and starch granules (Langton et al., 1999; Ford et al., 2004). It has been postulated that these granules may also make an important contribution in stabilizing the droplets against aggregation through a particle stabilization mechanism (Ford et al., 2004). The ability of egg components to stabilize emulsion droplets is discussed in more detail in Section 4.4.2.

#### 12.4.2 *Microstructure*

In general, emulsion-based dressings consist of oil droplets dispersed in an aqueous medium (Langton et al., 1999; Ford et al., 2004). Nevertheless, their properties can vary widely because of their different compositions and microstructures. The mean radius of the oil droplets varies from 1 to 40  $\mu\text{m}$ , and the oil content from nearly zero to over 80%, depending on the product (Ford et al., 2004). The type of emulsifier used to stabilize the system may also vary considerably from product-to-product, for example, small molecule surfactants, proteins, polysaccharides, or colloidal complexes. In some products the droplets are flocculated, whereas in others they are not. The continuous phase of dressings may or may not contain colloidal particles or other nondissolved suspended matter depending on the type of ingredients used as emulsifiers, stabilizers, texture modifiers, and flavorings. Consequently, dressings may exhibit a wide variety of different kinds of microstructures.



The oil content in mayonnaise is so high (75–84%) that the droplets are close packed and many of them have nonspherical shapes (Langton et al., 1999). The larger droplets tend to have a greater nonsphericity than the smaller ones, presumably because of their lower Laplace pressure and therefore greater deformability (Chapter 5). The droplets in mayonnaise typically have a mean radius of around 1–2  $\mu\text{m}$ , but the distribution of droplet sizes is usually rather broad, ranging from around 0.1 to over 10  $\mu\text{m}$ . This means that smaller droplets can pack efficiently between larger droplets, so that the emulsion can have a droplet concentration exceeding the theoretical maximum packing limit for monodisperse spherical particles (Langton et al., 1999; Ford et al., 2004). The oil droplets in mayonnaise are surrounded by an interfacial membrane that has an average thickness of around 14 nm, which is comprised of surface-active proteins and lecithin-protein granules from egg yolk (Langton et al., 1999; Ford et al., 2004). The aqueous phase may also contain a network of aggregated egg yolk granules, which may contribute to the stability and rheology of the product (Langton et al., 1999).

Salad dressings also have fairly high fat concentrations (30–60%) and relatively small mean droplet radii (1–2  $\mu\text{m}$ ). At the higher fat concentrations, the droplets tend to be packed fairly densely into the system and may be nonspherical (Ford et al., 2004). Pourable dressings, such as French, Italian, Russian, and Thousand island, tend to have lower fat contents (30–45%) and higher mean droplet radii (5–20  $\mu\text{m}$ ) than salad dressings. Consequently, the droplets are usually less densely packed and the droplets are spherical. When products are viewed by optical or electron microscopy it is often possible to observe nondissolved matter at the oil–water interface or dispersed in the aqueous phase, for example, egg yolk granules, starch granules, mustard particles, herbs, spices, cheese, and so on (Ford et al., 2004). In many systems it is observed that the droplets are flocculated with each other, which can be attributed to depletion or bridging flocculation induced by the presence of sufficiently high concentrations of thickening or gelling agents. Nevertheless, the flocculated droplets do not cream because of the high viscosity or yield stress of the aqueous phase and/or because they form a particle network. An optical microscopy picture of a typical salad dressing is shown in Figure 12.5, which shows highly polydisperse oil droplets suspended in an aqueous medium.

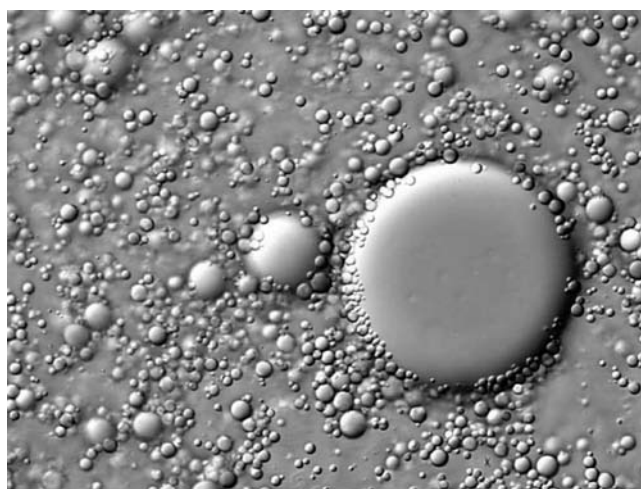


**Figure 12.5** Salad dressing evaluated using Differential Interference Contrast (DIC), a general contrast enhancement optical method which highlights differences in refractive indices in heterogeneous samples. Picture kindly supplied by Kraft Foods ©.

### 12.4.3 Production

The precise nature of the manufacturing process used to prepare a dressing depends on the product type. Dressings can be produced using either continuous or batch processes (Lopez, 1981; Hui, 1992). The various ingredients used to prepare the aqueous phase are often mixed together initially to ensure that they are adequately dissolved or dispersed, for example, water, vinegar, sweeteners, spices, and thickening agents. Sometimes powdered ingredients may be mixed together prior to incorporation into the aqueous phase. In some processing operations a part of the aqueous phase components is added at one stage, and the remainder is added at a later stage (Lopez, 1981). The aqueous phase may undergo some kind of heat treatment to facilitate the development of the functional properties of the thickening agent, for example, cook-up starches may need gelatinization. Any oil-soluble components that need to be incorporated into the product can be mixed with the oil phase prior to homogenization or with the oil and aqueous phases during the blending stage. High-speed blenders are used to produce dressings that contain relatively large droplet sizes ( $r > 5 \mu\text{m}$ ). A combination of a high-speed blender and a homogenizer (colloid mill or high-pressure valve homogenizer) is usually used to produce dressings with small droplet sizes, for example, mayonnaise and salad dressing (Hui, 1992). The product may then be heat-treated to inactivate microbes prior to packaging and storing. Special processing requirements are needed for some types of dressings (Hui, 1992). For example, in mayonnaise production small aliquots of oil phase may be slowly fed into a high-speed blender to form a course emulsion. The rate of addition of the oil must be carefully controlled to avoid phase inversion of the product. The course emulsion is then homogenized using a colloid mill to reduce its droplet size. It is usually important to avoid freezing, heating, or excessive mechanical agitation of dressings during storage and transport to avoid product breakdown (Dickinson and Stainsby, 1982).

### 12.4.4 Physicochemical properties

#### 12.4.4.1 Stability

The required stability of dressings may vary from a few minutes (e.g., products where separate oil and aqueous phases are mixed together immediately prior to usage by the consumer) to years (e.g., commercial mayonnaise). In general, the term stability means preserving the appearance, texture, and taste of a product throughout its anticipated shelf life. From an emulsion science perspective this usually involves preventing droplet coalescence, flocculation,\* and/or creaming. Nevertheless, there may also be chemical or biochemical changes in a product that also lead to quality deterioration, such as oxidation or hydrolysis reactions (Lopez, 1981).

Creaming is not usually a problem in dressings that have high fat contents (>50–60%) because the droplets are so closely packed together that they cannot move, for example, spoonable salad dressings and mayonnaise. In products with lower fat contents, creaming is usually prevented by adding thickening or gelling agents to the aqueous phase to slow down droplet movement, for example, gums or starches. These texture modifiers often promote droplet flocculation through a depletion or bridging mechanism; however, the system is still stable to creaming because the viscosity of the aqueous phase is so high (or there is a sufficiently high yield stress) that the flocs cannot move or they are trapped in a particle network.

The driving force for droplet flocculation in dressings depends on the product. In mayonnaise it is likely to be screening of electrostatic repulsion between droplets, whereas

\* In some cases flocculation may be desirable because it leads to a desirable texture for the product.

in many nontraditional dressings it may be depletion or bridging flocculation by biopolymers in the aqueous phase. Droplet flocculation is usually considered to be undesirable in food emulsions because it increases instability to creaming, but it may actually be desirable in dressings. Droplet flocculation increases the viscosity of the emulsion, or may even give it gel-like properties due to the formation of a three-dimensional network of aggregated particles (Parker et al., 1995; Manoj et al., 1998a,b), which may reduce the amount of other components required to modify the texture of the system.

Prevention of coalescence is of paramount importance in many salad dressings because it leads to the formation of free oil on the product surface, which is perceived as being undesirable. Coalescence is the result of droplets coming together and merging with each other (Section 7.6). In order for it to occur the droplets must come into close proximity, and the interfacial membranes surrounding the droplets must be disrupted so that the material from one droplet can flow into another. The most effective means of retarding or preventing coalescence are to prevent the oil droplets from getting too close together or having interfacial membranes that are resistant to rupture. Droplets can be prevented from coming into close proximity by generating sufficiently strong repulsive forces between them, for example, electrostatic, steric, hydration, particle, or structuring forces (Ford et al., 2004). The most important stabilizing force in a particular dressing depends on the type of emulsifier used (e.g., protein, polysaccharide, surfactant, colloid particle) and the environmental conditions (e.g., pH and ionic strength). Most dressings contain relatively high concentrations of salt so that the electrostatic repulsive forces are highly screened. Steric repulsion is therefore expected to be the dominant mechanisms in many systems, especially those stabilized by relatively thick layers of biopolymers or colloidal particles (Le Denmat et al., 2000). It has been proposed that particle stabilization is important in systems containing adsorbed colloidal particles at the interfacial membranes, such as egg yolk, spice, or starch granules (Ford et al., 2004). A stabilizing mechanism known as "structuring" has been proposed to account for the stability of some dressing products (Ford et al., 2004). This occurs due to the stratification of nonadsorbed colloidal particles (such as surfactant micelles, starch granules, biopolymer aggregates) between the emulsion droplets, which generates a short-range repulsive interaction.

Certain types of emulsifiers form highly viscoelastic interfacial membranes that are flexible but resistant to rupture, for example, polysaccharides, aggregated proteins, or colloidal particles. The presence of these interfacial membranes may protect droplets from coalescence, even when the droplets are in close contact for extended periods, as is the case in mayonnaise and salad dressings.

Commercially prepared dressings and mayonnaise are usually considered to be very safe with regard to microbial stability because foodborne pathogens do not grow in the acidic conditions present in these products, that is,  $\text{pH} < 4.4$  (Smittle, 1977, 2000). In addition, certain organic acids used in these products, such as acetic acid, are particularly effective at preventing microbial growth or killing added bacteria, presumably by chelating mineral ions essential for bacterial function. Many dressings also contain preservatives and antimicrobials to slow down bacterial growth, such as sodium benzoate or benzoic acid.

A variety of chemical degradation mechanisms can also occur in dressings during storage that will reduce their quality, for example, polysaccharide hydrolysis or lipid oxidation (Jacobsen, 1999). Lipid oxidation is the result of the interaction of unsaturated lipids with oxygen and leads to the generation of undesirable off-flavors and potentially harmful reaction products. Its progress can be retarded in dressings using a variety of different strategies, for example, adding chelating agents to sequester iron, incorporation of antioxidants, reducing the oxygen concentration, avoiding exposure to heat and light, avoiding prooxidants and interfacial engineering (McClements and Decker, 2000).

#### 12.4.4.2 Rheology

The rheological properties of dressings are one of the major factors that influence their perceived quality. The “pourability,” “flowability,” and “spreading” of dressings during their application, and the perceived “thickness” or “creaminess” of dressings during mastication depend strongly on their rheological characteristics (Mela et al., 1994; Wendin et al., 1997a,b, 1999; Wendin and Hall, 2001). The shelf life of dressings depends on the ability to reduce gravitational separation of emulsion droplets and other suspended matter, which depends mainly on the rheology of the aqueous phase. Rheology also plays an important role during the processing of this type of product, since it affects processes such as mixing, stirring, homogenization, and pumping through pipes. It is therefore important for food manufacturers to have a thorough understanding of the rheological properties of dressings and of the factors that determine these properties.

The rheology of most dressings is highly complex, depending on both the magnitude and duration of the stress applied (Franco et al., 1995a,b, 1997; Bower et al., 1999; Stern et al., 2001). Many dressings can be considered to behave as nonideal plastic materials. Below a critical yield stress ( $\tau_{cr}$ ) they are not permanently deformed on timescales of relevance for consumer applications. At these small stresses dressings behave like viscoelastic solids and can be characterized in terms of a complex modulus with real and imaginary parts (e.g.,  $G'$  and  $G''$ ). Above the yield stress, dressings flow and are permanently deformed once the applied stress is removed (Gallegos et al., 1992). At these relatively high stresses, dressings behave like viscoelastic liquids that exhibit strong shear-thinning characteristics. Their apparent viscosity may decrease both with increasing shear stress (pseudoplasticity) and with increasing time (thixotropy). Full characterization of the rheological properties of a dressing therefore depends on making a variety of different measurements, for example, determination of  $\tau_{cr}$  from stress versus strain measurements, determination of the complex modulus below  $\tau_{cr}$  from small strain oscillatory measurements, determination of the apparent viscosity versus shear stress above  $\tau_{cr}$  from shear flow measurements. It should be noted; however, that characterization of the rheological properties of dressings is often complicated due to slip, particle migration, sample history, and stress overshoot effects (Goshawk et al., 1998; Franco et al., 1998a; Plucinski et al., 1998; Guerrero et al., 2000).

The existence of a yield stress and shear-thinning rheological behavior is crucial for the successful application of dressings. Droplet creaming during storage is retarded or prevented by the yield stress or the extremely high viscosity of dressings at low shear stresses. The presence of a yield stress also means that the dressings will retain their shape after being poured or spread onto a product, rather than rapidly flowing away. Consumers use the perceived pourability, spreadability, thickness, and creaminess to judge the quality of a product. For example, a dressing should usually flow slowly from a container, rather than being runny like water. Some studies suggest that shear thinning plays an important role in determining the mouthfeel of dressings, whereas others suggest that it is the apparent viscosity of the product at conditions close to those experienced in the mouth (Morris, 1995b).

The bulk rheological characteristics of dressings, like other emulsions (Chapter 8), are largely determined by the rheological characteristics of the continuous phase and the properties of the emulsion droplets for example, their concentration, particle size distribution, and interactions. In high fat products ( $\phi = 0.4\text{--}0.8$ ), the existence of a yield stress and shear-thinning behavior is dominated by the characteristics of the oil droplets. The oil droplets are packed so closely together that there is a strong resistance to flow. At sufficiently high droplet concentrations the product gains solid-like characteristics, which can be characterized by a shear modulus (Franco et al., 1995a,b, 1997). The shear modulus increases with increasing droplet concentration and decreasing droplet size (Franco et al., 1995a,b,

Langton et al., 1999). In lower fat products ( $\phi = 0\text{--}0.4$ ), the droplets alone are unable to provide this yield stress and shear-thinning behavior. Instead, this must be achieved by adding texture modifiers (thickening or gelling agents) to the aqueous phase (Wendin and Hall, 2001). These texture modifiers are usually natural or chemically modified biopolymers that increase the solution viscosity either directly or indirectly. Biopolymers, such as gums or starches, modify the rheology *directly* by providing a small yield stress, greatly increasing the aqueous phase viscosity, and generating shear-thinning behavior. Biopolymers may also modify the rheology of dressings *indirectly* by altering the strength of the attractive forces between the droplets, thereby promoting droplet aggregation, for example, by depletion or bridging mechanisms (Parker et al., 1995). In this case, the rheology of the system depends on the strength of the droplet–droplet attraction and the structure of the flocs formed (Tuinier and de Kruif, 1999). At sufficiently high droplet concentrations, a three-dimensional network of aggregated droplets may extend throughout the system, which provides solid-like characteristics to the overall emulsion (Manoj et al., 1998a,b, 2000). In principle, surface-active biopolymers can also modify emulsion rheology indirectly by forming an interfacial membrane that is relatively thick compared to the droplet radius, thereby increasing the effective volume fraction of the droplets (Section 8.4.6).

In fat-reduced products, the objective is often to generate an apparent viscosity versus shear stress profile that mimics that of comparable full fat products so that their flow behaviors are similar, for example, pourability, spreadability, and mouthfeel. This is usually achieved by controlling the type, concentration, and interactions of one or more biopolymers incorporated into the aqueous phase (Clegg, 1996; Wendin et al., 1997a,b, 1999; Wendin and Hall, 2001).

#### 12.4.4.3 Appearance

Dressings tend to be optically opaque because the relatively high droplet concentration ( $\phi > 5\%$ ) leads to extensive light scattering (Chapter 10). When the fat content is reduced below about 5% the lightness of emulsions decreases appreciably, hence it is necessary to add nonfat particles that scatter light to fat-reduced dressings in order to create appearances similar to those observed in full fat products, for example, particulated proteins, polysaccharides, or their complexes. A variety of ingredients within mayonnaise and salad dressings naturally adsorb radiation in the visible region of the electromagnetic spectrum and therefore contribute to the color, for example, oils and egg yolk (Lopez, 1981). Additional colorants are added to some products to produce a more desirable overall appearance, for example, fruit juice, vegetable juice, caramel extract, annatto extract, or  $\beta$ -carotene.

#### 12.4.4.4 Flavor

The overall flavor of dressings is due to a combination of factors, including volatile odor molecules, nonvolatile taste molecules, and mouthfeel (Depree and Savage, 2001; Ford et al., 2004). The taste of mayonnaise and other dressings is largely determined by water-soluble or water-dispersible components such as acidulants (e.g., vinegar, lemon juice), sweeteners (natural or artificial), and seasonings (e.g., salt, mustard, pepper, paprika, onion, garlic). The aroma of dressings is determined by small volatile molecules, which may be associated with other major ingredients (e.g., oil, vinegar, lemon juice) or added as flavorings (e.g., herbs, spices). It should be noted that chemical degradation reactions may change the flavor profile of a dressing during storage. This change may be due to loss of desirable flavor components or due to formation of undesirable flavor components, for example, from lipid oxidation (Jacobsen, 1999a,b, Jacobsen et al., 1999). The desirable mouthfeel of dressings is contributed mainly by the emulsion droplets and thickening agents dispersed throughout the aqueous phase (Wendin et al., 1997a,b, 1999; Wendin and Hall, 2001).

One of the major problems associated with developing fat-reduced versions of conventional dressings is the change in the flavor profile due to removal of the fat droplets. The equilibrium partitioning and mass transfer kinetics of flavor molecules in O/W emulsions are strongly governed by the overall fat content (Chapter 9). In addition, fat droplets give dressings a “creamy” or “fatty” mouthfeel that is lost when they are removed to create fat-reduced products (Mela et al., 1994). It is often possible to replace at least some of this desirable mouthfeel by using thickening agents that give the product a high viscosity and shear-thinning behavior, and by using microparticulated biopolymer spheres that have similar dimensions to fat droplets. It is more difficult to mimic the odor and taste of conventional dressings once fat has been removed (Ford et al., 2004). When the fat content is reduced the partitioning and release rate of flavor compounds is changed, which changes the flavor profile. In addition, flavors can bind to certain types of proteins and polysaccharides, which may also change the flavor profile of the product.



---

# References

- Abismail, A., Canselier, J.R., Wilhelm, A.M., Delmas, H., Gourdon, C. (1999). Emulsification by ultrasound: Drop size distribution and stability. *Ultrasonics Sonochemistry*, **6**, 75.
- Adams, R.L., Mottram, D.S., Parker, J.K., Brown, H.M. (2001). Flavor-protein binding: Disulfide interchange reactions between ovalbumin and volatile disulfides. *Journal of Agricultural and Food Chemistry*, **49**, 4333.
- Adamson, A.W. (1990). *Physical Chemistry of Surfaces*, John Wiley & Sons, New York, NY.
- Agboola, S.O., Dalgleish, D.G. (1995). Calcium-induced destabilization of oil-in-water emulsions stabilized by caseinate or by  $\beta$ -lactoglobulin. *Journal of Food Science*, **60**, 399.
- Agboola, S.O., Dalgleish, D.G. (1996a). Kinetics of calcium-induced instability of oil-in-water emulsions: Studies under quiescent and shearing conditions. *Food Science and Technology — Lebensmittel Wissenschaft und Technologie*, **29**, 425.
- Agboola, S.O., Dalgleish, D.G. (1996b). Enzymatic hydrolysis of milk proteins used for emulsion formation. Part 1: Kinetics of protein breakdown and storage stability of the emulsions. *Journal of Agriculture and Food Science*, **44**, 3631.
- Agboola, S.O., Dalgleish, D.G. (1996c). Enzymatic hydrolysis of milk proteins used for emulsion formation. Part 2: Effects of calcium, pH and ethanol on the stability of the emulsions. *Journal of Agriculture and Food Science*, **44**, 3637.
- Agboola, S.O., Dalgleish, D.G. (1996d). Effects of pH and ethanol on the kinetics of destabilization of oil-in-water emulsions containing milk proteins. *Journal of the Science of Food and Agriculture*, **72**, 448.
- Aguilera, J.M., Stanley, D.W. (1990). *Microstructural Principles of Food Processing and Engineering*, Elsevier, Amsterdam.
- Akintayo, E.T., Esuoso, K.O., Oshodi, A.A. (1998). Emulsifying properties of some legume proteins. *International Journal of Food Science and Technology*, **33**, 239.
- Akoh, C.C., Min, D.B. (2002). *Food Lipids: Chemistry, Nutrition and Biotechnology*, Marcel Dekker, New York, NY.
- Alaimo, M.H., Kumosinski, T.F. (1997). Investigation of hydrophobic interactions in colloidal and biological systems by molecular dynamics simulations and NMR spectroscopy. *Langmuir*, **13**, 2007.
- Alber, T. (1989). Stabilization energies of protein conformation, in *Prediction of Protein Structure and the Principles of Protein Conformation*, Fasman, G.D., Ed., Plenum Press, New York, NY, p. 161.
- Allouche, J., Tyrode, E., Sadtler, V., Choplin, L., Salager, J.L. (2003). Emulsion morphology follow-up by simultaneous *in situ* conductivity and viscosity measurements during a dynamic temperature-induced transition inversion, in *Proceedings of the Third International Symposium on Food Rheology and Structure*, Fischer, P., Marti, I., Windhab, E.J., Eds., Laboratory of Food Process Engineering, Zurich, Switzerland, p. 19.
- Anandarajah, A., Chen, J. (1995). Single correction function for computing retarded van der Waals attraction. *Journal of Colloid and Interface Science*, **176**, 293.
- Ananthapadmanabhan, K.P. (1993). Protein-surfactant interactions, in *Interactions of Surfactants with Polymers and Proteins*, Goddard, E.D., Ananthapadmanabhan, K.P., Eds., CRC Press, Boca Raton, FL, p. 319.



- Andriot, I., Marin, I., Feron, G. (1999). Binding of benzaldehyde by  $\beta$ -lactoglobulin, by static headspace and high performance liquid chromatography in different physico-chemical conditions. *Lait*, **79**, 577.
- Andriot, I., Harrison, M., Fournier, N. (2000). Interactions between methyl ketones and  $\beta$ -lactoglobulin: Sensory analysis, headspace analysis, and mathematical modeling. *Journal of Agricultural and Food Chemistry*, **48**, 4246.
- Anema, S.G., Li, Y.M. (2003a). Association of denatured whey proteins with casein micelles in heated reconstituted skim milk and its effect on casein micelle size. *Journal of Dairy Research*, **70**, 73.
- Anema, S.G., Li, Y.M. (2003b). Effect of pH on the association of denatured whey proteins with casein micelles in heated reconstituted skim milk. *Journal of Agricultural and Food Chemistry*, **51**, 1640.
- Anton, M., Gandemer, G. (1999). Effect of pH on interface composition and on quality of oil-in-water emulsions made with hen egg yolk. *Colloids and Surfaces B: Biointerfaces*, **12**, 351.
- Anton, M., Beaumal, V., Gandemer, G. (2000a). Thermostability of hen egg yolk granules: Contribution of native structure of granules. *Journal of Food Science*, **65**, 581.
- Anton, M., Beaumal, V., Gandemer, G. (2000b). Adsorption at the oil-water interface and emulsifying properties of native granules from egg yolk: Effect of aggregated state. *Food Hydrocolloids*, **14**, 327.
- Anton, M., Le Denmat, M., Beaumal, V., Pilet, P. (2001). Filler effects of oil droplets on the rheology of heat-set emulsion gels prepared with egg yolk and egg yolk fractions. *Colloids and Surfaces B: Biointerfaces*, **21**, 137.
- Anton, M., Beaumal, V., Brossard, C., Llamas, G., Gandemer, G. (2002). Droplet flocculation and physical stability of oil-in-water emulsions prepared with hen egg yolk, in *Food Emulsions and Dispersions*, Anton, M., Ed., Research Signpost, Trivandrum, India.
- Aoki, H., Shirase, Y., Kato, J., Watanabe, Y. (1984). Emulsion stabilizing properties of soy protein isolates mixed with sodium caseinates. *Journal of Food Science*, **49**, 212.
- Arlauskas, R.A., Weers, J.G. (1996). Sedimentation field-flow fractionation studies of composition ripening in emulsion mixtures. *Langmuir*, **12**, 1923.
- Aronson, M.P. (1992). Surfactant induced flocculation of emulsions, in *Emulsions: A Fundamental and Practical Approach*, Sjblom, J., Ed., Kluwer Academic Publishers, The Netherlands, p. 75.
- Arvisenet, G., Voilley, A., Cayot, N. (2002). Retention of aroma compounds in starch matrices: Competitions between aroma compounds toward amylose and amylopectin. *Journal of Agricultural and Food Chemistry*, **50**, 7345.
- Asami, K. (1995). Evaluation of colloids by dielectric spectroscopy. *HP Application Note 380-3*, Hewlett Packard, Paolo Alto, CA.
- Atkins, P. (2003). *Atkin's Molecules*, 2nd ed., Cambridge University Press, Cambridge, UK.
- Atkins, P.W. (1994). *Physical Chemistry*, 5th ed., Oxford University Press, Oxford, UK.
- Atkinson, P.J., Dickinson, E., Horne, D.S., Richardson, R.M. (1995). Neutron reflectivity of adsorbed  $\beta$ -casein and  $\beta$ -lactoglobulin at the air/water interface. *Journal of the Chemical Society—Faraday Transactions*, **91**, 2847.
- Attard, P. (2003). Nanobubbles and the hydrophobic attraction. *Advances in Colloid and Interface Science*, **104**, 75.
- Aveyard, R., Binks, B.P., Clark, S., Fletcher, P.D.I. (1990). Cloud points, solubilization and interfacial tensions in systems containing nonionic surfactants. *Chemical Technology and Biotechnology*, **48**, 161.
- Awad, T., Sato, K. (2001). Effects of hydrophobic emulsifier additives on crystallization behavior of palm mid fraction in oil-in-water emulsion. *Journal of the American Oil Chemists Society*, **78**, 837–842.
- Awad, T., Sato, K. (2002). Acceleration of crystallisation of palm kernel oil in oil-in-water emulsion by hydrophobic emulsifier additives. *Colloids and Surfaces B: Biointerfaces*, **25**, 45.
- Awad, T., Hamada, Y., Sato, K. (2001). Effects of addition of diacylglycerols on fat crystallization in oil-in-water emulsion. *European Journal of Lipid and Science Technology*, **103**, 735.
- Azzam, R.M., Bachara, N.M. (1989). *Ellipsometry and Polarized Light*, North-Holland, Amsterdam.
- Azzam, M.O.J., Omari, R.M. (2002). Stability of egg white-stabilized edible oil emulsions using conductivity technique. *Food Hydrocolloids*, **16**, 105.

- Baianu, I.C. (1992). *Physical Chemistry of Food Processes, Vol. 1. Fundamental Aspects*, Van Nostrand Reinhold, New York, NY.
- Baianu, I.C., Pessen, H., Kumosinski, T.F. (1995). *Physical Chemistry of Food Processes: New Techniques, Structures and Applications*, Aspen Publishers, New York, NY.
- Bailey, A.E., Cannell, D.S. (1994). Practical method for calculation of multiple light scattering. *Physical Review E*, **50**, 4853.
- Baines, Z.V., Morris, E.R. (1989). Suppression of perceived flavor and taste by hydrocolloids, in *Food Colloids*, Bee, R.D., Richmond, P., Mingins, J., Eds., Royal Society of Chemistry, Cambridge, UK, p. 184.
- Baker, E.N., Hubbard, R.E. (1984). Hydrogen bonding in globular proteins. *Progress in Biophysics and Molecular Biology*, **44**, 97.
- Baker, R. (1987). *Controlled Release of Biologically Active Agents*, John Wiley & Sons, New York, NY.
- Bakker, J. (1995). Flavor interactions with the food matrix and their effects on perception, in *Ingredient Interactions: Effects on Food Quality*, Gaonkar, A.G., Ed., Marcel Dekker, New York, NY.
- Bakker, J., Mela, D.J. (1996). Effect of emulsion structure on flavor release and taste perception, in *Flavor-Food Interactions*, McGorin, R.J., Leland, J.V., Eds., American Chemical Society, Washington, DC, Chap. 4.
- Bakker, J., Boudaud, N., Harrison, M. (1998). Dynamic release of diacetyl from liquid gelatin in the headspace. *Journal of Agricultural and Food Chemistry*, **46**, 2714.
- Baldwin, R.W., Cloninger, M.R., Lindsay, R.C. (1973). Flavor thresholds for fatty acids in buffered solutions. *Journal of Food Science*, **38**, 528.
- Balinov, B., Mariette, F., Soderman, O. (2004). NMR studies of emulsions with particular emphasis on food emulsions, in *Food Emulsions*, 4th ed., Friberg, S., Larsson, K., Sjoblom, J., Eds., Marcel Dekker, New York, NY, Chap. 15.
- Banavara, D.S., Rabe, S., Krings, U., Berger, R.G. (2002). Modeling dynamic flavor release from water. *Journal of Agricultural and Food Chemistry*, **50**, 6448.
- Banks, W., Muir, D.D. (1988). Stability of alcohol containing emulsions, in *Advances in Food Emulsions and Foams*, Dickinson, E., Stainsby, G., Eds., Elsevier, London, UK, Chap. 8.
- Barfod, N.M. (1995). Methods for characterization of structure in whippable dairy based emulsions, in *Characterization of Foods: Emerging Techniques*, Gaonkar, A.G., Ed., Elsevier, Amsterdam, Chap. 3.
- Barfod, N.M., Krog, M. (1987). Destabilization and fat crystallization of whippable emulsions (top-pings) studied by pulsed NMR. *Journal of the American Oil Chemists Society*, **64**, 112.
- Barfod, N.M., Krog, N., Bucheim, W. (1987). Protein fat surfactant interactions in whippable emulsions, in *Food Emulsions and Foams*, Dickinson E., Ed., Royal Society of Chemistry, Cambridge, UK, p. 141.
- Barfod, N.M., Krog, N., Larsen, G., Bucheim, W. (1991). Effects of emulsifiers on protein-fat interaction in ice cream mix during ageing. Part I: Quantitative analysis. *Fat Science Technology*, **93**, 24.
- Barnes, H.A. (1994). Rheology of emulsions—a review. *Colloids and Surfaces*, **91**, 89.
- Barnes, H.A., Nguyen, Q.D. (2001). Rotating vane rheometry—review. *Journal of Non-Newtonian Fluid Mechanics*, **98**, 1.
- Barylko-Pilielna, N., Martin, A., Mela D.J. (1994). Perception of taste and viscosity of oil-in-water and water-in-oil emulsions. *Journal of Food Science*, **59**, 1318.
- Basaran, T., Demetriades, K., McClements, D.J. (1998). Ultrasonic imaging of gravitational separation in emulsions. *Colloids and Surfaces*, **136**, 169.
- Becher, P. (1957). *Emulsions: Theory and Practice*, Chapman & Hall, London, UK.
- Becher, P. (1983). *Encyclopedia of Emulsion Technology, Vol. 1. Basic Theory*, Marcel Dekker, New York, NY.
- Becher, P. (1985). Hydrophile-lipophile balance: An updated bibliography, in *Encyclopedia of Emulsion Technology*, Vol. 2, Becher, P., Ed., Marcel Dekker, New York, NY.
- Becher, P. (1996). HLB: Update III, in *Encyclopedia of Emulsion Technology*, Vol. 4, Becher, P., Ed., Marcel Dekker, New York, NY.
- Behrend, O., Ax, K., Schubert, H. (2000). Influence of continuous phase viscosity on emulsification by ultrasound. *Ultrasonics Sonochemistry*, **7**, 77.

- Bell, G.A. (1996). Molecular mechanisms of olfactory perception: Their potential for future technologies. *Trends in Food Science and Technology*, **7**, 425.
- BeMiller, J.N., Whistler, R.L. (1996). Carbohydrates, in *Food Chemistry*, 3rd ed., Fennema, O.R., Ed., Marcel Dekker, New York, NY, p. 157.
- Benichou, A., Aserin, A., Garti, N. (2001). Polyols, high pressure and refractive indices equalization for improved stability of W/O emulsions for food applications. *Journal of Dispersion Science and Technology*, **22**, 269.
- Benichou, A., Aserin, A., Garti, N. (2002a). Double emulsions stabilized by new molecular recognition hybrids of natural polymers. *Polymers for Advanced Technologies*, **13**, 1019.
- Benichou, A., Aserin, A., Garti, N. (2002b). Protein-polysaccharide interactions for stabilization of food emulsions. *Journal of Dispersion Science and Technology*, **23**, 93.
- Benjamins, J., Cagna, A., Lucassen-Reynders, E.H. (1996). Viscoelastic properties of triacylglycerol/water interfaces covered by proteins. *Colloid and Surfaces*, **114**, 245.
- Benjamins, J., Lucassen-Reynders, E.H. (1998). Surface dilational rheology of proteins adsorbed at air/water and oil/water interfaces. In: *Proteins at Liquid Interfaces*, Mobius, D., Miller, R., Eds., Elsevier Science, Amsterdam, Netherlands, 341.
- Ben-Naim, A. (1980). *Hydrophobic Interactions*, Plenum Press, New York, NY.
- Bentley, B.J., Leal, L.G. (1986). An experimental investigation of drop deformation and breakup in steady, two-dimensional linear flows. *Journal of Fluid Mechanics*, **167**, 241.
- Bergenholtz, J. (2001). Theory of rheology of colloidal dispersions. *Current Opinion in Colloid and Interface Science*, **6**, 484.
- Bergenstahl, G. (1997). Physicochemical aspects of an emulsifier functionality, in *Food Emulsifiers and Their Applications*, Hasenhuettl, G.L., Hartel, R.W., Eds., Chapman & Hall, New York, NY, Chap. 6.
- Bergenstahl, B.A., Claesson, P.M. (1997). Surface forces in emulsions, in *Food Emulsions*, 3rd ed., Friberg, S., Larsson, K., Eds., Marcel Dekker, New York, NY, p. 57.
- Berger, K.G. (1997). Ice cream, in *Food Emulsions*, 3rd ed., Friberg, S., K. Larsson, Eds., Marcel Dekker, New York, NY, Chap. 9.
- Bergethon, P.R. (1998). *The Physical Basis of Biochemistry*, Springer, New York, NY.
- Bergethon, P.R., Simons, E.R. (1990). *Biophysical Chemistry: From Molecules to Membranes*, Springer-Verlag, New York, NY.
- Berli, C.L.A., Quemada, D., Parker, A. (2002). Modelling the viscosity of depletion flocculated emulsions. *Colloids and Surfaces A: Physicochemical and Engineering Aspects*, **203**, 11.
- Berli, C.L.A., Quemada, D., Parker, A. (2003). Gel transition of depletion flocculated emulsions. *Colloids and Surfaces A: Physicochemical and Engineering Aspects*, **215**, 201.
- Besseling, N.A.M. (1997). Theory of hydration forces between surfaces. *Langmuir*, **13**, 2113.
- Beveridge, W.I.B. (1950). *The Art of Scientific Investigation*, Vintage Books, New York, NY.
- Bibette, J. (1991). Depletion interactions and fractionated crystallization for polydisperse emulsion purification. *Journal of Colloid and Interface Science*, **147**, 474.
- Bibette, J., Roux, D., Nallet, F. (1990). Depletion interactions and fluid-solid equilibrium in emulsions. *Physical Review Letters*, **65**, 2470.
- Bijsterbosch, B.H., Bos, M.T.A., Dickinson, E., van Opheusden, J.H.J., Walstra, P. (1995). Brownian dynamics simulation of particle gel formation: From argon to yoghurt. *Faraday Discussions*, **101**, 51.
- Billmeyer, F.W., Saltzman, M. (1981). *Principles of Color Technology*, 2nd ed., John Wiley & Sons, New York, NY.
- Billmeyer, F.W., Richards, L.W. (1973). Scattering and absorption of radiation by lighting materials. *Journal of Color and Appearance*, **2**, 4.
- Billsten, P., Carlsson, U., Elwing, H. (2003). Studies on the conformation of adsorbed proteins with the use of nanoparticle technology, in *Biopolymers at Interfaces*, 2nd ed., Malmsten, M., Ed., Marcel Dekker, New York, NY, p. 497.
- Binks, B.P. (1993). Emulsion-type below and above the CMC in AOT microemulsion systems. *Colloids and Surfaces A: Physicochemical and Engineering Aspects*, **71**, 167.
- Binks, B.P. (1998). Emulsions: Recent advances in understanding, in *Modern Aspects of Emulsion Science*, Binks, B.P., Ed., The Royal Society of Chemistry, Cambridge, UK, Chap. 1.
- Birch, G.G., Lindley, M.G. (1986). *Interactions of Food Components*, Elsevier, London, UK.

- Birker, P.J.M.W.L., Padley, F.B. (1987). Physical properties of fats and oils, in *Recent Advances in Chemistry and Technology of Fats and Oils*, Hamilton, R.J., Bhati, A., Eds., Elsevier, London, UK, Chap. 1.
- Blake, A. (2002). Communicating with Chemicals. *Chemistry of Taste: Mechanisms, Behaviors, & Mimics*, ACS Symposium Series, **825**, 58.
- Blijdenstein, T.B.J., Nicolas, Y., van der Linden, E., van Vliet, T., Paques, M., van Aken, G.A., Knaebel, A., Munch, J.P. (2003a). Monitoring the structure of flocculated emulsions under shear by DWS and CSLM, in *Proceedings of the Third International Symposium on Food Rheology and Structure*, Fischer, P., Marti, I., Windhab, E.J., Eds., Laboratory of Food Process Engineering, Zurich, Switzerland.
- Blijdenstein, T.B.J., Hendriks, W.P.G., van der Linden, E., van Vliet, T., van Aken, G.A. (2003b). Control of strength and stability of emulsion gels by a combination of long- and short-range interactions. *Langmuir*, **19**, 6657.
- Blonk, J.C.G., van Aalst, H. (1993). Confocal scanning light microscopy in food research. *Food Research International*, **26**, 297.
- Boek, E.S., Coveney, P.V., Lekkerkerker, H.N.W., vanderSchoot, P. (1997). Simulating the rheology of dense colloidal suspensions using dissipative particle dynamics. *Physical Review E*, **55**, 3124.
- Bohren, C.F., Huffman, D.R. (1983). *Adsorption and Scattering of Light by Small Particles*, John Wiley & Sons, New York, NY.
- Boistelle, R. (1988). Fundamentals of nucleation and crystal growth, in *Crystallization and Polymorphism of Fats and Fatty Acids*, Garti, N., Sato, K., Eds., Marcel Dekker, New York, NY, Chap. 5.
- Bomben, J.L., Bruin, S., Thijssen, H.A.C., Merson, R.L. (1973). Aroma recovery and retention in concentration and drying of foods. *Advances in Food Research*, **20**, 1.
- Boode, K. (1992). *Partial Coalescence in Oil-in-Water Emulsions*, Ph.D. Thesis, Wageningen Agricultural University, Wageningen, The Netherlands.
- Boode, K., Walstra, P. (1993a). Partial coalescence in oil-in-water emulsions. Part 1: Nature of the aggregation. *Colloids and Surfaces A: Physicochemical and Engineering Aspects*, **81**, 121.
- Boode, K., Walstra, P. (1993b). The kinetics of partial coalescence in oil-in-water emulsions, in *Food Colloids and Polymers: Stability and Mechanical Properties*, Dickinson, E., Walstra, P., Eds., Royal Society of Chemistry, Cambridge, UK, p. 23.
- Boode, K., Bispernick, C., Walstra, P. (1991). Destabilization of O/W emulsions containing fat crystals by temperature cycling. *Colloids and Surfaces*, **61**, 55.
- Boode, K., Walstra, P., Degrootmostert, A.E.A. (1993). Partial coalescence in oil-in-water emulsions. Part 2: Influence of the properties of the fat. *Colloids and Surfaces A: Physicochemical and Engineering Aspects*, **81**, 139.
- Bos, M.A., van Vliet, T. (2001). Interfacial rheological properties of adsorbed protein layers and surfactants: A review. *Advances in Colloid and Interface Science*, **91**, 437.
- Bos, M., Nylander, T., Arnebrant, T., Clark, D.C. Protein/emulsifier interactions, in *Food Emulsifiers and Their Applications*, Hasenhuettl, G.L., Hartel, R.W., Eds., Chapman & Hall, New York, NY, Chap. 5.
- Boudaud, N., Dumont, J.P. (1996). Interaction between flavor components and  $\beta$ -lactoglobulin, in *Flavor-Food Interactions*, McGorin, R.J., Leland, J.V., Eds., American Chemical Society, Washington, DC, Chap. 4.
- Bourne, M.C. (1997). *Food Texture and Viscosity: Concept and Measurement*. Academic Press, New York, NY.
- Bower, C., Washington, C., Purewal, T.S. (1997). The use of image analysis to characterize aggregates in a shear field. *Colloids and Surfaces A: Physicochemical and Engineering Aspects*, **127**, 105.
- Bower, C., Gallegos, C., Mackley, M.R., Madieto, J.M. (1999). The rheological and microstructural characterisation of the non-linear flow behaviour of concentrated oil-in-water emulsions. *Rheologica Acta*, **38**, 145.
- Bradley, R.L. (2003). Moisture and total solids analysis, in *Food Analysis*, 3rd ed., Nielsen, S.S., Ed., Kluwer Academic Publishers, New York, NY, Chap. 6.
- Brady, J.W. (1989). The role of dynamics and solvation in protein structure and function, in *Food Proteins*, Kinsella, J.E., Soucie, W.G., Eds., American Oil Chemists Society, Champaign, IL, Chap. 1.

- Brady, J.F. (2001). Computer simulations of viscous suspensions. *Chemical Engineering Science*, **56**, 2921.
- Brady, J.W., Ha, S.N. (1975). Molecular dynamic simulations of the aqueous solvation of sugars, in *Water Relationships of Foods*, Duckworth, R.B., Ed., Academic Press, London, UK, p. 3.
- Braginsky, L.M., Belevitskaya, M.A. (1996). Kinetics of droplets breakup in agitated vessels, in *Liquid-Liquid Systems*, Kulov, N.N., Ed., Nova Science, Commack, Chap. 1.
- Brakenhoff, G.J., van der Voort, H.T.M., van Spronsen, E.A., Nanninga, N. (1988). Three-dimensional imaging of biological structures by high resolution confocal laser scanning microscopy. *Scanning Microscopy*, **2**, 33.
- Brandt, L.A. (1999). Salad days for healthy dressings. Prepared Foods, october Issue.
- Brandt, L.A. (2002). Pouring on flavor in beverages. Prepared Foods, october Issue.
- Braudo, E.E., Plashchina, I.G., Kobak, V.V., Golovnya, R.V., Zhuravleva, I.L., Krikunova, N.I. (2000). Interactions of flavor compounds with pectic substances. *Nahrung-Food*, **44**, 173.
- Brauss, M.S., Linforth, R.S.T., Cayeux, I., Harvey, B., Taylor, A.J. (1999). Altering the fat content affects flavor release in a model yogurt system. *Journal of Agricultural and Food Chemistry*, **47**, 2055.
- Bremer, L.G.B. (1992). *Fractal aggregation in relation to formation and properties of particle gels*, Ph.D. Thesis, Wageningen Agricultural University, Wageningen, The Netherlands.
- Bremer, L.G.B., Bijsterbosch, B.H., Walstra, P., van Vliet, T. (1993). Formation, properties and fractal structure of particle gels. *Advances in Colloid and Interface Science*, **46**, 117.
- Brennan, J.G., Butters, J.R., Cowell, N.D., Lilly, A.E.V. (1981). *Food Engineering Operations*. Applied Science Publishers, London, UK.
- Brooker, B.E. (1995). Imaging food systems by confocal laser scanning microscopy, in *New Physico-chemical Techniques for the Characterization of Complex Food Systems*, Dickinson, E., Ed., Blackie Academic & Professional, London, UK, Chap. 2.
- Brooks, B.W., Richmon, H.N., Zerfa, M. (1998). Phase inversion and drop formation in agitated liquid-liquid dispersions in the presence of non-ionic surfactants, in *Modern Aspects of Emulsion Science*, Binks, B.P., Ed., The Royal Society of Chemistry, Cambridge, UK, Chap. 6.
- Brossard, C., Rousseau, F., Dumont, J.P. (1996). Flavour release and flavour perception in oil-in-water emulsions: Is the link so close? in *Flavour Science: Recent Developments*, Tayloer, A.J., Mottram, D.S., Eds., Royal Society of Chemistry, Cambridge, UK, p. 375.
- Bruin, S. (1999). Phase equilibria for food product and process design. *Fluid Phase Equilibria*, **158**, 657.
- Brujic, J., Edwards, S.F., Grinev, D.V., Hopkinson, I., Brujic, D., Makse, H.A. (2003a). 3D bulk measurements of the force distribution in a compressed emulsion system. *Faraday Discussions*, **123**, 207.
- Brujic, J., Edwards, S.F., Hopkinson, I., Makse, H.A. (2003b). Measuring the distribution of inter-droplet forces in a compressed emulsion system. *Physica A*, **327**, 201.
- Brun, J.M., Dalgleish, D.G. (1999). Some effects of heat on the competitive adsorption of caseins and whey proteins in oil-in-water emulsions. *International Dairy Journal*, **9**, 323.
- Buchheim, W., Dejmek, P. (1997). Milk and dairy-type emulsions, in *Food Emulsions*, 3rd ed., Larsson, K., Friberg, S., Eds., Marcel Dekker, New York, NY, Chap. 6.
- Buettner, A., Beer, A., Hannig, C., Settles, M., Schieberle, P. (2002). Physiological and analytical studies on flavor perception dynamics as induced by the eating and swallowing process. *Food Quality and Preference*, **13**, 497.
- Buffler, C.R. (1995). Advances in dielectric characterization of foods, in *Characterization of Food: Emerging Methods*, Gaonkar, A.G., Ed., Elsevier, Amsterdam, Chap. 10.
- Buffo, R.A., Reineccius, G.A. (2001). Shelf-life and mechanisms of destabilization in dilute beverage emulsions. *Flavour and Fragrance Journal*, **16**, 7.
- Buffo, R.A., Reineccius, G.A. (2002). Modeling the rheology of concentrated beverage emulsions. *Journal of Food Engineering*, **51**, 267.
- Buffo, R.A., Reineccius, G.A., Oehlert, G.W. (2001). Factors affecting the emulsifying and rheological properties of gum acacia in beverage emulsions. *Food Hydrocolloids*, **15**, 53.
- Buffo, R.A., Reineccius, G.A., Oehlert, G.W. (2002). Influence of time-temperature treatments on the emulsifying properties of gum acacia in beverage emulsions. *Journal of Food Engineering*, **51**, 341.
- Bujannenez, M.C., Dickinson, E. (1994). Brownian dynamics simulation of a multisubunit deformable particle in simple shear-flow. *Journal of the Chemical Society — Faraday Transactions*, **90**, 2737.

- Burova, T.V., Grinberg, N.V., Golubeva, I.A., Mashkevich, A.Y., Grinberg, V.Y., Tolstoguzov, V.B. (1999). Flavour release in model bovine serum albumin/pectin/2-octanone systems. *Food Hydrocolloids*, **13**, 7.
- Buscall, R., Goodwin, J.W., Hawkins, M.W., Ottewill, R.H. (1982). *Journal of the Chemical Society—Faraday Transactions*, **78**, 2889.
- Buttery, R.G., Ling, L.C., Guadagni, D.G. (1969). Volatilities of aldehydes, ketones and esters in dilute water solution. *Journal of Agriculture and Food Chemistry*, **17**, 385.
- Buttery, R.G., Bomden, J.L., Guadagni, D.G., Ling, L.C. (1971). Flavor compounds: Volatilities in vegetable oil and oil-water mixtures. Estimation of odor thresholds. *Journal of Agricultural and Food Chemistry*, **19**, 1045.
- Buttery, R.G., Guadagni, D.G., Ling, L.C. (1973). Flavor compounds: Volatilities in vegetable oil and oil-water mixtures. Estimation of odor thresholds. *Journal of Agricultural and Food Chemistry*, **21**, 198.
- Caessens, P.W.J.R., Gruppen, H., Slangen, C.J., Visser, S., Vorangen, A.G.J. (1999). Functionality of  $\beta$ -casein peptides: Importance of amphipathicity for emulsion-stabilizing properties. *Journal of Agriculture and Food Chemistry*, **47**, 1856.
- Caldwell, K.B., Goff, H.D., Stanley, D.W. (1992). A low temperature scanning electron microscopy study of ice cream. Part I: Techniques and general microstructure. *Food Structure*, **11**, 1.
- Callaghan, P.T., Jolley, K.W., Humphrey, R.S. (1983). Diffusion of fat and water in cheese as studied by pulsed field gradient nuclear magnetic resonance. *Journal of Colloid and Interface Science*, **93**, 521.
- Campanella, O.H., Peleg, M. (2002). Squeezing flow viscometry for nonelastic semiliquid foods — theory and applications. *Critical Reviews in Food Science and Nutrition*, **42**, 241.
- Campanella, O.H., Dorward, N.M., Singh, H. (1995). A study of the rheological properties of concentrated food emulsions. *Journal of Food Engineering*, **25**, 427.
- Campbell, I.J. (1989). The role of fat crystals in emulsion stability, in *Food Colloids*, Bee, R.D., Richmond, P., Miggins, J., Eds., Royal Society of Chemistry, Cambridge, UK, p. 272.
- Campbell, I., Norton, I., Morley, W. (1996). Factors controlling the phase inversion of oil-in-water emulsions. *Netherlands Milk and Dairy Journal*, **50**, 167.
- Canselier, J.R., Delmas, H., Wilhelm, A.M., Abismail, A. (2002). Ultrasound emulsification—an overview. *Journal of Dispersion Science and Technology*, **23**, 333.
- Caram-Lelham, N., Hed, F., Sundelof, L.O. (1997). Adsorption of charged amphiphiles to oppositely charged polysaccharides — a study of the influence of polysaccharide structure and hydrophobicity of the amphiphile molecule. *Biopolymers*, **41**, 765.
- Carey, M.E., Asquith, T., Linforth, R.S.T., Taylor, A.J. (2002). Modeling the partition of volatile aroma compounds from a cloud emulsion. *Journal of Agricultural and Food Chemistry*, **50**, 1985.
- Carlotti, M.E., Gallarate, M., Morel, S., Ugazio, E. (1999). Micellar solutions and microemulsions of odorous molecules. *Journal of Cosmetic Science*, **50**, 281.
- Carnie, S.L., Chan, D.Y.C., Stankovich, J. (1994). Computation of forces between spherical colloidal particles: Non-linear Poisson-Boltzmann theory. *Journal of Colloid and Interface Science*, **165**, 116.
- Carosso, M.L., Rowlands, W.N., Kennedy, R.A. (1995). Electroacoustic determination of droplet size and zeta potential in concentrated intravenous fat emulsion. *Journal of Colloid and Interface Science*, **174**, 405.
- Carr, J., Baloga, D., Guinard, J.-X., Lawter, L., Marty, C., Squire, C. (1996). The effect of gelling agent type and concentration on flavor release in model systems, in *Flavor-Food Interactions*, McGorin, R.J., Leland, J.V., Eds., American Chemical Society, Washington, DC, Chap. 9.
- Cebula, D.J., McClements, D.J., Povey, M.J.W., Smith, P.R. (1992). Neutron diffraction studies of liquid and crystalline trilaurin. *Journal of the American Oil Chemists Society*, **69**, 130.
- Cesero, A. (1994). The role of conformation on the thermodynamics and rheology of aqueous solutions of carbohydrate polymers, in *Water in Foods: Fundamental Aspects and Their Significance in Relation to the Processing of Foods*, Fito, P., Mullet, A., McKenna, B., Eds., Elsevier, London, UK, p. 27.
- Chaintreau, A., Grade, A., Munozbox, R. (1995). Determination of partition-coefficients and quantitation of headspace volatile compounds. *Analytical Chemistry*, **67**, 3300.

- Chanamai, R., McClements, D.J. (2000a). Impact of weighting agents and sucrose on gravitational separation of beverage emulsions. *Journal of Agricultural and Food Chemistry*, **48**, 5561.
- Chanamai, R., McClements, D.J. (2000b). Creaming stability of flocculated monodisperse oil-in-water emulsions. *Journal of Colloid and Interface Science*, **225**, 214.
- Chanamai, R., McClements, D.J. (2000c). Dependence of creaming and rheology of monodisperse oil-in-water emulsions on droplet size and concentration. *Colloids and Surfaces A: Physicochemical and Engineering Aspects*, **172**, 79.
- Chanamai, R., McClements, D.J. (2001a). Depletion flocculation of beverage emulsions by gum arabic and modified starch. *Journal of Food Science*, **66**, 457.
- Chanamai, R., McClements, D.J. (2001b). Prediction of emulsion color from droplet characteristics: Dilute monodisperse oil-in-water emulsions. *Food Hydrocolloids*, **15**, 83.
- Chanamai, R., McClements, D.J. (2002). Comparison of gum arabic, modified starch and whey protein isolate as emulsifiers: Influence of pH, CaCl<sub>2</sub> and temperature. *Journal of Food Science*, **67**, 120.
- Chanamai, R., Herrmann, N., McClements, D.J. (1999). Influence of thermal overlap effects on the ultrasonic attenuation spectra of polydisperse oil-in-water emulsions. *Langmuir*, **15**, 3418.
- Chanamai, R., Herrmann, N., McClements, D.J. (2000). Probing floc structure by ultrasonic spectroscopy, viscometry, and creaming measurements. *Langmuir*, **16**, 5884.
- Chanamai, R., Horn, G., McClements, D.J. (2002). Influence of oil polarity on droplet growth in oil-in-water emulsions stabilized by a weakly adsorbing biopolymer or a nonionic surfactant. *Journal of Colloid and Interface Science*, **247**, 167.
- Chang, C.M., Powries, W.D., Fennema, O. (1972). Electron microscopy of mayonnaise. *Canadian Institute of Food Science and Technology Journal*, **5**, 134.
- Chantrapornchai, W., Clydesdale, F., McClements, D.J. (1998). Influence of droplet size and concentration on the color of oil-in-water emulsions. *Journal of Agricultural and Food Chemistry*, **46**, 2914.
- Chantrapornchai, W., Clydesdale, F., McClements, D.J. (1999a). Theoretical and experimental study of spectra reflectance and color of concentrated oil-in-water emulsions. *Journal of Colloid and Interface Science*, **218**, 324.
- Chantrapornchai, W., Clydesdale, F., McClements, D.J. (1999b). Influence of droplet characteristics on the optical properties of colored oil-in-water emulsions. *Colloids and Surfaces A: Physicochemical and Engineering Aspects*, **155**, 373.
- Chantrapornchai, W., Clydesdale, F., McClements, D.J. (2001a). Influence of flocculation on optical properties of emulsions. *Journal of Food Science*, **66**, 464.
- Chantrapornchai, W., Clydesdale, F., McClements, D.J. (2001b). Influence of relative refractive index on optical properties of emulsions. *Food Research International*, **34**, 827.
- Chapman, D. (1965). *The Structure of Lipids*, Methuen, London, UK.
- Charlambous, G., Doxastakis, G. (1989). *Food Emulsifiers: Chemistry, Technology, Functional Properties and Applications*, Elsevier, Amsterdam.
- Charles, M., Rosselin, V., Beck, L., Sauvageot, F., Guichard, E. (2000a). Flavor release from salad dressings: Sensory and physicochemical approaches in relation with the structure. *Journal of Agricultural and Food Chemistry*, **48**, 1810.
- Charles, M., Lambert, S., Brondeur, P., Courthaudon, J.L., Guichard, E. (2000b). Influence of formulation and structure of an oil-in-water emulsion on flavor release, in *Flavor Release*, ACS Symposium Series 763, Roberts, D.D., Taylor, A.J., Eds., American Chemical Society, Washington, DC, p. 342.
- Chen, J., Anadarajah, A. (1996). Van der Waals attraction between spherical particles. *Journal of Colloid and Interface Science*, **180**, 519.
- Chen, J., Dickinson, E. (1993). Time-dependent competitive adsorption of milk proteins and surfactants in oil-in-water emulsions. *Journal of the Science of Food and Agriculture*, **62**, 283.
- Chin, C.J., Yiacoumi, S., Tsouris, C. (1998). Shear-induced flocculation of colloidal particles in stirred tanks. *Journal of Colloid and Interface Science*, **206**, 532.
- Chow, C.K. (1992). *Fatty Acids in Foods and Their Health Implication*. Marcel Dekker, New York, NY.
- Christenson, H.K., Claesson, P.M. (2001). Direct measurements of the force between hydrophobic surfaces in water. *Advances in Colloid and Interface Science*, **91**, 391.

- Christenson, H.K., Fang, J., Ninham, B.W., Parker, J.L. (1990). Effect of divalent electrolyte on the hydrophobic attraction. *Journal of Physical Chemistry*, **94**, 8004.
- Christian, S.D., Scamehorn, J.F. (1995). *Solubilization in Surfactant Aggregates*, Marcel Dekker, New York, NY.
- Christov, N.C., Ganchev, D.N., Vassileva, N.D., Denkov, N.D., Danov, K.D., Kralchevsky, P.A. (2002). Capillary mechanisms in membrane emulsification: Oil-in-water emulsions stabilized by Tween 20 and milk proteins. *Colloids and Surfaces A: Physicochemical and Engineering Aspects*, **209**, 83.
- Chrysam, M.M. (1996). Margarine and spreads, in *Bailey's Industrial Oil and Fat Products*, 5th Edition, Vol. 3, *Edible Oil and Fat Products: Products and Application Technology*, Hui, Y.H., Ed., John Wiley & Sons, New York, NY, Chap. 2.
- Claesson, P.M. (1987). Experimental evidence for repulsive and attractive forces not accounted for by conventional DLVO theory. *Progress in Colloid and Polymer Science*, **74**, 48.
- Claesson, P.M., Christenson, H.K. (1988). Very long range attractive forces between uncharged hydrocarbon and fluorocarbon surfaces in water. *Journal of Physical Chemistry*, **92**, 1650.
- Claesson, P.M., Blomberg, E., Froberg, J.C., Nylander, T., Arnebrant, T. (1995). Protein interactions at solid surfaces. *Advances in Colloid and Interface Science*, **57**, 161.
- Claesson, P.M., Blomberg, E., Poptoshev, E. (2001). Surface forces and emulsion stability, in *Encyclopedic Handbook of Emulsion Technology*, Sjoblom, J., Ed., Marcel Dekker, New York, NY, p. 305.
- Claesson, P.M., Blomberg, E., Poptoshev, E. (2004). Surface forces and emulsion stability, in *Food Emulsions*, 4th ed., Friberg, S., Larsson, K., Sjoblom, J., Eds., Marcel Dekker, New York, NY, Chap. 7.
- Claesson, P.M., Ederth, T., Bergeron, V., Rutland, M.W. (1996). Techniques for measuring surface forces. *Advances in Colloid and Interface Science*, **67**, 119.
- Clark, A.H. (1987). The application of network theory to food systems, in *Food Structure and Behaviour*, Blanshard, J.M.V., Lillford, P.J., Eds., Academic Press, London, UK, Chap. 2.
- Clark, A.H., Lee-Tuffnell, C.D. (1986). Gelation of globular proteins, in *Functional Properties of Food Macromolecules*, Mitchell, J.R., Ledward, D.A., Eds., Elsevier, London, UK, Chap. 5.
- Clausse, D. (1983). Dielectric properties of emulsions and related systems, in *Encyclopedia of Emulsion Technology*, Vol. 1. *Applications*, Becher, P., Ed., Marcel Dekker, New York, NY, Chap. 9.
- Clausse, D. (1985). Research techniques utilizing emulsions, in *Encyclopedia of Emulsion Technology*, Vol. 2. *Applications*, Becher, P., Ed., Marcel Dekker, New York, NY, Chap. 2.
- Clausse, D. (1998). Thermal behaviour of emulsions studied by differential scanning calorimetry. *Journal of Thermal Analysis and Calorimetry*, **51**, 191.
- Clausse, D., Fouconnier, B., Gomez, J.A. (2002). Ripening phenomena in emulsions—a calorimetry investigation. *Journal of Dispersion Science and Technology*, **23**, 379.
- Clegg, S.M. (1996). The use of hydrocolloid gums as mimetics, in *Handbook of Fat Replacers*, Roller, S., Jones, S.A., Eds., CRC Press, Boca Raton, FL, pp. 191.
- Clegg, S.M., Kilcast, D., Arazi, S. (2003). The structural and compositional basis of creaminess in food emulsion gels, in *Proceedings of the Third International Symposium on Food Rheology and Structure*, Fischer, P., Marti, I., Windhab, E.J., Eds., Laboratory of Food Process Engineering, Zurich, Switzerland.
- Clydesdale, F.M. (1975). Methods and measurements of food color, in *Theory, Determination and Control of Physical Properties of Food Materials*, Rha, C., Ed., D. Reidel Publishing, Boston, Chap. 14.
- Clydesdale, F.M., Francis, F.J. (1975). *Food Colorimetry: Theory and Applications*, AVI Publishing, Westport, CT.
- Coffey, D.G., Bell, D.A., Henderson, A. (1995). Cellulose and cellulose derivatives, in *Food Polysaccharides and Their Applications*, Stephan, A.M., Ed., Marcel Dekker, New York, NY, Chap. 5.
- Cofrades, S., Carballo, J., Careche, M., Colmenero, F.J. (1996). Emulsifying properties of actomyosin from several species. *Food Science and Technology—Lebensmittel-Wissenschaft und Technologie*, **29**, 379.
- Cohen Stuart, M.A. (2003). Macromolecular adsorption: A brief introduction, in *Biopolymers at Interfaces*, 2nd ed., Malmsten, M., Ed., Marcel Dekker, New York, NY, p. 1.
- Collins, K.D., Washabaugh, M.W. (1985). The Hofmeister effect and the behavior of water at interfaces. *Quarterly Reviews of Biophysics*, **18**, 323.



- Corredig, M., Dalgleish, D.G. (1995). A differential microcalorimetric study of whey proteins and their behaviour in oil-in-water emulsions. *Colloids and Surfaces B: Biointerfaces*, **4**, 411.
- Corredig, M., Dalgleish, D.G. (1996). Effect of temperature and pH on the interactions of whey proteins with casein micelles in skim milk. *Food Research International*, **29**, 49.
- Corredig, M., Dalgleish, D.G. (1999). The mechanisms of the heat-induced interaction of whey proteins with casein micelles in milk. *International Dairy Journal*, **9**, 233.
- Corthaudon, J.-L., Dickinson, E., Dalgleish, D.G. (1991a). Competitive adsorption of  $\beta$ -casein and nonionic surfactants in oil-in-water emulsions. *Journal of Colloid and Interface Science*, **145**, 390.
- Corthaudon, J.-L., Dickinson, E., Matsumura, Y., Clark D.C. (1991b). Competitive adsorption of  $\beta$ -lactoglobulin and polyoxyethylene sorbitan monostearate 20 at the oil-water interface. *Colloids and Surfaces*, **56**, 293.
- Corthaudon, J.-L., Dickinson, E., Matsumura, Y., Williams, A. (1991c). Influence of emulsifier on the competitive adsorption of whey proteins in emulsions. *Food Structure*, **10**, 109.
- Corthaudon, J.-L., Dickinson, E., Christie, W.W. (1991d). Competitive adsorption of lecithin and  $\beta$ -casein in oil-in-water emulsions. *Journal of Agriculture and Food Chemistry*, **39**, 1365.
- Coulter, T.P. (1996). *Food: The Chemistry of its Components*, 3rd ed., Royal Society of Chemistry Paperbacks, Cambridge, UK.
- Couper, A. (1993). Surface tension and its measurement, in *Physical Methods of Chemistry*, Vol. IXA, *Investigations of Surfaces and Interfaces*, Rossiter, B.W., Baetzold, R.C., Eds., John Wiley & Sons, New York, NY, Chap. 1.
- Coupland, J.N. (2002). Crystallization in emulsions. *Current Opinion in Colloid and Interface Science*, **7**, 445–450.
- Coupland, J.N., McClements, D.J. (1997). Physical properties of liquid edible oils. *Journal of the American Oil Chemists Society*, **74**, 1559.
- Coupland, J.N., McClements, D.J. (1996). Lipid oxidation in food emulsions. *Trends in Food Science and Technology*, **7**, 83.
- Coupland, J.N., McClements, D.J. (2001). Droplet size determination in food emulsions: Comparison of ultrasonic and light scattering techniques. *Journal of Food Engineering*, **50**, 117.
- Coupland, J.N., McClements, D.J. (2004). Analysis of droplet characteristics using low-intensity ultrasound, in *Food Emulsions*, 4th ed., Friberg, S., Larsson, K., Sjöblom, J., Eds., Marcel Dekker, New York, NY, Chap. 14.
- Coupland, J.N., Brathwaite, D., Fairley, P., McClements, D.J. (1997). Effect of ethanol on the solubilization of hydrocarbon emulsion droplets in nonionic surfactant micelles. *Journal of Colloid and Interface Science*, **190**, 71.
- Coupland, J.N., Dickinson, E., McClements, D.J., Povey, M.J.W., Rancourt de Mimmerand, C. (1993). Crystallization of simple paraffins and monoacid saturated triacylglycerols dispersed as an oil phase in water, in *Food Colloids and Polymers: Structure and Dynamics*, Dickinson, E., Walstra, P., Eds., Royal Society of Chemistry, Cambridge, UK.
- Coupland, J.N., Zhu, Z., Wan, H., McClements, D.J., Nawar, W.W., Chinachotti, P. (1996). Droplet composition affects the rate of oxidation of emulsified ethyl linoleate. *Journal of the American Oil Chemists Society*, **73**, 795.
- Crank, J. (1975). *The Mathematics of Diffusion*, Oxford University Press, London, UK.
- Creighton, T.E. (1993). *Proteins*, 2nd ed., W.H. Freeman, New York, NY.
- Curle, N., Davies, H.J. (1968). *Modern Fluid Dynamics*, Vol. 1: *Incompressible Flow*, D van Nostrand, London, UK.
- Dalgleish, D.G. (1989). Protein stabilized emulsions and their properties, in *Water and Food Quality*, Hardman, T.M., Ed., Elsevier, London, UK, Chap. 6.
- Dalgleish, D.G. (1995). Structure and properties of adsorbed layers in emulsions containing milk proteins, in *Food Macromolecules and Colloids*, Dickinson, E., Lorient, D., Eds., Royal Society of Chemistry, Cambridge, UK, p. 23.
- Dalgleish, D.G., Hallet, F.R. (1995). Dynamic light scattering – applications to food systems. *Food Research International*, **28**, 181.
- Dalgleish, D.G. (1996a). *Food Emulsions*, in *Emulsions and Emulsion Stability*, Sjöblom, J., Ed., Marcel Dekker, New York, NY, Chap. 5.
- Dalgleish, D.G. (1996b). Conformations and structures of milk proteins adsorbed to oil-water interfaces. *Food Research International*, **29**, 541.

- Dalgleish, D.G. (1997a). Adsorption of protein and the stability of emulsions. *Trends in Food Science and Technology*, **8**, 1.
- Dalgleish, D.G. (1997b). Structure-function relationships of caseins, in *Food Proteins and Their Applications*, Damodaran, S., Paraf, A., Marcel Dekker, New York, NY, Chap. 7.
- Dalgleish, D.G., Goff, H.D., Luan, B.B. (2002a). Exchange reactions between whey proteins and caseins in heated soya oil-in-water emulsion systems – behavior of individual proteins. *Food Hydrocolloids*, **16**, 295.
- Dalgleish, D.G., Goff, H.D., Brun, J.M., Luan, B.B. (2002b). Exchange reactions between whey proteins and caseins in heated soya oil-in-water emulsion systems – overall aspects of the reaction. *Food Hydrocolloids*, **16**, 303.
- Dalgleish, D.G. (2004). Food Emulsions: Their structures and properties, in *Food Emulsions*, 4th ed., Friberg, S., Larsson, K., Sjoblom, J., Eds., Marcel Dekker, New York, NY, Chap. 1.
- Dalgleish, D.G., West, S.J., Hallett, F.R. (1997). The characterization of small emulsion droplets made from milk proteins and triglyceride oil. *Colloids and Surfaces A: Physicochemical and Engineering Aspects*, **123**, 145.
- Damodaran, N.S. (1990). Interfaces, protein films and foams, in *Advances in Food and Nutrition Research*, Vol. 34, Kinsella, J.E., Ed., Academic Press, San Diego, CA, p. 1.
- Damodaran, N.S. (1994). Structure-function relationships of food proteins, in *Protein Functionality in Food Systems*, Hettiarachchy, Ziegler, G.R., Eds., Marcel Dekker, New York, NY, p. 1.
- Damodaran, N.S. (1996). Amino acids, peptides and proteins, in *Food Chemistry*, 3rd ed., Fennema, O.R., Ed., Marcel Dekker, New York, NY, pp. 321.
- Damodaran, N.S. (1997). Food proteins: An overview. *Food Proteins and Their Applications*, Marcel Dekker, New York, NY, Chap. 1.
- Damrau, E., Peleg, M. (1997). Imperfect squeezing flow viscosimetry of Newtonian liquids: Theoretical and practical considerations. *Journal of Texture Studies*, **28**, 187.
- Darling, D.F. (1982). Recent advances in the destabilization of dairy emulsions. *Journal of Dairy Research*, **49**, 695.
- Das, A.K., Ghosh, P.K. (1990). Concentrated emulsions—investigation of polydispersity and droplet distortion and their effect on volume fraction and interfacial area. *Langmuir*, **6**, 1668.
- Das, K.P., Kinsella, J.E. (1990). Stability of food emulsions: Physicochemical role of protein and non-protein emulsifiers, in *Advances in Food and Nutrition Research*, Vol. 34, Kinsella, J.E., Ed., Academic Press, San Diego, CA, p. 81.
- Dattatreya, B.S., Kamath, A., Bhat, K.K. (2002). Developments and challenges in flavor perception and measurement—a review. *Food Reviews International*, **18**, 223.
- Daubert, C.R., Foegeding, E.A. (2003). Rheological principles for food analysis, in *Food Analysis*, 3rd ed., Nielsen, S.S., Ed., Kluwer Academic, New York, NY, 503.
- Dave, J.V. (1969). Scattering of electromagnetic radiation by a large, absorbing sphere. *IBM Journal of Research and Development*, **13**, 302.
- Davidson, J.M., Linforth, R.S.T., Hollowood, T.A., Taylor, A.J. (1999). Effect of sucrose on the perceived flavor intensity of chewing gum. *Journal of Agricultural and Food Chemistry*, **47**, 4336.
- Davidson, J.M., Linforth, R.S.T., Hollowood, T.A., Taylor, A.J. (2000). Release of non-volatile flavor compounds in vivo, in *Flavor Release*, Roberts, D.D., Taylor, A.J., Eds., American Chemical Society, Washington, DC, p. 99.
- d'Avila, M.A., Shapley, N.C., Walton, J.H., Phillips, R.J., Dungan, S.R., Powell, R.L. (2003). Mixing of concentrated oil-in-water emulsions measured by nuclear magnetic resonance imaging. *Physics of Fluids*, **15**, 2499–2511.
- Davis, E.A. (1994a). Thermal analysis, in *Introduction to the Chemical Analysis of Foods*, Nielsen, S.S., Ed., Bartlett & Jones, Boston, Chap. 34.
- Davis, H.T. (1994b). Factors determining emulsion type: Hydrophile-lipophile balance and beyond. *Colloids and Surfaces A: Physicochemical and Engineering Aspects*, **91**, 9.
- Davis, R.H. (1996). Velocities of sedimenting particles in suspensions, in *Sedimentation of Small Particles in a Viscous Liquid*, Tory, E.M., Ed., Computational Mechanics Publications, Southampton, UK, Chap. 6.
- Davis, R.H., Schonberg, J.A., Rallison, J.M. (1989). The lubrication force between two viscous drops. *Physics of Fluids A*, **1**, 77.

- de Roos, A.L. (2000). Physicochemical models of flavor release in foods, in *Flavor Release*, Roberts, D.D., Taylor, A.J., Eds., American Chemical Society, Washington, DC, p. 126.
- de Roos, A.L., Walstra, P. (1996). Loss of enzyme activity due to adsorption onto emulsion droplets. *Colloids and Surfaces B: Biointerfaces*, **6**, 201.
- de Vries, A.J. (1963). Effect of particle aggregation on the rheological behaviour of disperse systems, in *Rheology of Emulsions*, Sherman, P., Ed., Pergamon Press, New York, NY.
- de Wit, J.N., van Kessel, T. (1996). Effects of ionic strength on the solubility of whey protein products: A colloid chemical approach. *Food Hydrocolloids*, **10**, 143.
- Dea, I.C.M. (1982). Polysaccharide conformation in solutions and gels, in *Food Carbohydrates*, Lineback, D.R., Inglett, G.E., Eds., AVI Publishing, Westport, Chap. 22.
- Deffenbaugh, L.B. (1997). Carbohydrate/emulsifier interactions, in *Food Emulsifiers and Their Applications*, Hasenhuettl, G.L., Hartel, R.W., Eds., Chapman & Hall, New York, NY, Chap. 4.
- Deibler, K.D., Acree, T.E. (2000). Effect of beverage base conditions on flavor release, in *Flavor Release*, Roberts, D.D., Taylor, A.J., Eds., American Chemical Society, Washington, DC.
- Deis, R.C. (1997). Reducing Fat: A Cutting-Edge Strategy. *Food Product Design*, Weeks Publishing, Northbrook, IL.
- Deis, R.C. (1997). Reducing Fat: A Cutting-Edge Strategy. *Food Product Design*, Weeks Publishing, Northbrook, IL.
- Delarue, J., Giampaoli, P. (2000). Study of interaction phenomena between aroma compounds and carbohydrate matrixes by inverse gas chromatography. *Journal of Agricultural and Food Chemistry*, **48**, 2372.
- Demetriades, K., Coupland, J.N., McClements, D.J. (1997a). Physical properties of whey protein stabilized emulsions as related to pH and NaCl. *Journal of Food Science*, **62**, 342.
- Demetriades, K., Coupland, J.N., McClements, D.J. (1997b). Physicochemical properties of whey protein stabilized emulsions as affected by heating and ionic strength. *Journal of Food Science*, **62**, 462.
- Demetriades, K., McClements, D.J. (1998). Influence of pH and heating on the physicochemical properties of whey protein stabilized emulsions containing a non-ionic surfactant. *Journal of Agricultural and Food Chemistry*, **46**, 3936.
- Demetriades, K., McClements, D.J. (1999). Flocculation of whey protein stabilized emulsions as influenced by dextran sulfate and electrolyte. *Journal of Food Science*, **64**, 206.
- Deminieri, B., Colin, A., Leal-Calderon, F., Bibette, J. (1998). Lifetime and destruction of concentrated emulsions undergoing coalescence, in *Modern Aspects of Emulsion Science*, Binks, B.P., Ed., The Royal Society of Chemistry, Cambridge, UK, Chap. 8.
- Depree, J.A., Savage, G.P. (2001). Physical and flavour stability of mayonnaise. *Trends in Food Science and Technology*, **12**, 157.
- Derjaguin, B.V. (1989). *Theory of Stability of Colloids and Thin Films*, Consultants Bureau, New York, NY.
- Derjaguin, B.V., Churaev, N.V., Muller, V.M. (1987). *Surface Forces*, Consultants Bureau, New York, NY.
- Dickinson, E. (1989). A model of a concentrated dispersion exhibiting bridging flocculation and depletion flocculation. *Journal of Colloid and Interface Science*, **132**, 274.
- Dickinson, E. (1992). *Introduction to Food Colloids*, Oxford University Press, Oxford, UK.
- Dickinson, E. (1993). Protein-polysaccharide interactions in food colloids, in *Food Colloids and Polymers: Stability and Mechanical Properties*, Dickinson, E., Walstra, P., Eds., Royal Society of Chemistry, Cambridge, UK, pp. 77.
- Dickinson, E. (1994). Colloidal aspects of beverages. *Food Chemistry*, **51**, 343.
- Dickinson, E. (1995). Emulsion stabilization by polysaccharides and protein-polysaccharide complexes, in *Food Polysaccharides and Their Applications*, Stephan, A.M., Ed., Marcel Dekker, New York, NY, Chap. 15.
- Dickinson, E. (1997). Properties of emulsions stabilized with milk proteins: Overview of some recent developments. *Journal of Dairy Science*, **80**, 2607.
- Dickinson, E. (1998). Rheology of emulsions: The relationship to structure and stability, in *Modern Aspects of Emulsion Science*, Binks, B.P., Ed., The Royal Society of Chemistry, Cambridge, UK, Chap. 5.
- Dickinson, E. (2000). Structure and rheology of simulated gels formed from aggregated colloidal particles. *Journal of Colloid and Interface Science*, **225**, 2.

- Dickinson, E. (2001). Milk protein interfacial layers and the relationship to emulsion stability and rheology. *Colloids and Surfaces B: Biointerfaces*, **20**, 197.
- Dickinson, E. (2003). Hydrocolloids at interfaces and the influence on the properties of dispersed systems. *Food Hydrocolloids*, **17**, 25.
- Dickinson, E., Davies, E. (1999). Influence of ionic calcium on stability of sodium caseinate emulsions. *Colloids and Surfaces B: Biointerfaces*, **12**, 203.
- Dickinson, E., Euston, S.R. (1991). Computer-simulation of bridging flocculation. *Journal of the Chemical Society — Faraday Transactions*, **87**, 2193.
- Dickinson, E., Everson, D.J., Murray, B.S. (1989). On the film-forming and emulsion-stabilizing properties of gum arabic: Dilution and flocculation aspects. *Food Hydrocolloids*, **3**, 101–114.
- Dickinson, E., Evison, J., Gramshaw, J.W., Schwöpe, D. (1994). Flavor release from a protein-stabilized water-in-oil-in-water emulsion. *Food Hydrocolloids*, **8**, 63.
- Dickinson, E., Galazka, V.B., Anderson, D.M.W. (1991). Emulsifying behavior of gum-arabic. Part 1: Effect of the nature of the oil phase on the emulsion droplet-size distribution. *Carbohydrate Polymers*, **14**, 373.
- Dickinson, E., Golding, M. (1997a). Rheology of sodium caseinate stabilized oil-in-water emulsions. *Journal of Colloid and Interface Science*, **191**, 166.
- Dickinson, E., Golding, M. (1997b). Depletion flocculation of emulsions containing unadsorbed sodium caseinate. *Food Hydrocolloids*, **11**, 13.
- Dickinson, E., Golding, M. (1998). Influence of alcohol on stability of oil-in-water emulsions containing sodium caseinate. *Journal of Colloid and Interface Science*, **197**, 133.
- Dickinson, E., Golding, M., Povey, M.J.W. (1997). Creaming and flocculation of oil-in-water emulsions containing sodium caseinate. *Journal of Colloid and Interface Science*, **185**, 515.
- Dickinson, E., Goller, M.I., McClements, D.J., Povey, M.J.W. (1990). Ultrasonic monitoring of crystallization in oil-in-water emulsions. *Journal of the Chemical Society—Faraday Transactions*, **86**, 1147.
- Dickinson, E., Goller, M.I., Wedlock, D.J. (1993d). Creaming and rheology of emulsions containing polysaccharide and non-ionic or anionic surfactants. *Colloids and Surfaces A: Physicochemical and Engineering Aspects*, **75**, 195.
- Dickinson, E., Goller, M.I., Wedlock, D.J. (1995). Osmotic pressure, creaming and rheology of emulsions containing non-ionic polysaccharide. *Journal of Colloid and Interface Science*, **172**, 192.
- Dickinson, E., Hong, S.K. (1994). Surface coverage of  $\beta$ -lactoglobulin at the oil-water interface: Influence of protein heat treatment and various emulsifiers. *Journal of Agriculture and Food Chemistry*, **42**, 1602.
- Dickinson, E., Hong, S.T. (1995a). Interfacial and stability properties of emulsions: Influence of protein heat treatment and emulsifiers, in *Food Macromolecules and Colloids*, Dickinson, E., Lorient, D., Royal Society of Chemistry, Cambridge, UK, p. 269.
- Dickinson, E., Hong, S.T. (1995b). Influence of water-soluble nonionic emulsifier on the rheology of heat-set protein-stabilized emulsion gels. *Journal of Agricultural and Food Chemistry*, **43**, 2560.
- Dickinson, E., Hong, S.T., Yamamoto, Y. (1996). Rheology of heat-set emulsion gels containing  $\beta$ -lactoglobulin and small-molecule surfactants. *Netherlands Milk and Dairy Journal*, **50**, 199.
- Dickinson, E., Hunt, J.A., Horne, D.S. (1992). Calcium induced flocculation of emulsions containing adsorbed  $\beta$ -casein or phosvitin. *Food Hydrocolloids*, **6**, 359.
- Dickinson, E., Iveson, G. (1993). Adsorbed films of  $\beta$ -lactoglobulin + lecithin at the hydrocarbon-water and triglyceride-water interfaces. *Food Hydrocolloids*, **6**, 553.
- Dickinson, E., Iveson, G., Tanai, S. (1993c). Competitive adsorption in protein stabilized emulsions containing oil-soluble and water-soluble surfactants, in *Food Colloids and Polymers: Stability and Mechanical Properties*, Dickinson, E., Walstra, P., Eds., Royal Society of Chemistry, Cambridge, UK, p. 312.
- Dickinson, E., Krishna, S. (2001). Aggregation in a concentrated model protein system: A mesoscopic simulation of beta-casein self-assembly. *Food Hydrocolloids*, **15**, 107.
- Dickinson, E., Matsumura, Y. (1991). Time-dependent polymerization of  $\beta$ -lactoglobulin through disulphide bonds at the oil-water interface in emulsions. *International Journal of Biology and Macromolecules*, **13**, 26.
- Dickinson, E., McClements, D.J. (1995). *Advances in Food Colloids*, Chapman & Hall, London, UK.

- Dickinson, E., McClements, D.J., Povey, M.J.W. (1991). Ultrasonic investigation of the particle size dependence of crystallization in n-hexadecane-in-water emulsions. *Journal of Colloid and Interface Science*, **142**, 103.
- Dickinson, E., Murray, B.S., Stainsby, G. (1988). *Journal of the Chemical Society—Faraday Transactions* **1**, **84**, 871.
- Dickinson, E., Owusu, R.K., Tan, S., Williams, A. (1993a). Oil-soluble surfactants have little effect on competitive adsorption of  $\alpha$ -lactalbumin and  $\beta$ -lactoglobulin in emulsions. *Journal of Food Science*, **58**, 295.
- Dickinson, E., Owusu, R.K., Williams, A. (1993b). Orthokinetic destabilization of a protein-stabilized emulsion by a water-soluble surfactant. *Journal of the Chemical Society—Faraday Transactions* **1**, **89**, 865.
- Dickinson, E., Radford, S.J., Golding, M. (2003). Stability and rheology of emulsions containing sodium caseinate: Combined effects of ionic calcium and non-ionic surfactant. *Food Hydrocolloids*, **17**, 211.
- Dickinson, E., Ritzoulis, C., Yamamoto, Y., Logan, H. (1999). Ostwald ripening of protein-stabilized emulsions: Effect of transglutaminase crosslinking. *Colloids and Surfaces B: Biointerfaces*, **12**, 139.
- Dickinson, E., Stainsby, G. (1982). *Colloids in Foods*, Elsevier, London, UK.
- Dickinson, E., Stainsby, G. (1988). Emulsion Stability, in *Advances in Food Emulsions and Foams*, Dickinson, E., Stainsby, G., Eds., Elsevier, London, UK, Chap. 1.
- Dickinson, E., Tanai, S. (1992). Temperature dependence of the competitive displacement of protein from the emulsion droplet surface by surfactants. *Food Hydrocolloids*, **6**, 163.
- Dickinson, E., Williams, A. (1994). Orthokinetic coalescence of protein-stabilized emulsions. *Colloids and Surfaces A: Physicochemical and Engineering Aspects*, **88**, 314.
- Dickinson, E., Yamamoto, Y. (1996). Viscoelastic properties of heat-set whey protein stabilized emulsion gels with added lecithin. *Journal of Food Science*, **61**, 811.
- Dijksterhuis, G.B., Piggott, J.R. (2000). Dynamic methods of sensory analysis. *Trends in Food Science and Technology*, **11**, 284.
- Dill, K.A. (1990). Dominant forces in protein folding. *Biochemistry*, **29**, 7133.
- Dimitrova, T.D., Leal-Calderon, F. (1999). Forces between emulsion droplets stabilized with Tween 20 and proteins. *Langmuir*, **15**, 8813.
- Divakar, S. (1998). Nuclear magnetic resonance spectroscopy in food applications: A critical appraisal. *Journal of Food Science and Technology—Mysore*, **35**, 469-481.
- Djerdjev, A.M., Beattie, J.K., Hunter, R.J. (2003). Electroacoustic study of the crystallization of n-eicosane oil-in-water emulsions. *Langmuir*, **19**, 6605.
- Doi, E. (1993). Gels and gelling of globular proteins. *Trends in Food Science and Technology*, **4**, 1.
- Donald, A.M. (2003). The use of environmental scanning electron microscopy for imaging wet and insulating materials. *Nature Materials*, **2**, 511.
- Doyen, K., Carey, M., Linforth, R.S.T., Marin, M., Taylor, A.J. (2001). Volatile release from an emulsion: Headspace and in-mouth studies. *Journal of Agricultural and Food Chemistry*, **49**, 804.
- Druaux, C., Voilley, A. (1997). Effect of food composition and microstructure on volatile flavour release. *Trends in Food Science and Technology*, **8**, 364.
- Ducker, W.A., Pashley, R.M. (1992). Forces between mica surfaces in the presence of rod-shaped divalent counterions. *Langmuir*, **8**, 109.
- Dufour, E., Haertle, T. (1990). Binding affinities of  $\beta$ -ionone and related flavor compounds to  $\beta$ -lactoglobulin: Effects of chemical modifications. *Journal of Agricultural and Food Chemistry*, **38**, 1691.
- Dukhin, A.S., Goetz, P.J. (1996). Acoustic and electroacoustic spectroscopy. *Langmuir*, **12**, 4336.
- Dukhin, A.S., Goetz, P.J., Wines, T.H., Somasundaran, P. (2000). Acoustic and electroacoustic spectroscopy. *Colloids and Surfaces A: Physicochemical and Engineering Aspects*, **173**, 127-158.
- Dukhin, S.S., Krietchamer, G., Miller, R. (1995). *Dynamics of Adsorption at Liquid Interfaces: Theory, Experiment and Application*, Elsevier, Amsterdam.
- Dukhin, S.S., Sjoblom, J. (1996). Kinetics of brownian and gravitational coagulation in dilute emulsions, in *Emulsions and Emulsion Stability*, Sjoblom, J., Ed., Marcel Dekker, New York, NY, Chap. 2.
- Dukhin, S.S., Sjoblom, J., Wasan, D.T., Saether, O. (2001). Coalescence coupled with either coagulation or flocculation in dilute emulsions. *Colloids and Surfaces, A—Physicochemical and Engineering Aspects*, **180**, 223.

- Duran, L., Costell, E. (1999). Perception of taste. Physiochemical and psychophysical aspects. *Food Science and Technology International*, **5**, 299.
- Eads, T.M. (1994). Molecular origins of structure and functionality in foods. *Trends in Food Science and Technology*, **5**, 147.
- Eastoe, J. (1995). Small-angle neutron scattering and neutron reflection, in *New Physicochemical Techniques for the Characterization of Complex Food Systems*, Dickinson, E., Ed., Blackie Academic & Professional, London, UK, Chap. 12.
- Edris, A.E. (1998). Preparation and stability of a protein stabilized orange oil-in-water emulsion. *Nahrung*, **1**, 19.
- Edwards, S.F., Lillford, P.J., Blanshard, J.M.V. (1987). Gels and networks in practice and theory, in *Food Structure and Behaviour*, Blanshard, J.M.V., Lillford, P.J., Eds., Academic Press, London, UK, Chap. 1.
- Egelhaaf, S., Olsson, U., Schurtenberger, P., Morris, J., Wennerstrom, H. (1999). Quantitative measurements of Ostwald ripening using time-resolved small-angle neutron scattering. *Physical Review E*, **60**, 5681.
- Elwell, M.W., Roberts, R.F., Coupland, J.N. (2003). Effect of homogenization and surfactant type on the exchange of oil between emulsion droplets. *Food Hydrocolloids*, **18**, 413.
- Elworthy, P.H., Florence, A.T., Macfarlane, C.B. (1968). *Solubilization by Surface-Active Agents and its Application in Chemistry and the Biological sciences*, Chapman & Hall, London, UK.
- Epstein, P.S., Carhart, R.R. (1953). The absorption of sound in suspensions and emulsions. *Journal of the Acoustical Society of America*, **25**, 553.
- Esselink, K., Hilbers, P.A.J., van Os, N.M., Smit, B., Karaborni, S. (1994). Molecular dynamics simulations of mode oil/water/surfactant systems. *Colloids and Surfaces A:—Physicochemical and Engineering Aspects*, **91**, 155.
- Estellé, P., Lanos, C., Melingé, Y., Servais, C. (2003). Squeezing flow for rheological characterisation of food materials, in *Proceedings of the Third International Symposium on Food Rheology and Structure*, Fischer, P., Marti, I., Windhab, E.J., Eds., Laboratory of Food Process Engineering, Zurich, Switzerland.
- Ettelaie, R. (2003). Computer simulation and modeling of food colloids. *Current Opinion in Colloid and Interface Science*, **8**, 415–421.
- Euston, S.R., Finnigan, S.R., Hirst, R.L. (2001). Heat-induced destabilization of oil-in-water emulsions formed from hydrolyzed whey protein. *Journal of Agricultural and Food Chemistry*, **49**, 5576.
- Evans, D.F., Wennerstrom, H. (1994). *The Colloidal Domain: Where Physics, Chemistry, Biology and Technology Meet*, VCH Publishers, New York, NY.
- Everett, D.H. (1988). *Basis Principles of Colloid Science*, Royal Society of Chemistry, Cambridge, UK.
- Evilevitch, A., Rescic, J., Jonsson, B., Olsson, U. (2002). Computer simulation of molecular exchange in colloidal systems. *Journal of Physical Chemistry B*, **106**, 11746.
- Evison, J., Dickinson, E., Owusu-Apenten, R.K., Williams, A. (1995). Formulation and properties of protein stabilized water-in-oil-in-water multiple emulsions, in *Food Macromolecules and Colloids*, Dickinson E., Lorient, D., Eds., Royal Society of Chemistry, Cambridge, UK, p. 235.
- Fabre, M., Aubry, V., Guichard, E. (2002). Comparison of different methods: Static and dynamic headspace and solid-phase microextraction for the measurement of interactions between milk proteins and flavor compounds with an application to emulsions. *Journal of Agricultural and Food Chemistry*, **50**, 1497.
- Faergemand, M., Krog, N. (2003). Using emulsifiers to improve food texture, in *Texture in Foods, Volume 1: Semi-Solid Foods*, McKenna, B.M., Ed., CRC Press, Boca Raton, FL, Chap. 10.
- Fainerman, V.B., Lucassen-Reynders, E., Miller, R. (1998). Adsorption of surfactants and proteins at fluid interfaces. *Colloids and Surfaces A: Physicochemical and Engineering Aspects*, **143**, 141.
- Fainerman, V.B., Zholob, S.A., Lucassen-Reynders, E.H., Miller, R. (2003). Comparison of various models describing the adsorption of surfactant molecules capable of interfacial reorientation. *Journal of Colloid and Interface Science*, **261**, 180.
- Fang, Y., Dalgleish, D.G. (1997). Conformation of  $\beta$ -lactoglobulin studied by FTIR: Effect of pH, temperature, and adsorption to the oil-water interface. *Journal of Colloid and Interface Science*, **196**, 292.
- Fang, Y., Dalgleish, D.G. (1998). The conformation of alpha-lactalbumin as a function of pH, heat treatment and adsorption at hydrophobic surfaces studied by FTIR. *Food Hydrocolloids*, **12**, 121.

- Fares, K., Landy, P., Guillard, R. (1998). Physicochemical interactions between aroma compounds and milk proteins: Effect of water and protein modification. *Journal of Dairy Science*, **81**, 82.
- Farinato, R.S., Rowell, R.L. (1983). Optical properties of emulsions, in *Encyclopedia of Emulsion Technology*, Vol. 1. *Basic Theory*, Becher, P., Ed., Marcel Dekker, New York, NY, Chap. 8.
- Fellows, P. (2000). *Food Processing Technology: Principles and Practice*, 2nd ed., Woodhead Publishers, Cambridge, UK.
- Fennema, O.R. (1977). Water and protein hydration, in *Food Proteins*, AVI Publishing, Westport, Chap. 3.
- Fennema, O.R. (1996a). *Food Chemistry*, 3rd ed., Marcel Dekker, New York, NY.
- Fennema, O.R. (1996b). Water and ice, in *Food Chemistry*, 3rd ed., Fennema, O.R., Ed., Marcel Dekker, New York, NY, Chap. 2.
- Fennema, O.R., Tannenbaum, S.R. (1996). Introduction to Food Chemistry, in *Food Chemistry*, 3rd ed., Fennema, O.R., Ed., Marcel Dekker, New York, NY, p. 1.
- Fisher, L.R., Parker, N.S. (1985). How do food emulsion stabilizers work? *CSIRO Food Research Quarterly*, **45**, 33.
- Fito, P., Mullet, A., McKenna, B. (1994). *Water in Foods: Fundamental Aspects and Their Significance in Relation to the Processing of Foods*, Elsevier, London, UK.
- Flack, E. (1997). Butter, margarine, spreads and baking fats, in *Lipid Technologies and Applications*, Gunstone, F.D., Padley, F.B., Eds., Marcel Dekker, New York, NY, pp. 265.
- Flint, O. (1994). *Food Microscopy: A Manual of Practical Methods, Using Optical Microscopy*, Springer Verlag, New York, NY.
- Floury, J., Desrumaux, A., Legrand, J. (2002). Effect of ultra-high-pressure homogenization on structure and on rheological properties of soy protein-stabilized emulsions. *Journal of Food Science*, **67**, 3388.
- Foegeding, E.A., Davis, J.P., Doucet, D., McGuffey, M.K. (2002). Advances in modifying and understanding whey protein functionality. *Trends in Food Science and Technology*, **13**, 151.
- Ford, L.D., Borwankar, R.P., Pechak, D., Schwimmer, B. (2004). Dressings and sauces, in *Food Emulsions*, 4th ed., Friberg, S., Larsson, K., Sjoblom, J., Eds., Marcel Dekker, New York, NY, Chap. 13.
- Formo, M.W. (1979). Physical properties of fats and fatty acids, in *Bailey's Industrial Oil and Fat Products*, Vol.1, 5th ed., Swern, D., Ed., John Wiley & Sons, New York, NY, Chap. 3.
- Foss, D.R., Brady, J.F. (2000). Brownian Dynamics simulation of hard-sphere colloidal dispersions. *Journal of Rheology*, **44**, 629.
- Fox, P.F. (1993). *Cheese: Chemistry, Physics, and Microbiology*, Chapman & Hall, London, UK.
- Fox, P.F., McSweeney, P.L.H. (1998). *Dairy Chemistry and Biochemistry*, Blackie Academic & Professional, UK.
- Fox, P.F., Condon, J.J. (1982). *Food Proteins*, Applied Science Publishers, London, UK.
- Fox, P.F., Guinee, T.P., Cogan, T.M., McSweeney, P.L.H. (2000). *Fundamentals of Cheese Science*, Aspen Publishers, Gaithersburg, MD.
- Francis, F.J. (1975). Basic concepts of colorimetry, in *Theory, Determination and Control of Physical Properties of Food Materials*, Rha, C., Ed., D. Reidel Publishing, Boston, MA, Chap. 14.
- Francis, F.J. (1995). Colorimetric properties of foods, in *Engineering Properties of Foods*, 2nd ed., Rao, M.A., Rizvi, S.S.H., Eds., Marcel Dekker, New York, NY, Chap. 10.
- Francis, F.J. (1998). Color analysis, in *Food Analysis*, 2nd ed., Nielsen, S.S., Ed., Aspen Publishers, Gaithersburg, MD, p. 599.
- Francis, F.J. (1999). *Colorants*, Eagen Press, St. Paul, MN.
- Francis, F.J. (2002). Food colorings, in *Colour in Food: Improving Quality*, MacDougall, D.B., Ed., CRC Press, Boca Raton, FL, p. 297.
- Francis, F.J., Clydesdale, F.M. (1975). *Food Colorimetry: Theory and Applications*, AVI Publishing, Westport, CT.
- Franco, J.M., Berjano, M., Gallegos, C. (1997). Linear viscoelasticity of salad dressing emulsions. *Journal of Agricultural and Food Chemistry*, **45**, 713.
- Franco, J.M., Berjano, M., Guerrero, A., Munoz, J., Gallegos, C. (1995a). Flow behavior and stability of light mayonnaise containing a mixture of egg-yolk and sucrose stearate as emulsifiers. *Food Hydrocolloids*, **9**, 111.

- Franco, J.M., Guerrero, A., Gallegos, C. (1995b). Rheology and processing of salad dressing emulsions, *Rheologica Acta*, **34**, 513.
- Franco, J.M., Gallegos, C., Barnes, H.A. (1998a). On slip effects in steady-state flow measurements of oil-in-water food emulsions. *Journal of Food Engineering*, **36**, 89.
- Franco, J.M., Raymundo, A., Sousa, I., Gallegos, C. (1998b). Influence of processing variables on the rheological and textural properties of lupin protein-stabilized emulsions. *Journal of Agricultural and Food Chemistry*, **46**, 3109.
- Frank, P. (2000). Premier salad dressings. *Food Product Design*.
- Frankel, E.N. (1991). Recent advances in lipid oxidation. *Journal of Food Science and Agriculture*, **54**, 495.
- Frankel, E.N. (1996). Evaluation of antioxidant activity of rosemary extracts, carnosol and carnosic acid in bulk vegetable oils and fish oil and their emulsions. *Journal of the Science of Food and Agriculture*, **72**, 201.
- Frankel, E.N. (1998). *Lipid Oxidation*, American Chemical Society, Washington, DC.
- Frankel, E.N., Huang, S.W., Kanner, J., German, J.B. (1994). Interfacial phenomena in the evaluation of antioxidants: Bulk oils versus emulsions. *Journal of Agriculture and Food Chemistry*, **42**, 1054.
- Franks, F. (1972–1982). *Water: A Comprehensive Treatise*, Vols. 1–7, Plenum Press, New York, NY.
- Franks, F. (1973). The solvent properties of water, in *Water: A Comprehensive Treatise*, Vol. 2, Franks, F., Ed., Plenum Press, New York, NY, Chap. 1.
- Franks, F. (1975a). The hydrophobic interaction, in *Water: A Comprehensive Treatise*, Vol. 4, *Aqueous solutions of amphiphiles and macromolecules*, Franks, F., Ed., Plenum Press, New York, NY, Chap. 1.
- Franks, F. (1975b). Water, ice and solutions of simple molecules, in *Water Relationships of Foods*, Duckworth, R.B., Ed., Academic Press, London, UK, p. 3.
- Franks, F. (1985a). Water and aqueous solutions: Recent advances, in *Properties of Water in Foods in Relation to Quality and Stability*, Simatos, D., Multon, J.L., Eds., Martinus Nijhoff Publishers, Dordrecht, p. 1.
- Franks, F. (1985b). Complex aqueous systems at subzero temperatures, in *Properties of Water in Foods in Relation to Quality and Stability*, Simatos, D., Multon, J.L., Eds., Martinus Nijhoff Publishers, Dordrecht, p. 497.
- Franks, F. (1991). Hydration phenomena: An update and implications for the food processing industry, in *Water Relationships in Foods: Advances in the 1980's and Trends for the 1990's*, Levine, H., Slade, L., Eds., Plenum Press, New York, NY, p. 1.
- Franzen, K.L., Kinsella, J.E. (1975). Physicochemical aspects of food flavouring. *Chemistry and Industry*, **21**, 505.
- Freeburg, E.J., Mistry, B.S., Reineccius, G.A., Scire, J. (1994). Stability of citral containing and citralless lemon oils in flavor emulsions and beverages. *Perfumer and Flavorist*, **19**, 23.
- Frei, R.W., MacNeil, J.D. (1973). *Diffuse Reflectance Spectroscopy in Environmental Problem-Solving*, CRC Press, Cleveland, OH.
- Frei, R.W., Frodyma, M.M., Lieu, V.T. (1975). Diffuse reflectance spectroscopy, in *Comprehensive Analytical Chemistry*, Svehla, G., Ed., Elsevier, Amsterdam, Chap. 3.
- Friberg, S.E. (1997). Emulsion stability, in *Food Emulsions*, 3rd ed., Friberg, S.E., Larsson, K., Eds., Marcel Dekker, New York, NY, p. 1.
- Friberg, S.E., El-Nokaly, M. (1983). Multilayer emulsions, in *Physical Properties of Foods*, Peleg, M., Bagley, E.B., Eds., AVI Publishing, Westport, CT, Chap. 5.
- Friberg, S.E., Larsson, K. (1997). *Food Emulsions*, 3rd ed., Marcel Dekker, New York, NY.
- Friberg, S.E., Larsson, K., Sjoblom, J. (2004). *Food Emulsions*, 4th ed., Marcel Dekker, New York, NY.
- Friel, E.N., Linforth, R.S.T., Taylor, A.J. (2000). An empirical model to predict the headspace concentration of volatile compounds above solutions containing sucrose. *Food Chemistry*, **71**, 309.
- Fromell, K., Huang, S.C., Caldwell, K. (2003). Scanning calorimetry in probing the structural stability of proteins at interfaces, in *Biopolymers at Interfaces*, 2nd ed., Malmsten, M., Ed., Marcel Dekker, New York, NY, p. 517.
- Frost, M.B., Dijksterhuis, G., Martens, M. (2001). Sensory perception of fat in milk. *Food Quality and Preference*, **12**, 327.
- Galazka, V.B., Dickinson, E., Ledward, D.A. (2000). Emulsifying properties of ovalbumin in mixtures with sulphated polysaccharides: Effects of pH, ionic strength, heat and high-pressure treatment. *Journal of the Science of Food and Agriculture*, **80**, 1219.



- Galema, S.A., Hoiland, H. (1991). Stereochemical aspects of hydration of carbohydrates in aqueous solutions: Density and ultrasonic measurements. *Journal of Physical Chemistry*, **95**, 5321.
- Gallegos, C., Berjano, M., Choplin, L. (1992). Linear viscoelastic behavior of commercial and model mayonnaise. *Journal of Rheology*, **36**, 465.
- Galluzzo, S.J., Regenstein, J.M. (1978a). Emulsion capacity and timed emulsification of chicken breast muscle myosin. *Journal of Food Science*, **43**, 1757.
- Galluzzo, S.J., Regenstein, J.M. (1978b). Role of chicken breast muscle proteins in meat emulsion formation—myosin, actin and synthetic actomyosin. *Journal of Food Science*, **43**, 1761.
- Gaonkar, A. (1995). *Characterization of Foods: Emerging Methods*, Elsevier, Amsterdam.
- Garrouch, A.A., Lababidi, H.M.S., Gharbi, R.B. (1996). Dielectric dispersion of dilute suspensions of colloid particles: Practical applications. *Journal of Physical Chemistry*, **100**, 16996.
- Garside, J. (1987). General principles of crystallization, in *Food Structure and Behaviour*, Blanshard, J.M.V., Lillford, P., Eds., Academic Press, London, UK, Chap. 3.
- Garti, N., Reichman, D. (1993). Hydrocolloids as food emulsifiers and stabilizers. *Food Microstructure*, **12**, 411.
- Garti, N. (1997). Progress in stabilization and transport phenomena of double emulsions in food applications. *Food Science and Technology—Lebensmittel-Wissenschaft und Technologie*, **30**, 222.
- Garti, N. (1999). Hydrocolloids as emulsifying agents for oil-in-water emulsions. *Journal of Dispersion Science and Technology*, **20**, 327.
- Garti, N., Benichou, A. (2001). Double emulsions for controlled-release applications: Progress and trends, in *Encyclopedic Handbook of Emulsion Technology*, Sjoblom, J., Ed., Marcel Dekker, New York, NY, p. 377.
- Garti, N., Benichou, A. (2004). Recent developments in double emulsions for food applications, in *Food Emulsions*, 4th ed., Friberg, S., Larsson, K., Sjoblom, J., Eds., Marcel Dekker, New York, NY, Chap. 10.
- Garti, N., Bisperink, C. (1998). Double emulsions: Progress and applications. *Current Opinion in Colloid and Interface Science*, **3**, 657.
- Garti, N., Sato, K. (1988). *Crystallization and Polymorphism of Fats and Fatty Acids*, Marcel Dekker, New York, NY.
- Garti, N., Yano, J. (2001). The roles of emulsifiers in fat crystallization, in *Crystallization Processes in Fats and Lipid Systems*, Garti, N., Sato, K., Eds., Marcel Dekker, New York, NY, p. 211.
- Gelin, B.R. (1994). *Molecular Modeling of Polymer Structures and Properties*, Hanser Publishers, Munich, Germany.
- Gilbert, A.N., Firestein, S. (2002). Dollars and scents: Commercial opportunities in olfaction and taste. *Nature Neuroscience*, **5**, 1043.
- Gilbertson, T.A., Damak, S., Margolskee, R.F. (2000). The molecular physiology of taste transduction. *Current Opinion in Neurobiology*, **10**, 519.
- Glicksman, M. (1982a). Background and classification, in *Food Hydrocolloids*, Vol. 1, Glicksman, M., Ed., CRC Press, Boca Raton, FL, Chap. 1.
- Glicksman, M. (1982b). Functional properties, in *Food Hydrocolloids*, Vol. 1, CRC Press, Boca Raton, FL, Chap. 3.
- Glicksman, M. (1982c). Food applications of gums, in *Food Carbohydrates*, Lineback, D.R., Inglett, G.E., Eds., AVI Publishing, Westport, CT, Chap. 15.
- Glicksman, M. (1983). Gums, in *Food Hydrocolloids*, Glicksman, M., Ed., CRC Press, Boca Raton, p. 7.
- Goddard, E.D., Ananthapadmanabhan, K.P. (1993). *Interactions of Surfactants with Polymers and Proteins*, CRC Press, Boca Raton, FL.
- Goff, H.D. (1993). Interactions and contributions of stabilizers and emulsifiers to development of structure in ice-cream, in *Food Colloids and Polymers: Stability and Mechanical Properties*, Dickinson, E., Walstra, P., Eds., Royal Society of Chemistry, Cambridge, UK, p. 71.
- Goff, H.D. (1997a). Instability and partial coalescence in whippable dairy emulsions. *Journal of Dairy Science*, **80**, 2620.
- Goff, H.D. (1997b). Instability and partial coalescence in dairy emulsions. *Journal of Dairy Science*, **80**, 2620.
- Goff, H.D. (1997c). Partial coalescence and structure formation in dairy emulsions, in *Food Proteins and Lipids*, American Chemical Society, S. Damodaran, Ed., Plenum Press, NY, p. 137.

- Goff, H.D. (1997d). Colloidal aspects of ice cream—a review. *International Dairy Journal*, **7**, 363.
- Goff, H.D. (2000). Controlling ice-cream structure by examining fat: Protein interactions. *Australian Journal of Dairy Technology*, **55**, 78.
- Goff, H.D. (2002). Formation and stabilization of structure in ice cream and related products. *Current Opinion in Colloid and Interface Science*, **7**, 432.
- Goff, H.D. (2003). Ice cream, in *Advanced Dairy Chemistry—1. Proteins*, 3rd ed. Fox, P.F., McSweeney, P.L.H., Eds., Kluwer Academic Publishers, New York, NY, p. 1063.
- Goff, H.D., Hartel, R.W. (2003). Ice cream and frozen desserts, in *Handbook of Food Freezing Technology*, Hui, Y.H., Ed., Marcel Dekker, New York, NY.
- Goff, H.D., Liboff, M., Jordon, W.K., Kinsella, J.E. (1987). The effect of polysorbate on the fat emulsion of ice-cream mix: Evidence from transmission electron microscopy studies. *Food Microstructure*, **6**, 193.
- Goff, H.D., Verespej, E., Smith, A.K. (1999). A study of fat and air structures in ice cream. *International Dairy Journal*, **9**, 817.
- Goodwin, J.W., Ottewill, R.H. (1991). Properties of concentrated colloidal dispersions. *Journal of the Chemical Society—Faraday Transactions*, **87**, 357.
- Gopal, E.S.R. (1968). Principles of Emulsion Formation, in *Emulsion Science*, Sherman, P., Ed., Academic Press, London, UK, Chap. 1.
- Goshawk, J.A., Binding, D.M., Kell, D.B., Goodacre, R. (1998). Rheological phenomena occurring during the shearing flow of mayonnaise. *Journal of Rheology*, **42**, 1537.
- Goubet, I., Dahout, C., Semon, E., Guichard, E., Le Quere, J.L., Voilley, A. (2001). Competitive binding of aroma compounds by beta-cyclodextrin. *Journal of Agricultural and Food Chemistry*, **49**, 5916.
- Goubet, I., Le Quéré, J.L., Sémon, E., Seuvre, A.M., Voilley, A. (2000). Competition between aroma compounds for the binding of  $\beta$ -cyclodextrins: Study of the nature of the interactions, in *Flavor Release*, ACS Symposium Series 763, Roberts, D.D., Taylor, A.J., Eds., American Chemical Society, Washington, DC, p. 246.
- Grab, W., Geffler, H. (2000). Flavourspace: A technology for measuring fast dynamic changes of flavor release during eating, in *Flavor Release*, ACS Symposium Series 763, Roberts, D.D., Taylor, A.J., Eds., American Chemical Society, Washington, DC, p. 33.
- Green, F.J. (1991). *Sigma-Aldrich Handbook of Stains, Dyes, and Indicators*, Aldrich, Milwaukee, WI.
- Green, R.J., Hopkinson, I., Jones, J.A.L. (1999). Conformational changes of globular proteins in solution and adsorbed at interfaces investigated by FTIR spectroscopy, in *Food Emulsions and Foams: Interfaces, Interactions and Stability*, Dickinson, E., Rodriguez-Patino, J.M., Eds., Royal Society of Chemistry, Cambridge, UK, pp. 285–295.
- Gregory, J. (1969). The calculation of Hamaker constants. *Advances in Colloid and Interface Science*, **2**, 396.
- Gregory, J. (1981). Approximate expressions for retarded van der Waals interaction. *Journal of Colloid Science*, **83**, 138.
- Grillo, I. (2003). Small-angle neutron scattering study of a world-wide known emulsion: Le Pastis. *Colloids and Surfaces A: Physicochemical and Engineering Aspects*, **225**, 153.
- Grinberg, V.Y., Tolstoguzov, V.B. (1997). Thermodynamic incompatibility of proteins and polysaccharides in solutions. *Food Hydrocolloids*, **11**, 145.
- Grosberg, A.Y., Khokhlov, A.R. (1997). *Giant Molecules*, Academic Press, San Diego, CA.
- Grover, G.S., Bike, S.G. (1995). Monitoring of flocculation in-situ in sterically stabilized silica dispersions using rheological techniques. *Langmuir*, **11**, 1807.
- Guerrero, A., Partal, P., Gallegos, C. (2000). Linear and non-linear viscoelasticity of low-in-cholesterol mayonnaise. *Food Science and Technology International*, **6**, 165.
- Guichard, E. (1996). Interactions between pectins and flavor compounds in strawberry jam, in *Flavor-Food Interactions*, McGorrian, R.J., Leland, J.V., Eds., American Chemical Society, Washington, DC, Chap. 11.
- Guichard, E. (2000). COST Action 96: Interaction of food matrix with small ligands influencing flavour and texture. *Food Research International*, **33**, 187.
- Guichard, E. (2002). Interactions between flavor compounds and food ingredients and their influence on flavor perception. *Food Reviews International*, **18**, 49.
- Guichard, E., Etievant, P. (1998). Measurement of interactions between polysaccharides and flavour compounds by exclusion size chromatography: Advantages and limits. *Nahrung-Food*, **42**, 376.

- Guichard, E., Langourieux, S. (2000). Interactions between  $\beta$ -lactoglobulin and flavour compounds. *Food Chemistry*, **71**, 301.
- Gunning, A.P., Mackie, A.R., Kirby, A.R., Morris, V.J. (2001). Scanning near field optical microscopy of phase separated regions in a mixed interfacial protein (BSA)-surfactant (Tween 20) film. *Langmuir*, **17**, 2013.
- Gunning, A.P., Mackie, A.R., Wilde, P.J., Morris, V.J. (2004a). Atomic force microscopy of emulsion droplets: Probing droplet-droplet interactions. *Langmuir*, **20**, 116.
- Gunning, P.A., Mackie, A.R., Gunning, A.P., Wilde, P.J., Woodward, N.C., Morris V.J. (2004b). The effect of surfactant type on protein displacement from the air-water interface. *Food Hydrocolloids*, **18**, 509.
- Gunstone, F.D. (1997). Fatty acids and lipids structure, in *Lipid Technologies and Applications*, Gunstone, F.D., Padley, F.B., Eds., Marcel Dekker, New York, NY, p. 1.
- Gunstone, F.D., Norris, F.A. (1983). *Lipids in Foods: Chemistry, Biochemistry and Technology*, Pergamon Press, Oxford, UK.
- Gunstone, F.D., Padley, F.B. (1997). *Lipid Technologies and Applications*, Marcel Dekker, New York, NY.
- Gurkov, T.D., Russev, S.C., Danov, K.D., Ivanov, I.B., Campbell, B. (2003). Monolayers of globular proteins on the air/water interface: Applicability of the volmer equation of state. *Langmuir*, **19**, 7362.
- Gurr, E. (1961). *Encyclopedia of Microscopic Stains*, Williams & Wilkins, Baltimore, MD.
- Gurr, M.I. (1997). Lipids and nutrition, in *Lipid Technologies and Applications*, Gunstone, F.D., Padley, F.B., Eds., Marcel Dekker, New York, NY, p. 79.
- Guyot, C., Bonnafont, C., Lesschaeve, I., Issanchou, S., Voilley, A., Spinnler, H.E. (1996). Effect of fat content oil odor intensity of three aroma compounds in model emulsions: Delta-decalactone, diacetyl, and butyric acid. *Journal of Agricultural and Food Chemistry*, **44**, 2341.
- Gwartney, E.A., Foegeding, E.A., Larick, D.K. (2000). The role of texture and fat on flavor release from whey protein isolate gels, in *Flavor Release*, ACS Symposium Series 763, Roberts, D.D., Taylor, A.J., Eds., American Chemical Society, Washington, DC, p. 355.
- Haahr, A.M., Bredie, W.L.P., Stahnke, L.H., Jensen, B., Refsgaard, H.H.F. (2000). Flavour release of aldehydes and diacetyl in oil/water systems. *Food Chemistry*, **71**, 355.
- Hallet, F.R. (1994). Particle size analysis by dynamic light scattering. *Food Research International*, **27**, 195.
- Halliwell, B., Gutteridge, J.M.C. (1991). *Free Radicals in Biology and Medicine*, 2nd ed., Clarendon Press, London, UK.
- Hansen, A.P., Booker, D.C. (1996). Flavor interactions with casein and whey protein, in *Flavor-Food Interactions*, McGorin, R.J., Leland, J.V., Eds., American Chemical Society, Washington, DC, Chap. 7.
- Hapke, B. (1993). *Theory of Reflectance and Emittance Spectroscopy*, Cambridge University Press, Cambridge, UK.
- Harden, J.L., Viasnoff, V. (2001). Recent advances in DWS-based micro-rheology. *Current Opinion in Colloid and Interface Science*, **6**, 438.
- Harper, W.J., Hall, C.W. (1976). *Dairy Technology and Engineering*, AVI Publishing, Westport, CT.
- Harrison, M. (1998). Effect of breathing and saliva flow on flavor release from liquid foods. *Journal of Agricultural and Food Chemistry*, **46**, 2727.
- Harrison, M. (2000). Mathematical models of release and transport of flavors from foods in the mouth to the olfactory epithelium, in *Flavor Release*, ACS Symposium Series 763, Roberts, D.D., Taylor, A.J., Eds., American Chemical Society, Washington, DC, p. 179.
- Harrison, M., Hills, B.P. (1997a). Mathematical model of flavor release from liquids containing aroma-binding macromolecules. *Journal of Agricultural and Food Chemistry*, **45**, 1883.
- Harrison, M., Hills, B.P. (1997b). Effects of air flow-rate on flavour release from liquid emulsions in the mouth. *International Journal of Food Science and Technology*, **32**, 1.
- Harrison, M., Hills, B.P., Bakker, J., Clothier, T. (1997). Mathematical models of flavor release from liquid emulsions. *Journal of Food Science*, **62**, 653.
- Harrison, M., Campbell, S., Hills, B.P. (1998). Computer simulation of flavor release from solid foods in the mouth. *Journal of Agricultural and Food Chemistry*, **46**, 2736.
- Hartel, R.W. (2001). *Crystallization in Foods*, Aspen Publishers, Gaithersburg, MD.

- Harvey, B.A., Brauss, M.S., Linforth, R.S.T., Taylor, A.J. (2000). Real time flavor from foods during eating, in *Flavor Release*, ACS Symposium Series 763, Roberts, D.D., Taylor, A.J., Eds., American Chemical Society, Washington, DC, p. 22.
- Harvey, B.A., Druaux, C., Voilley, A. (1995). Effect of protein on the retention and transfer of aroma compounds at the lipid water interface, in *Food Macromolecules and Colloids*, Dickinson, E., Lorient, D., Eds., The Royal Society of Chemistry, Cambridge, UK, p. 154.
- Hasenhuettl, G.L. (1997a). Overview of food emulsifiers, in *Food Emulsifiers and Their Applications*, Hasenhuettl, G.L., Hartel, R.W., Eds., Chapman & Hall, New York, NY, Chap. 1.
- Hasenhuettl, G.L. (1997b). Analysis of food emulsifiers, in *Food Emulsifiers and Their Applications*, Hasenhuettl, G.L., Hartel, R.W., Eds., Chapman & Hall, New York, NY, Chap. 3.
- Hasenhuettl, G.L., Hartel, R.W. (1997). *Food Emulsifiers and Their Applications*, Chapman & Hall, New York, NY.
- Hasted, J.B. (1972). Liquid water: Dielectric properties, in *Water: A Comprehensive Treatise*, Vol. 1, Franks, F., Ed., Plenum Press, Chap. 7.
- Hato, M., Maruta, M., Yoshida, T. (1996). Surface forces between protein A adsorbed mica surfaces. *Colloids and Surfaces A: Physicochemical and Engineering Aspects*, **109**, 345.
- Hau, M.Y.M., Gray, D.A., Taylor, A.J. (1996). Binding of volatiles to starch, in *Flavor-Food Interactions*, McGorin, R.J., Leland, J.V., Eds., American Chemical Society, Washington, DC, Chap. 10.
- Hauser, H. (1975). Lipids, in *Water: A Comprehensive Treatise*. Vol. 4, *Aqueous Solutions of Amphiphiles and Macromolecules*, Franks, F., Ed., Plenum Press, New York, NY, Chap. 4.
- Heath, H.B. (1978). *Flavor Technology: Profiles, Products, Applications*, AVI Publishing, Westport, CT.
- Heath, H.B., Reineccius, G. (1986). *Flavor Chemistry and Technology*, AVI Publishing, Westport, CT.
- Hedin, N., Furo, I. (2001). Ostwald ripening of an emulsion monitored by PGSE NMR. *Langmuir*, **17**, 4746.
- Heertje, I., Paques, M. (1995). Advances in electron microscopy, in *New Physicochemical Techniques for the Characterization of Complex Food Systems*, Dickinson, E., Ed., Blackie Academic & Professional, London, UK, Chap. 1.
- Heertje, I., vanAalst, H., Blonk, J.C.G., Don, A., Nederlof, J., Lucassen-Reynders, E.H. (1996). Observations on emulsifiers at the interface between oil and water by confocal scanning light microscopy. *Food Science and Technology—Lebensmittel-Wissenschaft und Technologie*, **29**, 217.
- Heinemann, C., Conde-Petit, B., Nuessli, J., Escher, F. (2001). Evidence of starch inclusion complexation with lactones. *Journal of Agricultural and Food Chemistry*, **49**, 1370.
- Hemar, Y., Horne, D.S. (1999). A diffusing wave spectroscopy study of the kinetics of Ostwald ripening in protein-stabilised oil/water emulsions. *Colloids and Surfaces B: Biointerfaces*, **12**, 239.
- Hemar, Y., Herrmann, N., Lemarechal, P., Hocquart, R., Lequeux, F. (1997). Effective medium model for ultrasonic attenuation due to the thermo-elastic effect in concentrated emulsions. *Journal de Physique II*, **7**, 637.
- Hemar, Y., Pinder, D.N., Hunter, R.J., Singh, H., Hebraud, R., Horne, D.S. (2003). Monitoring of flocculation and creaming of sodium-caseinate-stabilized emulsions using diffusing-wave spectroscopy. *Journal of Colloid and Interface Science*, **264**, 502.
- Herman, B., Tanke, H.J. (1998). *Fluorescence Microscopy*, 2nd ed., Bios Scientific Pub.
- Hermansson, A.M. (1988). Gel structure of food biopolymers, in: *Food Structure—Its Creation and Evaluation*, Blanshard, J.M.V., Mithchell, J.R., Eds., Butterworths, London, UK, Chap. 3.
- Hernandez, E., Baker, R.A. (1991). Turbidity of beverages with citrus oil clouding agent. *Journal of Food Science*, **56**, 1024.
- Hernandez, E., Baker, R.A., Crandall, P.G. (1991). Model for evaluating the turbidity in cloudy beverages. *Journal of Food Science*, **56**, 747.
- Hernqvist, L. (1984). On the structure of triglycerides in the liquid state and fat crystallization. *Fette Seifen Anstrichmittel*, **86**, 297.
- Hernqvist, L. (1990). Polymorphism of triglycerides: A crystallographic review. *Food Structure*, **9**, 39.
- Herrmann, N., McClements, D.J. (1999). Ultrasonic propagation in highly concentrated oil-in-water emulsions. *Langmuir*, **15**, 7937.
- Hiemenz, P.C., Rajagopalan, R. (1997). *Principles of Colloid and Surface Chemistry*, 3rd ed., Marcel Dekker, New York, NY.

- Hills, B.P., Manoj, P., Destruel, C. (2000). NMR Q-space microscopy of concentrated oil-in-water emulsions. *Magnetic Resonance Imaging*, **18**, 319.
- Hills, B.P., Tang, H.R., Manoj, P., Destruel, C. (2001). NMR diffusometry of oil-in-water emulsions. *Magnetic Resonance Imaging*, **19**, 449.
- Hlady, V., Buijs, J. (2003). Local and global optical spectroscopic probes of adsorbed proteins, in *Biopolymers at Interfaces*, 2nd ed., Malmsten, M., Ed., Marcel Dekker, New York, NY, p. 435.
- Hodate, Y., Ueno, S., Yano, J., Katsuragi, T., Tezuka, Y., Tagawa, T., Yoshimoto, N., Sato, K. (1997). Ultrasonic velocity measurement of crystallization rates of palm oil in oil-water emulsions. *Colloids and Surfaces A: Physicochemical and Engineering Aspects*, **128**, 217.
- Hodgins, D. (1997). The electronic nose: Sensor array-based instruments that emulate the human nose, in *Techniques for Analyzing Food Aroma*, Marsili, R., Ed., Marcel Dekker, New York, NY, p. 331.
- Hollingsworth, P. (1995). Food research: Cooperation is the key. *Food Technology*, **49**: 2, 67.
- Hollingsworth, K.G., Johns, M.L. (2003). Measurement of emulsion droplet sizes using PFG NMR and regularization methods. *Journal of Colloid and Interface Science*, **258**, 383.
- Hollowood, T.A., Davidson, J.M., DeGroot, L., Linforth, R.S.T., Taylor, A.J. (2002). Taste release and its effect on overall flavor perception. *Chemistry of Taste: Mechanisms, Behaviors, and Mimics*, ACS Symposium Series, **825**, 166.
- Hollowood, T.A., Linforth R.S.T., Taylor, A.J. (2000). The relationship between carvone release and the perception of mintyness in gelatine gels, in *Flavor Release*, ACS Symposium Series 763, Roberts, D.D., Taylor, A.J., Eds., American Chemical Society, Washington, DC, p. 370.
- Holt, W.J.C., Chan, D.Y.C. (1997). Pair interactions between heterogeneous spheres. *Langmuir*, **13**, 1577.
- Hone, J.H.E., Cosgrove, T., Saphiannikova, M., Obey, T.M., Marshall, J.C., Crowley, T.L. (2002). Structure of physically adsorbed polymer layers measured by small-angle neutron scattering using contrast variation methods. *Langmuir*, **18**, 855–864.
- Horike, S., Akahoshi, R. (1996). Solubilization mechanism of cis-3-hexenol and menthyl acetate into sodium dodecyl sulfate micelles, and the vapor pressure of these odorants. *Nippon Kagaku Kaishi*, **12**, 1033.
- Horne, D.S. (1995). Light scattering studies of colloid stability and gelation, in *New Physicochemical Techniques for the Characterization of Complex Food Systems*, Dickinson, E., Ed., Blackie Academic & Professional, London, UK, Chap. 11.
- Hsu, J.P., Nacu, A. (2003). Behavior of soybean oil-in-water emulsion stabilized by nonionic surfactant. *Journal of Colloid and Interface Science*, **259**, 374.
- Hu, M., McClements, D.J., Decker, E.A. (2003). Lipid oxidation in corn oil-in-water emulsions stabilized by casein, whey protein isolate, and soy protein isolate. *Journal of Agricultural and Food Chemistry*, **51**, 1696.
- Huang, S.-W., Frankel, E.N., Aeschbach, R., German, J.B. (1997). Partition of selected antioxidants in corn oil-in-water model systems. *Journal of Agriculture and Food Chemistry*, **45**, 1991.
- Huang, X., Kakuda, Y., Cui, W. (2001). Hydrocolloids in emulsions: Particle size distribution and interfacial activity. *Food Hydrocolloids*, **15**, 533.
- Huber, D.G., Regenstien, J.M. (1988). Emulsion stability studies of myosin and exhaustively washed muscle from adult chicken breast muscle. *Journal of Food Science*, **53**, 1282.
- Hui, Y.H. (1992). *Encyclopedia of Food Science and Technology*, John Wiley & Sons, New York, NY.
- Huidobro, A., Montero, P., Borderias, A.J. (1998). Emulsifying properties of an ultrafiltered protein from minced fish wash water. *Food Chemistry*, **61**, 339.
- Hunt, J.A., Dalgleish, D.G. (1994). Effect of pH on the stability and surface composition of emulsions made with whey protein isolate. *Journal of Food Science*, **59**, 2131.
- Hunt, J.A., Dalgleish, D.G. (1995). Heat stability of oil-in-water emulsions containing milk proteins: Effect of ionic strength and pH. *Journal of Food Science*, **60**, 1120.
- Hunt, J.A., Dalgleish, D.G. (1996). The effect of the presence of KCl on the adsorption behavior of whey-protein and caseinate in oil-in-water emulsions. *Food Hydrocolloids*, **10**, 159.
- Hunter, R.J. (1986). *Foundations of Colloid Science*, Vol. 1, Oxford University Press, Oxford, UK.
- Hunter, R.J. (1989). *Foundations of Colloid Science*, Vol. 2, Oxford University Press, Oxford, UK.
- Hunter, R.J. (1993). *Introduction to Modern Colloid Science*, Oxford University Press, Oxford, UK.

- Hunter, R.J. (1998a). Recent developments in the electroacoustic characterisation of colloidal suspensions and emulsions. *Colloids and Surfaces A: Physicochemical and Engineering Aspects*, **141**, 37.
- Hunter, R.J. (1998b). The electroacoustic characterization of colloidal suspensions, in *Handbook on Ultrasonic and Dielectric Characterization Techniques for Suspended Particles*, Hackley, V.A., Texter, J., Eds., American Chemical Society, Westerville, OH.
- Hunter, R.S., Harold, R.W. (1987). *The Measurement of Appearance*, 2nd ed., John Wiley & Sons Interscience Publication, New York, NY.
- Husband, F.A., Garrood, M.J., Mackie, A.R., Burnett, G.R., Wilde, P.J. (2001). Adsorbed protein secondary and tertiary structures by circular dichroism and infrared spectroscopy with refractive index matched emulsions. *Journal of Agricultural and Food Chemistry*, **49**, 859.
- Hussin, A.B.B.H., Povey, M.J.W. (1984). A study of dilation and acoustic propagation in solidifying fats and oils: Experimental. *Journal of the American Oil Chemists Society*, **61**, 560.
- Hutchings, J. (2002a). The perception and assessment of color, in: *Colour in Food: Improving Quality*, MacDougall, D.B., Ed., CRC Press, Boca Raton, FL, p. 9.
- Hutchings, J. (2002b). Calibrated color imaging analysis of foods, in *Colour in Food: Improving Quality*, MacDougall, D.B., Ed., CRC Press, Boca Raton, FL, p. 352.
- Hutchings, J.B. (1999). *Food Color and Appearance*, 2nd ed., Aspen Publishers, Gaithersburg, MD.
- Ikeda, S., Morris, V.J., Nishinari, K. (2001). Microstructure of aggregated and nonaggregated kappa-carrageenan helices visualized by atomic force microscopy. *Biomacromolecules*, **2**, 1331.
- Imeson, A. (1997). *Thickening and Gelling Agents for Food*, 2nd ed., Blackie Academic & Professional, London, UK.
- Isaacs, E.E., Huang, M., Babchin, A.J. (1990). Electroacoustic method for monitoring the coalescence of water-in-oil emulsions. *Colloids and Surfaces*, **46**, 177.
- Islam, A.M., Phillips, G.O., Sljivo, A., Snowden, M.J., Williams, P.A. (1997). A review of recent developments on the regulatory, structural and functional aspects of gum arabic. *Food Hydrocolloids*, **11**, 493.
- Israelachvili, J.N. (1992). *Intermolecular and Surface Forces*, Academic Press, London, UK.
- Israelachvili, J.N. (1994). The science and applications of emulsions—an overview. *Colloids and Surfaces*, **91**, 1.
- Israelachvili, J.N., Berman, A. (1995). Irreversibility, energy dissipation and time effects in intermolecular and surface interactions. *Israel Journal of Chemistry*, **35**, 85.
- Israelachvili, J.N., Pashly, R.M. (1984). Measurement of the hydrophobic interaction between two hydrophobic surfaces in aqueous electrolyte solutions. *Journal of Colloid Science*, **98**, 500.
- Israelachvili, J.N., Wennerstrom, H. (1996). Role of hydration and water-structure in biological and colloidal interactions. *Nature*, **379**, 219.
- Ivanov, I.B., Danov, K.D., Kralchevsky, P.A. (1999). Flocculation and coalescence of micron-size emulsion droplets. *Colloids and Surfaces A: Physicochemical and Engineering Aspects*, **152**, 161.
- Iwanami, Y., Tateba, H., Kodama, N., Kishino, K. (1997). Changes of lemon flavor components in an aqueous solution during UV irradiation. *Journal of Agricultural and Food Chemistry*, **45**, 463.
- Jackel, V.K. (1964). Über die funktionen des schuzkolloids. *Kolloid-Zeitschrift und Zeitschrift für Polymere*, **197**, 143.
- Jacobsen, C. (1999). Sensory impact of lipid oxidation in complex food systems. *Fett-Lipid*, **101**, 484.
- Jacobsen, C., Meyer, A.S., Adler-Nissen, J. (1998). Oxidation mechanisms in real food emulsions: Method for separation of mayonnaise by ultracentrifugation. *Journal of Food Lipids*, **5**, 87.
- Jacobsen, C., Meyer, A.S., Adler-Nissen, J. (1999a). Oxidation mechanisms in real food emulsions: Oil-water partition coefficients of selected volatile off-flavor compounds in mayonnaise. *Food Research and Technology*, **208**, 317.
- Jacobsen, C., Schwarz, K., Stockmann, H., Meyer, A.S., Adler-Nissen, J. (1999b). Partitioning of selected antioxidants in mayonnaise. *Journal of Agricultural and Food Chemistry*, **47**, 3601.
- Jacobsen, C., Timm, M., Meyer, A.S. (2001a). Oxidation in fish oil enriched mayonnaise: Ascorbic acid and low pH increase oxidative deterioration. *Journal of Agricultural and Food Chemistry*, **49**, 3947.
- Jacobsen, C., Hartvigsen, K., Thomsen, M.K., Hansen, L.F., Lund, P., Skibsted, L.H., Holmer, G., Adler-Nissen, J., Meyer, A.S. (2001b). Lipid oxidation in fish oil enriched mayonnaise: Calcium disodium ethylenediaminetetraacetate, but not gallic acid, strongly inhibited oxidative deterioration. *Journal of Agricultural and Food Chemistry*, **49**, 1009.

- Janestad, H., Wendin, K., Ruhe, A., Hall, G. (2000). Modelling of dynamic flavour properties with ordinary differential equations. *Food Quality and Preference*, **11**, 323.
- Janssen, J.J.M., Boon, A., Agterof, W.G.M. (1994). Influence of dynamic interfacial properties on droplet breakup in simple shear floes. *Fluid Mechanics and Transport Phenomena*, **40**, 1929.
- Jay, J.M. (2000). *Modern Food Microbiology*, 6th ed., Kluwer Academic Publishers, Norwell, MA.
- Jayme, M.L., Dunstan, D.E., Gee, M.L. (1999). Zeta potentials of gum arabic stabilised oil in water emulsions. *Food Hydrocolloids*, **13**, 459.
- Jaynes, E.N. (1983). Applications in the food industry: II, in *Encyclopedia of Emulsion Technology*, Vol. 2, Becher, P., Ed., Marcel Dekker, New York, NY, Chap. 6.
- Jenkins, P., Snowden, M. (1996). Depletion flocculation in colloidal dispersions. *Advances in Colloid and Interface Science*, **68**, 57.
- Jensen, R.G. (1995). *Handbook of Milk Composition*, Academic Press, San Diego, CA.
- Jo, C., Ahn, D.U. (1999). Fat reduces volatiles production in oil emulsion system analyzed by purge-and-trap dynamic headspace/gas chromatography. *Journal of Food Science*, **64**, 641.
- Jokela, P., Fletcher, P.D.I., Aveyard, R., Lu, J.R. (1990). The use of computerized microscopic image analysis to determine emulsion droplet size distribution. *Journal of Colloid and Interface Science*, **134**, 417.
- Jones, M.N., Chapman, M.N. (1995). *Micelles, Monolayers and Biomembranes*, John Wiley & Sons, New York, NY.
- Jones, S.A. (1996). Issues in fat replacement, in *Handbook of Fat Replacers*, Roller, S., Jones, S.A., Eds., CRC Press, Boca Raton, FL, Chap. 1.
- Jönsson, B., Lindman, B., Holmberg, K., Kronberg, B. (1998). *Surfactants and Polymers in Aqueous Solution*. John Wiley & Sons, Chichester, UK.
- Joshi, P. (2000). Physical aspects of color in foods. *Chemical Innovation*, **30**, 19.
- Joshi, P. (2002). Colour measurement of foods by colour reflectance, in *Colour in Food: Improving Quality*, MacDougall, D.B., Ed., CRC Press, Boca Raton, FL, p. 80.
- Jouenne, E., Crouzet, J. (2000a). Determination of apparent binding constants for aroma compounds with  $\beta$ -lactoglobulin by dynamic coupled column liquid chromatography. *Journal of Agricultural and Food Chemistry*, **48**, 5396.
- Jouenne, E., Crouzet, J. (2000b). Effect of pH on retention of aroma compounds by beta-lactoglobulin. *Journal of Agricultural and Food Chemistry*, **48**, 1273.
- Judd D.B., Wyszecki, G. (1963). *Color in Business, Science, and Industry*, 2nd ed., New York, NY, John Wiley & Sons.
- Jung, D.M., de Ropp, J.S., Ebeler, S.E. (2002). Application of pulsed field gradient NMR techniques for investigating binding of flavor compounds to macromolecules. *Journal of Agricultural and Food Chemistry*, **50**, 4262.
- Jung, D.M., Ebeler, S.E. (2003). Headspace solid-phase microextraction method for the study of the volatility of selected flavor compounds. *Journal of Agricultural and Food Chemistry*, **51**, 200.
- Kabalnov, A.S. (1998). Coalescence in emulsions, in *Modern Aspects of Emulsion Science*, Binks, B.P., Ed., The Royal Society of Chemistry, Cambridge, UK., Chap. 7.
- Kabalnov, A.S., Shchukin, E.D. (1992). Ostwald ripening theory: Applications to fluorocarbon emulsion stability. *Advances in Colloid and Interface Science*, **38**, 69.
- Kabalnov, A.S., Weers, J. (1996). Macroemulsion stability within the Winsor III region: Theory versus experiment. *Langmuir*, **12**, 1931.
- Kabalnov, A.S., Wennerstrom, H. (1996). Macroemulsion stability: The orientated wedge theory revisited. *Langmuir*, **12**, 276.
- Kabalnov, A.S., Weers, J., Arlauskas, R., Tarara, T. (1995). Phospholipids as emulsion stabilizers. Part 1: Interfacial tension. *Langmuir*, **11**, 2966.
- Kalab, M. (1981). Electron microscopy of milk products: A review of techniques. *Scanning Electron Microscopy*, **3**, 453.
- Kalab, M., Allan-Wojtas, P., Miller, S.S. (1995). Microscopy and other imaging techniques in food structure analysis. *Trends in Food Science and Technology*, **6**, 180.
- Kallay, N., Hlady, V., Jednacak-Biscan, J., Milonjic, S. (1993). Techniques for the study of adsorption from solution, in *Physical Methods of Chemistry*, Vol. IXA, *Investigations of Surfaces and Interfaces*, Rossiter, B.W., Baetzold, R.C., Eds., John Wiley & Sons, New York, NY, Chap. 2.

- Kandori, K. (1995). Applications of microporous glass membranes: Membrane emulsification, in *Food Processing: Recent Developments*, Gaonkar, A.G., Ed., Elsevier, Amsterdam.
- Karbstein, H., Schubert, H. (1995a). Developments in the continuous mechanical production of oil-in-water macro-emulsions. *Chemical Engineering and Processing*, **34**, 205.
- Karbstein, H., Schubert, H. (1995b). Basic criteria for the selection of emulsifying machines, in *Food Ingredients Europe Conference Proceedings*, Frankfurt a.M. S. 93.
- Karplus, M., Porter, R.N. (1970). *Atoms and Molecules: An Introduction for Students of Physical Chemistry*, Benjamin-Cummings Publishing, Menlo Park, CA.
- Kashchiev, D., Kaneko, N., Sato, K. (1998). Kinetics of crystallization in polydisperse emulsions. *Journal of Colloid and Interface Science*, **208**, 167.
- Kawakatsu, T., Kikuchi, Y., Nakajima, M. (1997). Regular-sized cell creation in microchannel emulsification by visual microprocessing method. *Journal of the American Oil Chemists Society*, **74**, 317.
- Kawakatsu, K., Trägårdh, G.; Trägårdh, C.H., Nakajima, M., Oda, N., Yonemoto, T. (2001). The effect of hydrophobicity of microchannels and components in water and oil phases on droplet formation in micro-channel water-in-oil emulsification. *Colloids and Surfaces A: Physicochemical and Engineering Aspects*, **179**, 29.
- Keane, M.A., Bowyer, M.C., Biggs, S.R., Galvin, K.P., Hosken, R.W. (2000). Particle size analysis of microfluidised dairy emulsions. *Australian Journal of Dairy Technology*, **55**, 94.
- Keikens, F. (1997). Optimization of electrical conductance measurements for the quantification and prediction of phase separation in O/W emulsions containing hydroxypropylmethylcelluloses as emulsifying agents. *International Journal of Pharmaceutics*, **146**, 239.
- Kellens, M., Meeussen, W., Reynaers, H. (1992). *Journal of the American Oil Chemists Society*, **69**, 906.
- Kelley, D.I., McClements, D.J. (2003). Interaction of bovine serum albumin with ionic surfactants in aqueous solutions. *Food Hydrocolloids*, **17**, 73.
- Keowmaneechai, E., McClements D.J. (2002a). Effect of  $\text{CaCl}_2$  and KCl on physicochemical properties of model nutritional beverages based on whey protein stabilized oil-in-water emulsions. *Journal of Food Science*, **67**, 665.
- Keowmaneechai, E., McClements D.J. (2002b). Influence of EDTA and citrate on physicochemical properties of whey protein-stabilized oil-in-water emulsions containing  $\text{CaCl}_2$ . *Journal of Agricultural and Food Chemistry*, **50**, 7145.
- Kerker, M. (1969). *The Scattering of Light and Other Electromagnetic Radiation*, Academic Press, New York, NY.
- Khatib, K.A., Herald, T.J., Aramouni, F.M., MacRitchie, E., Schapaugh, W.T. (2002). Characterization and functional properties of soy beta-conglycinin and glycinin of selected genotypes. *Journal of Food Science*, **67**, 2923.
- Kilcast, D., Clegg, S. (2002). Sensory perception of creaminess and its relationship with food structure. *Food Quality and Preference*, **13**, 609.
- Kim, H.J., Decker, E.A., McClements, D.J. (2002a). Impact of protein surface denaturation on droplet flocculation in hexadecane oil-in-water emulsions stabilized by  $\beta$ -lactoglobulin. *Journal of Agricultural and Food Chemistry*, **50**, 7131.
- Kim, H.J., Decker, E.A., McClements, D.J. (2002b). Role of postadsorption conformation changes of beta-lactoglobulin on its ability to stabilize oil droplets against flocculation during heating at neutral pH. *Langmuir*, **18**, 7577.
- Kim, H.J., Choi, S.J., Shin, W.S., Moon, T.W. (2003). Emulsifying properties of bovine serum albumin-galactomannan conjugates. *Journal of Agricultural and Food Chemistry*, **51**, 1049.
- Kim, Y.D., Morr, C.V., Schenz, T.W. (1996). Microencapsulation properties of gum arabic and several food proteins: Liquid orange oil emulsion particles. *Journal of Agricultural and Food Chemistry*, **44**, 1308.
- Kinsella, J.E. (1989). In *Flavor Chemistry of Lipid Foods*, Min, D.B., Smouse, T.H., Eds., American Oil Chemists Society, Champaign, IL, p. 376.
- Kinsella, J.E., Whitehead, D.M. (1989). Proteins in whey: Chemical, physical and functional properties. *Advances in Food and Nutrition Research*, **33**, 343.
- Kippax, P., Sherwood, J.D., McClements, D.J. (1999). Ultrasonic spectroscopy study of globule aggregation in parenteral fat emulsions containing calcium chloride. *Langmuir*, **15**, 1673.



- Kirby, A.R., Gunning, A.P., Morris, V.J. (1995). Atomic force microscopy in food research: A new technique comes of age. *Trends in Food Science and Technology*, **6**, 359.
- Kitakara, A., Watanabe, A. (1984). *Electrical Phenomenon at Interfaces: Fundamentals, Measurements and Applications*, Marcel Dekker, New York, NY.
- Kobayashi, I., Nakajima, M., Mukataka, S. (2003). Preparation characteristics of oil-in-water emulsions using differently charged surfactants in straight-through microchannel emulsification. *Colloids and Surfaces A: Physicochemical and Engineering Aspects*, **229**, 33.
- Kokini, J.L. (1987). The physical basis of liquid food texture and texture-taste interactions. *Journal of Food Engineering*, **6**, 51.
- Kong, L., Beattie, J.K., Hunter, R.J. (2001a). Electroacoustic study of *n*-hexadecane/water emulsions. *Australian Journal of Chemistry*, **54**, 503.
- Kong, L., Beattie, J.K., Hunter, R.J. (2001b). Electroacoustic determination of size and charge of sunflower oil-in-water emulsions made by high-pressure homogenizing. *Chemical Engineering and Processing*, **40**, 421.
- Kong, L., Beattie, J.K., Hunter, R.J. (2001c). Electroacoustic study of concentrated oil-in-water emulsions. *Journal of Colloid and Interface Science*, **238**, 70.
- Kong, L., Beattie, J.K., Hunter, R.J. (2003). Electroacoustic study of BSA or lecithin stabilised soybean oil-in-water emulsions and SDS effect. *Colloids and Surfaces B: Biointerfaces*, **27**, 11.
- Kortum, G. (1969). *Reflectance Spectroscopy: Principles, Methods, Applications*, Springer-Verlag, New York, NY.
- Kritchevsky, D. (2002). Fats and oils in human health, in *Food Lipids: Chemistry, Nutrition and Biotechnology*, Akoh, C.C., Min, D.B., Eds., Marcel Dekker, New York, NY, Chap. 17.
- Krog, M.J., Riisom, T.H., Larsson, K. (1983). Applications in the food industry: I., in *Encyclopedia of Emulsion Technology*, Vol. 2, Becher, P., Ed., Marcel Dekker, New York, NY, Chap. 5.
- Krog, N. (1997). Food emulsifiers, in *Lipid Technologies and Applications*, Gunstone, F.D., Padley, F.B., Eds., Marcel Dekker, New York, NY, pp. 521–534.
- Krog, N.J., Sparso, F.V. (2004). Food Emulsifiers: Their chemical and physical properties, in *Food Emulsions*, 4th ed., Friberg, S., Larsson, K., Sjoblom, J., Eds., Marcel Dekker, New York, NY, Chap. 2.
- Kulmyrzaev, A., Chanamai, R., McClements, D.J. (2000a). Influence of pH and  $\text{CaCl}_2$  on the stability of dilute whey protein stabilized emulsions. *Food Research International*, **33**, 15.
- Kulmyrzaev, A., Silvestre M.P.C., McClements, D.J. (2000b). Rheology and stability of whey protein stabilized emulsions with high  $\text{CaCl}_2$  concentrations. *Food Research International*, **33**, 21.
- Kulmyrzaev, A.A., Schubert, H. (2004). Influence of KCl on the physicochemical properties of whey protein stabilized emulsions. *Food Hydrocolloids*, **18**, 13.
- Kuznetsova, G.M., Kartasheva, Z.S., Kasaikina, O.T. (1996). Kinetics of limonene autooxidation, *Russian Chemical Bulletin*, **45**, 1592.
- Labows, J.N., Cagan, R.H. (1993). *Complexity of Flavor Recognition and Transduction*, ACS Symposium Series, **528**, 10.
- Lachaise, J., Mendiboure, B., Dicharry, C., Marion, G., Salager, J.L. (1996). Simulation of the over-emulsification phenomenon in turbulent stirring. *Colloids and Surfaces A: Physicochemical and Engineering Aspects*, **110**, 1.
- Land, D.G. (1996). Perspectives on the effects of interactions on flavour perception: An overview, in *Flavor-Food Interactions*, McGorin, R.J., Leland, J.V., Eds., American Chemical Society, Washington, DC.
- Landy, P., Courthaudon, J.L., Dubois, C., Voilley, A. (1996). Effect of interface in model food emulsions on the volatility of aroma compounds. *Journal of Agricultural and Food Chemistry*, **44**, 526.
- Landy, P., Rogacheva, S., Lorient D., Voilley, A. (1998). Thermodynamic and kinetic aspects of the transport of small molecules in dispersed systems. *Colloids and Surfaces B: Biointerfaces*, **12**, 57–65.
- Lang, J., Zana, R. (1987). Chemical relaxation methods, in *Surfactant Solutions: New Methods of Investigation*, Zana, R., Ed., Marcel Dekker, New York, NY.
- Langourieux, S., Crouzet, J. (1995). Protein-aroma interactions, in *Food Macromolecules and Colloids*, Dickinson, E., Lorient, D., Eds., The Royal Society of Chemistry, Cambridge, UK, p. 123.
- Langton, M., Jordansson, E., Altskar, A., Sorensen, C., Hermansson, A.M. (1999). Microstructure and image analysis of mayonnaises. *Food Hydrocolloids*, **13**, 113.

- Lapasin, R., Priel, S. (1995). *Rheology of Industrial Polysaccharides: Theory and Applications*, Blackie Academic & Professional, London, UK.
- Larison, K.D. (1992). *Handbook of Fluorescent Probes and Research Chemicals*, Molecular Probes, Eugene, OR.
- Larson, R.G. (1999). *The Structure and Rheology of Complex Fluids*, Oxford University Press, Oxford, UK.
- Larsson, K. (2004). Molecular organization in lipids and emulsions, in *Food Emulsions*, 4th ed., Friberg, S., Larsson, K., Sjoblom, J., Eds., Marcel Dekker, New York, NY, Chap. 3.
- Larsson, M., Larsson, K. (1997). Neglected aspects of food flavor perception. *Colloids and Surfaces A: Physicochemical and Engineering Aspects*, **123**, 651.
- Launay, B., Doublier, J.L., Cuvelier, G. (1986). Flow properties of aqueous solutions of polysaccharides, in *Functional Properties of Food Macromolecules*, Mitchell, J.R., Ledward, D.A., Eds., Elsevier, London, UK, Chap. 1.
- Lawler, P.J., Dimick, P.S. (2002). Crystallization and polymorphism of fats, in *Food Lipids: Chemistry, Nutrition and Biotechnology*, Akoh, C.C., Min, D.B., Eds, Marcel Dekker, New York, NY, Chap. 9.
- Lawson, H.W. (1995). *Food Oils and Fats: Technology, Utilization and Nutrition*, Chapman & Hall, New York, NY.
- Le Botlan, D., Wennington, J., Cheftel, J.C. (2000). Study of the state of water and oil in frozen emulsions using time domain NMR. *Journal of Colloid and Interface Science*, **226**, 16–21.
- Le Denmat, M., Anton, M., Beaumal, V. (2000). Characterisation of emulsion properties and of interface composition in O/W emulsions prepared with hen egg yolk, plasma and granules. *Food Hydrocolloid*, **14**, 539.
- Le Denmat, M., Anton, M., Gandemer, G. (1999). Protein denaturation and emulsifying properties of plasma and granules of egg yolk as related to heat treatment. *Journal of Food Science*, **64**, 194.
- Ledward, D.A. (1986). Gelation of gelatin, in *Functional Properties of Food Macromolecules*, Mitchell, J.R., Ledward, D.A., Eds., Elsevier, London, UK, Chap. 4.
- Lee, H.Y., McCarthy, M.J., Dungan, S.R. (1998). Experimental characterization of emulsion formation and coalescence by nuclear magnetic resonance restricted diffusion techniques. *Journal of the American Oil Chemists Society*, **75**, 463–475.
- Lee, S.Y., Morr C.V. (1992). Fixation and staining milkfat globules in cream for transmission and scanning electron microscopy. *Journal of Food Science*, **57**, 887.
- Lees, L.H., Pandolfe, W.D. (1986). Homogenizers, in *Encyclopedia of Food Engineering*, Hall, C.W., Farrall, A.W., Rippen, A.L., Eds., AVI Publishing, Westport, CT, p. 467.
- Lefevre, T., Subirade, M. (2003). Formation of intermolecular beta-sheet structures: A phenomenon relevant to protein film structure at oil-water interfaces of emulsions. *Journal of Colloid and Interface Science*, **263**, 59.
- Lehnert, S., Tarabishi, H., Leuenberger, H. (1994). Investigation of thermal phase inversion in emulsions. *Colloids and Surfaces A: Physicochemical and Engineering Aspects*, **91**, 227.
- Lehninger, A.L., Nelson, D.L., Cox, M.M. (1993). *Principles of Biochemistry*, 2nd ed., Worth Publishers, New York, NY.
- Leroux, J., Langendorff, V., Schick, G., Vaishnav V., Mazoyer, J. (2003). Emulsion stabilizing properties of pectin. *Food Hydrocolloids*, **17**, 455.
- Leuenberger, B.H. (1991). Investigation of viscosity and gelation properties of different mammalian and fish gelatins. *Food Hydrocolloids*, **5**, 353.
- Li, X., Cox, J.C., Flumerfelt, R.W. (1992). Determination of emulsion size distribution by NMR restricted diffusion measurement. *AIChE Journal*, **38**, 1671.
- Li, Z., Grun, I.U., Fernando, L.N. (2000). Interaction of vanillin with soy and dairy proteins in aqueous model systems: A thermodynamic study. *Journal of Food Science*, **65**, 997.
- Lian, G. (2000). Modeling flavor release from oil-containing gel particles, in *Flavor Release*, ACS Symposium Series 763, Roberts, D.D., Taylor, A.J., Eds., American Chemical Society, Washington, DC, p. 201.
- Lickiss, P.D., McGrath, V.E. (1996). Breaking the sound barrier. *Chemistry in Britain*, **32**, 47.
- Lindman, B. (2001). Physico-chemical properties of surfactants, in *Handbook of Applied Surface and Colloid Chemistry*, Vol. 1, Holmberg, K., Ed., John Wiley & Sons, Chichester, England, Chap. 19.

- Lindman, B., Carlsson, A., Gerdes, S., Karlstrom, G., Picullel, L., Thalberg, K., Zhang, K. (1993). Polysaccharide-surfactant systems: Interactions, phase diagrams and novel gels, in *Food Colloids and Polymers: Stability and Mechanical Properties*, Dickinson, E., Walstra, P., Eds., Royal Society of Chemistry, Cambridge, UK, p. 113.
- Lindsay, R.C. (1996a). Flavors, in *Food Chemistry*, 3rd ed., Fennema, O.R., Ed., Marcel Dekker, New York, NY, Chap. 11.
- Lindsay, R.C. (1996b). Food Additives, in *Food Chemistry*, 3rd ed., Fennema, O.R., Ed., Marcel Dekker, New York, NY, Chap. 12.
- Lines, R.W. (1994). The electrical sensing zone method (the Coulter principle), in *Liquid and Surface Bourne Particle Measurement Handbook*, Knapp, J.Z., Ed., Marcel Dekker, New York, NY.
- Linfield, W.M. (1976). *Anionic Surfactants: Parts I and II*, Marcel Dekker, New York, NY.
- Linforth, R.S.T. (2000). Developments in instrumental techniques for food flavour evaluation: Future prospects. *Journal of the Science of Food and Agriculture*, **80**, 2044.
- Linforth, R.S.T., Friel, E.N., Taylor, A.J. (2000). Modeling aroma release from foods using physico-chemical parameters, in *Flavor Release*, Roberts, D.D., Taylor, A.J., Eds., American Chemical Society, Washington, DC, p. 166.
- Lips, A., Campbell, I.J., Pelan, E.G. (1991). Aggregation mechanisms in food colloids and the role of biopolymers, in *Food Polymers, Gels and Colloids*, Dickinson, E., Ed., Royal Society of Chemistry, Cambridge, UK, p. 1.
- Lips, A., Westbury, T., Hart, P.M., Evans, I.D., Campbell, I.J. (1993). Aggregation mechanisms in food colloids and the role of biopolymers, in *Food Colloids and Polymers: Stability and Mechanical Properties*, Dickinson, E., Walstra P., Eds., Royal Society of Chemistry, Cambridge, UK, p. 31.
- Lissant, K.J. (1983). *Demulsification: Industrial Applications*, Marcel Dekker, New York, NY.
- Liu, M.X., Lee, D.S., Damodaran, S. (1999). Emulsifying properties of acidic subunits of soy 11S globulin. *Journal of Agricultural and Food Chemistry*, **47**, 4970.
- Liu, S., Masliyah, J.H. (1996). Rheology of suspensions, in *Suspensions: Fundamentals and Applications in the Petroleum Industry*, Schramm, L.L., Ed., American Chemical Society, Washington, DC, Chap. 3.
- Lloyd, N.E. (1959). Determination of surface-average particle diameter of colored emulsions by reflectance, and application to emulsion stability studies. *Journal of Colloid and Interface Science*, **14**, 441.
- Lobo, L. (2002). Coalescence during emulsification. Part 3: Effect of gelatin on rupture and coalescence. *Journal of Colloid and Interface Science*, **254**, 165.
- Lobo, L., Svereika, A. (2003). Coalescence during emulsification. Part 2: Role of small molecule surfactants. *Journal of Colloid and Interface Science*, **261**, 498.
- Lobo, L., Svereika, A., Nair, M. (2002). Coalescence during emulsification. Part 1: Method development. *Journal of Colloid and Interface Science*, **253**, 409.
- Lodge, J.F.M., Heyes, D.M. (1999). Rheology of transient colloidal gels by Brownian dynamics computer simulation. *Journal of Rheology*, **43**, 219.
- Loewenberg, M., Hinch, E.J. (1996). Numerical simulation of a concentrated emulsion in shear flow. *Journal of Fluid Mechanics*, **321**, 395–419.
- Loncin, M., Merson, R.L. (1979). *Food Engineering: Principles and Selected Applications*, Academic Press, New York, NY.
- Lopez, A. (1981). *A Complete Course on Canning. Book II – Processing Procedures for Canned Food Products*, The Canning Trade, Baltimore, MD, p. 380.
- Lovsey, S.W. (1984). *Theory of Neutron Scattering from Condensed Matter*, Clarendon Press, Oxford, UK.
- Lu, J.R. (2003). Neutron reflection study of protein adsorption at the solid-solution interface, in *Biopolymers at Interfaces*, 2nd ed., Malmsten, M., Ed., Marcel Dekker, New York, NY, p. 609.
- Lubbers, S., Landy, P., Voilley, A. (1998). Retention and release of aroma compounds in foods containing proteins. *Food Technology*, **52**, 68.
- Lübke, M., Guichard, E., Le Quéré, J.L. (2000). Infrared spectroscopic study of b-lactoglobulin interactions with flavor compounds, in *Flavor Release*, ACS Symposium Series 763, Roberts, D.D., Taylor, A.J., Eds., American Chemical Society, Washington, DC, p. 246.
- Lubke, M., Guichard, E., Tromelin, A., Le Quere, J.L. (2002). Nuclear magnetic resonance spectroscopic study of  $\beta$ -lactoglobulin interactions with two flavor compounds, gamma-decalactone and beta-ionone. *Journal of Agricultural and Food Chemistry*, **50**, 7094.

- Lucassen-Reynders, E.H., Benjamins, J. (1999). Dilational rheology of proteins adsorbed at fluid interfaces, in *Food Emulsions and Foams: Interfaces, Interactions and Stability*, Dickinson E., Rodriguez-Patino J.M., Eds., Royal Society of Chemistry, Cambridge, UK, p. 195.
- Lucassen-Reynders, E.H., Kuipers, K.A. (1992). The role of interfacial properties in emulsification. *Colloids and Surfaces*, **65**, 175.
- Luckham, P.F., Costello, B.A.L. (1993). Recent developments in the measurement of interparticle forces. *Advances in Colloid and Interface Science*, **44**, 193.
- Lundin, L., Williams, M.A.K., Foster, T.J. Phase separation in foods, in *Texture in Foods, Volume 1: Semi-Solid Foods*, McKenna, B.M., Ed., CRC Press, Boca Raton, FL, Chap. 3.
- Luyten, H., Jonkman, M., Klok, W., van Vliet, T. (1993). Creaming behaviour of dispersed particles in dilute xanthan solutions, in *Food Colloids and Polymers: Stability and Mechanical Properties*, Dickinson, E., Walstra P., Eds., Royal Society of Chemistry, Cambridge, UK, p. 224.
- Ma, Y., Varadan, V.K., Varadan V.V. (1990). Comments on ultrasonic propagation in suspensions. *Journal of the Acoustical Society of America*, **87**, 2779.
- MacDougall, D.B. (2002a). Introduction, in *Colour in Food: Improving Quality*, MacDougall, D.B., Ed., CRC Press, Boca Raton, FL, p. 1.
- MacDougall, D.B. (2002b). Colour measurement of food: Principles and practice, in *Colour in Food: Improving Quality*, MacDougall, D.B., Ed., CRC Press, Boca Raton, FL, p. 33.
- MacGregor, E.A., Greenwood, C.T. (1980). *Polymers in Nature*, John Wiley & Sons, New York, NY.
- MacKay, R.A. (1987). *Nonionic Surfactants: Physical Chemistry*, Schick, M.J., Ed., Marcel Dekker, New York, NY, p. 297.
- Mackie, A.R., Gunning, A.P., Wilde, P.J., Morris, V.J. (2000). Orogenic displacement of protein from the oil/water interface. *Langmuir*, **16**, 2242.
- Mackie, A.R., Gunning, A.P., Pugnali, L.A., Dickinson, E., Wilde, P.J., Morris, V.J. (2003). Growth of surfactant domains in protein films. *Langmuir*, **19**, 6032.
- Mackie, A.R., Gunning, A.P., Ridout, M.J., Wilde, P.J., Patino, J.R. (2001). *In situ* measurement of the displacement of protein films from the air/water interface by surfactant. *Biomacromolecules*, **2**, 1001.
- Macosko, C.W. (1994). *Rheology: Principles, Measurements and Applications*, VCH Publishers, New York, NY.
- Magdassi, S. (1996). *Surface Activity of Proteins: Chemical and Physicochemical Modifications*, Marcel Dekker, New York, NY.
- Magdassi, S., Kamyshny, A. (1996). Surface activity and functional properties of proteins. *Surface Activity of Proteins: Chemical and Physicochemical Modifications*, Magdassi, S., Ed., Marcel Dekker, New York, NY, Chap. 1.
- Mahanty, J., Ninham, B.W. (1976). *Dispersion Forces*, Academic Press, New York, NY.
- Malmsten, M. (2003). Ellipsometry and reflectometry for studying protein adsorption, in *Biopolymers at Interfaces*, 2nd ed., Malmsten, M., Ed., Marcel Dekker, New York, NY, p. 539.
- Malmsten, M., Lindstrom, A.-L., Warnheim, T. (1995). Ellipsometry studies of interfacial film formation in emulsion systems. *Journal of Colloid and Interface Science*, **173**, 297.
- Malone, M.E., Appelqvist, I.A.M. (2003). Gelled emulsion particles for the controlled release of lipophilic volatiles during eating. *Journal of Controlled Release*, **90**, 227.
- Malone, M.E., Appelqvist, I.A.M., Norton, I.T. (2003a). Oral behaviour of food hydrocolloids and emulsions. Part 1: Lubrication and deposition considerations. *Food Hydrocolloids*, **17**, 763.
- Malone, M.E., Appelqvist, I.A.M., Norton, I.T. (2003b). Oral behaviour of food hydrocolloids and emulsions. Part 2: Taste and aroma release. *Food Hydrocolloids*, **17**, 775.
- Malone, M.E., Appelqvist, I.A.M., Goff, T.C., Homan, J.E., Wilkins, J.P.G. (2000). A novel approach to the selective control of lipophilic flavor release in low fat foods, in *Flavor Release*, ACS Symposium Series 763, Roberts, D.D., Taylor, A.J., Eds., American Chemical Society, Washington, DC, p. 212.
- Manley, C.H. (1993). Psychophysiological effect of odor. *Critical Reviews in Food Science and Nutrition*, **33**, 57.
- Manoj, P., Fillery-Travis, A.J., Watson, A.D., Hibberd, D.J., Robins, M.M. (1998a). Characterization of a depletion-flocculated polydisperse emulsion. Part I: Creaming behavior. *Journal of Colloid and Interface Science*, **207**, 283.

- Manoj, P., Fillery-Travis, A.J., Watson, A.D., Hibberd, D.J., Robins, M.M. (1998b). Characterization of a depletion-flocculated polydisperse emulsion. Part II: Steady-state rheological investigations. *Journal of Colloid and Interface Science*, **207**, 294.
- Manoj, P., Fillery-Travis, A.J., Watson, A.D., Hibberd, D.J., Robins, M.M. (2000). Characterization of a polydisperse depletion-flocculated emulsion. Part III: Oscillatory rheological measurements. *Journal of Colloid and Interface Science*, **228**, 200.
- Marangoni, A.G. (2000). Elasticity of high-volume-fraction fractal aggregate networks: A thermodynamic approach. *Physical Review*, **62**, 13951.
- Marangoni, A.G., Narine, S.S. (1999). The influence of microstructure on the macroscopic rheological properties of soft materials. *Scanning*, **21**, 120.
- Marangoni, A., Narine, S. (2002). *Physical Properties of Lipids*, Marcel Dekker, New York, NY.
- Maranzano, B.J., Wagner, N.J. (2002). Flow-small angle neutron scattering measurements of colloidal dispersion microstructure evolution through the shear thickening transition. *Journal of Chemical Physics*, **117**, 10291.
- Marciani, L., Ramanathan, C., Tyler, D.J., Young, P., Manoj, P., Wickham, M., Fillery-Travis, A., Spiller, R.C., Gowland, P.A. (2001). Fat emulsification measured using NMR transverse relaxation. *Journal of Magnetic Resonance*, **153**, 1.
- Margolskee, R.F. (2002). Molecular mechanisms of taste transduction. *Pure and Applied Chemistry*, **74**, 1125.
- Marinova, K.G., Alargova, R.G., Denkov, N.D., Velev, O.D., Petsev, D.N., Ivanov, I.B., Borwankar, R.P. (1996). Charging of oil-water interfaces due to spontaneous adsorption of hydroxyl ions. *Langmuir*, **12**, 2045.
- Marra, J. (1986). *Journal of Colloid and Interface Science*, **109**, 11.
- Marshall, R.T., Goff, H.D., Hartel, R.W. (2003). *Ice Cream*, 6th ed. Kluwer Academic Publishers, New York, NY.
- Marsili, R. (1997). *Techniques for Analyzing Food Aroma*. Marcel Dekker, New York, NY.
- Martinet, V., Beaumal, V., Dalgalarondo, M., Anton, M. (2003). Emulsifying properties of and adsorption behavior of egg yolk lipoproteins (LDL and HDL) in O/W emulsions. *Recent Research Developments in Agricultural and Food Chemistry*, **37**, 103.
- Mathews (1999). Beverage flavorings and their applications, in *Food Flavorings*, 3rd ed., Ashurst, P.R., Ed., Aspen Publishers, Gaithersburg, MD, pp. 199–228.
- Mathews, R.G., Donald, A.M. (2002). Conditions for imaging emulsions in the environmental scanning electron microscope. *Scanning*, **24**, 75.
- Matsubara, T., Texter, J. (1986). *Journal of Colloid and Interface Science*, **112**, 421.
- Mayhill, P.G., Newstead, D.F. (1992). The effect of milkfat fractions and emulsifier type on creaming in normal-solids UHT recombined milk. *Milchwissenschaft*, **47**, 75.
- McCarthy, W.W. (1964). Ultrasonic emulsification. *Drug and Cosmetic Industry*, **94**: 6, 821.
- McCarthy, K.L., Kerr, W.L. (1998). Rheological characterization of a model suspension during pipe flow using MRI. *Journal of Food Engineering*, **37**, 11.
- McClements, D.J. (1989). *The use of ultrasonics for characterizing fats and emulsions*, Ph.D. Thesis, University of Leeds, UK.
- McClements, D.J. (1991). Ultrasonic characterization of emulsions and suspensions. *Advances in Colloid and Interface Science*, **37**, 33.
- McClements, D.J. (1994). Ultrasonic determination of depletion flocculation in oil-in-water emulsions containing a non-ionic surfactant. *Colloids and Surfaces A: Physicochemical and Engineering Aspects*, **90**, 25.
- McClements, D.J. (1996). Principles of ultrasonic droplet size determination. *Langmuir*, **12**, 3454.
- McClements, D.J. (1997). Ultrasonic characterization of foods and drinks: Principles, methods, and applications. *Critical Reviews in Food Science*, **37**, 1.
- McClements, D.J. (1998). Analysis of Food Emulsions, in *Food Analysis*, 2nd ed., Nielsen, S.S., Ed.. Aspen Publishers, Gaithersburg, MD, pp. 571–585.
- McClements, D.J. (2000). Comments on viscosity enhancement and depletion flocculation by polysaccharides. *Food Hydrocolloids*, **14**, 173.
- McClements, D.J. (2001). Emulsion Droplet Size Determination, in *Current Protocols in Food Analytical Chemistry*, Vol. 1, Wrolstad, R.E., Ed.. John Wiley & Sons, New York, NY, Section D3.3.

- McClements, D.J. (2002a). Theoretical prediction of emulsion color. *Advances in Colloid and Interface Science*, **97**, 63.
- McClements, D.J. (2002b). Colloidal basis of emulsion color. *Current Opinion in Colloid and Interface Science*, **7**, 451.
- McClements, D.J. (2002c). Modulation of globular protein functionality by weakly interacting cosolvents. *Critical Reviews in Food Science*, **42**, 417.
- McClements, D.J. (2003). The rheology of emulsion-based food products, in *Texture in Foods, Volume 1: Semi-Solid Foods*, McKenna, B.M., Ed., CRC Press, Boca Raton, FL, Chap. 1.
- McClements, D.J. (2004). Role of hydrocolloids as emulsifiers in foods, in *Gums and Stabilizers in the Food Industry*, Vol. 12, Springer Verlag, New York NY.
- McClements, D.J., Decker, E.A. (2000). Lipid oxidation in oil-in-water emulsions: Impact of molecular environment on chemical reactions in heterogeneous food systems. *Journal of Food Science*, **65**, 1270.
- McClements, D.J., Demetriades, K. (1998). An integrated approach to the development of reduced-fat food emulsions. *Critical Reviews in Food Science*, **38**, 511.
- McClements, D.J., Dungan, S.R. (1993). Factors that affect the rate of oil exchange between oil-in-water emulsion droplets stabilized by a non-ionic surfactant: Droplet size, surfactant concentration and ionic strength. *Journal of Physical Chemistry*, **97**, 7304.
- McClements, D.J., Dungan, S.R. (1997). Effect of colloidal interactions on the rate of interdroplet heterogeneous nucleation in oil-in-water emulsions. *Journal of Colloid and Interface Science*, **186**, 17.
- McClements, D.J., Povey, M.J.W. (1987). Solid fat content determination using ultrasonic velocity measurements. *International Journal of Food Science and Technology*, **22**, 491.
- McClements, D.J., Povey, M.J.W. (1988). Comparison of pulsed NMR and ultrasonic velocity techniques for determining solid fat contents. *International Journal of Food Science and Technology*, **23**, 159.
- McClements, D.J., Povey, M.J.W. (1989). Scattering of ultrasound by emulsions. *Journal of Physics D: Applied Physics*, **22**, 38.
- McClements, D.J., Chantapornchai, W., Clydesdale, F. (1998). Prediction of food emulsion color using light scattering theory. *Journal of Food Science*, **63**, 935.
- McClements, D.J., Dungan, S.R., German, J.B., Simoneau, C., Kinsella, J.E. (1993a). Droplet size and emulsifier type affect crystallization and melting of hydrocarbon-in-water emulsions. *Journal of Food Science*, **58**, 1148.
- McClements, D.J., Dungan, S.R., German, J.B., Kinsella, J.E. (1993b). Factors which affect oil exchange between oil-in-water emulsion droplets stabilized by whey protein isolate: Protein concentration, droplet size and ethanol. *Colloids and Surfaces A: Physicochemical and Engineering Aspects*, **81**, 203.
- McClements, D.J., Monahan, F.J., Kinsella, J.E. (1993c). Effect of emulsion droplets on the rheology of whey protein isolate gels. *Journal of Texture Studies*, **24**, 411.
- McClements, D.J., Monahan, F.J., Kinsella, J.E. (1993d). Disulfide bond formation affects the stability of whey protein stabilized emulsion. *Journal of Food Science*, **58**, 1036.
- McClements, D.J., Dickinson, E., Dungan, S.R., Kinsella, J.E., Ma, J.E., Povey, M.J.W. (1993e). Effect of emulsifiers type on the crystallization kinetics of oil-in-water emulsions containing a mixture of solid and liquid droplets. *Journal of Colloid and Interface Science*, **160**, 293.
- McClements, D.J., Povey, M.J.W., Dickinson, E. (1993f). Absorption and velocity dispersion due to crystallization and melting of emulsion droplets. *Ultrasonics*, **31**, 443.
- McClements, D.J., Han, S.W., Dungan, S.R. (1994). Interdroplet heterogeneous nucleation of super-cooled liquid droplets by solid droplets in oil-in-water emulsions. *Journal of the American Oil Chemists Society*, **71**, 1385.
- McClements, D.J., Hemar, Y., Herrmann, N. (1999). Incorporation of thermal overlap effects into multiple scattering theory. *Journal of the Acoustical Society of America*, **105**, 915.
- McClements, D.J., Herrmann, N., Hemar, Y. (1998). Influence of flocculation on the ultrasonic properties of emulsions: Theory. *Journal of Physics D: Applied Physics*, **31**, 2950.
- McClements, D.J., Povey, M.J.W., Jury, M., Betsansis, E. (1990). Ultrasonic characterization of a food emulsion. *Ultrasonics*, **28**, 266.

- McDonald, P.J., Ciampi, E., Keddie, J.L., Heidenreich, M., Kimmich, R. (1999). Magnetic-resonance determination of the spatial dependence of the droplet size distribution in the cream layer of oil-in-water emulsions: Evidence for the effects of depletion flocculation. *Physical Review E*, **59**, 874-884.
- McGee, H. (1984). *On Food and Cooking*, Simon & Schuster, New York, NY.
- McKenna, B.M., Lyng, J.G. (2003). Introduction to food rheology and its measurement, in *Texture in Foods, Volume 1: Semi-Solid Foods*, McKenna, B.M., Ed., CRC Press, Boca Raton, FL, Chap. 6.
- McNamee, B.F., O'Riordan, E.D., O'Sullivan, M. (1998). Emulsification and microencapsulation properties of gum arabic. *Journal of Agricultural and Food Chemistry*, **46**, 4551.
- McNulty, P.B. (1987). Flavor release—elusive and dynamic, in *Food Structure and Behaviour*, Blanshard, J.M.V., Lillford, P., Eds., Academic Press, London, UK.
- McNulty, P.B., Karel, M. (1973). Factors affecting flavour release and uptake in O/W emulsions: II Stirred cell studies. *Journal of Food Technology*, **8**, 319.
- Mei, L., Decker, E.A., McClements, D.J. (1998a). Evidence of iron association with emulsion droplets and its impact on lipid oxidation. *Journal of Agricultural and Food Chemistry*, **46**, 5072.
- Mei, L., McClements, D.J., Wu, J., Decker, E.A. (1998b). Iron-catalyzed lipid oxidation in emulsions as affected by surfactants, pH and NaCl. *Food Chemistry*, **61**, 307.
- Mela, D.J., Langley, K.R., Martin, A. (1994). Sensory assessment of fat content: Effect of emulsion and subject characteristics. *Appetite*, **22**, 67.
- Melik, D.H., Fogler, H.S. (1988). Fundamentals of colloidal stability in quiescent media, in *Encyclopedia of Emulsion Technology*, Vol. 3, Becher, P., Ed., Marcel Dekker, New York, NY, Chap. 1.
- Menon, W.B., Wasan, D.T. (1985). Demulsification, *Encyclopedia of Emulsion Technology*, Vol. 2, Applications, Becher, P., Ed., Marcel Dekker, New York, NY, Chap. 1.
- Mermelstein, N.H. (2002). Food research trends—2003 and beyond. *Food Technology*, **66**: 12, 30.
- Mewis, J., Macosko, C.W. (1994). Suspension rheology, in *Rheology: Principles, Measurements and Applications*, Macosko, C.W., Ed., VCH Publishers, New York, NY, Chap. 10.
- Mewis, J., Yang, H., Van Puyvelde, P., Moldenaers, P., Walker, L.M. (1998). Small-angle light scattering study of droplet break-up in emulsions and polymer blends. *Chemical Engineering Science*, **53**, 2231.
- Meyers, R.A. (2000). *Encyclopedia of Analytical Chemistry: Applications, Theory and Instrumentation*, Vol. 6, John Wiley & Sons, New York, NY, pp. 5299-5610.
- Mialon, V.S., Ebeler, S.E. (1997). Time-intensity measurement of matrix effects on retronasal aroma perception. *Journal of Sensory Studies*, **12**, 303.
- Michalski, M.C., Desobry, S., Hardy, J. (1998). Adhesion of edible oils and food emulsions to rough surfaces. *Food Science and Technology*, **31**, 495.
- Michel, B. 2004. *Optics of Small Particles and Inhomogeneous Materials*. ([www.unternehmen.com/Bernhard-Michel/eindex.html](http://www.unternehmen.com/Bernhard-Michel/eindex.html)).
- Middelberg, A.P.J., Bogle, D.L., Snoswell, M.A. (1990). Sizing biological samples by photosedimentation techniques. *Biotechnology Progress*, **6**, 255.
- Miettinen, S.M., Tuorila, H., Piironen, V., Vehkalahti, K., Hyvonen, L. (2002). Effect of emulsion characteristics on the release of aroma as detected by sensory evaluation, static headspace gas chromatography, and electronic nose. *Journal of Agricultural and Food Chemistry*, **50**, 4232.
- Miklavic, S.J., Ninham, B.W. (1990). Competition for adsorption sites by hydrated ions. *Journal of Colloid and Interface Science*, **134**, 305.
- Mikula, R.J. (1992). Emulsion characterization. *Emulsions: Fundamentals and Applications in the Petroleum Industry*, Schramm, L.L., Ed., American Chemical Society, Washington, DC, Chap. 3.
- Miles, C.A., Fursey, G.A.J., Jones, C.D.J. (1985). Ultrasonic estimation of solid/liquid ratios in fats, oils and adipose tissue. *Journal of the Science of Food and Agriculture*, **36**, 215.
- Miles, M.J., McMaster, T.J. (1995). Scanning probe microscopy of food-related systems, in *New Physicochemical Techniques for the Characterization of Complex Food Systems*, Dickinson, E., Ed., Blackie Academic & Professional, London, UK, Chap. 3.
- Miller D.D. (1996). Minerals, in *Food Chemistry*, 3rd ed., Fennema, O.R., Ed., Marcel Dekker, New York, NY, Chap. 9.

- Miller, R., Fainerman, V.B., Kragel, J., Loglio, G. (1997). Surface rheology of adsorbed surfactants and proteins. *Current Opinion in Colloid and Interface Science*, **2**, 578.
- Miller, R., Fainerman, V.B., Wustneck, R., Kragel, J., Trukhin, D.V. (1998). Characterisation of the initial period of protein adsorption by dynamic surface tension measurements using different drop techniques. *Colloids and Surfaces A: Physicochemical and Engineering Aspects*, **131**, 225.
- Miller, R., Fainerman, V.B., Makievski, A.V., Kragel, J., Grigoriev, D.O., Kazakov, V.N., Sinyachenko, O.V. (2000). Dynamics of protein and mixed protein/surfactant adsorption layers at the water/fluid interface. *Advances in Colloid and Interface Science*, **86** 39.
- Milling, A., Mulvaney, P., Larson, E. (1996). Direct measurement of repulsive van der Waals interactions using an atomic force microscope. *Journal of Colloid and Interface Science*, **180**, 460.
- Min, D.B., Boff, J.M. (2003). Crude fat analysis, in *Food Analysis*, 3rd ed., Nielsen, S.S., Ed., Kluwer Academic Publishers, New York, NY, Chap. 8.
- Mine, Y. (1998a). Emulsifying characterization of hens egg yolk proteins in oil-in-water emulsions. *Food Hydrocolloids*, **12**, 409.
- Mine, Y. (1998b). Adsorption behavior of egg yolk low-density lipoproteins in oil-in-water emulsions. *Journal of Agricultural and Food Chemistry*, **46**, 36.
- Mine, Y. (2002). Recent advances in egg protein functionality in the food system. *World Poultry Science Journal*, **58**, 31.
- Mine, Y., Noutomi, T., Haga, N. (1991). Emulsifying and structural-properties of ovalbumin. *Journal of Agricultural and Food Chemistry*, **39**, 443.
- Mishchuck, N.A., Sjoblom, J., Dukhin, S.S. (1995). Influence of retardation and screening on van der Waals attractive forces on reverse coagulation of emulsions in the secondary minimum. *Colloid Journal*, **57**, 785.
- Mishchuk, N.A., Sjoblom, J., Dukhin, S.S. (1996). The effect of retardation and screening of van der Waals attractive forces on the breaking of doublet of drops during sedimentation. *Colloid Journal*, **58**, 210.
- Mishchuk, N.A., Miller, R., Steinchen, A., Sanfeld, A. (2002). Conditions of coagulation and flocculation in dilute mini-emulsions. *Journal of Colloid and Interface Science*, **256**, 435.
- Mitchell, J.R., Ledward, D.A. (1986). *Functional Properties of Food Macromolecules*, Elsevier, London, UK.
- Moe, S.T., Draget, K.I., Gudmund, S.B., Smidsrod, O. (1995). Alginates, in *Food Polysaccharides and Their Applications*, Stephan, A.M., Ed., Marcel Dekker, New York, NY, Chap. 9.
- Mohan, S., Narsimhan, G. (1997). Coalescence of protein-stabilized emulsions in a high-pressure homogenizer. *Journal of Colloid and Interface Science*, **192**, 1.
- Molina, E., Papadopoulou, A., Ledward, D.A. (2001). Emulsifying properties of high pressure treated soy protein isolate and 7S and 11S globulins. *Food Hydrocolloids*, **15**, 263.
- Monahan, F.J., McClements, D.J., German, J.B. (1996). Disulfide-mediated polymerization reactions and physical properties of heated WPI-stabilized emulsions. *Journal of Food Science*, **61**, 504.
- Montagne, F., Braconnot, S., Mondain-Monval, O., Pichot, C., Elaissari, A. (2003). Colloidal and physicochemical characterization of highly magnetic O/W magnetic emulsions. *Journal of Dispersion Science and Technology*, **24**, 821.
- Moore, P.B., Langley, K., Wilde, P.J., Fillery-Travis, A., Mela, D.J. (1998). Effect of emulsifier type on sensory properties of oil-in-water emulsions. *Journal of the Science of Food and Agriculture*, **76**, 469.
- Moore, I.P.T., Dodds, T.M., Turnbull, R.P., Crawford, R.A. (2000). Flavor release from composite dairy gels: A comparison between model predictions and time-intensity experimental studies, in *Flavor Release*, ACS Symposium Series 763, Roberts, D.D., Taylor, A.J., Eds., American Chemical Society, Washington, DC, p. 381.
- Moran, D.P.J. (1994). Fats in spreadable products, in *Fats in Food Products*, Blackie Academic & Professional, London, UK.
- Moran, D.P.J., Rajah, K.K. (1994). *Fats in Food Products*, Blackie Academic & Professional, London, UK.
- Moreau, L., Kim, H-J., Decker, E.A., McClements, D.J. (2003). Production and characterization of O/W emulsions containing droplets stabilized by  $\beta$ -lactoglobulin-pectin membranes. *Journal of Agricultural and Food Chemistry*, **51**, 6612.
- Moros, J.E., Franco, J.M., Gallegos, C. (2002a). Rheological properties of cholesterol-reduced, yolk-stabilized mayonnaise. *Journal of the American Oil Chemists Society*, **79**, 837.



- Moros, J.E., Franco, J.M., Gallegos, C. (2002b). Rheology of spray-dried egg yolk-stabilized emulsions. *International Journal of Food Science and Technology*, **37**, 297.
- Morris, V.J. (1986). Gelation of polysaccharides, in *Functional Properties of Food Macromolecules*, Mitchell, J.R., Ledward, D.A., Eds., Elsevier, London, UK, Chap. 3.
- Morris, V.J. (1995a). Bacterial polysaccharides, in *Food Polysaccharides and Their Applications*, Stephen, A.M., Ed., Marcel Dekker, New York, NY, Chap. 11.
- Morris, E.R. (1995b). Polysaccharide rheology and in-mouth perception, in *Food Polysaccharides and Their Applications*, Stephen, A.M., Ed., Marcel Dekker, New York, NY, Chap. 16.
- Morris, V.J., Gunning, A.P., Kirby, A.R. (1999). *Atomic Force Microscopy for Biologists*, Imperial College Press, London, UK.
- Morris, V.J., Mackie, A.R., Wilde, P.J., Kirby, A.R., Mills, E.C.N., Gunning, A.P. (2001). Atomic force microscopy as a tool for interpreting the rheology of food biopolymers at the molecular level. *Food Science and Technology—Lebensmittel-Wissenschaft und Technologie*, **34**, 3.
- Moss, B.W. (2002). The chemistry of food colour, in *Colour in Food: Improving Quality*, MacDougall, D.B., Ed., CRC Press, Boca Raton, FL, p. 145.
- Mousa, H., Agterof, W., Mellema, J. (2001). Experimental investigation of the orthokinetic coalescence efficiency of droplets in simple shear flow. *Journal of Colloid and Interface Science*, **240**, 340.
- Mudgett, P.S., Richards, L.W. (1971). Multiple scattering calculations for technology. *Applied Optics*, **10**, 1485.
- Mukerjee, P. (1979). Solubilization in aqueous micellar systems, in *Solution Chemistry of Surfactants*, Vol. 1, Mittal, K.L., Ed., Plenum Press, London, UK.
- Mulder, H., Walstra, P. (1974). *The Milk Fat Globule: Emulsion Science as Applied to Milk Products and Comparable Foods*, Pudoc, Wageningen, The Netherlands.
- Muller, H.J., Hermel, H. (1994). On the relation between the molecular-mass distribution of gelatin and its ability to stabilize emulsions. *Colloid and Polymer Science*, **272**, 433.
- Mullin, J.W. (2001). *Crystallization*, 4th ed., Butterworth-Heinemann, Oxford, UK.
- Mulvaney, P., Perera, J.M., Biggs, S., Grieser, F., Stevens, G.W. (1996). The direct measurement of the forces of interaction between a colloid particle and an oil droplet. *Journal of Colloid and Interface Science*, **183**, 614.
- Munoz, V.A., Mikula, R.J. (1997). Characterization of petroleum industry emulsions and suspensions using microscopy. *Journal of Canadian Petroleum Technology*, **36**, 36.
- Muresan, S., van der Bent, A., de Wolf, F.A. (2001). Interaction of  $\beta$ -lactoglobulin with small hydrophobic ligands as monitored by fluorometry and equilibrium dialysis: Nonlinear quenching effects related to protein-protein association. *Journal of Agricultural and Food Chemistry*, **49**, 2609.
- Murphy, D.B. (2001). *Fundamentals of Light Microscopy and Electronic Imaging*, 1st ed., Wiley-Liss, New York, NY.
- Murray, B.S., Dickinson, E. (1996). Interfacial rheology and the dynamic properties of adsorbed films of food proteins and surfactants. *Food Science and Technology International*, **2**, 131.
- Murray, J.M., Delahunty, C.M., Baxter, I.A. (2001). Descriptive sensory analysis: Past, present and future. *Food Research International*, **34**, 461.
- Murrell, J.N., Boucher, E.A. (1982). *Properties of Liquids and Solutions*, John Wiley & Sons, Chichester, U.K.
- Murrell, J.N., Jenkins, A.D. (1994). *Properties of Liquids and Solutions*, 2nd ed., John Wiley & Sons, Chichester, UK.
- Myers, D. (1988). *Surfactant Science Technology*, VCH Publishers, Weinheim, Germany.
- Nahon, D.F., Harrison, M., Roozen, J.P. (2000). Modeling flavor release from aqueous sucrose solutions, using mass transfer and partition coefficients. *Journal of Agricultural and Food Chemistry*, **48**, 1278.
- Najbar, L.V., Considine, R.F., Drummond, C.J. (2003). Heat-induced aggregation of a globular egg-white protein in aqueous solution: Investigation by atomic force microscope imaging and surface force mapping modalities. *Langmuir*, **19**, 2880.
- Nakai, S., Li-Chan, E. (1988). *Hydrophobic Interactions in Food Systems*, CRC Press, Boca Raton, FL.
- Nakashima, T., Shimizu, M., Kukizaki, M. (2000). Particle control of emulsion by membrane emulsification and its applications. *Advances in Drug Delivery Reviews*, **45**, 47.

- Narine, S.S., Marangoni, A.G. (1999). Mechanical and structural model of fractal networks of fat crystal at low deformations. *Physical Review E*, **60**, 6991.
- Narsimhan, G., Goel, P. (2001). Drop coalescence during emulsion formation in a high-pressure homogenizer for tetradecane-in-water emulsion stabilized by sodium dodecyl sulfate. *Journal of Colloid and Interface Science*, **238**, 420.
- Nawar, W.W. (1996). Lipids, in *Food Chemistry*, 3rd ed., Fennema, O.R., Ed., Marcel Dekker, New York, NY, p. 225.
- Nettleton, J.A. (1995). *Omega-3 Fatty Acids and Health*, Aspen Publishers, Gaithersburg, MD.
- Newstein, M.C., Wang, H., Balsara, N.P., Lefebvre, A.A., Shnidman, Y., Watanabe H., Osaki, K., Shikata, T., Niwa, H., Morishima, Y. (1999). Microstructural changes in a colloidal liquid in the shear thinning and shear thickening regimes. *Journal of Chemical Physics*, **111**, 4827.
- Nielsen, S.R., Holst, S., Horsholm, C.H. (2002). Developments in natural colourings, in *Colour in Food: Improving Quality*, MacDougall, D.B., Ed., CRC Press, Boca Raton, FL, p. 331.
- Nielsen, S.S. (2003). *Food Analysis*, 3rd ed., Kluwer Academic Publishers, New York, NY.
- Nikitina, T.K., Nikitin, S.Y. (1990). Use of an acoustic method to study the interaction between lysozyme and sodium dodecyl sulfate. *Molecular Biology*, **24**, 656.
- Ninham, B.W., Yaminsky, V. (1997). Ion binding and ion specificity: The Hofmeister effect and Onsager and Lifshitz theories. *Langmuir*, **13**, 2097.
- Nino, M.R.R., Patino, J.M.R., Sanchez, C.C., Fernandez, M.C., Garcia, J.M. (2003). Physicochemical characteristics of food lipids and proteins at fluid–fluid interfaces. *Chemical Engineering Communications*, **190**, 15.
- Norde, W. (2003). *Colloids and Interfaces in Life Sciences*, Marcel Dekker, New York, NY.
- Norton, I.T., Frith, W.J. (2001). Microstructure design in mixed biopolymer composites. *Food Hydrocolloids*, **15**, 543.
- Noskov, B.A., Akentiev, A.V., Bilibin, A.Y., Zorin, I.M., Miller, R. (2003). Dilational surface viscoelasticity of polymer solutions. *Advances in Colloid and Interface Science*, **104**, 245.
- Nuchi, C.D., McClements, D.J., Decker, E.A. (2001). Impact of Tween 20 hydroperoxides and iron on the oxidation of methyl linoleate and salmon oil dispersions. *Journal of Food and Agricultural Chemistry*, **49**, 4912.
- Nussinovitch, A. (1997). *Hydrocolloid Applications: Gum Technology in the Food and Other Industries*, Blackie Academic & Professional, London, UK.
- Nylander, Y. (2004). Interactions between proteins and lipids, in *Food Emulsions*, 4th ed., Friberg, S., Larsson, K., Sjoblom, J., Eds., Marcel Dekker, New York, NY, Chap. 4.
- O'Brien, R.W., Cannon, D.W., Rowlands, W.N. (1995). Electroacoustic determination of particle size and zeta potential. *Journal of Colloid and Interface Science*, **173**, 406.
- O'Brien, R.W., Jones, A., Rowlands, W.N. (2003). A new formula for the dynamic mobility in a concentrated colloid. *Colloids and Surfaces A: Physicochemical and Engineering Aspects*, **218**, 89–101.
- O'Donnell, M. (1995). Controlling the fat: Whats new, whats to come. *Prepared Foods*, 65.
- O'Neill, T.E. (1996). Flavor binding to food proteins: An overview, in *Flavor-Food Interactions*, McGorin, R.J., Leland, J.V., Eds., American Chemical Society, Washington, DC, Chap. 6.
- Oakenfull, D., Pearce, J., Burley, R. (1997). Protein Gelation, in *Food Proteins and Their Applications*, Damodaran, S., Paraf, A., Eds., Marcel Dekker, New York, NY, Chap. 4.
- Odake, S., Roozen, J.P., Burger, J.J. (1998). Effect of saliva dilution on the release of diacetyl and 2-heptanone from cream style dressings. *Nahrung-Food*, **42**, 385.
- Odake, S., Roozen, J.P., Burger, J.J. (2000). Flavor release of diacetyl and 2-heptanone from cream style dressings in three mouth model systems. *Bioscience Biotechnology and Biochemistry*, **64**, 2523.
- O'Driscoll, B., Smyth, C., Altting, A.C., Visschers, R.W., Buckin, V. (2003). Recent applications for high-resolution ultrasonic spectroscopy. *American Laboratory*, **35**, 54.
- Okshima, H. (1994). Electrostatic interaction between two spherical colloidal particles. *Advances in Colloid and Interface Science*, **53**, 77.
- Olijve, J., Mori, F., Toda, Y. (2001). Influence of the molecular-weight distribution of gelatin on emulsion stability. *Journal of Colloid and Interface Science*, **243**, 476.
- Orr, C. (1988). Determination of particle size, in *Encyclopedia of Emulsion Technology*, Vol. 3, Becher, P., Ed., Marcel Dekker, New York, NY, Chap. 3.

- Overbosch, P., Afterof, W.G.M., Haring, P.G.M. (1991). Flavor release in the mouth. *Food Reviews International*, **7**, 137.
- Pacek, A.W., Moore, I.P.T., Nienow, A.W., Calabrese, R.V. (1994). Video technique for measuring dynamics of liquid-liquid dispersion during phase inversion. *AIChE Journal*, **40**, 1940.
- Pailthorpe, B.A., Russel, W.B. (1982). Retarded van der Waals interaction between spheres. *Journal of Colloid and Interface Science*, **89**, 563.
- Pal, R. (1992). Rheology of polymer thickened emulsions. *Journal of Rheology*, **36**, 1245.
- Pal, R. (1994). Techniques for measuring the composition (oil and water content) of emulsions—a state of the art review. *Colloids and Surfaces A: Physicochemical and Engineering Aspects*, **84**, 141.
- Pal, R. (1996). Rheology of emulsions containing polymeric liquids, in *Encyclopedia of Emulsion Technology*, Vol. 4, Becher, P., Ed., Marcel Dekker, New York, NY, Chap. 3.
- Pal, R. (2000a). Viscosity-concentration equation for emulsions of nearly spherical droplets. *Journal of Colloid and Interface Science*, **231**, 168.
- Pal, R. (2000b). Shear viscosity behavior of emulsions of two immiscible liquids. *Journal of Colloid and Interface Science*, **225**, 359.
- Pal, R. (2001). Evaluation of theoretical viscosity models for concentrated emulsions at low capillary numbers. *Chemical Engineering Journal*, **81**, 15.
- Pal, R., Yan, Y., Masliyah, J.H. (1992). Rheology of emulsions, in *Emulsions: Fundamentals and Applications in the Petroleum Industry*, Schramm, L.L., Ed., American Chemical Society, Washington, DC, Chap. 4.
- Palanuwech, J., Coupland, J.N. (2003). Effect of surfactant type on the stability of oil-in-water emulsions to dispersed phase crystallization. *Colloids and Surfaces A: Physicochemical and Engineering Aspects*, **223**, 251–262.
- Palanuwech, J., Potineni, R., Roberts, R.F., Coupland, J.N. (2003). A method to determine free fat in emulsions. *Food Hydrocolloids*, **17**, 55.
- Pandolfe, W.D. (1991). Homogenizers, in *Encyclopedia of Food Science and Technology*, John Wiley & Sons, New York, NY, p. 1413.
- Pandolfe, W.D. (1995). Effect of premix condition, surfactant concentration and oil level on the formation of oil-in-water emulsions by homogenization. *Journal of Dispersion Science and Technology*, **16**, 633.
- Pandolfe, W.D., Masucci, S.F. (1984). An instrument for rapid spectroturbimetric analysis. *American Laboratory*, **40**.
- Papenhuijzen, J.M.P. (1972). The role of particle interactions in the rheology of dispersed systems. *Rheologica Acta*, **11**, 73.
- Paraskevopoulou, A., Kiosseoglou, V., Alevisopoulos, S., Kasapis, S. (1999). Influence of reduced-cholesterol yolk on the viscoelastic behaviour of concentrated O/W emulsions. *Colloids and Surfaces B: Biointerfaces*, **12**, 107.
- Parker, A., Marin, M. (2000). A gas-liquid mass-transfer cell for studying flavor release, in *Flavor Release*, ACS Symposium Series 763, Roberts, D.D., Taylor, A.J., Eds., American Chemical Society, Washington, DC, p. 192.
- Parker, A., Vigouroux, F. (2003). Texture profiling with the vane: A general method for characterizing the rheology of shear sensitive soft foods, in *Proceedings of the Third International Symposium on Food Rheology and Structure*, Fischer, P., Marti, I., Windhab, E.J., Eds., Laboratory of Food Process Engineering, Zurich, Switzerland.
- Parker, A., Gunning, P.A., Ng, K., Robins, M.M. (1995). How does xanthan stabilise salad dressing? *Food Hydrocolloids*, **9**, 333.
- Parliament, T.H., McGorin, R.J. (2000). Critical flavor compounds in dairy products, in *Flavor Chemistry: Industrial and Academic Research*, ACS Symposium Series 756, Risch, S.J., Ho, C.T., Eds., American Chemical Society, Washington, DC, p. 44.
- Parsegian, V.A. (1993). Reconciliation of van der Waals Force measurements between phosphatidylcholine bilayers in water and between bilayer coated mica surfaces. *Langmuir*, **9**, 3625.
- Partmann, W. (1975). The effects of freezing and thawing on food quality, in *Water Relationships of Foods*, Duckworth, R.B., Ed., Academic Press, London, UK, p. 505.
- Pashley, R.M. (2003). Effect of degassing on the formation and stability of surfactant-free emulsions and fine teflon dispersions. *Journal of Physical Chemistry B*, **107**, 1714.

- Pashley, R.M., McGuiggan, P.M., Ninham, B.W., Evans D.F. (1985). Attractive forces between uncharged hydrophobic surfaces: Direct measurements in aqueous solutions. *Science*, **229**, 1088.
- Patino, J.M.R., Nino, M.R.R. (1999). Interfacial characteristics of food emulsifiers (proteins and lipids) at the air-water interface. *Colloids and Surfaces B: Biointerfaces*, **15**, 235.
- Patino, J.M.R., Ortiz, S.E.M., Sanchez, C.C., Nino, M.R.R., Anon, M.C. (2003a). Behavior of soy globulin films at the air-water interface. Structural and dilatational properties of spread films. *Industrial and Engineering Chemistry Research*, **42**, 5011.
- Patino, J.M.R., Nino, M.R.R., Sanchez, C.C. (2003b). Structure, miscibility, and rheological characteristics of beta-casein-monoglyceride mixed films at the air-water interface. *Journal of Agricultural and Food Chemistry*, **51**, 112.
- Paulaitis, M.E., Garde, S., Ashbaugh, H.S. (1996). The hydrophobic effect. *Current Opinion in Colloid and Interface Science*, **1**, 376.
- Pearce, K.N., Kinsella, J.E. (1978). Emulsifying properties of proteins: Evaluation of a turbidimetric technique. *Journal of Agricultural and Food Chemistry*, **26**, 716.
- Peleg, M. (1993). Fractals and foods. *Critical Reviews of Food Science and Nutrition*, **33**, 149.
- Penner, M.H. (1994a). Basic principles of spectroscopy, in *Introduction to the Chemical Analysis of Foods*, Nielsen, S.S., Ed., Jones & Bartlet, London, UK, Chap. 22.
- Penner, M.H. (1994b). Ultraviolet, visible and fluorescence spectroscopy, in *Introduction to the Chemical Analysis of Foods*, Nielsen, S.S., Ed., Jones & Bartlet, London, UK, Chap. 23.
- Petsev, D.N. (1998). Interactions and macroscopic properties of emulsions and microemulsions, in *Modern Aspects of Emulsion Science*, Binks, B.P., Ed., The Royal Society of Chemistry, Cambridge, UK, 1998, Chap. 10.
- Petsev, D.N. (2000). Theoretical analysis of film thickness transition dynamics and coalescence of charged miniemulsion droplets. *Langmuir*, **16**, 2093.
- Pettitt, D.J., Waybe, J.E.B., Nantz, J.R., Shoemaker, C.F. (1995). Rheological properties of solutions and emulsions stabilized with xanthan gum and propylene glycol alginate. *Journal of Food Science*, **60**, 528.
- Phillips, L.G., Barbano, D.M. (1997). The influence of fat substitutes based on protein and titanium dioxide on the sensory properties of lowfat milks. *Journal of Dairy Science*, **80**, 2726.
- Phillips, G.O., Williams, P.A. (1995). The use of hydrocolloids to improve food texture, in *Ingredient Interactions: Effect on Food Quality*, Gaonkar, A.G., Ed., Marcel Dekker, New York, NY, p. 131.
- Phillips, G.O., Williams, P.A. (2003). The use of hydrocolloids to improve food texture, in *Texture in Foods, Volume 1: Semi-Solid Foods*, McKenna, B.M., Ed., CRC Press, Boca Raton, FL, Chap. 11.
- Phillips, L.G., McGiff, M.L., Barbano, D.M., Lawless, H.T. (1995). The influence of fat on the sensory properties, viscosity, and color of low-fat milk. *Journal of Dairy Science*, **78**, 1258.
- Phipps, L.W. (1964). Heterogeneous and homogeneous nucleation in supercooled triglycerides and n-paraffins. *Transactions of the Faraday Society*, **60**, 1873.
- Phipps, L.W. (1985). *The High Pressure Dairy Homogenizer*, The National Institute for Research in Dairying, Reading, England.
- Phung, T.N., Brady, J.F., Bossis, G. (1996). Stokesian dynamics simulation of Brownian suspensions. *Journal of Fluid Mechanics*, **313**, 181.
- Piculell, L. (1995). Gelling carrageenans, in *Food Polysaccharides and Their Applications*, Stephen, A.M., Ed., Marcel Dekker, New York, NY, Chap. 8.
- Piggott, J.R. (1988). *Sensory Analysis of Foods*, 2nd ed., Elsevier, London, UK.
- Piggott, J.R. (2000). Dynamism in flavour science and sensory methodology. *Food Research International*, **33**, 191.
- Piggott, J.R., Simpson, S.J., Williams, S.A.R. (1998). Sensory analysis. *International Journal of Food Science and Technology*, **33**, 7.
- Pike, O.A. (2003). Fat characterization, in *Food Analysis*, 3rd ed., Nielsen, S.S., Ed., Kluwer Academic Publishers, New York, NY, p. 227.
- Pine, D.J., Weitz, D.A., Chaikin, P.M., Herbolzheimer, E. (1988). Diffusion wave spectroscopy. *Physical Review Letters*, **60**, 1134.
- Pine, D.J., Weitz, D.A., Zhu, X., Herbolzheimer, E. (1990). Diffusing Wave Spectroscopy: Dynamic light scattering in the multiple scattering limit. *Journal de Physique*, **51**, 2101.

- Pinfield, V.J., Dickinson, E., Povey, M.J.W. (1994). Modeling of concentration profiles and ultrasound velocity profiles in a creaming emulsion: Importance of scattering effects. *Journal of Colloid and Interface Science*, **166**, 363.
- Pinfield, V.J., Dickinson, E., Povey, M.J.W. (1997). Modeling of combined creaming and flocculation in emulsions. *Journal of Colloid and Interface Science*, **186**, 80.
- Plucinski, J., Gupta, R.K., Chakrabarti, S. (1998). Wall slip of mayonnaises in viscometers. *Rheologica Acta*, **37**, 256.
- Plucknett, K.P., Pomfret, S.J., Normand, V., Ferdinando, D., Veerman, C., Frith, W.J., Norton, I.T. (2001). Dynamic experimentation on the confocal laser scanning microscope: Application to soft-solid, composite food materials. *Journal of Microscopy-Oxford*, **201**, 279.
- Pomeranz, Y., Meloan, C.E. (1994). *Food Analysis*, 3rd ed., Chapman & Hall, New York, NY.
- Pothakamury, U.E., Barbosa-Canovas, G.V. (1995). Fundamental aspects of controlled release in foods. *Trends in Food Science and Technology*, **6**, 397.
- Povey, M.J.W. (1995). Ultrasound studies of shelf-life and crystallization, in *New Physicochemical Techniques for the Characterization of Complex Food Systems*, Dickinson, E., Ed., Blackie Academic & Professional, London, UK, Chap. 9.
- Povey, M.J.W. (1997). *Ultrasonic Techniques for Fluids Characterization*. Academic Press, San Diego, CA.
- Prescott, J. (1999). Flavour as a psychological construct: Implications for perceiving and measuring the sensory qualities of foods. *Food Quality and Preference*, **10**, 349.
- Prosser, A.J., Franes, E.I. (2001). Adsorption and surface tension of ionic surfactants at the air-water interface: Review and evaluation of equilibrium models. *Colloids and Surfaces A: Physicochemical and Engineering Aspects*, **178**, 1.
- Puff, N., Cagna, A., Aguié-Béghin, V., Douillard, R. (1998). Surface dilatational rheology of proteins absorbed at air/water and oil/water interfaces. *Journal of Colloid and Interface Science*, **208**, 405.
- Pugnaloni, L.A., Ettelaie, R., Dickinson, E. (2003). Growth and aggregation of surfactant islands during the displacement of an adsorbed protein monolayer: A Brownian dynamics simulation study. *Colloid Surface B*, **31**, 149–157.
- Pugnaloni, L.A., Dickinson, E., Ettelaie, R., Mackie, A.R., P.J. Wilde. (2004). Competitive adsorption of proteins and low-molecular-weight surfactants: Computer simulation and microscopic imaging. *Advances in Colloid and Interface Science*, **107**, 27–49.
- Qi, M., Hettiarachchy, N.S., Kalapathy, U. (1997). Solubility and emulsifying properties of soy protein isolates modified by pancreatin. *Journal of Food Science*, **62**, 1110.
- Quemada, D., Berli, C. (2002). Energy of interaction in colloids and its implications in rheological modeling. *Advances in Colloid and Interface Science*, **98**, 51.
- Rabe, S., Krings, U., Banavara, D.S., Berger, R.G. (2002). Computerized apparatus for measuring dynamic flavor release from liquid food matrices. *Journal of Agricultural and Food Chemistry*, **50**, 6440.
- Rabe, S., Krings, U., Berger, R.G. (2003). Dynamic flavour release from miglyol/water emulsions: Modelling and validation. *Food Chemistry*, **84**, 117.
- Race, S.W. (1991). Improved product quality through viscosity measurement. *Food Technology*, **45**, 86.
- Rahman, S. (1995). *Food Properties Handbook*, CRC Press, Boca Raton, FL.
- Rampon, V., Lethuaut, L., Mouhous-Riou, N., Genot, C. (2001). Interface characterization and aging of bovine serum albumin stabilized oil-in-water emulsions as revealed by front-surface fluorescence. *Journal of Agricultural and Food Chemistry*, **49**, 4046.
- Rampon, V., Genot, C., Riaublanc, A., Anton, M., Axelos, M.A.V., McClements, D.J. (2003a). Front-face fluorescence spectroscopy study of globular proteins in emulsions: Displacement of BSA by a nonionic surfactant. *Journal of Agricultural and Food Chemistry*, **51**, 2482.
- Rampon, V., Genot, C., Riaublanc, A., Anton, M., Axelos, M.A.V., McClements, D.J. (2003b). Front-face fluorescence spectroscopy study of globular proteins in emulsions: Influence of droplet flocculation. *Journal of Agricultural and Food Chemistry*, **51**, 2490.
- Rampon, V., Riaublanc, A., Anton, M., Genot, C., McClements, D.J. (2003c). Evidence that homogenization of BSA-stabilized hexadecane-in-water emulsions induces structure modification of the nonadsorbed protein. *Journal of Agricultural and Food Chemistry*, **51**, 5900.
- Rao, M.A. (1995). Rheological properties of fluid foods, in *Engineering Properties of Foods*, 2nd ed., Rao, M.A., Rizvi, S.S.H., Eds., Marcel Dekker, New York, NY, Chap. 1.
- Rao, M.A. (1999). *Rheology of Fluids and Semisolid Foods*, Kluwer Academic Publishers, New York, NY.

- Rao, V.N.M., Delaney, R.A.M., Skinner, G.E. (1995). Rheological properties of solid foods, in *Engineering Properties of Foods*, 2nd ed., Rao, M.A., Rizvi, S.S.H., Eds., Marcel Dekker, New York, NY, Chap. 2.
- Ratey, J.J. (2001). *A Users Guide to the Brain*, Vintage Books, New York, NY.
- Rawle, A. (2004). Basic principles of particle size analysis. *Technical Paper*, Malvern Instruments, Malvern, Worcs, England.
- Ray, A.K., Bird, P.B., Iacobucci, G.A., Clark, B.C. (1995). Functionality of gum arabic: Fractionation, characterization and evaluation of gum fractions in citrus oil emulsions and model beverages. *Food Hydrocolloids*, **9**, 123.
- Razumovsky, L., Damodaran, S. (2001). Incompatibility of mixing of proteins in adsorbed binary protein films at the air-water interface. *Journal of Agricultural and Food Chemistry*, **49**, 3080.
- Reddy, S.R., Fogler, H.S. (1981). Emulsion stability: Determination from turbidity. *Journal of Colloid and Interface Science*, **79**, 101.
- Reichardt, C. (1988). *Solvents and solvent effects in organic chemistry*, 2nd ed., VCH Publishers, Weinheim, Germany.
- Reid, J.S.G., Edwards, M.E. (1995). Galactomannans and other cell wall storage polysaccharides in seeds, in *Food Polysaccharides and Their Applications*, Stephan, A.M., Ed., Marcel Dekker, New York, NY, Chap. 6.
- Reiner, E.S., Radke, C.J. (1993). Double-layer interactions between charge-regulated colloidal surfaces—pair potentials for spherical-particles bearing ionogenic surface groups. *Advances in Colloid and Interface Science*, **47**, 59.
- Reiners, J., Nicklaus, S., Guichard, E. (2000). Interactions between  $\beta$ -lactoglobulin and flavour compounds of different chemical classes. Impact of the protein on the odour perception of vanillin and eugenol. *Lait*, **80**, 347.
- Reische, D.W., Lillard, D.A., Eitenmiller, R.R. (1998). *Food Lipids: Chemistry, Nutrition and Biotechnology*, Akoh, C.C., Min, D.B., Eds., Marcel Dekker, New York, NY.
- Reynolds, P.A., Gilbert, E.P., White, J.W. (2000). High internal phase water-in-oil emulsions studied by small-angle neutron scattering. *Journal of Physical Chemistry B*, **104**, 7012–7022.
- Rha, C.K., Pradipasena, P. (1986). Viscosity of proteins, in *Functional Properties of Food Macromolecules*, Mitchell, J.R., Ledward, D.A., Eds., Elsevier, London, UK, Chap. 2.
- Richmond, J.M. (1990). Cationic surfactants: Organic Chemistry. Marcel Dekker, New York, NY.
- Rizzieri, R., Baker, F.S., Donald, A.M. (2003). A tensometer to study strain deformation and failure behavior of hydrated systems via *in situ* environmental scanning electron microscopy. *Review of Scientific Instruments*, **74**, 4423.
- Roberts, I. (2003). In-line and on-line rheology measurements of food, in *Texture in Foods, Volume 1: Semi-Solid Foods*, McKenna, B.M., Ed., CRC Press, Boca Raton, FL, Chap. 7.
- Roberts, D.D., Taylor, A.J. (2000a). *Flavor Release*, ACS Symposium Series 763, American Chemical Society, Washington, DC.
- Roberts, D.D., Taylor, A.J. (2000b). Flavor release: A rationale for its study, in *Flavor Release*, ACS Symposium Series 763, Roberts, D.D., Taylor, A.J., Eds., American Chemical Society, Washington, DC, p. 1.
- Roberts, D.D., Acree, T.E. (1995). Simulation of retronasal aroma using a modified headspace technique—investigating the effects of saliva, temperature, shearing, and oil on flavor release. *Journal of Agricultural and Food Chemistry*, **43**, 2179.
- Roberts, D.D., Acree, T.E. (1996). Retronasal flavor release in oil and water model systems with an evaluation of volatility predictors, in *Flavor-Food Interactions*, McGorrin, R.J., Leland, J.V., Eds., American Chemical Society, Washington, DC, Chap. 16.
- Roberts, D.D., Elmore, J.S., Langley, K.R., Bakker, J. (1996). Effects of sucrose, guar gum and carboxymethylcellulose on the release of volatile flavor compounds under dynamic conditions. *Journal of Agricultural and Food Chemistry*, **44**, 1321.
- Roberts, D.D., Pollien, P., Watzke, B. (2003). Experimental and modeling studies showing the effect of lipid type and level on flavor release from milk-based liquid emulsions. *Journal of Agricultural and Food Chemistry*, **51**, 189.

- Robin, O., Britten, M., Paquin, P. (1994). Influence of the disperse phase distribution on the electrical conductivity of liquid O/W model and dairy emulsions. *Journal of Colloid and Interface Science*, **167**, 401.
- Robins, M.M. (2000). Lipid emulsions. *Grasas Y Aceites*, **51**, 26–34.
- Robins, M.M., Hibberd, D.J. (1998). Emulsion flocculation and creaming, in *Modern Aspects of Emulsion Science*, Binks, B.P., Ed., The Royal Society of Chemistry, Cambridge, UK, Chap. 4.
- Robinson, R.K. (1993). *Modern Dairy Technology: Advances in Milk Products*, 2nd ed., Elsevier, New York, NY.
- Robinson, R.K. (1994). *Modern Dairy Technology: Advances in Milk Processing*, 3rd ed., Elsevier, New York, NY.
- Robinson, G.W., Zhu, S.B., Singh, S., Evans, M.W. (1996). *Water in Biology, Chemistry and Physics: Experimental Overviews and Computational Methodologies*, World Scientific, Singapore.
- Roesch, R.R., Corredig, M. (2002a). Characterization of oil-in-water emulsions prepared with commercial soy protein concentrate. *Journal of Food Science*, **67**, 2837.
- Roesch, R.R., Corredig, M. (2002b). Texture and microstructure of emulsions prepared with soy protein concentrate by high-pressure homogenization. *Food Science and Technology*, **36**, 113.
- Rogacheva, S., Espinosa-Diaz, M.A., Voilley, A. (1999). Transfer of aroma compounds in water-lipid systems: Binding tendency of  $\beta$ -lactoglobulin. *Journal of Agricultural and Food Chemistry*, **47**, 259.
- Rogers, N.K. (1989). In *Prediction of Protein Structure and the Principles of Protein Conformation*, Fasman, G.D., Ed., Plenum Press, New York, NY, p. 359.
- Roland, A.M., Phillips, L.G., Boor, K.J. (1999). Effects of fat content on the sensory properties, melting, color, and hardness of ice cream. *Journal of Dairy Science*, **82**, 32.
- Roos, Y.H. (1995). *Phase Transitions in Foods*, Academic Press, San Diego, CA.
- Rosen, M.J. (1978). *Surfactants and Interfacial Phenomenon*, Wiley-Interscience Publishers, New York, NY.
- Roth, C.M., Lenhoff, A.M. (1996). Improved parametric representation of water dielectric data for Lifshitz theory calculations. *Journal of Colloid and Interface Science*, **179**, 637.
- Rother, M.A., Zinchenko, A.Z., Davis, R.H. (1997). Buoyancy-driven coalescence of slightly deformable drops. *Journal of Fluid Mechanics*, **346**, 117.
- Rouseff, R., Naim, M. (2000). Citrus flavor stability, in *Flavor Chemistry: Industrial and Academic Research*, ACS Symposium Series 756, Risch, S.J., Ho, C.T., Eds., American Chemical Society, Washington, DC, p. 44.
- Rousseau, D., Zilnik, L., Khan, R., Hodge, S. (2003). Dispersed phase destabilization in table spreads. *Journal of the American Oil Chemists Society*, **80**, 957–961.
- Rubio-Hernández, F.J., Carrique, F., Ruiz-Reina, E. (2004). The primary electroviscous effect in colloidal suspensions. *Advances in Colloid and Interface Science*, **107**, 51.
- Sader, J.E., Carnie, S.L., Chan, D.Y.C. (1995). Accurate analytic formulas for the double-layer interaction between spheres. *Journal of Colloid and Interface Science*, **171**, 46.
- Sadtler, V.M., Imbert, P., Dellacherie, E. (2002). Ostwald ripening of oil-in-water emulsions stabilized by phenoxy-substituted dextrans. *Journal of Colloid and Interface Science*, **254**, 355.
- Saether, O., Sjoblom, J., Dukhin, S.S. (2004). Droplet flocculation and coalescence in dilute oil-in-water emulsions, in *Food Emulsions*, 4th ed., Friberg, S., Larsson, K., Sjoblom, J., Eds., Marcel Dekker, New York, NY, Chap. 5.
- Saito, M. (2003). Optimization of emulsifying activity of soy protein isolate using computer-aided techniques. *Food Science and Technology Research*, **9**, 76.
- Salager, J.L. (1988). Phase transformation and emulsion inversion on the basis of the catastrophe theory, in *Encyclopedia of Emulsion Technology*, Vol. 3, Becher, P., Ed., Marcel Dekker, New York, NY, Chap. 1.
- Sanchez, M.C., Valencia, C., Franco, J.M., Gallegos, C. (2001). Wall slip phenomena in oil-in-water emulsions: Effect of some structural parameters. *Journal of Colloid and Interface Science*, **241**, 226.
- Sanchez, C.C., Ortiz, S.E.M., Nino, M.R.R., Anon, M.C., Patino, J.M.R. (2003). Effect of pH on structural, topographical, and dynamic characteristics of soy globulin films at the air-water interface. *Langmuir*, **19**, 7478.

- Santos, N.C., Castanho, M.A.R.B. (2004). An overview of the biophysical applications of atomic force microscopy. *Biophysical Chemistry*, **107**, 133.
- Sato, K. (1988). Crystallization of fats and fatty acids, in *Crystallization and Polymorphism of Fats and Fatty Acids*, Gardi, N., Sato, K., Marcel Dekker, New York, NY, p. 227.
- Schenkel, J.H., Kitchner, J.A. (1960). A test of the Derjaguin-Verwey-Overbeek theory with a colloidal suspension. *Transactions of the Faraday Society*, **56**, 161.
- Schenz, T.W. (2003). Thermal analysis, in *Food Analysis*, 3rd ed., Nielsen, S.S., Ed., Kluwer Academic Publishers, New York, NY, Chap. 31.
- Schirle-Keller, J.P., Reineccius, G.A., Hatchwell, L.C. (1994). Flavor interactions with fat replacers: Effect of oil type. *Journal of Food Science*, **59**, 813.
- Schmidt, R.K., Tasaki, K., Brady, J.W. (1994). Computer modeling studies of the interaction of water with carbohydrates. *Journal of Food Engineering*, **22**, 43.
- Schmitt, C., Sanchez, C., Desobry-Banon, S., Hardy, J. (1998). Structure and techno-functional properties of protein-polysaccharide complexes. *Critical Reviews in Food Science and Nutrition*, **38**, 689.
- Schokker, E.P., Dalgleish, D.G. (2000). Orthokinetic flocculation of caseinate-stabilized emulsions: Influence of calcium concentration, shear rate, and protein content. *Journal of Agricultural and Food Chemistry*, **48**, 198.
- Scholten, E., Tuinier, R., Tromp, R.H., Lekkerkerker, H.N.W. (2002). Interfacial tension of a decomposed biopolymer mixture. *Langmuir*, **18**, 2234.
- Schröder, V., Schubert, H. (1999). Production of emulsions using microporous ceramic membranes. *Colloids and Surfaces A: Physicochemical and Engineering Aspects*, **152**, 103.
- Schröder, V., Behrend, O., Schubert, H. (1998). Effect of dynamic interfacial tension on the emulsification process using microporous, ceramic membranes. *Journal of Colloid and Interface Science*, **202**, 334.
- Schubert, H. (1997). Advances in the mechanical production of food emulsions, in *Engineering and Food*, Jowitt, R., Ed., Sheffield Academic Press, Sheffield, UK, p. AA82.
- Schubert, H., Armbruster, H. (1992). Principles of formation and stability of emulsions. *International Chemical Engineering*, **32**, 14.
- Schubert, H., Ax, K. (2003). Engineering food emulsions, in *Texture in Foods, Volume 1: Semi-Solid Foods*, McKenna, B.M., Ed., CRC Press, Boca Raton, FL, Chap. 8.
- Schubert, H., Karbstein, H. (1994). Mechanical emulsification, in *Developments in Food Engineering. Part 1*, Yano, T., Matsuno, R., Nakamura, K., Eds., Blackie Academic & Professional, London, UK.
- Schubert, H., Lambrich, U. (2003). Membrane emulsification, in *Proceedings of the 34th Thematic Meeting, Membrane Emulsification-the Quest for the Perfect Membrane*, Wageningen, The Netherlands.
- Schubert, H., Ax, K., Behrend, O. (2003). Product engineering of dispersed systems. *Trends in Food Science and Technology*, **14**, 9.
- Schultz, K.W., Day, E.A., Sinnbuber, R.O. (1962). *Lipids and Their Oxidation*, AVI Publishing, Westport, CT.
- Sears, F.W., Salinger, G.L. (1975). *Thermodynamics, Kinetic Theory and Statistical Thermodynamics*, Addison-Wesley Publishing, Reading, MA.
- Seebergh, J.E., Berg, J.C. (1994). Depletion flocculation of aqueous, electrostatically stabilized latex dispersions. *Langmuir*, **10**, 454.
- Semenova, M.G., Antipova, A.S., Misharina, T.A., Golovnya, R.V. (2002). Binding of aroma compounds with legumin. Part I: Binding of hexyl acetate with 11S globulin depending on the protein molecular state in aqueous medium. *Food Hydrocolloids*, **16**, 557.
- Seuvre, A.M., Diaz, M.A.E., Voilley, A. (2000). Influence of the food matrix structure on the retention of aroma compounds. *Journal of Agricultural and Food Chemistry*, **48**, 4296.
- Seuvre, A.M., Diaz, M.A.E., Voilley, A. (2002). Transfer of aroma compounds through the lipidic-aqueous interface in a complex system. *Journal of Agricultural and Food Chemistry*, **50**, 1106.
- Shapley, N.C., d'Avila, M.A., Walton, J.H., Powell, R.L., Dungan, S.R., Phillips, R.J. (2003). Complex flow transitions in a homogeneous, concentrated emulsion. *Physics of Fluids*, **15**, 881.
- Sharma, R., Singh, H., Taylor, M.W. (1996a). Composition and structure of fat globule surface layers in recombined milk. *Journal of Food Science*, **61**, 28.



- Sharma, R., Singh, H., Taylor, M.W. (1996b). Recombined milk: Factors affecting the protein coverage and composition of fat globule surface layers. *Australian Journal of Dairy Technology*, **51**, 12.
- Shaw, D.J. (1980). *Introduction to Colloid and Surface Chemistry*, 3rd ed., Butterworths, London, UK.
- Shaw, P.E. (1986). The flavour of non-alcoholic beverages, in *Food Flavours, Part B: The Flavor Beverages*, Morton, I.D., MacLeod, A.J., Eds., Elsevier, Amsterdam.
- Sherman, P. (1968a). *Emulsion Science*, Academic Press, London, UK.
- Sherman, P. (1968b). General properties of emulsions and their constituents, in *Emulsion Science*, Sherman, P., Ed., Academic Press, London, UK, Chap. 3.
- Sherman, P. (1968c). Rheology of emulsions, in *Emulsion Science*, Sherman, P., Ed., Academic Press, London, UK, Chap. 4.
- Sherman, P. (1970). *Industrial Rheology with Particular Reference to Foods, Pharmaceuticals and Cosmetics*, Academic Press, London, UK.
- Sherman, P. (1982). Rheology of emulsions, in: *Encyclopedia of Emulsion Technology. Basic Theory*, Vol. 1, Becher, P., Ed., Marcel Dekker, New York, NY, Chap. 7.
- Sherman, P. (1995). A critique of some methods proposed for evaluating the emulsifying capacity and emulsion stabilizing performance of vegetable proteins. *Italian Journal of Food Science*, **1**, 3.
- Shi, W.H., Shi, W.Y., Kim, S.I., Liu, J., Aksay, I.A. (1990). Scaling behavior of the elastic properties of colloidal gels. *Physical Review A*, **42**, 4772.
- Shinoda, K., Friberg, S. (1986). *Emulsions and Solubilization*. John Wiley & Sons, New York, NY.
- Shinoda, K., Kunieda, H. (1983). Phase properties of emulsions: PIT and HLB, in *Encyclopedia of Emulsion Technology*, Vol. 1, Becher, P., Ed., Marcel Dekker, New York, NY, Chap. 5.
- Shoemaker, C.F., Nantz, J., Bonnans, S., Noble, A.C. (1992). Rheological characterization of dairy products. *Food Technology*, **46**, 98.
- Siano, S.A. (1998). Applications development with radio-frequency dielectric spectroscopy: Emulsions, suspensions and biomass, in *Handbook on Ultrasonic and Dielectric Characterization Techniques for Suspended Particles*, Hackley, V.A., Texter, J., Eds., American Chemical Society, Westerville, OH.
- Silvestre M.P.C., Decker, E.A., McClements, D.J. (1999). Influence of copper on the stability of whey protein stabilized emulsions. *Food Hydrocolloids*, **13**, 419.
- Simic, M.G., Jovanovic, S.V., Niki, E. (1992). Mechanisms of lipid oxidative processes and their inhibition, in *Lipid Oxidation in Food*, St. Angelo, A.J., Ed., American Chemical Society, Washington, DC, Chap. 2.
- Simoneau, C., McCarthy, M.J., Kauten, R.J., German, J.B. (1991). Crystallization dynamics in model emulsions from magnetic resonance imaging. *Journal of the American Oil Chemists Society*, **68**, 481.
- Simoneau, C., McCarthy, M.J., Reid, D.S., German, J.B. (1993). Influence of triglyceride composition on crystallization kinetics of model emulsions. *Journal of Food Engineering*, **19**, 365.
- Singer, N.S. (1996). Microparticulated proteins as fat mimetics, in *Handbook of Fat Replacers*, Roller, S., Jones, S.A., Eds., CRC Press, Boca Raton, FL, pp. 175–189.
- Singh, A.P., McClements, D.J., Marangoni, A.G. (2002). Comparison of ultrasonic and pulsed NMR techniques for determination of solid fat content. *Journal of the American Oil Chemists Society*, **79**, 431–437.
- Singh, S.K., Caram-Lelham, N. (1998). Thermodynamics of  $\kappa$ -carrageenan-amphiphilic drug interaction as influenced by specific counter-ions and temperature: A microcalorimetric and viscometric study. *Journal of Colloid and Interface Science*, **203**, 430.
- Sinton, S.W., Chow, A.W., Iwamiya, J.H. (1994). NMR imaging as a new tool for rheology. *Macromolecular Symposia*, **86**, 299.
- Sjoblom, J., Fordedal, H., Skodvin, T. (1996). Flocculation and coalescence in emulsions studied by dielectric spectroscopy, in *Emulsion and Emulsion Stability*, Sjoblom, J., Ed., Marcel Dekker, New York, NY, Chap. 8.
- Skoda, W., van den Tempel, M. (1963). Crystallization of emulsified triglycerides. *Journal of Colloid and Interface Science*, **18**, 568.
- Skodvin, T., Sjoblom, J., Saeten, J.O., Warnhim, T., Gestblom, B. (1994). A time domain dielectric spectroscopy study of some model emulsions and liquid margarines. *Colloids and Surfaces A: Physicochemical and Engineering Aspects*, **83**, 75.

- Skoog, D.A., West, D.M., Holler, F.J. (1994). *Analytical Chemistry: An Introduction*, 6th ed., Saunders College Publishing, Philadelphia, PE.
- Skvarla, J. (2001). Hydrophobic interaction between macroscopic and microscopic surfaces. Unification using surface thermodynamics. *Advances in Colloid and Interface Science*, **91**, 335.
- Sloan, A.E. (2003). Top 10 trends to watch and work on. *Food Technology*, **56**:4, 55.
- Smart, M.G., Fulcher, R.G., Pechak, D.G. (1995). Recent developments in the microstructural characterization of foods, in *Characterization of Foods: Emerging Techniques*, Gaonkar, A.G., Ed., Elsevier, Amsterdam, Chap. 11.
- Smith, A.L., Mitchell, D.P. (1976). The centrifuge technique in the study of emulsion stability, in *Theory and Practice of Emulsion Technology*, Smith, A.L., Ed., Academic Press, London, UK, Chap. 4.
- Smith, D.V., Margolskee, R.F. (2001). Making sense of taste. *Scientific American*, **284**, 32.
- Smith, D.V., St. John, S.J. (1999). Neural coding of gustatory information. *Current Opinion in Neurobiology*, **9**, 427.
- Smith, N.J., Williams, P.A. (1995). Depletion flocculation of polystyrene latices by water-soluble polymers. *Journal of the Chemical Society—Faraday Transactions*, **91**, 1483.
- Smittle, R.B. (1977). Microbiology of mayonnaise and salad dressing—review. *Journal of Food Protection*, **40**, 415.
- Smittle, R.B. (2000). Microbiological safety of mayonnaise, salad dressings and sauces produced in the United States: A review. *Journal of Food Protection*, **63**, 1144.
- Smolin, L.A., Grosvenor, M.B. (1994). *Nutrition: Science and Applications*, Saunders College Publishing, Fort Worth, TX.
- Soderberg, I., Hernqvist, L., Bucheim, W. (1989). Milk fat crystallization in natural milk fat globules. *Milchwissenschaft*, **44**, 403.
- Soderman, O., Bailnov, B. (1996). NMR self-diffusion studies of emulsions, in *Emulsions and Emulsion Stability*, Sjoblom, J., Ed., Marcel Dekker, New York, NY, Chap. 8.
- Soderman, O., Lonnqvist, I., Balinov, B. (1992). NMR self-diffusion studies of emulsion systems. Droplet sizes and microstructure of the continuous phase, in *Emulsions - A Fundamental and Practical Approach*, Sjoblom, J., Ed., Kluwer Publishers, Dordrecht, The Netherlands, p. 239.
- Sonntag, N.O.V. (1979a). Structure and composition of fats and oils, in: *Bailey's Industrial Oil and Fat Products*, Vol. 1, Swern, D., Ed., John Wiley & Sons, New York, NY, Chap. 1.
- Sonntag, N.O.V. (1979b). Reactions of fats and fatty acids, in *Bailey's Industrial Oil and Fat Products*, Vol. 1, Swern, D., Ed., John Wiley & Sons, New York, NY, Chap. 2.
- Sonntag, N.O.V. (1979c). Sources, utilization and classification of oils and fats, in *Bailey's Industrial Oil and Fat Products*, Vol. 1, Swern, D., Ed., John Wiley & Sons, New York, NY, Chap. 5.
- Sperry, P.R. (1982). A simple quantitative model for the volume restriction flocculation of latex by water-soluble polymers. *Journal of Colloid Science*, **87**, 375.
- Spicer, P.T., Pratsinis, S.E. (1996). Shear-induced flocculation: The evolution of floc structure and the shape of the size distribution at steady-state. *Water Research*, **30**, 1049.
- Srinivasan, M., Singh, H., Munro, P.A. (2000). The effect of sodium chloride on the formation and stability of sodium caseinate emulsions. *Food Hydrocolloids*, **14**, 497.
- Srinivasan, M., Singh, H., Munro, P.A. (2002). Formation and stability of sodium caseinate emulsions: Influence of retorting (121°C for 15 min) before or after emulsification. *Food Hydrocolloids*, **16**, 153.
- St. Angelo, A.J. (1989). A brief introduction to food emulsions and emulsifiers, in *Food Emulsifiers: Chemistry, Technology, Functional Properties and Applications*, Charalambous, G., Doxastakis, G., Eds., Elsevier, Amsterdam.
- St. Angelo, A.J. (1992). *Lipid Oxidation in Food*, American Chemical Society, Washington, DC.
- Stachurski, J., Michalek, M. (1996). The effect of the zeta potential on the stability of a non-polar oil-in-water emulsion. *Journal of Colloid and Interface Science*, **184**, 433.
- Stang, M., Karbstein, H., Schubert, H. (1994). Adsorption kinetics of emulsifiers at oil-water interfaces and their effect on mechanical emulsification. *Chemical Engineering and Processing*, **33**, 307.
- Stang, M., Schuchmann, H., Schubert, H. (2001). Emulsification in high-pressure homogenizers. *Engineering in the Life Sciences*, **1**, 151.
- Stanley, L., Flegler, J.W., Heckman, W., Klomparens, K.L. (1993). *Scanning and Transmission Electron Microscopy: An Introduction*, Oxford University Press, Oxford, UK.

- Stanley, N.F. (1995). Agars, in *Food Polysaccharides and Their Applications*, Stephan, A.M., Ed., Marcel Dekker, New York, NY, Chap. 7.
- Staples, E., Penfold, J., Tucker, I. (2000). Adsorption of mixed surfactants at the oil-water interface. *Journal of Physical Chemistry B*, **104**, 606-614.
- Stauffer, C.E. (1996). Emulsifiers for the food industry, in *Bailey's Industrial Oil and Fat Products*, 5th Edition, Vol. 3, *Edible Oil and Fat Products: Products and Application Technology*, Hui, Y.H., Ed., John Wiley & Sons, New York, NY, Chap. 12.
- Stauffer, C.E. (1999). *Emulsifiers*, Eagen Press Handbook, St. Paul, MN.
- Steffe, J.F. (1996). *Rheological Methods in Food Process Engineering*, 2nd ed., Freeman Press, East Lansing, MI.
- Steinhart, H., Stephan, A., Bucking, M. (2000). Advances in flavor research, HRC. *Journal of High Resolution Chromatography*, **23**, 489.
- Stephan, A., Steinhart, H. (2000). Bitter taste of unsaturated free fatty acids in emulsions: Contribution to the off-flavour of soybean lecithins. *European Food Research and Technology*, **212**, 17.
- Stephan, A., Bucking, M., Steinhart, H. (2000). Novel analytical tools for food flavours. *Food Research International*, **33**, 199.
- Stephen, A.M. (1995). *Food Polysaccharides and Their Applications*, Marcel Dekker, New York, NY.
- Stern, P., Valentova, H., Pokorný, J. (2001). Rheological properties and sensory texture of mayonnaise. *European Journal of Lipid Science and Technology*, **103**, 23.
- Stokes, D.J. (2001). Characterisation of soft condensed matter and delicate materials using environmental scanning electron microscopy (ESEM). *Advanced Engineering Materials*, **3**, 126.
- Stokes, D.J. (2003). Recent advances in electron imaging, image interpretation and applications: Environmental scanning electron microscopy. *Philos T Roy Soc A*, **361**, 2771.
- Stokes, D.J., Thiel, B.L., Donald, A.M. (1998). Direct observation of water-oil emulsion systems in the liquid state by environmental scanning electron microscopy. *Langmuir*, **14**, 4402.
- Stoll, S., Buffle, J. (1996). Computer-simulation of bridging flocculation processes: The role of colloid to polymer concentration ratio on aggregation kinetics. *Journal of Colloid and Interface Science*, **180**, 548.
- Stone, H., Sidel, J.L. (1993). *Sensory Evaluation Practices*, 2nd ed., Academic Press, San Diego, CA.
- Stone, H.A. (1994). Dynamics of drop deformation and breakup in viscous fluids. *Annual Review of Fluid Mechanics*, **26**, 65.
- Stoohart, P.H. (1995). Developments in the application of small angle neutron scattering to food systems, in *Characterization of Foods: Emerging Techniques*, Gaonkar, A.G., Ed., Elsevier, Amsterdam, Chap. 9.
- Strawbridge, K.B., Ray, E., Hallett, F.R., Tosh, S.M., Dalgleish, D.G. (1995). Measurement of the particle size distributions in milk homogenized by a microfluidizer—estimation of populations of particles with radii less than 100 nm. *Journal of Colloid and Interface Science*, **171**, 392.
- Sugiura, S., Nakajima, M., Yamamoto, K., Iwamoto, S., Oda, T., Satake, M., Seki, M. (2004). Preparation characteristics of water-in-oil-in-water multiple emulsions using microchannel emulsification. *Journal of Colloid and Interface Science*, **270**, 221.
- Suratkar, V., Mahapatra, S. (2000). Solubilization site of organic perfume molecules in sodium dodecyl sulfate micelles: New insights from proton NMR studies. *Journal of Colloid and Interface Science*, **225**, 32.
- Suzuki, K., Shuto, I., Hagura, Y. (1996). Characteristics of the membrane emulsification method with preliminary emulsification for preparing corn oil-in-water emulsions. *Food Science and Technology International*, **2**, 43.
- Suzuki, K., Hayakawa, K., Hagura, Y. (1999). Preparation of high concentration O/W and W/O Emulsions by the membrane phase inversion emulsification method. *Food Science and Technology Research*, **5**, 234.
- Swaigood, H.E. (1996). Characteristics of milk, in *Food Chemistry*, 3rd ed., Fennema, O.R., Ed., Marcel Dekker, New York, NY, Chap. 14.
- Swanson, N.L., Billard, D.B. (2000). Multiple scattering efficiency and optical extinction, *Physical Review E*, **61**, 4518.
- Swift, C.E., Lockett, C., Fryer, P.J. (1961). Comminuted meat emulsions—the capacity of meat for emulsifying fat. *Food Technology*, **15**, 469.

- Tadros, T.F. (1994). Fundamental principles of emulsion rheology and their applications. *Colloids and Surfaces*, **91**, 30.
- Tadros, T.F. (1996). Correlation of viscoelastic properties of stable and flocculated suspensions with their interparticle interactions. *Advances in Colloid and Interface Science*, **68**, 97.
- Tadros, T.F., Vincent, B. (1983). Liquid/liquid interfaces, in *Encyclopedia of Emulsion Technology*, Vol. 1, Becher, P., Ed., Marcel Dekker, New York, NY.
- Taisne, L., Walstra, P., Cabane, B. (1996). Transfer of oil between emulsion droplets. *Journal of Colloid and Interface Science*, **184**, 378.
- Tamime, A.Y. (2003). *Manual of Yogurt Making Technology*, Blackwell Scientific, New York, NY.
- Tamime, A.Y., Robinson, R.K. (1999). *Yoghurt : Science and Technology*, 2nd ed., Pergamon Press, New York, NY.
- Tan, C.T. (1998). Beverage flavor emulsion—a form of emulsion liquid membrane encapsulation, in *Food Flavors: Formation, Analysis and Packaging Influences*, Contis, E.T., Ed., Elsevier, New York, NY, p. 29.
- Tan, C.T. (2004). Beverage emulsions, in *Food Emulsions*, 4th ed., Friberg, S., Larsson, K., Sjoblom, J., Eds., Marcel Dekker, New York, NY, Chap. 12.
- Tanford, C. (1980). *The Hydrophobic Effect*, John Wiley & Sons, New York, NY.
- Taylor, P. (1995). Ostwald ripening in emulsions. *Colloids and Surfaces A: Physicochemical and Engineering Aspects*, **99**, 175.
- Tcholakova, S., Denkov, N.D., Ivanov, I.B., Campbell, B. (2002). Coalescence in lactoglobulin-stabilized emulsions: Effects of protein adsorption and drop size. *Langmuir*, **18**, 8960.
- Taylor, A.J. (1996). Volatile flavor release from foods during eating. *Critical Reviews in Food Science and Nutrition*, **36**, 765.
- Taylor, A.J. (1998). Physical chemistry of flavour. *International Journal of Food Science and Technology*, **33**, 53.
- Taylor, A.J., Linforth, R.S.T. (1996). Flavour release in the mouth. *Trends in Food Science and Technology*, **7**, 444.
- Taylor, A.J., Linforth, R.S.T. (2000). Techniques for measuring volatile release in vivo during consumption of food, in *Flavor Release*, ACS Symposium Series 763, Roberts, D.D., Taylor, A.J., Eds., American Chemical Society, Washington, DC, p. 8.
- Taylor, A.J., Linforth, R.S.T. (2001). Modeling flavour release through quantitative structure property relationships (QSPR). *Chimia*, **55**, 448.
- Taylor, A.J., Linforth, R.S.T., Harvey, B.A., Blake, B. (2000). Atmospheric pressure chemical ionisation mass spectrometry for in vivo analysis of volatile flavour release. *Food Chemistry*, **71**, 327.
- Tcholakova, S., Denkov, N.D., Sidzhakova, D., Ivanov, I.B., Campbell, B. (2003). Interrelation between drop size and protein adsorption at various emulsification conditions. *Langmuir*, **19**, 5640.
- ten Grotenhuis, E., Paques, M., van Aken, G.A. (2000). The application of diffusing-wave spectroscopy to monitor the phase behavior of emulsion-polysaccharide systems. *Journal of Colloid and Interface Science*, **227**, 495.
- Terpstra, M.E.J., Janssen, A.M., van Gemert, L.J., van Doorn, R.J.M., de Wijk, R.A., Weenen, H., van der Linden, E. (2003). Texture of mayonnaise and dressing; relations between sensory attributes and physical properties, in *Proceedings of the Third International Symposium on Food Rheology and Structure*, Fischer, P., Marti, I., Windhab, E.J., Eds., Laboratory of Food Process Engineering, Zurich, Switzerland.
- Texter, J., Beverly, T., Templar, S.R., Matsubara, T. (1987). Partitioning of para-phenylenediamines in oil-in-water emulsions. *Journal of Colloid and Interface Science*, **120**, 389.
- Thomas, J.C., Middelberg, A.P.J., Hamel, J.F. Snoswell, M.A. (1991). High resolution particle size analysis in biotechnology process control. *Biotechnology Progress*, **7**, 377.
- Thomson, D.M.H. (1986). The meaning of flavor, in *Developments in Food Flavours*, Birch, G.G., Lindley, M.G., Eds., Elsevier, London, UK, p. 1.
- Timms, R.E. (1991). Crystallization of fats. *Chemistry and Industry*, **342**.
- Timms, R.E. (1995). Crystallization of fats, in *Developments in Oils and Fats*, Hamilton, R.J., Ed., Blackie Academic & Professional, London, UK, Chap. 8.
- Tinoco, I., Sauer, K., Wang, J.C. (1985). *Physical Chemistry: Principles and Applications in Biological Sciences*, 2nd ed., Prentice-Hall, Englewood Cliffs, NJ.

- Toledano, O., Magdassi, S. (1998). Emulsification and foaming properties of hydrophobically modified gelatin. *Journal of Colloid and Interface Science*, **200**, 235.
- Tolstoguzov, V.B. (1996). Structure-property relationships in foods, in *Macromolecular Interactions in Food Technology*, Parris, N., Kato, A., Creamer, L.K, Pearce, J., Eds., American Chemical Society, Washington, DC, Chap. 1.
- Tolstoguzov, V.B. (1997). Protein-polysaccharide interactions, in *Food Proteins and Their Applications*, Damodaran, S., Paraf, A., Eds., Marcel Dekker, New York, NY, Chap. 6.
- Tornberg, E., Olsson, A., Perrson, K. (1997). Surface forces in emulsions, in *Food Emulsions*, 3rd ed., Friberg, S., Larsson, K., Eds., Marcel Dekker, New York, NY, p. 279.
- Tory, E.M. (1996). *Sedimentation of Small Particles in a Viscous Liquid*, Computational Mechanics Publications, Southampton, UK.
- Trainer, M.N., Freud, P.J., Leonardo, E.M. (1992). High-concentration submicron particle size distribution by dynamic light scattering. *American Laboratory*, July.
- Trubiano, P.C. (1995). The role of specialty food starches in flavor emulsions, in *Flavor Technology: Physical Chemistry, Modification, and Process*, Ho, C.T., Tan, C.T., Tong, C.H., Eds., American Chemical Society, Washington, DC, p. 199.
- Tse, K.Y. (1990). *Physical Stability of Flavor Emulsions*, Thesis, University of Minnesota, MN.
- Tse, K.Y., Reineccius, G.A. (1995). Methods to predict the physical stability of flavor-cloud emulsion, in *Flavor Technology: Physical Chemistry, Modification, and Process*, Ho, C.T., Tan, C.T., Tong, C.H., Eds., American Chemical Society, Washington, DC, p. 173.
- Tuinier, R., de Kruif, C.G. (1999). Phase separation, creaming and network formation of oil-in-water emulsions induced by an exocellular polysaccharide. *Journal of Colloid and Interface Science*, **218**, 201.
- Tung, M.A., Jones, L.J. (1981). Microstructure of mayonaisse and salad dressing, in *Studies of Food Microstructure*, Holcomb, D.N., Kalab, M., Eds., Scanning Electron Microscopy, AMF O'Hare, IL, p. 231.
- Tung, M.A., Paulson, A.T. (1995). Rheological concepts for probing ingredient interactions in food systems, in *Ingredient Interactions: Effects on Food Quality*, Gaonkar, A., Ed., Marcel Dekker, New York, NY.
- Tunon, I., Silla, E., Pascual-Ahuir, J.L. (1992). Molecular surface area and hydrophobic effect. *Protein Engineering*, **5**, 715.
- Turnbull, D., Cormia, R.L. (1961). Kinetics of crystal nucleation in some normal alkane liquids. *Journal of Chemical Physics*, **34**, 830.
- Urbina-Villalba, G., Garcia-Sucre, M. (2000). Brownian dynamics simulation of emulsion stability. *Langmuir*, **16**, 7975.
- Uriev, N.B. (1994). Structure, rheology and stability of concentrated disperse systems under dynamic conditions. *Colloids and Surfaces A: Physicochemical and Engineering Aspects*, **87**, 1.
- USDA (1994). *A Food Labeling Guide*, Center for Food Safety and Applied Nutrition, U.S. Food and Drug Administration, Washington, DC.
- Utsumi, S., Matsumura, Y., Mori, T. (1997). Structure-function relationships of soy proteins, in *Food Proteins and Their Applications*, Damodaran, S., Paraf, A., Eds., Marcel Dekker, New York, NY, Chap. 9.
- Vaessen, G.E.J., Stein, H.N. (1995). The applicability of catastrophe theory to emulsion phase inversion. *Journal of Colloid and Interface Science*, **176**, 378.
- van Aken, G.A. (2002). Flow-induced coalescence in protein-stabilized highly concentrated emulsions. *Langmuir*, **18**, 2549.
- van Aken, G.A. (2004). Coalescence mechanisms in protein-stabilized emulsions, in *Food Emulsions*, 4th ed., Friberg, S., Larsson, K., Sjoblom, J., Eds., Marcel Dekker, New York, NY, Chap. 8.
- van Aken, G.A., Blijdenstein, T.B.J., Hotrum, N.E. (2003). Colloidal destabilisation mechanisms in protein-stabilised emulsions. *Current Opinions in Colloid and Interface Science*, **8**, 371.
- van Boekel, M.A.J.S. (1981). Estimation of solid liquid ratios in bulk fats and emulsions by pulsed NMR. *Journal of the American Oil Chemists Society*, **58**, 768.
- van Boekel, M.A.J.S., Walstra, P. (1981). Stability of oil-in-water emulsions with crystals in the disperse phase. *Colloids and Surfaces*, **3**, 109.

- van Dalen, G. (2002). Determination of the water droplet size distribution of fat spreads using confocal scanning laser microscopy. *Journal of Microscopy-Oxford*, **208**, 116.
- van de Hulst, H.C. (1957). *Light Scattering by Small Particles*, John Wiley & Sons, New York, NY.
- van den Enden, J.C., Waddington, D., van Aalst, H., van Kralingen, C.G., Packer, K.J. (1990). Rapid determination of water droplet size distributions by PFG-NMR. *Journal of Colloid and Interface Science*, **140**, 105.
- van der Linden, E., Sagis, L., Venema, P. (2003). Rheo-optics and food systems. *Current Opinion in Colloid and Interface Science*, **8**, 349.
- van der Ven, C., Gruppen, H., de Bont, D.B.A., Voragen, A.G.J. (2001). Emulsion properties of casein and whey protein hydrolysates and the relation with other hydrolysate characteristics. *Journal of Agricultural and Food Chemistry*, **49**, 5005.
- van Duynhoven, J.P.M., Goudappel, G.J.W., van Dalen, G., van Bruggen, P.C., Blonk, J.C.G., Eijkelenboom, A.P.A.M. (2002). Scope of droplet size measurements in food emulsions by pulsed field gradient NMR at low field. *Magnetic Resonance in Chemistry*, **40**, pp. S51-S59.
- van Gunsteren, W.F. (1988). The role of computer simulation techniques in protein engineering. *Protein Engineering*, **2**, 5.
- van Holde, K.E. (1971). *Physical Biochemistry*, Prentice-Hall, Englewood Cliffs, NJ.
- van Holde, K.E. (1977). Effects of amino acid composition and microenvironment on protein structure, in *Food Proteins*, Whitaker, J.R., Tannenbaum, S.R., Eds., AVI Publishing, Westport, CT, Chap. 1.
- van Kalsbeek, H.K.A.I., Prins, A. (1999). Foam formation by food proteins in relation to their dynamic surface behavior, in *Food Emulsions and Foams: Interfaces, Interactions and Stability*, Dickinson E., Rodriguez-Patino, J.M., Eds., Royal Society of Chemistry, Cambridge, UK, p. 91.
- van Ruth, S.M. (2001). Methods for gas chromatography-olfactometry: A review. *Biomolecular Engineering*, **17**, 121.
- van Ruth, S.M., O'Connor, C.H. (2001a). Evaluation of three gas chromatography-olfactometry methods: Comparison of odour intensity-concentration relationships of eight volatile compounds with sensory headspace data. *Food Chemistry*, **74**, 341.
- van Ruth, S.M., O'Connor, C.H. (2001b). Influence of assessors' qualities and analytical conditions on gas chromatography-olfactometry analysis. *European Food Research and Technology*, **213**, 77.
- van Ruth, S.M., Roozen, J.P. (2000). Aroma compounds of oxidised sunflower oil and its oil-in-water emulsion: Volatility and release under mouth conditions. *European Food Research and Technology*, **210**, 258.
- van Ruth, S.M., Villeneuve, E. (2002). Influence of  $\beta$ -lactoglobulin, pH and presence of other aroma compounds on the air/liquid partition coefficients of 20 aroma compounds varying in functional group and chain length. *Food Chemistry*, **79**, 157.
- van Ruth, S.M., de Vries, G., Geary, M., Giannouli, P. (2002a). Influence of composition and structure of oil-in-water emulsions on retention of aroma compounds. *Journal of the Science of Food and Agriculture*, **82**, 1028.
- Van Ruth, S.M., King, C., Delarue, M., Giannouli, P. (2002b). Release of volatile compounds from emulsions: Influence of beta-lactoglobulin and pH. *Italian Journal of Food Science*, **14**, 145.
- van Ruth, S.M., King, C., Giannouli, P. (2002c). Influence of lipid fraction, emulsifier fraction, and mean particle diameter of oil-in-water emulsions on the release of 20 aroma compounds. *Journal of Agricultural and Food Chemistry*, **50**, 2365.
- van Ruth, S.M., Roozen, J.P., Posthumus, M.A., Jansen, F.J.H.M. (1999a). Volatile composition of sunflower oil-in-water emulsions during initial lipid oxidation: Influence of pH. *Journal of Agricultural and Food Chemistry*, **47**, 4365.
- van Ruth, S.M., Roozen, J.P., Posthumus, M.A., Jansen, F.J.H.M. (1999b). Influence of ascorbic acid and ascorbyl palmitate on the aroma composition of an oxidized vegetable oil and its emulsion. *Journal of the American Oil Chemists Society*, **76**, 1375.
- van Vliet, T. (1995). Mechanical properties of concentrated food gels, in *Food Macromolecules and Colloids*, Dickinson, E., Lorient, D., Eds., Royal Society of Chemistry, Cambridge, UK, p. 447.
- van Vliet, T., Walstra, P. (1989). Weak particle networks, in *Food Colloids*, Bee, R.D., Richmond, P., Mingins, J., Eds., Royal Society of Chemistry, Cambridge, UK, p. 206.
- Vanapalli, S.A., Coupland, J.N. (2001). Emulsions under shear—the formation and properties of partially coalesced lipid structures. *Food Hydrocolloids*, **15**, 507.

- Vanapalli, S.A., Coupland, J.N. (2004). Orthokinetic stability of emulsions, in *Food Emulsions*, 4th ed., Friberg, S., Larsson, K., Sjoblom, J., Eds., Marcel Dekker, New York, NY, Chap. 9.
- Vanapalli, S.A., Palanuwech, J., Coupland, J.N. (2002a). Influence of fat crystallization on the stability of flocculated emulsions. *Journal of Agricultural and Food Chemistry*, **50**, 5224.
- Vanapalli, S.A., Palanuwech, J., Coupland, J.N. (2002b). Stability of emulsions to dispersed phase crystallization: Effect of oil type, dispersed phase volume fraction, and cooling rate. *Colloids and Surfaces A: Physicochemical and Engineering Aspects*, **204**, 227–237.
- Vargas, W.E. (1999). Diffuse radiation intensity propagating through a particulate slab. *Journal of the Optical Society of America A—Optic Image Science and Vision*, **16**, 1362.
- Vargas, W.E. (2000). Optimization of the diffuse reflectance of pigmented coatings taking into account multiple scattering. *Journal of Applied Optics*, **88**, 4079.
- Vargas, W.E. (2002). Inversion methods from Kubelka-Munk analysis. *Journal of Optics A—Pure and Applied Optics*, **4**, 452.
- Vargas, W.E., Niklasson, G.A. (1997a). Generalized model for evaluating scattering parameters used in radiative transfer models. *Journal of the Optical Society of America A—Optics, Image Science and Vision*, **14**, 2243.
- Vargas, W.E., Niklasson, G.A. (1997b). Intensity of diffuse radiation in particulate media. *Journal of the Optical Society of America A—Optics, Image Science and Vision*, **14**, 2253.
- Vaughan, J.G. (1979). Food Emulsions, in *Food Microscopy*, Vaughan, J.G., Ed., Academic Press, London, UK.
- Verly, A., Tarabukinova, E., Haudin, J.M., Peuvrel-Disdier, E., Navard, P. (2003). Application of rheo-optical tools to the analysis of food structure under shear, in *Proceedings of the Third International Symposium on Food Rheology and Structure*, Fischer, P., Marti, I., Windhab, E.J., Eds., Laboratory of Food Process Engineering, Zurich, Switzerland.
- Vincent, B., Kiraly, Z., Obey, T.M. (1998). Emulsion formation by nucleation and growth mechanisms, in *Modern Aspects of Emulsion Science*, Binks, B.P., Ed., The Royal Society of Chemistry, Cambridge, UK, Chap. 3.
- Vladislavljevic, G.T., Schubert, H. (2003a). Preparation of emulsions with a narrow particle size distribution using microporous  $\alpha$ -alumina membranes. *Journal of Dispersion Science and Technology*, **24**, 811.
- Vladislavljevic, G.T., Schubert, H. (2003b). Influence of process parameters on droplet size distribution in SPG membrane emulsification and stability of prepared emulsion droplets. *Journal of Membrane Science*, **225**, 15.
- Vladislavljevic, G.T., Lambrich, U., Nakajima, M., Schubert, H. (2004). Production of O/W emulsions using SPG membranes, ceramic  $\alpha$ -alumina oxide membranes, microfluidizer and a silicon microchannel plate—a comparative study. *Colloids and Surfaces A: Physicochemical and Engineering Aspects*, **232**, 199.
- Vodovotz, Y., Vittadini, E., Coupland, J., McClements, D.J., Chinachoti, P. (1996). Bridging the Gap: Use of confocal microscopy in food research. *Food Technology*, **50**, 74.
- Vold, M.J. (1961). The effect of adsorption on the van der Waals interaction of spherical colloidal particles. *Journal of Colloid Science*, **16**, 1.
- Voragen, A.G.J., Pilnik, W., Thibault, J.F., Axelos, M.A.V., Renard, C.M.G.C. (1995). Pectins, in *Food Polysaccharides and Their Applications*, Stephan, A.M., Ed., Marcel Dekker, New York, NY, Chap. 10.
- Waddington, D. (1980). Some applications of wide line NMR in the oils and fats industry, in *Fats and Oils: Chemistry and Technology*, Hamilton, R.J., Bhati, A., Eds., Applied Science Publishers, London, UK, Chap. 2.
- Wagner, N.J. (1998). Rheo-optics, *Current Opinion in Colloid and Interface Science*, **3**, 391.
- Walstra, P. (1967). On the crystallization habit in fat globules. *Netherlands Milk and Dairy Journal*, **21**, 166.
- Walstra, P. (1968). Estimating globule-size distribution of oil-in-water emulsions by spectroturbidimetry. *Journal of Colloid and Interface Science*, **27**, 493.
- Walstra, P. (1983). Formation of emulsions, in *Encyclopedia of Emulsion Technology*, Vol. 1. Basic Theory, Becher, P., Ed., Marcel Dekker, New York, NY, Chap. 2.
- Walstra, P. (1987). Fat crystallization, in *Food Structure and Behaviour*, Blanshard, J.M.V., Lillford, P., Eds., Academic Press, London, UK, Chap. 5.

- Walstra, P. (1993a). Introduction to aggregation phenomenon in food colloids, in *Food Colloids and Polymers: Stability and Mechanical Properties*, Dickinson, E., Walstra, P., Eds., Royal Society of Chemistry, Cambridge, UK, p. 3.
- Walstra, P. (1993b). Principles of emulsion formation. *Chemical Engineering Science*, **48**, 333.
- Walstra, P. (1996a). Emulsion stability, in *Encyclopedia of Emulsion Technology*, Vol. 4, Becher, P., Ed., Marcel Dekker, New York, NY, Chap. 1.
- Walstra, P. (1996b). Disperse systems: Basic considerations, in *Food Chemistry*, 3rd ed., Fennema, O.R., Ed., Marcel Dekker, New York, NY, Chap. 3.
- Walstra, P. (1999). *Dairy Technology: Principles of Milk Properties and Processes*, Marcel Dekker, New York, NY.
- Walstra, P. (2003a). *Physical Chemistry of Foods*, Marcel Dekker, New York, NY.
- Walstra, P. (2003b). Studying food colloids: Past, present and future, in *Food Colloids, Biopolymers and Materials*, Royal Society of Chemistry, Cambridge, UK.
- Walstra, P., R. Jenness. (1984). *Dairy Chemistry and Physics*, John Wiley & Sons, New York, NY.
- Walstra, P., Smulder, P.E.A. (1998). Emulsion formation, in *Modern Aspects of Emulsion Science*, Binks, B.P., Ed., The Royal Society of Chemistry, Cambridge, UK, Chap. 2.
- Walstra, P., van Beresteyn, E.C.H. (1975). Crystallization of milk fat in the emulsified state. *Netherlands Milk and Dairy Journal*, **29**, 35.
- Wang, Z.L. (2003). New developments in transmission electron microscopy for nanotechnology. *Advanced Materials*, **15**, 1497.
- Watkins, S.M., German, J.B. (2002). Omega fatty acids, in *Food Lipids: Chemistry, Nutrition and Biotechnology*, Akoh, C.C., Min, D.B., Eds., Marcel Dekker, New York, NY, p. 559.
- Webb, M.R., Naeem, H.A., Schmidt, K.A. (2002). Food protein functionality in a liquid system: A comparison of deamidated wheat protein with dairy and soy proteins. *Journal of Food Science*, **67**, 2896.
- Wedzicha, B.L. (1988). Distribution of low-molecular weight food additives in dispersed systems, in *Advances in Food Emulsions*, Dickinson, E., Stainsby, G., Eds., Elsevier, London, UK, Chap. 10.
- Wedzicha, B.L., Zeb, A., Ahmed, S. (1991). Reactivity of food preservatives in dispersed systems, in *Food Polymers, Gels and Colloids*, Dickinson, E., Ed., Royal Society of Chemistry, Cambridge, UK, p. 180.
- Weers, J.G. (1998). Molecular diffusion in emulsions and emulsion mixtures, in *Modern Aspects of Emulsion Science*, Binks, B.P., Ed., The Royal Society of Chemistry, Cambridge, UK, Chap. 9.
- Wehling, R.L. (2003). Infrared spectroscopy, in *Food Analysis*, 3rd ed., Nielsen, S.S., Ed., Kluwer Academic Publishers, New York, NY, Chap. 24.
- Wei, Y.-Z., Kumbharkhane, A.C., Sadeghi, M., Sage, J.T., Tiam, W.D., Champion, P.M., Reiner, E.S., Radke, C.J. (1993). Double layer interactions between charge-regulated colloidal systems: Pair potentials for spherical particles bearing ionogenic surface groups. *Advances in Colloid and Interface Science*, **47**, 59.
- Wei, Y.-Z., Kumbharkhane, A.C., Sadeghi, M., Sage, J.T., Tiam, W.D., Champion, P.M., Radke, C.J., McDonald, M.J. (1994). Protein hydration investigations with high-frequency dielectric spectroscopy. *Journal of Physical Chemistry*, **98**, 6644.
- Weiss, T.J. (1983). *Food Oils and Their Uses*, 2nd ed., AVI Publishing, Westport, CT.
- Weiss, J., Liao, W. (2000). Addition of sugars influences color of oil-in-water emulsions. *Journal of Agricultural and Food Chemistry*, **48**, 5053.
- Weiss, J., McClements, D.J. (2000). Influence of Ostwald ripening on rheology of oil-in-water emulsions containing electrostatically stabilized droplets. *Langmuir*, **16**, 2145.
- Weiss J., McClements, D.J. (2001). Color changes in hydrocarbon oil-in-water emulsions caused by Ostwald ripening. *Journal of Agricultural and Food Chemistry*, **49**, 4372.
- Weiss, J., Cancelliere, C., McClements, D.J. (2000). Mass transport phenomena in oil-in-water emulsions containing surfactant micelles: Ostwald ripening. *Langmuir*, **16**, 6833.
- Weiss, J., Coupland, J.N., McClements, D.J. (1996). Solubilization of hydrocarbon droplets suspended in a non-ionic surfactant solution. *Journal of Physical Chemistry*, **100**, 1066.
- Weiss, J., Herrmann, N., McClements, D.J. (1999). Ostwald ripening of hydrocarbon emulsion droplets in surfactant solutions. *Langmuir*, **15**, 6652.



- Weitz, D.A., Pine, D.J. (1992). Diffusing-wave spectroscopy. *Dynamic Light Scattering*, Ed., Wyn-Brown, Open University Press, UK.
- Weitz, D.A., Zhu, X., Durian, D.J., Gang H., Pine, D.J. (1993). Diffusing wave spectroscopy: The technique and some applications, *Physica Scripta*, **T49**, 610.
- Wendin, K., Hall, G. (2001). Influences of fat, thickener and emulsifier contents on salad dressing: Static and dynamic sensory and rheological analyses. *Food Science and Technology*, **34**, 222.
- Wendin, K., Aaby, K., Edris, A., Ellekjaer, M.R., Albin, R., Bergenstahl, B., Johansson, L., Willers, E.P., Solheim, R. (1997a). Low-fat mayonnaise: Influences of fat content, aroma compounds and thickeners. *Food Hydrocolloids*, **11**, 87.
- Wendin, K., Solheim, R., Allmere, T., Johansson, L. (1997b). Flavour and texture in sourmilk affected by thickeners and fat content. *Food Quality and Preference*, **8**, 281.
- Wendin, K., Ellekjaer, M.R., Solheim, R. (1999). Fat content and homogenization effects on flavour and texture of mayonnaise with added aroma. *Food Science and Technology*, **32**, 377.
- Wendlandt, W.W. (1968). *Modern Aspects of Reflectance Spectroscopy*, Plenum Press, New York, NY.
- Whittle, M., Dickinson, E. (1997). Brownian dynamics simulation of gelation in soft sphere systems with irreversible bond formation. *Molecular Physics*, **90**, 739.
- Whittle, M., Dickinson, E. (2001). On simulating colloids by dissipative particle dynamics: Issues and complications. *Journal of Colloid and Interface Science*, **242**, 106.
- Whorlow, R.W. (1992). *Rheological Techniques*, 2nd ed., Ellis Horwood, New York, NY.
- Wickramasinghe, N.C. (1973). *Light Scattering Functions for Small Particles*, John Wiley & Sons, New York, NY.
- Wilde, P.J. (2000). Interfaces: Their role in foam and emulsion behaviour. *Current Opinion in Colloid and Interface Science*, **5**, 176.
- Williams, A., Janssen, J.J.M., Prins, A. (1997). Behaviour of droplets in simple shear flow in the presence of a protein emulsifier. *Colloids and Surfaces A: Physicochemical and Engineering Aspects*, **125**, 189.
- Williams, A.A. (1986). Modern sensory analysis and the flavour industry, in *Developments in Food Flavours*, Birch, G.G., Lindley, M.G., Eds., Elsevier, London, UK, p. 1.
- Williams, P.A., Phillips, G.O. (2003). The use of hydrocolloids to improve food texture, in *Texture in Foods, Volume 1: Semi-Solid Foods*, McKenna, B.M., Ed., CRC Press, Boca Raton, FL, Chap. 11.
- Wilson, H.J., Pietraszewski, L.A., Davis, R.H. (2000). Aggregation of charged particles under electrophoresis or gravity at arbitrary Peclet numbers. *Journal of Colloid and Interface Science*, **221**, 87.
- Wilson, R.H. (1995). Recent developments in infrared spectroscopy and microscopy, in *New Physicochemical Techniques for the Characterization of Complex Food Systems*, Dickinson, E., Ed., Blackie Academic & Professional, London, UK, Chap. 8.
- Wu, W.U., Hettiarachchy, N.S., Qi, M. (1998). Hydrophobicity, solubility, and emulsifying properties of soy protein peptides prepared by papain modification and ultrafiltration. *Journal of the American Oil Chemists Society*, **75**, 845.
- Wunderlich, B. (1990). *Thermal Analysis*, Academic Press, New York, NY.
- Wurzburg, O.B. (1995). Modified starches, in *Food Polysaccharides and Their Applications*, Stephan, A.M., Ed., Marcel Dekker, New York, NY, Chap. 3.
- Wustneck, R., Kragel, J., Miller, R., Fainerman, V.B., Wilde, P.J., Sarker, D.K., Clark, D.C. (1996). Dynamic surface tension and adsorption properties of beta-casein and beta-lactoglobulin. *Food Hydrocolloids*, **10**, 395.
- Wyszecki, G., Stiles, W.S. (1982). *Color Science : Concepts and Methods, Quantitative Data and Formulae*, 2nd ed., John Wiley & Sons, New York, NY.
- Xiong, Y.L. (1997). Structure-function relationships of muscle proteins, in *Food Proteins and Their Applications*, Damodaran, S., Paraf, A., Eds., Marcel Dekker, New York, NY, Chap. 12.
- Yaminsky, V.V., Jones, C., Yaminsky, F., Ninham, B.W. (1996a). Onset of hydrophobic attraction at low surfactant concentrations. *Langmuir*, **12**, 3531.
- Yaminsky, V.V., Ninham, B.W., Christenson, H.K., Pashley, R.M. (1996b). Adsorption forces between hydrophobic monolayers. *Langmuir*, **12**, 1936.
- Yan, Z.Y., McCarthy, M.J., Klemann, L., Otterburn, M.S., Finley, J. (1996). NMR applications in complex food systems. *Magnetic Resonance Imaging*, **14**, 979–981.

- Yazici, F., Akgun, A. (2004). Effect of some protein based fat replacers on physical, chemical, textural, and sensory properties of strained yoghurt. *Journal of Food Engineering*, **62**, 245.
- Ye, A.Q., Singh, H. (2001). Interfacial composition and stability of sodium caseinate emulsions as influenced by calcium ions. *Food Hydrocolloids*, **15**, 195.
- Ying, P.Q., Yu, Y., Jin, G., Tao, Z. (2003). Competitive protein adsorption studied with atomic force microscopy and imaging ellipsometry. *Colloids and Surfaces B: Biointerfaces*, **32**, 1.
- Yost, R.A., Kinsella, J.E. (1993). Properties of acidic whey protein gels containing emulsified butterfat. *Journal of Food Science*, **57**, 158.
- Young, S.L., Sarda, X., Rosenberg, M. (1993a). Microencapsulation properties of whey proteins. Part 1: Microencapsulation of anhydrous milk fat. *Journal of Dairy Science*, **76**, 2868.
- Young, S.L., Sarda, X., Rosenberg, M. (1993b). Microencapsulation properties of whey proteins. Part 2: Combination of whey proteins with carbohydrates. *Journal of Dairy Science*, **76**, 2878.
- Zhang, X., Davis, R.H. (1991). The rate of collisions due to Brownian or gravitational motion on small droplets. *Journal of Fluid Mechanics*, **230**, 479.
- Ziegler, G.R., Foegedding, E.A. (1990). The gelation of proteins, in *Advances in Food and Nutrition Research*, Vol. 34, Kinsella, J.E., Ed., Academic Press, San Diego, CA, p. 203.
- Zielinski, R.J. (1997). Synthesis and composition of food-grade emulsifiers, in *Food Emulsifiers and Their Applications*, Hasenhuettl, G.L., Hartel, R.W., Eds., Chapman & Hall, New York, NY, Chap. 2.
- Zobel, H.F., Stephan, A.M. (1995). Starch: Structure, analysis and application, in *Food Polysaccharides and Their Applications*, Stephan, A.M., Ed., Marcel Dekker, New York, NY, Chap. 1.



---

# Index

## A

- Absorbance, 434, 435
- Absorption, Light, 433–435, 440–444, 453, 457  
coefficient, 440–444
- Absorption, Ultrasonic, 489
- Adsorption, 179–191  
characterization of, 208–227  
competitive, 200–205  
conformational changes after, 189, 205–207  
displacement, 200–205  
energy barrier to, 190  
entropy, 180  
free energy, 180, 185, 197  
Gibbs adsorption isotherm, 184, 186  
ions, 191–192, 197  
isotherms, 182–186, 197, 202  
kinetics, 187–191, 224–225  
Langmuir adsorption isotherm, 184–186, 197, 202  
reversibility, 185  
surface activity, 187  
surface excess concentration, 182–184, 187  
surface pressure, 187
- Adsorption kinetics, 187–191, 224–225
- Agar, 156
- Aggregation, droplet, 5, 74, 86–92, 289–330  
flocculation, *see* Flocculation  
coalescence, *see* Coalescence  
partial coalescence, *see* Partial coalescence  
effect of colloidal interactions on, 53–56  
kinetics, 289–319
- Aggregation, molecular, 28, 39
- Alginate, 156, 159–160
- Amphiphilic biopolymers, 137–146
- Amphiphilic molecules, 4
- Analytical techniques, to characterize emulsion  
properties, 2–3, 461–514
- Anomalous diffraction theory, 442
- Antimicrobial agents, 171
- Antioxidants, 169–170
- Appearance, 431–460  
effect of colorant concentration 433–435, 456–457  
effect of colorant type 433–435, 456–457  
effect of droplet concentration, 433–435, 455–456  
effect of droplet size, 433–435, 455–456  
effect of droplet refractive index, 433–435, 456–457  
emulsion, 431–460  
human vision, 438  
light, interaction with matter, 432–438  
mathematical modeling of, 439–450  
measurement cell, 449–450  
measurement of, 450–454  
light scattering, 454  
sensory analysis, 454  
spectrophotometric colorimeters, 451–453  
trichromatic colorimeters, 453–454  
numerical calculations of color, 446–449  
optical properties of materials, 432–439  
polydispersity, 446  
reflectance, 442–444  
relative refractive index, 456  
scattering characteristics of emulsion droplets,  
440–442  
transmittance, 442–444  
tristimulus coordinates, 439, 445–446
- Aqueous phase characteristics, 428–429, 531–532; *see also* Water
- Aroma, 407–415; *see also* Flavor
- Atomic force microscopy, 473–475, 513
- Attenuation coefficient, ultrasonic, 489
- Attractive interactions, interdroplet  
depletion interactions, 74–78  
electrostatic interactions, 63–69  
hydrophobic interactions, 78–81  
van der Waals interactions, 56–62
- Attractive interactions, intermolecular  
electrostatic interactions, 30–33  
hydrogen bonds, 47–48  
hydrophobic interactions, 47–48, 118–121  
van der Waals interactions, 33–35
- Autocorrelation function, 482

## B

- Babcock method, fat analysis, 496
- Bancroft's rule, 130
- Benzene, 33

- Beverage emulsions, 526–533
    - composition, 526–529
    - microstructure, 529–530
    - physicochemical properties, 530
    - production, 530
  - Binding affinity, 147, 185
  - Bingham plastic, 352
  - Biochemical stability, 339–340
  - Biomodal distribution, 16
  - Biopolymers
    - blends, 165–167
      - coacervation, 166–167
      - incompatibility, 166–167
    - bridging, 301–302
    - conformation
      - at interface, 140, 180, 199–122
      - in solution, 138, 149–150
    - cross links, 154
    - depletion interactions, effect on, 75–76, 303–305
    - effective volume in solution, 149–150
    - emulsifiers, 122, 137–146, 266–267
      - types, 140–146
    - flavor, effect on, 395–397, 410–412
    - gelling agents, 153–158
      - types, 158–165
    - interaction with surfactants, 128
    - mouthfeel, 415–416
    - rheology, effect on, 149–153
    - salting out, 117
    - surface activity, 140, 266–267
    - thickening agents, 148–153
      - types, 158–165
    - viscosity, effect on, 149–153
  - Black-box approach, 24
  - Bond strength, 36
  - Bridging flocculation, 67–68, 301–302
  - Brominated vegetable oil, 172, 527
  - Brownian motion, 283
    - collisions due to, 292–294
  - Bulk compression, 343
  - Butan-2-one, 393
  - Butter, 522–523
- C**
- Calcium stearoyl lactylate, 123, 132
  - Calorimetry techniques, 213
  - Capillary rise, 229–230
  - Capillary viscometers, 360–361
  - Capillary wave
    - coalescence, effect on, 313–314
    - for surface tension measurement, 224
  - Carboxymethyl cellulose, 164
  - Carrageenan, 156, 158–159
  - Casein, 141–142, 158, 165
  - Cavitation, 245
  - Cavitational flow, 236
    - conditions, 245–246
  - Cellulose derivatives, 157, 163–164
  - Celluloses, modified, 145
  - Centrifugal sedimentation, 487–488
  - Centrifugation, 520
  - Charge, droplet, 68, 192, 198, 508–512
    - measurement, 508–512
      - electroacoustics, 510–512
      - particle electrophoresis, 508–509
    - surface charge density, 68, 192
    - surface potential, 68, 192
    - $\zeta$ -potential, 198, 508–512
  - Charge regulation, 64–66
  - Cheese, 525–526
  - Chelating agents, 169
  - Chemical stability, emulsion, 339–340
  - Chroma, 447
  - Churning, 522
  - Circular dichroism, 204, 208
  - Citric acid esters, 123
  - Cloud emulsions, beverage, 526
  - Cloud point, 126–127
  - CMC, *see* Critical micelle concentration
  - Coagulation, 291
  - Coalescence, 310–324
    - droplet aggregation, 6
    - factors affecting, 320–322
    - immediately after collision, 317
    - measurement of, 322–324
    - methods of controlling, 319–320
    - modeling droplet growth due to, 318–319
    - physical, molecular processes associated with, 311–313
    - physical basis of, 311–319
    - prevention of, 540
      - from primary minimum, 317–318
      - rate-limiting step, 316–318
      - from secondary minimum, 317
  - Collision efficiency, 296–298
  - Collision frequency, 292–296, 298
  - Collision mechanisms, relative importance of, 295–296
  - Colloidal interactions, 53–94, 384–385
    - characteristics of, 87
    - depletion interactions, 74–78
      - general characteristics of, 77–78
      - modeling of, 75–77
      - origin of, 74–75
    - droplet aggregation, 53–56
    - electrostatic interactions, 63–69
      - general characteristics of, 68–69
      - modeling, 63–68
      - origins of, 63
    - hydration interactions, 81–83
      - general characteristics of, 82–83
      - modeling, 81–82
      - origin of, 81
    - hydrophobic interactions, 78–81
      - general characteristics of, 81
      - modeling, 79–80
      - origin of, 78–79
    - influence on floc structure, 306
    - measurement of, 92–93
    - nonequilibrium effects, 85–86
      - continuous phase, hydrodynamic flow of, 85–86

- Gibbs-Marangoni effect, 86
  - interface, molecular rearrangements
    - at, 85
  - prediction of, 93
  - steric interactions, 69–74
    - general characteristics of, 73–74
    - modeling, 69–73
    - origin of, 69
  - thermal fluctuation interactions, 83–84
    - general characteristics of, 84
    - modeling, 84
    - origin of, 83–84
  - total interaction potential, 86–92
    - van der Waals/steric, 87–88
    - van der Waals/steric/electrostatic, 88–91
    - van der Waals/steric/electrostatic/depletion, 91–92
    - van der Waals/steric/electrostatic/hydrophobic, 91
  - van der Waals interactions, 56–62
    - general features of, 62
    - modeling, 56–62
    - origin of, 56
  - Colloid mill, 238, 250–251
  - Colloid vibration potential, 510–511
  - Color, *see* Appearance
  - Colorant type, concentration, 456–457
  - Colorimeters, 451–454
  - Color measurement, 450–454
    - light scattering, 454
    - sensory analysis, 454
    - spectrophotometric colorimeters, 451–453
    - trichromatic colorimeters, 453–454
  - Competitive adsorption, 200–205, 223
  - Complexity, food emulsions, 7–8
  - Component phases
    - properties of, droplet size and, 263–264
    - rheology of, 383–384
  - Computer modeling, liquid properties, 48–50
    - molecular dynamics techniques, 50
    - Monte Carlo techniques, 49–50
  - Computer simulation, rheology, 381–382
  - Configuration entropy, 180
  - Confocal laser scanning, 322, 468–470
  - Conformation
    - molecular, 45–47
      - compound interactions, 47–48
      - hydrogen bonds, 47–48
      - hydrophobic interactions, 48
  - Conformation entropy, 39, 180
  - Constant surface charge, 65
  - Constant surface potential, 65
  - Contact angles, 226–229
  - Continuous phase rheology, 286
  - Contrast, enhancement of, 467
  - Covalent interactions, 28–29, 305
  - Crank model, 404–406
  - Cream, 515–526
    - composition, 515–518
    - dairy products, 522–526
    - microstructure, 518–519
    - physicochemical properties, 520–522
    - production, 519–520
  - Creaming, *see* Gravitational separation
  - Creep, 353
  - Critical micelle concentration, 125–126
  - Crystal concentration, 328–329
  - Crystal growth, 105
  - Crystallinity, droplet, 499–508
    - dilatometry, 499–501
    - nuclear magnetic resonance, 501–504
    - thermal analysis, 504–506
    - ultrasonics, 506–508
  - Crystallization, 110–111
    - effects, 113–114
    - phase inversion, 337
  - Crystal morphology, 106
  - Curved interfaces, properties of, 225–226
- ## D
- Damar gum, 172–173, 527
  - Debye screening length, 59, 63–67, 192–195
  - Decaglycerol dioleate, 132
  - Decaglycerol hexaoleate, 132
  - Decaglycerol monooleate, 132
  - Demulsification, 265–267
    - biopolymer emulsifiers, 266–267
    - ionic surfactants, 266
    - methods of, 267
    - nonionic surfactants, 265–266
    - technique selection, 267
  - Density bottles, 497
  - Density measurements, 329
  - Depletion flocculation, 74–78, 303–305
  - Depletion interactions, 74–78, 303–305
    - examples of, 303–305
    - general characteristics of, 77–78
    - modeling of, 75–77
    - origin of, 74–75
  - Depletion technique, 87, 203
  - Detergent method, fat analysis, 496
  - Diacetyl tartaric acid esters, 123
  - Diameter, droplet, 9–17
  - Dielectric spectroscopy, 495
  - Differential scanning calorimetry, 329–330, 504–505
  - Differential thermal analysis, 505
  - Diffraction, anomalous, theory of, 442
  - Diffusing wave spectroscopy, 484–485
  - Diffusion coefficient, 189
  - Dilatant fluids, 348
  - Dilatometry, 499–501
  - Dilute emulsions, 442–443
  - Dilute systems, 365
  - Directions of research, factors influencing, 21–23
  - Discriminant methods, 421

- Disperse phase volume fraction, 3, 8–9, 382–383, 422–424, 495–499
    - alternative techniques, 499
    - density measurements, 496–498
    - electrical conductivity, 498–499
    - proximate analysis, 495–496
  - Displacement of emulsifiers, 202–204
  - DLVO theory, 90
  - Doppler shift spectroscopy, 483–484
  - Dressings, 533–543
    - composition, 534–537
    - microstructure, 537–538
    - physicochemical properties, 539–543
    - production, 539
  - Droplet aggregation, 53–56, 289–292
    - coalescence, 6
    - droplet-droplet encounters, 289
    - film rupture, 291–292
    - film thinning, 289–291
    - flocculation, 6
    - thin film formation, 291
  - Droplet charge, 17–18, 385–386, 508–512
    - electroacoustics, 510–512
    - particle electrophoresis, 508–509
    - surface charge density, 68, 192
    - surface potential, 68, 192
    - $\zeta$ -potential, 198, 508–512
  - Droplet coalescence, *see* Coalescence
  - Droplet creaming, *see* Gravitational separation
  - Droplet crystallinity, 18–19, 499–508
    - dilatometry, 499–501
      - nuclear magnetic resonance, 501–504
      - thermal analysis, 504–506
      - ultrasonics, 506–508
  - Droplet disruption, 237–246
    - emulsifier role, 246
    - nonideal fluid behavior role, 246
  - Droplet fluidity, 276
  - Droplet interactions, *see* Colloidal interactions
  - Droplet size, 9–17, 384, 424–426
    - controlling, 233–268
    - distribution, 9–17, 333, 465–495
    - emulsifier type, concentration, 261–263
    - energy input, effect on, 263
    - factors influencing, 261–265
    - measurement of, 465, 495
      - dielectric spectroscopy, 495
      - diffusing wave spectroscopy, 481–485
      - dynamic light scattering, 481–485
      - electrical pulse counting, 485–487
      - electroacoustics, 495
      - microscopy, 465–475
      - neutron scattering, 493–494
      - nuclear magnetic resonance, 492–493
      - sedimentation techniques, 487–488
      - static light scattering, 475–481
      - ultrasonic spectrometry, 488–492
    - reduction of, 285–286
  - Drop-volume method, 218–219
  - Du Nouy ring method, 215–216
  - Dynamic light scattering, 481–485
  - Dynamic rheometers, 361–363
  - Dynamic rheological tests, 354–356
- ## E
- Effective volume
    - biopolymers, 149, 304
    - droplets, 384–386
    - flocs, 308, 382
    - rheology, 150–152, 382–386
  - Efficiency of homogenization, 257–259
  - Egg proteins, 143–144
  - Egg yolk, 536–537
  - Elastic interaction, 72
  - Elastic solids
    - ideal, 342–344
    - nonideal, 344–345
    - types of deformations, 343
  - Electrical characteristics of interfaces, 64–68, 191–199, 508–512
    - double layer, 193–195
    - ion distribution, near charged interface, 193–198
    - measurement, 199, 508–512
      - electroacoustics, 510–512
      - particle electrophoresis, 508–509
    - origin of, 191–193
    - surface charge density, 68, 192
    - surface potential, 68, 192
    - $\zeta$ -potential, 198, 508–512
  - Electrical double layer, 193–195
  - Electrical pulse counting, 309, 323, 330, 335, 485–487
  - Electroacoustics, 495, 510–512
  - Electrolyte, influence on emulsion stability, 74
  - Electrolyte ions, 66–67, 114–117, 192
  - Electromagnetic interactions, 28
  - Electron microscopy, 309, 322, 470–473
  - Electron spin resonance, 329
  - Electrosonic amplitude, 510–511
  - Electrostatic interactions,
    - intermolecular, 30–33
    - interdroplet, 63–69
  - Electrostatic screening effects, 59, 63–68, 193–196, 298–301
  - Electrostatic stabilization, 74, 87
    - advantages, disadvantages of mechanisms, 74
  - Electroviscous effect, primary, 385–386
  - Emulsifiers, 122–148
    - amphiphilic biopolymers, 137–146
    - effectiveness, testing, 461–465
    - role of, 248–249
    - selection of, 146–148
    - surfactants, 122–137
  - Emulsifying capacity, 462–463
  - Emulsion formation, 233–268
    - demulsification, 265–267
      - biopolymer emulsifiers, 266–267
      - ionic surfactants, 266
      - methods of, 267
      - nonionic surfactants, 265–266
      - technique selection, 267

- droplet coalescence, 246–248
- droplet disruption, 237–246
- droplet size, factors influencing, 261–265
  - component phases, properties of, 263–264
  - emulsifier type, concentration, 261–263
  - energy input, 263
  - temperature, 264–265
- emulsifier, role of, 248–249
- future developments, 267–268
- homogenization, 233–236
- homogenization devices, 249–261
  - colloid mills, 250–251
  - comparisons, 259–261
  - high-pressure valve homogenizers, 251–253
  - high-speed mixers, 249–250
  - homogenization efficiency, 257–259
  - membrane homogenizer, 256–257
  - microchannel homogenizer, 256–257
  - microfluidization, 255–256
  - ultrasonic homogenizers, 253–255
- homogenizers, flow profiles in, 236–237
- physical principles, 237–249
- Emulsion ingredients, 95–174
  - antimicrobial agents, 171
  - antioxidants, 169–170
  - colorants, 172
  - emulsifiers, 122–148
    - amphiphilic biopolymers, 137–146
    - selection of, 146–148
    - surfactants, 122–137
  - fat replacers, 173
  - fats/oils, 96–112
    - bulk physicochemical properties, 98–100
    - chemical changes, 109–110
    - fat crystallization, 100–109
    - lipid selection, 110–112
    - molecular structure, organization, 98
  - flavors, 171
  - minerals, 168–169
  - selection of, factors influencing, 173–174
  - sequestrants, 169
  - texture modifiers, 148–168
    - gelling agents, 153–158
    - selection of, 167–168
    - thickening agents, 148–153
  - water, 112–122
    - aqueous phase, selection of, 121–122
    - bulk physicochemical properties, 113–114
    - molecular structure, organization, 112–113
    - organization of water molecules, influence of solutes, 114–121
    - physicochemical properties of solutions, influence of solutes on, 121
  - weighting agents, 172–173
- Emulsion instability, mechanisms of, 5–6, 269–340
- Emulsion mouthfeel, 415–416
- Emulsion properties
  - characterization of, 461–514
  - hierarchy of, 20–21
- Emulsion rheology, 341–388
  - attractive interactions, concentrated suspensions with, 376–380
  - colloidal interactions, 384–385
  - component phases, rheology of, 383–384
  - computer simulation of, 381–382
  - disperse phase volume fraction, 382–383
  - droplet charge, 385–386
  - droplet size, 384
  - factors influencing, 382–386
  - flocculated particles, dilute suspensions of, 370–372
  - flocculated systems, 376–380
  - future trends, 386–387
  - liquids, 345–351
  - long-range colloidal interactions, nonflocculated particles in absence of, concentrated suspensions of, 372–374
  - measurement of, 356–365
    - compression, 356–360
    - elongation, 356–360
    - empirical techniques, 364–365
    - shear measurements, 360–364
  - plastics, 351–352
  - properties of emulsions, 365–381
  - repulsive interactions, suspensions of nonflocculated particles with, 374–376
  - rigid nonspherical particles, dilute suspensions of, 368–370
  - rigid spherical particles, dilute suspensions of, 366–367
  - semisolid continuous phases, emulsions with, 380–381
  - solids, 342–345
  - viscoelastic materials, 353–356
- Emulsion stability, 269–340
  - biochemical, 339–340
  - chemical, 339–340
  - coalescence, 310–324
    - factors affecting, 320–322
    - measurement of, 322–324
    - methods of controlling, 319–320
    - physical basis of, 311–319
  - droplet aggregation, 289–292
    - droplet-droplet encounters, 289
    - film rupture, 291–292
    - film thinning, 289–291
    - thin film formation, 291
  - flocculation, 292–310
    - experimental measurement of, 309–310
    - methods of controlling, 298–305
    - physical basis of, 292–298
    - structure, properties, flocculated emulsions, 305–309
  - gravitational separation, 273–289
    - experimental characterization of, 286–289
    - methods of controlling, 284–286
    - physical basis of, 274–284
    - index of, 463–465
  - kinetic stability, 272–273



- Ostwald ripening, 330–335
  - experimental characterization of, 335
  - methods of controlling, 333–335
  - physical basis of, 331–333
- partial coalescence, 324–330
  - experimental characterization of, 329–330
  - methods of controlling, 327–329
  - physical basis of, 325–327
- phase inversion, 335–339
  - characterization of, 338–339
  - methods of controlling, 337–338
  - physical basis of, 336–337
- thermodynamic, 270–272
- Emulsions
  - appearance, 431–460
  - approaches to study of, 23–26
  - colloidal interactions, 53–94
  - complexity of, 7–8
  - composition of, ways to define, 95
  - dynamic nature of, 7
  - flavor, 389–430
  - formation, 233–268
  - general characteristics of, 3–8
  - ingredient partitioning, 6–7
  - ingredients, 95–174
  - interfacial properties, characterization, 175–232
  - molecular characteristics, 27–52
  - monodisperse, 9
  - polydisperse, 9
  - in practice, 515–544
  - properties, characterization of, 461–514
  - rheology, 341–388
  - stability, 269–340
- Energy barrier, 5, 290
- Energy densities, 259–260
- Energy efficiency, 258–259
- Energy input, droplet size and, 263
- Enthalpic contribution to, 64
- Entropy, 180
- Entropy effects, 38–41
- Environmental conditions, influence of, 321–322
- Equilibrium measurements, 417–420
- Equilibrium partition coefficients, of flavors in oil,
  - water, 393
- Ethanol, 33, 178, 393
- Ethoxylated monoglyceride, 132
- Ethylene glycol, 33
- Evaporation, 519
- Experimental error, possible sources of,
  - 363–364
- F**
- Fat crystallization, 100–109, 282
- Fat replacers, 173
- Fats, edible, crystallization of, 107–108
- Fats/oils, 96–112
  - bulk physicochemical properties, 98–100
  - chemical changes, 109–110
  - fat crystallization, 100–109
  - lipid selection, 110–112
  - molecular structure, organization, 98
- Fatty acid salts, 123
- Filamentous, particulate, distinguishing between,
  - 154–155
- Filled gels, 380–381
- Film rupture, 312–313
  - mechanisms of, 313–315
- Film stretching, 314
- Film thinning, 289–291
- Film tearing, 314–315
- Fish proteins, 143
- Flavor, 171, 389–430, 521–522, 532–533, 542–543
  - degradation, 339
  - emulsion, 389–430
    - beverage, 526
  - emulsion mouthfeel, 415–416
  - factors influencing, 422–429
    - aqueous phase characteristics, 428–429
    - disperse phase volume fraction, 422–424
    - droplet size, 424–426
    - interfacial characteristics, 426–427
    - oil phase characteristics, 427–428
  - measurement of, 417–422
    - nonvolatile flavor compounds, analysis of, 419–421
    - sensory analysis, 421–422
    - volatile flavor compounds, analysis of, 417–419
  - nonvolatile compounds, release, 402–407
  - in oil, water, equilibrium partition coefficients, 393
  - partitioning, 391–401
    - in absence of interfacial membrane, 397–398
    - flavor binding on partitioning, 395–397
    - flavor ionization, 394–395
    - homogeneous liquid, vapor, 391–392
    - in presence of interfacial membrane, 398–401
    - surfactant micelles, partitioning, 397
  - physicochemical processes, 389–390
  - physiological processes, 390
  - profile, 110
  - psychological processes, 390
  - release, 401–415
    - from emulsions, 412–415
    - from homogeneous liquids, 407–410
    - kinetics, 403–407
    - of volatile compounds, 407–415
- Floc structure
  - fractal geometry describing, 306–308
  - influence of colloidal interactions, 306
  - influence on emulsion properties, 308–309
- Flocculated particles, dilute suspensions of, 370–372
- Flocculated systems, 376–380
- Flocculation, 278–281, 286, 292–310
  - droplet aggregation, 6
  - experimental measurement of, 309–310
  - methods of controlling, 298–305
  - particles in suspensions, monitoring of, 485
  - physical basis of, 292–298
  - structure, properties, flocculated emulsions, 305–309
- Flow profiles, homogenizers, 236–237

Fluid spherical particles, dilute suspensions of, 367–368

Food emulsions, *see* Emulsions

Fractal dimension, 306–307

Fractal geometry, to describe floc structure, 306–308

Free energy

adsorption, 185

emulsion formation, 271–272

film rupture, 313

hole formation, 315

interfacial, 176

mixing, 41–43

nucleus formation, 103

surface, 176

transfer, 119

transition, 40, 46

Freeze-thaw stability, 74

Freezing, 321

Frequency distribution function

log-normal, 15–16

normal, 15

## G

Galactomannans, 161

Gas-liquid interface

in absence of solutes, 182–183

in presence of solutes, 183–184

Gases

bulk physicochemical properties of, 51

thermodynamic properties, 51

Gelatin, 157

Gelation, 153–158

Gellan gum, 157, 162–163

Gelling agents, 4, 153–158

molecular, functional properties of, 156

Gelting, 164–165

Gerber method, fat analysis, 496

Gibbs adsorption isotherm, 184, 186–187

Gibbs dividing surface, 183–184

Gibbs-Marangoni effect, 86, 305

Globular proteins, 158, 165

Glycerol dioleate, 132

Glycerol monolaurate, 132

Glycerol monoleate, 132

Glycerol monostearate, 132

Glycol monolaurate, propylene, 132

Glycol monostearate, propylene, 132

Gravitational sedimentation, 487

Gravitational separation, 273–289, 364

collisions due to, 294–295

creaming, 6

experimental characterization of, 286–289

methods of controlling, 284–286

physical basis of, 274–284

sedimentation, 6

Guar gum, 161

Gum arabic, 144, 161, 178

Gum karaya, 161

Gum tragacanth, 161

## H

Hamaker function, 57–62

Hard-shell model, 35

Head space analysis, volatile flavors, 417–419

Heat stability, emulsions, 302–303

Helix conformation, 46

Helix-to-coil transition, 46

Henderson-Hasselbach equation, 394

Heptan-2-one, 393

Heterodyne technique, 483–484

Heterogeneous charge distribution, 66

Heterogeneous nucleation, 101–105

primary, 101

secondary, 101

Heteropolymer, 137

Hexaglycerol dioleate, 132

High-pressure valve homogenizers, 251–253

High-speed mixer, 238, 249–250

HLB number, 130–133

Hole formation, 315–316

Homodyne technique, 483–484

Homogenization, 4, 233–268, 519

Homogenization devices, 249–261

colloid mills, 250–251

comparisons, 259–261

energy density, 259–260

energy efficiency, 258–259

flow profiles in, 236–237

high-pressure valve homogenizers, 251–253

high-speed mixers, 249–250

homogenization efficiency, 257–259

membrane homogenizer, 256–257

microchannel homogenizer, 256–257

microfluidization, 255–256

ultrasonic homogenizers, 253–255

types of, 238, 249–261

Homopolymer, 137

Hookean solid, 342

Hooke's law, 344, 357

HPLC, 417

Human vision, 438

Hydration, 116–118

Hydration interactions, 81–83

general characteristics of, 82–83

modeling, 81–82

origin of, 81

Hydration number, 116

Hydrocarbon chains, 123, 126

Hydrodynamic instabilities, 364

Hydrodynamic interactions, 85–86, 305

droplet collisions, 305

gravitational separation, 276

rheology, 366–373

Hydrolysis, 339

Hydrometers, 497–498

Hydrophile-lipophile balance, 131–133

Hydrophobic effect, 118–121

Hydrophobic interactions, 48, 78–81, 87, 120–121, 302–303  
 examples of, 302–303  
 general characteristics of, 81  
 modeling, 79–80  
 origin of, 78–79

## I

Ice cream, 523–524  
 Ideal elastic solid, 342  
 Ideal liquid, 345  
 Ideal plastic, 352  
 Immiscible liquids, 28  
*In vivo* analysis, flavor, 418–421  
 Induction forces, 33–34  
 Infrared spectroscopy, 204, 209, 496  
 Ingredient partitioning, emulsions, 6–7  
 Instability, emulsion, mechanisms of, 5–6  
 Interaction with biopolymers, 128–130  
 Interaction energies, 38–41  
 Interaction entropy, 180  
 Interaction of water with polar solutes, 117–118  
 Interactions, droplet, 512–513  
 Interdroplet pair potential, 53–57, 63–64, 69  
 Interface, adsorption to, 28  
 Interfacial activity, emulsion stabilization, 138–140  
 Interfacial characteristics, 426–427  
   in determining emulsion properties, 175  
 Interfacial composition, 147, 199–204, 184  
   characterization of, 202–204  
   factors influencing, 199–202  
 Interfacial electrical properties, 176  
 Interfacial energy, 176  
 Interfacial forces, 237–239  
 Interfacial membranes, 333–334, 516–518, 528–529, 536–537  
   disruption, prevention of, 328  
   influence of, 61–62  
   rupture, prevention of, 319–320  
 Interfacial properties, 17, 175–232  
   capillary rise, 229–230  
   contact angles, 226–229  
   curved interfaces, properties of, 225–226  
   electrical characteristics, 191–199  
   solute adsorption, 182–191  
 Interfacial rheology, 221–225  
   characterization of, 222–225  
   dilatational rheology, 223–225  
   factors influencing, 221–222  
   shear rheology, 222–223  
 Interfacial structure, 204–213  
   characterization of, 208–213  
   factors influencing, 204–208  
 Interfacial tension, 214–221  
   characterization of, 214–221  
   definition, 214  
   factors influencing, 214  
 Interference reflection techniques, 210  
 Intermediate-wavelength regime, 477  
 Intermolecular pair potential, 30–32, 35–38  
 Interpenetration, compression regime, 72

Ion binding, 66, 198  
 Ion bridging, 67–68  
 Ionic solutes, interaction of water with, 114–117  
 Ionic strength, 66  
   influence on electrostatic interactions, 66–67, 193–198, 298–301  
 Ionic surfactants, 266  
 Ionization, flavor, 394–395  
 Ions, adsorbed, 192  
 Irreversible binding, 401

## J

Jet homogenizer, 254

## K

Kinetic stability, 4–5, 270–273  
 Kinetics  
   droplet aggregation, 289–319  
   flavor release, 403–407  
 Krafft point, 126  
 Kubelka-Munk theory, 443–444

## L

Lactic acid esters, 123  
 Laminar flow, 236  
   conditions, 240–244  
 Laminar-viscous regime, 236  
 Langmuir adsorption isotherm, 184–186, 197  
 Langmuir trough measurements, 211–212  
 Laplace equation, 225  
 Laplace pressure, 237  
 Laser scanning confocal microscopy, 322, 468–470  
 Lecithin, 123, 137  
 Light, interaction with matter, 432–438  
 Light absorption, 433–435  
 Light scattering, 309, 323, 330, 335, 435–438, 454  
   static, neutron scattering, similarities between, 494  
 Lipid oxidation, 111, 169–170, 322, 339  
 Lipolysis, 109  
 Liquid-liquid interfaces, 176–179, 184  
 Liquid properties, computer modeling, 48–50  
   molecular dynamics techniques, 50  
   Monte Carlo techniques, 49–50  
 Liquids  
   bulk physicochemical properties of, 51  
   ideal, 345–346  
   nonideal, 346–351  
   rheology, 345–351  
   thermodynamic properties, 51  
 Log normal distribution, 15–16  
 Long-wavelength regime, 476–477  
 Low fat foods, 534

## M

Magnetic chaining, 513  
 Magnification, 465

- Many-flux theory, light scattering, 444
  - Margarine, 282
  - Mass transfer, flavors, 389–391, 403–429
  - Mastication, 402–416
  - Mathematical modeling of color, 439–450
  - Maximum bubble pressure method, 220–221
  - Maximum packing factor, rheology, 376, 384, 386
  - Mayonnaise, 533–543
  - Mean droplet size, 12–15
  - Measurement of flavor, 417–422
    - nonvolatile flavor compounds, analysis of, 419–421
    - sensory analysis, 421–422
    - volatile flavor compounds, analysis of, 417–419
  - Measurement of rheology, 356–365
    - compression, elongation, 356–360
    - empirical techniques, 364–365
    - shear measurements, 360–364
  - Meat proteins, 142–143
  - Mechanical viscometers, 361–363
  - Melting, 97–102, 107–108
  - Membrane homogenizer, 256–257
  - Membrane processing, 238
  - Meniscus, 229
  - Metastability, 4–5
  - Methanol, 33, 393
  - Methoxyl, 160
  - Micelles, 124–126
  - Microchannel homogenizer, 256–257
  - Microemulsions, 127, 272
  - Microfluidization, 238, 255–256
  - Microscopy, 465–475
    - atomic force, 209, 473–475
    - Brewster angle, 209–210
    - confocal laser scanning, 322, 468–470
    - electron, scanning, 209, 472, 473
    - electron, transmission, 209, 470–472
    - optical, 209, 465–470
  - Microstructure, *see* Particle size distribution and Microscopy
  - Mie theory, 441–442
  - Milk, 515–526
    - composition, 515–518
    - dairy products, 522–526
    - microstructure, 518–519
    - physicochemical properties, 520–522
    - production, 519–520
  - Milk proteins, 141–142
    - casein 141–142, 158, 165
    - whey, 141–142, 165
  - Minerals, 168–169
  - Mixing thermodynamics, 41–45
    - complications, 44–45
    - entropy change on, 43
    - overall free energy change on, 43–44
    - potential energy change on, 42–43
  - Molecular characteristics, 27–52
    - computer modeling, liquid properties, 48–50
    - molecular dynamics techniques, 50
    - Monte Carlo techniques, 49–50
    - interaction energies, 38–41
    - intermolecular pair potential, 35–38
    - measurement of, 50–51
    - mixing thermodynamics, 41–45
      - complications, 44–45
      - entropy change on, 43
      - overall free energy change on, 43–44
      - potential energy change on, 42–43
    - molecular conformation, 45–47
      - compound interactions, 47–48
      - hydrogen bonds, 47–48
      - hydrophobic interactions, 48
      - steric overlap interactions, 35
      - van der Waals interactions, 33–35
  - Molecular conformation, 45–47
    - compound interactions, 47–48
    - hydrogen bonds, 47–48
    - hydrophobic interactions, 48
  - Molecular interactions
    - covalent interactions, 28–29
    - electrostatic interactions, 29–33
    - origin, nature of, 28–35
  - Molecular organization, 27–28
  - Monodisperse emulsion, 9
  - Monoglycerides, 123, 136
    - organic acid esters of, 136
  - Monooleate, polyoxyethylene, sorbitan, 123, 132
  - Monopalmitate, polyoxyethylene, sorbitan, 132
  - Monostearate, polyoxyethylene, sorbitan, 123, 132
  - Mouthfeel, 415–416
    - biopolymers, 153, 162
    - fat crystals, 100
    - ice crystals, 113
  - Multiple emulsions, 4
  - Multiple scattering, 437
  - Multilayer formation, 146
  - Multivalent ions, 66–67, 299–301
- ## N
- N-dodecane, 178
  - Negative adsorption, 180
  - Nephelometer, 454
  - Neutron reflection, 210
  - Neutron scattering, 493–494
  - New analytical techniques, to characterize food
    - properties, 2–3
  - Newtonian liquid, 345
  - N-hexadecane, 178
  - N-octane, 178
  - Non-Newtonian liquid, 281–282
  - Nondilute systems, 276–278
  - Nonequilibrium effects, 85–86
    - continuous phase, hydrodynamic flow of, 85–86
    - Gibbs-Marangoni effect, 86
    - interface, molecular rearrangements at, 85
  - Nonideal plastics, 352
  - Nonideal solids, 344
  - Nonionic surfactants, 265–266
  - Nonpolar solutes, interaction of water with, 118–121
  - Nonspherical particles, dilute suspensions of, 368–370
  - Nonvolatile flavor compounds, analysis of, 419–421

Normal distribution, particle size, 15  
 Nuclear magnetic resonance, 492–493, 501–504  
 Nucleation,  
   heterogeneous nucleation, 101–105  
     primary, 101  
     secondary, 101  
   homogeneous, 104  
 Numerical calculations, color, 446–449

## O

Octanol, 393  
 Oil content, proximate analysis, 495–496  
 Oil-in-water emulsion, definition, 3  
 Oil quality, 111–112  
 Oiling off, 310, 319  
 Oils, *see* Fats/oils  
 Oleic acid, 132  
 Optical microscopy, 309, 322, 335, 465–468  
 Optical properties of materials, 432–439  
 Organization of water molecules, influence of solutes,  
   114–121  
 Orientation entropy, 180  
 Orientation forces, 34–35  
 Orientational entropy, 38  
 Oscillating drop method, 223  
 Oscillating U-tubes, 498  
 Osmotic pressure, 75–76  
 Ostwald ripening, 230–231, 330–335  
   experimental characterization of, 335  
   methods of controlling, 333–335  
   physical basis of, 331–333  
 Overflowing cylinder method, 224  
 Oxidation, 109  
 Oxidative stability, 111

## P

Pair potential  
   interdroplet, 54  
   intermolecular, 30  
 Parameters of food manufacturers, 146  
 Partial coalescence, 108, 324–330  
   experimental characterization of, 329–330  
   methods of controlling, 327–329  
   physical basis of, 325–327  
 Particle electrophoresis, 508–509  
 Particle size, 9–17  
   controlling, 233–268  
   distribution, 9–17, 333, 465–495  
   emulsifier type, concentration, 261–263  
   energy input, effect on, 263  
   factors influencing, 261–265  
   mathematical models, 15  
   mean, 12–15  
   measurement of, 465, 495  
     dielectric spectroscopy, 495  
     diffusing wave spectroscopy, 481–485  
     dynamic light scattering, 481–485  
     electrical pulse counting, 485–487  
     electroacoustics, 495  
     microscopy, 465–475  
     neutron scattering, 493–494  
     nuclear magnetic resonance, 492–493  
     sedimentation techniques, 487–488  
     static light scattering, 475–481  
     ultrasonic spectrometry,  
       488–492  
   presenting, 10–12  
   reduction of, 285–286  
   standard deviation, 12–15  
 Particulate, filamentous, distinguishment between,  
   154–155  
 Partitioning, flavor, 6–7, 391–401  
   binding, 395–397  
   ionization, 394–395  
   oil-water, 391–392  
   interfacial membrane, 398–401  
   surfactant micelles, 397  
 Pasteurization, 519  
 PCS, *see* Photon correlation spectroscopy  
 Peclet number, 381, 382  
 Pectin, 156, 160–161  
 Pendant drop methods, 217–218  
 Penetration theory, flavor, 407–415  
 Pent-2-one, 393  
 Phase inversion, 335–339  
   characterization of, 338–339  
   methods of controlling, 337–338  
   physical basis of, 336–337  
 Phase inversion temperature, 133–134  
 Photon correlation spectroscopy, 482–483  
 Physicochemical approaches, 24–25  
 Physicochemical properties of solutions, 121–130  
 PIT, *see* phase inversion temperature  
 Plant proteins, 144  
 Plastics, rheology, 351–352  
 Poisson-Boltzmann theory, 195–200  
 Polyglycerol esters, 123  
 Polymeric steric stabilization, 74  
 Polymorphism, 106–107  
 Polyol esters, fatty acids, 136–137  
 Polysaccharides, 144–145, 158–164, 320  
   enzymatic hydrolysis, 322  
 Potassium oleate, 132  
 Potential determining ions, 192  
 Primary minimum, 290  
 Properties of emulsions, 8–20  
   disperse phase volume fraction, 8–9  
   droplet charge, 17–18  
   droplet crystallinity, 18–19  
   droplet interactions, 19–20  
   hierarchy of, 20–21  
   interfacial properties, 17  
   particle size distribution, 9–17  
 Propylene glycol esters, 123  
 Protein-polysaccharide complexes, 146  
 Proteins, 140–144, 164–165  
   casein, 141–142, 158, 165  
   egg, 143–144

enzymatic hydrolysis, 322  
 fish, 143  
 meat, 142–143  
 plant, 144  
 soy, 144  
 whey, 141–142, 165  
 Pseudoplastic fluids, 348  
 Psychological processes, flavor, 390  
 Pulse-echo techniques, ultrasonic, 491–492

## R

Radius, droplet, 9–17  
 Rate-limiting step, coalescence, 316–318  
 Rayleigh-Gans-Debye theory, 442  
 Reductionism-integrationist approach, 25  
 Reflection spectrophotometry, 452–453  
 Refractive index, influence of, 448–449  
 Relative refractive index of droplets, 456  
 Release of flavor, 401–402, 401–415  
   of nonvolatile compounds, 402–407  
   of volatile compounds, 407–415  
 Repulsive interactions, interdroplet  
   electrostatic interactions, 63–69  
   hydration interactions, 81–82  
   steric, 69–74  
   thermal fluctuation interactions, 83  
 Repulsive interactions, intermolecular  
   electrostatic interactions, 29–33  
   steric overlap, 35  
 Reverse micelles, 124–125  
 Reversible binding, 400–401  
 Rheology, 341–388  
   attractive interactions, concentrated suspensions  
     with, 376–380  
   colloidal interactions, 384–385  
   component phases, rheology of, 383–384  
   computer simulation of, 381–382  
   disperse phase volume fraction, 382–383  
   droplet charge, 385–386  
   droplet size, 384  
   emulsion, 341–388  
   factors influencing, 382–386  
   floculated particles, dilute suspensions of,  
     370–372  
   floculated systems, 376–380  
   future trends, 386–387  
   interfacial, 221–225  
     characterization of, 222–225  
     factors influencing, 221–222  
   liquids, 345–351  
   long-range colloidal interactions, 372–374  
   measurement of, 356–365  
     compression, elongation, 356–360  
     empirical techniques, 364–365  
     shear measurements, 360–364  
   plastics, 351–352  
   properties of emulsions, 365–381  
   repulsive interactions, suspensions of  
     nonfloculated particles with, 374–376

rigid nonspherical particles, dilute suspensions  
   of, 368–370  
 rigid spherical particles, dilute suspensions  
   of, 366–367  
 semisolid continuous phases, emulsions with,  
   380–381  
 solids, 342–345  
   viscoelastic materials, 353–356  
 Rheometer gap effects, 363  
 Rheopectics, 350  
 Rigid nonspherical particles, dilute suspensions  
   of, 368–370  
 Rigid spherical particles, dilute suspensions of,  
   366–367  
 Rupture, interfacial membranes, prevention of, 319–320

## S

SAIB, 172–173, 527  
 Salad cream, 533–543  
 Salad dressing, 533–543  
 Salting out, 117  
 Scanning calorimetry, 329–330; *see also* Differential  
   scanning calorimetry  
 Scanning electron microscopy, 472–473  
 Scattering characteristics of emulsion droplets, color  
   and, 440–442  
 Scattering coefficient, light, 443  
 Scattering pattern, light, 138  
 Scattering methods, angular, 477–479  
 Schultz-Hardy rule, 299–300  
 Screening, *see* Electrostatic screening effects  
 Scientific approach, to understanding food emulsion  
   properties, 2  
 Scientific personnel, availability of, 22  
 Secondary electroviscous effect, 386  
 Secondary minimum, 290  
 Sedimentation, *see* Gravitational separation  
 Sedimentation techniques, 487–488  
 Seed gums, 156, 161  
 SEM, *see* Scanning electron microscopy  
 Semiempirical calibration approach, 450  
 Semisolid continuous phases, emulsions with, 380–381  
 Sensory analysis, color, 454  
 Sensory analysis, flavor, 421  
 Sensory analysis, texture, 387  
 Sequestrants, 169  
 Sessile drop methods, 217–218  
 SFC, *see* Solid fat content  
 Shear plane, 196–197  
 Shear-rate dependent nonideal liquids, 347–349  
 Shear strain, typical rates of, 347  
 Shear thickening, 348–349  
 Shear thinning,  
   biopolymer solutions, 152–153  
   emulsions, 348, 370–380  
 Short-wavelength regime, 477  
 Single scattering, 437  
 Size distribution, droplet, diffusing wave  
   spectroscopy, 481–485

- Size of droplet, 465–495
  - dielectric spectroscopy, 495
  - dynamic light scattering, 481–485
  - electrical pulse counting, 485–487
  - electroacoustics, 495
  - microscopy, 465–475
  - neutron scattering, 493–494
  - nuclear magnetic resonance, 492–493
  - sedimentation techniques, 487–488
  - static light scattering, 475–481
  - ultrasonic spectrometry, 488–492
- Small angle neutron scattering, 329
- Small molecule surfactants, 123
- Sodium lauryl sulfate, 132
- Sodium oleate, 132
- Sodium stearyl lactylate, 123, 132
- Soft-shell model, 35
- Solid fat content, 110
- Solids
  - bulk physicochemical properties of, 51
  - rheology, 342–345
  - thermodynamic properties, 51
- Solubilization, 127
- Solute adsorption to interfaces, 182–191
  - adsorbed, bulk solute concentrations, relationship between, 184–187
  - adsorption kinetics, 187–191
  - surface-active solutes, stipulating interfacial properties of, 187
  - surface excess concentration, 182–184
- Solutes
  - influence on physicochemical properties of solutions, 121
  - interfaces in presence of, 179–182
- Solution, surfactants in, molecular organization of, 124–125
- Sorbitan monolaurate, 132
- Sorbitan monooleate, 132
- Sorbitan monopalmitate, 132
- Sorbitan monostearate, 123, 132
- Sorbitan trioleate, 132
- Sorbitan tristearate, 123, 132
- Soy lecithin, 132
- Soy protein, 144
- Spans, 123
- Spatial arrangements of molecules, transitions between, 39
- Spectral transmittance, reflectance of emulsions, color and, 442–444
- Spectrophotometric colorimeters, 451–453
- Spectroscopy techniques, 209–210
- Spectroturbidimetric methods, 479
- Spherical particles, dilute suspensions of, 366–367
- Spin resonance, 329; *see also* Electron spin resonance
- Spinning drop method, 219–220
- Spontaneous hole formation, 314
- Squeezing flow viscometry, 359
- Stability, emulsion, 269–340
- Stability index, 463–465
- Starch, 145, 157, 163
- Static light scattering, 475–481
- Stearyl lactylate salts, 137
- Steric interactions, 69–74, 301
  - characteristics of, 73–74
  - distance dependence of, 72–73
  - modeling, 69–73
  - origin of, 69
- Steric overlap interactions, 35
- Stokes' law, 274–284
- Stokesian Dynamics, 381
- Strength of interactions, structural organization, within bulk liquid, 43–44
- Stress-strain curve, 358
- Structure breaker, 116
- Structure maker, 116
- Structural organization, within bulk liquid, strength of interactions, 43–44
- Structure, interfacial, 204–213
  - characterization of, 208–213
  - factors influencing, 204–208
- Succinic acid esters, 123
- Sucrose esters, 123
- Sucrose monoesters, 132
- Sucrose monolaurate, 132
- Sucrose trimesters, 132
- Supercooling, 101–102
- Surface activity, 147, 185–187
- Surface charge, 65
- Surface denaturation, 302
- Surface force measurements, 212–213
- Surface load, 147, 184
- Surface potential, 65
- Surface pressure, 147, 181
- Surface rheology, 221–225
- Surface tension, 176–179, 214–221
- Surfactant classification schemes, 130–135
- Surfactant-induced phase inversion, 336–337
- Surfactant micelles, partitioning, 397

## T

- Taste, 402–407; *see also* Flavor
- TEM, *see* Transmission electron microscopy
- Temperature, droplet size and, 264–265
- Tension, interfacial, 214–221
  - characterization of, 214–221
  - factors influencing, 214
- Texture, *see* Rheology
- Texture modifiers, 148–168
  - gelling agents, 153–158
  - selection of, 167–168
  - thickening agents, 148–153
- Thermal analysis, 504–506
- Thermal denaturation, 142–143, 302
- Thermal fluctuation interactions, 83–84
  - general characteristics of, 84
  - modeling, 84
  - origin of, 83–84
- Thermal stability, emulsions, 302–303
- Thermodynamic stability, 4–5, 270–272
  - vs.* kinetic stability, 4–5

Thermodynamics, mixing, 41–45  
     complications, 44–45  
     entropy change on, 43  
     overall free energy change on, 43–44  
     potential energy change on, 42–43  
 Thickening agents, 4, 148–153  
     molecular, functional properties of, 156  
 Thixotropic behavior, 350  
 Through-transmission, 492  
 Time-dependent nonideal liquids, 349–351  
 Total interaction potential, 86–92  
     van der Waals/steric, 87–88  
     van der Waals/steric/electrostatic, 88–91  
     van der Waals/steric/electrostatic/depletion, 91–92  
     van der Waals/steric/electrostatic/hydrophobic, 91  
 Translational entropy, 38  
 Transmission electron microscopy, 470–472  
 Transmission spectrophotometry, 451–452  
 Transmittance, 434  
 Tree gum exudates, 161  
 Triacylglycerol, 178; *see also* Fats/oils  
     “tuning-fork” structure, 98  
 Trichromatic colorimeters, 453–454  
 Triglycerol monostearate, 132  
 Trioleate, polyoxyethylene, sorbitan, 132  
 Tristearate, polyoxyethylene, sorbitan, 123, 132  
 Tristimulus coordinates, 439  
     spectral reflectance, transmittance, color and, 445–446  
 Turbidity, 438, 442–443  
 Turbulent flow, 236  
     conditions, 244–245  
 Turbulent-inertial regime, 236  
 Turbulent-viscous regime, 236  
 Tweens, 123

## U

Ultramicroscope, 467  
 Ultrasonic homogenizers, 253–255  
 Ultrasonic jet homogenizer, 238  
 Ultrasonic probes, 238  
 Ultrasonic spectrometry, 309, 323, 488–492  
 Ultrasonic velocity measurements, 329  
 Ultrasonics, 506–508  
 Undecan-2-one, 393  
 Universal Testing Machines, 356  
 UV-visible spectrophotometry, 451–452

## V

van der Waals interactions, interdroplet, 56–62, 87  
     features of, 62  
     modeling, 56–62  
     origin of, 56  
     total interaction potential, 87–88  
 van der Waals interactions, intermolecular, 33–35,  
 van der Waals/steric/electrostatic/depletion  
     interactions, total interaction potential, 91–92  
 van der Waals/steric/electrostatic/hydrophobic  
     interactions, total interaction potential, 91

van der Waals/steric/electrostatic interactions, total  
     interaction potential, 88–91  
 Vesicles, 124  
 Viscoelastic materials, rheology, 353–356  
 Viscometers, 361–364  
 Viscosity, 345  
     apparent, 347  
     biopolymer solutions, 148–153  
     concentrated emulsions, 372–380  
     creaming, 274–275, 286  
     dilute emulsions, 366–372  
     emulsions, 341–388  
     floculated emulsions, 308  
     gravitational separation, 274–275, 286  
     interfacial, 221–225  
     measurement, 361–364  
     sedimentation, 274–275, 286  
 Volatile flavor compounds, analysis of, 417–419

## W

Wall-slip effects, 363  
 Water, 112–122  
     aqueous phase, selection of, 121–122  
     bulk physicochemical properties, 113–114  
     molecular structure, organization, 112–113  
     organization of water molecules, influence of  
         solutes, 114–121  
     physicochemical properties of solutions, influence  
         of solutes on, 121  
 Water content, proximate analysis, 495–496  
 Water-in-oil emulsion, definition, 3  
 Weak flocculation, 74, 291  
 Weak nuclear interactions, 28  
 Weber number, 239–244  
 Weighting agents, 172–173  
     influence of, 284–285  
 Wetting, 226–228  
 Whey protein, 141–142, 165  
 Whipped cream, 522  
 Wilhelmy plate method, 216–217

## X

X-ray diffraction, 329, 330  
 Xanthan, 156, 161–162

## Y

Yield stress, 351–352  
 Yogurt, 524–525  
 Youngs modulus, 343  
 Young-Dupre equation, 227  
 Young-Laplace equation, 225

## Z

Zero interaction regime, 72  
 $\zeta$ -potential, 198–199, 508–512